IJACSA
WHERE WISDOM SHARES
International Journal of Advanced Computer Science and Applications

Volume 8 Issue 6
June 2017

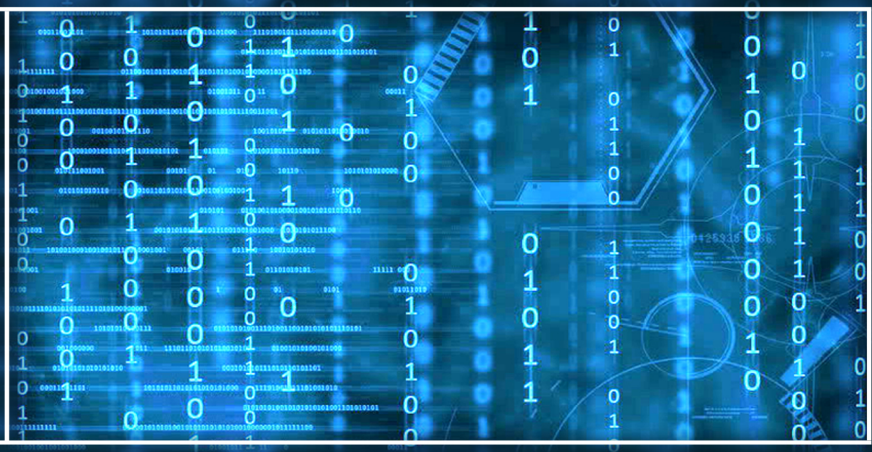

ISSN 2156-5570(Online)
ISSN 2158-107X(Print)

SAI
www.ijacsa.thesai.org

Editorial Preface

From the Desk of Managing Editor…

It may be difficult to imagine that almost half a century ago we used computers far less sophisticated than current home desktop computers to put a man on the moon. In that 50 year span, the field of computer science has exploded.

Computer science has opened new avenues for thought and experimentation. What began as a way to simplify the calculation process has given birth to technology once only imagined by the human mind. The ability to communicate and share ideas even though collaborators are half a world away and exploration of not just the stars above but the internal workings of the human genome are some of the ways that this field has moved at an exponential pace.

At the International Journal of Advanced Computer Science and Applications it is our mission to provide an outlet for quality research. We want to promote universal access and opportunities for the international scientific community to share and disseminate scientific and technical information.

We believe in spreading knowledge of computer science and its applications to all classes of audiences. That is why we deliver up-to-date, authoritative coverage and offer open access of all our articles. Our archives have served as a place to provoke philosophical, theoretical, and empirical ideas from some of the finest minds in the field.

We utilize the talents and experience of editor and reviewers working at Universities and Institutions from around the world. We would like to express our gratitude to all authors, whose research results have been published in our journal, as well as our referees for their in-depth evaluations. Our high standards are maintained through a double blind review process.

We hope that this edition of IJACSA inspires and entices you to submit your own contributions in upcoming issues. Thank you for sharing wisdom.

Thank you for Sharing Wisdom!

Managing Editor
IJACSA
Volume 8 Issue 6 June 2017
ISSN 2156-5570 (Online)
ISSN 2158-107X (Print)

Editorial Board

Reviewer Board Members

- **Aamir Shaikh**
- **Abbas Al-Ghaili**
  Mendeley
- **Abbas Karimi**
  Islamic Azad University Arak Branch
- **Abdelghni Lakehal**
  Université Abdelmalek Essaadi Faculté Polydisciplinaire de Larache Route de Rabat, Km 2 - Larache BP. 745 - Larache 92004. Maroc.
- **Abdul Razak**
- **Abdul Karim ABED**
- **Abdur Rashid Khan**
  Gomal Unversity
- **Abeer ELkorany**
  Faculty of computers and information, Cairo
- **ADEMOLA ADESINA**
  University of the Western Cape
- **Aderemi A. Atayero**
  Covenant University
- **Adi Maaita**
  ISRA UNIVERSITY
- **Adnan Ahmad**
- **Adrian Branga**
  Department of Mathematics and Informatics, Lucian Blaga University of Sibiu
- **agana Becejski-Vujaklija**
  University of Belgrade, Faculty of organizational
- **Ahmad Saifan**
  yarmouk university
- **Ahmed Boutejdar**
- **Ahmed AL-Jumaily**
  Ahlia University
- **Ahmed Nabih Zaki Rashed**
  Menoufia University
- **Ajantha Herath**
  Stockton University Galloway
- **Akbar Hossain**
- **Akram Belghith**
  University Of California, San Diego
- **Albert S**
  Kongu Engineering College
- **Alcinia Zita Sampaio**
  Technical University of Lisbon
- **Alexane Bouënard**
  Sensopia
- **ALI ALWAN**
  International Islamic University Malaysia
- **Ali Ismail Awad**
  Luleå University of Technology
- **Alicia Valdez**
- **Amin Shaqrah**
  Taibah University
- **Amirrudin Kamsin**
- **Amitava Biswas**
  Cisco Systems
- **Anand Nayyar**
  KCL Institute of Management and Technology, Jalandhar
- **Andi Wahju Rahardjo Emanuel**
  Maranatha Christian University
- **Anews Samraj**
  Mahendra Engineering College
- **Anirban Sarkar**
  National Institute of Technology, Durgapur
- **Anthony Isizoh**
  Nnamdi Azikiwe University, Awka, Nigeria
- **Antonio Formisano**
  University of Naples Federico II
- **Anuj Gupta**
  IKG Punjab Technical University
- **Anuranjan misra**
  Bhagwant Institute of Technology, Ghaziabad, India
- **Appasami Govindasamy**
- **Arash Habibi Lashkari**
  University Technology Malaysia(UTM)
- **Aree Mohammed**
  Directorate of IT/ University of Sulaimani
- **ARINDAM SARKAR**
  University of Kalyani, DST INSPIRE Fellow
- **Aris Skander**
  Constantine 1 University
- **Ashok Matani**
  Government College of Engg, Amravati
- **Ashraf Owis**
  Cairo University
- **Asoke Nath**

CONTENTS

Intelligent Security for Phishing Online using Adaptive Neuro Fuzzy Systems

G. Fehringer
Computer and Information Sciences
University of Northumbria
Newcastle upon Tyne, NE1 8ST, United Kingdom

P. A. Barraclough
Computer and Information Sciences
University of Northumbria
Newcastle upon Tyne, NE1 8ST, United Kingdom

***Abstract*—Anti-phishing detection solutions employed in industry use blacklist-based approaches to achieve low false-positive rates, but blacklist approaches utilizes website URLs only. This study analyses and combines phishing emails and phishing web-forms in a single framework, which allows feature extraction and feature model construction. The outcome should classify between phishing, suspicious, legitimate and detect emerging phishing attacks accurately. The intelligent phishing security for online approach is based on machine learning techniques, using Adaptive Neuro-Fuzzy Inference System and a combination sources from which features are extracted. An experiment was performed using two-fold cross validation method to measure the system's accuracy. The intelligent phishing security approach achieved a higher accuracy. The finding indicates that the feature model from combined sources can detect phishing websites with a higher accuracy. This paper contributes to phishing field a combined feature which sources in a single framework. The implication is that phishing attacks evolve rapidly; therefore, regular updates and being ahead of phishing strategy is the way forward.**

Keywords*—Phishing websites; fuzzy models; feature model; intelligent detection; neuro fuzzy; fuzzy inference system

I. INTRODUCTION

Phishing attacks are increasing rapidly costing the global economy billions of dollars per year [1]. Although various studies have concentrated on phishing attacks and used a variety of solutions in the recent years to combat phishing [2], [3]-[6] there is still a lack of accuracy in real-time causing vast amount of losses annually [7]. In general, detection techniques are classified in 2 main categories namely, URL blacklist-based and web-page feature-based. URL blacklist use human-verified URL based on server-side that performs URL matching with real-time website URLs to detect phishing websites. This category works on the principle of detecting phishing attacks and provide warning to users to prevent them from taking risky actions that could otherwise result in compromising their sensitive information. Although existing approaches are effective to some extent, effective generalisation to new threats is still a challenge. For instance, it was discovered that zero-hour protection provided by blacklist-based toolbar systems offers true-positive rate between 15% and 40% [8]. These systems can make users vulnerable to phishing threats. Moreover, statistics were posted in March 2009 stating that it takes 10 hours on average to verify submitted URLs [9]. This study proposes a novel Intelligent Phishing Security (IPS) using features and adaptive neuro fuzzy inference systems approach to combat the above limitations.

Feature-based approaches have been studied by researchers [10]-[12] using extracted features from sources such as web-pages and utilizes machine learning algorithms to enhance phishing detection systems, but inaccuracy is still a problem. Different to blacklist-based approaches, feature-based approaches can be generalized to new phishing attacks. However, feature-based approach has a tendency to have high false positives. Inaccuracy has been the main barrier in the existing phishing detection technologies [7].

Fuzzy rules techniques that models the qualitative side of human reasoning process with no precise quantitative analysis was extended to deal with imprecise conditions [13]. Fuzzy rules have been investigated by [13] and have found various practical applications in imprecise reasoning, control and in prediction. However, fundamentals of this method when dealing with data requires consideration. Particularly, there is a lack of effective feature models that cover specific and effective features.

The intelligent phishing security approach (IPS) is based on Adaptive neuro-fuzzy inference system (ANFIS), using features from a combined sources. ANFIS is chosen because it has ability to learn given features. While neural network handles features well, fuzzy logic deals with reasoning on a high level utilizing given features. This enables membership function parameters tuning for classification between phishing, suspicious and legitimate websites. The two combined feature sources 'phishing email and web-form' are used because they are main phishing targets. These enable effective feature extraction for training and testing sets. Phishing emails carry hyperlink that leads users to phishing web-form. The goal of web-form is to collect the main users sensitive information. The phishing e-web-form is not only used for classification, but also used for training and testing fuzzy models and to generate fuzzy rules as demonstrated in experiment section. This study is focused on answering: how can effective feature model be constructed to reduce inaccuracy in online transactions?

A. This research objectives are to:

1) Conduct relevant literature review in the relevant field.
2) Identify sources in order to extract effective features.
3) Perform feature preparation and normalization to a format suitable for the chosen tools.

4) Design and carry out experimental procedure based on Adaptive Neuro-Fuzzy Inference Systems with features.

5) Train and test fuzzy models using training and testing sets.

6) Compare the result with the existing methods in the field to measure the model's effectiveness.

This paper contributes to the field of phishing detection combined sources of features, phishing Email and phishing e-web-form in a single framework. This is novel as the idea has not been used in literature. Features are extracted from these sources to construct a feature model. This feature model is expected to reduce inaccuracy in existing detections.

The remaining sections are structured as: Section II critically reviews relevant literature in the field and describes phishing deception procedures. Section III describes the intelligent phishing security approach including sources and features identification, feature normalization and size, a description of ANFIS and fuzzy rules. Section IV describes the experimental procedures including intelligent phishing security structure and learning procedure, training and parameters, testing and membership functions. Results are presented in Section V. Section VI provides comparison and discussions. Section VII offers evaluation and conclusions including feature work.

II. Relevant Work

Although various solutions are available that models automatic phishing detection, major studies have focused on blacklist-based and feature-based approaches applying machine learning techniques to identify phishing sites.

A. Feature-based and Machine Learning Approaches

Ozarkar and Patwardhan [14] focused on feature-based applying machine learning methods to detect spam email. A set of conventional features model was used and summarized a prediction error rate using Associative Classification (AC) algorithms. Their method achieved 97.5% accuracy. The results indicated that C4.5 outperformed other algorithms with 5.76% average error-rates, which is relatively putting users at risk when faced with phishing attacks.

Zuhair [15] investigated different feature-based methods using different sizes based on 58 hybrid futures and four machine learning classifiers, including Naïve Bayes, DT, C4.5, and SVM to classify phishing websites effectively. The author's results revealed that the features were highly significant with a recommendation drawn that there is no golden filtering method that fits all classifications algorithms on the data sets used in the experiments. However, a better way forward should be provided from the finding.

Form's [16] study applied Support Vector Machine classifier to classify emails using a set of 9 structure-based and behaviour-based features. The method achieved 97.25% success rates, however it has a relatively small training dataset (1000 emails with 50% spam and 50% non-spam). In the attempt to improve feature-based approach, 27 features from [17] were used based on multi-class classification-based association rules (MCAR) and Association classification (AC) algorithm to assess the detection system. Their method classified webpages with more than 98.5% accuracy, but it was not clear how many rules were generated by employing the MCAR algorithm.

Moreover, work by [11] concentrated on feature-based approach to explore how rule-based classification data-mining techniques are applied in phishing site detection. They employed 450 legitimate and phishing websites for features extraction. By using JavaScript feature extractor, features related to the address bar were extracted. Rule-based classification algorithms employed C4.5, RIPPER, PRISM and Classification using Associate algorithm and 17 features to identify phishing attacks. Using experiment, C4.5 attained 5.76% error-rates, RIPPER obtained 5.94% errors and PRISM achieved 21.24% error rates. After reducing feature size to 9, classification based on association (CBA) achieved 4.75% error rates which was lower compared to other classifiers used. However, the features are not wide-ranging enough to cover phishing characteristics that users can experience in their daily browsing. Additional features could improve the system.

As seen above, Abdelhamid, Ayash and Tabatah [10] method explored data-mining utilizing Associate Classification algorithms such as Multi-class Associative Classification (MCAC), classification based on association (CBA), missing completely at random (MCAR), Multi-attribute co-cluster (MMAC), rule induction and decision trees algorithms including C4.5, PART, RIPPER with 16 features to distinguish between phishing and legitimate sites. The results attained are as follows: MCAC algorithm was misclassified by 0.8% error rates, C4.5 misclassified 1.24% error rates, RIPPER misclassified 1.86% errors and PART misclassified 4.46% error rates. Although MCAC achieved a high accuracy, their features have been extracted from one source only without considering all other different possible sources. In this case, more sources could improve features to detect emerging phishing attacks.

Another work explored feature-based approach [18] based on a neuro-fuzzy, using features extracted from five different sources (also known as inputs) to detect phishing websites accurately. Their approach achieved 98.5% accuracy, but suffered 1.5% error rates.

In the attempt to improve feature-based approaches, a neuro-fuzzy system was employed to deal with parameters in detecting phishing attacks [19]. Given that machine learning algorithms are parameter driven and parameters are difficult to tune. This applies to this study because in training and testing, parameters are tuned for a desirable outcome. The study used 300 features based on a neuro-fuzzy system to tune different parameters for the discovery of a desirable parameters. The method achieved 98.74% accuracy. The outcome can be used to increase user's confidence on tuning parameters.

Another area of study investigates email-based approaches. A method utilized 9 hybrid features of email header and body extracted from approximately 10000 emails divided equally between genuine and spam emails [4]. Their method applied J48 classification algorithm to classify phishing and legitimate emails. Their approach obtained 98.1% success with 1.9% false positives.

B. Blacklist-based approaches

In the attempt to improve URL blacklist-based approaches, PhishStorm was introduced to identify potential phishing websites [20]. Their approach applied machine learning classification, using lexical features including low-level domain, upper-level domain, path and query based on STORM and Bloom, and big data architectures. Their method attained 94.9% accuracy, but suffered 1.44% false positives. Although the use of data from parts of URL exhibits higher positive rates, features extracted from URLs alone are not comprehensive enough to detect phishing websites accurately due to variations of phishing characteristics and regular evolving techniques. Therefore, extracting data from various sources is a possible means to solve this issue.

Phishing Email classification model was explored to detect phishing [21]. The method applied text stemming and wordNet based on Knowledge discovery, data mining and text processing. Using Random forest algorithm achieved 99.1% accuracy, while 98.4% accuracy was achieved applying J48 algorithm. However, this method used 0.9 training data-set and the remaining 0.1 as testing data-set which is a very small data-size for testing using 10-fold-cross-validation measuring method.

Although blacklist-based approaches are largely utilized in industry due to low false-positives, these approaches cannot handle new phishing attacks [7] due to employing human-verified blacklist which takes longer to update. Also there is an ill-fame group known as "rock phish gang" that utilizes toolkits to make a large number of unique phishing URLs, placing extra pressure on blacklist-based techniques.

In contrast to blacklist-based, feature-based techniques exist to combat this problem. Mohammad, Thabtah and McCluskey [22] used automatically extracted features instead of manually extracted to predict phishing website. The method is said to be effective. However, using URL, IP addresses, adding prefix and suffix to request URL may not be adequate to detect evolving phishing.

In this paper, a feature-based approach is used based on adaptive neuro-fuzzy system with phishing e-web-form features. Specifically, 56 features in total are used. Thirty-four features are taken from the previous study [19] and twenty-two significant novel features are added from phishing e-web-form sources. Features are reduced to decrease redundant records in the training and testing sets and applied the state-of-the-art advanced machine learning algorithm. This should enables the construction of e-web form feature model to solve the errant problem of false positive rates and keep up with emerging phishing attacks.

C. Phishing deception procedures

In order to tackle phishing attacks effectively, it is important to understand how phishing works. Phishing attack is a deception that causes humans to take risky action. As shown in Fig. 1, phishing website attack takes the follow form:

1) **Step 1:** Attacker starts by constructing malicious websites with a form, and e-mail with hyperlink. The malicious sites and email are meant to look exact copies of known organization websites. For example, financial institute sites.

2) **Step 2:** Attacker sends malicious emails with a link pointing a user to malicious website.

3) **Step 3:** A user accesses malicious web form by clicking the link. After the user accessed malicious web form, the user types the required fields with sensitive information as requested on the form and clicks submit button.

The information goes to attacker, while the user believes it is received by a known financial institute.

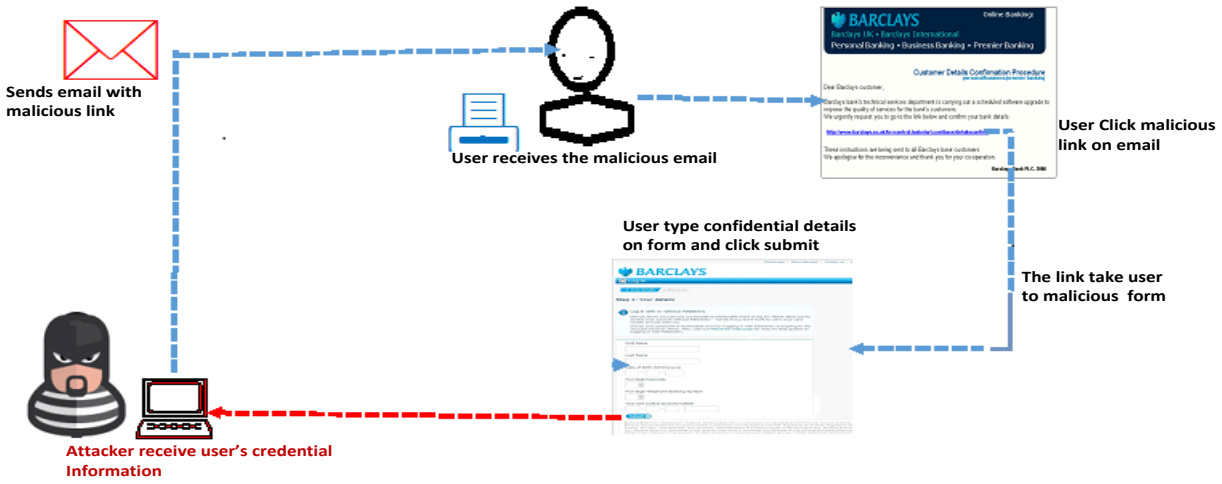

Fig. 1. Phishing deception process.

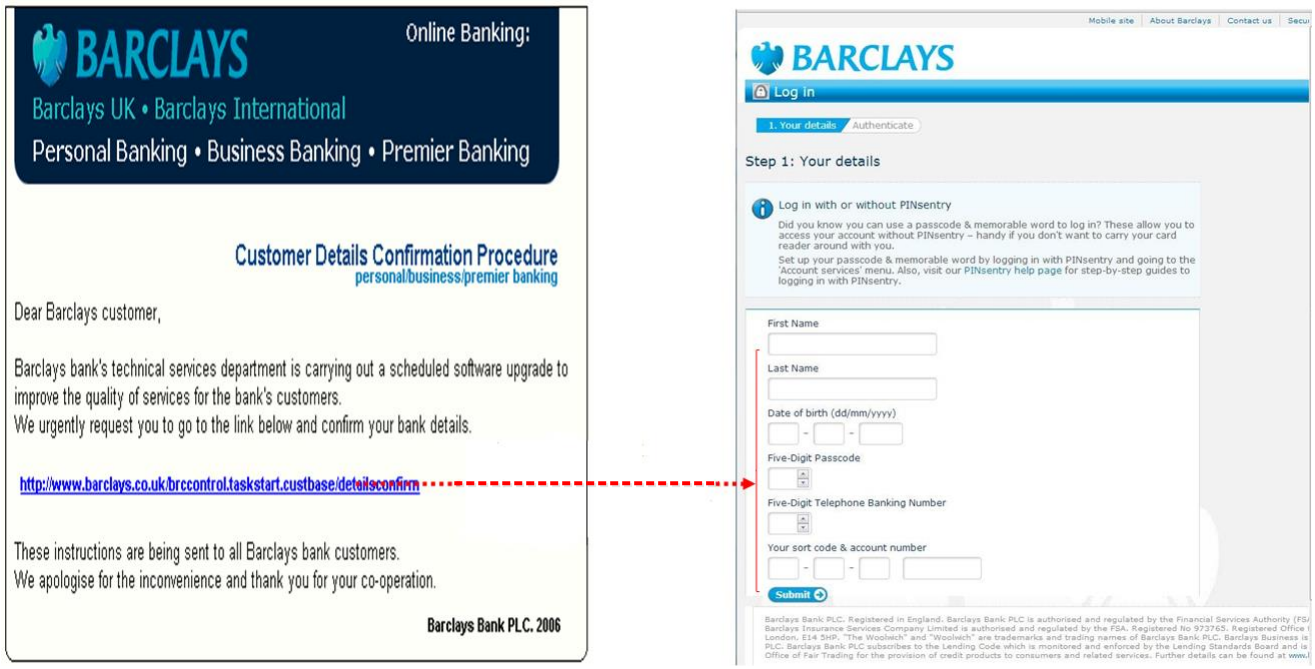

Fig. 2. Phishing attack methodology.

In summary, phishing website attack starts by a phisher creating a malicious website and a form with a hyperlink. The link is sent to users by email, which convince users to click a link that take victims to malicious websites with a form for users to fill in their sensitive details. Examples of phishing email and web-form imitating Barclays bank's genuine email and site are presented in Fig. 2(a) and 2(b).

III. Intelligent Phishing Security

The proposed intelligent phishing security (IPS) take the form of a zero order Sugeno type that consists of four main components, which include: features sources, features, adaptive neuro-fuzzy inference system (ANFIS). ANFIS consists of a rule base and a feature base that makes knowledgebase and a decision-making unit. ANFIS is used because it can learn and validate given features using IF-THEN fuzzy rules. The intelligent phishing security architecture is presented in Fig. 3. The construction of fuzzy rules and the process of the fuzzy inference are provided in detail in sections below. Input features enable fuzzy modelling and Gbell shape membership function to be used for its efficiency. As can be seen in the intelligent phishing architecture, the two sources are phishing emails and phishing web-forms jointly known as phishing e-web-forms

1) The sources are the core of the combined framework from which comprehensive features are extracted that is used to generate fuzzy models and to test the models.

2) Features are phishing website identifiers, which are utilized to classify between phishing, suspicious and legitimate websites. The features can be seen in Fig. 4.

3) A rule-base carries a number of fuzzy IF-Then statement.

4) The Takagi and Sugeno type rules are utilized because it is a zero order [23]. The output of every rule is a combination of linear, input and constant term. Whereas a final output is the weighted average of all rule's output.

5) An adaptive neuro-fuzzy inference system is a neural network with multilayers that performs fuzzy reasoning [13].

6) Features extracted from comprehensive sources are also known as identifiers to distinguish phishing website. The methodology choice is scientifically appropriate to meet the study's objectives.

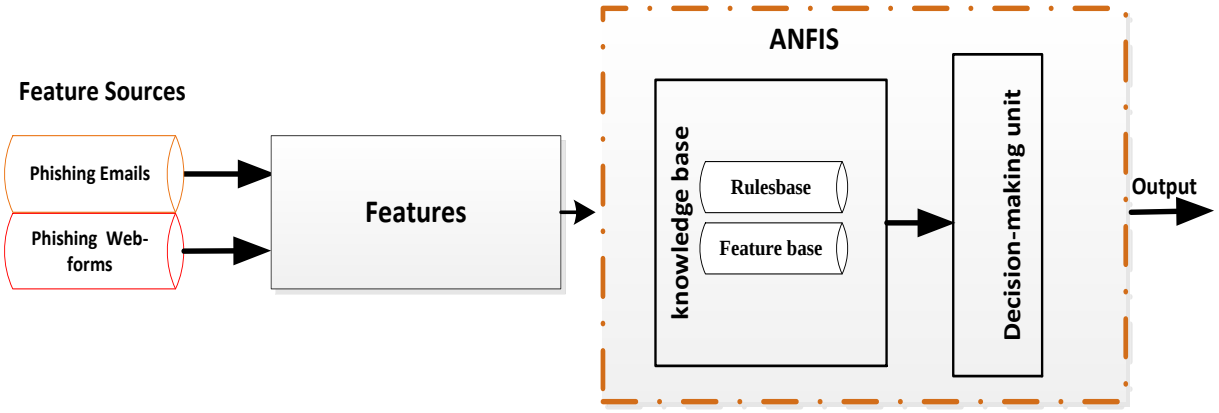

Fig. 3. Intelligent phishing security architecture

A. Sources and feature identification

To reduce phishing attacks, it is important to utilize effective techniques and identify important sources to extract comprehensive features that can detect phishing websites accurately. One hundred phishing emails that contain links to phishing websites and two hundred web-forms used to collect sensitive information from users are gathered to be the representative of sources to extract features. From these sources, 56 features were extracted in which 22 features are novel, while 34 features have been used in the previous work [19] as stated in the above section. These features are presented in Fig. 4. Emails and web-forms are selected from Millersmiles' website archive [24]. Millersmiles is one of the leading anti-phishing web services dedicated to maintain a large archive of phishing websites and emails. Other anti-phishing services that maintains huge archives for phishing websites is PhishTank [9]. The sources are chosen because new phishing attacks are added to them regularly and they supplement each other well.

B. Feature normalization

To comply with fuzzy inference system principles, variable ranges are determined. Intelligent phishing security has four main linguistic variables as detailed in Section D: Legitimate (low), suspicious (medium) and phishing (high). The degree of risk is the most important criteria to determine the accuracy of models. The average percentage accuracy should not exceed the limit acceptable in phishing detection. To determine the degrees of risk, feature's linguistic values (legitimate, suspicious and phishing) ranges are specified, the degree which are normalized to values within the range of (0, 1) by assigning the numerical value. Website are classified between legitimate, suspicious or phishing. Other values like 'very low' are not practical to use. Features are normalized since they are textual and the assigned values are used to define the level of risk of a website. Also, features are of different types. However, some tools for intelligent systems like MATLAB toolbox requires a specific type of data [12].

C. Feature size

Features size can vary depending on the type of measuring tool. However, features should have sufficient size that can be analyzed when using standard measurement method. If for instances, two-fold cross validation method is used, the features size should be split into two pairs with a reasonable amount in each pair. Therefore, 56 feature size are used for experiment in the intelligent phishing security is within the minimal sufficient amount. They are split into 28 training set and 28 testing set. These features are the most frequent phishing features found across all the two hundred phishing web-forms and a hundred phishing emails.

D. Adaptive neuro fuzzy inference system

Adaptive Neuro-Fuzzy Inference System (ANFIS) is a type of adaptive network that is functionally equivalent to Fuzzy inference systems. It combines both fuzzy logic principles and a neural network. It represents Sugeno Tsukamoto fuzzy models that utilize a hybrid learning algorithm. Its outputs depend on input data and the parameters relating to the neurons. ANFIS is used in this study not only because of its advantage of imprecise reasoning, but also for its suitable functionalities when modelling the intelligent phishing security fuzzy models [13].

E. Intelligent phishing security fuzzy rules

In phishing detection structure, there are inputs which are represented in the form of inputs as x , y and one output z. A single input is represented by two-fuzzy sets and the output by a first order polynomial then the rules are presented in the following form in Fig. 5:

Email	Features	Value range
Email	Security alert	
	Details confirmation	
	A transfer was attempted	[0, 0.3]
	Encrypt reference	
	Have your card ready to hand	
Personal Detail	Date of birth	
	Mobile phone number	
	Primary telephone number	
	Home address	[0.2, 0.6]
	Postal code	
	E-mail	
	e-mail password	
	Last name	
	First name	
Card secret Items	Start date	
	Expiration date	
	Credit card number	
	Sort code	
	Security number	
	Account number	
	Password	
	first digits of your password	
	second digits of your password	
	third digits of your password	
	fourth digits of your password	
	fifth digits of your password	
	sixth digits of your password	
	seven digits of your password	
	eighth digits of your password	
	ninth digits of your password	
	tenth digits of your password	
	eleventh digits of your password	[0.5,1]
	twelves digits of your password	
	Confirm your ID	
	Bank account number	
	Your card details	
	Card security code	
	3-digit security code	
	Card verification number	
	Membership number	
	Five-digit passcode	
	Memorable word	
	Mother maiden name	
	Card verification number	
	Personal logon	
	Telephone banking PIN	
	Telephone passcode	
	User code	[1]

Fig. 4. E-web-form Feature Model.

R_1:		Rule 1:	
IF	x is $A1$	IF	feature is security_alert
OR	y is $B1$	OR	feature is details_confirmation
	⋮		⋮
THEN	z is $C1$	THEN	Website is Legitimate
R_2:		Rule 2:	
IF	x is $A2$	IF	feature is credit_card_start_date
OR	y is $B2$	OR	feature is credit card_expiry_date
	⋮		⋮
THEN	z is $C2$	THEN	website is suspicious
R_3:		Rule 3:	
IF	x is $A3$	IF	feature is credit card_number
OR	y is $B3$	OR	feature is sort_code
	⋮		⋮
THEN	z is $C3$	THEN	website is phishing

Fig. 5. Rule representation.

Where x, y and z (feature and website) are linguistic variables, $A1$, $A2$, $A3$ (details_confirmation, credit_card_start-date and card_number) are linguistic values decided by fuzzy-set on the universe of discourse x; $B1$, $B2$ and $B3$ are fuzzy sets on the universe of discourse z (website).

IV. Experimental Procedures

The experiment for the intelligent phishing security (IPS) is based on an ANFIS, using 56 features as training and testing sets. The fuzzy system is used since it is best suited for feature-base fuzzy modeling. 56 comprehensive features are used for training and testing fuzzy models. A two-fold cross-validation method is employed which involves randomly splitting the features into two parts, training set and testing set. First, training is carried out on a training-set only once and testing is done on a test-set only once. Then the roles of training and testing sets are reversed. The results are assembled to get the average errors.

A. Phishing security structure and learning procedure

An Intelligent phishing security structure generated from phishing e-web-form features and ANFIS learning procedure can be seen in Fig. 6. It is equivalent to first-order Sugeno-fuzzy-model and is a multilayer network feedforward where every single neuron performs a specific function. It has six layers including: Layer I – input, Layer II – fuzzification, Layer III – fuzzy rule, Layer IV – normalization, Layer V – defuzzification and Layer VI – crisp output.

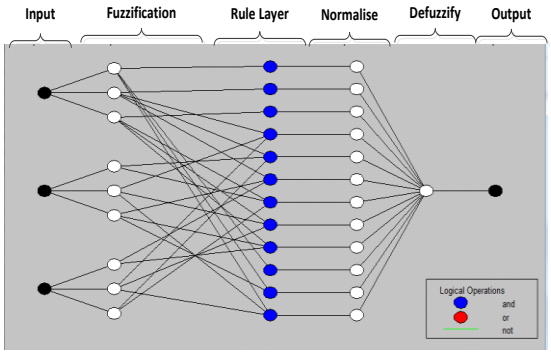

Fig. 6. Fuzzy structure with six layers.

The learning procedures take the following form:

a) Layer 1: This is the input. Neurons in Layer I transmit external inputs to Layer II. This is specified as $y_i^{(1)} = x_i^{(1)}$ (1) where the input is $y_i^{(1)}$ and the output in Layer I is $x_i^{(1)}$.

b) Layer II: This is the fuzzification. Neurons in Layer II perform fuzzification. The Sugneo model fuzzification have a Gbell shape activation function. This is specified as:

$$y_i^{(2)} = \frac{1}{\left(\frac{x_i^{(2)} - ai}{Ci}\right)^{2b_i}} \quad (2)$$

Where, the input is $x_i^{(2)}$ and the output is $y_i^{(2)}$ of neuron I Layer II, and a_i, b_i and c_i are parameters that control the center width and slope of the bell-shape function of neuron.

c) Layer III: This is a rule layer. Every neuron in Layer III matches a single fuzzy rule. A rule neuron receives inputs from fuzzification and calculates the execution strength of the rule it represents. Thus the output in Layer III is expressed as:

$$y_i^{(3)} = \prod_{j=1}^{k} x_{ji}^{(3)} \quad (3)$$

Where, inputs are $x_{ji}^{(3)}$ and $y_i^{(3)}$ are output of rule neuron in Layer III.

d) Layer IV: This is normalization. Every neuron in this layer receives outputs from the rule layer and the normalized execution strength of any given rule is calculated. Therefore, the output of Layer IV is expressed as:

$$y_i^{(4)} = \frac{x_{ii}^{(4)}}{\sum_{j=1}^{n} x_{ji}^{(4)}} = \frac{ui}{\sum_{j=1}^{n} uj} = {}_{ui} \quad (4)$$

where the input $x_{ji}^{(4)}$ from neuron j is allocated in Layer III to Layer IV.

e) Layer V: This is defuzzification. Every neuron in Layer V is linked to the normalisation neuron, as well as receives the initial input x_1 and x_2. A defuzzification neuron calculates the value of weight consequent of any given rules. It is specified as:

$$y_i^{(5)} = x_i^{(5)}\left[k_{i0} + k_{i1}x1 + k_{i2}x2\right] = u_i\left[k_{i0} + k_{i1}x1 + k_{i2}x2\right] \quad (5)$$

Where, the input is $x_i^{(5)}$ and the output in the defuzzification neuron is $y_i^{(5)}$ in Layer V. k_{i0}, k_{i1} and k_{i2} is a set of parameter consequent of rule I [25].

f) Layer VI: This is represented by a single neuron sum. The neuron calculates the total of outputs of every defuzzification and produces the overall output y which is specified as:

$$y = \sum_{i=1}^{n} x_i^{(6)} = \sum_{i=1}^{n} u_i \left[k_{i0} + k_{i1} x1 + k_{i2} x2 \right] \quad (6)$$

Indeed, the fuzzy structure is functionally equal to a first-order Sugeno-fuzzy model.

B. Training and parameters

To facilitate the learning of intelligent phishing security feature model, parameters are assigned. Membership functions assigned to each input is arbitrarily set to 3, Gbell shape was chosen, 30 epochs and learning optimization method known as hybrid. These parameters are identified carefully to optimize model performances. A training-set was presented to the input layer of the network in which the network propagates the inputs from layer to layer till it reaches the output layer. When it finds a different pattern from a desired output, an error is calculated and back-propagated through the network from the output layer to the input layer. When errors are propagated, weighting is modified. After training is complete, the training set is used only once to train the feature model.

C. Testing

Testing begins as the testing feature-set is presented in the input layer of the system. The neurons propagate the inputs from Layer 1 to every layer till it reaches the output layer. Since the measurement method is two-fold cross-validation, testing is completed. After which, roles are reversed and the testing set is used to train, while the training set is used to test models. The measurement at the testing stage is the final average measurement in which the model is evaluated for its merit. After the training and testing processes, outputs are achieved which are presented and discussed in sub-section *D* whereas results are displayed and discussed in Section V.

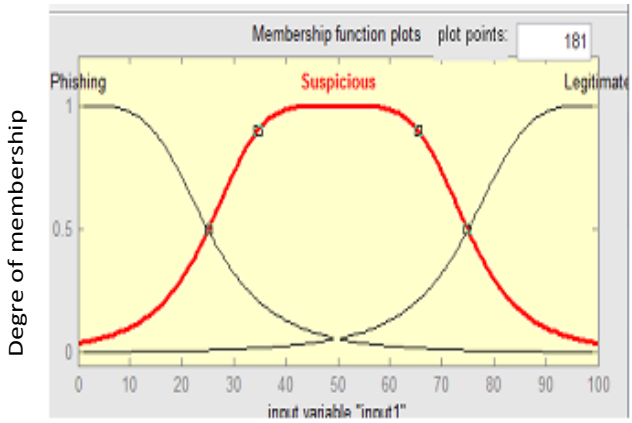

Fig. 7. Membership function using feature-set.

D. Membership functions

Due to efficiency, membership function (MFs) used is Generalized bell (Gbell) shape, while the default MF has triMFs. Membership function of fuzzy sets is a curve that defines how each point in the input space is mapped to a membership value between (0, 1) and the output can vary between (0, 100). The Gbell shape MF is illustrated in Fig. 7.

The intelligent phishing security membership function plot for feature model contains values including Low=Legitimate, Medium=Suspicious and High=Phishing:

Linguistic variables	Numerical value range
Legitimate	(0, 0, 0.3)
Suspicious	(0.2, 0.4, 0.5)
Phishing	(0.4, 0.6, 1)

This means legitimate features has a degrees of risk range between (0, 0.3). Phishing website has degrees of risk range between (0.4, 1). Suspicious has degrees of risk range between (0.2, 0.5). While an output with a risk between (0, 0.3) is classified as low in phishing detection, an output with a risk between (0.2, 0.5) is classified as medium and an output with a risk between (0.4, 1) is classified as high.

V. Results

Using two-fold cross-validation, training was first performed on a training set and tested on a testing set. The roles are reversed and training is performed on a testing set. This is presented in the graph in Fig. 8.

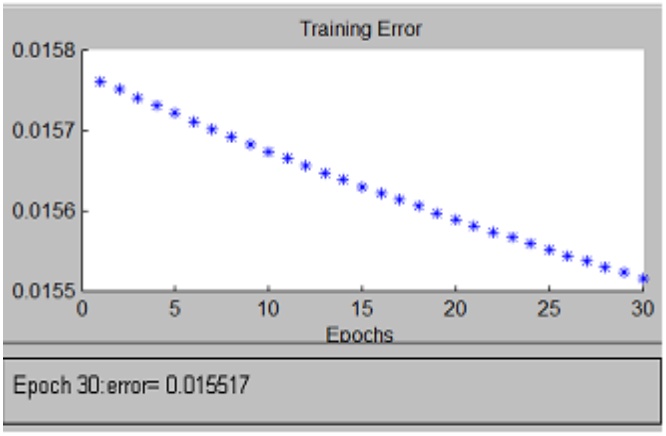

Fig. 8. Training results error rates.

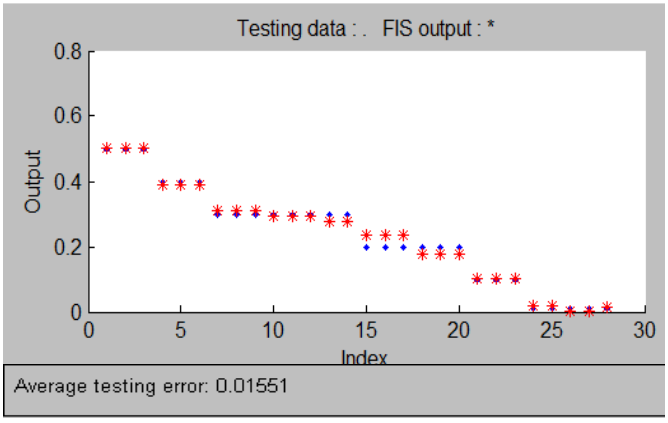

Fig. 9. Test results in error rate.

TABLE. I. A COMPARISON BETWEEN THE EXISTING AND THE IPS RESULTS

Authors	Approach	Feature size	Learning algorithm	Testing results
Form's Approach	Feature-based	9	SVM	97.25%
The IPS Approach	Feature-based	56	ANFIS	98.4%
Barraclough et al.	Feature-base	300	A neuro-fuzzy	98.74%

TABLE. II. RESULTS SUMMARY

Training & Testing	Training error	Testing error	Errors in 2 decimal point	Overall testing average accuracy in percentage
Experiments	0.015517	0.01551	1.6	98.4%
	0.015517	0.01551	1.6	

The estimation for training offered a single crisp output errors of 0.015517, which is lower and is equal to the first run. The overall training measure obtained an average of 1.6% error rate. This is illustrated in Table 1.

Similarly, after the training was completed, testing was performed on a testing set and the estimation for testing gave 0.01551 average testing errors. This is presented in the graph in Fig. 9. The roles are reversed and testing is performed on training set. The output errors produced is 0.01551 which is the same to the first run, an indication of valid results.

The results for each execution are summed-up and divided by two. When converted into a percentage and to two decimal places, the overall average error rates attained 1.6% for both training and testing. Thus, the overall testing average accuracy percentage is 98.4%, which is an excellent result. The summary of results is illustrated in Table 2.

VI. COMPARISON AND DISCUSSIONS

Since the intelligent phishing security (IPS) focuses in enhancing feature-based approaches, the study is similar with Form's study [16] in that both methods used features. The main difference is that IPS method employed 56 features based on ANFIS in comparison to Form's 9 features applying SVM classifier. As it can be seen in summary in Table 1, IPS results is comparable with Barraclough's results [19]. Although features differ in size, IPS method obtained an average accuracy of 98.4%, compared to Barraclough's method, which achieved 98.74% accuracy. Although Barraclough's result is higher by a small margin (0.3 per cent), their method used 300 feature size in comparison to 56 utilized in IPS. This can be explained that phishing evolves regularly and some become redundant. Therefore, a well selected IPS features have dealt with redundant record and are covering the specific sensitive information attackers capture from users. Hence, IPS has offered a promising results in-line with [19] results.

This result is important since it evaluates the effectiveness of phishing e-web-form feature model. This is the first study to demonstrate the effectiveness of phishing e-web-form features. Using two-fold cross-validation in testing allows estimating the validity of phishing e-web-form feature model and its generalization to new attacks. The results indicate that phishing e-web-form feature model can classify between phishing, suspicious and legitimate websites with higher accuracy.

VII. EVALUATION AND CONCLUSIONS

Keeping in mind that phishing strategy evolves regularity; it is a challenge that puts pressure on the existing detection systems. This would apply to the e-web form feature model if they are not updated regularly in future. The limitation in this study is that the evolving phishing characteristics identification is difficult to be automated, hence are manually selected.

This paper analyzed phishing e-web-form sources to identify and extract effective features to classify and detect emerging phishing websites. 56 features were used based on ANFIS algorithms. These features are specific to the main sensitive information that attackers acquire from users. The intelligent phishing security approach obtained promising results which demonstrates effectiveness of phishing e-web-form and feature model to classify and detect phishing websites with a higher accuracy. This is the first study to use phishing e-web-form framework, which is a source for effective features that has demonstrated effectiveness to detecting emerging phishing attacks accurately.

Future work would be to construct fuzzy rules that can be used to identify phishing websites, using human problem-solving methods. Based on the effective phishing e-web-form, an effective phishing detective system will be built to detect real-world phishing websites.

ACKNOWLEDGMENT

Our greatest thanks goes to the head of the department of Computer and Information Sciences and the School of Engineering and Environment in Northumbria University for providing a space and facilities during the process of the research.

REFERENCES

[1] D. Correa, "Fraud costs UK £193bn per year, rise in phishing attacks seen". Online available < https://www.scmagazineuk.com/fraud-costs-uk-193bn-per-year-rise-in-phishing-attacks-seen/article/531293/> Accessed on 22nd May 2017, published in May 2016.

[2] L. Fang, W. Bailing, H. Junheng, S. Yushan, and W. Yuliang, "A Proactive Discovery and Filtering Solution on Phishing Websites", IEEE International Conference on Big Data (Big Data), 2015.

[3] B. Kumar, P. Kumar, A. Mundra, and S. Kabra, "DC Scanner: Detecting Phishing Attack", IEEE Third International Conference on Image Information Processing, 2015.

[4] S. Smadi, N. Aslam, L. Zhang, R. Alasem, and M. A. Hossain, "Detection of Phishing Emails using Data Mining Algorithms", 9th

International Conference on Software, Knowledge, Information Management and Applications (SKIMA), 2015.

[5] Z. Dong, A. Kapadia, J. Blythe, and L. J. Camp, "Beyond the Lock Icon: Real-time Detection of Phishing Websites Using Public Key Certificates", APWG Symposium on Electronic Crime Research (eCrime), 2015.

[6] M. Aburrous and A. Khelifi, "Phishing Detection Plug-In Toolbar Using Intelligent Fuzzy-Classification Mining Techniques, International Journal of Soft Computing and Software Engineering [JSCSE], 2013, Vol. 3, pp. 54-61.

[7] G. Xiang, J. Hong, C. P. Rose, and Cranor, L. "Cantina+: A feature-rich machine learning framework for detecting phishing web

[8] Sites", ACM Transactions on Information and System Security (TISSEC*)*, 2011, 14 (2), pp. 2 - 21.

[9] S. Sheng, B. Wardman, G. Warner, L. Cranor, J. Hong, and C. Zhang, "An empirical analysis of phishing blacklists". In proceedings of the 6th conference on email and Anti-Spam. Mountain view, CA, USA, 2009.

[10] PhishTank. Statistics about phishing activity and phishTank usage. Online available <http://www.phishtank.com/stats.php. 2.2.4, 3.1, 4.4.2> Accessed on 15th November 2016.

[11] N. Abdelhamid, A. Ayash, and F. Tabatah, "Phishing Detection Based Associative Classification Data Mining", Expert System with Application, 2014, 41, pp. 5948-5959.

[12] R. Mohammad, T. L. McCluskey, and F. A. Thabtah, "Intelligent Rule based Phishing Websites Classification". IET Information Security, (2014) 8 (3). pp. 153-160. ISSN 1751-8709.

[13] M. Ajlouni, W. Hadi, and J. Alwedyan, "Detecting phishing websites using associative classification", European Journal of Business and Management, 2013, *5* (15), 36–40.

[14] N. Walia, H. Singh, and A.Sharma, "ANFIS : Adaptive Neuro-Fuzzy Inference System" A Survey," International Journal of Computer Applications (IJCA), 2015, vol. 123, pp. 32-38.

[15] P. Ozarkar and M. Patwardhan, "Efficient Spam Classification by Appropriate Feature Selection", International Journal of Computer Engineering and Technology (IJCET), ISSN 0976 – 6375 Vol. 4, (3), May – June 2013.

[16] H. Zuhair, A. Selamat, and M. Salleh, "Feature selection for phishing detection: a review of research," International Journal of Intelligent Systems Technologies and Applications, 2016, Vol. 15 (2) pp. 147–162.

[17] L. M. Form, K. L. Chiew, S. N. Szeand, and W. K. Tiong, "Phishing Email Detection Technique by using Hybrid Features", IT in Asia (CITA), 9th International Conference, 2015.

[18] M. Aburrous, M. A. Hossain, K. Dahal, and F. Thabtah "Intelligent phishing detection system for e-banking using fuzzy data mining," Expert Systems with Applications: An International Journal, 2010, pp. 7913-7921.

[19] P. A. Barraclough, M.A. Hossain, M. A. Tahir, G. Sexton, and N. Aslam. "Intelligent phishing detection and protection scheme for online transactions" Expert Systems with Applications, Vol. 40, (11) pp. 4697-4706, 2013,

[20] P. A. Barraclough, M.A. Hossain, M. A. Tahir, G. Sexton, and N. Aslam, "Parameter optimization for intelligent phishing detection using adaptive neuro-fuzzy" International Journal of Advanced Research in Artificial Intelligence (IJARAI), 2014, Vol. 3, (10), 2014

[21] S. Marchal, J. Francois, R. State, T. Engel, "PhishStorm: Detecting Phishing with Streaming Analytics," Network and Service Management, IEEE Transactions, 2014 , vol.11, (4), pp.458-471.

[22] A. F. Yasin, A. Abuhasan, "An Intelligent classification model for phishing email detection" International Journal of Network Security & Its Applications (IJNSA), 2016, Vol.8, No.4.

[23] R. M. Mohammad, F. A. Thabtah, and T. McCluskey, "An Assessment of Features Related to Phishing Websites using an Automated Technique,". In the 7th International Conference for Internet Technology and Secured Transactions (ICITST-2012), London, 2012.

[24] O. Celik and S. Ertugrul," Predictive human operator model to be utilized as a controller using linear", Neuro-fuzzy and fuzzy-ARX modeling techniques, Engineering Applications of Artificial Intelligence, 2010, (4) 23, pp. 595-603.

[25] Millersmiles, "the web's dedicated anti-phishing services". Online available < http://www.millersmiles.co.uk/> accessed on 14th November 2016.

[26] O. E. Dragomir, F. Dragomir, V. Stefan, and E. Minca, "Adaptive neuro-fuzzy inference systems as a strategy for predicting and controlling the energy produced from renewable sources". Energies, 2015, vol *8*, pp. 13047–13061

Multispectral Image Analysis using Decision Trees

Arun Kulkarni
Department of Computer Science
The University of Texas at Tyler
Tyler, Texas, USA

Anmol Shrestha
Department of Computer Science
The University of Texas at Tyler
Tyler, Texas, USA

***Abstract*—Many machine learning algorithms have been used to classify pixels in Landsat imagery. The maximum likelihood classifier is the widely-accepted classifier. Non-parametric methods of classification include neural networks and decision trees. In this research work, we implemented decision trees using the C4.5 algorithm to classify pixels of a scene from Juneau, Alaska area obtained with Landsat 8, Operation Land Imager (OLI). One of the concerns with decision trees is that they are often over fitted with training set data, which yields less accuracy in classifying unknown data. To study the effect of overfitting, we have considered noisy training set data and built decision trees using randomly-selected training samples with variable sample sizes. One of the ways to overcome the overfitting problem is pruning a decision tree. We have generated pruned trees with data sets of various sizes and compared the accuracy obtained with pruned trees to the accuracy obtained with full decision trees. Furthermore, we extracted knowledge regarding classification rules from the pruned tree. To validate the rules, we built a fuzzy inference system (FIS) and reclassified the dataset. In designing the FIS, we used threshold values obtained from extracted rules to define input membership functions and used the extracted rules as the rule-base. The classification results obtained from decision trees and the FIS are evaluated using the overall accuracy obtained from the confusion matrix.**

Keywords*—Decision trees; knowledge extraction; fuzzy inference system; Landsat imagery

I. INTRODUCTION

Many pixel-based classification and clustering algorithms have been developed to analyze Landsat images. These include the minimum distance classifier, maximum likelihood classifier (MLC), and non-parametric techniques such as the support vector machine (SVM), decision tree (DT), ensemble of decision trees, multi-layered perceptron model, fuzzy inference system, and fuzzy neural networks. The maximum likelihood classification algorithm is one of the most well-known algorithms. It assumes the normal distribution for reflectance values and calculates the mean vector and covariance matrix for each class using training set data. The classifier uses Bayes' rule to calculate posterior probabilities and assigns a pixel to the class with the highest posterior probability [1]. The SVM algorithm is appealing for Landsat data analysis because of its ability to successfully handle small datasets, often producing higher classification accuracy than traditional methods [2]. Vapnik [3] proposed the SVM algorithm. The use of a kernel for SVMs was suggested by Boser *et al.* [4]. The SVM is a binary classifier that assigns a sample to one of the two linearly separable classes. In the SVM algorithm two hyper-planes are selected so as not only to maximize the distance between the two classes but also not to include any points between them [5]. The SVM algorithm is extended to nonlinearly separable classes by mapping samples to a higher dimensional feature space. Huang *et al.* [6] have used the SVM algorithm to classify pixels in remotely sensed images. They have shown that for most training cases slightly higher accuracies were achieved when the model was trained with a randomly selected fixed number of samples for each class. Mitra *et al.* [7] have used the SVM algorithm for Landsat image analysis. Moumtrakis *et al.* [8] have provided a review of usage of SVM in remote sensing.

Neural networks are preferred for classification because of their parallel processing capabilities as well as learning and decision-making abilities. Several studies aimed at evaluating the performance of neural networks in comparison with traditional statistical methods to remote sensing applications are available. Benediktsson and Sveinsson [9] have used neural networks for feature extraction and classification for multisource data. Neural networks with learning algorithms such as backpropagation (BP) can learn from training samples and are used Landsat data analysis [10]-[16]. Laprade [17] has used the split-merge clustering algorithm for segmentation in aerial images. Hathaway and Bezdek [18] have used the fuzzy K-means for pixel classification in multispectral images. Pal *et al.* [19] and Kulkarni and McCaslin [20] have used fuzzy neural networks for classification of pixels in Landsat images. Neural networks provide a reasonable alternative to statistical methods for classifying pixels in Landsat images [21].

Decision trees represent another type of classification algorithm that is non-parametric in nature [22]. Pooja *et al.* [23] classified pixels in multispectral images using decision trees. They used C4.5 algorithm to implement the decision tree. However, they did not consider the problem of over-fitting. Hansen *et al.* [24] have suggested classification trees as an alternative to traditional land cover classifiers. Lowe and Kulkarni [25], [26] have used Random Forest and the decision tree for classification of pixels in Landsat data. They have considered two scenes that represent the Mississippi River bottom land and the Yellowstone forest areas. Random Forest algorithm is an ensemble of trees. In designing a decision tree the stopping criterion is that each terminal node represents samples of the same category or the height of the tree exceeds the specified limit. A major problem with a decision tree is that the tree can be built to fit training data perfectly. While the decision tree may accurately classify training data, it could be too trained to the training data that it may not perform well on the real world data. This problem is known as overfitting the training data and something one should be aware of in designing a decision tree. Overfitting of a tree may result in a number of misclassifications. Often the decision tree obtained

from the training samples needs to be pruned to be used as a model for classifying other pixels in the scene. Again the question arises as to what level we should prune the decision tree so that it can be used as a reliable model. In this paper, we implement decision trees using the C4.5 algorithm and classify pixels in a Landsat scene. We also considered the problem of overfitting the decision tree. To overcome the effect of overfitting, we used the method of pruning to improve classification accuracy. Also we consider the effect of sample size on classification accuracy. We used the MATLAB Machine Learning and Computer Vision toolboxes to implement the C4.5 algorithm, and we have chosen Landsat 8 Scene from Juneau, Alaska area. Furthermore, we extracted knowledge from the pruned decision tree regarding classification rules. To validate extracted rules, we built a fuzzy inference system (FIS) using the rules as the rule base and threshold values from the extracted rule set to define input fuzzy membership functions. We classified all samples from the training set data using the FIS and compared predicted and actual categories. Similar approach was proposed by Taylor *et al*. [27] for extracting knowledge from MARSI dataset. The work presented in this paper differs from the earlier work in [23], [26] in two aspects a) we have considered the problem of overfitting and b) we have validated extracted rules using the FIS. The outline of the paper is as: Section II explains the methodology. Section III describes the data set, implementation, and results, and Section IV provides conclusions.

II. METHODOLOGY

A. Decision Tree Classifiers

Decision tree (DT) classifiers are non-parametric classifiers that do not require any *a priori* statistical assumptions regarding distribution of data. The structure of a decision tree consists of a root node, some non-terminal nodes, and a set of terminal nodes. The data is recursively divided down the DT according to the defined classifier framework. A binary tree is a special case of a decision tree. Kulkarni [28] used a binary decision tree to classify pixels in multispectral images, where a subset of features was used at each non-terminal node to classify samples. To select the subset of features at each non-terminal node, the separability of the classes was used as the criterion. One of the most popular algorithms for constructing a decision tree is ID3 algorithm suggested by Quinlan [29]. The ID3 algorithm was developed for discrete attribute values. The basic idea in the ID3 algorithm is to construct a tree top-down from the root node. At the root node every attribute is tested, and the attribute that best classifies data is selected. The ID3 algorithm uses information gain to make a decision as to which attribute is the best. For each attribute, the information gain is calculated by finding the difference in entropy using (1), where D is the observation vector, m is the number of classes, and p_i is the probability that D belongs class i.

$$entropy\left(D\right) = -\sum_{i=1}^{m} p_i \log\left(p_i\right) \tag{1}$$

The information gain is calculated by subtracting the entropy before the split and after the split using (2), where A is the attribute being processed. In (2) v is the number of distinct values of attribute A, and $|D_j|/|D|$ shows the weight value of the j^{th} split. The process is repeated again for the remaining attributes.

$$Gain\left(A\right) = Info\left(D\right) - Info_A\left(D\right)$$

where

$$Info_A\left(D\right) = \sum_{j=1}^{v} \frac{\left|D_j\right|}{\left|D\right|} \times Info\left(D_j\right) \tag{2}$$

The ID3 Induction tree algorithm has proven to be effective when working with large datasets that have a number of features, where it is inefficient for human experts to process. C4.5 is a supervised learning algorithm that is descendent of the ID3 algorithm. C4.5 allows the usage of both continuous and discrete attributes.

The main problem with decision trees is overfitting. Mitchell [30] has defined overfitting as: Given a hypothesis space H, a hypothesis h in H is said to overfit the training data if there exists some other h' in H, such that h has a smaller error than h' over the training examples, but h' has a smaller error than h over the entire distribution of instances i. e. Hypothesis $h \in H$ overfits training data if there is an alternative hypothesis $h' \in H$ such that

$$error_{train}\left(h\right) < error_{train}\left(h'\right)$$

and

$$error_D\left(h\right) > error_D\left(h'\right) \tag{3}$$

where D denotes the entire distribution. Overfitting can decrease the accuracy of a decision tree on real world samples significantly. One method for dealing with overfitting in decision trees is pruning. Removing subtrees from a decision tree is known as pruning. Removing redundant subtrees makes the decision less specific yet performs the same as the original tree. The pruning algorithm goes through the entre tree and removes nodes and subtrees that have no negative effect on the classification accuracy, turning a subtree into leaf node with the common label. Once a decision tree is constructed, classification rules can be extracted by traversing from the root node to each leaf node. The split condition at a non-terminal node represents the antecedent part, and the leaf node represents the consequent part. To evaluate the accuracy of extracted rules, we built a fuzzy inference system (FIS) using the rules and reclassified the training set data.

B. Fuzzy Inference System

A fuzzy inference system (FIS) essentially defines a nonlinear mapping of the input feature vector into a scalar output using fuzzy rules. A general model of a fuzzy inference system (FIS) is shown in Fig. 1. The FLS maps crisp inputs

into crisp outputs. The FIS contains four components: fuzzifier, inference engine, rule base, and defuzzifier [20], [21].

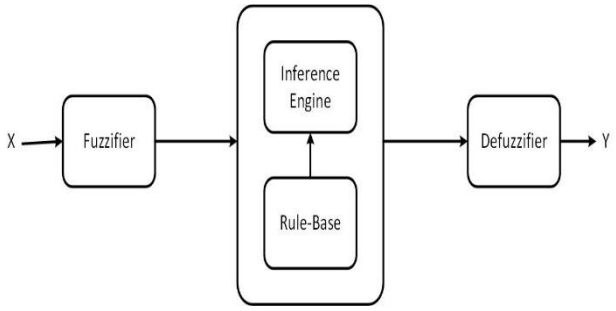

Fig. 1. Block diagram of a fuzzy inference system (FIS).

The mapping process is described below:

Step 1: The first step is to take inputs and determine the degree to which they belong to each of the appropriate fuzzy sets via membership functions.

Step 2: Once the inputs have been fuzzified, we know the degree to which each part of the antecedent has been satisfied for each rule.

Step 3: Apply the implication method. The input for the implication process is a single number given by the antecedent part, and the output is a fuzzy set.

Step 4: Aggregate all outputs. The output of the aggregation process is the combined output fuzzy set.

Step 5: Defuzzify. The input for the defuzzification process is an aggregated output fuzzy set and the output of this is a crisp value.

III. Implementation and Results

In this research work, we implemented decision trees and the fuzzy inference system (FIS) using MATLAB scripts from the machine learning and fuzzy logic tool boxes from the MATLAB 15a package and analyzed a Landsat scene.

A. Landsat Scene and Training set

We considered a Landsat scene obtained by the Landsat-8 Operational Land Imager (OLI) on June 13, 2016. The scene is from Juneau, Alaska area with the path and row numbers 58 and 19, respectively. We selected a subset of the original scenes of size 2000 rows by 2000 columns. In order to train the classifiers, we selected four classes: water, vegetation, ice-land, and glaciers [31]. Five training sets each consisting covering areas of the size 100 rows and 100 columns or 10,000 pixels, were selected. The total number of training samples were 50,000 representing five training sets. The classifiers were trained using the samples and reflectance data for bands 2 through 7 [25]. To train each classifier, we selected four classes. The color composite for a raw scene obtained with bands 5, 6, and 7 is shown in Fig. 2. The spectral signatures for classes: water, vegetation, ice-land, and glaciers are shown in Fig. 3. The 3D-scatter plot is shown in Fig. 4. To study the effect of overfitting of a decision tree on classification accuracy, we created two datasets. The first dataset contains 50,000 samples. The second dataset was obtained by adding noise to the first dataset.

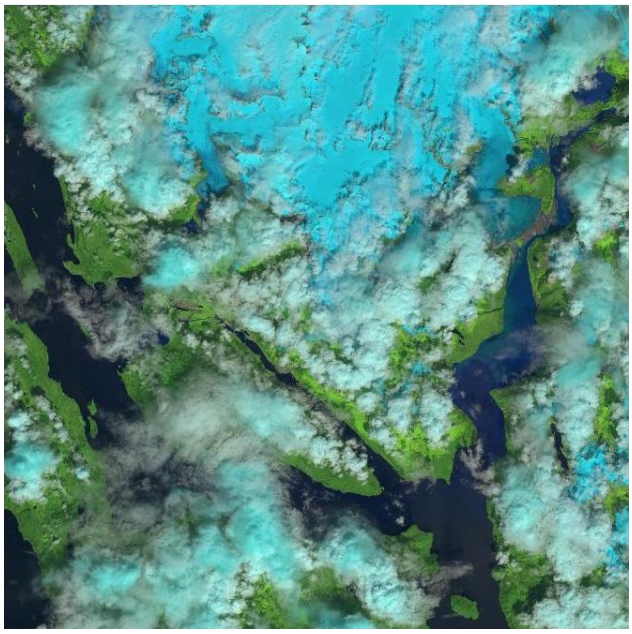

Fig. 2. Juneau Landsat -8 scenes (Raw Data).

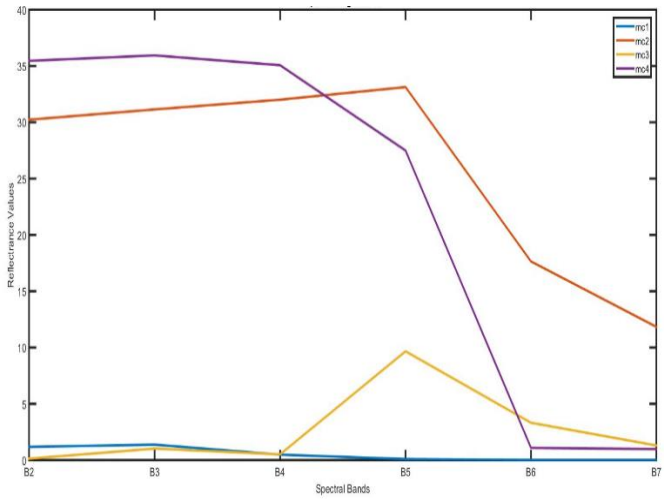

Fig. 3. Spectral signatures.

B. Decision Tree Implementation

We analyzed both data sets the clean and noisy datasets using full and pruned decision trees. We used the C4.5 algorithm from MATLAB machine learning toolbox. Noisy data samples or outliers often lead to overfitting in decision trees. To evaluate the effect of sample size, we used randomly selected samples. We used from ten percent to ninety percent randomly selected samples for training, and evaluated all samples with each decision tree. Fig. 5 and 6 show the full decision tree and the pruned decision tree, respectively.

The graphs for the overall accuracy of the original and noisy datasets are shown in Fig. 7 and 8, respectively. In Fig. 7 and 8 the x-axis represents the percentage of randomly selected samples that are used for training the classifier, and the y-axis represents the classification accuracy when all samples in the dataset are classified.

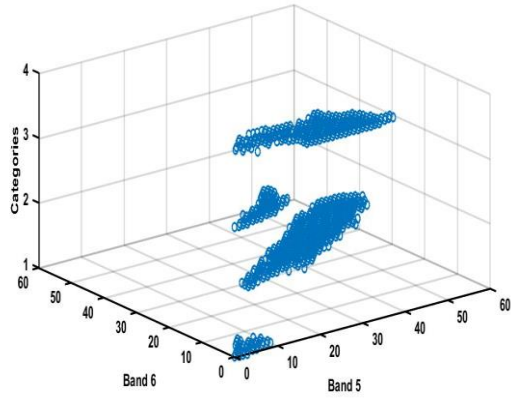

Fig. 4. Scatter plot.

C. Extracting Classification Rules from Decision Tree

Once we build a decision tree, classification rules can be extracted from the decision tree by traveling down from root node to a leaf node. The arcs of a decision tree represent the antecedent part and the category at the leaf node represents the consequent part of the rule.

We can extract a number of classification rules using the full decision tree. The pruned tree is a generalized version of an over-fitted full tree. The rules represent knowledge extracted from the pruned tree. To validate the extracted rules we built the FIS using the rules as a rule base. To implement the FIS the rules were modified by using the term sets, as the FIS requires rules to be defined using term sets. The modified rule set is used as a rule-base for the FIS.

The classified output obtained with the pruned decision tree is shown in Fig. 9. The colors blue, orange, green, and brown represent categories: water, vegetation, ice-land, and glaciers, respectively.

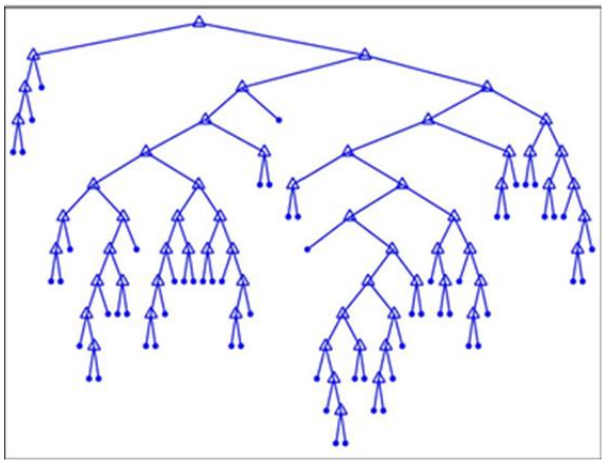

Fig. 5. Full decision tree.

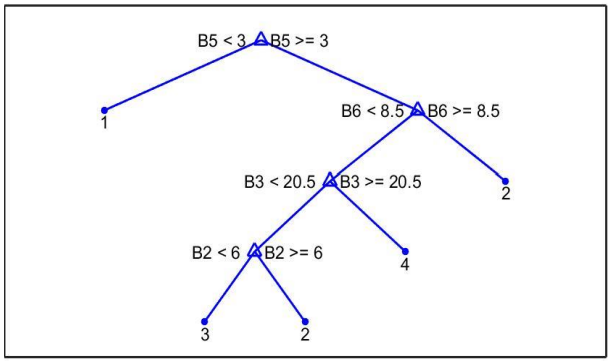

Fig. 6. Pruned decision tree.

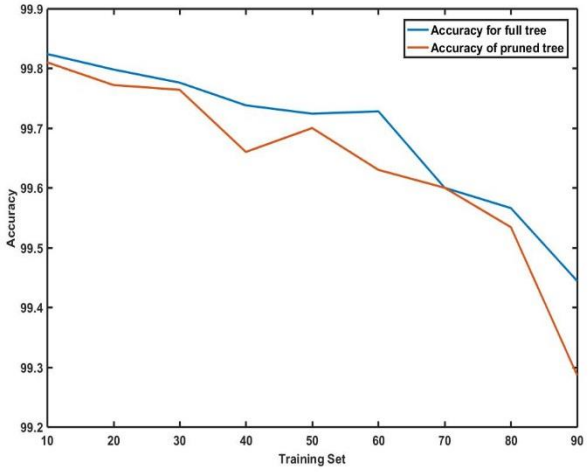

Fig. 7. Accuracy with the full decision tree and pruned decision tree using clean data.

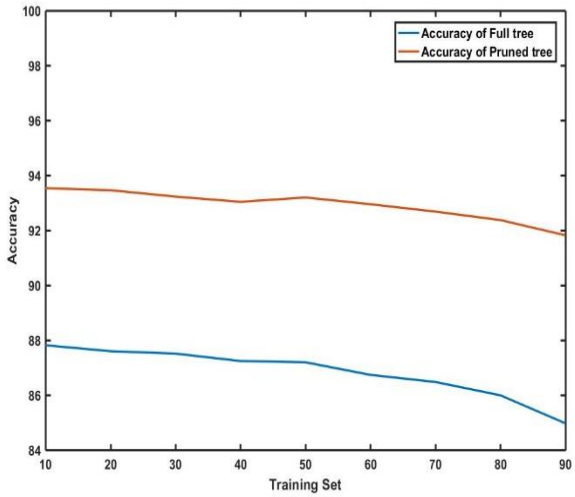

Fig. 8. Accuracy with the full decision tree and pruned decision tree for noisy data.

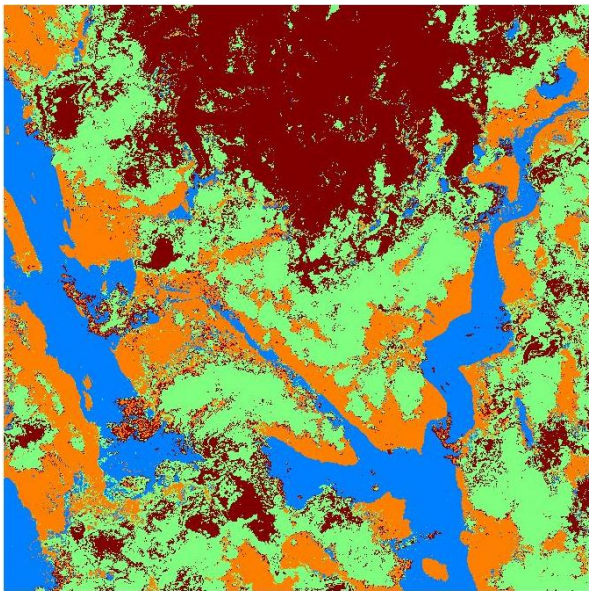

Fig. 9. Classified output with the pruned decision tree.

```
Rule 1: If Band5 < 3 Then Class = Water
Rule 2: If Band5 >= 3 AND Band 6 >= 8.5
        Then Class = Vegetation
Rule 3: If Band5 >= 3 AND Band 6 < 8.5
        AND Band3 > 20.5 Then Class = Glacier
Rule 4: If Band5 >= 3 AND Band 6 < 8.5 AND
        Band3 < 20.5 AND Band2 < 6
        Then Class = Iceland
Rule 5: If Band5 >= 3 AND Band 6 < 8.5
        AND Band3 < 20.5 AND Band2 >= 6
        Then Class = Vegetation
```

Fig. 10. Extracted rules from pruned decision tree.

```
Rule 1: If Band5 = Low Then Class = Water
Rule 2: If Band5 = High AND Band6 = High
        Then Class = Vegetation
Rule 3: If Band5 = High AND Band6 = Low
        AND Band3 = High Then Class = Glacier
Rule 4: If Band5 = High AND Band6 = Low
        AND Band3 = Low
        AND Band2 = Low Then Class = Iceland
Rule 5: If Band5 = High AND Band6 = Low
        AND Band3 = Low AND Band2 = High
        Then Class = Vegetation
```

Fig. 11. Rules for the fuzzy inference system.

D. Fuzzy Inference System

Creating an FIS in MATLAB fuzzy logic toolbox consists of three main steps: 1) defining term sets and fuzzy membership functions for each input; 2) defining term sets and membership functions for the output; and 3) creating the rule-base that implements the inference engine. In the present example we developed the FIS with four inputs and one output. The inputs represent the four features: Band2, Band3, Band5, and Band6 reflectance values. We selected these four features because the extracted rule set contains these features. For each feature we used two term sets with labels Low and High. To define the membership functions, we used threshold values from the rule set in Fig. 10. It can be seen from the rule set shown in Fig. 11 that each variable has used these two term-sets.

The membership functions for Band2, Band3, Band5 and Band6 are shown in Fig. 12(a)-12(d). Fig. 13 shows the output membership functions. Since we have four categories we have chosen four term sets to represent four categories water, vegetation, ice-land, and glaciers. We have created the rule-base by entering using a verbose representation. The fuzzifier converts the input crisp values to input membership values. Depending upon the input fuzzy membership values firing strength for each rule is determined by applying fuzzy operators to antecedent parts. It is possible that for a given input vector more than one rule may get fired. The firing strength of each rule determines the shape of the corresponding output membership function. The reshaped output membership functions are aggregated to form the output fuzzy set, which then is defuzzified to get a crisp output.

The process of generating an output fuzzy set is shown in Fig. 14. Fig. 15 shows the mapping surface. The output of the FIS is then presented to the post-processor block. The post-processor converts the crisp output values to categories. The range of the output membership functions is defined from 0 to 10. In the output fuzzy membership functions values from 0 to 2.5 represent water, values from 2.5 to 5 represent vegetation, values from 5 to 7.5 represent ice-land, and values from 7.5 to 10 represent glaciers.

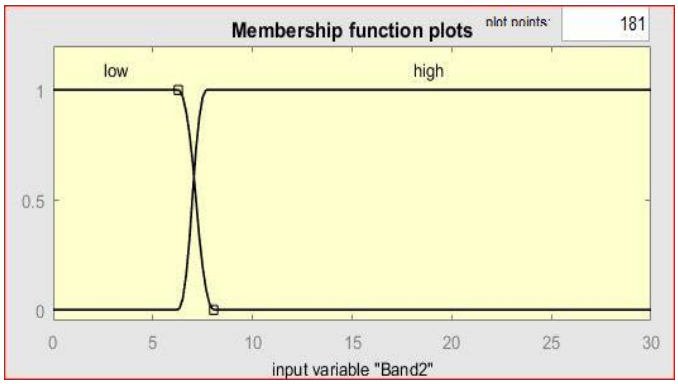

Fig. 12. (a) Membership functions for Band2.

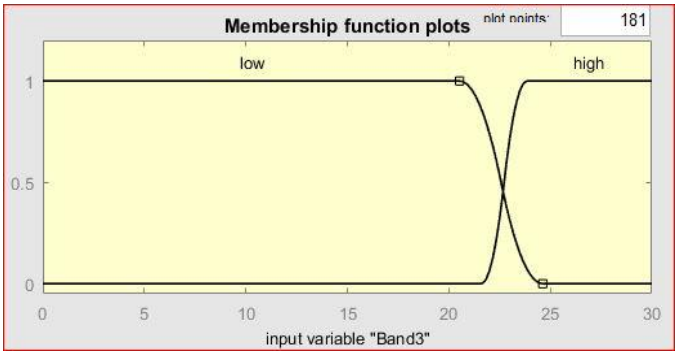

Fig. 12. (b) Membership functions for Band3.

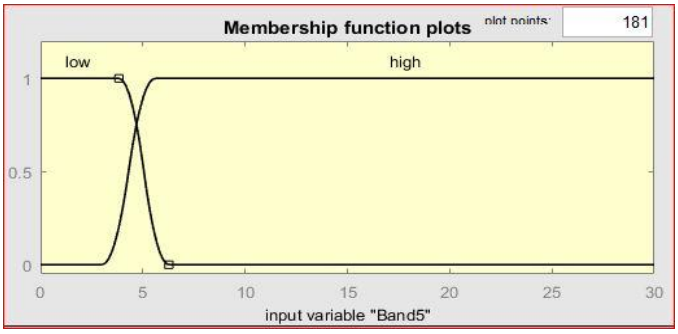

Fig. 12. (c) Membership functions for Band5.

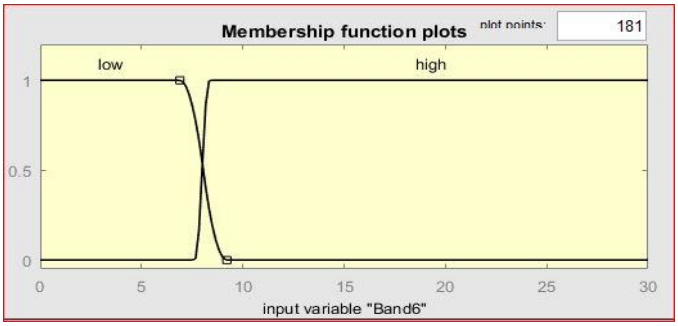

Fig. 12. (d) Membership functions for Band6.

We classified 50,000 samples from the clean and noisy datasets using the FIS and compared the output of the FIS with actual categories. The confusion matrices for clean and noisy datasets are shown in Tables 1 and 2, respectively. We calculated the overall efficiency using the confusion matrix [32]. Rows in the confusion matrix represent actual categories and columns represent the estimated categories by the FIS. The diagonal values in the confusion matrix show the number of samples that are correctly classified by the FIS. The overall classification accuracy with the FIS was 95.59 percent for the training set data without noise and 80.23 percent for the noisy data set.

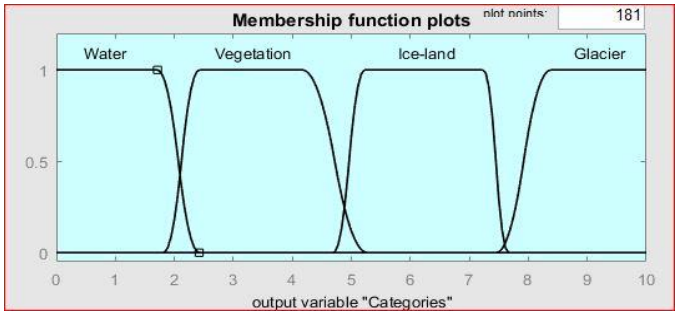

Fig. 13. Output membership functions.

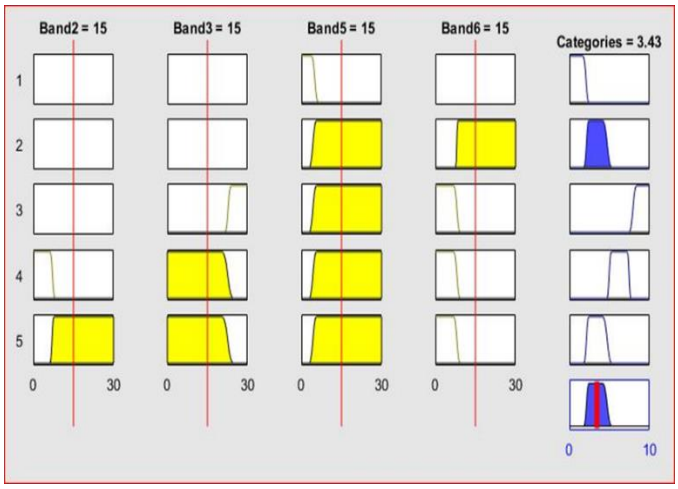

Fig. 14. Firing of rules and the process of aggregation.

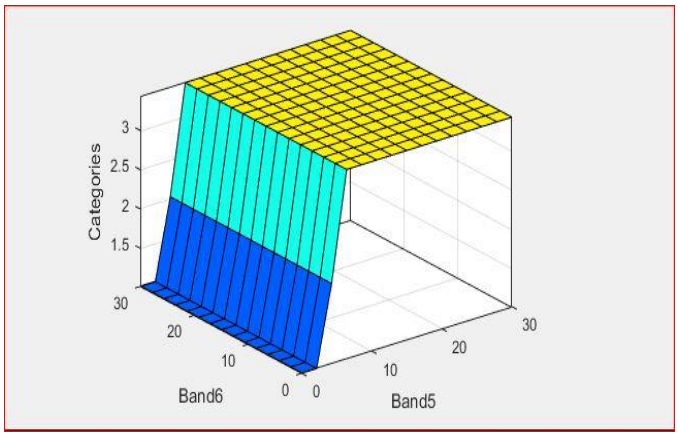

Fig. 15. Mapping surface for the fuzzy inference system.

TABLE. I. CONFUSION MATRIX FOR FIS WITH CLEAN DATA

	Water	Vegetation	Ice-land	Glacier
Water	18663	1301	36	0
Vegetation	12	9924	63	1
Ice-land	182	335	9483	0
Glacier	1	214	59	9726

TABLE. II. CONFUSION MATRIX FOR FIS WITH NOISY DATA

	Water	Vegetation	Ice-land	Glaciers
Water	16673	3240	84	0
Vegetation	2002	7985	15	1
Ice-land	153	358	7609	1878
Glaciers	30	191	1933	7848

IV. CONCLUSION

In this research work, we implemented decision trees using the C4.5 algorithm to classify pixels in the Landsat-8 image. Also, we extracted classification rules from the pruned decision tree and evaluated the rules by implementing the FIS. One of the main concerns in decision tree classifiers is that often decision trees are over-fitted, when the training dataset is noisy or contains anomalies in the form of outliers. We generated training set data by selecting training set areas from the scene. To study the effect of overfitting we added noise to the original training set data. We selected five levels for the pruned decision tree because the resulting decision tree represented all categories. Fig. 7 and 8 show the effect of sample size and overfitting. It can be seen from the graphs in Fig. 7 and 8 that the classification accuracy decreases as the percent of randomly selected samples that are used to train the classifier increases. Fig. 8 shows the pruned tree classifier performs better than the full tree classifier for noisy training set data. The pruned tree represents the generalized version of the full decision tree classifier.

The decision trees were implemented using the C4.5 algorithm because the algorithm works with attribute values that are continuous. In the pruned decision tree decisions at each non-terminal node are made using threshold values. To implement an FIS with the extracted rules, we needed to convert the extracted rules that use term sets such as Low and High instead of threshold values. In implementing the FIS, the threshold values from the extracted rule set were used to define fuzzy membership functions for input features. We classified all data samples with the FIS and obtained 95.59 and 80.23 percent overall accuracy for clean and noisy datasets, respectively.

In conclusion, decision trees represent an alternative to conventional algorithm to classify pixels in Landsat images. Furthermore, we can extract knowledge in terms of classification rules from the decision tree. The extracted rules provide a rule-base for the FIS. It is possible to use a combination of rules obtained from multiple sources such as neural networks, decision trees, and an expert's knowledge to implement the rule base in the FIS.

The future work includes 1) developing an algorithm to find the number of levels for pruning the decision tree that yield high accuracy for test data; 2) exploring the possibility of reducing the number of features; and 3) building the FIS with rules that are extracted using multiple methods such as neural networks and decision trees.

ACKNOWLEDGMENT

The authors are thankful to Dr. Stephen Rainwater for his constructive suggestions.

REFERENCES

[1] R. O. Duda, P. E. Hart, and D. G. Stork, Pattern classification. Wiley New York, 1973.

[2] P. Mantero, G. Moser, and S. B. Serpico, "Partially supervised classification of remote sensing images through SVM-based probability density estimation," IEEE Transactions on Geoscience and Remote Sensing, vol. 43, no. 3, pp. 559-570, 2005.

[3] V. N. Vapnik and S. Kotz, Estimation of dependences based on empirical data. Springer-Verlag New York, 1982.

[4] B. E. Boser, I. M. Guyon, and V. N. Vapnik, "A training algorithm for optimal margin classifiers," in Proceedings of the fifth annual workshop on Computational learning theory, 1992, pp. 144-152: ACM.

[5] German Alba, "Remote sensing classification algorithms, algorithm analysis applied to land cover change" Master in Emergency Early Warning and Response Space Applications, CONAE, Argentina, 2014, pp 1-21.

[6] C. Huang, L. Davis, and J. Townshend, "An assessment of support vector machines for land cover classification," International Journal of remote sensing, vol. 23, no. 4, pp. 725-749, 2002.

[7] P. Mitra, B. U. Shankar, and S. K. Pal, "Segmentation of multispectral remote sensing images using active support vector machines," Pattern recognition letters, vol. 25, no. 9, pp. 1067-1074, 2004.

[8] G. Mountrakis, J. Im, and C. Ogole, "Support vector machines in remote sensing: A review," ISPRS Journal of Photogrammetry and Remote Sensing, vol. 66, no. 3, pp. 247-259, 2011.

[9] J. Benediktsson and J. Sveinsson, "Feature extraction for multisource data classification with artificial neural networks," International journal of remote sensing, vol. 18, no. 4, pp. 727-740, 1997.

[10] K. Chen, Y. Tzeng, C. Chen, and W. Kao, "Land-cover classification of multispectral imagery using a dynamic learning neural network," Photogrammetric Engineering and Remote Sensing, vol. 61, no. 4, pp. 403-408, 1995.

[11] G. Foody, "Supervised image classification by MLP and RBF neural networks with and without an exhaustively defined set of classes," International Journal of Remote Sensing, vol. 25, no. 15, pp. 3091-3104, 2004.

[12] W. Y. Huang and R. P. Lippmann, "Neural Net and Traditional Classifiers," in Neural Information Processing Systems, pp. 387–396, 1988.

[13] S. J. Eberlein, G. Yates, and E. Majani, "Hierarchical multi-sensor analysis for robotic exploration," in SPIE 1388, Mobile Robots, vol. 1, pp. 578-586, 1991.

[14] A. Cleeremans, D. Servan-Schreiber, and J. L. McClelland, "Finite state automata and simple recurrent networks," Neural computation, vol. 1, no. 3, pp. 372-381, 1989.

[15] S. E. Decatur, "Application of neural networks to terrain classification," in International Joint Conference on Neural Networks, 1989, vol. 1, pp. 283–288.

[16] A. D. Kulkarni and K. Lulla, "Fuzzy neural network models for supervised classification: multispectral image analysis," Geocarto International, vol. 14, no. 4, pp. 42-51, 1999.

[17] R. H. Laprade, "Split-and-merge segmentation of aerial photographs," Computer Vision, graphics, and Image Processing, vol. 44, no. 1, pp. 77-86, 1988.

[18] R. J. Hathaway and J. C. Bezdek, "Recent convergence results for the fuzzy c-means clustering algorithms," Journal of Classification, vol. 5, no. 2, pp. 237-247, 1988.

[19] S. K. Pal, R. K. De, and J. Basak, "Unsupervised feature evaluation: A neuro-fuzzy approach," IEEE Transactions on neural networks, vol. 11, no. 2, pp. 366-376, 2000.

[20] A. Kulkarni and S. McCaslin, "Knowledge discovery from multispectral satellite images," IEEE Geoscience and Remote Sensing Letters, vol. 1, no. 4, pp. 246-250, 2004.

[21] A. D. Kulkarni, “Neural-fuzzy models for multispectral image analysis,” Applied Intelligence, vol. 8, no. 2, pp. 173-187, 1998.

[22] M. Ghose, R. Pradhan, and S. S. Ghose, “Decision tree classification of remotely sensed satellite data using spectral separability matrix,” International Journal of Advanced Computer Science and Applications, vol. 1, no. 5, 2010.

[23] A. P. Pooja, J. Jayanth, and K. Shivaprakash, “Classification of RS data using decision three approach”, International Journal of Computer Applications, vol 23, no. 3, pp 7-11, 2011.

[24] M. Hansen, R. Dubayah, and R. DeFries, "Classification trees: an alternative to traditional land cover classifiers,” International journal of remote sensing, vol. 17, no. 5, pp. 1075-1081, 1996.

[25] B. Lowe and A. D. Kulkarni. “Multispectral image analysis using Random Forest”, International Journal on Soft Computing (IJSC), vol. 6, no.1, pp. 1-14, 2015.

[26] A. D. Kulkarni, B. Lowe. “Random forest algorithm for land cover classification”. International Journal on Recent Innovations Trends in Computing and Communication, vol. 4, no. 3, pp. 58-63, 2016.

[27] C. Taylor, A. Kulkarni, and K. Mokhtar, "Knowledge Extraction from Metacognitive Reading Strategies Data Using Induction Trees," International Journal of Advanced Computer Science & Applications, vol. 1, no. 7, pp. 269-274, 2016.

[28] Kulkarni, A. D. (1983). Categorization of multispectral data using binary tree classifiers. Proceedings of the International Symposium on Machine Processing of Remotely Sensed Data at LARS, Purdue University, pp 609-612.

[29] J. R. Quinlan, "Induction of decision trees," Machine learning, vol. 1, no. 1, pp. 81-106, 1986.

[30] T. Mitchell, Machine Learning, WCB/McGraw-Hill, Boston, MA, pp. 52-80, 1997.

[31] "Land Remote Sensing Image Collections". Remotesensing.usgs.gov. N.p., 2017. Web. 26 Mar. 2017.

[32] R. G. Congalton, “A review of assessing the accuracy of classifications of remotely sensed data,” Remote Sensing of Environment, vol. 37, no. 1, pp. 35–46, 1991.

Sentiment Analysis on Twitter Data using KNN and SVM

Mohammad Rezwanul Huq
Dept. of Computer Science and Engineering
East West University
Dhaka, Bangladesh

Ahmad Ali
Dept. of Computer Science and Engineering
East West University
Dhaka, Bangladesh

Anika Rahman
Dept. of Computer Science and Engineering
East West University
Dhaka, Bangladesh

***Abstract*—Millions of users share opinions on various topics using micro-blogging every day. Twitter is a very popular micro-blogging site where users are allowed a limit of 140 characters; this kind of restriction makes the users be concise as well as expressive at the same time. For that reason, it becomes a rich source for sentiment analysis and belief mining. The aim of this paper is to develop such a functional classifier which can correctly and automatically classify the sentiment of an unknown tweet. In our work, we propose techniques to classify the sentiment label accurately. We introduce two methods: one of the methods is known as sentiment classification algorithm (SCA) based on k-nearest neighbor (KNN) and the other one is based on support vector machine (SVM). We also evaluate their performance based on real tweets.**

***Keywords*—Support Vector Machine (SVM); k-nearest neighbor (KNN); Grid Search; Confusion matrix; ROC graph; Hyperplane; Social data analysis**

I. INTRODUCTION

These days social networks, blogs, and other media produce a huge amount of data on the World Wide Web. This huge amount of data contains crucial opinion related information that can be used to benefit for businesses and other aspects of commercial and scientific industries. Manual tracking and extracting this useful information from this massive amount of data is almost impossible. Sentiment analysis of user posts is required to help taking business decisions. It is a process which extracts sentiments or opinions from reviews which are given by users over a particular subject, area or product in online. We can categorize the sentiment into two types: 1) positive or 2) negative that determine the general attitude of the people to a particular topic. Our principal goal is to correctly detect sentiment of tweets as more as possible. This paper has two main parts: the first one is to classify sentiment of tweets by using some feature and in the second one we use machine learning algorithm SVM [1]. In both the cases, we use five-fold cross validation method to determine the accuracy. We propose two approaches for sentiment analysis. One of the technique facilitates KNN and the other uses SVM. Both techniques work with same dataset and same features. For both SCA and SVM we calculate weights based on different features. Then in SCA, we build a pair of tweets by using different features. From that pair, we measure the Euclidian distance for every tweet with its counterpart. From those distance we only consider nearest eight tweets label to classify that tweet. On the other hand in SVM, build a matrix from the calculated weights based on different features and by applying PCA (principal component analysis) [2], we try to find k eigenvector with the largest Eigen values. From this transformed sample dataset we try to find the best c and best gamma by using grid search technique [3] to use in SVM. Finally, we apply SVM to assign the sentiment label of each tweet in the test dataset. In both algorithms, we use confusion matrix [4] to calculate the accuracy.

Later, we compare our two techniques in respect to an accuracy level of detecting the sentiment accurately. We found that Sentiment Classifier Algorithm (SCA) performs better than SVM.

II. RELATED WORK

Researchers have paid attention to this problem to some extent. In this paper [5], authors looking at popular micro-blogging Twitter, here the authors build models for two classifying tasks. These are a binary task of classifying sentiment into positive, negative classes and three-way task means to classify sentiment into positive, negative and neutral classes. They also performed an experiment with unigram model, a feature based model, and a tree kernel-based model. They were combining unigrams with their features and features with the tree kernel. In this paper, they presented extensive feature analysis of the 100 features they propose.

In this work [6], authors proposed an approach to automatically detect sentiment on Twitter messages (Tweets) and also proposed two-step sentiment analysis classification method for Twitter. First, they classified messages as a subjective and objective category and further distinguishes the subjective tweets as positive or negative. For creating these classifiers, instead of using manually annotated data to compose the training data as regularly supervised approaches, they leverage sources of noisy labels as their training data. These noisy labels were provided by a few sentiment detection websites over Twitter data. For better utilizing these sources, it is important to verify the potential value of using and combining them. A more robust feature set that captures a more abstract representation of tweets and it is composed by meta-information associated to words and specific characteristics of how tweets are written is also proposed by the authors. In Meta-features, they map a given word in a tweet to its part-of-speech using a part-of-speech dictionary as POS tags are good indicators for sentiment tagging. An

effective and robust sentiment detection approach for Twitter messages is presented by this paper which uses biased and noisy labels as input to build its models. The main limitations of our approach are the cases of sentences that contain antagonistic sentiments.

By investigating the utility of linguistic features for detecting the sentiment of Twitter messages, the author of this paper [7] evaluate the usefulness of existing lexical resources as well as features to capture information about the informal and creative language used in micro-blogging. For building training data they take a supervised approach but leverage existing hashtags in Twitter data. In their experiment, they use three different corpora of Twitter messages. For development and training, they use hashtagged dataset (HASH) and the emoticon dataset (EMOT). There are three steps for preprocessing the dataset. They are: 1) tokenization, 2) normalization and 3) parts-of-speech (POS) tagging and they also use a variety of features for their classification and experiment. They use unigrams and bigrams for the baseline and they also include features typically used in sentiment analysis such as sentiment lexicon and POS features. The features are n-gram, lexicon features, part-of-speech features, micro-blogging features.

Their experiments [8] show that part-of-speech features may not be useful for sentiment analysis in the micro-blogging domain. Features from an existing sentiment lexicon were somewhat useful in conjunction with micro-blogging features. For automatically classifying the sentiment of Twitter messages, in this paper, the authors introduce a novel approach and they classified these messages as either positive or negative with respect to a query term. For this reason, they build a framework that treats classifiers and feature extractors as two distinct component. This framework allows them to easily try out different combinations of classifiers and features extractors and then normalizing the effect of query terms along with corresponding tweets. Their assumption is that users prefer to perform sentiment analysis on a product and not of a product. By Stripping out the emoticons causes the classifier to learn from other features such as unigrams and bigrams present in the tweet. An interesting side effect of their feature is that they use non-emoticon to determine the sentiment. They consider emoticons as noisy labels because they are not perfect while defining the correct sentiment of a tweet. For example, @BATMANNN :(I love chutney..... Without the emoticon, most people would probably consider this tweet to be positive. Tweets with these types of mismatched emoticons are used to train our classifiers because they are difficult to filter out from our training data. The Twitter language model has many unique properties such as using rnemes and links and taking advantage of the following properties to reduce the feature space. They also use support vector machine classification technique. Here their output data are two sets of vectors of size m. Each entry in the vector corresponds to the presence of feature. In this paper, they show that machine learning algorithms (Naive Bayes, maximum entropy classification, and support vector machines) can achieve high accuracy for classifying sentiment when using this method.

III. WORKING PROCEDURES

We use a variety of features for our classification experiments. For the baseline, we use word feature, n-gram feature, pattern feature and punctuation feature [9]. Finally, we also include another key based feature. After calculating weight based on features for each tweet, we use our techniques.

In **Word Feature,** each word in tweet considered as a binary feature [10]. For counting the word feature of a tweet, it compares with a dictionary which is used to detect which words are stop words and which are not. Stop words [11], [12] are out of consideration. Otherwise, every word is considered for word feature. Moreover, if we encounter sequences of two or more punctuation symbols inside a tweet, we consider them as word features [13]. Additionally, the common word RT, which means "retweet", does not constitute a feature because it may appear in the majority of tweets inside the dataset. When we calculate word feature weight we calculate is as $ws = \frac{Nf}{coun(f)}$ where *Nf* represents the number of feature present in the tweet and count (f) represent the number of total feature present in the whole dataset. We use this formula for all the features of our experiment.

In **N-Gram Feature,** a sequence of 2-5 consecutive words in a sentence is regarded as a binary n-gram feature. The tweet which contains more rare words that have a higher weight than which contain common words and it has made a greater effect on the classification task.

In **Pattern Features,** the words are divided into three categories. They are high-frequency words (HFWs), content words (CWs) and regular words (RWs). When a word frequency is considered as *f* which frequency in the dataset is represent as *frf* and it will be considered as a high-frequency word if *frf* > *FH*. On the other hand, if *frf* < *FC*, then *f* is considered to be a content word and the rest of the words are considered as regular words. The word frequency is calculated from all the words of the dataset and it is estimated from the training set rather than from an external corpus. We treat as HFWs all consecutive sequences of punctuation characters as well as URL, REF, TAG and RT meta-words for pattern extraction as they play an important role in pattern detection. A pattern is an ordered sequence of HFWs and slots for content words. The upper bound for FC is set to 1000 words per million and the lower bound for FH is set to 10 words per million. FH is set to 100 words per million and we provide a smaller lower bound as the experimental evaluation produced better results. Observing that the FH and FC bounds allow overlap between some HFWs and CWs. By addressing this issue, we follow a simple strategy as described next. If $f_{rf} \in \left(FH, FH + \frac{FC}{2}\right)$ the word is classified as HFW; otherwise, $f_{rf} \in \left[FH + \frac{FC}{2}, FC\right)$ the word is classified as CW. We seek for patterns containing 2-6 HFWs and 1-5 slots for CWs. Moreover, we require patterns to start and to end with HFWs, thus a minimal pattern is of the form (HFW)(CW slot)(HFW).

TABLE. I. ACCURACY OF ALL ALGORITHMS OVER 1000 TWEETS

Method	Number of tweets	Precision	Recall	F-Score	TPR	FPR	Accuracy
Algorithm [9]	1000	0.81	0.76	0.78	0.79	0.13	79.99%
KNN with normalization (4 features)	1000	0.83	0.75	0.79	0.81	0.14	80.80%
KNN with normalization and keyword base(5 features)	1000	0.85	0.81	0.83	0.68	0.17	84.32%
SVM with (4 features	1000	0.56	0.69	0.61	0.78	0.49	58.79%
SVM with normalization (4 features)	1000	0.55	0.73	0.62	0.80	0.52	58.39%
SVM with normalization and keyword base (5 features)	1000	0.62	0.79	0.70	0.79	0.50	67.03%
SVM with normalization and keyword base (5 features) with grid search	1000	0.72	0.89	0.80	0.70	0.30	77.97%

In **Punctuation Feature,** the last feature type is divided into five generic features as: 1) tweet length in words, 2) number of exclamation mark characters in the tweet, 3) number of question mark characters in the tweet, 4) number of quotes in the tweet, and 5) number of capital/capitalized words in the tweet. The weight *wp* of a punctuation feature p is defined as $wp = (3 * Np)/(Mp * (Mw + Mng + Mpa))$, where *Mw*; *Mng*; *Mpa* declare the maximal values for word, n-gram and pattern feature groups, respectively. So, *wp* is normalized by averaging the maximal weights of the other feature types.

In the **Key-based feature,** we use a list [14] where there are 18000 words with its sentiment strength whose range falls within 1 to -1. Based on these words strength, we calculate the key based feature weight [15].

IV. EXPERIMENTAL RESULT & PERFORMANCE EVALUATION

In this section, based on the result of Sentiment Classification Algorithm (SCA) and Support Vector Machine we try to evaluate the performance of different algorithms. Our key parameters to evaluate performance are Accuracy, Recall, and Precision, etc. We have used a few open source machine learning library [16]-[18] during performance evaluation.

Here we give the accuracy of all algorithms on 1000 tweets. From the result, there are four attributes whose are precession, recall, F-Score, and Accuracy. Precision (also called positive predictive value) is the fraction of retrieved instances that are relevant while recall (also known as sensitivity) is the fraction of relevant instances that are retrieved. Both precision and recall are therefore based on an understanding and measure of relevance. F-score is calculated from precision and recall. According to the result, we can get an overview of the performance of the algorithms for different size of the dataset but for better analysis, we should compare the results based on a different parameter which is easily represented via graphs.

A. Performance Evaluation Based on Accuracy

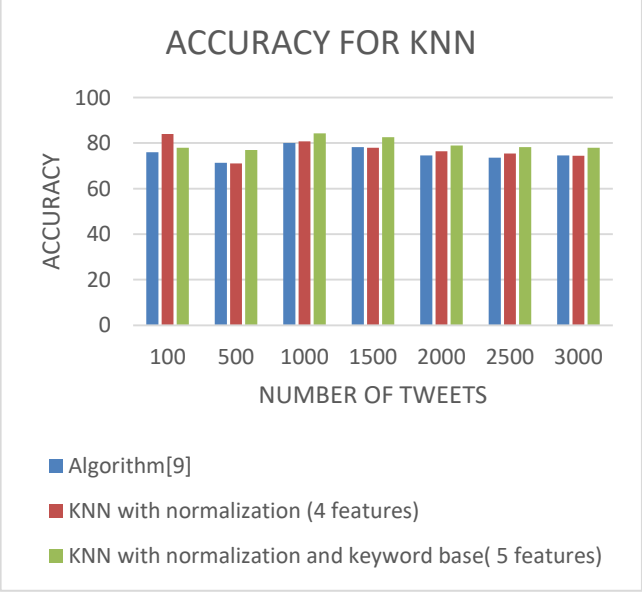

Fig. 1. Accuracy of KNN.

From Fig. 1, we can see that this graph show the accuracy of different versions of KNN for different size of the dataset. From the graph, we can see that when we use the original version of KNN with four features we get an accuracy which is increasing for all the dataset when we normalize the dataset. It is much more increasing when we add a feature name keyword-based feature.

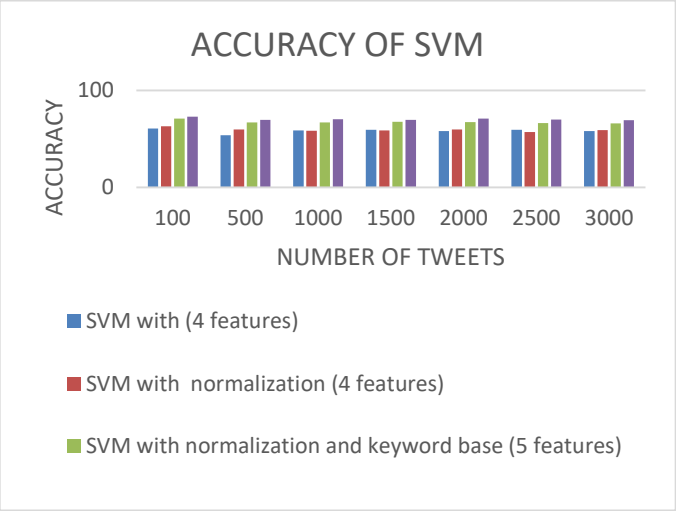

Fig. 2. Accuracy of SVM.

This graph (Fig. 2) shows the accuracy of the SVM. From the graph, we see that the accuracy of SVM with four features is around 60 percent for different size of the dataset. This is increased by normalization of the dataset. When we add another feature, keyword base features its accuracy much more increasingly and finally, we get accuracy around 70% by using grid search for every dataset.

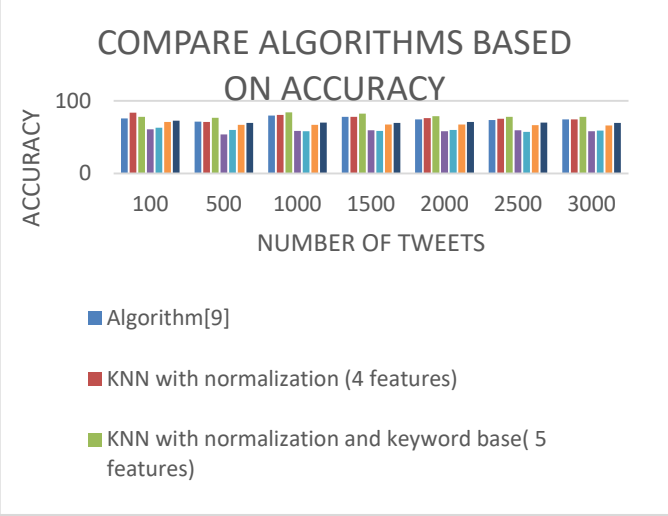

Fig. 3. Comparing algorithms based on accuracy.

From Fig. 3, we see that the accuracy of different versions of KNN is always higher than the accuracy of the different versions of SVM. From the accuracy, we see that KNN performs better than SVM for all the dataset.

If we only consider the accuracy only then it may be misleading us. Sometimes a model has greater predictive power on the problem with lower accuracy may be desirable to select.

If we consider a problem where there exist a large class imbalance and there may be a model which can predict the value of the majority and high classification accuracy achieved by it but this kind of model is not useful in the problem domain.

For this reason, we need to consider some additional measures like as precession, recall to evaluate a classifier.

B. Performance Evaluation based on Precision

When evaluating classifiers it is also necessary to consider the precession because precession can be thought as a measure of classifier exactness. A low precession indicates a large number of false positive. Sometimes it may occur that a classifier has low accuracy but it gives high precision. In a problem where exactness is more important than the high accuracy than the precession evaluating is very important.

Precision is calculated from the number of true positives divided by the number of true positives and false positives

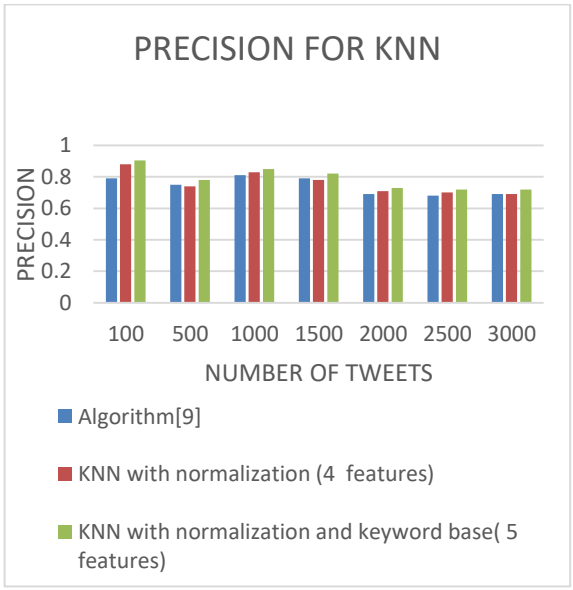

Fig. 4. Precision of KNN.

From Fig. 4, we see that the precision of the original KNN (four features) is lower than the updated version of KNN which also contains four features but the dataset is normalized. The precision is also much more increases by adding another feature keyword base feature with the previous version of KNN.

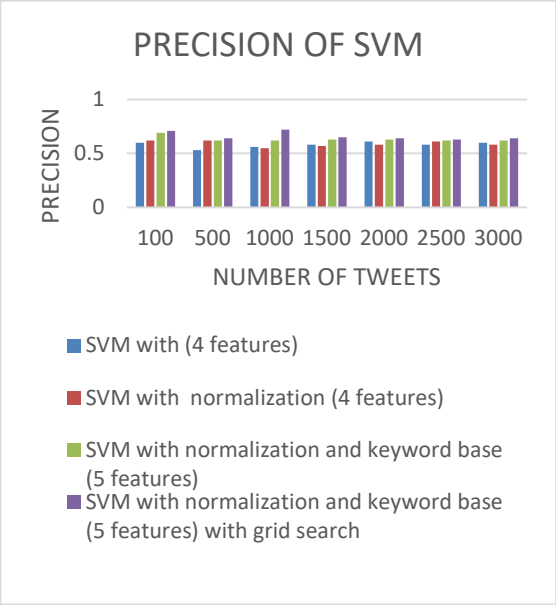

Fig. 5. Precision of SVM.

Fig. 5 contains the information about the precision of different version of SVM. When we measure the precision of SVM with four features we get precision which can be increased by normalizing it. It goes much higher when we add another feature and using grid search.

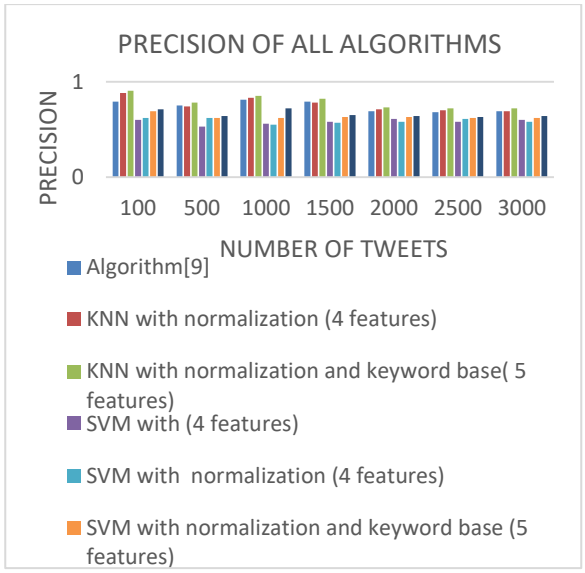

Fig. 6. Comparing algorithms based on precision.

As the precision of different versions of KNN is higher than the different versions of SVM (from Fig. 6), we can conclude that based on precision, KNN performs better than SVM.

C. Performance Evaluation Based on Recall

The recall is also important in classifier performance evaluation. It can be considered as a measure of a classifier's completeness and a low recall indicates many false negatives.

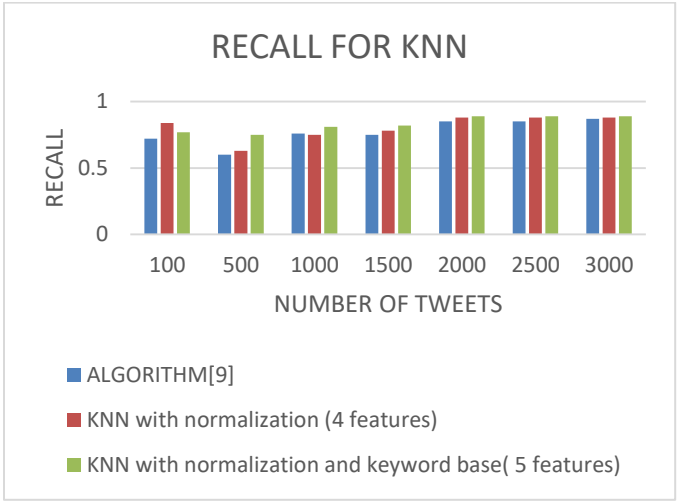

Fig. 7. Recall for KNN.

The recall is calculated from the number of true positives divided by the number of true positive and the number of false negatives.

The different versions of KNN provide good recall for different size of the dataset as shown in Fig. 7. As we modify the version of KNN, recall is increased than the previous version and it goes up to around 90% which is satisfactory.

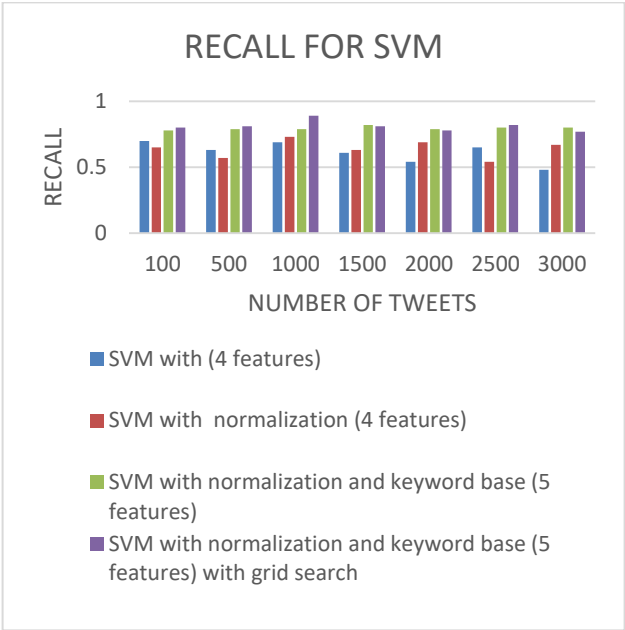

Fig. 8. Recall for SVM.

Performance based on recall is also good for the different versions of SVM as shown in Fig. 8. As version upgraded recall is also increased. SVM with four features without normalization and with normalization version recall is around 60% to 70% and it is going to 80 up when we added another feature and using grid search.

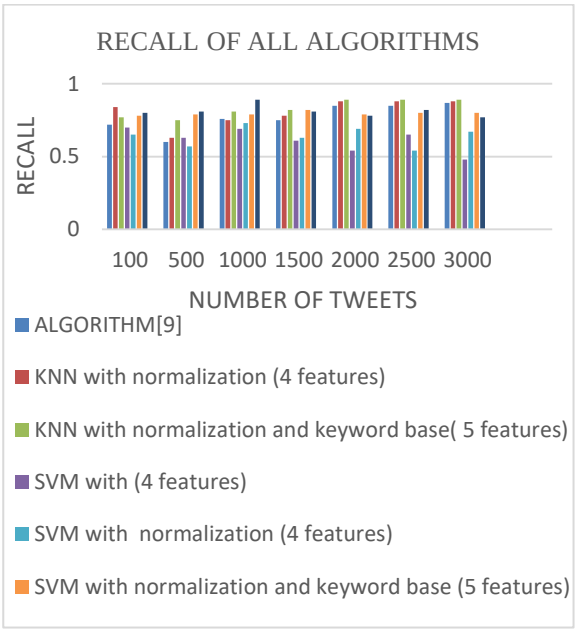

Fig. 9. Comparing algorithms based on recall.

From Fig. 9 which indicates the comparison among different versions of KNN and SVM, we see that the last two versions of SVM and KNN almost close to each other and the percentage are very good.

D. ROC Graph for Performance Evaluation

For selecting classifiers based on their performance receiver operating characteristics (ROC) graph is a good technique [19]. By plotting the true positive rate (TPR) against the false positive Rate (FPR) the curve is created. The true positive rate indicated the sensitivity or probability of detection and false positive rate indicate the fall-out or probability of false alarm.

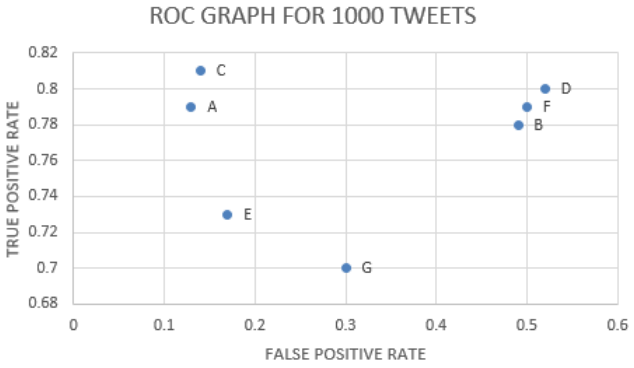

Fig. 10. ROC graph for 1000 tweets.

A: Original (KNN) (4 features).

B: KNN with normalization (4 features).

C: KNN with normalization and keyword base (5 features).

D: SVM with (4 features).

E: SVM with normalization (4 features).

F: SVM with normalization and keyword base (5 features).

G: SVM with normalization and keyword base (5 features) with grid search.

Fig. 10 shows the performance of the algorithms for 1000 tweets. We know that according to the ROC graph the performance of an algorithm is better than the other algorithms if its true positive rate is high and false positive rate is low. Based on this, if we plot the true positive rate in Y-axis and false positive rate in X-axis then we get a point in a two-dimensional plane for an algorithm. The more the algorithm is left and upper side the performance of the algorithms is better than the other algorithms. Fig. 10 shows A, C, and E performance better compared with other algorithms. According to the ROC graph, the algorithm is the best for which the data point is northwest corner compare to other algorithms that algorithm is best. But in our figure, no data point can fulfill the requirement. But we can easily say that B, D, and F perform worse than other algorithms. As G has less True positive rate than B, F, and D it has also less false positive rate compared to them. Comparing between A and C algorithms A has less true positive rate and false positive rate than C but for the C True positive rate is much more increases than the false positive rate increase.

We can see from all the graphs draw based on different parameters all time KNN always performs better than SVM. There are some reasons behind this kind of performance. Those reasons are given below.

SVM performs better when the number of dimensions is very high. But in our experiment, we only use five features and every data point represents in five dimensions. For a lot of points in few dimensions, SVM cannot perform better.

As the tweets are collect randomly and it is not guaranteed that which dataset we use as training dataset the number of positive and negative tweets are equal. It may also produce highly imbalanced dataset when we use k-fold-cross validation algorithm. Imbalance dataset means the difference between the number of positive and negative tweets is very high in the training dataset.

Learning factor c and gamma vary based on the dataset. Finding the best pair of c and gamma for a particular dataset is very tough. We try to find the best c and gamma by using grid search algorithm from some particular values of c and gamma. Grid search algorithm returns the best pair of c and gamma but there may exist better c and gamma.

SVM always assumes a hyperplane exist between the classes. But sometimes it may be very difficult to determine the hyperplane for the position of the data point in the dataset.

V. Conclusion and Future Work

Sentiment analysis based on micro-blogging is still in the developing stage and far from complete. As an example a positive sentiment is “It is a nice Day!” and a negative sentiment is “it is a horrible day!” In this paper, we will try to find out the positive and negative sentiment on Twitter data.

Currently, we have worked with a simple model and in our work, we design our classifier with only a few features like n-

gram feature, pattern feature, punctuation feature, keyword-based feature and word feature. We also use machine learning algorithm SVM (support Vector Machine). We also use KNN classifier and calculate the accuracy of all algorithms. In this paper, we are focusing on dividing the tweets into positive and negative sentiment. In our work, we see that sentiment classifier algorithm (SCA) performs better than SVM.

In future, we would study further many related problems. For this, we will try to improve our models by adding some extra features. In this paper, we work with only the English tweets and we are not considering the emoticons tweet. So our next plan is to work with other language tweets and add the emoticons tweets. Apart from this, we will also try to detect another sentiment label of human being and at the same time, we will work with a big amount of tweets. From this, we can say that our future work list may contain the following actions:

- *Adding some extra features*: Adding some features will helps us to detect sentiment more correctly and provide a better result than the present result.
- *Working with others language*: In our work, we use Java language and Java JAR files. In future, we can use different language.
- *Working with emoticons tweets*: We only work with text tweets. In future, we need to work with text tweets as well as emoticons tweets.
- *Focusing on detecting another sentiment label of human being*: We only work with positive and negative sentiment label. We will extend our work to consider other sentiment labels.
- *Working with a lot of tweets*: In future, we would like to work with a dataset which contains a large number of tweets.
- *Accuracy calculation and performance evaluation*: In current work, we use confusion matrix for calculating accuracy and performance evaluation. In future Apply others machine learning algorithms to calculate accuracy and performance evaluation.
- *Working with real world problems*: Given an efficient sentiment label, we will try to see how it can be applied to solving real-world problems. As for example, predicting presidential election, estimating product reputation, etc.

In this paper, we are mainly focusing on general sentiment analysis like the positive and negative sentiment. There is the potential of work in the field of sentiment analysis and we will try to use our knowledge in this field. On the other hand, we would like to compare sentiment analysis with other domains.

REFERENCES

[1] AnalyticsVidhaya: https://www.analyticsvidhya.com/blog/ 2015/10/ understaing-support-vector-machine-example-code/ (accessed on 12/11/16)

[2] Sebastianraschka:http://sebastianraschka.com/Articles/ 2014_pca_step_by_step.html(accessed on 10/11/16)

[3] StackOverflow:http://stackoverflow.com/questions/19335165/cross-validation-and-grid- Search (accessed on 10/11/16)

[4] Cs.uregenia: http://www2.cs.uregina.ca/~dbd/cs831/notes/ confusion_matrix.html (accessed on 10/11/16)

[5] Apoorv Agarwal, Boyi Xie,Ilia Vovsha, Owen Rambow, Rebecca Passonneau: Sentiment Analysis of Twitter Data. In: Proceedings of the workshop on Language in Social Media (LSM), pages 30-38, 2011.

[6] Luciano Barbosa, Junlan Feng: Robust Sentiment Detection on Twitter from Biased and Noisy Data. In 23rd International Conference on Computational Linguistics, 2010.

[7] Efthymios Koulompis, Theresa Wilson, Johanna Moore: Twitter Sentiment Analysis: The Good the Bad and the OMG!.In: Proceeding of the Fifth International AAAI Conference on Weblogs and Social Media, 2011.

[8] Hassan Saif, Yulan He and Harith Alani: Semantic Sentiment Analysis of Twitter. In: Proceedings of the 11th International Semantic Web Conference, 2012.

[9] Nikolaos Nodarakis, Athanasios Tsakalidis, Spyros Siouts, Giannnis Tzimas: Large Scale Sentiment Analysis on Twitter with Spark. In: Proceedings of the First International Workshop on Multiengine Data Analytics, 2016.

[10] Archive.org:https://archive.org/details/twitter/cikm_2010 (accessed on 07/07/2016)

[11] Sentiment140: http://help.sentiment140.com/api (accessed on 10/07/2016)

[12] Github:https://github.com/aababu/sentiment-analysis/blob/master/stopword.txt (accessed on (29/11/16)

[13] Adam Bermingham, Alan F. Smeaton: Classifying sentiment in microblogs: is brevity an advantage? In: Proceedings of the 19th International Conference on Information and Knowledge Management, ACM, 2010, pp. 1833-1836.

[14] Michael Gamon. Sentiment classification on customer feedback data: noisy data, large feature vectors, and the role of linguistic analysis. In: Proceedings of the 20th International Conference on Computational Linguistics, 2004.

[15] Github:https://github.com/aababu/sentiment-analysis/blob/master/wordstrength.txt(accessed on 29/11/16)

[16] Sourceforge:https://sourceforge.net/projects/java-ml/files/java-ml/ (accessed on 10/08/16)

[17] Java2s: http://www.java2s.com/Code/Jar/l/Downloadlibsvm317sourcesjar.htm (accessed on 11/08/16)

[18] Java2s: http://www.java2s.com/Code/Jar/j/Downloadjama103jar.htm (accessed on 12/08/16)

[19] Tom Fawcett: ROC Graphs: Notes and Practical Considerations for Data Mining Researchers. In: Journal of Pattern Recognition Letters – Special issue in Roc analysis in pattern recognition archive, 2006.

Handwritten Digit Recognition based on Output-Independent Multi-Layer Perceptrons

Ismail M. Keshta
Department of Computer Engineering
King Fahd University of Petroleum and Minerals
Dhahran, Saudi Arabia

***Abstract*—With handwritten digit recognition being an established and significant problem that is facing computer vision and pattern recognition, there has been a great deal of research work that has been undertaken in this area. It is not a trivial task because of the big variation that exists in the writing styles that have been found in the available data. Therefore both, the features and the classifier need to be efficient. The core contribution of this research is the development of a new classification technique that is based on the MLP, which can be identified in handwritten documents as the binary digits '0' and '1'. This technique maps the different sets of various input data onto the MLP output neurons. An experimental evaluation of the technique's performance is provided. This evaluation is based on the well-known 'Pen-Based Recognition of Handwritten Digits' dataset, which is comprised of a total of 250 handwriting samples that are taken from 44 writers. The results obtained are very promising for such an approach in accurate handwriting recognition.**

Keywords*—Handwritten digit recognition; Pattern classification; Neural network mode; Two-class classification; Accuracy; Binary data

I. INTRODUCTION

The method of handwritten digit recognition both recognizes and classifies handwritten digits from (0-9) without there being any human interaction at all. It is a computer's ability to first receive and then interpret this handwritten input intelligently from a number of sources, including photographs, paper documents, touch screens and a number of other similar devices [1]. In fact, recognizing the handwritten digits of people has been an important field of progressive research for the last few decades and studied intensely as a challenging problem [1]-[3]. Researchers have achieved a number of results by using different algorithms, such as K-Nearest-Neighbors (KNNs), Neural Networks (NNs), etc. [2], [3].

Handwritten digit recognition remains a vital area because of its huge practical applications, as well as the important financial implications [1] [2]. It is promising in a wide range of application domains, including online handwriting recognition on computer tablets; zip code recognition to help sort posted mail, as well as the verification of signatures on cheques in order to thwart any attempts at bank fraud, etc. Handwritten digit recognition is also widely used in a number of academic institutions to process their examination papers [1], [3].

The handwriting recognition process faces certain challenges [4]-[7]. The biggest one is that the handwritten images' various dimensions have to be normalized and/or processed in order for them to fall within the system's boundary specific requirements. Thus, the challenges of handwritten digit recognition do not just result from the many different ways in which a single digit can be written, but also arise from the various different requirements that are imposed by the applications that are specifically used [1], [2]. In addition, there are the varying degrees of thickness of people's handwriting and the writing's different positions when it comes to the sample's margins [8]-[10]. Moreover, Akhtar *et al.* [1] indicated that as people's various writing styles will depend on their age, qualifications, mode, background, etc. handwritten digit recognition is a relatively complex research task and the format of handwritten digits will have a big impact on classification and/or identification, as the various subjects will all use different styles of writing. In fact, even digits that have been written by the same person at different times were also found to vary [11], [12]. Therefore, it is almost impossible to develop a generic recognizer that is able to recognize an infinite number of writers' handwritten digits.

As part of this research, we investigated a number of different handwritten digit recognition schemes and presented various existing methods after reviewing a number of recent researches related to this field. A classification technique that is based on MLP was also proposed. This was done in order to recognize both the binary digits of '0' and '1' in a series of handwritten documents. This technique was implemented in Java and then tested on the Pen-Based Recognition of Handwritten Digits dataset.

As part of the proposed approach, the number of hidden neurons depends on the number of input features (including the bias), which is in contrast to other approaches wherein the number of hidden layer units depends on the number of output neurons. As a result, the proposed approach provides for a more concise network for the recognition task. Furthermore, the ultimate goal is binary digit classification, which finds applications in digital system design and human subject identification.

The rest of this paper is organized as follows. Section II provides a literature survey of recent approaches proposed for handwritten digit recognition. Section III elaborates upon the proposed MLP-based classification technique. Section IV discusses the simulation results obtained. Finally, a conclusion and future directions for research are all summarized in Section V.

II. HAND WRITING RECOGNITION APPROACHES

This section describes some of the existing approaches for handwritten digit recognition.

A. Clustering approaches

The aim of the research done by the authors in [12] is to use the genetic algorithm for clustering digit for handwriting digit recognition. It uses the famous genetic algorithm clustering method based on the phenomenon of natural selection in genetic evolution, i.e., mating and mutation. Starting from an initial population of arbitrary samples of handwriting, a group of new and elite individuals are generated through random selection. There are three main operations or phases in the genetic algorithm, namely, selection, cross over and mutation. The proposed hand digit recognition includes three aspects: digital image pre-processing, feature extraction, and identification.

The authors found that the genetic algorithm has a higher clustering accuracy than the Backpropagation neural network; in addition, the experiment carried out shows that genetic algebra requires less training time than the BP NN. In [13], the scheme proposed uses the following procedure for conducting the clustering task. The procedure involves three steps: 1) Image pre-processing, 2) Feature extraction, and 3) Clustering of digits. In the image pre-processing phase, the following sub-tasks are needed, namely, binarization, smoothing and de-noising, image normalization and refinement.

In the binarization stage, the image is transformed into a grey scale version that contains only two kinds of values, 0 or 1. The smoothing and de-noising task is needed to fine-tune the binary output for noise removal/smoothing. The third task, which is image normalization, is needed because text sizes and their positions differ from person to person, thus the characters need to be normalized. The final sub task is refinement, which is mainly needed for reduction of the original binary matrix into a value that can be easily stored. This is done by obtaining an approximate graph formed by a simple curve with the original. Secondly, feature extraction; the method used in this paper is the principal component analysis (PCA), which is statistical feature extraction that uses the full data in the second order statistical information for data feature extraction and reduction of dimensionality. The authors use the k-means clustering algorithm to partition N observations into K clusters, in which each observation belongs to the cluster with the nearest mean.

B. Feature extraction methods for Handwritten Digit Recognition

The authors in [14] propose an algorithm that uses two dimensional hidden Markov models for a handwritten digit recognition algorithm. Their main idea is based on the combination of tropical geometry and algebraic statistics in order to determine the Markov model parameters. The main task is to compute the distance between the unclassified images and prototypes in a certain way. For that purpose, they used the k-nearest neighbors technique.

The authors in [15] proposed a method to extract the features of one-number Persian images and subsequently used a neural network with three layers for classification. Their method has the capability of extraction of the ideal features for one number in an image even if there is a rotation, changing in the size and noise. The proposed method has four main components, namely, frame finding, classification, feature extraction and finally recognition using neural network. The first step, which is frame finding, narrows the digits and extracts the features of that narrowed digit. Classification is used to classify the narrowed digits into two categories/classes. The two categories are digits 1, 2, 3, 4, 6 and 9 that have a 1-like base and the other digits that are 0, 5, 7 and 8. Feature extraction is used to extract the features based on direction and accumulation techniques. Finally, the recognition is done using the multi-layer perceptron neural network with a feed-forward algorithm used for the final recognition of the number.

C. Neural Network for Digit Recognition

The authors in [16] present an intensive and complete representation for the two main types of neural networks, which are the backpropagation networks and radial basis function networks. They also attempt to compare the capabilities of these two types of neural networks based on a digit image recognition problem. The authors use 10 digit images, from “0” to “9”. Each image consists of 8×7=56 pixels. The authors highlight the architecture for the neural networks based on the digit image recognition problem. For backpropagation networks they have 56 inputs, 10 outputs and no hidden layer. Their architecture for the RBF neural network has 56 inputs, 10 outputs and an additional layer that consist of 10 units for each data image; this is because the 10 input image data can be classified into 10 clusters.

In [11] and [15]-[17], all schemes use the MLP backpropagation method in classification of the handwritten digits. In the propagation phase, data propagation involves the following steps: 1) forward propagation of a training pattern’s input through the neural network in order to generate the propagation’s output activations, and 2) backward propagation of the propagation’s output activations through the neural network using the training pattern’s target in order to generate the deltas of all output and hidden neurons.

The authors of [18] aim to analyze the effect of two backpropagation (BP) algorithms: simple BP and BP with momentum, on a handwritten digit recognition task. They analyze the relationship between the learning rate and the accuracy of the handwritten digit recognition task using two backpropagation schemes. It is very important to note that the choice of the learning rate is critical for the design of a BP neural network. The main distinction between the simple backpropagation and backpropagation with momentum is in the way the weights are updated; the latter (BP with momentum) uses an additional term, which is the momentum. They provided two results. The first one was by using the simple BP algorithm and the other using BP with momentum for different learning rates and different number of hidden neurons: 150 iterations are used in both BPs. The results show that the accuracy of the network increases as the learning rate increases from 0 and approaches 1, but the accuracy decreases as the learning rate decreases for any number of hidden neurons in the hidden layer.

III. The Proposed MLP-Based Digit Recognition Technique

After describing some of the existing approaches for handwritten digits recognition in Section II, this section describes the proposed classification technique based on the Multilayer Perceptron (MLP) algorithm, for identifying binary digits '0' and '1' in handwritten documents. Also, under the same section, the implemented algorithm is pointed out. In addition, simulation setups for the proposed scheme that are used for evaluating the performance of the implementation are described in this section.

A. Dataset

In this research work, the "Pen-Based Recognition of Handwritten Digits" dataset [19] is used. It is a digit database that was prepared from handwritten numeric digits. It is a collection of 250 samples from 44 different writers. The writers are advised to write 250 digits in a casual order inside boxes of 500 x 500 tablet pixel resolution. Each screen contains five boxes, with the digit to be written displayed above; subjects are told to write only inside the boxes. 10992 instances exist in this dataset with 16 input features [19], [20]. The calculation for these features was based on basis of (X, Y) coordinates of the pen at a particular instance. The dataset contains 10 classes. It is important to point out that all input attributes are integers in the range (0-100). The last attribute in this dataset is the class label that is an integer in the range (0-9) [21]. It is important to point out that the dataset was filtered based on the class label in order to include only digits 0 and 1 and exclude the other digits from (2-9).

From the literature, it can be concluded that the authors of [12] used genetic algorithm for clustering digit samples in order to implement handwriting digit recognition. The genetic algorithm has a faster convergence rate than the back propagation neural network methods; it involves complexities in its implementation and includes many randomization processes. Another method is the use of k-means clustering algorithm [13], which has the problem of deciding on the members of the initial cluster. The proposed approach focuses on the use of a classification technique based on the Multilayer Perceptron (MLP) for identifying binary digits '0' and '1' in handwritten documents, with neural structure being independent of the size of the output layer.

It is important to point out that the training algorithm for the MLP neural network employs a technique which makes the number of hidden units in the hidden layer equal to the number of the input neurons which includes nodes for the features and bias. In other words, the difference between the proposed approach and approaches proposed by Yu *et al.* in [13] and others for handwriting digit recognition is that in the approach, the number of the hidden units depends on the number of the elements in the input vector regardless of the number of the outputs, whereas the other techniques rely on the number of the outputs. For example, if the number of features is 4 then the number of hidden units will be 10 based on the previous approaches because of having ten digits (i.e., 0–9), while in the proposed technique the number of hidden units will be five corresponding to four features and one bias regardless of the number elements in the output vector. Therefore, for identifying binary digits '0' and '1' in handwritings, the previous approaches require only two hidden units in the hidden layer regardless of how many features are used, while the proposed approach requires the number of the hidden units to be the same as the number of the features plus one for bias.

```
1)  /**Initializing steps**/
2)  Initialize all weights to small random values and Take the
    feature vector and bias as Input vector.

3)  /**propagate the input features and bias of the training
    pattern k to determine the MLP's output [steps 4-14]**/
4)  for i ← 0 to (number of features +1 )
5)      hiddenU[i] ←0
6)      for j ←0 to (number of features +1 )
7)          hiddenU[i]← hiddenU[i]+  trainPattern[k][ j]*
    IH_Weights[j][i]
8)      end for
9)      hiddenU[i] ← tanh (hiddenU[i])
10) end for
11) predOut  ← 0
12) for i ←0 to (number of features +1 )
13)     predOut ← predOut + hiddenU[i]+ HO_Weights[i]
14) end for

15) /**calculate the error for the pattern k, step 16**/
16) Error_inPatternK= predOut  - actual [k]

17) /**update weights hidden-output, steps (18-21) **/
18) for i ←0 to (number of features +1 )
19)     delta = Error_inPatternK * hiddenU[i]
20)     HO_Weights[i] ← HO_Weights [i]- delta;
21) end for

22) /**update weights input-hidden, steps (23-31)**/
23) for i ← 0 to (number of features +1 )
24)     for j←0 to (number of features +1 )
25)         x←1-(hiddenU[i] * (hiddenU[i])
26)         x← x* HO_Weights [i] * Error_inPatternK
27)         x←x* trainPattern[k][ j]
28)         change ←x
29)         IH_Weights[j][i]= IH_Weights[j][i]-change
30)     end for
31) end for
```

Fig. 1. Pseudo-code for the proposed binary digit recognizer.

However, for the proposed approach, the network size depends on the number of features; thus, this approach gives a more concise network when the recognition task is extended to 0-9.

B. The Implemented MLP algorithm

The main steps of the algorithm in the training phase for the MLP network are as follows: given an input pattern X from the dataset, this value is forward propagated to the output of the MLP network, and is compared with the desired output; the error signal between the output of the network and the desired

response is then back propagated to the network, and adjustments are made on the synaptic weights. The same procedure is repeated for the next input vector until all the training patterns are passed through the neural network [22]-[24]. The pseudo-code for the implemented training MLP algorithm is provided in Fig. 1. It illustrates the main steps needed for propagating the input features and bias of a training pattern k as shown in [step lines 4-14]. Line 16 calculates the error in current pattern k. For updating the weight, we have two stages, namely updating the weights hidden-output as in steps 18-21, and updating the weights in the input to hidden layer interconnections, as in steps 23-31.

C. Experimental work

2-Feature Experiment: The first experiment was performed using only two features, namely, Feature 6 and Feature 14 for digits 0 and 1. That means, the number of inputs is two for the two features and one input for the bias. So, the number of inputs is three in total for each input pattern. Therefore, the size of the input training array is (number of input Patterns X 3). It is considered that only one hidden layer in both experiments. In the first experiment, the number of inputs is three (two inputs for Features + one for bias), i.e., three units in the hidden layer as shown in Fig. 2. For the input weight to hidden layer interconnection, it is a 2-D array of size equal to number of input patterns times 3. The output weights are presented as a 1-D array of size three. Finally, it is also assumed that they have only one unit at the output layer.

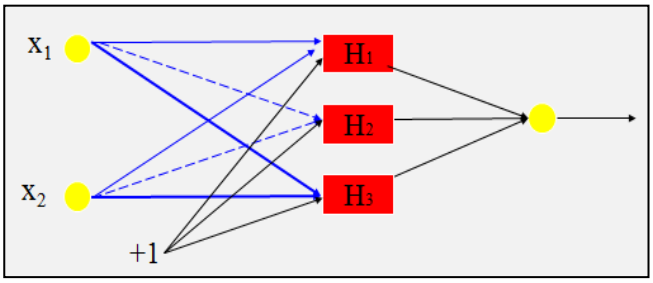

Fig. 2. MLP implemented structure for experiment 1.

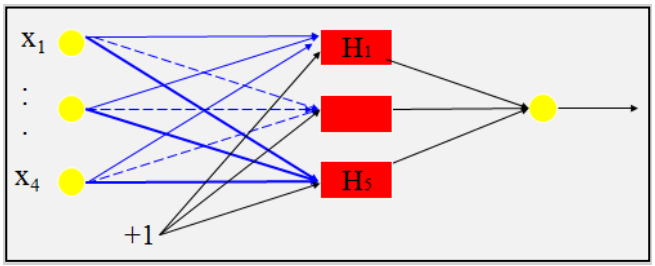

Fig. 3. MLP implemented structure for experiment 2.

4-Feature Experiment: For the second experiment, four features are used, namely, Feature 5, Feature 6, Feature 8 and Feature 14 for digits 0 and 1. Thus, the number of inputs is four for each feature and one input for the bias. So, five inputs in total can be seen for each input pattern. Therefore, the size of the input training array is equal to number of input patterns times 5. Five units in the hidden layer are used as illustrated in Fig. 3. The size of the input weight to hidden layer array is equal to number of input patterns times 5. The size of the output weight array is five. Similar to the first experiment, only one unit is used at the output layer.

IV. Summary and Discussion of Results

Fig. 4, 5 and TABLE. I summarize the results obtained through simulation of both the setups. In TABLE. I, the error levels are shown, when applying the proposed approach on the Pen-Based Recognition of Handwritten Digits dataset. The salient aspects that require analysis are the numbers of correctly/incorrectly classified instances.

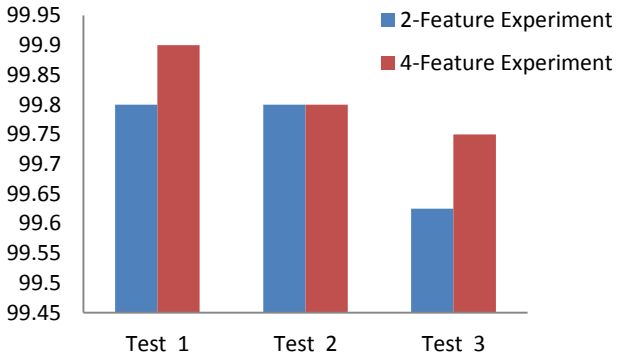

Fig. 4. Accuracy of the classifier for all the tested scenarios.

As shown on the obtained results, the implemented MLP performs better when four features are included instead of having just two features. In the case that the four features are included and the network is trained on the whole dataset and then tested again on the whole dataset, we got the highest identification rate of 99.9%. However, under the same test option, if two features are included, the percentage of correctly classified instances was around 99.8%.

In the second test option where the network is trained on half of the dataset and test on the other half, there is no clear difference between including four features or just having two, with the implementation yielding similar results for both cases. For the last test, test 3, including four features yields better performance than having just two features by merely 0.15%. It is important to highlight that the value of back propagation learning rate for all the tests was set as 0.7. Several other values for the learning rate were tried but because they yielded degraded performance; it is selected to be 0.7 as the optimal value for the conducted experiments.

TABLE. I. ACCURACY OF THE IMPLEMENTED MLP BASED ON THE FEATURE SIZES

Feature sizes	Experiment no.	Number of instances used for training	Number of instances used for testing	Correctly classified	Incorrectly classified	Accuracy%
With only two features F6 and F14	Experiment 1:Test 1	1000	1000 (same dataset used for training)	998	2	99.8
	Experiment 1: Test 2	500 (train in the first 500 instances)	500 (Test on the remaining ones)	499	1	99.8
	Experiment 1: Test 3	200 (train in the first 200 instances)	800 (Test on the remaining ones)	797	3	99.6
With four features F5,F6,F8 and F14	Experiment 2: Test 1	1000	1000 (same dataset used for training)	999	1	99.9
	Experiment 2: Test 2	500 (train in the first 500 instances)	500 (Test on the remaining ones)	499	1	99.8
	Experiment 2: Test 3	200 (train in the first 200 instances)	800 (Test on the remaining ones)	798	2	99.75

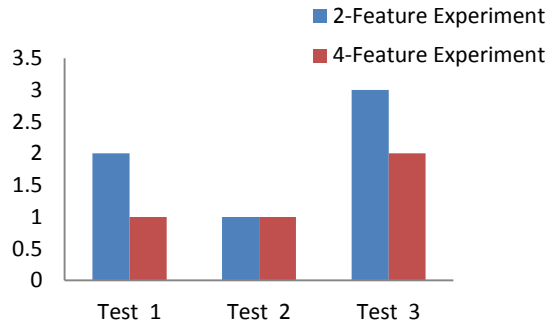

Fig. 5. Number of false classifications for the three tests and the two experiments.

V. CONCLUSIONS & FUTURE WORK

In this paper, an MLP-based approach for identifying human handwriting samples is proposed. The proposed scheme provides an inner setup of the neural network different from existing research work done in the recent past.

The approach is output-independent, and provides for a hidden layer neuron structure, which is dependent only on the input layer. Two sets of experiments were conducted for testing the effectiveness of the proposed technique. The first approach accepts only two features as inputs and the second includes four features as inputs. In addition, the first sets of experiments were conducted using two features only and training and testing repeated on the same dataset. The second set of experiments bifurcated the data set into two sets of size 500 each. Training was done on one half, with testing done on the other. From the experiments conducted above, it can be concluded that the MLP back-propagation technique based on output-independence is an excellent classifier for handwritten digit classification; furthermore, it is evident from the above results that selection of higher number of features gives more classification accuracy as opposed to using fewer features.

As part of future work, we plan to evaluate the performance of the proposed classification technique that is based on the MLP under other benchmarking datasets. In addition, we intend to study the effect of attribute selection and transfer function selection on the outcome of the classifier.

REFERENCES

[1] Akhtar, Muhammad Suhail, and Hammad A. Qureshi, "Handwritten digit recognition through wavelet decomposition and wavelet packet decomposition." Digital Information Management (ICDIM), 2013 Eighth International Conference on. IEEE, 2013.

[2] Niu, Xiao-Xiao, and Ching Y. Suen. "A novel hybrid CNN–SVM classifier for recognizing handwritten digits." Pattern Recognition 45.4 (2012): 1318-1325.

[3] Ali, Syed Salman, and Muhammad Usman Ghani. "Handwritten Digit Recognition using DCT and HMMs." Frontiers of Information Technology (FIT), 2014 12th International Conference on. IEEE, 2014.

[4] Jackson, J.E. (1991). A User's Guide to Principal Components (Wiley).

[5] Jollife, Ian. "Principal component analysis." New York: Springer-Verlag., 2002.

[6] Mohebi, Ehsan, and Adil Bagirov. "A convolutional recursive modified Self Organizing Map for handwritten digits recognition." Neural Networks 60 (2014): 104-118.

[7] Khatri, Sunil Kumar, Shivali Dutta, and Prashant Johri. "Recognizing images of handwritten digits using learning vector quantization artificial neural network." Reliability, Infocom Technologies and Optimization (ICRITO) (Trends and Future Directions), 2015 4th International Conference on. IEEE, 2015.

[8] Wu, J. (2012). "Advances in K-means clustering: a data mining thinking." Springer Science & Business Media..

[9] Khan, M. E. (2015). "K-means clustering."

[10] Juanying Xie, Shuai Jiang 2010, "A simple and fast algorithm for global K-means clustering", 2010 Second International Workshop on Education Technology and Computer Science,

[11] Decong Yu, Lihong, Ma. "Digit Recognition Based on Multi-features", IEEE Systems and Design Engineering Symposium, 2007.

[12] Ye Xu, Dezhan Liu: Clustering research of handwritten digit recognition by genetic algorithm. BIC-TA 2010: 291-297.

[13] Xu Ye, Zhang Wei, "On a Clustering Method for Handwritten Digit Recognition" Third International Conference on Intelligent Networks and Intelligent Systems 2010.

[14] Wierer, J., Boston, N., "A Handwritten Digit Recognition Algorithm using Two- Dimensional Hidden Markov Models for Feature Extraction," Acoustics, Speech and Signal Processing, 2007. ICASSP 2007. IEEE International Conference on, Volume 2, 15-20 April 2007 Page(s): II-505 - II-508.

[15] Rasul Enayatifar and Mehdi Alirezanejad 2011 "Off Line Handwriting Digit Recognition by Using Direction and Accumulation of Pixels" International Conference on Computer and Software Modeling IPCSIT vol.14 (2011) IACSIT Press, Singapore.

[16] Hao Yu, Tiantian Xie, Michael Hamilton, and Bogdan Wilamowski "Comparison of Different Neural Network Architectures for Digit Image Recognition" 4th Conference on Human System Interactions HSI-2011, Yokohama, Japan, May19-21, pp. 98-103, 2011

[17] Marzieh Moradi, Mohammad Ali Poormina, Farbod Razzazi: FPGA Implementation of Feature Extraction and MLP Neural Network Classifier for Farsi Handwritten Digit Recognition.EMS 2009: 231-234

[18] Abbas, Q.; Ahmad, J.; Bangyal, W.H., "Analysis of learning rate using BP algorithm for hand written digit recognition application" Information and Emerging Technologies (ICIET), 2010 International Conference on Communication, Networking & Broadcasting.

[19] Alpaydin, E., and Fevzi Alimoglu. "Pen-based recognition of handwritten digits data set." University of California, Irvine, Machine Learning Repository. Irvine: University of California (1998).

[20] Suebsing, Anirut, and Nualsawat Hiransakolwong. "A novel technique for feature subset selection based on cosine similarity." Applied Mathematical Sciences 6.133 (2012): 6627-6655. APA

[21] Ji Qian, Dongping Qian, Mengjie Zhang ―A Digit Recognition System for Paper Currency Identification Based on Virtual Instruments‖ IEEE Transactions, 1-4244-0555-6/06,2006

[22] Gurney, Kevin. "An introduction to neural networks." CRC press, 1997.

[23] Khan, Y., "Partial discharge pattern analysis using PCA and back-propagation artificial neural network for the estimation of size and position of metallic particle adhering to spacer in GIS." Electr. Eng. 98(1):29–42, 2016

[24] Lin, B. S., Wu, H. D., and Chen, S. J., "Automatic wheezing detection based on signal processing of spectrogram and back-propagation neural network." J. Healthcare Eng. 6(4):649–672, 2015.

Process Improvements for Crowdsourced Software Testing

Sultan Alyahya, Dalal Alrugebh
Information Systems Department
King Saud University, Riyadh, Saudi Arabia

***Abstract*—Crowdsourced software testing has been a common practice lately. It refers to the use of crowdsourcing in software testing activities. Although the crowd testing is a collaborative process by nature, there is no available research that provides a critical assessment of the key collaboration activities offered by the current crowdsourced testing platforms. In this paper, we review the process used in the crowd testing platforms including identifying the workflow used in managing the crowd testing process starting from submitting testing requirements and ending with reviewing testing report. Understanding the current process is then utilized to identify a set of limitations in the current process and has led to propose three process improvements (improving assigning crowd manager, improving building test team, monitoring testing progress). We have designed and implemented these process improvements and then evaluated them using two techniques: 1) questionnaire and 2) workshop. The questionnaire shows that the process improvements are significantly sound and strong enough to be added to crowd testing platforms. In addition, the evaluation through conducting a workshop was useful to assess the design and implementation of the process improvements. The participants were satisfied with them but asked for further modifications. Nevertheless, because crowd testing requires participation from a large number of people, the automation suggested improving managing the current process which was highly appreciated.**

Keywords*—Software testing; crowdsourcing, crowd testing; process improvement; tool

I. Introduction

In the last few years, a recent software testing strategy called crowdsourced testing has become a common practice and has been increasingly introduced into software development organizations. Crowdsourced testing refers to the use of crowdsourcing in software testing activities. It differs from the traditional approach; in this, testing is carried out by a larger number of testers from different places as crowd test team which can be consisted of professional testers, novice testers, real application users and subject matter experts, rather than by a limited number of in-house testing professionals [1].

According to Bruce Sterlings [2]: "*The best software is that which has been tested by thousands of users under thousands of different conditions, over the years*". This is almost impossible with the classical testing approach.

Crowdsourced testing has three main components [3]:

1) *The crowd testers*: the individuals who carry out the testing.

2) *The crowd seekers*: project owners who submit the projects for testing.

3) *An intermediation platform*: building a link between crowd testers and crowd seekers. This serves as a crowdsourcing enabler that allows customers to express their needs and individuals making up the crowd to respond to these needs.

There are many research papers that explore the use of crowdsourced testing platforms in the various types of testing such as usability testing [4], performance testing [5], GUI testing [6], etc.

However, although the crowd testing is a collaborative process by nature, there is no available research that provides a critical assessment of the key collaboration activities offered by the current crowdsourced testing platforms. Mao *et al*. [7] mention that the coordination and communication issue in the current platforms has not been explored yet. They state:

"both the resources and development process need to be coordinated. For example, geographically distributed and transient crowd workers need to reach a consistent understanding of the tasks required of them. Without coordination, it may be quite problematic".

In this paper, we will review the process used in the crowdsourced testing platforms including identifying the workflow used in managing the crowd testing process starting from submitting testing requirements and ending with reviewing testing report. Understanding the process used is the first step towards assessing the current platforms and then providing process improvements for them.

The remainder of this paper is organized as: Section II provides some background information about the crowdsourced testing and discusses the related work. Section III describes the current crowdsourced testing process. Observations on the current process are discussed in Section IV while process improvements are proposed in Section V and the evaluation is presented in Section VI. Their implementation is shown in Section VII and finally, the paper concludes in Section VIII.

II. Background and Related Work

A. Crowdsourced Software Testing

Crowdsourced software testing (also known as 'crowdsourced testing' and 'crowd testing') is to outsource testing activities to testers recruited from a large pool of individuals. It overcomes the limitations of the conventional

in-house testing that is restricted to the knowledge of a small set of solvers and thus is limited in terms of quality and efficiency [8].

Crowd testing is not a replacement for conventional testing, but a supplement solution done by people who are not directly involved in the project. They can be from different geographical and cultural backgrounds performing exploratory testing, identify defects, and provide user experience feedback.

Crowd testing is successfully implemented by using crowdsourcing platforms. These platforms play a key role in managing the process of crowd testing as will be clarified in Section III.

TABLE. I. CROWD SOURCED TESTING PLATFORMS

Application Name	Types of Tests Offered
Utest	• Functional • Security • Usability • Load • Localization
Crowdsourced Testing	• Functional • Usability • Localization
Pay4Bugs	• Functional • Localization
Mob4Hire	• Usability • Functional
99tests	• Functional • Security • Load • Automation
Passbrains	• Functional • Compatibility • Security • Localization • Usability
TestCloud	• Functional
Feedback Army	• Usability

uTest [9] claims to be the largest community for software testing. In addition to this one, the most discussed crowd testing platforms in the literature includes crowdsourced testing [10], Pay4bugs [11], Mobile4Hire [12], 99tests [13], Passbrains [14], TestCloud [15] and Feedback Army [16] (shutdown October 2016). Table 1 lists the types of testing offered by these platforms.

The role of each member in crowd testing platforms is described below:

1) *Crowd Testing Manager*: Crowd testing manager is a person who manages the community of the crowdsourced software testing, including building test teams and providing learning and engagement experiences for crowd testers.

2) *Test Team Leader*: Test team leader is responsible for the performance and management of a group of crowd testers in a given project and ensuring that the needs of the crowd seekers are met. The test team leader is also the escalation point for all bugs and technical fault.

3) *Crowd Testers*: Crowd testers are the heart line of crowdsourced software testing to execute testing activities. Crowd testers can be from different levels as well as from domain experts or potential users.

In current crowd testing platforms, each crowd tester has a profile with basic information and project preferences. The basic information is about crowd testers' demographic information and their experience with several testing types (functional, load, etc.), operating system, test automated tools and hardware [3].

4) *Crowd Seekers (Customer)*: Crowd seeker is the project owner who crowdsources the testing activities to the crowd.

B. Related Work

The use of crowdsourced testing has been studied with several types of testing activities, such as usability testing, performance testing and GUI testing.

With usability testing, the existing work attempts to evaluate the crowdsourced usability testing against the traditional approach in terms of its capability for detecting usability problems [4].

Musson *et al*. [5] demonstrate the value of using crowd testing to measure real-world performance and how it can mitigate the problem of finding various user behaviors and execution environments for testing software in various regions in the world.

Dlstra *et al*. [6] consider using crowd testing to make continuous GUI testing. They have described a method for crowdsourcing of GUI tests based on instantiating the system under test in virtual machines that are served by a geographically dispersed pool of workers.

The literature discussed above aim to evaluate the suitability of using crowdsource concept in testing activities. However, they do not consider making an assessment to the current crowdsourced testing process.

Furthermore, many research papers have focused on developing a theoretical basis for the crowdsourced software engineering in general. The authors in [17] propose Metropolis Model. They argue that the classical software development models (e.g. waterfall, agile models) are not suitable for Crowdsourced Software Engineering. Tsai *et al*. [18] summarized the commonalities in different Crowdsourced Software Engineering processes and proposed an architecture for cloud-based software crowdsourcing.

In addition to the fact that these papers do not concentrate on crowd testing in particular, they merely provide generic-level frameworks to use crowdsourcing in software engineering without any assessment of the process used in the current crowdsourcing platforms.

III. Current Crowd Sourced Testing Process

The platforms listed in Table 1 have been reviewed to understand the current process of crowd testing. The current crowd testing platforms share the same common workflow shown in Fig. 1. We considered making high granularity of analysis in order to provide a unified workflow that all the crowd testing platforms meet.

In order to provide a comprehensive review of the current platforms, we have used the following methods:

1) Registering and participating in the surveyed platforms (i.e. mainly as crowd testers).
2) Watching demos explaining the platforms' functionalities.
3) Reading the formal descriptions of the platforms.
4) Asking direct questions through relevant community boards.

The activities used in these platforms are described below:

a) *Submit the project*: The crowd seekers submit software project for testing and specify the business needs and goals clearly. At this stage, the crowd seeker needs to submit: the targeted software, required testing types, required operating system platforms and required testing automation tools.

b) *Review the submitted project by crowd manager*: The crowd manager reviews the project based on the requirements of the crowd seeker, crowd manager designs test plan that includes estimation of testing size, testing effort and testing cost.

c) *Announce the project*: After the crowd manager reviews the submitted project, an announcement will be sent to the crowd testers based on: their performance (i.e., quantity and quality of bugs they submit) and the frequency of participation in test cycles. In addition, there are many factors go into test cycle invitations such as the crowd's available hardware, software and geography location.

d) *Review project specification by crowd testers*: When crowd testers receive a test cycle invitation, they will have the option to either accept or decline the project opportunity. They must accept a test cycle to be able to report bugs and test cases. On the other hand, if they are not available for testing or perhaps they are not interested in a particular test cycle, they have the option to decline the invitation.

If the invitation is ignored, this will impact negatively on the crowd testers' rating. It is also important that crowd testers review all instructions and documentation before they start testing to avoid "out of scope" bugs, which can lower crowd testers' rating too.

e) *Build test team*: The crowd manger reviews the list of crowd testers interested to work in the test cycle. He verifies their information and makes sure they satisfy the required qualifications to participate.

The crowd manger recruits crowd testers based on matching customer requirements of hardware and software with crowdsourced testers' evaluation, available resources and demographic information.

After crowd testers are selected based on the review, they are then presented with the test cases associated with a particular test cycle. Under "Available Test Cases", crowd tester can view which test cases are available to claim based on testing environment and pre-determined rules set by the crowd seeker (e.g., specific number of testers per environment, specific number of pending test cases per tester).

f) *Assign crowd test team leader*: Test team leader is selected by crowd manager to work under the guidance of a crowd manager. For each test cycle, the leader recommends approval/rejection of incidents to increase the value of the final report (i.e., by improving the output and minimizing the noise level).

g) *Test the project*: In this activity, crowd testers start testing using the required types of devices, operating systems and software.

h) *Submit incident testing report*: It is the responsibility of the crowd tester to create an incident, link it to a corresponding script, and assign an initial severity and status.

The incidents are composed of the following:

i) Incident title and description of the issue.
ii) Actions and steps performed, numbered and clearly written, showing how the user arrived at the bug location.
iii) Environment information containing information, such as the operating system used browser and URL from where the bug is found.
iv) Attachments showing the issue either in picture or in video.

i) *Evaluate the incidents by crowd leader*: It is the responsibility of the crowd leader to review the severity of the incidents and modify status as incidents progress through the test cycle. The incidents may be pushed to one of two other states called "Pending Approval" or "Pending Rejection".

j) *Update crowd testers rating by crowd manager*: Based on incident reports evaluation, these reports may have a positive impact on crowd testers rating if the identified bugs are classified as "exceptionally valuable", "very valuable" or "somewhat valuable". On the other side, "rejected bugs" have a standard negative impact on crowd testers' rating.

k) *Prepare testing reports*: At this step, depending on the crowd seeker's feedback, the incidents may be moved into "Approved" or "Rejected". In addition, experience and lesson learned are documented and notifications are sent to close out any activities related to the project.

l) *Review final report*: Incidents exported, tester feedbacks, test summary and recommendations are handed to customer for final review.

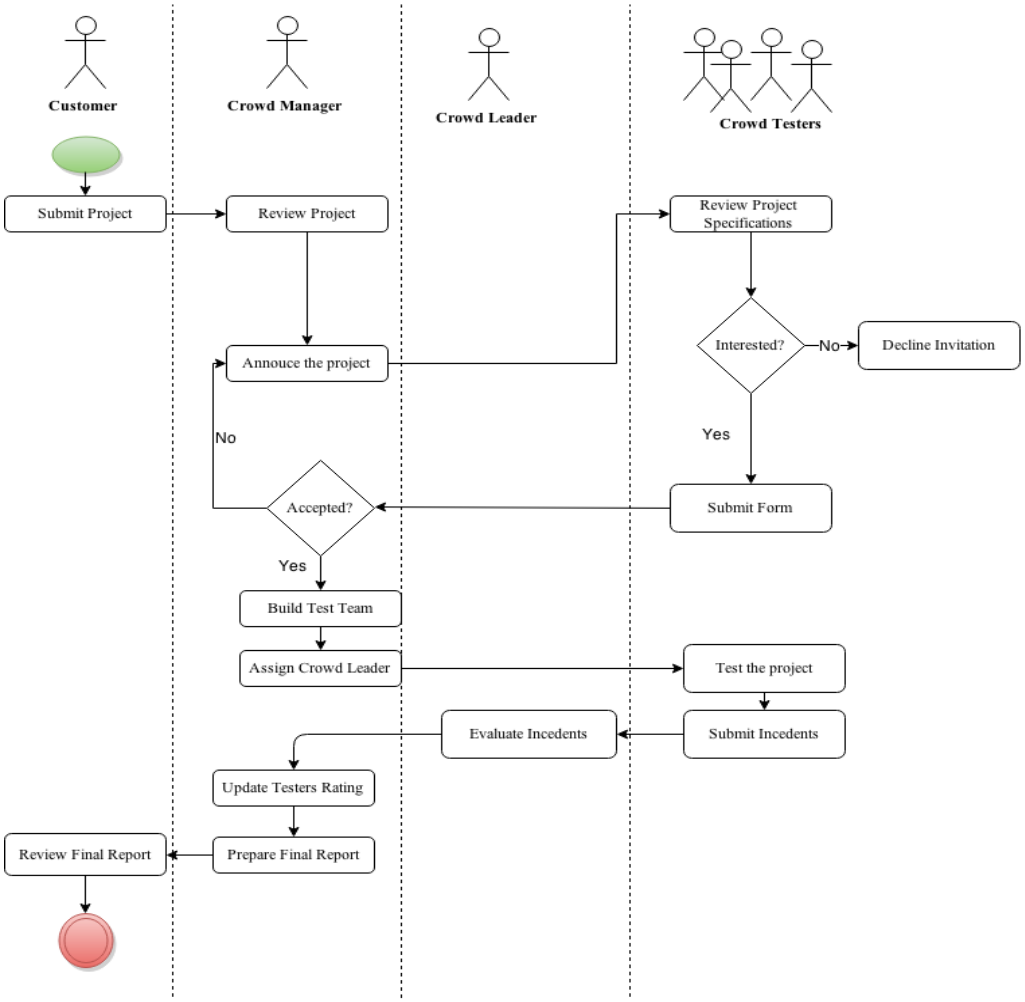

Fig. 1. Crowdsourced software testing workflow.

IV. Observations on the Current Process

The study of the current process used in crowdsourced testing reveals several observations that we believe can be source of weaknesses. These observations are:

1) Crowd mangers are assigned manually. In crowdsourced testing, it is common that multiple projects share the same crowd managers; hence, with the manual process used to assign crowd managers, the allocation can be inefficient (i.e., some crowd managers can overwork while others wait for new assignments).

2) Building the testing team is carried out manually. Reviewing the list of interested crowd testers and matching their capabilities with the test requirements are time consuming specially for large projects (i.e., some projects can receive hundreds of candidate participants).

3) There is a lack of mechanisms for monitoring the progress of crowd testers. They may accept to participate but then disappear or do not submit any test report.

V. Proposed Process Improvements

Based on the process observations listed in Section IV, we propose in this section a set of process improvements to be implemented in a crowdsourced testing computer application (CSTCA). These are listed below:

Process Improvement 1: Improving Assigning Crowd Manager

A resource allocation process is needed to allocate projects to the free crowd managers (or the least loaded). In our proposed process improvement, an automatic assignment of project crowd is offered based on their availability and preferences in testing types or testing environments. The most available one will be the primary crowd manager of a new project.

Fig. 2 presents the process of assigning crowd manager. After crowd seeker submits a software project with an estimate of the expected date of delivery, the system will send automatic notification to crowd managers based on testing requirements (e.g., testing type/environment). If a crowd manager accepts the project, they should provide an estimate about when they will be available to start testing the project. The system then assigns a crowd manager based on the best availability.

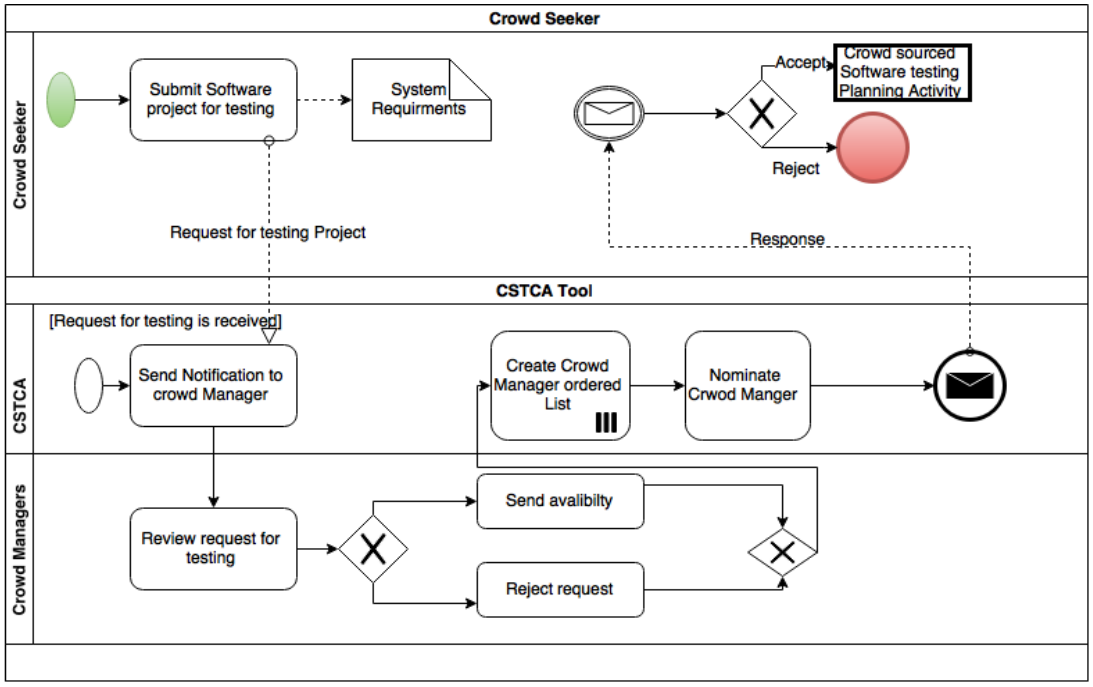

Fig. 2. The workflow of the proposed Process Improvement 1.

Process Improvement 2: Improving Building Test Team

To avoid the limitations of the manual building of a test team, the system will pick up the most relevant crowd testers automatically.

Fig. 3 presents this process improvement. The system announces the project for those who meet the project requirements. After crowd testers register for a project, the system will accept the maximum allowed number of crowd testers based on crowd testers' availability and rate.

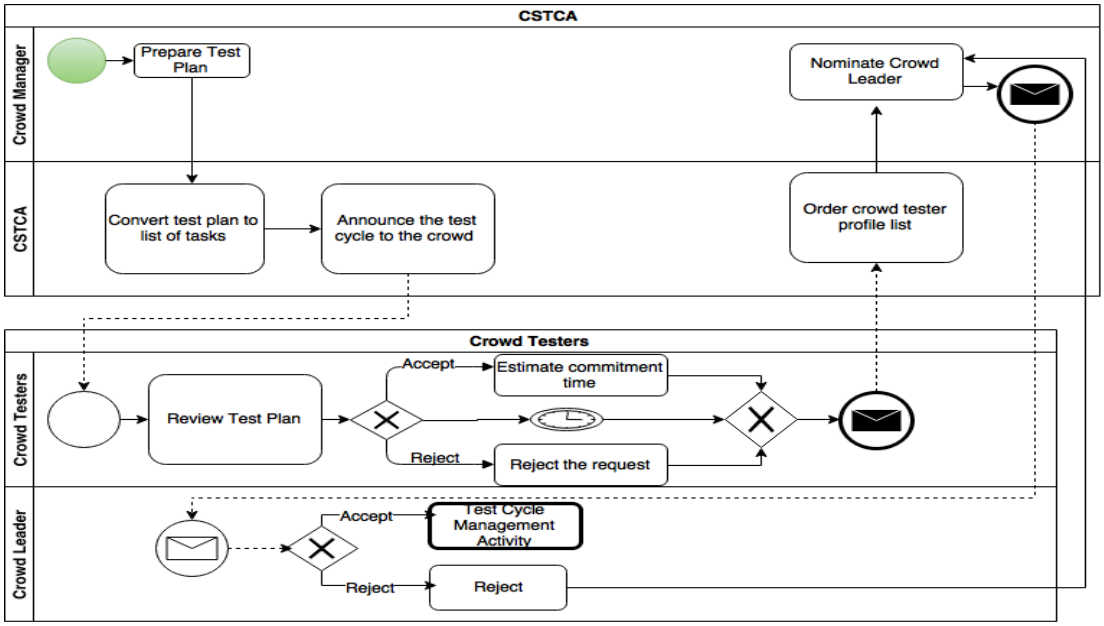

Fig. 3. The workflow of the proposed Process Improvement 2.

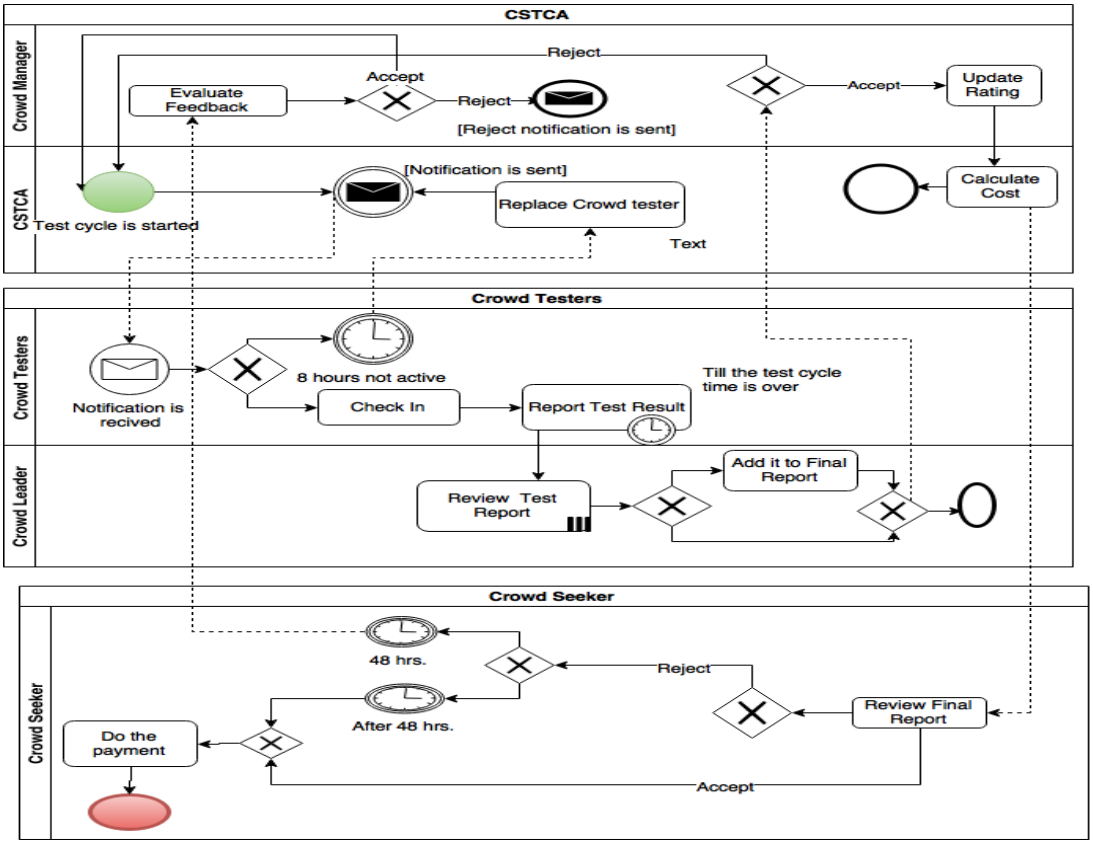

Fig. 4. The workflow of the proposed Process Improvement 3.

Process Improvement 3: Monitoring Testing Progress

To minimize the problem of having non-productive crowd testers, a process improvement is proposed to monitor the work of crowd testers and flag those who are not active.

Fig. 4 shows that if the crowd tester does not login or be active for a specific period of a work day (e.g., 8 hours), the system will exclude him and send invitation to other crowd testers.

The process can encourage crowd testers to accept a test cycle invitation only if they are willing to spend appropriate amount of time to accomplish the assigned test cases.

VI. IMPLEMENTATION

As a proof of concept, we have developed a research-based crowdsourced testing computer application (CSTCA).

CSTCA is designed as multi-layer architecture as shown in Fig. 5. The layers of the architecture are the Presentation Tier (i.e., User Interfaces), Domain Tier and Data Tier (i.e., Database).

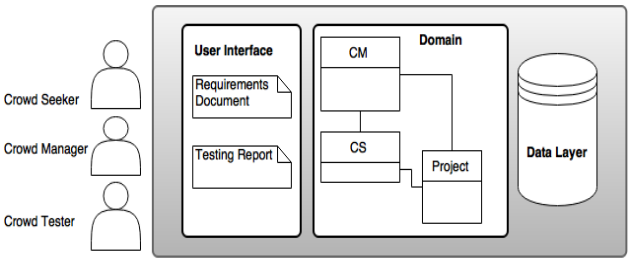

Fig. 5. The architecture of CSTCA.

For the sake of brevity, the implementation of the second process improvement (Improving Building Test Team) is only shown here. This process starts by preparing a test plan by a project plan. Fig. 6 shows the screen of preparing test plan. The test plan will include the estimation of minimum number of crowd testers should be participated in a test cycle with the start and end dates of the test cycle.

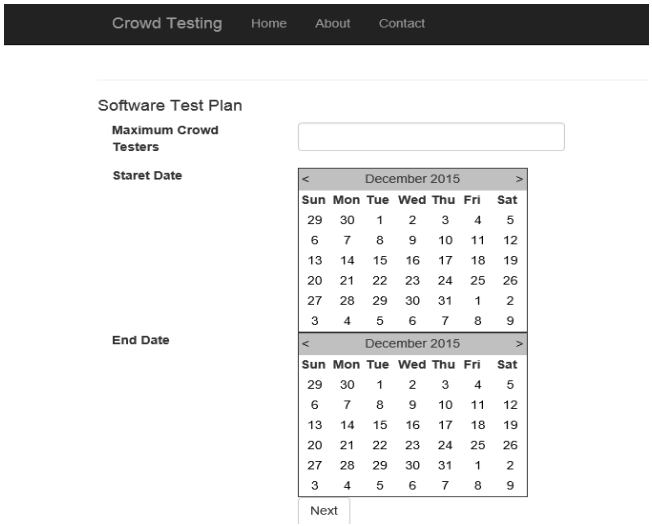

Fig. 6. Preparing the test plan.

The test plan includes a list of test cases to be performed by crowd testers. Fig. 7 shows the screen of adding test cases. The test case should include test case title, description, priority and number of minimum crowd testers needed.

Once the test cycle is created by crowd manger, notifications will be sent automatically to crowd testers based on their availability, rate and their preferences in testing types or testing environments.

The crowd testers have the option to accept or reject an invitation. If the invitation is accepted by a crowd tester, he will be asked to estimate the total number of hours he can spend in the test cycle as shown in Fig. 8.

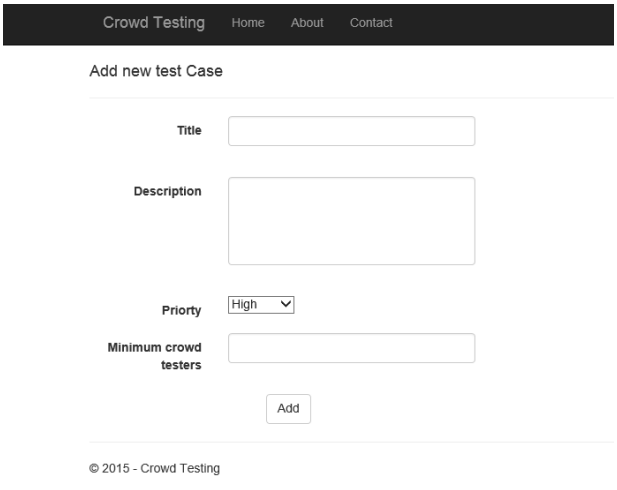

Fig. 7. Test case form.

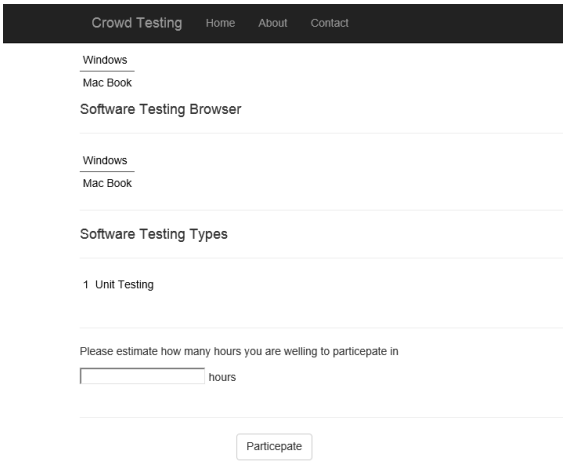

Fig. 8. Reviewing project details by crowd tester.

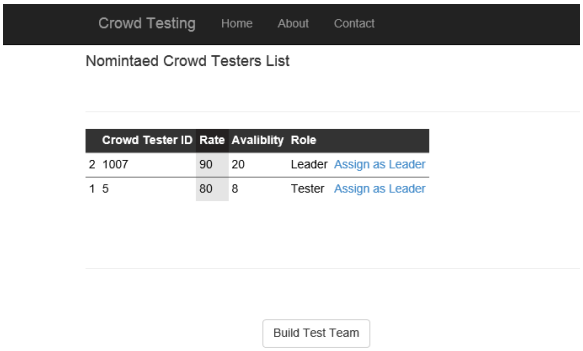

Fig. 9. Testing team is built.

The crowd manger will have the option to build test team by one click. The system will select the crowd testers based on their availability, rate and testing type preferences. The crowd leader will be assigned automatically based on his rate. To provide more flexibility, the crowd manger will have the option to change the crowd leader if needed as shown in Fig. 9.

VII. EVALUATION

This section details the evaluation of the proposed process improvements. A combination of questionnaire and workshop methods is used for the evaluation.

The main purpose of the questionnaire is to make sure that the identified process improvements are sound and strong enough to be added as part of the crowdsourced software testing process. Furthermore, the main purpose of the workshop is to go deeply inside the new processes and identify any limitations which can affect the applicability of them.

A. Questionnaire

Although it seems to us that there is some value in introducing the three suggested process improvements, we believe it is necessary to ask people who actually work in the problem domain about their opinions regarding the need for these process improvements.

We have selected twelve domain experts to answer a short questionnaire. It is taken into account that the selected people must have strong background about the domain of crowd testing. It also considered that they have diverse roles as shown in Fig. 10 (i.e., includes people with the roles: crowd seeker, crowd leader, crowd manager and crowd testers).

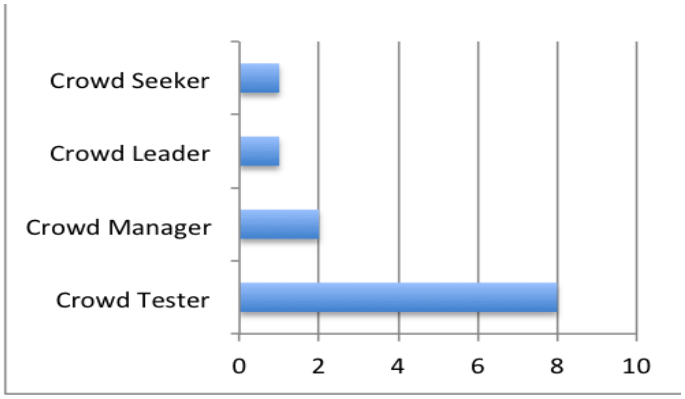

Fig. 10. Roles of the domain experts.

Feedback about Process Improvement 1:

We asked the domain experts to evaluate the need for improving the process of identifying the right crowd manager from their experience. The feedback is shown in Fig. 11. Two third of them agree that this improvement will be useful.

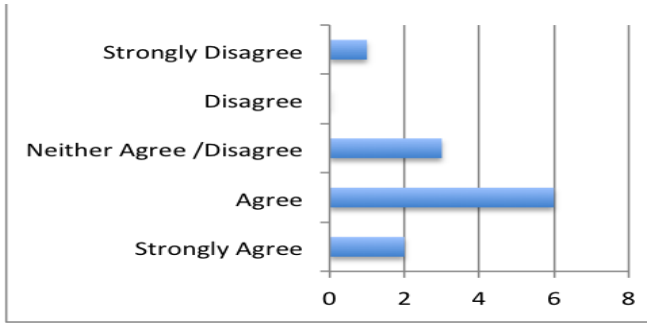

Fig. 11. Results of evaluating Process Improvement 1.

Feedback about Process Improvement 2:

The domain experts have evaluated the process of automating building test teams (Fig. 12). Ten out of twelve agree that this improvement will be useful.

Feedback about Process Improvement 3:

The idea of monitoring the testing process has also been evaluated by the domain experts as shown in Fig. 13. Again here, two third of them agree that this improvement will be useful.

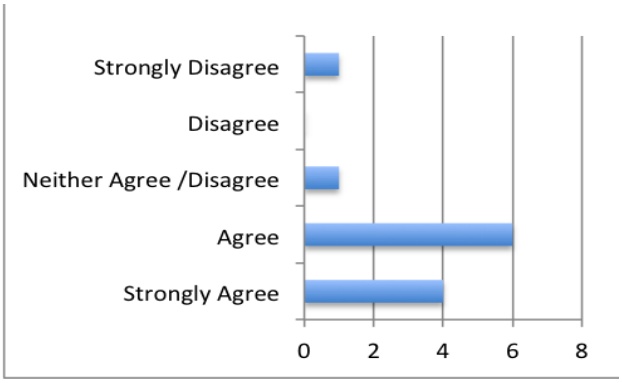

Fig. 12. Results of evaluating Process Improvement 2.

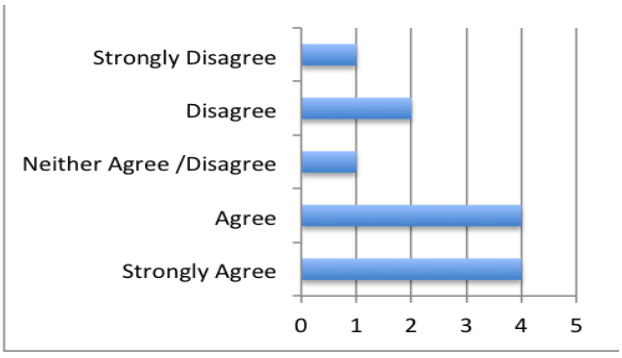

Fig. 13. Results of evaluating Process Improvement 3.

As we mentioned earlier, the purpose of the questionnaire is to have general view about the validity of the process improvements we suggested. It is clear from the results that the majority of the domain experts believe that the process improvements are useful. The results were encouraging for us to move to the stage of designing and implementing the proposed process improvements.

B. Workshop

Workshop Setup

A technical workshop is carried out to evaluate the design and implementation of the new process improvements. Two software process engineers and four domain experts have been invited for the workshop. They have been handed a handbook describing the process design and implementation in advance. The workshop is set to complete in one hour and a half so that each process improvement takes about half an hour. The room is equipped with a data show to provide live demo to the attendees.

Workshop Session

With each process improvement, the moderator has explained in details the proposed process workflow and displayed a demo about the corresponding feature. Afterwards, questions were received to make sure that the participants eliminate any ambiguity about the proposed process improvements. Then, the workshop discussion started. The theme of the discussion focus on three main questions directed to the participants:

1) What is your opinion about the design and

implementation provided to improve the process of assigning crowd manager?

2) What is your opinion about the design and implementation provided to improve the process of building test team?

3) What is your opinion about the design and implementation provided to improve the process of monitoring testing progress?

Workshop Findings

The workshop session was useful to assess the proposed process improvements. The participants believe that the modifications carried out will improve the current process of crowd testing. All the participants appreciate the automation part of the process improvement and they believe that it will add value to the crowd testing platforms. Examples of their words are:

"Rather than waiting for project managers to decide on which one should take the responsibility of a new project, why do not we set criteria for the selection and make that automatic … it speeds up the process."

"We send invitation to all testers, it takes time to filter the responses and decide who should be involved … automatic creation of test team can be great feature".

Furthermore, for the workflow of Process Improvement 1 (Fig. 2), the participants believe that, instead of asking project managers about their availability in the mid of the assignment process, it would be better that they register their availability in advance. This can shorten the assignment process.

In addition, with regard to the workflow of Process Improvement 2 (Fig. 3), the participants mentioned that it is necessary to avoid the full automation of creating a test team. They suggested that the project manager should review the names of the nominated crowd testers after it is automatically identified by the system. They believe that many human-based factors can determine the relationship between crowd managers and crowd testers especially if they have experience of working together in old projects (e.g., socio-cultural factors, trust, etc.) which can affect the success of the test project.

Finally, the participants stated that the third process improvement (Fig. 4) will solve the problem of having many testers accept test invitation but then disappear. However, they suggested relaxing the condition that judges whether a crowd tester is productive in a project or not. They argue that it is the crowd manager who should determine first the acceptable amount of time allowed before excluding a crowd tester; then the system can automate the exclusion task. They consider the length of project and the planned completion date of project as important factors in this matter.

VIII. CONCLUSIONS

This paper narrows the research gap regarding studying crowd testing process. It reviewed the current workflow used in crowd testing platforms and proposed three process improvements.

The questionnaire shows that the process improvements are significantly sound and strong enough to be added to crowd testing platforms. In addition, the evaluation through conducting a workshop was useful to assess the design and implementation of the process improvements. The participants were satisfied with them but asked for further modifications. Nevertheless, because crowd testing requires participation from large number of people, the automation suggested to improve managing the current process was highly appreciated.

This research focuses only on crowd testing. Future research will investigate examining the process of using crowdsourcing concept in other software engineering phases, such as requirements engineering.

REFERENCES

[1] D. Speidel and M. Sridharan, "A framework and research agenda for crowdsourced testing," 2013.

[2] B. Zajac, "The Hacker Crackdown," *Comput. Fraud* , vol. 1994, pp. 18–19, 1994.

[3] M. Sharma and R. Padmanaban, *Leveraging the Wisdom of the Crowd in Software Testing*. CRC Press, 2014.

[4] C. Schneider and T. Cheung, "The power of the crowd: Performing usability testing using an on-demand workforce," in *Information Systems Development*, Springer, 2013, pp. 551–560.

[5] R. Musson, J. Richards, D. Fisher, C. Bird, B. Bussone, and S. Ganguly, "Leveraging the crowd: How 48,000 users helped improve Lync performance," *IEEE Softw.*, vol. 30, no. 4, pp. 38–45, 2013.

[6] E. Dolstra, R. Vliegendhart, and J. Pouwelse, "Crowdsourcing GUI tests," in *Proceedings - IEEE 6th International Conference on Software Testing, Verification and Validation, ICST 2013*, 2013, pp. 332–341.

[7] K. Mao, L. Capra, M. Harman, and Y. Jia, "A Survey of the Use of Crowdsourcing in Software Engineering," *RN*, vol. 15, p. 1, 2015.

[8] S. Zogaj, U. Bretschneider, and J. M. Leimeister, "Managing crowdsourced software testing: a case study based insight on the challenges of a crowdsourcing intermediary," *J. Bus. Econ.*, vol. 84, no. 3, pp. 375–405, 2014.

[9] "uTest." [Online]. Available: https://www.utest.com/. [Accessed: 01-Dec-2016].

[10] "Crowdsourced Testing." [Online]. Available: https://crowdsourcedtesting.com. [Accessed: 01-Dec-2016].

[11] "Pay4bugs." [Online]. Available: https://www.pay4bugs.com/. [Accessed: 01-Dec-2016].

[12] "Mobile4Hire." [Online]. Available: http://www.mob4hire.com/. [Accessed: 01-Dec-2016].

[13] "99tests." [Online]. Available: https://99tests.com/. [Accessed: 01-Dec-2016].

[14] "Passbrains." [Online]. Available: https://www.passbrains.com/. [Accessed: 01-Dec-2016].

[15] "TestCloud." [Online]. Available: https://www.xamarin.com/test-cloud.

[16] "Feedback Army." [Online]. Available: http://feedbackarmy.com/. [Accessed: 01-Dec-2016].

[17] R. Kazman and H.-M. Chen, "The metropolis model a new logic for development of crowdsourced systems," *Commun. ACM*, vol. 52, no. 7, p. 76, 2009.

[18] W. T. Tsai, W. Wu, and M. N. Huhns, "Cloud-based software crowdsourcing," *IEEE Internet Computing*, vol. 18, no. 3. Institute of Electrical and Electronics Engineers Inc., pp. 78–83, 2014.

Glaucoma-Deep: Detection of Glaucoma Eye Disease on Retinal Fundus Images using Deep Learning

Detection of Glaucoma by Abbas Q

Qaisar Abbas
College of Computer and Information Sciences,
Al Imam Mohammad Ibn Saud Islamic University (IMSIU),
Riyadh 11432, Saudi Arabia

***Abstract*—Detection of glaucoma eye disease is still a challenging task for computer-aided diagnostics (CADx) systems. During eye screening process, the ophthalmologists measures the glaucoma by structure changes in optic disc (OD), loss of nerve fibres (LNF) and atrophy of the peripapillary region (APR). In retinal images, the automated CADx systems are developed to assess this eye disease through segmentation-based hand-crafted features. Therefore in this paper, the convolutional neural network (CNN) unsupervised architecture was used to extract the features through multilayer from raw pixel intensities. Afterwards, the deep-belief network (DBN) model was used to select the most discriminative deep features based on the annotated training dataset. At last, the final decision is performed by softmax linear classifier to differentiate between glaucoma and non-glaucoma retinal fundus image. This proposed system is known as Glaucoma-Deep and tested on 1200 retinal images obtained from publically and privately available datasets. To evaluate the performance of Glaucoma-Deep system, the sensitivity (SE), specificity (SP), accuracy (ACC), and precision (PRC) statistical measures were utilized. On average, the SE of 84.50%, SP of 98.01%, ACC of 99% and PRC of 84% values were achieved. Comparing to state-of-the-art systems, the Nodular-Deep system accomplished significant higher results. Consequently, the Glaucoma-Deep system can easily recognize the glaucoma eye disease to solve the problem of clinical experts during eye-screening process on large-scale environments.**

***Keywords*—Fundus imaging; glaucoma; diabetic retinopathy; deep learning; convolutional neural networks; deep belief network**

I. INTRODUCTION

Glaucoma is the main reason of visual disability across the world [1] and it has no cure. At an early stage, if it is not detected then it can definitely be the cause of permanent blindness. There are cures to prevent the vision loss if it is recognized at an early stage. Since, it is a salient chronic eye disease that develops permanent blindness. In recent years, the glaucoma is rapidly increasing even in urban regions. By the year of 2020 [2], it was estimated that it might be affected 79 million people in the world. Thus, it is important to do eye screening for detecting of glaucoma. The eye screening process is expected to tedious and time consuming task due to checkup of every individual patients, which is generally large.

For ophthalmologists to do better eye screening process, the computer-aided diagnostics systems (CADx) [3] are developed to provide a cost effective solution to the patients. As a result, the automated CADx screening systems have capability to reduce time and effort wasted on the analysis of glaucoma eye disease. It is also important to develop CADX systems using image analysis [4] for clinical experts to differentiate between normal and glaucoma retinal images because it is difficult for ophthalmologists to make this discrimination as shown in Fig. 1. As shown in this figure, the CUP boundary is affected due to glaucoma eye disease. This effect can be determined through the cup to disc ratio (CDR). According to the literature survey, the classification of retinal fundus images into normal and glaucomatous stages is a significance problem due to large population of screening.

There is another indicator for glaucoma eye disease that is known as peripapillary atrophy (PPA). In case of PPA affect, a change in intensity adjoining the disc boundary can be observed clearly. The Fig. 2 depicts the effect of PPA on glaucomatous retinal fundus region-of-interest (ROI) image. It can observe from this figure that the PPA appears as a variation in the disc boundary and similar to rim thinning.

(a) (b)

Fig. 1. An example of visually presented glaucoma: (a) normal retinal image, (b) glaucoma.

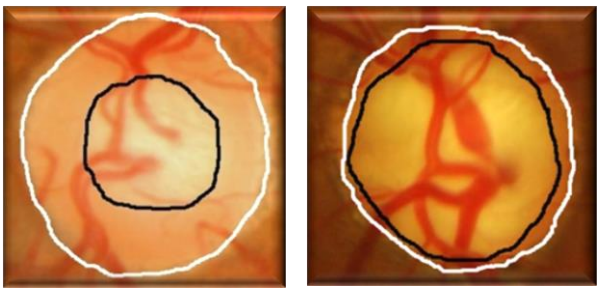

(a) (b)

Fig. 2. Sample of normal (a) fundus image and glaucomatous (b) OD region-of-interest (ROI) image showing the effect of rim dilution due to the glaucoma eye disease.

In the past studies, the authors presented a solution to automatic detect and classify glaucoma through the cup to disc ratio (CDR) and extraction of texture features. Accordingly, it is very difficult for the CADx system to segment the CUP and OD regions in a robust manner. To extract features, there is a need to segment the OD and CUP regions so it needs lots of image processing techniques. After defining image features, there is also need a domain-expert knowledge to select most discriminative features. Therefore, the detection of glaucoma is a challenging task for ophthalmologists and CADx systems.

In contrast to segmentation-based approaches, the authors detect glaucoma eye disease through image features around OD region. In those approaches, the authors pre-assumed that the morphological changes in OD caused by the disease, can be encoded using the statistical image features, so removing the need to accurately recognize cup and disc borders. Hence in this paper, a deep-learning base features were automatically extracted, selected and classified using a modern deep-learning classifiers without the need of understanding about domain-expert knowledge in image processing tasks.

The rest of the paper is organized as: In Section II, the related work is presented. In the next Section III, the utilize dataset and the propose methods are discussed in detail whereas in Section IV, the experiments are described to analyze the impact on detection performance. Finally, the paper is concluded in Section V.

II. Related Work

Glaucoma is detected through segmentation-based and features learning-based approaches. However in this paper, the features learning-based approaches are briefly described in the subsequent paragraphs. In particular, the modern deep-learning algorithms utilized in the past studies to automatically detect glaucoma eye disease are mentioned here.

In [5], the authors developed a convolutional neural network (CNN) architecture to automate the detection process of glaucoma. The CNN model is having multilayer architecture which belongs to the class of deep-learning algorithms. In that study, the authors make a clear differentiation between glaucoma and non-glaucoma patterns through hierarchical representation of features by CNN model. They used six multilayers of CNN model and divided into four convolutional layers along with two fully-connected layers. They performed experiments on ORIGA and SCES datasets and achieved 0.8321 and 0.887 of AUC values, respectively for detection of glaucoma eye disease. The authors reported that this developed system obtained accomplished better results compared to state-of-the-art systems. The smallest version of this paper [6] was also represented in conference.

Another version of deep-learning (DL) algorithm was developed in [7] to detect glaucoma eye diseased through the extraction of different features, such as 52 total deviation, mean deviation, and pattern standard deviation values. The authors utilized DL classifier such as a deep feed-forward neural network (FNN). However, the authors combined this DL classifier with other old machine learning classifiers such as random forests (RF), gradient boosting, support vector machine, and neural network (NN). Therefore, the authors presented deep ensemble solution for detecting of glaucoma disease. The authors reported that the 92.5% of AUC value was obtained through a deep FNN classifier.

There was another different approach presented in [8]. The authors utilized the structure of optic disc (OD) to analyze the glaucoma and other eye diseases such as retinal vein occlusion. The authors claimed that the OD is an essential to local the macula and main vascular arcade from retinal fundus images. In the past studies, the authors used OD properties and spatial relationship between OD and the main vascular arcade to diagnostic the eye disease. However in that paper, the authors used the structure of OD abnormalities and deep-learning algorithm to determine the glaucoma eye disease.

In [9], a novel algorithm was developed to detect glaucoma using support vector machine (SVM) instead of using advanced deep-learning algorithm along with hybrid feature set. The authors also detected color and texture features from retinal fundus images and some other properties of CDR of OD/CUP ratio to determine the severity-level of glaucoma eye disease. This developed approach was evaluated on 100 patients and they obtained the average sensitivity and specificity of are 100 and 87 %, respectively.

The authors developed an automatic solution for the detection of glaucoma by using features [10] learning through deep-learning algorithm on retinal fundus images. The authors utilized CNN model to learn the features with linear and nonlinear activation function. They used glaucoma and non-glaucoma patterns to differentiate for training of CNN model. They performed experiments on the ORIGA and SCES datasets and reported 0.838 and 0.898 of AUC values, respectively. In [11], the authors performed image processing techniques to automatic detection of glaucoma eye disease through ensemble machine learning classifiers. In that paper, the authors presented a system to segment optic disc, extract of texture feature in different color models and classified them by multilayer perceptron (MLP) model.

To improve OCT-based glaucoma diagnosis in [12], the authors used two ML learning algorithms, such as ANN and SVM with input on retinal nerve fiber layer thickness (RNFLT). In that study, the authors researched on 90 healthy persons and 62 glaucoma patients. It concluded that there was no statistically significant differences between ANNs and SVMs and reported the best ROCs for both ANN (0.982, 95% CI: 0.966–0.999) and VM (0.989, 95% CI: 0.979–1.0).

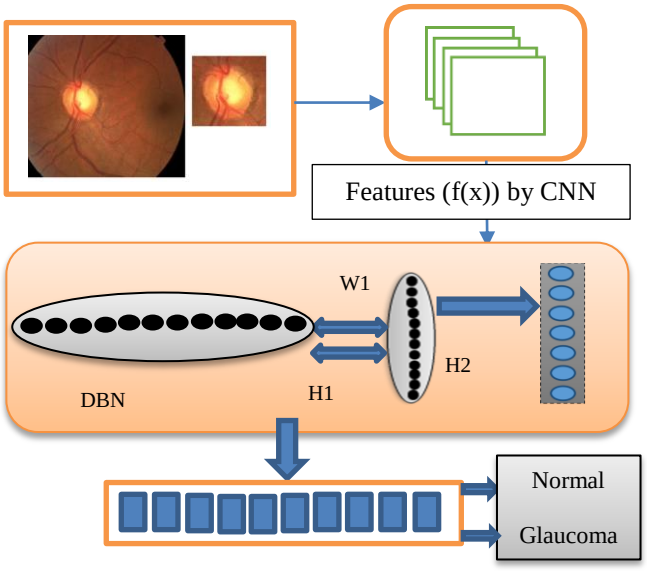

Fig. 3. Systematic flow diagram of proposed Glaucoma-Deep system tested on 1200 retinal fundus images.

TABLE I. SELECTED 1200 RETINAL FUNDUS IMAGES FOR DIAGNOSIS OF GLAUCOMA EYE DISEASES FROM DIFFERENT ONLINE AND PRIVATE SOURCES

No.	Glaucoma dataset		
	Dataset Name	***Normal***	***Glaucoma***
1	DRIONS-DB	50	60
2	sjchoi86-HRF	300	101
3	HRF-dataset	15	15
4	PRV-Glaucoma	235	424
Total		**600**	**600**

III. METHODOLOGY

The systematic flow diagram of proposed Glaucoma-Deep system is visually represented in Fig. 3. The Glaucoma-Deep system contains four main steps such as automatic detection of region=of-interest (ROI), extraction of deep features, optimization of features and classification phases. These steps are explained in detail in the upcoming subsections.

A. Acquisition of Glaucoma-datasets

To test and evaluate the Glaucoma-Deep system, the dataset of 1200 retinal fundus images (normal of 600 and glaucoma of 600) were acquired from different public and private resources. The information about these data sources is mentioned in Table 1. The first 110 images were collected from online web source named as DRIONS-DB [13]. In DRIONS-DB dataset, there were 110 fundus images that were belonging to the Ophthalmology Service at Miguel Servet Hospital, Saragossa (Spain). Each image size was 600 x 400 and 8 bits/pixel and the ground truth was provided by two medical experts in the form of papillary contour points. Another publicly available dataset sjchoi86-HRF (High Resolution Fundus) [14] was used to detect and diagnose Glaucoma eye disease.

The sjchoi86-HRF dataset was normal of 300 and glaucoma of 101 retinal fundus images. The HRF-dataset was also used to automatic diagnosis the glaucoma disorder [15]. In this study, the 15 retinal fundus images for each category are considered in both normal and glaucoma. Instead of publically available data sources, the private dataset of PRV-Glaucoma was also collected from a central hospital. The PRV-Glaucoma dataset was contained 235 normal and 424 glaucoma images.

A clinical expert was requested to make the difference between these two categories and validate and provide ground truth about the image level annotation as normal and confirm case of glaucoma.

B. Region-of-interest (ROI)

The color fundus images are acquired in the form of RGB image and the high intensity region-of-interest (ROI) image is extracted automatically from the green plane. This ROI region contains the OD and CUP regions. From each image, the ROI of size (300 x 300) pixels with radius 150 is utilized to extract deep features by using deep-learning algorithms.

C. Extraction of deep features

The best variants of deep-learning algorithms have many applications in practice such as in bioinformatics, computer vision and medical image processing. For example, the convolutional neural network (CNN) [16] is having the framework of deep-learning algorithm used to extract the pixel-level features in a multi-layer form that are defined automatically from an image. In the past few years, the CNN model achieved best performance compare to manually tune classification algorithms. Yet, there are still many properties of CNNs that researchers are determined to recognize.

In recent years, the CNNs model is used to understand the feature maps represented by an image. In deep-learning models, the CNNs is describing the best feature-map without manually defined domain-expert methodologies of image processing algorithms. The features defined by CNN model is known as deep-invariant features that are acquired from different layers also known as visual features. The output layer is responsible for generating the final features-map that can be used in the training process for classification tasks. However, the features-map generated by CNN model is not optimized. In particular, a pre-trained CNN model is having capability to extract features that are invariant and achieves better results compared to handcrafted features.

Accordingly, the CNN model is used to extract the deep invariant features from the segmented region-of-interest (ROI) of size (300 x 300) pixels and then generate a features-map in different layers. In these experiments, the dataset of 1200 ROIs is used and therefore, the CNN model generated the huge amount of features-vector that is further needed to optimize.

D. Optimization of deep features

These invariant features (IFs) that are extracted through convolutional neural network (CNN) deep-learning model are optimized through supervised deep-belief network (DBN) [17] deep-learning algorithm. The CNN algorithm is just used to describe the features in distributed fashion organize and then the DBN model is used to optimize the features for best

classification tasks. The DBN model is used to assist the final classification decision between normal and glaucoma eye disease on 1200 retinograph images.

For the optimization purposes, the three layers from deep belief nets (DBNs) are utilized along with step. In DBNs, the first layer is already trained from 40% ROI images contained normal and glaucoma category. On 1200 ROI images, the training of DBN is performed one layer at a time through learning the features that provided the bases for the upcoming layer and so on. In the DBNs model, there is also another fine-tuning step which is employed to improve the performance of features selection step. As shown in Fig. 3, there are many hidden (H1) layers of DBNs model that are stacked together to show a deep-neural network in a tree-like features representation of the training dataset.

E. Classification of deep features

For classification of deep and optimize features, the soft-max linear classifier is used to best describe the differentiation between normal and glaucoma ROI images. The softmax classifier is generally used to recognize the classes in deep-learning algorithms. The softmax linear classifier is used in this paper to find out the differentiation between these two classes.

IV. Experimental Results

The Glaucoma-Deep system was tested on a personal Laptop with an Intel core i7 CPU @ 3.35 GHz and 8 GB of random access memory (RAM). The Glaucoma-Deep program was implemented in MATLAB® 2016b and the results were also statistically calculated through MATLAB®.

The dataset of 1200 retinal fundus images including normal of 600 and glaucoma of 600 were acquired from different public and private resources to test and evaluate the performance of Glaucoma-Deep system. The information about these data sources is mentioned in Table 1. From 1200 retinal fundus images, the region-of-interest (ROI) was automatically segmented that serves as a feature extraction phase. The manual prediction was used to train and test the deep-learning classifiers that provided by an expert ophthalmologist as a ground truth. The proposed Glaucoma-Deep algorithm is compared to its corresponding ground truth images in two category problems, such as normal and glaucoma eye.

The statistical measures, such as sensitivity (SE), specificity (SP), accuracy (ACC) and precision (PRC) metrics were performed for achieving the numerical results. The performance of proposed Glaucoma-Deep algorithm is analyzed with the following parameters that are mathematically described in the following equations:

$$\text{Sensitivity (SE)} = TP/(TP+FN) \quad (1)$$

$$\text{Specificity (SP)} = TN/(TN+FP) \quad (2)$$

$$\text{Accuracy (ACC)} = (TP+TN)/(TP+FN+TN+FP) \quad (3)$$

$$\text{Precision (PRC)} = TP/(TP+FP) \quad (4)$$

These performance parameters are calculated on the 1200 ROIs retinal fundus images based on ground truth and the results obtained by Glaucoma-Deep system. The achieved results are listed in Table 2, where, TP denotes true positive, FP denotes false positive, FN is false negative and TN is true negative. True positive refers to the correctly identified normal and glaucoma ROI image. True negative refers to the wrongly identified normal and glaucoma classes. Whereas, false positive refers to the correctly identified classes and false negative refers to the wrongly identified classes. The entire Glaucoma-Deep algorithm was run on the 1200 retinal ROI images and results for normal and glaucoma categories were achieved. The results are reported in Table 2 based on 10-fold cross validation test and the dataset is divided into 40% for training and 60% for testing to check its viability in a large-scale environments.

Table 2 shows the performance comparisons of the proposed Glaucoma-Deep methodology in terms of sensitivity (SE), specificity (SP), accuracy (ACC) and precision (PRC) statistical measures. On average, the SE of 84.50%, SP of 98.01%, ACC of 99% and PRC of 84% values were achieved. As displayed in Table 2, the Glaucoma-Deep system obtained 85.17% of SE, 98.45% of SP, 99.00% of ACC and 82.01% of PRC in case of normal retinal eye. However, the Glaucoma-Deep system reported 83.50%, SP of 99.25%, ACC of 99.01% and 87.05% of PRC values in case of glaucoma eye disease. These results are comparable to state-of-the-art systems; the Nodular-Deep system is accomplished significant higher results. Consequently, the Glaucoma-Deep system can easily recognize the glaucoma eye disease to solve the problem of clinical experts during eye-screening process in a large-scale environment.

TABLE II. Results Obtained by Glaucoma-Deep System On the Selected 1200 Retinal Fundus Images For Diagnosis Of Glaucoma Eye Diseases

No.	Detection of Glaucoma eye disease				
	Category	***SE*** [a]	***SP*** [b]	***ACC*** [c]	***PRC*** [d]
1	Normal	85.17	98.45	99.00	82.01
2	Glaucoma	83.50	99.25	99.01	87.05
Average		**84.50%**	**98.01%**	**99%**	**84%**

[a] Sensitivity, [b] Specificity, [c] Accuracy and [d] Precision

TABLE III. Performance Comparision Results With State-of-the-Art Deep-Learning Methods for Diagnosis of Glaucoma Eye Diseases

Cited	Detection of Glaucoma eye disease		
	Methodologies	***Accuracy***	***Year***
[5]	CNN [a]	83.00%	2015
[7]	FFN [b]	92.00%	2016
[9]	SVM [c]	87.00%	2016
[11]	CNN [a]	90.00%	2016
Glaucoma-Deep (CNN, DBN [d], Softmax)		**99.0%**	**2017**

[a] Convolutional neural network, [b] Feed-forward neural network, [c] Support vector machine, [d] Deep-belief network

Table 3 reported the comparison results of state-of-the-art systems for classification of normal and glaucoma eye disease in the recent years. As displayed in this table, the proposed

Glaucoma-Deep system achieved higher statistical values compared to other four state-of-the-art computational methods for recognizing glaucoma eye disease. The reason behind is that the integration of CNN, DBN and softmax deep-learning classifiers can recognize the glaucoma without doing automatic or manual segmentation of OD and CUP area.

These experimental results indicate that the proposed Glaucoma-Deep system can be used to diagnosis glaucoma eye disease and assists the ophthalmologists to reduce the pressure of very large screening environment. The current studies focused on either local or global feature-based or segmentation of OD/CUP areas approaches. No current efforts have been made to integrate the deep-learning algorithms to combine the strengths of both the approaches. In this paper, the advanced form of automatic system is proposed to diagnose the glaucoma eye disease through deep-learning techniques.

The deep-learning based classification of glaucoma eye disease is provided best performance as reported in Table 2. In the previous approaches, the authors focused on segmenting and measuring the OD and CUP ratios. However in real, the segmentation of OD and CUP regions is a challenging task for automatic computerize system. Therefore, the deep-learning based methods may improve the performance of eye screening process and insist the ophthalmologists to correctly diagnosis the eye disease. The superior performance of this proposed the Glaucoma-Deep system which is achieved over CDR-based classification approaches, shows the importance of expanding the scope of analysis to multiple factors in glaucoma assessment.

V. CONCLUSIONS

In this paper, the advanced machine deep-learning algorithms are used to diagnose Glaucoma based on retinal fundus images without using segmentation-based hand-crafted features. To develop Glaucoma-Deep system, the convolutional neural network (CNN) unsupervised architecture is applied on 1200 images to extract the features through multilayer from raw pixel intensities. Afterwards, the deep-belief network (DBN) model is used to select most discriminative deep features based on the annotated training dataset. At last, the classification decision is performed by softmax linear classifier to differentiate between glaucoma and non-glaucoma images. To evaluate the performance of Glaucoma-Deep system, the sensitivity (SE), specificity (SP), accuracy (ACC), and precision (PRC) statistical measures were utilized. On average, the SE of 84.50%, SP of 98.01%, ACC of 99% and PRC of 84% values were achieved. Comparing to state-of-the-art systems, the Nodular-Deep system is accomplished significant higher results. Consequently, the Glaucoma-Deep system can easily recognize the glaucoma eye disease to solve the problem of clinical experts during eye-screening process in a large-scale environment.

Glaucoma-Deep system offers great promising results but still, there are certain areas open to do further research. In the future, the Glaucoma-Deep system will be tested on large-scale glaucoma-datasets to test its applicability in practice.

ACKNOWLEDGMENT

The author would like to thank an ophthalmologist to manually annotate the three regions and verified them from each retinograph images.

REFERENCES

[1] E. Dervisevic, S. Pavljasevic, A. Dervisevic, S.S. Kasumovic, “Challenges In Early Glaucoma Detection,” Med Arch., vol. 70, pp. 203–207, June 2016.

[2] R. Bock, J. Meier, L. G. Nyl, G. Michelson, “Glaucoma risk index: automated glaucoma detection from color fundus images,” Medical Image Analysis, vol. 14, pp. 471–481, 2010.

[3] J.E.W. Koh, U. Rajendra Acharya, Y. Hagiwara, U. Raghavendra, J. Hong Tan, S. Vinitha Sree et al, “Diagnosis of retinal health in digital fundus images using continuous wavelet transform (CWT) and entropies,” Computers in Biology and Medicine, vol. 84, pp. 89–97, May 2017.

[4] A. Anton, M. Fallon, F. Cots, M. A Sebastian, A. Morilla-Grasa et al., “Cost and Detection Rate of Glaucoma Screening with Imaging Devices in a Primary Care Center,” Clinical Ophthalmology, vol. 11, pp. 337–346, May 2017.

[5] X. Chen, Y. Xu, D. Wing Kee Wong, T. Yin Wong, J. Liu, “Glaucoma detection based on deep convolutional neural network,” IEEE Eng Med Biol Soc, pp. 715–718, Annual Conf., August 2015.

[6] X. Chen, Y. Xu, D. W. Kee Wong, T. Y. Wong and J. Liu, “Glaucoma detection based on deep convolutional neural network,” International Conference of the IEEE Engineering in Medicine and Biology Society (EMBC), Milan, pp. 715–718, 37th Annual Conference, 2015.

[7] R. Asaoka, H. Murata, A. Iwase, M. Araie, “Detecting Preperimetric Glaucoma with Standard Automated Perimetry Using a Deep Learning Classifier,” Ophthalmology, vol. 123, pp. 1974–1980, September 2016.

[8] H.S. Alghamdi, H.L. Tang, S.A. Waheeb, T. Peto, “Automatic Optic Disc Abnormality Detection in Fundus Images: A Deep Learning Approach,” OMIA3 (MICCAI 2016), pp. 10–17, Athens, October 2016.

[9] A. A. Salam, T. Khalil, M.U. Akram, A. Jameel and I. Basit, “Automated detection of glaucoma using structural and non structural features,” Springerplus, vol. 5, pp. 1–22, 2016.

[10] X. Chen, Y. Xu, S. Yan, D. Wong, T. Wong, and J. Liu, “Automatic Feature Learning for Glaucoma Detection Based on Deep Learning,” MICCAI (3), vol. 9351 of Lecture Notes in Computer Science, pp. 669–677, 2015.

[11] M. Claro, L. Santos, W. Silva Fl´avio Ara´ujo, N. Moura, “Automatic Glaucoma Detection Based on Optic Disc Segmentation and Texture Feature Extraction,” Clei Eletronic Journal, vol. 19, pp. 1–10, August 2016.

[12] D. Bizios, A. Heijl, J. Leth Hougaard and B. Bengtsson, “Machine learning classifiers for glaucoma diagnosis based on classification of retinal nerve fibre layer thickness parameters measured by Stratus OCT,” Acta Ophthalmologica, vol. 88, pp. 44–52, January 2010.

[13] E.J. Carmona, M. Rincón, J. García-Feijoo and J. M. Martínez-de-la-Casa, “Identification of the optic nerve head with genetic algorithms,” Artificial Intelligence in Medicine, vol. 43, pp. 243–259, 2008.

[14] sjchoi86-HRF dataset: https://github.com/sjchoi86/retina_dataset/tree/master/dataset. [Access date: 26/1/2017].

[15] High-Resolution Fundus (HRF) Image Database. https://www5.cs.fau.de/research/data/fundus-images/, [access date: 2/1/2016].

[16] G.W. Yang, and J. Hui-Fang, “Multiple Convolutional Neural Network for Feature Extraction,” International Conference on Intelligent Computing, pp. 104–114. Springer International Publishing, 2015.

[17] A. Qaisar, “DeepCAD: A Computer-Aided Diagnosis System for Mammographic Masses Using Deep Invariant Features,” Computers, vol.5,pp.1–15,2016.

GPC Temperature Control of A Simulation Model Infant-Incubator and Practice with Arduino Board

E. Feki
University of Tunis El Manar,
Faculty of Science,
UR17ES11 LAPER, 2092 Tunis,
Tunisia

M. A. Zermani
University of Tunis El Manar,
Faculty of Science,
UR17ES11 LAPER, 2092 Tunis,
Tunisia

A. Mami
University of Tunis El Manar,
Faculty of Science,
UR17ES11 LAPER, 2092 Tunis,
Tunisia

***Abstract*—The thermal environment surrounding preterm neonates in closed incubators is regulated via air temperature control mode. At present, these control modes do not take account of all the thermal parameters involved in a pattern of incubator such as the thermal parameters of preterm neonates (birth weight < 1000 grams). The objective of this work is to design and validate a generalized predictive control (GPC) that takes into account the closed incubator model as well as the newborn premature model. Then, we implemented this control law on a DRAGER neonatal incubator with and without newborn using microcontroller card. Methods: The design of the predictive control law is based on a prediction model. The developed model allows us to take into account all the thermal exchanges (radioactive, conductive, convective and evaporative) and the various interactions between the environment of the incubator and the premature newborn. Results: The predictive control law and the simulation model developed in Matlab/Simulink environment make it possible to evaluate the quality of the mode of control of the air temperature to which newborn must be raised. The results of the simulation and implementation of the air temperature inside the incubator (with newborn and without newborn) prove the feasibility and effectiveness of the proposed GPC controller compared with a proportional–integral–derivative controller (PID controller).**

***Keywords*—Incubator; neonatal; model; temperature; Arduino; GPC**

I. INTRODUCTION

For many years, incubators have been used to create a comfortable and healthful hygrothermal environment for neonates. Within this context, a neonatal incubator contributes to better newborns [1]. The newborn premature needs favourable conditions to ensure minimum energy expenditure as well as a safe temperature range; therefore the neonatal incubator is considered to be one device which will ensure a thermoneutral environment [2], [3]. In closed type incubators, the internal temperature can be completely controlled. This property decreases the neonate temperature variance due to large differences between the air and the skin temperature.

Most authors have limited their research to a mathematical model [3]-[5] useful for a computer simulation of the neonate-incubator system with classical controller (ON-OFF or PID); [6] developed a simulator of neonatal energy transfer to provide a convenient and precise comparison of sensible heat loss in the incubator. [7] describes the fundamental equations involved in the thermal exchange between infants and their environment. [8] has developed a theoretical model of infant incubator dynamic for the analysis of the factors that influence neonatal thermoregulation.

Reference [9] has developed a comprehensive mathematical model of the closed-loop newborn incubation system in a manner that takes into account all the exchange relations. This model is exploited to perform simulations by Matlab/Simulink. The PID controller is used to control the simulation model for each mode; air servo controlled and skin servo controlled.

Other authors have used the mathematical model of the infant-incubator with a more advanced controller (fuzzy logic or predictive) but without taking into account all of the interactions between a premature infant and an incubator. [10] has developed a fuzzy logic control which integrates two inputs (incubator air temperature and infant's skin temperature) to control the heating. The controller is tested on a mathematical simulation model of the neonatal incubator.

Reference [11] presents a theoretical modelling on the thermal behaviour of the premature infant (only the thermal exchanges of the incubator on the infant are considered). Air temperature and humidity, which play a prominent role in convective and evaporative exchanges, are calculated by a coupled transfer function. Additionally, a decoupling of the generalized predictive controller (DGPC) was proposed in order to obtain optimal thermal conditions for immature newborns.

The primary objective of this study is to develop a mathematical model used for a computer simulation that can predict the future temperature calculated continuously and design an appropriate controller to reduce heat loss by evaporation.

For this reason, two models have been developed and described. The first model is a physical model that takes into account all the interactions between the premature infant and the incubator. This model is based on physical and biological equations developed by the work of [8], [9], but modified according to the characteristics of the incubator used in the experiment (Drager 8000C). The main modification is to estimate a new mathematical model of the heating system using system identification method. Therefore the complete infant incubator system is subdivided into six homogeneous compartments: infant's core, infant's skin, incubator's heater,

incubator's wall, incubator's mattress, and incubator's environmental conditions. A computer simulation for each compartment of the system will be presented and developed using the Matlab/Simulink environment. These Simulink models are then interlocked via internal loops (called interactions), i.e., input and output data fully interlocked.

The second model, based on input-output measurements used in empirical and statistical approaches, will be useful for designing and simulating incubator environment controllers.

The climatic parameters of the neonatal incubator are temperature and humidity, but in this work, we limit ourselves only to the temperature in order to simplify the process. Therefore the incubator process becomes a SISO system (single input, single output). The input is the control signal applied to the heater and the output is air temperature inside the incubator. Its transfer function was identified using recursive identification methods. The validation of the model is performed with the comparison of the results to a series of clinical tests described in the medical literature [12].

Closed incubators that are used in intensive care are usually equipped with a conventional regulation (ON-OFF or PID) [13], [14]. These types of controllers still have little robust capability compared to adaptive controllers. The infant-incubator process encounters multiple challenges in the operating environment of the system, such as changing the physical model of the incubator as a result of interactions between the premature infant and its environment and also external disturbances [15], [16] due to the opening of the access door during a medical intervention. In addition, the disadvantage of the PID controller is finding the right parameters, compensating for the system's delay as well as making a stability study. Indeed, an essential question remains: is it possible to ensure an appropriate environment for prematurely born infants using an advanced control strategy, and maintain precisely the output temperature set by the doctor without significant variation over time, regardless of the disturbance?

Therefore, the objective of this study is to answer this question, using predictive control, so it is necessary to have a precise model for the system. The modelling consists in developing a set of equations in order to describe a phenomenon in a reproducible and stimulable way. The nonlinearities that exist in the system and which are represented as parametric uncertainty can be solved using adaptive control. Therefore, we designed and realized a control system based on a microcontroller (Arduino board).

The rest of the paper is organized as: first, the thermodynamic mathematical model of premature infants placed in an infant incubator will be developed; the aim of the proposed model is to develop and study the heat exchange relationships between the infant, its environment and the different compartments of the neonatal incubator. Secondly, applied feedback control systems using GPC control is described in order to control the infant's air temperature. The control of heating element is applied under the constraints of the air temperature and the power of the actuator. In addition, skin temperature and core temperature are monitored because the simulation of the model with MATLAB-Simulink allows us to see these parameters. Finally, an explanation of the incubator process containing the temperature control circuit is used to obtain a simulation and implementation results, and a comparative study between PID and GPC control was carried out in order to show the performance of each strategy.

II. Methodology of Model Development

In nursing care, the major concern in newborns after birth is to provide them with appropriate thermo-neutral environments, in order to ensure a body temperature within the normal range between 36.5° C and 37.5° C. This can only be realized when newborns are placed in thermoregulation devices, which are also called "infants warmers".

In this section, a spatially lumped mathematical model for an infant incubator will be developed. The laws of conservation of heat and mass will be used in order to obtain the physical model. As a result, the complete infant incubator system will be subdivided into six homogeneous compartments; the neonate core, skin, incubator air space, heater, wall, and mattress (Fig. 1).

Several assumptions were made in the development of the model. Each compartment was assumed to be homogeneous in all properties throughout its substance. All airflow fields in the incubator were assumed to be uniform. The baseline metabolic rate for each size infant was assumed to be that which enabled the infant to maintain his/her own body temperature while in a non-functional incubator.

The conduction of heat from the mattress to the incubator Q_{mat}, was assumed to be negligible. The model developed to describe the rate of change of temperature over time in each of these compartments. The model equations, based upon the law of conservation of energy, were:

$$\frac{dT_c}{dt} = \frac{Q_{met} - Q_{sen} - Q_{lat} - Q_{cd} - Q_{bc}}{M_c.C_{pc}} \quad (1)$$

$$\frac{dT_s}{dt} = \frac{Q_{cd} + Q_{bc} - Q_{mc} - Q_{scv} - Q_{se} - Q_{sr}}{M_s.C_{ps}} \quad (2)$$

$$\frac{dT_a}{dt} = \frac{Q_{scv} + Q_{se} + Q_{ht} + Q_{sen} + Q_{lat} - Q_{acv} - Q_{mat}}{M_a.C_{pa}} \quad (3)$$

$$\frac{dT_w}{dt} = \frac{Q_{acv} + Q_{sr} - Q_{cvo} - Q_{ro}}{M_w.C_{pw}} \quad (4)$$

$$\frac{dT_m}{dt} = \frac{Q_{mc} + Q_{mat} - Q_{ic}}{M_m.C_{pm}} \quad (5)$$

$$\frac{dT_{\square a}}{dt} = \frac{\theta}{C} \quad (6)$$

The differential operator D=d/dt is used, hence (1) can be written as follows:

$$T_c = \frac{Q_{met} - Q_{sen} - Q_{lat} - Q_{cd} - Q_{bc}}{M_c.C_{pc}.D} \quad (7)$$

Equation (7) describes the heat flow rate using the heat transfer relationships associated with the infant's body. Each one of the terms of energy rate (in watt) in this equation can be determined as follows. The core of the newborn body produces heat; its expression is:

$$Q_{met} = M_{rst} \times S_a \quad (8)$$

Concerning the tidal volume and the respiratory rate, we can determine the equations for respiration losses as follows:

$$Q_{sen} = IV \times m \times C_{pa} \times \rho_a \times (T_{ex} - T_a) \quad (9)$$

With: Q_{sen}, is the rate of sensible heat energy due to breathing.

$$Q_{lat} = IV \times m \times hfg \times \rho_a \times (\mathcal{W}_{ex} - \mathcal{W}_a) \quad (10)$$

With: Q_{lat}, is the latent heat energy by a newborn due to breathing.

In fact, the core loses heat by conduction through the skin layer. Therefore, the rate of conduction heat transfer between core and skin can be written as follows:

$$Q_{cd} = \frac{(T_c - T_s) \times K_c \times S_a}{\left({}^{m}/_{(\rho_c \times S_a)}\right)} \quad (11)$$

All parameters in (11) are defined in the nomenclature. The convective heat lost by the core blood circulation was determined as described in (12):

$$Q_{bc} = (T_c - T_s) \times \rho_{bl} \times bf \times C_{pb} \times V_{cb} \quad (12)$$

Q_{bc}, is the rate of convective heat transfer between core and skin via blood.

We adopt the differential operator D in (2), the infant's skin temperature can be written as:

$$T_s = \frac{Q_{cd} - Q_{bc} - Q_{mc} - Q_{scv} - Q_{se} - Q_{sr}}{M_s.C_{ps}.D} \quad (13)$$

Where, Q_{cd}, Q_{bc} are given in (11) and (12), respectively, while the rate of conductive heat loss from the skin in contact with the mattress Q_{mc} can be determined by:

$$Q_{mc} = A_s \times K_{mat} \times (T_s - T_m)/th_m \quad (14)$$

In addition, the difference in temperature between the skin and the airspace causes convective heat losses in the skin. This can be determined by:

$$Q_{scv} = h_{scv} \times A_{cv} \times (T_s - T_a) \quad (15)$$

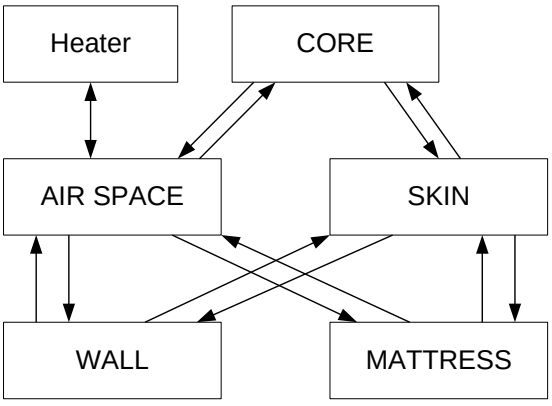

Fig. 1. The neonate-incubator system can be divided into six distinct homogeneous compartments.

The water loss from the skin to the air space through evaporation is inversely proportional to the ambient partial pressure of water vapour. The rate of evaporative heat transfer between skin and incubator air Q_{se} (in watt) can be determined by:

$$Q_{se} = \frac{hfg \times m \times E_{vap} \times \rho_{h2o}}{86400} \quad (16)$$

The skin also loses heat to the walls of the incubator by radiation. Thus, the rate of radiant heat losses can be determined by:

$$Q_{sr} = A_r \times \sigma \times \varepsilon_s \times [(T_s + 273.15)^4 - (T_\omega + 273.15)^4] \quad (17)$$

Using D-operator in (3), the temperature of the air space can be written as:

$$T_a = \frac{Q_{scv} + Q_{se} + Q_{\square t} + Q_{sen} + Q_{lat} - Q_{acv} - Q_{mat}}{M_a.C_{pa}.D} \quad (18)$$

The baby's skin Q_{scv} allows the airspace of the incubator to gain heat by convection.

Equation (15) is determined by this coefficient and also by the heating compartment Q_{ht} (rate of convective heat energy supplied to the hood).

Concerning the heater modelling, the process is assumed to be adiabatic (i.e., no heat losses) and air absorbed all the heat generated, the temperature of the heated air can be determined as follows:

$$Q_{\square t} = \dot{m}_a C_{pa} (T_{\square a} - T_a) \quad (19)$$

Where $\dot{m}_a$ is the mass flow rate of the incubator air, kg/sec.

Q_{se} is a vaporized energy that is caused by water loss from the skin that occurs through evaporation in the airspace. Q_{se} can be determined using (16).

It should be noted that the air compartment undergoes heat loss by convection through the walls of the incubator, this coefficient (Q_{acv}) being defined by the following relationship:

$$Q_{acv} = \square_{acv} A_{wi} (T_a - T_w) \quad (20)$$

Also, the mattress is heated convectively by air. Not the totality of the area of the mattress is the convective heated, therefore, the expression of the area not covered by the infant can be written as follows:

$$Q_{mat} = \square_{acv} A_{net} (T_a - T_m) \quad (21)$$

With Q_{mat} is the rate of convective heat transfer between incubator air and mattress.

Using D-operator in (4), the temperature of the wall is determined as follows:

$$T_w = \frac{Q_{acv} + Q_{sr} - Q_{cvo} - Q_{ro}}{M_w.C_{pw}.D} \quad (22)$$

The convective heat transfer coefficient between the walls of the incubator and the environment is determined as follows:

$$Q_{cvo} = \square_{cvo} A_{wi} (T_w - T_e) \quad (23)$$

Concerning energy loss from radiation, the heat transfer rate from the walls to the environments can be expressed as follows [17]:

$$Q_{ro} = A_{wi} \times \sigma \times \varepsilon_w \times [(T_w + 273.15)^4 - (T_e + 273.15)^4] \quad (24)$$

Using D-operator in (5), the mattress temperature T_m can be written as:

$$T_m = \frac{[Q_{mc} + Q_{mat} - Q_{ic}]}{M_m . C_{pm} . D} \quad (25)$$

Using equations (14) and (21), the energy rate Q_{mc} and Q_{mat} are then determined, and heat transfer rate from the mattress to the incubator Q_{ic} is assumed to be negligible.

Assume the temperature of the incubator before heat is transferred to be T_{ha}. The temperature of the incubator after heat is transferred to be T_{hai}.

Heat transferred to the incubator to be $dq = C dT_{ha}$

C = heat capacity.

By dividing both sides by dt:

$$\frac{dq}{dt} = \theta = C \frac{dT_{\square a}}{dt} \quad (26)$$

Equation (26) represents the rate of heat transfer inside the incubator. This rate is governed by a thermal resistance R. This follows a law similar to the law of Ohm:

$$\theta = \frac{(T_{\square ai} - T_{\square a})}{R} \quad (27)$$

Where, R is the thermal resistance in Kelvin per watt. Using 26 and 27 so we have:

$$C \frac{dT_{\square a}}{dt} = \frac{(T_{\square ai} - T_{\square a})}{R} \quad (28)$$

$$\frac{dT_{\square a}}{dt} = \frac{(T_{\square ai} - T_{\square a})}{C.R} \quad (29)$$

Where the time constant of the system is RC so we have:

$$\frac{dT_{\square a}}{dt} = \frac{(T_{\square ai} - T_{\square a})}{\tau} \quad (30)$$

Using the Laplace transform "p" we have:

$$p.T_{\square a} = \frac{(T_{\square ai} - T_{\square a})}{\tau} \quad (31)$$

$$T_{\square a}(\tau . p + 1) = T_{\square ai} \quad (32)$$

$$\frac{T_{\square a}}{T_{\square ai}}(p) = \frac{1}{(\tau . p + 1)} \quad (33)$$

The relationship between the applied voltage (U) and the temperature generated by an electrical heater is linear.

$$T_{\square ai} = K \times U \quad (34)$$

So we have:

$$\frac{T_{\square a}}{U}(p) = \frac{K}{(\tau p + 1)} \quad (35)$$

Where K is called the steady state gain and τ is called the time constant will be defined during the modelling of the heating element in Section V.

III. Implementation of Predictive Control

In this section, GPC will be well described for a single input-output process based on a CARIMA model.

The standard cost function used in GPC with constraints is expressed by (36).

$$J = \sum_{i=N_1}^{N_2} \delta(i)[\hat{y}(k+i) - w(k+i)]^2 + \sum_{i=1}^{N_u} [\lambda(i) \Delta u(k + i - 1)]^2 \quad (36)$$

Where, N_1 and N_2 are respectively the minimum and the maximum of the prediction horizon, N_u is the control horizon, $\hat{y}(\mathrm{k+i})$ is the prediction process output, $w(k+1)$ is the reference signal and $\Delta \mathrm{u(k+i-1)}$ is the sequence of the future control increments that have to be calculated.

Implicit constraints on Δu are placed between $\mathrm{N_u}$ and $\mathrm{N_2}$ as:

$$\Delta u(k + i - 1) = 0, \qquad N_u < i \leq N_2 \quad (37)$$

The parameters $\delta(i)$ and $\lambda(i)$ are weighting factors that affect the future behaviour of the controlled process [18]-[20].

A. Calculation of the Optimal Control

The aim of the predictive control is to calculate a sequence of future control increments $[\Delta u(k),\ \Delta u(k+1), \dots]$ so that the criterion (36) is minimized. To facilitate the calculation, it is necessary to transform the criterion (36) to a matrix form.

The form of the output of the prediction model is expressed as the sum of the free response y_0 and the forced response y_n.

$$\hat{y} = y_n + y_0 \quad (38)$$

The forced response is the multiplication of the Jacobian matrix of the model with the vector of the future control increment.

$$y_n = G \Delta u \quad (39)$$

Where,

$$\begin{bmatrix} g_1 & 0 & 0 & \dots & 0 \\ g_2 & g_1 & 0 & \dots & 0 \\ g_3 & g_2 & g_1 & \dots & 0 \\ \vdots & \vdots & \vdots & \ddots & \vdots \\ g_{N_2} & g_{N_2-1} & g_{N_2-2} & \dots & g_{N_2-N_u+1} \end{bmatrix} \quad (40)$$

The elements of this matrix are the values of the steps sequence.

Using (38) and (39) the predictor in a vector form is given by:

$$\hat{y} = G \Delta u + y_0 \quad (41)$$

The cost function (36) can be modified to the form below:

$$J = (\hat{y} - w)^T (\hat{y} - w) + \lambda \Delta u^T \Delta u = (G \Delta u + y_0 - w)^T (G \Delta u + y_0 - w) + \lambda \Delta u^{\mathrm{T}} \Delta u \quad (42)$$

Where, w is the trajectory to follow.

B. Computation of Predictor Second Order System with Time-Delay

The nominal model with d steps time-delay is considered as

$$F(z^{-1}) = \frac{B(z^{-1})}{A(z^{-1})} z^{-d} = \frac{b_1 z^{-1} + b_2 z^{-2}}{1 + a_1 z^{-1} + a_2 z^{-2}} z^{-d} \quad (43)$$

The model can be also written in the form

$$A(z^{-1})y(k) = z^{-d}B(z^{-1})u(k) \quad (44)$$

The CARIMA is the most used model in generalized predictive control that can be obtained from a nominal model given by the (43) by adding a disturbance model.

$$A(z^{-1})y(k) = z^{-d}B(z^{-1})u(k) + \frac{C(z^{-1})}{\Delta}n_c(k) \quad (45)$$

Where, d is the dead time and $n_c(k)$ is a non-measurable random disturbance that is assumed to have zero mean value and constant covariance and the operator delta is $1 - z^{-1}$. Inverted delta is then an integrator.

The polynomial $C(z^{-1})$ will be further considered as $C(z^{-1}) = 1$.

To compute the control action, we must determine the predictions of $d + 1$ to $d + N_2$. The output at time $(k + t)$ will be:

$$y(k+t) = \frac{B(z^{-1})}{A(z^{-1})}u(k+t-d-1) + \frac{C(z^{-1})}{A(z^{-1})\Delta(z^{-1})}n_c(k+t) \quad (46)$$

The Euclidean algorithm applied to the second term of (40) gives the following equation:

$$\frac{C(z^{-1})}{A(z^{-1})\Delta(z^{-1})} = L(z^{-1}) + z^{-1}\frac{H(z^{-1})}{A(z^{-1})\Delta(z^{-1})} \quad (47)$$

Using (40) and (41) we assume that the term related to the disturbance is zero, the optimal predictor of the output is written as follows:

$$\hat{y}(k+t) = \frac{L_t(z^{-1})B(z^{-1})\Delta(z^{-1})}{C(z^{-1})}u(k+t-d-1) + \frac{H(z^{-1})}{C(z^{-1})}y(k) \quad (48)$$

A second Diophantine equation decomposes the predictor in two terms: a first term based on the current output, old orders, the system output and a second term dependent on future orders.

$$\frac{\sigma(z^{-1})}{C(z^{-1})} = G_t(z^{-1}) + z^{-1+d}.\frac{R_t(z^{-1})}{C(z^{-1})} \quad (49)$$

With:

$$\sigma(z^{-1}) = L_t(z^{-1})B(z^{-1}) \quad (50)$$

The optimal predictor of the output is written as follows:

$$\hat{y}(k+t) = G_t(z^{-1})\Delta(z^{-1})u(k+t-d-1) + \frac{H(z^{-1})}{C(z^{-1})}y(k) + \frac{R_t(z^{-1})}{C(z^{-1})}\Delta(z^{-1})u(k-1) \quad (51)$$

Where: $G_t(z^{-1})$, $H(z^{-1})$, $R_t(z^{-1})$, and $L_t(z^{-1})$ are polynomial solutions to the Diophantine equations.

The matrix formulation is represented as follows:

$$\hat{y}(k) = \hat{G}\Delta u(k) + \frac{\hat{H}}{C(z^{-1})}y(k) + \frac{\hat{R}}{C(z^{-1})}\Delta u(k-1) \quad (52)$$

With:

$$y_n = \hat{G}\Delta u(k) \quad (53)$$

$$y_0 = \frac{\hat{H}}{C(z^{-1})}y(k) + \frac{\hat{R}}{C(z^{-1})}\Delta u(k-1) \quad (54)$$

The cost function (36) can be modified to the form below:

$$J = (\hat{y} - w)^T\delta(\hat{y} - w) + \lambda\Delta u^T\Delta u = (G\Delta u + y_0 - w)^T\delta(G\Delta u + y_0 - w) + \lambda\Delta u^T\Delta u \quad (55)$$

C. Constrained formulation

The amplitude of the control signal $u(k)$ is an important object for imposing constraint; we can be expressed by means of the following inequality:

$$u_{min} \le u \le u_{max} \quad (56)$$

Where, u_{min} and u_{max} are respectively the lower threshold and the upper threshold of the control.

The restrictions on the increase of the control signal take a very simple form and can be expressed by means of the inequality:

$$-\Delta u_{min} \le \Delta u \le \Delta u_{max} \quad (57)$$

Where, $\Delta u_{min}\ and\ \Delta u_{max}$ represent the lower and upper derivative threshold of the control inputs.

On the horizon controller N_u, can be written:

$$\begin{aligned} &-\Delta u_{min} \le \Delta u(k) \le \Delta u_{max} \quad (58)\\ &-\Delta u_{min} \le \Delta u(k+1) \le \Delta u_{max}\\ &\quad\vdots\\ &-\Delta u_{min} \le \Delta u(k+N_u-1) \le \Delta u_{max} \end{aligned}$$

Or in the condensed form:

$$\begin{bmatrix} I \\ -I \end{bmatrix}\Delta u \le \begin{bmatrix} b \\ -c \end{bmatrix} \quad (59)$$

With, I is identity matrix of dimension $(N_u \times N_u)$, and

$$b = [\Delta u_{max}\ \cdots\ \Delta u_{max}]^T \quad (60)$$

$$c = [\Delta u_{min}\ \cdots\ \Delta u_{min}]^T \quad (61)$$

$$\Delta u = [\Delta u(k) \cdots \Delta u(k+N_u-1)]^T \quad (62)$$

The vector of horizon control can be written according to the control constraints:

$$\begin{aligned} &u_{min} - u(k-1) \le \Delta u(k) \le u_{max} - u(k-1) \quad (63)\\ &u_{min} - u(k-1) \le \Delta u(k) + \Delta u(k+1) \le u_{max} - u(k-1)\\ &\quad\vdots\\ &u_{min} - u(k-1) \le \Delta u(k) + \cdots + \Delta u(k+N_u-1)\\ &\quad\le u_{max} - u(k-1) \end{aligned}$$

Or in the condensed form:

$$\begin{bmatrix} T \\ -T \end{bmatrix}\Delta u \ge \begin{bmatrix} -p \\ -h \end{bmatrix} \quad (64)$$

Where, T is a lower triangular matrix, dimension $(N_u \times N_u)$.

$$\text{And } p = \left[[u_{min} - u(k-1)] \cdots [u_{min} - u(k-1)]\right]^T \quad (65)$$

$$\text{And } h = \left[[u_{max} - u(k-1)] \cdots [u_{max} - u(k-1)]\right]^T \quad (66)$$

$$\text{And } \Delta u = [\Delta u(k) \cdots \Delta u(k+N_u-1)]^T \quad (67)$$

We can rewrite the two inequalities (59) and (64):

$$\begin{bmatrix} I \\ -I \\ T \\ -T \end{bmatrix}\Delta u \le \begin{bmatrix} -b \\ -c \\ p \\ -h \end{bmatrix} \quad (68)$$

$$\hat{y} = G\Delta u + y_0 \quad (69)$$

The problem of minimization of the criterion J with constraints is writing:

$$J = \frac{1}{2}\Delta u^T Q_2 \Delta u + Q_1^T \Delta u + Q_0 \quad (70)$$

With :

$$Q_2 = 2G^T G + \lambda I \quad (71)$$

$$Q_1^T = 2(y_0 - w)^T G \quad (72)$$

$$Q_0 = (y_0 - w)^T (y_0 - w) = const \quad (73)$$

The synthesis of the control law GPC consists in minimizing the criterion J. The latter cannot be performed by the analytical methods. To solve the problem of optimization of a quadratic criterion under constraints, we used the "fmincon" function of MATLAB.

IV. Incubator Process Description

In order to research issues related to incubators temperature and to test the results discussed in this paper, a neonatal incubator DRAGER 8000C from Maternal and Neonatal Unit of Rabta-Tunisia is described.

The main points related to such equipment are mentioned in this section. The pilot plant has these parts: a transparent cabinet (41.2cm height, 80.6cm length and 44cm width); a heater (400Watt), a fan is on all the time. The heater is modified to allow external control with a dimmer (infinitely variable control).

All infant incubators work on the same principle. A fan blows filtered ambient air over a heating element and a water container [21], but in our case, the water container of the incubator was emptied in order to control only the temperature.

The hardware realization of the temperature control circuit is proposed. Fig. 2 illustrates the diagram of the designed electrical circuits. The design consists mainly of a temperature sensor, an Arduino Uno board and a heating power module (dimmer with zero detectors). These parts are explained in more detail in the following paragraphs.

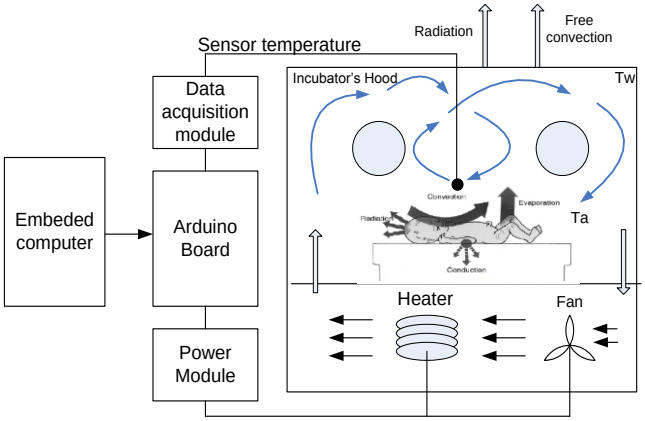

Fig. 2. Schematic of the incubator process with experimental arrangement.

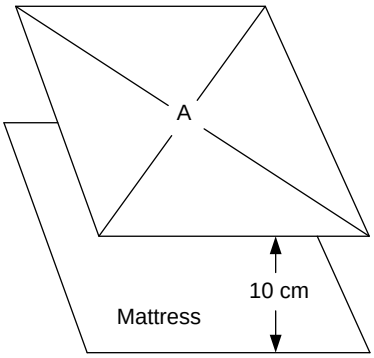

Fig. 3. Location of the point of measurement of the mattress in accordance with the standard NBR-IEC 601-2-19.

A. Temperature Sensing

The LM35DZ is a temperature sensor that delivers an output voltage linearly proportional to the Celsius temperature (+10 mV/°C). This sensor is selected because no further external calibration is required; its accuracy is ± 1/4 ° C. It operates at 4-30 V. In this experiment, the LM35DZ was connected to a 5V DC power supply. The temperature was considered an important parameter in neonatal incubators. This parameter was measured at point A, located 10 cm above the surface of the mattress with the same low horizontal position, as shown in Fig. 3 [22].

B. Arduino Board

The Arduino Uno is a microcontroller card based on the ATmega328. This card has 14 I/O pins (6 pins of which can be used as PWM outputs), 6 analogue input pins, 16 MHz ceramic resonator, USB connection, power socket, ICSP header and reset button [23], [24].

The Arduino board is selected to design the heat control circuit; it is able to acquire the temperature by means of the analogue input (for example the temperature inside the incubator Ta), also to vary the power of the control devices through a dimmer (for example the power of the heating system) in order to accomplish some real operations (e.g., temperature control of an incubator). The data acquisition module uses analogue inputs that operate at a 10-bit resolution, which provides a scale from 0 to 1023.

The ready structure of the Arduino is the most advantageous compared to the other card. This card is delivered in a complete package including a microcontroller, a 5V regulator, an oscillator, a serial communication interface and headers for connections. In addition, Arduino is easily connected to Matlab/Simulink which is a powerful tool to identify, model our process then, to synthesize the corrector or even to implement other more advanced control laws. The Arduino was programmed using the IDE software. The program allows the Arduino to perform the ambient environment regulation within the incubator through the dimmer control of the heating system.

C. Heater and control module

The heating system plays an important role in all closed incubators. This system compensates for any loss of

temperature. Generally, the heating system is an electrical resistance that converts electrical energy into heat. For our experiment, the heating system of the incubator is used but with another design of its control circuit [25].

This section presents a phase control method implemented on Arduino microcontroller to control power delivered to AC loads by using TRIAC.

Varying the root means square (rms) value of voltage supply results in varying of power delivered to the AC loads [26]. Varying the rms value of supply voltage could be done by using a TRIAC [27]. TRIAC is a bidirectional silicon controlled rectifier (SCR) or thyristor. Unlike SCR, TRIAC could conduct current in both directions which make them convenient to regulate the AC voltage. Fig. 4 shows TRIAC output voltage waveform.

The main circuit could be separated to two parts, zero-crossing detector and AC load driver circuit. The zero-crossing detector [28] is the upper part with an optocoupler, bridge rectifier, and two current limiting resistors.

The load rms voltage is same as the TRIAC's output rms voltage. The TRIAC's output rms voltage is related to delay angle, α [29] which is represented as:

$$V_{L(rms)} = V_s\sqrt{\frac{1}{\pi}\left[(\pi-\alpha)+\frac{sin2\alpha}{2}\right]} \quad (74)$$

Where, $V_{L(rms)}$ = TRIAC rms output voltage

V_s = Supply voltage

α = delay angle, in radian

According to Fig. 2, it is noted that the heater control is divided into several modules, which is presented in the following Fig. 5.

The lower part is the AC load driver constructed by the TRIAC, the MOC3021 optocoupler with the resistor (1kΩ). If the load is inductive (such as a motor) then the combined resistors-capacitors (RC) will be added to the circuit and connected in parallel to the TRIAC with a 39Ω resistor and a 0.01μF capacitor. The snubber circuit is excluded in Fig. 5 as a resistive load is used in this paper.

In the phase, control technique is implemented, and Arduino is programmed to fire the gate pulses to TRIAC for a number of microseconds. After a period of time the main supply voltage crosses zero. Therefore, a zero crossing detector (ZCD) is necessary to detect when the sinusoidal supply voltage goes through zero [29]. This could avoid the unpredictable time for TRIAC conducts or in other words, during what part of the sinusoidal wave the TRIAC is turn on and lead to the unpredictable power of loads. The pulses generated by the ZCD acts as interrupt signals to the Arduino microcontroller [30]. Arduino microcontroller is then firing a pulse to the TRIAC. By controlling the time delay between zero crossing point and firing gate pulses to TRIAC, the power delivered to the AC load is controlled smoothly and effectively.

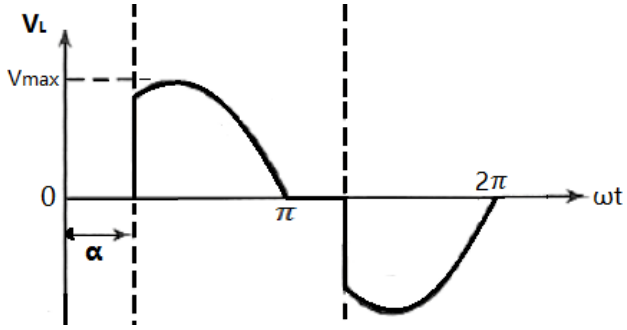

Fig. 4. TRIAC Output Voltage Waveform.

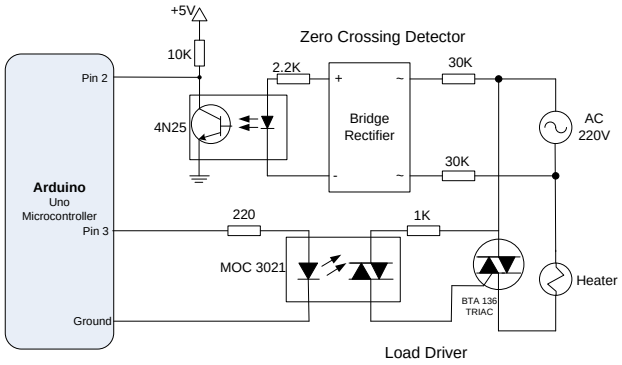

Fig. 5. Phase control technique circuit diagram.

To protect the Arduino microcontroller from being damaged by high voltage, an optocoupler MOC3021 is placed in between the microcontroller and TRIAC to isolate the high voltage side of loads and low voltage side of the Arduino microcontroller.

D. Arduino interfaces Matlab / Simulink

There are three ways to interface the Arduino board with Matlab/Simulink, namely:

1) Programming the Arduino Uno card as an interface card.

2) Using the ArduinoIO package.

3) Using the Arduino Target Package.

In this work, we use the first method. The solution uses the functions offered by the Arduino language which allows to send and to acquire binary data via the serial port (USB) and, on the other hand, to develop under Simulink a program to process or visualize those data.

The Arduino functions for this configuration are shown in Table 1.

TABLE. I. ARDUINO FUNCTIONS

Function name	Function description
available ()	Get the number of bits (characters) available to read from the serial port. These data are stored in the buffer that can back up 64 bit.
read ()	Allows reading of incoming bits on the serial port (data acquisition).
write ()	Allows the writing of the bits on the serial port (sends data)
attachInterrupt ( )	An interruption to detect zero crossing

TABLE. II. SIMULINK BLOCKS

Blocks name	Blocks description
Serial Configuration	Configuration of the serial port parameters
Serial Send	Sends binary data via the serial port
Serial Receive	Acquisition of binary data via the serial port
Temperature processing	This block treats the acquisition of the temperature by ensuring the conversion of the received voltage to a temperature
Control processing	This block processes the data sent by the corrector by ensuring the conversion of (0-100%) into unit8 (0-128)

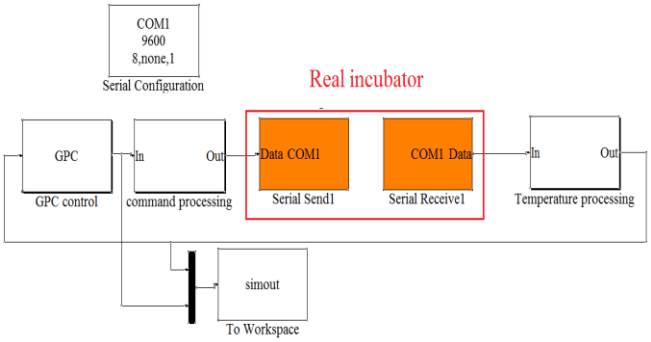

Fig. 6. Simulink model of real-time temperature control.

The Simulink blocks used to process or visualize those data are shown in Table 2.

The Arduino card handles communication with the real process and Simulink. In Simulink, we implemented the feedback loop containing the corrector and the temperature processing from the sensor. The block diagram, corresponding to the operation of the acquisition and temperature control chain, developed under Simulink is represented by Fig. 6.

V. RESULTS

A. Heating element modelling

The heating model of the incubator is considered as an input-output box. This model has, respectively, the electrical power of the radiator and the temperature in the heater as input-output variables. Knowing that the system can be modelled as a causal, linear and time invariant system, the model can be expressed as a transfer function given by (35).

The mathematical model was determined by applying an input of step type $U = 100\%$ to the input of the system, which presents the maximum control power provided. The functional diagram, corresponding to the operation of the acquisition chain and to the thermal treatment of the heating resistor, developed under Simulink is represented by Fig. 7.

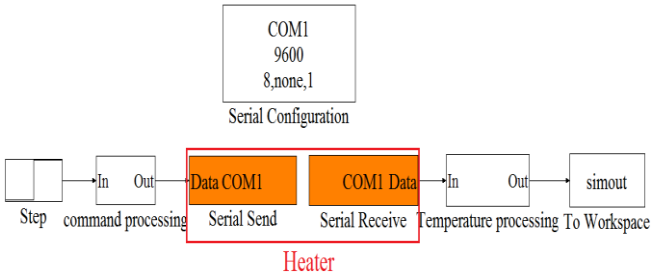

Fig. 7. Simulink blocks for the acquisition and treatment of the heater temperature.

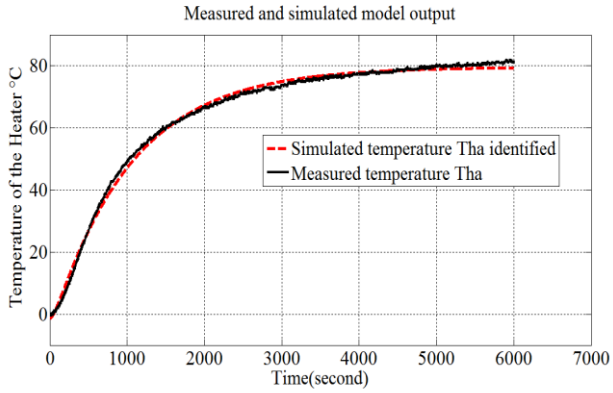

Fig. 8. Real and estimated heater temperature.

The results of this test are shown in Fig. 8. After determining the response of the system, the determination of the transfer function is made using System Identification Tool.

$$\frac{T_{ha}}{U}(p) = \frac{0.8077}{(1127.3p+1)} \quad (75)$$

To validate the obtained model, we compare it with the actual measurement carried out as shown in Fig. 8.

B. Model of the incubator subsystem with newborn

The newborn incubator consists essentially of 6 compartments in total, as shown in Fig. 9.

A Simulink open-loop model is developed as shown in Fig. 10. This developed model includes the six compartments mentioned in the previous section (Method) with a single input power U and a single controlled output Ta.

Knowing that the newborn input indicates the presence of premature and H% indicates the humidity in (%), in our case, it is equal to 80%.

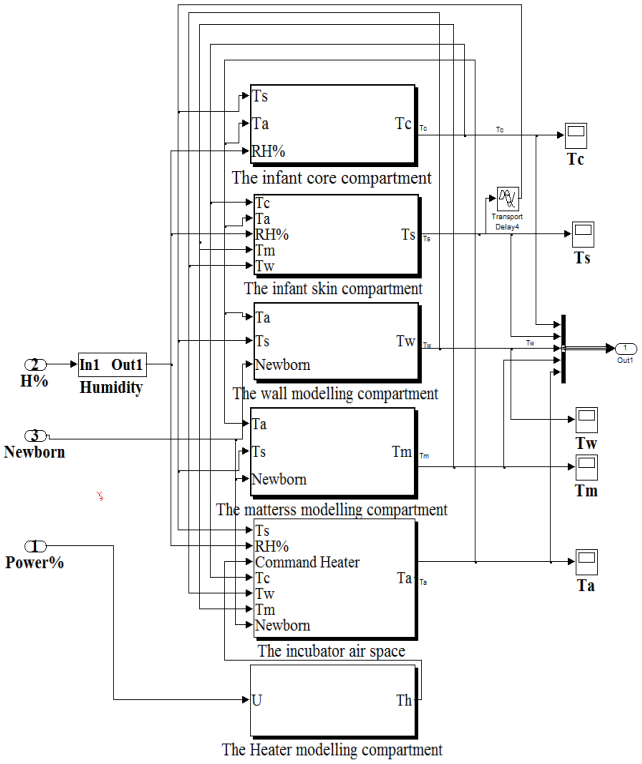

Fig. 9. Combined system compartments.

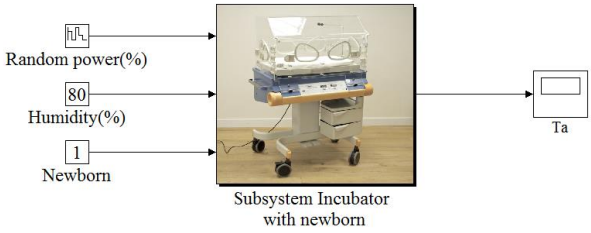

Fig. 10. Open loop infant-incubator system.

If it is assumed that in the operating region of the system is considered as linear and invariant in time, it can, therefore, be expressed as a transfer function. To linearize the Simulink model and to convert it into a transfer function, we applied a random input signal type step to the heater zones, which covers the entire range of control as shown in Fig. 11. After determining the response of the system, the determination of the transfer function is made using System Identification Tool. The process model with transfer function is:

$$Hc(p) = \frac{T_a}{U}(p) = Kp\frac{1+Tz*p}{1+2*Zeta*w*p+(w*p)^2}e^{(-Td*p)} \quad (76)$$

With: $Kp = 0.21378,\ w = 434.56,\ Zeta = 1.5511,\ Td = 30, Tz = -50.432$

The results of combining the baby and incubator measured showed good agreement with the simulated model as shown in Fig. 12.

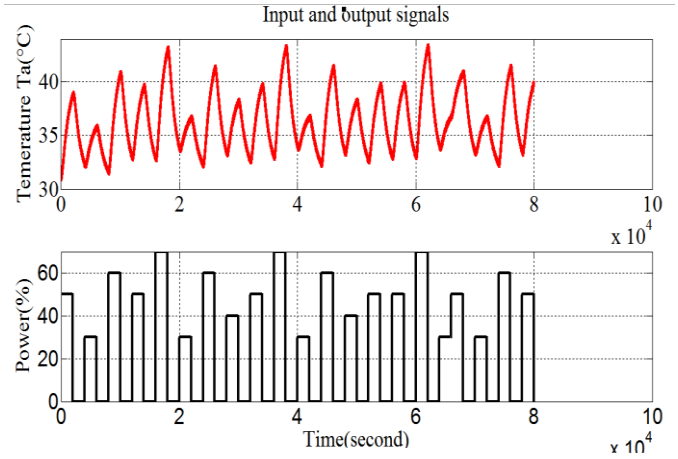

Fig. 11. Input and output signals.

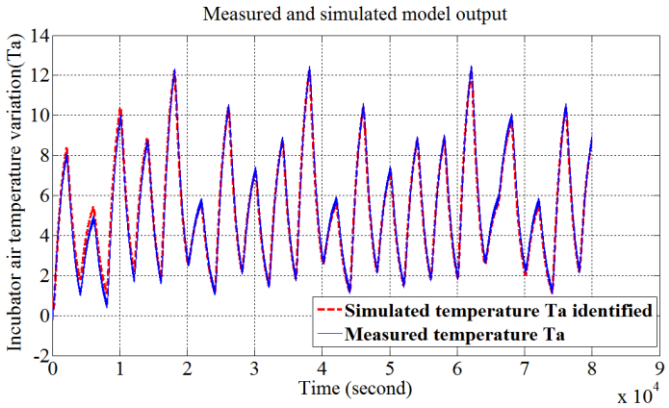

Fig. 12. Measured and estimated air temperature.

Systems controlled by digital controllers are always inherently physical systems. On the other hand, generalized predictive control is often used with a discrete prediction model used to perform predictions in a discrete manner with a sampling period Te. In order to establish the discretization, we exploited the $c2d$ function of Matlab which makes it possible to obtain the discrete equivalent of a continuous transfer function with the integration method as an argument:

$$Hd = c2d(Hc, 20, 'zoh')$$

The discrete transfer function Hd is:

$$Hd(z) = \frac{-0.0004957z^2+0.0003543z+0.0005633}{z^2-1.865z+0.867} \quad (77)$$

C. GPC and PID control with and without newborn

Having established the model of the incubator with a newborn, we focused our efforts on the more detailed description and critical assessment of the controlled incubator system. In order to verify the improved performance of the proposed approach (GPC) compared to PID control, the main parameters are presented in Table 3.

TABLE. III. GPC AND PID PARAMETERS

Control/Parameter	P	I	D	N_2	N_u	λ
GPC	-	-	-	12	1	0.1
PID	10	0.005	0	-	-	-

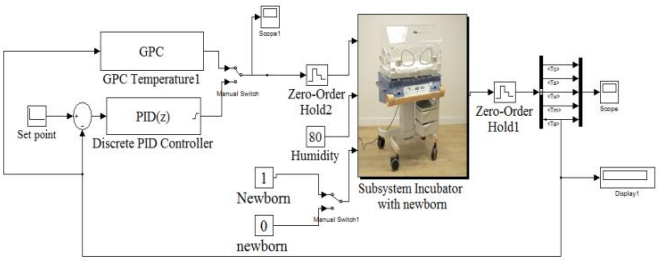

Fig. 13. Closed loop infant-incubator system.

The diagram of the simulation is shown in Fig. 13. This is a closed loop system whose elements of the direct chain are the two controllers GPC, PID and the child incubator system.

The input energy varies between 0-100% equivalent to 0 and 400 Watt. The set point is 37°C. A manual switch is used to switch at will according to the regulation mode requested GPC or PID with or without a baby.

To find the optimal parameters of the PID controller, we tested various parameters using the Matlab/Simulink toolbox, and the best parameters were used. $Kp = 10$, $Ki = 0.005$, and $Kd = 0$, which can be deduced from the results.

For GPC, taking into account the sampling period and the time constant, the prediction horizons were set to $N_2 = 12$.

The reasonable choice of the control horizon N_u that provides a compromise between the degree of stability and system performance must be less than N_2. In our case and based on the simulation results we have set $N_u = 1$. In addition, the choice of the weighting factor of the control increments is based on [31] $\lambda = 0.2422$.

The GPC and PID controllers have been applied and implemented to the closed incubator system with and without a newborn. The aims objective of this works is to evaluate the quality of the mode of control of the air temperature to which newborn must be raised. To validate the control system, we set the simulation time at 22 hours, whose air temperature begins at 27°C and the set point is set at 37°C. Also we introduced a perturbation to the system. This perturbation is modelled as five hours opening of the incubator ports.

In the first experiment, the incubator without the baby model was used to simulate the system using PID and GPC air control. Then we keep the same parameters of each controller and we reproduce the same experiment but with an incubator occupied by a baby.

It can be deduced from the results illustrated in Fig. 14 that the GPC has a fast transient response. Also, the robustness of this strategy can be illustrated through the low overshoot and the high efficiency of fluctuation rejection. This is not the case of PID control that gave an undesirable transient response in terms of low steady state error, short rise time, short settling time and low overshoot.

When the 5 hours opening of the incubator ports was simulated, time recovery for the air temperature was 2 minutes with GPC control and 5 minutes with PID.

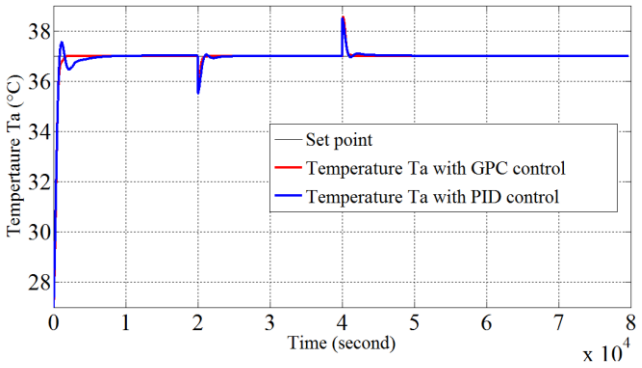

Fig. 14. Close loop step response of air temperature with GPC and PID control without premature.

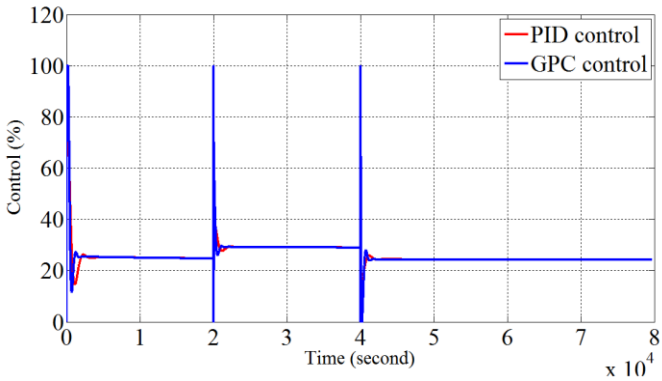

Fig. 15. Step response – Heater power closed-loop with GPC and PID control without premature.

Fig. 15 shows the evolution of the control signal of GPC and PID. These signals represent the oscillation of the heater power between 0–100 (%).

In the case without a baby, all heat flows related to the baby in the global model are cancelled. Initial conditions related to the child correspond to those of a preterm infant with a gestation period of 28 weeks and a rectal temperature (skin) of 35.5°C.

After determining the best parameters for each controller without baby mode, we now proceed to the global simulation of the child-incubator system and proceed to the presentation of the results. In baby mode, the manual switch is closed so that the GPC or PID controller is in the direct chain and the second manual switch that indicates the presence of the baby is closed.

In this case, all heat flows related to the baby in the global model are cancelled. Initial conditions related to the child correspond to those of a preterm infant with a gestation period of 28 weeks and a rectal temperature (skin) of 35.5°C.

The control of the air temperature gives the result in Fig. 16. After 1100 seconds GPC respects the set point (37°C) when PID respects the same set point after 5000 seconds.

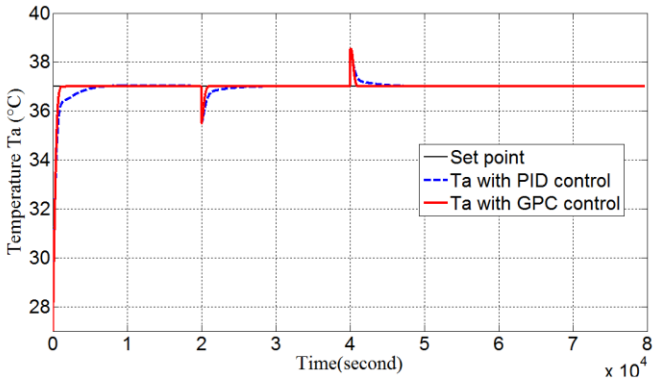

Fig. 16. Close loop step response of air temperature with GPC and PID control with premature.

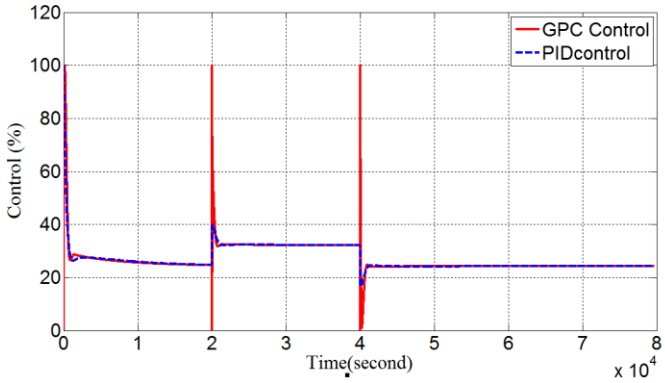

Fig. 17. Step response – Heater power closed-loop with GPC and PID control with premature.

The step response of the input signals of PID and GPC control that flows to the infant incubator system is demonstrated in Fig. 17. These signals represent the oscillation of the heater power between 0–100 (%) upon the variation of the output temperature inside the incubator.

Fig. 18 shows the results of the simulation of the skin temperature and the core temperature, respectively. The initial skin and core temperature are 35°C. It grows to achieve good stability and reaches respectively 36.5 and 37 °C after 8 hours. The variation in core temperature of the preterm infant respectively with PID and GPC control air temperature. The core body temperature downs to around 34.7°C, which is lower than the initial value and it increases rapidly again to 37°C. This core body temperature is comparable with the mean of empirical clinical results reported for the preterm newborn with gestational age 29 ±2 weeks and birth weight <1000 grams.

Similarly, with respect to the core temperature as shown in Fig. 18, the variation of the temperature of the skin of the premature infant is illustrated respectively with the regulation of the air temperature GPC and PID. The skin temperature decreases to around 34.3°C and rises promptly to reach 36.6°C.

In addition, in GPC control, the rise time of the infant's core and skin temperature is more than the rise time with PID control (Fig. 18), which shows that there is a very smooth rise in core and skin temperature before it reaches the steady value. During the interval [2000s, 4000s] sampled, the hand ports incubator was opened and the internal temperature initially dropped then recovered the optimal value.

The margin of temperature between the core and the skin of newborn varies from 0.1° C to 0.4° C. This is comparable with the results obtained in simulations presented in Fig. 18. In our case, the margin between the skin and core temperature is 0.3°C. Consequently, it may be considered that the performance of the global model including the air servo control is satisfactory.

Where, T_r is the rise time, T_p is peak time, T_{st} is the settling time, and M_p is the overshoot.

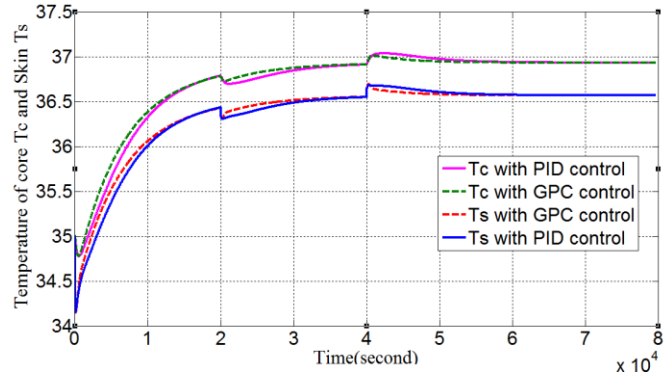

Fig. 18. Infant skin and core temperature variation with GPC and PID control.

TABLE. IV. RESULT OF TEST

Control/Parameter	T_r (sec)	T_p (sec)	T_{st}(sec)	M_p (%)
GPC without premature	760	-	1260	-
PID without premature	720	1140	3440	5,6
GPC with premature	660	-	990	-
PID with premature	920	-	3900	-

It can be deduced from Table 4 that the regulation of the neonatal incubator to the desired temperature in the shortest possible time with minimum or no overshoot, short rise time, small peak time and short settling time is provided by the GPC controller. This controller showed robustness against perturbations and parametric changes related to the prematurely associated with the system.

By comparing the results obtained by the two modes of temperature control with and without the baby, we find that the temperature control with GPC brings about better results than a PID. The GPC makes it possible to obtain a greater stability of the thermal environment thus reducing thermal stress, or decreasing the energy expenditure.

The real process of the newborn incubator with experimental set-up for the acquisition of air temperature is shown in Fig. 19.

The responses of the experiments with the PID and the GPC controllers are presented in Fig. 20 without a newborn. The step magnitude for the air temperature was 37°C and it was applied with a sample time of 20 seconds, totalizing 10000 seconds of the experiment.

For the GPC controller, the step response of the incubator system presents a rapid settling time and a smaller overshoot. Unlike the PID controller, the system has shown a faster settling time, but an undesirable overshoot.

Based on the best performance of the tuning obtained by simulations result, it is important to note that the GPC controller is more efficient than PID controller.

Table 5 shows the required metabolic rates and the incubator model coefficients.

Fig. 19. Real process of neonatal incubator.

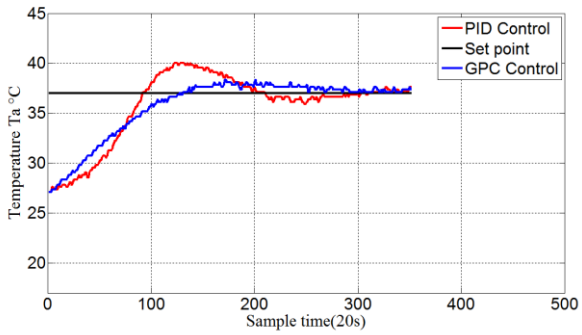

Fig. 20. Temperature responses in the experiment with the GPC and with PID methods.

VI. CONCLUSIONS

One of the most important questions addressed by this study is "How the interference between the newborn and the incubator influences the regulation of the air temperature in the incubator?" In this direction, the combined newborn incubator model has been developed and described. This model was based on physical equations, biological data and real measurements with identification method. To answer this question, the feedback system is developed for the Simulink model using Generalized Predictive Control (GPC) and compared with PID control.

Nomenclature

A_{cv}	Surface area of skin exposed to the air, m^2
A_{net}	Area of the mattress not covered by the infant, m^2
A_r	Surface area of the neonate's local segment normal to the incubator wall, m^2
A_s	Surface area of skin in contact with the mattress, m^2
A_{wi}	Surface area of the incubator walls, m^2
bf	Blood flow rate parameter, sec^{-1}
C_{pa}	Specific heat of air, $J.Kg^{-1}.°C^{-1}$
C_{pb}	Specific heat of the blood, $J.Kg^{-1}.°C^{-1}$
C_{pc}	Specific heat of the core, $J.Kg^{-1}.°C^{-1}$
C_{pm}	Specific heat of moist air, $J.Kg^{-1}.°C^{-1}$
C_{ps}	Specific heat of the skin, $J.Kg^{-1}.°C^{-1}$
C_{pw}	Specific heat of the wall, $J.Kg^{-1}.°C^{-1}$
$Evap$	The evaporation loss from the skin of the infant to the environment, $mL/kg/day$
$hacv$	Heat transfer coefficient for forced convection, $J.m^{-2}.°C^{-1}$
$hcvo$	The convective heat transfer coefficient for free convection, $W.m^{-2}.°C^{-1}$
hfg	Latent heat of the water, $J.Kg^{-1}$
h_{scv}	Heat transfer coefficient for infant skin, $W.m^{-2}.°C^{-1}$
IV	Inspired second volume, $mL/kg \times sec$
K_c	Thermal conductivity of the core, $W.m^{-1}.°C^{-1}$
K_{mat}	Thermal conductivity of the mattress, $W.m^{-1}.°C^{-1}$
m	Mass of the infant, Kg
M_a	Mass of the incubator air, kg
M_c	Mass of the core, kg
M_m	Mass of the mattress, kg
M_{rst}	Resting metabolic rate at the thermo neutral zone for the 1st week of life, W/m^2
M_s	Mass of the skin, kg
M_w	Mass of the wall, kg
S_a	Surface area of the local body segment, m^2
T_x	Temperature of compartment x
th_m	Mattress thickness, m
V_{cb}	Blood volume, mL
w_a	Humidity ratio of the inhaled air
w_{ex}	Humidity ratio of the exhaled air
ρ_a	Air density, kg/mL
ρ_{bl}	Blood density, kg/mL
ρ_c	Core density, kg/m^{-3}
$\rho_{\square 2o}$	Water density, kg/mL
σ	Stefan-Boltzmann constant, $5.64 \times 10^{-8}\text{W/m}^2.\text{K}^4$
ε_s	Radian emissivity of the skin, assumed to be 1.0
ε_w	Radian emissivity of the wall-Plexiglass
Subscripts	
c	Subscript for the neonate core, °C
s	Subscript for the neonate skin, °C
a	Subscript for the incubator air space, °C
w	Subscript for the incubator walls, °C
m	Subscript for the heated air entering the incubator, °C
ex	Subscript for the exhaled air, °C
ha	Subscript for the heated air, °C

Taking into account the interactions between the model of the newborn and the model of the incubator, we have managed to control the incubator temperature with and without a newborn in the shortest feasible time with minimum overshoot, short rise time, small peak time and short settling time. These results prove that our Simulink model (incubator newborn) developed under the predictive controller GPC is satisfactory. The results that we present for the combined baby-incubator

model were only tested with static conditions in Simulink. In addition, experiment results of PID and GPC without baby confirmed that the predictive approach is able to cope with the given control problem. As a future work, the GPC and the PID methods can be applied to a commercial incubator with a calorimetric newborn [32].

TABLE. V. REQUIRED METABOLIC RATES AND THE INCUBATOR MODEL COEFFICIENTS

A_{cv}	$0.0765m^2$	Measured
A_{net}	$0.2019m^2$	Measured
A_r	$0.0427m^2$	Measured
A_s	$0.0085m^2$	Leblanc
A_{wi}	$1.3988m^2$	Measured
bf	$0.003531\ l/sec$	Derived
C_{pa}	$1007\ J/kg.C$	Yunus
C_{pb}	$3840\ J/kg.C$	Yunus
C_{pc}	$3470\ J/kg.C$	Yunus
C_{pm}	$1757\ J/kg.C$	Yunus
C_{ps}	$1900\ J/kg.C$	Yunus
C_{pw}	$1297\ J/kg.C$	Yunus
$hacv$	$0.1131W/m^2.C$	Yunus
hfg	$2419000\ J/kg$	Yunus
IV	$3.667mL/kg.sec$	Yunus
K_c	$0.51W/m.C$	Leblanc
K_{mat}	$0.04184\ W/m.C$	Al-Taweel
m	$0.900kg$	Leblanc
M_m	$0.2575\ kg$	Al-Taweel
M_c	$0.85kg$	Al-Taweel
M_{rst}	$24.8\ W/m^2$	Wheldon
M_s	$0.05kg$	Derived
M_w	$9.98kg$	Yunus
S_a	$0.085m^2$	Leblanc
th_m	$0.02735m$	Al-Taweel
V_{cb}	$80*m\ (mL)$	Christopher
ρ_a	$1.145 * 10^{-6}$kg/mL	Simon
ρ_{bl}	1.06E-3kg/mL	Bernd Fischer
ρ_c	$1080kg/m^3$	Leblanc
$\rho_{\square 2o}$	$0.001\ kg/mL$	Simon
σ	$5.67E\text{-}08W/m^2.K^4$	Leblanc
ε_s	0.97	Simon
ε_w	0.86	Simon

REFERENCES

[1] H. Gustavo, C. Oliveira, Luis. H. Ushijima, "A Hybrid Predictive Control Scheme for Hygrothermal Process", Proceedings of the 17th World Congress, The International Federation of Automatic Control, Seoul, Korea, July 6-11, 2008.

[2] J. Medeiros, J. M. Pires, A. A. Moura, O.M. Almeida, "Certification of Neonatal Incubator Sensors through an Inferential Neural Network", Sensors, vol. 13, 2013, pp. 15613-15632.

[3] G. H. C. Oliveira, M. F. Amorim, and C. Pacholok. "A real-time predictive scheme for controlling hygrothermal conditions of neonate incubators",. In Proc. of the IFAC Symposium on Modelling and Control of Biomedical Systems, Reims/France, 2006.

[4] ML. Bernd Fischer, A. Meister, "The thermoregulation of infants: modeling and numerical simulation", BIT Numerical Mathematics, 2001; vol. 41(5), pp. 950-966.

[5] R. D. Rojas, E. L. Dove, "A mathematical model of premature baby thermo-regulation and infant incubator dynamics", International Conference on Simulation Modelling in Bioengineering, 1996, pp. 23-38.

[6] J. S. Ultman, S. Berman, P. Kirlin, J. M. Vireslovic, C. B. Baer, K. H. Marks, "Electrically heated simulator for relative evaluation of alternative infant incubator environments", Med. Instrum., 1988, vol. 22(1), pp.33-8.

[7] M. H. LeBlanc, "The physics of thermal exchange between infants and their environment", AAMI Technology Assessment Report, Feb. 1987. Vol. 21 (No.1), pp. 11-15.

[8] B. N. Simon, Jr. Narender, P. Reddy, A. Kantak, "A theoretical model of infant incubator dynamics", journal of biomechanical engineering, vol. 116, August 1994, pp. 263-269.

[9] Y. A. Al-Taweel "A simulation model of infant–incubator–feedback system with humidification and temperature control"; Thesis, The Faculty of Engineering and Science of Auckland University of Technology. August 2006.

[10] N. P. Reddy, G. Mathur, S. I. Hariharan, "Toward a fuzzy logic control of the infant incubator", Annals of Biomedical Engineering, 2009, vol. 37(10), pp. 2146–2152.

[11] M. A. Zermani, E. Feki, A. Mami, "Building simulation model of infant-incubator system with decoupling predictive control", IRBM 35, 2014, pp. 189-201.

[12] P. Chessex, S. Blouet, J. Vaucher, "Environmental temperature control in very low birth weight infants (less than 1000 grams) cared for in double-walled incubators", J. Pediatr., 1988, vol. 113(2), pp.373-80.

[13] A. De Silva, M. Jayathilake, A. Galgomuwa, S. Peiris, L. Udawatta, T. Nanayakkara, "High performance temperature controller for infant incubators", International Conference on Information and Automation, New York 2006, pp. 115-120.

[14] M. A. Zermani, E. Feki, A. Mami, "Application of Adaptive Predictive Control to a Newborn Incubator", American J. of Engineering and Applied Sciences, vol. 4(2), 2011, pp. 235-243.

[15] K. A. Thomas,. R. Burr, "Preterm infant thermal care: differing thermal environments produced by air versus skin servo-control incubators", J. Perinatol, june 1999, pp. 264-270.

[16] J. A. D. Pinto, E. A. Cordova, C. B. C. Lévano, "Design and implementation of a digital PID temperature controller for neonatal incubator ESVIN", Journal of Mechanics Engineering and Automation, vol. 5, 2015, pp. 167-172.

[17] Yunus. A. Cengel, "Heat Transfer : A practical Approach", Second Edition ed: McGraw-Hill, 2002.

[18] E. F. Camacho, C. Bordons, "Model Predictive Control", Edition : Springer-Verlag, New York, 1998.

[19] D. W. Clarke, C. Mohtadi, PS. Tuffs, "Generalized predictive control: I. The basic algorithm", Part I, Automatica, vol. 23(2), 1987, pp. 137-148.

[20] M. Kubalcik, V. Bobal, "Predictive control of time-delay processes", 26th European Conference on modelling and simulation, june 2012, Koblenz, Germany.

[21] Dräger. Incubator User Manual; Drager_Incubator_8000SC, Germany, 2017; English. Available online: http://www.frankshospitalworkshop.com/equipment/documents/infant_incubators/user_manuals/Drager_Incubator_8000SC_-_User_manual.pdf (accessed on 04 March 2017).

[22] E. J. L. Costa, R. C. S. Freire, J. B. A. Silva, C. M. P. Cursino, C. R. Oliveira, B. A. M. Pereira, R. F. L. Silva, "Humidity control system in newborn incubator", XIX IMEKO World Congress Fundamental and Applied Metrology, Portugal, septembre 2009, pp. 1760-1764.

[23] F. Chabni, R. Taleb, A. Benbouali, M.A. Bouthiba, "The Application of Fuzzy Control in Water Tank Level Using Arduino", IJACSA, vol. 7, No. 4, 2016, pp. 261-265.

[24] J. Oxer, H. Blemings, "Practical Arduino: Cool Projects for Open Source Hardware", Eds. Apress, 2009.

[25] L. Siang Tat, Y. Kah Haur, "Remote AC Power Control by Using Microcontroller", Journal of Telecommunication, Electronic and Computer Engineering, vol. 8, No. 12, 2016, pp. 53-58.

[26] H. Abramowitz, "Phase-Control Alternatives for Single-Phase AC Motors Offer Smart, Low-Cost, Solutions", Power Systems World, AirCare Automation, 2013.

[27] M. H. Rashid, "Power Electronics Handbook", Academic Press. 2001.

[28] A. Gupta, R. Thakur, S. Murarka, "An Efficient Approach to Zero Crossing Detection Based On Opto-Coupler", International Journal of Engineering Research and Applications, vol. 3, Issue 5, 2013, pp. 834-838.

[29] S. Ali AL-Mawsawi, N.Allaith, H. Qassim, S. Dhiya, "An Accurate Formula for the Firing Angle of the Phase Angle Control in Terms of the Duty Cycle of The Integral Cycle Control", Journal of Automation & Systems Engineering, 2012, pp. 30-35.

[30] Y. V. Niranjan Kumar, P. Hima Bindu, A. Divya Sneha, A. Sravani, "A Novel Implementation of Phase Control Technique for Speed Control of Induction Motor Using ARDUINO", International Journal of Emerging Technology and Advanced Engineering, Volume 3, Issue 4, 2013, pp. 469-473.

[31] R. B. Abdenour, P. Borne, M. Ksouri, F. Msahli, "Identification et commande numérique des procédés industriels", Paris, France: Eds. Technip; 2001.

[32] AE. Wheldon, "Energy balance in the newborn baby: use of a manikin to estimate radiant and convective heat loss", Phys Med Biol, vol. 27(2), 1982, pp. 285-96.

Intelligent Hybrid Approach for Android Malware Detection based on Permissions and API Calls

Altyeb Altaher, Omar Mohammed Barukab
Department of Information Technology, Faculty of Computing and Information Technology-Rabigh,
King Abdulaziz University, P.O. Box 344,
Jeddah, Saudi Arabia

***Abstract*—Android malware is rapidly becoming a potential threat to users. The number of Android malware is growing exponentially; they become significantly sophisticated and cause potential financial and information losses for users. Hence, there is a need for effective and efficient techniques to detect the Android malware applications. This paper proposes an intelligent hybrid approach for Android malware detection using the permissions and API calls in the Android application. The proposed approach consists of two steps. The first step involves finding the most significant permissions and Application Programming Interfaces (API) calls that leads to efficient discrimination between the malware and good ware applications. For this purpose, two features selection algorithms, Information Gain (IG) and Pearson CorrCoef (PC) are employed to rank the individual permissions and API's calls based on their importance for classification. In the second step, the proposed new hybrid approach for Android malware detection based on the combination of the Adaptive neural fuzzy Inference System (ANFIS) with the Particle Swarm Optimization (PSO), is employed to differentiate between the malware and goodware Android applications (apps). The PSO is intelligently utilized to optimize the ANFIS parameters by tuning its membership functions to generate reliable and more precise fuzzy rules for Android apps classification. Using a dataset consists of 250 goodware and 250 malware apps collected from different recourse, the conducted experiments show that the suggested method for Android malware detection is effective and achieved an accuracy of 89%.**

Keywords*—Android malware detection; features selection; fuzzy inference system; particle swarm optimization

I. INTRODUCTION

Recently, the use of smartphones in all aspects of our daily lives is increasing continuously. The global shipments of smartphones hit a record 1.4 billion in 2015 [1]. This number has grown 12% compared with the last year. The massive popularity of smartphones have been accompanied with a potential increase in the number of malwares. With Android dominating 82.8% of the market in 2015 [2], Android become the main goal for mobile malware. The number of Android malware applications is increasing continuously. The total number of malware attacking the mobile devices increased more than three times in 2015, compared to that of 2014 [3]. The dangerous threats targeting mobile devices in 2015 were ransomware. Malware can access all the resources in the attacked mobile device, and data stealers, like business malware.

Google's Play store is a market for Android apps, also there are many other third-party stores for Android apps. The Android apps developers use the Google's Play and third-party stores to publish the apps they developed, and make it available for download and install by users. Detecting the huge number of Android malware and isolating them from application markets is potential and great challenging issue. Very recently in 2016, a significantly sophisticated new form of Android ransomware/Android.Lockdroid.E is detected by Symantec, this variant of ransomware malware employs the accessibility tapjacking method to pose a real threat for more than 67% of Android devices [4].

Several research efforts have been presented for malware detection depending on the Android permissions used in the app. However, using Android permissions only is not enough for accurate detection of malware [5], [6]. Moreover, the existence of permissions in the Android application's Manifest.xml is not evident that it has been used by app code [7], [8]. On the other hand, some researches [9] consider the API level information only to get the features from big data set, but it requires a large number of features for the discrimination between malware and goodware apps. Moreover, efficient detection of the new and ever-evolving Android malware is a continues challenge. To address these challenges, this paper proposes a new hybrid method for Android malware detection based on the hybridization of the Adaptive neural fuzzy Inference System (ANFIS) with the Particle Swarm Optimization (PSO). This paper has the following contributions:

1) Finding the most significant permissions and API calls that lead to efficient categorization of malware and goodware apps.
2) Designing and implementing a new hybrid approach for Android malware detection based on the combination of (ANFIS) with (PSO).
3) An accurate dataset was collected which consists of 250 goodware and 250 malware apps from different resources including Google's play.

The rest of this paper is structured as: Section 2 presents the related work. Section 3 introduced the employed features and feature selection methods. Section 4 explains the proposed method for Android malware detection. Section 5 presents the experimental results and discussion. Section 6 includes the conclusion and future work.

II. Related Work

Android malware detection has been a very active research area in the recent years. The two main approaches for Android malware analysis are static and dynamic analysis [10]. Static analysis examines the Android application without executing it. Many static analysis approaches for Android malware detection have been proposed [11]-[15]. For example, Kirin's approach [12], explores the used permissions in the Android app to determine their maliciousness. Stowaway [13] examines API calls to detect Malware applications and Risk Ranker [14] statically classifies applications based on different security risks. In 2014, DREBIN proposed by Arp *et al*. [15], it detects the Android malware application by performing application analysis using different features such as permissions, API calls, network address, hardware access, etc. Examples for static analysis tools include Smali [16] and Androguard [17], which facilitate the static analysis of Android apps. However, the static analysis approaches are unable to detect malwares that use dynamic code loading obfuscation techniques.

The dynamic analysis examines the Android application by monitoring its behavior during execution. A number of dynamic analysis approaches have been proposed for Android malware detection [18]-[22]. DroidScope and TaintDroid proposed in [21] and [22], they monitor the application during its running in a protected environment (similar to the java sand box concept), by exploring different components of the application. Dynamic analysis approaches require many resources compared with static analysis, which made them unsuitable for the limited resources of the mobile devices.

Machine learning approaches also have been proposed for Android malware detection, motivated by the problem of manually creating and updating detection models for Android malware. Aafer *et al*. [23] used machine learning approach to classify Android apps as malware or goodware. They compared the malware detection accuracy of four classifiers using the API calls and permissions as features for Android application. Shabtai *et al*. [24] used six machine learning based classifiers for Android malware detection, namely, k-Means, NB, DT, decision tree, BN, logistic regression and histogram using the Andromaly framework. Andromaly achieved a 99.9% accuracy rate using the information gain algorithm for features selection and decision tree classifier. The main disadvantage of Andromaly is using self-written Android malware applications to test it. In contrast, 250 real-world malware apps were used in our approach.

Dini *et al*. in [19] combined the system calls in kernel with system calls in user level. They used features set consisting of 12 system calls and the K-nearest neighbors (KNN) as classifier for Android malware detection. Dini *et al*. achieved an accuracy of 93% using 10 Android malwares. The main disadvantage of this approach is its inability to detect malware that use root permissions to avoid the system call. Therefore, Android API calls and permissions are used in this research rather than using system calls only. Zhao *et al*. in [25] used the Support Vector machine learning method to develop RobotDroid in order to detect unknown Android malware. RobotDroid depends on the hidden payment services and the privacy information leakage. They considered three malware types, namely, Plankton, DroidDream and Gemini. Consequently, this approach is limited to the considered Android malware types only. Amos *et al*. proposed STREAM in [26], it employs several machine learning classifiers to detect Android malware based on a set of features such as permissions , memory and battery usage. However, the features set collected from Android emulator, which is not accurate as real Android device [27]. In this work, we used features collected from real-world malware and goodware apps.

Our proposed approach is related to these methods and uses comparable features for detecting malicious applications, such API calls and permissions. However, it differs in two main aspects from previous research: First, we find the most significant permissions and API calls that leads to efficient discrimination between the malware and goodware applications. Second, we design and implement a new hybrid classifier for efficient Android malware detection based on combining (ANFIS) [35] with the PSO.

III. Overview

A. Android Permissions

Android uses the permission system to regulate the application's access to the resources and data in the mobile device, such as camera, storage and internet access. Android permissions offer the security characteristics by restricting certain tasks an application can execute [28]. The selection of the most suitable permissions corresponding to the tasks performed by the application is the ultimate responsibility of the developer. The shortage of knowledge about the permissions could guide developers to add in essential and excessive permissions to the application which may leads to over privileged Android application [29] that make users stop installing the application. Moreover, adding in essential permissions makes the application similar to malware [30], causing re-delegation attacks [31]. Furthermore, the shortage of knowledge about permissions makes the user uncertain about the decision of installing the application. Currently available information about permissions is not quite enough to support the users decision regarding the installation of application [32]. Since the used permissions and API calls in the application reflect the behavior of the app, it is believed that it is potentially feasible to detect the malware application by exploring the patterns of used permissions and API calls, and help both developers and users in getting better understanding of permissions and API calls.

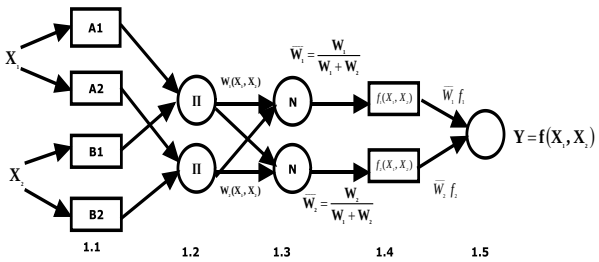

Fig. 1. Artificial neuro fuzzy inference system architecture.

B. Android API Calls

APIs are functions used by the developers to interact with Android operating system. Since there are many Android APIs, it is more appropriate to consider specific APIs frequently used by malware and enable them to access Smartphone's sensitive resources, rather than considering all APIs used in the app's source code. Seo *et al*. [33] examined malware apps and specified suspicious APIs frequently used by malware. They compared the number of suspicious APIs in malware applications with the number of suspicious APIs in goodware apps. In this paper, the suspicious APIs from the malware and goodware apps were extracted and used as part of the features set. The selected suspicious APIs are similar to the subspecies APIs defined in [33], [15], examples of the selected suspicious APIs include, API calls for accessing important information such as getSubscriberId()and getDeviceId(), and API calls for getting accessibility services which can activate several types of malicious payloads. Finding the rank of the importance of API calls and permissions in terms of categorization of malware and goodware application, and evaluating the efficiency of our proposed hybrid approach PSO-ANFIS for malware detection, are main challenges of this research work.

C. Artificial Neuro Fuzzy Inference System (ANFIS)

Artificial Neuro Fuzzy Inference System (ANFIS) is proposed by Jang *et al*. [34] and it became one of the well-known researches related to fuzzy inference systems in the recent years. ANFIS associates the advanced reasoning and explanation of fuzzy logic with the powerful computation and learning capabilities of neural networks [34]. There are many architectures for neuro-fuzzy networks, however, the most dominant architectural models are the Mamdani and the Takagi Sugeno (TSK). TSK model uses a single-spike as the output membership function while Mamdani model uses a fuzzy set. The ANFIS used in this paper is based on TSK model. Fig. 1 shows example for ANFIS architecture that consists of five layers with two inputs X1 and X2 and one output Y.

The rule base consists of Takagi–Sugeno fuzzy rules as follows:

R1=IF x1 is μ1i AND x2 is μ2i THEN fij = pijx1 + qijx2 + rij

Where, x1 and x2 are the input for the ANFIS, conditions specified in the IF part are called antecedent, and conditions in the THEN part are called the consequence. ANFIS consists of five layers [34].

Layer One: Crisp input data entered into the ANFIS are transformed into linguistic expressions. Membership function (μ) is used to transform the inputs into linguistic expressions, there are several types of membership functions. In this paper, Gaussian membership function is used because it leads to more smooth model behavior. The Gaussian membership function is defined as follow:

$$O_i^1 = \beta(X) = \exp\left(-\frac{1}{2}\frac{(X-C)^2}{\sigma^2}\right) \quad (1)$$

Where, Oi's are the outputs of this layer. σ and C represent the variance and the center of the Gaussian membership function, respectively. This layer includes parameters called antecedent parameters, which are tuned by ANFIS for obtaining results that are more accurate.

Layer 2: This layer determines the level of accuracy of the statements specified in antecedent parts, which is also called the firing strength, using the following equation.

$$O_i^3 = \frac{w_i}{\sum_i w_i} \quad (2)$$

Layer 3: This layer normalizes all the firing strengths computed in the former layer (Wi), where it computes the proportion of the ith rule's firing strength to the all rules firing strengths using the following equation:

$$O_i^3 = \frac{w_i}{\sum_i w_i} \quad (3)$$

Layer 4: This layer contains the consequent portion of the fuzzy rules, the influence of each rule in the final output is defined as:

$$O_i^4 = \overline{W_i} f_i = \overline{W_i}(m_i X_1 + n_i X_2 + r_i) \quad (4)$$

Where, mi, ni, and ri are the consequent parameters. The consequent parameters and the antecedent parameters in the first layer, are tuned by ANFIS in the learning process to decrease the differences between the output and the target result.

Layer 5: This is the defuzzification layer where all the rules generated for one output are collected and defuzzified into numerical outputs, according to a weighted average sum as follow:

$$O_i^5 = Y = \sum_i \overline{W_i} f_i = \overline{W_1} f_1 + \overline{W_2} f_2 = \frac{\sum_i W_i f_i}{\sum_i W_i} \quad (5)$$

D. The Particle Swarm Optimization (PSO)

The particle swarm optimization (PSO) is a well-known method for searching, which is grounded on the behavior of bird flocking. In PSO, each possible answer for the optimization issue can be considered as a point in the population, the point is called a particle. The particle propagates in the population with a specified speed which is tuned based on its movement knowledge and its companions' movement knowledge. Each particle is assigned a fitness value specified based on the objective function and records its current position and current best position (recorded as pbest). The pbest can be considered as the particle's own moving experience. Moreover, each particle records the global best position (recorded as gbest, which is the best value in pbest) of the total collection. The gbest can be considered as its companions' movement knowledge for the particle [35], [36]. Let xi (t) represent the location of a particle i in the population at time t. Then, the particle's location is adjusted by the addition of the velocity, vi to the current location:

$$x_i(t) = x_i(t) + v_i(t) \quad (6)$$

$$v_i(t) = c_1 r_1\big(pbest(t) - x_i(t)\big) + c_2 r_2\big(gbest(t) - x_i(t)\big) \quad (7)$$

Where, c1 and c2 represent the acceleration coefficients, r1 and r2 are random vectors.

IV. The Proposed Approach for Android Malware Detection

This section explains our methodology for the detection of Android malware. First, the used dataset is introduced. Second, we used the Information Gain (IG) and Pearson CorrCoef (PC) to find the most significant permissions and API calls that leads to efficient discrimination between the malware and goodware applications. Third, the proposed hybrid PSO-ANFIS is utilized to classify the Android apps as either goodware or malware.

A. The Used Dataset

To build an accurate and reliable model capable of efficiently classifying the Android applications as malware or goodware, an accurate and well-labeled dataset is required. We used a recent data set contains 250 benign applications collected from Google's play, the free online malware detection tool VirusTotal [36] is used to confirm that the collected apps are benign. The data set also contains 250 malware applications which have been downloaded from Genome project [37] and Drebin dataset [15], all the malware apps are confirmed as malware using the VirusTotal. In this paper, we considered the permissions and API calls used in the app as features to classify the applications as either goodware or malware.

B. Features selection

In this section, the most significant permissions and API calls that leads to efficient discrimination between the malware and goodware applications are selected. For this purpose, two features ranking algorithms, namely, Information Gain (IG) and Pearson CorrCoef (PC) are employed to rank the individual permissions and API calls based on their importance for classification. Based on the static analysis method, we used free analysis tools like android-apktool, dex2jar and jd-gui to extract the API calls and permissions from the goodware and malware applications. Java language is used to develop Android applications and they are generated as Android Application Package (APK) files. APK package consists of files required for running the application. The files in the APK include the following:

DalVik Executable (DEX) file: This is a file generated by the compilation of the Java source code.

Manifest file: A file holding the Android application characteristics such as permissions, the activities, and intents.

eXtensible Markup Language (XML) file: A file defining the components of the user interface layout and the used values.

Resource file: A file consists of resources needed by applications like sound files and images.

- *Information Gain Ratio (IGR)*

Information Gain Ratio method extracts the correlation between Android API calls and permissions, it gives the maximum scoret to the most potential permissions based on the class of malware and goodware Android apps belonging to IGR [38], the IGR equations are explained as follows:

$$gain\_r(X, C) = \frac{gain\_r(X,C)}{split\_info(C)} \quad (8)$$

$$split\_info(C) = \sum_i \left(\frac{|C_i|}{|C|}\right) log \frac{|C_i|}{|C|} \quad (9)$$

Where, gain_r (X,C) denotes the gain ratio of the feature X occurrence in the class C. Ci and |Ci| represent the occurrence of feature X in class C, the ith sub-class of C and the total number of features in Ci, respectively.

- *The Pearson CorrCoef*

Pearson CorrCoef computes the relation between feature X and class C by

$$R(X, C) = \frac{cov(X,C)}{\sqrt{var(X)var(C)}} \quad (10)$$

Where, R(P;A) = 0 means the independency of feature P and class A, R(P;A) = 1 means the top positive correlation of feature P and class A and R(P;A) = -1 means the top negative correlation. In our paper, R(P;A) = 1 means that the application which request the feature P is highly suspected as malware app, while R(P;A) = -1 means requesting the feature P leads to classify the applications as goodware.

C. PSO-based ANFIS

The proposed approach PSO-ANFIS intelligently combines ANFIS method and PSO algorithm for the optimization of Android malware detection, by tuning the parameters of membership function to achieve the highest malware detection accuracy. ANFIS utilizes the IF-Then fuzzy rules in mapping the inputs to outputs, the level of ANFIS accuracy is significantly affected by tuning its network structure and parameters [40]. There is a strong relation between the accuracy and the used membership functions. This paper aims to tune the Gaussian membership function to improve the accuracy of ANFIS by getting the best learning parameters and minimum number of fuzzy rules. The best learning parameters which minimize the difference between the target data and ANFIS output, can be obtained by minimizing the Root Mean Square Error (RMSE) as follows:

$$J = \left[\sum_{m=1}^{\alpha} \frac{(R_m - y_m)^2}{\alpha}\right]^{\frac{1}{2}} \quad (11)$$

Where, α represents the number of training data items, Rm is the input value and ym is the predicted value. The Performance criterion RMSE depends on the center and the width of the Gaussian membership function (Ci, σi). The RMSE is considered as an objective function and its minimization is the research problem in this study. PSO is a potential optimization technique to enhance the performance of ANFIS [41]. In this paper, PSO algorithm is utilized intelligently to realize the minimization of the objective function of ANFIS which is the error between the predicted class of Android malware and the actual class, by tuning the membership functions of ANFIS. Fig. 2 shows the structure of the proposed hybrid PSO-ANFIS approach, each learning process of ANFIS represents one particle and the parameters of the membership functions that effect the ANFIS performance represent the particle dimensions.

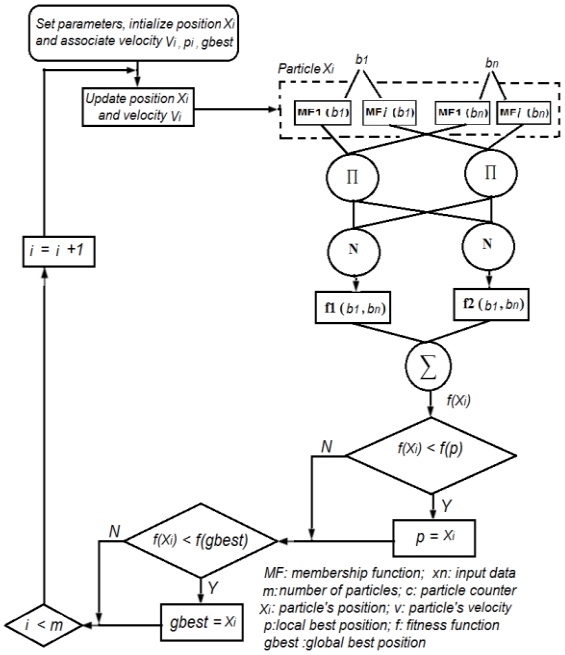

Fig. 2. The proposed POS-ANFIS classifier.

The steps of the hybrid PSO-ANFIS approach are explained as follows:

Step 1: Set initial value for the number of iterations C =1, randomly initialize the position Xiand velocity Viof the i-th particle in the search space using (6) and (7), respectively.

Step 2: Compute the objective function of ANFIS using (8) and use it as a fitness function (f_i) for the proposed PSO-ANFIS.

Step 3: IF the fitness function of the i-th particle in position X $f(X_i)$ is better than the fitness function of the same particle in the local best position f (Pi) THEN

$P_i = X_i$.
ELSE
IF the fitness function of the i-th particle in position X $f(X_i)$ is better than the fitness function of the same particle in the global best position$f(gbest)$ THEN
Gbest = Xi

Step 4: IF the fitness function of global best position$f(gbest)$ is best than stopping criteria OR the particle counter C is greater than the total number of iterations m THEN

Stop
ELSE
Go to Step 2

V. Experiments and Results Discussion

To conduct the experiments the dataset is separated into two sets testing set and training set. The five-fold cross-validation technique is selected to split the dataset. In order to evaluate the performance of the proposed approach for Android malware detection, we selected the 24 permissions and API calls features according to their significance for the discrimination, using the Pearson CorrCoef (PC) and Information Gain (IG) algorithms. We applied our proposed approach PSO-ANFIS on the selected features. The performance of our proposed approach PSO-ANFIS is compared with the well-known system ANFIS system. ANFIS is selected for comparing our proposed PSO-ANFIS with, because it proofs efficiency in many classification tasks and it is similar to PSO-ANFIS in terms of fuzzy rules type. The classification accuracy of the two classifiers is compared in terms of the Root Mean Square Error (RMSE). Root Mean Square Error measures the dissimilarity between values obtained by the classifier and the observed values:

$$RMSE = \sqrt{\frac{1}{2}\sum_{i=1}^{n}(M_i - P_i)^2} \qquad (12)$$

The total accuracy obtained by the cross-validation is calculated based on the average of the RMSE in the five-folds method as follows:

$$CVA = \frac{1}{m}\sum_{i=1}^{m} R_i \qquad (13)$$

Where, CVA is the accuracy based on the cross-validation, m is the number of the used folds, and Ri is the calculated RMSE of each fold. The evaluation of the fuzzy inference classifier requires the separation of its output into two main classes. To evaluate our proposed POS-ANFIS, we separated its continuous output by determining a threshold in the range between one and zero, to categorize the malware and goodware apps. In this experiment, four threshold values have been determined: 0.10, 0.25, 0.35 and 0.40. The classification results based on the selected features are compared in terms of Accuracy (ACC) and obtained error rate. The following confusion matrix used to classify the Android application as malware (1) or goodware (0).

		Actual	
		1	0
Classified	1	TP	FP
	0	FN	TN

Where,

TP: correct classification of malware as malware

FP: incorrect classification of malware as goodware

FN: incorrect classification of goodware as malware

TN: correct classification of goodware as goodware.

TABLE. I. MOST FREQUENTLY USED FEATURES IN MALWARE AND GOODWARE APPLICATIONS AND THEIR RANK OF IMPORTANCE

Information Gain Algorithm			**Pearson CorrCoef Algorithm**		
Rank	***Score***	***Feature***	***Rank***	***Score***	***Feature***
1	0.2746	READ_PHONE_STATE	1	0.5811	READ_PHONE_STATE
2	0.2743	getDescription	2	0.5563	RECEIVE_BOOT_COMPLETED
3	0.2537	AccessibilityNodeProvider	3	0.5542	SYSTEM_ALERT_WINDOW
4	0.2537	AccessibilityNodeInfo	4	0.5403	getDescription
5	0.2537	AccessibilityRecord	5	0.5186	AccessibilityRecord
6	0.2537	AccessibilityStateChangeListener	6	0.5186	AccessibilityNodeProvider
7	0.2537	AccessibilityManager	7	0.5186	AccessibilityNodeInfo
8	0.2529	SYSTEM_ALERT_WINDOW	8	0.5186	AccessibilityManager
9	0.2366	RECEIVE_BOOT_COMPLETED	9	0.5186	AccessibilityStateChangeListener
10	0.0816	SEND_SMS	10	0.3151	SEND_SMS
11	0.0776	INTERNET	11	0.3115	INTERNET
12	0.0473	ACCESS_NETWORK_STATE	12	0.2544	ACCESS The STATE Of NETWORK
13	0.0414	WRITE_EXTERNAL_STORAGE	13	0.2378	WRITE In The EXTERNAL STORAGE
14	0.0124	READ_SMS	14	0.1283	READ_SMS
15	0.0112	WRITE_SETTINGS	15	0.0427	WRITE_SETTINGS
16	0.0109	getResolveInfo	16	0.0161	getResolveInfo
17	0.0101	KILL_BACKGROUND_PROCESSES	17	0.0104	KILL_BACKGROUND_PROCESSES
18	0.0019	WAKE_LOCK	18	0.0041	WAKE_LOCK
19	0.0012	getSettingsActivityName	19	0.0040	getSettingsActivityName
20	0.0010	GET_TASKS	20	0.0004	GET_TASKS

TABLE. II. COMPARISON OF TESTING AND TRAINING RMSE FOR BOTH ANFIS AND PSO-ANFIS

Fold #	**ANFIS**		**PSO-ANFIS**	
	Testing RMSE	**Training RMSE**	**Testing_RMSE**	**Training RMSE**
1	0.3318	0.3476	0.1574	0.1168
2	0.3221	0.3296	0.1161	0.1053
3	0.3159	0.3282	0.1458	0.1245
4	0.3147	0.3156	0.1494	0.1265
5	0.3113	0.3396	0.1359	0.1184

Table 1 above shows the most frequently used features in malware and goodware applications and their rank of importance. It is observed that using the Information gain and Pearson CorrCoef Algorithm yield the same subset of 15 features, signifying that the results of ranking are consistent. The most requested permissions are associated with accessing phone state, connecting to the Internet, checking the connectivity of the network, monitoring the device booting, writing to external storage and messages related permissions. Moreover, most of the applications requested the SYSTEM_ALERT_WINDOW permission and accessibility services APIs. They enable an application to create windows that can be shown on top of other applications and even execute tasks on them, these abilities made them an extremely attractive target for malware developers to perform tapjacking attacks. A significantly sophisticated new form of Android ransomware/Android.Lockdroid.E is detected [4], this variant of ransomware malware employs the accessibility tapjacking method to pose a real threat for more than 67% of Android devices.

Table 2 above shows the testing and training RMSE for both ANFIS and PSO-ANFIS using the features selected by the proposed dual-stage method based on the five-fold cross-validation. A low RMSE depicts greater malware detection accuracy, so the classifier that generates lower RMSE is considered as a better classifier for the differentiation between the malware and goodware applications. It can be observed from Table 2 that the proposed PSO-ANFIS achieves lowest RMSE for both testing and training in all five-folds.

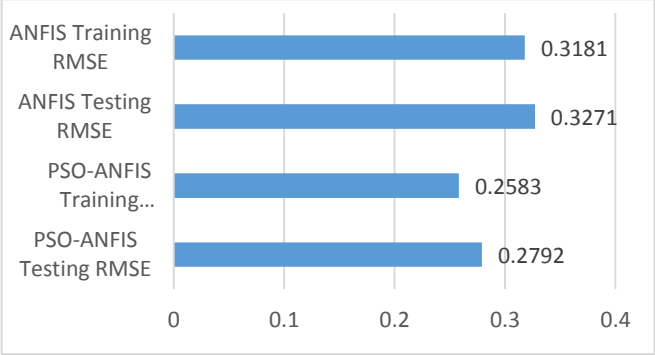

Fig. 3. The accuracy of cross-validation in terms of RMSE.

TABLE. III. CLASSIFICATION ACCURACY OF PSO-ANFIS AND ANFIS

Threshold	**Accuracy**		**Error**	
	PSO-ANFIS	**ANFIS**	**PSO-ANFIS**	**ANFIS**
0.10	45 %	41%	55 %	59%
0.25	63 %	50%	37 %	50%
0.35	66 %	54%	34 %	46%
0.40	89%	69%	11 %	31%

TABLE. IV. THE PERFORMANCE OF THE PROPOSED APPROACH COMPARED WITH OTHER APPROACHES

Classification approach	**Accuracy**
PSO-ANFIS	89%
K-ANFIS [39]	75%
Droid Permission Miner [42]	87%
Puma [5]	86.41%.

Table 3 above shows the performance of PSO-ANFIS and ANFIS for each threshold in terms of accuracy and error rates. We can see that the proposed classifier PSO-ANFIS achieved better results than ANFIS for all thresholds. These results confirm the suitability of PSO algorithm in minimizing the error between the predicted class of Android application and the actual class, by tuning the membership functions of ANFIS. Fig. 3 shows a comparison between the values of CVA for PSO-ANFIS and ANFIS. It is clear from Fig. 3 that the results from PSO-ANFIS are significantly better. For example, the CVA of RMSE value of PSO-ANFIS testing is 0.2792 which is smaller than the CVA value of ANFIS testing which is 0.3271. Also, the CVA of RMSE value of PSO-ANFIS training is 0.2583 which is smaller than the CVA value of ANFIS training which is 0.3181. All these results confirm that PSO-ANFIS system outperforms ANFIS. The performance of our proposed approach has been compared with other comparable approaches, including our previous research [39] and other approaches [5], [42] as shown in Table 4.

VI. Conclusion

Accurate detection of Android malware has been an important issue in recent years. In this study, we found that the most significant permissions and API calls lead to efficient discrimination between the malware and goodware applications. For this purpose, two features ranking algorithms, Information Gain (IG) and Pearson CorrCoef (PC) are employed to rank the individual permissions and API calls based on their importance for classification. In addition, we proposed a new hybrid method for Android malware detection based on the combination of the Adaptive neural fuzzy Inference System (ANFIS) with the Particle Swarm Optimization (PSO). Using dataset consists of 250 malware and 250 goodware collected from different recourse, the proposed approach achieved classification accuracy of 89% which is better than the classification accuracy of ANIS and other approaches. For future work ensemble of classifiers will be considered to improve the classification accuracy of Android apps.

Acknowledgement

This work was supported by the Deanship of Scientific Research (DSR), King Abdulaziz University, Jeddah, under Grant No. (G-160-830-37). The authors, therefore, gratefully acknowledge the DSR technical and financial support.

References

[1] Rawal, Priyanka, Alka Awasthi, and Shekhar Upadhayay. “Creating a Hunger Driven Smartphone Market by Xiaomi.” International Journal of Engineering Science, pp. 11250-11255,2017.

[2] Azfar, Abdullah, Kim-Kwang Raymond Choo, and Lin Liu. “Forensic taxonomy of android productivity apps.” Multimedia Tools and Applications .76, no. 3 ,pp. 3313-3341, 2017.

[3] Kambourakis, Georgios, Dimitrios Damopoulos, Dimitrios Papamartzivanos, and Emmanouil Pavlidakis. “Introducing touchstroke: keystroke‐based authentication system for smartphones.” Security and Communication Networks, 9, no. 6, pp. 542-554, 2016.

[4] Narudin, Fairuz Amalina, Ali Feizollah, Nor Badrul Anuar, and Abdullah Gani. “Evaluation of machine learning classifiers for mobile malware detection.” Soft Computing, 20, no. 1, pp.343-357, 2016

[5] Sanz, B., Santos, I., Laorden, C., Ugarte-Pedrero, X., Bringas, P. G., & Álvarez, G. Puma: Permission usage to detect malware in android. InInternational Joint Conference CISIS’12-ICEUTE´ 12-SOCO´ 12 Special Sessions, Springer Berlin Heidelberg, pp: 289-298, 2013.

[6] Wei, X., Gomez, L., Neamtiu, I., & Faloutsos, M. Permission evolution in the android ecosystem. In Proceedings of the 28th Annual Computer Security Applications Conference, ACM, pp: 31-40,2012.

[7] Sharma, Akanksha, and Subrat Kumar Dash. Mining API Calls and Permissions for Android Malware Detection. In *Cryptology and Network Security*, Springer International Publishing, pp: 191-205, 2014.

[8] Grace, M. C., Zhou, Y., Wang, Z., & Jiang, X. Systematic Detection of Capability Leaks in Stock Android Smartphones. In NDSS ,Vol. 14,. pp. 19,2012.

[9] Aafer, Y., Du, W., & Yin, H. Droidapiminer: Mining api-level features for robust malware detection in android. In International Conference on Security and Privacy in Communication Systems ,Springer International Publishing, pp: 86-103,2013.

[10] Egele, Manuel, Theodoor Scholte, Engin Kirda, and Christopher Kruegel. “A survey on automated dynamic malware-analysis techniques and tools.” ACM Computing Surveys (CSUR) 44, no. 2,pp. 6, 2012.

[11] Enck, W., Octeau, D., McDaniel, P., & Chaudhuri, S. A Study of Android Application Security. In USENIX security symposium,Vol. 2 ,pp. 2. 2011.

[12] Enck, W., Ongtang, M., & McDaniel, P. On lightweight mobile phone application certification. In Proceedings of the 16th ACM conference on Computer and communications security, ACM, pp: 235-245, 2009.

[13] Felt, A. P., Chin, E., Hanna, S., Song, D., & Wagner, D. Android permissions demystified. In Proceedings of the 18th ACM conference on Computer and communications security ,ACM, pp.627-638,2011.

[14] Grace, M., Zhou, Y., Zhang, Q., Zou, S., & Jiang, X. Riskranker: scalable and accurate zero-day android malware detection. In Proceedings of the 10th international conference on Mobile systems, applications, and services, ACM, pp. 281-294, 2012.

[15] Arp, D., Spreitzenbarth, M., Hubner, M., Gascon, H., Rieck, K., & Siemens, C. E. R. T. DREBIN: Effective and Explainable Detection of Android Malware in Your Pocket. In NDSS, 2014.

[16] J. Freke. An assembler/disassembler for android’s dex format. Google Code, http://code.google.com/p/smali/, visited February, 2013.
Desnos, A., & Gueguen, G. Android: From reversing to decompilation. Proc. of Black Hat Abu Dhabi, pp.77-101, 2011

[17] Burguera, I., Zurutuza, U., & Nadjm-Tehrani, S. Crowdroid: behavior-based malware detection system for android. In Proceedings of the 1st ACM workshop on Security and privacy in smartphones and mobile devices ACM, pp. 15-26,2011.

[18] Dini, G., Martinelli, F., Saracino, A., & Sgandurra, D. MADAM: a multi-level anomaly detector for android malware. In International Conference on Mathematical Methods, Models, and Architectures for Computer Network Security ,Springer Berlin Heidelberg,pp. 240-253, 2012.

[19] Zhou, Y., Wang, Z., Zhou, W., & Jiang, X. February. Hey, you, get off of my market: detecting malicious apps in official and alternative android markets. In NDSS ,Vol. 25, No. 4, pp. 50-52,2012.

[20] Yan, L. K., & Yin, H. DroidScope: Seamlessly Reconstructing the OS and Dalvik Semantic Views for Dynamic Android Malware Analysis. In USENIX security symposium, pp. 569-584,2012.

[21] Enck, W., Gilbert, P., Han, S., Tendulkar, V., Chun, B. G., Cox, L. P., ... & Sheth, A. N. TaintDroid: an information-flow tracking system for realtime privacy monitoring on smartphones. ACM Transactions on Computer Systems (TOCS), 32(2), 2014.

[22] Aafer, Y., Du, W., & Yin, H. Droidapiminer: Mining api-level features for robust malware detection in android. In International Conference on Security and Privacy in Communication Systems, Springer International Publishing, pp. 86-103, 2013.

[23]] Shabtai, A., Kanonov, U., Elovici, Y., Glezer, C., & Weiss, Y. “Andromaly”: a behavioral malware detection framework for android devices. Journal of Intelligent Information Systems, 38(1), pp. 161-190, 2012.

[24] Zhao, M., Zhang, T., Ge, F., & Yuan, Z. RobotDroid: A Lightweight Malware Detection Framework On Smartphones. JNW, 7(4), pp. 715-722,2012.

[25] Amos B, Turner H, White J. Applying machine learning classifiers to dynamic android malware detection at scale. In: Proceedings of the 9th international wireless communications and mobile computing conference (IWCMC), Sardinia, Italy, pp. 1666–1671, 2013.

[26] Raffetseder T, Kruegel C, Kirda E. Detecting system emulators.In: Proceedings of the 10th international conference ISC, Valparaíso, Chile, pp. 1–18,2007.

[27] Android, "Andriod developers guides,"

[28] http://developer.android.com/guide/topics/security

[29] Felt, A. P., Chin, E., Hanna, S., Song, D., & Wagner, D. Android permissions demystified. In Proceedings of the 18th ACM conference on Computer and communications security ,ACM, pp. 627-638, 2011.

[30] Grace, M. C., Zhou, Y., Wang, Z., & Jiang, X. Systematic Detection of Capability Leaks in Stock Android Smartphones. In NDSS ,Vol. 14, pp. 19,2012.

[31] Felt, A. P., Wang, H. J., Moshchuk, A., Hanna, S., & Chin, E. Permission Re-Delegation: Attacks and Defenses. In USENIX Security Symposium , 2011.

[32] Kelley, P. G., Consolvo, S., Cranor, L. F., Jung, J., Sadeh, N., & Wetherall, D. A conundrum of permissions: installing applications on an android smartphone. In Financial Cryptography and Data Security ,Springer Berlin Heidelberg, pp. 68-79,2012.

[33] Seo, S. H., Gupta, A., Sallam, A. M., Bertino, E., & Yim, K. Detecting mobile malware threats to homeland security through static analysis. Journal of Network and Computer Applications, 38, pp. 43-53,2014.

[34] Jang, J. S. ANFIS: adaptive-network-based fuzzy inference system. IEEE transactions on systems, man, and cybernetics, 23(3), pp. 665-685, 1993

[35] Trelea, I. C. The particle swarm optimization algorithm: convergence analysis and parameter selection. Information processing letters, 85(6), pp. 317-325, 2003.

[36] Kennedy, J., & Eberhart, R. Particle swarm optimization, IEEE International of first Conference on Neural Networks, 1995.

[37] Jarabek, Chris, David Barrera, and John Aycock. "ThinAV: truly lightweight mobile cloud-based anti-malware." In Proceedings of the 28th Annual Computer Security Applications Conference, pp. 209-218, 2012.

[38] Zhou, Y. and Jiang, X. Dissecting android malware: Characterization and evolution. In Security and Privacy (SP), 2012 IEEE Symposium on ,pp. 95-109, 2012.

[39] Mori, T. Information gain ratio as term weight: The case of summarization of IR results. Proceedings of the 19th International Conference on Computational Linguistics, (COLING '02), Association for Computational Linguistics, pp. 1-7,2002.

[40] Abdulla, S., & Altaher, A. Intelligent Approach for Android Malware Detection. KSII Transactions on Internet and Information Systems (TIIS), 9(8),pp. 2964-2983, 2015.

[41] Jiang, H.M., Kwong, C.K., Ip, W.H. and Wong, T.C. Modeling customer satisfaction for new product development using a PSO-based ANFIS approach. Applied Soft Computing, 12(2), , pp.726-734,2012.

[42] T.Fushiki. Estimation of prediction error by using K-fold cross-validation, Statistics and Computing,vol.21, pp.137-146,2011.

[43] Aswini, A.M., Vinod, P. Droid Permission Miner: Mining Prominent Permissions for Android Malware Analysis. In: 5th International Conference on the Applications of the Digital Information and Web Technologies (ICADIWT 2014), pp. 81–86 ,2014.

Insight to Research Progress on Secure Routing in Wireless Ad hoc Network

Jyoti Neeli
Dept of Information Science & Engineering
Global Academy of Technology
Bengaluru,
India

N K Cauvery
Professor & HOD
Dept. of Information Science of Engineering
RV College of Engineering,
Bengaluru, India

***Abstract*—Wireless Ad hoc Network offers a cost effective communication to the users free from any infrastructural dependencies. It is characterized by decentralized architecture, mobile nodes, dynamic topology, etc. that makes the network formation typically challenging. In the past decade, there has been a series of research work towards enhancing its routing performance by addressing various significant problems. This manuscript mainly orients around the progress being made in the line of secure routing protocol, which is still a bigger issue. The paper discusses different approaches undertaken by existing literature towards discrete security problem and explores the effective level of security. The study outcome of the paper finds that progress towards wireless ad hoc network is still very less and there is a need to come up with robust security framework. The paper also discusses the research gap being identified from the existing techniques and finally discusses the future work direction to address the certain unsolved problem.**

***Keywords*—Attacks; confidentiality; secured routing; integrity; mobile ad hoc network; wireless ad hoc network**

I. INTRODUCTION

Wireless ad hoc network consists of autonomous nodes that are interconnected by themselves without any presence of infrastructure [1]. It is highly useful for offering robustness communication with minimal cost. The sustenance of wireless ad hoc network is quite high irrespective of any adverse deployment area [2]. For this reason, there is wide range of applications using ad hoc network e.g. recovery from natural disaster, combat, and military application, community network, etc. However, there are multiple challenges in the design principle of the wireless ad hoc network. It is essential that a wireless network should overcome the issue about physical medium, e.g., maximized bit rate, restricted range, noise, the minimal range of transmission, etc. As the nodes perform its mobility in the wireless ad hoc network, it is quite imperative that communication status and routing behavior will also change accordingly giving rise to dynamic topology. The presence of shared uncontained medium in a wireless network may also pose a significant security challenge while performing routing in the ad hoc environment [3]. Apart from this, energy has always been the peak problem associated with routing protocols in the wireless ad hoc network. Although there is various existing study to address such problem, the problems are not completely been solved. It is because usage of radio interfaces, directional antenna, and wireless technology are already shrouded with various security loopholes that are yet under the desk of researchers. The prominent attacks on the wireless ad hoc network are basically of two types, i.e., 1) routing-disruption attacks, and 2) resource-consumption attacks. The routing disruption-based attack is initiated by forwarding counterfeited beacon to mislead the route formation. Similarly, the resource-consumption based attack is responsible for initiating an attack that leads to unwanted drainage of energy or consumption of channel capacity. Although, the wireless ad hoc network uses both public and private key for performing encryption, usage of the public key is found more than private keys. This is because the implementation of the private key during distribution is quite difficult to be achieved in the presence of dynamic topology. There is another approach called Statistically Unique Cryptographically Verifiable (SUCV) that allows the nodes to select their addresses after generating public and private pairs of keys. However, this approach is found ineffective to address the problem of key set up [4]. Usage of Certificate Authority (CA) is another frequently used approach to secure the communication in the wireless ad hoc network. Therefore, there are multiple numbers of challenges being associated with the secure routing in the wireless ad hoc network. It is significantly felt that there is no efficient modeling for addressing secure routing issue. Study towards modeling will allow the system to evaluate the type of attackers as well as catch hold of the malicious node, which are very less being prioritized in existing techniques. Existing routing technique have proved potential improvement in security features but at the cost of computational complexity. Therefore, this paper discusses the three prominent forms of wireless ad hoc network i.e., mesh network, mobile ad hoc network, and vehicular ad hoc network. Although, wireless sensor network and delay tolerant protocol is also a significant form of ad hoc network, it has made some strong security implementation and is less considered when it comes to ad hoc environment. So, this manuscript doesn't discuss any research progress towards secure routing for wireless sensor network. Section II discusses security challenges followed by a discussion of existing techniques in Section III. Section IV discusses research gap while Section V briefs about the conclusion and tentative future direction of the research in secure routing in the wireless ad hoc network.

II. Security Challenges in Wireless Ad Hoc Network

The inherent characteristics of the wireless ad hoc network, itself, give rise to various forms of security challenges while performing routing operation. Some of the essential security challenges are as follows:

1) There is higher feasibility for a communication line to become victim of link attacks that could be in either of the form, i.e., messaging replay, impersonation, eavesdropping, etc. All these illegitimate operation offers a form of an access towards the confidential information. An intruder can directly corrupt the message or tamper the message using active attacks. All these adversarial operation leads to potential damage of integrity, availability, non-repudiation, and availability.

2) Normally, the nodes in wireless adhoc network don't have effective physical security that leads it to a very vulnerable condition in hostile environment. Hence, it is unwise to consider that origination of the intrusion could possibly happen from outside only. In order to maintain highest level of resiliency, ad hoc network are demanded to possess a distributed architecture without any central actor.

3) The wireless ad hoc network is also characterized by the dynamic topology that will mean that the nodes are performing, joining and leaving the defined network very frequently.

III. Secure Routing in Wireless Ad Hoc Network

A secure routing protocol over the wireless ad hoc network is not only meant for offering security features but also should keep communication performance in mind (Fig. 1). It has been seen that existing routing protocols can quite well cater up to the need of dynamic topology of ad hoc network, but they are highly incapable of resisting the malicious attacks.

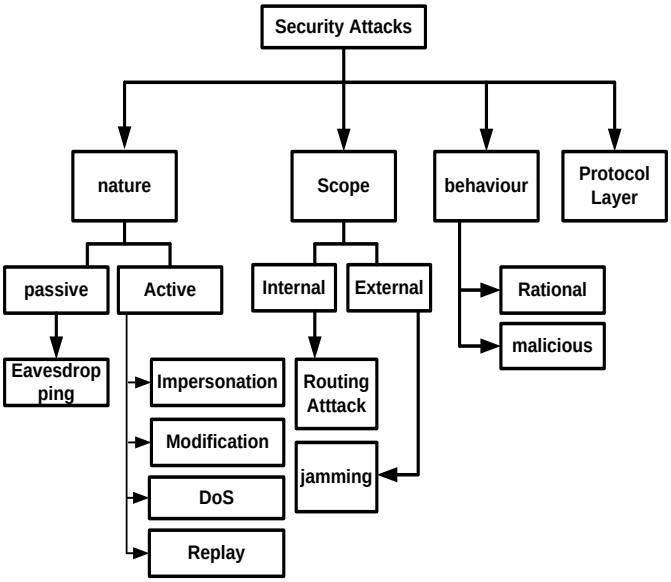

Fig. 1. Security intrusion in wireless ad hoc network.

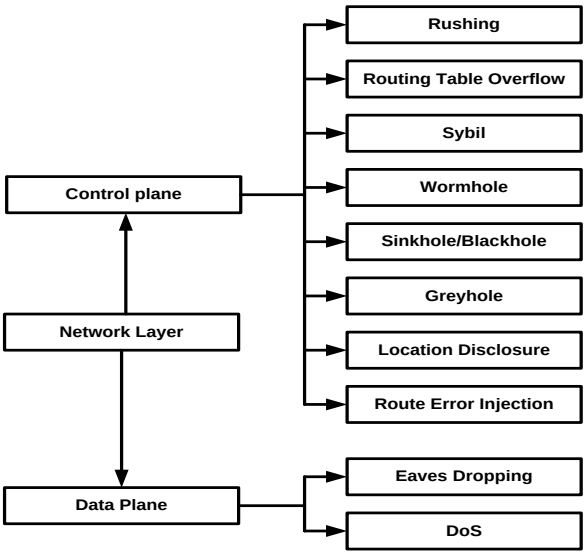

Fig. 2. Taxonomies of attacks on network layer

A closer look into the security attack taxonomies will show that there are essentially four types of intrusion in routing operation of wireless ad hoc network, i.e., attacks based on nature, attacks based on scope, behaviour-related attacks, and attacks on protocol layers. The frequently heard attacks of active and passive type come under nature-based attacks. Routing attacks come under internal attack while jamming attack comes under external attack. There are also behavioural-based attacks. The protocol layer-based attacks are classified depending on multiple layers, i.e., physical layer (jamming), MAC layer (flooding, MAC spoofing, replay attack), network layer (wormhole, control plane attack, sinkhole, blackhole, denial of service, eavesdropping), TCP layer (flooding and de-synchronization based attack). Attack associated with protocol layer particularly is more affected on network layer where the majority of the secure routing is implemented. Fig. 2 shows the taxonomies of attacks over network layer.

Basically, to resist such attacks, a secure routing protocol in the wireless ad hoc network is designed that are of two types: i.e., (1) *proactive* and (2) *reactive* form. *Secure Efficient Distance Vector Routing* (SEAD) [5] and *Secured Link State Protocol* (SLSP) [6] are two prominent protocols in proactive routing. SEAD is designed using destination sequence distance vector and is essentially meant for resisting jamming attacks, denial-of-service attacks, or any other forms of attacks that result in valuable resource consumption. The routing message is authenticated using the sequence number in SEAD. One of the major limitations of SEAD protocol is its dependencies of trusted entity that performs distribution of symmetric key in the network. Such phenomenon may give rise to bottleneck issue in the network. The next secured protocol SLSP is designed using link state protocol approach that aims to discover an effective topology followed by dissemination of packets of link state. It uses one-way hash function and neighbor lookup protocol for broadcasting state information. Unfortunately, SLSP is incapable of resisting colluding attacks, e.g., blackhole and wormhole attacks.

TABLE. I. CHARACTERISTICS OF SECURED ROUTING PROTOCOL

Protocol	Feature	Can resist	Cannot resist
SEAD	-Trusted Third Party (TTP) -Authentication using hop-by-hop -Hash function	-Rushing attack -Denial-of-Service	-Wormhole attack -Blackhole attack -Location disclosure
SLSP	-Threshold cryptography -Neighbour Lookup Protocol -Certification of Public keys by TTP	-Spoofing -Denial-of-Service	-Wormhole attack -Blackhole attack -Location disclosure
SAR	-Usage of different keys -Enhanced AODV implementation	-Rushing Attack -Routing Attack -Blackhole Attack	-Denial-of-Service -Wormhole Attack -Location disclosure
SRP	-Enhancement of Dynamic Source Routing -MAC is used for authentication Route Request and Route Reply	-Rushing Attack -Poisoning Attack -Routing Table Attack	-Denial-of-Service -Wormhole Attack -Location disclosure
SAODV	-Usage of Digital Signature -One-way Hash Chain -Enhancement of AODV	-Route Reply Attack -Rushing Attack -Replay Attack -Poisoning Attack -Routing Table Attack	-Denial-of-Service -Wormhole Attack -Blackhole Attack -Location disclosure
ARIADNE	-Secret Shared Key -Clock Synchronization -Authentication (end-to-end) -Dependency of key distribution center	-Selective Packet Dropping -Rushing Attack -Poisoning Attack -Routing Table Attack	-Denial-of-Service -Wormhole Attack -Blackhole Attack -Location disclosure
ARAN	-Uses TTP -Apriori secure link information among the nodes	-Spoofing -Rushing Attack -Illegitimate node participation	-Route Request Attack -Denial-of-Service -Flooding Attack -Wormhole Attack -Blackhole Attack
SEAODV	-Enhancement of AODV -Message Authentication (hop-by-hop) -Bloom's key	-Rushing Attack -Flooding Attack	-Denial-of-Service -Wormhole Attack -Blackhole Attack -Location disclosure

The reactive protocols make use of flooding of route request message and further classified into 6 types: i.e., 1) *Security-aware Ad hoc Routing* (SAR) [7], 2) *Secure Routing Protocol* (SRP) [8], 3) *Secure Ad hoc On-demand Distance Vector* (SAODV) [9], 4) *A Secure On-demand Routing Protocol for Ad hoc Network* (ARIADNE) [10], 5) *Authenticated Routing for Ad hoc Network* (ARAN) [11], and 6) *Secured Enhanced AODV* (SEAODV) [12]. The numbers of secure routing techniques are more in reactive form as compared to proactive form. Therefore, we briefly discuss its characteristics in Table 1.

There are also other forms of taxonomies of intrusion when it comes to secure routing protocol in the wireless ad hoc network. We find that design of secure routing is done by *prevention* and *identification* approach. Some good example prevention-based routing approaches are i) ARAN (using asymmetric cryptography), ii) SAR and SRP (using symmetric cryptography), iii) SEAD and ARIADNE (using one-way hash chain), iv) SLSP and SAODV (hybrid approach). Similarly, secure routing protocols based on identification are as follows e.g. i) Byzantine algorithm [13], ii) CORE algorithm [14], iii) CONFIDANT algorithm [13], and iv) WatchDog and Pathrater [15]. However, in the vehicular network, the trust factor is extensively used. The secure routing techniques in vehicular network consist of *infrastructure based* and *self-organizing based trust*. The majority of the existing secure routing protocols towards trust-based approaches mainly use precise location of the source, cryptographic authentication using public key infrastructure, repudiation of transmitter's identity, message transmission of other vehicular nodes, and validation of infrastructure. The existing techniques towards securing communication in the wireless ad hoc network mainly attempts to offer security toward the broadcasted information that bears sender's information during route discovery process. The routing techniques are also meant to provide identification of the type of attacks especially about the spoofed or forfeited information during ad hoc communication. A greedy-based technique is one of the frequently used in the wireless ad hoc network. However, apart from securing the communication link, these reported existing protocols are consistently used in research work by different forms. Still, the biggest hurdle is that they are not completely capable of mitigating denial-of-service, wormhole attack, blackhole attack, location disclosure attack, etc. The next section highlights some recent work carried out in the secure routing protocol.

IV. EXISTING TECHNIQUES OF SECURE ROUTING

Studies towards evolving up a secured routing mechanism in the wireless ad hoc network have various variations of techniques as well as approaches. The existing security techniques are designed for addressing explicit problems about security loopholes. We discuss only the significant research techniques published during 2010 to till date. For effective discussion, we brief the existing research contributions to different categories of the wireless ad hoc network below.

A. Studies in Wireless Mesh Network

A Wireless Mesh Network (WMN) is a type of ad hoc network where multiple nodes are connected to each other in a mesh topology. It is characterized by multiple communication paths to ensure zero link breakage as well as it also ensures highest link quality by minimizing the spatial distance among the nodes [16]. The best part is WMN can be combined with

existing standards, e.g., IEEE 802.15/16/11, sensor network, the internet, etc. to offer data communication service. However, WMN suffers from significant security problems on routing as it highly depends on adopting multicast routing schemes. Such schemes are never safe for active intrusions. Most recent, the work carried out by Matam and Tripathy [17] have used digital signatures for developing a secure routing mechanism to resist wormhole attack in WMN. The study outcome was compared with some of the conventional routing scheme to find better security performance. Another significant problem associated with WMN is involvement of multiple operators that results in zero cooperation finally leading to malicious behavior of a node. This problem has been addressed by Subhash and Ramachandram [18] who enhanced the feature of Ad hoc On-Demand Distance Vector (AODV) for constructing a trust and reputation model. The technique implements an algorithm to evaluate trust followed by recommendation of trust and selection of secured trusted path. The above-mentioned problems of multiple operator involvements also lead to intrusion of privacy in WMN as the attacks based on network layers are too high in it. This problem was found to be addressed by Meganathan and Palanichamy [19] who have used cross-layer approach with group signature scheme to resist such attacks. The technique also uses dynamic reputation for building subjective logic while performing route discovery in WMN. Adoption of the cross layer has been seen in the study of Bansal *et al.* [20] for developing a unique intrusion detection system. Such problems of intrusion can be counter-measured by including strong authentication protocol. Li *et al.* [21] have presented a public key encryption for enhancing the operability of Kerberos protocol by using arbitrary numbers. Hybridizing is another mechanism found out by certain researcher, e.g., Avule *et al.* [22] for strengthening security in WMN. This technique appends fields of message extension to the frame elements of selected route. The study outcome shows good communication performance for the smaller network. For the larger network, WMN uses hop-by-hop communication that is highly prone to cyber-attack. This problem was addressed by Gharavi and Hu [23] by using a dynamic update strategy towards the distribution of the secure key. The technique utilizes hash-based encryption to cipher the secure messages against Denial-of-Service attacks in WMN. There is already a default routing protocol in WMN that are found to be protected by various existing research-based secured routing technique. Tan *et al.* [24] have evaluated the strength of existing security approaches. The study outcome speaks of non-availability of robust security feature while routing in WMN.

B. Studies in Mobile Ad hoc Network

Mobile Ad hoc Network (MANET) is another type of wireless ad hoc network where each mobile node are also considered to be the router. It has highly decentralized architecture and characterized by dynamic topology. These inherent characteristics are itself possessed as a great security threat to its routing protocols. Although there are various existing studies towards secured routing in MANET [25], there is no single standard protocol being found 100% resilient against complex intrusion. In this regards, AODV is being used various researchers for incorporating security in MANET. Alkhamisi and Buhari [26] have enhanced the AODV by introducing multipath-based and trust-based communication in it. The technique is responsible for monitoring the communication behavior of a mobile node followed by computation of trust factor for identification of intrusion. Discussion of trust-model was also seen in the studies of Rikli and Alnasser [27] who have developed a centralized architecture to compute trust. Another bigger problem within MANET secure routing is the adoption of multicast communication strategy that drains high energy and overshoots delay and overheads. This problem was addressed by Madhusudhanan *et al.* [28] by introducing key management exclusively for multicast routing. This technique utilizes encryption techniques with the session key for forwarding the data using multicast routing over fixed interval for rekeying. Security problems about multicast routing in MANET have been addressed by Vijendran and Gripsy [29]. This technique assists in on-demand discovery. Multicast routing also leads the location information quite vulnerable in MANET. Research in this direction has been carried out by Saravanan and Sakthivel [30] who have used a digital signature with a time stamp for carrying out authentication. A private key crypto-system has been introduced with a symmetric key for ensuring sufficient privacy of location information in MANET. There are also schemes that perform repeated encryption process to resists attacks. One such scheme is found in the work of Wu *et al.* [31] where symmetric encryption is used without any need to change source node protocol. Sekaran and Parasuraman [32] have used Advanced Encryption Standard (AES) algorithm to secure communication while disseminating location information within it. The technique is resistive against any attack that causes depletion of the energy of the mobile node at any cause. Study towards addressing anonymity problems in communication for ad hoc network has been carried out by Yuan [33]. The technique renders all the communication nodes along with the intermediate node anonymous using the public key. The technique is found to be completely independent of any additional key establishments. Sagheer and Taher [34] have used identity-based encryption over AODV to offer secured routing. A similar form of study was also carried out by Wan *et al.* [35] where author have addressed the privacy problems as well as unlink ability issue in communication over MANET. The technique mainly uses identity-based encryption and group signature to retain potential privacy.

C. Studies in Vehicular Ad hoc Network

Vehicular Ad hoc Network (VANET) is another form of wireless ad hoc network that is characterized by infrastructure less and applies multihop network for providing communication. The study of VANET considers two forms of actors i.e. Road Side Unit (RSU) and On-Board Unit (OBU). A vehicle node is normally termed as OBU which has communicated with another OBU using RSU [36]. Hence, as faster security operations are required in VANET system that can normally be offered by Public Key Infrastructure (PKI). Unfortunately, these mechanism suffers from serious pitfalls, and hence it is not much applicable in VANET system (however, it is much better in another form of the wireless system e.g. wireless sensor network). Study on this direction was carried out by Tan *et al.* [37] by introducing a unique key management approach. The technique uses asymmetric

encryption mechanism for controlling the computational cost. The technique allows concatenating identity and its respective public key for OBU as well as RSU that results in the elimination of revocation list of certificates. Another key management strategy has been introduced by Vijayakumar *et al*. [38] that center around trusted authority to perform communication. The technique introduces a dual authentication approach for resisting illegitimate vehicular node from entering VANET system. Similarly, key management is also carried out using dual manner for effective dissemination of group key. The study contributes to cost-effective mechanism to add or revoke user in VANET. Study towards strengthening authentication mechanism is also discussed by Wang *et al*. [39] along with privacy problems. The technique uses biological password as well as decentralized digital certificate to perform authentication. In cryptography, ensuring fault tolerance is one of the challenging tasks especially in VANET system. Research towards implementing fault tolerant communication system has been carried out by Li *et al*. [40]. The author uses the Light Encryption Device (LED) principle that was originally implemented by Guo *et al*. [41]. The technique is claimed to support 64-128 bit encryption key that is similar to AES performance. Ultimately, the study finds the vulnerability factor of LED in VANET system. However, one of the biggest impediments towards VANET security is to even identify the extent of malicious information in dissemination process. A research attempt of Li and Song [42] has introduced a methodology using trust factor for identification of the malicious node as well as malicious data. Lo, and Tsai [43] have used Elliptical Curve Cryptography (ECC) as well as an identity-based signature mechanism to secure the communication system in VANET. The scheme mainly focuses on efficient authentication process between RSU and Vehicular nodes. Study towards group key dissemination scheme is presented by Park and Seo [44]. The technique constructs protocols for securing a vehicle to vehicle communication along with the assurance of system integrity. Tan *et al*. [45] have introduced filtering algorithm based on the fuzzy logic-based approach to computing the trust factor of a node in VANET. An interesting technique has been presented by Tripathi *et al*. [46] towards privacy problems in VANET system by incorporating private key encryption. Uniquely, the technique uses multilingual translation mechanism for encoding the messages. Yang *et al*. [47] have used reputation-based approach along with Dempster-Shafer evidence theory for identifying the selfish node. The technique is also found to address the energy problems too along with security features. Abumansoor and Boukerche [48] have addressed the security problem arising from the location of non-line of sight in VANET. The summary of the existing techniques to secure the wireless ad hoc network is sown below in Table 2.

TABLE. II. SUMMARY OF EXISTING TECHNIQUES TO SECURE WIRELESS AD HOC NETWORK

	Authors	Problems	Techniques	Contribution	Limitation
Wireless Mesh Network	Matam [17]	Wormhole attack	Digital signature	Resistive against routing loop attack, Route corruption attack, metric manipulation attack.	It doesn't offer faster response time for large network
	Subhash [18]	Node misbehaviour	Trust and reputation	Accurate trust recommendation	Trust model offer significant overhead
	Meganathan [19]	Network layer attacks	Cross layer, ID based encryption, group signature	Ensure privacy, security, reliability	Lower response rate, computational complex
	Bansal *et al*. [20]	Detection of malicious behaviour	Cross layer,	Resistive towards low intensity attack and can identify switching behaviour	Outcomes are not benchmarked
	Li *et al*. [21]	Authentication	Enhancing Kerberos protocol using public key cryptography	Public keys are kept separated from higher calculation of cost	No benchmarking of outcomes, less consideration of mobility.
	Avule *et al*. [22]	Security attacks	Adding fields to frames of selected path	Protect both mutable and non-mutable fields, good communication performance	Not applicable to large scale networks
	Gharavi [23]	Cyber-attack, denial-of-service	Hash based encryption	Simplified encryption technique	Only subjective to denial of service attack
	Tan *et al*. [24]	Comparative study of existing secure routing	Comparative analysis	Existing techniques are not robust	-
Mobile Ad hoc Network (MANET)	Alkhamisi [26]	Attack identification & isolation	Enhancing AODV, adding trust	Enhances throughput	Less effective benchmarking, behaviour to large & sparse network is not found
	Rikli [27]	Attack identification	Trust-based modeling	Claimed to detect all types of attackers	Recursive functions will lead to complexity and overhead It is subjective approach to sensor network only.

	Madhusudhanan *et al*. [28]	Security in multicast routing	Key management, fixed interval for rekeying, session key	Minimizes overhead of rekeying	Rekeying generates memory overflow in dense network
	Vijendran [29].	Security in multicast routing	Dynamic mobile point relay, location	Claimed to be energy efficient	Delay and overhead could possibly shoot up in real-time file transmission as well as in large network.
	Saravanan [30]	Privacy of location in multicasting, identity-spoofing attack	Symmetric key, digital signature	Ensure location anonymity	Not applicable for variable bit rate traffic, less evidence to prove key strength
	Wu *et al*. [31]	Routing attack	Double encryption	Have low complexity	Not applicable to variable bit rate traffic, not tested over large scale network.
	Sekaran [32]	Security and seamless communication	AES protocol	Good communication performance	Outcome is not benchmarked, algorithm complexity over not is not testified
	Yuan [33]	Packet analysis attack, anonymity problems of nodes, active attacks, denial-of-service	Public key encryption	Zero dependency of extra key establishment	Uses RSA
	Taher [34]	Security for nodes	Identity-based encryption	Simple technique	Not applicable for larger network with increased node mobility
	Wan *et al*. [35]	Anonymity	Identity-based encryption, group signature	Better packet delivery performance	Not applicable for larger network with increased node mobility
Vehicular Ad hoc Network (VANET)	Tan *et al*. [37]	PKI problems	Asymmetric encryption	Control computational cost, reduced time for key generation	High storage cost
	Vijayakumar *et al*. [38]	Authentication, key management	Fuzzy logic, dual approach for group keying and authentication	Computationally cost effective	Doesn't address node location privacy, constructed fuzzy rule-set cannot cover up entire dynamic scene of communication.
	Wang *et al*. [39]	Authentication, privacy	Biological password, decentralized certificate authority	Significant control over computational cost, minimizes overheads	Resilient to only denial-of-service
	Li *et al*. [40]	Assessing fault for LED	Mathematical analysis	Study finds LED to be vulnerable	Study focused on side-channel attack
	Li [42]	Identification of data trust	Trust management scheme	Better precision performance	Chances of increased overhead on large network
	Lo [43]	Privacy in VANET	Identity-based signature, ECC	Reduced time consumption	Iterative process will lead to space complexity
	Park [44]	Securing group communication	Constructed protocol to protect group key	Faster response time, scalable performance	Outcomes not benchmarked
	Tan *et al*. [45]	Attacks in data plane of VANET	Fuzzy logic	Detects and resist well for attacks in data plane	Constructed fuzzy rule-set cannot cover up entire dynamic scene of communication.
	Tripathi *et al*. [46]	Privacy in VANET	Multilingual translational	Very simple technique to implement	Not resistive against node capture attack or key compromise attack.
	Yang *et al*. [47]	Selfish node in VANET	Dempster Shafer, Reputation	Faster response time for decision making	Space complexity not addressed
	Abumansoor [48]	Security over non-line of sight	Collaborative protocol	Maintains integrity in localization services	Protocol doesn't work if there is no shared neighbor node.

V. RESEARCH GAP

From the previous section, it has been seen that there are various attempts being made towards addressing secure routing problems in the wireless ad hoc network. Table 1 has discussed the contribution along with limitations of each approaches being studied. There is no doubt that all the above-mentioned techniques have some significant contribution that assists the future researchers potentially; however, it cannot be ignored that each technique of existing literature is also associated with certain limitation. In this section, we will point out certain research gap, which we felt that it could have been addressed in the past but was not found so because of unknown reason. The significant research gaps are as follows:

A. Unbalanced Focus in Research Technique

It could be notably understood that there are discrete forms of secure routing techniques and trust/reputation-based approach is common to find in the wireless ad hoc network. The majority of the research using trust has used it only for choosing the secured route that is found matching with certain trust conditions. Unfortunately, such schemes are not found to balance the anticipated communication need (e.g., throughput) of a node in the generic environment of the wireless ad hoc network. Similarly, we also find that the methodologies of designing intrusion detection system are quite specific to a type of wireless ad hoc network that will mean its dependencies over the specific form of network. It will also mean that such scheme may be very particular to one type of wireless ad hoc network and cannot be exchanged with each other. This will pose a practical implementation of the wireless ad hoc network in real-time while working on the collaborative network. Another observation is that all the trust-based approaches have been remodeled and novelty is still missing. Hence, there is a need that such techniques should be seriously designed by re-defining the generic environment of the wireless ad hoc network.

B. Frequent Usage of AODV

The majority of the studies towards secure routing over the wireless ad hoc network is constructed on the top of frequently used AODV as routing protocol. Well, the problem is AODV suffers from the problem of stale data while routing and it can significantly generate control overhead. Existing study doesn't enhance AODV but just add security on the top of it that eventually means that still the legacy communication problems in a new protocol are allowed to be continued unnoticed. It was also known that usage of AODV or applying any form of remodeling it with sophisticate cryptography (e.g., hashing, ECC, symmetric encryption, etc.) will only lead to bandwidth consumption that has never been found to be testified while evaluating security strength in the existing system. There is far better and efficient routing protocol in wireless ad hoc network, e.g., Optimized Link State Routing (OLSR) which could also be used in secure routing. However, the trend is more on AODV while implying security features.

C. Missing Feature in Attack Identification and Isolation Techniques

Maximum category of the existing literature is focused on using the principle of attack identification and isolation. However, we find that such schemes are all focused on particular types of attack and that will mean that they are not capable of resisting another form of attack. The second problem in all these approaches is that they consider single intruders while routing and so existing system fails to address the security breach problem that may occur in the presence of dual colluding intruders. The third potential problem in this regard is that all the cryptographic based approach are shown to have a successful outcome when it comes to identification of attacks. However, there are no significant studies where the malicious nodes have been identified effectively. Certain studies which introduces selfish node may turn out to be regular node after accomplishing its objective, and hence existing techniques fails to discretize the form of attack while constructing the secure routing principle.

D. Less Focus on Computational Complexity

Existing techniques using digital signatures can potentially lead to communication overhead and possibly invite other forms of attack, which they are not meant to resist. The process of signing the message involves computational cost that may increase exponentially with increase in network sizes. There is also a possibility of lack of spontaneous network as such technique will require nodes to have apriori information about each other for facilitating sharing of public keys.

E. No Significant Initiative towards Optimization

We find that cost-effective optimization process is not being incorporated in the existing research techniques towards securing routing in the wireless ad hoc network. Without optimization technique, it is quite impossible for cost effectively plan the equilibrium between security computation and communication performance under any adverse scenario of intrusion. Hence, there is an emergent need for such research direction.

VI. CONCLUSION & FUTURE WORK

According to the theory, the wireless ad hoc network is one of the best alternative ways to establish connectivity in the region which doesn't have any form of infrastructure. However, establishing communication among the nodes is not that easy task in the ad hoc network as these nodes are consistently moving and forming a dynamic topology. The conventional study says that in MANET and rural VANET system, the node could move in any arbitrary direction; however, in the case of urban VANET system the path is very well defined. All this will mean that the applicability of the routing protocols in wireless ad hoc network differs in different forms of the network. This pattern is also same for secure routing protocols. First of all, there is extremely less progress made towards evolving up with secure routing techniques in the wireless ad hoc network, and the only handful of names of routing protocol exists in present time. This document has reviewed some of the recently implemented routing protocols to mitigate attacks in the wireless mesh network, mobile ad hoc network, and vehicular ad hoc network. We also find that there is significant research gap explored from existing literature, e.g., unbalanced focus in research technique, frequent usage of AODV, missing a feature in attack identification and isolation techniques, less focus on computational complexity, no

significant initiative towards optimization. So, our future work direction will be towards addressing such explored problems.

Our first initiative toward future research work will be to develop a secure routing protocol to address some lethal attacks. This review finding suggests that certain lethal attacks, e.g., wormhole attack, black hole attack, location disclosure, and denial-of-service are rarely addressed by existing secured routing techniques. Our future idea will be to evolve up with an analytical modeling that formulates a virtual decoy node to capture the attacker as well as isolate the attacker. A novel adversarial model will be designed based on the features of above-mentioned attacks. Our second research initiative will also be to explore the feasibility of coming up with cost effective optimization model as it is quite a few to find in existing literature.

REFERENCES

[1] N. Chaki, R. Chaki, "Intrusion Detection in Wireless Ad-Hoc Networks", CRC Press, pp. 258, 2014

[2] M.A. Matin, "Handbook of Research on Progressive Trends in Wireless Communications and Networking", IGI Global, pp. 592, 2014

[3] S. Khan, J.L. Mauri, "Security for Multihop Wireless Networks", CRC Press, pp. 538, 2016

[4] F. Anjum, P. Mouchtaris, "Security for Wireless Ad Hoc Networks", John Wiley & Sons, pp.316, 2007

[5] Y.-C. Hu, D.B. Johnson, and A. Perrig, "SEAD: secure efficient distance vector routing for mobile wireless ad hoc networks", In Proceedings of the 4th IEEE Workshop on Mobile Computing Systems and Applications (WMCSA'02), Callicoon, NY, USA, pp. 3 – 13, 2002

[6] P. Papadimitratos and Z. J. Hass, "Secure link state routing for mobile ad hoc networks", In Proceedings of the Symposium on Applications and the Internet Workshops (SAINT'03 Workshops), pp.379-383, Washington DC, USA, 2003

[7] S. Yi, P. Naldurg and R. Kravets, "Security-aware ad hoc routing for wireless networks", Proceedings of the ACM Symposium on Mobile Ad Hoc Networking and Computing (MobiHoc'01), Long Beach, CL, USA, pp.299 – 302, 2001

[8] P. Papadimitratos and Z. J. Haas, "Secure routing for mobile ad hoc networks", In Proceedings of the SCS Communication Networks and Distributed Systems Modeling and Simulation Conference (CNDS'02), San Antonio, TX, USA, pp. 27-31, 2002

[9] M. G. Zapata and N. Asokan. "Securing ad hoc routing protocols", In Proceedings of the 1st ACM Workshop on Wireless Security, Atlanta, GA, USA, pp. 1-10, 2002

[10] Y.-C. Hu, A, Perrig, and D. Johnson, " Ariadne: a secure on-demand routing protocol for ad hoc networks", In Proceedings of ACM Annual International Conference on Mobile Computing (MobiCom'02), Atlanta, GA, USA, pp. 21 – 38, 2002

[11] K. Sanzgiri, B. Dahill, B.N. Levine, C. Shields, and E.M. Belding-Royer, "A secure routing protocol for ad hoc networks", In Proceedings of the 10th IEEE International Conference on Network Protocols (ICNP'02), Paris, France, pp. 78 – 87, 2002

[12] C. Li, Z. Wang, and C. Yang, "Secure routing for wireless mesh networks", International Journal of Network Security, vol 13, no 2, pp. 109-120, 2011

[13] M. Yu, M. Zhou and W. Su, "A Secure Routing Protocol Against Byzantine Attacks for MANETs in Adversarial Environments," in IEEE Transactions on Vehicular Technology, vol. 58, no. 1, pp. 449-460, 2009.

[14] P. Tomar, P.K. Suri, M.K. Soni, "A Comparative Study for Secure Routing in MANET", International Journal of Computer Applications, Vol.4(5), pp.17-22, 2010

[15] "Chapter 11 Detecting Bad Behaviors", http://perso.crans.org/raffo/papers/phdthesis/thesisch11.html, Retrieved 16th June-2017

[16] S. Misra, S.C.Misra, I.Zhang, "Guide to Wireless Mesh Networks", Springer Science & Business Media, pp.528, 2009

[17] R. Matam and S. Tripathy, "Secure Multicast Routing Algorithm for Wireless Mesh Networks", Journal of Computer Networks and Communications, pp.11, 2016

[18] P. Subhash and S. Ramachandram, "Trust Based HWMP Protocol in High-Performance Wireless Mesh Networks", work, vol.5(6), pp. 11-25, 2016

[19] N.T. Meganathan and Y. Palanichamy, "Privacy Preserved and Secured Reliable Routing Protocol for Wireless Mesh Networks", The Scientific World Journal, pp.12, 2015

[20] D. Bansal, S. Sofat and P. Kumar, "Distributed cross layer approach for detecting multilayer attacks in wireless multi-hop networks," *2011 IEEE Symposium on Computers & Informatics*, Kuala Lumpur, pp. 692-698, 2011

[21] M. Li, X. Lv, W. Song, W. Zhou, R. Qi, and H. Su, "A novel identity authentication scheme of wireless mesh network based on improved kerberos protocol", In Distributed Computing and Applications to Business, Engineering and Science (DCABES), 13th International Symposium, pp. 190-194, 2014.

[22] M. Avula, S-G. Lee, and S-M. Yoo, "Security Framework for Hybrid Wireless Mesh Protocol in Wireless Mesh Networks", TIIS, vol. 8, no. 6, pp.1982-2004, 2014

[23] H. Gharavi and B. Hu, "4-way handshaking protection for wireless mesh network security in smart grid", In Global Communications Conference (GLOBECOM), pp. 790-795, 2013

[24] W.K. Tan, S-G. Lee, J.H. Lam, and S-M. Yoo, "A security analysis of the 802.11 s wireless mesh network routing protocol and its secure routing protocol" Sensors, vol. 13, no. 9, pp.1553-11585, 2013

[25] J. Loo, J.L.Mauri, J. H.Ortiz, "Mobile Ad Hoc Networks: Current Status and Future Trends", CRC Press, pp.538, 2016

[26] A. O. Alkhamisi and S. M. Buhari, "Trusted Secure Adhoc On-demand Multipath Distance Vector Routing in MANET," *IEEE 30th International Conference on Advanced Information Networking and Applications (AINA)*, Crans-Montana, pp. 212-219, 2016

[27] R. Nasser-Eddine, and A. Alnasser, "Lightweight trust model for the detection of concealed malicious nodes in sparse wireless ad hoc networks", International Journal of Distributed Sensor Networks, Vol. 12, no. 7, pp.1-16, 2016

[28] B. Madhusudhanan, S. Chitra, and C. Rajan, "Mobility based key management technique for multicast security in mobile ad hoc networks," The Scientific World Journal, pp.10, 2015

[29] A.S. Vijendran and J. V. Gripsy, "Enhanced secure multipath routing scheme in mobile adhoc and sensor networks", In Current Trends in Engineering and Technology (ICCTET), 2nd International Conference, pp. 210-215, 2014.

[30] T.R. Saravanan, and P. Sakthivel, "Location privacy protection for secure multicasting in MANET", In Recent Advances in Electronics & Computer Engineering (RAECE), National Conference, pp. 59-64, 2015

[31] X. Wu, X. Zhu and F. Kong, "Routing and Data Security Scheme Based on Double Encryption in Mobile Ad Hoc Networks," *Fifth International Conference on Instrumentation and Measurement, Computer, Communication and Control (IMCCC)*, Qinhuangdao, pp. 1787-1791, 2015

[32] R. Sekaran and G.K. Parasuraman, "A Secure 3-Way Routing Protocols for Intermittently Connected Mobile Ad Hoc Networks", The Scientific World Journal, pp.13, 2014

[33] W. Yuan, "An anonymous routing protocol with authenticated key establishment in wireless ad hoc networks", International Journal of Distributed Sensor Networks, pp. 10, 2014

[34] A.M. Sagheer and H. M. Taher, "Identity Based Cryptography for secure AODV routing protocol", In Telecommunications Forum (TELFOR), 2012 20th, pp. 198-201, 2012

[35] Z. Wan, K. Ren and M. Gu, "USOR: An Unobservable Secure On-Demand Routing Protocol for Mobile Ad Hoc Networks," in *IEEE Transactions on Wireless Communications*, vol. 11, no. 5, pp. 1922-1932, May 2012.

[36] Al-S.K.Pathan, "Security of Self-Organizing Networks: MANET, WSN, WMN, VANET", CRC Press, pp. 638, 2016

[37] H. Tan, M. Ma, H. Labiod, A. Boudguiga, J. Zhang and P. H. J. Chong, "A Secure and Authenticated Key Management Protocol (SA-KMP) for Vehicular Networks," in *IEEE Transactions on Vehicular Technology*, vol. 65, no. 12, pp. 9570-9584, 2016.

[38] P. Vijayakumar, M. Azees, A. Kannan and L. Jegatha Deborah, "Dual Authentication and Key Management Techniques for Secure Data Transmission in Vehicular Ad Hoc Networks," in *IEEE Transactions on Intelligent Transportation Systems*, vol. 17, no. 4, pp. 1015-1028, 2016

[39] F. Wang, Y. Xu, H. Zhang, Y. Zhang and L. Zhu, "2FLIP: A Two-Factor Lightweight Privacy-Preserving Authentication Scheme for VANET," in *IEEE Transactions on Vehicular Technology*, vol. 65, no. 2, pp. 896-911, 2016.

[40] W. Li, W. Zhang, D. Gu, Y. Tao, Z. Zhao, Z. Liu, "Impossible Differential Fault Analysis on the LED Lightweight Cryptosystem in the Vehicular Ad-Hoc Networks," in *IEEE Transactions on Dependable and Secure Computing*, vol. 13, no. 1, pp. 84-92, 2016.

[41] J. Guo, T. Peyrin, A. Poschmann and M. Robshaw, "The LED Block Cipher", Springer, pp. 326-341, 2011

[42] W. Li and H. Song, "ART: An Attack-Resistant Trust Management Scheme for Securing Vehicular Ad Hoc Networks," in *IEEE Transactions on Intelligent Transportation Systems*, vol. 17, no. 4, pp. 960-969, 2016.

[43] N. W. Lo and J. L. Tsai, "An Efficient Conditional Privacy-Preserving Authentication Scheme for Vehicular Sensor Networks Without Pairings," in *IEEE Transactions on Intelligent Transportation Systems*, vol. 17, no. 5, pp. 1319-1328, 2016.

[44] Y. H. Park and S. W. Seo, "Fast and Secure Group Key Dissemination Scheme for Out-of-Range V2I Communication," in *IEEE Transactions on Vehicular Technology*, vol. 64, no. 12, pp. 5642-5652, 2015.

[45] S. Tan, X. Li and Q. Dong, "A Trust Management System for Securing Data Plane of Ad-Hoc Networks," in *IEEE Transactions on Vehicular Technology*, vol. 65, no. 9, pp. 7579-7592, 2016.

[46] V. K. Tripathi and S. Venkaeswari, "Secure communication with privacy preservation in VANET- using multilingual translation," *2015 Global Conference on Communication Technologies (GCCT)*, Thuckalay, pp. 125-127, 2015

[47] Y. Yang, Z. Gao, X. Qiu, Q. Liu, Y. Hao, and J. Zheng, "A hierarchical reputation evidence decision system in VANETs", International Journal of Distributed Sensor Networks, pp.4, 2015

[48] O. Abumansoor and A. Boukerche, "A Secure Cooperative Approach for Nonline-of-Sight Location Verification in VANET," in *IEEE Transactions on Vehicular Technology*, vol. 61, no. 1, pp. 275-285, Jan. 2012

AUTHOR'S PROFILE

Jyoti Neeli, is currently a research scholar in RV College of Engineering, Bengaluru working as an Associate Professor in Department of Information Science & Engineering Global Academy of Technology, Bengaluru. She has completed her M. Tech in Computer Science & Engineering from VTU. She has 15 years of experience in teaching and 6 years in R&D. Her area of interest includes Computer networks, Software testing, Mathematical models.

Dr. N K Cauvery, is Professor and Head of Department of Information Science & Engineering, RV College of Engineering, Bengaluru. She has completed her Ph. D from VTU with research title as *"Routing in Computer Network using Genetic Algorithm".* She has 17 years of experience in teaching and 7 years in R&D. She has published papers both in national & international conferences. Her area of interest includes Computer network, Compiler Design, Genetic Algorithm.

Environments and System Types of Virtual Reality Technology in STEM: A Survey

Asmaa Saeed Alqahtani
Department of Computer Science
Najran University
Najran, Saudi Arabia

Dr. Lamya Foaud Daghestani
Department of Computer Science
King Abdulaziz University
Jeddah, Saudi Arabia

Prof. Lamiaa Fattouh Ibrahim
Department of Computer Science
King Abdulaziz University
Jeddah, Saudi Arabia

***Abstract*—Virtual Reality (VR) technology has been used widely today in Science, Technology, Engineering and Mathematics (STEM) fields. The VR is emerging computer interface distinguished by high degrees of immersion, trustworthy, and interaction. The goal of VR is making the user believe, as much as possible, that he is within the computer-generated environment. The VR has become one of the important technologies to be discussed regarding its applications, usage, and its different types that can achieve huge benefits in the real world. This survey paper introduces detail information about VR systems and requirements to build correct VR environment. Moreover, this work presents a comparison between system types of VR. Then, it presents the tools and software used for building VR environments. After that, we epitomize a road of the map for selecting appropriate VR system according to the field of applications. Finally, we introduce the conclusion and future predictions to develop the VR systems.**

Keywords*—Virtual reality; 3D graphics; immersion; 3D images; navigation; multimedia

I. Introduction

In most of the sciences which contained concepts and principles of 3D images, there is a need to represent it using the technology of VR. The VR is a natural extension to 3D computer graphics consisted of 3D manufacturing and design tools to create and design computer-aided engineering [1], [2].

The VR has become one of the important technologies to be discussed regarding its applications, usage, and its different types that can achieve huge benefits in the real world. The VR considered as full visualization environment using appropriate computer technologies. In most of the learning environment, the VR becomes possible for many learners or trainees to simulate the real world. The benefits of this technology often start with computer graphics and continue for long times.

The VR allows the user and learner to watch the external world by different dimensions as its real world in and to try things that are not accessible in real life or even not yet created [3]. Also, it could be said that the VR depends on the internet networks and simulation that can help trainers or educators to interact through motion, embodiment and graphical images that idealize persons. So, VR can be defined in general as computer graphics that allowing to see the unseen and provides new shrewdness into the underlying data [4].

Many years ago, educators started to explore VR as a powerful multimedia for the education. The VR allows for continuing and growing social interaction that can enhance cooperative learning. VR can adapt and grow to meet different user needs.

The next section discusses concepts of VR. Section 3 represents the emergence of VR till date. After that Section 4 discusses VR applications, then Section 5, VR requirements. Section 6 discusses essential elements of VR environments. Section 7 talks about the literature review. Section 8 discusses the VR software and tools. Section 9 shows the navigation in VR environments. Section 10 represents benefits and limitation of VR technology. Section 11 summarizes the road map of this survey. The paper's conclusion is presented in Section 12.

II. Concepts of Virtual Reality

The use of 3D as it is a virtual world in education is to increase because the 3D virtual world has a strong sense of existence even in remote participants, and because it increases the social awareness and communication of human [5].

Many researchers have previously talked about the term of VR. In this section, we will highlight some of the most prominent and important definitions concerning the term VR.

The VR is emerging computer interface distinguished by high degrees of immersion, trustworthy, and interaction. The goal of VR is making the user believe, as much as possible, that he is within the computer-generated environment [6].

According to [7], the VR is "technology that allows us to create environments where we can interact with any object in real time, and that has been widely used for training and learning purposes." The integration some of technologies and hardware such as computers and graphics software can generate the technology of VR. So, the VR can be summed up as it is a progressing computer interface to allow the user to be immersed in a simulated environment generated by a computer.

Over and above, the VR can be defined as it is a system according to [2], which said that the VR is "human–computer environments in which users are immersed in and able to perceive, act and interact with a three-dimensional world." The VR has no criterion definition that makes it considered as a difficult task. VR can be an oxymoron as it denoted by some school of intellect as "reality that does not exist" [8]. There are many names used interchangeably with the VR. These names can be Virtual Environment, Artificial Reality, Virtual Worlds, Artificial Worlds, or Cyberspace.

The Virtual Environment (VE) defined as a digital space in which a user's movement is tracked and his or her surroundings playback, or numerals composed and offered to the senses, by those movements. For instance, when educators start using computer playtimes it can be noticed that handlebar movement can be followed and tracked and his or her character moves forward, rendering a new environment [9].

III. Emergence of VR Technology

The term VR came from Jaron Lanier, who is the founder of VPL Research. However, it was in 1965 that Ivan Sutherland published a paper entitled "The Ultimate Display" which described how one day; the computer would provide a window into virtual worlds [3].

VR came into public consciousness as a medical toy with equipment's including kid's MX Motocross, helmet, glove, and others which were discriminatory determined from the wider public and the price of this system will not be expensive. After that the companies, which produce the system of VR, directed to develop and provide the system for the data collected and analyzing it. This usage could be indicated that the VR often used in the application that is based on 3D space for analyzing and in the visualization of overall physical dimensions. The data used in VR substantially integrated due to the ability of VR to display 3D data with sounds and touch information [10].

The emergence of VR can be highlighted at the following main points [3]:

A. Sensorama (invited in 1957, Morton Heilig)

Sensorama is a machine patented in 1962. The system of Sencorama consisted of multi sensors that could make a chromatic film that previously recorded to be augmented by clear sound, smell, the wind and related vibration. The Sensorama was the first way to explore the system of VR. It had most of the features of such environment, but without interaction [11]. Fig. 1 shows the Sensorama machine. The Sensorama allow people to enter in the style of an interactive cinema [12].

B. The Ultimate Display (invented in 1965, Ivan Sutherland)

Sutherland tried to suggest a definitive solution for the VR. The suggestion aimed to make system consists of interactive graphics, with sound, smell, and force feedback as the construction of an artificial world. Fig. 2 shows the proposed ultimate display.

The ultimate display suggests using like a Head Mounted Display (HMD) to be as a window for the VR [13]. Sutherland said in his words about the ultimate display, it as "room within which the computer can control the existence of matter. A chair displayed in such a room would be good enough to sit in. Handcuffs displayed in such a room would be confining, and a bullet displayed in such a room would be fatal." [12], [14].

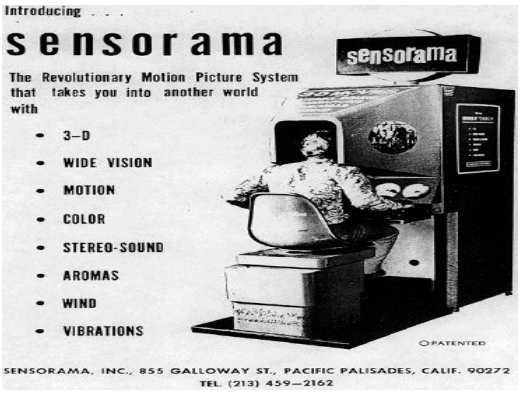

Fig. 1. Sensorama simulator device, [15].

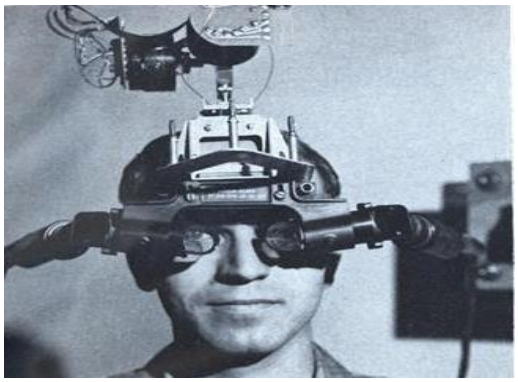

Fig. 2. The ultimate display, [16].

C. The Sword of Damocles

The Sword of Damocles is neither system nor the early concept of the VR. It considered as the first hardware of VR. The first Head Mounted Display (HMD) constructed by Sutherland. It contains sounds as stereo updated due to the position and navigation of the user. It is the implementation of the ultimate display.

D. GROPE

GROPE is "The first prototype of a force-feedback system realized at the University of North Carolina (UNC) in 1971". According to the notion of Sutherland's system, the UNC developed a system to force feedback devices and allow users feel simulated computer force [17], [11]. Fig. 3 shows the example of a force feedback device. It consists of a simple glove with a specific structure to give sensible feedback with "mechanically complex exoskeletal hand masters" [11].

GROPE aimed to combine both haptic display and visual one to produce a GROPE system. The latest prototype of GROPE is shown in Fig 4. It consisted of "ceiling-mounted arm coupled with a computer and was used by the chemists for a drug-enzyme docking procedure" [11].

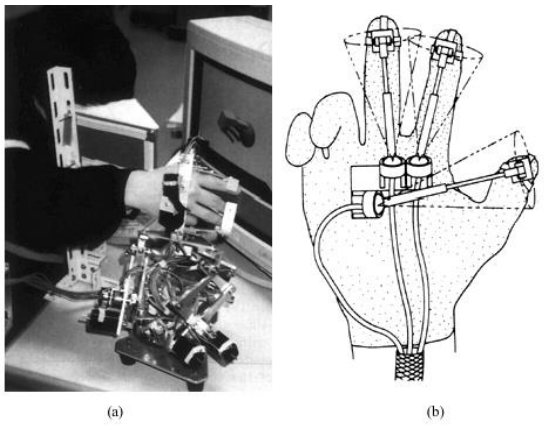

Fig. 3. Force feedback hand masters: (a) Master Manipulator, (b) force feedback structure for the data glove), [11].

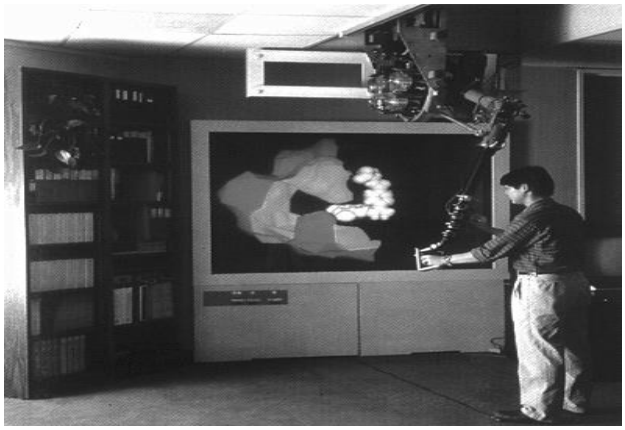

Fig. 4. GROPE force feedback display, [11], [16].

E. VIDEOPLACE (invented in 1975, by Myron Krueger)

It is "a conceptual environment, with no existence." The VIDEOPLACE artificially created to allow the computer device to control the relationship, the images of users and the places in the scene of the graphic. The imagination shadow of users in VIDEOPLACE system is determined by the camera that posted on a screen. The user in this system can interact with other participants objects [11].

Fig. 5 shows the concept and components of video place. It consists of two rooms next to each other and in any place, camera captures the gesture of participants, a projection screen to control and monitor the movements of users. The images of users are seen by other participants in the second room. Each of the participants in both rooms can interact with the images of each other. The user can interact with images of himself, can zoom it, move it, rotate it, and shrunk it. The user also can interact with graphically represented [18].

F. VCASS (developed in 1982, Thomas Furness)

Furness developed the "Visually Coupled Airborne Systems Simulator." It is a sophisticated flight simulator. The graphics are describing targeting used in this system by a fighter pilot who wears a Head Mounted Display (HMD [19]).

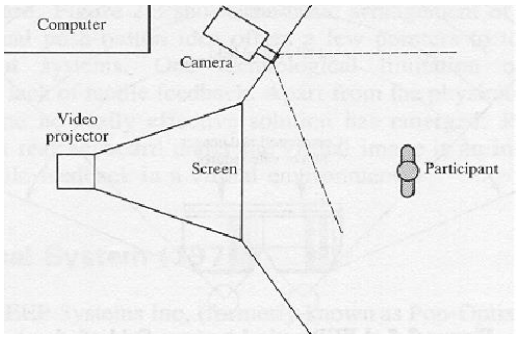

Fig. 5. Video place, [16].

G. VIVED (created in 1984)

VIVED is an abbreviation of "Virtual Visual Environment Display" that created at NASA Ames with a stereoscopic monochrome HMD. VIVED was created to allow a person to describe his digital world for other people and see it as 3D space [19]. Fig. 6 shows an example of VIVED.

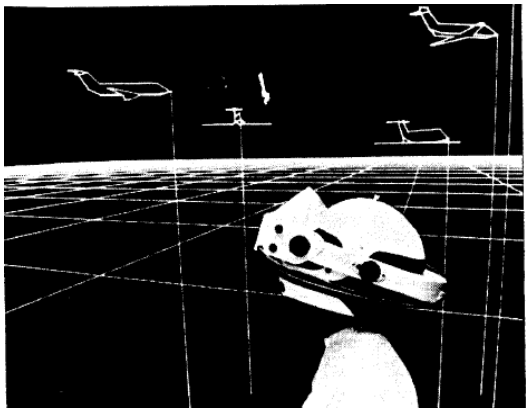

Fig. 6. VIVED, [19].

H. VPL (DataGlove created in 1985 and the Eyephone HMD created in 1988)

VLP is a company who manufactures and created DataGlove and Eyephone HMD as the first commercially available hardware of VR for the public. The DataGlove was used as an input device. The Eyephone is a head mounted display unit and used to give the user the feeling of immersion [20].

I. BOOM (created in 1989, Fake Space Labs)

Binocular Omni-Orientation Monitor (BOOM) is "a small box containing two CRT monitors that can be viewed through the eye holes." In the system of BOOM, the user can take the small box with his/her eye movements, move it through virtual environments and keep track of the box by the eye orientation [17]. Fig. 7 shows the BOOM machine.

J. UNC walk-through project (created in 1980)

This project was proposed at the University of North Carolina. Many of VR hardware are built to enhance the quality of the UNC Walk-through system such as, "HMDs, optical trackers and the Pixel-Plane graphics engine" [10].

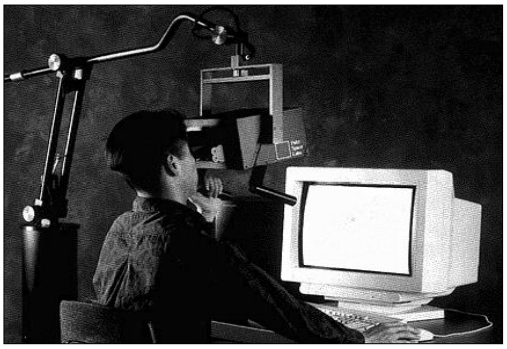

Fig. 7. The Binocular Omni-Orientation Monitor (BOOM), image by [17].

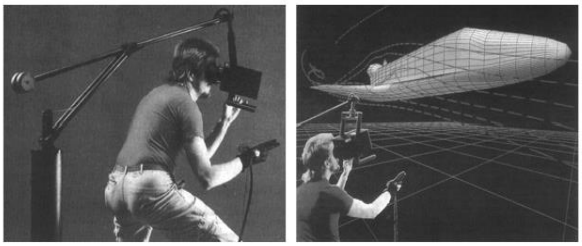

Fig. 8. Example for the Exploration of airflow using Virtual Wind Tunnel developed at NASA Ames: (a) outside view, (b) inside view [10], [11].

K. Virtual Wind Tunnel (created in 1990)

Virtual Wind Tunnel developed to allow the monitoring and investigation of flow fields included with BOOM and DataGlove. The Virtual Wind Tunnel is developed at NASA Ames [3]. Fig. 8 shows an example of the Virtual Wind Tunnel. This type of VR helps scientists to utilize a DataGlove to input and manipulate "the streams of virtual smoke in the airflow around a digital model of an airplane or space shuttle. Moving around (using a BOOM display technology) they can watch and analyze the dynamic behavior of air flow and easily find the areas of instability" [10].

L. CAVE (invented in 1992)

CAVE is "a VR and scientific visualization system." It uses stereoscopic pictures on the walls of the room instead of using HMD. In CAVE system, the user has to wear LCD shutter glasses "active shutter glasses" [14]. Fig. 9 shows the general structure of the CAVE. It consists of three walls and one door as the fourth wall "flat screens" with projectors to form four projection surfaces. In the CAVE "projection on all six surfaces of a room allows users to turn around and look in all directions. This allows the user to interact with a virtual environment in ways with a better sense of full immersion." [17].

IV. Applications of VR

Recently, the improvement of software and hardware of computer leads to develop and improve the VR technology and its applications. It has often been used by all the sides and fields of our daily life. Nowadays the user of VR technology is being used in most fields such as education, engineering fields, architectural design, medical practice, games, aerospace, different sports, warlike simulation and many other areas [21].

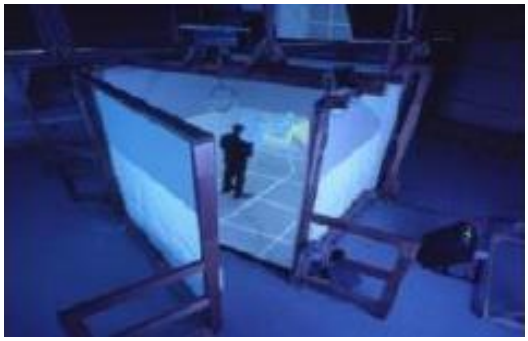

Fig. 9. Cave Automatic Virtual Environment (CAVE), [17].

The VR applications can be summarized as the following:

A. Medicine

One of the most important and practical uses of VR technique is that it can be used in the field of medicine for a variety of tasks including computational neuroscience, molecular modeling, treating phobias, ultrasound echography, and others. The using of VR will certainly achieve a saving in both cost and time in a practical way in the process of both teaching and training. Another medical application area include VR training simulations that can be used to develop surgeons surgical skills, the main advantage being that no harm will come to animals or human being [22].

Education and Training

The VR has long been used for education, training and various simulators have been developed for all types of tasks such as planes operation, submarines, power plants, tanks, helicopters, ships, cranes, trains, surgery, cars and air traffic control [23].

Entertainment and Sport

It can also be said that VR can be applied in the field of sport, for instance, a round of golf can be played using large projection screens in which golf player must direct his ball towards a virtual green. Moreover, a bicyclist can also use VR systems to improve their visual experience when using cycling machines by using large projection screens that update the display according to the speed of that bicyclist. TV cartoons are starting to make use of real-time VR, for example, the BBC's Ratz the Cat, from a children's television program, is animated in real-time during a live broadcast using a tracking system on the puppeteer [21], [22].

B. Engineering and Architecture

One of the most important usage for VR is the field of engineering. In other words, descriptions of engineering components can be viewed as lifeless drawings or static perspective projections, some of which were animated along a set path through a 3D model. Researcher in [22] indicated that the application of VR had enabled components to be virtually made, examined, gathered and tested with low cost and low time-consuming prototype production. For instance, architects can use VR to take themselves, or their clients, for a walk through the rooms or buildings they are designing. This allows the architect and client to get a real feel for the design and

allows for possible design changes to be visualized. The advantage of using VR for walk-through instead of CG animations is that the viewer is not restricted to a set path; they can explore the virtual design freely [23].

C. Data Visualization

Data visualization is the use of graphical representations of information to make certain characteristics or values more apparent. The Data visualization is especially the case for visualizing complex 3D data sets such as those arising from Computational Fluid Dynamics (CFD) calculations. Data is usually visualized by mapping geometric objects, such as arrows or particle clouds, to the data values. For example, to visualize air flow, arrows could be mapped to the data values where their width could represent volumetric flow rate, color represents temperature and direction represent the direction of air flow [22], [24].

D. Augmented Reality

Augmented Reality (AR) "is an upgrade of VR where synthetic stimuli (computer- generated visual, audio or haptic information) are superimposed onto real-world stimuli. [24]" Using this application allows learners to understand and perceive the displayed the invisible information. For example, in the medicine field, during the surgery, there is artificially displaying the information from the interior of the body on the appropriate. Another example of using augmented reality is displaying the main information on a screen in industrial and martial devices. Augmented reality is also used in tourism, advertising, and in a mobile phone. In a mobile phone, this application can determine the location of the user, introduce for the user information about the nearest street with all places and landmarks [24].

E. Designing

Designing using VR is not limited to a specific field. VR can be used to design the driving simulator, copying, and simulation of famous buildings that users can walk through a virtual historical building, in gaming and allow the user to interact with other users and exchange displays information with others [24].

F. Construction progress monitoring

Construction progress monitoring has been recognized as one of the key elements that lead to the success of a construction project. On the other word, by performing advanced control, exact measurement and other suitable procedures and steps can be fulfilled in the specific time [25]. Accordingly, it will certainly be easy to enable the performance to be as close as possible to the desired outcome even if the structure performance significantly deviates from the main design. Nevertheless, the ways of data acquisition nowadays and its use in construction progress monitoring has tended to be manual and time-consuming. The complicated nature of construction works makes the detailed progress monitoring challenging. Current construction progress monitoring methods involve submission of periodic reports and compelled by their dependence on manually dense processes and limited support for recording visual information [26]. Recently, the techniques of image based visualization allow using reporting construction progress by using "interactive and visual approaches" [27].

The virtual models can be useful both in face-to-face classes and in distance learning using E-learning technology. VR technique can easily provide chances to transfer technical education in ways not possible through traditional methods, thereby expanded the range of tools available to students to allow more educators and subjects are getting benefits. On the other hand, Birzina *et al*. [28] argued that to make a didactic application be used as an E-learning tool, it should be reusable, accessible, durable and interoperable.

V. The VR Requirements

Based on the definitions mentioned above and after having a look at the history of VR technologies, we would like to indicate and understanding the requirement of VR. According to [29] who asked the following question "if one were to create a VR that behaves like our world, what would be the requirements?" The researcher answered saying that the "information processing constancy" should be supposed by one and it operates the same trend for word processing regarding information processing in our world involves discrete management, certain processes for arithmetic matters, limited memory treatment. Accordingly, VR processing assumed to work the same way. The research [29] also indicated to the following requirements that are:

A. Finite processing allocations

This requirement means that the processing creates the VR conducts as the real world around us allocates the processing in limited "finite" quantities. The finite processing allocations assumed that each amount of time, space, and power has a "finite information capacity."

Autonomy: Autonomy here means the VR assumed to conduct by itself as the real world behaves without external data and information input [29].

B. Consistent self-registration

This requirement means the VR conducts like the reality to register itself systematically to internal "observers." The reality registered when light from the world interacts with our eyes, also in the same world. For a VR to "register itself" as we do, internal interactions must be consistent on each local "observer [29]".

C. Calculability

Calculability requirement means the VR conducts like the real world that should calculate at all time. The source in the system of VR should enclose each calculation does finite and not tend to infinity. For example, "the processing demands of some many-body calculations explode to incalculability".

All these above requirements affect the system to be VR. The requirements are like constraints for making VR in the real world.

Another researcher [30] indicated in his research that the three primary requirements to develop the environment of the VR are:

1) Performance: The VR environment requires low latency with a high rate of the frame. It is inconvenient for the user if the performance of VR environments is poor. Then, the

systems of VR have to get the benefits of available resources such as special graphics hardware and processors [30].

2) Flexibility: The devices and software used in development, VR environment should adjust with that devices and software configurations. That configuration has to be new [30].

3) Ease of use: The required VR environment to be developed has to be learned and configure easily by the user. "The Application Programming Interfaces (APIs) and languages used to create applications should be cleanly designed and should hide as much of the system's underlying complexity as possible" [30].

The interaction technique by the users of all three types of VR systems is one requirement of the user interface for the users of VR technologies. The requirements are input, output, and the interaction [24]. Interaction in VR systems is essential because it "outlines the mapping path between the user and the VR environment and determines how the environment will react when the user interacts using the input devices" [31]. The interaction technique gives the users the ability to navigate and travel in the virtual environment.

There are three types of interaction technique as it is tracking technique in VR systems. The types are navigation, object selection and manipulation, and system control (view control) [24], [32].

Navigation means choosing an orientation in space or place to determine the specific location of an object [33]. Navigation is tracking that allows users to move and travel inside virtual environments [24].

The navigation task of interaction furthermore divided into three main categories. The categories of navigation are exploration, searching, and maneuvering. Navigation with all its categories allows the user to locate the standpoint at more beneficial points to perform a particular task [31].

Object selection and manipulation enables the user to track a specific object in VR environment by using the hand of the user and to choose an object for manipulation. The user can perform the selection by gestures of hands, head orientation, eyes direction, or by using input devices such as mouse, keyboard, or joysticks [24], [32].

System control (view control) is called interactivity [34]. System control allows the user to communicate with a virtual environment (3D world) and allowing the communication among different users [24]. System control acts like a command performed to change the action of the system or the mode of interaction [31].

VI. Essential Elements of VR

The system of VR essentially has four basic elements. These elements determined by researchers Sherman and Craig [35]. The elements are the following:

1) Virtual World: It is a world generated by a computer. The virtual world consists of objects and principles of space. Those objects and principles integrated with each other by relationships.

2) Immersion: It makes the sensibility of the world as the user lives inside it and can touch it. Immersion not being just seen the world without sense it.

3) Sensory feedback: This element allows the user to reach a sensible result based on what is the input by the user. The sensibility result also based on the user place, action, and navigation.

4) Interactivity: This fourth element is responsible for offering the realization and for representing the virtual world. It allows the user to interact with objects in virtual world place.

These four elements are the basic elements in the VR system by using a computer.

VII. Types of VR Systems and Hardware

The different types of the VR systems are classified according to different usage of technological supply. Those various supplies and equipment are represented in various displayed hardware and interaction devices. "VR systems are classified according to the level of immersion they provide, ranging from semi-immersive (or desktop) VR to fully immersive VR to augmented reality (AR)" [31].

The different types of VR systems that use various technological devices and perform different functions are shown through the following explanation:

A. Immersion Systems (Fully-immersive)

The immersion type of VR systems requires the user to wear a data glove and HMD that tracks the user's head movements that then changes the view [22], [24]. CAVE is an example of fully immersion technology. CAVE designed and implemented to deal and treatment the challenges of creating a one-to-many visualization tool that utilizes large projection screens [32].

This type of VR system encases the audio and visual perception of the user in the virtual world and cuts out all outside information so that the experience is fully immersive. This type of technology is expensive and has some disadvantages, including less determining images, burden and environmental problems concerning simulators [31]. The user using full immersion of VR technology has the ability of feeling of being part of the virtual environment. An example of using this type of VR is in a virtual walk-through of buildings as one application of full immersion [8].

The examples of using full immersion of VR are shown in Fig. 10. It represents the "Light Vehicle Simulator" of fully immersed used for training purposes. This type of simulator allows users to learn how to deal with and respond to emergencies and risks when the user is driving the vehicles on mine sites [32].

Fig. 10. Example of using the light vehicle simulator in full immersion VR.

Fig. 11. An example of using only a computer in desktop VR system.

B. Non-Immersive system

The non-immersive system is often called desktop virtual reality (without any input devices) and based on the displayed screens as it is a window to the virtual world without additional devices such as HMD, and it is sometimes called Window on World (WoW) systems [3], [36]. The most widely used VR system is the desktop system that consists of a standard computer monitor to display the virtual world. Although these systems provide a lower level of presence and perhaps interaction, they can achieve satisfactory levels of graphic quality, user comfort and convenience and lower costs [22], [34].

The desktop VR system is the least types of immersion and lowest cost of the VR systems. Non-immersive type of VR is the least sophisticated components and mostly used in education [8].

Examples of desktop VR systems are video games and other examples represented in Fig. 11. It shows the non-immersion system based on the screen that contains only 3D display without any interaction. It combines VR with real-world attributes by integrating computer graphic objects into a real-world scene, but without interacting with objects that in screen [31].

Another form of desktop VR system is a virtual world. It used in education to support the learning and enhance the user to understand and observe the information. Pull together systems of the virtual world provides interactions among humans through many avatars [31]. Many of open-source software packages such as "Second Life, Active World, Open Simulator, and Open Croquet" are available to construct virtual worlds [37].

C. Semi-Immersive system

The third type of VR systems also called hybrid systems. The semi-immersive is a development desktop VR and include additional devices such as Data Gloves. It keeps the simplicity of the desktop VR system, but with a high level of immersion and using physical models [8]. In semi-immersive, the displayed virtual environment is set up onto the recognized real environment [24]. For building semi-immersive system, the requirement is displaying, tracking sensors, and user interfaces [32].

The semi-immersive system consists of VR and real world attributes by embodying objects of computer graphic into the scene of the reality. The input to this type of system is entered and controlled by the users such as a mouse, keyboard, interaction styles, glasses, and joystick [31]. It allows the user to interact by using the hands and sometimes wear glasses or DataGloves.

The displayed information such as text, graphs, and images are jutting onto the transparent screen to allow the user to interact with the real environment. An example of using hybrid systems is shown in Fig. 12. Fig. 13 represents example for semi-immersive systems [38], [39].

Fig. 12. Example of semi-immersive, (1) projection screen, laptop, and I-glasses; (2) conventional monitor, keyboard, and mouse, [31].

The following Table 1 displayed the main differences among the three types of immersion VR system:

TABLE. I. COMPARISONS AMONG THE THREE TYPES OF VR SYSTEMS

	Fully-immersive	Semi-Immersive	Non-immersive
Resolution	High	High	Medium - Low
Sense of mersion	Low-Non	Medium - High	Low
Interaction	Low	Medium	High
Price	Lowest cost	Relatively Expensive	Very Expensive

TABLE. II. CATEGORIES OF VR SOFTWARE ACCORDING TO ITS FINANCIAL VALUE

Free of Charge Software	Inexpensive Software	Moderately Expensive Software	Expensive Software
Software products that are free (commonly referred to as freeware or shareware) are copyrighted, and commercial use is often restricted. Examples include Alice, DIVE, and the common VR Modeling Language (VRML).	Computer games are classified within the commercial VR programs. This type of programs is currently at the forefront of VR technology. The games can feature realistic graphics and sound, interaction, are distributed cheaply and are used by millions of people. 3D editors are also available which allow players to modify and even create their own 3D worlds for these game environments.	The software in this category does not require any expert hardware beyond the basic computer system. It has many of excellent professional packages, three of which are World Tool Kit, which is a toolkit consisting of a library of programming functions, VR Toolkit which is an authoring package and Macromedia Director Shockwave Studio.	The VR software packages in this category are typically aimed at the professional market and can often require high computer specifications; these are known as a workstation or Rackable Systems Inc, which nowadays is known as Silicon Graphics International (SGI) system. These categories often demand much expensive hardware, such as that used in flight simulators.

VIII. VR SOFTWARE AND TOOLS

According to increasing and using the VR technology in many fields around the world, the tools and software to develop and use VR systems are available and still growing. To realize the applications of VR systems, the software is the key factor to recognize those applications [23].

There are two main types of VR software available: toolkits and authoring systems. Some of the VR applications are the framework, while others are complete development environments [22], [40]. Every VR environment is created and constructed by many aspects (modeling, coding, and then executing) and these aspects should be integrated into a single package [30].

The first type includes special programs for library usage that allows a proficient programmer to create a VR application by introducing a set of functions (Toolkits). However, the authoring systems are a simple program created without having recourse to detailed programming, but with graphical interfaces. In Table 2, there are some VR toolkits and authoring software applications available as shown through the following points, ranging from software packages that are free to use for those that are expensive [22]:

The software of VR technology has four main components that are "3D modeling software, 2D graphics software, digital sound editing software and VR simulation software" according to Onyesolu [40].

A. 3D modeling software

It is a program used to inspire 3D images using a computer and then build geometry objects in VR environments. Examples of tools used in this component of software are:

1) Autodesk 3d Max: It has another name that is 3D Studio MAX. It is extensive with many sides 3D application used in film, TV, video games and architecture. It works with Windows and Apple Macintosh operating system.

2) GL Studio: It makes interactive 3D graphics with the user interface. GL Studio based on a programming language that is C++ and OpenGL source code to create virtual worlds with interfaces.

3) Electric Image Animation System (EIAS): Creates animated 3D environments. Mostly it used to generate films such as Hollywood that used it extensively.

4) Maya: Maya software is used in to create the movie, and on TV, and to create gaming industry with the 3D virtual world. It is compatible with many operating systems Windows, Linux, and Mac. Many other examples such are Massive, Cobalt, Cinema 4D, and AC3D. It can call either 2D graphics editor or drawing program. It used to play and operate objects in 3D constructions to support the visual details.

B. 2D graphics software

The 2D graphics software creates images, diagrams and manipulates it by using the mouse, graphics tablet, or similar hardware.

This type of 2D software is also used in drawings such as electrical, electronic diagrams, topographic maps, and fonts in a computer. It is a program used to integrate the components of VR and how its objects conduct and set the rules to guide VR environment to follow it.

C. VR simulation software

An example of this simulation software is OpenSimulator (OpenSim). It is a 3D application server to create a 3D environment; it has many tools for developers to improve and build various applications such as chat application among avatars. OpenSim supports many programming languages such as Linden Scripting Language, C#, and JScript and VB.NET to develop the application.

Another example of VR simulation is Ogoglio. It is an open source 3D graphical stage used to build online spaces for artistic collaboration. It is considered as scripting language similar to Javascript. It is compatible with Windows, Linux, Solaris operating system and can run on any browser.

Another example is Flexsim DS. It is considered the advanced 3D simulation recently. FlexSim DS used to build distributed VR environments through networks.

D. Digital sound editing software

This type of editing software is used to edit and mix sounds in VR environments with other objects available in the same environment. Examples of sound editing software are Audiobook Cutter Free Edition, Creative Wavestudio, FlexiMusic Wave Editor, Goldwave, Media Digitalizer, and mp3DirectCut. VR environments can be constructed and build 3D objects with animation and user interfaces with integrated a programming language with the language of VR that is VR Modelling Language (VRML) [41]. VRML is a modeling language written easily to represent Scalable Vector Graphics (SVG). VRML can be used alone and viewed on a player or a viewer or onto a Web browser with an additional plug-in to run

it [42]. Most of the 3D environments and the interactive virtual world constructed and created by using VRML language that has improved through different versions since its inception in 1994 [43].

Nowadays, VRML became one of the most common 3D languages and filed to construct VR. VRML mostly used according to feature that it can easily access data structure essentially. VRML files can be downloaded and executed on a computer independently. However, it needs an additional plug-in to run and operate on any player or viewer [34].

IX. NAVIGATION IN VR ENVIRONMENT

The VR consists of 3D objects as any another animated 3D image. There are three components which distinguish between the VR and other 3D objects and multimedia such as television and multimedia. Three main components to make VR are: navigation, immersion, and interaction [31], [44].

1) Navigation: It is the essential tool for the usability in the VR. It is the main part to form virtual environments [45]. The navigation task allows the user to move from one place to another one in the VR. It provides the user the guidance about the destination and place of 3D objects [46], [44].

2) Immersion: It allows the user the feel of sense and presence as in the real world. The feeling of immersion could bring by the 3D objects, by the interaction with it, and by the navigation through the VR environment.

3) Interaction: It is done between the user and the objects in the virtual world to give the user the feeling of presence and the feel of acting within the reality environment in real time [31].

In the VR, the main component which leads to the other components is the navigation. The navigation behaviors in VR allow the user to interact and manipulate the 3D objects by input/output devices. The devices in a semi-immersive (developed desktop VR) are like mouse, keyboard, 3D mouse, and joystick. These allow the navigation in VR to improve the spatial presence (cognitive map) of the user [47], [48].

The cognitive map means the mental images. The first term of the cognitive map used by Tolman to mean the cognitive map is the description of the mental representation of spatial information and it is the internal (mentally) representation of spatial environments [49]. The cognitive map used to solve the spatial problems (visualization) such that we need in our research by the navigation as many types of research conclude it [50], [51].

The interaction in VR has three types of tasks. The tasks are navigation, manipulation (selecting), and system control [31]. The navigation task as we know is moving from one point to another among 3D objects in VR. It allows the movement between many different locations in the virtual world. The navigation task consists of two components that are [52], [53], [31]:

1) Travel (the motor component): means the movement from one particular location in virtual space to another one.

2) Wayfinding (the cognitive component): means the process of connection to find the paths in VR to travel through it. The wayfinding and travel build up and improve the cognitive map (spatial visualization).

Moreover, the navigation task classified into three categories that are maneuvering, search tasks and exploration allows the user to navigate (move) and travel from one viewpoint in VR to another point of view.

The manipulation (selecting) is selecting a specific object in VR and by choosing the user can start the manipulations such as rotate, zoom in, zoom out, and flying over the objects. Selecting allows the user to apply a specific command for the selected object and to change the attributes of the selected object. The third component is system control. It is the changing of the state of a system or mode of interaction [31], [44].

The navigation, cognitive map, and wayfinding have a relationship with each other. The navigation and wayfinding improve the cognitive map (spatial skill) to solve the spatial problems. The navigation and wayfinding are terms used interchangeably to refer to "a person's abilities, both cognitive and behavioral, to reach spatial destinations" [54].

The wayfinding is one component of the navigation task. Wayfinding does not mean the travel over the objects, but it means the tactical part of manipulation to allow the user of VR to apply the third part of VR environment in our model which we will build the system according to the framework of cognitive theory by Daghestani. The motion refers to the term of travel that allows users to move the objects in the virtual world [55]-[57].

So, the cognitive map by navigation and wayfinding helps to improve the visualization ability and skill in the VR to visualize the paths, locations, detail of objects and its features. The cognitive map allows the person to remember and visualize the structure of objects and its locations in the VR [54]. The navigation is the result of exploration, manipulation and searching in the virtual environments. According to the navigation, the spatial awareness (spatial visualization) is improved [58].

The navigation in VR and specifically in desktop VR (semi-immersive) can be done by the six degrees of freedom (6DoF). The navigation with 6DoF as shown in Fig. 13 support the spatial reasoning by allowing students to manipulate a model to examine its parts, scan its features, display many objects that make one solid model and compare these objects, define the spatial styling of an object [38].

The six DOF means can see the object from six sides that are: up-down; left-right; forward-back; pitch; yaw; and roll, and allow users to navigate and manipulate the objects in the VR environments.

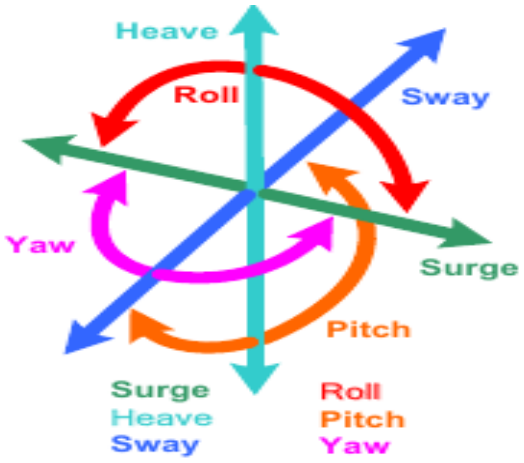

Fig. 13. Six degrees of freedom.

X. Benefits and Limitation of VR

Among the prominent advantages and benefits of VR, as it can help to change the circumstances surrounded the users or trainers to make them live in the actual situations saving both time and cost. In other words, VR can help to allow users in viewing world that is modeled inside computers and enable them to test and try things that are not normally accessible in our world or not yet formed [59].

The main advantages of VR could be as the following [32], [21], [22], [60]-[62]:

1) Any systems in technique could have many features that are either too small or large. The VR allow the user to monitor, control, and observe that feature in the normal scale system.

2) VR allows the user to feel and sense the "non-real time." Non- real time means a case or situation either offered in fast time or slow.

3) VR is safe more than the real world. So, it is used to enhance the education, training tools and experience. VR introduces the students with realism and interactivity.

4) Simulate the interaction and its speed or faster that in the real world.

5) Most of the systems in VR give the users opportunities to repeat the task until the user fulfills that task professionally with desired skills.

6) The virtual environment is much safer than the real environments.

7) VR technology gives the users of VR the ability of observations and monitoring from many numbers of views.

8) VR technology support and enhance the distance learning and avoid real danger, break the limitations of time, provides a riches of educational resources for students to allow them to explore learning independently. It enhances the self-learning.

9) VR is the most technology used to improve the engineering training, architected, and in the company of road and street, not only in engineering but also in medicine and education environments as we see in VR applications.

10) VR does not require users to present in the same place of training any system simulation that the user can train even if he/she is in another country.

11) By using 3D simulation in VR technology, the cultural information could be presented in 3D models from many angles. It allows people to sense and understand social science, landscape, and traditions of the real world.

Those advantages are not only the benefits of VR technology, but it could be the main characteristics of VR. The advantages of VR could not be counted so that the above features could be as many examples of its benefits.

However, there is no doubt that VR has been facing some noticeable, limitations and obstacles. As VR allows users to interact in real-time, this benefit needs a computer process to manipulate the virtual world with real-time as in reality. "The changes made on the virtual prototype will have to be reflected in real time; otherwise the best visual effects produced by this technology will be completely lost" [63].

Some types of VR system require much more money to create it such as in full-immersion system. Moreover, the VR technology should be improved and developed permanently as the world and techniques are increasing and improving.

XI. Road of the Map for Selecting Appropriate VR System According to the Field of Applications

The features and drawback of each type of VR system depends on what application is used. Some application is extremely useful if it is implemented using fully, while it has not benefitted if it is implemented using non-immersive.

To clarify what we mean, we make a table for the applications with all three systems to show when the system is good or low to use the application. Table 3 illustrates the type of systems and whether it is appropriate or inappropriate according to the application used.

XII. Conclusion and Future Works

The importance of using the VR came according to the increasing demand for the invention with the correct perception of what studied in higher education for many majors. Some of these majors are math, computer science, medicine, and for sure in engineering.

The VR technology is introduced as an educational environment as innovation tool to enhance learners to be able to increase and improve the value of their solutions for solving the problem in complex life. The complex problem can be broken into small problems by breaking the complex problem leads learners to produce a unique solution, realistic and practical [64].

In this paper, we illustrate the concepts of VR systems and applications. We represented the requirements and essential elements to build a complete VR environment. Benefits and limitation of VR are also introduced in this survey paper.

A road map for choosing appropriate VR system according to the required application is finally presented based on the discussed VR systems, applications, and tools. For the future work, we advise selecting a VR system based on many criteria

such as price, the level of immersion, and goals of VR application.

For the future work, we will present another survey paper to compare among VR, AR, and Mixed Reality (MR) [8]. The MR combined both VR and AR. The MR keeps the feeling about the reality and generated virtual environment at the same time. An example of MR is Microsoft HoloLens. Moreover, it is proposed to use the MR in STEM fields which allows more interactions between the user and objects of the virtual environment.

TABLE. III. THE USING OF SYSTEM OF VR ACCORDING TO THE APPLICATIONS

Field	Fully-immersive	Semi-immersive	Non-immersive
Medicine	Not effective to use fully-immersive in medicine and will be very expensive	Use it in making surgery; no harm will come to animals or human being. Not costly for each autopsy's experiment Can take the training many times by using the system. However, it will not be helpful if fully-immersive or non-immersive	It will not be useful if we use this system for medicine
Education and Training	Fully-immersive is appropriate for training such as driving, submarines, ships, cranes, and flight by making flight simulator. It does not make useful and leads to the goal for training if it used semi or non-immersive.	In education, such as engineering, drawing, cooking, soon, the semi-immersive is the most efficient system for education.	Non-immersive system such as AR is good to show animated images, or convert images to video from capture the page of a lesson in education.
Entertainment and Sport	Fully-immersive for specific entertainment will be effective. Such as seeing the sea with the animal inside it. Some games for companies to enjoy people and tourists to see new places by using CAVE.	For sports and 3d game (PlayStation)	Non-immersive is appropriate for entertainment such AR video game, TV cartoons, and football.
Engineering and Architecture	Fully immersive using to see the way of specific building to simulate it.	For engineering, the semi-immersive system is effective to visualize the 3D objects.	After designing the virtual buildings, using non-immersive to show the rooms and furniture to check the correctness of conception.
Data Visualization	There will no benefits if using fully-immersive for data visualization such as the direction of rains; Color represents temperature and direction represent the direction of air flow and clouds.	Mostly there is no need for interacting with data visualization because we use the VR for monitoring in data visualization.	Data visualization is the use of graphical representations of information to make certain characteristics or values more apparent. Use non-system in mapping geometric objects, such as arrows or particle clouds, to the data values.
Augmented Reality	AR specifically used for the non-immersive system.	AR specifically utilized for the non-immersive system.	AR used for non-immersive. For example, in the medicine field, during the surgery, there is artificially displaying the information from the interior of the body at the appropriate. Another example of using AR is displaying the main information on a screen in industrial and martial devices. AR also used in tourism, advertising, and in a mobile phone.
Designing	Fully-immersive VR can be used to design the driving simulator, copying, and simulation of famous buildings that users can walk through a virtual historical building.	Designing of 3D objects in (engineering) will be affected if the semi-immersive system uses it.	Show 3D models for the others. 3D design allows users to interact with other users and exchange displays information with others
Construction progress monitoring	Monitoring not within the system, but monitoring by being far, no in the place and obtain more time. Therefore, it effective by monitoring the progress of data or working during the desktop VR.	The techniques of image-based visualization allow using reporting construction progress by using "interactive and visual approaches "such as (monitoring the traffics inroads) and to go to another road or place by clicking and interacting with the desktop display.	Non-immersive with Construction progress monitoring enable the performance to be as close as possible to the wanted outcome even if the construction performance significantly deviates from the main design.

REFERENCES

[1] S. Jayaram, H. I. Connacher, and K. W. Lyons, "Virtual assembly using VR techniques," Computer-Aided Design, vol. 29, no. 8, pp. 575–584, 1997.

[2] S. Borsci, G. Lawson, and S. Broome, "Empirical evidence, evaluation criteria and challenges for the effectiveness of virtual and mixed reality tools for training operators of car service maintenance," Computers in Industry, vol. 67, pp. 17–26, 2015.

[3] S. Mandal, "Brief Introduction of VR & its Challenges," 2013.

[4] J. C. Roberts, "On encouraging multiple views for visualization," in Information Visualization, 1998. Proceedings. 1998 IEEE Conference on, 1998, pp. 8–14.

[5] L. Rapanotti and J. G. Hall, "Design concerns in the engineering of virtual worlds for learning," Behaviour & Information Technology, vol. 30, no. 1, pp. 27–37, 2011.

[6] J. T. Bell and H. S. Fogler, "The investigation and application of VR as an educational tool," in Proceedings of the American Society for Engineering Education, 1995.

[7] A. Rodriguez, B. Rey, M. Clemente, M. Wrzesien, and M. Alcañiz, "Assessing brain activations associated with emotional regulation during VR mood induction procedures," Expert Systems with Applications, vol. 42, no. 3, pp. 1699–1709, 2015.

[8] O. Bamodu and X. M. Ye, "VR and VR System Components," Advanced Materials Research, vol. 765, pp. 1169–1172, 2013.

[9] J. Fox, D. Arena, and J. N. Bailenson, "VR: a survival guide for the social scientist," Journal of Media Psychology, vol. 21, no. 3, pp. 95–113, 2009.

[10] J. Novak-Marcincin, M. Kuzmiakova, and K. Al Beloushy, "VR TECHNOLOGIES AND VIRTUAL MANUFACTURING IN MANUFACTURING ENGINEERING.," Scientific Bulletin Series C: Fascicle Mechanics, Tribology, Machine Manufacturing Technology, vol. 23, no. 100, 2009.

[11] T. Mazuryk and M. Gervautz, "VR-history, applications, technology and future," 1996.

[12] J. Sharpe and R. Self, "Computers for Everyone," Computers for Everyone, vol. 1, no. 1, 2015.

[13] O. Bimber and R. Raskar, Spatial augmented reality: merging real and virtual worlds. CRC Press, 2005.

[14] F. Rebelo, E. Duarte, P. Noriega, and M. M. Soares, "24 VR in Consumer," Human Factors and Ergonomics in Consumer Product Design: Methods and Techniques, p. 381, 2011.

[15] J. W. V. De Faria, E. G. Figueiredo, and M. J. Teixeira, "History of VR and its use in medicine," Revista de Medicina, vol. 93, no. 3, pp. 106–114, 2015.

[16] G. Welch, "VR History ." 2015.

[17] M. Vafadar, "VR: Opportunities and Challenges," History of VR and its use in medicine, 2013.

[18] P. L. Weiss, H. Sveistrup, D. Rand, and R. Kizony, "Video capture VR: A decade of rehabilitation assessment and intervention," Physical Therapy Reviews, vol. 14, no. 5, pp. 307–321, 2009.

[19] S. S. Fisher, M. McGreevy, J. Humphries, and W. Robinett, "Virtual environment display system," in Proceedings of the 1986 workshop on Interactive 3D graphics, pp. 77–87, 1987.

[20] Z. Zivkovic, "Optical-flow-driven gadgets for gaming user interface," in Entertainment Computing-ICEC 2004, Springer, pp. 90–100, 2004.

[21] R. Hui-Zhen and L. Zong-Fa, "Application and Prospect of the VR Technology in College Ideological Education," in Intelligent Systems Design and Engineering Applications, 2013 Fourth International Conference on, pp. 125–128, 2013.

[22] C. Cox, "The use of computer graphics and VR for visual impact assessments," 2003.

[23] W. Jin, "VR technology in the design of the space environment research," in Control, Automation and Systems Engineering (CASE), 2011 International Conference on, 2011, pp. 1–4.

[24] M. Mihelj, D. Novak, and S. Beguvs, VR Technology and Applications. Springer, 2014.

[25] H. Son and C. Kim, "3D structural component recognition and modeling method using color and 3D data for construction progress monitoring," Automation in Construction, vol. 19, no. 7, pp. 844–854, 2010.

[26] S. Roh, Z. Aziz, and F. Peña-Mora, "An object-based 3D walk-through model for interior construction progress monitoring," Automation in Construction, vol. 20, no. 1, pp. 66–75, 2011.

[27] A. Z. Sampaio, "VR Technology Applied in Teaching and Research in Civil Engineering Education."

[28] R. Birzina, A. Fernate, I. Luka, I. Maslo, and S. Surikova, "E-learning as a Challenge for Widening of Opportunities for Improvement of Students' Generic Competences," E-Learning and Digital Media, vol. 9, no. 2, pp. 130–142, 2012.

[29] B. Whitworth, "The physical world as a VR," arXiv preprint arXiv:0801.0337, 2008.

[30] A. Bierbaum and C. Just, "Software tools for VR application development," Course Notes for SIGGRAPH, vol. 98, 1998.

[31] L. Daghestani, "The Design, Implementation and Evaluation of a Desktop VR for Teaching Numeracy Concepts via Virtual Manipulatives," 2013.

[32] M. A. Muhanna, "VR and the CAVE: Taxonomy, interaction challenges and research directions," Journal of King Saud University-Computer and Information Sciences, 2015.

[33] T. Sulbaran and N. C. Baker, "Enhancing engineering education through distributed VR," in Frontiers in Education Conference, 2000. FIE 2000. 30th Annual, vol. 2, p. S1D–13, 2000.

[34] W. Cartwright and M. P. Peterson, Multimedia cartography. Springer, 2007.

[35] P. Brey, "VR and computer simulation," The Handbook of Information and Computer Ethics, p. 361, 2008.

[36] N. Sala, "Multimedia and VR in architecture and in engineering education," in Proceedings of the 2nd WSEAS/IASME International Conference on Educational Technologies, Bucharest, Romania, vol. 22, 2006.

[37] J. Kaplan and N. Yankelovich, "Open Wonderland: an extensible virtual world architecture," Internet Computing, IEEE, vol. 15, no. 5, pp. 38–45, 2011.

[38] S. Sua, A. Chaudhary, B. Geveci, W. Sherman, H. Nieto, L. Francisco-Revilla, and others, "VR enabled scientific visualization workflow," in Everyday VR (WEVR), 2015 IEEE 1st Workshop on, pp. 29–32, 2015.

[39] E. T. Solovey, J. Okerlund, C. Hoef, J. Davis, and O. Shaer, "Augmenting spatial skills with semi-immersive interactive desktop displays: do immersion cues matter?," in Proceedings of the 6th Augmented Human International Conference, pp. 53–60, 2015.

[40] M. O. Onyesolu, I. Ezeani, and O. R. Okonkwo, A Survey of Some VR Tools and Resources. INTECH Open Access Publisher, 2012.

[41] X. Fang, D. Zheng, H. He, and Z. Ni, "Data-driven heuristic dynamic programming with VR," Neurocomputing, 2015.

[42] F. Ziwar and R. Elias, "VRML to WebGL Web-based converter application," in Engineering and Technology (ICET), International Conference on, 2014, pp. 1–6, 2014.

[43] J. Martin-Gutierrez, M. Garcia-Dominguez, C. Roca Gonzalez, and M. M. Corredeguas, "Using different methodologies and technologies to training spatial skill in Engineering Graphic subjects," in Frontiers in Education Conference, 2013 IEEE, pp. 362–368, 2013.

[44] J. ao A. onio M. P. Joaquim Armando Pires Jorge, "Direct Interactive 3D Modeling in a Semi-Immersive Environment," 2013.

[45] G. Opriessnig, "User-defined mapping functions and collision detection to improve the user-friendliness of navigation in a VR environment," in Information Visualization, 2003. IV 2003. Proceedings. Seventh International Conference on, pp. 446–451, 2003.

[46] J. Ma, H. Zhu, and J. Gong, "Study of navigation based on intelligent avatar with mobile VR," in Wireless, Mobile and Multimedia Networks, 2006 IET International Conference on, pp. 1–4, 2006.

[47] T. D. Parsons, C. G. Courtney, M. E. Dawson, A. A. Rizzo, and B. J. Arizmendi, "Visuospatial processing and learning effects in VR based mental rotation and navigational tasks," in Engineering Psychology and

Cognitive Ergonomics. Understanding Human Cognition, Springer, pp. 75–83, 2013

[48] M. Muhaiyuddin, N. Diyana, and D. R. Awang Rambli, "Navigation in image-based VR as the factor to elicit spatial presence experience," in Technology Management and Emerging Technologies (ISTMET), 2014 International Symposium on, pp. 349–354, 2014.

[49] S. K. Semwal, "Wayfinding and navigation in haptic virtual environments," in null, p. 143, 2001.

[50] P. Hafner, C. Vinke, V. Hafner, J. Ovtcharova, and W. Schotte, "The impact of motion in virtual environments on memorization performance," in Computational Intelligence and Virtual Environments for Measurement Systems and Applications (CIVEMSA), 2013 IEEE International Conference on, pp. 104–109, 2013.

[51] G. Wallet, H. Sauzéon, F. Larrue, and B. N'Kaoua, "Virtual/real transfer in a large-scale environment: impact of active navigation as a function of the viewpoint displacement effect and recall tasks," Advances in Human-Computer Interaction, vol. 2013, p. 8, 2013.

[52] B. S. Santos, P. Dias, A. Pimentel, J.-W. Baggerman, C. Ferreira, S. Silva, and J. Madeira, "Head-mounted display versus desktop for 3D navigation in VR: a user study," Multimedia Tools and Applications, vol. 41, no. 1, pp. 161–181, 2009.

[53] E. Suma, S. L. Finkelstein, M. Reid, S. V. Babu, A. C. Ulinski, L. F. Hodges, and others, "Evaluation of the cognitive effects of travel technique in complex real and virtual environments," Visualization and Computer Graphics, IEEE Transactions on, 2010.

[54] K. Patel and S. Vij, "Spatial navigation in virtual world," Advanced knowledge based systems: model, applications and research, TMRF e-Book, pp. 101–125, 2010.

[55] D. A. Bowman and L. F. Hodges, "An evaluation of techniques for grabbing and manipulating remote objects in immersive virtual environments," in Proceedings of the 1997 symposium on Interactive 3D graphics, 1997.

[56] N. G. Vinson, "Design guidelines for landmarks to support navigation in virtual environments," in Proceedings of the SIGCHI conference on Human Factors in Computing Systems, 1999.

[57] C.-H. Tang, W.-T. Wu, and C.-Y. Lin, "Using VR to determine how emergency signs facilitate way-finding," Applied ergonomics, vol. 40, no. 4, pp. 722–730, 2009.

[58] G. A. Satalich, "Navigation and wayfinding in VR: Finding the proper tools and cues to enhance navigational awareness," 1995.

[59] M. J. Williams, "Application of VR for risk assessment and training in the minerals industry," 2000.

[60] A.-H. G. Abulrub, A. N. Attridge, M. Williams, and others, "VR in engineering education: The future of creative learning," in Global Engineering Education Conference (EDUCON), IEEE, 2011.

[61] H. Chen, K. Feng, C. Mo, S. Cheng, Z. Guo, and Y. Huang, "Application of Augmented Reality in Engineering Graphics Education," in IT in Medicine and Education (ITME), 2011 International Symposium on, vol. 2, pp. 362–365, 2011.

[62] G. Li and B. Zhang, "The application and advantages of VR technology in cultural resources communication," in 2011 International Conference on Multimedia Technology, 2011.

[63] A. Jimeno and A. Puerta, "State of the art of the VR applied to design and manufacturing processes," The International Journal of Advanced Manufacturing Technology, vol. 33, no. 9, pp. 866–874, 2007.

[64] I. Kartiko, M. Kavakli, and K. Cheng, "Learning science in a VR application: The impacts of animated-virtual actors' visual complexity," Computers & Education, vol. 55, no. 2, pp. 881–891, 2010.

Phishing Websites Classification using Hybrid SVM and KNN Approach

Altyeb Altaher
Faculty of Computing and Information Technology in Rabigh,
King Abdulaziz University, Jeddah, Saudi Arabia

***Abstract*—Phishing is a potential web threat that includes mimicking official websites to trick users by stealing their important information such as username and password related to financial systems. The attackers use social engineering techniques like email, SMS and malware to fraud the users. Due to the potential financial losses caused by phishing, it is essential to find effective approaches for phishing websites detection. This paper proposes a hybrid approach for classifying the websites as Phishing, Legitimate or Suspicious websites, the proposed approach intelligently combines the K-nearest neighbors (KNN) algorithm with the Support Vector Machine (SVM) algorithm in two stages. Firstly, the KNN was utilized as a robust to noisy data and effective classifier. Secondly, the SVM is employed as a powerful classifier. The proposed approach integrates the simplicity of KNN with the effectiveness of SVM. The experimental results show that the proposed hybrid approach achieved the highest accuracy of 90.04% when compared with other approaches.**

Keywords*—Information security; phishing websites; support vector machine; K-nearest neighbors

I. Introduction

Phishing is a serious threat that is potentially dangerous to the internet users. Phishing is a sort of semantic attack and attacks are targeting social or financial achievements [1]. In phishing attack, attackers attempt to trick and take money from the users of the internet by sending them e-mails instead of using malware software. First a fake web site which looks like the legitimate website is made by the attacker. Then users are requested to access the fake website and the attacker takes their money and important information. Phishing attacks become advanced continually as attackers find innovative methods and adapt their policies consequently. The most common method for phishing is e-mail. Phishing e-mails utilize different strategies to deceive the internet users into releasing their personal information such as account number, passwords and usernames. For example, requesting the user to validate his bank account information by providing his bank information to be compromised. The growing complexity of these approaches makes it difficult to protect users from phishing attacks [1]. The Anti-Phishing Working Group (APWG) is a group which gathers the phishing data from several sources, stated that phishing attacks continue spreading, as there were 69,533 unique phishing websites counted in December 2016, 80% of theses phishing attacks were targeting the online payment divisions [2].

Heuristic approach for phishing website detection [3]-[6] explores the content, structure and URL of phishing websites, finds the phishing websites features and develop an approach to identify phishing sites. The advantages of this method are the high speed and it generates less false negative or false positive. An attacker can avoid the filter and can achieve his target and get the user credentials when he understands the heuristic method strategy. The approach for phishing website detection based on visual similarity [7], [8] matches the suspicious website visual object such as text and images with original domain visual object. If the matching is less than definite threshold it is considered as legitimate site else as phishing. This method is not fast if matched with heuristic approach since it matches the suspicious website with the visual contents of all the legitimate websites.

The fast evolution of advanced phishing methods developed by professional attackers enabled the new phishers to build phishing websites using phishing software tools, which are offered in the internet. Therefore, the use of traditional anti-phishing approaches is not enough for efficient detection of phishing websites [8]. To limit the growing of phishing attacks, there is a need for effective and efficient solution. In this paper, a hybrid approach based on the combination of SVM and KNN is proposed to detect phishing webpages. The contributions of our paper are as follows:

1) To explore the potential of data mining techniques for phishing websites classification.
2) To propose a hybrid KNN-SVM approach for phishing websites classification
3) To validate and evaluate the performance of the proposed hybrid KNN-SVM approach for phishing websites classification and compare it with existing works.

The rest of the paper is structured as: Section 2 shows the related work. Section 3 explains the proposed hybrid approach for phishing websites classification. Section 4 presents the experimental results. Finally, Section 5 concludes our paper.

II. Related Work

Several research efforts were conducted to safe the users from the phishing websites. There are several approaches for phishing websites detection including machine learning [9], blacklists, visual similarity calculation [7] and classification of URL feature and domain name exploration. Our paper belongs to the first area. However, we also present a brief overview of the other fields to provide background to our research. In [1], Purkait provided a comprehensive phishing detection literature which introduced a complete review about the phishing detection techniques.

Google Safe Browsing [10] utilizes a blacklist phishing detection approach. The suspected uniform resource locator (URL) is matched in the blacklist to check its existence, if it is found in the blacklist the suspected URL is categorized as phishing website, else it will be categorized as valid website. The main drawback in this method is that phishing websites that are not exist in blacklist are not identified. The phishing websites appears for the first time is not presented in blacklist are named Zero day phishing sites. This approach could raise the false negative percentage. Cantina is proposed by Zhang *et al*. In [11], it is an approach for phishing website detection depends on the text in the website. The Term Frequency–Inverse Document Frequency (TF-IDF) method is employed on the text in website to identify the phishing attacks. The top five terms based on the TF-IDF is sent to search unit and compared with the results obtained by searching unit using the suspicious link. Their results show that the proposed approach detected 89% of the phishing sites. This approach cannot detect the phishing websites when the text in the website is substituted with images.

In [12] the authors proposed an approach for phishing website detection. The authors have carefully chosen six structural-features of the website, and then the Support-Vector-Machine algorithm is utilized to decide if the website is phishing website or legitimate website. The accuracy of the classification of this approach was 84%. However, this approach mentioned significant features that can potentially help in defining the legitimate website. Moreover, it is not affected by prior familiarity of the user about computer security techniques. Aburrous *et al.* [13] proposed an intelligent phishing detection approach based on Fuzzy data-mining algorithms, they used 27 features for phishing website detection and achieved an accuracy of 83.7%. However, the features used in their proposed approach are inadequate. Xiang and Hong in [14] proposed an approach for phishing websites detection based on linear classifier. Their approach employed the Domain Object Model and Hyper-Text Mark-up language with 10 attributes to classify phishing sites. Their results attained an accuracy of 89%.

BaitAlarm [15] utilizes the visual features contrast to categorize legitimate and phishing websites. Phishing attacks usually employ similar designs to reproduce the layout of the real website so authors employed Cascading Style Sheets (CSS) for classifying phishing websites. The authors considered a valid site and matched with many phishing sites signifying the necessity of whitelist. The drawback of BaitAlarm is that calculation cost of CSS style and matching with the records of whitelist is excessively high.

III. The Proposed Hybrid KNN-SVM Approach for Phishing Websites Classification

In this section, we present the techniques that have been employed in this paper for the classification of the phishing websites.

A. K-Nearest Neighbors (KNN)

KNN is an effective supervised learning method for many problems including security techniques [16]. K-nearest neighbor is based on the clustering of the elements that have the same characteristics; it decides the class category of a test example based on its k neighbor that is near to it. The value of k in the KNN depends on the size of dataset and the type of the classification problem [17]. Fig. 1 shows that KNN classifies the target based on its neighbors.

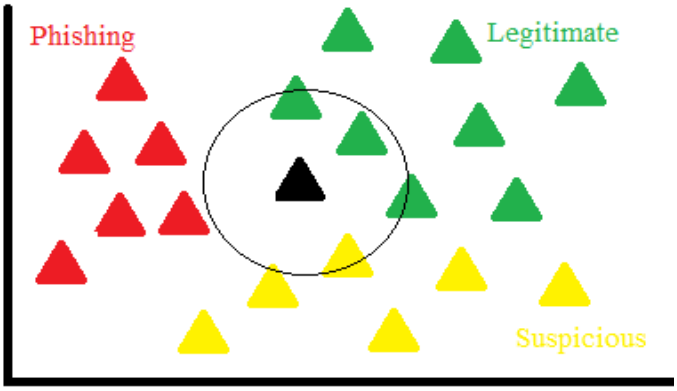

Fig. 1. A k-nearest neighbor (KNN) classifier

KNN is explained as follows:

Find the nearest elements from the test data *a* to training data K based on euclidean distance to calculate the distance. For two elements in k dimensional space, $a = [a1, a2, \ldots, ak]$ and $y = [b1, b2, \ldots, bk]$, the Euclidean distance based on the two elements can be computed by using (1) :

$$d(a,b) = \sqrt{\sum_{i=1}^{k}(b_i - a_i)^2} \quad (1)$$

After collecting the k-nearest neighbors, the majority of the k-nearest neighbors will be considered as a class for the test data.

B. Support Vector Machine (SVM)

SVM is a machine learning technique based on supervised learning and appropriate to both regression and classification [18]. The SVM is considered a modern technique achieving fast acceptance due to the good results achieved in a many fields of data mining problems, based on its solid foundation in statistical learning theory. SVM is a classification technique based on the statistical learning, which successfully utilized in many applications of nonlinear classification and large datasets and issues [19]. SVM classifiers employ the hyper-plane to isolate categories. Every hyper-plane is determined by its direction (w), the precise position in space or a threshold is (b), (xi) denotes the input array of constituent N and indicates the category. A set of the training cases are shown in (2) and (3).

$$(x1, y1), (x2, y2), \ldots, (xk, yk); xi \epsilon R^d \quad (2)$$

K represents the number of training dataset and d denotes the number of the dimensions of the input dataset. The function of decision is specified as follows:

$$f(x, w, b) = sgn\big((w.xi) + b\big), w\epsilon\, R^d,\ \text{b}\,\epsilon\, R \quad (3)$$

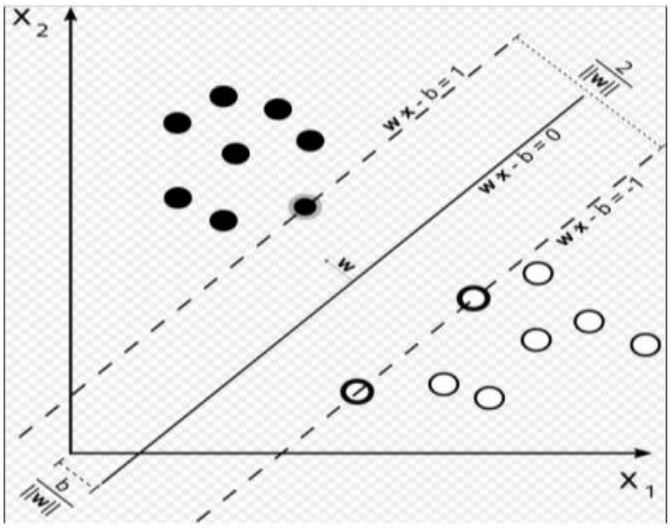

Fig. 2. SVM for phishing websites classification

One of the advantages of employing the SVM for training the system is its ability to work with multi-dimensional data. SVM is a classifier that takes a given labeled training data as input and outputs an optimal hyperplane which classifies new examples. SVM makes a hyperplane between data sets by maximizing the margin as shown in Fig. 2

C. The Proposed Hybrid KNN-SVM Approach for Phishing Website Detection

This paper proposes an integration of nearest neighbor classifier and support vector machine for phishing website detection. The proposed KNN-SVM hybrid classification approach can be used effectively for phishing website detection with low computational complexity in the training and detection stage. The lower computational complexity property is gained from KNN classification approach that does not require construction of a feature space. KNN algorithm has been used in the proposed hybrid approach KNN-SVM as the first step in the phishing website detection, and then the SVM method is employed in the second stage as a classification engine of this hybrid model. Fig. 3 shows the proposed KNN-SVM hybrid approach for phishing website detection.

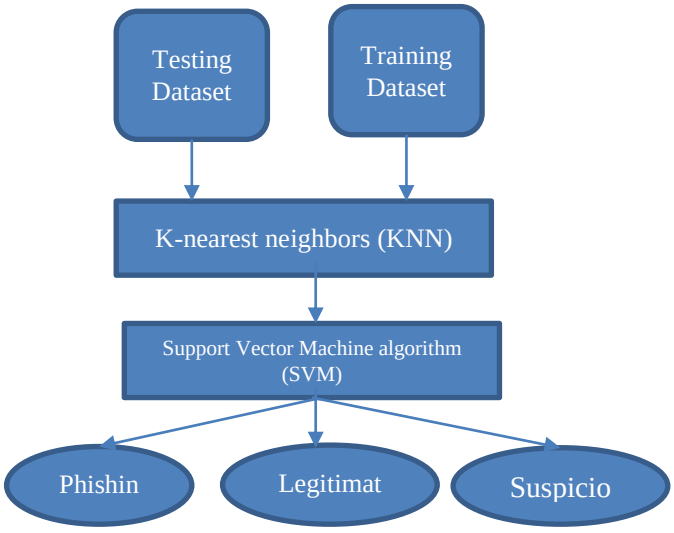

Fig. 3. The proposed hybrid approach for phishing website detection

IV. Experimental Results and Discussion

In our study, we used a dataset prepared by Abdelhamid *et al*. [20]. The dataset contains more than 1353 samples collected from different sources, each sample record consists of nine different features plus the class which is Phishing, Legitimate or Suspicious website. The used features in the dataset are explained in Table 1.

To evaluate the effectiveness of the proposed hybrid KNN-SVM approach for phishing website detection, two classification metrics were considered, the Accuracy and Recall.

Accuracy: Accuracy is a well-known measure for the classification assessment. It is known as the proportion of correctly classified samples to the total number of samples, whereas the error rate uses wrongly classified rather than correctly. Equation (4) shows the mathematical formula for accuracy.

$$Accuracy = \frac{(TN+TP)}{(TN+FP)+(TP+FN)} \quad (4)$$

TABLE I. Description of the Features Used in the Dataset

Feature	Description
IP Address	The existence of IP address in the URL domain name indicates that someone is attempting to access the personal information.
URL Length	Phishers redirect the user's submitted information by hiding the suspicious part of the URL to differentiate between legitimate and phishing URLs based on the URL length, Mohammad *et al* in [4] proposed that if the length of URL is more than 54 symbols the URL is classified phishy.
Pop Up Window	Generally, genuine sites do not request users to send their private information through secondary window.
Request URL	A webpage commonly contains characters, audio files, videos and images. Usually, these entities are uploaded in the webpage using the similar server hosting the webpage. When the entities are loaded from other domain, the webpage is possibly suspicious.
web_traffic	The traffic rate in Legitimate websites is usually high because they are used frequently. The traffic rate of phishing websites is usually low because they used rarely.
Fake HTTPs protocol	Using HTTPs protocol to transfer Important information indicates that the user is surely linked with a true website. Phishers could employ a false HTTPs protocol to trick the users.
URL of anchor	Like the URL, and differs in the links in the webpage which may possibly connect to another domain unlike the domain entered in the URL address bar.
Server Form Handler (SFH)	When the user send the data, the webpage will send the data to the server for processing. Usually, the information is handled from the same domain that hosting the website. Phishers try to send the information to fake domain.

Where, True Positive (TP): The number of phishing websites correctly classified as phishing websites.

False Positive (FP): The number of phishing websites classified as legitimate websites.

True Negative (TN): The number of legitimate websites classified as legitimate websites.

False Negative (FN): The number of legitimate websites classified as phishing websites.

Recall: Recall is the ratio of correct items that were selected. Equation (5) presents the mathematical formula for recall.

$$Recall = \frac{TP}{(TP+FN)} \quad (5)$$

The experiments conducted using the training and testing datasets to assess the performance of the proposed hybrid KNN-SVM approach for phishing websites detection. The total dataset is divided into two parts: 20% for testing and 80% for training. The proposed hybrid KNN-SVM approach combines the advantages of both SVM and KNN classifiers. The experiments compared the performance of proposed hybrid KNN-SVM approach with that of basic SVM, Naïve Bayes, Neural Network, Decision tree and basic KNN.

As shown in Fig. 4, the proposed hybrid KNN-SVM approach achieved the highest accuracy of 90.04% and outperform the other machine learning classifiers, which indicates the advantage of the proposed hybrid KNN-SVM approach. The performance of the proposed KNN-SVM is better than those of the SVM (83.76%) and KNN (87.45%), separately. Consequently, the proposed KNN-SVM can better classify the phishing websites than a single classifier. Also, Fig. 4 shows that the other machine learning classifiers including Naïve Bayes, Neural Network, DT and KNN achieved lower accuracy of 83.10%, 87.08%, 83.76%, 86.72%, 87.45%, respectively.

Fig. 5 demonstrates the recall results of the proposed hybrid KNN-SVM outperform the all other machine leaning classifiers, namely the Naïve Bayes, Neural Network, SVM, DT and KNN. The recall is calculated for the three classes: phishing, legitimate and suspicious, then the average recall for all the classes is presented. The proposed KNN-SVM achieved the highest average recall of 89.08%, while the Naïve Bayes, Neural Network, SVM, DT and KNN achieved an average recall of 64.41%, 80.65%, 58.56%, 64.89% and 84.78%, respectively as shown in Table 2.

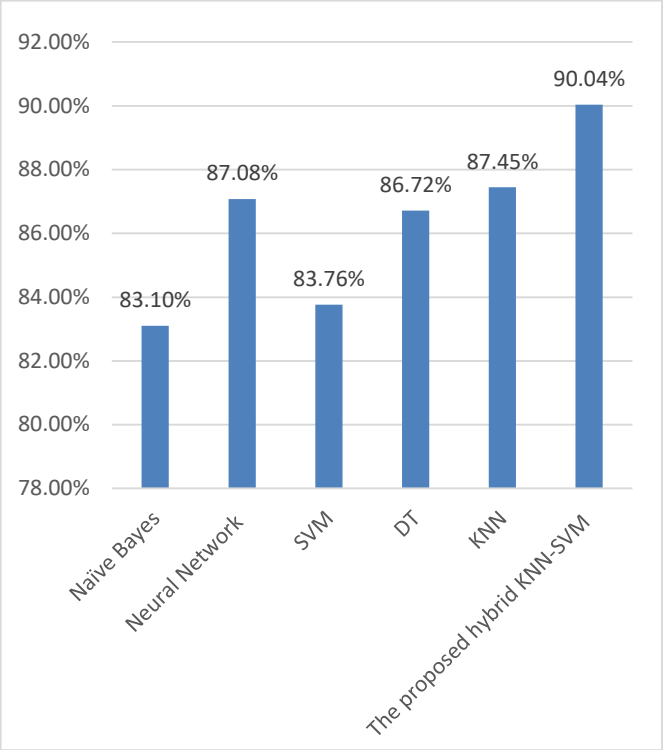

Fig. 4. Performance comparison between the proposed hybrid KNN-SVM and other approaches in terms of accuracy

TABLE II. COMPARISON OF THE RECALL ACHIEVED BY THE PROPOSED HYBRID KNN-SVM AND OTHER DATA MINING CLASSIFIERS

Used approach	Suspicious	Legitimate	Phishing	AVG
Naïve Bayes	17.65%	85.29%	90.30%	64.41%
Neural Network	66.67%	83.96%	91.33%	80.65%
SVM	0.00%	83.02%	92.67%	58.56%
DT	13.33%	88.68%	92.67%	64.89%
KNN	80.00%	83.02%	91.33%	84.78%
The proposed hybrid KNN-SVM	86.67%	90.57%	90.00%	89.08%

TABLE III. PERFORMANCE COMPARISON BETWEEN THE PROPOSED HYBRID KNN-SVM AND EXISTING APPROACHES

The approach	Accuracy
SVM based approach by Pan etal. [12]	84%
An intelligent phishing detection approach based on Fuzzy data-mining algorithms by Aburrous *et al* [13]	83.7%.
Text based approach By Zhang etal. [11]	89 %
phishing websites detection based on linear classifier by Xiang and Hong in [14]	89 %
The proposed hybrid KNN-SVM	90.04%

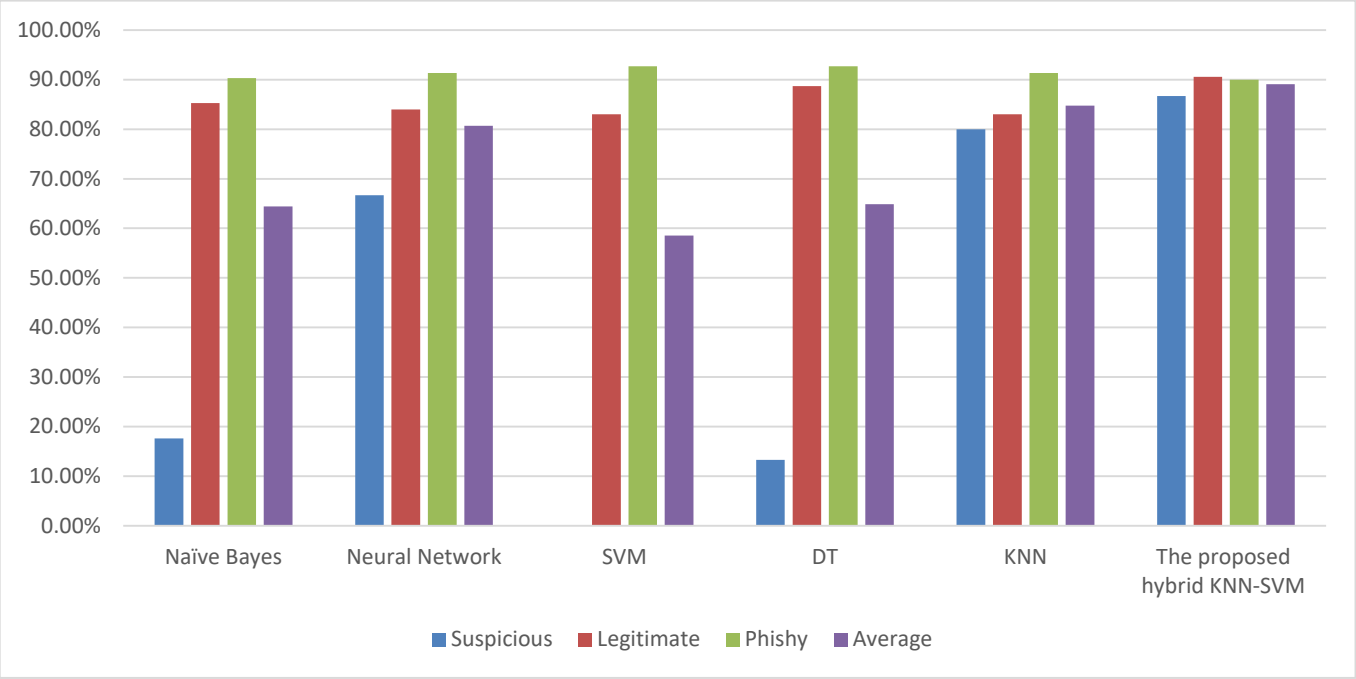

Fig. 5. Performance comparison between the proposed hybrid KNN-SVM and other approaches in terms of recall

The proposed hybrid approach is also compared with other related approaches as show in Table 3, it is clear form Table 3 that the proposed hybrid KNN-SVM approach achieved the highest accuracy of 90.04% and performs better than the other approaches. Among the listed related works, the intelligent phishing detection approach based on Fuzzy data-mining algorithms proposed by Aburrous *et al* [13] achieved the lowest accuracy of 83.7%. Text based approach proposed by Zhang *et al*. [11] and the phishing websites detection based on linear classifier proposed by Xiang and Hong [14], achieved performance close to the performance of our proposed hybrid KNN-SVM.

V. Conclusion

Detection of Phishing websites is an active research area due to its significant importance for both individuals and organizations, because phishing websites can cause potential financial loses. Artificial Intelligence techniques have been used successfully in many fields and it offer potential possibility to classify the fishing websites. This paper proposed a hybrid approach for classifying the websites as Phishing, Legitimate or Suspicious, the proposed approach combines the K-nearest neighbors (KNN) algorithm with the support vector machine algorithm (SVM). The proposed approach integrates the effectiveness and simplicity of KNN with the powerful of SVM. Thus, the proposed hybrid KNN-SVM gains the advantages of combining KNN with SVM and avoids their own drawbacks when they used separately. The experimental results show that the proposed hybrid approach achieved an accuracy of 90.04%. For the future, we will consider more advanced data mining techniques for the classification of the phishing websites.

References

[1] Purkait, Swapan. “Phishing counter measures and their effectiveness–literature review.” Information Management & Computer Security 20.5 , pp.382-420,2012.

[2] Anti-Phishing Working Group,2016. Phishing Activity Trends Report—4th Quarter 2016. http://docs.apwg.org/reports/apwg_trends_report_q4_2016.pdf

[3] Joshi, Yogesh, Samir Saklikar, Debabrata Das, and Subir Saha. “PhishGuard: a browser plug-in for protection from phishing.” In Internet Multimedia Services Architecture and Applications, 2008. IMSAA 2008. 2nd International Conference on, pp. 1-6. IEEE, 2008.

[4] Mohammad, Rami M., Fadi Thabtah, and Lee McCluskey. “An assessment of features related to phishing websites using an automated technique.” In Internet Technology And Secured Transactions, 2012 International Conference for, pp. 492-497. IEEE, 2012.

[5] ALmomani, Ammar, Tat-Chee Wan, Ahmad Manasrah, Altyeb Altaher, Eman Almomani, Karim Al-Saedi, Ahmad Alnajjar, and Sureswaran Ramadass. “A survey of learning based techniques of phishing email filtering.” International Journal of Digital Content Technology and its Applications 6, no. 18 (2012): 119..

[6] Chou, Neil, Robert Ledesma, Yuka Teraguchi, and John C. Mitchell. “Client-Side Defense Against Web-Based Identity Theft.” In NDSS. 2004.

[7] Fu, Anthony Y., Liu Wenyin, and Xiaotie Deng. “Detecting phishing web pages with visual similarity assessment based on earth mover's distance (EMD).” IEEE transactions on dependable and secure computing 3, no. 4 (2006).

[8] Rao, Routhu Srinivasa, and Syed Taqi Ali. “A computer vision technique to detect phishing attacks.” In Communication Systems and Network Technologies (CSNT), 2015 Fifth International Conference on, pp. 596-601. IEEE, 2015.

[9] Whittaker, Colin, Brian Ryner, and Marria Nazif. “Large-Scale Automatic Classification of Phishing Pages.” In NDSS, vol. 10, p. 2010. 2010.

[10] Safe Browsing API – Google Developer, [Online] Available at https://developers.google.com/safe-browsing/

[11] Zhang, Yue, Jason I. Hong, and Lorrie F. Cranor. "Cantina: a content-based approach to detecting phishing web sites." In Proceedings of the 16th international conference on World Wide Web, pp. 639-648. ACM, 2007.

[12] Pan, Ying, and Xuhua Ding. "Anomaly based web phishing page detection." In Computer Security Applications Conference, 2006. ACSAC'06. 22nd Annual, pp. 381-392. IEEE, 2006.

[13] Aburrous, Maher, M. Alamgir Hossain, Fadi Thabatah, and Keshav Dahal. "Intelligent phishing website detection system using fuzzy techniques." In Information and Communication Technologies: From Theory to Applications, 2008. ICTTA 2008. 3rd International Conference on, pp. 1-6. IEEE, 2008.

[14] Xiang, Guang, and Jason I. Hong. "A hybrid phish detection approach by identity discovery and keywords retrieval." In Proceedings of the 18th international conference on World wide web, pp. 571-580. ACM, 2009.

[15] Mao, Jian, Pei Li, Kun Li, Tao Wei, and Zhenkai Liang. "BaitAlarm: detecting phishing sites using similarity in fundamental visual features." In Intelligent Networking and Collaborative Systems (INCoS), 2013 5th International Conference on, pp. 790-795. IEEE, 2013.

[16] Tavallaee, Mahbod, Ebrahim Bagheri, Wei Lu, and Ali A. Ghorbani. "A detailed analysis of the KDD CUP 99 data set." In Computational Intelligence for Security and Defense Applications, 2009. CISDA 2009. IEEE Symposium on, pp. 1-6. IEEE, 2009.

[17] Bremner, David, Erik Demaine, Jeff Erickson, John Iacono, Stefan Langerman, Pat Morin, and Godfried Toussaint. "Output-sensitive algorithms for computing nearest-neighbour decision boundaries." Discrete & Computational Geometry 33, no. 4 , pp.593-604, 2005.

[18] Suthaharan, Shan. "Support Vector Machine." In Machine Learning Models and Algorithms for Big Data Classification, pp. 207-235, 2016.

[19] Hussain, Hanaa, Khaled Benkrid, and HÜSEYİN ŞEKER. "Novel dynamic partial reconfiguration implementations of the support vector machine classifier on FPGA." Turkish Journal of Electrical Engineering & Computer Sciences 24, no. 5 ,pp. 3371-3387, 2016

[20] Abdelhamid, Neda, Aladdin Ayesh, and Fadi Thabtah. "Phishing detection based associative classification data mining." Expert Systems with Applications 41, no. 13, pp.5948-5959, 2014.

On Arabic Character Recognition Employing Hybrid Neural Network

Md. Al-Amin Bhuiyan
Dept. of Computer Engineering
King Faisal University
Al Ahsa, Saudi Arabia

Fawaz Waselallah Alsaade
Dept. of Computer Engineering
King Faisal University
Al Ahsa, Saudi Arabia

***Abstract*—Arabic characters illustrate intricate, multidimensional and cursive visual information. Developing a machine learning system for Arabic character recognition is an exciting research. This paper addresses a neural computing concept for Arabic Optical Character Recognition (OCR). The method is based on local image sampling of each character to a selected feature matrix and feeding these matrices into a Bidirectional Associative Memory followed by Multilayer Perceptron (BAMMLP) with back propagation learning algorithm. The efficacy of the system has been justified over different test patterns of Arabic characters. Experimental results validate that the system is well efficient to recognize Arabic characters with overall more than 82% accuracy.**

***Keywords*—Arabic characters; Arabic OCR; image histogram; BAMMLP; hybrid neural network**

I. INTRODUCTION

Arabic language occupies a significant role in mass communication. Over 200 million people speak in Arabic language as mother tongue [1], and more than one billion people exercise it for multifarious religion-oriented matters. Arabic character recognition, therefore, has become one of the exciting areas of research. In spite of its emergent interests in this area, no appropriate solution is presented due to the distinct and intricate characteristics of Arabic scripts.

Numerous research articles have been cited in scientific journals in the field of recognizing English, Chinese, Japanese, Latin, Indian and Bangla characters [2]-[8]. A minute development, however, has been attained in the recognition of Arabic characters, principally owing to their cursive behavior [9]. A simple method for Arabic character recognition system was proposed by Abdelwadood *et al*. [10] where segmentation of Arabic characters were performed by dynamic windowing and correlation were employed to recognize Arabic alphabets. AbdelRaouf *et al*. offered a comprehensive study on multi-modal Arabic corpus for OCR development [11]. Dreuw *et al*. proposed a hidden Markov model based OCR system [12]. Oujaoura *et al*. proposed a Zernike moments based Walsh Transformation for feature extraction and employed neural networks for classification of Arabic characters [13]. Abulnaja and Batawi have proposed a fault-tolerant method to increase the success rate of Arabic character recognition [14]. With cursive styles, Alkhateeb *et al*. [15] employed hidden Markov model for Arabic alphabet identification. Vaseghi *et al*. [16] presented a holistic approach to recognize handwritten Farsic/Arabic word employing discrete Markov chain and Kohonen feature map for Arabic character recognition. Al-Taani *et al*. [17] analyzed the structural features of Arabic characters and made a decision tree learning approach for character identification.

AbdelRaouf *et al*. [18] have proposed the Haar cascade classifier approach which employs discrepancies between rectangular sub-windows to collect features of the Arabic characters. Although the characters with diagonal shapes were prominent while considering the rotated features, but character with other orientations were poorly recognized by their method. Elnagar and Bentrcia [19] have used a neural network to validate the over-segmentation problem in Arabic character recognition and proposed a heuristic-based rule to accumulate strokes for accurate segmentation of characters. Supriana and Nasution [20] have implemented binarization and median filter for Arabic character recognition. They employed Hilditch operator for thinning combined by two templates, one to prevent redundant tail and the other one to eliminate redundant interest points. During segmentation, they employed line segmentation by horizontal projection by connected pixel components, and letter segmentation by Zidouri algorithm. For feature extraction, they used 24 features. Parvez and Mahmoud [21] have segmented the Arabic texts into words and sub-words to extracted the dots and have developed an Arabic handwriting script recognition by means of morphological procedures and fuzzy polygon matching algorithm. Mohammad *et al*. [22] employed three hidden Marcov model skewed windows: aligned to the left, right, and vertical, and combined the effects employing a set of arrangements: addition law, majority vote and multilayer perceptron. Al-Helali and Mahmoud [23] have processed the delayed strokes of Arabic characters and proposed a framework for Arabic character recognition. Although they evaluated the statistical features of Arabic characters but they did not consider the connectivity problems, variability, and style change of text.

This paper proposes a BAMMLP approach for Arabic character recognition that is commenced on local image sampling by converting each Arabic character into a selected $M \times N$ feature matrix. The system is organized with a Bidirectional Associative Memory (BAM) and a Multi-Layer Perception (MLP). The remainder of the article is organized as: Section II describes salient features of Arabic scripts, Section III describes the proposed Arabic OCR algorithm, Section IV highlights the architecture of BAMMLP network, Section V outlines the experimental results, and finally the conclusion section outlines the overall conclusions of the article.

II. Salient Features of Arabic Characters

Arabic scripts are written from right to left and are always cursive [24], [25]. There are 28 basic characters and each character has multiple forms depending on its place in the word. Table 1 shows the 28 Arabic characters with their numerous forms: Isolated, Beginning, Middle, and End forms.

TABLE. I. Arabic Characters

SL	Characters	Isolated	Begining	Middle	End
1	Alif	ا	ا	ـا	ـا
2	Baa	ب	بـ	ـبـ	ـب
3	Taa	ت	تـ	ـتـ	ـت
4	Thaa	ث	ثـ	ـثـ	ـث
5	Jeem	ج	جـ	ـجـ	ـج
6	Hha	ح	حـ	ـحـ	ـح
7	Kha	خ	خـ	ـخـ	ـخ
8	Dal	د	د	ـد	ـد
9	Thal	ذ	ذ	ـذ	ـذ
10	Raa	ر	ر	ـر	ـر
11	Zay	ز	ز	ـز	ـز
12	Seen	س	سـ	ـسـ	ـس
13	Sheen	ش	شـ	ـشـ	ـش
14	Sad	ص	صـ	ـصـ	ـص
15	Dhad	ض	ضـ	ـضـ	ـض
16	Tta	ط	طـ	ـطـ	ـط
17	Ttha	ظ	ظـ	ـظـ	ـظ
18	Ain	ع	عـ	ـعـ	ـع
19	Ghain	غ	غـ	ـغـ	ـغ
20	Faa	ف	فـ	ـفـ	ـف
21	Gaf	ق	قـ	ـقـ	ـق
22	Kaf	ك	كـ	ـكـ	ـك
23	Lam	ل	لـ	ـلـ	ـل
24	Meem	م	مـ	ـمـ	ـم
25	Noon	ن	نـ	ـنـ	ـن
26	Ha	ه	هـ	ـهـ	ـه
27	Waw	و	و	ـو	ـو
28	Yaa	ي	يـ	ـيـ	ـي

While writing separately, each Arabic character is patterned in an isolated style and is implied in three different styles when it is joined with other characters. Fig. 1 shows some characters whose isolated forms are distinguished from the Beginning, Middle, and End forms. Characters possessing the same shape but vary in number of dots provide the similar characteristics.

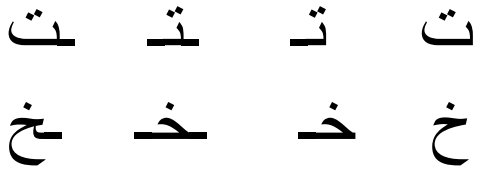

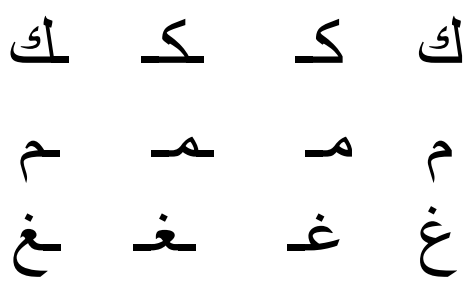

(a) End (b) Middle (c) Beginning (d) Isolated

Fig. 1. Characters whose isolated forms are distinguished from their Beginning, Middle, and End forms.

Arabic scripts belong to the following features [1]:

1) The texts are being written from right to left.
2) Different characters have different sizes.
3) Different characters have different number of dots. Some characters have dots located in the upper side, some have in the lower side, some contain one dot, some contain two dots, some contain three dots, and some characters even do not have any dot.
4) The same character appears in diverse profiles depending on its location in the word.
5) Within a word, every character is usually joined to the preceding character. However, there are six characters that do not attach to the preceding character. These characters have only the Isolated and End forms.
6) Some Arabic words consist of sub-words. Example, the word رسول contains three sub-words: a character ر, the second sub-word سو and finally the character ل.
7) During formation of words, some characters appear with different compound strings. For example, Noon followed by Alif is written (ـنا) rather than (ـن ا), Lam in the middle of a word is often written as (ـلـ), Ta (ـتـ) and ha (ـهـ) has other different shapes which are (ة) and (ه), respectively, like in the word "word" (كـلـمـة), (ك ل م ة) and in the word "Lost" (تـاه) and not (ت ا هـ).

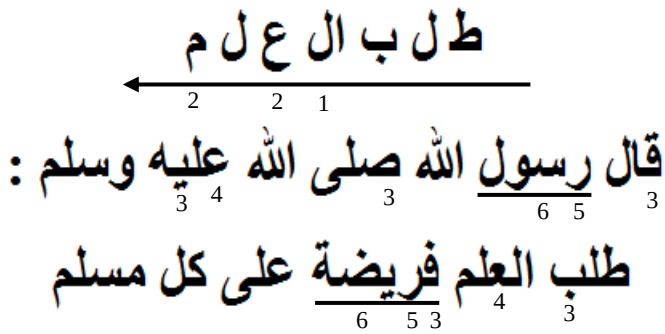

Fig. 2. Features of Arabic script.

Fig. 2 illustrates a precise summary of the striking features of Arabic scripts: 1) written from right to left; 2) different characters have different sizes; 3) different characters have different number of dots, some characters even do not contain any dot; 4) the same character appears with different profiles;

5) some characters are not connected to the succeeding characters; 6) some words consist of sub-words.

III. Arabic Character Recognition

Since the Arabic alphabets possess diverse profiles at different positions of a word and most letters contain one, two, or three dots, the proposed Arabic OCR algorithm, therefore, employs a two stage method: the first stage serves for dots identification; and the second stage is dedicated for recognizing the main shape of the characters. The reason behind dots identification is to reduce the complexity of the problem domain. Since some characters have different number of dots above or below the basic skeleton but have the similar shapes, as shown in Fig. 3, so counting the dots and identification of the basic shape reduces the search space.

(a) Noon (b) Thaa (c) Taa (d) Baa

Fig. 3. Similar characters with different number of dots.

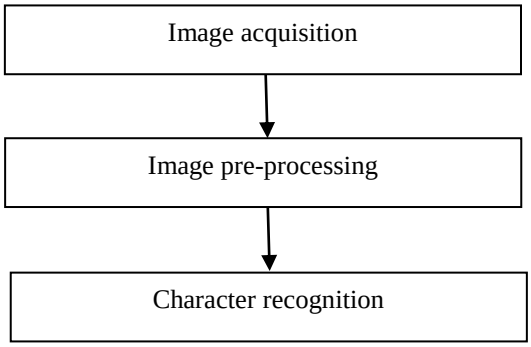

Fig. 4. Steps employed for the proposed Arabic character recognition system.

To recognize the main shape of characters, the system employs a three steps procedure, as shown in Fig. 4.

Step 1: *Image acquisition*: The proposed Arabic OCR system is commenced on image acquisition process that scans the texts in 600 dots per inch and the generated images are being saved in .pgm files. This research employs popular Arabic words for image database. After scanning, images of the characters are being Affine (scaling, translation and rotation) transformed [26].

Step 2: *Image pre-processing*: The input images sometimes may be corrupted by various sources of noise. If the noise is not suppressed, it may cause incorrect results. Therefore, these images are filtered by median filter to remove noise and then converted into binary image for processing.

Step 3: *Image recognition*: This step involves word segmentation, character segmentation and recognition steps.

Arabic characters are being segmented by histogram analysis and baseline detection method. The baseline is described by one or more rows with the higher number of black pixels on them compared to other lines. Baselines are being detected by employing histogram construction in counting the number of black pixels followed by white pixels in a single line, as shown in Fig. 5. Subsequently, each line is considered separately for segmenting the words.

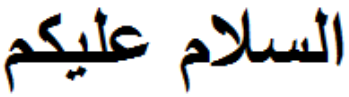

(a) An Arabic script image.

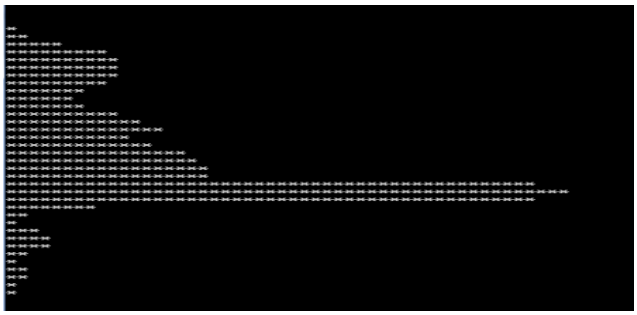

(b) Histogram of the image (a)

Fig. 5. Baseline detection.

IV. BAMMLP Network

The BAMMLP is the hybridization of two neural networks: 1) Bidirectional Associative Memory (BAM) network and 2) Multilayer Perceptron (MLP). The design of the BAMMLP network [27] is illustrated in Fig. 6.

Once the image pre-processing is done, the Arabic characters are patterned in a 20×20 matrix and subjected to the input of the BAM network. Thus the matrix pattern is characterized as vectors of 400 neurons. The BAM accepts an input pattern as a vector and generates an associated vector to reduce the size. To develop the BAM, a correlation matrix is created for each pattern pair. The BAM disseminates the input Vector ***A*** to the ***B*** layer where the net input is computed as:

$$y_k = \sum_{j=1}^{N} x_j w_{jk} \tag{1}$$

and control the output values by the thresholding function:

$$y_k(p+1) = \begin{cases} +1 & if\ y_k > 0 \\ y_k(p) & if\ y_k = 0 \\ -1 & if\ y_k < 0 \end{cases} \tag{2}$$

for k=1, 2, …, N.

The pattern ***B*** formed in the Y layer is then disseminated back to the X layer computing the net input as:

$$x_j = \sum_{k=1}^{M} y_k w_{jk} \tag{3}$$

and decide the output values as:

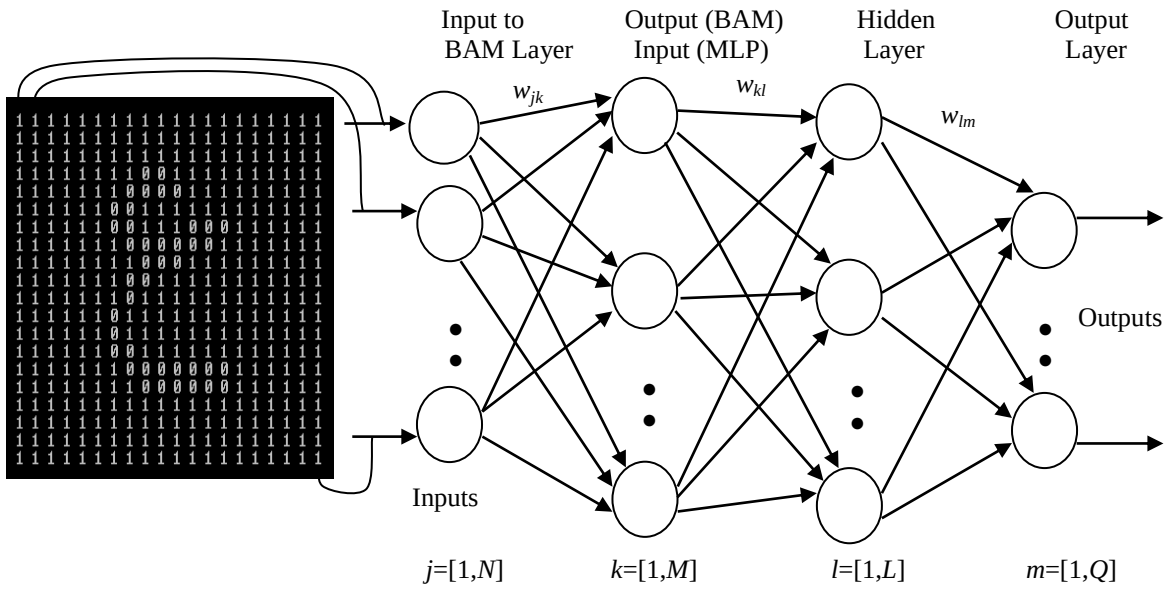

Fig. 6. Architecture of hybrid neural network.

$$x_j(t+1) = \begin{cases} +1 & if\ x_j > 0 \\ x_j(t) & if\ x_j = 0 \\ -1 & if\ x_j < 0 \end{cases} \quad (4)$$

The output of the BAM layer is subjected to the input of the MLP. The Multi-layer Perceptron (MLP) is being trained by back-propagation algorithm [28], [29].

Step 1: *Initialization*: Initialize the network with all the weights and threshold parameters of the MLP to small random numbers.

Step 2: *Activation*: Activate the MLP by subjecting the training set $y_k, k = [1, M]$ and the expected outputs $y_m, m = [1, Q]$. Compute the activation of neurons in the *l* and *m* layers:

$$y_l(z) = sigmoid\left[\sum_{k=1}^{M} y_k(z) \times w_{kl}(z) - \theta_l\right], \quad (5)$$

$$y_m(z) = sigmoid\left[\sum_{l=1}^{L} y_l(z) \times w_{lm}(z) - \theta_m\right], \quad 6)$$

where *sigmoid* is the sigmoidal activation function, w_{kl} and w_{lm} are the weights between neuron *k* is the input layer of MLP and neuron *l* in the hidden layer, and neuron *l* is the hidden layer and neuron *m* in the output layer, respectively. θ_l and θ_m are the threshold values of the respective neurons.

Step 3: *Weight modification*: Modify the weights of the MLP disseminating the errors in the backward direction.

Step 4: *Iteration*: Increase iteration *i* by one, loop back to Step 2 and repeat the process until the error value reduces to the desired level.

For reorganizing Arabic characters, all the characters of Arabic dictionary need not train. Only the basic or mainstream characters (without dots) need to be trained. All other characters can be assessed by means of the information about the position and number of dots containing the characters.

V. Experimental Results

The efficacy of the approach has been validated with numerous Arabic texts of different resolutions. Our system is capable of segmenting and identifying characters in images of various orientations and background conditions. Experiments are carried out on an Intel Core ™ i5-2390T CPU @ 2.70 GHz PC with 4 GB MB RAM. The Arabic character recognition system has been implemented employing Visual C++ programming language. Fig. 7 illustrates the program snapshot for a typical Arabic character individually.

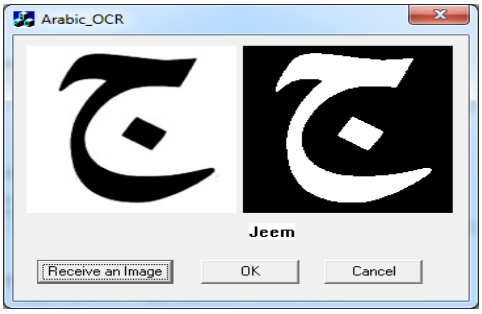

Fig. 7. Snapshot of the software interface for Arabic character recognition.

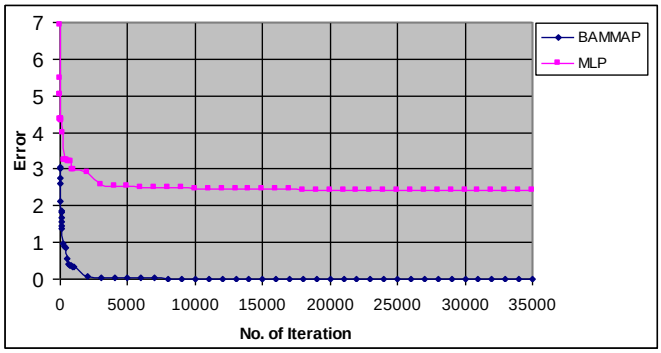

Fig. 8. Error versus iteration.

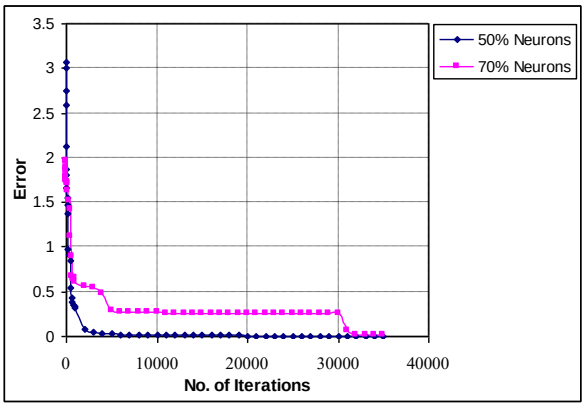

Fig. 9. Error versus iteration graph for BAMMLP.

The learning outcome of the hybrid network has been tested with different experiments. For each character images, investigations were accomplished with 5 training and 3 test images. There was no overlap between the training and test image sets. First the system was implemented employing the multilayer perceptron with back propagation algorithm. Then BAMMLP was employed to train and recognize the Arabic characters. The MLP was trained with back-propagation learning algorithm employing the parameters: learning rate 0.1 and momentum 0.25, for 35000 iterations. During training session, the algorithm runs until the error value reduces to the desired threshold level of 0.001. The error versus iteration graphs for both BAMMLP and MLP are jointly shown in Fig. 8.

The graphs imply that the errors reduce exponentially. Although for BAMMLP, the error value reduces to 0.01 at 1996 iterations, it still remains 0.264 even after 35000 iterations. The graphs reveal that the BAMMLP network outperforms the MLP in terms of minimum number of iterations to train the Arabic characters. Fig. 9 shows the error versus iteration graph for BAMMLP for 50% and 70% neurons with respect to the input layer, respectively. Obviously, as the number of neurons in the hidden layer is less, there is less computational cost and recognition process becomes faster. But for accuracy, we need more neurons in the hidden layer. So there is always a trade off in choosing the number of neurons in the hidden layer. For this experiment, the learning process achieved the expected threshold level within less than 5,000 iterations while choosing the number of neurons in the hidden layer to be 50% of the number of neurons in the input layer. On the contrary, considering 70% neurons in the hidden layer, the same threshold level is being achieved after 30,000 iterations. Therefore, the number of neurons in the hidden layer was chosen as 50% of the number of neurons in the input layer for recognizing Arabic characters. Later on, the BAMMLP hybrid neural network was used to recognize characters randomly, as shown Fig. 10.

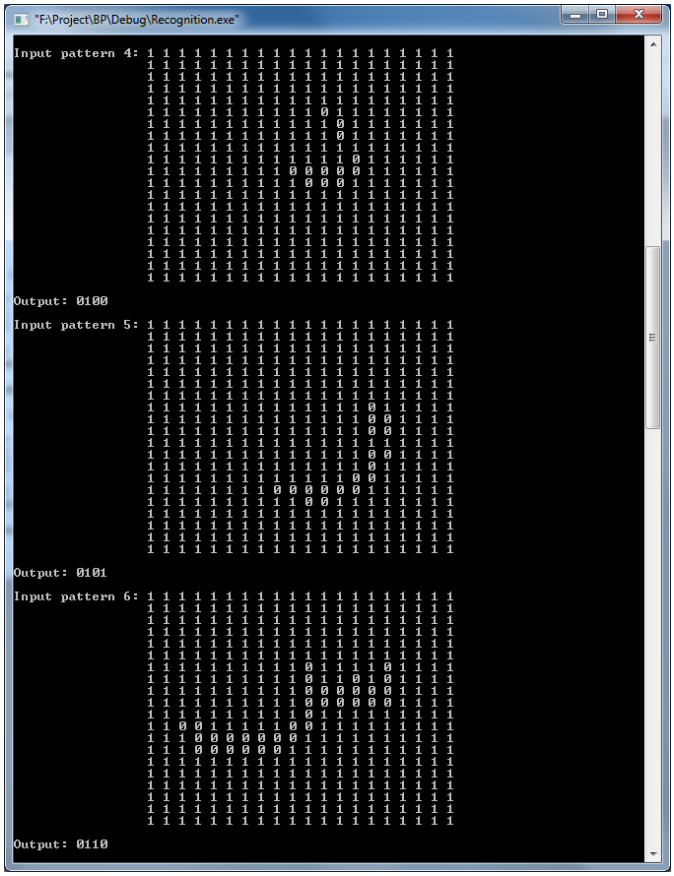

Fig. 10. Recognition of three test images (,ر,ض)

Experiments were conducted separately for Arabic character recognition for four different forms: Isolated, Beginning, Middle, and End form and their outcomes are furnished in the Table 2.

TABLE. II. ACCURACY FOR DIFFERENT FORMS OF ARABIC CHARACTERS

Isolated form	Beginning form	Middle form	End form
91.5%	90.5%	82.71%	84.29%

The recognition rate for different Arabic characters in isolated form is shown in Fig. 11.

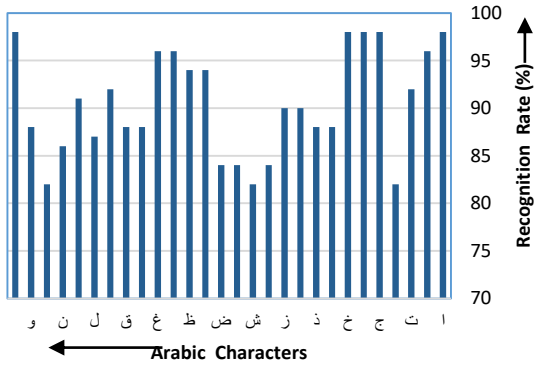

Fig. 11. Recognition rate for different Arabic characters in isolated form.

VI. CONCLUSIONS

An efficient Arabic character recognition system has been presented through a hybrid neural network which consists of a BAM and a multilayer perceptron. The system is very fast and is able to carry out the recognition in less than 1ms for all forms of Arabic characters, which demonstrates that the method is an appropriate one for real-time applications. Our next approach will be to recognize Arabic number plate identification for any desired application, including black-lists, white-lists, and alarm functions.

ACKNOWLEDGMENT

The authors would like to express their gratitude to the Deanship of Scientific Research, King Faisal University, Saudi Arabia, for the financial support of the project No 150169.

REFERENCES

[1] A. Hassin, X.L. Tang, J.F. Liu and W. Zhao, "Printed Arabic character recognition using HMM", Journal of Computer Science and Technology, Vol. 19, No. 4, pp. 538-543, 2004.

[2] M.R. Gupta, P.N. Jacobson, E.K. Garcia, "OCR binarization and image pre-processing for searching historical documents", Pattern Recognition, Vol. 40, pp. 389 – 397, 2007.

[3] Y. Yang, X. Lija, and C. Chen, "English character recognition based on feature combination", Procedia Engineering, Vol. 24, pp. 159-164, 2011.

[4] X.-D. Zhou, D.-H. Wang, F. Tian, C.-L. Liu, and M. Nakagawa, "Handwritten Chinese/Japanese text recognition using semi-Markov conditional random fields", IEEE Trans. Pattern Analysis and Machine Intelligence, vol. 35, no. 10, pp. 2484–2497, 2013.

[5] Q.-F. Wang, F. Yin, and C.-L. Liu, "Handwritten Chinese text recognition by integrating multiple contexts", IEEE Trans. Pattern Analysis and Machine Intelligence, vol. 34, no. 8, pp. 1469–1481, 2012.

[6] C.-L. Liu, F. Yin, D.-H. Wang, and Q.-F. Wang, "Online and offline handwritten Chinese character recognition: Benchmarking on new databases," Pattern Recognition, vol. 46, no. 1, pp. 155–162, 2013.

[7] M. Kumar, M.K. Jindal and R.K. Sharma, "Review on OCR for handwritten Indian scripts character recognition", Advances in Digital Image Processing and Information Technology Communications in Computer and Information Science, Vol. 205, pp. 268-276, 2011.

[8] T. Hashem, M. Asif and M.A. Bhuiyan, "Handwritten Bangla digit recognition employing hybrid neural network approach", Proc. of 16th International Conference on Computer and Information Technology (ICCIT), pp. 360-365, 2014.

[9] B. Al-Badr and S. Mohmoud, "Survey and bibliography of Arabic text recognition", Signal processing, Vol. 4, pp. 49-77, 1995.

[10] M. Abdelwadood, S. Ahmed, J. Al-Azzeh, M. Abu-Zaher, N. Al-Zabin, T. Jaber, O. Aroob, and H. Myssa'a, "An optical character recognition", Contemporary Engineering Sciences, Vol. 5, No. 11, pp. 521 – 529, 2012.

[11] C. AbdelRaouf, T. Higgins, T. Pridmore and M. Khalil, "Building a multi-modal Arabic corpus (MMAC)", International Journal on Document Analysis and Recognition, Vol. 13, pp. 285-302, 2010.

[12] P. Dreuw, D. Rybach, G. Heigold and H. Ney, "RWTH OCR: A large vocabulary optical character recognition system for Arabic scripts", Guide to OCR for Arabic Scripts Chapter, Part II: Recognition, Springer, London, UK, pp. 215-254, 2012.

[13] M. Oujaoura, R.E. Ayachi, M. Fakir, B. Bouikhalene and B. Minaoui, "Zernike moments and neural networks for recognition of isolated Arabic characters", International Journal of Computer Engineering Science, Vol. 2, pp. 17-25, 2012.

[14] O. Abulnaja and Y. Batawi, "Improving Arabic optical character recognition: accuracy using n-version programming technique", Canadian Journal on Image Processing and Computer Vision, Vol. 3, pp. 44-46, 2012.

[15] J.H. Alkhateeb, J. Ren, J. Jiang, H. Al-Muhtaseb, "Offline handwritten Arabic cursive text recognition using hidden Markov models and re-ranking", Pattern Recognition Letters, Vol. 32, No. 1, pp. 1081-1088, 2011.

[16] B. Vaseghi and S. Hashemi, "Farsi/Arabic handwritten word recognition using discrete HMM and self-organiaing feature map", International Congress on Informatics, Environment, Energy and Applications, IPCSIT, Vol. 38, No. 1, pp. 55-62, 2012.

[17] A. T. Al-Taani, S. and Al-Haj, "Recognition of on-line Arabic handwritten characters using structural features", Journal of Pattern Recognition Research, Vol. 1, pp. 23-37, 2010.

[18] A. AbdelRaouf, C.A Higgins, T. Pridmore and M.I. Khalil, "Arabic character recognition using a Haar cascade classifier approach", Pattern Analysis and Application, Vol. 19, pp. 411–426, 2016.

[19] A. Elnagar and R. Bentrcia, "A recognition-based approach to segmenting Arabic handwritten text", Journal of Intelligent Learning Systems and Applications, Vol. 7, No. 1, pp. 93-103, 2015.

[20] I. Supriana and A. Nasution, "Arabic character recognition system development", Procedia Technology, Vol. 11, pp. 334 – 341, 2013.

[21] M.T. Parvez and S.A. Mahmoud, "Arabic handwriting recognition using structural and syntactic pattern attributes", Pattern Recognition, Vol. 46, pp. 141–154, 2013.

[22] R.A. Mohamad, L. Likforman-Sulem, C. Mokbel, Combining slanted-frame classifiers for improved HMM-based Arabic handwriting recognition, IEEE Transactions on Pattern Analysis and Machine Intelligence, Vol. 31, No. 7, pp. 1165–1177, 2009.

[23] B.M. Al-Helali and S.A. Mahmoud, "A statistical framework for online Arabic character recognition", Cybernetics and Systems: An International Journal, Vol. 47, No. 6, pp. 478–498, 2016.

[24] G.A. Abandah and K.S. Younis, "Handwritten Arabic character recognition using multiple classifiers based on letter form", Proc. 5th IASTED Int'l Conf. on Signal Processing, Pattern Recognition and Applications (SPPRA), pp.128-133, 2008.

[25] K. Addakiri and M. Bahaj, "On-line handwritten Arabic character recognition using artificial neural network", International Journal of Computer Applications, Vol. 55, No. 13, pp. 42-46, 2012.

[26] M.A.Bhuiyan and H. Hama, "Identification of Actors Drawn in Ukiyoe Pictures, Pattern Recognition, vol. 35, no. 1, pp. 93-102, 2002.

[27] A. Khatun and M.A. Bhuiyan, "Neural network based face recognition with Gabor filters", International Journal of Computer Science and Network Security, Vol. 11, No. 1, pp. 71-76, 2011.

[28] S.K. Saha, M. Shamsuzzaman and M.A. Bhuiyan, "On Bangla character recognition", Proc of 13th International Conference on Computer and Information Technology (ICCIT), pp. 436-439, 2010.

[29] M. Negnevitsky, Artifical Intelligence - A Guide to Intelligent Systems, Addision-Wesley Inc., Pearson Edition, London, England, 2002.

Cross-Layer-Based Adaptive Traffic Control Protocol for Bluetooth Wireless Networks

Sabeen Tahir
Department of Information Technology,
Faculty of Computing and Information Technology,
King Abdulaziz University, Jeddah 21589, Makkah,
Saudi Arabia

Sheikh Tahir Bakhsh
Department of Computer Science,
Faculty of Computing and Information Technology,
King Abdulaziz University, Jeddah 21589, Makkah,
Saudi Arabia

***Abstract*—Bluetooth technology is particularly designed for a wireless personal area network that is low cost and less energy consuming. Efficient transmission between different Bluetooth nodes depends on network formation. An inefficient Bluetooth topology may create a bottleneck and a delay in the network when data is routed. To overcome the congestion problem of Bluetooth networks, a Cross-layer-based Adaptive Traffic Control (CATC) protocol is proposed in this paper. The proposed protocol is working on backup device utilization and network restructuring. The proposed CATC is divided into two parts; the first part is based on intra-piconet traffic control, while the second part is based on inter-piconet traffic control. The proposed CATC protocol controls the traffic load on the master node by network restructuring and the traffic load of the bridge node by activating a Fall-Back Bridge (FBB). During the piconet restructuring, the CATC performs the Piconet Formation within Piconet (PFP) and Scatternet Formation within Piconet (SFP). The PFP reconstructs a new piconet in the same piconet for the devices which are directly within the radio range of each other. The SFP reconstructs the scatternet within the same piconet if the nodes are not within the radio range. Simulation results are proof that the proposed CATC improves the overall performance and reduces control overhead in a Bluetooth network.**

***Keywords*—Bluetooth; scatternet; multi-layer; resolving bottleneck; reducing control overhead component**

I. INTRODUCTION

Improvements in wireless technologies have enhanced our daily life. A number of mobile devices can interconnect through wireless technology and exchange different types of data (text, voice, and video) [1]. Bluetooth is an open standard that has the ability to connect heterogeneous mobile devices. A basic communication unit of Bluetooth is piconet, which consists of eight active Bluetooth nodes. A piconet is created through sharing the same frequency hopping sequence and synchronization, where one Bluetooth node becomes the master and remaining nodes act as slaves. An active Bluetooth device may perform the role of master, slave or bridge. Slave nodes cannot communicate directly with each other; they always need a master node support for communication, as the master node always handles all communications within a piconet [2], [3]. The communication within a piconet is also called intra-piconet communication. Bluetooth devices transmit their data packets over Time Division Duplex (TDD) [4].

Bluetooth also allows communication within multiple piconets, which is known as a scatternet. Where a relay or bridge device provides communication among different piconets, a bridge node can be Master-Slave (M/S) or Slave-Slave (S/S) [5]. A bridge node is responsible for transporting messages between piconets so that the resources should not be restricted [6]. Bluetooth efficient communication can be achieved through a role switching technique [7], which can be used for different requirements. A role switching operation divides one piconet into multiple piconets; splitting operation increases the number of piconets and bridge nodes. Using an example in Fig. 1(a), before executing a splitting role switch operation, there is one piconet having one master with six slave nodes. Fig. 1(b) shows how a role switch operation splits one piconet into two piconets P_1 and P_2 by changing the roles of the devices, where node C and F perform the master role and node A is used as a bridge between two piconets.

A merge role switch operation combines different piconets into a single piconet [8], [9]. As shown in Fig. 1(b), two piconets (P_1 and P_2) are connected through an intermediate node *A*. Nodes (*B, C, D, E, F, G*) are in the range of node A. According to the role switch operation, node A performs the master role and merges two piconets into a single piconet. Fig. 1(a) shows how a bridge node becomes a master and masters (*C* and *F*) change their roles from master to slave. A role switch operation can be applied on Bluetooth device to take over the resource of other device. During this operation, devices can change their roles from slave to master and vice versa. As shown in Fig. 1(c), node *D* and *G* become masters and node *A* acts as a slave node, with two independent piconets.

Many researchers proposed scatternet formation protocols [10]-[14] to decrease scatternet formation time or increase the probability of making a scatternet, but an efficient scatternet formation protocol is missing. This paper designs a well-organized protocol for a Bluetooth scatternet that minimizes the delay and efficiently uses the network resources. The proposed CATC controls and shares the traffic load of master and bridge nodes in a distributed manner. The role-switching operations are performed dynamically for congestion handling on an affected link.

Deanship of Scientific Research (DSR) in King Abdulaziz University, under grant No. (611-271-D1435).

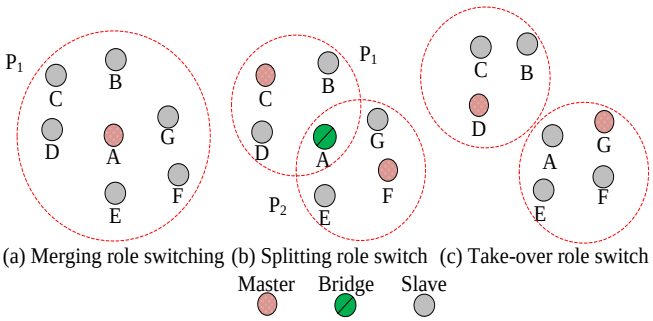

Fig. 1. Different configurations of Bluetooth network.

The paper is organized as: The background is discussed in Section 2. To control traffic load in Bluetooth network, a protocol is proposed in Section 3. The results of the proposed CATC are presented in Section 4 using NS-2 [15] and UCBT [16]. The paper is concluded in Section 5.

II. Related Work

The traffic bottleneck is an important issue in Bluetooth, which is caused by a master or bridge node. Within a piconet, all slaves communication is possible through the master node, while scatter communication is achieved through intermediate relay node [17]. A huge number of devices may cause congestion and delay in the Bluetooth scatternet. The slave device cannot communicate with each other, master is always involved in intra-piconet communication among slaves. Therefore, master's energy and mobility have a critical role in the piconet. In the same way, bridge node mobility and energy has a crucial role for inter-piconet communication. Failure of a bridge node may disconnect the whole network. Many researchers have proposed different techniques for a Bluetooth scatternet, i.e., relay optimization, congestion avoidance, and scheduling. Each technique has its own benefits and limitations [1], [18], [19]. Through a literature survey, some relevant existing research works have been analyzed in this research work.

Dynamic piconet restructuring protocol (PRP) [20] is proposed for Bluetooth networks. PRP locally regulates the traffic on the master node. PRP shares master node load by forming new piconets of slave nodes that can communicate directly, where one slave node acts as a master and others act as slaves. During the restructuring operation, the slave node with light traffic flow will be selected as the new master. For example, as shown in Fig. 2(a), nodes (*A, B*), (*E, F*) and (*B, C*) are communicating through a master *G*. According to PRP, when traffic load is detected by the master node, it performs piconet restructuring using a role switching operation as shown in Fig. 2(b).

It is analyzed that PRP provides a solution for congestion problem on a master node through sharing the load, but it creates serious problems. It loses active member addresses due to breaking the existing link between slaves and master. During transmission, if new joins the piconet, the master assigns all remaining active member addresses to new nodes. Once the communication is over the nodes cannot join the existing master due to unavailability of active member address. Frequent piconets construction also consume extra resources. At it creates new piconets for all communicating pairs without considering whether they are frequently communicating or not. The new nodes cannot communicate with the node already changed their state, therefore, the new nodes have to wait until nodes to return to their original states.

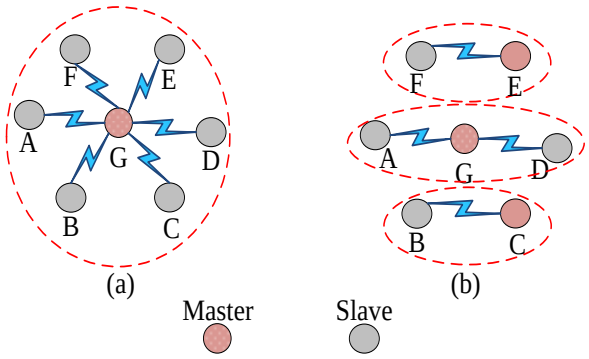

Fig. 2. Traffic flow analysis before and after role switching.

Subsequently, Dynamic Congestion Control (DCC) [21] has been proposed as another solution for avoiding bottleneck problems in a scatternet through backup relay (BR). If several links use a single bridge it creates a bottleneck. The master monitors the load and delay on the bridge node. The master gets relay load and a number of links from relay table. When the master observes bottleneck in the piconet, it shares the load through BR. As shown in Fig. 3, multiple links passing through M_1 the data traffic load can be determined by the master. As different piconets are communicating through bridge node B_1, the master activates the *BR* to share the load. It provides a solution for intra-piconet congestion inter-piconet congestion it still missing. When there is a bottleneck on B_1, but the master in P_1 cannot find the congestion due to distributed traffic, it fails to avoid inter-piconet congestion. As shown in Fig. 3, all traffic load is passing through B_1. Although *BR* is available the load is distributed, *BR* is not activated by M_1. In distributed load, DCC does not allow parallel transmissions.

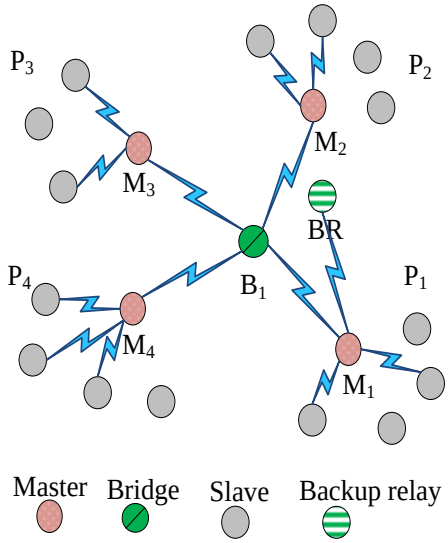

Fig. 3. Scatternet formation using DCC Protocol.

III. The Proposed Cross-Layer-Based Adaptive Traffic Control (CATC) Protocol

This section discusses the proposed CATC protocol for intra-piconet and inter-piconet congestion avoidance. The proposed protocol consists of two parts; in the first part, role switching techniques are used to overcome the problem of intra-piconet congestion avoidance. In the second part, FBB is used to control the bridge load that overcomes the bottleneck problem of inter-piconet congestion.

A. Intra-piconet traffic load and dynamic role switching operation

In this section, intra-piconet traffic load handling is presented. The intra-piconet traffic load is handled through PFP and SFP.

1) Intra-piconet load handling through Piconet Formation within Piconet

Large numbers of connections passing through the master node within a piconet may create congestion. The incoming data traffic is called Download Traffic (*DTr*), and the outgoing data traffic is called Upload Traffic (*UTr*). The traffic load in a piconet is calculated as follows:

$$DTr = \sum_{i=1}^{n} a_{i1} \quad for\ i = 1, 2, 3, \ldots n \quad where\ n \leq 8 \qquad (1)$$

$$UTr = \sum_{j=1}^{n} a_{1j} \quad for\ j = 1, 2, 3, \ldots n \quad where\ n \leq 8 \qquad (2)$$

$$TT = DTr + UTr = \sum_{i=1}^{n} a_{i1} + \sum_{j=1}^{n} a_{1j} \qquad (3)$$

where *DTr* and *UTr* calculate incoming and outgoing traffic respectively. The total traffic (*TT*) load on a master node is calculated through the sum of (1) and (2).

The proposed protocol maintains a Master Traffic Flow Table (*MTFT*) to monitor traffic load. The *MTFT* maintains the information of all incoming and outgoing data traffic going through the master within a piconet as recorded in Table 1. A threshold (θ) value is used for congestion handling on the master node. When a master gets *TT* it compares to θ, where θ = 90 slots. The traffic load is calculated after receiving or transmitting data between a new pair. In the next step, master marks the most frequent (*MF*) communicating nodes that reach the limit of the threshold value. Hence, the CATC performs network restructuring using a taking-over role switching operation. When the master node determines higher traffic load is greater than θ, it performs a role switch operation by sending a request packet to the pair of *MF* communicating nodes within the piconet. When the master node receives uplink data, it checks in the *MTFT*; if the number of active connections is more than three, the master node calculates *TT*. A pair of nodes having the highest traffic load is marked as the *MF* communicating pair.

The role switch request packet contains the node *ID* and clock-offset of the nodes. On receiving the role switch request, the source node enters into Page state and destination node enters into Page Scan state to create a new piconet. In the next step, the master node changes both nodes mode into park mode, to save active member addresses and reduce unnecessary switching control overhead. Once the communication ends, the nodes come back into their original states and send a request to the master node to restore their original states as active slaves. As the master node maintains the list of nodes for temporary connections, the original active member addresses are reserved by the master node. Hence, the nodes can come back to their original states without losing their connection.

Using an example, Fig. 4(a) shows, node (*I*, *J*) and (*A*, *B*) are marked as *MF* communicating pairs by M_1 and M_2 respectively. Therefore, a piconet restructuring request is sent to the slave nodes by the master nodes. As a result, after piconet restructuring, slave nodes *J* and *A* become auxiliary masters; the new connections of the most frequently communicating nodes are shown in Fig. 4(b). The data traffic flow of *the* M_2 is maintained in Table 1 among different nodes, where *MF* represents a heavy traffic flow, 1 is used for normal traffic, and Ø means there is no data exchange between nodes.

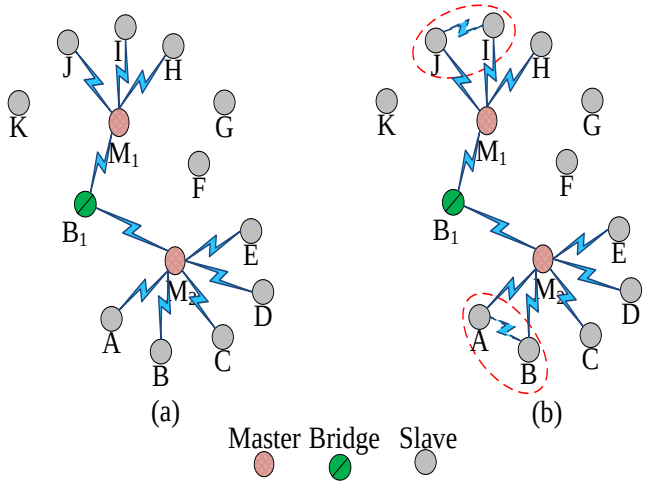

Fig. 4. (a) Before role switching operation (b) After role switching operation.

TABLE. I. Data Traffic Flow Analysis on Master M_2

ID	A	B	C	D	E	F	B_1	M_2
A	Ø	MF	Ø	Ø	Ø	Ø	Ø	1
B	MF	Ø	1	Ø	Ø	Ø	Ø	1
C	Ø	Ø	Ø	1	1	Ø	Ø	1
D	Ø	Ø	1	Ø	1	Ø	Ø	1
E	Ø	Ø	1	1	Ø	Ø	Ø	1
F	Ø	Ø	Ø	Ø	Ø	Ø	Ø	Ø
B_1	Ø	Ø	Ø	Ø	Ø	Ø	Ø	Ø
M_2	1	1	1	1	1	Ø	1	Ø

2) Intra-piconet traffic load handling through Scatternet Formation within Piconet (SFP)

The proposed SFP creates a scatternet within a piconet. On receiving a role switch request, source and destination nodes enter Page and Page Scan state respectively and try to create a new link. As the paging procedure needs 1.28 *s*, after executing twice paging procedure if nodes fail to establish the new link. The source node sends a link fail message to the master node. On receiving the source node link fail message, the master requests connected slave nodes to enter into Inquiry state and create a new connection, where all slave nodes enter into the Inquiry Scan state and listen to the source and the destination nodes. A node that can connect both source and destination nodes performs a bridge role and executes a splitting role switching operation by making a scatternet within a piconet. During SFP operation, an intermediate node is selected as an auxiliary bridge (*AxB*) and a pair of source and destination nodes are selected as auxiliary masters. An intermediate node between source and destination can be selected as an auxiliary bridge.

The SFP operation is explained through Fig. 5. Nodes H and F are marked as MF communicating nodes in the piconet but both are not within the direct radio range of each other. Thus, node G performs an A x B role, while the source node H and the destination node F perform an *AxM* role. In Table 2, according to the Fig. 5, the master node updates the Node Information Table (*NIT*) for *MF* communicating nodes, which are in the same piconets but cannot communicate directly so they need an intermediate node.

TABLE. II. NODE INFORMATION TABLE (NIT) FOR P1 AFTER SFP

ID	Clock-offset	Device-role	Download traffic	Upload traffic
F	C-offset (F)	AxM	70	80
G	C-offset (G)	AxB	150	150
H	C-offset (H)	AxM	80	70

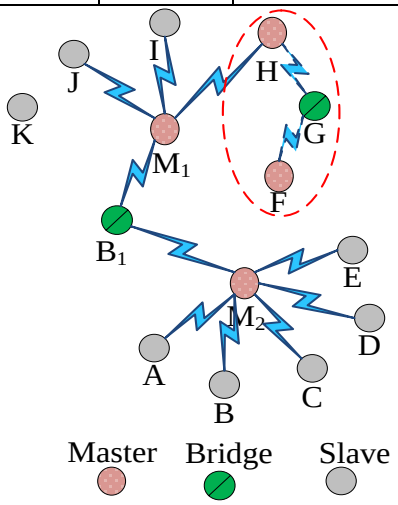

Fig. 5. Sharing of traffic load by making scatternet within the piconet.

B. Inter-piconet traffic load handling on the bridge node through Fall-Back Bridge (FBB)

When multiple piconets are connected through a single bridge, it may create a bottleneck in the network due to the unavailability of a bridge. The inter-piconet problem is solved through FBB. At the same time, a maximum of seven master devices can connect to a bridge device. According to the Bluetooth specification, a bridge node shares its time with all connected masters. Therefore, at the same time, only one master node's traffic can flow through the bridge node. Due to unavailability of a bridge node, inter-piconet congestion seriously affects network performance. The proposed CATC maintains a Bridge Traffic Flow Table (*BTFT*) (Table 3) to store the traffic load of masters that passes through the bridge node. As the bridge device receives/transmits data from master devices if a bridge device receives the data from a master device, it is called Bridge Download Traffic (*BDTr*); similarly, if the bridge device transmits data to the master device, it is called Bridge Upload Traffic (*BUTr*). The traffic load on a bridge (*CB*) device can be calculated as follows:

$$CB = BDTr + BUTr$$

$$= \sum_{i=1}^{n} a_{i1} + \sum_{j=1}^{n} a_{1j} \quad for\ i\ \&j = 0, 1, ..n\ where\ n < 8 \qquad (4)$$

If higher traffic load is detected by a bridge node, it requests masters to activate a backup node. On receiving the request, master finds a FBB; if any master node has a FBB, then it sends a request to the bridge node to activate its connection with the required master node. The FBB is activated when a single bridge node is not sufficient for an efficient communication between piconets. Thus, parallel transmissions are allowed between piconets for well organized and smooth communication. Meanwhile, the master node sends the active bridge node into the park mode. As shown in Fig. 3(a), B_1 connects multiple nodes and creates a bottleneck. The heavy traffic flow does not allow parallel transmission in a scatternet, and thus, B_1 creates the bottleneck, as one master node sends data through B_1, and others wait for B_1 to become free. As shown in Fig. 6, node A is selected as FBB for P_2 and P_3 and node *D* is selected as FBB for P_1 and P_2. The dotted lines show the temporary links where traffic is shared and the bottleneck problem is resolved through activation of FBB. Master nodes update the *NIT* and send FBB to park mode; once communication ends successfully, FBBs return to their original states.

TABLE. III. BRIDGE TRAFFIC FLOW TABLE FOR B_1

ID	M_2	M_3	M_4	M_5	B_1
M_2	Ø	MF	1	1	1
M_3	MF	1	1	1	1
M_4	1	1	Ø	1	1
M_5	1	1	1	Ø	1
B_1	1	1	1	1	Ø

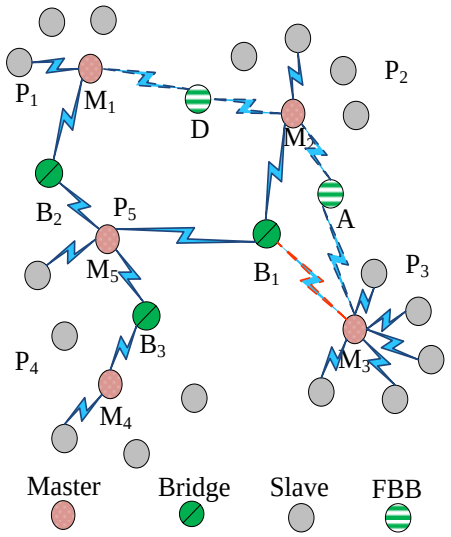

Fig. 6. Scatternet formation after activation of FBB.

IV. Performance Analysis

The proposed protocol is compared against PRP and DCC protocols. To assess the performance, the CATC is simulated in the University of Cincinnati Bluetooth (UCBT) [16], which is a ns-2 [15] based Bluetooth simulator. UCBT is an open source and publicly available which can support mesh-formed Bluetooth scatternet and implemented most Bluetooth protocol stacks [22]. The time interval between different frequencies is 625μs.

A. Simulation setup

The parameters used in the proposed protocol simulation are listed in Table 4. For simulation, the number of Bluetooth nodes is varied from 10 to 100 and 48 node pairs are used [23].

TABLE. IV. Simulation Parameters

Parameters	Assessment
Traffic Model	CBR
Number of nodes	10 - 100
Bluetooth nodes pairs	48
Simulation time	1000 s
Network Dimension	80 m x 80 m
Data packet type	DH3, DH5
Communication range	10 m
Scheduling algorithm	Round Robin
Bridge scheduling algorithm	Maximum Distance Rendezvous Point
Packet size	349 Bytes
Inquiry time	10.24 s
Paging time	128 – 256 s
Packet interval	0.15
Queue length	50 packets

B. Simulation results and discussion

In this sub-section, the simulation results are discussed. The simulation was run ten times and results are obtained using those ten simulations. After getting the comparison results, it was found that the proposed CATC protocol outperformed the existing PRP and DCC protocols.

During the communication, it was observed that, when the number of passing links increased through a single bridge node, the proposed CATC activates a FBB that shares the traffic load. The CATC allows the parallel transmission to reduce the wait time and improve network performance. In the holding mode when one pair of devices transmits remaining pairs are blocked. As DCC and PRP both are proposed to handle congestion, but, it is observed that the DCC is efficient for intra-piconet traffic load. When traffic load increases on a master node, it activates a bridge node for load balancing. In the contrary, the PRP solves bottleneck problem by creating extra piconets within the piconet. It creates a new piconet for each new communicating pairs. As shown in Fig. 7, the CATC shares the traffic load more efficiently compared to DCC and PRP. There are total twenty available bridges and 84 connections, the PRP uses 12 bridges, the DCC 14, and the CATC uses 18 bridge nodes. Therefore, the traffic load has been successfully shared; which improves the overall performance.

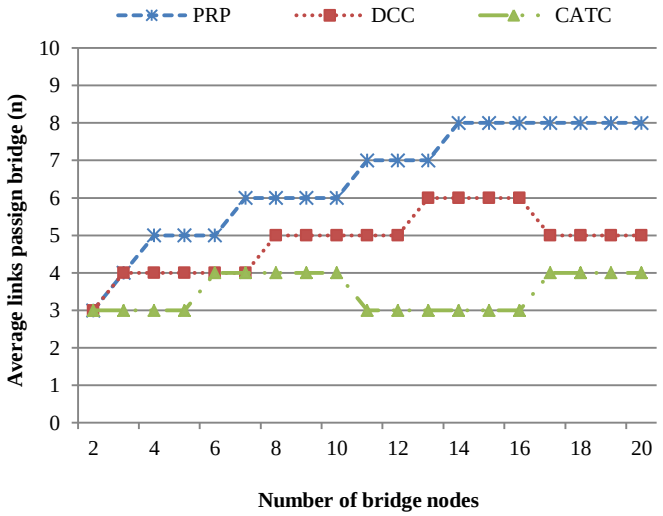

Fig. 7. Average links passing through bridge nodes vs. Number of bridges.

A large number of nodes in a scatternet increasing the master polling time. To increase efficiency, PRP frequently performs piconet restructuring for all connections. It provides the solution for congestion on the master node, but it increases the network delay. On the contrary, DCC avoids congestion, within an intra-piconet but it does not provide any solution inter-piconet. It is analyzed a large number of connections passing through a bridge node create a bottleneck and increase network delay. The CATC shares the traffic load on the master and bridge nodes. The total delay of protocols is shown in Fig. 8 and it is observed that CATC has less delay compared to PRP and DCC protocols. The throughput of the CATC, PRP,

and DCC protocols was compared and it was observed that the CATC protocol showed better results than the PRP and DCC protocols. The PRP and DCC protocols consume more control packets compared to the CATC protocol. The CATC allows the parallel transmission because it efficiently manages traffic load in the intra-piconet and inter-piconet to improve overall network throughput. When a bridge creates bottleneck the CATC activates the FBB for an efficient communication between the piconets. As shown in Fig. 6, when a larger number of links pass through B_1 it creates a bottleneck, to avoid bottleneck node A is selected as a FBB for P_2 and P_3, and node D is selected as FBB for P_1 and P_2. Fig. 9 shows the throughput of the CATC is higher compared to PRP and DCC.

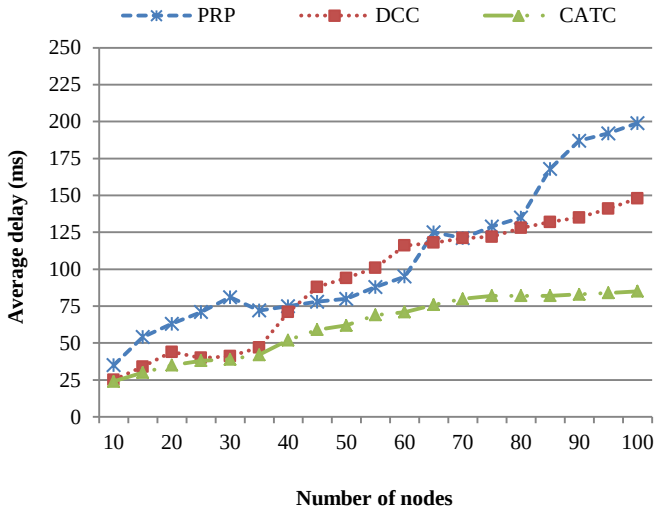

Fig. 8. Average delay vs. Number of nodes.

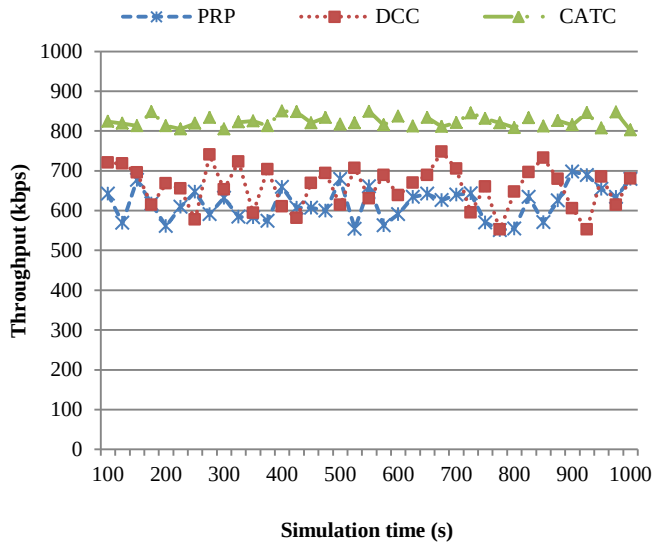

Fig. 9. Network throughput vs. Time.

Bluetooth has limited resources, and therefore, efficient resource utilization is key to network performance. The CATC does not frequently perform the network restructuring within the piconet, and therefore, it uses a lower number of control packets. The PRP frequently creates new piconets within the piconet and makes new links so that each time during synchronization, the Bluetooth devices use extra control packets. In contrast, the DCC protocol overcomes the delay problem within the piconet through activating a backup device that is utilizing extra control packets. Fig. 10 shows that the PRP and DCC's inefficient resource utilization causes more control packets compared to the CATC protocol. Also the number of blocking users increases due to the unavailability of intermediate nodes. As PRP makes new piconets frequently within the piconet and if other devices need to communicate with the devices which have changed their roles, it could block more users. The CATC protocol creates efficient links for intra-piconet and inter-piconet communication so it decreases the rate of blocking users. When the CATC protocol performs network restructuring, it changes the mode of the device in the park mode. After successful transmissions, it changes back into the original states. From Fig. 11, it can be seen that the CATC protocol performs better than the PRP and DCC protocol in terms of blocking connections about 15%.

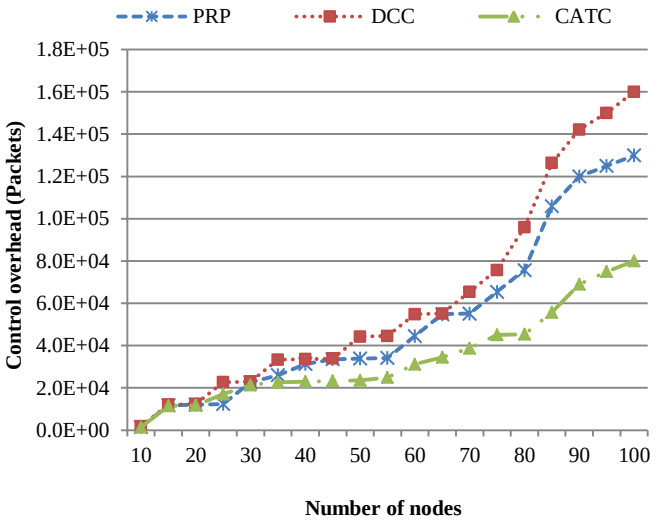

Fig. 10. Control packet overhead vs. Number of nodes.

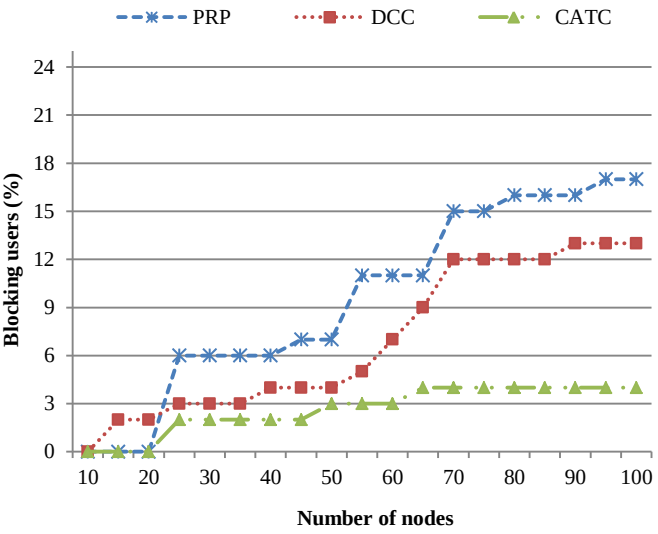

Fig. 11. Blocking users vs. Number of nodes.

V. CONCLUSIONS AND FUTURE WORK

This paper has proposed a Cross-layer-based Adaptive Traffic Control protocol for Bluetooth network. The proposed CATC protocol shares the master load through network restructuring and the bridge load through FBB. The CATC creates PFP if nodes are within the range. If the source and destination are not within 10 m CATC creates SFP to reduce traffic load on the master node. On the contrary, the CATC activates FBB to overcome bottleneck problem of a bridge node and allow parallel transmission in the scatternet. Simulation results show that the CATC protocol outperforms existing protocols in terms of minimizing the total delay, control overhead, and a number of blocked users.

In future work, this research work will be extended by using some additional parameters for comparison. In addition, the network traffic load can be shared by reducing the hop count based on the role switch operations.

ACKNOWLEDGEMENT

The authors are thankful to the Deanship of Scientific Research (DSR) at King Abdulaziz University for funding this project, under grant No. (611-271-D1435).

REFERENCES

[1] M. J. Sataraddi, et al., "Priority Based Scheduler for Bluetooth Network," in Advances in Computing, Communication, and Control. vol. 361, S. Unnikrishnan, et al., Eds., ed: Springer Berlin Heidelberg, 2013, pp. 356-365.

[2] Bluetooth_specificaiton. (2015). Bluetooth SIG, "Specification of the Bluetooth System", http://www.bluetooth.com, June 2010.

[3] G. Aldabbagh, et al., "QoS-Aware Tethering in a Heterogeneous Wireless Network using LTE and TV White Spaces," Computer Networks, vol. 81, pp. 136-146, 2015.

[4] Y. Chih-Min and Y. Yin-Bin, "Reconfigurable Algorithm for Bluetooth Sensor Networks," Sensors Journal, IEEE, vol. 14, pp. 3506-3507, 2014.

[5] S. Sharafeddine, et al., "A scatternet formation algorithm for Bluetooth networks with a non-uniform distribution of devices," Journal of Network and Computer Applications, vol. 35, pp. 644-656, 2012.

[6] J. Decuir, "Bluetooth Smart Support for 6LoBTLE: Applications and connection questions," Consumer Electronics Magazine, IEEE, vol. 4, pp. 67-70, 2015.

[7] T. Klajbor, et al., "A new role-switching mechanism optimizing the coexistence of bluetooth and Wi-Fi networks," Telecommunication Systems, pp. 1-11, 2010.

[8] G. Aldabbagh, et al., "Distributed dynamic load balancing in a heterogeneous network using LTE and TV white spaces," Wireless Networks, pp. 1-12, 2015.

[9] S. T. Bakhsh, et al., "Self-Schedule and Self-Distributive MAC Scheduling Algorithms for Next-Generation Sensor Networks," International Journal of Distributed Sensor Networks, 2015.

[10] C. M. Yu and J. H. Lin, "Enhanced bluetree: A mesh topology approach forming bluetooth scatternet," Wireless Sensor Systems, IET, vol. 2, pp. 409-415, 2012.

[11] C. M. Yu, "Global configured method for blueweb routing protocol," Communications, IET, vol. 6, pp. 69-75, 2012.

[12] J.-W. Lin and W.-S. Wang, "An efficient reconstruction approach for improving Bluetree scatternet formation in personal area networks," Journal of Network and Computer Applications, vol. 33, pp. 141-155, 2010.

[13] G. Ramana Reddy, et al., "An efficient algorithm for scheduling in bluetooth piconets and scatternets," Wireless Networks, vol. 16, pp. 1799-1816, 2010/10/01 2010.

[14] S. Bakhsh, "A Self-organizing Location and Mobility-Aware Route Optimization Protocol for Bluetooth Wireless," Journal of King Saud University-Computer and Information Sciences, pp. 239-248, 2016.

[15] E. Hossain, "The Network Simulator (NS-2)". http://www.isi.edu/nsnam/ns/ns-build.html, 2016.

[16] D. Agrawal and Q. Wang, "University of Cinicinnati Bluetooth simulator (UCBT)" http://www.cs.uc.edu/~cdmc/ucbt/, 2016.

[17] S. T. Bakhsh, et al., "Adaptive Sleep Efficient Hybrid Medium Access Control algorithm for next-generation wireless sensor networks," EURASIP Journal on Wireless Communications and Networking, vol. 2017, pp. 84-94, 2017.

[18] P. A. Laharotte, et al., "Spatiotemporal Analysis of Bluetooth Data: Application to a Large Urban Network," Intelligent Transportation Systems, IEEE Transactions on, vol. 16, pp. 1439-1448, 2015.

[19] J. Nieminen, et al., "Networking solutions for connecting bluetooth low energy enabled machines to the internet of things," Network, IEEE, vol. 28, pp. 83-90, 2014.

[20] G.-J. Yu and C.-Y. Chang, "Congestion control of bluetooth radio system by piconet restructuring," Journal of Network and Computer Applications, vol. 31, pp. 201-223, 2008.

[21] S. Tahir Bakhsh, et al., "Dynamic Congestion Control through backup relay in Bluetooth scatternet," Journal of Network and Computer Applications, vol. 34, pp. 1252-1262, 2011.

[22] F. Subhan, et al., "Indoor positioning in bluetooth networks using fingerprinting and lateration approach," in International Conference on Information Science and Applications (ICISA), pp. 1-9, 2011.

[23] P. Johansson, et al., "Rendezvous scheduling in Bluetooth scatternets," presented at the IEEE International Conference on Communications, 2002.

A Comparative Study on the Effect of Multiple Inheritance Mechanism in Java, C++, and Python on Complexity and Reusability of Code

Fawzi Albalooshi
Department of Computer Science
University of Bahrain
Kingdom of Bahrain

Amjad Mahmood
Department of Computer Science
University of Bahrain
Kingdom of Bahrain

***Abstract*—Two of the fundamental uses of generalization in object-oriented software development are the reusability of code and better structuring of the description of objects. Multiple inheritance is one of the important features of object-oriented methodologies which enables developers to combine concepts and increase the reusability of the resulting software. However, multiple inheritance is implemented differently in commonly used programming languages. In this paper, we use Chidamber and Kemerer (CK) metrics to study the complexity and reusability of multiple inheritance as implemented in Python, Java, and C++. The analysis of results suggests that out of the three languages investigated Python and C++ offer better reusability of software when using multiple inheritance, whereas Java has major deficiencies when implementing multiple inheritance resulting in poor structure of objects.**

***Keywords*—Reusability; complexity; Python; Java; C++; CK metrics; multiple inheritance; software metrics**

I. INTRODUCTION

Inheritance is one of the fundamental concepts of object-oriented (OO) software development. There are two types: single and multiple. Single inheritance is the ability of a class to inherit the features of a single super class with more than a single inheritance level i.e. the super class could also be a subclass inheriting from a third class and so on. Multiple inheritance, on the other hand, is the ability of a class to inherit from more than a single class. For example, a graphical image could inherit the properties of a geometrical shape and a picture. Stroustrup [1], [2] states that multiple inheritance allows a user to combine independent concepts represented as classes into a composite concept represented as a derived class. For example, a user might specify a new kind of window by selecting a style of window interaction from a set of available interaction classes and a style of appearance from a set of display defining classes.

There is wide debate on the usefulness of multiple inheritance and whether the complexities associated with it justify its implementation. Though some researchers such as Stroustrup [1], [2] are convinced that it can easily be implemented. He states that multiple inheritance avoids replication of information that would be experienced with single inheritance when attempting to represent combined concepts from more than one class. Booch [3] asserts that it is good to have inheritance when you need it. According to Booch, there are two problems associated with multiple inheritance and they are how to deal with name collisions from super classes, and how to handle repeated inheritance. He presents solutions to these two problems. Other researchers [4] suggest that there is a real need for multiple inheritance for efficient object implementation. They justify their claim referring to the lack of multiple subtyping in the ADA 95 revision which was considered as a deficiency that was rectified in the newer version [5]. It is clear that multiple inheritance is a fundamental concept in object-orientation. The ability to incorporate multiple inheritance in system design and implementation will better structure the description of objects modeling, their natural status and enabling further code reuse as compared to single inheritance.

Java, C++, and Python are three widely used OO programming languages in academia and industry. Java has secured its position as the most widely used OO programming language due to many reasons including its network-centric independent platform and powerful collection of libraries known as Java APIs (Application Programming Interface). Nevertheless, Java has a limitation when it comes to implementing multiple inheritance. C++ is another widely used programming language and is considered to be the most comprehensive due to its support to a variety of programming styles such as procedural, modular, data abstraction, object-oriented and generic programming [1], [2]. It supports single and multiple inheritance in which a child class can inherit the properties of a single parent class and multiple parents. Python is a powerful object-oriented general-purpose programming language created by Guido van Rossum [6]. It has wide range of applications from Web development to scientific and mathematical computing to desktop graphical user Interfaces. It is a simple language; open source, portable across platforms, extensible and embeddable, interpreted, and has large standard libraries to solve common tasks. Similar to C++ single and multiple inheritance is supported by Python. An empirical study on the use of inheritance in Python systems was carried out by Orru *et al*. [7]. More details about the implementation of multiple inheritance in these languages are discussed in Section 2.

To the best of our knowledge there has been no studies comparing the complexity and reusability of commonly used object-oriented programming languages. In this paper, we present implementation of multiple inheritance and use CK

(Chidamber and Kemerer) [8] metrics to study the complexity and reusability of multiple inheritance as implemented in Python, Java, and C++. For this purpose, we used a sample design and code from real-life systems involving multi-level multiple inheritance and its implementation.

The rest of the paper is organized as: Section 2 presents the implementation of multiple inheritance in Java, C++, and Python. Section 3 details the complexity and reusability analysis for the three languages. It discusses software metrics and how they are applied in the measurement of the complexity and reusability followed by a discussion of the results. In Section 4 we address the current use of multiple inheritance in open source software and the impact of such practice on its complexity and reusability and Section 5 concludes the paper.

II. Multiple Inheritance Implementation in Java, C++, and Python

In Java, a class can singly inherit the properties of another class. Java does not support multiple inheritance of classes, but it supports multiple inheritance of interfaces [9]. A strong reason that prevents Java from extending more than one class is to avoid issues related to multiple inheritance of attributes from more than one level which is referred to as the 'diamond problem' [10]. This is a situation that occurs when implementing multiple inheritance in which a class inheriting from two or more super classes with a common ancestor. The super classes inherit the common ancestor method(s) and/or attribute(s). This results to their child class to inherit multiple versions of the same method(s) and/or attribute(s) (one from each super class). Thus, a conflict arises during program execution involving the child class on which version of the same inherited method/attribute to use. Java interfaces do not have a state, thus do not pose such a threat. The more recent Java 8 compiler resolves the issue of which default method a particular class uses, however this solution has its limitations. To overcome Java's shortcoming in implementing multiple inheritance, researchers investigated compromised solutions. Two of the most commonly used approaches are termed as approximation [11] and delegation [12] of multiple inheritance. C++ overcomes the diamond problem with the use of virtual inheritance. Program 1(b) shows the implementation of multiple inheritance in C++ for the Java example shown in Program 1(a). In Python the diamond problem is nicely resolved using the "Method Resolution Order" approach which is based on the "C3 superclass linearization" algorithm. Program 1(c) shows the implementation of multiple inheritance in Python.

```
class A { // The primary class to be inherited
    public string a() { return a1();}
    protected string a1() {return "A";}
}
interface IB {
// Second class to be inherited declared as an interface
    public string b(IB self);
    public string b1();
}
class B implements IB{
 // Implementation class for the interface IB
    public string b(IB self) {return self.b1(); }
    protected string b1() {return "B";}
}

class C extends A implements IB {
// Subclass inheriting from A and implementing IB's interface
    B b; // Innerclass as composition relationship
    public string b(IB self) {return b.b(this); }
    protected string b1() {return "C";}
    protected string a1() {return "C";}
}
```

Program 1(a): Approximating multiple inheritance in Java.

```
class A { // The primary class to be inherited
    public string a() { return a1();}
    protected string a1() {return "A";}
}

class B { // Implementation class for the interface IB
    public string b() {return self.b1(); }
    protected string b1() {return "B";}
}

class C extends A, B {
    protected string b1() {return "C";}
    protected string a1() {return "C";}
}
```

Program 1(b): Multiple inheritance in C++.

```
class A:
  def  a(self): (return a1();)
  def a1(): (return "A")

class B(A):
  def  b(self): (return b1();)
  def b1(): (return "B")
```

```
class C(A,B):
    def b1(): (return "C")
    def a1(): (return "C")
```

Program 1(c): Multiple inheritance in Python.

Thirunarayan *et al*. [11] proposed approximating multiple inheritance in Java by enabling a subclass C to inherit from a single superclass A and to implement an interface IB that is implemented by a class B in an effort to simulate multiple inheritance in Java. The example in Program 1(a) outlines the authors' solution to approximating multiple inheritance in Java. The class B is then incorporated as an inner class (with composition relationship) in the class C. This approach however suffers from a number of shortcomings such as, limited code reuse, limited support for polymorphism and difficult implementation of overriding. Polymorphism could not be fully supported due to the fact that class C may not support all methods in B. Any change in class B will require changes to the interface IB and to the class C. Overriding cannot easily be implemented with inner classes such as B and may require the modification of the parent class.

Tempro and Biddle [12] suggest that delegation can be used to simulate multiple inheritance in Java. Their solution is similar to that presented by Thirunarayan *et al.* [11] as shown in Program 1(a) in which the class B is incorporated as an inner class within C and declaring an object b to implement it. They demonstrate that protocol conformance can be achieved by single inheritance and the use of Java's capability that allows multiple implementation of Java interface classes. The technique they use is called 'interface-delegation' which require a child class to inherit from a single parent class and implements and delegates to as many interface classes resulting to the child class reusing all the parent classes. There are a number of drawbacks of this approach. The first is that in some cases the amount of code needed to achieve reuse is almost as much as the code being reused. The second is the difficulty in accessing objects imposed by the solution which renders classes to be highly coupled and less cohesive. Thirdly, protected fields and methods of the delegation object are only accessible to extending classes and, fourthly, the programmer does not have control over class libraries such as Java Core API thus creating interfaces for such classes is not possible; and finally, delegation can be problematic in the presence of self-calls. The authors recommend that every class intended for reuse by inheritance (such as Java Core API library of classes) should also have a matching interface to enable such an approach in simulating multiple inheritance to be applicable. It is important to note that the main use of interface classes in Java is to define uniform interfaces. An interface class can only have signatures of 'public' operations with no data members. When used for the purpose of inheritance all operations must be defined in the class that implements the interface and so do the attributes. This limitation results to repeated coding of the interface operations and the definition of necessary attributes whenever an interface is used. This act is the inverse advantage of code reuse the primary advantage of inheritance.

III. Complexity and Reusability Analysis of Python, Java, and C++

A number of software metrics have been proposed to analyze the complexity and reusability of object-oriented programming languages. In this section we review the metrics and then we analyze the complexity and reusability of Python, Java, and C++.

A. Software Metrics

A software metric measures or quantifies a software characteristic such as number of classes or lines of code or the number of operations, etc. They help software developers and managers to track the status of software specification or implementation [13]. Metrics for OO software have been a major research topic for more than two decades. A survey carried out by Genero *et al.* [14] presented nine different initiatives to establish metrics for OO software such as CK [8], Li and Henry [15], MOOD (Metrics for Object Oriented Design) [16], Lorenz and Kidd[17], Briand *et al.* [18], Marchesi [19], Harrison *et al.* [20], Bansiya and Davis [21], and Genero *et al*. [22]. More recently other researchers such as Amalarethinam and Hameed [23], Ibrahim *et al*. [24] and Abu Bakar [25] have also reviewed metrics for OO software. The CK [8] set of metrics has gained wide acceptance due to the fact that it was empirically tested by many researchers such as that reported in [26]-[29]. The originators of the CK [8] metrics realized the need for software measures or metrics to manage the software development process. They proposed a suite of six metrics for OO design and demonstrated their feasibility for process improvement. These are Weighted Methods per Class (WMC), Depth of Inheritance Tree (DIT), Number of Children (NOC), Coupling between Object Classes (CBO), Response for a Class (RFC), and Lack of Cohesion in Methods (LCOM). WMC is the number of methods defined in a class including methods, constructors and destructor. The larger the number of methods in a class the greater the impact on children this is due to the fact that the methods will be inherited by the children. Classes with large number of methods are application specific which limits their reuse. DIT is calculated as the max path from root to node. Deeper trees present greater design complexities as more classes are inherited. The potential reuse of inherited methods is increased but there is a risk in predicting their behavior. The more NOC a class has the more important it is and therefore must carefully be designed and tested due its high impact on others. CBO is calculated as the number of classes to which each class is coupled. The more coupling the less a class becomes reusable due to its dependability on other classes. RFC is calculated as the number of methods in the class in addition to the number of methods called by methods in the same class. The larger the number of methods invoked as a response to a message the more complex becomes a class in addition to increasing the complexity of testing and debugging. LCOM is calculated as the count of the number of methods pairs whose similarity is 0 minus the count of methods pairs whose similarity is not 0, or more precisely (number of pair of methods that have no common attribute)-(number of pair of methods that have common attribute). Cohesiveness of a method is desirable since it promotes encapsulation. Chidamber *et al.* [30] demonstrate the use of CK metrics for managers responsible of software

development efforts. Their advantage in predicting parts of the system that may be problematic as early as in the design or during implementation stages is presented. The empirical results across three financial services applications showed that metrics data can be collected on systems that were written in a variety of programming languages and on systems that were not yet coded. Another set of popular metrics was the MOOD [16] which was later extended to MOOD2 [31]. The set consists of six metrics for OO software. For the measurement of encapsulation Method Hiding Factor (MHF) and Attribute Hiding Factor (AHF) are proposed. To measure inheritance Method Inheritance Factor (MIF) and Attribute Inheritance Factor (AIF) metrics are proposed. The Coupling Factor (CF) measures coupling and the Polymorphism Factor (PF) measures polymorphism. The authors demonstrate how they can be used to measure systems. They assert that their set of metrics operate at the system level and are complementary to the CK metrics that operate at the class level.

B. The Sample Application

To determine the exact difference in implementing multiple inheritance in Python, Java and C++, we devised a sample application as shown in Fig. 1. There are eight classes all together starting with Person, Student, and Parent classes at the first level with each having one attribute and its associated get and set methods. At the second level three more classes are defined. They are: FullTimeEmployee, FullTimeStudent, and FullTimeParent. FullTimeEmployee having an attribute and its associated get and set methods. FulTimeStudent and FullTimeParent are inheriting from two first level classes (multiple inheritance) each. Unlike the FullTimeEmployee class which declares the employee related attribute and inherits from Person the FullTimeStudent and FullTimeParent in addition to inheriting from Person each inherit from another class Student and Parent, respectively. This is because the Student and Parent classes are further reused by the StudentEmployee and ParentStudentEmplyee classes, and to avoid the "diamond problem" the Student and Parent classes are independently declared (not inheriting from Person) which will otherwise occur if one or more child classes inherit from one of them and at the same time inherit from Person (or another class that already inherits from it) such as StudentEmployee and ParentStudentEmployee as shown in Fig. 1. StudentEmpolyee class is at the second level and ParentStudentEmployee is in the third with an attribute each and set and get methods for each of the attributes.

Fig. 2 shows the Java implementation for the same set of classes and similarly to the C++ implementation the "diamond problem" between the classes is avoided. All Java classes have the same set of attributes and their associated (set and get) methods for the same classes in the C++ implementation. However, to achieve multiple inheritance in the FullTimeStudent, FullTimeParent, StudentEmployee, and ParentStudentEmployee classes the inner-object approach was used. Each of these classes would inherit from one and contain an object of type the other class as shown in Fig. 2. For each inner-object an additional data member and a set and a get method had to be declared to access its attribute.

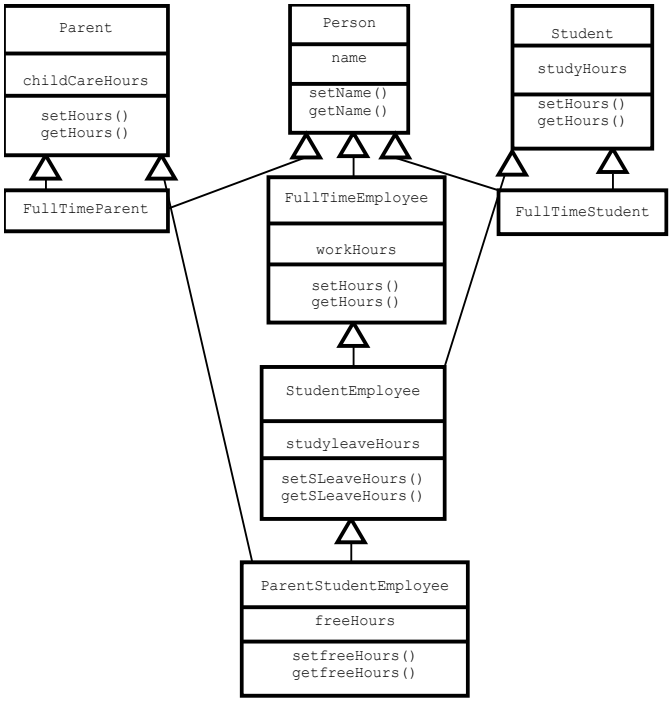

Fig. 1. C++ class diagram.

Thus each of the four classes had an additional attribute (inner-object) and two additional methods (for the single attribute in the inner-object) each Using the approach recommended by Thirunarayan *et al*. [11] and Tempro and Biddle [12] will require the declaration of additional interface classes which for the purpose of our study will increase the number of declared classes. We therefore chose to minimize classes so that the comparison is more precise. Fig. 3 shows the Python class diagram for the same implementation classes presented in Fig. 1 and 2. The sample design used to measure the difference in implementing multiple inheritance can easily be implemented in the three languages and has four situations of multiple inheritance to enable us to precisely calculate the associated metrics in the different implementations.

C. Applying the Metrics

To compare the three implementations, we used the six CK metrics [8] as discussed in Section 3.1. Table 1 shows the values for CK set of metrics for the Python, Java and C++ implementations. The classes that inherit from more than one super class are underlined. Details on how the tabulation values are calculated are presented in the following two paragraphs:

For Java implementation WMC is 2 for the classes Person, Student, Parent, FullTimeEmployee, FullTimeStudent and FullTimeParent whereas WMC is 4 for StudentEmployee and ParentStudentEmployee. DIT is 0 for Person, Student and Parent classes. It is 1 for FullTimeEmployee, FullTimeStudent and FullTimeParent, 2 for StudentEmployee and 3 for ParentStudentEmployee. NOC is 3 for Person, 0 for Student, Parent, FullTimeStudent, FullTimeParent and ParentStudentEmployee. Its 1 for FullTimeEmployee and StudentEmployee. CBO is 0 for Person, Student, Parent, and FullTimeEmployee.

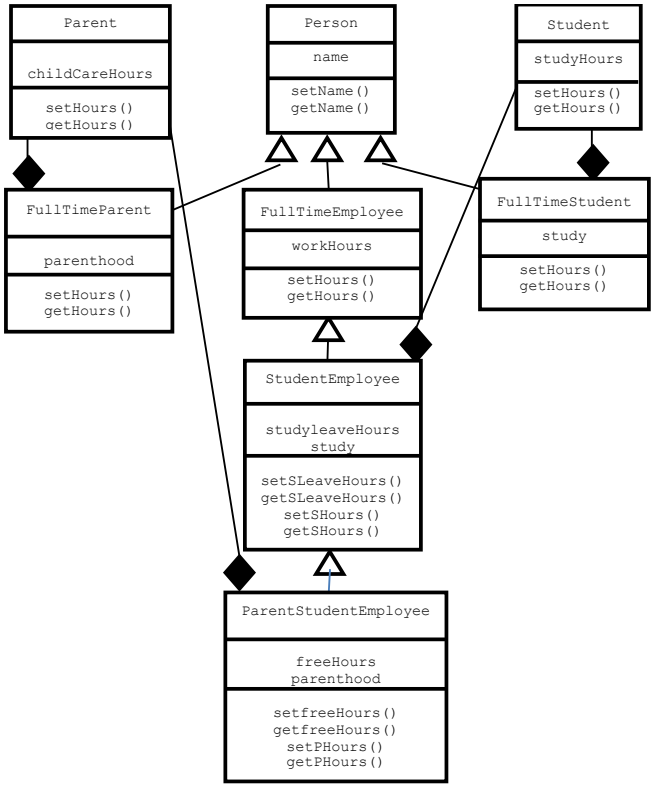

Fig. 2. Java class diagram.

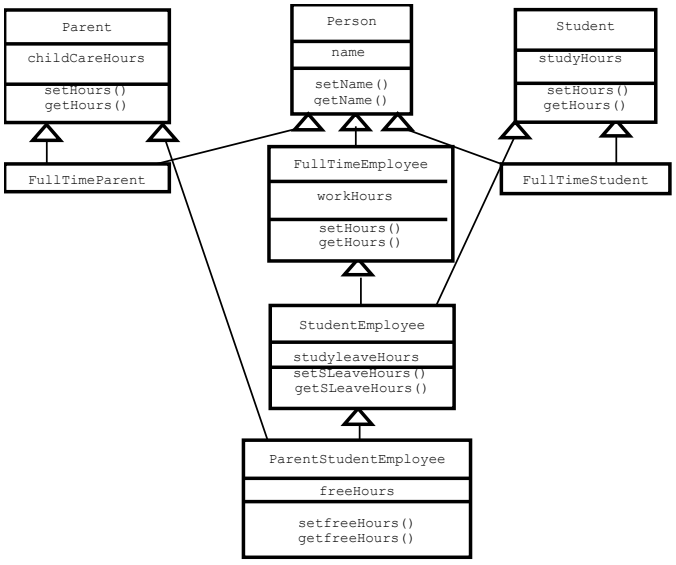

Fig. 3. Python class diagram.

It is one for FullTimeStudent, FullTimeParent, StudentEmployee and ParentStudentEmployee. This is because FullTimeStudent and StudentEmployee have an inner object of type Student each so does FullTimeParent and ParentStudentEmployee have an inner object of type Parent each. RFC and LCOM measure for the classes is the same as WMC due to the simplicity of our sample programme.

TABLE. I. CK METRICS FOR JAVA, C++ AND PYTHON CLASSES

Class	WMC			DIT			NOC			CBO			RFC			LCOM		
	Java	C++	Python	Java	C++	Python	Java	C++	Python	Java	C++	Python	Java	C++	Python	Java	C++	Python
Person	2	2	2	0	0	0	3	3	3	0	0	0	2	2	2	2	2	2
Student	2	2	2	0	0	0	0	2	2	0	0	0	2	2	2	2	2	2
Parent	2	2	2	0	0	0	0	2	2	0	0	0	2	2	2	2	2	2
FullTimeEmployee	2	2	2	1	1	1	1	1	1	0	0	0	2	2	2	2	2	2
FullTimeStudent	2	0	0	1	1	1	0	0	0	1	0	0	2	0	0	2	0	0
FullTimeParent	2	0	0	1	1	1	0	0	0	1	0	0	2	0	0	2	0	0
StudentEmployee	4	2	2	2	2	2	1	1	1	1	0	0	4	2	2	4	2	2
ParentStudentEmolyee	4	2	2	3	3	3	0	0	0	1	0	0	4	2	2	4	2	2
Total:	20	12	12	8	8	8	5	9	9	4	0	0	20	12	12	20	12	12

As it is primarily designed to investigate the difference in implementing multiple inheritance between the three languages. For the Python and C++ implementation, WMC is to 2 for Person, Student, Parent, FullTimeEmployee, StudentEmployee and ParentStudentEmployee. In addition to inheriting from Person, FullTimeStudent and FullTimeParent inherit methods from Student and Parent classes respectively therefore have no methods of their own and WMC for them is 0. In the same way StudentEmployee and ParentStudentEmployee inherit from more than one class and require to define less new methods than the Java implementation. DIT measure remained the same as the Java implementation, its 0 for Person, Student and Parent classes; 1 for FullTimeEmployee, FullTimeStudent and FullTimeParent; 2 for StudentEmployee; and 3 for ParentStudentEmployee. NOC for Student and Parent classes differ than that in the Java implementation, the rest of the classes have the same measure. It is 3 for Person; 2 for Student and Parent; 1 for FullTimeEmployee and StudentEmployee; and 0 for FullTimeStudent, FullTimeParent and ParentStudentEmployee. The Pyhton and C++ implementation has 0 coupling resulting to a 0 CBO measure for all classes. Similarly to the Java classes RFC and LCOM measure for the C++ classes is the same as WMC, but the classes FullTimeStudent, FullTimeParent, StudentEmployee and ParentStudentEmployee measured less than the Java implementation due to their ability to inherit from more than one class without the need for extra methods. We used the combined metrics to investigate the reusability of classes as proposed by Goel and Bhatia [32] and the results are given in Table 2.

TABLE. II. CK REUSABILITY METRICS FOR JAVA, C++ AND PYTHON CLASSES

Class	DIT+NOC			CBO+LCOM			WMC + RFC		
	Java	C++	Python	Java	C++	Python	Java	C++	Python
Person	3	3	3	2	2	2	4	4	4
Student	0	2	2	2	2	2	4	4	4
Parent	0	2	2	2	2	2	4	4	4
FullTimeEmployee	2	2	2	2	2	2	4	4	4
FullTimeStudent	1	1	1	3	0	0	4	0	0
FullTimeParent	1	1	1	3	0	0	4	0	0
StudentEmployee	3	3	3	5	2	2	8	4	4
ParentStudentEmolyee	3	3	3	5	2	2	8	4	4
Total:	13	17	17	24	12	12	40	24	24

D. Discussion

The metrics' values presented in Table 1 show that the Java implementation has higher values for WMC, CBO, RFC, and LCOM for all four classes inheriting from two parents. The higher the value of each of these metrics, the less desirable is the code as discussed in Section 3.1 resulting to the Python and C++ implementations to be more desirable than Java. DIT remained unchanged in all implementations. However, NOC in the Python and C++ implementations is higher which is a desirable characteristic due to the fact that classes could have more than one child.

Reusability is the most fundamental benefit achieved with the use of inheritance. According to Booch [3] any artefact of software development can be reused, including code, design, scenarios, and documentation, but classes serve as the primary linguistic vehicle for reuse. Classes when properly designed and implemented can be used again (reused) in new development projects reaching up to 70% in some projects. Thus the more classes are efficiently developed to be reusable the more time and effort can be saved in new projects. More recent researchers such as Gupta and Dashore [33] and Goel and Bhatia [32] have also appreciated the importance of OO software reusability. The first developed a tool to measure reusability and the latter investigated the measurement of the reusability of a class and in particular the use of the CK metrics for this purpose. Goel and Bhatia [32] combined the six metrics with each other and came up with three new metrics to measure the reusability of a class. The first combined metric was the DIT and NOC. They believe that the deeper the depth of a class the more potential for reuse, thus DIT has a positive effect on reusability. Also a particular value of NOC has a positive impact on reuse. Therefore, the increase in DIT in combination with NOC has a positive effect on reusability. The second combined metric is CBO and LCOM. Coupling has negative impact on reusability so does the lack of cohesion which increases complexity and has negative effect on reusability. Therefore, these two metrics have an inverse effect on reusability, the higher CBO+LCOM the less reusable is the class. The third was the combination of WMC and RFC metrics. The higher the number of methods is (WMC) the more is the impact on children. Such classes tend to be application specific thus limiting their reuse. The higher RFC the more complex a class is thus having negative effect on its reusability. The higher WMC+RFC the less reusable a class is. Their observations on the indications of the CK metrics of a software system were formerly highlighted by the metrics originators [8]. These set of metrics' values for our implementations are presented in Table 2. The classes that inherit from more than one class (thus implementing multiple inheritance) are underlined.

Analysis of the results based on the combined metrics approach proposed by Goel and Bhatia [32] clarifies the differences between the three implementations further. Table 2 shows that the Python and C++ implementations have major advantages. The DIT metric's values for all implementations are identical, but the NOC's are different. The Python and C++ implementations have higher NOC value by 4 counts this is because the Student and Parent classes have two children each as a result of inheritance by the FullTimeStudent, FullTimeParent, StudentEmployee and ParentStudentEmployee classes as shown in Fig. 1 and 3. In the Java implementation the same two classes are declared as inner-objects for the same four classes. Therefore, the Python and C++ implementations have a positive measure over Java for this combined metric. For the second combined metric, the CBO value for the Java implementation is 1 for each of the four classes inheriting from two due to the fact that each inherits from one and incorporates the other as an inner-object. LCOM in the Java implementation as shown in Table 1 is also higher by 8 due to the need for methods to access the data members of the inner objects in the multiple inheriting four classes, two for each inner object. Therefore, CBO+LCOM values for the Java implementation double the Python and C++ by 12 counts as shown in Table 2. As a result, the Java implementation is less reusable as discussed in the previous section. The third metric is the combination of WMC and RFC. They both have higher values in the Java implementation by 8 counts each for the same reason LCOM increased. Resulting to the two metrics having 16 counts extra in the Java implementation than in Python and C++ is shown in Table 2. All four multiple inheriting classes increased by 4 each in the Java implementation thus resulting for them to be considered less reusable as discussed in the previous section.

IV. Multiple Inheritance in Open Source Software

In this section we present our investigation of the use of multiple inheritance in big open source software. For this purpose, we selected JRE and Eclipse, two of the largest open source systems that were analyzed by Tempero *et al*. [34]. The authors found substantial unnecessary overriding present in all applications. Their results assert that in the applications they examined the number of classes that inherit something in addition to number of classes that override something are roughly equivalent to the number of classes in the application as a whole. Two of the biggest applications they presented were JRE and Eclipse. Their empirical study was based on the Qualitas Corpus [35] open source code repository.

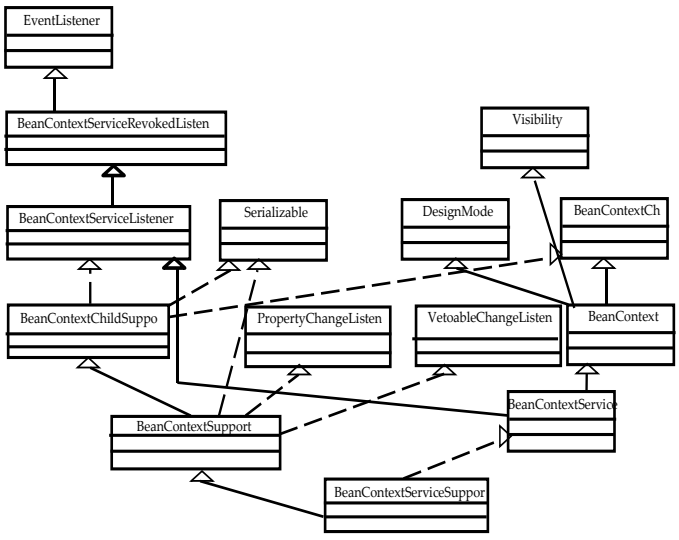

Fig. 4. JRE class diagram.

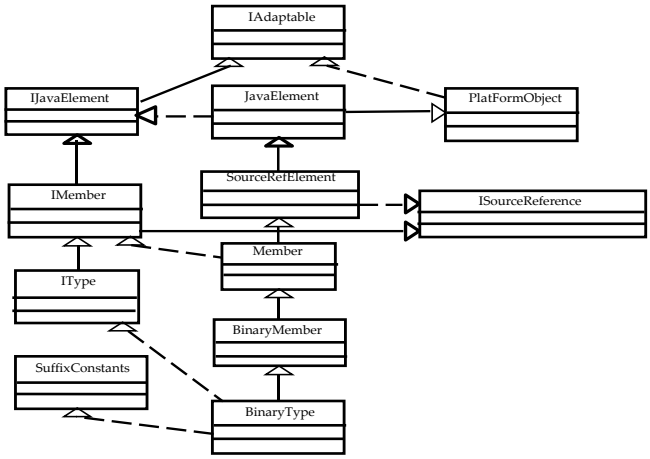

Fig. 5. Eclipse example design.

For our study, the source code of both the applications was downloaded from SourceForge [36]. We used StarUML [37] to reverse engineer the code to UML designs. Fig. 4 shows the UML design reverse engineered from parts of Java code for the Java beans context from JRE. Fig. 5 shows the UML design reverse engineered from parts of open source code for the Eclipse JDT. Both applications follow a similar approach to implement multiple inheritance in which a class inherits from another and delegates from one or more interfaces to simulate multiple inheritance. The process of delegation requires the inheriting class to implement the interface class(es).

A critical analysis of both implementations shows high DIT reaching to six levels in Fig. 5 with a low number of direct children-NOC for each subclass. Furthermore, delegation necessitates interface class operations' definition in inheriting/implementation classes which increases coupling and reduces the class's cohesion thus increasing CBO, LCOM, and WMC metrics as we discuss in Section 3.4. The increase in WMC has a relative impact on the increase in RFC as shown in our experimental results in Table 1. Both implementations show high DIT thus an increase in design complexity. The object-oriented programming community does not recommend more than three levels due to the complexity it invites when maintaining the code. On the contrary, high number of children breadthwise is recommended and increases the importance of the parent class, but due to the inheritance limitation imposed by Java NOC is low resulting to a negative impact on reuse. The increase in CBO and LCOM further negatively effects reuse so does the increase in WMC and RFC. Both implementations further suffer from the diamond problem. The first implementation is in BeanContextSupport and BeanContextServicesSupport classes and the second is in the JavaElement, Member and BinaryType classes.

To further demonstrate the difference between Java and C++/Phython implementations of multiple inheritance we developed the class diagram shown in Fig. 6 as a possible implementation in C++ of the design shown in Fig. 5 without reducing the number of classes as they are part of a bigger system. The new design improves the original implementation in a number of ways. Firstly, the diamond problem is not present anymore and the number of relationships dropped from 15 to 11.

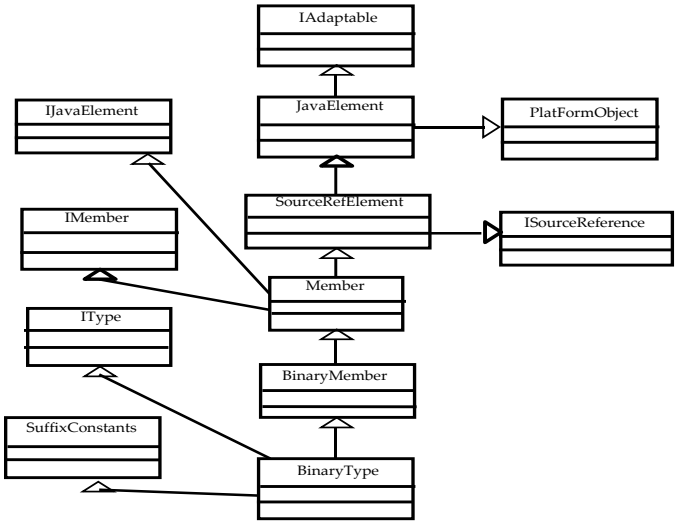

Fig. 6. Redesign of the Eclipse example.

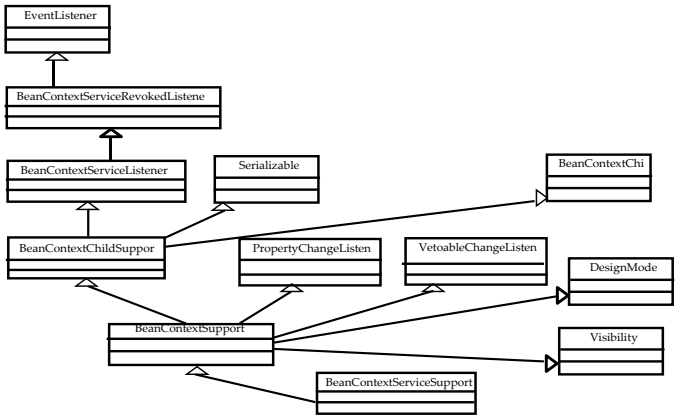

Fig. 7. Redesign of the JRE example.

Secondly, the operations of interface classes in Fig. 5 and associated attributes in the implementation classes need to be defined only once in Fig. 6. In affect coupling is reduced and the classes are more cohesive thus, CBO and LCOM metrics values are reduced. Furthermore, the number of operations defined in the classes is reduced because they are now fully inherited (with their implementations) which greatly reduces the values of WMC and RFC metrics and finally DIT is optimized. These major improvements to the partial code will reduce its complexity and increase its reusability indicating that much more benefits is gained if the whole application is to be redesigned for it to be implemented in a language such as C++ or Python. An analysis of the redesign of the JRE example shown in Fig. 7 presents a similar picture. The diamond problem present in a number of classes in the design in Fig. 4 disappeared; the number of classes and relationships between them is less; and operations and attributes need to be defined only once resulting to less values for CBO, LCOM, WMC and RFC for the design.

V. CONCLUSION

The paper presents an important issue faced by OO software developers. Using Java, Python and C++, we

presented the effect of the programming language on the resultant software. The case discussed in this paper in multiple inheritance for which a program was designed to determine the difference in the implementations. For a fair comparison, the diamond problem was avoided in order not to advantage the C++ and Python implementations. We used the CK metrics to measure the complexity and the combined metrics proposed by Goel and Bhatia to measure reusability. The results clearly affirm that the Java implementation is less reusable. The Python and C++ implementations have a higher NOC indicating the ability of the classes to become better parents for multiple classes, which is considered as positive measure of reusability. CBO and LCOM in the java implementation doubled the Python and C++ clearly suggesting that the latter two implementations have better reusability. The higher count of WMC in combination with RFC for the Java implementation further asserts that the Python and C++ implementations are more reusable. The outcome of the experiment presented in this paper confirms the concerns raised by a number of researchers about the Java implementation (or simulation) of multiple inheritance. We also demonstrated the negative effect of the use of simulated multiple inheritance in big open source industrial software.

REFERENCES

[1] Stroustrup, B. Multiple inheritance for C++. The C/C++ Users Journal, 1999.

[2] Stroustrup, B. The C++ Programming Language, Fourth Edition. Addison-Wesley, 2013.

[3] Booch, G. Object-oriented analysis and design with applications, 2nd Edition, Addison-Wesley, 1998.

[4] Ducournau, R.; Morandat, F.; Privat J. Emprical assessment of object-oriented implementations with multiple inheritance and static Typing, in OOPSLA 2009, Orlando, Florida, USA, October 25-29 2009, ACM.

[5] Taft, S. T.; Duff, R. A.; Brukardt, R. L.; Ploedereder, E.; Leroy, P. Eds. Ada 2005 reference manual: language and standard libraries. In LNCS 4348 ,Springer, 2006.

[6] Lutz, M. Learning Python, 5th Edition. Published by O'Reilly Media, Inc. (June), CA, USA, 2013.

[7] Orru M.; Tempro E.; Marchesi M. (2015) How Do Python Programs Use Inheritance? In A Replication Study. Software Engineering Conference (APSEC), Asia-Pacific. 2015, 1-4 Dec.

[8] Chidamber, S. R.; Kemerer, C. F. A Metrics Suite for Object Oriented Design, IEEE Transactions on Software Engineering, 1994, Vol 20, No. 6.

[9] Flanagan, D. Java in a NUTSHELL, 3rd Edition, O'Reilly & Associates, Inc.; 1999.

[10] Gosling, J.; Joy, B.; Steele, G.; Bracha, G.; Buckley, A. The Java language specification – Java SE, 7th Edition, Oracle America, Inc. 2013.

[11] Thirunarayan, K.; Kniesel, G.; Hampapuram, H. Simulating multiple inheritance and generics in Java, Computer Languages, 1999, Volume 25, Issue 4, 189-210, (Elsevier Science Ltd).

[12] Tempro E.; Biddle, R. Simulating multiple inheritance in Java, The Journal of Systems and Software, 2000, 55, pp. 87-100, (Elsevier Science Inc.).

[13] Vogelsang, A.; Fehnker, A.; Huuck, R.; Reif, W. Software Metrics in Static Program Analysis. In the International Conference on Formal Engineering Methods. Springer Berlin Heidelberg, 2010, pp 485-500.

[14] Genero, M.; Piattini, M.; Calero, C. A Survey of Metrics for UML Class Diagrams, Journal of Object Technology, 2005, Vol. 4., No. 9, pp 59-92, http://www.jot.fm/issues/issue_2005_11/article1, (ETH Zurich).

[15] Li, W.; Henry, S. Object-Oriented Metrics that Predict Maintainability, Journal of Systems and Software, 1993, Vol. 23, No. 2, pp. 111-122.

[16] Harrison, R.; Counsell, S. J.; Nithi, R. V. An Evaluation of the MOOD Set of Object-Oriented Software Metrics, IEEE Transactions on Software Engineering, 1998, Vol. 24, No. 6.

[17] Lorenz, M.; Kidd, J. Object-Oriented Software Metrics: A Practical Guide, Prentice Hall, Englewood Cliffs, New Jersey, 1994.

[18] Briand, L.; Devanbu, W.; Melo, W. An investigation into coupling measures for C++. In 19th International Conference on Software Engineering (ICSE 97), Boston, USA, 1997, pp. 412-421.

[19] Marchesi, M. OOA Metrics for the United Modeling Language. In 2nd Euromicro Conference on Software Maintenance and Reengineering, 1998, pp. 67-73.

[20] Harrison, R.; Counsell, S.; R. Nithi, R. Coupling Metrics for Object-Oriented Design. In 5th International Software Metrics Symposium Metrics, 1998, pp. 150-156.

[21] Bansiya, J.; Davis, C. A. Hierarchical Model for Object-Oriented Design Quality Assessment, IEEE Transactions on Software Engineering, 2002, Vol. 28, No. 1, pp. 4-17.

[22] Genero, M.; Piattini, M.; Calero, C. Early Measures for UML Class Diagrams, L'Object, 2001, Vol. 6, No. 4, (Hermes Science Publications), pp. 489-515.

[23] Amalarethinam D. I. George; Hameed P.H. Maitheen Shahul. Analysis of Object Oriented Metrics on a Java Application. International Journal of Computer Applications, 2015, Volume 123, Number 1.

[24] Ibrahim Ahmed Abd ElHalim; Kamal Amr; Hassan Hesham. Object Oriented Metrics and Quality Attributes: A Survey. In INFOS'16, Giza, Egypt, May 09-11 2016, published by ACM.

[25] Abu Bakar N. S. A. The Analysis of Object-Oriented Metrics in C++ Programs. Lecture Notes on Software Engineering, 2016, Volume 4, Number 1.

[26] Basili, V. R.; Briad, L. C.; Melo, W. L. A Validation of Object-Oriented Design Metrics as Quality Indicators, IEEE Transactions Software Engineering, 1996, vol. 22, pp. 751-761.

[27] Cartwright, M.; Shepperd, M. An Empirical Investigation of Object-Oriented Software System, IEEE Transactions on Software Engineering, 2000, Volume 26, Issue 8, Page 786-796.

[28] Pant, Y.; Henderson-Sellers, B.; Verner, J. M. Generalization of Object-Oriented Components for Reuse: Measurement of Effort and Size Change, J. Object-Oriented Programming, 1996, vol. 9, pp. 19-41.

[29] Hirama Kechi. Software Complexity Analysis Based on Shannon Entropy Theory and C&K Metrics. IEEE Latin America Transactions, 2016, Volume 14, Issue 5.

[30] Chidamber, S. R.; Darcy, D. P.; Kemerer, C. F. Managerial Use of Metrics for Object-Oriented Software: An Exploratory Analysis, IEEE Transactions on Software Engineering, 1998, Vol. 24, No. 8.

[31] Abreu, F. B.,; Cuche, J. S. Collecting and Analyzing the MOOD2 Metrics. In workshop on Object-Oriented Product Metrics for Software Quality Assessment (ECOOP'98), Brussels, Belgium, pages 258-260, July 21st 1998.

[32] Goel, B. M.; Bhatia, P. K Analysis of Reusability of Object-Oriented System using CK Metrics. International Journal of Computer Applications, 2012, Vol. 60, No. 10, pp 32-36.

[33] Gupta A.; Dashore P. An Approach to Analyse Software Reusability of Object Oriented Code. International Journal of Research in Science & Engineering, 2017, Volume 3, Issue 1.

[34] Tempero, E.; Counsell, S.; Noble, J. An Empirical Study of Overriding in Open Source Java. In ACSC'10 proceedings of the 33rd Australasian Computer Science Conference, Brisbane, Australia, January 2010, pp 3-12.

[35] Tempero, E.; Anslow, C.; Dietrich, J. The Qualitas Corpus: A Curated Collection of Java Code for Empirical Studies. In Software Engineering Conference (APSEC), 2010 17th Asia Pacific, January 2011, pp 336-345.

[36] Sourceforge. Available online: https://sourceforge.net/ (12/4/2017).

[37] StarUml 5.0. Available online: http://staruml.software.informer.com/5.0/ (12/4/2017)

Fast Hybrid String Matching Algorithm based on the Quick-Skip and Tuned Boyer-Moore Algorithms

Sinan Sameer Mahmood Al-Dabbagh
Department of Parallel and Distributed Processing
School of Computer Sciences Universiti Sains Malaysia
(USM), 11800 Pulau Pinang,
Malaysia

Mustafa Abdul Sahib Naser
Department of Software Engineering and Information Technology,
Al-Mansour University College,
Baghdad, Iraq

Nuraini bint Abdul Rashid (PhD)
Associate Professor, Department of Computer Sciences,
College of Computer & Information Sciences,
Princess Nourah bint Abdulrahman University, KSA.

Nawaf Hazim Barnouti
Al-Mansour University College
Baghdad,
Iraq

***Abstract*—The string matching problem is considered as one of the most interesting research areas in the computer science field because it can be applied in many essential different applications such as intrusion detection, search analysis, editors, internet search engines, information retrieval and computational biology. During the matching process two main factors are used to evaluate the performance of the string matching algorithm which are the total number of character comparisons and the total number of attempts. This study aims to produce an efficient hybrid exact string matching algorithm called Sinan Sameer Tuned Boyer Moore-Quick Skip Search (SSTBMQS) algorithm by blending the best features that were extracted from the two selected original algorithms which are Tuned Boyer-Moore and Quick-Skip Search. The SSTBMQS hybrid algorithm was tested on different benchmark datasets with different size and different pattern lengths. The sequential version of the proposed hybrid algorithm produces better results when compared with its original algorithms (TBM and Quick-Skip Search) and when compared with Maximum-Shift hybrid algorithm which is considered as one of the most recent hybrid algorithm. The proposed hybrid algorithm has less number of attempts and less number of character comparisons.**

Keywords*—*Hybrid algorithm; string matching algorithm; Tuned Boyer-Moore algorithm; quick-skip search algorithm; Sinan Sameer Tuned Boyer Moore-Quick Skip Search (SSTBMQS)

I. INTRODUCTION

String matching, which involves locating all occurrences of a particular pattern in a large text, is considered one of the primary problems in computer science. Basically, the string matching algorithm accepts two inputs, namely, a short string called a pattern and a long string called a text. The pattern string is usually compared with the text string to determine if the former is a substring of the latter [1], [2]. Although many algorithms and strategies have been developed to solve this problem, scientists still attempt to develop far more efficient methods. String matching algorithms are extensively employed in different computer applications, such as information retrieval, DNA sequence, Web search engines, and artificial intelligence [3].

In the last two decades, string matching algorithms have elicited considerable attention, particularly when applied in various computer applications, such as text processing, DNA analysis, antivirus software, and anti-spam software. Such amount of attention may be attributed to the rapid growth of technology [4]. Current improvements in existing technologies pose numerous challenges to string matching algorithms [5]. String matching algorithms are of two types: exact and approximate string matching [4]. This research focuses on on-line exact string matching algorithms.

String matching algorithms are the basic components of existing applications, such as text processing, intrusion detection, search analysis, information retrieval, and computational biology [6]. All these applications involve a large amount of data because of the advancement in technology; moreover, all these applications involve different types of alphabets. Therefore, researchers continue to reiterate the need for significant string matching algorithms that can address different types of alphabets and large amounts of data [7].

Hybrid string matching approach was introduced to overcome the limitation of existing exact string matching algorithms. The former involves merging two or more algorithms. The Quick-Skip Search hybrid algorithm and Tuned Boyer-Moore algorithm are suitable for identifying all appearances of a pattern in a large text. However, both algorithms have limitations. The Quick-Skip Search hybrid algorithm consists of Skip Search and Quick Search algorithms. The latter exhibits good efficiency when large alphabets with a small pattern are utilized in the comparison operation, whereas the former exhibits good performance when small alphabets and a long pattern are employed [8].

However, the Skip Search algorithm consumes much time when a short DNA pattern and protein database are employed [7]. By contrast, the Tuned Boyer-Moore algorithm consumes much time when a long pattern of DNA alphabet is employed [7]. This algorithm has two disadvantages. First, it does not examine m−text characters to specify a starting search point as

the first step. Second, in the case of mismatch or entire pattern match, the shifting distance depends on a fixed shift value obtained in the preprocessing phase; this fixed shift value does not change until the text window reaches the end of the text. One of the advantages of this algorithm is that it checks the rightmost character in the text window as the first step before character comparison is implemented.

By contrast, the quick-skip search algorithm does not check the rightmost character in the text window as the first step before character comparison is implemented. The advantage of this algorithm is that it examines m − text characters to specify a starting search point as the first step; in the case of mismatch or entire pattern match, the shifting distance value depends on the Skip Search bucket and Quick Search bad character table. The larger shift value is adopted.

Owing to the contradictory behavior of the two algorithms, the important issue for this research is *"how to harness the significant advantages of the positive features of the two algorithms, overcome their performance weaknesses, and solve the string matching problem effectively during sequential and parallel stages for any alphabet type and any pattern length?"*

The remaining of the paper is structured as: Section 2 presents the look at of several hybrid algorithms. Section 3 the design principle of the proposed hybrid algorithm is discussed in detail. Moreover, an example is outlined in Section 4 to trace the hybrid algorithm. Section 5 discusses the experimental results of the hybrid algorithm when compared with its original algorithms and when compared with Maximum-Shift hybrid algorithm. In Section 6 summarizes the conclusion and suggests a future work that can be performed to improve the hybrid algorithm.

II. Previous Works

Numerous studies on the string matching problem have been conducted continuously over the years to develop new efficient algorithms. These efficient algorithms are expected to reduce the work performed in each attempt, increase the amount of shift, and reduce the number of character comparisons during each attempt. Algorithms that acquire the positive properties and exclude the negative properties of original algorithms are called hybrid algorithms. The next subsections discuss some of these hybrid string matching algorithms.

SSABS algorithm [9] explained the advantage of combining two well-known exact string matching algorithms, namely, Quick Search and Raita. The new hybrid string matching algorithm exploits the fact that the dependency between neighboring characters is stronger than that between other characters. Therefore, putting off the comparisons of the neighboring characters would be better, which forms the fundamental idea of the new proposed algorithm. During the searching phase, which is similar to the Raita algorithm's searching phase, the rightmost character in the pattern is compared with the corresponding character in the text to determine if they match. The leftmost character in the pattern is then compared with the matched position character in the text. If they match, then the remaining characters are compared from right to left until a match or mismatch is observed in all $m-2$ characters. The shifting value to the sliding window after complete match or mismatch is determined based on the Quick Search bad character table.

Berry Ravindran-Fast Search (BRFS) algorithm, Yong [10] presented a new hybrid algorithm called BRFS by combining BR and Fast Search (FS) algorithms. Similar to most exact string matching algorithms, BRFS consists of preprocessing and searching phases. The preprocessing phase is constructed by computing the maximum shift value from BM good suffix shift (bmGs) and BR bad character (brBc) table. The searching phase depends on the searching method of the Fast Search algorithm, which performs comparison from right to left. After a complete match or mismatch, the sliding window shifts to the right side depending on the shift value provided by the preprocessing phase. The BRFS algorithm exhibits good performance in cases that involve small alphabets and long patterns. Hence, this algorithm is appropriate for use in applications related to biological sequence search.

Berry Ravindran-Skip Search (BRSS) Algorithm Berry Ravindran-Skip Search (BRSS) algorithm [11] is a combination of Berry Ravindran and Skip Search (SS) algorithms. The preprocessing phase consists of building the bucket list for the SS algorithm and the (brBc) table. The process to calculate the shift value in the preprocessing phase aims to have highest shift value to shift pattern throughout the searching phase. The combination of the two algorithms improves the other's weaknesses. The BR algorithm provides optimum shift values through the use of two successive characters positioned after the rightmost character of the text window. However, the BR algorithm does not examine m-text characters to specify a starting search point as a first step. By contrast, the SS algorithm begins by examining m-text characters during the searching phase to assign the starting search point in the text characters prior to the matching process. The drawback of the SS algorithm comes from using all the locations of the examining character in the bucket list table in case of a match or mismatch. The BRSS hybrid algorithm shows the benefit of combining the two algorithms by reducing the total work performed in each attempt and the overall computational time.

Quick-Skip Search Hybrid Algorithm [12] developed another hybrid algorithm based on the Quick Search (QS) algorithm. The combination of Quick Search and Skip Search algorithms allows each algorithm to complement the other. The resultant algorithm is called Quick-Skip Search hybrid algorithm. Similar to the two original algorithms, the effectiveness of the resultant hybrid algorithm can be found in the preprocessing and searching phases. The preprocessing phase of the Quick-Skip Search hybrid algorithm consists of building two shifting value tables, namely, the bad character table for the Quick Search algorithm and the bucket list for the Skip Search algorithm. The searching phase of the hybrid algorithm depends on the original algorithms searching phase with some update related to matching operation (the searching process is performed in different orders). Throughout the searching phase, the decision on how much distance is required to shift the sliding window if a mismatch or a complete match is found between the pattern and text characters depends on selecting a large shift value from the Quick Search and Skip

Search shift values. The algorithm is effective for any alphabet type and pattern length.

Quick Search, Zuh-Takaoka and Boyer Moore-Horspool (Maximum-Shift) Algorithm [13] proposed a hybrid string matching algorithm called Maximum-Shift hybrid algorithm. This new hybrid algorithm is a combination of three existing algorithms, namely, QS, ZT, and Horspool. The Maximum-Shift hybrid algorithm consists of three phases: preprocessing, maximum shift, and searching phases. The pre-processing phase, which preprocesses the input pattern to be useful during the matching process, consists of building the shifting value tables of the QS bad character table and the (ztBc) table.

The two inputs to the maximum shift phase are the QS and ZT shift values. The output from this phase is considered the maximum shift value between these two inputs to shift the pattern to a longer distance and subsequently reduce the number of attempts and the total number of character comparisons. The searching phase depends on QS and modified Horspool algorithms. The searching phase of the Maximum-Shift hybrid algorithm follows the searching phase orders of the QS algorithm with some updates related to the matching process.

During the searching phase, the hybrid algorithm searches the text string from left to right and utilizes the idea of the Horspool algorithm with a slight modification by comparing the two rightmost characters of the pattern with the text window characters as an initial step before searching the remaining characters P[m −2] from left to right. The algorithm produces better results compared with the three original algorithms and also when compared with another two hybrid algorithms (BR and Smith) in terms of minimizing the number of attempts and character comparisons [13].

The author [14] in 2017 proposed a new hybrid algorithm its name ABSBMH, which is a result of combining the good features of the two well know algorithms the modified Horspool and SSABS hybrid algorithms, which are a single and hybrid algorithm respectively. In the preprocessing phase the ABSBMH hybrid algorithm generates the Quick Search bad character table (qsBc) as the SSABS algorithm do which is beneficial to calculate the shifting distance during the searching phase. In the searching phase the ABSBMH algorithm depending on the SSABS and modified Horspool searching phase algorithms, the ABSBMH algorithm inspects not only the rightmost character in the text window, but it checks the last two characters in the text window with its corresponding position in the pattern characters to inspect if it matches or mismatch, if it matches the algorithm start search the remaining characters from left to right.

III. The Proposed Algorithm

The contribution of this research is discussed in this section, that is, a solution to the string matching problem that involves proposing a sequential hybrid algorithm that blends two existing algorithms to develop an efficient sequential hybrid algorithm.

The proposed hybrid algorithm, SSTBMQS algorithm, is the key point of this study. This algorithm comprises two phases: the preprocessing and searching phases. In the preprocessing phase, the pattern characters are preprocessed to collect information to be used in the searching phase to decrease the number of characters compared and the number of attempts. The preprocessing and searching phases, which consist of seven steps for the proposed hybrid algorithm, are summarized in the next subsections, as shown in Fig. 1.

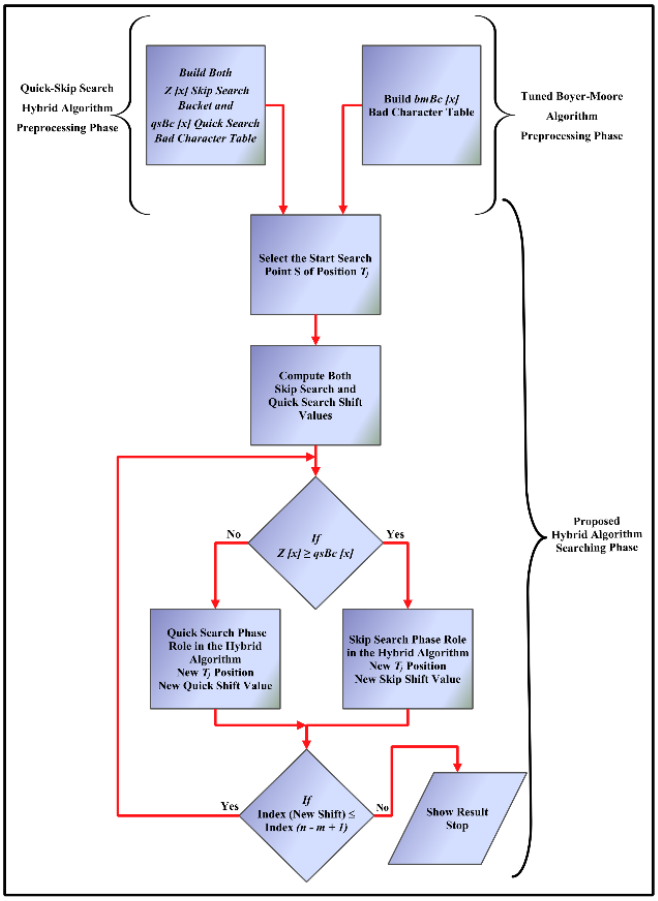

Fig. 1. Flowchart for SSTBMQS hybrid algorithm overview.

A. Preprocessing Phase

To construct the preprocessing phase for SSTBMQS algorithm, the preprocessing phase for the Quick-Skip Search hybrid algorithm and the Tuned Boyer-Moore algorithm must be built first. The Quick-Skip Search hybrid algorithm preprocessing phase consists of building the QS bad character table and the SS bucket separately. The two preprocessing phases were not combined into one preprocessing phase because of the reverse behavior of the preprocessing phase for the QS and SS algorithms. Bad character table of QS stores all the rightmost indexes for each character in the pattern. The SS bucket contains all the leftmost indexes for each character in the pattern. Moreover, the bad character table for the Tuned Boyer-Moore algorithm consists of all the first rightmost appearances for each character in the pattern after scanning and indexing the pattern from right to left, starting with the rightmost character in the pattern, which always has the index 0. As a result, the preprocessing phase of SSTBMQS algorithm builds the preprocessing phase from each original algorithm.

B. Searching Phase

The searching phase of SSTBMQS algorithm depends on the technique used in the original algorithms, such as searching using different orders, with some development during the matching operation. During the matching operation, if a mismatch or an entire pattern string match occurs, the algorithm shifts the pattern according to the shift value from the original Quick-Skip Search hybrid algorithm. Basically, the searching phase of the hybrid algorithm follows these seven steps:

Step 1: Similar to the original Quick-Skip Search hybrid algorithm, this stage starts by examining the $m-text$ characters to specify a possible starting search point *S*. The starting search point has a T_j position in the text characters, where both *j* and the pattern length *(m)* have the same size. Initially, after selecting the T_j position in the text characters, At this point, the SSTBMQS algorithm starts performing the alignment operation between the text characters and the pattern characters in such a way that permits the alignment of the character at the T_j position with its corresponding location in the bucket list. Also, as an initial step the SSTBMQS algorithm computes the shift value of the Quick-Skip Search hybrid algorithm, which contains the shift value for the Skip Search phase and Quick Search phase, because the underlying structure of SSTBMQS algorithm has two searching phases (Skip Search and Quick Search).

The SSTBMQS algorithm examines both shift values and uses the searching phase, which has the maximum shift value. When the alignment between the text characters and the pattern characters is performed, the character located at the T_j position does not appear in the pattern characters. Thus, the algorithm continually shifts the pattern characters to the following T_j position in the text character. This operation skips numerous unnecessary attempts, consequently minimizing the total number of character comparisons and avoiding the alignment of the leftmost character of the pattern with the leftmost character of the text at the beginning of the searching phase.

Step 2: The SSTBMQS algorithm calculates the T_d value, where *d* is the difference between the T_f position and the T_j position. T_f is the position of the inspection character, where *f* is the location of the last character in the $m-text$ characters. The T_f position is determined in the next step. The T_d value is calculated depending on two circumstances:

1) If the character at position T_j occurs in the last position in the bucket, T_d is calculated from Equation (1) after being subtracted from the last character index, which is equal to the pattern length minus one $(m-1)$ from the last T_j position in the bucket. Then, the algorithm moves directly to **Step 3**.

$$T_d = (m-1) - (\text{The last } T_j \text{ position in the bucket}) \quad (1)$$

2) Whenever the character at position T_j is not at the last position in the bucket, the T_d value is calculated using Equation (2) after subtracting the last character index, which is equal to the pattern length minus one $(m-1)$ from the current T_j position of the bucket.

$$T_d = (m-1) - (\text{The current } T_j \text{ position of the bucket}) \quad (2)$$

This process continues to execute until all positions of the character at T_j position in the bucket are processed. The algorithm moves to the **Step 3**.

Step 3: This step comes after determining the T_d value in **Step 2**. In this step, the algorithm determines the location of T_f, where *f* is the location of the last character in the $m-text$ characters, which is often called the inspection character. To determine the location of T_f, the SSTBMQS algorithm adds the T_d value to the current position of T_j in the text characters, as shown in Equation (3).

$$T_f = (\text{The current position of } T_j \text{ in the text characters}) + T_d \quad (3)$$

Step 4: The SSTBMQS algorithm verified whether a match is possible between the pattern and the text characters by checking the inspection character (which occurs at T_f in the text). If the value of this character after referring to the (bmBc[a]) table is equal to (0) (that is, the last character in the pattern matches its corresponding character at the T_f position in the text), where the value (0) in the (bmBc[a]) table is given only for the rightmost character in the pattern, The most significant property of the Tuned Boyer-Moore algorithm is the unique zero value given to the rightmost character in the pattern. Therefore, the value of the rightmost character in the (bmBc) table is always (0). The algorithm moves to **Step 5**. Otherwise, the algorithm goes to **Step 6**. By performing this process, the algorithm verifies whether a match is possible between the rightmost character in the pattern and its corresponding character at the T_f position in the text without opening the text window and without performing a comparison operation. The latter is considered the most costly portion of a string matching algorithm, that is, when the algorithm verifies whether the character in the pattern occurs in the text window [15]. This process will reduce the number of character comparisons, as well as the number of attempts.

Step 5: This step is accomplished if the inspection character at T_f equals (0) from the (bmBc[a]) table. Thus, a match between the pattern and the text characters is possible. At this step, comparisons occur between the pattern and text characters by opening a text window that is equal to pattern length *(m)*. The first comparison operation is performed from the leftmost character in the pattern to the corresponding character position in the text window to the right side. If a mismatch or a complete pattern match occurs, the SSTBMQS algorithm moves to the following step.

Step 6: In this step, the SSTBMQS algorithm computes the shift values for both the SS and QS algorithms. SSTBMQS hybrid algorithm computes the SS shift value in different ways depending on two circumstances:

1) When the SSTBMQS algorithm checks the character at the T_j position and determines that the character appears in the last location of the bucket, the SS value is computed using (4) after the first bucket location of the character that appears in the next T_j position is distinguished in the text characters. This position is considered the following start search point.

$$SS\_shift = m + \text{current } T_j \text{ position (from bucket)} - \text{the next } T_j \text{ position} \quad (4)$$

2) When the T_j position does not appear in the last location of the bucket, the SS shift value is computed by using a subtracting operation performed between the following location value from the current location value of this character in the bucket.

SSTBMQS algorithm is used to compute the QS shift value depending on the character that follows the rightmost character of the text window. This character is used as an index that refers to the shift value stored in the QS bad character table, which represents the value of the rightmost occurrence of this character in the pattern.

SSTBMQS algorithm has two searching phases (Skip Search and Quick Search). At this point, SSTBMQS algorithm computes the shift values of the Skip Search and Quick Search phases. SSTBMQS algorithm examines both shift values and uses the searching phase, which has the maximum shift value. In other words, if the SS shift value is larger than or equal to the QS shift value, SSTBMQS algorithm depends on the Skip Search phase and goes to **Step 2**, as shown in Fig. 2. Otherwise, if the QS shift value is larger, then the SSTBMQS algorithm goes to **Step 7**.

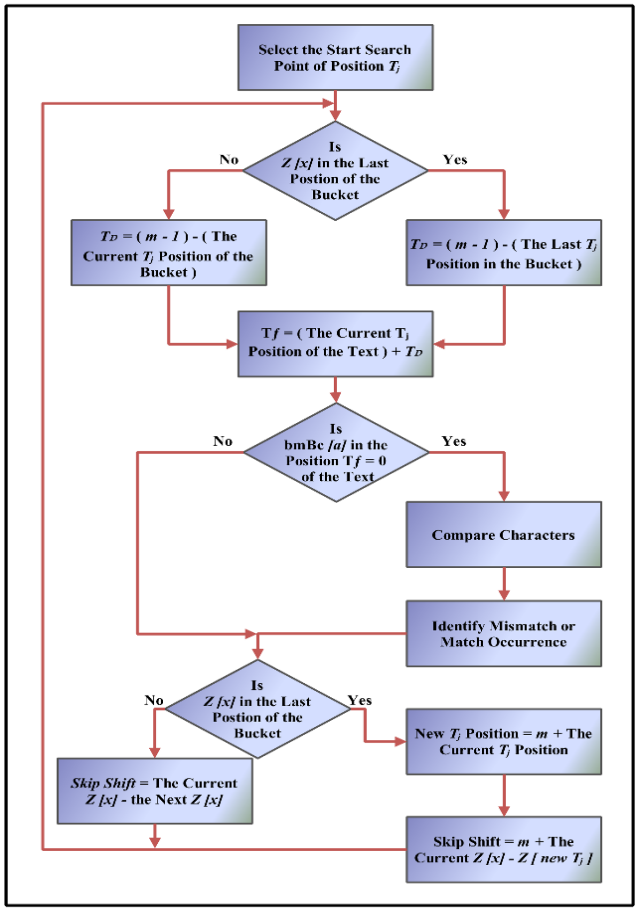

Fig. 2. Flowchart for Skip Search Phase Role in the SSTBMQS algorithm.

Step 7: This step is employed when SSTBMQS algorithm depends on the Quick Search phase. The Quick Search phase computes the T_j position depending on two circumstances.

1) When the value of the character is positioned next to the rightmost character of the text window is lower than or equivalent to pattern length *(m)*, the new T_j position computes the current T_j position in the text character to become equivalent to that positioned immediately next to the window, which is considered to be the new beginning search point. Then, the algorithm moves to **Step 2**, as presented in the following condition.

If (QS_Shift > SS_Shift) & (QS_Shift ≤ m)

Then

New T_j Position = First Position after the Window

2) When the Quick Search phase checks the shift value of the character that follows the rightmost character of the text window and it is larger than pattern length *(m)*, the new T_j position is computed by summing the current T_j position in the text and is made equal to the character position immediately next to the text window plus the value of pattern length *(m)* as presented in the following condition.

If (QS_Shift > SS_Shift) & (QS_Shift > m)

Then

New T_j Position = First Position after the Window + m

However, after the new T_j position is computed, if the character positioned at the new T_j position does not appear in the pattern characters, SSTBMQS algorithm continually shifts the pattern to the following potential beginning search point, and SSTBMQS algorithm goes into **Step 2**. Fig. 3 shows the functionality of the Quick Search phase throughout the searching phase of SSTBMQS algorithm. All of the steps of the searching phase are repeated until the window is placed beyond *(n − m + 1)*.

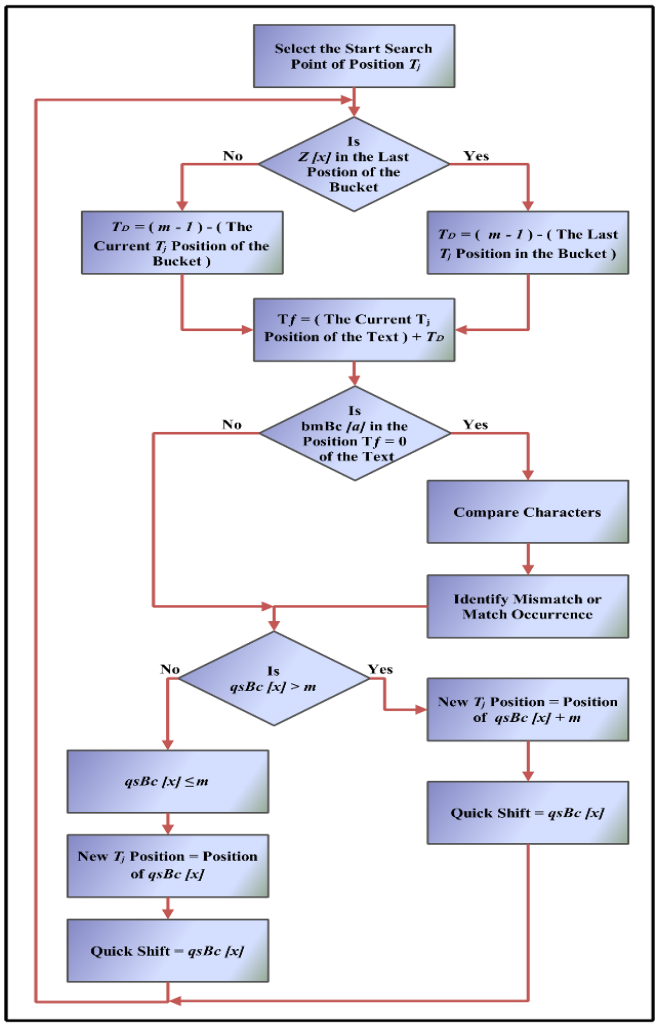

Fig. 3. Flowchart for Quick Search Phase Role in the SSTBMQS algorithm.

IV. SSTBMQS Algorithm Tracing Example

This section demonstrates an example of tracing by using SSTBMQS algorithm. The example shows the steps of the preprocessing and searching phases of SSTBMQS algorithm. Two strings are used as input: text and a pattern, as displayed in Fig. 4.

Text = " A D F T C D C T D A D A A T A A M A C A G C T T C A C G A C D F C C A C G A

C M A C "

Pattern = "A C G A C M A C "

The text length n = 42

The pattern length m = 8

The alphabet set $\sum = (A, C, D, F, G, M, T)$ *of size* $\sigma = 7$

Fig. 4. Algorithm Inputs.

The preprocessing phase of SSTBMQS algorithm is built by constructing the pre-processing phase for the two original algorithms: The Quick-Skip Search hybrid algorithm and the TBM algorithm. The Quick-Skip Search hybrid algorithm is used to build the SS buckets and the QS bad character table, whereas the TBM algorithm is used to build the (bmBc[a]) bad character table for the input pattern, as shown in Fig. 5.

X	Z[x]
A	(6, 3, 0)
C	(7, 4, 1)
D	Φ
F	Φ
G	(2)
M	(5)
T	Φ

Skip Search Buckets

X	A	C	D	F	G	M	T
qsBc[x]	2	1	9	9	6	3	9

Quick Search Bad Character Table

X	A	C	D	F	G	M	T
bmBc[x]	1	0	8	8	5	2	8

Tuned Boyer-Moore Bad character Table

Fig. 5. Preprocessing phase.

The searching phase starts by choosing the start search point, which is at location T_j in the text, as shown in Fig. 6.

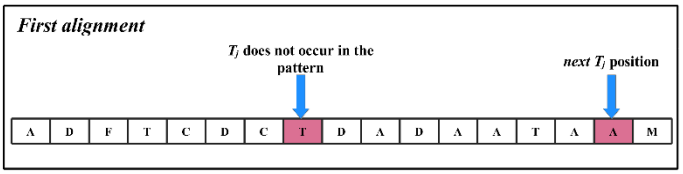

Fig. 6. First Alignment.

In the first alignment, the chosen beginning point (T) does not exist in the pattern. SSTBMQS algorithm checks the following potential starting point (A), as mentioned in **Step 1** of Section III. In the second alignment (see Fig. 7), the shift value is calculated by subtracting the next position value from the current position value of the character (A) that appears in the SS bucket, as explained in the second circumstance in **Step 6** in Section III.

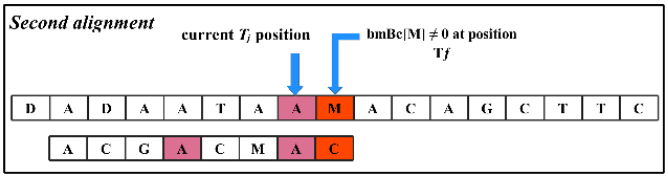

Fig. 7. Second Alignment.

Shift = Skip Shift = 6 - 3 = 3

SSTBMQS algorithm checks the character at position T_f in the (bmBc[M] 6= 0), which is found to be unequal to 0. By performing this process, SSTBMQS algorithm avoids opening a text window and reduces the number of attempts, as well as the number of character comparisons, as explained in **Step 4** in Section III. SSTBMQS algorithm then computes the shift value of the SS shift value = 3, where the QS shift value = 2 from the QS bad character table. SSTBMQS algorithm depends on the SS shift value, as explained in **Step 6** in Section III.

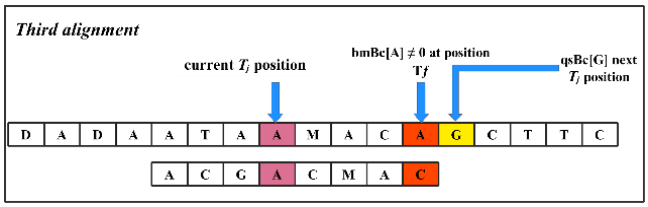

Fig. 8. Third Alignment.

Shift = Quick Search bad character table = 6

The third alignment shows a situation in which SSTBMQS algorithm depends on the QS shift value, which is equal to the position of the character (G) in the pattern (see Fig. 8). After checking the character (A) at position T_f in (bmBc[A] 6= 0), as mentioned previously in **Step 4** in Section III, the new T_j position becomes equivalent to the position of the character (G) in the text characters, as explained in the first circumstance of **Step 7** in Section III.

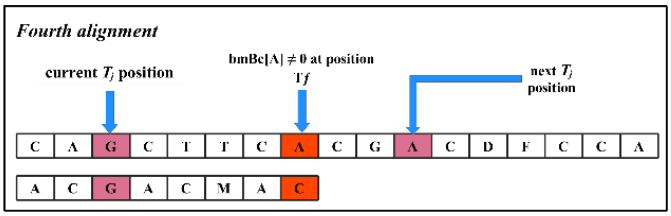

Fig. 9. Fourth Alignment.

Shift = Skip Shift = 8 + 2 - 6 = 4

The value of the character (A) in the TBM bad character table is equal to (1). Thus, a match between the pattern and the text characters is impossible (see Fig. 9). The SSTBMQS algorithm computes shift value depending on the shift value from the SS bucket. The (G) character at position T_j appears in the last position of the bucket. SSTBMQS algorithm computes the shift value by adding the value of the (G) character in the SS bucket to the pattern length *(m)*. Then, the summation is subtracted from the first value of the character at position T_j from the bucket, as explained in the first circumstance of **Step 6** in Section III.

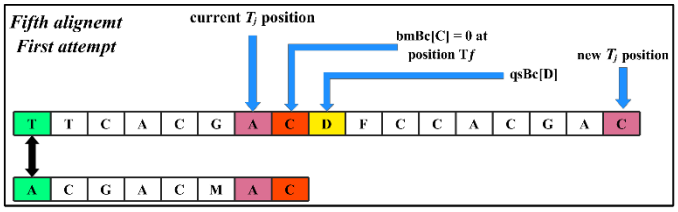

Fig. 10. Fifth Alignment and First Attemp.

Shift = Quick Search bad character table = 9

In the fifth alignment the character (C) at position T_f equals (0) in the (bmBc[c] = 0) bad character table. Thus, matching can possibly occur between pattern and text characters. SSTBMQS algorithm opens a text window and starts comparing characters from left to right, considering the first attempt, as shown in Fig. 10. After a mismatch occurs, SSTBMQS algorithm computes both SS and QS shift values. The QS shift value becomes larger than the SS shift value. By computing for the shift value of the character (D), which is equal to (9) in the QS bad character table, the QS shift value becomes larger than the pattern length *(m)*. Thus, the new T_j position becomes equal to the summation of the current (qsBc[D]) and the pattern length *(m)*, as explained in the second circumstance of **Step 7** in Section III.

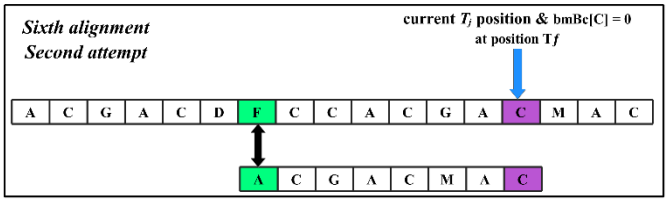

Fig. 11. Sixth Alignment and Second Attempt.

Shift = Skip Shift = 7 - 4 = 3

The sixth alignment shows a situation in which the pattern aligns its character (C) at position T_j that is, at the same time, the T_f position. After examining the (bmBc[C]=0), SSTBMQS algorithm opens a text window and starts comparing characters from left to right, considering the second attempt (see Fig. 11). SSTBMQS algorithm depends on the SS shift value by subtracting the next position value from the current position value of the character (C) in the SS bucket, as explained in the second circumstance of **Step 6** in Section III.

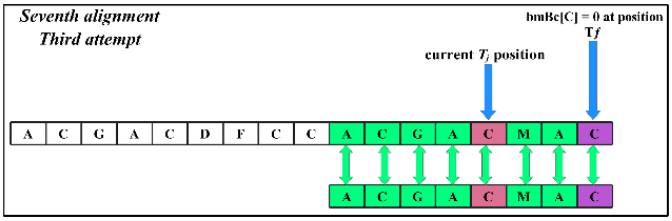

Fig. 12. Seventh Alignment and Third Attempt.

In the seventh alignment, SSTBMQS algorithm first examines the value of the character (C) at the T_f position in the TBM bad character table (bmBc[C] = 0) and finds it to be equal to (0). Then, SSTBMQS algorithm starts comparing the characters from left to right until all characters' match, considering the third attempt as explained in Fig. 12.

Number of attempts = 3
Number of characters' comparison = 10

V. Results and Discussion

This section presents the experimental design adopted in this study for the sequential version of SSTBMQS algorithm. The execution of the sequential program, performance and evaluation are discussed.

A. Experimental Databases

DNA sequence, protein sequence, and English text datasets are used in this work to evaluate the results of the sequential version of SSTBMQS algorithm with the two original algorithms. Such datasets are chosen because they are defined

as a benchmark standard that demonstrates the typical utilization of string matching applications. They also vary in alphabet size; thus, a variety of algorithm behavior with different alphabet sizes can be evaluated. The data size chosen for testing the sequential behavior of SSTBMQS algorithm with the two original algorithms is 100 MB.

a) DNA Sequence

DNA sequence is created from a long string that holds hereditary information arranged in a sequence of four nucleotides represented by four uppercase letters. Usually, adenine is indicated by (A), thymine is indicated by (T), guanine is indicated by (G), and cytosine is indicated by (C) [$\sum$ = (A, C, G, T) and $\sigma = 4$]. To examine the algorithm behavior in a small alphabet size, DNA sequence is considered in this study. Database is downloaded from Gutenberg Project [16].

b) Protein Sequence

Protein sequence is composed of 20 amino acids indicated by uppercase characters [$\sum$ = (A, C, D, E, F, G, H, I, K, L, M, N, P, Q, R, S, T, V, W, Y) and $\sigma = 20$]. Protein sequence has an essential responsibility in biochemistry science, especially in protein structure and functionality.

c) English Text

English text data type comprises over 100 various alphabet types split into English language (lowercase and uppercase), numbers, and samples. The large size of this alphabet data type allows testing the algorithm behavior in such a large dataset. This data type is gathered from the Gutenberg Project [16].

B. Performance and Evaluation

The major goal of this research is to offer an effective algorithm to be utilized basically with different string matching applications. Two common factors are typically considered to evaluate the performance of a string matching algorithm with different applications [17]. The two factors are presented below.

a) Total Number of Character Comparisons

This factor refers to the summation of exact comparison that occurs between the pattern and characters of text window. The algorithm with a significantly less number of character comparisons is identified as a powerful algorithm with better performance.

b) Total Number of Attempt

This factor denotes the distance that a pattern needs to skip along the entire assigned text. When the amount of attempts is significantly less, the overall performance of an algorithm is better. These two factors are used as a basis to evaluate the efficiency of the sequential version of SSTBMQS algorithm and to specify its overall performance with various datasets implemented.

C. Sequential Program Execution

The sequential program of SSTBMQS hybrid algorithm with the two sequential original string matching algorithms (i.e., TBM and Quick-Skip Search) is examined on each kind of dataset outlined in part (A) of Section V. The three algorithms are run using a personal computer with 2.4 GHZ Inter®Core™with 7 cores and 8 GB RAM. The operating system used is Microsoft Windows 8 Single language, which is a 64-bits operating system. Microsoft visual studio 2010 is utilized to write down the codes. The compiler used to build and run the codes is visual C++ compiler.

This section elucidates the evaluation results acquired from executing the sequential programs of SSTBMQS algorithm when compared with TBM and Quick-Skip Search hybrid algorithms. As indicated in Table 1, TBM is a single algorithm used in developing SSTBMQS algorithm of this study. Quick-Skip Search and Maximum-Shift are both hybrid algorithms.

Quick-Skip Search is used in developing SSTBMQS algorithm. Maximum-Shift consists of QS, BMH, and ZT algorithms. The results of Maximum-Shift are compared with those of SSTBMQS algorithm and the two chosen string matching algorithms. This hybrid algorithm is chosen for comparison because it is considered as one of the latest hybrid algorithm in the literature. The QS algorithm that is included in developing Quick-Skip Search hybrid algorithm is also used to develop the Maximum-Shift hybrid algorithm. All the algorithms indicated above are elucidated in Section II of this research.

These algorithms are evaluated according to the total numbers of character comparisons and number of attempts. As mentioned previously in part (A) of Section V, various kinds of datasets are employed, which are DNA sequence, protein sequence, and English text. The patterns are selected randomly from the words inside each dataset and have various lengths that range from 8 to 100 [10], where 8 and 10 are short patterns; 20, 30, 40, 50, 60, 70, 80, 90, and 100 are long patterns [13]. Each pattern length is searched five times, and the average is obtained. The Maximum-Shift hybrid algorithm results are generated from [13] (Table 1).

TABLE. I. RELATIONSHIP AMONG TBM, QUICK-SKIP SEARCH, MAXIMUM-SHIFT, AND THE PROPOSED ALGORITHM

Algorithms	***Algorithm Type***	***Underlying Structure***	***Relationship with the Proposed Algorithm***
Tuned Boyer-Moore (TBM)	Single algorithm	TBM	Used in the preprocessing and searching phases
Quick-Skip Search algorithm	Hybrid algorithm	QS+Skip Search	Used in the preprocessing and searching phases
Maximum-Shift (Max-Shift)	Hybrid algorithm	QS+BMH+ZT	Used the QS in the preprocessing phase

D. Analyzing Number of Character Comparisons

Based on the empirical results presented in Fig. 13 to 15, DNA alphabet delivers a great number of character comparisons, especially when the size of pattern length is short. This behavior is due to the structure nature of the DNA alphabet itself, which considers a small alphabet size. The DNA alphabet structure consists of four characters, thereby leading to a small shift distance of pattern during the searching operation of pattern string into text string. The use of a small

size of alphabet in implementing algorithms causes considerable exact matching between inspected pattern string and text window, particularly when utilizing short pattern lengths. Subsequently, the amount of character comparisons is influenced by the size of the alphabet used.

For all algorithms with all dataset types, the results show that when pattern lengths increase, the total number of character comparisons decreases significantly. This behavior is due to the increasing amount of shift distance provided by the algorithms when a mismatch occurs. Based on this observation, the DNA dataset is excluded, especially for TBM algorithm. The performance of TBM algorithm in DNA dataset shows an unstable behavior, which is due to a fixed shift value provided by this algorithm that leads to a small shift of pattern after a mismatch occurs. Furthermore, DNA dataset generates small numbers in TBM bad character table, which leads to a small shift of pattern during an unrolled operation in each attempt. This condition can be considered another reason for the unstable behavior provided by TBM algorithm that tends to increase the total number of character comparisons.

In protein and English datasets, the performance of Quick-Skip Search hybrid algorithm surpasses that of Maximum-Shift hybrid algorithm when a short pattern length is used. This result is ascribed to that the Maximum-Shift hybrid algorithm starts the searching phase without checking T_j starting point. The probability of T_j position character taking place in pattern characters is low when using medium and large alphabet sizes for protein and English datasets, respectively. The results of protein and English datasets also show that the Maximum-Shift hybrid algorithm beats the Quick-Skip Search hybrid algorithm in 30 to 100 pattern lengths.

This behavior is due to employing both QS and ZT preprocessing phases to obtain a maximum shift distance to shift a pattern when a mismatch or a complete match occurs. The largest shift value can be obtained from the QS algorithm preprocessing phase, which is equal to the pattern length plus one, when the character following the rightmost character of text window is not occurring in the pattern characters. However, ZT preprocessing phase depends on two consecutive rightmost characters in the text window to calculate the shift distance value. Using these methods avoids many unnecessary potential numbers of character comparisons during the matching process of Maximum-Shift hybrid algorithm.

Quick-Skip Search hybrid algorithm utilizes QS algorithm preprocessing phase with Skip buckets to determine the next position of pattern string in text string. Maximum-Shift hybrid algorithm strongly beats Quick-Skip Search hybrid algorithm when 30 to 100 pattern lengths are used. The Quick-Skip Search hybrid algorithm uses the Skip buckets with the QS algorithm in the preprocessing phase. The disadvantage of the Skip Search algorithm is used all the positions of the character at position T_j in the bucket list in case of match or mismatch occurs. On the contrary, the Maximum-Shift hybrid algorithm uses the preprocessing phase of ZT algorithm, which is viewed as a highly effective algorithm with small alphabet size data type.

SSTBMQS algorithm outperforms all other algorithms by producing a less number of character comparisons for all pattern lengths and data types. Such a good performance is due to three reasons. First, the algorithm employs Quick-Skip Search preprocessing phase to determine the next position of a pattern in text string after a mismatch occurs. Second, the algorithm starts the searching phase by checking the occurrence of character at Tj position in pattern characters, which is considered a starting search point before actual comparison. Third, the algorithm employs modified TBM matching operation characteristic by checking the character at T_f position before starting a comparison operation.

The results of the SSTBMQS algorithm are better than those of the two original algorithms and Maximum-Shift hybrid algorithm in all pattern lengths and data types. The good performance of the SSTBMQS algorithm implies that the integration of the two original algorithms provides a new hybrid algorithm with better performance.

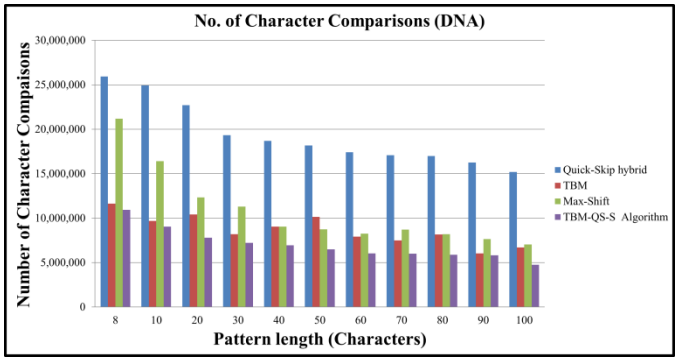

Fig. 13. Number of Character Comparisons in DNA Sequence Data.

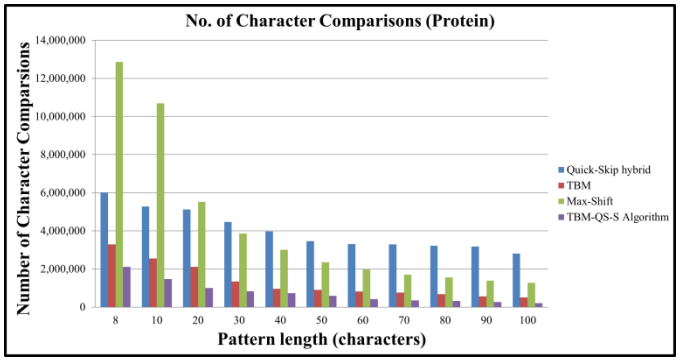

Fig. 14. Number of Character Comparisons in Protein Sequence Data.

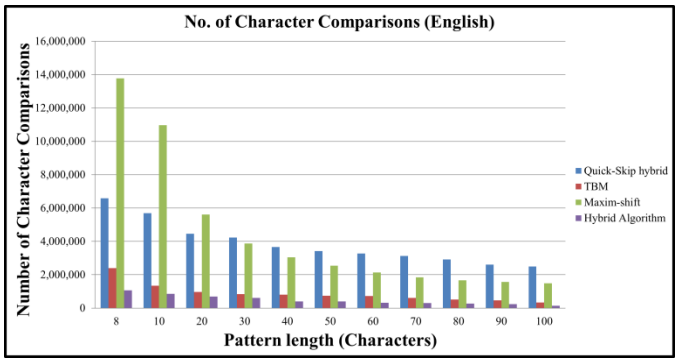

Fig. 15. Number of Character Comparisons in English Text Data.

E. Analyzing Number of Attempts

The empirical results presented in Fig. 16 to 18, show the behavior of TBM, Quick-Skip Search, Maximum-Shift, and SSTBMQS algorithms when using with DNA sequence, protein sequence, and English text data types. The results show that all the algorithms have a stable behavior in medium and large sizes for protein and English alphabets, respectively. Generally, the total number of attempts is decreased when pattern lengths increase. In short, pattern lengths and the Quick-Skip Search hybrid algorithm outperform the Maximum-Shift hybrid algorithm. This result is due to the characteristic of the Quick-Skip Search hybrid algorithm, that is, it starts the searching phase by checking the probability of occurrences of the character at T_j position in the pattern characters. This probability decreases when alphabet size increases. Hence, the Quick-Skip Search hybrid algorithm surpasses the Maximum-Shift hybrid algorithm in a short pattern length with protein and English alphabets.

The Maximum-Shift hybrid algorithm does not start the searching phase by checking T_j position to specify the starting search point. DNA alphabet is accordingly excluded because of its small size, which consists of only four characters, and the ordering of the characters in the pattern itself, which increases the probability of occurrences of the character at T_j position in the pattern. Thus, a small shift distance to the pattern is generated across the text string. The Maximum-Shift hybrid algorithm generally outperforms the Quick-Skip Search hybrid algorithm in long pattern, especially from 30 to 100 pattern lengths. This result is due to using ZT preprocessing function, which uses two rightmost characters at the text window to compute the shift distance and is considered as a powerful function with small alphabets.

The TBM algorithm shows a stable behavior in protein and English alphabets by decreasing the total number of attempts, which is related to the alphabet size of the dataset being used. DNA dataset is excluded because of the size of DNA alphabet, which increases the probability of finding inspection character, which is the position of the rightmost character in text window that is equal to zero in the TBM bad character table. This behavior will lead to many exact matching processes between the pattern and text characters, which contributes in increasing the total number of attempts.

The results of the SSTBMQS algorithm indicate that it outperforms all other algorithms in all pattern lengths and with any alphabet sizes. This good behavior is related to its good properties acquired from integrating the two original algorithms. The hybrid algorithm starts the searching phase by checking the occurrence of the character at T_j position in the pattern characters. When the size of the alphabet used is large, the probability of the character occurrence at T_j position is low. The Quick-Skip Search preprocessing function is used to compute a maximum shift distance to shift the pattern long distance when a mismatch or a complete pattern match occurs.

Before performing matching operations, the character at T_f position is checked that is the position of the rightmost character at the text window. If the character at T_f position equals to zero in the TBM bad character table, then the SSTBMQS algorithm starts a character comparison. If the character at T_f position is not equal to zero value, then the SSTBMQS algorithm skips opening text window and starts character comparison. This technique contributes in reducing the total number of attempts. Therefore, SSTBMQS algorithm utilizes the significant advantages and excludes the disadvantages of the two original algorithms by producing a minimal number of attempts.

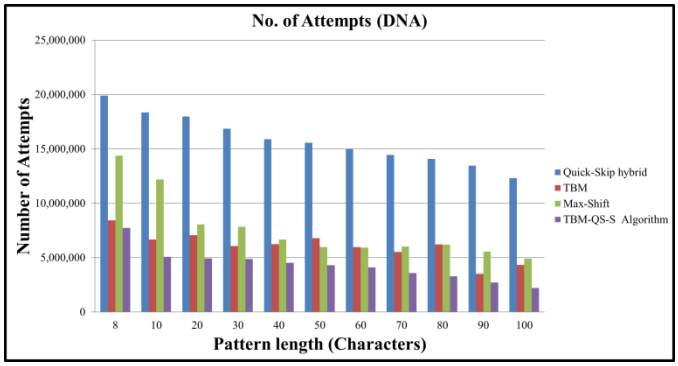

Fig. 16. Number of Attempts in DNA Sequence.

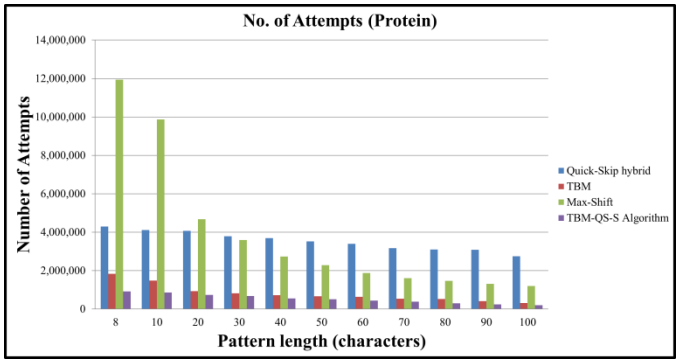

Fig. 17. Number of Attempts in Protein Data Type.

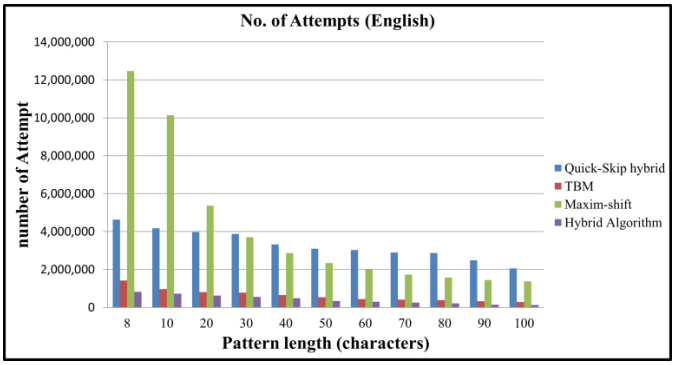

Fig. 18. Number of Attempts in English Text Data Type.

VI. Conclusion and Future Work

This section presents the conclusion from achieving the objective of this study, that is, integrating two existing algorithms (i.e., TBM and Quick-Skip Search) to produce an efficient hybrid string matching algorithm called SSTBMQS. Particularly, this study aims to extract the good properties from the two original algorithms. The SSTBMQS algorithm uses the shift values produced from the preprocessing phase of the

Quick-Skip Search hybrid algorithm to compute the next expected position of the pattern during the searching phase.

In the searching phase, the SSTBMQS algorithm examines *m−text* characters to specify a starting search point before the actual character comparisons. This process avoids performing many unnecessary attempts, which reduces the total number of attempts. The SSTBMQS algorithm also utilizes modified TBM matching operation during the searching phase by checking the character at T_f position in the TBM bad character table before performing character comparisons and starting an attempt. Consequently, the total numbers of character compassions and attempts are significantly reduced.

Two parameters are used to evaluate the performance of the sequential version of the SSTBMQS algorithm, which are the total numbers of character comparisons and attempts. In Section V, the SSTBMQS algorithm is compared with three algorithms, namely, TBM and Quick-Skip Search as original algorithms and Maximum-Shift as hybrid string matching algorithm. Comparisons are performed in different datasets (DNA sequence, Protein sequence, and English text) with different pattern lengths. The SSTBMQS algorithm outperforms all other algorithms by producing fewer total numbers of attempts and character comparisons. In future work, the running time of SSTBMQS algorithm should be enhanced by parallelizing it on the GPU using CUDA library.

REFERENCES

[1] Michailidis, Panagiotis D., and Konstantinos G. Margaritis. "On-line string matching algorithms: Survey and experimental results." *International journal of computer mathematics* 76.4 411-434, (2001).

[2] Al-Dabbagh, Sinan Sameer Mahmood, et al. "Parallel Quick Search Algorithm for the Exact String Matching Problem Using OpenMP." *Journal of Computer and Communications* 4.13 (2016): 1.

[3] Raju, S. Viswanadha, A. Vinaya Babu, and M. Mrudula. "Backend engine for parallel string matching using boolean matrix." *Parallel Computing in Electrical Engineering, 2006. PAR ELEC 2006. International Symposium on*. IEEE, 2006.

[4] Kumar, K. S. M. V., S. Viswanadha Raju, and A. Govardhan. "A Survey of Parallel Algorithms for Text Matching In Large Databases and Hardware Implementations." International Journal of Engineering and Innovative Technology (IJEIT) 1(2): 2277–3754, 2012.

[5] Hassan, Atif Agha. "Mixed heuristic algorithm for intelligent string matching for information retrieval." *Computational Intelligence and Multimedia Applications, 2005. Sixth International Conference on*. IEEE, 2005.

[6] Kun, Bi, et al. "A practical distributed string matching algorithm architecture and implementation." *World Acad Sci Eng Technol* 10 (2005): 1307-6884, 2005.

[7] AbdulRazzaq, A. A., Rashid, N. A., Hasan, A. A. and Abu-Hashem, M. A. The Exact String Matching Algorithms Efficiency Review, Global Journal on Technology 4(2): 576–589, 2013.

[8] Naser, Mustafa Abdul Sahib, and Mohammed Faiz Aboalmaaly. "Quick-Skip search hybrid algorithm for the exact string matching problem." *International Journal of Computer Theory and Engineering* 4.2 (2012): 259.

[9] Sheik, S. S., et al. "A fast pattern matching algorithm." *Journal of Chemical Information and Computer Sciences* 44.4, 1251-1256, 2004.

[10] Huang, Yong, et al. "A fast exact pattern matching algorithm for biological sequences." *BioMedical Engineering and Informatics, 2008. BMEI 2008. International Conference on*. Vol. 1. IEEE, 2008.

[11] Almazroi, Abdulwahab Ali. "A fast hybrid algorithm approach for the exact string matching problem via berry ravindran and alpha skip search algorithms." *Journal of Computer Science* 7.5 (2011): 644.

[12] Naser, Mustafa Abdul Sahib, and Mohammed Faiz Aboalmaaly. "Quick-Skip search hybrid algorithm for the exact string matching problem." *International Journal of Computer Theory and Engineering* 4.2 (2012): 259.

[13] Kadhim, Hakem Adil, and NurAini AbdulRashidx. "Maximum-shift string matching algorithms." *Computer and Information Sciences (ICCOINS), 2014 International Conference on*. IEEE, 2014.

[14] Al-Dabbagh, Sinan Sameer Mahmood, and Nawaf Hazim Barnouti. "A New Efficient Hybrid String Matching Algorithm to Solve the Exact String Matching Problem."

[15] Charras, Christian, and Thierry Lecroq. *Handbook of exact string matching algorithms*. King's College, 2004.

[16] Kärkkäinen, Juha, and Joong Chae Na. "Faster filters for approximate string matching." *2007 Proceedings of the Ninth Workshop on Algorithm Engineering and Experiments (ALENEX)*. Society for Industrial and Applied Mathematics, 2007.

[17] Thathoo, Rahul, et al. "TVSBS: A fast exact pattern matching algorithm for biological sequences." *Current Science* 91.1 (2006): 47-53.

Multi-Criteria Wind Turbine Selection using Weighted Sum Approach

Shafiqur Rehman
Center for Engineering Research
King Fahd University of Petroleum & Minerals
Dhahran, Saudi Arabia

Salman A. Khan
Computer Engineering Department
University of Bahrain
Sakhir, Bahrain

***Abstract*—Wind energy is becoming a potential source for renewable and clean energy. An important factor that contributes to efficient generation of wind power is the use of appropriate wind turbine. However, the task of selecting an appropriate, site-specific turbine is a complex problem. The complexity is due to the presence of several conflicting decision criteria in the decision process. Therefore, a decision is sought such that best tradeoff is achieved between the selection criteria. With the inherent complexities encompassing the decision-making process, this study develops a multi-criteria decision model for turbine selection based on the concepts of weighted sum approach. Results indicate that the proposed methodology for finding the most suitable turbine from a pool of 18 turbines is effective.**

Keywords*—Wind turbine; renewable energy; weighted sum method; multi-criteria decision-making

I. INTRODUCTION

The exponential growth in population, materialistic life styles, and fast industrialization has resulted in higher demand for energy. However, the awareness and sensitivity of deteriorating environmental changes have prompted the use of renewable and cleaner sources of energy to safeguard the life of our very planet. In recent years, substantial research has been devoted to develop systems and techniques that would enhance utilization of renewable energy sources. Such sources primarily include wind, solar, geothermal, and hydro, among others. Of these energy sources, wind power technology has emerged as a promising commercial alternative to the fossil fuel based energy [1]-[3]. The advantages of wind energy in comparison with traditional methods of power generation (e.g. coal, gas, or nuclear plants, etc.) lie in fast deployment and commissioning of wind farms. This is attributed to wind turbines which require minimal operation and maintenance attention and cost. In addition, the operational age of turbines lasts between 20 and 25 years which are quite cost effective. Furthermore, wind power harnessing is not restricted by geographical boundaries [4], [5], a case which is not prevalent with the fossil fuel based energy generation systems.

A recent report by Global Wind Energy Council [6] indicates that substantial progress has been made by several countries with regard to exploitation of wind energy. The statistics suggest that at the end of 2016, the global generation of wind energy reached 486,600 MW. This denotes an increase of around 2700% compared to that of year 2000. Just in a period of one year from 2015 to 2016, the cumulative wind power generation increased by 12.5% from 432,680 MW in 2015 to 486,749 MW. China currently leads the global market with addition of 23,328 MW of wind power to its national grid in 2016. Other prominent followers are USA, Germany, India, and Brazil adding 8,203, 5,443, 3,612 and 2,014 MW respectively in year 2016. Other countries such as France, Turkey, the Netherlands, UK and Canada are also catching up with the wind power generation. However, Africa and the Middle East are lagging behind, though some initiatives have recently been taken in some regions [6].

A fundamental challenge in harnessing wind energy is the maximization of energy output from turbines. It is a challenge since fluctuations arising in the speed of wind have a negative impact on energy generation [7]. The speed of wind depends heavily on geographical location, climatic conditions, topography, and height above ground level (AGL). In a typical setup, speed of wind is measured between 8 to 12 meters AGL. The tower height at which the turbine rotor is mounted is referred to as hub height. Since more wind is absorbed at higher hub heights, generally high hub heights are desired in a typical wind farm layout setting. However, the maximum hub height has a threshold due to installation, technical, maintenance, and economic issues. Another factor that affects the generation of energy is rotor diameter. While a bigger rotor diameter is associated with higher energy generation, rotor with smaller diameter is desired again due to cost and maintenance issues.

In addition to hub height and rotor diameter, the factors of cut-in wind speed and rated wind speed also have impact on energy output of a turbine. Cut-in wind speed refers to minimum wind speed at which the turbine starts functioning, while rated wind speed is referred to as the wind speed at which the turbine produces its maximum rated energy. It is desirable to have low values of cut-in wind speed and rated wind speed so that the turbine can operate in low windy sites. However, turbines with bigger rotor diameter are considered appropriate since they have large swept area, which in turn generates more power. In addition, turbines with higher rated capacity (the maximum power that can be generated by a turbine) require bigger rotor diameter. Thus, there is a need for a decision approach in order to find an optimal tradeoff between all the factors (a.k.a. decision criteria).

The rest of this paper is organized as: A review of relevant literature is given in Section 2. Novelty of the proposed work is discussed in Section 3. The research method

is presented in Section 4. The discussion as how goal programming is applied to the problem considered herein is given in Section 5. Section 6 provides the results and discussion. Finally, a conclusion is given in Section 7.

II. Literature Review

Significant attention has been given to wind turbine selection problem in during the past two decades. A qualitative approach was adopted by Sarja and Halonen [8] who interviewed domain experts. Their research identified various turbine selection criteria such as product reliability and availability, production frequency of the vendor, cost, and maintenance patterns. Perkin *et al*. [9] utilized a genetic algorithm to find the most suitable turbine while employing various selection criteria such as rotor radius, generator size, hub height, and pitch angle. Nemes and Munteanu [10] proposed a system reliability based model to compare nine different turbine types. A particle swarm optimization based algorithm was proposed by Chowdhury *et al*. [11] for turbine selection. They considered a single turbine type while employing energy production capacity as the selection criterion. Firuzabad and Dobakhshari [12] used turbine reliability as the decision criterion in a probabilistic model that they developed. The proposed approach was tested on five turbine types. Bencherif *et al*. [13] developed a Weibull distribution based analytical approach and considered 24 different turbines models while using capacity factor as the decision criterion. Montoya *et al*. [14] proposed a Pareto-ranking based genetic algorithm to choose the best turbine. Their decision model considered power output and deviation in daily power output as the selection criteria. In an approach proposed by Chowdhury [15], more than 120 turbine types were considered while using cost of energy as the turbine selection criterion. Martin [16] assumed a hypothetical wind turbine to optimize the rotor-to-generator ratio and developed a simple support tool considering numerous wind conditions. Bekele and Ramayya [17] considered a site-specific turbine selection with blade design as the decision criterion. They proposed a genetic algorithm to optimize their model. Helgason [18] conducted a study on several potential sites in Iceland. For selection of turbines, cost of energy was used as the decision criterion and 47 different turbine models were considered. A genetic algorithm was proposed by Eke and Onyewudiala [19] for site-specific turbine selection. The aim was to maximize power generation while blade thickness, twist, and cord were used in the optimization model. A genetic algorithm was also employed by Jureczko *et al*. [20] for turbine design with the consideration of give design objectives. These objectives were generated output, blade structure stability, blade vibrations, blade material cost, and blade strength requirements.

Aljowder [21] proposed a turbine selection methodology using six different turbine models and used capacity factor as the decision criterion. El-Shimy [22] proposed a site-specific turbine selection methodology while considering average power output, capacity factor, and turbine performance index as the decision variables. Dong *et al*. [23] considered turbine selection while considering turbine cost and integrated matching indices as the optimization criteria. The proposed model was applied to genetic algorithm, differential evolution, and particle swarm optimization. An analytic hierarchy process (AHP) based approach [24] was proposed by Shirgholami *et al*. [25] who identified over 30 decision criteria, but only a subset of these criteria could be used in the selection process depending on the site-specific conditions. Bagocius *et al*. [26] proposed a weighted sum based approach for turbine selection for offshore wind farms. They considered five decision factors which were yearly energy generation, maximum power generated in the area, nominal power of the wind turbine, investments, and CO_2 emissions. Lee *et al*. [27] proposed a multi-criteria decision approach while considering economic issues, environmental aspects, technical challenges, and machine characteristics as the major decision criteria. Four turbines, with all having almost the same rated power, were considered. Du *et al*. [28] proposed a turbine selection approach based on SCADA data analysis.

A turbine selection approach was proposed by Khan and Rehman [29], [30] who used fuzzy logic based multi-criteria decision approach considering three criteria. Subsequently, a fuzzy logic based turbine selection strategy consisting of six criteria was also proposed by them [31]. However, one limitation of these studies was the use of fuzzy decision making in which selection of an appropriate fuzzy operator is a challenge. It is due to the fact that different fuzzy operators may result in different decisions. This issue is overcome in the current study through the use weighted sum approach which does not suffer from such issues.

III. Novelty of the Proposed Work

The review of studies in Section 2 points towards several limitations of the research as far as wind turbine selection is concerned. A number of studies [10]-[18], [21] assumed a simple decision model where a single criterion was considered in the decision process, and therefore lacks a realistic scenario where multiple factors affect the decision process. Another limitation of the studies was in terms of use of computationally expensive methods. Numerous studies used genetic algorithms, differential evolution, particle swarm optimization, and non-linear programming [15]-[24], [26], [27]. Despite the fact that these approaches generally provide efficient solutions, they are computationally expensive. Another limitation observed in various studies [4], [16]-[21], [23], [24], [26], [27], [29], [30] was the use of limited number of turbines and/or lack of consideration of variety of turbines. This aspect limits the comprehensiveness of the concerned studies. One more issue that prevails in the existing studies is the use of decision factors for which information is not easily accessible (e.g. production volume, system reliability indices, maintenance schedules, blade shape, product reliability, visual impact, and political stability, among many others) [8]-[12], [16]-[24], [26]. Use of such parameters make the turbine selection process a complex one, and in many cases, impractical. Finally, one key limitation of those reported studies which assumed multi-criteria decision-making was that they did not focus on the fundamental requirement of conflict and incommensurability among the decision-criteria [8], [9], [14], [18]-[20], [22]-[24], [27]. Conflict refers to the situation where improvement in one (or more) criterion (criteria) has a negative impact on the other

criteria. Incommensurability issues arise when decision criteria are of different magnitudes and units.

With the aforementioned observations, our proposed turbine selection approach, which is based on the weighted sum method [32], has several novel aspects and addresses the concerns present in the above studies. The proposed approach develops a turbine selection model considering five simple, yet important decision criteria, while taking into account the issues of conflict and incommensurability. These criteria are easily and readily available for any commercially available turbine, thus simplifying the proposed approach. Unlike many previous studies which used complex and time-inefficient techniques, the weighted sum method is simple and provides solutions in linear time, making the proposed approach computationally efficient. In addition, 18 turbines from a variety of manufacturers have been considered, thus enhancing the comprehensiveness of results. It is also important to mention that the proposed scheme is also scalable and robust; criteria as well as the types of turbines can be added or deleted easily according to the requirements of the designer, without affecting the computational efficiency.

IV. Research Method

The research is based on an empirical study and uses five important decision criteria as identified from the literature survey. The decision criteria are hub height, rated speed of wind, cut-in speed of wind, rotor diameter, and turbine rated output. These criteria are used to develop the desired decision model based on the weighted sum method. First, using the data, the upper limit for each criterion is determined. Then, a normalized value of each criterion with respect to its corresponding upper limit is calculated. Finally, all normalized values are added together using the weighted sum approach (explained in next section). The minimum value of weighted sum is then taken as the best solution found.

V. Application of Weighted Sum Method to Wind Turbine Selection

Multi-criteria decision-making (MCDM) is substantially employed to tackle decision problems in which multiple and conflicting decision criteria are considered in the decision process. Several approaches, such as weighted sum method, goal programming, compromise programming, and fuzzy logic have been proposed in literature to solve MCDM problems. Weighted sum method has been widely used by researchers due to its simple approach and time efficiency [33]. To apply weighted sum approach to MCDM problems, a fundamental requirement is to aggregate criteria such that an overall decision function is formed (represented as a scalar value). However, this process highlights the need to overcome incommensurability of criteria, due to which different criteria cannot be combined into a single decision function. Therefore it is necessary to convert all criteria to a unit-less, uniform scale. This is done by normalizing each criterion such that the value of the criterion lie in a 0 – 1 range. Then, weights are assigned to each normalized criterion according to the desire of the decision maker. Finally, all weighted values of criteria are added. Mathematically, the aim is to maximize (in case of a maximization problem) or minimize (in case of a minimization problem) the following equation:

$$\sum_{i=1}^{K} w_i f_i(x) \quad (1)$$

Where, K represents the number of decision criteria and w_i represents the weight of the i^{th} criterion. Furthermore, $w_i \geq 0$ for all $i = 1, \ldots, K$. In addition, the sum of all weights should be equal to 1, that is, $\sum_{i=1}^{K} w_i = 1$.

In order to apply the weighted sum approach using the five decision criteria, the upper limit for each criterion is required for the purpose of normalization of criteria. Note that we are dealing with a minimization problem. That is, our interest is finding the turbines that have minimum values of hub height, rotor diameter, cut-in speed of wind, and rated speed-of wind. However, the criterion of turbine rated power requires maximization. Therefore, the inverse of this criterion is taken such that the criterion is also considered for minimization. The normalized criteria are weighted and added. The resulting equation, as given below, is then used for the decision.

$$w_1\left(\frac{hub\ height}{\max hub\ height}\right)+ w_2\left(\frac{rotor\ diameter}{\max rotor\ diamter}\right)+ w_3\left(\frac{cut-in\ speed}{\max cut-in\ speed}\right)+ w_4\left(\frac{rated\ speed}{\max rated\ speed}\right)+ w_5\left[1-\left(\frac{rated\ power}{\max rated\ power}\right)\right] \quad (2)$$

Since equal preference is given to each criterion, and there are five criteria, all weights were assigned the same value of 0.2. Furthermore, normalization was done using the upper limits given in the last row of Table 1. These limits were determined using the maximum value of each criterion given in the 2nd last row of Table 1.

VI. Results and Discussion

A C++ based program was developed to perform the simulations. The simulator performs the multi-criteria decision-making calculations using the input data and the weighted sum model of (2) to generate the decision output. Eighteen different turbine models with different rated powers and manufacturers were considered. Technical data of these turbines is given in Table 1.

Table 2 shows the individual normalized values for each criterion, along with the weighted sum value (calculated using (2)) in the last column of the table. It is observed from this table that Fuhrlander FL 600 has the minimum weighted sum of 0.575, indicating that this is the best turbine among all turbines. The table also indicates that a potential alternative to Fuhrlander FL 600 is Ecotecnia 80/200 with a weighted sum of 0.578. Note that Fuhrlander FL 600 has a rated capacity of 600 KW while Ecotecnia 80/200 has a rated power of 2000 KW. Therefore, the designer has a choice between turbines of high and low values of rated power. Furthermore, Suzlon S.52/600 is the worst turbine with the highest weighted sum of 0.706.

TABLE. I. TECHNICAL SPECIFICATIONS OF TURBINES [31]

Turbine	Minimum Hub Height (m)	Rotor Diameter (m)	Cut-in Speed of wind (m/s)	Rated Speed of wind (m/s)	Rated Power (KW)
Fuhrlander FL 600	50	50	2.5	11	600
Hyosung HS50	50	50	3.5	11	750
RRB Energy PS 600	48	47	3.5	15	600
Suzlon S.52/600	75	52	4	13	600
Unison U57	68	57	3	10.5	750
Vestas V47	55	47	4	13	660
Windflow 500	29	33	6	14	500
AAER A-1000	70	58	4	12	1000
DeWind D6 64m	60	64	2.5	12.3	1250
Mitsubishi MWT62	69	61.4	3.5	12.5	1000
Nordex N54/1000	60	54	3.75	14	1000
Suzlon S.62/1000	65	62	3	12	1000
Vensys 62-1200	69	62	2.5	11.5	1200
AAER A-2000-84	65	84	3.25	12	2000
DeWind D8.1	80	80	3	13.5	2000
Ecotecnia 80/2000	70	80	3	12	2000
REpower MM92	79	92	3	12.5	2000
Suzlon S.88/2000	80	88	4	14	2000
Maximum	**80**	**92**	**6**	**15**	**2000**
Upper limit	**85**	**95**	**7**	**16**	**2100**

TABLE. II. COMPARISON OF TURBINES USING THE WEIGHTED SUM

Turbine	Normalized Hub Height	Normalized Rotor Diameter	Normalized Cut-in Speed of wind	Normalized Rated Speed of wind	Normalized Rated Power	Weighted Sum
Fuhrlander FL 600	0.588	0.526	0.357	0.688	0.714	0.575
Hyosung HS50	0.588	0.526	0.500	0.688	0.643	0.589
RRB Energy PS 600	0.565	0.495	0.500	0.938	0.714	0.642
Suzlon S.52/600	0.882	0.547	0.571	0.813	0.714	0.706
Unison U57	0.800	0.600	0.429	0.656	0.643	0.626
Vestas V47	0.647	0.495	0.571	0.813	0.686	0.642
Windflow 500	0.341	0.347	0.857	0.875	0.762	0.637
AAER A-1000	0.824	0.611	0.571	0.750	0.524	0.656
DeWind D6 64m	0.706	0.674	0.357	0.769	0.405	0.582
Mitsubishi MWT62	0.812	0.646	0.500	0.781	0.524	0.653
Nordex N54/1000	0.706	0.568	0.536	0.875	0.524	0.642
Suzlon S.62/1000	0.765	0.653	0.429	0.750	0.524	0.624
Vensys 62-1200	0.812	0.653	0.357	0.719	0.429	0.594
AAER A-2000-84	0.765	0.884	0.464	0.750	0.048	0.582
DeWind D8.1	0.941	0.842	0.429	0.844	0.048	0.621
Ecotecnia 80/2000	0.824	0.842	0.429	0.750	0.048	0.578
REpower MM92	0.929	0.968	0.429	0.781	0.048	0.631
Suzlon S.88/2000	0.941	0.926	0.571	0.875	0.048	0.672

VII. CONCLUSION

An essential requirement for an efficient wind farm design is the selection of most suitable turbines such that maximum power can be harnessed with minimal effort and cost. However, selection of a suitable wind turbine from a pool of off-the-shelf available turbines is not an easy task since the decision-making process is governed by many criteria. Among several decision criteria, five important criteria are hub height, turbine rotor diameter, cut-in and rated wind speeds of a turbine, and turbine rated output. This study proposed a multi-criteria decision-making approach for the turbine selection problem using the weighted sum approach. The proposed approach was motivated by the inherent limitations of previous studies. These limitations were due to simple decision models using a single criterion, use of computationally complex techniques, lack of variety of turbines, and complex decision criteria. The effectiveness of the proposed strategy was analyzed with its application to a number of wind turbine types from several manufacturers. Results indicate that Fuhrlander FL 600 was the best turbine, followed by Ecotecnia 80/200.

As a future work, we intend to perform an analysis of effects of weights assigned to different criteria as mentioned in the context of (2). Furthermore, we also intend to perform a comparative analysis of our weighted sum approach with other techniques such as goal programming and fuzzy logic.

ACKNOWLEDGMENTS

The support of Deanship of Research at King Fahd University of Petroleum & Minerals, Saudi Arabia, is acknowledged under project number IN 141039.

REFERENCES

[1] S. Rehman, M. Baseer, J. Meyer, M. Alam, M. Alhems, A. Lashin, and N. AlArifi, "Suitability of utilizing small horizontal axis wind turbines for off grid loads in Eastern Region of Saudi Arabia". Energ. Explor. Exploit., vol. 34, no. 3, pp. 449–467, March 2016.

[2] M. Baseer, J. Meyer, S. Rehman, M. Alam, M. L. Al-Hadhrami, and A. Lashin, "Performance evaluation of cup-anemometers and wind speed characteristics analysis". Renew. Energ., vol. 86, pp. 733–744, Feb. 2016.

[3] M. Baseer, J. Meyer, M. Alam, and S. Rehman, "Wind speed and power characteristics for Jubail industrial city, Saudi Arabia", Renew. Sust. Energ. Rev., vol. 52, pp. 1193–1204, December 2015.

[4] S. Khan, "An automated decision-making approach for assortment of wind turbines—a case study of turbines in the range of 500 kW to 750 kW". Int. J. Comput. Netw. Tech. 2015, vol. 3, no. 2, pp. 75–81, May 2015.

[5] S. Rehman, and N. Al-Abbadi, "Wind power characteristics on the north west coast of Saudi Arabia" Energ. Env., vol. 20, no. 8, pp. 1257–1270, December 2009.

[6] Global Wind Statistics, GWEC 2016, http://www.gwec.net/wp-content/uploads/2017/02/1_Global-Installed-Wind-Power-Capacity-MW-%E2%80%93-Regional-Distribution.jpg (Accessed on 28 February 2017)

[7] S. Khan, and S. Rehman, "Iterative non-deterministic algorithms in on-shore wind farm design: A brief survey". Renew. Sust. Energ. Rev., vol. 19, pp. 370–384, March 2013.

[8] J. Sarja, and V. Halonen, "Wind turbine selection criteria: a customer perspective", J. Energ. Power. Eng., vol. 7, pp. 1795-1802, September 2013.

[9] S. Perkin, D. Garrett, D, and P. Jensson, "Optimal wind turbine selection methodology: A case-study for Búrfell, Iceland", Renew. Energ., vol. 75, pp. 165–172, March 2015.

[10] C. Nemes, and F. Munteanu, "Optimal selection of wind turbine for a specific area". In Proceedings of the IEEE 12th International Conference on Optimization of Electrical and Electronic Equipment, Brasov, Romania, pp. 1224–1229, May 2010.

[11] S. Chowdhury, J. Zhang, A. Messac, and L. Castillo, L, "Optimizing the arrangement and the selection of turbines for wind farms subject to varying wind conditions". Renew. Energ., vol. 52, pp. 273–282, April 2013.

[12] M. Firuzabad, and A. Dobakhshari. "Reliability-based selection of wind turbines for large-scale wind farms", Int. J. Electr. Electron Eng., vol. 3, no. 2, pp. 114-120, February 2009.

[13] M. Bencherif, B. Brahmi, and A. Chikhaoui, "Optimum selection of wind turbines", Sci. J. Energ. Eng., vol. 2, no. 4, pp. 36–46, August 2014.

[14] F. Montoya, F. Manzano-Agugliaro, S López-Márquez, Q. Hernández-Escobedo, and C. Gil, "Wind turbine selection for wind farm layout using multi-objective evolutionary algorithms". Expert Syst. Appl., vol 41, no. 15, pp. 6585–6595, November 2014.

[15] S. Chowdhury, A. Mehmani, J. Zhang, and A. Messac, "Market suitability and performance tradeoffs offered by commercial wind turbines across differing wind regimes", Energ., vol. 9, no. 5, pp. 352–383, May 2016.

[16] K. Martin, M. Schmidt, S. Shelton, and S. Stewart, "Site specific optimization of rotor/generator sizing of wind turbines", ASME Energy Sustainablility Conference., 2007, pp. 1123–1130.

[17] A. Bekele, and A. Ramayya, "Site specific design optimization of horizontal axis wind turbine based on minimum cost of energy for Adama I wind farm", Int. J. Eng. Res. Tech., vol. 2, no. 7, pp. 862–870, July 2013.

[18] K. Helgason, "Selecting optimum location and type of wind turbines in Iceland", Master's Theses, Reykjavík University, Reykjavík, Iceland, 2012.

[19] G. Eke, and J. Onyewudiala, "Optimization of wind turbine blades using genetic algorithm", Global J. Res. Eng., vol. 10, no. 7, pp. 22–26, December 2010.

[20] M. Jureczko, M. Pawlak, and A. Mezyk, "Optimisation of wind turbine blades", J. Mat. Process. Tech., vol, 167, no. 2, pp. 463–471, August 2005.

[21] F. Jowder, "Wind power analysis and site matching of wind turbine generators in Kingdom of Bahrain", Appl. Energ., vol. 86, no. 4, pp. 538–545, April 2009.

[22] M. El-Shimy, "Optimal site matching of wind turbine generator: Case study of the Gulf of Suez region in Egypt" Renew. Energ., vol. 35, no.8, pp. 1870–1878, August 2010.

[23] Y. Dong, J. Wang, H. Jiang, and X. Shi, "Intelligent optimized wind resource assessment and wind turbines selection in Huitengxile of Inner Mongolia, China", Appl. Energ., vol. 109, pp. 239–253, September 2013.

[24] R. Saaty, "The analytic hierarchy process—what it is and how it is used", Math. Modelling, vol. 9, no.3, pp. 161-176, May 1987.

[25] Z. Shirgholami, S. Zangeneh, and M. Bortolini, "Decision system to support the practitioners in the wind farm design: A case study for Iran mainland", Sust. Energ. Tech. Assess., vol. 16, pp. 1–10, August 2016.

[26] V. Bagočius, E. Zavadskas, Z. Turskis, "Multi-person selection of the best wind turbine based on the multi-criteria integrated additive multiplicative utility function", J. Civil Eng. Manage., vol. 20, no. 4, pp. 590–599, July 2014

[27] A. Lee, M. Hung, H. Kang, and W. Pearn, "A wind turbine evaluation model under a multi-criteria decision making environment", Energ. Convers. Manage.,vol. 64, pp. 289–300, December 2012.

[28] M. Du, J. Yi, P. Mazidi, L. Cheng, and J. Guo, "A parameter selection method for wind turbine health management through SCADA data", Energ., 2017, vol. 10, no. 2, pp. 253-267, February 2017.

[29] S. Khan, and S. Rehman, "On the use of unified and-or fuzzy aggregation operator for multi-criteria decision making in wind farm design process using wind turbines in 500 kW–750 kW range", In Proceedings of the IEEE International Conference on Fuzzy Systems, Brisbane, Australia, pp. 1–6, June 2012.

[30] S. Khan, and S. Rehman, S, On the use of Werners fuzzy aggregation operator for multi-criteria decision making in wind farm design process using wind turbines in 1000 kW–1200 kW range. In Proceedings of the International Clean Energy Conference, Quebec, 2012, pp. 163–170, June 2012.

[31] S. Rehman, and S. Khan, "Fuzzy logic based multi-criteria wind turbine selection strategy—a case study of Qassim, Saudi Arabia. Energ., vol. 9, no. 11, pp. 872-898, October 2016.

[32] S. Gass, and T. Saaty, "The computational algorithm for the parametric objective function" Nav. Res. Log. vol. 2, no. 1, pp. 39–45, March 1955

[33] C. A. Coello-Coello. "A comprehensive survey of evolutionary-based multiobjective optimization techniques" Knowl. Inform. Syst., vol. 1, no. 3, pp. 269 – 308, August 1999.

An Adaptive CAD System to Detect Microcalcification in Compressed Mammogram Images

Ayman AbuBaker
Electrical and Computer Engineering Dept.
Applied Science Private University
Amman, Jordan

***Abstract*—Microcalcifications (MC) in mammogram images are an early sign for breast cancer and their early detection is vital to improve its prognosis. Since MC appears as small dot in the mammogram image with size less than 1 mm and maybe easily overlooked by the radiologist, the Computer Aided Diagnosis (CAD) approach can assist the radiologist to improve their diagnostic accuracy. On the other hand, the mammogram images are a high resolution image with large image size which makes difficult the image transfer through the media. Therefore, in this paper, two image compressions techniques which are Discrete Cosine Transform (DCT) with entropy coding and Singular Value Decomposition (SVD) were investigated to reduce the mammogram image size. Then a novel adaptive CAD system is used to test the quality of the processed image based on true positive (TP) ratio and number of detected false positive (FP) regions in the mammogram image. The proposed adaptive CAD system used the visual appearance of MC in the mammogram to detect a potential MC regions. Then five texture features are implemented to reduce number of detected FP regions in the mammogram images. After implementing the adaptive CAD system on 100 mammogram images from USF and MIAS databases, it was found that the DCT can reduce the image size with a high quality since the ratio of TP is 87.6% with 11 FP/regions while in SVD the TP ratio is 79.1% with 26 FP/regions.**

Keywords*—Mammogram image; texture features; Discrete Cosine Transform (DCT); Singular Value Decomposition (SVD)

I. INTRODUCTION

Nowadays, breast cancer has become the second leading cause of cancer deaths in women after lung cancer [1]. In 2007, about 40460 women and 450 men died from breast cancer in the United States [1]. Breast cancer's death rates continue to decline primarily in young women less than 50 years old [1], [2]. These declines are believed to be the result of earlier detection, through screening and increased awareness, as well as improved treatment.

Radiologist used three methods to diagnose breast cancer tumors: mammography, fine needle aspirate and surgical biopsy. The Mammography is specialized medical imaging that uses a low-dose x-ray system to see inside the breasts. A mammography exam, called a mammogram, aids in the early detection and diagnosis of breast diseases in women. The malignant sensitivity of mammography has a reported between 68% and 79% [3]. In fine needle aspirate biopsy (FNAB), a flexible needle that is thinner than ones used for blood tests is employed. The needle is guided into the area of the breast change while the doctor is feeling (palpating) the lump to extract some lump fluids. These fluids extracted from the breast lump are inspected under the microscope and diagnosed as benign or malignant. The sensitivity of this method varying from 65% to 98% [3], since cancer lumps are sometimes missed or benign cells are taken from near a cancer. Surgical biopsy is more evasive and costly but it is the only test that can confirm malignancy.

Most of the researchers try to focus in detection one or more of abnormal structures in mammogram images which are microcalcifications, circumscribed masses and speculated lesions [4]. Therefore, many researchers investigate many approaches to automatically and accurately detect these tumors in the mammogram images.

Approximately 65% of women who undergo biopsy for histopathologic diagnosis as a second stage in detecting the breast cancer are found to be healthy, which was a false positive result from diagnosis mammogram images [5]. These false positives may be due to different circumstances such as poor image quality, eye fatigue, or oversight by the radiologist. Therefore, the Computer Aided Diagnosis (CAD) which is the application of computational techniques that is used to solve the problem of interpreting mammogram images [6], [7]. The CAD system is usually used as a second mammogram reader. However, the final decision regarding the likelihood of the presence of a cancer and patient management is left to the radiologist.

Microcalcification is one of the most difficult detection tumors by the radiologists since its size less than 1 mm. Therefore, mammogram images have a high resolution in order to show the microcalcification clearly for the radiologist. As a result, the digital mammogram image is one of the medical images that varies in the size between 8 MB and 55 MB based on the breast size. In this case, image compression techniques is crucial to easily process and transfer these images. At the same time, it is important to maintain the mammogram image details which are mirocalcficaitions as in the original image.

The main objective of this paper is to evaluate the performance of the proposed adaptive CAD system that will be

implemented on two different images' compression techniques which are Discrete Cosine Transform (DCT) with entropy coding and Singular Value Decomposition (SVD) techniques. Moreover, the mammogram image quality resulted from both compression techniques will be evaluated using the adaptive CAD system based on True Positive (TP) ratio and number of detected False Positive (FP) regions.

In this paper, mammogram database that are used in this work is described in Section II. A brief literature survey is presented in Section III. An adaptive CAD system implementation on two different compression techniques is introduced in Section IV. While Section V presents the algorithm evaluations. Finally, concluding remarks are given in Section VI.

II. DATABASE

One hundred mammogram images are collected from both University of South Florida (USF) and MIAS databases. USF mammogram images are collected from different medical schools. Then they were scanned using high resolution (3000 pixel × 4500 pixel and 16- bit pixel depth). The MIAS database also been used in this work, where 40 % of the MC mammogram images from this database. This database were collected from the United Kingdom National Breast Screening Program. The mammogram images have been expertly diagnosed and the positions of the MCs in each image are recorded.

In this paper, 60 USF and 40 MIAS MC mammogram images are used in order to be processed on the proposed algorithm.

III. LITERATURE REVIEW

Reduction image size such as mammography, multimedia and electronic publishing is a critical stage in processing such these images [7], [8]. Many techniques are available to magnify or reduce images ranging from linear interpolation to cubic spline interpolation [8]-[11].

Image interpolation is one of image reduction techniques that has a central role in many applications [12], [13]. These techniques change digital image size according to the nature of the display device. Chuah and Leou [14] presented three categories of image interpolation techniques which are static image interpolation [15], [16]; multi-frame image interpolation [11], [17]; and image sequence (video) interpolation [17].

Many authors investigate different types of interpolation techniques to reduce the image size as in Herasa, *et al*. [18]. They investigate three interpolation methods to reduce the image size which are linear, bi-cubic and the parametric spline method. Then they try to compare between them using the visual appearance which was a compromise between the previous two methods. Then a robust algorithm OPED for the reconstruction of images from Radon data using these interpolation methods were build. The results show that the performance of bi-cubic interpolation were better than other interpolation techniques showed significantly lower Normalized Mean Square Error (NMSE) comparing with other methods.

On the other hand, other authors modified the algorithm of interpolation processing such in Kim, *et al*. [19]. They were proposed a new image scaling algorithm called the Winscale algorithm. In this algorithm a scaling (up/down) is used based on an area pixel model rather than a point pixel model. As a result, the Winscale algorithm produced effective results for image processing systems that required high visual quality and low computational complexity. However, its performance was similar to the bi-linear interpolation technique [20]. An adaptive algorithm to interpolate low resolution image frames was proposed by Chuah and Leou [14]. In this algorithm, two nonlinear filters were used to generate high-frequency components iteratively that were lost during the implementation of the resolution reduction procedure, then a blocking artefacts-reduction scheme was adopted to improve the image quality. Abe and Iiguni [21] investigated the discrete cosine transform (DCT) in down-sampled images and proposed high-resolution (HR) image restoration from a down-sampled low-resolution (LR) image using the discrete cosine transform (DCT). Their algorithm showed a superior performance compared to cubic spline interpolation in the HR image restoration as long as the amount of the additive noise was small.

Another authors used image interpolation techniques that was followed by a re-sampling process in order to reduce the image size. These techniques used in image reduction that utilizes the mean of each non-overlapping 8×8 pixel neighborhood [22]. This blurred the breast boundary since the boundary was averaged with the background. As a result, an important breast regions such as microcalcification are lost which means that there are a significant loss of the information in the original mammogram images.

IV. PROPOSED ALGORITHM

CAD system is used to identify regions where abnormalities may be found. Therefore, some researchers have suggested that a combination of computer plus radiologist can produce better results than a radiologist alone, and have concluded that CAD systems can be used to prompt radiologists [23]. Recently, some studies have suggested that a CAD system and a radiologist could be used as an alternative to using two radiologist film readers to look at each mammogram case [23], [24].

CAD systems can improve the performance of a radiologist by detection the MC in the mammogram image with minimum number of false positive regions. So, in order to have a robust CAD system, a preprocessing image size reduction is needed to speed up and easily transfer the mammogram images. Therefore, in this work, the mammogram image size is reduced using two image compression techniques which are SVD and DCT. Then an adaptive CAD system is investigated to evaluate the performance of these image compression techniques based on TP ratio and FP regions. The proposed work stages are summarized in Fig. 1.

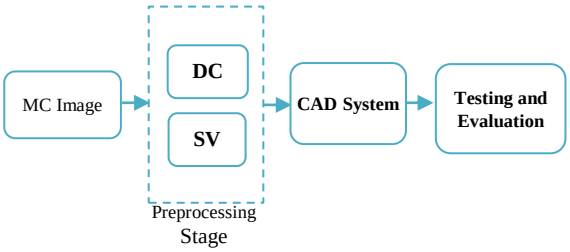

Fig. 1. The paper work flowchart.

A. Preprocessing Stage

The growth in social media and multimedia increases the need to transfer and save multimedia files. The mammogram images are part of these files that have large image size with high resolution. Compression the mammogram images is crucial to be transferred or processed but without degradation the image quality. In this paper, two types of image compression techniques were be used as in [25] which are SVD and DCT.

1) Singular Value Decomposition (SVD)

SVD is one of the image compression techniques which take high data set dimensions and reduces it to fewer dimensions with retaining the original substructure of the data. In this work, the SVD technique is applied on 100 mammogram images from both USF and MIAS database as in [25]. Fig. 2, show the result of the processed mammogram images using SVD compression technique.

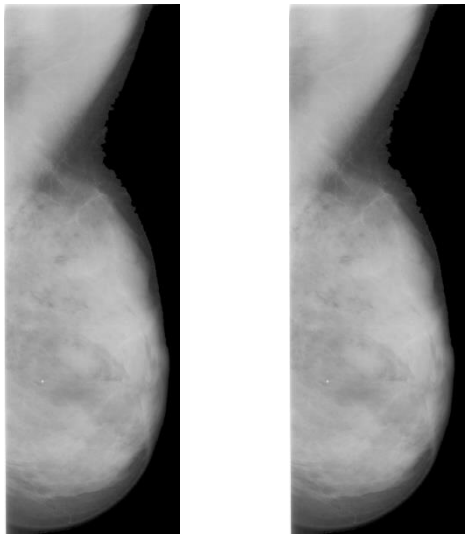

(A) Original image ***(B) SVD image***

Fig. 2. Mammogram image compression using SVD.

The mammogram images were processed using SVD at different threshold value and found that the best singular value is in the range of 150-160 singular values. The maximum image compression ratio was 42% with high quality image appearance.

B. Discrete Cousin Transform (DCT)

As a DCT works in a frequency domain, the image is initially transformed from the spatial domain to frequency domain. Then the image is separated into parts of differing frequencies. These image frequencies presented as a sum of sinusoids of varying magnitude and frequencies. DCT is high energy compact so the most significant image information is concentrated in few coefficient of DCT.

One hundred mammogram images are also processed using the DCT technique in order to compare between these compression techniques. The DCT image compression is applied as in [25]. Fig. 3 show the result of implementing the DCT compression technique on the mammogram images.

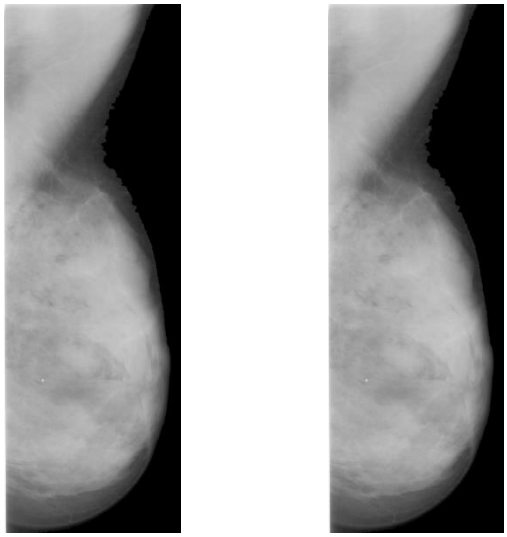

(A) Original image ***(B) DCT image***

Fig. 3. Mammogram image compression using DCT.

After many trials, it was found that the average of the best threshold value is 10 where the image appearance is good. The DCT can successfully reduce the mammogram image size by 62% of the original image.

C. Proposed Adaptive CAD System

This section presents the novel adaptive CAD technique that is implemented on the two types of compressed mammogram images. The CAD system performance in detecting the MCs in mammogram images for each one of the image compression techniques will be recorded in this paper. The proposed CAD system is mainly divided into two stages. In the first stage a potential MC regions (PMR) will be detected based on the MC appearance on the mammogram images. Then, in stage 2, five texture feature will be generated to reduce number of the detected FP regions in the mammogram image consequently increase the CAD system sensitivity in detection the MC in the mammogram images. The following subsection will present the steps in detecting the MC in compressed mammogram images.

1) Detection of Potential MC Region

MCs are one of most difficult cases in diagnosis by the radiologist since they are appear as small regions, with intensity values higher than their surrounding background in mammogram images. Usually the MCs size is less than 1 mm [26]. So, the proposed CAD algorithm is designed to be sensitive in detecting MC in compressed mammogram images.

Therefore, two dynamic concentric masks are used to detect potential MC regions as shown in Fig. 4. So, the potential peak (MCs) will be when an average value of the inner mask is greater than the average of the outer mask excluding the inner mask pixels values.

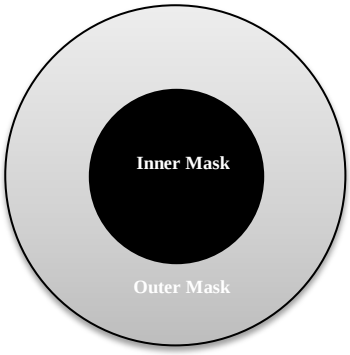

Fig. 4. Two concentric masks.

In [27] the mask size for both inner and outer mask are set to be fixed based on image resolution. Where the image resolution of the USF and MIAS databases are 45 µm × 45 µm and 50 µm × 50 µm respectively. Based on the image resolution, an inner mask was design to be in a radius of 9 pixels. Also, the suitable outer mask is design to be in a radius of 13 pixels. These concentric masks are processed on different USF and MIAS mammogram images and the CAD system can effectively detect a potential MC regions.

In this work, the MCs size in the image will be changed corresponding to the image compression technique since the image compression change the image resolution. Therefore, the proposed CAD system is designed using two dynamic concentric masks. The masks size will be varied based on the image resolution.

In preprocessing stage, the mammogram images are processed using SVD and DCT compression techniques. So we have to datasets which are 100 SVD mammogram images and 100 DCT mammogram images. These images are individually processed using the first stage of the proposed adaptive CAD system and the MC regions are tested for each image. As a result, the algorithm can successfully detect the PMC regions in both SVD and DCT mammogram images as shown in Fig. 5.

As shown in Fig. 5, the PMC regions are detected but with large number of FP regions which will reduce the proposed CAD system sensitivity. Therefore, five texture features are generated for each detected PMC region in order to reduce number of detected FP regions as will be presented in the next section.

2) FP Reduction Algorithm

In order to have a high sensitive CAD system, number of detected FP regions should be very low. This can be achieved by using five texture features which are mean, entropy, standard deviation, moment and kurtosis. These five texture features are implemented on *actual* TP MC regions that copped manually from 100 mammogram images. As a result, a dataset of the *actual* TP features is generated. This dataset is used to classify the detected PMC to TP and eliminate FP regions from the mammogram images.

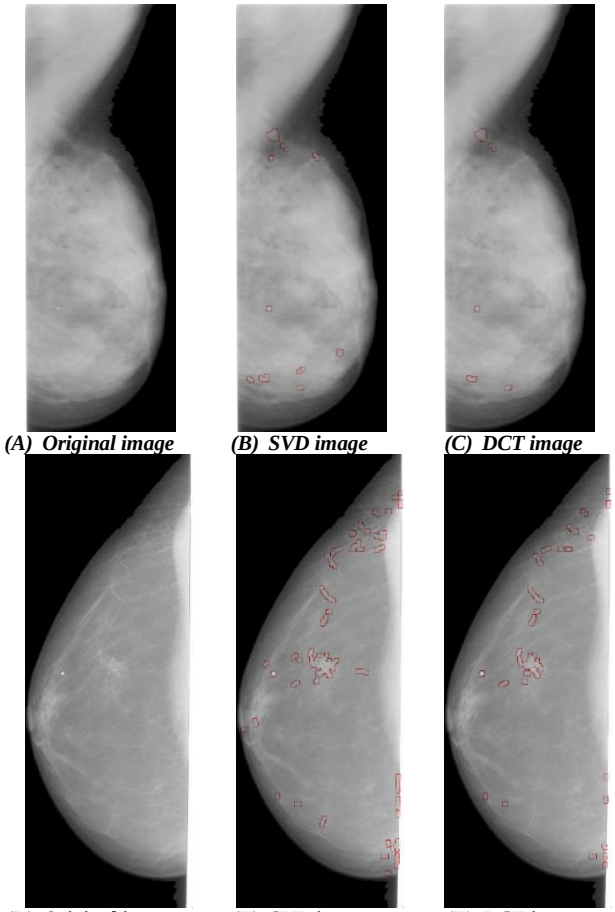

Fig. 5. Detected PMC regions in SVD and DCT compressed images.

In order to investigate feature extraction algorithm, initially, the histogram probability ***P(i)*** that is calculated from the intensity histograms renormalized was implement on each *actual* TP and FP cluster as in (1).

$$P(i) = \sum_{i=40}^{240} h(i) / MN \quad (1)$$

Where, *h(i)* is the intensity histogram and *M, N* are the image region's height and width respectively.

Then five features are calculated and modified considering the upper and lower grey levels of the MC (range from 40 to 240 grey levels) in the mammogram images as shown in (2) to (6).

1) The Modified Mean Feature (µ)

$$\mu = \sum_{i=40}^{240} iP(i) \quad (2)$$

2) The Modified Entropy Feature(E)

$$E = -\sum_{i=40}^{240} P(i)\log_2[P(i)] \quad (3)$$

3) The Modified Standard Deviation Feature (σ)

$$\sigma = \sqrt{\sum_{i=40}^{240} (i-\mu)^2 P(i)} \quad (4)$$

4) The Modified third order of moment Feature (M3)

$$M_3 = \sum_{i=40}^{240} (i-\mu)^3 P(i) \quad (5)$$

5) The Modified Kurtosis Feature (K)

$$K = \sigma^{-4} \sum_{i=40}^{240} (i-\mu)^4 P(i) - 3 \quad (6)$$

The texture feature algorithm is again implemented on 100 mammogram images. The results show that texture feature algorithm can successfully reduce the detected FP regions in the mammogram images as shown in Fig. 6.

V. Algorithm Evaluation

The adaptive CAD system is implemented on 100 mammogram images resulted from both SVD and DCT image compression techniques. Initially, the CAD system is implemented to detect the PMC regions in the mammogram images and the TP and FP regions are recorded for both SVD and DCT techniques as shown in Table 1. Then texture feature CAD system is implemented on SVD and DCT mammogram images. Also the TP and FP regions are recorded as shown in Table 1.

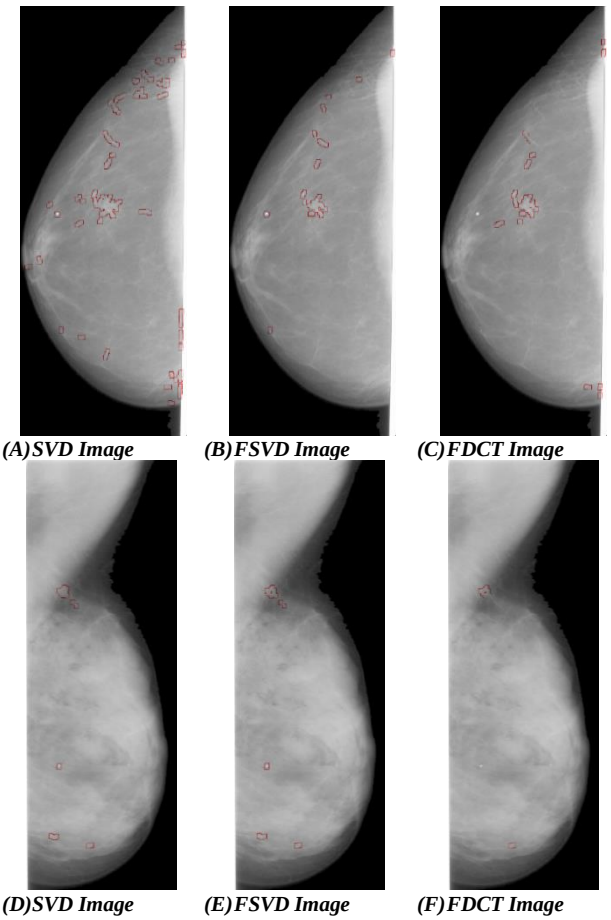

(A) SVD Image *(B) FSVD Image* *(C) FDCT Image*

(D) SVD Image *(E) FSVD Image* *(F) FDCT Image*

Fig. 6. Processed SVD and DCT compressed images after implementing texture features.

TABLE. I. Comparison between SVD and DCT Image Compression Techniques based on TP and FP Regions

Image Name	SVD		SVD *Feature*		DCT		DCT *Feature*	
	TP (%)	FP	TP (%)	FP	TP (%)	FP	TP	FP
A_1116_1.LEFT_CC	79	30	76	10	83	18	83	2
A_1874_1.RIGHT_MLO	71	16	70	7	80	12	79	3
A_1894_1.RIGHT_MLO	69	65	68	31	82	53	82	9
A_1178_1.LEFT_CC	85	120	81	24	93	87	93	18
Average of 100 mammogram images	79.6	81	79.1	26	87.9	49	87.6	11

As shown in Table 1, the proposed CAD system can effectively detect the MC in the mammogram image in both DCT and SVD image compression techniques. In SVD the average values for TP for 100 mammogram images is 79.1% with minimum FP regions 26 clusters, whereas in DCT the average values for 100 mammogram images is 87.6% with 11 FP clusters. As a result, the DCT image compression techniques is better the SVD image compression technique in maintaining a small details in the image. So the image quality of the DCT is better than SVD since the performance of the CAD system show good result when using the DCT image compression technique.

VI. Conclusions

A novel adaptive CAD system is proposed in this paper. The proposed CAD system is used to test the image quality resulted from SVD and DCT image compression techniques. Initially, SVD and DCT image compression techniques are used to reduce 100 selected MC mammogram images from both USF and MIAS databases. The resulted images which are SVD and DCT mammogram images are processed using adaptive CAD system. The proposed CAD system can effectively detect most of the MC regions as a PMC but number of FP regions were extremely high. So, five texture features are used to reduce the detected FP regions in the mammogram images. As a result, the adaptive CAD system with texture features can successfully detect the MC in the mammogram images with minimum number of FP regions.

After implementing the proposed adaptive CAD system on 100 mammogram images from USF and MIAS database, it was found that the performance of the DCT image compression technique is better than SVD image compression techniques. The results show that the proposed CAD system can effectively detect the MC in DCT mammogram image with ratio 87.6% TP and 11 FP/regions while in SVD mammogram images the TP ratio was 79.1% with 26 FP/regions.

Acknowledgment

The author is grateful to the Applied Science Private University, Amman, Jordan, for the full financial.

References

[1] American Cancer Society, “Cancer Facts and Figures 2007,” Atlanta, Ga: American cancer Society, 2007.

[2] V. Vogel, “Breast cancer prevention: a review of current evidence,” Ca. Cancer J. Clinic, 2000, pp.156–170.

[3] O.L. Mangasarian, “Breast cancer diagnosis and prognosis via linear programming,” Oper. Res., Springer, Vol. 43, pp. 570-577, 1995.

[4] S. Liu, and E.J. Delp, "Multiresolution detection of stellate lesions in mammograms," Proc. IEEE Intl. Conf. Image Processing, Santa Barbara, 1997, pp. 109-112.

[5] D. B. Kopans, "The positive predictive value of mammography," AJR Am J Roentgenol, Vol. 158, pp. 521–526, 1992.

[6] K. Doi, H. MacMahon, S. Katsuragawa, RM Nishikawa, Y. Jiang, "Computer-aided diagnosis in radiology: potential and pitfalls," Radiology, Elsevier, Vol. 31, pp. 97–109, 1999.

[7] ML. Giger, "Computer-aided diagnosis of breast lesions in medical images," IEEE Computer Science Eng, Vol. 2, pp. 39–45, 2000.

[8] A. Aldroubi, M. Unser and M. Eden, "Cardinal spline filters: Stability and convergence to the ideal sinc interpolation," IEEE Signal Process, Vol. 28, 1992, pp. 127-138.

[9] M. Unser, A. Aldroubi and E. Eden, "Fast B-spline transforms for continuous image representation and interpolation," IEEE Trans. Pattern Anal. Machine Intell., Vol. 13, 1991, pp. 277-285.

[10] M. Unser, A. Aldroubi and M. Eden, "Enlargement or reduction of digital images with minimum loss of information," IEEE Trans. Image Processing, Vol. 4, 1995, pp. 247-258.

[11] R. kumar Mulemajalu , Shivaprakash Koliwad, "Lossless compression of digital mammography using base switching method", J. Biomedical Science and Engineering, 2009, 2, 336-344

[12] Z. Liang, Xiangying Du, Jiabin Liu, Yanhui Yang, Dongdong Rong, Xinyu Yao & Kuncheng Li, "Effects Of Different Compression Techniques On Diagnostic Accuracies Of Breast Masses On Digitized Mammograms", Acta Radiologica, Vol. 49, No.(7), 2009, 747-751.

[13] W.K. Pratt, "Digital Image Processing," 3rd edition, Johm Willey & Sons Inc, 1991.

[14] C.S. Chuah, and J.J. Leou, "An adaptive image interpolation algorithm for image/video processing," Pattern Recognition, Elsevier, Vol. 34, 2001, pp. 2383-2393.

[15] H.S. Hou, and H.C. Andrews, "Cubic splines for image interpolation and digital altering," IEEE Trans. Acoust. Speech Signal Process, ASSP, Vol. 26, 1978, pp. 508-517.

[16] R.R. Schultz, and R.L. Stevenson, "A Bayesian approach to image expansion for improved definition," IEEE Trans. Image Process., Vol. 3, 1994, pp. 233-242,.

[17] A.J. Patti, M.I. Sezan and A.M. Tekalp, "High-resolution image reconstruction from a low-resolution image sequence in the presence of time-varying blur," Proc. IEEE Intl. Conf. Image Processing, Austin, TX, 1994, pp. 343-347.

[18] Hugo de las Herasa, Oleg Tischenkoa, Yuan Xub, Christoph Hoeschena, "Comparison of interpolation functions to improve a rebinning-free CT-reconstruction algorithm," IEEE of Medical Physics, Vol. 4, 2007, pp. 430-445,.

[19] C.H. Kim, S.M. Seong, J.A. Lee and L.S. Kim, "Winscale: An image-scaling algorithm using an area pixel model," IEEE Trans. Circuits and Systems for Video Technology, Vol. 13, No. 6, 2003, pp. 1-4.

[20] E. Aho, J. Vanne, K. Kuusilinna and T.D. Hämäläinen, "Comments on Winscale: An image-scaling algorithm using an area pixel model," IEEE Trans. Circuits and Systems for Video Technology, Vol. 15, No.3, 2005, pp. 345-355.

[21] Y. Abe, Youji Iiguni, "Image restoration from a down-sampled image by using the DCT," IEEE of Signal Processing Vol. 87, 2007, pp. 2370–2380.

[22] M. Masek, "Hierarchical segmentation of mammograms based on pixel intensity," Ph.D. Thesis, The University of Western Australia, Australia, 2004

[23] A. A. AbuBaker, R. S. Qahwaji, M.J. Aqel, M. H. Saleh, "Efficient Pre-processing of USF and MIAS Mammogram Images," Journal of Computer Science, Science Publications, Vol. 3, No. 2, pp. 67-75, 2006.

[24] A. A. AbuBaker, R.S. Qahwaji, M.J. Aqel, M.H. Saleh, "Mammogram Image Size Reduction Using 16-8 bit Conversion Technique," International Journal of Biomedical Sciences, Enformatica, Vol. 1, No. 2, pp. 103-110, 2006.

[25] A. Abubaker, "Adaptive Enhancement Technique for Cancerous Lung Nodule in Computed Tomography Images", International Journal of Engineering and Technology (IJET), Vol 8, No 3, 2016, pp. 1444-1450.

[26] H.S.Sheshadri and A.Kandaswamy, "Computer Aided diagnosis of digital mammograms," ACM Information Technology Journal, Vol. 5, No. 2, 2005, pp. 342-346.

[27] A. AbuBaker. "Automatic Detection of Breast Cancer Microcalcifications in Digitized X-ray Mammograms". Ph.D., thesis, School of Informatics, University of Bradford-UK. (2008).

A Learner Model for Adaptable e-Learning

Moiz Uddin Ahmed
Department of Computer Science
Allama Iqbal Open University
Islamabad, Pakistan

Nazir Ahmed Sangi
Department of Computer Science
Allama Iqbal Open University
Islamabad, Pakistan

Amjad Mahmood
Department of Computer Science
University of Bahrain
Bahrain

***Abstract*—The advancement in Information and Communication Technology (ICT) has provided new opportunities for teaching and learning in the form of e-learning. However, developing specialized contents, accommodating profiles of learners, e-learning pedagogy and available ICT infrastructure are the real challenges that need to be properly addressed for any successful e-learning system. The adaptability in an e-learning system can be used to address many of these challenges and issues. This paper proposes a learner model for adaptable e-learning model. The proposed model is based on the findings of a survey conducted to investigate the profiles and preferences of the local learners. The conceptual framework highlights the layered model of adaptable e-learning with the knowledge level of learners as the foundation layer. The foundation layer is derived from four components of adaptable e-learning, i.e., domain, program pedagogy, student model and technology interface. The learner algorithm retrieves the adaptable contents from the domain model by analyzing the learner information stored in the student model. The e-assessment is part of the program pedagogy and the assessment results are used to control the presentation and navigation of adaptable contents during the learning process. The model has been tested on a Computer Science course offered by Allama Iqbal Open University, Islamabad, Pakistan at Post Graduate Diploma level. The results show that the proposed adaptable e-learning model has significantly improved the knowledge level of the learners.**

***Keywords*—E-learning; adaptable; pedagogy; learning styles; e-assessment**

I. Introduction

E-learning refers to electronic means of education through the use of computers, Internet and media technologies [1]. In recent years, e-learning has become more popular [2]-[4] and its use in educational sector, especially in distance education, is increasing [5]. But at the same time, e-learning is posing many challenges because most of the e-learning systems provide teaching rather than learning [6]. Therefore, there is a need to build e-learning models that are adaptable, interactive and localized.

Localization is the process of adapting e-learning functional properties and content presentation to accommodate the needs and requirements of local learners [7]. The localized applications need to be built upon the international e-learning standards in order to get technology acceptance by local learners and teachers [8]. Adaptivity under localized conditions creates more effective learning scenarios by focusing on the needs and learning styles of individual students [9]. It provides appropriate lessons to a learner, when needed. According to Brusilovsky [10], adaptivity is significant for e-learners because they might differ in their strengths and weaknesses while grasping a knowledge concept. It can tailor a learning path based on their needs, requirements and learning styles [11] .

The development of specialized e-learning models is a real challenge in distant learning environment for a developing country like Pakistan. Various issues such as development of specialized contents suitable for local learners and its delivery under local ICT infrastructure should be properly addressed [12]-[13]. The major contribution of this research is development of an adaptable e-learning model that not only fulfills the needs of localized environment but is also in compliance with international standards such as IEEE Learning Object Metadata (LOM) and IMS Learner Information Package (LIP). The theoretical models are explored to derive the important parameters of adaptable e-learning. A unique instructional pedagogy has been implemented that converts the teaching approaches into sequence of learning activities. An algorithm has been proposed for content presentation and navigation control. The delivery and communication tools of MOODLE Learning Management System (LMS) are used to implement the proposed adaptable model.

The rest of the paper is organized as: Section II presents the literature review, Section III discusses e-learning survey results conducted from the students of Allama Iqbal Open University (AIOU), Section IV presents the proposed adaptive model and discusses its major components, and Section V presents the experimental results followed by conclusions in Section VI.

II. Literature Review

Early e-learning systems used computers as self-contained teaching machines in order to provide instructional support to a group of learners [14]. However, these systems were lacking in analyzing the needs of a particular student; and therefore were unable to provide personalized assistance [15]. As computer technology became more advanced, researchers began to think about the development of more advanced and innovative learning systems in the form of adaptive e-learning [16]. Brusilovsky and Miller [17] divided adaptive e-learning systems into two major categories: Intelligent Tutoring Systems (ITS) and Adaptive Hypermedia (AH). Intelligent Tutoring Systems are specialized learning systems which facilitate the process of learning based on individual student's needs. They are problem-specific and provide alternate instruction methods [18]. Adaptive Hypermedia works along intersection of hypertext (hypermedia) and user modeling. They are curriculum specific, focus on course modules and construct a model of users based on their personality,

interaction and attitudes [19]. While developing adaptive systems there is an important aspect that "what can be adapted?" The literature review provides the answer by denoting the classes of adaptive presentation and adaptive navigation. The adaptive presentation displays contents on hypermedia. The techniques of adaptive presentation are adaptive text presentation, adaptive multimedia presentation and adaptation of modality. On the other hand adaptive navigation controls the interconnection between the content elements. The techniques for adaptive navigation controls are direct guidance, link sorting, link hiding, link annotation, link generation and map adaptation [17].

One of the most prevalent areas of adaptive hypermedia is the Adaptive Educational Hypermedia Systems (AEHS). These are online systems used for teaching and learning of online students [20]. These systems use adaptive hypermedia techniques to adjust the learning contents according to the required knowledge goals. There are three core components of AEHS: content model, instructional model and learner model [21]. The content model deals with the course domain and includes course topics, content levels, learning outcome and details of the tasks performed by learners. The instructional model aims at the pedagogy of the learning system. It uses information from content model and learner model and selects the appropriate content for the learner. The learner model keeps track of information about the learner. It takes the parameters from learner's personality and applies statistical inference about their knowledge level [22]. The personality comprises of profiles and learning styles of students, which deal with different aspects of perceiving and processing information by different people [23]. The major models of learning styles have been identified on the basis of theoretical importance and used in research and development work. The important theories include Visual Auditory, Kinesthetic (VAK) [24], Felder-Silverman [25] and Kolb [26] learning style theory.

Adaptable e-learning has been an area of researchers' interest since long time, therefore a number of studies have been proposed. These studies revolve around three important aspects, i.e., content authoring, pedagogical considerations and user modeling approaches. Content authoring tools are specialized software applications used for aligning and arranging learning contents. There are large number of content authoring tools which includes TANGOW [27], AHA [28], AMAS [29], GRAPPLE [30], and MOT [31]. All these tools are diverse in nature therefore the selection of right tool for the right subject requires detailed analysis and testing. The matching with subject domain and requirement of specific group of learners are important issues. Some tools are complicated and difficult to use by non-technical users [32]. The pedagogical designs in authoring tools are also difficult to implement [33]. Due to importance of online teaching methods the pedagogy has been an important consideration for adaptive e-learning [34]-[35]. Although every tool define a set of pedagogical rules to present adaptive content, the pedagogy of e-learning varies due to institutional policies, domain of study and assessment criteria. A predefined pedagogy may not be suitable for every program of study therefore there is a need of a generalized model which can be adapted to institutional polices.

The modeling of the user activities is another important consideration of the researchers in adaptable e-learning. There are two important techniques that may be used to implement learner model: knowledge-based and behavioral-based [36]. These approaches are used to generate adaptation rules for the generation of adaptive content. The knowledge-based technique comprises of structured and unstructured information about the students. The initial data for knowledge-base is obtained through questionnaires, user profile, preferences and learning styles [37]. The behavioral-based is the range of actions and reactions of students during interaction with the learning system. The behavior modeling may be implemented through overlay and perturbation model [38]. Both the knowledge-based and behavioral-based techniques have been considered for the development of adaptive e-learning systems [39]-[43], yet they differ in domain knowledge, complexity, pedagogy and user interface technology. They also diverge in practice, the range of sophistication, and level of details. Most of the adaptive e-learning systems and models are being developed and practiced for specialized domains mainly in higher learning institutions. The adoption of such adaptable e-learning models is not easy due to variety of issues such as lack of instruction design models for e-learning [12], non-availability of localized contents, power failure [44], Internet bandwidth [45], English language competency level [46] and different norms among teaching and learning communities. Therefore, there is a dire need and growing demand to develop a generalized adaptable learner model, which can easily be replicated in a local environment. This motivation encourages us to present a learner model for adaptable e-learning that not only complies with international e-learning standards like IEEE LOM & IMS LIP but is also suitable for locally available ICT environment in order to fulfill needs of local learners.

III. Profiles and Preferences of Local Learners

E-learning can be more effective if it is adapted to the needs of learners. Therefore, before developing the e-learning framework, local learners are investigated to determine their ICT capacity and preferences about adaptable e-learning. A questionnaire is developed and validated through consultation of experts from education and technology. The questionnaire was distributed among the four hundred students of the Bachelor of Science in Computer Science BS (CS) and the Post Graduate Diploma in Computer Science PGD (CS). The CS program is selected because its students have the competency in using and comprehending computer applications. Furthermore, the CS programs have a flavor of e-learning mode of education in selected courses with representation in urban, semi urban and rural areas of the country. These responses are analyzed using SPSS and results are given below.

A. Demographics

The demographic results show that 80.6 % of respondents are male and 19.4% are female with majority of students in the age group of 21-30 years as shown in Table 1. The majority of the respondents (73.4%) are living in urban areas, whereas 9.9 % in semi-urban, and 16.7 % in rural areas.

TABLE I. STUDENTS' DEMOGRAPHIC PROFILE

Variable	Frequency	% Frequency
Gender		
Male	203	80.6
Female	49	19.4
Total	252	100
Age Group		
Less than 21	45	17.9
21 – 30	180	71.4
31 – 40	21	8.3
More than 40	6	2.4
Total	252	100
Location		
Urban	185	73.4
Semi-urban	25	9.9
Rural	42	16.7
Total	252	100
Program of Study		
BS (CS)	180	71.4
PGD (CS)	72	28.6
Total	252	100

B. Accessibility to ICT Devices

The analysis of respondents on accessibility to ICT devices is given in Table 2. The results show that computers and laptops are most accessible among all devices. However, these are slightly less accessible in rural and semi urban areas as compared to urban areas. The latest devices such as iPad are rarely used by the respondents. The interesting fact is that TV and Radio are found to be more in use in semi urban areas. However, their usage for education is less than that of computers and laptops. The analysis reveals that ICT devices are highly accessible to the local learners, which is an encouraging sign for the implementation of e-learning. The significant level (p value) for computer/laptop is less than 0.05 which rejects the null hypothesis when the hypothesis is true. Similar analysis is found in cases of mobile phones, CD/DVD player and TV/Radio. It reveals that strong association exists between the location and accessibility variables. The p-value is greater in case of iPad but has no significance because iPad is rarely used by the respondents as given in Table 2.

C. Accessibility to Internet

The analysis of respondents' accessibility to Internet is given in Table 3. The results show that the broadband Internet connection at home is the highest available facility with a mean value of 3.71. The Internet in an institution/office and via mobile is found another closer option. Internet at cafe and Internet dial up options obtain low scores. It means that students can participate in e-learning activities with ease because of Internet availability at their homes and offices. The p-value analysis shows that the broadband Internet connection has the highest significant level. It implies that the strong association does not exist between the location and Internet variables and Internet is available in urban, semi-urban and rural areas of the country.

D. Adaptable E-learning Preferences

The adaptable e-learning preferences have been investigated to determine the opinion of students about personalized learning with special assistance to weak learners. The analysis of respondents on adaptable preferences is given in Table 4. The respondents prefer locally prepared material in simple English language. They want freedom and control, while browsing educational contents and participating in online activities. They also want format of contents which matches their learning styles. The results further reveal that the respondents prefer adaptable features to expedite their learning skills. The majority of learners want personalized learning with their favorite format of contents. They want special assistance during online education. The mean values have shown significant preferences of students towards adaptable e-learning.

The results are quite encouraging as accessibility to ICT devices and Internet connection are on a high scale. Most of the students have computers and laptops with broadband Internet connection. There is an enormous potential for the growth of online education as public infrastructure is available to support modern distance learning mode. The results reveal us the need for localized and adaptable e-learning model.

TABLE II. ACCESSIBILITY TO COMMONLY USED ICT DEVICES BY LOCATION

N= 252

ICT Devices	Urban		Semi Urban		Rural		Chi Square	df	p-value
	Mean	SD	Mean	SD	Mean	SD			
Computer/Laptop with Internet	4.32	1.01	4.16	0.94	3.69	1.28	32.458	8	.000
Mobile Phone	3.88	1.25	3.96	1.37	3.55	1.17	19.203	8	.014
iPad	1.92	1.26	1.96	1.31	1.55	1.13	8.75	8	.364
CD/DVD Player	2.54	1.33	3.36	1.29	2.62	1.32	17.209	8	.028
TV/Radio	3.04	1.39	3.84	1.37	2.74	1.50	15.723	8	.047

TABLE III. INTERNET ACCESS

Internet Connectivity Options	Mean	SD	Chi-Square	Df	p-value
Internet Dialup at home	2.62	1.54	19.489	8	.012
Broadband (e.g.DSL) at home	3.71	1.40	46.429	8	.000
Internet at institution/office	3.18	1.36	6.624	8	.578
Mobile Internet	2.97	1.32	5.073	8	.750
Wireless Internet	3.15	1.48	17.184	8	.028
Internet at café	2.01	1.21	13.49	8	.096

TABLE IV. ADAPTABLE E - LEARNING PREFERENCES

Adaptable E-learning Preferences	Mean	SD
Course materials should be developed locally	3.71	1.19
Course materials should be in simple language	4.15	1.00
Course materials should be presented in learner led manner	3.92	0.98
E-course materials should match the learning style	4.00	1.00
Instructions should be available on different medium of instructions (e.g. Text, multimedia, Radio, TV, Mobile, and Internet etc.)	3.94	1.08
E-Learning can provide batter learning by incorporating adaptive features	3.90	0.98
AIOU should promote personalized e-learning	4.04	1.02
The learning content which is presented as per my favorite format improve my learning	3.99	0.94
I need special academic assistance during online education	4.10	1.05

IV. PROPOSED ADAPTABLE LEARNER MODEL

In this section, our proposed adaptable learner model is being presented. The proposed model is based on the findings of survey conducted to investigate the profiles and preferences of the local learners as presented in Section III. The proposed adaptable learner model, as shown in Fig. 1 can be conceptualized in the perspective of layered technology of software engineering with knowledge as the foundation layer. This layer glues personality, domain and pedagogy layers with the blend of technology interface. It enables the functionality of key process areas for smooth delivery of course instructions, contents and learning activities. The key process areas coordinate gradually to increase the knowledge level of learners and ensure the quality of learning.

If the knowledge and software engineering models are interwoven, the adaptable e-learning can be made flexible and interactive in nature. It helps to maximize the students' participation in a particular course (domain of learning). It is, therefore, a combination of both education and technology, integrated for the purpose of knowledge transfer through teacher specified domain (content) and pedagogy (learning activities) using the interface of delivery and communication.

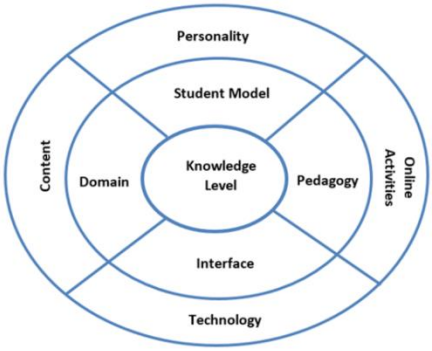

Fig. 1. Layered approach of proposed adaptable e-learning model.

The student model plays a pivotal role in knowledge transfer and the use of ICT for teaching and learning processes. Its goal is to improve the knowledge level of learners by using the adaptable contents. The components of each layer are given in Fig. 2 and are described below.

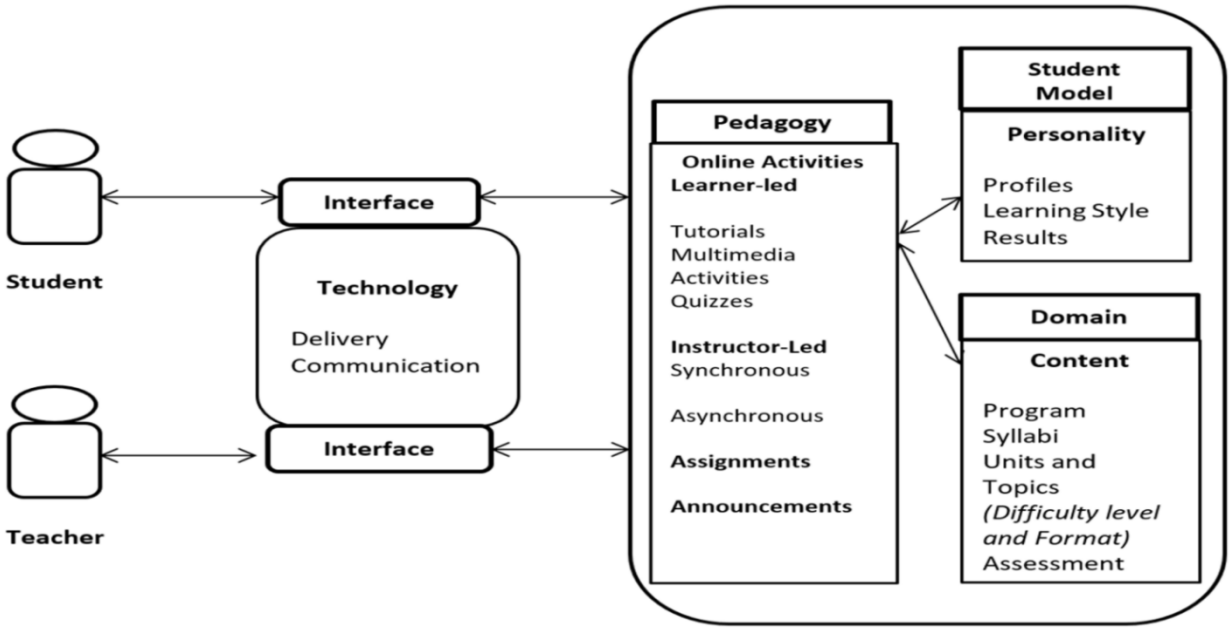

Fig. 2. Proposed learner model of adaptable e-learning.

A. Domain Model

The Domain Model is the main component of our proposed adaptable e-learning model. It is composed of information about program, syllabi (curriculum sequence) and courses. Each course is divided into coherent concepts referred to as unit, which is further divided into related topics and sub-topics. The metadata is adopted from IEEE LOM metadata standard for learning objects [47]. Each unit has been tailored up to three levels of knowledge depth. The beginner level comprises of the basic concepts of the topic. The moderate level defines the topic in more detail and the advance level covers the expert domain knowledge. The granularity level is defined on the topic level which is the finest level of granularity in terms of size and concepts and can be re-used in other courses as shown in Fig. 3. Additionally, for each difficulty level, three formats of the contents are proposed to match with visual, auditory and kinesthetic learning styles.

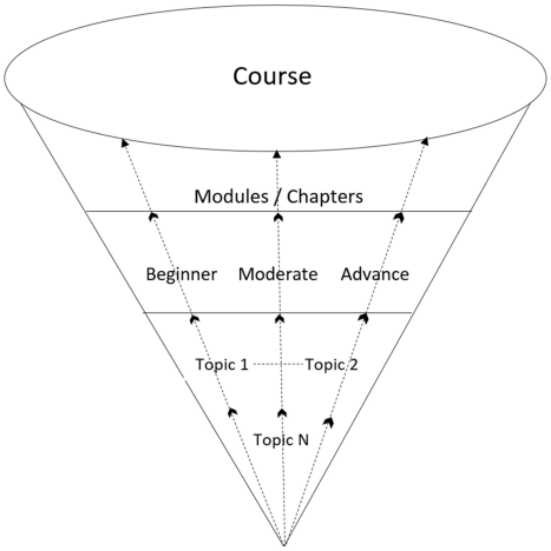

Fig. 3. Granularity of adaptable content.

These formats include tutorials, multimedia instructions and activities as shown in Fig. 4. The tutorial is an instructional lesson that explains the key concepts of a topic. It is consist of a series of content-pages linked via hyperlinks that gradually develop the concepts. The tutorials are authored in the form of webpages connected through hyperlinks using authoring tool of MOODLE LMS. They are used to facilitate students with visual learning style. Multimedia instructions are developed through a combination of text, audio, video and animation. Multimedia electronic courseware is used to develop hypermedia instructions to assist students with visual and auditory learning styles. The multimedia components are assembled in a Shock Wave Flash (SWF) file using Flash Macromedia tool. The text, audio, video, image, table, figure, and animation are synchronized in SWF files and are uploaded by using MOODLE LMS. The activities (such as quizzes and assignments) are developed to let the student learn concepts by doing exercises and assignments. It enables students to apply actions on various concepts and situations by using their critical thinking ability. These activities are used to facilitate students with kinesthetic learning styles. The activities are also compiled as webpages using MOODLE LMS authoring tools.

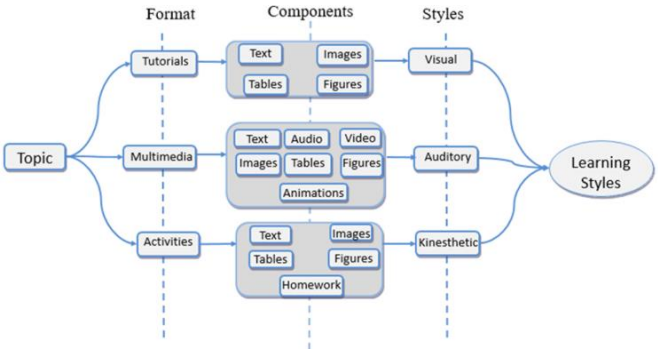

Fig. 4. Format of contents and learning styles.

B. Student Model

The student model collects information related to leaners as shown in Fig. 5. The metadata is adopted from IMS Learner Information Package [48]. The profiles are comprised of personal information, location and profession. The device accessibility determines the availability of commonly used ICT devices to local learners. The Internet access determines the availability of Internet to the local learners. The preferences of learners are determined to find out their level of inclination towards technology based learning. The performances are based on the evaluation results of pop-up quizzes. The learning style captures information about visual, auditory and kinesthetic learning styles.

The assessment quizzes are developed with content levels for each unit of the course. The stereotypes are defined on the basis of student's achievements in quiz results (following university grading system) as shown in Table 5:

Students who achieve the quiz percentage less than 60 are categorized as beginner with knowledge level, K =1. The other category K = 2 is of moderate learner with percentage in quiz greater or equal to 60 and less than 80. The advance level of learners, K =3 have percentage greater or equal to 80. The learners who acquire the knowledge level K = 3 can move to the next level of topic as per algorithm. The information of student model is stored at backend in MySQL database of MOODLE LMS.

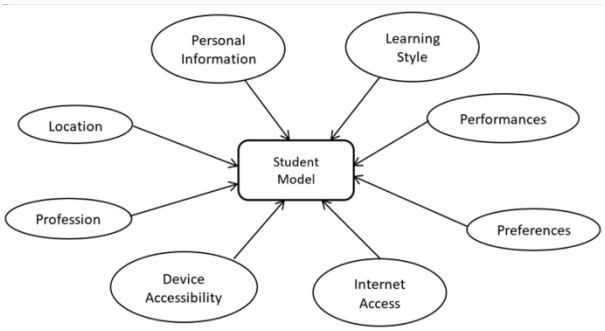

Fig. 5. Student model.

TABLE V. STUDENT'S STEREOTYPE

Stereotype	Interval	Knowledge
Beginner	K(X) < 60	K = 1
Moderate	60 ≤ K(X) < 80	K = 2
Advance	80 ≤ K(X) ≤ 100	K = 3

C. Pedagogy

The course pedagogy is hybrid and composed of both the learner led and the instructor led online activities blended with face to face program workshop. The course calendar, outline and contents and assessments are uploaded by the instructor. The instructor support is available to the students in the form of synchronous online tutorial sessions and asynchronous discussions using forum under instructor led mode. The announcements are made from time to time during the semester. The learner interface is customized for learners to participate in adaptable e-learning activities under learner led mode. The orientation of adaptable e-learning methodology is given during the orientation workshop. The program workshop is arranged in the mid of the semester as a supplement in order to take additional tutorial classes. Both workshops are face-to-face and part of the program pedagogy.

D. Algorithm for Adaptable Content Presentation and Navigation Control

The proposed leaner model utilizes the information stored about each learner to decide content presentation and navigation control. The proposed algorithm shown in Fig. 6 is used to decide the presentation of contents and learning activities. The index i indicates the unit number (or chapter number) and index j indicates the content level. The index k indicates the knowledge level of learners. Every topic starts with the beginner level content of a unit/chapter that is provided in three formats as discussed in previous section. The presentation of contents is followed by an evaluation quiz to assess knowledge level of students. The quiz results are used to assess the achieved knowledge level of learners (beginner, moderate or advance). If the learners achieved knowledge level is beginner or moderate then he/she is required to browse the content and appear in the quiz again until he/she achieves the advance level of knowledge. After completing three levels of knowledge of a unit, learner can move to next unit. Note that the adaptation rules (Steps 6 and 7 of the algorithm) control the display of pages from the domain model using student's assessment data from the student model. The navigation control uses the link enabling and disabling customization in MOODLE to control the learning activities.

E. Interface

The Interface is a platform for learners and instructors to interact with adaptable e-learning system. The prototype of proposed research model is implemented using MOODLE Learning Management System (LMS). MOODLE is an open source LMS based on Hypertext Preprocessor (PHP) server based technology which uses MySQL database at the backend. The teacher interface is customized to control the adaptable e-learning mechanism. A new file was created in MOODLE content directory comprising of the proposed algorithm. This algorithm is called by extending the existing presentation and navigation functionality. Once the contents are uploaded by the teacher the algorithm controls the sequence of activities as per rules discussed in content presentation method. The selected screen shot of the homepage is shown in Fig. 7 and it comprises of virtual class room (tool for synchronous communication), links of news & discussion forums, assignments and course outlines.

Step 1. Initialize unit number i = 1

Step 2. initialize content level j = 1

Step 3. initialize student knowledge level k = 1

Step 4. Present level j content of unit i

Step 5. Start quiz and generate result (percentage marks obtained by the student)

Step 6. Evaluate knowledge level k of learner using the following rules

IF obtained marks < 60 then k=1

ELSE IF obtained marks ≥ 60 and < 80 then k=2

ELSE k=3

ENDIF ENDIF

Step 7. IF k=1 or k=2 Then go to step 4

ELSE IF j = 3 then

i = i +1 // next unit

go to step 2

ELSE

j = j +1 //next content level

Go to step 4

Fig. 6. Algorithm for adaptable content presentation.

Fig. 7. A course homepage under adaptable e-learning.

V. Experimental Results

The adaptable e-learning model is tested on software engineering course of PGD (CS) program offered at AIOU. There were 78 students enrolled from different cities of the country who participated in learner-led and instructor-led activities. The results show that the performance of students improves significantly as he/she progresses in the said course as shown in Fig. 8.

The analysis reveals that the average marks in first attempt in each quiz are less than the average marks in all (total number of attempts in each quiz) and the last attempt. It is due to the reason that the first attempt of quiz was started with the beginner level of each topic where students had little knowledge related to the topic. They repeated the lessons and improved their percentage in the second attempt of each quiz. The process continued till they achieved the highest marks in last attempt of each quiz. The overall result comparison was made with the previous groups of the same course and shown in Fig. 9.

The students of adaptable e-learning batch 5 have shown better performance as compared to the previous batches. In this batch, 13 % of the students got A+ grade which is second highest in the last five years results. The majority of students (41 %) fall between B or C grades which is also higher in percentage as compared to the previous groups. The absent (failure) rate has also dropped to 34%. This analysis is encouraging as students' learning has improved through the use of proposed adaptable e-learning model.

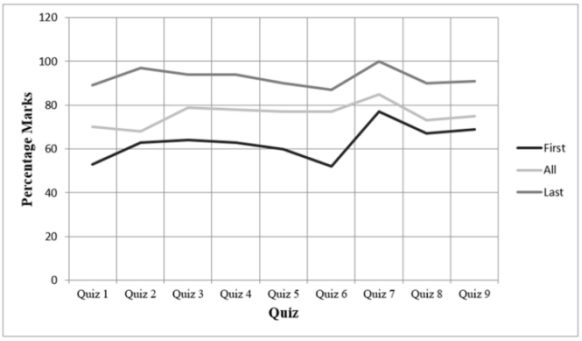

Fig. 8. Average marks in first, all and last attempts.

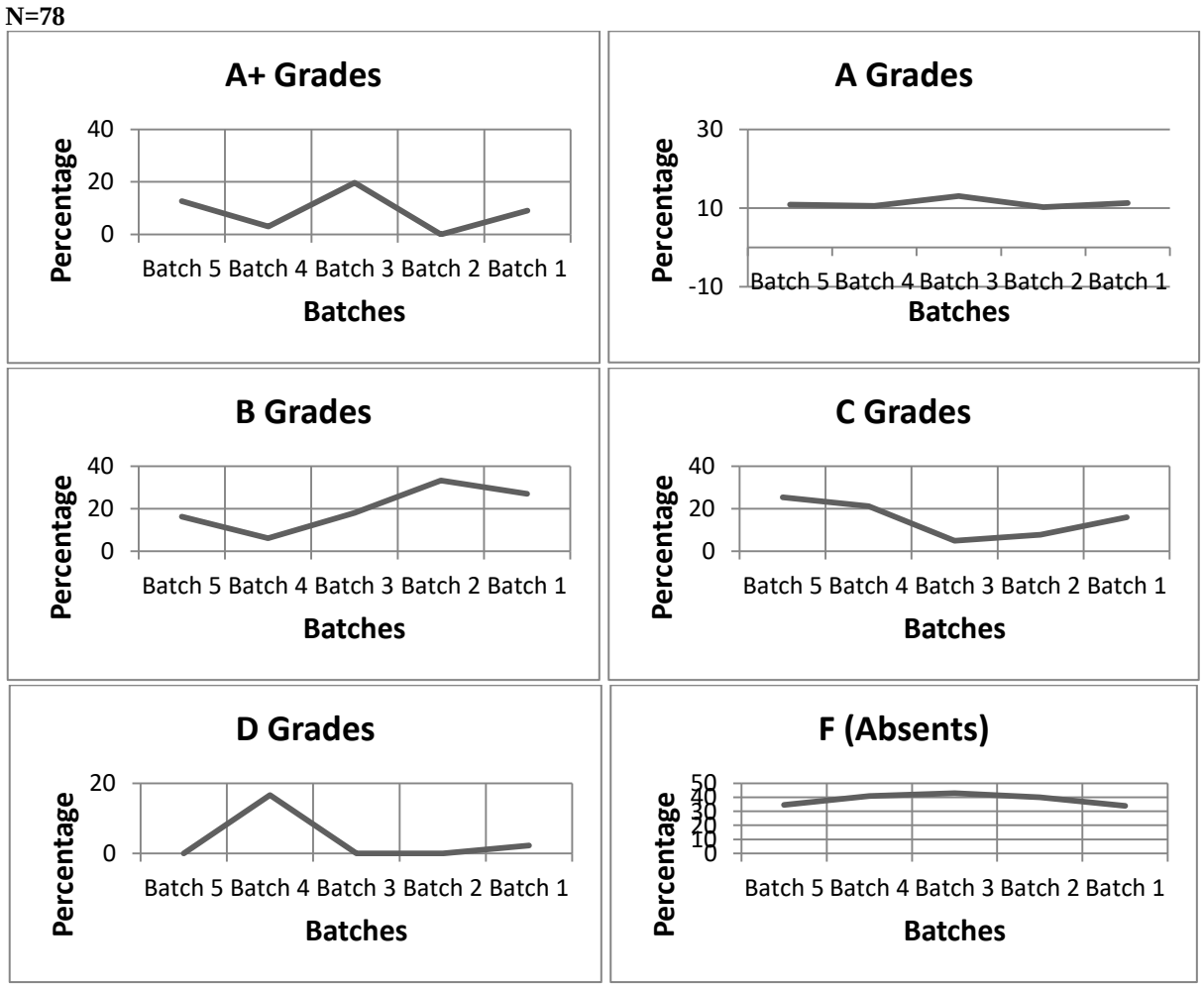

Fig. 9. Overall result comparison from the previous groups.

VI. Conclusion

An adaptable e-learning model has been proposed in this paper. The compliance with e-learning standards has been assimilated for the wider acceptance among the local academic community. A survey of local learners is conducted to determine the profiles, preferences and learning styles. The local parameters are incorporated to fulfill the learning needs and styles. The model is based on domain, pedagogy, technology interface and local learners' profiles. The model has been implemented on a course with development of localized, standardized e-learning contents and their delivery over the local ICT infrastructure under the unique program pedagogy. The examination results reveal that the proposed adaptable e-learning model has a significant impact on the performance of students. The performance of the class has improved overall as compared to previous batches of the same course and the failure rate has also dropped sheer.

Future work will deal with the development of academic repository of different formats of digital contents associated with the difficulty levels of knowledge. The development of

question databank and creation of adaptive test shall be a part of the future work. The decision support system shall also be linked with the student participation and performance so that the system may advise students on the basis of their requirements and needs. This research provides a common ground for the future research based on adaptive and adaptable e-learning.

ACKNOWLEDGEMENT

This research work was made possible through the feedback and support from faculty, staff and students of AIOU. We are also thankful to internal and external reviewers for their comments and suggestions.

REFERENCES

[1] G. Puri, "Critical success Factors in e-Learning -An Empirical Study", *International Journal of Multidisciplinary Research*, vol. 2, no. 1, pp. 149-161, 2012.

[2] S. R. Harandi, "Effects of E-learning on Students' Motivation", *Procedia-Social and Behavioral Sciences*, vol. 181, pp. 423-430, 2015

[3] P.F. Ellis, and K. D. Kuznia, "Corporate E-learning Impact on Employees", *Global Journal of Business Research*, vol. 8, no. 4, pp. 1-15, 2014.

[4] J. L. Moore, C. D. Dean, and K.Galyen, "E-Learning, Online learning, and Distance Learning Environments: Are they the same?" *Journal of Internet and Higher Education*, vol. 14, pp. 129–135, 2011.

[5] J. Wang, D. Solan and A. Ghods, "Distance Learning Success: A perspective from Socio-Technical Systems Theory", *Behaviour & Information Technology*, vol. 29, no. 3, pp. 321-329, 2010

[6] H. Rana, Rajiv, M. Lal, "E-learning: Issues and Challenges", International *Journal of Computer Applications*, vol. 97, no. 5, pp. 20-24, 2014

[7] P. Mohammed and P. Mohan, "A Case Study of the Localization of an Intelligent Tutoring System", *Paper presented at second International Workshop on Learning Technologies for the Developing World in conjunction with AIED 2013*, Memphis, USA, 2013.

[8] J. Cos, R. Toval, J. L. Fernández-Alemán, J. M. Carrillo-de-Gea and J. Nicolas, "Internationalization Requirements for E-learning Audit Purposes", *In Global Engineering Education Conference, 2012*

[9] P. Ardimento, N. Boffoli, N. Convertini, and G. Visaggio, ed. "Decision Table for Adaptive E-learning Systems in Education in a Technological World", *Communicating Current and Emerging Research and Technological Efforts*. 127-134, A. Méndez-Vilas, 2011.

[10] P. Brusilovsky, "Adaptive Hypermedia, an Attempt to Analyze and Generalize. Lecture Notes in Computer Science", Springer- Verlag, Berlin, Germany, pp. 288–304, 1996.

[11] B. Radenkovic, M. Despotovic, Z. Bogdanovic, and D. Barac, "Creating Adaptive Environment for E- learning Courses", *Journal of Information and Organizational Sciences*, vol. 33, no. 1, pp. 179-189, 2008

[12] K. Daud, "Development of Multimedia Instruction Objects for Delivery in a Localized E-Learning Environment", *Dissertation Defense*, Allama Iqbal Open University, Islamabad, 2009

[13] N. Sangi, "Access Strategy for Blended E-learning: An AIOU Case Study", *Journal of the Research Center for Educational Technology (RCET)*, vol. 5, no. 2, pp. 75-91, 2009

[14] F. Chukwunonso, R. B. Ibrahim, A. B. Selamat, A. Idama, and W. A. Gadzama, 'The Impact of the Internet and the World Wide Web on Distance and Collaborative Learning", *In Eighth International Multi-Conference on Computing in the Global Information Technology*, Nice, France, 2013

[15] G. Woodill, "Where is the Learning in E-learning?", *Educational Psychology Interactive*, Valdosta, GA, 2004.

[16] J. Vélez, R. Fabregat, S. Nassiff, J. Petro, and A. Fernandez, "Integrated User Model in Adaptive Virtual Learning Environment", *World Conference on E-Learning in Corporate, Government, Healthcare and Higher Education, Las Vegas, United States*, pp. 3275-3284, 2008.

[17] P. Brusilovsky, and P. Miller, ed. Course Delivery Systems for the Virtual University, "*Access to Knowledge: New Information Technologies and the Emergence of the Virtual University"*, Amsterdam: Elsevier Science, pp. 167- 206, 2001

[18] A. Alla, "Advances in Intelligent Tutoring Systems: Problem-Solving Modes and Model of Hints", *International Journal of Computers, Communications & Control*, vol. 1, pp. 48-55, 2007.

[19] H. Mohamed, T. Bensebaa, and P. Trigano, "Developing Adaptive Intelligent Tutoring System based on Item Response Theory and Metrics", *International Journal of Advanced Science and Technology*, vol. 43, pp. 1-14, 2012.

[20] P. Brusilovsky, "Developing Adaptive Educational Hypermedia Systems: From Design Models to Authoring Tools", *In Authoring tools for advanced technology Learning Environments*, Springer Netherlands, pp. 377-409, 2003

[21] S. Oxman, and W. Wong, "Adaptive Learning Systems", [White Paper], *DV X Innovations, DeVry Education Group, Integrated Education Solutions*, 2014, Available online at: from http://snapwiz.com/wp-content/uploads/2014/03/DVx_Adaptive_Learning_White_Paper.pdf

[22] V. Shute, and B. Towle, "Adaptive E-learning", *Educational Psychologist*, vol. 38, no. 2, pp. 105-114, 2003

[23] H. Pashler, M. McDaniel, D. Rohrer, and R. Bjork, "Learning Styles: Concepts and Evidence", *Psychological Science in the Public Interest*, vol. 9, no. 3, pp. 105-119, 2008.

[24] S. Gholami, and M. S. Bagheri, "Relationship between VAK Learning Styles and Problem Solving Styles regarding Gender and Students' Fields of Study", *Journal of Language Teaching and Research*, vol. 4, no. 4, pp. 700-706, 2013

[25] R.M. Felder and L.K. Silverman, "Learning and Teaching Styles in Engineering Education", *Journal of Engineering Education*, vol. 78, no. 7, pp. 674–681, 1998.

[26] D.A. Kolb, 1984. Experiential Learning: Experience as the Source of Learning and Development, New Jersey, Prentice-Hall, Englewood Cliffs, 1984.

[27] R. M. Carro, E. Pulido, and P. Rodríguez, "Adaptive Internet-based learning with the TANGOW system", In Computers and Education in the 21st Century, Springer Netherlands, pp. 127-135, 2000.

[28] P. De Bra, , N. Stash, D. Smits, C. Romero, S. Ventura, "Authoring and management tools for adaptive educational hypermedia systems: The AHA! case study", Studies in Computational Intelligence, vol. 62, pp. 285-308. Springer, 2007

[29] C. Gaffney, O. Conlan,, and V. Wade, "The amas authoring tool 2.0: A ux evaluation", In Proceedings of the 25th ACM conference on hypertext and social media, pp. 224-230, 2014.

[30] M. Hendrix, P. De Bra, M. Pechenizkiy, D. Smits, and A. Cristea, "Defining adaptation in a generic multi layer model: CAM: The GRAPPLE Conceptual Adaptation Model", In European Conference on Technology-Enhanced Learning EC-TEL., Maastricht, The Netherlands, 2008.

[31] A.Cristea, and C. Stewart, "Authoring of Adaptive Hypermedia. Advances in Web-Based Education: Personalized Learning Environments", Information Science Publishing, 2004.

[32] D. Vassileva, B. Bontchev, B. Chavkova, and V. Mitev, "Software construction of an authoring tool for adaptive e-learning platforms", *In Fourth Balkan Conference in Informatics*, Thessaloniki, Greece, 2009.

[33] M. Harrigan, M. Kravcik, C. Steiner, and V. Wade, "What do academic users really want from an adaptive learning system?", In *Proceedings of the 17th International Conference on User Modeling, Adaptation, and Personalization (UMAP); formerly UM and AH.*, Trento, Italy, 2009.

[34] C. Watson, F. W. Li, and R. W. Lau, "A pedagogical interface for authoring adaptive e-learning courses", In Proceedings of the second ACM international workshop on Multimedia technologies for distance leaningACM, , pp. 13-18, 2010.

[35] C. Swertz, A.Schmölz, A. Forstner, F.Heberle,, P. A. Henning, A. Streicher,... and S. Zander, "A Pedagogical Ontology as a Playground in

Adaptive Elearning Environments", In GI-Jahrestagung, pp. 1955-1960, 2013

[36] A. C. Martins, L. Faria, C., V. Carvalho and E. Carrapatoso, "User Modeling in Adaptive Hypermedia Educational Systems", Journal of Educational Technology & Society, vol. 11, no. 1, pp. 194-207, 2008

[37] O. Bourkoukou, E .El Bachari, and M. El Adnani, "A Personalized E-Learning Based on Recommender System", *International Journal of Learning and Teaching*, vol. 2, no. 2, 2016.

[38] P. L. Nguyen, "A User Modeling System for Adaptive Learning", *Journal of Standard Scientific Research and Essays*, vol. 2, no. 4, pp. 65-209, 2014

[39] C. Giovannella, and S. Carcone, "A new application to detect "emotional perception and styles" of primary school children, and their evolution with age", In Proceedings of 11th International conference on advanced learning technologies, ICALT 2011, Athens, USA, 2011

[40] D. Vassileva, "Adaptive e-learning content design and delivery based on learning styles and knowledge level", *Serdica Journal of Computing*, vol. 6, no. 2, pp. 207-252, 2012.

[41] M. Lamia, and L. M. Tayeb, Discovering Learner Styles in Adaptive e-Learning Hypermedia Systems, *Journal of Universal Computer Science*, vol. 19, no. 11, pp. 1522-1542, 2013.

[42] A. Adetunji, and A. Ademola, "A Proposed Architectural Model for an Automatic Adaptive E-Learning System Based on Users Learning Style", *International Journal of Advanced Computer Science and Applications*, vol. 5, no. 4, 2014.

[43] M. S. Halawa, E. M. R. Hamed, and M. E. Shehab, "Personalized E-learning recommendation model based on psychological type and learning style models", In Intelligent Computing and Information Systems (ICICIS), 2015 IEEE Seventh International Conference, pp. 578-584, 2015

[44] N. Sangi, "Electronic Assessment Issues and Practices in Pakistan: A Case Study", *Journal of Learning, Media and Technology*, vol. 33, no. 3, pp. 191-206, 2008

[45] A. R. Sajid, and T. Hassan, "ICTs in Learning: Problems faced by Pakistan", *Journal of Research and Reflections in Education*, vol. 7, no. 1, pp. 52 -64, 2013

[46] I. A. Qureshi, K. Ilyas, R. Yasmin, and M. Whitty, "Challenges of Implementing E-learning in a Pakistani University", *Journal of Knowledge Management & E-Learning*, 4(3), 310-324, 2012

[47] P. Barker, "What is IEEE Learning Object Metadata/IMS Learning Resource Metadata?", *Cetis Standards briefings series, 2005*.

[48] LIP, *IMS Learner Information Package Specification*, 2008.

Implementation of the RN Method on FPGA using Xilinx System Generator for Nonlinear System Regression

Intissar SAYEHI
University of Tunis Elmanar, Faculty of Mathematical, Physical and Natural Sciences of Tunis
Laboratory of Electronics and Microelectronics, (E. µ. E. L), FSM, Monastir, Tunisia

T. Saidani and B. Bouallegue
University of Monastir,
Faculty of Sciences of Monastir
Laboratory of Electronics and Microelectronics, (E. µ. E. L), Tunisia

Okba TOUALI
University of Monastir,
National Engineering School of Monastir, Tunisia
Laboratory LARATSI, ENIM, Monastir, Tunisia

Mohsen MACHHOUT
University of Monastir, Faculty of Sciences of Monastir
Laboratory of Electronics and Microelectronics, (E. µ. E. L), Tunisia

***Abstract*—In this paper, we propose a new approach aiming to ameliorate the performances of the regularization networks (RN) method and speed up its computation time. A considerable rapidity in totaling calculation time and high performance were accomplished through conveying difficult calculation charges to FPGA. Using Xilinx System Generator, a successful HW/SW Co-Design was constructed to accelerate the Gramian matrix computation. Experimental results involving two real data sets of Wiener-Hammerstein benchmark with process noise prove the efficiency of the approach. The implementation results demonstrate the efficiency of the heterogeneous architecture, presenting a speed-up factor of 40-50 orders of time, comparing to the CPU simulation.**

Keywords*—Machine learning; Reproducing Kernel Hilbert Spaces (RKHS); regularization networks; FPGA; HW/SW Co-simulation; systolic array architecture; PT326; Wiener-Hammerstein benchmark

I. INTRODUCTION

In the last decade, Kernel methods [1] like Support Vector Machine (SVM), Regularization Networks (RN) and Kernel Principle Component Analysis (KPCA) [2] have become typical to perform nonlinear systems identification. Comparing with the traditional method, such as Neural Networks [3], [4], Voltera series [5], and the Kernel methods present an attractive alternative. They are well founded in a rigid mathematical structure of Reproducing Kernel Hilbert Spaces (RKHS) [6], [7], it overcomes convex optimization problems. Furthermore, they are complete nonlinear regressors that necessitate simply reasonable computational complexity.

Kernel methods like Support Vector Machines (SVM) [8] proved a high efficiency in various fields because it reveals some disadvantages that have to be tackled appropriately in each appliance especially for big data sets. Recently, several learning algorithms as the regularization networks (RN) are inspired from the support vector machine and affected from the need of reaching algorithms simpler to implement by simplifying the quadratic programming QP problem in training SVMs, which can be hard to solve.

The RN is most promising theoretically and practically but suffers from the equality between the number of model parameters and observations.

In this paper, an efficient Regularization Network model was contributed for identifying nonlinear systems based on random observations. A successful FPGA HW/SW Co-Design for accelerating the Gramian matrix computation was developed. Moreover, to avoid the information redundancy in the training data set, an efficient statistical method was employed to extract the useful information describing the most frequently occurring observations.

An application to a known challenging nonlinear system proves the rapidity and the low-resource-consuming hardware of this model for modeling in RKHS space.

The paper is structured as: Firstly, the background of this work is presented and discussed the different categories of SVM implementations on FPGA board and its inefficiencies and weakness. Then, we briefly evoke some basic concepts from learning theory for identification of nonlinear systems in reproducing Kernel Hilbert Space (RKHS). After discussing RKHS proprieties and the representer theorem, the regularization networks is described as a machine learning. Then we present the designing tools exploited for the HW/SW Co-design. After describing the move from RN algorithm to RN model and the statistical Data Preprocessing method, we introduce the acceleration of Gramian matrix computation and we discuss the co-simulation performances. For better understanding, the basic principles of systolic array architecture and the serial multiplication were explained with simple examples. Finally, we validate the work on a challenging nonlinear system: the Wiener-Hammerstein benchmark with process noise. We deal with the main results

concerning time and error. Finally, we conclude with some comments and perspectives.

II. Background and Related Work

Kernel methods have become powerful tools for classification and regression tasks due to its capability to be trained from past examples and continually adapt to new situations. In term of performances and aptitude to generalization the Support Vector Machine (SVM) excels the other Kernel method. Unfortunately the high computational cost of the SVM running time is critically reliant on the training dataset size and the problem's dimension. Also the quadratic programming (QP) techniques are a severe and computationally expensive task. There were much software like Sequential Minimum Optimization (SMO) and SVMLIGHT [9] have been proposed to resolve these problems analytically but don't give an enormous amelioration for real-time embedded systems. Consequently, special hardware architectures are ordered to convene limitations as inadequate resources exploitation plus little power consumption. That's motivates researchers to implement this method on programmable device to accelerate the computation time especially in case of online training.

The embedded digital systems like microcontroller, Digital Signal Processors (DSPs) or Field Programmable Gate Arrays (FPGAs) permit attaining greater resource-performance relation, but necessitating a careful implementation design. The FPGAs are potent and greatly parallel processing and allows a great flexibility and efficiency for different applications. Lately they have showing considerable performance against the General Purpose Processors (GPPs) for a lot of purpose like machine learning algorithms [10], [11]. In addition, Graphics Processing Unit (GPU) presents a further proposal for elevated performance computing [12]. Comparing the FPGA and GPU implementations of diverse algorithms and applications was the subject of many studies [13], [14]. In the majority of times, FPGAs confirmed greater performance. Even though GPUs profit from lower cost and shorter development time prejudiced against to FPGAs, they are inferior to FPGAs in terms of power consumptions. Next, we reviewed existing and new practices in hardware implementations aiming efficient implementations of the SVM model on FPGA. It could be approximately classed in two major groups. The first one called FPGA hardware accelerator which implemented only one phase: training or validation phase. The second group enclosed the FPGA implementations of SVM for classification and regression.

A. FPGA: Hardware Accelerator

The training phase of the SVM algorithm has attracted a community of investigators to exploit hardware accelerators aiming a diminution in whole training time. J. Filho, *et al*. [15] proposed a dynamically reconfigurable SVM architecture that supports different sizes of training datasets. A modular architecture was designed through the SMO algorithm to obtain dynamic reconfiguration. The authors employed the hardware-friendly Kernel function proposed in [16] and so the Coordinate Rotation Digital Computer (CORDIC) algorithm for Kernel computations. The platform exploited was Xilinx Virtex-IV (XC4VLX25). The proposed reconfigurable architecture attained 22.38% area economy with good enough reconfiguration time punishment. To study the consequence of fixed-point data representation on accuracy and classification mistake, three diverse learning benchmarks were implemented and accomplished speeding up factors of more than 12.53 times quicker than the software implementation for the entirety training time.

L. Martinez, *et al*. [17] designed a heterogeneous architecture to accelerate SVM training phase. To reduce the dot-product computation time, these operations were affected by the hardware coprocessor of Xtreme DSP Virtex- IV whereas the hierarchy of SMO algorithm was implemented in GPP. This application was a classification of the ADULT dataset by the linear Kernel function. The expected coprocessor design reached an acceleration of 178.7x comparing software results. In another method, the SVM was trained offline on software and then the trained data were imported for exploitation for online classification on hardware (FPGA board). There was a variety of techniques using different implementations methods. The authors in [18] were proposed an embedded hardware SVM implementation on FPGA board: Xilinx Virtex-5, Spartan-3E. Thanks to the hardware friendly Kernel function [16], the hardware design was made easier and simpler targeting satellite onboard applications. In the same way, the multiplication process was substituted by simple shift operations that verified lower resources exploitation of 167 slices. This hardware design proved its efficiency in Satellite onboard application based on NASA database.

B. FPGA platform for both SVM classification and regression

It was an intelligent idea to use the same platform for different task: classification and regression.

The work of authors in [19] presented an excellent design for an elevated performance and low resource consumption for support vector classification and regression. The proposed architecture has been considered as general use for embedded applications, where the number of support vectors and the resolution of the parameters can be arranged. In addition, there is not a limit to the dimension of the input vectors and the number of support vectors but the size of the FPGA. The performance of this design was tested for a multi classification problem on a basic COIL database and for regression problem on sinus cardinal function. In both cases, the average error rate for the hardware is between 0% and 0.02 %, which means that the SVM gives better results when using the hardware then MATLAB.

An additional hardware architecture for SVM algorithm was offered for classification and regression problems [20] and established on the hardware friendly Kernel [16]. A tree structure founded on common Sum of Absolute Differences (SAD) unit was used for diminishing clock cycles. Beginning simulation study was executed on the accuracy of input parameters by selecting fixed-point arithmetic, caring the same classification accuracy level with no failure.

The designers were aiming a diminution in hardware complication and power consumption through executing SVM on FPGA with different ways instead of conventional

algorithm. They presented a different approach to surmount this difficulty but the SVM still a complex method especially when solving the quadratic programming problem which is computationally expensive mission. In this work we suggest to implement a Kernel method inspired from SVM which is the regularization networks (RN). It is simpler and easier to implement and gives similar performances.

In next paragraph, we present the theoretical basis of this method and its advantages.

III. Modeling Nonlinear System in Reproducing Kernel Hilbert Space (RKHS)

A. Overview of Statistical Learning Theory (SLT)

The principle of the Statistical Learning Theory [21] is to find such function f modeling a system from a set of observations

$O = \{(x_i , y_i)\}$, i =1..N composed of inputs x_i and outputs y_i . This function has to reproduce the comportment of the system by minimizing the functional risk.

$$R(f) = \int_{X,Y} V(y, f(x))P(x, y)dxdy \quad (1)$$

The term V(y,f(x)) is named cost function. It determines the variation among system output yi and the estimated output f(x). The couple (X, Y) is composed of a random vectors and (xi, y i) are independents samples. The risk R(f) cannot be expected caused by ignoring P(x, y). To resolve that difficulty we have to diminish the following term:

$$R_{emp}(f) = \frac{1}{N}\sum_{i=1}^{N} V(y_i, f(x_i)) \quad (2)$$

However the frank minimization of $R_{emp}(f)$ in the functions space H don't provide better estimation of R(f) minimization and may leads to over fitting. As a solution, Vapnik advanced the theory of structural risk minimization (SRM). It punishes the empirical risk through a function estimating the complexity of reserved model. This conducts to minimizing the restriction definite by this equation:

$$\min_{f \in H} D(f) = \frac{1}{N}\sum_{i=1}^{N} V(y_i, f(x_i)) + \lambda \quad (3)$$

Where the first term measure how well the function (f) fits the given data and the second term is the squared norm of (f) in the RKHS space H, which controls the complexity (smoothness) of the solution. The parameter λ is the regularization parameter that balances the tradeoff between the two terms.

The more significant is the solution regularity and not the value of λ. while it is not obvious to minimize the restraint (3) on any random function space H, whatsoever is it with finite or infinite dimension. Consequently, to conquer this trouble, the space H will be regarded as a RKHS.

B. Reproducing Kernel Hilbert Space (RKHS) and the representer theorem

We assume that X a random variable is estimated in the space $E \subset \mathbb{R}^d$ and we expect the existence of a function K named Kernel function $K : E^2 \to \mathbb{R}$ which is symmetric and positive definite. Accordingly, there is [1] a function $\phi : E \to H$ that:

$$K(x, x')) = \langle \phi(x), \phi(x') \rangle_H \quad (4)$$

H is the Reproducing Kernel Hilbert Space (RKHS) [7] of Kernel K. Such space acquired distinguishing properties:

$$\forall x \in E \text{ and } f \in H \quad \langle K(x,.), f \rangle_H = f(x) \quad (5)$$

- *Thanks to representer theorem [22] the resolution of the optimization difficulty offered by (3) in this space is specified by:*

$$f_{opt} = \sum_{i=1}^{N} a_i K(x_i, .) \quad (6)$$

There are many types of Kernel functions which can be considered as:

1) Linear Kernel

$$K(x, x')) = x \times x' \quad (7)$$

2) Polynomial Kernel

$$K(x, x')) = (1 + \langle x, x' \rangle)^{\eta} \quad (8)$$

Where, $\eta \in \mathbb{R}^*$ and $\langle x, x' \rangle$ is an Euclidian scalar product.

3) Radial Basis Function (RBF) Kernel

$$K(x, x')) = e^{\frac{\|x - x'\|^2}{2\sigma^2}} \quad (9)$$

Where, σ is a real positive parameter.

4) Sigmoid Kernel

$$k(x, y) = \tanh(\alpha . x^T . y + c) \quad (10)$$

The slope alpha and the intercept constant c are two adjustable parameters in the sigmoid Kernel.

C. Learning Machine: Regularization networks (RN)

Machine is one of the most recent research areas of data mining. The algorithm exploited to approximate the parameters a_i in (5) is entitled learning machine like regularization network (RN) [23]. The exploited algorithm to calculate approximately the parameters a_i is the regularization network (RN). Compared to other Kernel method that optimize the parameters iteratively like support vector regression (SVR) the RN takes less time and offer excellent performances in term of generalization ability. As exposed, the optimization problem (3) can be resolved thanks to the Kernel trick:

$$\|f\|_H^2 = \sum_{i=1}^{N}\sum_{j=1}^{N} a_i a_j K(x_i, x_j) \quad (11)$$

The cost function to be minimized by the RN is:

$$V(y_i, f(x_i)) = (y_i - f(x_i))^2 \quad (12)$$

The optimal function given by (5), where the sequence $\{a_i\}$ is:

$$a_i = \sum_{i=1}^{N} (G + \lambda)_{ij}^{-1} y_j \quad (13)$$

Where, $G \in \mathbb{R}^{N \times N}$ is the Gramian matrix associated to the Kernel function K , $G_{ij} = (K(x_i, x_j)), i, j = 1, ..., N$ and Y is the output vector. On the other hand, in matrix form:

$$A = (G + \lambda NI)^{-1} Y, A = (a_1, ..., a_N)^T, Y = (y_1, ..., y_N)^T \quad (14)$$

To simplify the understood of this method, the next section describes the move from RN algorithm to RN model and presents the designing tools and with explanation of the different components of the HW/SW Co-design.

IV. Proposed HW/SW Co-Simulation Method

A. Designing Tools

The used tools are MATLAB R2013a with Simulink from MathWorks [24], System Generator 14.7 for DSP and ISE 14.7 from Xilinx. The System Generator runs within the Simulink as simulation environment, which is part of MATLAB mathematical package. Simulink is an interactive software for modeling, simulating, and analyzing dynamical linear and nonlinear systems in continuous time, sampled time, or a hybrid of the two Systems. Thanks to the incorporation of MATLAB and Simulink, we can simulate, analyze, and revise our models in either environment at any point.

Xilinx System Generator [25] provides a set of Simulink blocks special for several hardware operations that could be implemented on various Xilinx FPGAs. These blocks can be used to simulate the functionality of the hardware system using Simulink environment. One of the advantages of Xilinx System Generator is the capability of generating HDL code directly from your designs.

Xilinx System Generator employs fixed-point format to describe all numerical values in the system and it provides some blocks to transform data provided from the software side of the simulation environment (Simulink) and the hardware side (System Generator blocks). This is an essential concept to understand throughout the design process using Xilinx System Generator. In the next section, we explain the steps of RN algorithm and how we transform it to a model that facilitates the hardware implementation.

B. Regularization Networks: from algorithm to model

An algorithm is a predetermined set of rules for conducting computational steps that produce a computational effect. Whereas, a model is a framework for expressing algorithms build from mathematical equations that is suitable for a hardware implementation. The development of a model in such way affords a simply understood system analysis for the models customers. Fig. 1 presents the conceptual model of the RN.

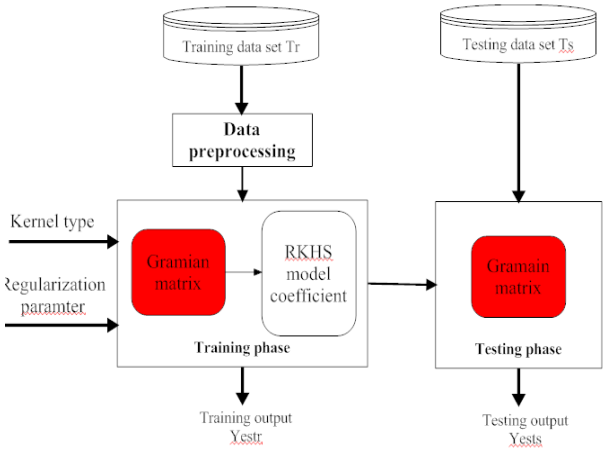

Fig. 1. Conceptual model of regularization networks.

In our case, the move from RN algorithm to RN model provides efficient conveyance of system details and allows easy extracting of system specifications. The modeling steps pass from necessary improvement through design, implementation, and testing. We obtain an executable model that can be continually developed. After model development, simulation shows whether the model works correctly.

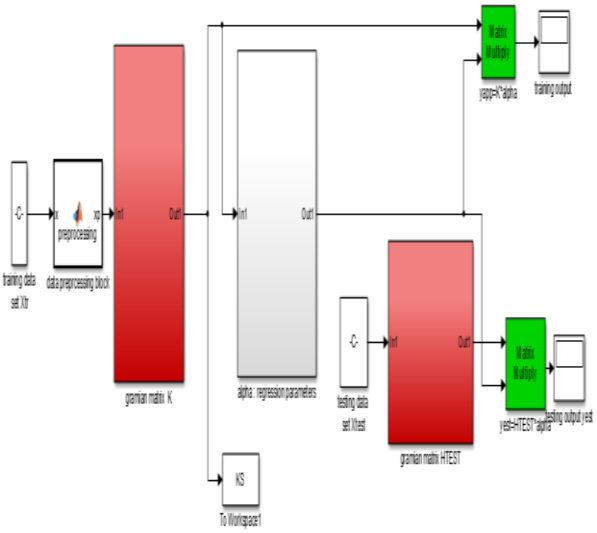

Fig. 2. System generator project for regularization networks co-simulation.

The main goal of the RN modeling is the assigning of complex computation tasks to the hardware. In fact, while software and hardware implementation supplies are integrated with the model, for instance fixed-point and timing behavior, the code could be generated for embedded exploitation and

generate test benches for system verification, saving time and evading manually coded errors. Fig. 2 presents the Simulink Co-simulation model. It contains Simulink and Xilinx system generator components. The red blocks in the figure are executed by the FPGA and the others executed through Simulink.

The adopted approach allows connecting designs straightforwardly to requirements and combining testing with design to constantly identify and correct errors. The reconfigurability of the FPGA and the flexibility of the different blocks of SIMULINK allow the identification of infinity of systems. In the next sections, we will specify the blocks function.

C. Data Preprocessing

The problem of RN method is that the total of parameters is identical to the number of observations. Therefore, to reduce the number of parameters, the number of observations must be reduced and must be a measure of the data spread. Generally, in supervised learning the data are generated by experimental measurement. Whereas, experimentation often makes multiple measurements of the same thing and it is subject to error.

Also, the sampling period of experimental process is small and so the variance of the data sets is small. In this case, the Statistical and mathematical tools [26] as the mean, the median and mode for data quantitative analysis can describe the central tendency of the data set and extract useful information without redundancy. The suitable tool for this work is the mode because it is a statistical term that refers to the most frequently occurring number found in data set of observations. It is found by identifying the most occurring rate in the data set most often representing the data. If the range is big, the central tendency is not as representative of the data as it would be if the range was mall.

Therefore, we can divide the data set in categories as shown in Fig. 3. The mode requires only those values of the data points which can be put into categories. The new chosen data set is composed of the mode of each category.

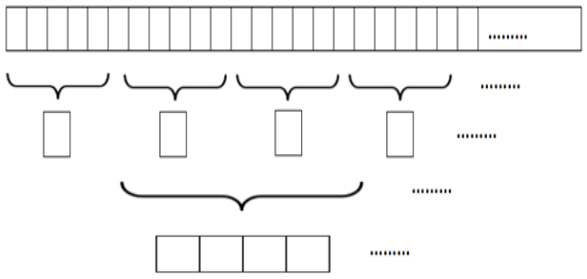

Fig. 3. Scheme of data reduction.

The frequency of each category is the number of data points whose values are in that category, and the mode is the category with the highest frequency. It is possible that more than one category share the highest frequency in which case the data is multimodal. In the training phase, we create a MATLAB function block called Data Preprocessing that receives a large data set and after statistical treatment; produces the data set for Gramian matrix computation. To demonstrate the efficiency of this approach, we executed different testing scenarios to compare between the performances of the real data and the treated data. The PT 326 [27] works as the hair dryer. It heats the air from the atmosphere from 30ºC to 60ºC. In the simulation, we used a single database input/single output (SISO) in the time domain of PT326 process. In previous work [28] a comparative study was established between two Kernel methods; SVM and RN. The consequences demonstrate the competence of the learning algorithms and confirm the excellence of the SVR method in obtaining minimal prediction error and advantage of the RN to gain the calculation time. Approximately, the performances of SVM can be reached by the RN when the data sets are large and with exploitation of a hardware platform for acceleration. Therefore, the choice of implementing the RN method as based on this study. Especially that RN is simpler to implement. In next work, we call the RN method using the reduction method RNR (Reduced). To compare RN to RNR, we employ the same dataset; 100observations for the training phase and 200 new observations for the validation phase. For the RNR, the 100 observations will be reduced to only 10. After obtaining the RKHS model coefficients, the validation data set was chosen randomly and without any treatment to augment the aptitude of generalization of the RKHS model. The Kernel used is polynomial. The optimal parameter λ of the machine learning was obtained by a cross validation technique and it is equal to 0.0001. To evaluate numerically the model performances, we exploit the Normalized Mean Squared Error (NMSE):

$$NMSE = \frac{\sum_{i=1}^{N}(y(i)-\tilde{y}(i))^2}{\sum_{i=1}^{N}(y(i))^2} \quad (15)$$

Where, y(i) is the system output and $\tilde{y}(i)$ is the predicted output. In Table 1 the variation of corresponding Normalized Mean Square Error (NMSE) are cited for each method.

TABLE. I. COMPARING THE RN AND RNR PERFORMANCES

	Kernel type	**EQMN Training**	**EQMN Testing**
RN	Polynomial	8.6768	0.0056
RNR		0.0045	3.9030.10-05

For the same dataset and with the same Kernel and machine learning parameter, the NMSE of RNR is much lower than the NMSE of RN. Thanks to the efficient statistical reduction method.

The following figures (Fig. 4 & 5) show the tough resemblance between the real and expected output for the two methods.

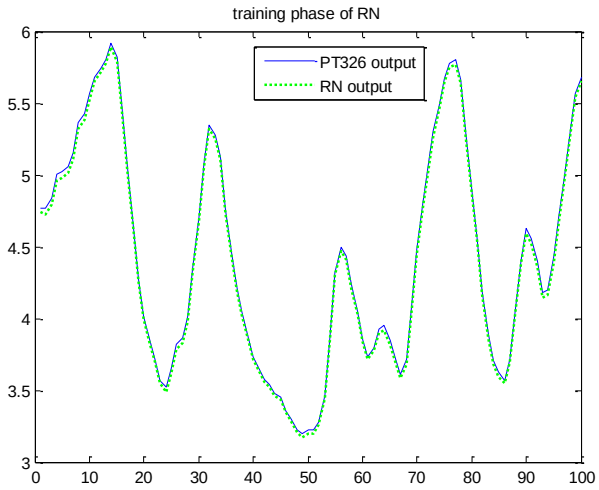

Fig. 4. Training phase of RN and RNR.

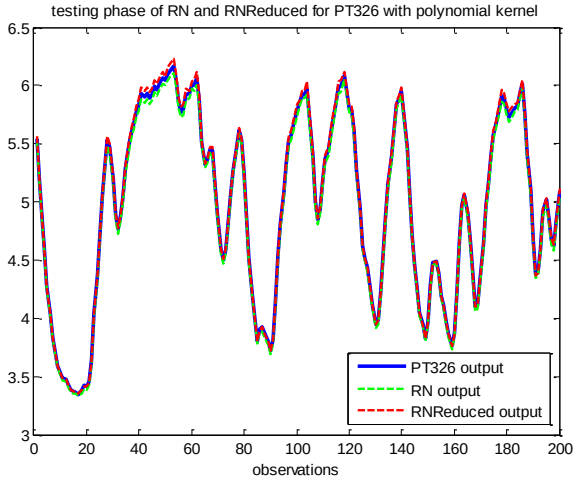

Fig. 5. The testing phase of RN and RNR.

This technique was capable to build a vigorous model for nonlinear system identification. The efficiency of this approach resides in the use of new observations in the testing phase and also facilitates the Gramian matrix implementation in the next section.

D. Accelerating the Gramian matrix computation by a Hardware/Software co-simulation

The Gramian matrix computation is a computationally intensive operation in RN algorithm. Critical speed–up in computation time can be attained by assigning computation tasks to hardware. We present the adopted approach for Gramian matrix computation and its basic principles.

1) *Systolic array architecture for Gramian matrix computation:* The Parallel Matrix Multiplication [29]-[31] has much different identification. In this work, we use the systolic array architecture for the Gramian matrix computation. A systolic array architecture is produced by the interconnection of a set of attached data processing units (DPU) in a regular way [32], [33]. In parallel, each unit or cell receives data from its upstream neighbors to calculate a part of the result. After that it saves the result inside itself and bypasses it downstream neighbors as shown in Fig. 6.

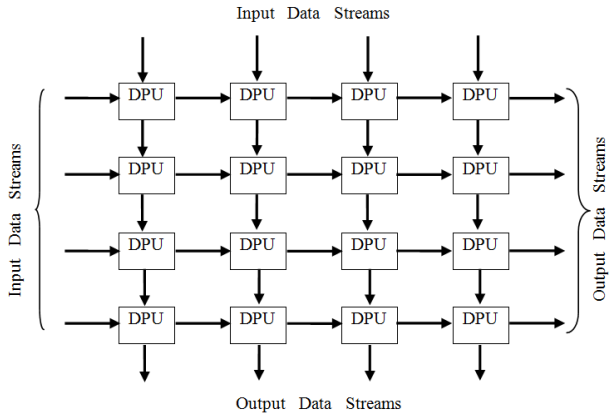

Fig. 6. Principle of systolic array architecture.

The systolic array conception is a mixture between an algorithm and a circuit that implements it. The systolic arrays rely on synchronous data transfers. The individual nodes in systolic array architecture are triggered by the arrival of new data and always treat the data in exactly the same way. We exploit the advantages of this architecture for the implementation of the Gramian matrix on hardware platform. In next paragraph, we explain the proper approach for the matrix computation and the employment of the systolic array method for implementation.

2) Basic principles of serial multiplication: The Gramian matrix $G \in \mathbb{R}^{N\times N}$ *is like that:*

$$G_{ij} = (K(x_i, x_j)), i, j = 1,...,N \quad (16)$$

Where, N is the number of observations and K is the Kernel function that can be chosen either as linear or polynomial Kernel. The Gramian matrix has to be calculated in the training and testing phase. As the input vector **X** can be 1-Dimensional or 2-Dimensional Array, we proposed two Architectures for Gramian matrix computation.

At first, we look at the 1-Dimensional vector multiplication respecting its general constitution. According to the expression of polynomial Kernel with first order:

$$G_{ij} = K(x_i, x_j) = (x_i \times x_j + 1)^{\eta}; i, j = 1,...,N, \eta = 1 \quad (17)$$

It consists to multiply the column vector X(n×1) containing *n* rows and one column with its transpose X^t and add one to the product. In this case, the product of an n dimensional column vector (n×1) by its transpose (row vector (1 × n)) is the Gramian matrix G. That is an (n × n) symmetric and squared matrix. Mathematically, it is presented by the following relationship:

$$G(i, j) = X(i) \times X_t(j) + 1 \quad (18)$$

The key idea here is to calculate the matrix G using the column vector X and its transpose the row vector X^t. The dimension of the given matrices depends on the application.

For efficient implementation and maximum speed-up, the matrix computation is based on systolic array architecture by broadcasting elements of vector X and multiplying it by the corresponding elements of vector X^t. As a simple example, supposing that the vector X is like that: X=[1 2 3] and its transpose X^t =[1 2 3]. The steps of multiplication are shown in Fig. 7.

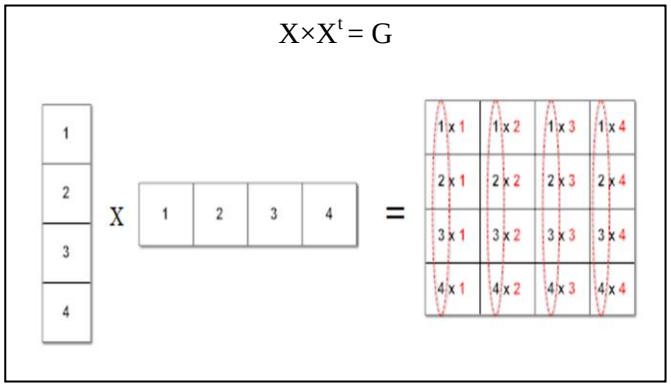

Fig. 7. Example of 1-Dimensional vector multiplication.

From this example, it can be observed that C (i) the i^{th} column of the matrix G is the product of the column vector X by the i^{th} element of this vector:

$$C(i) = X \times X(i)$$

Also for the 2-Dimensional Array, the example of input vector:

X(n×2)

Multiplied by its transpose X^t is presented in Fig. 8:

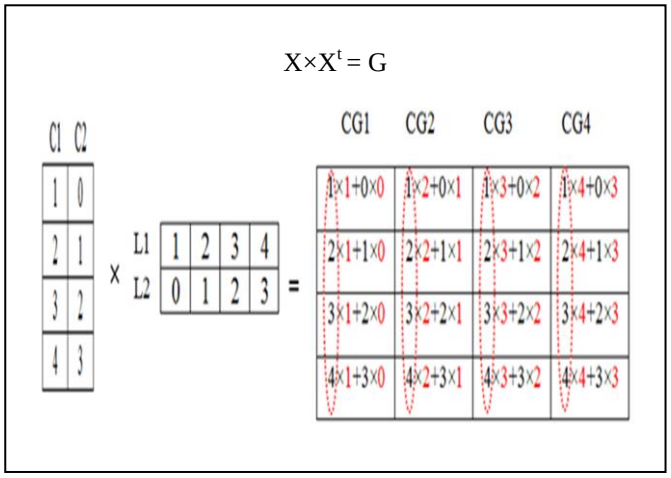

Fig. 8. An example of 2-Dimensional vector multiplication.

Concluding from this example, the expression of Gramian matrix with 2-dimensional vector is a concatenation of column vectors CG.

The i^{th} column of G is the result of sum and product of columns (L1 and L2) and rows (C1 and C2). We can generalize the calculation of each column vector CG of Gramian matrix G as follow:

$$CG(i) = C1 \times L1(i) + C2 \times L2(i) \quad (19)$$

As the input vector X will be streamed the column and rows have no real mean so the previous expression will be modified:

$$CG(i) = C1 \times C1(i) + C2 \times C2(i) \quad (20)$$

The sequence of operations involved in the serial multiplication is as follows:

1) Streaming the elements of column vector X by the input buffer.

2) Calculating the i^{th} column of the matrix G by multiplying each element of the streaming vector by its i^{th} element.

3) Accumulating the multiplier output and writing back the results to the output buffers.

4) Concatenating the n columns to construct the matrix G.

The Fig. 9 represents the system generator blocks for (10×10) Gramian matrix computation using 2-d vector with polynomial Kernel (second order).

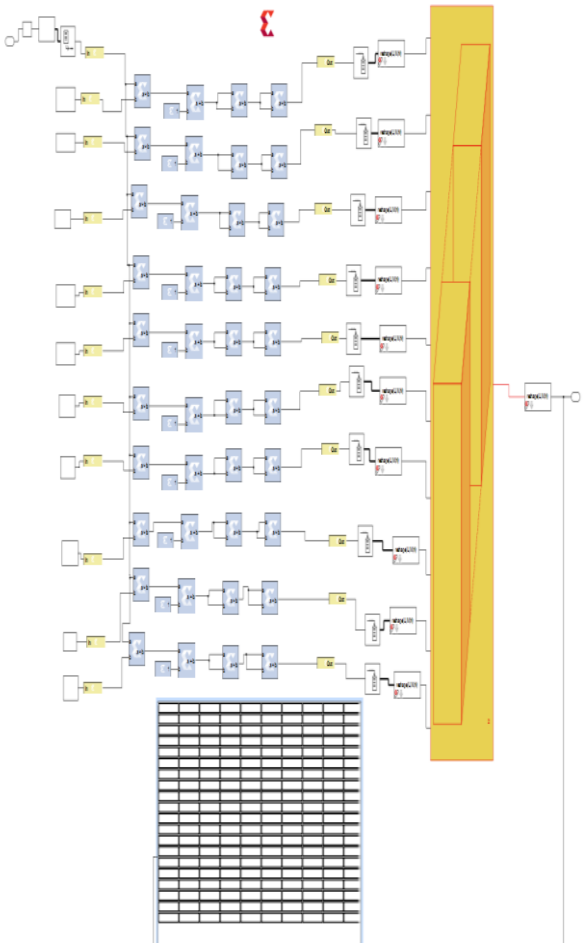

Fig. 9. System generator blocks for Gramian matrix computation.

Before passing to Fig. 10, the type of Kernel function can be selected by a manual switcher. The sigmoid and polynomial Kernels are implemented as shown in Fig. 10:

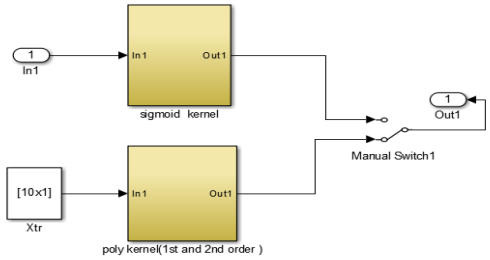

Fig. 10. Selection of Kernel function.

For the polynomial Kernel, it can be chosen for the first or second order by a manual switcher as in Fig. 11:

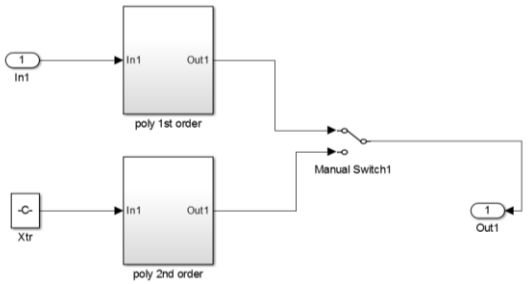

Fig. 11. Selection of the degree of polynomial Kernel function.

The design is able to calculate the Gramian matrix for any system. The user has just to enter the process observations and select the Kernel type. For the regularization parameter, it could be calculated away or in simulation to choose the suitable value. Next, the RN HW/SW Co-design (RN-Cosim) will be tested on a challenging nonlinear system with process noise.

V. Implementation Results and Analysis

A. The Hardware/Software co-simulation steps

In this work, the RN-Cosim co-design was performed using Xilinx System Generator and the Nexys 2 board, which is a complete circuit board and equipped to exploit the circuit development platform based on a Xilinx Spartan 3E FPGA. As shown in Fig. 12, the on-board high-speed USB2 port, jointly with a collection of I/O devices, data ports, and development connectors, enable the conception of a wide range of designs without the demand for any supplementary components.

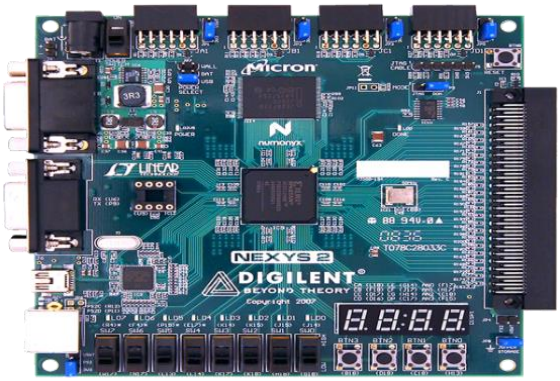

Fig. 12. The Nexys 2-board.

After completing the hardware system, the Simulink environment was exploited to verify functionality of the system. Simulink presents a very supple simulation environment that allows building different testing scenarios. After verifying the functionality of the RN-Cosim model for the different hardware component, the generation of Co-simulation module is executed. While building the hardware system, ISE flow generates a bit-stream that will be later used to configure the FPGA. When the compilation is completed, a new library is created including one block that includes all the functionality required for the system to be executed on the FPGA. The generated library encapsulates the hardware implementation of the RN-Cosim model, which is linked to a bit-stream that will be downloaded into the FPGA during Co-Simulation. The different hardware component is replaced by the new block from the Co-simulation library. Fig. 13 contains the final blocks for the Gramian matrix computation.

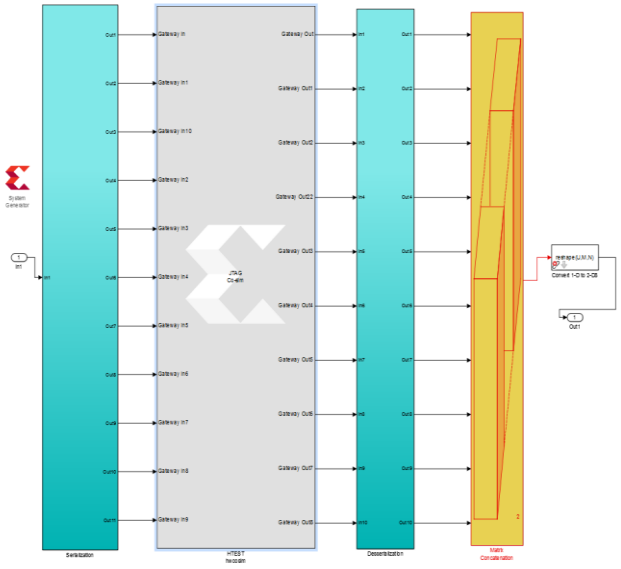

Fig. 13. System generator blocks using JTAG hardware co-simulation block for Gramian matrix computation.

The two blue blocks after and before the hardware co-simulation block, assure the serialization and deserialization of matrix. Then the FPGA is connected to the system generator via the Digilent USB JTAG Cable.

When the design is ready for co-simulation, system generator will first download the bit-stream associated with the block. Once the download completes, system generators reads the inputs from Simulink simulation environment and send them to the design on the board using the JTAG connection. System generator then reads the output back from JTAG and sends it to Simulink for displayed. When simulation is completed, the results should be displayed as shown and the results can be verified by comparing the simulation output to the expected output. The model chosen is a challenging nonlinear system identification; Wiener-Hammerstein benchmark with process noise.

B. *Description of the process and analysis of the implementations results*

The nonlinear system to be modeled is the Wiener-Hammerstein benchmark with process noise [34]. This system is challenging nonlinear system identification due to the process noise present in the system. Moreover, the static nonlinearity is not directly accessible from neither the measured input or output, and the output dynamics are difficult to invert due to the presence of a transmission zero.

The Wiener-Hammerstein benchmark is a well-known block oriented system. As illustrated in Fig. 14, it contains a static nonlinearity f(x) that is sandwiched in between two LTI blocks R(s) and S(s).

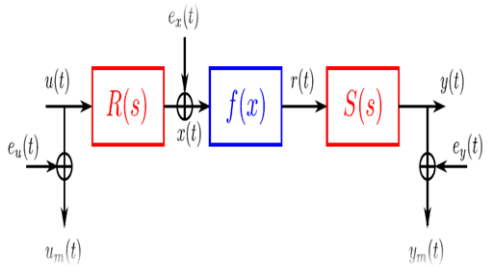

Fig. 14. The Wiener-Hammerstein system with process noise.

The presence of the two LTI blocks results in a problem that is harder to identify. The additive process noise $e_x(t)$ is filtered white Gaussian noise sequence.

The input and output signals of the system are:

1) *r : reference signal, signal loaded into the generator,*
2) *u: measured input signal,*
3) *y: measured output signal,*
4) *f_s: the sample frequency.*

Fig. 15 presents the plot of the measured output signal *y* versus the measured input signal *u* from a thousand of values with sampling time one second.

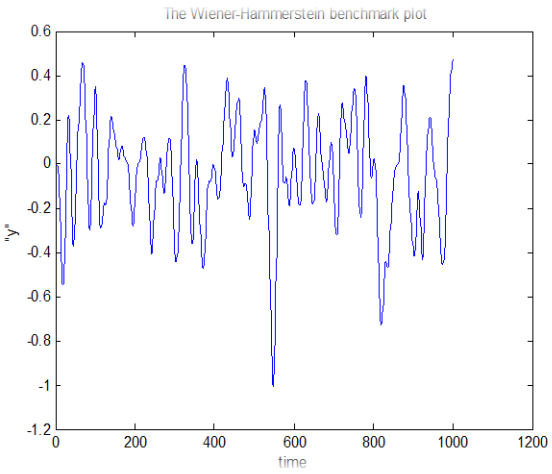

Fig. 15. The plot of Wiener-Hammerstein benchmark with process noise.

To construct the RKHS model, 100 observations are employed for the training phase that will be reduced to only 10 observations. Then, 100 new observations are randomly chosen for the validation phase. The data used for testing phase are not statistically treated. The Kernels used are of type: polynomial (first and second order) and sigmoid. The input vector is a 2-dimensional vector. The optimal parameter λ of the machine learning was obtained by a cross validation technique and it is equal to 0.0001.

By examining the plots in Fig. 16, it can be remarked that the two models outputs (RNR and RN-Cosim) are in concordance with the Wiener benchmark output in the training and testing phase. Comparing to benchmark process, the deviation of the RNR and RN- Cosim is small. This illustrates the excellent performances of the projected identification method.

Table 2 gives the computation time (CT) and NMSE in training and testing phase of RNR algorithm and RN-Cosim with sigmoid and polynomial Kernel.

TABLE. II. COMPARING NMSE AND CT OF RNR AND RN-COSIM

	Kernel type	**NMSE Training**	**NMSE Testing**	**CT(s)**
RNR	Polynomial	6.7980e-09	3.1847e-09	1.3884
RN-Cosim		3.1850e-07	7.1274e-07	0.033066
RNR	Sigmoid	7.9972e-09	3.1847e-08	1.4196
RN-Cosim		3.1850e-07	1.3886e-07	0.034018

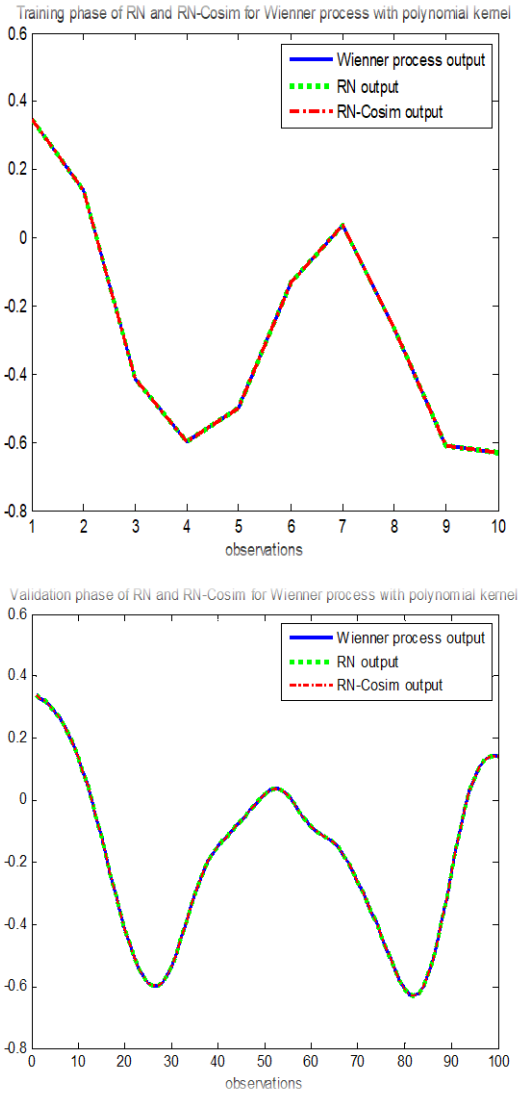

Fig. 16. Training and validation phase of RN and RN-Cosim.

In terms of the model accuracy, the two models are excellent but the RNR gives the lower NMSE comparing to RN-Cosim that uses the fixed point arithmetic. The reduction method based on statistical treatment improves the model accuracy because the reduced data set reflects the central tendency of data that decreases the model error and increases its capacity of generalization.

Considering the simulation speed, compared with RNR algorithm execution, the proposed RN-Cosim co-simulation gives more than 40 times speedup.

Note that, in both cases of sigmoid and polynomial Kernel, RN-Cosim gives significant simulation speedups thanks to the association of Gramian matrix computation to hardware and the immediate execution of the whole model contrary to the sequential algorithm execution. The properties of our co-design are listed in Table 3.

TABLE. III. COMPARING NMSE AND CT OF RNR AND RN-COSIM

	Kernel type	NMSE Training	NMSE Testing	CT(s)
RNR	Polynomial	6.7980e-09	3.1847e-09	1.3884
RN-Cosim		3.1850e-07	7.1274e-07	0.033066
RNR	Sigmoid	7.9972e-09	3.1847e-08	1.4196
RN-Cosim		3.1850e-07	1.3886e-07	0.034018

As seen from Table 4, the resulting architecture requires about 406 slices with 11% utilization from the available resources and about 48 Bonded IOBs with 19% utilization. Whereas the utilization of slice Flip Flop are approximately insignificant and negligible. The proposed architecture has low complexity and low resources consumption that enhanced effectiveness in area and provide a good choice in terms of low-cost hardware. The implemented RN-Cosim co-design reaches 50 MHz as maximum frequency.

TABLE. IV. FPGA RESOURCES UTILIZATION IN THE HW/SW CO-SIMULATION

Logic utilization	Used	Available	Utilization
Number of slices	406	3584	11 %
Number of slice Flip Flops	16	7168	1 %
Number of Bonded IOBs	48	251	19 %
Number of GCLKS	2	24	8 %

Since the current implementation, it is possible to solve various nonlinear system identification tasks in the RKHS space.

VI. CONCLUSION AND FUTURE WORK

This article proposed efficient method of HW/SW Co-simulation using Xilinx system generator. The basic principle of the contribution is to improve the RKHS model performances and to accelerate the computation task by including hardware in the loop. Also we developed a new reduction method to decrease the model errors. The experiments prove that the co-design reach more than 40 times speedup compared with the RN algorithm.

The principal improvement of this advance is the opportunity of modeling and confirming the overall system inside the identical design environment. Moreover, Simulink offers a friendly graphics interface for flexible modeling and simulation. The design was well organized into hierarchical modules including the hardware and software components that require rigorous verification all along the design flow.

Future works will incorporate the use of the Xilinx System Generator development devices for the implementation of another Kernel method like KPCA. As development in our co-

design, new Kernel function will be added in order to increase the simulation accuracy. We will also apply RN-Cosim to systems that are more complex with other FPGA type.

REFERENCES

[1] Bernhard Scholkopf and Alexander J. Smola, "Learning with Kernels: Support Vector Machines, Regularization, Optimization, and Beyond", MIT Press Cambridge, MA, USA 2001

[2] Yingwei Zhang, "Enhanced statistical analysis of nonlinear processes using KPCA, KICA and SVM", Chemical Engineering Science, Volume 64, Issue 5, March 2009, Pages 801-811.

[3] Mikhail Z. Zgurovsky , Yuriy P. Zaychenko, "Neural Networks", Chapter in The Fundamentals of Computational Intelligence: System Approach Volume 652 of the series Studies in Computational intelligence pp 1-37 Date: 02 July 2016.

[4] Alaa F. Sheta, " A Comparison between Regression, Artificial Neural Networks and Support Vector Machines for Predicting Stock Market Index ", communication on (IJARAI) International Journal of Advanced Research in Artificial Intelligence, Vol. 4, No.7, 2015

[5] C.A. Schmidt , S.I. Biagiola, J.E. Cousseau , J.L. Figueroa, "Volterra-type models for nonlinear systems identification" Journal of Applied Mathematical Modelling Volume 38, Issues 9–10, 1 May 2014, Pages 2414–2421.

[6] Cristian Preda, "Regression models for functional data by reproducing kernel Hilbert spaces methods", Journal of Statistical Planning and Inference Volume 137, Issue 3, 1 March 2007, Pages 829–840.

[7] Sergios Theodoridis "Learning in Reproducing Kernel Hilbert Spaces", Machine Learning, A Bayesian and Optimization Perspective 2015, Pages 509–583.

[8] C.BURGES, "A Tutorial on Support Vector Machines for Pattern Recognition." Review 1–43 on Kluwer Academic Publishers, Boston. Manufactured in The Netherlands.

[9] John C. Platt. Sequential Minimal Optimization: A Fast Algorithm for Training Support Vector Machines. Technical report, Advances in kernel methods - support vector learning, 1998.

[10] X.Zhang, Y.Zhang: " GPU Implementation of Parallel Support Vector Machine Algorithm with Applications to Intruder Detection" JOURNAL OF COMPUTERS, VOL. 9, NO. 5, MAY 2014

[11] "System Generator for DSP": Getting Started Guide.

[12] "Medical Image Processing on The GPU–Past, Present and Future," Medical Image Analysis, vol. 17, pp. 1073-1094,2013.

[13] S. Asano, T. Maruyama, and Y. Yamaguchi, "Performance Comparison of FPGA, GPU and CPU in Image Processing," in International Conference on Field Programmable Logic and Applications, 2009. FPL 2009, 2009, pp. 126-131.

[14] E. Fykse, "Performance Comparison of GPU, DSP and FPGA Implementations of Image Processing and Computer Vision Algorithms in Embedded Systems," M.Sc. thesis, Department of Electronics and Telecommunications, Norwegian University of Science and Technology, 2013.

[15] J. G. Filho, M. Raffo, M. Strum, and W. J. Chau, "A General-Purpose Dynamically Reconfigurable SVM," in 2010 VI Southern Programmable Logic Conference (SPL),2010, pp. 107-112.

[16] D. Anguita, S. Pischiutta, S. Ridella, and D. Sterpi, "Feed-Forward Support Vector Machine without Multipliers," IEEE Transactions on Neural Networks, vol. 17, pp. 1328-1331, 2006.

[17] L. Bustio-Martínez, R. Cumplido, J. Hernández-Palancar, and C. Feregrino-Uribe, "On the Design of a Hardware-Software Architecture for Acceleration of SVM's Training Phase," in Advances in Pattern Recognition, ed: Springer,2010, pp. 281-290.

[18] A. H. M. Jallad and L. B. Mohammed, "Hardware Support Vector Machine (SVM) for Satellite on-Board Applications," in 2014 NASA/ESA Conference on Adaptive Hardware and Systems (AHS), 2014, pp. 256-261.

[19] K. Nagarajan, B. Holland, A. D. George, K. C. Slatton, and H. Lam, "Accelerating Machine-Learning Algorithms on FPGAs using Pattern-Based Decomposition," Journal of Signal Processing Systems, vol. 62, pp. 43-63, 2011.

[20] X. Pan, H. Yang, L. Li, Z. Liu, and L. Hou, "FPGA Implementation of SVM Decision Function Based on Hardware-friendly Kernel," in International Conference on Computational and Information Sciences , ICCIS 2013 Proceedings, 2013, pp. 133-136.

[21] V.Vapnik, "An Overview of Statistical Learning Theory" , IEEE TRANSACTIONS ON NEURAL NETWORKS, VOL. 10, NO. 5, SEPTEMBER 1999.

[22] Wahba G. "An introduction to model building with Reproducing Kernel Hilbert Spaces". Technical report No. 1020. Department of Statistics, University of Wisconsin-Madison; 2000.

[23] Theodoros Evgeniou, Massimiliano Pontil, Tomaso Poggio, "Regularization Networks and Support Vector Machines" review on journal of Advances in Computational Mathematics (1999).

[24] Inc., T. M.: "Embedded MATLAB User's Guide" The MathWorks Inc, 2007.

[25] "System Generator for DSP Getting Started Guide" UG639 (v 14.3) October 16, 2012

[26] Chris Tsokos and Rebecca Wooten, " Basic Statistics" The Language and Art of Math 2016, Pages 265–327

[27] 'Air Temperature Control', Laboratory Manual .

[28] Intissar Sayehi, Okba Touali, Belgacem Bouallegue,

[29] Rached Tourki. "A comparative study of two kernel methods: Support Vector Regression (SVR) and Regularization Network (RN) and application to a thermal process PT326", 2015 16th International Conference on Sciences and Techniques of Automatic Control and Computer Engineering (STA), 2015

[30] Albert-Jan N. Yzelman, Dirk Roose, Karl Meerbergen, "Sparse Matrix-Vector Multiplication: Parallelization and Vectorization", Multicore and Many-Core Programming Approaches 2015, Pages 457–476.

[31] Urban Borštnika, Joost VandeVondeleb, Valéry Webera, Jürg Huttera, "Sparse matrix multiplication: The distributed block-compressed sparse row library" Parallel Computing Volume 40, Issues 5–6, May 2014, Pages 47–58

[32] Marco Maggioni and Tanya Berger-Wolf, " Optimization techniques for sparse matrix–vector multiplication on GPUs" Journal of Parallel and Distributed Computing Volumes 93–94, July 2016, Pages 66–86.

[33] H. L. P. Arjuna Madanayake, Student Member, IEEE, and Len T. Bruton, Fellow, IEEE, " A Systolic-Array Architecture for First-Order 3-D IIR Frequency-Planar Filters" , IEEE TRANSACTIONS ON CIRCUITS AND SYSTEMS—I: REGULAR PAPERS, VOL. 55, NO. 6, JULY 2008.

[34] Wei Jin, Chang N. Zhang and Hua Li, " MAPPING MULTIPLE ALGORITHMS INTO A RECONFIGURABLE SYSTOLIC ARRAY" , published in Electrical and Computer Engineering journal from Canadian Conference CCECE 2008 on 4-7 May 2008, pages 001187 – 001192, ISSN - 0840-7789.

[35] M. Schoukens, J.P. Noel, "Wiener-Hammerstein benchmark with process noise", Workshop on Nonlinear System Identification Benchmarks on April 25-27, 2016, Brussels, Belgium.

A Parallel Genetic Algorithm for Maximum Flow Problem

Ola M. Surakhi
Computer Science Department
University of Jordan
Amman-Jordan

Mohammad Qatawneh
Computer Science Department
University of Jordan
Amman-Jordan

Hussein A. al Ofeishat
Computer Science Department
Al-Balqa applied university Jordan
Amman-Jordan

***Abstract*—The maximum flow problem is a type of network optimization problem in the flow graph theory. Many important applications used the maximum flow problem and thus it has been studied by many researchers using different methods. Ford Fulkerson algorithm is the most popular algorithm that used to solve the maximum flow problem, but its complexity is high. In this paper, a parallel Genetic algorithm is applied to find a maximum flow in a weighted directed graph, by finding the objective function value for each augmenting path from the source to the sink simultaneously in the parallel steps in every iteration. The algorithm is implemented using Message Passing Interface (MPI) library, and results are conducted from a real distributed system IMAN1 supercomputer and were compared with a sequential version of Genetic-Maxflow. The simulation results show this parallel algorithm speedup the running time by achieving up to 50% parallel efficiency.**

***Keywords*—Flow network; Ford Fulkerson algorithm; Genetic algorithm; Max Flow problem; MPI; multithread; supercomputer**

I. INTRODUCTION

A flow network is a directed graph where each edge has a capacity and receives a flow. The amount of flow on an edge cannot exceed the capacity of the edge, and it must satisfy the restriction that the amount of flow into a node equals the amount of flow out of it, except when it is a source, which has more outgoing flow, or sink, which has more incoming flow [1]. The flow networks can represent many real-life situations like fluids in pipes for city water distribution, traffic in roads and more.

The maximum flow problem is one of the several well-known basic problems for combinatorial optimization in weighted directed graphs [2]. It involves finding a feasible flow from the source to the sink in a maximum flow network. The Ford-Fulkerson algorithm is the most widely used algorithm for solving maximum flow problem. The main idea of the algorithm is to find a path through the graph from the source (start node) to the sink (end node), in order to send a flow through this path without exceeding its capacity. Then we find another path, and so on. A path with available capacity is called an augmenting path [3], [4]. The time complexity of the Ford-Fulkerson algorithm is high. Therefore, a variety of researches have been applied to solve maximum flow problem using different methods and techniques [5].

In this paper, Genetic algorithm is applied in parallel to accelerate the process of finding the maximum flow problem and increasing the availability of high computer performance. Two conditions must be satisfied on the maximum flow problem: 1) The flow at each edge must not exceeds its capacity. 2) At each vertex, the incoming flow must be equal to the outgoing flow. The algorithm is implemented using MPI which is a standard library for message passing that can be used to develop portable parallel programs using C, C++ or FORTRAN [6], [7]. The evaluation is done in terms of the speed and parallel efficiency according to different network data size and different number of processors. The results were conducted using IMAN1 supercomputer which is Jordan's first and fastest supercomputer. It is available for the use of academia and industry in the region of Jordan. It provides multiple resources and clusters to run and test High Performance Computing (HPC) codes [7], [8].

The rest of this paper is organized as: Section 2 presents some related works to the maximum flow problem. Section 3 reviews the maximum flow problem. Section 4 introduces the sequential and parallel Genetic algorithm, and Section 5 presents the conclusion and future works.

II. RELATED WORKS

The maximum flow problem has been studied by many researchers because of its importance for many areas of applications, such as communication networks, Airline scheduling, computer sciences, electrical powers, tracks and more. Ford Fulkerson proposed the first pseudo code for solving maximum flow problem by finding the augmenting path [3], [4]. Other methods translate the maximum flow problem into maximal flow problem in layered network [9]. [10] introduced the push and re-label method which maintains a pre-flow and updates it through-push operations. The re-label operation perform the fine-grain updates of the vertex distances. Orlin [11] presents improved polynomial time algorithms for the max flow problem defined on a network with n nodes and m arcs, and shows how to solve the max flow problem in O(nm) time, improving upon the best previous algorithm due to [12] who solved the max flow problem in O(nm logm/(n log n) n) time. Genetic algorithm was also applied to solve max flow optimization problems. [2], each solution is represented by a flow matrix. The fitness function is defined to reflect two characteristics: balancing vertices and the saturation rate of the flow. Starting with a population of randomized solutions, better and better solutions are sought through the genetic algorithm. Optimal or near optimal solutions are determined with a reasonable number of

iterations compared to other previous GA applications. In [13], the CRO algorithm was implemented to solve the maximum flow problem. The proposed algorithm showed a better performance with a complexity of O(I E2), for I iterations and E edges.

III. Maximum Flow Problem

The flow network is a directed graph with two distinguished nodes; source and sink. Each edge between two nodes has a non-negative capacity and receives a flow where amount of flow on an edge cannot exceed its capacity as shown in Fig. 1.

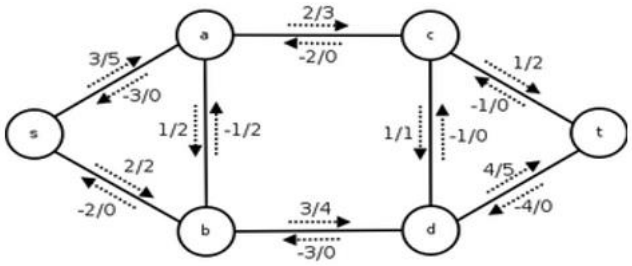

Fig. 1. An example of flow network [1].

For a directed graph G = (V, E), with source node S and a sink node T, and every edge e = (u,v) ∈ E has a non-negative, real-valued capacity c(u,v). The flow of the network is an integer valued function f that must satisfy following three properties for all nodes u and v:

1) Capacity constraints: f(u,v) ≤ c(u,v). The flow on each edge cannot exceed its capacity.

2) Skew symmetry: f(u,v) = −f(v,u). The flow from u to v must be the opposite of the net flow from v to u and f(u,u) =0.

3) *Flow conservation:* $\sum_{v \in V} f(s, v) = 0$,

4) the flow into a vertex must also flow out except for

5) the source, that "produces" flow, and the sink, which "consumes" flow.

The incoming flow to the node is equal to the outgoing flow from the node and thus the flow is conserved. Also, the total amount of flow going from source s equals total amount of flow into the sink t. the value of the flow is given by (1):

$$| f | = \sum_{v \in V} f(s, v) = \sum_{v \in V} f(v, t) \quad (1)$$

The maximum flow problem involves finding a flow from the source to the sink that is maximum to route as much flow as possible from s to t in the network.

IV. Sequential and Parallel Genetic Algorithm for Maximum Flow Problem

A. An overview of Genetic Algorithm

Genetic algorithm (GA) is a search based optimization algorithm inspired by the principle of genetics and natural selection. It begins with a population of possible solution to some problem which can be represented as a set of binary bit strings. Each individual in the population is assigned a fitness value based on its objective function value of the problem. The GA modified the population by applying the three main operations of it; reproduce, crossover and mutate to produce new children similar to natural genetic operators.

1) ***Reproduction*** *selects the best individual string from the population and discards the bad ones according to the fitness value. The best individuals are those having more chances to survive in the next generation.*

2) ***Crossover*** *includes two steps. First, select randomly two bit strings to be the parents of the new bit strings.*

Second, choose a place (crossover site) in the bit string and exchanges all characters of the parents after that point. The process tries to artificially mix the genetic of the parents and reproduce the mating process.

3) ***Mutation*** *changes the genes of the individual parents for the bits that didn't changed by the previous operations due to its absence from the generation, a 0 to 1 and vise versa.*

The genetic algorithm repeats these three operations until reaching the termination condition.

The pseudo code of GA is shown in Fig. 2.

B. Sequential GA for maximum flow problem

The GA has been applied to solve maximum flow optimization problems [2]. In [2], a flow matrix is used to represent each solution. The fitness function is defined to reflect two characteristics: 1) balancing vertices; and 2) the saturation rate of the flow.

```
(1) initialise population;
(2) evaluate population;
(3) while (!stopCondition) do
(4)     select the best-fit individuals for reproduction;
(5)     breed new individuals through crossover and mutation operations;
(6)     evaluate the individual fitness of new individuals;
(7)     replace least-fit population with new individuals;
```

Fig. 2. Generic pseudocode of a genetic algorithm [14].

Starting with a population of randomized solutions, the GA is applied for a reasonable number of iteration till reaching the optimal or near optimal solutions.

In this paper, a sequential implementation for GA is applied to find maximum flow problem with a different network size. The algorithm is implemented using Intel core I7-3632QM CPU2.20GHz, 8GB of RAM and windows 7 64 bits. The application programs were written in C language and executed on Net-Beans IDE 8.1. As mentioned before, the GA has three main operations; Reproduction (or Selection), Crossover and Mutation. The details of the implementation are discussed here.

For a graph, G with n vertices and m edges: G is represented by the flow capacity matrix, $C = [c_{ij}]$, i, j = 1, n.

Each solution is represented by a flow matrix $F = [f_{ij}]$, i, j = 1, n. The initial flow was generated randomly.

Selection step: There are different steps for selection. Through our approach, the probability to select some individual depends on its fitness value. We select half of all the individuals after calculating its fitness, then it will be ranked based on the fitness value, and from 0 to N/2 of the individuals will be selected.

Cross Over step: There are many ways to do crossover. Through our solution we make a cross over between selected population. We divide the population into two halves: F1 and F2. The crossover is done between the first half of F1 and the second half of F2 to produce S1, and crossover between first half of F2 with second half of F1 to produce S2, from this cross over new population was generated.

Mutation Step: A new population with full of individuals created after selection and crossover steps.

Some of them are directly copied, while others are produced by crossover. All the individuals should not be exactly the same. In order to ensure that a loop through all the alleles of all the individuals, and if that allele is selected for mutation, we can either change it by a small amount or replace it with a new value. The probability of mutation is usually between 1 and 2 tenths of a percent.

These steps will be repeated until reaching to maxflow value for selected generation. There fitness function used here is same as an objective function which is used to calculate Maxflow from source node to sink each iteration. These different steps will be repeated to select new population with new values for Maxflow from source to sink node.

The initialization step is important, through this step, different values must be defined and specified, like number of iteration, population size and mutation ratio. Number of iterations are important to achieve enhancement of solution at each iteration as GA is heuristic. Our experiment use different population size. The initial network size was 5000. The experiment was repeated by increasing the number of nodes, and stopped when it equals to 15,200 nodes as it consumes memory efficiency and space. The time needed to find max flow value is in seconds and shown in Table 1.

For the sequential implementation, the complexity depends on the population size and number of generations. And it can be defined as O(npg) where p is the population size and g is the number of generations.

C. Parallel GA for maximum flow problem

Finding the maximum flow value in a network graph can be done by running two main steps: 1) as long as there is a flow path from the source to the sink with a capacity c less than its flow value f, find this path; 2) change the flow accordingly. If no augmenting path exists, then we get the maximum flow. For a large network size with large number of nodes and arcs, dividing the graph into subgraph will enhance the running time needed to find the maximum flow value. In this case, the graph will be divided to a number of sub graph with a source and sink nodes for each one, every subgraph then, can be implemented in one processor to find its maximum flow value. The number of subgraphs will be equal to the number processors and the degree of concurrency will equal to the number of augmenting paths divided by number of processors as follows:

TABLE. I. TIME NEEDED FOR SEQUENTIAL GA TO FIND MAXFLOW VALUE WITH DIFFERENT NUMBER OF NODES

No. of nodes	Time/second
1000	0
2000	1
3000	1
4000	2
5000	3
6000	4
6300	4
7000	6
7700	7
8000	8
8300	9
8602	9
9000	10
10000	12
10400	14
11000	14
11400	15
11600	17
11800	21
12000	23
12200	29
12400	35
12800	39
13000	40
13400	50
14000	94
14200	147
14600	261
14800	343
15000	417
15200	480

Parallelism = total number of augmenting path/number of processors (2)

The implementation was done on Message Passing Interface (MPI) library, and results are conducted from a real distributed system IMAN1 supercomputer. The first implementation was done with one processor and then with two processors which reduced the time to half compared with the sequential time needed to solve maxflow problem as

shown in Fig. 3, then the number of processors were increased to 4, 8, 12, 16, 24 and 32, respectively. The initial network size 5000 and is increased repeatedly to reach 35,000 nodes. The implementation results are shown in Table 2.

The results show that using up to 4 processors in parallel can achieve a better result with a large network size, as the C language can measure the time with seconds only, we could not catch the enhancement in the running time when the number of nodes equals 5000 to 9000, the implementation gave an equal running time for 2 and 4 processors which could be less than the measured one if the estimated time was in millisecond. As the network size increased the running time reduced one or two seconds, a comparison between the running time for parallel maxflow-Genetic with 2 and 4 processors can be shown in Fig. 4.

TABLE. II. THE IMPLEMENTATION RESULTS FOR RUNNING MAXFLOW-GENETIC ON 1, 2, 4, 8, 12, 16, 24 AND 32

No of nodes	Time with 1-P	Time with 2-P	Time with 4-P	Time with 8-P	Time with 12-P	Time with 16-P	Time with 24-P	Time with 32-P
5,000	3	2	2	2	4	4	4	4
6,000	4	3	2	3	3	4	4	5
7,000	5	4	4	5	5	5	6	7
8,000	8	5	5	6	7	8	10	10
9,000	10	6	6	6	7	8	10	10
10,000	12	8	7	8	8	8	11	11
11,000	15	10	8	10	10	13	13	14
12,000	18	12	9	12	15	16	16	18
13,000	21	13	11	13	15	17	18	19
14,000	23	15	12	16	16	17	20	20
15,000	27	17	14	17	18	18	18	22
20,000	48	31	40	31	31	37	38	39
25,000	74	49	48	49	49	57	59	59
30,000	107	70	69	70	70	73	73	85
35,000	146	93	93	94	94	97	97	101

Using two-processors enhanced the efficiency of the system by reducing the running time to half as shown in Fig. 3.

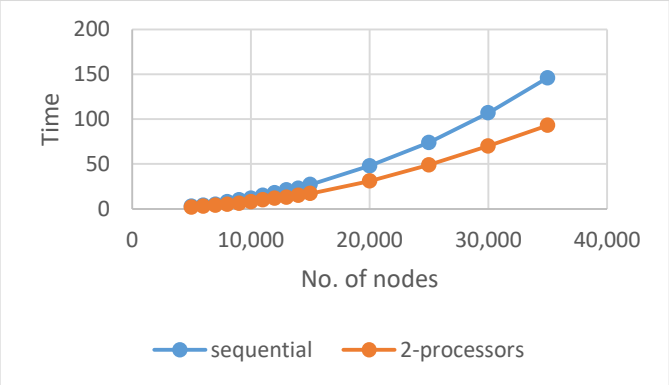

Fig. 3. Running time for parallel maxflow-Genetic with 1 and 2 processors.

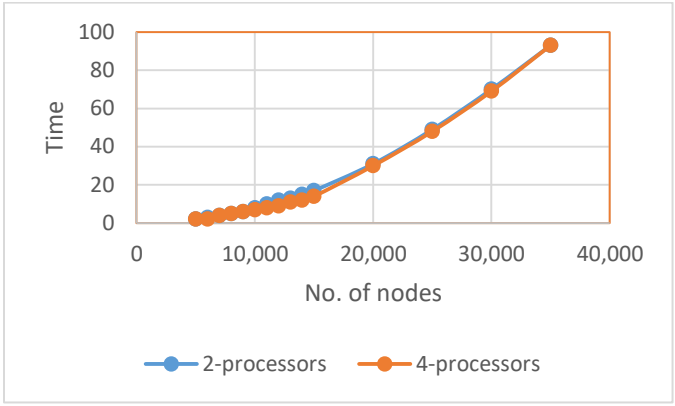

Fig. 4. Running time for parallel maxflow-Genetic with 2 and 4 processors.

Another important result could be noticed from Table 2. It shows that using more processors in parallel to solve maximum flow problem using GA could not give a better enhancement. It shows that using more processors in parallel to solve maximum flow problem using GA could not give a better enhancement. The speed up for this implementation is given in the following equation:

Speedup = sequential processing time/ parallel processing time (2)

Using (2) to find the speedup when using 2 and 4 processors give a result of 2. Fig. 5 shows the average speed up when using 1, 2, 4, 8, 12, 16, 24 and 32 processors.

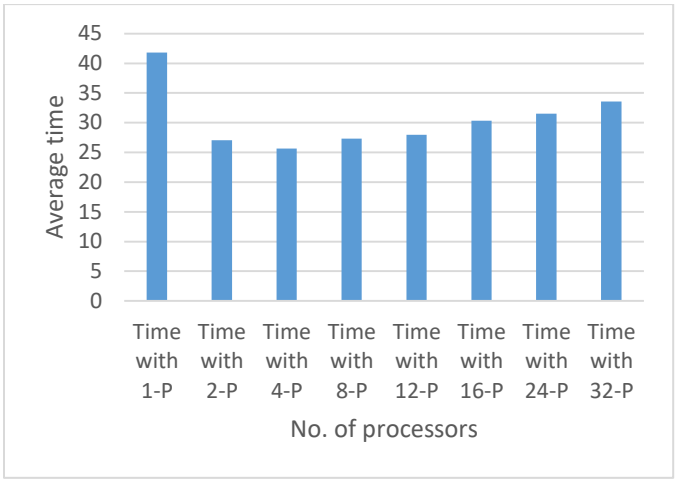

Fig. 5. Average speed up using 1, 2, 4, 8, 12, 16, 24 and 32 processors for parallel Maxflow-Genetic.

For 8, 12, 16, 24 and 32 processors, the running time increased by one second as the network size increased, which is close to the running time when using 4 processors. That's because of the communication between the processors to send and receive data. As the network size increase and the number of processors increase, the communication between the processors increased, which take more time than the time needed for execution. The running time for parallel maxflow-Genetic using 8, 12, 16, 24 and 32 processors are shown in Fig. 6.

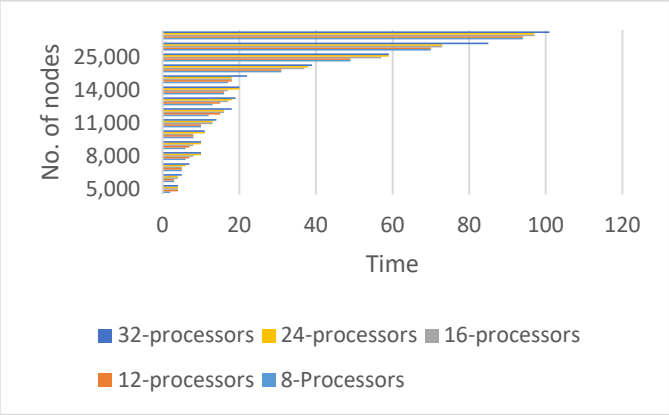

Fig. 6. Running time for parallel maxflow-Genetic with 8, 12, 16, 24 and 32 processors.

D. Parallel GA for maxflow problem in multi core processor

The parallel maxflow-Genetic has been applied on a multi core processors. That idea is similar to the parallel implementation on the distributed system, but in this case, the graph is divided over different number of threads, each of these threads work on separated core of CPU cores. Each subgraph has a set of augmenting paths, so each thread will calculate maximum flow value for its own nodes. The experiment was done with 2 threads, 4 and 6 threads respectively with a network size started initially with 5000 nodes and repeated 9 times till the number of nodes reached 12,000 with increasing by 1000 each time. The implementation was done using C programming language, on Intel Core I7-3632 QM CPU@2.20 GH with 8 GB internal memory.

The results show a better enhancement in the running time when compared with the time needed to find maxflow value with a sequential version of the maxflow-Genetic. The results are shown in Table 3 and Fig. 7.

TABLE. III. RUNNING TIME FOR MAXFLOW-GENETIC WITH 2, 4 AND 6 THREADS

No. of nodes	SEQ	2TH	4TH	6TH
5000	5	3	2	2
6000	6	3	3	3
7000	8	4	3	3
8000	9	5	4	4
9000	11	8	6	6
10000	13	9	7	7
11000	18	12	9	9
11500	23	16	16	12
12000	38	21	16	14

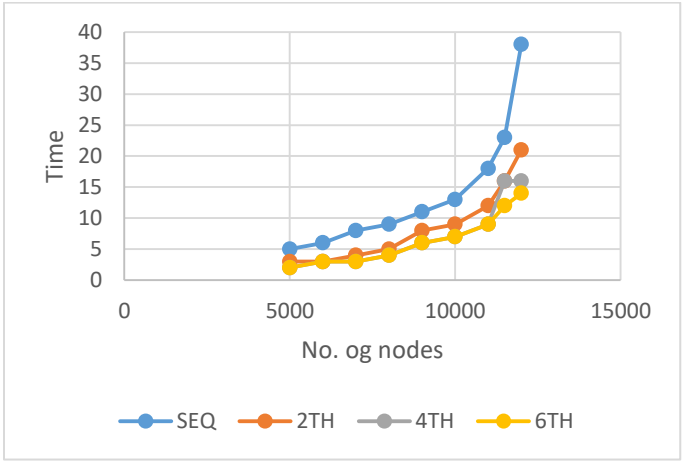

Fig. 7. Running time for maxflow-Genetic with 2, 4 and 6 threads.

V. CONCLUSIONS AND FUTURE WORKS

In this paper, a parallel genetic algorithm has been implemented to solve maxflow problem. The implementation was done using open MPI library on IMAN1 supercomputer. The evaluation of the algorithm includes a different network size which starts from 5000 to 14,000 nodes. The results are compared with the sequential version of the algorithm and show a good enhancement in terms of the running time and system performance. Another implementation was done on a multi-core processor by dividing the graph into a set of subgraphs where each sub graph runs on its own thread. The results show a better enhancement in the running time when compared with the time needed to find maxflow value with a sequential version of the maxflow-Genetic.

As a future work, another heuristic, meta-heuristic or evolutionary algorithm could be used to find the maximum flow problem, like Chemical Reaction Optimization algorithm. The parallel implementation of the algorithm could be compared with the proposed one, and the results will be compared in terms of accuracy and performance.

REFERENCES

[1] Zhipeng Jiang, Xiaodong Hu, and Suixiang Gao, “A Parallel Ford-Fulkerson Algorithm For Maximum Flow Problem’.

[2] Munakata, T. and Hashier, D.J. “A genetic algorithm applied to the maximum flow problem”, Proc. 5thInt. Conf. Genetic Algorithms, 1993, pp. 488-493.

[3] Ford jr., L.R., Fulkerson, D.R., “Maximal flow through a network”. Can. J. Math. 8(3), 1956, pp. 399-404.

[4] L.R. Ford, Jr. and D.R. Fulkerson, Flows in Networks, Princeton, NJ: Princeton University Press, 1962.

[5] T. H. Cormen, C. E. Leiserson, R. L. Rivest and C. Stein, Introduction to Algorithms, 3rd ed., The MIT Press, 2009.

[6] http://www.iman1.jo/iman1/, Accessed on (2014) July 10.

[7] M. Jeon and D. Kim, “Load-Balanced Parallel Merge Sort on Distributed Memory Parallel Computers”, Proceedings of the IEEE International Parallel and Distributed Processing Symposium, IPDPS.02, (2002).

[8] M. Saadeh, H. Saadeh, M. Qatawneh, "Performance Evaluation of Parallel Sorting Algorithms on IMAN1 Supercomputer" , International Journal of Advanced Science and Technology Vol.95 (2016), pp.57-72.

[9] Dinic, E.A., "Algorithm for solution of a problem of maximum flow in networks with power estimation". Sov. Math. Doklady. 11(8), 1970, pp. 1277-1280.

[10] R.K. Ahuja, T. L. Magnanti, and J. B. Orlin., Network Flows: Theory, Algorithms, and Applications, Prentice Hall, 1993.

[11] V. King, S. Rao, and R. Tarjan, "A faster deterministic maximum flow algorithm", In Proceedings of the 8th Annual ACM–SIAM Symposium on Discrete Algorithms, 1992, pp. 157–164.

[12] J.A. McHugh, Algorithmic Graph Theory, Englewood Cliffs, NJ: Prentice-Hall 1990, Chapter 6.

[13] R.Barham, A.Sharieh, A.Sliet. "Chemical Reaction Optimization for Max Flow Problem", (IJACSA) International Journal of Advanced Computer Science and Applications, Vol. 7, No. 8, 2016.

[14] MahmoodA.Rashid,M.A.HakimNewton,Md.TamjidulHoque, AbdulSattar, "Mixing Energy Models in Genetic Algorithms for On-Lattice Protein Structure Prediction", Hindawi Publishing Corporation Bio Med Research International, Volume 2013,Article ID 924137,15 pages.

Design of a High Speed Architecture of MQ-Coder for JPEG2000 on FPGA

Taoufik Salem Saidani
Department of Computer Sciences
Faculty of Computing & Information Technology
Northern Border University, Rafha, Saudi Arabia

Hafedh Mahmoud Zayani
Department of Information System
Faculty of Computing & Information Technology
Northern Border University, Rafha, Saudi Arabia

***Abstract*—Digital imaging is omnipresent today. In many areas, digitized images replace their analog ancestors such as photographs or X-rays. The world of multimedia makes extensive use of image transfer and storage. The volume of these files is very high and the need to develop compression algorithms to reduce the size of these files has been felt.**

The JPEG committee has developed a new standard in image compression that now also has the status of Standard International: JPEG 2000. The main advantage of this new standard is its adaptability. Whatever the target application, whatever resources or available bandwidth, JPEG 2000 will adapt optimally. However, this flexibility has a price: the JPEG2000 perplexity is far superior to that of JPEG. This increased complexity can cause problems in applications with real-time constraints. In such cases, the use of a hardware implementation is necessary. In this context, the objective of this paper is the realization of a JPEG2000 encoder architecture satisfying real-time constraints. The proposed architecture will be implemented using programmable chips (FPGA) to ensure its effectiveness in real time. Optimization of renormalization module and byte-out module are described in this paper. Besides, the reduction in computational steps effectively minimizes the time delay and hence the high operating frequency.

The design was implemented targeting a Xilinx Virtex 6 and an Altera Stratix FPGAs. Experimental results show that the proposed hardware architecture achieves real-time compression on video sequences on 35 fps at HDTV resolution.

***Keywords*—MQ-Coder; High speed architecture; FPGA; JPEG2000; VHDL**

I. Introduction

The current development of computer networks and the dramatic increase in the speed of processors reveal many new potentialities for digital imaging. Whether in the medical, commercial or military field, new applications are emerging each with its specificities. The JPEG Group has developed a new, more flexible and better image encoding standard: JPEG2000 [1]. It is built around a wide range of image compression and display tools. This makes the algorithm appealing to many applications, whether for Internet broadcasting, medical imaging or digital photography [2].

The main JPEG2000 coding steps are shown in Fig. 1. Several features are available for encoding, such as progressive quality and/or resolution reconstruction, fast random access to compressed image data, and the ability to encode different regions of the image called regions of interest (ROI).

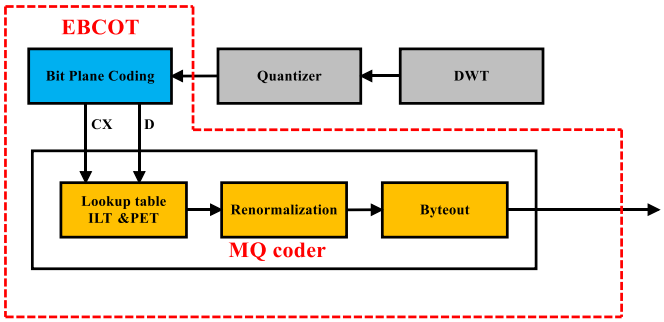

Fig. 1. Overview of JPEG2000 coding process.

The JPEG2000 standard can be broken down into several successive blocks. The original image is cut into tiles after the component transformation. All the tiles are then transformed into wavelets (transformation with or without loss), independently of each other [3]. The wavelets used in the JPEG2000 standard are bi-orthogonal, that is to say different wavelets are used for decomposition and reconstruction. Two types of bi-orthogonal wavelets are used: wavelets of Daubechies 9/7 and Le Gall 5/3 [4], [5]. These two wavelets are chosen according to the type of compression desired, lossless or lossy. Le Gall 5/3 wavelets used to perform a reversible transform are used for lossless compression. The wavelets of Daubechies 9/7 allowing realizing a reversible transform are used only for lossy compression.

The coefficients of the block-code undergo quantization and the quantized coefficients are decomposed into bit planes. The quantification minimizes the number of bits necessary for coding the supplied coefficients of the preceding block, by retaining only the minimum number of bits making it possible to obtain a certain quality level [6], [7].

Based on the wavelet decomposition technique, JPEG2000 is very different from previous standards and has many advantages that will allow it to be adopted in a wide range of applications, or even to be extended to video encoding. In contrast, this type of compression requires much more computational power than the original JPEG process, which makes software implementations irrelevant when very fast processing is required. Fig. 2 shows the comparison between JPEG and JPEG2000 in terms of performance. We note that the performance of JPEG2000 is greater than those of JPEG standard.

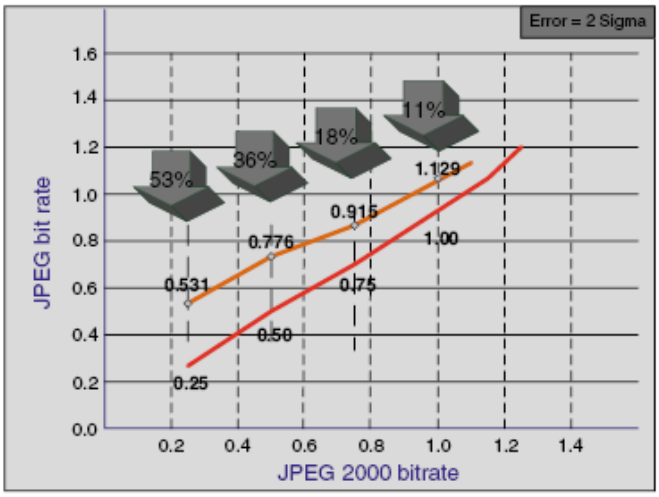

Fig. 2. Comparison between JPEG and JPEG2000 in terms of performance.

Due to many successive processes, JPEG2000 requires more computing power to achieve encoding and decoding speeds similar to JPEG. A hardware solution is therefore indispensable for fast applications.

The JPEG2000 image compression standard was created to meet the new requirements arising from the diversification of applications in the multimedia field. The many features that it offers bring a new breath to this sector. However, they have led to an increase in the complexity of the algorithm compared with existing standards. Faced with this complexity, a hardware encoder is the solution that allows satisfying the real-time constraints of certain applications.

This paper presents an FPGA-based accelerator core for JPEG2000 encoding. Comparison with various FPGA implementations is provided.

Contributions in this work are listed as follows:

1) The proposed high speed efficient MQ-coder architecture modifies the probability estimation (Qe) representation to minimize the memory consumption. The modification in probability estimation reduces the bitwise representation to 13 bit.

2) Due to the less memory occupation, the time and power required for the hardware-based JPEG2000 compression are reduced. Thereby, the operating speed is improved (more operating frequency) with the help of proposed MQ encoder for real time image processing.

3) The minimization in bitwise representation in proposed architecture of MQ coder reduces the count of memory elements to (32 9 13) 416 that leads to the preservation of silicon (Si) area further in the compact chip development.

4) The optimization of Renormalization and Byteout modules help speeding up the proposed architecture.

The remainder of this paper is decomposed into six sections. After the introduction, Section 2 details the JPEG2000 MQ encoder. Previously proposed hardware architectures for MQ-coder are described in Section 3. Section 4 describes the proposed hardware architecture of MQ coder. In Section 5, experiments and results are detailed. Finally, this paper is concluded in Section 6.

II. JPEG2000 MQ-CODER

The arithmetic coder used in JPEG2000, called the MQ encoder, takes as inputs the binary values D and the associated contexts CX resulting from the preceding step of binary modeling of the coefficients, and this in the order of the coding passes. Fig. 3 shows the arithmetic encoder inputs and outputs.

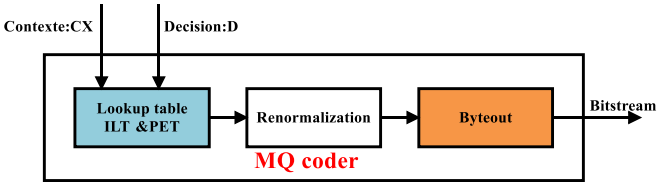

Fig. 3. The inputs and outputs of MQ-Coder.

Rather than representing the intervals associated with the probabilities of “0” or “1”, it was chosen to represent the data using the LPS (Less Probable Symbol) and MPS (More Probable Symbol) symbols, respectively representing the probabilities occurrence of the minority and majority species. Obviously, it is necessary to keep track of the meaning attributed to one or the other of the variables “0” or “1” is the minority species.

Thus the current interval is represented by the interval 1, which is then divided into two sub-intervals corresponding to the minority and majority species. From a representation point of view, LPS is always given as a lower interval. Each binary decision, represented by a bit, is divided recursively. The divisions are made to estimate the probability of Elias: MPS and LPS.

The binary sequence from the MQ is divided into a number of packets. Each of them contains the bit-stream corresponding to the same component, the same resolution level, the same quality layer and the same spatial zone of the resolution level. The spatial areas of each resolution level are called precincts. Each of the packets is preceded by a header containing information allowing identifying very precisely the data conveyed by this packet.

Four different progress orders are defined in JPEG 2000. They make it possible, during the decoding, to obtain in priority either the data of the same component, or those of the same resolution level, or those of the same quality layer, or those of the same spatial zone of the image.

In JPEG2000, the realization of the arithmetic coder is performed by means of an index table. The table represents the LPS probability estimate (Qe). For each input pair (decision, context), we look for the most probable symbol in a variable containing the different states. As each state is represented in the index table, the context can be associated with the index of the table. On its side, the decoder has the index replica of the table, which makes it possible to carry out the decoding.

The Finite state Machine (FSM) with 47 states defines the Probability Estimation Table structure clearly. The number of calculations to obtain the coding information and the utilization of resources are high that degrade the hardware performance. The hardware modeling of MQ-coder contains the following limitations:

5) Low clock frequency.
6) Consumption of LUTs and registers is more.
7) High hardware resource requirements.

A large number of context and decision pairs in MQ encoder shift the parallel operation into a serial operation; such a new architecture is called high-speed MQ encoder architecture. The storage of transformed coefficients in code block consumes more registers that lead to large flip-flop (FF) requirement. Hence, the reduction in code block based on the context pair probability estimation reduces the number of lookup tables (LUTs) and slice registers that leads to less memory consumption. The motivation behind the research work proposed in this paper is the reduction in memory, time and power consumption by reducing the size of the bitwise representation.

III. Related Works

The main advantage of JPEG 2000 was to combine most of these qualities, allowing using it in a very wide range of applications. This flexibility, coupled with a very high compression efficiency, unfortunately has a price. Moreover, some applications have real-time aspects which impose very high flow constraints.

An architecture composed of three stages is proposed by Mei *et al*. in [5]. When implemented on an APEX20K FPGA board, it operates with 37.27 MHz. Indeed in this architecture, if the state MPS occurs then two symbols will be coded simultaneously, if not a single symbol will be coded.

Shi *et al*. [8] proposed a MQ-coder hardware core that allows treating two symbols. Indeed, this architecture is based on the following hypothesis: a maximum of two offsets occurs when there is a renormalization operation. The architecture proposed in [9] is composed by three blocks. The first block is responsible for initializing register A at 0x8000, register C at 0, table MPS (Cx) at 0 and index table in ILT RAM, and perform all arithmetic operations. The second block is used to shift the registers A and the register C and to decrement the counter CT by 1. If CT = 0, the third block will be activated and the register B will be emitted as compressed data. The proposed architecture was implemented on a Startix FPGA and works at a frequency of 83.271 MHz.

The complexity of the JPEG 2000 algorithm is a problem for these real-time applications. In [10], the author indicates that in view of current technology, it is not possible for purely software implementations to respect the constraints imposed by these real-time applications. This is the reason why a growing number of companies and researchers are interested in (partially) hardware-related achievements of the standard, in which the computing resources have been optimized and the memory requirements reduced.

Below we give an overview of the hardware achievements to date and the results obtained.

As part of the PRIAM project, Thales Communications has developed an implementation of a JPEG 2000 encoder on an MPC74XX processor. This is studied in [11]. The MPC74XX processor is based on a PowerPC architecture (RISC type processor) to which is added a vector calculation unit called AltiVec. This allows multiple data sets to be processed in parallel in a single instruction.

Unlike the other blocks in the decoding chain, the entropy coder, due to its non-systematic behavior, is complex to optimize by means of vectorial instructions. This achievement gives overall very good results, but the entropy coder, requiring 400 cycles per 8-bit pixel, is truly the “bottleneck” of the system.

Bonaldi [12] has been working on the creation of a mixed software-hardware encoder. The medium used is the ARM-VIRTEX card of the DICE unit. An input rate of 6.6 Mbps for the entropy encoder is especially supported. Moreover, everything concerning the formation of the bit-stream is carried out in software, on the ARM. This approach of Co-Design is very judicious and is moreover widely supported by the literature.

The Amphion company offers an ASIC encoder-decoder available since 2003 [13]. Amphion announces speeds of 480 Mbps at encoding and 160 Mbps at decoding. This embodiment has interesting characteristics, such as the few constraints on the format of the input images, a division of tasks between hardware and software and an architecture compatible with the AMBA bus, which allows easy integration into other systems.

Analog devices [14] offer the ADV-JP2000. This circuit operates at a maximum 20 MHz frequency including a 5/3 wavelet transform (no 9/7) and an entropy encoder. The circuit is not fully compliant with the standard. The ADV-JP2000 offers two modes of operation: encodes and decodes. In the encode mode it accepts a single tile and generates the stream of code-blocks conforming to the standard. The ADV-JP2000 communicates via an asynchronous protocol but also allows an interrupt mode. Finally, the circuit supports the DMA mode.

Zhang *et al*. [15] proposed an architecture composed of four stages and three parts (P1, P2, P3). Indeed, P1 is implemented in Stage 1 to determine the new value of Qe when A < (0x8000). The P2 is called in Stage 2 and Stage 3, because the latter updates the Reg A and Reg C and also to perform the arithmetic operations and the offset operations. Finally, the P3 is used in Stage 4 to realize the bit stuffing when the counter CT is equal to 0. The processing frequency of this architecture was 110 MHz on an Altera FPGA card.

IV. Proposed Architechture

The proposed architecture of the encoder is shown by the block diagram of Fig. 4. The pairs (C, D) are received by the MQ coder as input and a sequence of bytes called ByteOutReg are provided as output. This architecture consists of two parts: the part of the prediction of the probability of the symbol to be

coded composed of 2 RAMs (ICX, MPS) and 4 ROMs (NMPS, NLPS, Switch, Qe), and the coding part which is composed of a state machine.

The four ROMs are not updated during coding operation. The pairs (CX, D) are first sequentially read. Subsequently, the CX context will be transmitted over the bus address of the ICX RAM and the MPS RAM. Then the value of I(CX) and MPS(CX) will be read. Then the I(CX) index will be delivered to the four ROMs. The mps_D will be executed with signal D, which causes the LPS_en signal to be generated. If this signal is equal to one then the CODELPS state will be carried out otherwise the CODEMPS state will take place.

The updating of the ICX RAM depends essentially on the signal Ren_out. Indeed this signal will set to one if the renormalization is carried out. However, the MPS RAM will update if the LPS_SW signal is equal to one. The Probability estimation architecture is shown in Fig. 5.

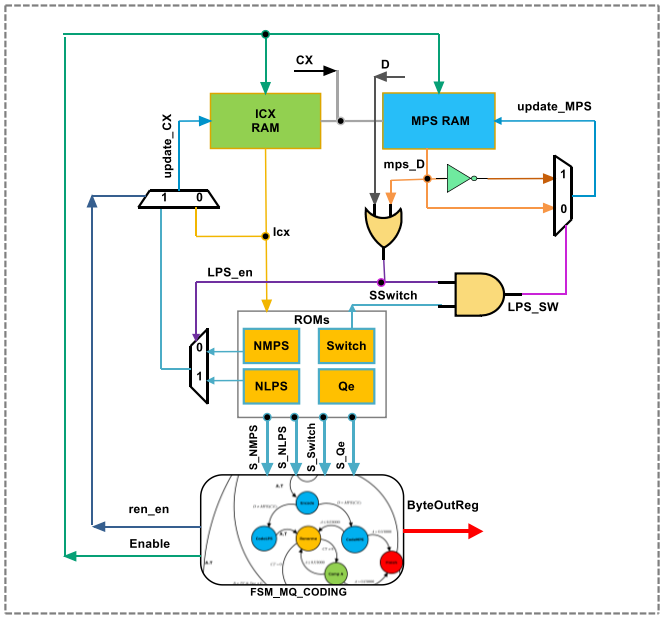

Fig. 4. MQ-Coder architecture.

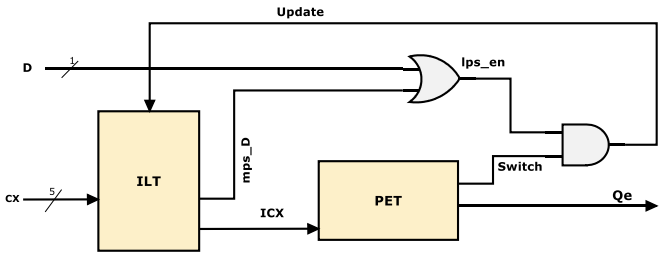

Fig. 5. Probability estimation architecture.

We are then interested in the coding part to manage the process of the coding by a machine of finite states by substituting the various sub-algorithms by states. The outputs depend on the current state and the inputs and react directly to changes in inputs. Fourteen states have been set up in order to describe the MQ encoder process. Fig. 6 shows the MQ-Coder state machine. The states used in this state machine are as follows:

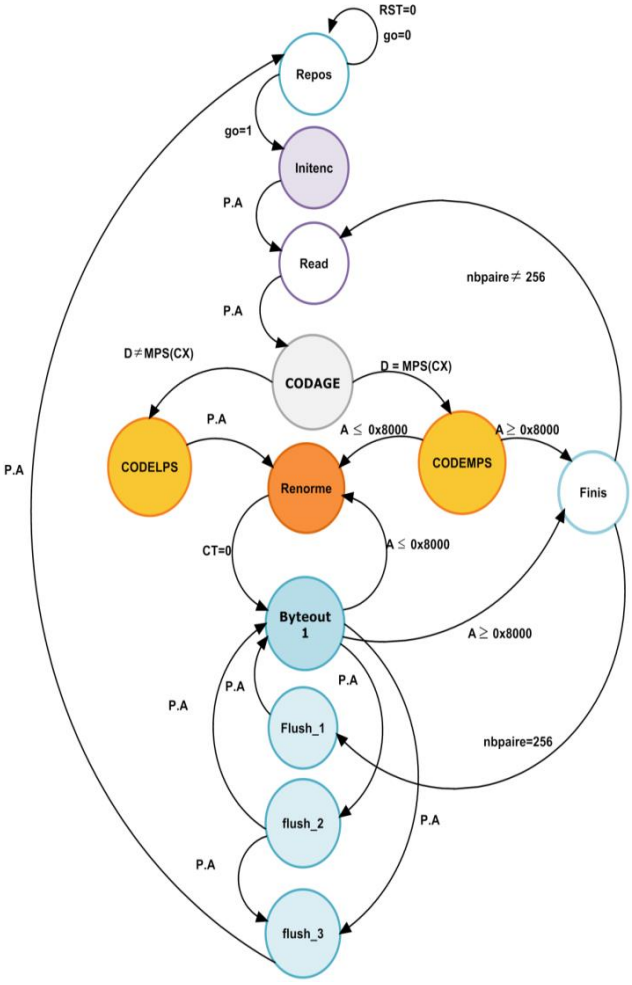

Fig. 6. MQ-Coder State machine.

8) **Repos:** This state essentially depends on the input "go", if go = 1 it switches to the state INITENC otherwise it remains in the same state.

9) **Initenc**: In this state, register Reg_A at (0x8000), register Reg_C at 0 and counter CT at 12 are initialized. Then the MPS RAM is filled with 0s and the RAM of the indexes by the 19 possible values of the context CX. Then you will automatically play (Read). The index/probability tables should be presented in the memory before coding begins.

10)**Read:** In this state, the context is read to deduce the value of the corresponding MPS (Cx) according to the table initialized in INITENC. We also read Decision D.

11)**CODAGE**: If Decision D = MPS (Cx), it switches to the CODEMPS state otherwise it goes to the CODELPS state.

12)**CODEMPS**: The register Reg_A is adjusted to Qe_reg. Then Reg_A is compared to (0x8000). If Reg_A is less than (0x8000), the index will be updated according to the NMPS table of the context index and the Renorme state will be used. If register Reg_A is greater than (0x8000), we add

the probability Qe_reg to the register Reg_C and we will pass to the Finis state.

13)**Finis**: In this state if the even number (number of pairs (CX, D) lu) is equal to 256 then we pass to the flush state, otherwise the next state will be Read.

14)**CODELPS**: In this state, register Reg_A to Reg_A-Qe_reg is adjusted. Then, if Reg_A is greater than Qe_reg then the register Reg_A takes the value of Qe_reg, otherwise we add the probability Qe_reg to the register Reg_C. The condition of inversion of the intervals is always checked. If a SWITCH is required, the direction of the MPS will be reversed. The index will take a new value according to the NLPS table and it will change to the Renorme state.

15)**Renorme**: The contents of Reg_A and Reg_C will be replaced by a simple left shift. This shift repeats until the value of Reg_A is raised above (0x8000). The counter CT containing the number of shifts of Reg_A and Reg_C will then be decremented at each offset. When the counter CT reaches 0 (CT was initially at 13, i.e., 13 left offsets were made at Reg_A and Reg_C), it will pass to byteout1 and if Reg_A is still less than (0 x 8000), we will return to the Renorme state as soon as we have finished with byteout. The optimization of the Renormalization procedure is presented in Fig. 7.

16)**Byteout1**: This state can be called in two states either in the Renorme state when the shift counter CT becomes equal to zero, or also at the end of the coding when the registers flush. The optimization of the Byteout procedure is presented in Fig. 8.

17)**FLUSH**: This is the state we reach towards the end of the encoding (in our case if nbpair = 256). The FLUSH procedure contains two calls to Byteout1 and two calls to Setbit; hence, the idea of subdividing it into three states: the first is flush_1 which ends with a call to byteout1, the second is flush_2 (same principle of fulsh_1) and the third is flush_3.

a) **Flush_1**: This state contains two sub-states, the first is the Setbit, the second is byteout1. First we make a call to the state Setbit then we apply an offset to the register Reg_C, then we make a call to byteout1 and we end by making a call to flush_2.

i) **Setbit:** In this state, the Reg_C register shift is automatically changed to byteout1, regardless of the Reg_C register value (i.e., Reg_C is lower or higher than TEMPC).

b) **Fluch_2**: This state has the same principle of the state flush_1 but this time we pass to state flush_3.

c) **Flush_3:** This state contains the end of the flush, when the first end marker 0xFF has to be inserted. The next state will be rest.

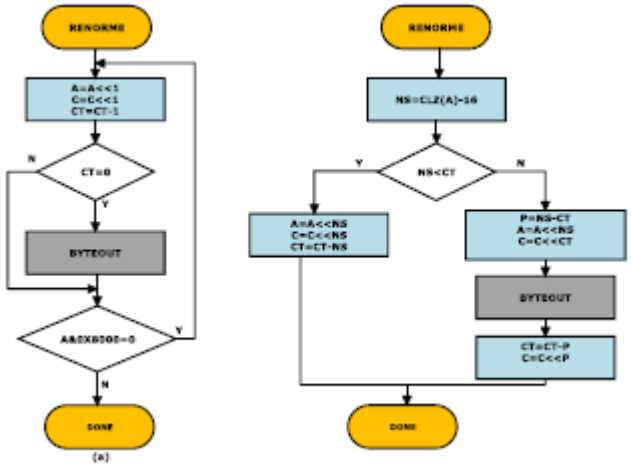

Fig. 7. (a) Original RENORME architecture (b) Optimized RENORME architecture.

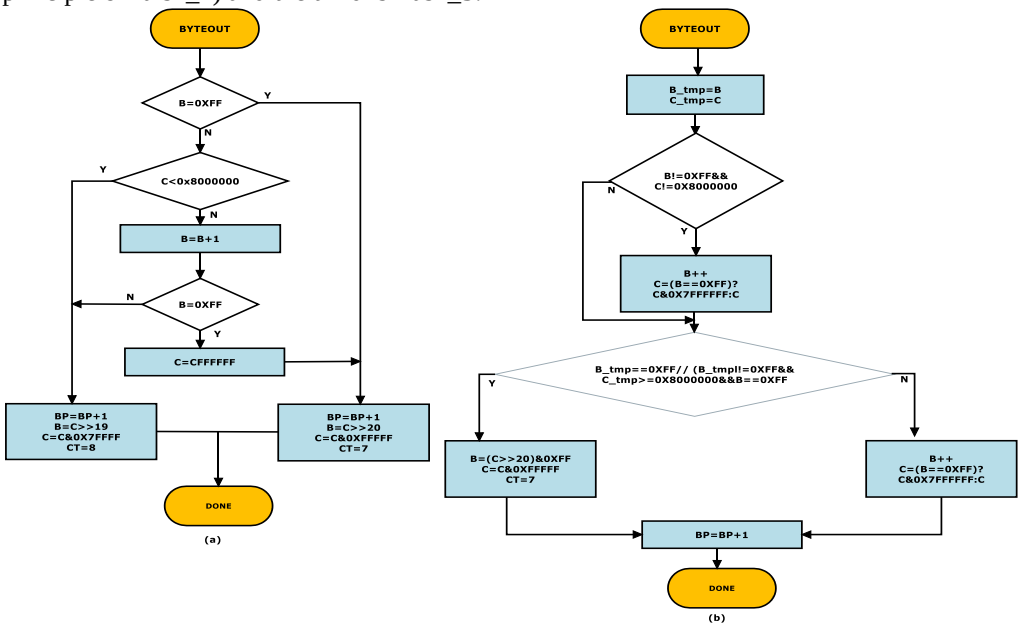

Fig. 8. (a) Original BYTEOUT architecture (b) Optimized BYTEOUT architecture.

V. Experimental Results

A. Simulation

Simulation of the proposed design, using VHDL HDL, is carried out with Mentor graphic.

ByteOutReg bytes coincide with those in column B and the parameters IDCX, MPS, Qe_reg, Reg_A, Reg_C and Reg_CT have evolved appropriately. This result has been well verified and we have chosen to take a sequence to visualize it in simulation and explain it in parallel. For the sake of clarity in Fig. 9, we have chosen to display some signals in the simulation flow that are the following: the compressed data Byteout_Reg, the index IDCX, the counter Reg_CT, the probability Qe_reg and states. Table 1 summarizes the simulation results of the MQ encoder: either from decision n° 28 to decision n° 34.

B. Synthesis Results

Implementation of the proposed design was made on Xilinx Virtex Family Platforms: XC6SLX75T, XC5LX30T and XC4VLX80 devices. We have used the Xilinx ISE tools version 14.1 .The synthesis results of the architecture is shown in Table 2. The proposed MQ encoder design gives the best result, in terms of hardware resources such as (the number of LUTs consumed, slices and Flip-Flop) and frequency of operation when implemented on a platform Virtex 6. Concerning the frequencies obtained, we note that our architecture meets the criteria real-time.

The design has a maximum frequency of 423.2MHz on the Virtex 6 (XC6SLX75T) device.

C. Comparison

A comparative study with other existing designs in the literature has been made. The Virtex 4 XC4VFX140 platform is used for this comparison. The performance comparison of our design with the architecture proposed in [16] is shown Table 3. Our proposed design codes frames in real time at a frequency of 244.475 MHz and requires only 455 slices.

The throughput of some architecture of MQ coders compared with our proposed architecture is presented in Table 4. It is calculated from the reported symbol consumption rate and operating frequency. It is found that our architecture encodes frames with a frequency 3.31 and 2.29 times higher than that of architecture [16] and [17] respectively.

Table 5 shows the comparisons of logic area, memory requirement, and estimated memory area of several previous works [5], [7], [15]-[20]. The total area of the proposed architecture is less than that of each previous work. However, the hardware cost of the word based architecture is larger than the proposed architecture. The proposed design can code 40 frames per second for high definition TV of 1920p at 254.84 Mhz on Stratix II.

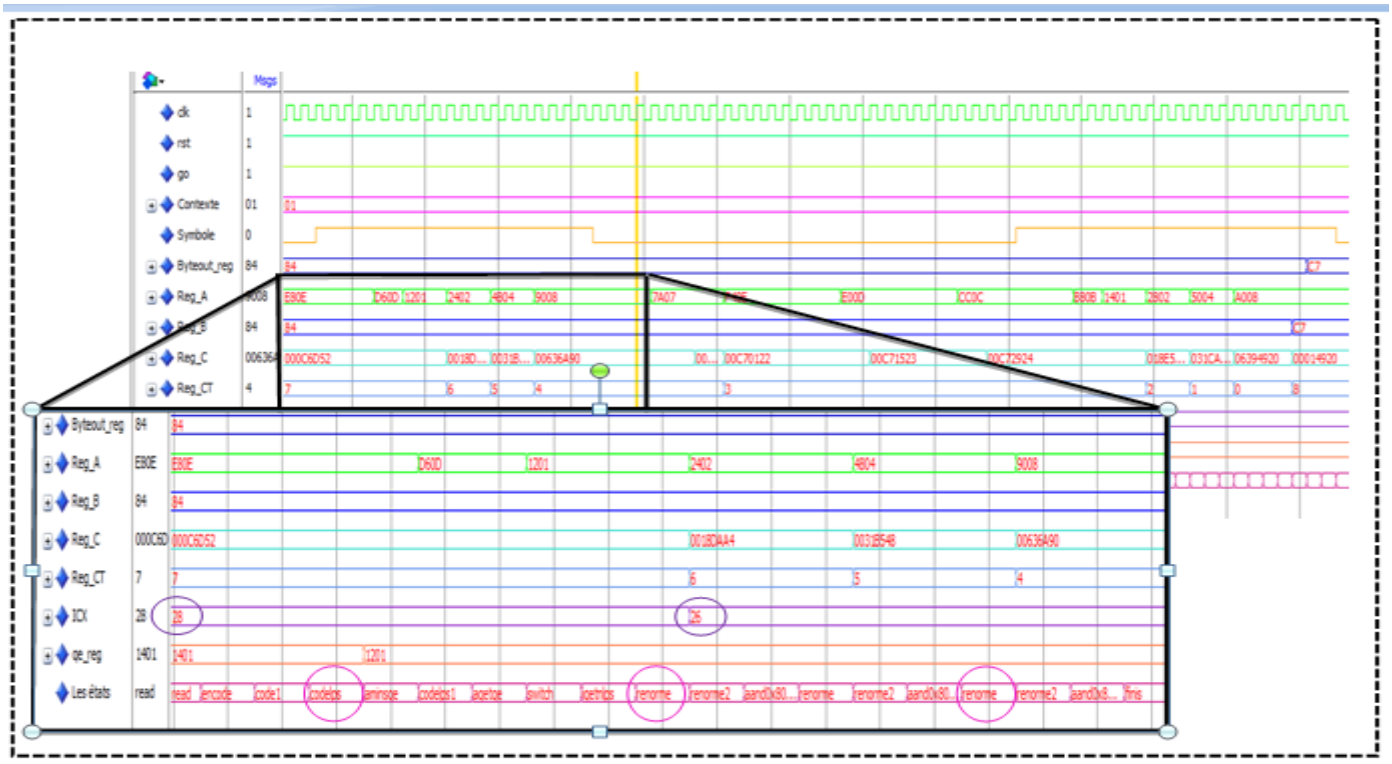

Fig. 9. Wave simulation for MQ coder architecture.

TABLE. I. EXAMPLE EXTRACTED FROM THE SIMULATION OF THE MQ ENCODER

Symbole	D	IDCX	Reg_A	Reg_C	CT	Byteout_Reg
10	1	28	0xE80E	0x000C6D52	7	0x84
11	0	26	0x9008	0x00636A90	4	0x84
12	0	27	0xF40E	0x00C70122	3	0x84
13	0	27	0xE00D	0x00C71523	3	0x84
14	1	27	0xCC0C	0x00C72924	3	0xC7
25	0	25	0xA008	0x00014920	8	0xC7
26	0	25	0x8807	0x00016121	8	0xC7

TABLE. II. RESULTS OF SYNTHESIS

Used Platform	XC6SLX75T	XC5VLX50T	XC4VLX80
Maximum Frequency (MHz)	423.2	336,304	264.2
No. of 4 input LUTs	540/343680	523/28800	766/71680
Total used slices	251/687360	247/28800	396/35840
Total FF slices	177/693	176/659	247/71680

TABLE. III. PERFORMANCE COMPARISON

Used FPGA	XC4VFX140	
Architecture	Proposed	Architecture [15]
Max. Frequency (MHz)	244.475	185.43
Used slices	455	495
Used FF slices	292	392
Used 4 input LUTs	865	893
Used BRAMs	1	2

TABLE. IV. THE THROUGHPUT OF SOME DESIGNS TESTED ON VIRTEX 4 X4VFX140

Used FPGA	XC4VFX140 (Virtex4)		
Design	Number of pairs	Frequency (Mhz)	Throughput (MS/s)
Design [7]	2	50.1	100.2
Design [21]	1	185.43	185.43
Design [18]	1.23	53.92	66.38
Design [19]	2	48.3	96.6
Proposed	1	244.475	244.475

VI. CONCLUSION

This paper discussed the problems in the real-time implementation of FPGA-based MQ coder architecture. The MQcoder utilization in both encoding and decoding stages performs the probability estimation of coefficients and optimization of Renorme and Byteout modules. The increase in computational overhead required more power and energy consumption. This paper provides the reduction in the bitwise computation to reduce the number of computational steps. The minimization in computational steps decrease the power and time delay. The proposed PET architecture reduced the bitwise representation from 13 bit to 12 bit that provided the reduction in memory elements from 416 to 348 compared to the existing MQ-coder architecture. Therefore, the size of PET ROM is 1376 bits. An embedded architecture of MQ Coder for JPEG2000 is designed and implemented in this paper. The implementations carried out during this work allowed us to know that the proposed architecture of the MQ encoder operates with a frequency of 423.2 MHz on Virtex6 XC6SLX4 device and that it can code 40 frames per second for the high-definition TV application. The proposed architecture is easily expandable to 2048×1080 resolution video at 45 fps. It can be used in several applications such as Internet broadcasting, medical imaging and digital photography. Moreover, the processing time was improved by about 13.6% in comparison with well-known architectures from literature.

ACKNOWLDGMENTS

The authors wish to acknowledge the approval and the support of this research study by the grant N° CIT-2016-1-6-F-5718 from the Deanship of the Scientific Research in Northern Border University, Arar, KSA.

TABLE I. COMPARISON WITH OTHER MQ CODER ARCHITECTURES

Architecture	FAGA family	Device used	Clk (MHz)	No. of LEs	Symbol/Clk	Throughput (MS/s)
[5]	APEX20K	EP20K600EFC672-3.	37.27	1256	2	74.54
[7]	Stratix	N/A	50.10	1596	2	100.2
[15]	Stratix	N/A	40.53	12649	2	81.6
[20]	Stratix II	EP2S15F484C3	106.2	1321	2	212.4
[22]	APEX20K	EP20K1000EFC672-1X.	9.25	14711	1	9.25
[23]	Stratix	N/A	27.05	761	1	57.05
[24]	Stratix	N/A	106.02	1267	2	210
[16]	Stratix	EP2S90F1020I4.	58.56	1488	2	117
[17]	Stratix	EP1S10B672C6.	145.9	824	1	145.9
Proposed	Stratix II	EP2S15F484C3	254.84	603	1	254.84

REFERENCES

[1] JPEG 2000 image coding system, ISO/IEC International Standard 15444-1. ITU Recommendation T.800, (2000).

[2] D. S. Taubman and M. W. Marcellin. JPEG2000 Image Compression Fundamentals, Standards, and Practice (2002).

[3] T. Acharya and P. Tsai, JPEG2000 Standard for Image Compression: Concepts, Algorithms and VLSI Architectures, J. Wiley & sons (2005).

[4] JASPER Software Reference Manual, ISO/IEC/JTC1/SC29/WG1N2415.

[5] K. Mei, N. Zheng, C. Huang, Y. Liu, Q. Zeng, VLSI design of a high-speed and area-efficient JPEG 2000 encoder, IEEE Transactions on Circuits and Systems for Video Technology 17 (8) (2007) 1065–1078.

[6] Horrigue, L., Saidani, T., Ghodhbani, R., Dubois, J., Miteran, J.,Atri, M.: An efficient hardware implementation of MQ decoder of the JPEG2000. Microprocess. Microsyst. 38, 659–668 (2014)

[7] L. Liu, N. Chen, H. Meng, L. Zhang, Z. Wang, H. Chen, A VLSI architecture of JPEG 2000 encoder, IEEE Journal of Solid-State Circuits 39 (11) (2004) 2032–2040.

[8] Jiangyi Shi, Jie Pang, Zhixiong D Yunsong Li. A Novel Implementation of JPEG2000 MQ-Coder Based on Prediction, International Symposium on Distributed Computing and Applications to Business, Engineering and Science, 2011. pp:179-182.

[9] Kishor Sarawadekar and Swapna Banerjee, VLSI design of memory-efficient, high-speed baseline MQ coder for JPEG 2000, Integration, the VLSI Journal, Elseiver. Vol 45, January 2012, Pages 1-8. DOI: 10.1016/j.vlsi.2011.07.004.

[10] J. Hunter. Digital cinema reels from motion JPEG 2000 advances, janvier 2003. http ://www.eetimes.com/story/OEG20030106S0034.

[11] C. Le Barz and D. Nicholson. Real time implementationof JPEG 2000 . june 2002.

[12] C. Bonaldi and Y. Renard. Conception et réealisation d'un codeur JPEG 2000 sur une carte Virtex-ARM . Laboratoire de Microélectronique (DICE), UCL, june 2001.

[13] Amphion. CS6590 JPEG 2000 codec preliminary product brief , October 2002. http ://www.amphion.com.

[14] D.Taubman and M.W.Marcellin, JPEG2000 - Image Compression Fundamentals, Standards and Practice, Kluwer Academic Publishers, Nov. 2001.

[15] K. Liu, Y. Zhou, Y. Song Li, J.F. Ma, A high performance MQ encoder architecture in JPEG2000, Integration, the VLSI Journal 43 (3) (2010) 305–317.

[16] P. Zhou, Z. Bao-jun, High-throughout hardware architecture of MQ arithmetic coder, in: 10th IEEE International Conference on Signal Processing (ICSP), 2010.

[17] K. Sarawadekar, S. Banerjee, An Efficient Pass-Parallel Architecture for Embedded Block Coder in JPEG 2000 . IEEE Trans. Circuits Systems. Video Technology, 22 (6) (2011) 825-836.

[18] Michael Dyer, David Taubman and Saeid Nooshabadi. Concurrency Techniques for Arithmetic Coding in JPEG2000. IEEE Transactions on Circuits and Systems for Video Technology, 2006, vol.53, pp. 1203–1213.

[19] Kishor Sarawadekar and Swapna Banerjee, "LOW-COST, HIGHPERFORMANCE VLSI DESIGN OF AN MQ CODER FOR JPEG 2000" ICSP2010, 2010, pp.397-400.

[20] Nandini Ramesh Kumar · Wei Xiang · Yafeng Wang, Two-Symbol FPGA Architecture for Fast Arithmetic Encoding in JPEG 2000, Journal of Signal Processing Systems, 69(2)(2012)213–224.

[21] Saidani, T., Atri, M., Khriji, L., Tourki, R.: An efficient hardware implementation of parallel EBCOT algorithm for JPEG2000. J. Real-Time Image Process. 11, 1–12 (2013).

[22] Varma,H.Damecharla,A.Bell,J.Carletta,G.Back,A fast JPEG2000 encoder that preserves coding efficiency:the splitarithmetic encoder, IEEE Transactions on Circuits and Systems—Part I:RegularPapers55(11)(2008) 3711–3722.

[23] M. Dyer, S. Nooshabadi, D. Taubman, Design and analysis of system on a chip encoder for JPEG 2000, IEEE Transactions on Circuits and Systems for Video Technology 19 (2) (2009) 215–225.

[24] N.R. Kumar, W. Xiang, Y. Wang, An FPGA-based fast two-symbol processing architecture for JPEG 2000 arithmetic coding, in: IEEE International Con- ference on Acoustics Speech and Signal Processing (ICASSP) 2010, 2010, pp. 1282–1285.

One-Year Survival Prediction of Myocardial Infarction

[1]Abdulkader Helwan, [2]Dilber Uzun Ozsahin
[1,2]Department of Biomedical Engineering, Near East University, Near East Boulevard, TRNC, Nicosia, 99138 Cyprus

[3]Rahib Abiyev, [4]John Bush
[3,4]Department of Computer Engineering, Near East University, Near East Boulevard, TRNC, Nicosia, 99138 Cyprus

***Abstract*—Myocardial infarction is still one of the leading causes of death and morbidity. The early prediction of such disease can prevent or reduce the development of it. Machine learning can be an efficient tool for predicting such diseases. Many people have suffered myocardial infarction in the past. Some of those have survived and others were dead after a period of time. A machine learning system can learn from the past data of those patients to be capable of predicting the one-year survival or death of patients with myocardial infarction. The survival at one year, death at one year, survival period, in addition to some clinical data of patients who have suffered myocardial infarction can be used to train an intelligent system to predict the one-year survival or death of current myocardial infarction patients. This paper introduces the use of two neural networks: Feedforward neural network that uses backpropagation learning algorithm (BPNN) and radial basis function networks (RBFN) that were trained on past data of patients who suffered myocardial infarction to be capable of generalizing the one-year survival or death of new patients. Experimentally, both networks were tested on 64 instances and showed a good generalization capability in predicting the correct diagnosis of the patients. However, the radial basis function network outperformed the backpropagation network in performing this prediction task.**

Keywords*—Machine learning; myocardial infarction; backpropagation; radial basis function network; generalization; one-year survival prediction

I. Introduction

Myocardial is simply described as thick muscular wall of the heart whereas, infarction is simply referred to dead portion of tissue caused by loss of blood supply; a localized necrosis. Hence, myocardial infarction describes the dead portion of thick muscular wall of the heart induced by a loss of blood supply. In cardiovascular system, the heart is the main organ which also includes different types of blood vessels. Coronary arteries are some of the most important vessels in cardiovascular system. These arteries take oxygen-rich blood to the heart as well as all other organs in the body. Gradual buildup of plaque blocks or narrows the arteries as a result; the blood flowing to the heart decreases significantly or stops completely. This may lead to myocardial infarction.

Irreversible necrosis in acute myocardial infarction of heart muscle secondary to prolonged ischemia is the most deadly presentation of coronary arteries disease. Usually, imbalance between oxygen supply and demand leads to infarction which is most often caused by thrombus formation and plaque rupture in a coronary vessel, leading to an acute reduction in the blood supply to a portion of the myocardium [1]. Myocardial infarction may lead to diastolic or systolic dysfunction and may increase the susceptibility to arrhythmias and other complications such as ischemic, mechanical, embolic and inflammatory disturbances [2]. Because of the high cost of care, effective drugs and treatments, the prevention of myocardial infarction is a desirable goal. To predict the likelihood of myocardial infarction many factors such as laboratory data, history and physical examination findings are used. Some of the results have been hopeful but none of these studies were successful in accurately predicting the likelihood of myocardial infarction [3], [4].

At some point in the past, the myocardial infarction patients suffered heart attacks. Some patients survived and are still alive but some died since they could not withstand the attack. Researchers that studied this problem addressed the prediction from the other variables whether or not the patient will survive or not for at least one-year.

The proposed research is targeted to investigating the use of backproagation neural network (BPNN) and radial basis function network (RBFN) in learning the past clinical and historical data of patients who had myocardial infarction and use them to generalize or predict the one-year survival or death of new patients. Acknowledging the importance of the prediction of survivals after myocardial infarction as well as the lack of sufficient studies designed to test methods of prediction, the implementation of this research work prompts to compare the capability of two types of neural networks to perform this prediction task, i.e. predict the one-year survival of patients who have myocardial infarction.

Both networks are trained using data of some patients who suffered myocardial infarction. These data include some historical attributes that show if patients have survived or not for one year. Other attributes are correspondent to some medical variables that indicate some abnormalities in patient vital conditions. This helps the networks to learn historical and medical data of both types of patients, i.e., the ones who survived at one year and those who died before or at one year. Both networks are evaluated and showed a good capability in predicting the one-year survival or death of myocardial infarction patients when tested on unseen data.

II. The Proposed Methodology

Artificial neural networks have opened new horizons in learning about the natural history of diseases and predicting

cardiac disease. In this work, we propose the use of two types of artificial neural networks to predict the one-year survival of patients who suffer myocardial infarction. All the patients suffered heart attacks at some point in the past. Some are still alive and some are not. Therefore, this work is to develop an intelligent system that will be trained using a database of many patients who have had myocardial infarction [5]. The database consists of 11 parameters as inputs such as survival period after infarction, a measure of contractility around the heart, etc. The parameters used in the dataset are shown in Table 1. As shown in Table 1 some parameters are historical data such as the survival and still-alive variables, when taken together, indicate whether a patient survived for at least one year following the myocardial infarction. The other attributes are clinical data correspondent to some medical variables which help the network to find differences in the two classes.

For output, one attribute is used to show if the patient has survived for one year or not. Upon training, the system will be capable of predicting whether the patient is going to survive for one year or will die before as shown in Fig. 1.

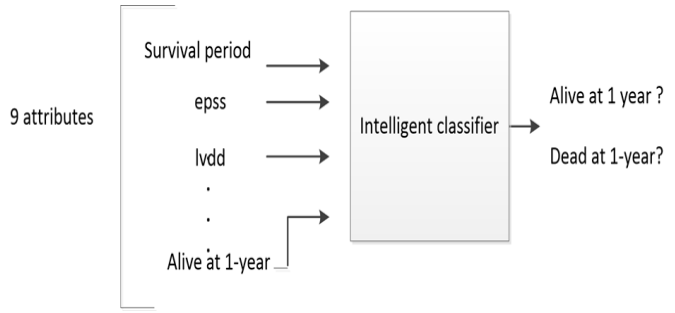

Fig. 1. Proposed prediction system.

A. Database Description

The database consists of 131 cases of different patients obtained for the public online database [5]. The data consist of 13 attributes that indicate the patient's conditions after having myocardial infarction; however, three of them were discarded since they make no sense and don't contribute to the network learning because they have no relation or indication to the myocardial disease. The three attributes are the patient name, group and other derivative variable that has no usage or benefits. Note that it was recommended to discard these three parameters by the database developers. Those parameters are described in Table 1. As seen in Table 1, some attributes are medical variables such as the occurrence of myocardial infarction pericardial-effusion which represents the fluid found around the myocardium, in addition to some other clinical parameters such as the wall-motion-score and wall-motion-index, etc.

Some other attributes such as survival and still-alive can be considered as historical data that show if the patients have survived or not at one year. These two parameters in addition to the other clinical attributes can be enough for the prediction of the one-year survival of myocardial infarction patients.

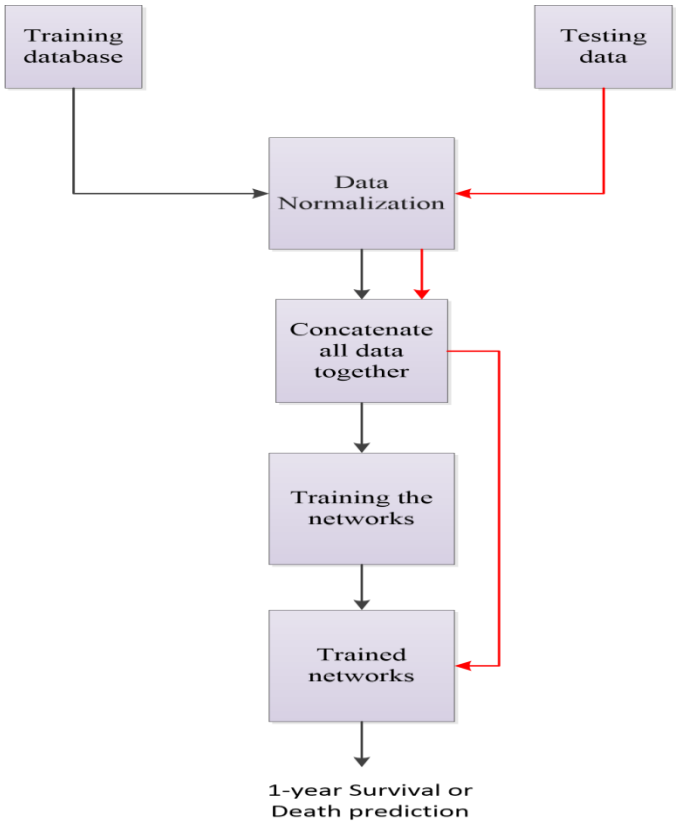

Fig. 2. Flowchart of the developed network system.

Fig. 2 represents a flowchart that illustrates the proposed system for the prediction of one-year survival myocardial infarction.

Input coding

Among the 10 attributes used, 9 are considered as inputs and one as output which is the variable that shows if the patient has survived or not at one year. Basically, the pre-processing stage of the data includes the normalization of input features or attributes into the range of 0 to 1 so that they be suitable to be fed into the networks. Equation (1) shows how the data were normalized. It should be noted that this equation is used in case where the data are all positive; which is our case here.

$$ND = \frac{Parametervalue - \min value}{Rangeof\ attributevalue} \quad (1)$$

Where, ND represents the normalized data.

Output coding

One of the data attributes is used as output since it shows if the patient has survived or not after having myocardial infarction. Therefore, the output was coded such that two neurons are used. Thus, one of these neurons switches on to one of the two classes; survive or not at one year (Table 2).

TABLE. I. DATABASE DESCRIPTION

Attribute	Attribute Description
Survival	The number of months patient survived (has survived, if patient is still alive). Because all the patients had their heart attacks at different times, it is possible that some patients have survived less than one year but they are still alive.
still-alive	A binary variable. 0=dead at end of survival period, 1 means still alive
age-at-heart-attack	Age in years when heart attack occurred
Pericardial effusion	Binary. Pericardial effusion is fluid around the heart. 0=no fluid, 1=fluid
fractional-shortening	A measure of contractility around the heart lower numbers are increasingly abnormal
Epss	E-point septal separation, another measure of contractility. Larger numbers are increasingly abnormal.
lvdd	Left ventricular end-diastolic dimension. This is a measure of the size of the heart at end-diastole. Large hearts tend to be sick hearts.
wall-motion-score	A measure of how the segments of the left ventricle are moving
wall-motion-index	Equals wall-motion-score divided by number of segments seen. Usually 12-13 segments are seen in an echocardiogram.
alive-at-1	Boolean-valued. Derived from the first two attributes. 0 means patient was either dead after 1 year or had been followed for less than 1 year. 1 means patient was alive at 1 year.

TABLE. II. OUTPUT CODING AND CLASSES

Output classes	Coding
Dead at 1-year	[1 0]
Alive at 1-year	[0 1]

III. BPNN TRAINING

The back propagation algorithm is a sort of supervised learning scheme. The neural network that uses such a learning algorithm is referred to as a back propagation neural network. BP algorithm is one of the most popular ANN algorithms. Rojas, (1996) in [6] claimed that BP algorithm could be packed up to four major steps. Once the weights chosen randomly, compute of necessary corrections are done by back propagatio algorithm. The algorithm can be expressed in the followin four steps [7]:

1) Computation of feed-forward.
2) Back propagation to the output layer.
3) Propagation to the hidden layer.
4) Weight updates.

While the function error value may become small enough, the algorithm is stopped. It considers being the basic formula for BP algorithm. With the variations proposed by other scientists, Rojas definition seems to be fairly accurate and simple to follow. The last step, weight updates is happening throughout the algorithm [8]. Equations (2) & (3) are used to update the output-hidden layer weights and input-hidden layer weights, respectively.

$$W_{jh}\,(new) = W_{jh}\,(old) + \eta\Delta_j O_h + \alpha[\partial W_{jh}\,(old)] \quad (2)$$

$$W_{hi}\,(new) = W_{hi}\,(old) + \eta\Delta hO_i + \alpha[\partial W_{hi}\,(old)] \quad (3)$$

Where, δWjh(old) represents the previous weight change, and η is the learning rate. ΔjOh stands for the error signal for output layer neurons, Wjh represent the weights that feed the output layer, and Whi are weights that feed the hidden layer [9].

Furthermore, η stands for the learning rate of the network which should has a value of range between 0 and 1. The α stands for the momentum rate which is added to increase the convergence speed of the network [10]. The backpropagation neural network is trained on 67 of 131 instances of patients who have had myocardial infarction. The number of parameters used in the database is 9; therefore the number of inputs neurons in the input layer is 9 where each one represents a different attribute as shown in Fig. 3. The number of neurons in the input layer is 2 since the proposed system is to classify two classes: death at 1 year, or alive at one year. The number of hidden neurons was taken as 100 by experience.

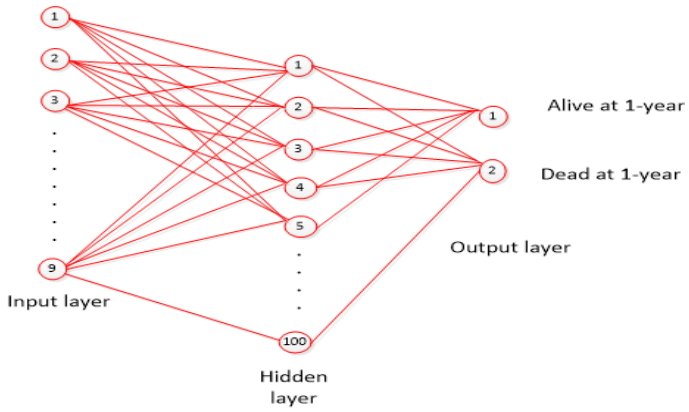

Fig. 3. The BPNN architecture.

Table 3 represents the training and testing set which consists of patients from two classes. It also shows the total number of database instances used for each set.

TABLE. III. TRAINING AND TESTING DATA

Data	Dead	Alive	Total
Training	45	22	67
Testing	44	20	64
Total	89	42	131

The pre-processing of the inputs data take place first in the system so that the data are normalized to values between 0 and 1 before feeding into network. Once the data are normalized, they are fed into a backpropagation neural network, respectively with their targets. Table 4 shows the input parameters values, as well as the training time of the network.

TABLE. IV. INPUT NETWORK PARAMETERS

Network data	Values
Number of training images	67
Number of hidden neurons	100
Activation function	Sigmoid
Learning rate (η)	0.3
Momentum rate (α)	0.7
Epochs	1000
Training time (secs)	20 sec
Mean square error (MSE) reached	0.012

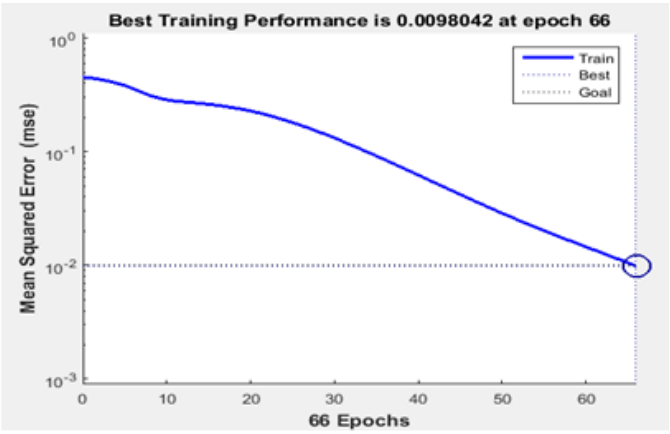

Fig. 4. Error variation with the iteration number (BPNN).

Fig. 4 shows the learning curve of the trained network. It can be seen that the network learned well since the error is decreasing after each epoch or iteration. The network has reached an error of 0.012 at epoch 66 which is good enough for this phase. It should be noted that the time taken for the network to learn and achieve the minimum square error is 20 seconds shown in Table 4.

IV. RBFN TRAINING

A radial basis function network is somehow different from the back propagation neural networks especially, in the way the weights in the hidden layer are updated. The output layer of a RBFN can be seen as that of a BPNN with linear activation functions [10]. Radial functions are simply a class of functions. In principle they could be employed in any sort of model linear or nonlinear and any sort of network single layer or multilayer. The output layer consists of neurons which combine linearly the bases computed in the hidden layer.

The motivation behind RBFN and some other neural classifiers is based on the knowledge that pattern transformed to a higher-dimensional space which is nonlinear is more probable to be linearly separable than in the low-dimensional vector representations of the same patterns (cover's separability theorem on patterns) [11].

The output of neuron units are calculated using k-means clustering similar algorithms, after which Gaussian function is applied to provide the unit final output. During training, the hidden layer neurons are centered usually randomly in space on subsets or all of the training patterns space (dimensionality is of the training pattern) [10]; after which the Euclidean distance between each neuron and training pattern vectors are calculated, then the radial basis function (also or referred to as a kernel) applied to calculated distances. The radial basis function is so named because the radius distance is the argument to the function [12].

$$Weight = RBFN(dis\tan ce) \quad (4)$$

It is to be noted that while other functions such as logistic and thin-plate spline can be used in RBFN networks, the Gaussian functions is the most common. During training, the radius of Gaussian function is usually chosen; and this affects the extent to which neurons have influence considering distance.

The best predicted value for the new point is found by summing the output values of the RBF functions multiplied by weights computed for each neuron [12]. The equation relating Gaussian function output to the distance from data points (r>0) to neurons center is given below.

$$\Phi(r) = e^{\frac{-r^2}{2\sigma^2}} \quad (5)$$

Where, σ is used to control the smoothness of the interpolating function [11]; and r is the Euclidean distance from a neuron center to a training data point.

Similarly, same data are used for the RBFN where 67 and 36 instances of data are used for training and testing, respectively. Table 5 shows the parameters values set during the training phase of this network. As seen in Table 5; the network is trained with 50 hidden neurons and spread constant of 0.5.

It is observed that RBFN with 50 hidden neurons and spread constant of 0.5 reached the lowest mean square error (MSE) (0.0330) in a very short time of 10 seconds. Moreover, this network was capable of reaching that low MSE with only 50 maximum epochs which is smaller than that of BPNN. Moreover, it is observed that this network was able to learn and converge in a shorter time than that of BPNN. The learning curve for RBFN is shown in Fig. 5.

TABLE. V. RBFN TRAINING PARAMETERS

Network parameter	RBFN
# of training samples	67
# hidden neurons	50
Spread constant	0.5
Maximum epochs	50
Training time (secs)	10
Mean Square Error reached	0.0330

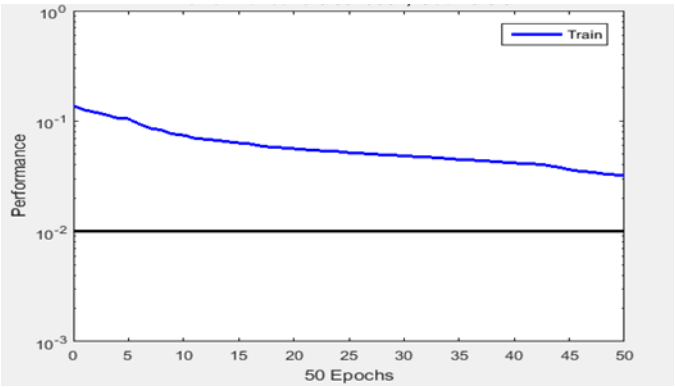

Fig. 5. Learning curve of the RBF network.

V. RBFN TRAINING

The networks were tested on a dataset of 64 records or patients; 44 for dead at one year, and 20 for alive at one year. Table 5 represents the total prediction rate of the designed one-year survival myocardial infarction prediction system. Note that the prediction rate shows the capability of the trained network to generalize, i.e., to predict the correct diagnosis while tested with unseen data. This prediction rate is defined as the total number of correctly classified instances of patient of the two classes divided by the total number of patients or instances.

Table 6 shows the backpropagation network's training and testing recognition rate of each set and class of data. It represents the number of cases that were accurately classified by the network in the training and the testing phases. In addition, it shows the percentage of instances that were not correctly classified by the network during the testing phase.

TABLE. VI. TOTAL PREDICTION RATE

Networks		Total number of data (patients)	Number of correctly classified cases	Prediction rate
BPNN	Training	67	66	66/67 98.5%
	Testing	64	61	95.3%
	Total	131	127	96.9%
RBFN	Training	67	67	67/67 100%
	Testing	64	62	96.8%
	Total	131	127	98.5%

The experimental results of the developed one-year survival myocardial infarction prediction system were as follows: 98.5% using the training data set (67), and 95.3% using the testing data set (64) for the BPNN. While, for the radial basis function network the training and testing classification rate results were 100% and 96.8%, respectively. The overall prediction rate for BPNN and RBFN was eventually calculated to be 96.9% and 98.5%, respectively.

Both networks successfully classified the two classes consistent with the clinical data. The RBF network was capable to achieve a better performance in predicting the correct diagnosis of the unknown data. Moreover, it was found that the RBF network's performance was the highest in the testing phase, as well as during training. On the other hand, this network reached a mean square error of 0.0330 which is higher than that of the BPNN "0.012". However, the BPNN required a longer training time "20 seconds" to reach that error than that of RBFN which achieved its lowest mean square error in "10 seconds". Note that the difference of the training time was not that high between both types of networks; however, the maximum number of iterations needed for the BPNN "1000 epochs" to converge was roughly higher than that of the RBFN "50 epochs".

VI. CONCLUSION

The deficiency in the myocardial infarction survival prediction systems was the motivation behind this work. In spite of the unreliability of survival prediction systems of myocardial infarction patients, our work showed that an intelligent system can learn from the past data of patients who suffered this disease to be capable of generalizing the correct diagnosis (survival or death at one year) of new myocardial infarction patients. This study compared the capability of two neural networks: BPNN and RBFN, to perform this task. As a result, both networks learned accurately to predict the two classes: dead at one year and survived at one year. However, one network "RBFN" outperformed the other "BPNN" when generalizing or predicting the diagnosis of the unseen instances. This outperformance was in terms of accuracy, training time, and number of maximum iterations needed for the network to converge.

REFERENCES

[1] G. Davì and C. Patrono, "Platelet activation and atherothrombosis", *New England Journal of Medicine*, 357, 24, 2482-2494, 2007.

[2] AS. Mullasari, P. Balaji, and T. Khando, "Managing complications in acute myocardial infarction", *Journal of the Association of Physicians of India* 59, pp. 43-8, 2011.

[3] BW. Karlson, J. Herlitz, O. Wiklund, A. Richter, and A. Hjalmarson, "Early prediction of acute myocardial infarction from clinical history, examination and electrocardiogram in the emergency room". *The American journal of cardiology* 68 (2), pp. 171-175, 1991.

[4] T. Mocan, L. Agoşton-Coldea, M. Gatfossé, S. Rosenstingl, LC. Mocan, and DL. Dumitraşcu, "A new prediction score for myocardial infarction: MINF SCORE",. *Romanian Journal of Internal Medicine* 46, pp. 145-151, 2008.

[5] M. Lichman, UCI Machine Learning Repository [http://archive.ics.uci.edu/ml]. Irvine, CA: University of California, School of Information and Computer Science. 2013.

[6] R. Rojas. Neural Networks-A Systematic Introduction Springer-Verlag. New York. (1996).

[7] A. Helwan, and DP. Tantua, IKRAI: Intelligent Knee Rheumatoid Arthritis Identification. International Journal of Intelligent Systems and Applications 8, pp. 18-24, 2016.

[8] A. Helwan,. and D. Ozsahin, "Sliding Window Based Machine Learning System for the Left Ventricle Localization in MR Cardiac Images", *Applied Computational Intelligence and Soft Computing*, 2017, doi:10.1155/2017/3048181.N.

[9] A., Helwan, & R. Abiyev, "Shape and Texture Features for the Identification of Breast Cancer", In *Proceedings of the World Congress on Engineering and Computer Science*, 2016.

[10] P. Strumiłło and W. Kamiński, "Radial basis function neural networks: theory and applications", *Neural Networks and Soft Computing - Advances in Soft Computing*, 19, pp. 107-119, 2003.

[11] A. Helwan, A. Khashman, E. O. Olaniyi, O. K. Oyedotun, & , O. A. Oyedotun, "Seminal Quality Evaluation with RBF Neural Network", *Bulletin of the Transilvania University of Brasov, Series III: Mathematics, Informatics, Physics*, 9, 2, 2016.

[12] S. Garg, K. Patra, and SK. Pal, D. Chakraborty, "Effect of different basis functions on a radial basis function network in prediction of drill flank wear from motor current signals", *Soft Computing* 12, pp. 777-787, 2008.

A Collaborative Approach for Effective Requirement Elicitation in Oblivious Client Environment

Muhammad Kashif Hanif
Department of Computer Science
Government College University
Faisalabad, Pakistan

Nauman Ul Haq
Department of Computer Science
Government College University
Faisalabad, Pakistan

Muhammad Umer Sarwar
Department of Computer Science
Government College University
Faisalabad, Pakistan

Muhammad Ramzan Talib
Department of Computer Science
Government College University
Faisalabad, Pakistan

Arfan Mansoor
Software Architecture and Product Line Group, Ilmenau University of Technology, Ilmenau, Germany

Nafees Ayub
Department of Computer Science
Government College University
Faisalabad, Pakistan

***Abstract*—Acquiring the desired requirements from customer through requirement elicitation process is a big deal as entire project depends on this initial important activity. Poor requirement elicitation affects software quality. Various factors in the oblivious client environment like culture, linguistic, gender, nationality, race and politics; can affect the final deliverables. The interaction of complex values, attitudes, behavioral norms, beliefs and communication approaches by stakeholders with different values may lead towards misunderstanding and misinterpretation. This could lead towards failure or dissatisfaction of the final outcome which might cause loss to both parties. The project requires redesign or modification that could take extra time and cost to get the desired results. The oblivious nature of the client's working environment is the major cause of poor requirement elicitation. This study focuses the issues in oblivious client environment where client is reluctant to provide desired information. This work proposes a novel requirement elicitation model for effective software development in oblivious client environment. The quality improvement results of software after using this model were verified using a qualitative survey.**

Keywords*—Requirement elicitation; oblivious client; software development; quality improvement; elicitation model

I. INTRODUCTION

The purpose of Requirement Engineering (RE) in software development is to produce a quality requirement specification report that contains the information without any ambiguity [1]. The detail provided in this report should be complete, accurate, verifiable and must be modifiable when required. The process goes well sometimes but often led towards downfall or failure of complete project due to incomplete or misinformation from the user and causes the loss in terms of huge maintenance or up-gradation charges. Thus requirement elicitation is the most critical phase in the development of the software [2], [3]. This crucial process of gathering requirements from the customers is most important because of which whole working of the project is to be planned, organized and managed. Any error while collecting information could lead towards major loss of developer's efforts, time and quality of the project. The facts and reasons which have been observed often in misunderstanding of information are due to many reasons among of which behavioural factor, cognitive behaviour, emotionality and social factors are most common [1], [4].

Another major factor which has been noticed is the locality of the customers as the living standards and environment is most important for the customer to provide accurate information to the developers so that the development team could lead towards successful solution of the problem [5]. The major area that is focused in this research study is the effect of various factors due to which efficiency of the final outcome is considered poor. It has been commonly noticed that the customer in our locality is unaware of the technicalities regarding software developments for the environment in which the software is to be developed. The client simply rushes towards the developer to get their desire product without knowing about the actual requirements which are desired by the analyst for the development procedure.

Correspondence to acquire necessities is a lengthy process that proceeds all through the life cycle of a project. Focuses in [6]-[9] have demonstrated that a considerable level of the difficulties confronted when designing the requirement in software development identify with organizational and social elements rather to the technical factors.

The important phase of the elicitation always effect the results of the system as the whole working of the system is determined by this valuable activity. The oblivious nature of the client is definitely the main reason behind the poor elicitation procedure as the analyst feels discomfort when client fails in describing his requirements. These unclear requirements must be purified before including them into the desired solution. The approach adopted in this effort designs a mechanism that detects the effectiveness of user requirements whether a given information to analyst is valid or not. The purification process moves on till an effective requirement is defined with the effective collaboration of the client as both parties agree on a common point.

As the nature of projects always vary from department to department and business to business, the requirement is always unclear to our analysts and professionals [3]. Once they work

on incomplete and unclear information, the project most often leads towards dissatisfaction or incompleteness for the desired customers and the developers have to work again to repeat the activity of development that always causes a high cost for mitigating the risks in the software [10]. Thus this research study is aimed to understand the levels of customers in our society and to create such a mechanism or approach that could make the developers successful in gathering accurate and meaningful information from the customers. So the best quality of the software could be achieved with minimum effort and time.

II. Related Work

Several researchers have studied the issues and challenges in agile requirement elicitation [1], [2], [10]-[12]. Kumar outlined different circumstances confronted by experts in software requirement gathering process and proposed elicitation technique for the purpose of suitable requirement engineering [12]. The suggested technique focused face to face communication and conducting meetings. Outcome: Iterative characteristic of agile RE makes it different from other software process models [1]. Sillitti and Succi conducted case studies for the organizations those follow the standard agile methods like XP and SCRUM and those who do not follow the standard methods at different level. These organizations adopted different agile practices like Face-to-Face Communication, Iterative RE, Extreme Prioritization, Constant Planning, Prototyping, Reviews & Test, and Test-Driven Development [2].

The requirement elicitation technique depends upon situation faced by analyst [12]. Kumar [13] highlighted the famous and most useable practice for software development. He has outlined the factors affecting requirement elicitation. The major factors were environment for which the software is developed and domain of the project. Lucia and Abdallah suggested techniques to solve the challenges of agile requirements engineering practices in large projects. They have also discussed the requirements traceability problem and the relationships between the traceability and refactoring processes [2].

The analysis done in [14] recommended practices to enhance agile RE. The RE process should consider different perspectives to utilize different meeting schemes, patterns, early consideration of non-functional requirements, adoption of requirement administration practices, and isolate environment setup and product development. Mennatallah and Ramadan investigated the agile RE practices in different software development organizations [13]. Davey and Parker classified the problems in requirement elicitation process [15]. Inayat *et al*. discussed 17 agile RE practices. The difficulties of agile RE are cost, schedule estimation, non-practical necessities, and client support [10].

The research work activities observed in [2], [12], [13] focused on the problem in agile software procedures like scrum, XP and proposed elicitation techniques. The practices in [13], [15] worked on various perspectives and classification of problems to offer new techniques for RE. The approach adopted here in our study focused on basic principle of software development but the difference between other approaches and our approach is that the model proposed in this research follows an iterative approach to purify the requirements for effective software development. The focus in [16] specified various requirement elicitations techniques with use of special use case diagrams in embedded systems. Practices performed in [17] focused on defining various requirement engineering responsibilities and efforts in agile development and role of engineers.

The related research work indicated above by many people shows their efforts in getting effective requirement elicitation. Many of these people focused on various circumstances and proposed there methods to deal with a certain situation. Some of the approaches described above focused on face to face communication with the customers and suggested various techniques to get good requirements for software development. This present approach is a detailed approach for acquiring perfect requirements from the customer as it is based on total involvement of the client until the requirement is cleared. This elicitation model is purely focused on purifying requirements till the acceptance which is main theme and differs from all other approaches for requirement elicitation.

III. Requirement Elicitation Process Challenges

The desired behaviour of the system is expressed as the requirements which are necessary for the completion of the task. A complete set of requirements contain information about various elements, objects or entities that are linked to system forming the behaviour of system in different situations. Requirement elicitation is considered to be the most important and crucial phase of the software development as whole the system depends on this important activity and errors during this activity becomes very hard to handle once the system is deployed. The thinking approach of the engineers in this regard is that, gathering required information is an easy task and they need not to be bothered about this but the reality is totally against this. Some of the main issues that affect the requirement elicitation process while software development are:

1) The conflict of statements between different stakeholders while eliciting the requirements could be the reason as various users in the same working environment might have different mind-sets and their opinion could be contradictory regarding a certain requirement.

2) Unnecessary requirements are one of the big problems in the requirement elicitation process as the client is not technically strong while eliciting proper requirements. The addition of such useless requirements becomes difficult to accommodate and require elimination at last with giving extra time.

3) The ambiguities in various requirements are major issues as the client is unaware about the outcomes of the system and provide those requirements which create a high level of ambiguity.

4) Sometimes the client is unclear about the requirements because the system is not seen by the client. The response of customer fails to explain the importance of the issue for which the system is to be developed.

5) A rough idea in the mind of client about a system that he has seen somewhere is also a big issue as the client is inspired by a system that might be opposite to his own. The requirements and the feature in both scenarios may differ and can cause analyst problems to properly elicit the requirements.

6) If the client is not sure about the final outcome of the desired system, it would be difficult for the developers to design a system according to the best satisfaction levels of client. So a system analyst must be sure about the background knowledge of the system and must also create a scenario in the mind of client before implementation.

7) Communication gap between the two parties is always noticed as the client environment vary from the development team with respect to his language, culture, behavioural norms, education level, locality, etc. These things must be kept in mind so that best requirement could be gathered.

8) Timely meetings and responses to the development team are always focused for best requirements. The client must provide desired information when required without hesitation and must give proper time and attention.

This work focuses to overcome the issues in the process of requirement elicitation. The obliviousness in the client level could affect the project badly. The software development activity can lead toward effectiveness with less defects and errors by focusing on these and other common soft issues in elicitation process.

The fundamental objective of this proposed activity is to make the elicitation activity more efficient during the initial phase. Once the requirements to be included in the main system are clear, concise and accurate; overall performance of the system will definitely satisfactory. So the goal of the work done in this approach is to simply provide a novel way of elicitation procedure through understanding the problem statement and purifying the requirement in more clear way.

IV. METHODOLOGY

The research activity was conducted in a step by step approach. The major activities adopted to get the results were divided into separate phases:

1) Pre-investigation and study of the problem
2) Meetings and interviews with the stakeholders
3) Prioritizing the issues for proposed methodology
4) Process model design for elicitation in oblivious client environment
5) Evaluation of the model

A. Pre-Investigation and Study of the Problem

Pre-investigation of the issues due to which software analysts face problem to understand the actual meanings of the client requirements. The activity of investigating the major causes in poor elicitation from users was conducted using a market survey. A questionnaire was designed related to some common issues in the minds of software analyst and then this questionnaire was floated in the market to get the opinions of the people, weather those people were actually effected by the obliviousness of the clients or not. The results of the questionnaire confirmed that the elicitation activity was heavily affected by the poor cooperation of the clients while communicating them for requirements. The results of the question are mentioned in the Fig. 1 that clearly shows how the elicitation activity in oblivious environment is affected by the client. The results of the survey are taken from different market experts in the field. The survey was conducted using electronic resources and by manual method of acquiring opinions from various technical people. The list of people who responded in this attempt contains 49 people who actually made this research possible by carrying the view that the software is always affected by the obliviousness of the client when the client fails to answer adequately due to lack of technical knowledge, self-interest, social factors and many other reasons as mentioned earlier. The results of respondents are as below shown by the respondent's outcomes in percentage values.

The results clearly show the effect of the oblivious clients that they definitely affect the performance of the desired system. The expert people in software field mostly agreed on the questions that were asked regarding poor elicitation from the client.

As it is clearly shown by the results of the questionnaire in Fig. 1 that the process of elicitation is heavily affected by the oblivious nature of the user and majority of the respondents declared that main reason of poor elicitation is due to the non-cooperative nature of the client due to which the final outcome suffers seriously. Focusing on the results of the market survey regarding poor elicitation issues in oblivious client environment; this research study purpose a working solution for better elicitation technique through elicitation model for oblivious client.

B. Meetings and interviews with the stakeholders

To verify the real issues regarding poor elicitation by client in oblivious environment; meetings sessions were conducted with development team experts and analysts to get more detail about the issues they face during elicitation phase. The results of the meeting sessions and interviews depicts that the developers society feel the same problem as it was noticed with the results of market survey through questionnaire. The related questions were asked to the stakeholders in the field of technical expertise and the respondents expressed the answers in favour to this study that the projects were mostly flopped due to negligence of client.

C. Attitude towards meaningful elicitation process.

The results indicated that non-cooperative behaviour, unclear vision, lack of technical knowledge about software were the major causes of the software failure at first attempt. Due to these reasons the project might have to rebuild and make changes again and again to satisfy the customer.

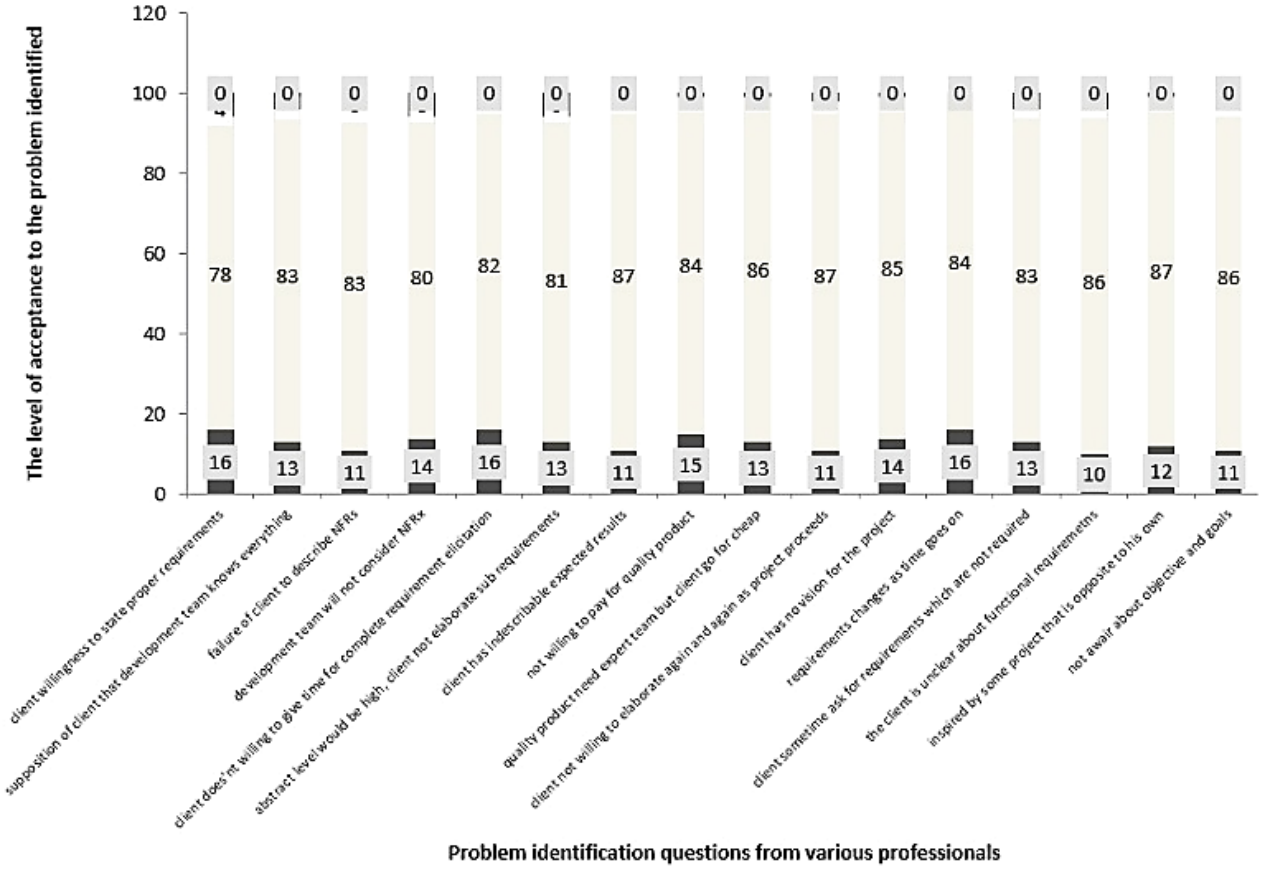

Fig. 1. Field survey graph of oblivious requirements.

D. Prioritizing the issues for proposed methodology

The core activity is to identify and prioritize the main causes due to which projects were heavily suffered. In this phase the identified problems in the oblivious client environment which were reasons behind poor elicitation were prioritize on the basis of results gathered from market survey through questionnaire and meeting sessions. The rankings were made according to the respondent's results and effect of that issue over the project life. The idea for this activity was to propose the desired effective methodology so that the elicitation method could become more effective to acquire desired requirements from customer.

E. Process model design for elicitation in oblivious client environment

The process model for making the elicitation activity in the oblivious client environment more effective is carried out through the designing of a comprehensive approach show in Fig. 2. The collaborative structure of identifying effective requirement from customer is carried out by following an elicitation process model for users who have lake of technical expertise and interests in defining the requirements properly. The process model is designed in a way that the analyst can acquire detailed information from client by realizing the importance of requirement engineering to the client. The process of requirement elicitation is based on the prior technique of software development that is based on standard SDLC format. Once the activity of elicitation comes into play; the role of this effective model comes to purify the best effective requirement using the proposed iterative approach in Fig. 3. The requirements are purified till the agreement between the analyst and client comes to final stage, whether to accept or reject certain requirement. The process goes similar for all oblivious requirements and finally gives the best suitable effective requirements for further activities of software development.

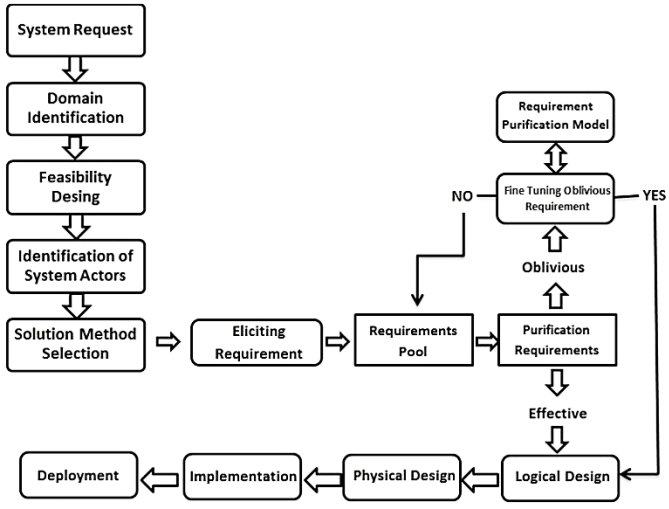

Fig. 2. Requirement elicitation model for requirement purification.

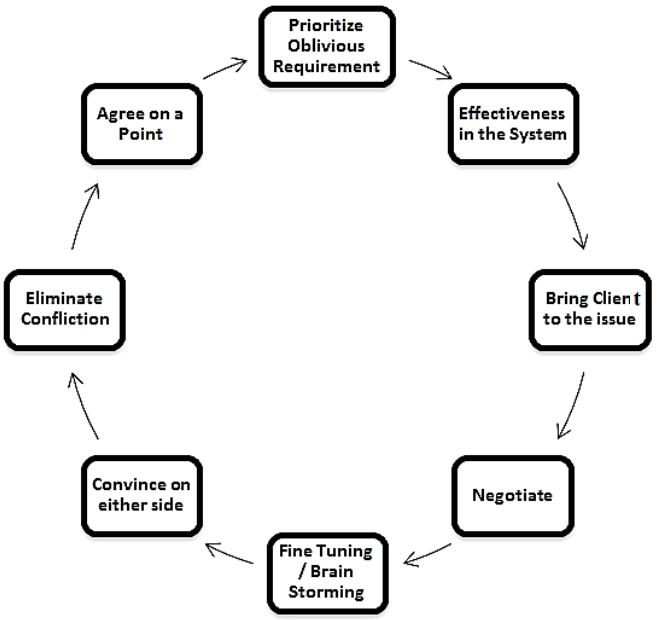

Fig. 3. Iterative approach for requirement purification.

The elicitation model for collaborative approach in this research study is expressed in Fig. 4 which depicts various activities in the elicitation phase.

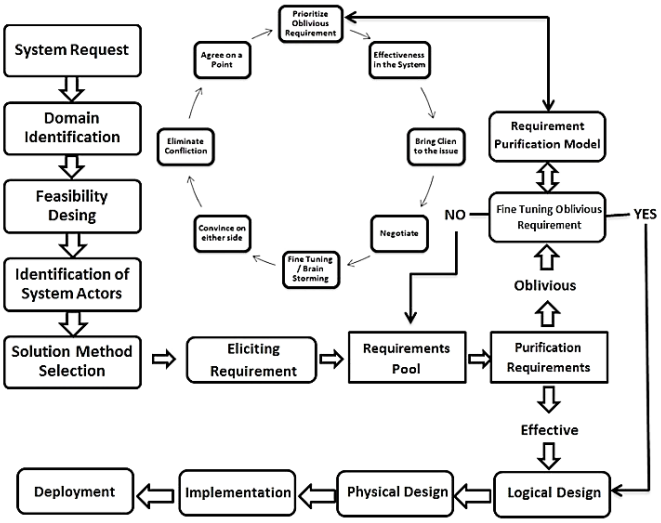

Fig. 4. Elicitation model for oblivious requirements.

F. Prioritizing the issues for proposed methodology

Fig. 4 illustrates the elicitation model for oblivious client environment shown above describe in detail process of communicating with customer for gathering effective requirements for software development. The activity of software development gets started with the system request as the client gets into the working environment of the system experts. The client request for developing software for his organization gets into the identification of the system as the developers or analysts wants to get familiarity with the system for which the request has been initiated. A feasibility report regarding the various estimations of the system is designed further to elaborate the system in more detail. The system is logically portioned according to the feasibility structure of the system so that various modules of the system could be analyst in attempt to acquire various functionalities. In the further step of this purposed system different actors of the system are identified to know the actual stakeholders of the system who will actually participate in the system requirement understanding. The list of all stakeholders is identified in this activity to make sure all the actors are nominated to whom the requested system is concerned about. Depending upon the nature of system request, domain problem of the system, feasibility analysis and the stakeholders identification; a solution method is chosen that will actually leads towards rest of the development activity. This development approach uses agile development approach to develop the system as agile approach is best suitable way to design the solution with active collaboration of the customer during project life.

As the main focus of this research study is focused on effective requirement elicitation from oblivious client environment, this proposed model leads towards elicitation requirement model in the next step to acquire the effective requirements for the further process of software development in the selected agile development method. This model suggests that the requirements from the different stakeholders must be kept into a requirements pool after initial elicitation phase, so that these could be categorized or ranked as the effective requirements with respect to desired solution or not. The client may express various kinds of requirements which are not associated to the system or he may not be able to answer effectively what the system demands. So the requirements must be purified before these are considered final for the desired solution to be developed.

The idea behind the purification of requirements in the elicitation phase is to determine whether the collected pool of requirements are effective set of requirements or these are oblivious sort of requirements that become part of requirements pool due to negligence of the client or misinterpretation. The model suggests a solution for the oblivious requirements that these sorts of requirements must be fine-tuned before these become part of the system that is under development. The refinement module of this system goes for the cyclic procedure to identify the nature of the requirement which is oblivious. This system suggest that these kind of requirements must be categorized and prioritize according to their importance in the system weather these could become part of the desired solution or these are mere due to uncertainty of the client. Depending upon the priority of the oblivious requirement, the client is further communicated in this approach to negotiate on the issue for realizing the fact why the client is interested in such sort of requirement. The process of brainstorming moves on until the parties agree on a single point and the issue is finally considered as a part of valid requirement or it is eliminated.

The process of identifying the effective requirements from the oblivious requirements goes on until the list of valid and effective requirements are finally adopted in this approach for the final solution to be prepared. Once the list of all effective requirements is updated the system moves towards the logical designing of the system so that it could be mapped into the physical model of the desired system. Since the physical design

of the desired system is purified using the proposed approach the system could be now implemented and deployed into the client environment with effective and efficient requirements.

G. Evaluation of the model

For the purpose of model evaluation, regarding the effectiveness and feasibility in the real life problem, the results were examined by evaluating responses from the questionnaires given to the experienced people in software development field and developers who were working in this field for at least more than five years, so that they can provide their feedback after using the system proposed for requirement elicitation in the said approach. Around hundred people were examined after using this approach and there observations were noted. The main focus was there on system analysts, requirement engineers and software developing people so that this system could be evaluated through their response by using this approach after number of times. The valuable opinion of these experienced people was then collected to make a statistical observation for the purpose of evaluating this proposed system.

The assessment scale of the system to verify the outcomes generated by this system was again referred to as strongly agree: means user is strongly agree to the outcomes generated after using this system; agree: means the user is satisfied with the results of this system; partially agree: means the user is willing to some extent that this solution is efficient; disagree: refers that the user is not satisfied with this approach. The outcomes of the questionnaires clearly dominated the results of first category that proved the effectiveness of the system as the large number of respondents went in support of this approach. The quality improvement results are shown here in the graph that clearly depicts the improvement in the efficiency of the final results after using this proposed model. The respondents clearly indicated the amount of change in quality before and after using this quality model for purifying requirement elicitation procedure.

TABLE I. STATISTICAL RESULTS WITH NOMINAL DATA SETS

	satisfaction_level	quality_rate	overall_satisfaction	comparison_other	overall_performance
Mean	4.42	1.28	4.14	3.84	3.98
Median	5.00	1.00	4.00	4.00	4.00
Mode	5.00	1.00	4.00	4.00	4.00
Std. Deviation	.882	.536	.857	.841	.914
Variance	.779	.287	.735	.709	.836

The statistical results indicate the interest of respondents in the favour of proposed elicitation model for requirements gathering (Table 1). The descriptive measures of statistics are taken from the outcome of questionnaires which was given to respondents for the purpose of evaluation of proposed elicitation model. The important measures of central tendency like mean, median, mode, standard deviation and variance are calculated from the data. The results clearly show the interest of respondents in favour of the proposed system as the satisfaction level, quality rate, overall satisfaction/performance are well above the high levels of interest showing high mean and median rates along with the high value of mode in resultant data. The standard deviation and variances of the said questions also depicts the high interest and similarity among the respondents.

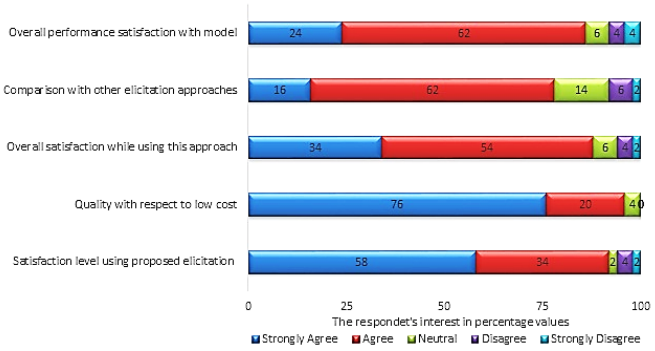

Fig. 5. Evaluation results of proposed model.

The results shown in Fig. 5 summarize the interest of respondents against the questions which they were asked to evaluate the proposed model with respect to different satisfaction levels. In the above data the questions were related like satisfaction level, quality with respect to rate and comparison with other elicitation techniques. The respondents were given five different values to evaluate after using the model criteria for elicitation. Most favourable outcomes were considered to be strongly agree, agree and neutral. After collecting the outcome the results can be seen as the percentage values of the respondents. The results clearly depicts that high percentages of respondents went into the favour of the proposed system against said questions. There were a very little number of respondents which opposed or went neutral. The high results with big numbers in favour of model efficiency and satisfaction proved it to be the suitable working elicitation model for the purpose of requirement gathering.

TABLE II. STATISTICAL RESULTS WITH ORDINAL DATA SETS

	quality_purification	satisfaction_purification	satisfaction_working	easy_elicitation	relation_goodproject
Mean	8.20	8.46	8.14	8.16	7.92
Median	8.00	9.00	8.00	8.00	8.00
Mode	8.00	9.00	8.00	8.00	8.00
Std. Deviation	.782	.734	.833	.976	.804
Variance	.612	.539	.694	.953	.647

The results observed in Table 2 describe the various levels of satisfaction from the respondents in the market. Different questions related to software satisfaction were asked again after adopting the proposed elicitation model for software development. The level of measuring was again set to get the response from the respondents which was categorized very high, high, medium, low and very low. The results show in the table above against each question clearly dominates in favour of the proposed model as large number of respondents positively agreed with high satisfaction level while eliciting requirements from clients using this model. The statistical

descriptive measures in above table shows the high rate of acceptance against each question that show the interest of the professionals in the proposed elicitation model for requirement gathering.

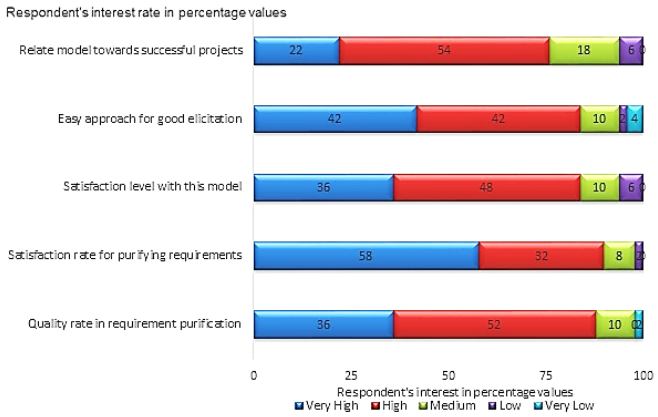

Fig. 6. Elicitation model evaluation results using ordinal set *data*.

The results in Fig. 6 graphical representation show that the respondents favoured this proposed model in close to high level of acceptance. In each question which they were asked, the respondents mostly agree that the satisfaction level with respect to quality in elicitation and customer satisfaction is at top levels. As the results indicate many of high percentages are towards the acceptance level of the users. A very few numbers were there who were either neutral or not satisfied but their percentages are very few in numbers which is closely near to ignorable levels.

TABLE III. STATISTICAL RESULTS WITH SCALE DATA SETS

	customer_satisfaction_level	customer_involvement	detailed_approach	enough_sufficient	Improvement_rate	chance_failure	Recommendation_other
Mean	.96	.94	.920	.96	.90	.06	.88
Median	1.00	1.00	1.00	1.00	1.00	.00	1.00
Mode	1.00	1.00	1.00	1.00	1.00	.00	1.00
Std. Deviation	.197	.239	.274	.19	.30	.23	.32
Variance	.039	.058	.075	.039	.092	.058	.108

In this evaluation procedure the data sets were used to measure the importance of the elicitation model using an interrogative approach (Table 3). The respondents were given only two choices to make their decision in favour of against various evaluation questions which were again satisfaction levels, customer involvement, efficiency, improvement rate and recommendation feature of this model to other people. The idea was to understand the importance of this model as in this category there were only two choice 'yes' or 'no'. The first answer was to evaluate high acceptance of the model and second answer was to purely see a negative response from the respondents. The results in Table 3 clearly indicate that a big average and number of respondents replied these questions in favour of this model by clicking their option to word 'yes'. The statistical measures shown in above table dominate the results as it shows the interest of the people in positive way towards using this approach for requirement elicitation.

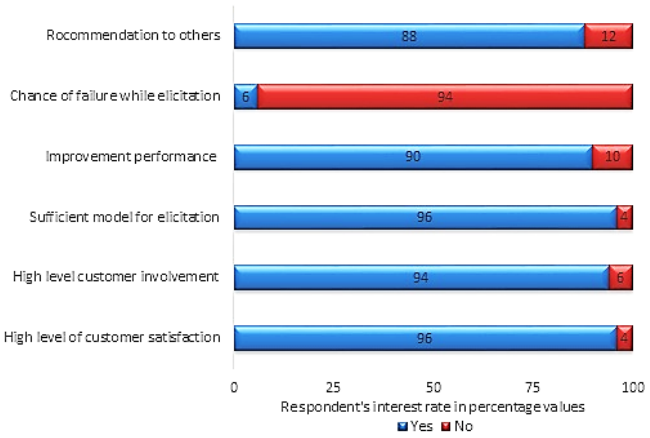

Fig. 7. Acceptance results detail using elicitation approach.

The graphical representation of the evaluation results against variety of questions in Fig. 7 shows the importance of this elicitation approach. The data shows the interest of people in this technique as they highly preferred this model to be recommended to other. The chance of failure in getting necessary requirements for software development was noted to be very low and it indicate the model high sufficient for purifying the requirements. The data gathered in above graphical representation clearly depicts that this model supports high level of customer involvement and due to that involvement the satisfaction level of the clients to be at very high levels.

The overall evaluation of this proposed elicitation model after gathering opinions from expert people shows that this approach is effective in purifying the requirement for software development. The results depicts the high percentages in favour of this proposed elicitation model as big number of expert people observed this approach as good for software development and requirement elicitation. The requirements for software development were initially understood whether clearly or not, and then those were purified by using a purification cyclic approach. This made this approach a better solution for requirement purification.

V. CONCLUSION

The process of requirement elicitation faces numerous problems while collecting the requirements from stakeholders during software development activity. This paper elaborates a comprehensive approach to overcome the challenges faced during elicitation process in oblivious client environment. As this model compared with other traditional elicitation model techniques the efficiency level and defectiveness level is much less in this proposed model. The evaluation of the system is performed using standard SDLC model but the elicitation activity is executed through this proposed elicitation model for obliviousness in client environment. As the initial activity is conducted in efficient manner, further development procedure gets smooth performance in effective manner with few chances

of defects. The deficiency level and rate of poor elicitation is far less than compared to the standard elicitation methods. The foremost benefit of using this proposed model is that the requirements are fully purified before implementing into the main system. The customer can clearly feel the system requirements, their importance and can definitely state his mind at any level by identifying issues. Since the purified requirements are part of the system, further there is no issue to gather requirements as it become easy to collect requirements with this model. Hence this research approach and suggested model for effective elicitation is efficient in the process of software development. By taking the proposed model as the base for quality software development, this work could be extended towards other software development activities. Software quality testing, risk management and software estimations could also be suggested as future work by focusing on this model.

REFERENCES

[1] A. Sillitti, and G. Succi, "Requirements engineering for agile methods, Engineering and Managing Software Requirements", Berlin Heidelberg, Springer, pp. 309-326, 2005.

[2] A. Lucia, and O. Abdallah "Requirements engineering in agile software development", Journal of Emerging Technologies in Web Intelligence, 3, pp. 212-220, 2010.

[3] E. Hull, K. Jackson,and J. Dick,"Requirements engineering", London, Springer, 2005.

[4] O. Isamet, "Requirements Elicitation Techniques: Comparative Study", International Journal of Recent Development in Engineering and Technology, 2013.

[5] F. Paetsch, E. Armin, and F. Maurer, "Requirements engineering and agile software development", IEEE 21st International Workshop on Enabling Technologies, pp. 308-308 2012.

[6] B. Elizabeth, K. Wnuk, and B. Regnell, "Requirements are Slipping through the Gaps", In Proceeding(s) of the Requirements Engineering conference (RE), pp. 37-46, 2011.

[7] N. Pa, and M. Zin, "Requirement Elicitation: Identifying the Communication Challenges between Developer and Customer", International Journal of New Computer Architectures and their Applications (IJNCAA), vol 1, pp. 371-383 2011.

[8] N. Pa, and M. Zin, "Managing Communication Challenges in Requirements Elicitation", In Proceeding(s) of the Second International Conference Kuantan, Pahang, Malaysia, Part III, CCIS, pp. 803-811, 2011.

[9] R. Fuentes-Fernández, J. Gómez-Sanz, and J. Pavón, "Understanding the human context in requirements elicitation", Journal Requirements Engineering, Springer-Verlag New York, vol.15, pp. 267-283 2010.

[10] H. Elshandidy, and S. Mazen, "Agile and Traditional Requirements Engineering", A Survey. International Journal of Scientific & Engineering Research, vol. 9, 2013.

[11] S. Inayat, S. Salim, S. Marczak, M. Daneva, and S. Shamshirband, "A systematic literature review on agile requirements engineering practices and challenges", Computers in Human Behavior, 2014.

[12] S. Kumar, "Analysis of Factors Involved in Choosing Requirement Elicitation Techniques for Agile Methodology", International Journal in IT and Engineering, vol.3, 2015.

[13] H. Mennatallah, and D. Ramadan, "Investigation of Adherence Degree of Agile Requirements Engineering Practices in Non-Agile Software Development Organizations", International Journal of Advanced Computer Science and Applications, vol.6 , 2015.

[14] S. Bose, M. Kurhekar, and J. Ghoshal, "Agile Methodology in Requirements Engineering", SET Labs Briefings Online, 2008.

[15] B. Davey, and K. Parker, "Requirements elicitation problems: A literature analysis. Issues in Informing Science and Information Technology", vol.12, pp. 71-82, 2015.

[16] E. Nasr, J. McDermid, and G. Bernat, "Eliciting and Specifying Requirements with Use Cases for Embedded Systems", International Workshop on Object-Oriented Real-Time Dependable Systems, 2002.

[17] V. Tripathi, and A. Goyal, "Agile Requirement Engineer: Roles and Responsibilities. International Journal of Innovative Science, Engineering & Technology", vol.3, pp. 213-219, 2014.

An Empirical Investigation into Blended Learning Effects on Tertiary Students and Students Perceptions on the Approach in Botswana

Gofaone Kgosietsile Kebualemang
Faculty of Computing
Botho University
Gaborone, Botswana

Alpheus Wanano Mogwe
Faculty of Computing
Botho University
Gaborone, Botswana

***Abstract*—The aim of the research was to conduct an empirical investigation into blended learning (BL) effects on tertiary students and students' perceptions on the approach. This purpose was objective driven, following three objectives which were identified as 1) to assess the impact of BL on students enrolled in Tertiary institutions; 2) to assess tertiary students' perceptions on the BL mode; and lastly 3) to establish the extent to which BL is accepted in a typical institution or university learning environment. An extensive literature review exercise was carried out which led to identification of two research questions to be used to meet the objectives and the purpose of the study. The research questions were 1) Does blended learning (BL) transform learners' attitudes towards learning and improves results? 2) Does blended learning (BL) revolutionizes learners' critical thinking levels and dispositions? Through the research the authors were specifically trying to elucidate and understand the BL mode and the effects it has on students, and their perceptions on it. The researcher followed the quantitative approach with the aid of using a questionnaire to further understand the effects of BL mode on students and their perceptions on the same, after reviewing several literatures. The findings indicated that the BL mode has a positive impact on the students, and students' perceptions on the BL mode were also positive. These findings led to positive conclusions on the BL mode, substantiating the literature review findings on the same. In the light of the findings, and the objectives of the study, the authors concluded the study by proposing a framework which could be used for monitoring BL effects on tertiary students and students' perceptions on the approach, as the results from the study indicated a positive outlook on the BL mode.**

Keywords—Blended learning; blended learning effects; Students' perceptions

I. INTRODUCTION

Blended learning (BL) has become an integral part of modern education. This has seen many institutions of higher learning providing a new perspective in education delivery and attainment through the use of blended learning mode. With this mode, a new phrase "the world is flat" was coined [1], meaning attainment of education has become accessible to everyone everywhere – global students [2], [3].

Blended learning is an integration of the online mode with the traditional mode of face-to-face to offer class activities in a pedagogically valuable planned manner [2], [4]-[7]. The mode involves certain portions of the activities of face-to-face being replaced through the usage of online activities [2], [8]. This diverse mode gives institutions a variety of educational approaches to use. With many institutions moving to this mode, the traditional way of face to face has seen its decline in institutions which are techno-savvy and oriented. BL growth and impact is currently undisputable in the educational field [9].

Various literatures indicate a rise in its usage both in institutions of higher education and or tertiary institutions [2], [5], [10]-[12]. It has become an acceptable pedagogical approach which is believed to change the whole educational scenario and the traditional classroom set up. Many benefits have been touted such as but not limited to pedagogical richness, access to knowledge and social interaction. In addition, some challenges have been noted such as but not limited to financial constraints to set up technologies related to usage of BL. These challenges, though, they have not hampered some of the tertiary institutions in Botswana to adopt the usage of the BL mode. Botho University is one institution which stands as an example of the provision of such mode. Other institutions have been lagging behind to embrace this mode.

II. BACKGROUND TO THE PROBLEM

A. Background Scenario

Botswana has made strides in education, with enrollment numbers indicating an increase on yearly basis and tertiary institutions accounting for 11.4% [13]. The delivery mode in many tertiary institutions has remained a traditional one, involving face-to-face with little or none at all to integrate modern technologies such as the usage of online technologies to supplement the educational system. Botho University is one institution which has embraced the use of BL, and it is vital to investigate how this has impacted students.

BL is being embraced all over the world [9]. Therefore, educational institutions in Botswana need to rethink on the inclusion of the blended learning mode. Institutions ought to embrace BL trends for reform, or face decline in their educational goals due to the use of the outdated approach only. Moreover, other studies [14], [15] have indicated the dynamism brought by technology in peoples' everyday lifestyles together with its importance in education and learning.

It would be argued that the assimilation of technology into an institutional teaching and delivery mode is an asset to its educational needs but when institutions lag in its embracement, causes to that should be identified. Thus, questions remain on why are Botswana institutions lagging behind in implementation of BL mode? What are the effects of BL on students? What are the students' perceptions on BL? Therefore, this study seeks to understand the BL effects on tertiary students and their perceptions on the same.

B. Problem Statement

The lagging behind of institutions in Botswana to embrace blended learning is a concern which ought to be investigated. Therefore, it is important to understand the effects of BL on tertiary students and students' perceptions on the approach on the institutions that have embraced BL mode. Understanding its effects on students and students' perception will pave way to know whether this influences the lagging behind of institutions to embrace the same. Due to the blended learning mode being a new educational delivery mode, it has not been tested or vigorously investigated in the Botswana scope, hence the lingering problem is the effects of this mode on tertiary students and students' perceptions on the approach.

III. Aim And Objectives

A. Aim

The study is aimed at conducting an empirical investigation into blended learning effects on tertiary students and students' perceptions on the approach.

B. Objectives

1) To assess the impact of BL on students enrolled in Tertiary institutions
2) To assess tertiary students' perceptions on the BL mode.
3) To establish the extent to which BL is accepted in a typical institution or university learning environment.

IV. Research Questions

1) Does blended learning (BL) transform learners' attitudes towards learning and improve results?
2) Does blended learning (BL) revolutionize learners' critical thinking levels and dispositions?

V. Literature Review

A. What is blended learning mode

Blended learning (BL) is the modern way of delivering education to students. Various authors agree that BL mode is an integration of the online mode with the traditional mode of face-to-face to offer class activities in a pedagogically valuable planned manner which provides flexibility [6], [16], [17]. In addition, other authors [1], [2], [8], [9], [18] support the findings related to the positives of the BL mode. The mode involves certain portions of the activities of face-to-face being replaced through the usage of online activities [2], [19].

This diverse mode gives institutions a variety of educational approaches to use which at the same time complement each other. With many institutions moving to this mode, the traditional way of face to face has seen its decline in institutions which are techno-savvy and oriented.

B. Blended learning mode around the world

There is a rise in the use of the BL mode. BL has become the acceptable pedagogical approach which is believed to change the whole educational scenario and the traditional classroom set up. Many benefits have been touted such as but not limited to pedagogical richness, access to knowledge and social interaction. In addition, some challenges have been noted such as but not limited to financial constraints to set up technologies related to usage of BL. These challenges, though, they have not hampered institutions around the world to introduce BL mode as seen from the following discussion.

Blended learning has found its way around the world. It has become a must inclusion component in the curriculum developments and educational learning. Institutions are rapidly infusing it into their education system. So and Bonk [18] have noted the increase of usage of the BL mode around the world. This has been attributed highly to the growth of usage of online and internet related gadgets. Different institutions around the world have embraced the concept, from both developed to developing countries, and BL has shown to be of positive developments in those institutions and countries.

In many of the developed and developing nations, institutions have embraced the use of blended learning. Kwak [17] states that there has been an increase of universities offering BL mode with an increase of many students embracing it. In the United Kingdom, Open University is one of the universities known for its employment of the BL mode [20]. It has helped students with greater access to educational opportunities. The use of the BL mode has helped to restructure education delivery and training programs. Amity University in India has also extensively utilized the BL mode technologies for greater access to the students' population.

C. Blended learning effects on students

A study carried in Iran [16], showed that BL mode has positive effects on the students. The study further showed that students easily associated and embraced a mode which included both the traditional face-to-face and the technology related mode, in which BL mode was the fit. Thus, the findings have shown a positive correlation between the usage of the BL mode and its effects on students' performance in class [17]. Kwak [17] note the importance of the BL mode environment in relation to the positive outcomes of students' results.

Mersal and Mersal [19] noted that BL mode utilizes two or more complementary approaches in the delivery of education to students. Through a study [19], BL mode was found to be effective and providing an improvement regarding satisfactory level of achievement in the education setup. Thus, this further shows the relevancy and importance of this mode in changing the educational scope to the positive scope. There was an improvement from the students who utilized BL mode in relation to course and teaching methods satisfaction [19], the same findings reached and concluded by other authors [21], [22].

Therefore, it can be argued that both the students' ways of learning and the subsequent quality of learning is closely related and forms part of their learning experiences and the embracement of the mode of learning they encounter. With the technology having broken the barriers of education attainment, the traditional way of learning which was constrained to class rooms and face-to-face learning, is by itself not enough in this modern era. It shows that alone it cannot meet the learners' expectations hence it draws on the negative side, but its infusion to modern ways of learning leading to a BL mode makes this a more robust learning approach. These are the same conclusions reached by Owston [23]. Students have shown that BL mode offers convenience, is more engaging and offers a better perspective of learning which gave a positive feedback on the overall satisfaction with BL mode. Thus, BL mode contributes more to students' attitudes towards course/subjects when it is compared to the traditional learning models. With it, it nurtures student critical disposition and levels leading to a positive correlation between student attitudes towards subjects or courses being undertaken.

VI. Methodology

Following a systematic approach in data collection is an important aspect in research [24]. Saunders [25] states that a methodology is a requirement for every research being conducted. This is sustained by other authors [26]-[28]. According to Oates [29], a selection of a methodology follows a careful analysis of various elements or factors, in which one of them is working well with other methods and research tools. This would help to deem the methodology suitable for the study to be conducted.

The most common methodologies are the qualitative and quantitative methodologies. These two methodologies can be used together to form what is known as a mixed methodology approach. Both this approaches have got advantages and disadvantages as they address various research issues. The researcher chose to follow the quantitative approach to complete this study.

According to Chilisa and Preece [28], quantitative approach is an approach driven by the investigators questions in which various issue perspectives are collected from the subjects' view point in line with the questions posed by the investigator [30]. It follows suitable techniques and metrics per problem statement. Through this approach there is a heavy reliance on numerical and statistical analysis, which is the strongest strength of the quantitative approach which helps it to evade biasness in a study [27], [31], [32].

Thus, the above argument, sustains the argument that the quantitative approach is regarded as a rigid approach which is not subject to bias through subjective interpretations [26], [33]. This approach employs a variety of techniques such as self-completion questionnaires, surveys, and structured observations to fulfill its mandate. The researcher employed self-completion questionnaire technique, with a structured questionnaire designed and developed for usage to obtain responses.

Patton and Cochran [34] states that utilization of self-completion questionnaire coupled with the quantitative approach makes it easier to measure and analyze data. This leads to a conducive and simple platform to measure the attitudes, behaviors and performance of respondents. This can then be easily changed into quantifiable graphs and charts. Moreover, the usage of this approach coupled with the questionnaire technique, helps to reach a wider audience and capture more data to be used [25], [35]. The researcher used a larger audience to ameliorate the downside associated with this approach. Attention was put in place to ensure the relevance and integrity of the study so that there is no diversion from the core mandate through the usage of a pilot study.

The main drawback for the quantitative methodology is the skills needed to comprehend the various formulae and numbers during the data analysis [29].

VII. Sampling

According to Terre Blanche [36] and Kumar [37] it is vital to locate a population to carry the sample on. A sample constitutes a portion which becomes the target population representing the overall population [36], [37]. This portion becomes the basis for estimating a fact, outcome or situation to represent a larger population. A population constitutes of all members to which the study makes a reference to, and are able to be part of it [37]. The sampled population was taken from Botho University in Gaborone with the target population being all Botho University students. The sample was done in Botho University, Gaborone. The sample helps to reduce costs as only a limited number of people are involved in the study. Carrying out research on a bigger population or whole population is expensive both in terms of resources, time and money. This sample is selected through a probability or non-probability method. A variety of decision making criteria are followed to reach conclusion on the specified sample such as the behavior of the targeted audience, their background, location and type of people.

As for this study, the researcher with the aid of online sample size calculators sampled 200 participants using a confidence interval of ±3 with confidence level set at 95%. The threshold for the needed sample size was 169 with a distribution of 200 participants. The researcher distributed 200 questionnaires in Botho University Gaborone campus. During distribution, no cognizant efforts were put into consideration in relation to gender or age.

The authors used a simple random sampling technique for distribution of the questionnaire. Chilisa and Preece [28] states that this is one of the basic sampling techniques which gives equal chances of inclusion and participation to each and every member of the general population.

VIII. Results Findings and Analysis

Presentation of this section closely follows the layout of the questionnaire. The questionnaire was divided into three parts, namely, 1) usage of Blended learning and its assistance in knowledge gaining; 2) Blended learning and my attitude to learning; and 3) Blended learning on results. These parts had their own sub-questions in likert scale of Strongly Agree, Agree, Neutral, Disagree and Strongly Disagree.

Table 1 shows that 200 questionnaires were distributed and, 189 (94%) were collected from the participants of the study. 6% which is a total of 11 were not brought back due to un-foretold reasons from participants. The threshold of the study wanted at least 169 (84.5%) of questionnaires collected, and this was met with the collection of 94% of the questionnaires surpassing the threshold by 9.5%.

TABLE. I. QUESTIONNAIRE SUMMARY

Questionnaire Summary		
	Raw Numbers	***%***
Brought Questionnaire	189	94%
Questionnaire Not Brought	11	6%
Total Questionnaire Given Out	200	100%

A. Part A: Usage of Blended learning and its assistance in knowledge gaining

This is the first part of the questionnaire, and it had six (6) questions. The objective of this part was to understand from the participants how blended learning impact on knowledge gaining. The questions were:

1) I enjoy using blended learning.
2) Blended learning improves my access to class content and interaction with other learners.
3) Blended learning improves my access to module content.
4) The use of blended learning components enhanced each other.
5) The use of web resources is useful for my modules/subjects.
6) The technologies used for blended learning (videos, web, audios, internet) are helpful in my course.

For questions in this section, it can be noted that participants agreed that BL mode impacted positively on their knowledge gaining sustaining the findings by Kwak [17]. Refer to summarized findings section (Section IX of this document) for column charts presentation as per the questions. Respondents for question 1 noted at 52% that they agreed with the question as shown in Fig. 1. They showed that they enjoyed using BL mode, followed by 30% who strongly agreed to being satisfied of using the BL mode. A total of 82% enjoyed BL mode usage compared to 12%. In question 2 depicted by Fig. 2, a total of 95% of the respondents are in the affirmative of the question with only 5% opposing it and 2% remaining neutral. Both these analyses indicate a strong confirmation of other studies [8], [19], [38].

Participants at an aggregate of 93% affirmed to the question stand with 41% strongly agreeing that BL improved access to module content, and 52% agreed to the same (refer to Fig. 3). 3% remained neutral and 5% made of 3% disagreeing and 2% strongly disagreeing represented those who opposed the question. For question 4 an aggregate of 95% of the respondents agreed with the question, as indicated in Fig. 4 and 3% opposed the question. 2% of the respondents remained neutral in this question. Participants agreed that BL mode web resources and technologies were helpful at 100% for both question 5 and 6 (refer to Fig. 5 and 6, respectively). The findings sustain Mersal and Mersal [19] findings together with those of Nagel [2] that BL Modes components enhance each other to offer greater access to learning resources and class contents [39].

From the respondents, it can be concluded that the Usage of Blended learning and its assistance in knowledge gaining as addressed in Part A of the questionnaire and summarised findings in Fig. 1 to 6, it is of importance to respondents. Respondents have overwhelmingly affirmed to the questions which were asked under this part, also sustaining the findings under the literature review which indicated that BL mode when correctly applied it will lead to satisfaction of students [2], [19], [21].

B. Part B: Blended learning and my attitude to learning

Under part B of the questionnaire, the researcher sought to understand how BL impacted on student attitude. This part had five questions, and below is the presentation of the findings from the questions. The questions were:

1) Blended learning has improved my Analytical skills.
2) Blended learning has helped me to be Open-Minded in approaching my course/program learning.
3) Blended learning has increased my Inquisitiveness to foster my understanding of the course/program.
4) Blended learning has increased my Self-Confidence in the course /program.
5) Blended learning has helped me to grow and be creative in my course/program in fostering innovation and problem solving.

For questions in this section it can be noted that participants agreed that BL mode has a positive impact on students' attitudes, further cementing other findings from other authors [16], [40]. Refer to summarized findings section (Section IX of this document) for pie charts presentation as per the questions.

Majority of the respondents in question 7 (refer to Fig. 7), sought to capture (if BL mode improved students' analytical skills at a combined 93%) agreed of a BL mode, positive impact on their analytical skills. 6% of the respondents remained neutral with 1% disagreeing. Fig. 8 shows results for question 8. In question 8, 56% of the respondents agreed to the question with 34% strongly agreeing to make a total of 90% of the respondents who concurred that BL had a positive impact of making them to be open minded on their approach to their studies. 6% remained and 3% disagreed. This also sustains the findings by various authors from various studies who have shown that BL mode impacts positively on students' analytical skills and open thinking [19], [38], [41].

In question 9, 92% of the respondents agreed that the BL mode helped them to further being inquisitive to understand their course with 5% remaining neutral and 3% opposed as indicated by Fig. 9. The analysis for question 10 as depicted in the results in Fig. 10 indicates that at 64%, respondents strongly agreed that BL mode increased their self confidence in their course, with 31% agreeing to the same making a total of 95% of the respondents who agreed that BL mode has a

positive impact of increasing their self-confidence with 3% remaining neutral and 2% disagreeing. Fig. 11, indicating question 11 feedback shows that 62% strongly agreed to the question with 31% agreeing to it, bringing the affirmative respondents to a total of 93%, who agreed that BL mode helped students to grow and be creative in their course/program to foster innovation and problem solving. Only 5% remained neutral and a combined 2% opposed it.

The analysis shows that majority of the respondents affirmed to the questions under this part and concurred that Blended learning mode changed their attitudes to the best in relation to their learning activities. These findings sustain the findings in the literature review [19], [38], [41] that BL mode has a positive impact to students and it changes their attitudes for the best [2], [19], [23].

C. Part C: Blended learning on results

This was the last portion of the questionnaire which sought to understand how BL impacted on students' results and performance. This had six questions which were:

1) With blended learning, I received too much feedback from my instructors.
2) Blended Learning fostered more interaction between me and other students and the instructor.
3) The responses received helped me to focus and learn more deeply.
4) With blended learning I have improved my module/subject results.
5) Blended learning has impacted positively on the growth of my course/program GPA.
6) I enjoy using blended learning mode and would recommend it for others.

The results indicated that BL mode has a positive impact on students learning and results. Refer to summarized findings section (Section IX of this document) for column and pie charts presentation as per the questions. The questions under this section concurred with findings from various studies [17], [19], [22] that BL mode helps improve results. An individual analysis of the questions under this section found out that for question 12, respondents agreed that BL mode had an impact on the instructor feedback at 94% (refer to Fig. 12). This included a combined 46% of those who strongly agreed and 48% who agreed. 3% remained neutral with a combined 3% opposing the question. For question 13, respondents at 41% strongly agreed that BL mode fostered more interaction between learners themselves and the instructor, followed by 54% who agreed, as indicated in Fig. 13. A total of 95% agreed that BL has a more positive impact in that regard with 2% and 1% disagreeing and strongly disagreeing, respectively. 2% of the respondents remained neutral on this question. Respondents under question 13 agreed at 87% that BL mode had the effect of making students focus and learn more deeply with 8% remaining neutral and 5% opposing (refer to Fig. 14).

Question 15 and 16 were focused onto the results and GPA of the students. The respondents in this question noted in the affirmative of BL mode positive impact on their results with 100% affirming that due to BL mode they have improved their results (refer to Fig. 15). Respondents at 65% indicated that they strongly agreed that BL mode has a positive impact on the growth of their GPA followed by 31% who agreed and 4% who remained neutral. That is a total of 96% of the respondents agreed that BL mode has a positive impact on the growth of GPA as indicated in Fig. 16.

With respondents showing a positive outlook for the BL mode, and appreciation, many of the respondents at 96% agreed that they enjoyed using BL mode and would recommend it for others with 4% remaining neutral on the same (refer to Fig. 17). Respondents of the questionnaire indicated that they have been exposed to BL mode for at least a minimum of a year, as indicated in Fig. 18 below.

The findings of this section sustain the literature review, in which BL mode is attributed to positive results in students. Various studies have been carried out to check how BL mode impacted students' results, and it has been concluded to be a positive impact, hence the same findings in this study. A study by Mersal [19] indicated that students performed better in a BL mode set up due to its richness in providing various modes for learning. Delialioğlu [39] also notes that students' engagement in BL mode environments provides a positive growth in relation to performance. Bliuc [42] highlights the relationship between social identity, mode/approaches to learning, and academic performance as factors-and concludes that BL mode environment is more advantageous.

IX. Charts Summarised Findings

This portion presents the analyzed findings in charts and graphs for better understanding of the previously discussed section. It augments what has already been discussed.

Part A Questions: Usage of Blended learning and its assistance in knowledge gaining

Column charts below are for all questions in Part A of the questionnaire. Refer to results findings and analysis (Section VIII) for analysis of part A.

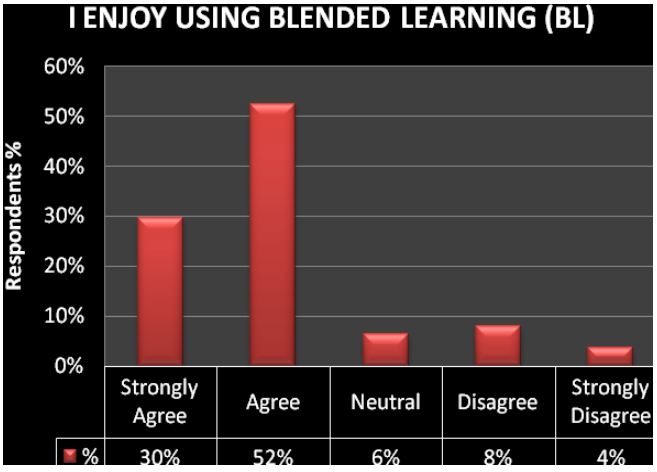

Fig. 1. Question 1 column chart

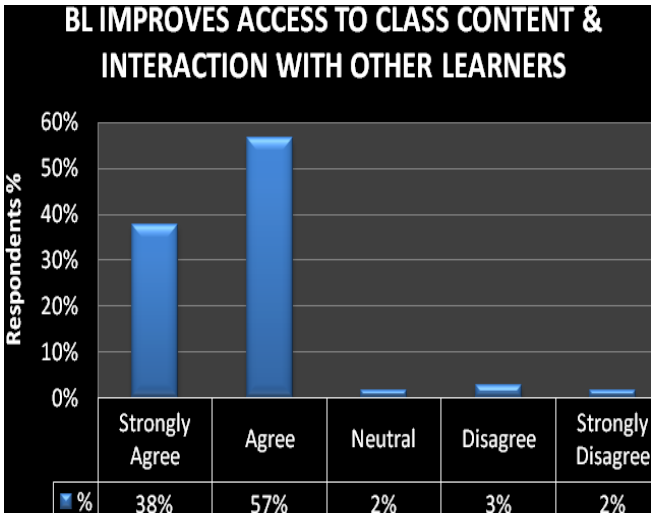

Fig. 2. Question 2 column chart

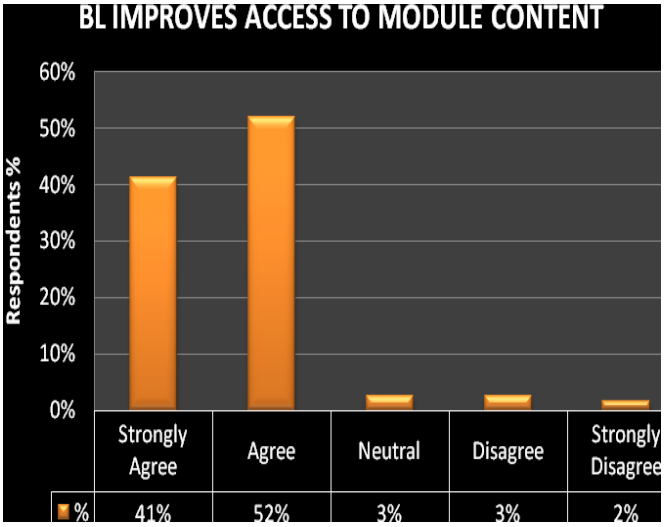

Fig. 3. Question 3 column chart

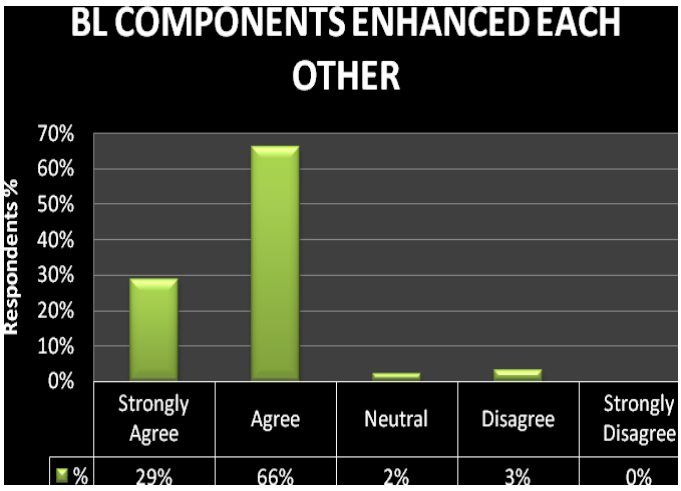

Fig. 4. Question 4 column chart

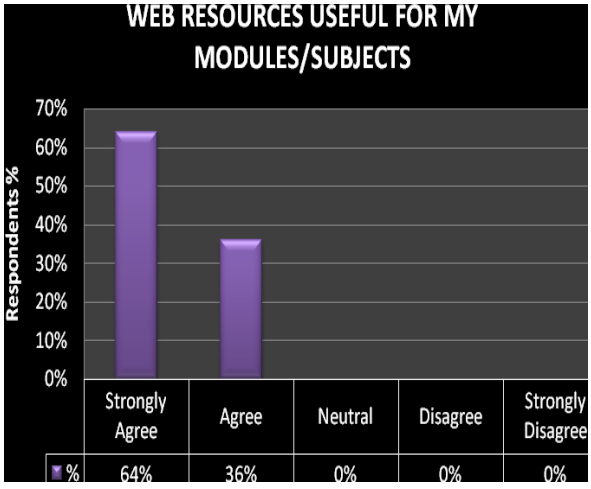

Fig. 5. Question 5 column chart

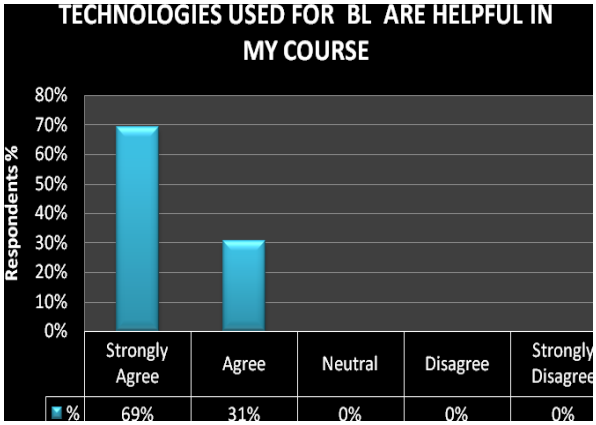

Fig. 6. Question 6 column chart

Part B Questions: Blended Learning and my attitude to learning

Pie charts below are for all questions in Part B of the questionnaire. Refer to results findings and analysis (Section VIII) for analysis of Part A.

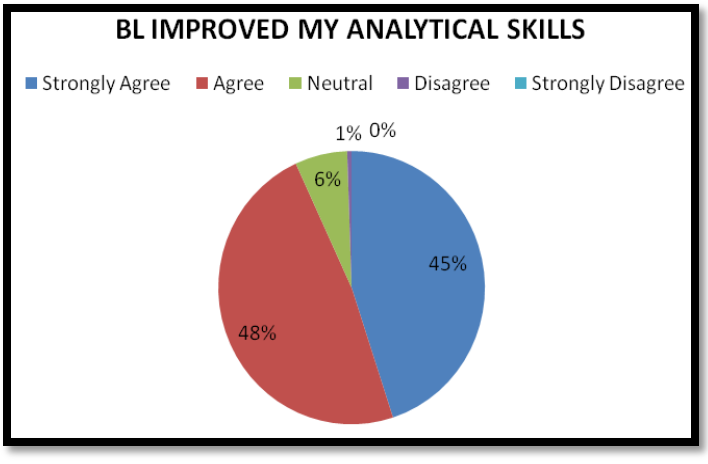

Fig. 7. Question 7 pie chart.

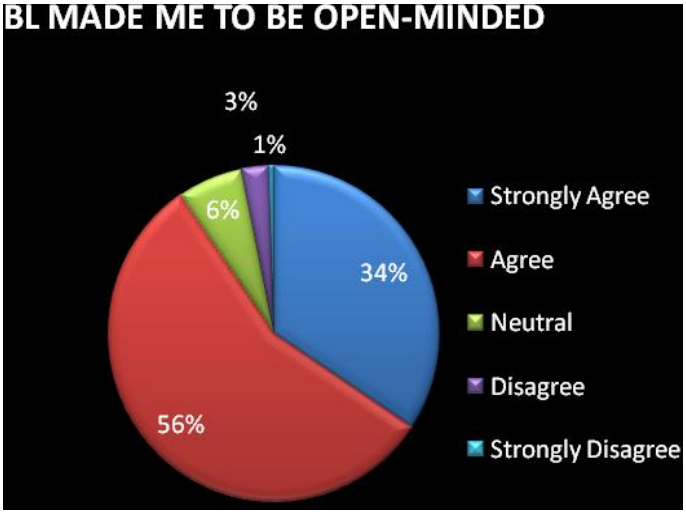

Fig. 8. Question 8 pie chart

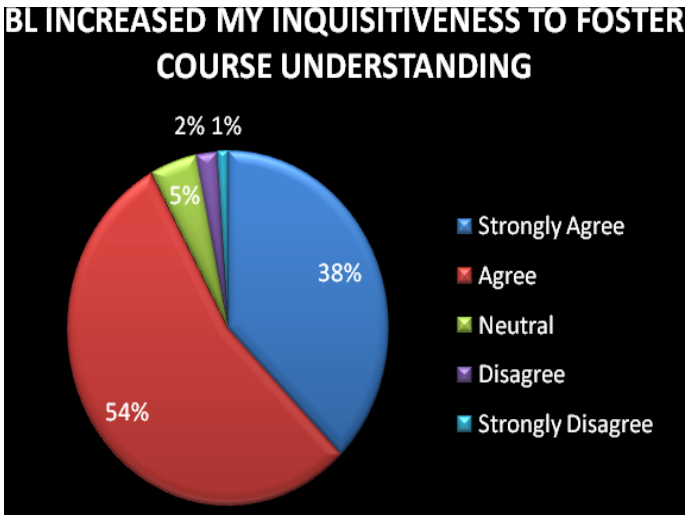

Fig. 9. Question 9 pie chart

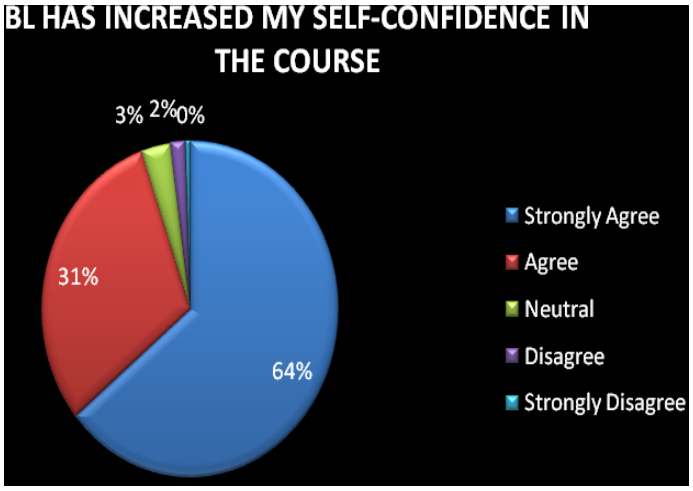

Fig. 10. Question 10 pie chart

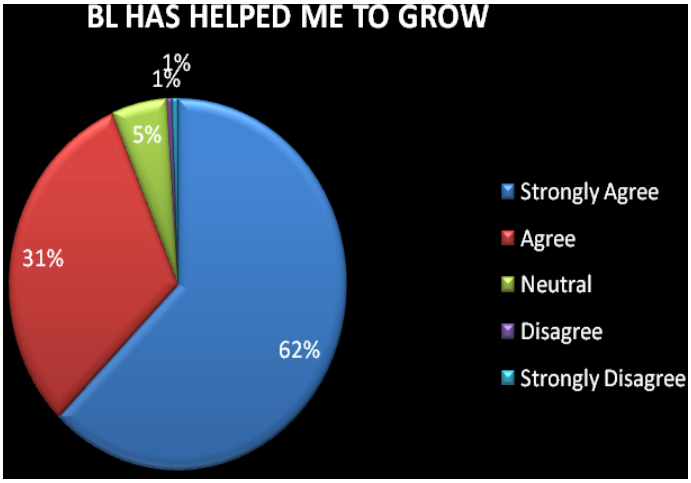

Fig. 11. Question 11 pie chart

Part C Questions: Blended learning on results

Pie charts below are for all questions in Part C of the questionnaire. Refer to results findings and analysis (Section VIII) for analysis of Part C.

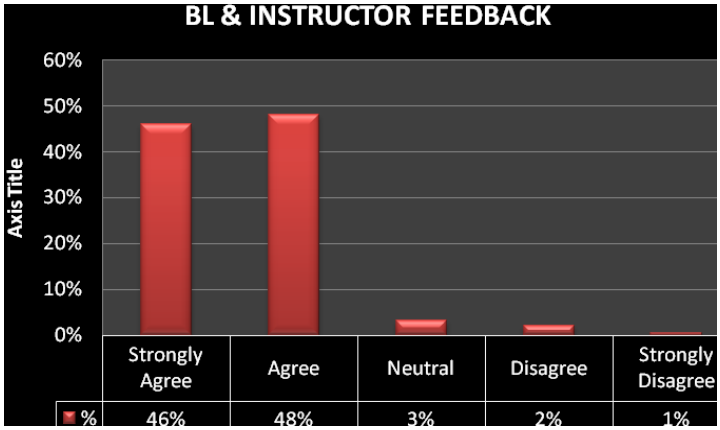

Fig. 12. Question 12 Column chart

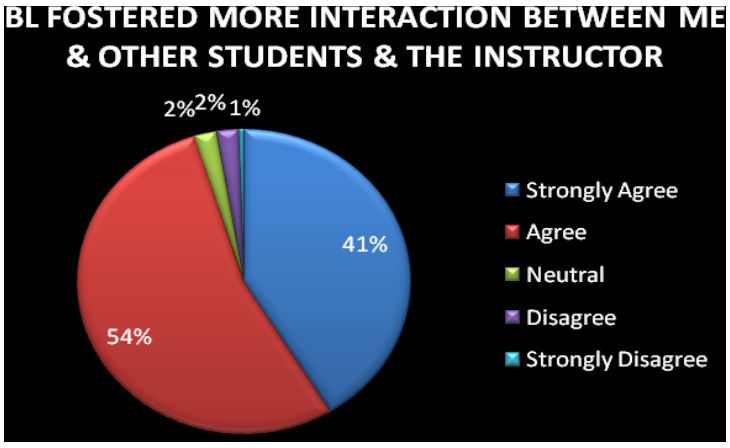

Fig. 13. Question 13 pie chart

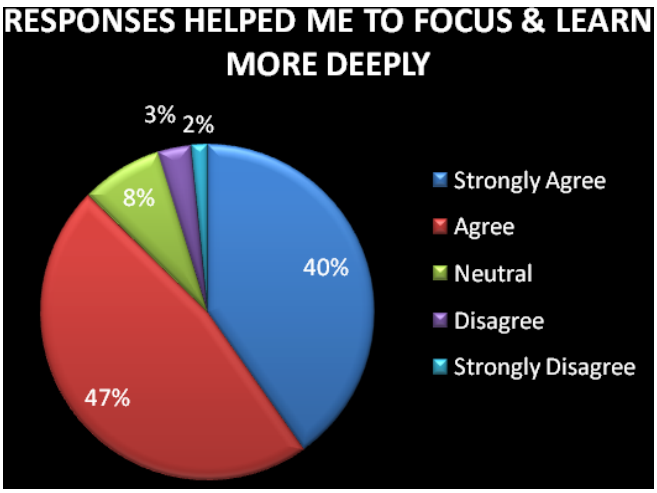

Fig. 14. Question 14 pie chart

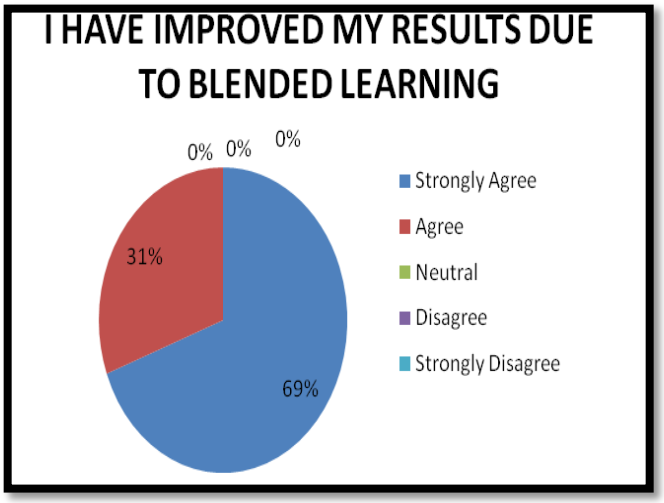

Fig. 15. Question 15 pie chart

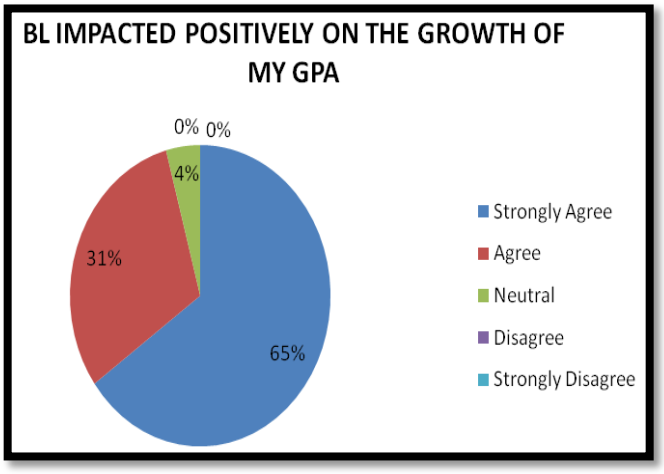

Fig. 16. Question 16 pie chart

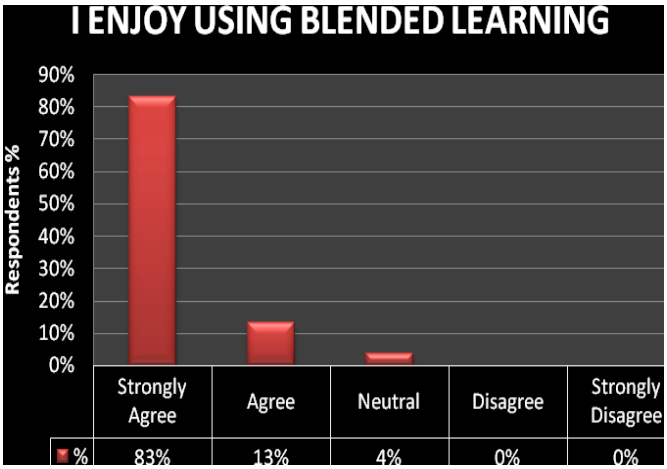

Fig. 17. Question 17 Column chart

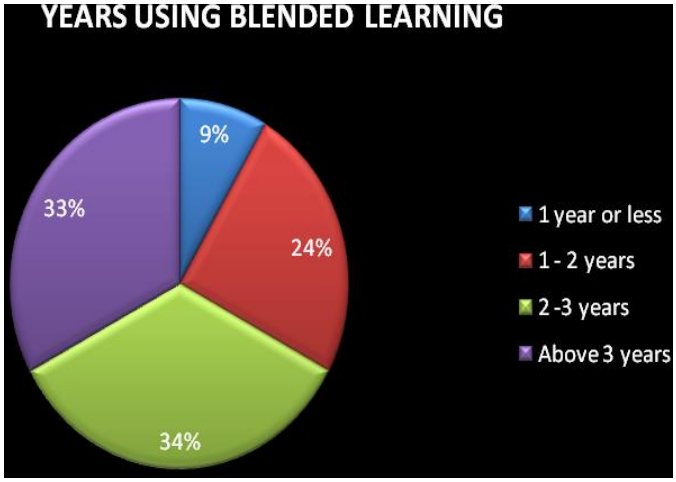

Fig. 18. Years using BL mode

X. PROPOSED FRAMEWORK

A. Framework Introduction

Upon completion of the presentation of results and analysis of the results, the researchers concluded by proposing a framework to monitor BL effects on students and students' perceptions on the same, as shown in Fig. 19. The framework takes note of the research questions and objectives of this study. Its input factors include the student factors, institution factors and the BL mode factors.

The authors combined the theoretical, logical and rational approaches to be able to develop the proposed framework [43] [44]. To establish the criteria and standards of the framework, the authors followed the literature review findings related to various BL frameworks, BL effects on students and perceptions with support from the participants of the questionnaire from Botho University.

The framework is modeled to indicate that the input factors which could affect the students' perceptions on the BL mode and the effects of the BL mode on students are the students, the institution and the BL mode. A triangulation of these factors is observed. The institutional factors, which include the institution characteristics, support and students' performance

expectation plays an integral role in bridging the gap between the student and the BL mode to be used. The BL mode factors include among characteristics, internal and external factors, relevance, ease of use, quality output. These factors should constantly be monitored to ensure they complement the students' factors of student characteristics, students' perceptions and performance expectation together with the university factors. When all the factors are in mutual understanding of each other then they would foster an environment of acceptance and usage which would yield a positive effect on students and a positive perception.

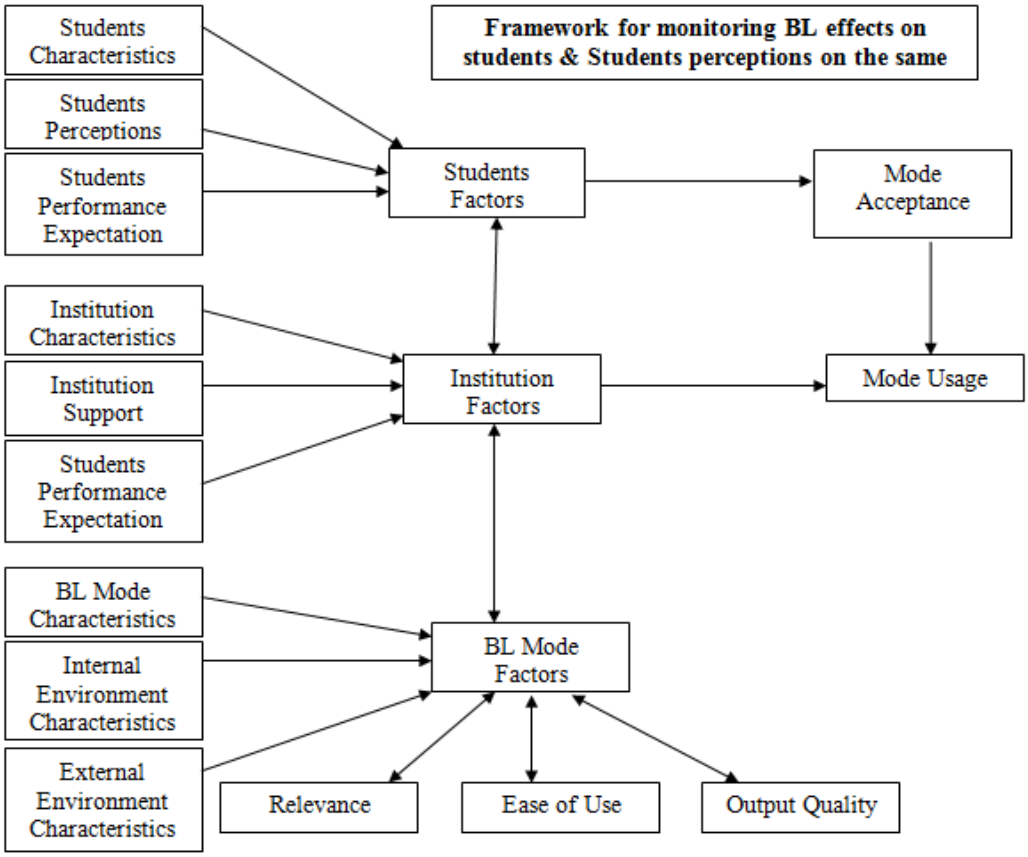

Fig. 19. Proposed framework

B. Intended Use of the framework

The framework would be used to BL mode effects on students and students' perceptions on the BL mode. The main purpose of the framework is to continual usage and appreciation of BL mode through a continuous process of referencing to the three inputs factors and their associated elements. It is essential for the Students, Institution and BL mode factors to be known and revised timely to ensure the integrity of the BL mode remains in place. The dynamism of today's education could impact individual entity factors, thus changing their known scope; hence an updating of them is important. Moreover, there should be a mutual balance between the Student, institution and BL mode factors hence, changes on the individual entities would necessitate a revision to ensure the framework still serves its purpose. When all the individual factors are in harmony, then acceptance of the mode by students and its usage is recognized.

C. Implications of the proposed framework

To realize the full potential of the framework in the academic setup, the following should be taken into consideration on its utilization.

1) The framework is meant to be an influential tool in the acceptance and (continual) usage of BL mode in institutions. It is imperative for all concerned stakeholders to engage with one another (students and institutions) to be able to identify and outline their factors and engage for constructive BL mode initiatives.

2) The framework act as a check tool. BL mode technologies keep on changing due to the nature of the technological setup of the modern-day society, hence it is important to continually check the relevance of the BL mode factors and elements and encourage the adoption of such technologies in line with relevance, ease of use and quality needed. Moreover, it would help institutions to re-align and determine areas of expertise and find ways of mutually assimilating BL mode in their areas and how they can be further developed for support of such in accordance with the various characteristics and or factors of the student cohort.

3) The framework is intended to act as a call up initiative in the Botswana educational set up for formation of research and discussion initiatives around the BL practice in tertiary institutions. This would ensure common understanding

and expectation from all stakeholders at policy and system levels for finding ways to provide support mechanisms such as but not limited to resources, infrastructure and technologies for the growth of the BL mode in Botswana and its appreciation.

XI. Recommendation

It is recommended that Institutions in Botswana review their curricula and find ways of adopting and assimilating the BL mode in their learning process.

With evidence that BL mode plays an important role in the student learning process, it is recommended that institutions, the private sector and the government of Botswana channel funds to the research of the utilization of BL mode.

XII. Conclusion

It is concluded that the purpose of the study was achieved. The purpose was to investigate the effects of the BL mode on the students and the students' perceptions on the BL mode. This was achieved through meeting and addressing of the objectives and research questions outlined earlier. The study concludes that BL mode is important to students learning process. The evidence from the research carried shows that BL mode helps in knowledge gaining, and positively transforms learners' attitudes towards learning whilst also improve students' results. It also revolutionizes learners' critical thinking levels and dispositions. It is also concluded that there is acceptance of BL mode in a typical institution or university learning environment, as indicated by appreciation and satisfaction of respondents to the BL mode. Thus, it is highly appreciated. Therefore, in conclusion, BL mode has positive effects on tertiary students, and the students view it positively on their learning journey.

XIII. Future Work

More work need to be done on identifying why the institutions in Botswana are behind in the adoption of BL mode despite it having a favorable appeal to the students' community. Not only is it favorable, but studies as indicated in the literature review portion of this study it helps in attitudes molding and improvement of learners' results. In addition, studies should be carried out to identify the embracement of the BL mode in supporting the various learners (slow and quick learners). More work needs to be done on the proposed framework, as there are several positive implications this study and the proposed framework could have on the learning scope in Botswana.

As for the institutions not yet utilizing the BL mode, it is their opportunity to put in place the proposal of using such and follow the framework for identification and realization of BL mode. Those utilizing BL mode, could use the framework to re-evaluate their standing as per the current set up and find ways to moderate their findings. In addition, the researcher hopes to provide other researchers an opportunity to trial the framework. This framework is a proposed conceptual framework which relies heavily on the literature review and questionnaire findings, and as such a trial is needed with researchers own context to validate its standing and improvement.

The research was also constrained to the BL mode effects on students, and perceptions of students on the same, thus more need to be done to include all the relevant stakeholders. In this case, staff with focus on lecturers or academics, institutions management should be included. The views and perceptions of stakeholders lead to a more robust scope.

Acknowledgment

We would like to thank our sponsor Botho University for the continued support in upholding research. We also extend our appreciation to the Botho University community and the public for their input. Our greatest appreciation goes to the participants of this study, and finally our families.

References

[1] Friedman, T. L. (2005). The world is flat: A brief history of the twenty-first century. New York: Farrar, Straus, and Giroux.

[2] Nagel, D. (2009). Meta-analysis: Is blended learning most effective. The Journal Newman

[3] Wagner, T. (2008). The global achievement gap. New York: Basic Books.

[4] Garrison, D. R. and Kanuka, H. (2004). Blended learning: uncovering its transformational potential on higher education. Internet and Higher Education, 7, 95-105.

[5] Garrison, D. R., and Vaughan, N. D. (2008). Blended learning in higher education: Framework, principles, and guidelines. San Francisco: Jossey-Bass.

[6] Garrison, R., Anderson, T. and Archer, W. (2001). Critical thinking, cognitive presence, and computer conferencing in distance education. American Journal of Distance Education, 15(1), 7-23.

[7] Picciano, A. G., & Dziuban, C. D. (Eds.). (2007). Blended learning research perspectives. Needham, MA: The Sloan Consortium.

[8] Laster, S., Otte, G., Picciano, A. G., and Sorg, S. (2005). Redefining blended learning. Paper presented at the Sloan-C workshop on blended learning, Chicago, IL.

[9] Mayadas, A., John, B., and Paul, B. (2009). Online education today. Science, 323(5910), 85-89.

[10] Dziuban, C., Hartman, J. and Moskal, P. (2004). Blended learning. Educause Review, 2004(7), 1-7.

[11] Graham, C. R. (2006). Blended learning systems. In C. Bonk (Ed.), The handbook of blended learning. Global perspectives and local designs (pp. 3-21). San Francisco: Pfeiffer.

[12] Shea, P. (2007). Towards a conceptual framework for learning in blended environments. In Blended Learning Research perspectives (pp. 19-36). Needham, MA: The Sloan Consortium.

[13] Republic of Botswana, (2012). Population of Towns, Villages and Associated Localities-Education. Gaborone: Government Printer.

[14] Wang T (2011),Developing Web-based assessment strategies for facilitating junior high school students to perform self-regulated learning in an e-Learning environment, Computers and Education,57, pp1801-1812.

[15] Rhema, A., and Miliszewska, I. (2014). Analysis of student attitudes towards e-learning: The case of engineering students in Libya. Issues in Informing Science and Information Technology, 11, 169-190.

[16] Kalantarrashidi, S.A., Mahammadpour, E. and Sahraei, F. Effect of Blended Learning Classroom Environment on Student's Satisfaction. Journal of Education and Training Studies.Vol. 3, No. 5; September 2015

[17] Kwak, D.W., Menezes, F.M. and Sherwood, C. (2013). Assessing the impact of blended learning on student performance.

[18] So, H.-J., & Bonk, C. J. (2010). Examining the Roles of Blended Learning Approaches in Computer-Supported Collaborative Learning

(CSCL) Environments: A Delphi Study. Educational Technology & Society, 13 (3), 189–200.

[19] Mersal, F.A. and Mersal, N.A. Effect of Blended Learning on Newly Nursing Student's Outcomes Regarding New Trends in Nursing Subject at Ain Shams University. American Journal of Educational Research, 2014, Vol. 2, No. 11.

[20] Duhaney, D. C. (2004). Blended learning in education, training, and development. Performance Improvement, vol. 43, no. 8, pp. 35-38.

[21] Li Z., Tsai M., Tao J., Lorentz C. Switching to blended learning: The impact on students' academic performance. Journal of Nursing Education and Practice, 2014, Vol. 4, No. 3. 245-251.

[22] Melton, B., Graf, H., Chopak-Foss J. Achievement and Satisfaction in Blended Learning versus Traditional General Health Course Designs. International Journal for the Scholarship of Teaching and Learning, 2009; 3 (1), 1-13.

[23] Owston, R., York, D. and Murtha, S. Student perceptions and achievement in a university blended learning strategic initiative. Internet and Higher Education XXX (2013).

[24] Cohen, L., Manion, L. and Morrison, K. (2000). Research methods in education. 5th ed. London: RoutledgeFalmer.

[25] Saunders, M. et al. (2010). Organizational Trust: A Cultural Perspective. Cambridge: Cambridge University Press.

[26] Babbie, E.R. (2004). The practice of social research. Thomson/Wadsworth. Belmont, CA.

[27] Babbie, E.R., Halley, F. and Zaino, J. (2003). Adventures in social research: data analysis using SPSS 11.0/11.5 for Windows. 5th ed. California: Pinee Forge Press.

[28] Chilisa, B. and Preece, J. (2005). Research methods for adult educators in Africa: Pearson South Africa.

[29] Oates, B.J. (2006). Researching Information Systems and Computing. London: Sage.

[30] Bryman, A, Bell, E, 2007, Business Research Methods, 2nd edition. Oxford University Press.

[31] Creswell, J.W. (2003). Research design: a qualitative, quantitative and mixed method Approaches. 2nd ed. California: Sage Publications Inc.

[32] Creswell, J.W. (1994). Research design: qualitative and quantitative approaches. Thousand Oaks, CA: Sage Publications.

[33] Baker, T.L. (1994), Doing Social Research (2nd Edn.), New York: McGraw-Hill Inc.

[34] Patton and Cochran (2002). A Guide to Using Qualitative Research Methodology Available from http://fieldresearch.msf.org/msf/bitstream/10144/84230/1/Qualitative%20research%20methodology.pdf (Accessed 13August 2016)

[35] Ackroyd, S. and J. A. Hughes, Data Collection in Context (1981) Longman

[36] Terre Blanche, M., Durrheim, K., and Painter, D. (Eds.) (2006). Research in practice: applied method for the social science. 2nd ed. Cape Town: University of Cape Town (Pty) Ltd.

[37] Kumar, R. (1996).Research Methodology: A Step-by Step Guide for Beginners. Longman, Australia

[38] Pérez-Marín, D. And Pascual-Nieto, I. (2012). A Case Study on the Use of Blended Learning to Encourage Computer Science Students to Study. Journal of Science Education and Technology, 21(1), 74-82.

[39] Delialioğlu, D. (2012). Student Engagement in Blended Learning Environments with Lecture-Based and Problem-Based Instructional Approaches. Journal of Educational Technology & Society, 15(3), 310-322.

[40] Lim, D.H. and Morris, M.L. (2009). Learner and Instructional Factors Influencing Learning Outcomes within a Blended Learning Environment. Journal of Educational Technology & Society, 12(4), 282-293.

[41] Hamilton, J. and Tee, S. Smart utilisation of tertiary instructional modes. Computers and Edcuation 54 (2010) Computers & Education, 54, 4, pp. 1036-1053, Computers & Applied Sciences Complete, EBSCOhost

[42] Bliuc, A., Ellis, R., Goodyear, P. And Hendres, D. (2011). Understanding student learning in context: Relationships between university students' social identity, approaches to learning, and academic performance. European Journal of Psychology of Education, 26(3), 417-433.

[43] Brown, F. G. (1983) Principles of Educational Design and Psychological Testing, 3rd edn, Hoilt, Rinehart, and Winston, New York.

[44] Friedenberg, L. (1995) Psychological Testing: Design, Analysis and Use, Allyn and Bacon, Boston, MA.

MAC Protocol with Regression based Dynamic Duty Cycle Feature for Mission Critical Applications in WSN

Gayatri Sakya
Department of Electronics and Communication Engineering
JSS Academy of Technical Education,
NOIDA, U.P., India

Dr. Vidushi Sharma
Department of Information and Communication Technology
Gautam Buddha University,
Greater Noida, U.P., India

***Abstract*—Wireless sensor networks demand energy efficient and application specific medium access control protocol when deployed in critical areas which are not frequently accessible. In such areas, the residual energy of nodes also become important along with the efficient data delivery. Many techniques using adaptive duty cycle approach are suggested by researchers to improve the data delivery performance of protocols. As low duty cycle introduces delay and high duty cycle causes energy losses in the network so duty cycle adaptation according to the distribution of nodes near event occurring area, traffic behaviour and remaining energy of the nodes may be done for energy saving as well as efficient data delivery performance. After analysing the S-MAC protocol performance in critical scenarios for the residual energy, throughput and packet delivery ratio, this paper suggests an improved mission critical MAC protocol called MC-MAC which uses novel regression based adaptive duty cycle approach. The duty cycle is given by the regression pattern of traffic while considering the performance of SMAC protocol for residual energy, throughput and packet delivery ratio. The analytical model of MC-MAC protocol is given accordingly and the performance analysis shows that the proposed MC-MAC protocol saves 40% energy of whole network and also 20% energy of the critical nodes in the mission critical path till base station, as compared to SMAC protocol. Very few improved MAC protocols provide mechanism to save the residual energy of critical nodes and hence to improve the lifetime of critical path. As MC-MAC protocol considers the throughput and packets delivery ratio (also along with residual energy) for calculating the regression formula for duty cycle based on traffic, so it is better than other critical MAC protocols which does trade-off of energy with throughput and packet delivery ratio.**

Keywords*—Regression based adaptive duty cycle approach; mission critical MAC; analytical model; performance analysis

I. INTRODUCTION

The wireless sensor networks consists of sensor nodes deployed in large numbers to gather information and send it to base station for further actions. These nodes consist of microcontrollers, sensors and transceivers and are battery operated as shown in Fig. 1.

The nodes are battery powered so power saving is the biggest challenge to researchers in wireless sensor networks for increasing lifetime of the network once the nodes are deployed.

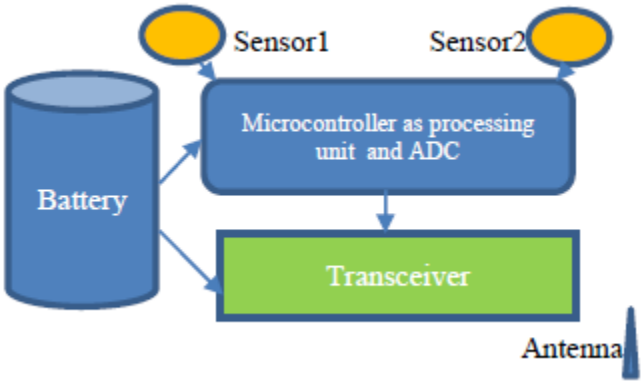

Fig. 1. Architecture of wireless sensor node.

The nodes are battery operated and most of the energy is consumed by the transceiver of the node in communication [1]. Nowadays wireless sensor networks are widely used in some critical applications like gas leakage detection, surveillance of border, patients monitoring system, monitoring volcanic activities, tsunami alert system, etc. Wireless sensor nodes which are deployed once, need to stay active for years to gather information which they sends to base stations. So apart from the data delivery performance, the residual energy of nodes plays an important role to keep the network path alive till base station nodes. The protocol stack for wireless sensor networks is not standardized because of the infinite applications of sensor nodes in almost all the fields of engineering and sciences. According to diversified applications of sensor networks, the existing protocols at MAC layer need to be designed differently which can meet the demand of fast response in mission critical areas along with energy saving. In mission critical applications, traffic load increases suddenly on nodes near event occurring area and they need to send information to base station in timely and reliable fashion. Several MAC protocols were proposed based on the existing basic IEEE 802.11 MAC protocol for wireless LAN [1]. Some protocols introduced periodic listing mechanism, some changed the contention mechanism and some protocols introduced adaptive listening mechanism to make it suitable for wireless sensor networks. But very few protocols talked about the MAC protocol suitable for critical applications of wireless

sensor network which is the need of the hour. The Sensor MAC (SMAC) [2] protocol is the most popular contention based wireless sensor network MAC protocol which introduced the periodic listen and sleep mechanism to save energy of the node. This protocol is already implemented and tested on hardware. The Sensor MAC protocol is an improvement of 802.11 MAC with sleep/awake mechanism to avoid the idle listening problem in 802.11 MAC protocol. The sensor MAC protocol performs well in slow traffic but in high traffic introduces sleep delay because of its periodic sleeping mechanism. Many improvements are done on Sensor MAC protocol to improve its performance but very few researchers have studied the Sensor MAC protocol performance in mission critical scenarios. This motivated to test the performance of SMAC protocol for mission critical applications and then to propose a new model for the mission critical MAC protocol. Medium access control protocols can save energy by intelligently using the transceiver power using periodic sleeping when there is no traffic, by avoiding collision and retransmission of packets and also by avoiding control packet overhead using one RTS/CTS pair to send data.

Mission critical applications are applications running in volcanic areas, in oceans or surveillance applications on border where quick response is required. These areas are not accessible frequently or instantly so the nodes cannot be replaced easily. The lifetime of network and the data delivery performance without delay is utmost importance So the residual energy of the sensor nodes and hence network lifetime is very essential .This paper analyses the Sensor MAC protocol for mission critical scenarios and based on these results proposes a new MC-MAC protocol model suitable for mission critical scenarios. Toward this goal, a novel approach based on regression is used for making MC-MAC protocol adaptive to the traffic scenarios while considering the residual energy of nodes and other mission critical performance parameters.

The paper is divided into various sections. In Section 2, the literature review and motivation for designing MC-MAC protocol is discussed. Section 3 represents the MC-MAC protocol model methodology. Section 4 gives the analytical model and performance analysis of the proposed protocol model and compares it with the basic Sensor MAC protocol. Section 5 discusses the conclusion of the work and Section 6 finally ends with the future scope of the work.

II. Related Work

Literature Review and Motivation

To develop a new protocol, the fundamental contention based Sensor MAC protocol is critically analyzed and thereafter its improvements are also reviewed which motivated to design a new model of mission critical MAC protocol.

A. Sensor MAC protocol critical analysis

S-MAC [2] protocol uses periodic listen and sleep mechanism for increasing the lifetime of the node. The frame interval is divided into listen time and sleep time as shown in Fig. 1.The nodes periodically wake up and the go to sleep to avoid the idle listening. During the sleep period node turns off its transceiver which saves maximum amount of energy. The listen period is fixed in SMAC and the duty cycle is controllable parameter varying from 1% to 100%. The improvements on 802.11 MAC is done to avoid idle listening using periodic listen-sleep of nodes, to avoid overhearing by turning off the transceiver after hearing RTS/CTS packets destined for other node and control packets overhead reduction by using single pair of RTS/CTS packet for transmission of data available. The duty cycle of the Sensor-MAC protocol is fixed during the initial deployment and is not changed when the traffic load and residual energy of the node changes. This makes it unsuitable for mission critical applications where high traffic rate signifies some important information to be delivered and immediate response is sought. So to minimize sleep delay the value of duty cycle should be increased, keeping constraint of residual energy of the node.

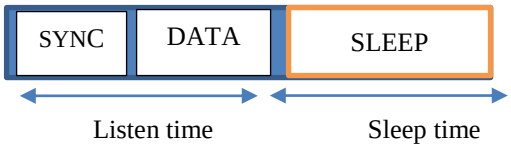

Fig. 2. SMAC frame.

The SMAC frame time is the sum of listen time and sleep time as shown in Fig. 2 and hence the energy saving in SMAC with periodic sleep is directly proportional to sleep time. The duty cycle of S-MAC is given by (1).

$$\text{Duty cycle (d)} = (\text{Listen Time}) / (\text{Listen Time} + \text{Sleep Time}) \quad \ldots\ldots\ldots (1)$$

Now from (1), it's implied that at low duty cycle, the sleep time in a frame will be relatively more and hence the energy will be saved. The future directions from [2] are also concluded as to limit the sleep period for decreasing the latency. The energy consumption in intermediate nodes is more because of SYNC overhead. Also the border nodes can follow multiple schedules, so they have to wakeup multiple times which consumes more energy. The Sensor MAC protocol uses message passing technique which should provide a limit on the number of times the extensions is given for the lost frames, in case of dead receiver.

B. Improved MAC protocols based on adaptive duty cycle approach.

Wei Ye, *et al*. in 2004 suggested an improvement on Sensor MAC protocol which used coordinated adaptive listening of the nodes to improve the latency [3]. In this protocol the neighboring nodes who overhears RTS and CTS packets wakeup for a short period of time after transmission. So if the node is next hop node, its neighbor will be able to pass data to it instead of waiting for the scheduled wakeup time. The drawback is that all the neighboring nodes who overhear RTS/CTS packets will awake for short period, which results in energy consumption. So latency is improved at the cost of residual energy of nodes.

In 2004, P. Lin, *et al.* proposed DSMAC protocol [4]. DSMAC protocol also tune the duty cycle of nodes according to the delay and residual energy of the node. The multiple duty cycle concept is used in DSMAC to improve the latency but at the cost of energy consumption, with not much improvement in

energy seen at high traffic rates. The mission critical scenarios are not taken care where suddenly the traffic rate increases on occurrence of an event.

In 2005, [5] Yang, *et al*. suggested utilization based tuning of duty cycle in their protocol. In U-MAC the duty cycle of the nodes are tuned based on the utilization function which calculated the load on each node. In U-MAC the forwarding node will always have the more utilization and hence all-time its duty cycle will be higher so soon it will die out even at low traffic loads. Hence, U-MAC protocol does not provide solution to improve the network lifetime in mission critical scenarios.

In 2006 Demirkol, *et al*. discussed the sensor network properties which should be taken care while designing the MAC protocols [6]. The authors discussed various many other existing MAC protocols which include contention based and contention free like TDMA approach also. TDMA approach has the feature of collision free access to channel but the network is not adaptable to topology changes when new nodes inserted or existing node dies out. Because of short range, the wireless sensor networks are dense networks. The main challenge of wireless sensor network is energy efficient sharing of communication channel. Multiple nodes in the same region want to transmit information to other nodes. The channel access mechanism thus primarily classified the medium access protocols as contention based, contention free and hybrid which use both the concepts.

Another challenge is confronted when wireless sensor nodes are used in critical application in last few years. Along with the energy efficiency, the throughput and packet loss rate also considered as important parameters for protocol performance in critical scenarios. In wireless sensor network applications, nodes play different roles like source nodes, intermediate nodes and the sink nodes. According to the location of event the role of the nodes changes in network. So if the role of nodes changes according to the scenarios, fixed sleep-listen schedule as in S-MAC will result in energy waste in nodes when no data packets to be forwarded by the nodes and also increase the buffer size on the nodes which are taking part in transmission. So further this work concentered on the existing protocols which used adaptive duty cycle approach.

In 2010, Mishra, *et al*. tuned the slot time in the contention window in listen period for adaptive listening but used a complex fuzzy based approach [7]. As the nodes have very less storage capacity so two fuzzy algorithms used in the paper may be replaced by some simple techniques.

In 2012, Suriyanchai, *et al*. [8] did the study and classification of MAC protocols on the basis of reliability and timely data delivery performance. The mission critical MAC protocol performance parameters based on reliability can be the packet loss rate and packet delivery ratio and the throughput signifies the data delivery in time.

In 2012, Hsu, Tz-Heng, *et al*. in [9] also gave the dynamic traffic aware MAC protocol based on tuning the duty cycle, they concentrated more on the data transmission rate and latency but the energy consumption is extremely increased in their protocol, which is not suitable for the mission critical case.

In 2013, Sakya G, *et al*. performed the analysis of SMAC protocol for single hop scenario in ns 2.35 [10].

In 2013, G. Sakya, *et al.* studied the popular SMAC in ns-2.35 for various packet arrival rates at different values of duty cycles in multi-hop scenario [11] also. The SMAC protocol is tested from low traffic rates to very high traffic rates in multi-hop scenario. It is observed that the residual energy reaches maximum if the duty cycle is 20% under high traffic rates (.01s to .1s packet inter arrival time) along with the optimum performance of packet delivery ratio and throughput. The authors concluded that under mission critical scenarios if the value of duty cycle is made high, then the residual energy can be saved as compared to low duty cycle. Tuning of duty cycle with respect to certain parameters in MAC protocol is the technique which may be used to improve the residual energy, throughput and packet delivery ratio of the network and also of the individual nodes.

In 2013, adaptive duty cycle control is also done by Byun, *et al*. They proposed the tuning of sleep time based on the queue management feedback control system to achieve efficient performance in heavy traffic [12].

In 2015, Donghong Xu and Ke Wang, *et al.* in proposed EA-MAC, an adaptive traffic aware MAC protocol based on correlation of nodes [13]. They also made duty cycle adaptive based on the bases of predicted flow on the node. The protocol performance in terms of energy consumption is very similar to S-MAC protocol, so in spite of having better throughput, delay and packet loss rate the protocol is not suitable for applications in which nodes cannot be replaced frequently, once deployed.

In 2016, G. Sakya, *et al*. analyzed the performance of SMAC in grid scenario and suggested improvements on SMAC to make it suitable for critical applications in grid scenario [14].

To develop the required mission critical MAC protocol, this paper analyzes the performance of S-MAC protocol for residual energy, throughput and packet delivery ratio and studied the data pattern and its behavior. Differing from other proposed protocol, it proposes to tune the duty cycle based on the output parameters like residual energy, throughput and packet delivery ratio under different traffic scenarios using novel regression technique. The analytical model is prepared for performance analysis of the proposed model. The proposed protocol is designed with the following objectives:

1) To save the residual energy of the network, the duty cycle of only selected nodes in event occurring area with high traffic is made high. It takes into consideration the residual energy of node also.

2) Duty cycle allocation is based on regressive analysis of Sensor MAC protocol performance parameters throughput, packet delivery ratio and residual energy with respect to traffic and duty cycle. This is done to improve the overall performance of the protocol.

3) Analytical model is developed to show the effect of this novel duty cycle adaptation approach on the residual energy saving of mission critical MC-MAC protocol.

III. MC-MAC PROTOCOL DESIGN

MC-MAC protocol is based on the novel approach where the results obtained from the S-MAC protocol analysis in mission critical applications for residual energy, throughput and packet delivery ratio are used to make the duty cycle adaptive. The duty cycle is made adaptive according to the observed regressive behavior of it based on traffic while considering the performance of the mission critical parameters for residual energy, throughput and packet delivery ratio.

This work consider first a multi-hop scenario of consists of 11 nodes with one source and one sink as shown in Fig. 3. The node 0 (source node) generates the packets at different time interval in the range .01s to 50s. All nodes have initial energy of 1000 joules. The performance of SMAC protocol is tested in ns-2.35. The nodes are places 200m apart and the routing protocol used is DSR. The CBR packets of size 80 bytes are used for data transmission. The queue size is taken as maximum 50 packets. The simulation runs for 10,000 second each time. The data generated in the trace file is used to summarize the performance of the protocol. The parameters considered in energy model are based on [14], [15].

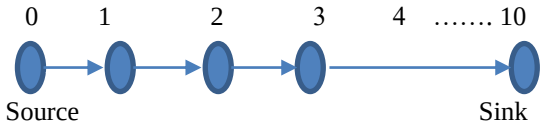

Fig. 3. Network topology

The duty cycle values are varies and the performance of S-MAC protocol is tested under different scenarios. The impact of changing the duty cycle according to the traffic loads is observed and presented in Table 1.

TABLE. I. SMAC PROTOCOL PERFORMANCE

Duty cycle %	Packet inter arrival time (seconds)	Residual energy in (Joules)	Packet delivery ratio (%)	Throughput (Kbps)
20	.1	1304.286	60.4222	0.13
30	.1	1048.182	57.9378	0.2
40	**.1**	**688.1242**	**84.8014**	**0.28**
20	1	1292.846	52.2422	0.06
30	**1**	**1102.84**	**54.6851**	**0.06**
40	1	789.1993	57.3691	0.06
20	**10**	**1002.848**	**84.3318**	**0.06**
30	10	550.9717	57.9378	0.06
40	10	368.9273	94.7644	0.06
20	**20**	**751.0417**	**89.8551**	**.03**
30	20	386.1013	95.0413	0.03
40	20	240.8189	97.0874	0.03

It has been observed in Table 1 that under high traffic rates, for efficient throughput and packet delivery ratio, the duty cycle must be 40%. But along with that to make the protocol energy efficient we have to take care of the energy loss because of this high duty cycle. So in mission critical scenarios, where the traffic rate increases suddenly, we should choose high value of duty cycle for efficient data transmission. In order to save energy, in medium traffic loads, we can choose the duty cycle value as 20%, to have efficient data transmission.

Also, it has been observed that at larger packet inter arrival time at 40s, the energy saving is 1151.221 joules and also the throughput and packet delivery ratio is .01 kbps and 82.5% at 10% duty cycle.

As regression is a measure of average relationship between two or more variables in terms original units of data so we applied this analysis to choose the duty cycle in different scenarios in the wireless sensor networks. The above data is summarized and the following regression expression for duty cycle factor is obtained in Table 2.

From the results obtained from Table 2, the relation between the packet arrivals rate (packets/second) and the duty cycle is obtained as follows:

*Duty cycle factor = (.20953116) * traffic (packets/second) + 20.83677* .... (2)

The duty cycle will be modified in the synchronization module of the protocol which modifies the synchronization packet and sends the synchronization packet to its neighbors at the next synchronization period. The synchronization packet incudes the information about the traffic rate of the node. The duty cycle allocation to the nodes in the network can be done based on this formula calculated. The duty cycle of SMAC protocol can be allocated dynamically to the nodes based on this expression, which takes care of all the output parameters like residual energy, throughput and packet delivery ratio. The sudden increase in the traffic of certain nodes occurs when they send data frequently on the occurrence of event. So according to the traffic only selected nodes tune their duty cycle and send the updated schedule in the synchronization packet to their neighbors.

To minimize the synchronization problem the algorithm uses duty cycle values only 10%, 20% and 40%. So the changed duty cycle will not affect the communication among nodes whose duty cycle is unaffected.

The duty cycle factor is calculated dynamically using (2).

1) If (Duty cycle factor ≥ 30) then assign duty cycle as 40%.

2) If (15 ≤ Duty cycle factor ≤ 30) then assign duty cycle as 20%.

3) If (Duty cycle factor < 15) then assign duty cycle as 10%. Since the base duty cycle is 10%.

TABLE. II. REGRESSION ANALYSIS OF SMAC PROTOCOL

	Coefficients	Standard Error	t Stat	P-value	Lower 95%	Upper 95%	Lower 95.0%	Upper 95.0%
Intercept	20.8367754	3.879835	5.370531	0.001711	11.34316	30.33039	11.34316	30.33039
packets/s	0.209531116	0.109188	1.91899	0.103411	-0.05764	0.476705	-0.05764	0.476705

Tuned duty cycle is the multiple of this base duty cycle, so the nodes which are in base duty cycle will be unaffected. Before sending the synchronization packet to its neighbours the sending node first checks the traffic rate which signifies the load on the node. According to the above algorithm it will modify the existing duty cycle and send the modified duty cycle to the neighbouring nodes. If the traffic on the node is high, then the duty cycle will be high of the node and it synchronizes with the other neighbours too. Without using the complex fuzzy algorithm, this regression technique will modify intelligently the duty cycle of nodes with high traffic. The high traffic signifies the occurrence of an event which must be reported to the base station without much delay.

In such model very few nodes in the whole network will be on high duty cycle during the time of communication and rest other will be able to preserve their energy while working in the normal mode of 20% or 10% duty cycle.

Mission critical applications demand quick reporting of the event to base station. So there should be an intelligent strategy to manage the nodes from one duty cycle to another.

A. Analytical Model

The paper has already discussed the strategy of tuning the duty cycle of the selected nodes in MC-MAC protocol mechanism. So in this model, we have considered the case where only selected nodes tune their duty cycle when event occurs, rest all other nodes remain unaffected. Then we have analyzed the energy performance of the proposed protocol and compared it with simple SMAC protocol.

B. Assumptions

1) There are ρ nodes in the wireless sensor network deployed for monitoring in mission critical region.

2) Only M nodes are tuning their duty cycle, rest other nodes are unaffected.

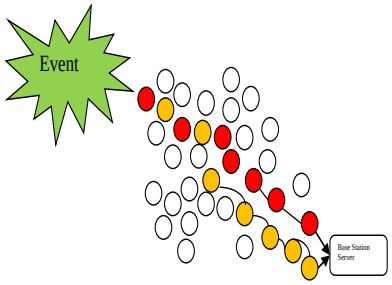

Fig. 4. Nodes with tuned duty cycle

Figure 4 shows that when an event occurs, the traffic increases on the selected nodes in an area. So to reduce the sleep delay, the duty cycle of the selected nodes is tuned based on traffic and residual energy. This reduces the sleep delay and also increases the lifetime of the critical area nodes.

Table 3 describes the notations used to for the analytical model. Here λ_{10} considers the Time in which node considers 10% duty cycle in seconds. Another λ_{20} considers the Time in which node considers 20% duty cycle in seconds and λ_{40} considers the Time in which node considers 40% duty cycle in seconds.

Following equations define the parameters:

λ_{10} =T* $\boldsymbol{\mu_1}$;
λ_{20} = T* $\boldsymbol{\mu_2}$;
λ_{40} = T* $\boldsymbol{\mu_3}$;

The energy dissipation of node in active state is given as in (3).

$$E_{\_active} = I_{d+} T_{r+} R_d \quad \ldots. (3)$$

The duty cycle of the node is given by (4).

$$d = [(L / C)*100] \rightarrow C = [(L/ d)*100 \quad \ldots. (4)$$

Hence Cycle Time for 10% duty cycle is given as (5).

$$C_{10} = S_{10} + L \rightarrow S_{10} = (C_{10} - L) \quad \ldots. \quad (5)$$

Now, Energy consumed in 10% duty cycle is given by (6).

$$\Pi_{10} = (L* E_{\_active})) + (S* S_l) \quad \ldots. \quad (6)$$

Number of frames for 10% duty cycle in total time is given by (7).

$$\alpha_{10} = (\lambda_{10} / C_{10}) \quad \ldots \quad (7)$$

So, in a similar way, α_{20} and α_{40} are obtained. Now Energy consumed by node during $\boldsymbol{\lambda_{10}}$ when it was operating under 10% duty cycle is obtained from (8).

$$E_{n10} = (\Pi_{10} * \alpha_{10}) \quad \ldots.. (8)$$

Similarly energy consumed by node in 20% and 30% duty cycle are obtained by (9) and (10).

$$E_{n20} = (\Pi_{20} * \alpha_{20}) \quad \ldots. (9)$$

$$E_{n40} = (\Pi_{40} * \alpha_{40}) \quad \ldots (10)$$

TABLE. III. NOTATIONS AND THEIR MEANINGS

S. No	Notation	Meaning
1.	T	Total time in seconds
2.	E_{nt}	Total energy consumed by the node in total time T
3.	$\rho(N+M)$	Total nodes in the network
4.	λ_{10}	Time in which node considers 10% duty cycle in seconds
5.	λ_{20}	Total time which node considers 20% duty cycle in seconds
6.	λ_{40}	Total time in which node considers 40% duty cycle in seconds
7.	μ_1	probability of the node to be in 10% duty cycle during the total time
8.	μ_2	that probability of the node to be in 20% duty cycle during the total time
9.	μ_3	that probability of the node to be in 40% duty cycle during the total time
10.	Π_{10}	Energy consumed in 10% duty cycle
11.	Π_{20}	Energy consumed in 20% duty cycle
12.	Π_{40}	Energy consumed in 40% duty cycle
13.	S_l	Sleep power(15µW)
14.	I_d	Idle power (14.4mW) for Mica Motes
15.	T_r	Transmission power(36.0mW) for Mica Motes
16.	R_d	Receive power (14.4mW) for Mica Motes
17.	$E_{\_active}$	energy dissipation of node in active state
18.	d	Duty cycle
19.	L	Listen Time
20.	C	Cycle Time in seconds
21.	C_{10}	Cycle Time for 10% duty cycle
22.	S_{10}	Sleep Time for 10% duty cycle
23.	α_{10}	Number of frames for 10% duty cycle (frame10) in total time
24.	α_{20}	Number of frames for 20% duty cycle (frame20) in total time
25.	α_{40}	Number of frames for 40% duty cycle (frame40) in total time
26.	E_{n10}	Energy consumed by node during λ_{10} when it was operating under 10% duty cycle.
27.	E_{n20}	Energy consumed by node during λ_{20} when it was operating under 20% duty cycle.
28.	E_{n40}	Energy consumed by node during λ_{40} when it was operating under 40% duty cycle.
29.	Ω_m	Residual energy of node taking part in mission critical data transmission
30.	Ω_t	Residual energy of all mission critical nodes
31.	Ω_n	Residual energy node in 10% duty cycle
32.	Ω_{nt}	Residual energy of all nodes in 10% duty cycle
33.	$\Omega_{network}$	Residual energy of network
34.	N	Number of nodes in 10% duty cycle
35.	M	Number of nodes taking part in mission critical data transmission

Now Total energy consumed by node in total time T is given by $E_{nt} = E_{n10} + E_{n20} + E_{n40}$. .... (11)

The residual energy of node taking part in mission critical data transmission is now given as (12).

$\Omega_m = (E_{initial} - E_n)$ ... (12)

So, Residual energy of all mission critical nodes is:

$\Omega_t = (\Omega * M)$ .... (13)

The value of residual energy of one node operating in 10% duty cycle for total time is obtained using the analytical model implemented in MATLAB, so Ω_n =935.065 J and hence residual energy of all nodes in 10% duty cycle is given by (14).

$\Omega_{nt} = (935.065 * N)$ ..... (14)

Also residual energy of network is given by:

$\Omega_{network} = \Omega_t + \Omega_{nt}$ ..... (15)

From this model by changing the values of μ_1, μ_2 and μ_3 in the different traffic scenario, a remarkable improvement is shown in the residual energy of the individual node and the whole network. The values to the μ_1, μ_2 and μ_3 are assigned initially and found the regression pattern for μ_1, μ_2 and μ_3 also based on packet inter arrival time on the nodes. Based on this regression pattern, the values of μ_1, μ_2 and μ_3 can be obtained and the model can be tested for any mission critical scenario.

IV. Performance Analysis

A. Input Parameters

To analyse the performance of proposed MC-MAC protocol model we have considered high traffic scenario to low traffic scenario range as given in Tables 4 and 5. Corresponding to that the probability value of duty cycle ***(μ_1, μ_2, and μ_3)*** is considered. The duty cycle values are assumed on the basis of observations obtained in analysis of SMAC protocol.

For S-MAC protocol, the duty cycle ***(μ_1, μ_2, μ_3)*** are presented in Table 5. Since the duty cycle is initialized only once and is same for all the nodes during whole transmission so ***(μ_1, μ_2, μ_3)*** values will be chosen as in Table 5.

Based on the regression pattern obtained in Table 5, the value of μ_1 can be given as in (16).

$\mu_1 = (-0.02321) * (\text{packets/s}) + 0.411847$ ..... (16)

The value of μ_2 can be given by (17).

$\mu_2 = (-0.02433) * (\text{packets/s}) + 0.434356$ .... (17)

And the value of μ_3 can be given as in (18).

$\mu_3 = (0.047539) * (\text{packets/s}) + 0.153797$ ... (18)

With the help of these regression equations we can obtain infinite pattern of μ1, μ2, μ3 in mission critical applications and can check the energy saving performance for various cases.

TABLE. IV. Input Parameters for MC-MAC Protocol Model

Scenarios	Packet inter arrival time in seconds	μ1	μ2	μ3
Very High traffic rate	0.1	0.2	0.2	0.6
High traffic rate	1	0.2	0.3	0.5
Medium traffic rate	10	0.2	0.6	0.2
Medium traffic rate	20	0.4	0.6	0
Low traffic rate	50	0.8	0.2	0

TABLE. V. Input Parameters for SMAC Protocol Model

Scenarios	Packet inter arrival time in seconds	μ1	μ2	μ3
Very high traffic rate	0.1	0	0	1
High traffic rate	1	0	0	1
Medium traffic rate	10	0	1	0
Medium traffic	20	0	1	0
Low traffic scenario	50	1	0	0

B. Result Analysis

Table 6 represents the Residual energy of whole network in mission critical applications. Table 7 represents the results obtained for average residual energy of individual node in S-MAC and MC-MAC protocols when they operate in mission critical area.

TABLE. VI. Residual Energy Of Network In Mission Critical Scenario

S. no	Packet inter-arrival time (seconds)	Residual energy of the network for MC-MAC in joules	Residual energy for S-MAC in joules
1	0.1	87805	48157
2	1	88583	48157
3	10	90915	87028
4	20	92729	87028
5	50	93247	93506.5

TABLE. VII. Average Residual Energy of Nodes Operating in Mission Critical Scenarios

S.No	Packet inter-arrival time (seconds)	Residual energy of single node (MC-MAC) in Joules	Residual energy of single node (S-MAC) in Joules
1	0.1	650.011	481.57
2	1	688.882	481.57
3	10	805.495	870.28
4	20	896.194	870.28
5	50	922.108	935.065

The performance comparison of proposed MC-MAC protocol and the basic S-MAC protocol is given in Fig. 5 for the individual node and in Fig. 6 for whole network.

This analyzed the behavior of MC-MAC protocol when after an event certain selected nodes tune their duty cycle, rest are unaffected.

In SMAC, if protocol is tuned for high duty cycle of 40% for mission critical applications, then the node always work in 40% duty cycle and consumes more energy than normal mode whereas in MC-MAC, the model considered the node to work in 40% duty cycle for maximum time (given by probability μ3) but not all the time when an event occurs.

The percentage energy saving in very high traffic rate scenarios (mission critical scenarios) for individual node is calculated as 16.84%.In high traffic (1s), the per node energy saving is around 20.7%. In medium traffic (10 packets/s) , when SMAC nodes work in 20% duty cycle, in MC-MAC for some time (given by probability μ3) nodes work in 40% duty cycle also. Hence it is seen that SMAC saves energy.

At low traffic rates, the performance of these nodes are same as in SMAC protocol. Since the nodes saves their energy in high traffic rates so, the network lifetime increases in MC-MAC protocol.

The percentage energy saving in very high traffic rate for whole network is 39.65% as shown in Fig. 6. In high traffic (1s), the energy saving for whole network it is 40.43%.These results differ from other improved SMAC protocols as here the work considered the efficient data transmission as one important consideration while tuning the duty cycle. For simple applications, the performance of MC-MAC protocol is almost similar to SMAC protocol.

V. CONCLUSION

In this paper, we have analysed the basic SMAC protocol for residual energy, throughput and packet delivery ratio and proposed a novel approach of duty cycle adaptation based on regression pattern according to traffic. In SMAC protocol the duty cycle is fixed but the proposed MC-MAC protocol is made intelligent to dynamically change its duty cycle according to the regression formula based as a function of packet arrival rate.

The analytical model shows the behavior of the proposed mission critical MC-MAC protocol and is compared with the popular S-MAC protocol. The analytical model is based on the assumption that nodes operating in mission critical conditions will not always operate in high duty cycle. They will tune their duty cycle according to the traffic and residual energy of the nodes. The analytical results shows that the energy performance of the proposed protocol are almost improved by 40% for the whole network and by 20% for the average energy of individual node operating in mission critical environment. Since the algorithm considers the throughput, packet delivery ratio and the residual energy for obtaining the regression pattern of the duty cycle so it's different from other existing protocols. Recent proposed protocols provide the energy efficiency but at the cost of throughput and packet delivery ratio. This protocol considers the throughput and packet delivery ratio initially to calculate the duty and still saves 40% energy of the network in mission critical scenario.

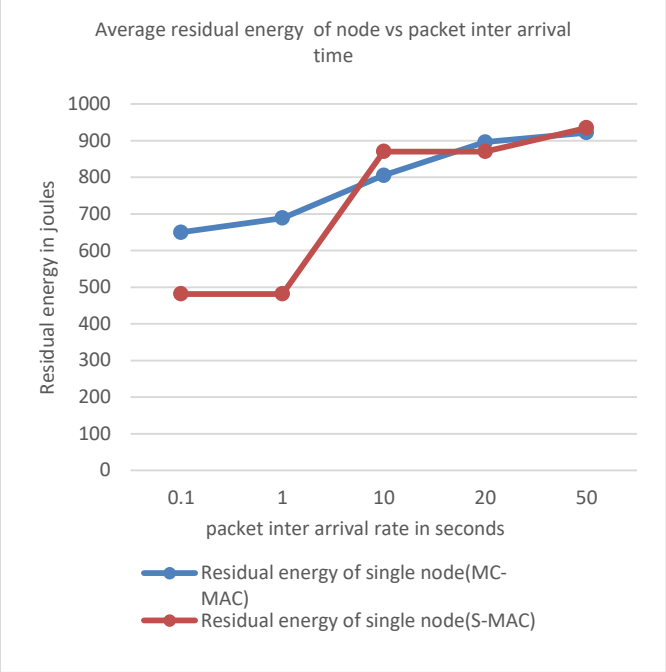

Fig. 5. Comparison of residual energy of node in MC-MAC and simple SMAC.

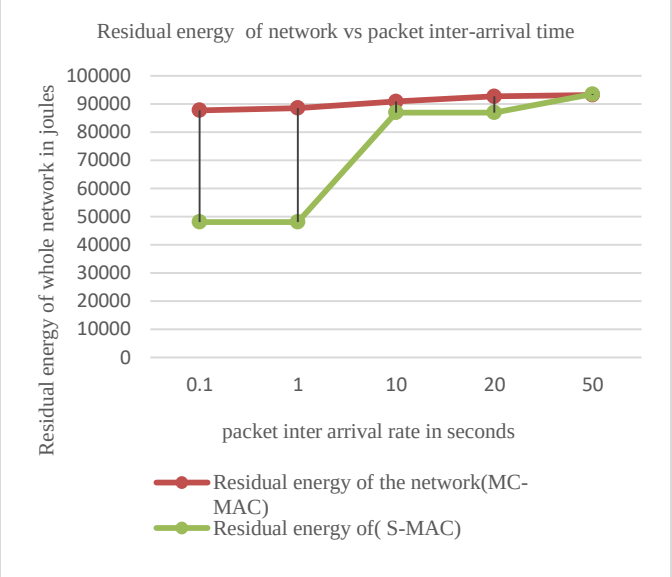

Fig. 6. Comparison of residual energy of network in MC-SMAC and simple SMAC.

Most of the proposed protocols are tested only for low traffic rates and hence the packet arrival time considered above 1 second. But this proposed protocol talks about the high traffic rates and packet inter arrival time below 1 second. So the proposed protocol is suitable for mission critical scenarios, where traffic tare suddenly become high.

VI. FUTURE SCOPE

The analytical model gives an idea of tremendous energy saving without deteriorating the data transmission performance of protocol. In SMAC protocol the nodes keep on sending the data without entering into sleep state after they win the contention till the end of data packets in queue of node. The sleep delay occurs only when the packets arrive at the node after the listen period. The packets wait in the queue for next listen period. In further work the proposed protocol will be implemented in ns-2 to analyse the actual energy, throughput and packet delivery ratio performance which includes this effect of not entering into sleep state when channel node has already occupied the channel for data transmission. The work will be extended to include the node selection algorithm for selecting the nodes which will send the synchronization packets to neighbouring nodes. Also the duty cycle tuning algorithm will be enhanced to include the actual load in the queue of node and its residual energy to calculate the duty cycle. This will make the MC-MAC protocol more suitable for mission critical applications by reducing the synchronization overhead and the traffic in the network in critical areas.

REFERENCES

[1] Akyildiz I. F., Su W., Sankarasubramaniam Y., Cayirci E., “A Survey on Sensor Networks,” IEEE Communications Magazine, Vol. 40, Issue 8, pp. 102-114, August 2002.

[2] Ye W., Heidemann J., Estrin D., “An energy-efficient MAC protocol for wireless sensor networks,” Proc. IEEE INFOCOM, New York, NY, pp. 1567–1576, June 2002.

[3] Ye W., Heidemann J., Estrin D., “Medium Access Control With Coordinated Adaptive Sleeping for Wireless Sensor Networks,” IEEE/ACM Transactions on Networking, vol. 12, no. 3, pp. 493 – 506, June 2004.

[4] P. Lin, C. Qiao and X. Wang, “Medium access control with a dynamic Duty cycle for sensor networks,” 2004 IEEE Wireless Communications And Networking Conference (IEEE Cat. No.04TH8733),2004, pp.1534-1539Vol.3.doi10.1109/WCNC.2004.1311671

[5] Shih-Hsien Yang, Hung-Wei Tseng, E. H. K. Wu and Gen-Huey Chen, "Utilization based duty cycle tuning MAC protocol for wireless sensor networks," GLOBECOM '05. IEEE Global Telecommunications Conference, 2005. St. Louis, MO, 2005, pp. 5 pp.-3262.

[6] Demirkol I., Ersoy C., Alagöz F, “MAC protocols for. Wireless Sensor Networks: a Survey,” IEEE Communications Magazine, vol. 44, no. 4, pp.115-121, April 2006.

[7] Sudip Misra and Debashish Mohanta, “Adaptive listen for energy-efficient medium access control in wireless sensor networks,”*Multimedia Tools Appl.* 47, 1 (March 2010), 121-145.

[8] Suryachai P.,Roedig U.,Scott A., “A Survey of MAC Protocols for Mission-Critical Applications in Wireless Sensor Networks”, IEEE Communication Surveys & Tutorials, vol. 14, no. 2, Second Quarter, 2012

[9] Hsu TH, Kim TH, Chen CC, Wu JS., “ A dynamic traffic-aware duty cycle adjustment MAC protocol for energy conserving in wireless sensor networks.” International Journal of Distributed Sensor Networks. 2012 Feb 26.

[10] Sakya G, Sharma V, Jain PC., “ Analysis of SMAC protocol for mission critical app lications in wireless sensor networks.” In Advance Computing Conference (IACC), 2013 IEEE 3rd International 2013 Feb 22 ,pp. 488- 492.

[11] Sakya G, Sharma V., “ Performance analysis of SMAC protocol in wireless sensor networks using network simulator (Ns-2),” In International Conference on Heterogeneous Networking for Quality, Reliability, Security and Robustness 2013 Jan 11 (pp. 42-51). Springer Berlin Heidelberg.

[12] Heejung Byun, Soogook Son, and Jungmin So. , “ Queue management based duty cycle control for end-to-end delay guarantees in wireless sensor networks.”, *Wirel. Netw.* 19, 6 (August 2013), 1349-1360.

[13] Donghong Xu,Ke Wang , “An adaptive traffic MAC protocol based on correlation of nodes”, EURASIP Journal on Wireless Communications and Networking. December 2015, 2015:258

[14] RF Monolithics Inc., http://www.rfm.com/, ASH Transceiver TR3000 Data Sheet.

[15] Gayatri Sakya, Vidushi Sharma and Trisha sawhney, “An Improved MAC Model for Critical Applications in Wireless Sensor Networks ,”International Journal of Engineering Technology, Management and Applied Sciences, Volume 4, Issue 6, ISSN 2349-4476,June 2016,pp.120-124.

An Internet-based Student Admission Screening System utilizing Data Mining

Dolluck Phongphanich and Wirat Choonui
Department of Science and Technology,
Suratthani Rajabhat University,
Suratthni, Thailand

***Abstract*—This study aimed to propose an internet-based student admission screening system utilizing data mining in order for officers to reduce time to evaluate applicants as well as for the faculty to use less human resources on screening applicants that meets their proficiency and criteria of each department. Another benefit is that the system can help applicants efficiently choose a specialization that is suitable to their proficiency and capability. The system used a decision tree based classification method. Prior to system development, six models were created and tested to find the most efficient model which would later be applied for development of internet-based student admission screening system. The first three of six models employed a k-fold cross validation technique, while the remaining three models use a percentage split test technique. Experiment results revealed that the most efficient model was the data classification model that uses Percentage Split (80), which provided the precision of 87.90%, recall of 87.80%, F-measure of 87.60% and accuracy of 87.82%. To make the efficient student admission screening system, this experiment selected a data classification model that implements Percentage Split (80).**

Keywords*—Classification method; data mining; decision tree; student admission screening

I. Introduction

Undergraduate student admission of educational institutions in Thailand is crucial because it directly affects to education management, budget planning for institution administration and education management, and lastly educational quality and standard indicator of each university that mainly concentrates on students. The efficient student admission as well as nurturing students throughout their enrolled curriculum until they complete the study in high quality under a specified timeframe are therefore what the institutions realize and pay attention to [1]. Faculty of Science and Technology, Suratthani Rajabhat University continuously receives a lot of applications and new students can enroll to the faculty in various ways. Each academic year, the university has to advertise itself in different ways, such as a roadshow and direct admission at high schools, billboard advertising, admission advertising via radio and newspapers, so as to gain a huge volume of applications, and this gives the institution more opportunity to get a number of candidates with appropriate knowledge and capabilities for further examination to finally select those candidates as new students of the university.[1]

Nonetheless, each student admission requires a number of personnel to evaluate student's profile so as to screen the right applicants given each department's criteria. And since criteria are different from one department to another, each student admission screening takes time and sometimes the screening does not serve unqualified students in accordance with a department's criteria, due to the fact that staffs evaluating those applicants are not from the department where students apply for. This results in maintaining a student status for an entire curriculum. That is, students are unable to complete the program or even finally drop out from studying.

This study aimed at developing an internet-based student admission screening system utilizing data mining to help reduce time as well as a number of personnel for evaluating applicants to select ones in accordance with their capability and criteria specified by each department. Besides, this system would help applicants choose the right specialization conforming to their proficiency and capability. The system was developed by analyzing student profiles to create six decision models for a decision tree based classification method, which is efficient and one of popular techniques for data mining. Those six models came from different modeling techniques: the first three models used a k-fold cross validation technique, while the next three models implemented a percentage split test technique. All models were then compared to each other to select the most efficient model for developing an internet-based student admission screening system. This student admission screening system will not only help save time and human resources on application screening, but also help applicants decide to select a specialization for studying which most fits with their characteristics and the university's objectives.

The next topics will describe related literature, research methodology, discussion of findings, and conclusion, respectively.

II. Literature Review

Sumitra Nuanmeesri develops an information system to

The Research and Development Institute of the Suratthani Rajabhat University (*sponsors*).

[1] Suratthani Rajabhat University, Department of Computer Science, "Recruitment Regulations for Students Admission", 2016, [Online] Available: http://www.sci.sru.ac.th/qts/devop.php.

forecast student admission via the internet with the aim of correctly and accurately forecasting student admission. As part of research methodology, the researcher creates and tests seven forecast models.[2] Three of those models use a k-fold cross validation technique, while the next three of the models employ a percentage split technique, and the last one apply a technique of separating data for training and testing a model. From the experiment, the technique of separating data for training and testing a model serves better performance on forecasting students than any other modeling technique as the former has the accuracy of 94%, precision of 94.30%, recall of 94.00% and F-measure of 93.70%. Decision tree classification rules underlying the most efficient model are utilized as part of development of information system to forecast student admission via the internet. The system is then evaluated by two sample groups comprising of experts (4 persons) and personnel (40 persons) based on mean and standard deviation. System performance evaluation shows that the average of experts was 4.17 while the average of personnel was 4.34. It can be concluded that the information system has satisfactory performance and can be applied to forecast student admission.

Supatkul Phakkachokh [2] applies data mining techniques to develop a model for selecting high school program with the objectives of discovering factors influencing selection of study program as well as capability to complete the chosen program successfully by using data mining techniques. Data used in this study is from study result of each subject and questionnaire on study program selection of high school students. A sample group consists of 850 students of Satri Si Suriyothai School enrolled in academic year 2012. The result shows that a high school study program selection model can represent what factors influence on study program selection and provide the accuracy of study program suggestion of 79.76%. It can be conclude from the model that a score of junior high school's basic subjects, including Thai language, mathematics, science, social studies, religion and culture and English language, as well as grade point average (GPA) are factors directly affecting to study program selection and success in completing the chosen program.

Raywadee Sakdulyatham adapts data mining techniques in knowledge based creation for education achievement prediction of Ratchaphruek College students to predict the right specialization so that academic advisors to use derived rules for providing academic advices.[3] Data used for modeling includes personal details and registration data of students from all of four specializations under Faculty of Business Administration, including Marketing, Business Computer, Management and Hotel and Tourism Management. The outcome is a model for analyzing student learning behaviors in each department which suggests that a study result of core finance subject group impacts to study result of restricted elective subject groups of Business Computer and Hotel and Tourism Management most, whereas a study result of core business subject group impacts to a study result of restricted elective subject groups of Marketing and Management most. Apart from that, a study result forecasting model was created for each specialization. The prediction model of study result for Business Computer has an accuracy of 73.49%, model for Marketing has an accuracy of 83.58%, model for Management has an accuracy of 78.12% and model for Hotel and Tourism Management has an accuracy of 86.67%.

Utcharaporn Juthapart, Kant Charoenjit and Phayung Meesad [1] adapt data mining techniques for providing suggestions of specialization selection to students, since most of students lack knowledge, understanding and experience about choosing a specialization, so they decide to pursue the inappropriate one. The technique adopted in this study is a decision tree algorithm, which is similar to that of Sumitra Nuanmeesri. Both researchers categorize grades into three groups: High (grade A, B+ and B), Medium (grade C+ and C) and Low (grade D+, D and F). Findings revealed that using a decision tree algorithm to categorize students of all specializations is very efficient as all models have an accuracy of more than 80%.

Teerapong Sungsri [3] applies the concept of data mining for analyzing candidates' profile and then stores the analysis result in a database for planning of future student admissions. The research comprises of two modules. The first module is for analysis of specialization selection behavior by using a simple k-means clustering technique, which results in four behavioral groups. The second module is for searching for association rules among groups of applicant behaviors by applying an Apriori algorithm with a confidence of 0.9. The second module is for comparing two models forecasting a number of new students. One model is created by a decision tree algorithm which is similar to Utcharaporn Juthapart, Kant Charoenjit and Phayung Meesad [1] and Sumitra Nuanmeesri with accuracy of 93.76%, while the other model is created by a multilayer perception-based artificial neural network model with accuracy of 93.60%.

From all related researches aforementioned, a classification technique, which is one of data mining techniques currently popular, is applied on educational data with the use of decision tree algorithm for modeling. Although this study applies a decision tree based classification techniques like related literature, but this study is differentiated from the others in a way to create a model and objectives of utilizing data from a model to develop an internet-based student admission screening system to facilitate related personnel as well as to help applicants make a decision on selecting a specialization appropriate to their proficiency. The next section will describe research methodology.

III. METHODOLOGY

A methodology of this research was divided into two stages. The first stage will be data analysis using data mining and the second stage will be development of internet-based student admission screening system. Both stages will be presented in the following sections.

[2] S. Nuanmeesri, "Developing Information System to Forecast the Student Admission via the Internet". Suan Sunandha Rajabhat University (In Thai), 2012. [Online]. Available: http://www.eresearch.ssru.ac.th/bitstream/123456789/330/1/ird_036_55%20%281%29.pdf.

[3] R. Sakdulyatham, "Utilizing Data Mining Techniques in Knowledge Based Creation for Education Achievement Prediction of Ratchaphruek College Students. (In Thai), 2009. [Online]. Available: http://www.rpu.ac.th/ebook/54/54-4.pdf (2009).

A. Data analysis using data mining

We followed Cross-Industry Standard Process for Data Mining (CRISP-DM) (shown in Fig. 1) which has six phases as follows:

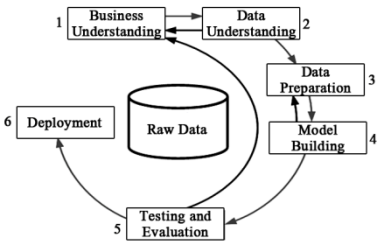

Fig. 1. Cross-industry standard process for data mining [4].

1) Business understanding and data understanding

The first and second phase of CRISP-DM is business understanding and data understanding, respectively. For business understanding, we targeted that this experiment helps facilitate personnel on quickly screening applicants regarding to criteria defined by Faculty of Science and Technology, helps reduce a number of personnel for evaluating candidate qualifications, aids students on choosing a specialization that meets their proficiency, thereby reducing student dropouts, as well as helps planning for future student admissions. And in terms of data understanding, we studied data files managed by Office of the Registrar by looking into data characteristics and validating not only data integrity, but also possibilities of using data for analysis.

2) Data preparation

The third phase is about data preparation which covers activities to improve data quality prior to analysis by using a decision tree algorithm. Those activities include verification of data integrity and completeness, data cleaning which includes feature verifications in terms of missing value, noisy data, errors and outliers, as well as data inconsistencies. Data preparation of this research can be explained below.

At the beginning, data collection was performed on 984 data files of new students of each specialization of Faculty of Science and Technology, Suratthani Rajabhat University, including a student ID, full name, national ID, address, contact telephone number, highest level of education, selected specialization for an undergraduate study, score from each subject taken in a high school education, such as mathematics, science and English language, and GPA per semester. The data files were during academic year 2010-2012.

The next step was to perform data cleaning and preparation by removing some features in the sample to keep only necessary features for further analysis, which in this study included a highest level of education, selected specialization for an undergraduate study, score from each subject taken in a high school education, such as mathematics, science and English language, and GPA per semester. For a study result of main subjects, an average score of each subject group would be determined by considering a score for five semesters. For example, a mathematics subject group 1st – 5th semester was 6 periods a decision tree algorithm and student admission criteria set by Faculty of Science and Technology, Suratthani Rajabhat University.

For the last step of data preparation, data would be transformed to a proper format for further analysis by applying a decision tree algorithm on continuous and discrete quantitative data; for instance, a score of each subject and average score across five semesters are continuous data, so to prepare data for data mining, the quantitative data had to be transformed to a nominal scale as presented in Table 1. To illustrate, suppose that a student gets a score within 0.00-0.90, a nominal value will be F, meaning that the student fails to pass the criteria. For a score within 1.00-1.49, a nominal value will be T, meaning that the student's score is terrible. For a score within 1.50-1.99, a nominal value will be L, meaning that the student's score is low. For a score within 2.00-2.49, a nominal value will be M, meaning that the student's score is medium. For a score within 2.50-2.99, a nominal value will be G, meaning that the student's score is good. Lastly, for a score within 3.00-4.00, a nominal value will be E, meaning that the student is excellent, respectively.

TABLE. I. SPECIFIES A VALUE IN EACH SCORE SCALE

Score Scale	Value
0.00-0.90	Fail (F)
1.00-1.49	Terrible (T)
1.50-1.99	Low (L)
2.00-2.49	Medium (M)
2.50-2.99	Good (G)
3.00-4.00	Excellent (E)

3) Modeling

The fourth phase is model creation or so called modeling. An algorithm used to analyze a sample to build a model is J48 decision tree classifier. J48 decision tree is one of the decision tree families that can construct a tree for the purpose of improving prediction accuracy and produce both decision tree and rule-sets; The J48 decision tree classifier is among the most popular and powerful decision tree classifiers [5]. In this phase, we created six models. Model 1 to Model 3 used a k-fold cross validation technique, which partitions a sample into k equal sized sub samples. The first subsample is retained for testing a model, while the remaining k – 1 sub samples are used as training data. The cross-validation process is then repeated k times (folds). Model 4 to Model 6 used a percentage split test technique, which separates data into two parts: the first part is for testing while the second part is for training. More specifically, Model 1 partitioned data into five sub-samples equally, kept the first sub sample for testing and left 2nd – 5th sub-sample for training, and then repeated for five folds. Similarly, Model 2 partitioned data into 10 sub-samples equally and Model 3 partitioned data into 100 sub-samples equally. Model 4 slated the sample in 70:30 ratios, meaning 70% of an original sample was used for training whereas the remaining 30% of an original sample was used for testing. Similar to Model 4, Model 5 slated the sample in 80:20 ratios and Model 6 slated the sample in 90:10 ratios. WEKA software was used to develop models, and after that those models were compared to each other in the area of accuracy, precision, recall and F-measure to find the most efficient one for development of internet-based student admission screening

system which will be described in the next stage. Performance of each of six models was presented in Table 2.

TABLE. II. PRESENTS PERFORMANCE OF EACH MODEL

Modeling	Times(Seconds)	Precision (%)	Recall (%)	F-Measure(%)	Accuracy (%)
Cross validation (5 folds)	0.11	88.00	88.50	87.40	87.50
Cross validation (10 folds)	0.02	87.90	87.40	87.30	87.40
Cross validation (100 folds)	0.02	88.10	87.60	87.50	87.60
Percentage Split (90)	0.00	88.50	87.80	87.50	87.76
Percentage Split (80)	0.10	87.90	87.80	87.60	87.82
Percentage Split (70)	0.00	87.40	87.10	86.90	87.12

4) Testing and evaluation

The fifth phase is about testing and evaluation of generated models to see the efficiency, error and level of accuracy of each model so as to get the right model for real usage. Evaluation is measured in terms of precision, recall, F-measure and accuracy. In this stage, the accuracy of each model is compared to that of other models to find the most efficient one. All measures can be derived from a confusion matrix as presented in Fig. 2 and calculated by using below formulas:

		Predicted Class	
		Class=Yes	Class=No
Actual Class	Class= Yes	True Positive (TP)	False Negative (FN)
	Class= No	False Positive (FP)	True Negative (TN)

Fig. 2. Shows a confusion matrix.

1) Precision of a particular model can be measured by considering each class [6].

$$Precision = TP/(TP + FP) \quad (1)$$

2) Recall of a particular model can be measured by considering each class.

$$Recall = TP/(TP + FN) \quad (2)$$

3) F-measure is a measurement of precision and recall at the same time for a particular model by considering each class [5].

$$F\text{-}measure = (2 \times Precision \times Recall)/(Precision + Recall) \quad (3)$$

4) Accuracy is a measurement of integrity of a particular model by considering every class [5].

$$Accuracy = (TP+TN)/(TP+TN+FP+FN) \quad (4)$$

5) Deployment

The sixth phase is an application of research findings. In this study, the most efficient model selected as an input of the next stage was a model implemented Percentage Split (80).

B. Development of internet-based student admission screening system utilizing data mining

The system was a web application based on PHP programming language and underlying database run on MySQL. The data analysis result from data mining in the first section was used together with student admission criteria of Faculty of Science and Technology's curriculums, which conforms to the university's targets. The system has two main functions. The first main function is for general users who can use the system to help suggest a specialization provided by the faculty according to their proficiency. This suggestion can be used to support decision making on applying an undergraduate program. The second main function is for personnel who can do basic screening from applicants' profile to see whether they pass the faculty's criteria by inputting a profile of each applicant or importing multiple applicants at once. Details of all functionalities will be further discussed in results and discussion section below.

IV. RESULTS AND DISCUSSION

In this study, we will present the results in two sections. The first section is about data analysis using data mining techniques and the second section is about development of student admission screening system that utilize data mining techniques.

A. Data analysis by using data mining techniques

In this section, modeling was done by using decision tree methods. All six models were compared in terms of accuracy, precision, recall and F-measure. A performance comparison was shown in Fig. 3.

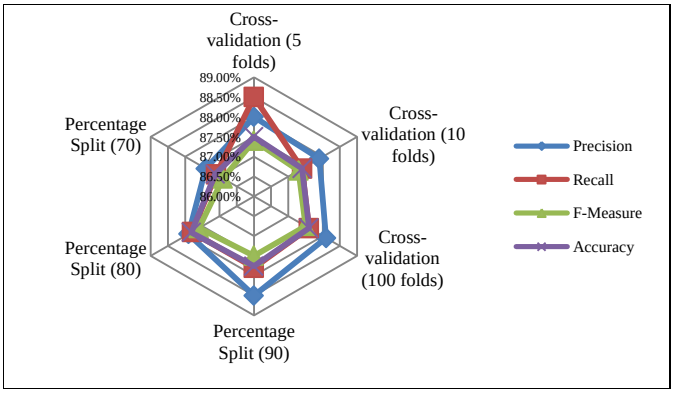

Fig. 3. Graphically presents performance of each model.

From an experiment of classification by using six models implementing different techniques, it was found from a comparison on precision, recall, F-measure and accuracy of all six models that all models gave the similar result shown in Table 3.

TABLE. III. PERFORMANCE OF EACH MODEL

Modeling	Order	Precision (%)	Recall (%)	F-Measure (%)	Accuracy (%)
Cross-validation (5 folds)	4	88.00 (3)	88.50 (1)	87.40 (4)	87.50 (4)
Cross-validation (10 folds)	5	87.90 (4)	87.40 (5)	87.30 (5)	87.40 (5)
Cross-validation (100 folds)	3	88.10 (2)	87.60 (4)	87.50 (2)	87.60 (3)
Percentage Split (90)	2	88.50 (1)	87.80 (2)	87.50 (2)	87.76 (2)
Percentage Split (80)	1	87.90 (4)	87.80 (2)	87.60 (1)	87.82 (1)
Percentage Split (70)	6	87.40 (6)	87.10 (6)	86.90 (6)	87.12 (6)

When considering each aspect, it was found from the experiment that the model with highest precision (represented in %) was 90 Percentage Split (88.50), followed by Cross validation (100 folds) (88.10), Cross validation (5 folds) (88.00), Cross validation (10 folds) and Percentage Split (80) (both at 87.90), and lastly Percentage Split (70) (87.40).

In terms of recall (represented in %), the experiment revealed that a model with highest recall was Cross validation (5 folds) (88.50), followed by Percentage Split (90) and Percentage Split (80) (both at 87.80), Cross validation (100 folds) (87.60), Cross validation (10 folds) (87.40), and Percentage Split (70) (87.10), respectively.

Next, for F-measure (represented in %), the model with highest F-measure was Percentage Split (80) (87.60), followed by Cross validation (100 folds) which gets the same F-measure as Percentage Split (90) (87.50), Cross validation (5 folds) (87.40), Cross validation (10 folds) (87.30), and lastly Percentage Split (70) (86.90).

Finally, as per accuracy (represented in %), the model with highest accuracy was Percentage Split (80) (87.82), followed by Percentage Split (90) (87.76), Cross validation (100 folds) (87.60), Cross validation (5 folds) (87.50), Cross validation (10 folds) 87.40, and Percentage Split (70) (87.12).

B. *Development of internet-based student admission screening system utilizing data mining*

They are of two types: component heads and text heads. This section will present user interfaces of the internet-based student admission screening system, which comprises of two sections.

1) General user section.
2) Officer section.

1) General user section

General users can use this internet-based student admission screening system to know a guideline in selecting a specialization respecting to their proficiency and capability. To tailor the guideline for users, the system will predict from a level of study results from a high school education based on a model from data mining and admission criteria of the faculty, which conform to the university targets. An input screen for general users is shown in Fig. 4.

A screen in Fig. 4 is for general users to input study results, which will be used by the system to suggest a specialization based on the student's proficiency. To do so, an applicant has to choose (subject) a designated specialization in Preferred Specialization (in case of not preferring any specializations, the system will perform analysis for all specializations) and select an education background. Then, the user has to fill in a score of each subject group for each of four semesters and average score of each subject group for all four semesters in the fifth semester row.

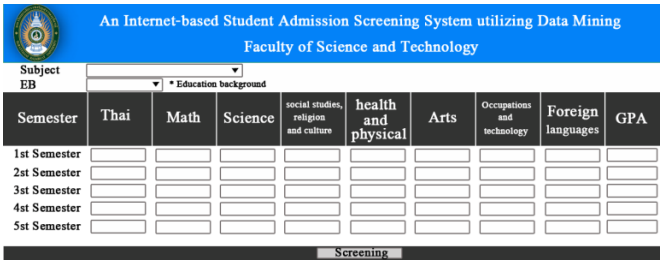

Fig. 4. An input screen for general users.

The most important data for screening is GPA of the fifth semester or GPA of the recent semester, in which the user is required to specify. After the user fills then click Screening, the system will display a screening result as shown in Fig. 5.

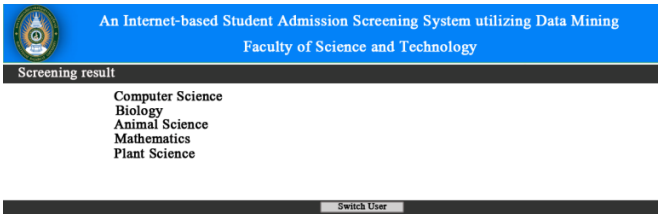

Fig. 5. Screening result.

2) Officer section

Officer section can use this internet-based student admission screening system to evaluate applicants as well as for the faculty to use less human resources on screening applicants that meets their proficiency and criteria of each department. The officer section was shown in Fig. 6. Three main menus for officers include:

1) Additional Subject.
2) Individual Screening.
3) Importing a CSV File.

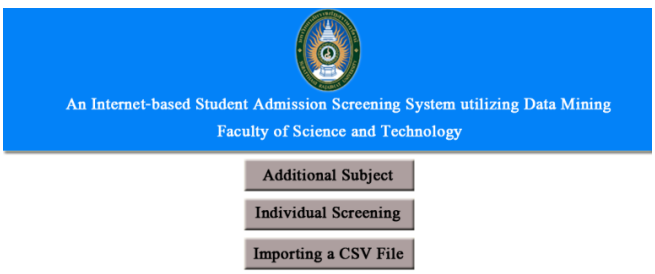

Fig. 6. Main menu for officers.

a) Additional Subject: Additional Subject is for searching and adding additional subjects in case that users would like to collect information of additional subjects from students. More specifically, the user can add and record additional information by using a screen shown in Fig. 7.

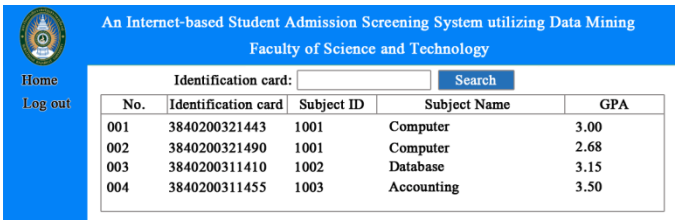

Fig. 7. An additional subject searching screen.

b) Individual Screening: Individual Screening is for officers to record a student profile which comprises of personal details; educational background and address as shown as an example in Fig. 8.

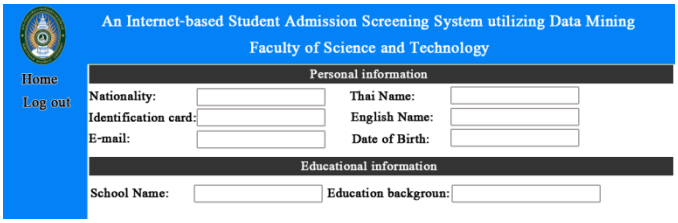

Fig. 8. An input screen to record a student profile for screening.

In terms of educational background, a study result is collected based on subject groups, including Thai language; mathematics; science; social studies, religion and culture; health and physical education; arts; occupations and technology and foreign languages and GPA. In case that a school or college does not provide ones of subject groups, an average grade of those subject groups can be blank. Indeed, the most important piece for screening is GPA of 5th semester or GPA of the recent semester, which will be retrieved by the system from the educational background section.

c) Importing a CSV File: Importing a CSV File is for officers to do screening of multiple applicants at once by inputting a number of student profiles. To use this function, an officer has to convert data into a CSV file with the condition that the CSV file must have a record with a given format as shown in Fig. 9.

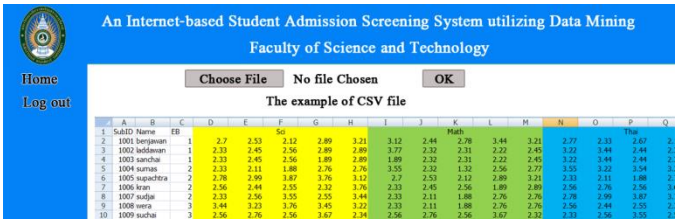

Fig. 9. A CSV file import screen.

V. Conclusion

The development of internet-based student admission screening system utilizing data mining used J48 decision tree to create a model through WEKA software, and then used the result for system development. 984 data sets of undergraduate applicants of Faculty of Science and Technology, Suratthani Rajabhat University during academic year 2010-2012 were used as samples for analysis. The system would help officers reduce time to do screening, help the faculty use less personnel for a screening process to find the right ones corresponding to their proficiency as well as criteria set by each department, leading to receive new qualified students aligning with a target group of each department. Moreover, this system would help applicants efficiently choose the right specialization according to their proficiency and capability. In addition, data from analysis can be used to make a decision on education management and budget planning for institution administration and learning management.

In this section, summary of this research will be described in the first section and suggestions will be discussed in the second section below.

A. Conclusion and discussion

This student admission screening system has a limitation of bring a model up to date, since it is developed based on applicants of academic year 2010-2012. If in the future some subjects are changed or added to in a given curriculum, the result from generated models may be incorrect.

B. Suggestion

1) Parameter settings in WEKA software results in different generations of classification rules or models; therefore, researchers should fine tune settings and use a large amount and variety of data for training and testing models in order to increase integrity and accuracy of screening.

2) This research idea can be improved and applied to similar works or used by another faculty, since capabilities of storing student profiles from the screening system, as well as recording a grade and additional subjects of applicants are in place.

C. Future work

In future work, we may adopt other data-mining techniques, such as anomaly detection or classification-based association, to gain more knowledge of the undergraduate applicants in Faculty of Science and Technology. We also plan to use data sets of undergraduate applicants from all departments of Suratthani Rajabhat University and compare the results with the data set from Faculty of Science and Technology.

Acknowledgment

We gratefully acknowledge financial support from the Research and Development Institute of the Suratthani Rajabhat University. We would like to express thanks to the Office of Academic Promotion and Registration as well as Department of Science and Technology, SRU for giving the information in this research and highly appreciates Dr. Nara Phongphanich, lecturer in Maejo University, Thailand for providing us advice during this study.

REFERENCES

[1] U. Juthapart, K. Charoenjit and P. Meesad, "Using Data Mining Technique to Selecting Majors for Students at the Faculty Information Technology Phetchaburi Rajabhat University". Joint Conference on ACTIS & NCOBA 2015, Jan 30-31, Nakhon Phanom, Thailand. ISSN: 1906-9006.

[2] S. Phakkachokh, "A Model for Selecting High School Program by Considering the Primary Subject Records Using Data Minig Techniques", Master's Thesis, Department of Science in Web Engineering, Faculty of Information Technology, Dhurakij Pundit University, 2013.

[3] T. Sungsri, "The Behavior Analysis on the Applying Major Selection and the Comparison of Model to Forecast the Numbers of New Students Using Data Mining Technique". The Tenth National Conference on Computing and Information Technology (In Thai), NCCIT2014 :pp.963-968, 2015.

[4] D. L. Olson and D. Denlen, "Advanced Data Mining Techniques., Springer-Verlag". ISBN 978-3-540-76916-3, 2008.

[5] J. Han and M. Kamber, "Data Mining: Concepts and Techniques", 2nd ed., Morgan Kaufmann publishers, San Francisco: CA, 2006.

[6] L. H. Witten, E. Frank and M. A. Hall, "Data Mining Practical Machine Learning Tools and Techniques", 3nd ed., Burlington, USA: Morgan Kaufmann publishers, 2011.

EVOTLBO: A TLBO based Method for Automatic Test Data Generation in EvoSuite

Mohammad Mehdi Dejam Shahabi
Software Engineering Lab., Department of Computer Engineering and Information Technology
Shiraz University of Technology
Shiraz, Iran

S. Ehsan Beheshtian
Software Engineering Lab., Department of Computer Engineering and Information Technology
Shiraz University of Technology
Shiraz, Iran

S. Parsa Badiei
Software Engineering Lab., Department of Computer Engineering and Information Technology
Shiraz University of Technology
Shiraz, Iran

Reza Akbari
Software Engineering Lab., Department of Computer Engineering and Information Technology
Shiraz University of Technology
Shiraz, Iran

S. Mohammad Reza Moosavi
Department of Computer Science, Engineering and Information Technology
Shiraz University
Shiraz, Iran

***Abstract*—Now-a-days software has a great impact on different aspects of human life. Software systems are responsible for safety of major critical tasks. To prevent catastrophic malfunctions, promising quality testing techniques should be used during software development. Software testing is an effective technique to catch defects, but it significantly increases the development cost. Therefore, automated testing is a major issue in software engineering. Search-Based Software Testing (SBST), specifically genetic algorithm, is the most popular technique in automated testing for achieving appropriate degree of software quality. In this paper TLBO, a swarm intelligence technique, is proposed for automatic test data generation as well as for evaluation of test results. The algorithm is implemented in EvoSuite, which is a reference tool for search-based software testing. Empirical studies have been carried out on the SF110 dataset which contains 110 java projects from the online code repository SourceForge and the results show that the TLBO provides competitive results in comparison with major genetic based methods.**

Keywords*— *EvoSuite; TLBO; test data generation

I. INTRODUCTION

In order to reduce software testing cost, automated test generation methods are used. These methods could be categorized into three classes based on the test data generation method used: random search algorithms, dynamic symbolic execution, and evolutionary optimization algorithms.

Dynamic Symbolic Execution (DSE) is the interpretation of programs using symbolic values for input arguments to explore code paths. A path is distinguished by logical conditions on the input values. A model for the condition is defined by a program input that follows the path described by the condition [1]. The drawback is path explosion which means that the number of feasible paths grows exponentially with an increase in program size.

Evolutionary algorithms are used to formulate the testing problem as an optimization problem. Search algorithms are used to find answers based on a cost function. These evolutionary algorithms, such as genetic and simulated annealing, try to find the best test suite that maximizes the coverage in the software under test. The commonly used evolutionary algorithm in the literature is the GA and its extensions (i.e., 73% of related papers). The mentioned reason is just the popularity of GA and its applications in various problems and fields [2]. There is no evidence to prove GA superiority in performance.

In our research, we applied other meta-heuristic algorithms and the proposed TLBO method is based on swarm intelligence for the evolutionary purpose of test data generation. Moreover according to the surveys on type of testing in software engineering, almost 75% of the researches done in this field discuss results on structural testing [2]. Despite what the majority of papers discuss, object oriented testing is used in this paper to evaluate the performance of our method. This is due to the recent trend in object oriented design, programming and object oriented testing in software engineering in the recent years.

Search-based techniques are appropriate for the automated generation of unit tests. There are search-based tools like AUSTIN for C programs [3] or EvoSuite for Java programs [4]. EvoSuite is a promising tool for automatic software testing that optimizes whole test suites towards satisfying a coverage

criterion [5]. A coverage criterion represents a finite set of coverage goals (described in Section II-B).

The TLBO algorithm is implemented based on EvoSuite tool. The performance of the TLBO algorithm on the SF100 corpus of open source classes shows enhanced coverage in 4 coverage criterions in the generated test data.

The rest of the paper is organized as: In Section II, basic concepts have been described. Section III provides related works and the background for the proposed method. The TLBO algorithm is proposed in Section IV. In Section V the empirical studies for the proposed method is presented and finally in Section VI the paper is concluded and some ideas have been suggested to inspire future researches.

II. BASIC CONCEPTS

A. Test Data Generation

The objective of test data generation is to have a test suite that maximizes a coverage criterion [6]. A test suite contains a set of test cases each of which specifies the inputs, a sequence of statements and execution conditions to test different behaviors of the code under test, and the predicted results. Finding test input data is a challenging task. Constraint based techniques and search based methods are two promising methods in test data generation. Constraint based techniques use static and dynamic symbolic execution methods to generate appropriate input for test cases. The disadvantages of constraint based techniques include low scalability, inability to manage the dynamic aspects of a unit under test, and the type of constraints they can handle.

On the other hand, using search algorithms, an optimization problem is solved to generate test cases and suitable input for them. Search based methods can handle a variety of domains and are very scalable. However these methods get stuck in local optima and degrade when the search landscape offers insufficient guidance. Our approach for automatically generating test input data is a search based evolutionary algorithm, guided by a fitness function.

B. Coverage Criteria

Coverage criterions determine the goals to be covered for the search algorithm. Each test suite is optimized for performance in a certain criterion. There are many criterions in software testing (e.g., line, mutation, and exception). Based on the previous works in unit testing, four criterions have been used in this paper, namely: line coverage, branch coverage, method coverage and output coverage [7]. Line coverage presents the executed lines in the code. Branch coverage [8] is the number of branches covered by the test, like branches of conditional statements. Method coverage represents the methods invoked by the test case and Output coverage is a complementary coverage to the method coverage as it checks the output of the methods and tries to capture different outputs by changing the corresponding input [7].

C. Fitness Function

In search based software testing a fitness function determines how good a test suite is regarding the optimization objective, which is usually defined by a certain coverage criterion. In addition to checking whether a coverage goal is achieved, a fitness function also provides additional information to guide the search toward covering it.

Method coverage is among basic coverage criteria. This criterion requires the test suite to invoke every method in the class under test at least once. This can be done by direct calls in test cases which appears as a statement or by indirect calls. For regression test suites, it is important that each method is also invoked directly. For a set of goals in a particular coverage criterion, X, the search algorithm generates a test suite that maximizes the number of the covered goals. Fitness functions calculate a fitness value to guide the search toward a goal. Usually the approach level A and branch distance d are employed for this purpose.

The approach level $A(t,x)$ for a given test t on a coverage goal $x \in X$ is defined as the minimal number of control dependent edges in the control dependency graph between the target goal and the control flow that is represented by the test case. The branch distance $d(t,x)$ means how far a predicate in a branch x is from being evaluated as true [9].

In branch coverage criterion, the fitness function to minimize the approach level and branch distance between a test t and a branch coverage goal x is defined as:

$$f(t,x) = A(t,x) + v(d(t,x)) \quad (1)$$

Where, v is any normalizing function in the range (0, 1) [10].

Another basic coverage criterion is line coverage which will satisfy by executing all the lines in the class under test [7]. For this purpose, a fitness function for the line coverage criterion uses branch distance to estimate how far a predicate is from evaluating to the expected outcome. For example, given a predicate $x==10$ and an execution with value 5, the branch distance for the expected outcome being true would be |10-5|=5. Branch distances can be calculated by applying a set of standard rules [8], [11]. To optimizing a test suite (rather than a single test case) toward satisfying line coverage criterion, the fitness function needs to calculate the branch distance for all branches. The line coverage fitness value of a test suite can be calculated by executing all test cases, and for each executed statement calculating the minimum branch distance among all of the branches that are control dependencies to that statement. Hence, the line coverage fitness function is defined as:

$$Fitness_{line}(test\ suite) = v(|total\ lines - covered\ lines|) + \sum_{b \in B} v(d_{\min}(b, suite)) \quad (2)$$

Where, v is any normalizing function, $d_{min}(b,suite)$ is the minimum distance and B is the set of control dependent branches.

For some methods, method coverage, line and branch have similar fitness values. In this case, unit tests are written to cover not only the input values of methods but also the output (returned) values. This criterion can help to improve fault

detection capability [12]. To determine output criterion coverage goals, the following function maps methods' return type to abstract values.

$$O(type) = \begin{cases} \{true, flase\} & if\ type \equiv boolean \\ \{-,0,+\} & if\ type \equiv number \\ \{alphabet, digit,*\} & if\ type \equiv char \\ \{null\ , \neq null\} & other\ wise \end{cases} \quad (3)$$

To satisfy this criterion for each abstract value $V \in O(type)$, a test suite should contain at least one test case which when executed calls a method that returns a value that is characterized by V.

D. Problem representation

Evolutionary algorithms, employing global search methods, are used for optimization of test data generation problem. The representation used in our proposed method is the same problem representation used in EvoSuite. Test suites and test cases are both formulated as chromosomes containing genes. A test suite chromosome consists of test cases that test a class in a specific criterion. A test case respectively includes statements that cover a goal or set of goals in that criterion. Statements are categorized into five groups: method calls; primitive statements that declare a variable; constructor statements that create classes; field statements that access public members of a class and assignment statements which assign a value to a variable.

E. Mutation

Mutation is the occasional random alteration of a gene in a chromosome which alters some features with unpredictable effect on coverage. In a test-suite level, mutation is done by randomly generating test cases and adding them to the set. This random generation is similar to the initial population generation in an evolutionary algorithm. In test-case level, mutation is done by adding or removing or changing the statements in the test case [13], [14].

For method call statements this is done by adding extra method calls or removing the existing ones. The change is completed by calling a method with a different value for its arguments. For constructor statements either a different object is created or another constructor of the class is used or the input value for the constructor is changed. For primitive statements mutation can be done by changing the type of the variable or declaring new ones. Mutation on field statements can be done by accessing a different member of the class with the same or different type. In mutating an assignment statement, the assigned value can be changed.

III. Related Works

Automatic test data generation has been proposed to both increase the precision of software testing and decrease the cost of software testing. Various tools are available based on the proposed methods. In a survey presented by Ali, *et al.* 450 articles have been reviewed and almost 75% of them have carried out their research on unit testing [2]. They mentioned that 73% of the papers used genetic algorithms and 14% of the papers used simulated annealing algorithms. Although genetic algorithms perform better than local search algorithms, but there is no evidence to show that they perform better than global search algorithms. On top of all the reasons mentioned, there are lots of ready tools that adopt GA and are easily accessible for everyone.

In another survey by Harman, *et al*. the history of test data generation and automatic test data generation using evolutionary algorithms has been reviewed [15]. Harman have some recommendations in the paper: using search algorithms on generating test data for testing non-functional features in a software; using search algorithms on establishing the test strategy; using multiple-goal algorithms on generating test data to optimize multiple features in a software.

The literature review of automatic test data generation can be categorized under three subsections of random test data generation, dynamic symbolic execution and search based software testing. However we focus on the search based software testing. One of the major issues of test data generation is the generation of the initial population. The initial population has an influence on both the final solution and the number of generations [16]. In the paper presented by Pachauri and Srivastava [17], three methods were introduced to sort branches to be chosen as goals for coverage.

The work presented by Fraser and Arcuri [5], shows that the whole test suite approach achieves up to 18 times the coverage than the traditional approach which would target coverage goals individually. This method also generates test suites that are up to 44% smaller due to the prevention of the search redundancy and overlapped coverage of goals. In traditional methods for selecting one goal at a time, it is assumed that all the importance of goals is equal and the goals are independent. In contrary the whole test suite generation method targets a coverage criterion rather than a coverage goal. This solves several issues including the collateral coverage problem (i.e., the accidental coverage of the remaining targets [18]), and the effect of selecting goals in a specific order is inevitable in the traditional method.

In the work done by Suresh and Rath [19], a method was proposed to extract basic paths from Control Flow Graph (CFG) by genetic algorithms. In this method after identifying the basic paths, test data is generated to cover them. In the work presented by Bueno, *et al.* [20], a new method was proposed to generate the test cases as different from each other as possible. In this method a cost function that determines the difference between test cases tries to maximize this difference. In addition to solving this function with their own proposed algorithm, it has also solved with genetic and simulated annealing algorithms and the results have been compared.

In another work by Hermadi, *et al.* [21], a new stopping condition has been introduced. This method stops the search if there are paths in the software and there is no test case that can reach them. These conditions have been tested in 20 software data sets and the results are compared with other stopping conditions. In the work done by Pachauri, *et al.* [22], a parallel algorithm has been proposed based on master-slave model and genetic algorithm to generate test data. In this method master selects a path for each slave based on "Path prefix" strategy. Slaves then generate test data to cover that

path using genetic algorithm. The results on two software show high precision in the generated data. It is noticeable that this method uses distributed techniques to generate test data.

Another paper on optimizing meta-heuristic algorithms has been presented by YueMing, *et al.* [23]. In this method that is based on particle swarm algorithms, the particles are divided into two groups, each having its own search method. This method has shown better performance both in execution time and in the quality of generated test cases. In the proposed method by Hoseini, *et al.* [24], the sequence diagram has been used as the input instead of the control flow graph. This method identifies basic paths in the software and generates test data to cover them using genetic algorithm. One key feature of this method is that is carries out the test before the development phase.

Reference [25] has used genetic algorithm to generate a sequence of method and constructor invocations of a class to test it. Then using a multiple-goal approach optimizes the length and the number of instructions in the test cases. Another idea in this article is to use previously generated test data as the initial population for the genetic algorithm to optimize them further. Results show a better performance than the manual method and some of other automatic methods. Change analysis test is technique that puts bugs in a software deliberately to realize if the generated test cases can detect it. If not, existing test cases should be modified or further test cases are required.

Zeller [26] have proposed a method to generate test data for detecting changes in object oriented classes. In this method test data are optimized for finding the most bugs rather than having the most coverage. In this work 'NTEST' has been introduced as way of generating test data for change analysis test, based on object oriented programs. Using change analysis test rather than structural testing, not only the place in code that needs testing is acquired but also what should be tested there is specified.

To combine the two methods of test data generation, search based algorithms and constrained based algorithms, a hybrid solution is proposed by Fraser [27] that works based on genetic algorithm. The algorithm evolves a set of answers chosen by the fitness function toward gaining the most coverage. To speed up the algorithm and avoid the search being confined to local optimizations, a mutation operator was introduced to be added to the GA. What this mutation does is the dynamic execution based on limitations. Instead of random alternations in the chromosomes genes (bytes) or blindly changing the input for methods in the generated test cases, the mutation is done based on the execution path's properties of the chromosome. By doing this a new path is formed in the search space and as a result increases the coverage. Results show a 28% improvement compared to search based methods and a 15% improvement to the limitation based methods. In the work done by Koleejan, *et al.* [28], a method is presented based on genetic and particle swarm algorithms. The main goal of this paper is to optimize the performance of the previous methods by generating multiple test cases in every iteration. Results show that the implemented algorithms perform better than the previous methods.

Arcuri and Fraser have shown the challenges of applying EvoSuite to randomly selected open source projects from SourceForge [29]. This research is of importance because many similar tools are tested with just a few hand selected cases and as a result they are optimized for those specific classes and are not to be generalized. Working with automated search based software testing tools in a real and industrial level project is the ultimate goal of software testing, which is achieved by EvoSuite, however there are challenges that require the testers' attention. The everlasting problems like seeding, tuning and bloat control have been fairly addressed in EvoSuite due to its years of development and surprised encounters with unexpected behaviors the developers had to deal with. Moreover for an industrial scale software regression testing is vital. This is achieved by generating test cases with assertions which capture the current behavior of the software. In addition to that test cases need to be readable by users, because no matter how good a test case is in finding failures, a user needs to check the test cases to ensure that failures found are caused by real faults and not because of the violation of a precondition and also to check the assertions to make sure that the captured behavior is correct. This readability is achieved by several methods. For example In case of variables with large values, EvoSuite tries to make them smaller using a binary method. Moreover naming the variables with proper understanding names or dedicating individual lines to them are also deliberated to make the generated test case as clear and readable as possible. To make analyzing the data easier, test data coverage results are in the form of CSV (comma separated values) files. Every column represents a coverage criterion and every row represents a class in the project.

In recent years many successful applications of swarm intelligence based methods have been reported by researchers. It seems that these methods have the potential to be applied in a broad range of software engineering problems such as software testing. Based on our knowledge there are a few swarm intelligence based methods applied for test data generation in EvoSuite. Hence, this work is aimed to design a swarm intelligence based method for automatic test data generation in EvoSuite.

IV. The Proposed Method

In this section, the proposed EvoTLBO algorithm is described in details. The pseudo code of the proposed algorithm is represented in Fig. 1. The proposed EvoTLBO algorithm is based on standard TLBO which is known as a swarm intelligence algorithm [30]. TLBO has been presented to optimize continues problems. Hence, we need to adapt it for discrete search space. In other words, the movement operator of TLBO is changed to suit moving of individuals in a discrete space. The algorithm has three phases: initialization, update, and termination.

Solution representation plays an important role in success of a population based method. Here, as mentioned before in Section II-D, the same representation which is presented by EvoSuite is used. As can be seen from Fig. 2, every individual is represented as a chromosome and attributes of each individual is determined by its genes. In terms of test data

generation, test cases and test suites are both represented as chromosomes. On the test suite level, a chromosome's genes correspond to test cases. On the test case level, genes are statements in a test case. Statements can be method call, constructor, primitive statement, filed, assignments, etc.

Initialize number of students, termination condition
While (termination condition not met)
  Calculate the mean of decision variables
  Identify the best solution as teacher //in our case the best test case or test suite based on the criterion
  Identify the movement percentage based on the average and a random number //sets the movement parameter
  Modify solution based on best solution //moving towards the teacher
  $X_{new} = X_{old} + r(X_{teacher} - (T_F)Mean)$ //movement formula based on the movement percentage
  If the new solution better than existing
    Accept the solution //continues to move toward a student
    Mutate the solution
  Else
    Reject the solution //doesn't change the solution
  End If
  Select two solutions randomly X_i and X_j
  If X_i better than X_j
    $X_{new} = X_{old} + r(X_i - X_j)$ //move toward a better student or solution
  Else
    $X_{new} = X_{old} + r(X_j - X_i)$ //move away from a worse student or solution
  End If
  If the new solution better than existing
    Accept the solution
    Mutate the solution
  Else
    Reject the solution
  End If
End While
Return best solution

Fig. 1. Pseudo code of the proposed EvoTLBO algorithm.

A. Initialization

The algorithm receives number of individuals and termination condition as inputs. The process starts with a randomly generated initial population. For this purpose, the initial solutions generated by the EvoSuite are used.

B. Update (teaching phase)

The algorithm has two main phases of teaching and learning that simulates the teaching and learning in a classroom. The teacher is the best student of the class. The whole class works together to reach the best level of knowledge (best answer).

This means that social knowledge is shared between individuals through best solution ever found. In the teaching phase, every student moves toward the teacher. For this purpose, the average of decision variable is computed and each individual is updated using the following equation:

$$X_{new} = X_{old} + r(X_{teacher} - (T_F)Mean) \quad (4)$$

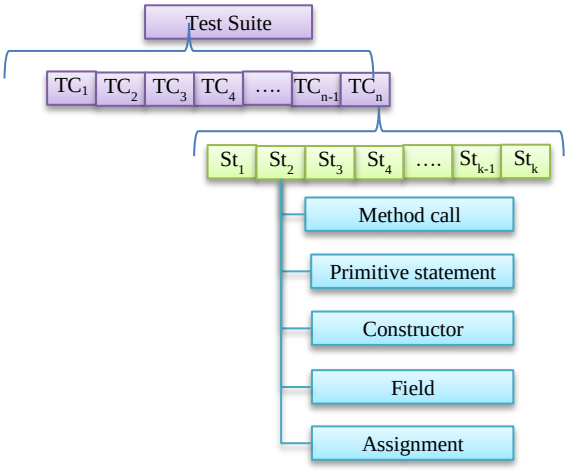

Fig. 2. Solution representation

Where, X_{new} and X_{old} are the new and old position of the

individual, r is a random number, $X_{teacher}$ is the position of the teacher, and $(T_F)Mean$ is the mean of decision variables. This parameter shows that the knowledge of all the individuals are used to update solutions. Using social knowledge in appropriate way (as used in EvoTLBO) can help the algorithm perform better in search space.

The movement operator in EvoTLBO is changed in a way that makes it applicable to a discrete search space of the test data generation problem. The proposed movement strategy changes each individual's attributes with regards to another member to make one look similar to the other. This change is done by obtaining attributes of one individual and adding a portion (set as a parameter) of them to the other one.

The general model for movement considers that individual i wants to move towards individual j. Each individual represents a test suite which is consisted of an array of test cases. The number of test cases in an individual is considered as its position in the search space. For the sake of simplicity, an example is presented in Fig. 3.

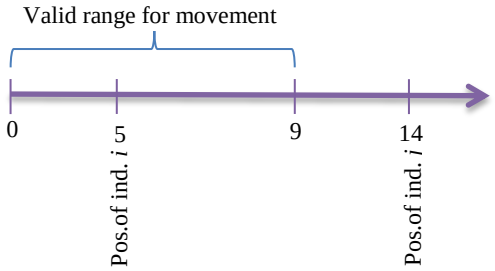

Fig. 3. An example of movement pattern.

Assume that individual *i* contains 5 test cases and individual *j* contains 14 test cases where both of them have two test cases in common. The positions of individuals *i* and *j* are 5 and 14 in the search space respectively. The difference between these two individuals is 7 because they have 2 common test cases. Based on this assumption, any movement pattern such as (4), (5), and (6) can be used.

What happens when moving one member closer to the other one is that some of the destination's attributes (i.e., test cases or statements) are copied and added to the source, leaving the destination as it is. Adding test cases or statements from one individual to the other is done by copying genes between chromosomes.

This movement works on both test suite and test case levels. On the test suite level, to decide which test cases are added to a test suite, they are prioritized based on their coverage. Test cases with exclusive goal coverage have higher priority. However, on test case level there is no prioritization.

After movement, the updated solutions are mutated using the same scenario given in Section II-E. The mutation helps the method to explore more regions to find better solutions.

C. Update (learning phase)

The teaching phase is followed by the learning phase in which the students tutor each other. In the teaching phase, all the members move toward the teacher. In the learning phase, a classmate is chosen randomly for each individual, and then they are compared in terms of their fitness. Actually, in case of the teaching phase, the individual is paired with the teacher in the movement operator meaning that it would get more like the teacher in that phase. If the random classmate's score (fitness value) is higher, then the individual moves toward it using following equation:

$$X_{new} = X_{old} + r(X_i - X_j) \quad (5)$$

In contrary if the randomly selected classmate has a lesser score, the individual gets further from it and closer to the teacher as:

$$X_{new} = X_{old} + r(X_j - X_i) \quad (6)$$

The unified random selection of the classmates results in searching a wider range of the search area, because not all the students move particularly toward the best-known member. Also, as in every movement operator, during movement the two individuals involved are maintained and no new members are generated.

After movement, the updated solutions are mutated using the same scenario given in Section II-E.

D. Termination

At the end of every iteration, the whole population is evaluated and if the minimum requirement (i.e., specific coverage percentage) is found in a member, the algorithm ends. On the other hand if there is no such member, the algorithm chooses the best individual as the teacher and continues into its evolutionary iterations. As these iterations can go on continually, in addition to the members' qualification, there are other stopping conditions like the number of iterations or time limit.

V. Performance Study

The performance of the proposed movement strategy is studied in this section. As shown in the results, there have been improvements in four criteria.

A. Tool Selection

The automation of software testing is done by various tools. The performance study of the proposed method is done by implementing and integrating it into the "EvoSuite" platform. Three of the well-known tools are briefly introduced here. One of the tools that also works on java programs is "Randoop" which generates the test cases mostly random and making assertions based on the feedback it gets from the execution of the test cases. Another random based tool is "T3". The basis of this tool is on random generation of test data sequences these sequences are saved and can be used for regression testing. In addition to that, T3 also performs "pair-wise" testing. "JTExpert" is another tool for java programs which uses search algorithms to generate a test suite. The drawback of this tool is that it only generates tests for branch coverage criterion and also has a lower overall performance in comparison to EvoSuite.

Regarding EvoSuite's performance among other similar tools, it has participated in the "9th International Workshop on

Search-Based Software Testing" and has achieved the highest overall score on the benchmark classes among the other tools [31]. It is noticeable that EvoSuite has close coverage to the manual method but at a fraction of time in generating them.

B. EvoSuite

EvoSuite is the tool of focus in this research. This tool generates test cases for codes written in java by using assertions to examine the integrity of the code [4].

To achieve this, EvoSuite has a hybrid method to generate test suites and optimizes them through an evolutionary process to satisfy a coverage criterion. EvoSuite suggests oracles for the generated test suites in the form of assertions. These small but effective assertions capture the behavior of the software to help the developer detect potential deviation. EvoSuite works on byte code which means that it doesn't need the source code. Test cases are evolved using evolutionary algorithms like Genetic and TLBO. One of the advantages of EvoSuite to other competitors is that it uses a whole test suite approach in which the evolutionary process tries to satisfy multiple coverage goals at the same time. This method and other challenges of using this tool in the real world are explained further, later in this section.

EvoSuite works on a master-slave architecture which enables parallel processing. This feature means that for example, calculating fitness value for a population can be done on different cores of a system or even on separate systems. This feature can help the performance of this tool effectively specially in large projects. In this architecture, a main process starts multiple sub-processes that do the actual search for the best test data. The communication between these processes is done by TCP, which makes EvoSuite independent from the signals of the operating system it is running on.

C. Dataset

Given that proving the performance of evolutionary algorithms is mathematically almost impossible, the performance in these cases is measured by empirical studies. There are challenges in using empirical methods. One of the important ones is to make sure that a technique which performs well under certain circumstances in the laboratory can also perform as well in real world problems. In literature, most of the works don't use a systematic method to choose the data set. In the matter of test data generation, there are many open source software available online. In [32] SF110 a set of 110 java projects were randomly selected from SourceForge code repository for automatic test data generation studies. This data set is also used by the EvoSuite development team. Since studying all the 22 thousand classes of this data set could take up to 1000 days, 50 random classes from SF110 is randomly selected to study the performance of the proposed EvoTLBO algorithm. The selected classes are shown in the table below. Classes are numbered in order to compare the coverage results.

TABLE. I. 50 CLASSES USED FOR TEST DATA GENERATION

Class #	Class Name
1	geo.google.mapping.AddressToUsAddressFunctor
2	com.werken.saxpath.XPathLexer
3	httpanalyzer.ScreenInputFilter
4	corina.formats.TRML
5	corina.map.SiteListPanel
6	lotus.core.phases.Phase
7	org.dom4j.tree.CloneHelper
8	org.dom4j.util.PerThreadSingleton
9	macaw.presentationLayer.CategoryStateEditor
10	org.fixsuite.message.view.ListView
11	com.browsersoft.openhre.hl7.impl.config.HL7SegmentMapImpl
12	com.lts.caloriecount.ui.budget.BudgetWin
13	com.lts.io.ArchiveScanner
14	com.lts.swing.table.dragndrop.test.RecordingEvent
15	com.lts.swing.thread.BlockThread
16	de.outstare.fortbattleplayer.gui.battlefield.BattlefieldCell
17	org.sourceforge.ifx.framework.complextype.RecChkOrdInqRs_Type
18	org.sourceforge.ifx.framework.complextype.PassbkItemInqRs_Type
19	umd.cs.shop.JSListSubstitution
20	jigl.image.utils.LocalDifferentialGeometry
21	org.sourceforge.ifx.framework.element.Fee
22	com.lts.xml.MapElement
23	weka.gui.beans.TrainTestSplitMaker
24	weka.filters.unsupervised.attribute.RandomProjection
25	com.lts.swing.table.rowmodel.tablemodel.RowModelTableModel
26	net.sourceforge.squirrel_sql.fw.datasetviewer.ColumnDisplayDefinition
27	org.gudy.azureus2.core3.util.ShellUtilityFinder
28	org.gudy.azureus2.core3.torrentdownloader.impl.TorrentDownloaderManager
29	jcmdline.UsageFormatter
30	net.sourceforge.squirrel_sql.fw.sql.ISQLExecutionCallback
31	br.com.jnfe.base.ICMSST

Class #	Class Name
32	glengineer.agents.setters.FunctionsOnSequentialGroupAndElement
33	org.sourceforge.ifx.framework.element.ForExDealStatusInqRq
34	org.sourceforge.ifx.framework.element.BankAcctTrnImgRevRs
35	com.aelitis.azureus.core.download.DownloadManagerEnhancer
36	corina.browser.Row
37	corina.graph.DensityPlot
38	com.browsersoft.openhre.hl7.impl.parser.HL7CheckerStateImpl
39	org.bouncycastle.asn1.DERUTCTime
40	module.RuleSet
41	net.kencochrane.a4j.DAO.Cart
42	org.petsoar.security.Address
43	org.sourceforge.ifx.framework.pain001.simpletype.DocumentType1Code
44	corina.prefs.components.BoolPrefComponent
45	jaw.gui.ProcessarEntidades
46	org.jcvi.jillion.fasta.pos.PositionFastaRecord
47	de.huxhorn.lilith.data.access.AccessEvent
48	com.sap.netweaver.porta.mon.StopCommand
49	org.sourceforge.ifx.framework.element.DevDepType
50	org.sourceforge.ifx.framework.complextype.DepAcctStmtRevRs_Type

D. Algorithm Configurations

All of the algorithms start with an initial population of size 50 which is generated with the random method mentioned in the literature. The algorithms have 2 minutes to run each time. In addition to timeout, a certain coverage percentage (i.e., 100%) is also a stopping condition. Each of the classes have been processed in 10 iterations to ensure reliable results.

The total time required for runs is calculated as follows:

$$Iterations * Coverage\ criterion * Classes * Execution\ time = 10 * 4 * 50 * 2 = 66\ hours$$

In addition to the common settings, each algorithm has its own specific configurations which are set as follows: for the genetic algorithm, selection is rank and crossover is single point. In the proposed EvoTLBO method, the teaching factor is selected as 0<random<2.0.

E. Experimental Results

Standard GA and Monotonic GA which are built into the EvoSuite tool by its developing team are used for comparing the results of the proposed EvoTLBO algorithm in 4 coverage criterions of Branch, Line, Method and Output. Two factors have been used for performance comparison, the number of classes which the algorithm has achieved the highest coverage in and the percentage of the total number of covered goals. These two factors are shown in the last row of the table for each algorithm. For every table the first column is the class number correspondent to Table 1. For every algorithm the first column is the coverage percentage in that class and the second column is the ratio of the covered goals to the total number of goals for that class in the specified criterion.

Branch coverage: The results of applying the EvoTLBO algorithm with the suggested movement operator in it are presented in Table 2. The table shows the results in branch coverage criterion. Standard GA has the highest score in terms of covering the most number of classes. This algorithm has the highest coverage in 36 classes in 12 of which achieving exclusive coverage that no other algorithm has. The monotonic GA algorithm gets the second rank by achieving highest coverage in 28 classes and exclusive coverage in only 3 cases. The proposed EvoTLBO algorithm does not show a good performance compared to the two genetic algorithms, it achieves the highest coverage in 24 classes alongside with the other two and it has exclusive coverage in only two classes. Regarding the goal coverage independent of which class they are in, all three algorithms have close performance. There are a total of 2101 goals in this criterion in all of the classes combined. Although the ranking stays the same, but the 62.67% of standard GA at first is close to 59.21% of the EvoTLBO at last.

TABLE. II. BRANCH COVERAGE RESULTS

#	Standard GA		Monotonic GA		EvoTLBO	
1	20.00%	(6/30)	20.00%	(6/30)	20.00%	(6/30)
2	85.99%	(416.2/484)	86.84%	(420.3/484)	85.12%	(412/484)
3	100.00%	(5/5)	94.00%	(4.7/5)	98.00%	(4.9/5)
4	24.78%	(22.3/90)	21.89%	(19.7/90)	19.56%	(17.6/90)
5	0.65%	(1/153)	0.65%	(1/153)	0.59%	(0.9/153)
6	72.86%	(20.4/28)	100.00%	(28/28)	100.00%	(28/28)
7	100.00%	(4/4)	100.00%	(4/4)	100.00%	(4/4)
8	85.71%	(6/7)	85.71%	(6/7)	85.71%	(6/7)
9	8.33%	(1/12)	7.50%	(0.9/12)	7.50%	(0.9/12)
10	5.26%	(4/76)	5.26%	(4/76)	4.21%	(3.2/76)
11	100.00%	(12/12)	100.00%	(12/12)	100.00%	(12/12)

#	Standard GA		Monotonic GA		EvoTLBO	
12	12.50%	(4/32)	12.50%	(4/32)	10.63%	(3.4/32)
13	71.33%	(32.1/45)	69.78%	(31.4/45)	57.78%	(26/45)
14	99.67%	(29.9/30)	100.00%	(30/30)	97.67%	(29.3/30)
15	98.89%	(8.9/9)	97.78%	(8.8/9)	98.89%	(8.9/9)
16	82.54%	(58.6/71)	81.83%	(58.1/71)	65.07%	(46.2/71)
17	100.00%	(34/34)	100.00%	(34/34)	100.00%	(34/34)
18	100.00%	(28/28)	100.00%	(28/28)	100.00%	(28/28)
19	92.86%	(6.5/7)	88.57%	(6.2/7)	90.00%	(6.3/7)
20	91.56	(181.2/198)	88.28	(174.7/198)	95.70	(189.4/198)
21	100.00%	(2/2)	100.00%	(2/2)	100.00%	(2/2)
22	100.00%	(1/1)	100.00%	(1/1)	100.00%	(1/1)
23	66.23%	(70.2/106)	64.62%	(68.5/106)	54.72%	(58/106)
24	41.71%	(65.9/158)	41.39%	(65.4/158)	37.34%	(59/158)
25	0.00%	(0/0)	0.00%	(0/0)	0.00%	(0/0)
26	90.41%	(44.3/49)	90.82%	(44.5/49)	91.02%	(44.6/49)
27	80.00%	(7.2/9)	88.89%	(8/9)	88.89%	(8/9)
28	78.82%	(40.2/51)	74.31%	(37.9/51)	71.18%	(36.3/51)
29	0.00%	(0/0)	0.00%	(0/0)	0.00%	(0/0)
30	0.00%	(0/0)	0.00%	(0/0)	0.00%	(0/0)
31	0.00%	(0/0)	0.00%	(0/0)	0.00%	(0/0)
32	0.00%	(0/0)	0.00%	(0/0)	0.00%	(0/0)
33	100.00%	(2/2)	100.00%	(2/2)	100.00%	(2/2)
34	100.00%	(2/2)	100.00%	(2/2)	100.00%	(2/2)
35	8.53%	(9.3/109)	3.85%	(4.2/109)	7.34%	(8/109)
36	57.59%	(33.4/58)	58.79%	(34.1/58)	50.17%	(29.1/58)
37	17.65%	(3/17)	17.65%	(3/17)	17.65%	(3/17)
38	92.86%	(97.5/105)	91.24%	(95.8/105)	80.86%	(84.9/105)
39	99.71%	(33.9/34)	99.12%	(33.7/34)	98.53%	(33.5/34)
40	0.00%	(0/0)	0.00%	(0/0)	0.00%	(0/0)
41	23.08%	(9/39)	23.08%	(9/39)	23.08%	(9/39)
42	100.00%	(11/11)	100.00%	(11/11)	100.00%	(11/11)
43	100.00%	(2/2)	100.00%	(2/2)	100.00%	(2/2)
44	0.00%	(0/6)	0.00%	(0/6)	0.00%	(0/6)
45	100.00%	(1/1)	100.00%	(1/1)	100.00%	(1/1)
46	100.00%	(18/18)	100.00%	(18/18)	100.00%	(18/18)
47	100.00%	(134/134)	100.00%	(134/134)	92.54%	(124/134)
48	100.00%	(2/2)	100.00%	(2/2)	100.00%	(2/2)
49	100.00%	(2/2)	100.00%	(2/2)	100.00%	(2/2)
50	100.00%	(26/26)	100.00%	(26/26)	100.00%	(26/26)
	36	62.67%	28	62.55%	24	59.21%

Line coverage: In Table 3 the results are based upon the line coverage criterion. The monotonic GA has achieved the highest coverage in 30 cases 7 of which were exclusive to this algorithm. The standard GA holds the second place closely with just 1 less class. Although EvoTLBO algorithm has the third place but it still has competitive results as it achieves the highest coverage in 25 classes along with others and has exclusive coverage in 4 classes. The same ranking goes for goal coverage percentage. The two genetic algorithms have close scores with less than 1 percent difference and the EvoTLBO algorithm has coverage more than 2 percent lower.

TABLE. III. LINE COVERAGE RESULTS

#	Standard GA		Monotonic GA		EvoTLBO	
1	27.03%	(10/37)	27.03%	(10/37)	26.76%	(9.9/37)
2	86.74%	(308.8/356)	87.67%	(312.1/356)	87.08%	(310/356)
3	98.18%	(10.8/11)	97.27%	(10.7/11)	98.18%	(10.8/11)
4	44.87%	(70/156)	48.53%	(75.7/156)	31.41%	(49/156)
5	0.43%	(1/232)	0.43%	(1/232)	0.39%	(0.9/232)
6	100.00%	(20/20)	100.00%	(20/20)	100.00%	(20/20)
7	38.46%	(5/13)	38.46%	(5/13)	38.46%	(5/13)
8	79.13%	(18.2/23)	80.00%	(18.4/23)	78.26%	(18/23)
9	0.00%	(0/46)	0.00%	(0/46)	0.00%	(0/46)
10	3.64%	(8/220)	3.64%	(8/220)	3.64%	(8/220)
11	100.00%	(26/26)	100.00%	(26/26)	100.00%	(26/26)
12	26.92%	(28/104)	26.92%	(28/104)	26.92%	(28/104)
13	81.36%	(53.7/66)	81.97%	(54.1/66)	62.88%	(41.5/66)
14	94.19%	(69.7/74)	94.05%	(69.6/74)	96.89%	(71.7/74)
15	72.69%	(18.9/26)	73.08%	(19/26)	72.69%	(18.9/26)
16	78.85%	(102.5/130)	87.08%	(113.2/130)	72.54%	(94.3/130)
17	100.00%	(51/51)	100.00%	(51/51)	100.00%	(51/51)

#	Standard GA		Monotonic GA		EvoTLBO	
18	100.00%	(42/42)	100.00%	(42/42)	100.00%	(42/42)
19	93.00%	(9.3/10)	90.00%	(9/10)	93.00%	(9.3/10)
20	87.66	(326/372)	87.25	(324.5/372)	92.47	(343.9/372)
21	100.00%	(2/2)	100.00%	(2/2)	100.00%	(2/2)
22	0.00%	(0/0)	0.00%	(0/0)	0.00%	(0/0)
23	70.38%	(112.6/160)	67.94%	(108.7/160)	65.81%	(105.3/160)
24	52.68%	(125.9/239)	53.35%	(127.5/239)	50.54%	(120.8/239)
25	0.00%	(0/0)	0.00%	(0/0)	0.00%	(0/0)
26	95.80%	(95.8/100)	95.80%	(95.8/100)	96.00%	(96/100)
27	93.75%	(7.5/8)	100.00%	(8/8)	100.00%	(8/8)
28	90.20%	(45.1/50)	89.00%	(44.5/50)	88.80%	(44.4/50)
29	0.00%	(0/0)	0.00%	(0/0)	0.00%	(0/0)
30	0.00%	(0/0)	0.00%	(0/0)	0.00%	(0/0)
31	0.00%	(0/0)	0.00%	(0/0)	0.00%	(0/0)
32	0.00%	(0/0)	0.00%	(0/0)	0.00%	(0/0)
33	100.00%	(2/2)	100.00%	(2/2)	100.00%	(2/2)
34	100.00%	(2/2)	100.00%	(2/2)	100.00%	(2/2)
35	10.16%	(18.6/183)	5.79%	(10.6/183)	13.28%	(24.3/183)
36	66.63%	(57.3/86)	65.93%	(56.7/86)	58.95%	(50.7/86)
37	8.51%	(4/47)	8.51%	(4/47)	8.30%	(3.9/47)
38	86.54%	(165.3/191)	85.39%	(163.1/191)	77.38%	(147.8/191)
39	100.00%	(55/55)	98.91%	(54.4/55)	98.91%	(54.4/55)
40	0.00%	(0/0)	0.00%	(0/0)	0.00%	(0/0)
41	39.06%	(50/128)	39.06%	(50/128)	39.06%	(50/128)
42	100.00%	(15/15)	100.00%	(15/15)	100.00%	(15/15)
43	100.00%	(2/2)	100.00%	(2/2)	100.00%	(2/2)
44	21.43%	(3/14)	21.43%	(3/14)	21.43%	(3/14)
45	0.00%	(0/0)	0.00%	(0/0)	0.00%	(0/0)
46	100.00%	(26/26)	100.00%	(26/26)	100.00%	(26/26)
47	100.00%	(86/86)	100.00%	(86/86)	100.00%	(86/86)
48	12.50%	(1/8)	12.50%	(1/8)	10.00%	(0.8/8)
49	100.00%	(2/2)	100.00%	(2/2)	100.00%	(2/2)
50	100.00%	(39/39)	100.00%	(39/39)	100.00%	(39/39)
	29	57.32%	30	57.52%	25	55.04%

Output coverage: The results of output coverage are presented in Table 4. On the number of classes with the highest coverage, standard GA scores 29 cases with 7 exclusive highest coverage. Monotonic GA achieves highest coverage in 24 classes with exclusive coverage in 3 cases. EvoTLBO ranked at last scores 21 on highest coverage with only 2 exclusively covered classes. Regarding the total goals in this criterion, of all the 1056 goals, standard GA being at the top covers 49.57% of them. EvoTLBO with the least score, covers 47.91% of the goals.

TABLE. IV. OUTPUT COVERAGE RESULTS

#	Standard GA		Monotonic GA		EvoTLBO	
1	50.00%	(2/4)	50.00%	(2/4)	50.00%	(2/4)
2	39.01%	(55.4/142)	38.59%	(54.8/142)	38.59%	(54.8/142)
3	66.67%	(2/3)	66.67%	(2/3)	66.67%	(2/3)
4	6.06%	(2/33)	6.06%	(2/33)	6.06%	(2/33)
5	0.00%	(0/0)	0.00%	(0/0)	0.00%	(0/0)
6	0.00%	(0/0)	0.00%	(0/0)	0.00%	(0/0)
7	0.00%	(0/0)	0.00%	(0/0)	0.00%	(0/0)
8	50.00%	(1/2)	50.00%	(1/2)	50.00%	(1/2)
9	0.00%	(0/0)	0.00%	(0/0)	0.00%	(0/0)
10	0.00%	(0/0)	0.00%	(0/0)	0.00%	(0/0)
11	63.64%	(7/11)	63.64%	(7/11)	63.64%	(7/11)
12	0.00%	(0/77)	0.00%	(0/77)	0.00%	(0/77)
13	80.00%	(4/5)	78.00%	(3.9/5)	80.00%	(4/5)
14	48.67%	(14.6/30)	33.00%	(9.9/30)	50.67%	(15.2/30)
15	0	(0/0)	0.00%	(0/0)	0.00%	(0/0)
16	83.33%	(10/12)	83.33%	(10/12)	83.33%	(10/12)
17	100.00%	(40/40)	100.00%	(40/40)	99.00%	(39.6/40)
18	100.00%	(33/33)	100.00%	(33/33)	99.70%	(32.9/33)
19	100.00%	(2/2)	100.00%	(2/2)	100.00%	(2/2)
20	48.90	(93.8/192)	46.30	(88.8/192)	50.31	(96.5/192)
21	100.00%	(2/2)	100.00%	(2/2)	100.00%	(2/2)
22	0.00%	(0/0)	0.00%	(0/0)	0.00%	(0/0)
23	37.78%	(17/45)	38.89%	(17.5/45)	35.78%	(16.1/45)
24	32.03%	(25.3/79)	33.16%	(26.2/79)	28.99%	(22.9/79)

#	Standard GA		Monotonic GA		EvoTLBO	
25	0.00%	(0/0)	0.00%	(0/0)	0.00%	(0/0)
26	85.21%	(60.5/71)	83.38%	(59.2/71)	82.68%	(58.7/71)
27	44.44%	(4/9)	44.44%	(4/9)	44.44%	(4/9)
28	10.69%	(9.3/87)	10.11%	(8.8/87)	9.89%	(8.6/87)
29	0.00%	(0/0)	0.00%	(0/0)	0.00%	(0/0)
30	0.00%	(0/0)	0.00%	(0/0)	0.00%	(0/0)
31	0.00%	(0/0)	0.00%	(0/0)	0.00%	(0/0)
32	0.00%	(0/0)	0.00%	(0/0)	0.00%	(0/0)
33	100.00%	(2/2)	100.00%	(2/2)	100.00%	(2/2)
34	100.00%	(2/2)	100.00%	(2/2)	100.00%	(2/2)
35	3.78%	(3.1/82)	1.22%	(1/82)	2.68%	(2.2/82)
36	47.78%	(12.9/27)	44.07%	(11.9/27)	41.85%	(11.3/27)
37	80.00%	(4/5)	80.00%	(4/5)	80.00%	(4/5)
38	94.63%	(51.1/54)	91.48%	(49.4/54)	81.11%	(43.8/54)
39	68.42%	(13/19)	67.89%	(12.9/19)	65.79%	(12.5/19)
40	0.00%	(0/0)	0.00%	(0/0)	0.00%	(0/0)
41	50.00%	(6/12)	50.00%	(6/12)	50.00%	(6/12)
42	100.00%	(15/15)	100.00%	(15/15)	100.00%	(15/15)
43	100.00%	(2/2)	100.00%	(2/2)	100.00%	(2/2)
44	0.00%	(0/0)	0.00%	(0/0)	0.00%	(0/0)
45	52.76%	(15.3/29)	53.45%	(15.5/29)	49.66%	(14.4/29)
46	60.00%	(9/15)	60.00%	(9/15)	59.33%	(8.9/15)
47	93.24%	(69/74)	93.24%	(69/74)	93.24%	(69/74)
48	0.00%	(0/3)	0.00%	(0/3)	0.00%	(0/3)
49	100.00%	(2/2)	100.00%	(2/2)	100.00%	(2/2)
50	100.00%	(26/26)	100.00%	(26/26)	100.00%	(26/26)
	29	49.57%	24	48.58%	21	47.91%

Method coverage: The coverage of methods is the last criterion used for comparison. The results of method coverage are presented in Table 5. In this criterion EvoTLBO performs better than the other two by achieving the highest coverage in 44 classes and exclusively covering 11 classes with the highest coverage percentage. Standard GA and monotonic GA both cover 35 classes with highest coverage alongside each other and EvoTLBO. The only case which standard GA has exclusive coverage is number 35. Monotonic GA doesn't cover any classes exclusively. Regarding the total goal coverage, EvoTLBO again has the first rank with 90.08% coverage. The two genetic algorithms have very close coverage percentage.

TABLE. V. METHOD COVERAGE RESULTS

#	Standard GA		Monotonic GA		EvoTLBO	
1	100.00%	(3/3)	100.00%	(3/3)	100.00%	(3/3)
2	100.00%	(44/44)	100.00%	(44/44)	100.00%	(44/44)
3	100.00%	(2/2)	100.00%	(2/2)	100.00%	(2/2)
4	72.00%	(3.6/5)	80.00%	(4/5)	82.00%	(4.1/5)
5	50.00%	(1/2)	50.00%	(1/2)	50.00%	(1/2)
6	100.00%	(2/2)	100.00%	(2/2)	100.00%	(2/2)
7	25.00%	(1/4)	25.00%	(1/4)	100.00%	(4/4)
8	100.00%	(4/4)	100.00%	(4/4)	100.00%	(4/4)
9	20.00%	(1/5)	20.00%	(1/5)	20.00%	(1/5)
10	33.33%	(1/3)	33.33%	(1/3)	23.33%	(0.7/3)
11	100.00%	(8/8)	100.00%	(8/8)	100.00%	(8/8)
12	11.11%	(1/9)	20.00%	(1.8/9)	28.89%	(2.6/9)
13	50.00%	(4/8)	50.00%	(4/8)	78.75%	(6.3/8)
14	100.00%	(16/16)	100.00%	(16/16)	100.00%	(16/16)
15	76.67%	(4.6/6)	81.67%	(4.9/6)	83.33%	(5/6)
16	100.00%	(8/8)	100.00%	(8/8)	100.00%	(8/8)
17	100.00%	(34/34)	100.00%	(34/34)	100.00%	(34/34)
18	100.00%	(28/28)	100.00%	(28/28)	100.00%	(28/28)
19	100.00%	(3/3)	100.00%	(3/3)	100.00%	(3/3)
20	100.00%	(19/19)	100	(19/19)	100	(19/19)
21	100.00%	(2/2)	100.00%	(2/2)	100.00%	(2/2)
22	100.00%	(1/1)	100.00%	(1/1)	100.00%	(1/1)
23	100.00%	(23/23)	100.00%	(23/23)	100.00%	(23/23)
24	75.00%	(24/32)	76.88%	(24.6/32)	86.25%	(27.6/32)
25	100.00%	(2/2)	100.00%	(2/2)	100.00%	(2/2)
26	93.75%	(30/32)	93.75%	(30/32)	99.69%	(31.9/32)
27	100.00%	(4/4)	100.00%	(4/4)	100.00%	(4/4)
28	100.00%	(10/10)	100.00%	(10/10)	100.00%	(10/10)
29	100.00%	(4/4)	100.00%	(4/4)	100.00%	(4/4)
30	0.00%	(0/1)	0.00%	(0/1)	0.00%	(0/1)

#	Standard GA		Monotonic GA		EvoTLBO	
31	0.00%	(0/6)	0.00%	(0/6)	0.00%	(0/6)
32	0.00%	(0/8)	0.00%	(0/8)	0.00%	(0/8)
33	100.00%	(2/2)	100.00%	(2/2)	100.00%	(2/2)
34	100.00%	(2/2)	100.00%	(2/2)	100.00%	(2/2)
35	33.08%	(4.3/13)	22.31%	(2.9/13)	26.15%	(3.4/13)
36	90.00%	(9/10)	90.00%	(9/10)	95.00%	(9.5/10)
37	75.00%	(3/4)	75.00%	(3/4)	82.50%	(3.3/4)
38	100.00%	(42/42)	100.00%	(42/42)	100.00%	(42/42)
39	99.23%	(12.9/13)	100.00%	(13/13)	100.00%	(13/13)
40	100.00%	(1/1)	100.00%	(1/1)	100.00%	(1/1)
41	100.00%	(7/7)	100.00%	(7/7)	100.00%	(7/7)
42	100.00%	(11/11)	100.00%	(11/11)	100.00%	(11/11)
43	100.00%	(2/2)	100.00%	(2/2)	100.00%	(2/2)
44	33.33%	(1/3)	33.33%	(1/3)	30.00%	(0.9/3)
45	90.63%	(14.5/16)	87.50%	(14/16)	92.50%	(14.8/16)
46	100.00%	(8/8)	100.00%	(8/8)	100.00%	(8/8)
47	100.00%	(34/34)	100.00%	(34/34)	100.00%	(34/34)
48	50.00%	(1/2)	50.00%	(1/2)	80.00%	(1.6/2)
49	100.00%	(2/2)	100.00%	(2/2)	100.00%	(2/2)
50	100.00%	(26/26)	100.00%	(26/26)	100.00%	(26/26)
	35	87.41%	35	87.47%	44	90.08%

VI. Conclusion And Future Works

In this work, a method based on TLBO has been proposed to generate test data automatically. The proposed method was applied on 50 randomly selected classes in EvoSuite. The performance of EvoTLBO method was compared with the two methods of standard GA and monotonic GA. The results showed that EvoTLBO is efficient and provides competitive results in comparison with the other methods.

The experience gained on working with different evolutionary algorithms has given us a wider perspective on this matter. Knowing the challenges of software testing and software quality validation, suggestions to improve the results further are made. Given the performance of swarm intelligence algorithm, more empirical studies using a larger number of classes are suggested. Extending EvoTLBO with new movement patterns and social models may result better performance. Analyzing other swarm intelligence paradigm algorithms like bats in generating test data is suggested. Other optimization paradigm algorithms for test data generation could be studied. Proposing a movement method in the search space of swarm intelligence algorithms for solving object oriented test problems is of importance. It is recommended to present a method to change the discrete space of the algorithm to a continuous form to implement the movement. Since evolutionary algorithms are dependent on their initial parameters values, empirical studies on tuning these parameters by comparing the execution results of different values is recommended. Utilizing multiple goal optimization algorithms in generating test data, to approach all the goals at the same time. Using fitness functions to generate tests for non-functional properties of software is a need. Further analysis of other tools like Randoop is recommended.

References

[1] J. P. Galeotti, G. Fraser, and A. Arcuri, “Improving search-based test suite generation with dynamic symbolic execution,” 2013 IEEE 24th Int. Symp. Softw. Reliab. Eng. ISSRE 2013, pp. 360–369, 2013.

[2] S. Ali, L. C. Briand, H. Hemmati, and R. K. Panesar-Walawege, “A systematic review of the application and empirical investigation of search-based test case generation,” IEEE Trans. Softw. Eng., vol. 36, no. 6, pp. 742–762, 2010.

[3] K. Lakhotia, M. Harman, and H. Gross, “AUSTIN: A Tool for Search Based Software Testing for the C Language and Its Evaluation on Deployed Automotive Systems,” in 2nd International Symposium on Search Based Software Engineering, 2010, pp. 101–110.

[4] G. Fraser and A. Arcuri, “EvoSuite : Automatic Test Suite Generation for Object-Oriented Software,” Proc. 19th ACM SIGSOFT Symp. 13th Eur. Conf. Found. Softw. Eng., pp. 416–419, 2011.

[5] G. Fraser and A. Arcuri, “Evolutionary Generation of Whole Test Suites,” 2011 11th Int. Conf. Qual. Softw., pp. 31–40, 2011.

[6] P. McMinn, “Search-Based Software Testing: Past, Present and Future,” in Proceedings of the 2011 IEEE Fourth International Conference on Software Testing, Verification and Validation Workshops, 2011, pp. 153–163.

[7] J. M. R. J. C. M. V. G. F. A. Arcuri, “Combining Multiple Coverage Criteria in Search-Based Unit Test Generation,” 2015.

[8] P. McMinn, “Search-based software test data generation: A survey,” Softw. Test. Verif. Reliab., vol. 14, no. 2, pp. 105–156, 2004.

[9] J. M. Rojas, M. Vivanti, A. Arcuri, and G. Fraser, A detailed investigation of the effectiveness of whole test suite generation. 2016.

[10] M. Barros and Y. Labiche, “Search-Based Software Engineering: 7th International Symposium, SSBSE 2015 Bergamo, Italy, September 5-7, 2015 Proceedings,” Lect. Notes Comput. Sci. (including Subser. Lect. Notes Artif. Intell. Lect. Notes Bioinformatics), vol. 9275, pp. 77–92, 2015.

[11] B. Korel, “Automated software test data generation,” IEEE Trans. Softw. Eng., vol. 16, no. 8, pp. 870–879, Aug. 1990.

[12] N. Alshahwan and M. Harman, “Coverage and Fault Detection of the Output-uniqueness Test Selection Criteria,” in Proceedings of the 2014 International Symposium on Software Testing and Analysis, 2014, pp. 181–192.

[13] H. Sthamer and P. Morgannwg, “The Automatic Generation of Software Test Data Using Genetic Algorithms,” no. November, 1995.

[14] P. Tonella, “Evolutionary Testing of Classes,” pp. 119–128.

[15] M. Harman, Y. Jia, and Y. Zhang, “Achievements , open problems and challenges for search based software testing,” 8th IEEE Int. Conf. Softw. Testing, Verif. Valid., no. Icst, 2015.

[16] H. Maaranen, K. Miettinen, and M. M. Mäkelä, “Quasi-random initial population for genetic algorithms,” Comput. Math. with Appl., vol. 47, no. 12, pp. 1885–1895, 2004.

[17] A. Pachauri and G. Srivastava, “Automated test data generation for branch testing using genetic algorithm: An improved approach using branch ordering, memory and elitism,” J. Syst. Softw., vol. 86, no. 5, pp. 1191–1208, 2013.

[18] G. Fraser and A. Arcuri, “Whole test suite generation,” IEEE Trans. Softw. Eng., vol. 39, no. 2, pp. 276–291, 2013.

[19] Y. Suresh and S. Rath, "A Genetic Algorithm based Approach for Test Data Generation in Basis Path Testing," Int. J. Soft Comput. Softw. Eng., vol. 3, no. 3, pp. 326–332, 2014.

[20] P. M. S. Bueno, M. Jino, and W. E. Wong, "Diversity oriented test data generation using metaheuristic search techniques," Inf. Sci. (Ny)., vol. 259, pp. 490–509, 2014.

[21] I. Hermadi, C. Lokan, and R. Sarker, "Dynamic stopping criteria for search-based test data generation for path testing," Inf. Softw. Technol., vol. 56, no. 4, pp. 395–407, 2014.

[22] A. Pachauri, "Towards a parallel approach for test data generation for branch coverage with genetic algorithm using the extended path prefix strategy Towards a Parallel Approach for Test Data Generation for Branch Coverage with Genetic Algorithm using the Extended Path," no. March, 2016.

[23] D. YueMing, W. YiTing, and W. DingHui, "Particle swarm optimization algorithm for test case automatic generation based on clustering thought," in Cyber Technology in Automation, Control, and Intelligent Systems (CYBER), 2015 IEEE International Conference on, 2015, pp. 1479–1485.

[24] B. Hoseini and S. Jalili, "Automatic test path generation from sequence diagram using genetic algorithm," Telecommun. (IST), 2014 7th Int. Symp., pp. 106–111, 2014.

[25] G. Fraser and A. Zeller, "Mutation-driven Generation of Unit Tests and Oracles," 2010.

[26] G. Fraser and A. Zeller, "Exploiting common object usage in test case generation," Proc. - 4th IEEE Int. Conf. Softw. Testing, Verif. Validation, ICST 2011, pp. 80–89, 2011.

[27] J. Malburg and G. Fraser, "Combining Search-based and Constraint-based Testing."

[28] C. Koleejan, B. Xue, and M. Zhang, "Code Coverage Optimisation in Genetic Algorithms and Particle Swarm Optimisation for Automatic Software Test Data Generation," pp. 1204–1211, 2015.

[29] G. Fraser and A. Arcuri, "txtUnknown - Unknown - EvoSuite On The Challenges of Test Case Generation in the Real World.txt.pdf."

[30] R. V. Rao, V. J. Savsani, and D. P. Vakharia, "Teaching–learning-based optimization: A novel method for constrained mechanical design optimization problems," Comput. Des., vol. 43, no. 3, pp. 303–315, 2011.

[31] G. Fraser, "EvoSuite at the SBST 2016 Tool Competition," pp. 10–13, 2016.

[32] G. Fraser and C. Science, "A Large Scale Evaluation of Automated Unit Test Generation Using EvoSuite," ACM Trans. Softw. Eng. Methodol., vol. 24, no. 2, p. 8, 2014.

An Investigation into the Suitability of k-Nearest Neighbour (k-NN) for Software Effort Estimation

Razak Olu-Ajayi
Department of Computer Science,
University of Hertfordshire
Hatfield, UK

***Abstract*—Software effort estimation is an increasingly significant field, due to the overwhelming role of software in today's global market. Effort estimation involves forecasting the effort in person-months or hours required for developing a software. It is vital to ideal planning and paramount for controlling the software development process. However, there is presently no optimal method to accurately estimate the effort required to develop a software system. Inaccurate estimation leads to poor use of resources and perhaps failure of the software project. Effort estimation also plays a key role in deducing cost of a software project. Software cost estimation includes the generation of the effort estimates and project duration to predict cost required to develop software project. Thus, effort is very essential and there is always need to enhance the accuracy as much as possible. This study evaluates and compares the potential of Constructive COst MOdel II (COCOMO II) and k-Nearest Neighbor (k-NN) on software project dataset. By the analysis of results received from each method, it may be concluded that the proposed method k-NN yields better performance over the other technique utilized in this study.**

Keywords*—Software effort estimation; machine learning; k-Nearest Neighbor; Constructive COst MOdel II

I. INTRODUCTION

Since the invention of computers, a vast number of people find themselves reliant on computers. Computers are appearing in nearly every aspect of our lives, such as transportation, banking, education, communication as well as personal health. In general, computers are making things easier for us, for example, working electronically from home, socialising with long distance friends. While a computer is merely a box of circuits that achieve software level tasks for its user, software is simply a set of instructions which enables the computer to perform specified tasks.

Despite the growing popularity of software, there are still issues been encountered in various aspect of its development which has been receiving attention from several researchers. In 1968, software engineering emerged at a meeting in a discussion of what was then called 'software crisis' [1]. It became apparent that developer approaches to software development did not scale up to large and complex software systems. These issues were unreliable, cost overrun, and late delivery [2]. Many software projects still suffer from inaccurate estimation hence they are delivered late or worse still abandoned.

For example, in April 1990, the Regional Information Systems Plan (RISP) for the Wessex Regional Health Authority was abandoned, five years after it started. By this time, £43 million had already been expended on the project and out of which £20 million was confirmed wasted. RISP was meant to accomplish integration across the health region. The failure of the project was attributed to the ambiguous definition of the scope which resulted in difficulties in handling and budgeting the expenditure of the project [3].

In this paper, an empirical study and comparison of two models on NASA dataset [4]. K-Nearest Neighbour and Constructive COst MOdel II (COCOMO II) are the methods which are utilised in this work. These methods have seen an explosion of interest over years and hence it is important to analyse the performance of these methods. These methods have been analysed on datasets collected from 90 projects.

The paper is organized as: Section 2 summarizes the related work. Section 3 explains the research background, i.e, describes the dataset used for the estimation of effort and also explains various performance measures. Section 4 presents the research methodology followed in this paper. The results of the models estimated for software effort estimation and the comparative analysis are given in Section 5. The paper is concluded in Section 6. Finally, the future research is discussed in Section 7.

II. RELATED WORK

Software Effort Estimation is one of the most significant fields in software engineering and has repeatedly drawn the attention of researchers and practitioners towards addressing the on-going problem of inaccurate estimates in software development. Software effort estimation requires high accuracy, but it is difficult to achieve accurate estimates. Software effort estimation also plays a key role in determining cost of a software project. Software cost estimation includes the generation of the effort estimates and project duration in order to compute cost required to develop software project. There are various Software Estimation Techniques which fall in the following categories: Expert Judgment, Algorithmic Models, Machine Learning, Empirical techniques, Regression techniques and Theory-based techniques.

Enhancing the accuracy of effort estimation remains an intricate problem because it is difficult to deduce which technique produces more accurate estimation on which dataset [5]. According to software effort estimation technique survey, it is concluded that there is no single technique that can lead

us to unambiguous results [6].

Several models have been proposed for Software effort estimation, e.g., Slim, Cocomo, Estimacs, Function Point Analysis (FPA), Spans, Costar etc. In any case, none of the models proposed have been outstandingly successful in precisely predicting the effort required to develop a particular software product [7].

Many machine learning methods have been the subject of comparison to seeking an accurate estimation model for software development effort [8]. Several studies comparing techniques have been conducted for software effort estimation. From 17 different organisations dataset of 299 software projects were used from which they were divided randomly into 249 training cases and 50 test cases [9]. Desharnais compared using function points Analysis (FPA) with Artificial Neural Networks (ANN), Case-Based Reasoning (CBR) and Regression Models. Desharnais concluded that Artificial Neural Networks model performs more effectively than the other techniques.

Jain and Malhotra (2011) compared Linear regression, Support Vector Machine (SVM), Artificial Neural Network (ANN), Decision tree and Bagging using 499 projects. The result showed that Decision tree is the best among the other techniques at predicting effort required to develop a software.

Over the years, machine learning has been producing good results in numerous fields and like the majority of the effort prediction research, these reports assess the accuracy of effort estimation models. The significant distinction between this report and the current research attempt is that it goes into the comparison of the traditionally utilized algorithmic model of software effort estimation with a popular machine learning technique not currently researched by most.

III. RESEARCH BACKGROUND

A. Feature Sub Selection Method

The data we have used is obtained from Promise data repository. The NASA dataset originally comprises of 93 instances, however, 90 of these instances are chosen after disregarding unusable instances. The disregarded instances are that of the organic software projects, given the number of instances, they would not be sufficient to implement the proposed technique. Each of this projects are described by 15 effort multipliers and are measured on the scale of six categories ranging from very low to extra high. The 90 project chosen consist of 69 semi-detached and 21 embedded software projects.

B. Machine Learning Method

After data refinement, the projects are then divided into training sets and test set on a ratio of 7:3 (Given a dataset of size "B", divided into a training set of size (Y=|Y set| <= B) and the test set of size (X = B – Y=|Y set|). Thus 70% was used for the training set and 20% was used for the test set.

The selected training set of semi-detached software projects are 48 projects and the remaining 21 projects are used as test set. Likewise, the selected training set of embedded software projects are 15 projects and the remaining 6 projects are used as test set. The two techniques (k-NN and COCOMO II) are both implemented in the MATLAB environment [10] and the estimated effort of the test set is generated and compared with the equivalent actual effort in the original dataset to verify the estimation capability of the method. For the k-NN technique, the estimated effort is generated using the Euclidean distance function and then different values of k used to examine which value produces better results while for the COCOMO II technique, effort is estimated using the COCOMO II formula for both the semi-detached and embedded software projects.

C. Performance Measures

The following evaluation criterion has been used to evaluate the estimate capability. Amongst all these stated criterions, the most frequently utilised for performance measure are the PRED (n) and MMRE. Hence, these two measures are used in the comparison of our results with the results of preceding researches.

1) *Mean Magnitude of Relative Error (MMRE)* is a measure of the average error given by an estimation system. It is achieved through the average of the Magnitude of Relative Error (MRE), MRE is calculated as the summation of the absolute difference between the actual effort and the predicted effort divided by the actual effort.

$$MMRE = \frac{1}{n}\sum_{i=1}^{n}\frac{|AE_i - PE_i|}{AE_i}$$

Where, PE_i is the predicted effort achieved for the i^{th} test data:

AE_i is the actual effort collected for the i^{th} test data

n is the total number of projects in the test set.

2) *Root Mean Squared Error (RMSE)* is a regularly utilised measure of differences between estimated value of the model and the actual perceived value. It is obtained through the square root of the Mean Square Error (MSE), MSE is calculated as the squared difference between the actual effort and the predicted effort.

$$RMSE = \sqrt{\frac{1}{n}\sum_{i=1}^{n}(AE_i - PE_i)^2}$$

Where, PE_i is the predicted effort achieved for the i^{th} test data:

AE_i is the actual effort collected for the i^{th} test data

n is the total number of projects in the test set.

3) *Mean Absolute Error (MAE)* is the measure of how far the predicted values are from actual values. It is calculated as the mean of the absolute errors between predicted and actual effort.

$$MAE = \frac{1}{n}\sum_{i=1}^{n}|AE_i - PE_i|$$

Where, PE_i is the predicted effort achieved for the i^{th} test

data:

AE_i is the actual effort collected for the i[th] test data

n is the total number of projects in the test set.

4) *Relative Absolute Error (RAE)* is the total absolute error made relative to what the error would have been if the estimate just had been the average of the actual values. It is obtained through the summation of the absolute difference between actual and predicted effort divided by the summation of the absolute difference between actual and mean of actual.

$$RAE = \frac{\sum_{i=1}^{n} |AE_i - PE_i|}{\sum_{i=1}^{n} |AE_i - AE_m|}$$

Where, PE_i is the predicted effort achieved for the i[th] test data:

AE_i is the actual effort collected for the i[th] test data

AE_m is the average of the actual effort collected for the i[th] test data

n is the total number of projects in the test set.

5) *Root Relative Squared Error (RRSE)* is calculated by dividing the RMSE by summation of the squared difference between actual values and mean of actual values. Therefore, the smaller the values the better.

$$RRSE = \sqrt{\frac{\sum_{i=1}^{n}(AE_i - PE_i)^2}{\sum_{i=1}^{n}(AE_i - AE_m)^2}}$$

Where, PE_i is the predicted effort achieved for the i[th] test data:

AE_i is the actual effort collected for the i[th] test data

AE_m is the average of the actual effort collected for the i[th] test data

n is the total number of projects in the test set.

6) *Correlation Coefficient* is the statistical measures of the strength and direction of a relationship between two variables. It indicates the strength of the relationship. The higher the value of correlation coefficient, the stronger the relationship.

$$Cov(AE, PE) = \frac{1}{n}\sum_{i=1}^{n}(AE_j - \overline{AE})(PE_j - \overline{PE})$$

$$\sigma_a = \sqrt{\frac{\sum_{i=1}^{n}(AE_j - \overline{AE})^2}{n}} \qquad \sigma_p = \sqrt{\frac{\sum_{i=1}^{n}(PE_j - \overline{PE})^2}{n}}$$

$$C_j = \frac{Cov(AE, PE)}{\sigma_a . \sigma_p}$$

Where, PE_i is the predicted effort achieved for the i[th] test data:

AE_i is the actual effort collected for the i[th] test data

$\overline{AE}$ is the mean of the actual effort collected for the i[th] test data

$\overline{PE}$ is the mean of the predicted effort collected for the i[th] test data

n is the total number of projects in the test set.

7) *Prediction Accuracy (PRED (n))* is an indicator of the percentage of estimates that are within n% of the actual values. It is obtained from the relative error which is the absolute difference between the actual and predicted effort. It is expressed as the ratio of the test data with relative error (RE) less than or equal to x percent to the total number of projects in the test set. Hence, the larger the value of PRED (n), the better it is. n should be 25% and a good prediction system ought to attain this accuracy level 75% of the time. [11]

$$PRED(x) = \frac{t}{n}$$

Where, t is the value of relative error (RE) where the test data has:

less than or equal to x.

n is the total number of projects in the test set.

IV. Research Methodology

In this paper, one machine learning technique and one algorithmic model is used in order to predict effort. K-Nearest Neighbour and COCOMO II have seen an explosion of interest over the years, and have successfully been applied in various areas.

A. K-Nearest Neighbour

K-Nearest Neighbour (k-NN) algorithm is a non-parametric machine learning method for classification that predicts objects class by classifying objects centred on the k nearest training examples in the feature space [12]. K-Nearest Neighbour is recognised for its ability to produce good results in clinical outcome prediction such as Cancer prediction.

The k-nearest neighbour (k-NN) classifies new cases with previously stored available cases on the basis of similarity measure (e.g., Distance functions). It is a type of instance-based learning where the function is only approximated locally and all calculation is postponed until classification. The k-Nearest Neighbour (k-NN) gathers historical data known as the training data set, and utilises this data collected to make estimates for new test data, and then, the k-nearest data of the training dataset are achieved. Based on the data attribute of the nearest records, an estimate is made for the new data.

The k-Nearest Neighbour (k-NN) classification algorithm expands this procedure by utilising a predefined number ($k \geq 1$) of the nearest training instances as opposed to utilising only a single instance. *k* is a user-defined constant of positive integers, usually small. For instance, in a self-organizing map (SOM), all nodes are representatives of a cluster of similar points, irrespective of their density in the original training data. K-Nearest Neighbour(k-NN) can then be applied.

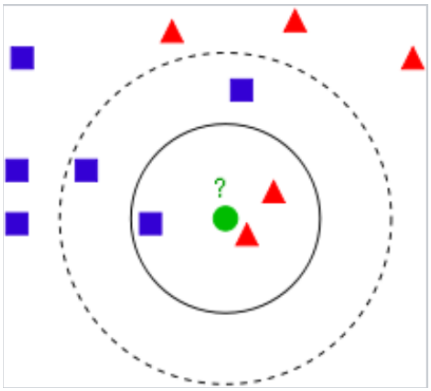

Fig. 1. Example of k-NN classification [13].

The test sample (green circle) ought to be classified either to the top class of blue squares or to the lower class of red triangles. When k = 3 (solid line circle) it is allotted to the red triangles because there are 2 triangles and just 1 square inside the inner circle. In the event that k = 5 (dashed line circle) it is allotted to the blue squares (3 squares versus 2 triangles inside the external circle) [13].

In k-Nearest Neighbour (k-NN) classification (Fig. 1), the estimated label is dictated by the voting for the nearest neighbours to the test label, that is, the most common label in the set of the chosen k instances is returned. The quality of the estimation relies upon the distance measure.

The generally used distance function is the Euclidean Distance.

$$Euclidean = \sqrt{\sum_{i=1}^{k}(x_i - y_i)^2}$$

Where, k is the user-defined constant

i is the number of instances

x and y are the vectors of each instance.

B. COCOMO II Model

COnstructive COst MOdel II (COCOMO II) is an estimation method that enables one to predict cost, schedule and effort when planning the development of a new project. The COCOMO techniques represents a model-based, data driven, parametric method that executes a fixed model method [14]. Thus, COCOMO produces a fixed estimation model which has been formed on organisational project data by utilising statistical regression, which signifies parametric and data driven techniques. COCOMO II is the latest version of the original COCOMO also known as COCOMO 81.

In 1981, the original COCOMO model was created by Dr. Barry Boehm using a multiple regression analysis. This was derived from the evaluation and scrutiny of 63 software development projects [15]. The use of the effort estimation equation to predict the number of person-months or person-hours needed to develop a project is the most essential calculation in the COCOMO model [15]. The model applies to three types of software projects (Table 1) [16]:

Organic projects – These are projects that consist of relatively small teams with lots of experience with less stringent requirements.

Semi-detached projects – These are projects that consist of medium teams with diversified experience working with a combination of stringent and less stringent requirements.

Embedded projects – These are projects developed with stringent requirements and team, that have little experience in the project area. It is also a mixture of organic and semi-detached projects.

TABLE I. TYPES OF SOFTWARE PROJECT [16]

Software project	**a**	**b**
Organic	2.4	1.05
Semi-Detached	3.0	1.12
Embedded	3.6	1.21

The original COCOMO model equation for computing effort is as follows:

$$Effort(E) = a \times (KLOC)^{b} \times EAF$$

Where, KLOC is the estimated size (number of lines of code) of the software project (expressed in thousands).

The coefficients a, b are dependent on which type of software project is being developed.

EAF (Effort Adjustment Factor) is the product of all the effort drivers. Effort is calculated in person months and it is a function of development criterion productivity, some effort drivers, and software size.

V. ANALYSIS RESULT

A. Model Prediction Result

The k-Nearest Neighbour (k-NN) and COCOMO II techniques have been used for estimating the efforts required to develop a software project using NASA dataset. Effort was estimated for both semi-detached and embedded software project. Seven performance measures have been utilised to compare the results gotten from these models. These measures are Mean Magnitude-Relative-Error (MMRE), Root-Mean Square-Error (RMSE), Mean Absolute Error (MAE), Relative Absolute Error (RAE), Relative Root Square Error (RRSE), Correlation Coefficient and PRED (25). The technique holding low values of MMRE, RMSE, MAE, RAE, and RRSE and high values of PRED (25) and correlation coefficient is considered to be the best among others.

TABLE II. RESULT

Performance Measures	Semi-Detached Software Project		Embedded Software Project	
	COCOMO II	k- Nearest Neighbour (k-NN)	COCOMO II	k- Nearest Neighbour (k-NN)
Mean Magnitude Relative Error (MMRE)	1.07	**0.54**	**1.70**	7.84
Root mean squared error (RMSE)	20266.30	**3189.30**	**1501.24**	5961.46
Mean absolute error (MAE)	1198.20	**393.70**	**429.36**	1378.92
Relative absolute error (RAE)	1.98	**0.65**	**0.20**	0.65
Root relative squared error (RRSE)	4.47	**0.70**	**0.21**	0.84
Correlation coefficient	**0.91**	0.76	**0.998**	0.98
PRED (25) %	23.81	**28.57**	**33.33**	16.67

The plots in Fig. 2 to 5 display the results of k-Nearest Neighbour (k-NN) and COCOMO II on semi-detached and embedded software project. In these plots, the purple curve represents the estimated values and the orange curve represents the actual values. The closer, the actual and estimated value curves are the lower, the error and the better the technique.

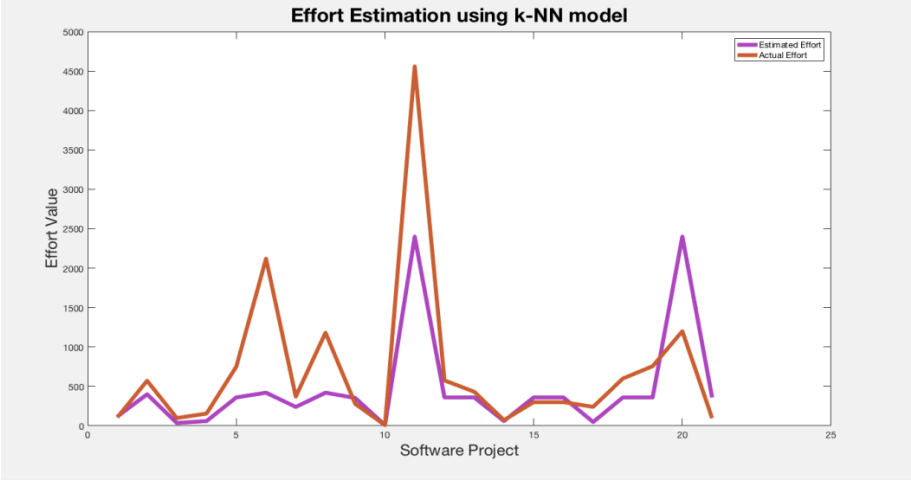

Fig. 2. Result using the k-Nearest Neighbour (k-NN) for Semi-Detached software project.

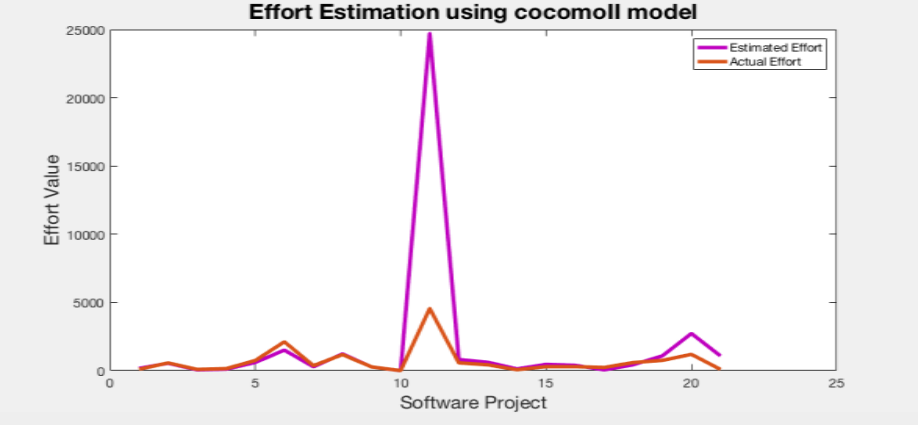

Fig. 3. Result using the COCOMO II for Semi-Detached software project.

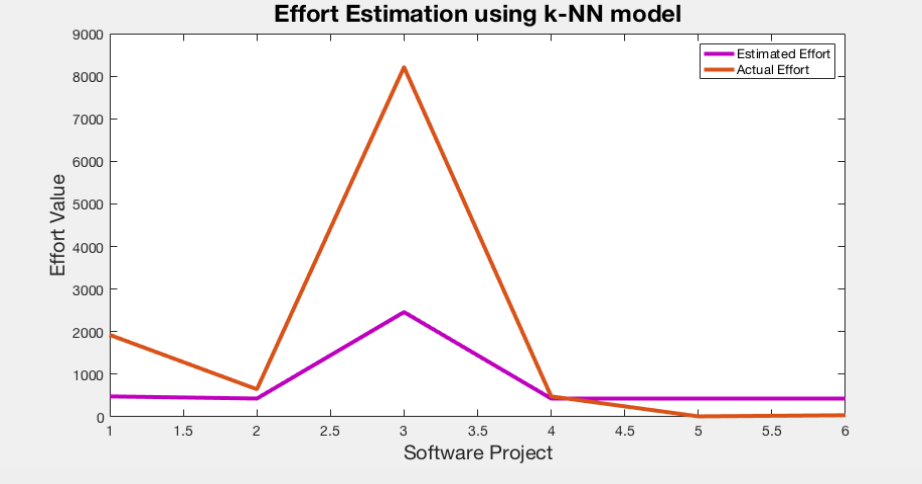

Fig. 4. Result using the k-Nearest Neighbour (k-NN) for Embedded software project.

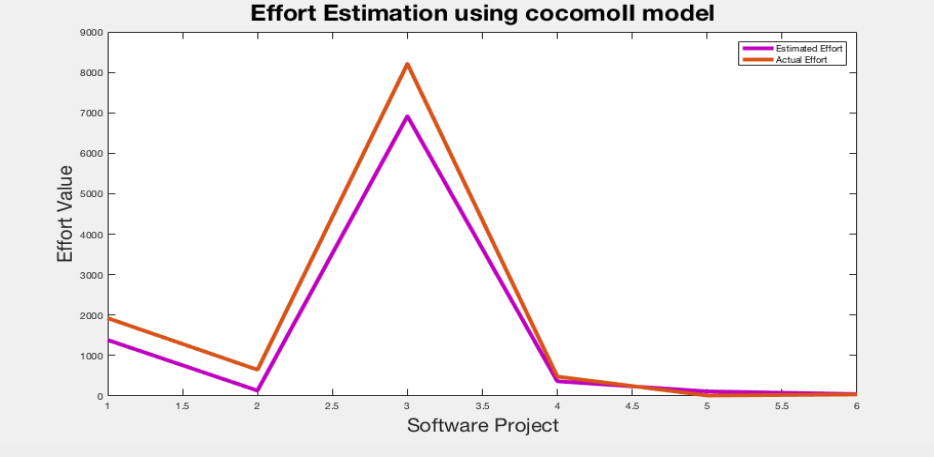

Fig. 5. Result using the COCOMO II for Embedded software project.

VI. CONCLUSION

In this research, the k-Nearest Neighbour (k-NN) and COCOMO II techniques have been used in predicting software development effort. Results were obtained using the NASA dataset acquired from Promise software engineering repository and are displayed in Table 2 above. The two techniques (k- NN and COCOMO II) were applied to the semi-detached and embedded software project and the method with lower error and higher accuracy is considered as better suited for estimating effort. There are various estimation techniques, although, no one method is necessarily better or worse than the other. It is difficult to decide which technique is right for which dataset [17].

The embedded software project dataset consists of 15 historical training data and 6 test set while semi-detached software project dataset consists of 48 historical training data and 21 test set. The results show that the k-Nearest Neighbour (k-NN) was the best technique for estimating the effort with MMRE value 0.54 and PRED (25) value 28.57% for the semi-detached software project. Hence, the NULL hypothesis H_0 should be accepted. Although, for the embedded software project the results show COCOMO II to be the best method with MMRE value 1.70 and PRED (25) value 33.33%. Thus, the Alternate hypothesis H_A should be accepted.

This result shows that k-NN is better when applied to the semi-detached software project and worse for embedded software project. This, however, does not signify that the type of software project has any effect on the method utilised. Thus indicating that the nature of data is important and this is true for most machine learning techniques. Small data makes over-fitting harder to avoid which is by far the most common problem in applied machine learning [18], and the outliers could mislead the training process thereby affecting the results too. In comparison to the previous study by Jain and Malhotra (2011), several machine learning methods such as decision tree, linear regression, bagging etc. were analysed on a larger dataset and produced good results.

The plot in Fig. 3 above shows an extreme overestimation of the semi-detached project which is with regards to the high rating scale of the effort driver in the dataset.

The first research question was “Which of the two techniques (k-NN and COCOMO II) produces better estimates?” Considering this question through the result obtained from both software projects, this question can, in

fact, have multiple answers: the k-NN technique performs better when there is a substantial amount of data. The lack of data makes k-NN unsuitable for use and as shown in Fig. 5 above, the COCOMO II model produces better estimates when analysed on the embedded project dataset because the nature of data has no effect on the algorithmic model.

The second research question was "Which of the two techniques (k-NN and COCOMO II) has stronger relationship between its estimated and actual value?" The result in Table 2 above shows that COCOMO II model has a stronger relationship with a correlation coefficient of 0.91 for semi-detached project and 0.998 for the embedded project.

Software practitioners and researchers may apply the k-Nearest Neighbour (k-NN) method for effort estimation where there is adequate data.

VII. FUTURE RESEARCH

Researchers have examined various machine learning techniques which are producing good results in different domains. However, the proposed technique has not received adequate attention in the field of software effort estimation. It would be useful to compare this k-Nearest Neighbour (k-NN) technique with other techniques such as Artificial Neural Network (ANN), Decision Tree, Neuro- Fuzzy (NF) etc. being examined by numerous researchers.

For future research, this methodology can further be explored on some large datasets to improve the validity of the produced results. Also, the performance of the proposed estimation method could be enhanced by making further modifications regarding small data by utilising the "leave one out" cross validation process, boot strapping and many more resampling techniques.

REFERENCES

[1] P. Naur, and B. Randell, "Software Engineering." 1969.

[2] I. Sommerville, "Software engineering." 9th ed. Addison-Wesley. 2011.

[3] M. Jeffcott, and C. Johnson, "The Use of a Formalised Risk Model in NHS Information System Development." 2002.

[4] Promise. Available: http://promisedata.org/repository/.

[5] A. Jain, and R. Malhotra, "Software Effort Prediction using Statistical and Machine Learning Methods." IJACSA, Vol.2, pp. 145-152, 2011.

[6] H. Rastogi, and S. Dhankhar "A survey on Software Effort Estimation Techniques" IEEE Xplore Document. *5th International Conference - Confluence The Next Generation Information Technology Summit (Confluence)*, pp.826-830, 2014.

[7] C. Kemerer, "An empirical validation of software cost estimation models." Communications of the ACM, Vol.30, pp.416-429, 1987.

[8] Y. Kim, and K. Lee, "A Comparison of Techniques for Software Development Effort Estimating." 2017.

[9] J. Desharnais, G. Wittig and G. Finnie, "A comparison of software effort estimation techniques: Using function points with neural networks, case-based reasoning and regression models." *Journal of Systems and Software*, vol.39, pp.281-289, 1997.

[10] Matlab.Available: https://uk.mathworks.com/products/matlab-online.html

[11] F. Ferrucci, C. Gravino, R. Oliveto, and F. Sarro, "Using Evolutionary Based Approaches to Estimate Software Development Effort." 2010.

[12] K. Conley, and D. Perry, "A Recommendation Engine for Picking Heroes in Dota 2."

[13] S. Ananthi, and D. Sathyabama, "Spam Filtering Using K-NN." Journal of Computer Applications, Vol.2, pp.20-23, 2009.

[14] A. Trendowicz, and R. Jeffery, "Software Project Effort Estimation." 1st ed. 2014.

[15] B. Boehm, "Software Engineering Economics." 1st ed. New York: Prentice-Hall Inc. pp.200- 217, 1981.

[16] S. Sehra, J. Kaur, and S. Sehra, "Effect of Data Preprocessing on Software Effort Estimation." International Journal of Computer Applications, Vol.69, pp.33-36, 2013.

[17] P. Rijwani, D. Santani, and S. Jain. "Software Effort Estimation: A Comparison Based Perspective." IJAIEM Vol.3, pp.18-29, 2014.

[18] J. Brownlee, "How to Identify Outliers in your Data -Machine Learning Mastery." 2013.

AUTHORS PROFILE

Razak Olu-Ajayi: He is a student at the Department of Computer Science, University of Hertfordshire. He received his bachelor's degree in Computer Science from Babcock University, Ogun, Nigeria. He is currently studying his masters in software engineering at the University of Hertfordshire, Hatfield, United Kingdom. His research interests are in software Estimation, improving software quality, statistical and adaptive prediction models.

An Adaptive Solution for Congestion Control in CoAP-based Group Communications

Fathia OUAKASSE, Said RAKRAK
Applied Mathematics and Computer Science
Laboratory (LAMAI)
Cadi Ayyad University
Marrekesh, Morocco

***Abstract*—The use of lightweight devices and constrained resources like Wireless Sensors Network (WSN) makes patterns traffic in the Internet of Things (IoT) different from the ones in conventional networks. One of the most emerging messaging protocols used to address the needs of these lightweight IoT nodes is Constrained Application Protocol (CoAP). CoAP presents a lot of advantages compared to other IoT application layer protocols; it ensures group communication via multicast communications between a server and multiple clients. Nevertheless, it doesn't support a group communication from a client to multiple servers; it relies on multiple unicasts to do so. Regarding the fact that these constrained devices communicate via a large amount of messages and notifications, network congestion occurs. This paper proposes an adaptive congestion control algorithm designed for group communications using unicast between a client and multiple servers. Simulated results show that the proposed mechanism can appropriately achieve higher performances in terms of response time and packet loss.**

***Keywords*—Internet of Things (IoT); Constrained Application Protocol (CoAP); congestion control; group communication; multicast; unicast**

I. INTRODUCTION

Recently, WSNs have been widely deployed in many IoT applications in order to measure, control or detect physical and environmental events like pressure, humidity, temperature and pollution levels, as well as other critical parameters. Applications usually used to send queries to concerned sensors to retrieve values periodically from the measurements or detections. Moreover, it is estimated that by the year of 2020 more than 26 billion devices will be connected to satisfy a wide range of IoT applications [1].

However, in recent critical applications of WSN that require intervention, such as home automation, industry process control, healthcare, environment monitoring, smart grid, and ambient assisted living, the challenge is getting information when an event of interest occurs in order to intervene in real-time. In this context, the publish/subscribe model [2] is the most appropriate model covering these requirements. Furthermore, one of the most important protocols based on this model is CoAP [3]. Indeed, CoAP is the most appropriate protocol for lightweight devices and constrained resources in terms of memory, energy, and computing. Thus, CoAP has been widely used in different application fields for resource constrained networks and M2M applications such as smart grid [4], building and home automation [5], smart cities [6] and in the healthcare industry, in which CoAP presents many applications, as an illustration, a mechanism for health monitoring using a wearable Sensor to provide real-time updates of the patient's status via CoAP protocol is presented in [7].

In many IoT application fields, in addition to unicast communication, nodes should be addressed in groups, so in order to manage the needs of multiple communications between different and several devices, CoAP supports group communication [8].

However, CoAP ensures multicast communication in one sense, from a server to multiple clients, but in the other sense; from a client to multiple servers; it relies on unicast communications. This has led to the problem of network congestion [9]. Network congestion in CoAP represents the great limitation that hinders the proper functioning of this protocol and causes the loss of packets. It can also significantly damage the performance of a network, manifesting in increased packet latencies, while a network may even become useless if the congestion collapse occurs [10].

To resolve this problem, researchers propose to insert a delay between consecutive requests. In this paper, an improved adaptive congestion control for group communication between a single client and multiple servers in CoAP is proposed. The principle of our improvement consists of the estimation of a delay to introduce between two requests; our formula adapts the calculation of the delay to network conditions because it is based on an estimated average link delay. Simulation results show that our proposition can appropriately achieve higher performances in terms of response time and packet loss.

The remainder of this paper is organized as: A brief presentation of the main aspects of CoAP protocol including reliability and security are presented as background in the second section. Then, in the third section, related works to group communication in CoAP including multicast and unicast group communications are described, also the problem of network congestion in group communication is discussed. Afterwards, in the fourth section, the proposed improved congestion control algorithm is detailed and a simulation of our proposition results is drawn using NS2 network simulator is presented. Finally, a conclusion and some future directions are closing up our paper in the fifth section.

II. CoAP Background

CoAP has been designed by the Internet Engineering Task Force (IETF) to support IoT with lightweight messaging for devices operating in a constrained environment. CoAP is an application layer protocol based on a REST architecture. It defines two kinds of interactions between end-points: 1) The client/server model which provides as well two interaction types: a) a one-to-one interaction which means request/reply and b) a multi-cast interaction; when a Client wants to interrogate servers it makes requests to servers, servers send back responses. Like HTTP, Clients have the ability to manage resources using requests: GET, PUT, POST and DELETE to perform Create, Retrieve, Update, and Delete operations. 2) A publish/subscribe model called the observer model [11], where a server, playing the role of the publisher, sends messages of notifications as publications to an observer, playing the role of subscriber, about a resource (event) that the subscriber is interested in receiving.

Unlike HTTP, CoAP doesn't run over TCP, it runs over UDP. Communication between clients and servers is afforded through connectionless datagrams. Retries and reordering are implemented in the application stack. UDP broadcasts and multicasts are also allowed by CoAP for addressing [12]. Otherwise, CoAP is considered more suitable for the IoT domain, this is going back to the fact that it is possible to build sufficiently basic error checking and verification for UDP to make sure that messages arrive without the significant communication overhead as in the case of TCP [13]. An overview architecture of CoAP protocol is drawn in Fig. 1.

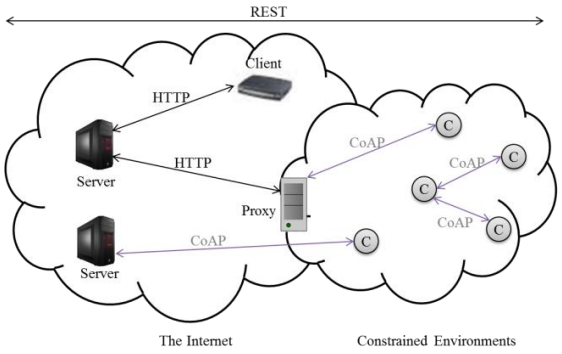

Fig. 1. An overview architecture of CoAP protocol.

CoAP utilizes four message types: 1) confirmable; 2) non-confirmable; 3) reset; and 4) acknowledgment, where two among them concern reliability messages. The reliability of CoAP consists of a confirmable message and a non-confirmable message [14]. In the case of a confirmable message an acknowledgment message (ACK) is sent to the sender from the intended recipient as shown in Fig. 2(a), else the message is retransmitted. This is just a confirmation that the message is received, but it doesn't confirm that its contents were decoded correctly. However, a non-confirmable message is fire and forget, i.e., no reception confirmation as shown in Fig. 2(b) [15].

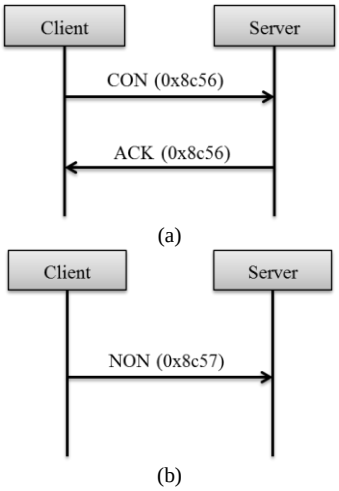

Fig. 2. (a) Reliable message transport (b) Unreliable message transport.

Since SSL/TLS are not available to provide security in UDP, CoAP uses Datagram Transport Layer Security (DTLS) on top of its UDP transport protocol for transfers of data [12].

III. Group Communication CoAP-Based

In the IoT, applications use group communication to make transactions between its different nodes, this goes back to the fact that nodes should be addressed either individually or in groups.

In many IoT applications, nodes addressed in group, i.e., a one to many communication patterns is essential to meet the needs of the application. Furthermore, in some applications, to increase the accuracy and the reliability of gathered data, it is important to collect information from more than one sensor. Moreover, the information gathered at the same time from many sensors may be very crucial to decide the appropriate way to intervene in situations which require real time intervention. So, all these scenarios and others require a communication with a group of sensors as recognized in the Charter of IETF CoRE Working Group [16].

A. Unicast group communications CoAP-based

In [17], authors propose to use an alternative unicast-based group communication solution for communication between CoAP devices. In order to facilitate the manipulation of a group of resources used by multiple smart objects, they create an intermediate level of aggregation. The group of resources is called an entity, the resources themselves are called the entity members and the component that manages these entities is called the Entity Manager (EM). By using a single CoAP request, an entity can be manipulated and thanks to the EM, entities that are created from groups of resources residing on CoAP servers can be maintained inside the Low power and Lossy Networks LLN. On the other hand, the EM acts as a proxy between the client and the constrained devices, thus clients on the Internet can create new entities and manipulate

them by requests via the EM. This latter analyses and verifies the client requests and then route them to the suitable constrained devices based on CoAP, after receiving responses, EM combines them according to the needs of the client and sends back an aggregated response to the client [18]. Fig. 3 shows an overview of the involved components.

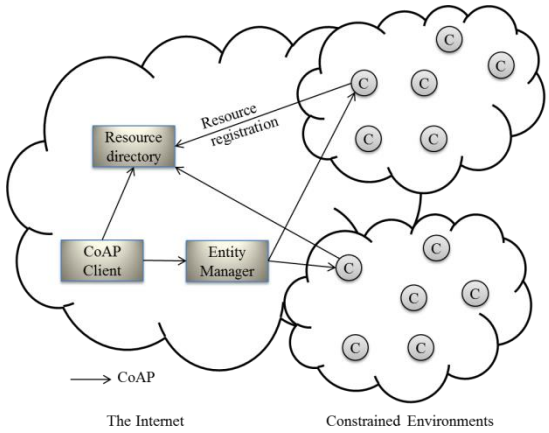

Fig. 3. The process of the creation of entities by clients on the entity manager.

Moreover, in [17] authors have introduced the notion of profiles which allows the client to give more details about the behavior of the created entities. The most advantage of this approach is its reliability; this goes back to the fact that it relies on unicast messages based on CoAP reliability mechanism.

However, in [19], authors gave a solution called SeaHttp for unicast-based group communication, where they proposed two additional methods called BRANCH and COMBINE to substitute the role of the entity manager and enable nodes to join and leave groups by themselves. This will benefit by reducing the number of messages. However, it can present some difficulties from viewpoint of the implementation in existing networks as a lack of flexibility.

B. Multicast group communications CoAP-based

As mentioned above, the IETF CoRE working group has first recognized the need to support a non-reliable multicast message. Thus, they have developed a specification for Group Communication for CoAP in RFC 7390 [20] to explain how we can use the CoAP protocol in a group communication context. Indeed, Group communication based on CoAP consists of sending a single non-confirmable message to multiple nodes grouped into a specific group using UDP/IP multicast for the requests, and unicast UDP/IP for the responses (if there was any). This means that all the nodes grouped in this group receive the same exact message.

It was proved that the use of multicast communication for sending requests is very efficient but it does not impact the number of responses sent by the destination nodes since these are sent as unicasts.

In the same context, authors in [21] presented an alternative lightweight forwarding algorithm for efficient multicast support in LLNs. This allows reducing a number of requests in the LLN since it sends one request to multiple destinations at the same time instead of a unicast for each destination.

C. Congestion control in group communications

The problem of congestion happens when the traffic load offered to a network approaches the network capacity [22]. This phenomenon is one of the main obstacles that still hinder the well-functioning of many protocols and thus impacts directly the efficiency of the communication. On the other hand, requests in group communication using CoAP engender a multitude of responses from different nodes, potentially causing congestion. Therefore, both the group communication multicast-based requests and the group communication CoAP unicast-based responses to these multicast requests must be conservatively controlled.

Indeed, CoAP must handle the congestion control by itself because it is based on UDP. Unlike HTTP which is based on TCP where a proper end-to-end congestion control is provided, CoAP offers a basic congestion control in the case of unicast messages [23].

In addition to the basic congestion control in unicast communications, the core CoAP specification also defines congestion control mechanism to be able to handle congestion control in case of multicast communications (requests from a server to multiple clients). Indeed, it defines a random delay called leisure which consists of a period of time delay inserted between multiple multicast requests. This leisure could be either a default value used by the server or it can be computed according to the following formula:

$$\text{Leisure} = S*G/R \quad (1)$$

Where, G is an estimated group size, R is a target data transfer rate R and S is an estimated response size.

Nevertheless, in the case when a single client is communicating with multiple servers using unicasts, CoAP does not specify a congestion control mechanism. To overcome this situation, authors in [17] proposed a simple solution consisting of a delay inserted between consecutive requests; this led to a limitation in the rate at which requests are sent.

In the following paper, we propose an improved formula to calculate the estimated delay to introduce between requests in order to reduce the network congestion.

IV. The Proposed Approach

Experiences show that communications via unicasts between a single client and multiple servers automatically engender a congestion of the network. In order to reduce the problem of congestion, we propose, in this paper, a simple adaptive solution based on the leisure defined in the RFC 7390 [20].

A. Adaptive solution to network condition

Indeed, the fact that the CoAP congestion control, designed for group communication between a single client and multiple servers, doesn't take into consideration the link delay to calculate the delay to insert between consecutive multicast requests, this leads to a congestion control mechanism insensitive to network conditions.

So, in this paper, in order to improve the delay and to adapt the behavior of our solution to network conditions, we propose

a delay between unicast requests depending on the link delay and the estimated group size as shown in the following formula:

$$D = \text{average link delay} * G / G-1 \quad (2)$$

Furthermore, the link delay represents the behavior of the network; if it increases, it means that congestion is more likely to happen, so in order to manage this problem, the estimated delay between unicast requests has to increase. On the other hand, if the link delay decreases, it means that the network is more available and the delays between requests have to be short adapting its behavior to the condition of the network.

B. Simulated results

In order to evaluate the performance of our proposed solution, we perform, in this section, simulations. Moreover, in order to figure out the performance of our proposed estimated delay to insert between unicast requests for group communications between a single client and multiple servers, we carry our evaluations on a NS2 simulator.

Our simulations are performed in terms of the average response; time taken by servers to respond to unicast communication, the jitter; the variation in the delay of the received messages and the packet loss ratio resulted from group communication.

The parameters considered in this simulation are detailed in Table1.

TABLE. I. SIMULATION PARAMETERS CONSIDERED IN OUR APPROACH

Parameter	**Value**
Nodes number	10 to 40 nodes
Packet size	1 Ko
Link speed	3 Mbps
Link delay	5 to 30ms
Simulation duration	10s

Fig. 4 shows the average response time according to several group sizes of servers to respond to unicast communications initiated by a single client. As expected, the average response time increases as the link delay increases proportionally to the group size. Furthermore, initially, in low link delay, all the group sizes have slightly the same average response time. Afterward, graphs for all of the group sizes start to increase following approximately the same curve variation, this is due to the fact that congestion is likely to happen causing more retransmissions delays, the thing that led to the increase in the average response time.

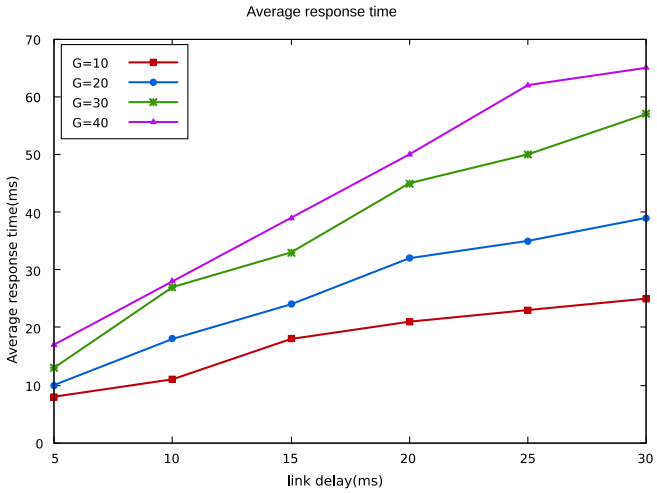

Fig. 4. Average response time according to link delays using several group sizes.

As discussed in the previous figure, the increases in link delay according to the increase of group size have slightly the same impact on the jitter variation as shown in Fig. 5.

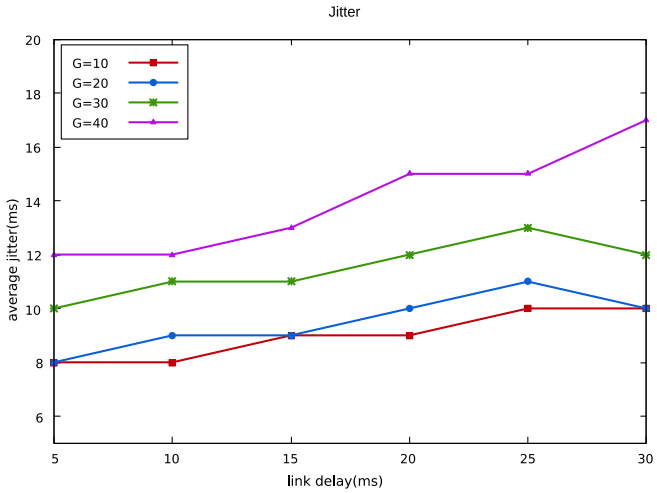

Fig. 5. Average jitter time according to link delays using several group sizes.

Indeed, using large groups can cause immediately network congestion. The reason for this is that with the increase in group size, the density of the nodes typically also increases, and as a result, congestion occurs in the network. Nevertheless, Fig. 6 shows that the average of packet loss stays less than 20% under the worst network conditions (link delay = 30 ms

and group size = 40), this is thanks to the use of the adaptive delay inserted between consecutive requests proposed in this paper.

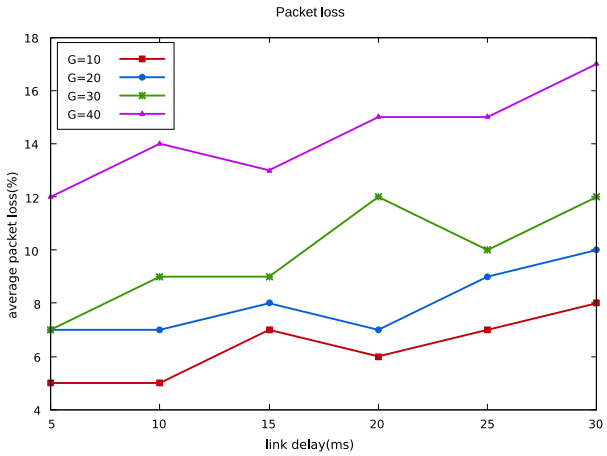

Fig. 6. Average packet loss time according to link delays using several group sizes.

Thanks to its flexibility and its ability to adapt its behavior to different network conditions, our proposition consistently presents high performances and short response times; it has the ability to increase the number of successful transactions and to decrease the packet loss ratio. Consequently, the proposed congestion control algorithm can maintain high performance and reduce the network congestion in almost all the considered scenarios.

V. Conclusion

The Internet of Things (IoT) is now offering the ability to transfer data over a network without requiring human-to-human or human-to-computer interaction. It is connecting different devices in our entourage through the use of WSN based on different protocols. One of the most appropriate protocols for lightweight devices and constrained resources in terms of memory, energy, and computing is CoAP. However, in such a network, the problem of congestion is very frequent especially in the case of group via unicast communications. Nevertheless, authors propose solutions for congestion control insensitive to network conditions, the thing which lowers its performances. The challenge is to design a congestion control mechanism for CoAP group communications between a single client and several servers suitable to ensure safe network operation while using network resources efficiently. Thus, in this paper, we present an improved congestion control algorithm, adaptive to network condition for the calculation of the delay to introduce between consecutive requests. In order to evaluate the performance of our proposed solution, we draw simulations under NS2 simulator. Simulated results show that our proposition can appropriately achieve higher performances in terms of response time and packet loss. Future works will consist of applying the idea of the paper to devices in a mobile environment in order to evaluate its performance in such environment.

Acknowledgment

I acknowledge the support provided by my supervisor Pr. Said RAKRAK and the members of the laboratory LAMAI (Laboratory of Mathematics Applied and Informatics) of the Faculty of Science and Technology-Cadi Ayyad University-Marrakesh.

References

[1] P. Middleton, P. Kjeldsen, J. Tully, “Forecast The Internet of Things,” Worldwide, Gartner, Inc., Tech. Rep. 2013.

[2] P.T. Eugster, P.A. Felber, R. Guerraoui, A.M. Kermarrec, “The many faces of publish/subscribe,” ACM Computing Survey. 35: 114–131, 2003.

[3] Z. Shelby, H. Hartke, C. Bormann, “Constrained Application Protocol (CoAP) drafietf core coap 18,” RFC 7252, Ver. 17, 18, 2013.

[4] S. In-Jae, E. Doo-Seop, S. Byung-Kwen, “The CoAP-based M2M gateway fordistribution automation system using DNP3.0 in smart grid environment,” IEEE International Conference on Smart Grid Communications (SmartGridComm), Miami, Florida, 2015.

[5] O. Bergmann, K.T. Hillmann, S.A. Gerdes, “CoAP-gateway for smart homes,” IEEE International Conference on Computing, Networking and Communications (ICNC), Maui, Hawaii, pp 446-450, 2012.

[6] J. Krimmling, S. Peter, “Integration and evaluation of intrusion detection for CoAP in smart city applications,” IEEE Conference on Communications and Network Security (CNS), San Francisco, CA, USA, pp 73-78, 2014.

[7] J. Joshi, D. Kurian, S. Bhasin, S. Mukherjee, P. Awasthi, S. Sharma, S. Mittal, “ Health Monitoring Using Wearable Sensor and Cloud Computing,” International Conference on Cybernetics, Robotics and Control (CRC), Hong Kong, China, pp 104 – 108, 2016.

[8] I. Ishaq, J. Hoebeke, I. Moerman, P. Demeester, “Observing CoAP groups efficiently,” Ad Hoc Networks, vol. 37, P2, pp. 368-388, 2016.

[9] H. Yuan, N. Yugang, G. Fenghao, “Congestion Control for Wireless Sensor Networks: A survey,” Control and Decision Conference, Changsha, China, pp 4853-4858, 2014.

[10] V. Paxson, M. Allman, “Computing TCP's Retransmission Timer,” RFC 2988, 2000.

[11] K. Hartke, “Observing Resources in CoAP Draft-Ietf-Core-Observe-06,” RFC 7641, Ver. 06, 2012.

[12] T. Jaffey, “MQTT and CoAP, IoT Protocols,” Eclipse, 2014.

[13] P. Masek, J. Hosek, K. Zeman, F. Kröpfl, “Implementation of True IoT Vision: Survey on Enabling Protocols and Hands-On Experience,” International Journal of Distributed Sensor Networks, Article ID 8160282, pp. 1-18, 2016.

[14] E.G. Davis, A. Calveras, I. Demirkol, “Improving Packet Delivery Performance of Publish/Subscribe Protocols in Wireless Sensor Networks,” Journal of sensors, vol. 13, pp. 648-680, 2013.

[15] X. Chen X, “Constrained Application Protocol for Internet of Things,” 2014.

[16] Constrained RESTful Environments charter charter-ietf-core-02.

[17] I. Ishaq, J. Hoebeke, F. Van den Abeele, I. Moerman, P. Demeester, “Flexible Unicast-Based Group Communication for CoAP-Enabled Devices,” Sensors, vol. 14, no. 6, pp. 9833-9877, 2014.

[18] I. Ishaq, J. Hoebeke, I. Moerman, P. Demeester, “Experimental Evaluation of Unicast and Multicast CoAP Group Communication,” Sensors, vol. 16, no. 7, pp. 9833-9877, 2016.

[19] C.D. Hou, D. Li, J.F. Qiu, H.L. Shi, L. Cui, “SeaHttp: A Resource-Oriented Protocol to Extend REST Style forWeb of Things,” Computer Sciences Technology Journal, vol. 29, pp. 205–215, 2014.

[20] A. Rahman, E. Dijk, “Group Communication for the Constrained Application Protocol (CoAP),” RFC 7390, 2014.

[21] M. Antonini, S. Cirani, G. Ferrari, P. Medagliani, M. Picone, L. Veltri, “Lightweight multicast forwarding for service discovery in low-power IoT networks,” In Proceedings of 22nd International Conference on Software, Telecommunications and Computer Networks (SoftCOM), Split, Croatia, 17–19, pp. 133–138, 2014.

[22] R. Bhalerao, S.S. Subramanian, J. Pasquale, "An Analysis and Improvement of Congestion Control in the CoAP Internet-of-Things Protocol," Annual Consumer Communications & Networking Conference (CCNC), Las Vegas, USA, pp. 889 – 894, 2016.

[23] C. Bormann, A. Betzler, C. Gomez, I. Demirkol, "CoAP Simple Congestion Control/Advanced, draft bormann-core-cocoa-00," Ver. draft-bormann-core-cocoa, 2016.

An Analytical Model for Availability Evaluation of Cloud Service Provisioning System

Fatimah M. Alturkistani
Information System Department
Imam Mohammed bin Saud University
Riyadh, Saudi Arabia

Saad S. Alaboodi
Information System Department
King Saud University
Riyadh, Saudi Arabia

***Abstract*—Cloud computing is a major technological trend that continues to evolve and flourish. With the advent of the cloud, high availability assurance of cloud service has become a critical issue for cloud service providers and customers. Several studies have considered the problem of cloud service availability modeling and analysis. However, the complexity of the cloud service provisioning system and the deep dependency stack of its layered architecture make it challenging to evaluate the availability of cloud services. In this paper, we propose a novel analytical model of cloud service provisioning systems availability. Further, we provide a detailed methodology for evaluating cloud service availability using series/parallel configurations and operational measures. The results of a case study using simulated cloud computing infrastructure illustrates the usability of the proposed model.**

Keywords*—Cloud computing; availability evaluation; series and parallel configuration; infrastructure as service

I. INTRODUCTION

Infrastructure as service (IaaS) cloud providers, such as Amazon Web Service and Microsoft Azure, deliver on-demand computational resources from large pools of equipment installed in a cloud service provider's data centers. The requests submitted by the cloud customers are provisioned and released if the cloud has enough available resources. Conversely, customers expect cloud services to be available whenever they need them, just like electricity or telephone connectivity. This expectation requires cloud service providers to regularly assess their infrastructure for probable failures and reduce the amount of time needed to recover from such failures.

Typically, a cloud service provider offers a service level agreement (SLA) stipulating the service provider's performance and quality in several ways. For example, an SLA may include a metric specifying the availability of the cloud service. Before committing an SLA to the cloud customers, the service provider needs to carry out an availability assessment of the infrastructure on which the cloud service is hosted [1], [2]. Most of the cloud providers offer approximately 99.99% of availability in their SLA. However, real data shows that the actual value of the availability of these providers is much lower [3], [4].

Hence, to reduce the overall cloud downtime and to provide a reliable estimate of service availability, cloud service providers need to assess the availability characteristics of their data centers in responsible and dependable manner. This assessment can be done through controlled experiments, large-scale simulations, and via analytical models [5], [1]. In a massive system such as cloud computing, conducting repetitive experiments or simulations is likely to be costly and time-consuming. Although analytical models can be cost and time-effective, accurate analytical modeling must deal with a large number of system states, leading to the state space explosion problem [6].

The primary contribution of this study is to propose a novel analytical model for evaluating the availability of cloud service provisioning systems focusing on IaaS. The proposed model is architecture-based; it relies on National Institute of Standards and Technology - Cloud Computing Reference Architecture (NIST-CCRA), the well-known cloud computing reference architecture [7]. NIST-CCRA provides an abstraction for cloud service provisioning system that can be used to model the logical interaction of failures within the system.

Consequently, availability is evaluated at two levels: the system-level and the component-level. At the system-level, reliability block diagrams (RBDs) are used to model the system's failures by considering series/parallel arrangements of the cloud components/subsystems. At component-level, availability is determined by probabilistic model and operational measures. Failure and repair data are modeled and analyzed using probability distributions and statistical inferences. Then, operational measures are derived and used to estimate component's availability.

A simulation approach is used to develop and verify the proposed analytical model. CloudSim [8] is used to simulate cloud infrastructure and the underlying components, while FTCloudSim [9], an extension of CloudSim, is used to simulate different failure scenarios using the fault injection technique. Also, BlockSim [10] and Weibull++ [11] are used for availability analysis and interpretation of results.

The rest of the paper is structured as: Section 2 presents relevant background information. Section 3 describes the proposed analytical model, and Section 4 presents conclusions and suggested future work.

II. BACKGROUND

A. NIST-based Cloud Service Provisioning System

According to NIST-CCRA, there are explicit processes and activities that cloud service providers need to perform to ensure reliable cloud service provisioning. Through service

orchestration, a cloud service provider operates the underlying cloud service infrastructure that supports its customers. The NIST defines service orchestration as "the composition of system components to support the cloud provider activities in arrangement, coordination, and management of computing resources in order to provide cloud services to cloud consumers" [11].

Service orchestration has three main components, which are arranged in layers: 1) the service layer (SL); 2) the resource abstraction and control layer (RACL); and 3) the physical layer (PL). The horizontal positioning of these layers reflects the relationships between them; upper-layer components depend on adjacent lower-layer components to provide a service. For instance, the RACL provides virtual cloud resources on top of the PL and supports the SL.

Likewise, in the SL, services can be modeled as three-layered components representing three types of services that have been universally accepted: 1) software as a service (SaaS); 2) platform as a service (PaaS); and 2) IaaS. A cloud service provider may define interface points in all three service models or just a subset. For instance, the platform component (i.e., PaaS) can be built upon the infrastructure component (i.e., IaaS) to support the software component (i.e., SaaS) where cloud service interfaces are exposed.

Although NIST-CCRA does not represent the system architecture for a particular cloud system, a specific cloud service provisioning system such as an IaaS provider or an IaaS broker can be modeled using NIST-CCRA [12]. Pereira, *et al*. [13] used NIST-CCRA to design a cloud-based architecture by refining the system's logical architecture. The suggested method involves 1) the selection of the NIST architectural component for which the respective coverage in the system's logical architecture needs to be analyzed; 2) analysis of the system's components into logical architecture including the respective architectural elements (AEs); and 3) the refinement and development of a new logical architecture in the cloud context by mapping the system's AEs to NIST-CCRA AEs.

B. Availability Evaluation in Cloud Computing

Cloud architecture has been studied using various techniques from reliability theory including RBDs, stochastic Petri nets (SPNs), fault trees, and Markov chains [13]-[17]. The availability of cloud computing architecture has been modeled in various ways using RBD techniques. In addition, analytical modeling has been used to estimate the availability of cloud system architectures including virtualized simple architecture and virtualized redundant architecture [18].

By considering the virtualization in the cloud, RBDs can also be applied to full virtualization, OS virtualization, and paravirtualization (see Fig. 1).

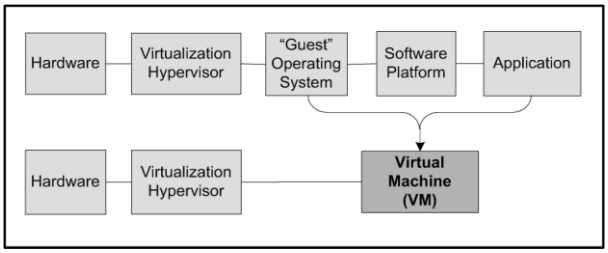

Fig. 1. Canonical virtualization *RBD.*

However, the dynamic nature of cloud computing requires the use of more rigorous modeling such as Markov modeling. Thus further analysis of availability in the context of system-level virtualization is needed.

Therefore, Dantas, *et al*. [19] used a hierarchical heterogeneous model based on RBD and a Markov reward model to describe non-redundant and redundant Eucalyptus architectures. Consequently, closed-form equations are obtained to compute the availability of those systems according to the rule of composition of series and parallel components. With respects to virtualization, availability model of a non-virtualized and virtualized system is presented using a hierarchical analytic model in which fault tree is used in the upper-level and homogeneous continuous-time Markov chains are used in the lower-level [20].

In another study, Silva, *et al*. adopted a hybrid modeling approach to deal with the complexity of the cloud system; RBDs are used for system-level dependability, whereas operational measures, such as mean time to failure (MTTF) or mean time between failure (MTBF), and mean time to repair (MTTR), are obtained for subsystem and component-level dependability.

III. MODELLING FORMALISM

A. System Representation and Basic Assumptions

Based on NIST-CCRA, let us consider the following two cloud implementation scenarios that can be used by a cloud service provider. In the first scenario, a cloud service provider may implement a high-level service model (i.e., SaaS) by using the interface points defined in the lower layers. For example, SaaS applications can be built on top of PaaS components, and PaaS components can be built on top of IaaS components. A real-world example of this is Google's cloud offerings. They offer a variety of SaaS products (e.g., Gmail, Google Search, Google Maps, Google Apps) using PaaS components (Google App Engine) that are run operationally on Google's cloud IaaS (Google's cloud platform) [7], [21]. As per NIST-CCRA, the dependency relationships among SaaS, PaaS, and IaaS components are represented graphically as components stacked on top of each other (see Fig. 2 (a)). A stack is a clearly defined structure that implies a series of interconnected systems that

transport data between each other to provide a certain function or service [22]. Therefore, similar to modeling large-scale distributed systems [23], [24] and other cloud platforms [19], [25], [26] the cloud service provisioning system is represented as a simple series system using an RBD (see Fig. 2 (b)).

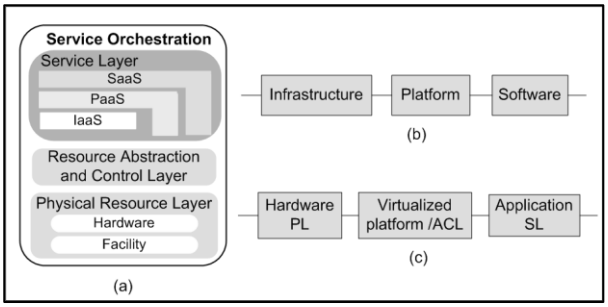

Fig. 2. NIST-CCRA service orchestration model.

In the second scenario, a cloud service provider may choose to provide an SL without the support of the lower-layer interface points. For example, a SaaS application can be implemented and hosted directly on top of cloud resources rather than using an IaaS virtual machine. A real-world example is salesforce.com, which provides both SaaS and PaaS products. The SaaS layer is built using the well-defined interface components from the PaaS. However, in this case, no IaaS layer is offered. SaaS is run directly on the resource abstraction layer with no explicit IaaS components. As per NIST-CCRA, the angling of the components indicates that each of the service components can stand alone and can be implemented directly on top of the cloud RACL and PL [7]. Hence, the cloud service provisioning system is represented as a simple series system using an RBD (see Fig. 2 (c)).

B. Cloud Service Provisioning Availability Model

In this model, the availability of the system is specified concerning the availability of the various components. Following a bottom-up approach, the availability at the component-level is determined using operational measures (i.e., MTBF and MTTR).

The logical relationship between individual components is considered to estimate the system-level availability, and it is expressed graphically using RBD. Table 1 set the definition of the notations that have been used in the availability modeling.

Let us consider a cloud service provisioning system denoted by CSP that consists of a set of subsystems $C = \{C_i, i = 1,2,3\}$ in which CSP success depends on the success of every subsystem C_i. Given the serial configuration as shown in Fig. 2, the availability of CSP denoted by A_{CSP} is written by [27]

$$A_{CSP} = \prod_{i=1}^{3} A_i, \tag{1}$$

Where, A_i is the availability of subsystem i. Recall that in NIST-CCRA, a cloud service provisioning system consists of three ordered layers, PL, RCAL, and SL.

Likewise, each subsystem C_i consists of a set of components $C_i = \{C_{i,j}, i = 1,2,3, j = 1,..,n_i\}$, where $C_{i,j}$ denotes the j^{th} component of the i^{th} subsystem, and n_i denotes the total number of components in subsystem i. Let us assume that the success of each subsystem C_i depends on the success of every individual component $C_{i,j}$.

TABLE. I. DEFINITION OF NOTATIONS

Notation	Definition
$_{SP}$	Cloud service provisioning system's overall availability value
	Availability of subsystem i
$_j$	Availability of component $C_{i,j}$
$_j$	Component j at subsystem i
	Total number of components at subsystem i
	$= \{C_{i,j}, i = 1,2,3, j = 1,..,n_i\}$, set of components for subsystem i
$X_{i,j}$	A random variable representing the time to failure of the j^{th}component of the i^{th} subsystem, $i = 1,2,3$ and $j = 1,..,n_i$
(t)	Availability of component $C_{i,j}$as a function over time
(t)	Failure density function for component $C_{i,j}$
$F_{i,j}$	Mean time to failure for component $C_{i,j}$
$R_{i,j}$	Mean time to repair for component $C_{i,j}$
$_j$	A random variable representing the time to repair of the j^{th}component at the i^{th} subsystem, $i = 1,2,3$ and $j = 1,..,n_i$
(t)	Repair density function for component $C_{i,j}$

Given this serial configuration, the availability of subsystem C_i denoted by A_i is given by

$$A_i = \prod_{j=1}^{n_i} A_{i,j}. \tag{2}$$

At the component-level, probability distributions are used for modeling operational data such as time to failure (TTF) and time to repair (TTR). Failure data can be used to make statements about the probability model, either in terms of the probability distribution itself or in terms of its parameters or some other characteristics.

Availability is the probability of a system/component being up (i.e., providing the service) at a specific instant of time t [24].

It is often expressed using (3), with many different variants [28], [29].

$$A = \frac{Uptime}{Uptime + Downtime}, \tag{3}$$

Where, *Uptime* refer to a capability to perform the task and *Downtime* refer to not being able to perform the task. However, the classification of availability is somewhat flexible and is largely based on the types of downtimes used in the computation and on the relationship with time. This study focused on inherent availability to determine the component-level availability. Inherent availability is the steady-state availability when considering only the corrective maintenance downtime of the system. Usually, this is the type of availability that companies use to report the availability of their products (e.g., computer servers) because they see downtime other than actual repair time as out of their control and too unpredictable.

Inherent availability used some operational measures from reliability theory: MTTF or MTBF and MTTR [18].

Now, let us assume that components failure data (i.e., TTF and TTR) is collected and preliminary analysis is performed using descriptive statistics and statistical inferences. Statistical inferences aim to draw inferences from the collected data in a meaningful way concerning some characteristics failure rates, MTTF, MTTR and related quantities. As probabilistic assumptions regarding the failure data play an important role in reliability and availability analysis [30], failure data (or at least assume the means of the sample data) usually assumed to follow well-known distributions (e.g., exponential, Weibull, lognormal).

Let $MTTF_{i,j}$ be a mean time to failure of the j^{th}component at the i^{th} subsystem, $i = 1,2,3$ and $j = 1,..,n_i$, $X_{i,j}$ is the random variable that represents the TTF of that component, and $f_{i,j}(t)$ is the probability density function of the component's failure time, then $MTTF_{i,j}$ is defined as the expected value of the random variable $X_{i,j}$ such that [24], [29]

$$MTTF_{i,j} = E[X_{i,j}] = \int_0^\infty t\, f_{i,j}(t)dt. \quad (4)$$

For a repairable component, $MTBF_{i,j}$ is used rather than $MTTF_{i,j}$ and defined similarly.

On the other hand, MTTR is used to measure the amount of time it takes to get a component running again after a failure [18]. Let $Y_{i,j}$ is the random variable that represents the TTR of the j^{th} component at the i^{th} subsystem, $i = 1,2,3$ and $j = 1,..,n_i$, and $g_{i,j}(t)$ is the probability density function of the component's repair time, then the component's $MTTR_{i,j}$ can be defined as [24]

$$MTTR_{i,j} = E[Y_{i,j}] = \int_0^\infty t g_{i,j}(t)dt. \quad (5)$$

Now, let us consider $C_{i,j}$ which represent the j^{th} component at i^{th} subsystem, $i = 1,2,3$ and $j = 1,..,n_i$, the availability of component $C_{i,j}$ denoted by $A_{i,j}$ is given by [18], [31]

$$A_{i,j} = \frac{MTTF_{i,j}}{MTTF_{i,j} + MTTR_{i,j}}. \quad (6)$$

C. Modeling Cloud System Availability with Redundant Components

Redundancy in cloud service provision system (e.g., hardware redundancy, software redundancy, and application redundancy) can also be modeled using RBD. The simplest example of redundancy could be achieved by combining two components in a parallel subsystem (i.e., server, storage, and virtual machine). The subsystem only fails if both components fail.

Let us consider n_i components in a cloud subsystem i with parallel composition, the subsystem availability A_i can be computed as follows

$$A_i = 1 - \prod_{j=1}^{n_i}(1 - A_{i,j}), \quad (7)$$

Where, $A_{i,j}$ is the availability of j^{th} individual component within the subsystem i. Further, the availability of more complex configuration (e.g., series-parallel configuration) can be obtained by combining the rules defined for series and parallel configuration [25].

D. Numerical example

To demonstrate NIST-based availability modeling and analysis numerically, let us consider the RBD of the IaaS provisioning system (IPS) depicted in Fig. 3. The objective is to obtain the average availability of the system after one year of operation (i.e., 8,760 hours).

The availability of the IPS, denoted by A_{IPS}, is the product of the availabilities of its subsystem i such that

$$A_{IPS} = A_1 \times A_2 \times A_3. \quad (8)$$

Where, A_1, A_2, and A_3 represent the availability of the hardware, virtualized platform, and application subsystems, respectively.

The availability of the hardware subsystem, denoted by A_1, is determined by the availability of its constituent components: power, network, storage, processor, and memory. Hence, A_1 is written as

$$A_1 = A_{1,1} \times A_{1,2} \times A_{1,3} \times A_{1,4} \times A_{1,5}. \quad (9)$$

Where, $A_{1,1}$, $A_{1,2}$, $A_{1,3}$, $A_{1,4}$, and $A_{1,5}$ represent the availability of power, network, storage, processor, and memory, respectively.

Likewise, the availability of virtualized platform A_2 is given by

$$A_2 = A_{2,1} \times A_{2,2} \times A_{2,3} \times A_{2,4}. \quad (10)$$

Where, $A_{2,1}$, $A_{2,2}$, $A_{2,3}$, and $A_{2,4}$ represent the availability of the hypervisor, VM, virtualized operating system, and middleware.

At component-level, let us assume that probability distributions model of failure data (i.e., TTF and TTR) are used to estimate the MTBF and MTTR for each component using (4) and (5), respectively to be shown in Fig. 4. Consequently, component availability is determined by substituting the values of MTBF and MTTR for the component in (6). Then, at the subsystem level, availability is analyzed based on system RBDs as follow:

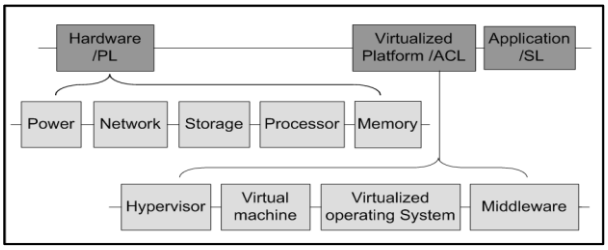

Fig. 3. IaaS provisioning system RBD.

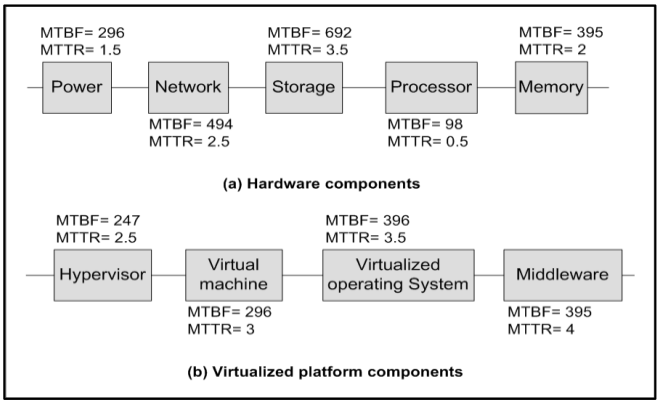

Fig. 4. MTBF and MTTR for IPS components.

Hardware availability A_1 is determined by substituting the values of its constituent component availabilities in (9), leading to

$$\begin{aligned} A_1 &= [MTBF_{1,1}/(MTBF_{1,1} + MTTR_{1,1})] \\ &\times [MTBF_{1,2}/(MTBF_{1,2} + MTTR_{1,2})] \\ &\times [MTBF_{1,3}/(MTBF_{1,3} + MTTR_{1,3})] \\ &\times [MTBF_{1,4}/(MTBF_{1,4} + MTTR_{1,4})] \\ &\times [MTBF_{1,5}/(MTBF_{1,5} + MTTR_{1,5})] \end{aligned}$$

$$\begin{aligned} &= [296/(296 + 1.5)] \\ &\times [494/(494 + 2.5)] \\ &\times [692/(692 + 3.5)] \\ &\times [98/(98 + 0.5)] \\ &\times [395/(395 + 2)] \end{aligned}$$

$$=0.975.$$

Virtualized platform availability A_2 is determined by substituting the values of components availabilities in (10), leading to

$$\begin{aligned} A_2 &= [MTBF_{2,1}/(MTBF_{2,1} + MTTR_{2,1})] \\ &\times [MTBF_{2,2}/(MTBF_{2,2} + MTTR_{2,2})] \\ &\times [MTBF_{2,3}/(MTBF_{2,3} + MTTR_{2,3})] \\ &\times [MTBF_{2,4}/(MTBF_{2,4} + MTTR_{2,4})] \end{aligned}$$

$$\begin{aligned} &= [247/(247 + 2.5)] \\ &\times [296/(296 + 3)] \\ &\times [396/(396 + 3.5)] \\ &\times [395/(395 + 4)] \end{aligned}$$

$$=0.961.$$

For application, let us assume that MTBF=329 and MTTR=5, then application availability A_3 is determined by substituting the values of the MTBF and MTTR of the application in (6), leading to

$$A_3 \quad 29/(329 + 5)$$

$$.986.$$

Subsequently, by substituting the values of A_1, A_2, and A_3, in (8), the availability of IPS is given by

$$A_{IPS} \quad .975 \times 0.961 \times 0.986$$

$$.924.$$

Using the RBD model and all the failure and repair characteristics, the IPS is simulated for 30,000 hours of operation (using BlockSim). After running the simulation for 30,000 hours, the relevant metrics are obtained. The point availability after one year of operation (i.e., $t = 8{,}670$) is estimated to be 93.6000%, whereas the mean availability after one year of operation is estimated to be 92.3134% (see Fig. 5), which corresponds to the analytical result obtained for mean system availability (i.e., $A_{IPS} = 0.924$). The subsystems mean availabilities are estimated to be 98.47% for application, 79.50% for hardware, and 69.19% for virtualized platform; these results correspond with those obtained using the analytical method (see Fig. 6).

Modeling and analyzing the IPS availability often carries significant value in boosting the efforts to improve availability, performing a trade-off analysis in system design or suggesting the most efficient way to operate and maintain the system.

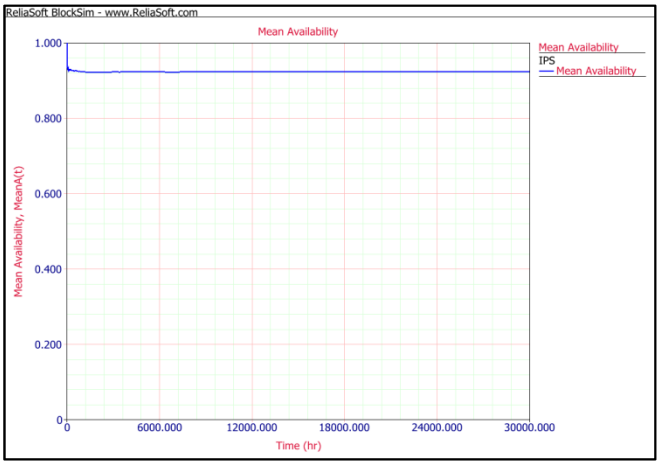

Fig. 5. Simulation results of IPS mean system availability.

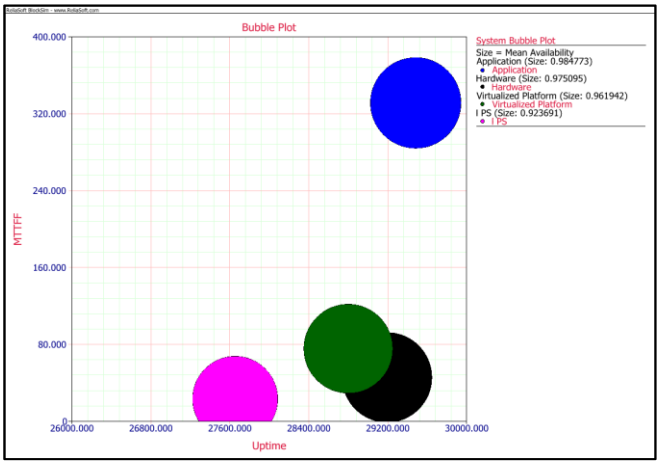

Fig. 6. Bubble plot of IPS subsystems mean availability with respects to mean time to first failure (MTTFF) and uptime.

IV. Testing and Validation

A. Approach

Because obtaining real-life failure data is extremely difficult as a result of the sensitive nature of these data, a simulation approach is used to test and validate the proposed model (Fig. 7). First, CloudSim is used to create a computerized duplication of real cloud infrastructure that is suitable for modeling probabilistic systems. Host, virtual machine (VM), and cloudlet are considered to be the infrastructure components that constituted the cloud service provisioning system.

For the experimental simulation, one data center is considered with different numbers of hosts using a 16-port fat-tree data center network and a corresponding number of VMs. Simultaneously, a Linux environment with x86 architecture is used as the operating environment and Xen as the virtual machine manager (VMM).

By investigating the architectural model of the cloud service provisioning system in CloudSim, the availability of IaaS requires an available host, VM, and cloudlet. Thus, the simulated IaaS cloud system can be modeled in a simple series system. Second, based on the previous study conducted by Zhou, *et al.* [8], multiple host failures are injected into the simulated system. Likewise, by considering some failure scenarios described by Nita, *et al.* [31], VM and cloudlet failures are introduced, and then failure and repair data are collected for availability analysis. Next, for the purpose of component availability modeling, Weibull++ is used to model component failure and repair data (i.e., TTF and TTR). A goodness-of-fit test is used to determine the corresponding distribution and estimate its parameters.

BlockSim is then used to model the cloud infrastructure availability at the system-level using an RBD. The cloud infrastructure system is modeled as a simple series diagram, which referred to as the base model (see Fig. 8). Failure and repair distributions are fed into BlockSim, and Monte Carlo simulations are done for 300,000-time units. Moreover, three more models representing different scenarios are created for comparison with the base model, and the model was showing the greatest availability is selected.

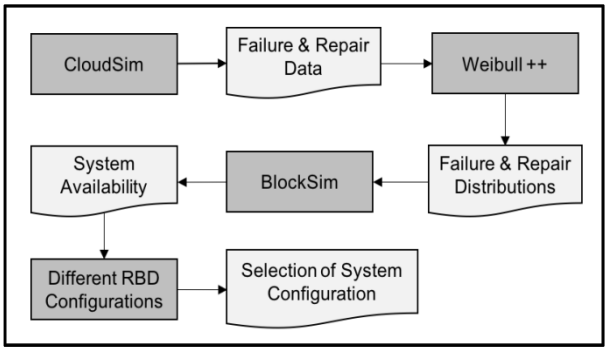

Fig. 7. Testing and validation approach.

B. Results and Discussion

The simulations show that failure data at the component-level (host, VM, and cloudlet) were successfully fitted to a Weibull distribution. The parameters of each distribution were estimated using regression analysis. For instance, Fig. 9 shows the Weibull probability plot for host failure data. In the probability plot, the shape parameter (beta) is estimated based on the fitted-line slope. The scale parameter (eta) is the time at which a specific percentage of the population has failed. The correlation coefficient (rho) is a measure of how well the linear regression model fits the data. Furthermore, VM repair data were the best fit with the lognormal distribution and a two-sided confidence level of 90% (see Fig. 10). In contrast, both the host and cloudlet have constant values for repair that are 10,800 hours and 300 hours, respectively.

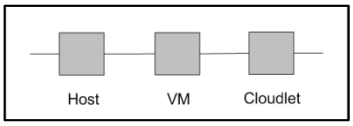

Fig. 8. Base model RBD.

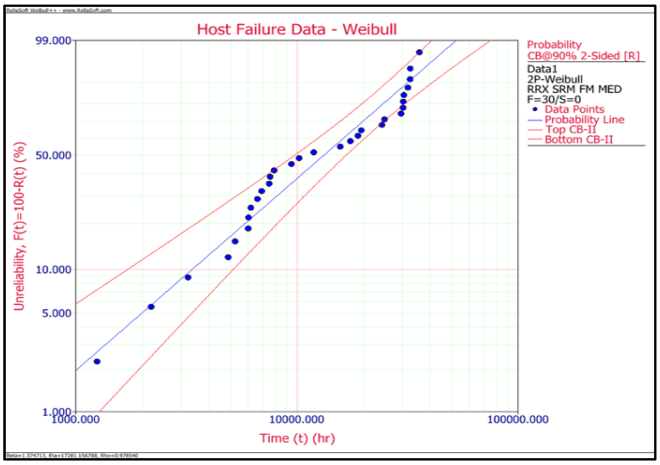

Fig. 9. Host failure data Weibull probability plot.

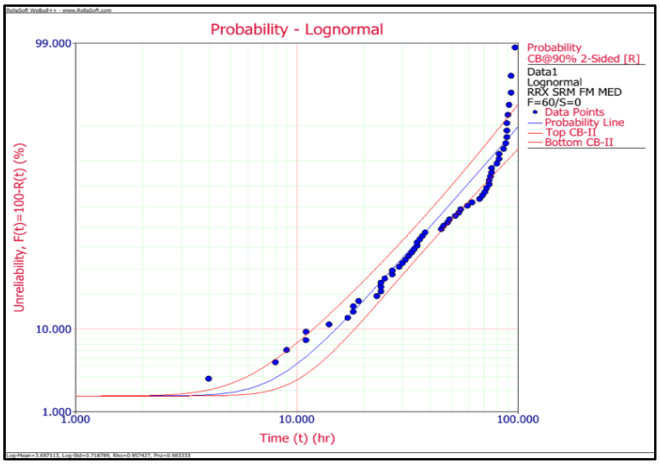

Fig. 10. VM repair data lognormal probability plot.

The failure and repair data distributions with associated parameters were used to feed several simulation models that were built using BlockSim and configured in four different models.

A base model was built in simple series and configured using the data provided by Weibull++. Table 2 shows the base model block configurations detailing the inputs for each block (i.e., host, VM, and cloudlet) on the availability model and the corrective task.

At the simulation end time (300,000-time units), the base model achieved an availability of 0.590767. Hence, to improve the system availability (i.e., to fulfill the customer's requirements), a sensitivity analysis is performed to study the impact of the repair rate and standby configuration (i.e., redundancy technique) on the overall system availability.

In the second model, host repair time was improved in the base model to determine its impact on overall system availability. The results showed that at the simulation end time (300,000-time units), availability is increased to 0.722.

In the third model, the base model was improved by using standby configurations. The base model was rebuilt with a standby container that included three base model systems; one system was active, and two were on standby (see Fig. 11). It is assumed that the switching reliability is 100%. The standby simulation results showed an improvement in overall system availability.

For instance, at the simulation end time (300,000-time units), system availability was 0.977. Also, a fourth model was created by applying a standby configuration to the second model in which the host repair time is improved. The results showed an improvement in overall system availability. At the simulation end time (300,000-time units), availability had increased to 0.996313. Fig. 12 shows the mean availability of the four models.

TABLE. II. BASE MODEL CONFIGURATIONS

Configuration	Attribute	Host	VM	Cloudlet
Reliability Model	Distribution	2P-Weibull	2P-Weibull	2P-Weibull
	Beta	1.37	1.43	1.46
	Eta	17281	17136	16260
Corrective Task	Distribution	Constant	Lognormal	Constant
	Parameter 1	10800	3.7 (log mean)	300
	Parameter 2	NA	0.72 (log-std)	NA
	Restoration	As good as new	As good as new	As good as new
	Task result	Bring item down	Bring item down	Bring item down

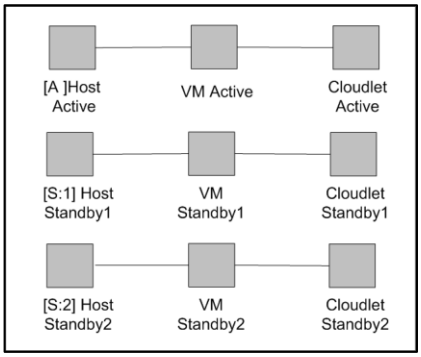

Fig. 11. Base model with standbys RBD.

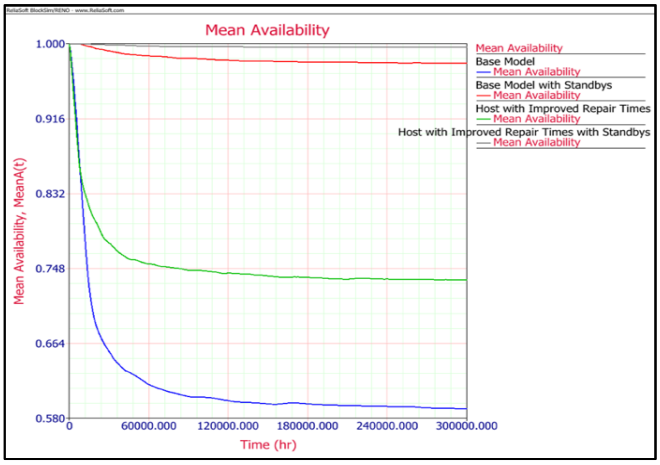

Fig. 12. Mean availability overlay plot for all models.

V. Conclusions and Future Work

This paper's primary contribution is a proposed model for evaluating the availability of cloud service provisioning systems. The model relies on NIST-CCRA, the well-known cloud computing reference architecture, to define cloud subsystems/components and the logical relationships among them. Using mature modeling techniques from reliability theory that can provide the operational measures that are so desirable today, we were able to quantify component-level availability. Furthermore, by considering series/parallel arrangements of the cloud system components, RBD was used to model system-level availability. The proposed model has some limitations imposed by the characteristics of RBDs. In future research, a dynamic RBD [30] will be adopted to consider the dynamic behavior of a cloud system. Other cloud scenarios such as cloud federation will also be modeled in future studies.

References

[1] F. Longo, R. Ghosh, V. K. Naik, and K. S. Trivedi, "Availability Analysis of IaaS Cloud Using Analytic Models," Achieve. Fed. Self-Manageable Cloud Infrastructures Theory Pract. IGI Glob., pp. 134–136, 2012.

[2] A. Undheim, A. Chilwan, and P. Heegaard, "Differentiated Availability in Cloud Computing SLAs," 2011 IEEE/ACM 12th Int. Conf. Grid Comput., pp. 129–136, Sep. 2011.

[3] A. Croll, Cloud performance from the end user perspective. 2011.

[4] G. P. Gibilisco, "Model-Based Availability Evaluation of Multi-Cloud Applications," University of Illinois at Chicago, 2013.

[5] F. Longo, R. Ghosh, V. K. Naik, K. S. Trivedi, and I. B. M. T. J. Watson, "A Scalable Availability Model for Infrastructure-as-a-Service Cloud," in Dependable Systems & Networks (DSN), 2011 IEEE/IFIP 41st International Conference on. IEEE, 2011.

[6] R. Ghosh, F. Longo, F. Frattini, S. Russo, and K. S. Trivedi, "Scalable Analytics for IaaS Cloud Availability," IEEE Trans. CLOUD Comput. VOL.2, vol. 2, no. X, pp. 1–14, 2014.

[7] V. Lo Faso, "Understanding NIST ' s Cloud Computing Reference Architecture : Part II Understanding NIST ' s Cloud Computing Reference Architecture : Part II," Global Knowledge, 2014. .

[8] R. N. Calheiros, R. Ranjan, A. Beloglazov, and A. F. De Rose, "CloudSim : a toolkit for modeling and simulation of cloud computing environments and evaluation of resource provisioning algorithms," Software. Pract. Exp. 41.1, no. August 2010, pp. 23–50, 2011.

[9] A. Zhou, S. Wang, Q. Sun, H. Zou, and F. Yang, "FTCloudSim: A Simulation Tool for Cloud Service Reliability Enhancement Mechanisms," Proc. Demo Poster Track ACM/IFIP/USENIX Int. Middleware. Conf., p. 2:1--2:2, 2013.

[10] "BlockSim: System Reliability and Maintainability Analysis Software Tool," ReliaSoft Corporation. .

[11] ReliaSoft Corporation, "Weibull++: Life Data Analysis (Weibull Analysis) Software Tool," 2017. [Online]. Available: http://weibull.reliasoft.com.

[12] J. Teixeira, C. E. Salgado, and R. J. Machado, "Modeling an IaaS Broker Based on Two Cloud Computing Reference Models," 2016 IEEE Int. Conf. Cloud Eng. Work., pp. 166–171, 2016.

[13] M. Ribas, A. S. Lima, N. Souza, T. Engenharia, and S. Paulo, "Assessing Cloud Computing SaaS adoption for Enterprise Applications using a Petri net MCDM framework," Netw. Oper. Manag. Symp. (NOMS), IEEE., 2014.

[14] G. Callou, P. Maciel, D. Tutsch, and J. Araújo, "A Petri Net-Based Approach to the Quantification of Data Center Dependability," Petri Nets - Manuf. Comput. Sci., pp. 313–336, 2012.

[15] R. Jhawar, V. Piuri, and I. Universit, "Fault Tolerance Management in IaaS Clouds," 2012 IEEE First AESS Eur. Conf. Satell. Telecommun., pp. 1–6, 2012.

[16] D. S. Kim, F. Machida, and K. S. Trivedi, "Availability Modeling and Analysis of a Virtualized System," 2009 15th IEEE Pacific Rim Int. Symp. Dependable Comput., pp. 365–371, Nov. 2009.

[17] B. Silva, P. Maciel, E. Tavares, and A. Zimmermann, "Dependability Models for Designing Disaster Tolerant Cloud Computing Systems," in Dependable Systems and Networks (DSN), 43rd Annual IEEE/IFIP International Conference on. IEEE, 2013.

[18] R. Bauer, E., Adams, Reliability and Availability of Cloud Computing. 2012.

[19] J. Dantas, R. Matos, J. Araujo, and P. Maciel, "Models for Dependability Analysis of Cloud Computing Architectures for Eucalyptus Platform," Int. Trans. Syst. Sci. Appl., vol. 8, no. December, pp. 13–25, 2012.

[20] D. S. Kim, F. Machida, and K. S. Trivedi, "Availability modeling and analysis of a virtualized system," 2009 15th IEEE Pacific Rim Int. Symp. Dependable Comput. PRDC 2009, pp. 365–371, 2009.

[21] A. Lenk, M. Klems, J. Nimis, S. Tai, and T. Sandholm, "What's inside the cloud? An architectural map of the cloud landscape," Proc. 2009 ICSE Work. Softw. Eng. Challenges Cloud Comput. CLOUD 2009, pp. 23–31, 2009.

[22] S. Kristopher, "Living in the Cloud Stack – Understanding SaaS, PaaS, and IaaS APIs," Nordic APIs, 2016. .

[23] K. Weyns and M. Höst, "Case Study on Risk Analysis for Critical Systems with Reliability Block Diagrams," in 10th International IT Systems for Crisis Response and Management (ISCRAM) Conference. ISCRAM, 2013, no. May, pp. 693–702.

[24] Gabriele Manno, "Reliability modelling of complex systems: an adaptive transition system approach to match accuracy and efficiency," University of Catania, 2012.

[25] B. Wei, C. Lin, and X. Kong, "Dependability Modeling and Analysis for the Virtual Data Center of Cloud Computing," 2011 IEEE Int. Conf. High Perform. Comput. Commun., pp. 784–789, Sep. 2011.

[26] T. Thanakornworakij, R. F. Nassar, and C. Leangsuksun, "A Reliability Model for Cloud Computing for High-Performance Computing Applications," in European Conference on Parallel Processing. Springer Berlin Heidelberg, 2013, pp. 474–483.

[27] G. Callou, P. Maciel, D. Tutsch, and J. Araújo, "A Petri Net-Based Approach to the Quantification of Data Center Dependability," Petri Nets-Manufacturing Comput. Sci. InTech, 2012.

[28] T. Humble, Availability, Reliability, Maintainability, and Capability. Triplex Chapter of the Vibrations Institute. Humble, TX: Barringer and Associated Inc, 1997.

[29] A. Alkasem and H. Liu, "Research Article A Survey of Fault-tolerance in Cloud Computing : Concepts and Practice," Sch. Comput. Sci. Technol. , Harbin Inst. Technol. China, vol. 11, no. 12, pp. 1365–1377, 2015.

[30] ReliaSoft, "Reliability Basics: Availability and the Different Ways to Calculate It." .

[31] V. K. Katukoori, "Standardizing Availability Definition," Univ. New Orleans, New orleans, La., USA, p. 21, 2007.

Network Packet Classification using Neural Network based on Training Function and Hidden Layer Neuron Number Variation

Imam Riadi
Department of Information System
Ahmad Dahlan University
Yogyakarta,
Indonesia

Arif Wirawan Muhammad
Department of Information Technology
Ahmad Dahlan University
Yogyakarta, Indonesia

Sunardi
Department of Electrical Engineering
Ahmad Dahlan University
Yogyakarta,
Indonesia

***Abstract*—Distributed denial of service (DDoS) is a structured network attack coming from various sources and fused to form a large packet stream. DDoS packet stream pattern behaves as normal packet stream pattern and very difficult to distinguish between DDoS and normal packet stream. Network packet classification is one of the network defense system in order to avoid DDoS attacks. Artificial Neural Network (ANN) can be used as an effective tool for network packet classification with the appropriate combination of numbers hidden layer neuron and training functions. This study found the best classification accuracy, 99.6% was given by ANN with hidden layer neuron numbers stated by half of input neuron numbers and twice of input neuron numbers but the number of hidden layers neuron by twice of input neuron numbers gives stable accuracy on all training function. ANN with Quasi-Newton training function doesn't much affected by variation on hidden layer neuron numbers otherwise ANN with Scaled-Conjugate and Resilient-Propagation training function.**

***Keywords*—Classification; DDoS; neural; network; training; function; hidden; layer**

I. Introduction

Distributed denial of service (DDoS) is a structured network attack coming from various sources and fused to form a large packet stream. DDoS attacks, generally utilizing resources from the slave computer coordinated by the attacker to decrease the target network resources causing legitimate client cannot access these resources. DDoS packet stream pattern behaves as normal packet stream pattern and it is very difficult to distinguish between DDoS and normal packet stream [1].

DDoS packet stream with a large volume causes the target system cannot handle and end up with a loss of resources such as system shutdown, loss of data, moreover, the system loses the overall of owned services [2], [3]. Network packet classification is one of network defense system in order to avoid DDoS attacks [4]. Network packet classification can be carried out by utilizing Artificial Neural Network (ANN) method.

Network packet classification for DDoS attacks detection in TOR network using ANN carried on research [5] by utilizing optimization of a sinusoidal function as a feature extractor of the network packet. ANN used in [6] with Resilient-Backpropagation function combined with the ensemble of classifier outputs method and Neyman-Pearson cost minimization strategy for detection of DDoS attack based on DARPA and KDDCUP datasets. Research [7] adopted the ANN method to detect DDoS attacks based on darknet traffic. TCP/80 and UDP/53 packets used as input and optimized by Locally Sensitive Hashing methods. ANN used in [8] to recognize illegal packets in the network, by taking advantage of the Backpropagation functions. TCP, ICMP, and UDP packet used as inputs in the [8]. Research [9] proved that the ANN method can be used to detect a new type of DDoS attack, in Hadoop and HBase environment.

Based on earlier research regarding packet classification with ANN, this study focuses on the ANN training function to find out the best training function layer for packet classification. DDoS dataset published by the Center for Applied Internet Data Analysis (CAIDA) and network normal dataset published by Ahmad Dahlan University Networks Laboratory are used in this study.

II. Packet Classification Approach

The study of packet classification with artificial neural network applying variation of training function and hidden layer neuron number, involves steps as seen on Fig. 1.

1) Get network DDoS dataset and Normal dataset from CAIDA and Ahmad Dahlan University Networks Laboratory in .pcap format.

2) Extract network packet, using statistical method to get network features, that are average packet size, number of packets, time interval variance, packet size variance, packet rate, and number of bytes.

3) Train ANN with three training function (Quasi-Newton, Resilient-Propagation, Scaled-Conjugate).

4) Classification result comparison using accuracy, mean-squared error (mse), and iteration parameters.

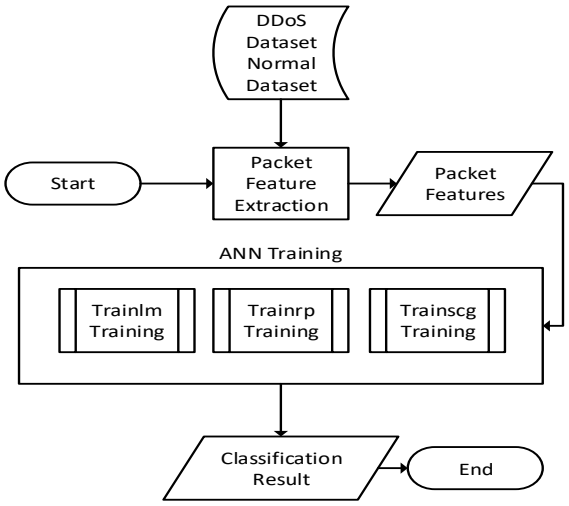

Fig. 1. Steps of network packet clasification.

Accuracy is the ratio between the addition of normal and DDoS packet that is recognized by the system and compared to the overall packet data. Mean square error (mse) is the most ANN important parameter for performance evaluation of training functions parameters [10]. Mean square error reflects an absolute error of ANN training output pattern with desired output pattern. The iterations reflect the time taken by ANN to reach convergence also a tradeoff indicator between training time and convergence.

III. ANN COMPONENTS FRAMEWORK

A. Network Packet Features

To classify the network packet, the first step is extracted from the network feature of the dataset. The aim of feature extraction is to measure certain attributes in original data that distinguish one input pattern from another pattern. In this study, network packet stream extracted to six features based on statistical method. Those six features are:

1) *Average packet size*: The longer DDoS attack occurs, then it is always followed by a rise in the value of average packet size [11].

2) *Number of packets*: DDoS attacks overwhelm a target computer network by sending many packets at a certain time lag. DDoS always result in high number of the packet [11].

3) *Time interval variance*: DDoS attack delivers packages in large numbers occurred in a certain time span, the value of time interval variance will be smaller and nearly zero. Time interval variance stated as (1) [12].

$$t_c{}^2 = \frac{\sum(t_n - t)^2}{n} \quad (1)$$

Where t_n is time of a packet received and $\bar{t}$ is the rate of time a packet is received.

4) *Packet size variance*: The normal traffic resulting high packet size variance values within DDoS attacks resulting close to zero packet size variance value, due to the monotony packet size that sent to target. Packet size variance stated as (2) [12].

$$p_c = \sqrt{\frac{\sum(p_n - \bar{p})^2}{n}} \quad (2)$$

Where, p_n is received packet size, and $\bar{p}$ is packet size rate.

5) *Packet rate*: Packet rate reflects the number of packets sent by the source address to a destination address within a specific time frame as stated on (3) [12].

$$p_c = n_p \, x \, \frac{1}{(t_e - t_x)} \quad (3)$$

Where n_p is the number of packets, t_e is end time a packet is received, t_s is the initial time a packet is received.

6) *Number of bytes*: DDoS attack always increases the number of bytes in constant [12].

B. Training Function

There are numbers of batch training algorithms which can be used to train an Artificial Neural Network [13]. The most used training algorithms are:

1) Newtonian training function is fast to reach convergence than conjugate gradient methods, but Newton's method is complex and time-consuming to compute the Hessian matrix for feed forward neural networks [14], [15]. Based on Newton's method there a new class of method is called a Quasi-Newton method (Matlab trainlm) which doesn't require calculation of second derivatives. The Quasi-Newton method updates a Hessian matrix in each iteration of the algorithm [16], [17].

2) Resilllent-Propagation training function (Matlab trainrp) refers to the gradient-descent algorithm that removes the effect of partial derivative magnitude from the activation function. In this case a partial derivative of the activation function is used to determine the direction of the neural network weights, whereas the magnitude of the partial derivatives has no effect on the weight changes. So that the weight changes of the neural network can become more stable in achieving the minimum gradient [15].

3) Scaled-Conjugate training function (Matlab trainscg) refers to the conjugate-gradient algorithm that exploits the gradient's negative direction to match the weight changes of the neural network layer so that it affects the number of iterations the neural network takes to achieve convergence [15].

C. ANN Layer Scheme

There is no certainty that the best number of neurons and hidden layers are used to resolve a problem with an ANN [18]. Based on that reason, this study does some variation on hidden layer neuron numbers as seen on Table 1.

TABLE. I. HIDDEN LAYERS VARIATION

Type	Input Neurons	Hidden Layer Neuron Variations	Output Neurons
1.	6	3	2
2.	6	6	2
3.	6	12	2
4.	6	13	2

D. Comparison Parameters

Accuracy, mean-squared error, and iteration parameters was used in this research for classification performance analysis.

1) Accuracy is the ratio between recognition result of DDoS and normal packet data compared to the overall packet data.

2) Mean-squared error (mse), reflect an absolute error of ANN training actual output pattern with desired output pattern.

3) Iteration reflect the time that takes by ANN to reach convergence [16].

IV. Result

Experiments were carried out on Matlab 2010R environment running on Windows 7 64-bit. Experimental dataset consists of 500 DDoS traffic data and 500 Normal traffic data by six features. In purpose of ANN training, dataset was divided by default on Matlab 2010R into 70% sets for training, 15% sets for validation, and 15% sets for testing. Distribution of dataset for training, validation, and testing was created by random function (Matlab dividerand) to avoid the bias tendency in the sample pattern.

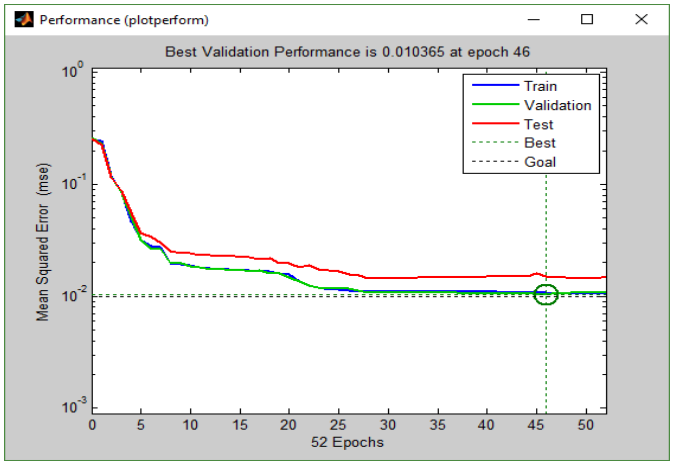

Fig. 2. Quasi-Newton Training Result on Layer 6-(3)-2.

Sigmoid transfer function used in the hidden and output layer. The basic parameters epoch = 20000, performance function = mse, goal = 0.01, maximum fail = 6, minimum gradient = 1.00e-10, mu = 1.00e+10 were used in the training process. For simplification purpose, the result for each training function displayed only for ANN layer 6-(3)-2. Quasi-Newton method (Matlab trainlm) training result for ANN layer 6-(3)-2 presented on Fig. 2. Scaled-Conjugate method (Matlab trainscg) training result for ANN layer 6-(3)-2 presented on Fig. 3.

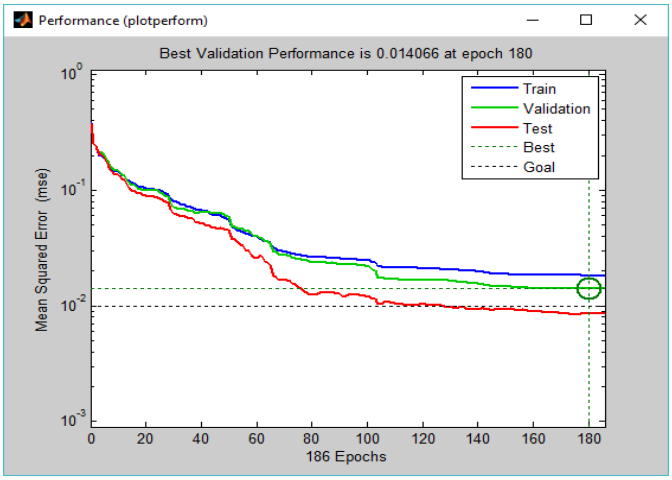

Fig. 3. Scaled-Conjugate Training Result on Layer 6-(3)-2.

Resilient-Propagation method (Matlab trainrp) training result for ANN layer 6-(3)-2 presented on Fig. 4.

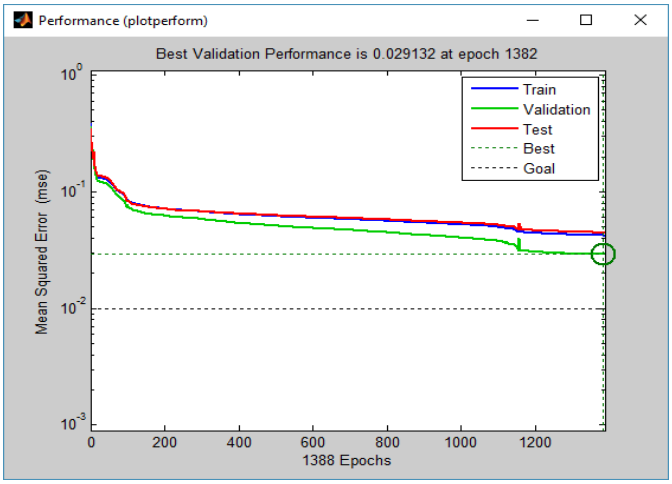

Fig. 4. Resilient-Propagation Training Result on Layer 6-(3)-2.

All training result stated that there was no overtraining faced on ANN scheme.

E. Accuracy

Quasi-Newton training function (Matlab trainlm) resulted stable accuracy value against all ANN layer schemes as stated on Fig. 5. The highest accuracy value 0.996 (99.6%) was achieved by ANN with Scaled-Conjugate training function (Matlab trainscg) under 6-(3)-2 layer scheme and also ANN with Quasi-Newton training function (Matlab trainlm) under 6-(12)-2 layer scheme. However, the Scaled-Conjugate training function (Matlab trainscg) resulted less consistent value on other ANN layer schemes. Based on Fig. 5 best classification accuracy was given by ANN with the number of hidden layer neurons by 1/2n and 2n. Where, n is the number of input nurons.

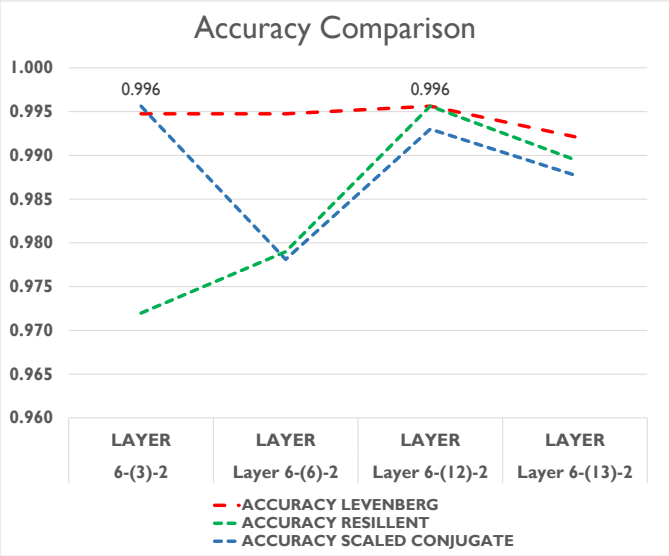

Fig. 5. Accuracy comparison.

The number of hidden layers neuron by 2n gives stable accuracy on all training function, as compared to Kolmogorov's theory that stated the best number of hidden layer neurons to solve ANN problem is 2n + 1 which produce accuracy value that tends to be low on this experiments.

F. Mean-Squared Error

As stated From Fig. 6, the conclusion that can be drawn is as follows:

1) Quasi-Newton (Matlab trainlm) training function resulted small average mse value on all ANN layer schemes compared to the Scaled-Conjugate (Matlab trainscg) and Resilient-Propagation (Matlab trainrp) training functions.

2) The number of neurons in the hidden layer don't have a significant effect on MSE value for Quasi-Newton (Matlab trainlm) training functions.

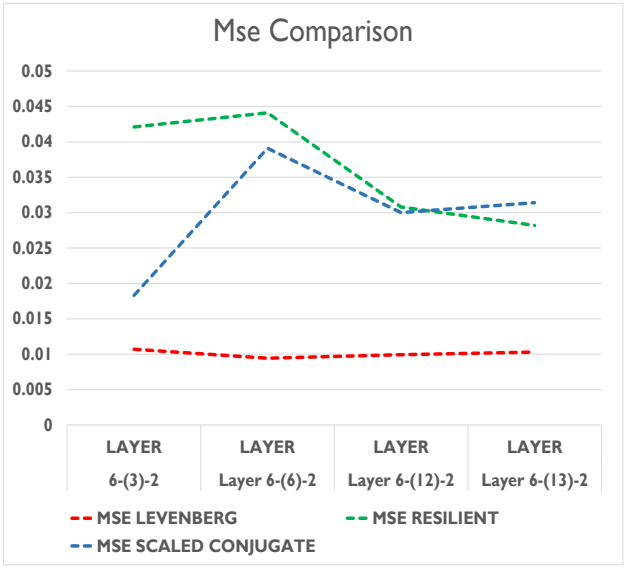

Fig. 6. MSE comparison.

3) The number of neurons in the hidden layer have a significant effect on MSE value for Scaled-Conjugate (Matlab trainscg) and Resilient-Propagation (Matlab trainrp) training functions.

4) More number of neurons in hidden layer can reduce MSE value for Resilient-Propagation (Matlab trainrp) training functions.

5) More number of neurons in hidden layer otherwise increases MSE value on Scaled-Conjugate (Matlab trainscg) training functions.

G. Iteration

ANN with Quasi-Newton (Matlab trainlm) training function has fewer iterations compared to Scaled-Conjugate (Matlab trainscg) and Resilient-Propagation (Matlab trainrp) training functions for all ANN schemes. ANN with Quasi-Newton (Matlab trainlm) training function is fast to reach convergence than conjugate gradient methods and efficient in time. Fig. 7 stated that the number of neurons in the hidden layer don't have a significant effect on ANN convergence speed for Quasi-Newton (Matlab trainlm) and Scaled-Conjugate (Matlab trainscg) training functions. However, the Resilient-Propagation (Matlab trainrp) training function affected with the number of neurons in the hidden layer, more number of neurons in hidden layer can increase convergence speed.

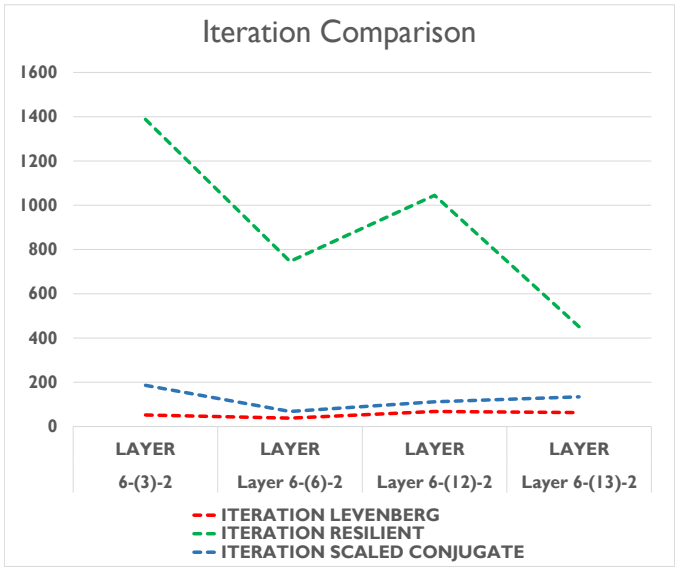

Fig. 7. Iteration comparison.

V. Future Work and Conclusion

Artificial neural network can be used as an effective tool for network packet classification with the appropriate combination hidden layer and training functions. This study found best classification accuracy (99.6%) was given by ANN with the number of hidden layer neurons by 1/2n for Matlab trainscg training function and 2n for Quasi-Newton (Matlab trainlm) training function. Where, n is the number of input neurons. The number of hidden layers neuron by 2n gives stable accuracy on all training function. Quasi-Newton (Matlab trainlm) training function is fast to reach convergence and

doesn't much affected by number of hidden layer neurons variation. The significant differences on MSE value is found by applying variation of hidden layer neurons numbers in the neural network trained by Scaled-Conjugate and Resilient-Propagation training function. More number of neurons in hidden layer can reduce MSE value for Resilient-Propagation (Matlab trainrp) training functions and more number of neurons in hidden layer otherwise increases MSE value on Scaled-Conjugate (Matlab trainscg) training functions. In this study, the best suitable number of neurons in hidden layer is 2n, because it gives stable accuracy on all training function.

The results obtained from this study can be used as a basic reference to determine the effective number of hidden layers neuron in building a network packet classification system based on artificial neural network. Further, the study will be improved on other parameters like increasing the sample size of input patterns presented to the network, reducing error goal and use more training method.

REFERENCES

[1] Mahadev, V. Kumar, and K. Kumar, "Classification of DDoS Attack Tools and its Handling Techniques and Strategy at Application Layer," 2016 2nd Int. Conf. Adv. Comput. Commun. Autom., pp. 1–6, 2016.

[2] S. H. A. Ali, S. Ozawa, T. Ban, J. Nakazato, and J. Shimamura, "A Neural Network Model For Detecting DDoS Attacks Using Darknet Traffic Features," 2016 Int. Jt. Conf. Neural Networks, no. November 2014, pp. 2979–2985, 2016.

[3] A. Iswardani and I. Riadi, "Denial of Service Log Analysis Using Density K-Means Method," J. Theor. Appl. Inf. Technol., vol. 83, no. 2, pp. 299–302, 2016.

[4] I. Riadi, A. W. Muhammad, and Sunardi, "Neural Network-Based DDoS Detection Regarding Hidden Layer Variation," J. Theor. Appl. Inf. Technol., vol. 95, pp. 1–9, 2017.

[5] T. Ishitaki, D. Elmazi, Y. Liu, T. Oda, L. Barolli, and K. Uchida, "Application of Neural Networks for Intrusion Detection in Tor Networks," Proc. - IEEE 29th Int. Conf. Adv. Inf. Netw. Appl. Work. WAINA 2015, pp. 67–72, 2015.

[6] M. Kale and D. . Choudhari, "DDOS Attack Detection Based on an Ensemble of Neural Classifier," IJCSNS Int. J. Comput. Sci. Netw. Secur., vol. 14, no. 7, pp. 122–129, 2014.

[7] S. H. A. Ali, S. Ozawa, T. Ban, J. Nakazato, and J. Shimamura, "A Neural Network Model for Detecting DDoS Attacks using Darknet Traffic Features," 2016 Int. Jt. Conf. Neural Networks, no. November 2014, pp. 2979–2985, 2016.

[8] A. Saied, R. E. Overill, and T. Radzik, "Detection of Known and Unknown DDoS Attacks Using Artificial Neural Networks," Neurocomputing, vol. 172, pp. 385–393, 2015.

[9] T. Zhao, D. C. T. Lo, and K. Qian, "A Neural Network Based DDoS Detection System Using Hadoop and HBase," Proc. - 2015 IEEE 17th Int. Conf. High Perform. Comput. Commun. pp. 1326–1331, 2015.

[10] H. Demuth, Neural Network Toolbox Users Guide, Sixth Ed., vol. 24, no. 1. Natick, Massachuset: The MathWorks, Inc, 2002.

[11] C. J. Hsieh and T. Y. Chan, "Detection DDoS Attacks Based On Neural-Network Using Apache Spark," 2016 Int. Conf. Appl. Syst. Innov. IEEE ICASI 2016, pp. 1–4, 2016.

[12] T. P. Thwe Thwe Oo, "A Statistical Approach To Classify And Identify DDoS attacks Using UCLA Dataset," Int. J. Adv. Res. Comput. Eng. Technol., vol. 2, no. 5, p. 1766, 2013.

[13] N. Pise and P. Kulkarni, "Algorithm Selection for Classification Problems," SAI Computing Conference 2016, pp. 203–211, 2016.

[14] Y. H. Hu and J.-N. Hwang, Handbook of Neural Network Signal Processing, First Edit. New York: CRC Press, 2002.

[15] S. Haykin, Neural Networks and Learning Machines, vol. 3. 2008.

[16] M. Anthony and P. L. Bartlett, Neural Network Learning : Theoretical Foundations, First Edit. New York: Cambridge University Press, 2009.

[17] F. Soares and A. M. F. Souza, Neural Network Programming With Java : Unleash The Power Of Neural Networks By Implementing Professional Java Code. 2016.

[18] C.-J. Hsieh and T.-Y. Chan, "Detection DDoS Attacks Based on Neutral-Network Using Apache Spark," Natl. Chin-Yi Univ. Technol. Taichung, Taiwan, pp. 1–4, 2015.

Classifying Natural Language Text as Controlled and Uncontrolled for UML Diagrams

Nakul Sharma
Research Scholar, Dept. of Computer Science and Engineering
K L University,
Vijayawada, India

Prasanth Yalla
Professor, Dept. of Compute Science and Engineering,
K L University,
Vijayawada, India

***Abstract*—Natural language text fall within the category of Controlled and Uncontrolled Natural Language. In this paper, an algorithm is presented to show that a given language text is controlled or uncontrolled. The parameters and framework is provided for UML diagram's repository. The parameter for controlled and uncontrolled languages is provided.**

Keywords—Natural Language Processing; UML Diagrams; Software Engineering

I. Introduction

Natural Language processing is using computer to process text which is readable and understood by humans. The processing in NLP requires natural language text to be given as input [1]. This input is can be classified as controlled or uncontrolled. NLP techniques are more effective in case of controlled languages instead of uncontrolled languages. The controlled language can be in form of plain text or any formal specification such BPNF. The authors had developed code for the removal of noise in the given the text [2].

In this work, Classifying Controlled Language (CCL) methodology is proposed. CCL methodology takes as input a natural language input and verifies using wordnet, framenet and StanfordNLP parser for checking if the language is controlled or not. The controlled languages has host of advantages which are missing in the uncontrolled language. This work is in continuation with the TextToUML (TTU) methdology presented earlier [3].

Our contribution is hence given as following:-

1) Providing a sample textual description for the class and activity diagrams.
2) Classifying the textual description as controlled and uncontrolled for UML Diagrams.

II. Problem Definition

The problem relates to giving the appropriate input for generating UML diagrams. There have been considerable efforts or converting text to UML diagrams [6-8]. The textual description for class and activity diagrams is not presented by any researcher.

Use of textual description is extensively done for use-case diagrams [4]. The simple text in any natural language is understood by large population of people if they are native to it. In order to achieve universal programmability, use of text [5] can be done as it can be understood by humans. This implies everyone gets a chance to code while everything else being done by the computer.

Table-1 provides list of papers which have usage of textual description in UML diagrams or in related fields.

TABLE. I. Textual Description in UML Diagram

Sr. No.	*Title*	*Topic Discussed*	*Domain*
1	Implemented domain model generation [6]	UML Diagram Generati-on using NLP Software	Software Design , Requirement Engineering and NLP
2	Requirement Specifications Using Natural Languages [7]	Software Require-ments using Textual specification	Software Analysis Specification
3	Generating Natural Language Specifications from UML Class Diagrams [8]	UML Diagram generation using NLP Software	Software Design Specification
4	Generally class models through controlled requirements [9]	UML Diagram generatin-g using NLP Software	Software Analysis Specification, Software Design Specification
5	Generating UML Diagrams from Natural Language Specification [10]	UML Diagram generati-n using NLP software	Software Design Specification
6	Natural Language Processing based automated system for UML Diagrams generation [11]	UML Diagram generation using NLP software	Software Analysis Specification, Software Design Specification
7	SVBR Business Rules Generation from Natural Language Specification[11]	Requirement gathering using NL specification	Software Analysis Specification, Software Design Specification

There are following benefits of using textual description for the UML diagrams:-

1) Natural Language Text is known to humans.
2) Natural Language Text is understood by humans.

3) Subject to less interpretation and speculation if the text is controlled.
4) Understood by large number of audience.
5) Possible to derive many applications of automation.
6) More comfort of understanding
7) Most convenient form of expressing information.

Figure-1 lists the advantages of textual description. The level of comfort is more for a human readable text. The level of comfort goes down as the specification moves away from the human readable text. The machine readable code is most difficult to interpret and understand.

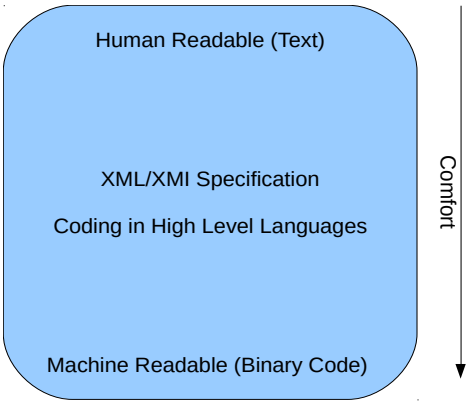

Fig. 1. Advantages of Textual Description

The following research questions were not extensively addressed in the literature review:-

RQ-1. What are the textual descriptions which describe the UML diagrams?

RQ-2. Is it possible to provide a textual specification for the entire UML diagrams?

RQ-3. How can Natural Language Text be classified as Controlled and Uncontrolled for UML Diagrams ?

The previous literature did not focus on the classifications according the domain level [13,14].

III. Problem Solution

A. Textual Description of UML Diagrams

Cockburn et.al. provides a use case template which is exhaustive example of an textual description [4]. While the use case template is specific only to use case diagrams no other diagrams have such description. UML diagram are developed when the analysis phase is about to finish and design phase gets started. Generally, the phases in SDLC are always overlapping and hence it is not feasible to tell when the analysis phase has started and when it will finish. Textual description allows automation to be made possible in early phases of SDLC. This can be made possible by generating textual descriptions of all the different artefacts, processes, methods, tools in SDLC.

B. UML Diagram Basic Usage

There exists a textual specification in form of textual use case template which is helpful in generating the use case UML Diagram [4]. Use case diagram generation is hence easy to automate. But there is no other description available. This explanation answers the research question- RQ-1. For answering the second question (RQ-2), we gave a sample textual description for the class and activity diagrams. The description was evaluated using StanfordNLP parser.

Textual Description - Class Diagram

A class diagram consists of two main features as [15]:-

1) Components of the class
   a) These are names, variables and operations.
2) Relationships with other classes.
3) These include relationships such as dependency, realization etc.

The class description should describe all the situations in which the class participates. The class diagram can be drawn from both the problem as well as solution domain. Hence, it has classes in both problems as well as solution domain must be properly described so that the problem can be automated. A sample description of the class diagram containing the above mentioned variables is available in Annexure A.

Textual Description – Activity Diagrams

1) An Activity diagram mainly focuses on the behavior of a set of objects [15]. A textual description for activity diagram should hence contain following parts:-
   a) Objects
      It includes the names of objects.
   b) Associated workflows.
2) A sample description of the activity diagram containing the above mentioned variables is available in Annexure A.

3) The textual description is first parsed using the Stanford NLP parser. The result is classified as Controlled Language and Uncontrolled language for the generation of UML diagrams.

Rules for Use Case Diagrams

For the input scanned using Stanford Parser:-

1) check the occurrence of/index of NN and NNP words these may constitute use case.
2) If it follows Subject Verb Object, the subject becomes actor.
3) If a sentence contains occurance of NNS, NNS becomes check the hierarchy in wordnet.
4) If in a sentence VB occurs get its index as it is a potentially a use case.

The above rules are applied for generating text ready to be fed into the system.

Rules for Class Diagrams

For the input scanned using Stanford Parser

1) check the occurance of/index of NN and NNP words these may constitute Class.
2) If it follows Subject Verb Object, the subject becomes class.

3) If a sentence contains occurance of NNS, NNS becomes check the hierarchy in wordnet.

4) If in a sentence VB occurs get its index as it is a potentially a use case.

Multiple sentences containing the same subjects are not considered for developing classes.

The whole process is divided into pre and post-processing of the text as shown in Figure-2.

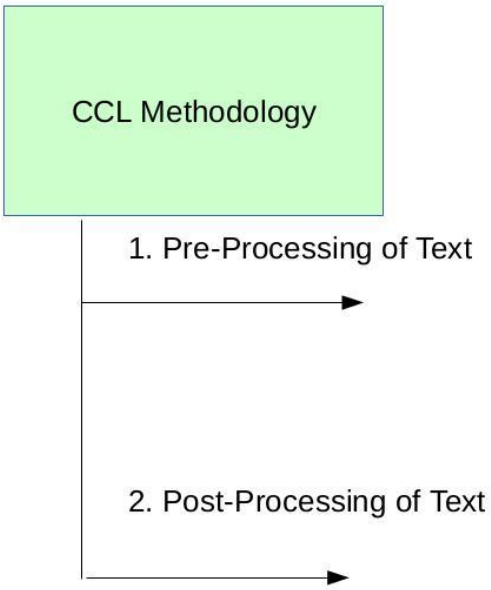

Fig. 2. CCL Methodology Steps

The CCL methodology encompasses two important phases: pre-processing and post-processing of text.

TABLE. II. SOFTWARE USED FOR PRE-PROCESSING STAGE

Sr. No.	*Operation Carried Out*	*Software's Used/Methodology used*	*Explanation*
1	Cleaning of Text	nltk	Cleaning involves removing of the special characters
2	Stemming	Algorithm Used	Stemming involves removing the stop words and reducing it to the base form.
3	Syntactic Feature Extraction	Stanford Parser, WordNet, Basic Rules	Parser parses the text be developing dependency tree and the result given to wordnet for evaluation
4	Subject/Domain Level Feature Extraction	Named Entity Recognition	For extracting person, names, nouns,

The table-II shows the software's used in the pre-processing stage of CCL methodology along with the explanation of the work done at each level.

TABLE. III. SOFTWARE USED FOR POST-PROCESSING STAGE

Sr. No.	*Operation Carried Out*	*Software's Used/Methodology used*	*Explanation*
1	Lookup Relevance	UML Repository	A Repository for activity, class and use case diagram is created along with its glossary for the purpose of checking the candidate actors, activities. (Annexure A)
2	Diagram Ready Text	UML Repository + Implementation Rules	Regenerating text to be fed into system for UML Diagram generation

IV. APPLICATION OF WORK

This work can be applied to several approaches which utilize textual information as input:-

1) Human User Textual Notation (HUTN) is a recent specification given by Object Management Group (OMG). That specification is also in textual format.[16]. The CCL methodology can be applied to it.

2) Software Requirement Specification, Requirement Document, Use Case Description, Acceptance Test Cases are the artifact on which CCL can be applied in analysis phase.

3) Software Design Specification, UML Diagrams, Test Cases are the artifact on which CCL can be applied.

4) Test cases and test manuals are the areas in which CCL algorithm can be applied.

5) Maintenance logs, user complaints, customer executive logs are also areas in which CCL can be applied.

6) UML Lookup Repository can be expanded to include other domains in Software Engineering for the purpose of generating useful information or for automation.

ACKNOWLEDGMENT

The authors are indebted to the HoD, faculties and staff of Computer Science and Engineering Department at K L University for giving the requisite amount of resources in making this research paper. The authors are also indebted to their forgiving all support and help in life.

Annexure A

Class diagrams Sample Descriptions

A person is a living entity. A person plays indoor and outdoor games. Acceptance is another operation of a person. A person goes to sleep. A passenger is special case of a person. A passenger buys a ticket from source to destination station. A person feeds his name address into the reservation form. Transaction details are also fed by the passenger.

Activity diagrams Sample Descriptions

A passenger goes to a railway counter. The passenger books the tickets by filling the source and destination details and by paying the transaction fees. The passenger boards the

train ticket for which ticket is reserved. The passenger does not board any other train and reaches the destination station.

UML Repository Table

The repository was developed using the basic information pertaining to the UML Diagram.

		Likely Related To		
Sr. No.	***Words***	***Use Case Diagrams***	***Class Diagram***	***Activity Diagram***
1	Abstract	Y	Y	Y
2	Abstract Class	-	Y	-
3	Abstract operation	-	Y	Y
4	Abstraction	Y	Y	Y
5	Action Sequence	-	-	Y
6	Action State	-	-	Y
7	Activation	-	-	-
8	Activity Diagram	-	-	Y
9	Active Class	-	Y	-
10	Active Object	-	-	Y
11	Activity	-	-	Y
12	Activity Final	-	-	Y
13	Actor	Y	Y	-
14	Aggregation	Y	Y	-
15	Artifact	Y	Y	Y
16	Association	Y	Y	-
17	Association Class	Y	Y	-
18	Attribute	Y	Y	-
19	Cardinality	Y	Y	-
20	Class	-	Y	-
21	Class Diagram	Y	Y	-
22	Classifier	-	Y	-
23	Collaboration	-	Y	-
24	Components	-	Y	-
25	Constraint	Y	Y	-
26	Dependency	Y	Y	Y
27	Encapsulation	Y	Y	Y
28	Expansion	Y	Y	Y
29	Extend	Y	Y	-
30	Final	-	Y	-
31	Flow			
32	Fork	Y	Y	-
33	Generalization	Y	Y	-
34	Generalization Tree	Y	Y	-
35	Guard	Y	-	-
36	Inheritance	-	Y	-
37	Initial node	-	Y	-
38	Interface	-	Y	-
39	Join	-	-	Y
40	Link	-	-	Y
41	Merge	-	Y	-
42	Message	Y	Y	-
43	Metadata	-	Y	
44	Metamodeling	-	Y	-
45	Modeling	-	Y	-
46	Multiplicity	-	Y	-
47	Namespace	-	Y	-
48	Navigable	Y	Y	-
49	Object Constraint Language	-	Y	-
50	Object Diagram	Y	Y	Y
51	Operation	Y	Y	
52	Package	-	-	-
53	Realization	Y	Y	-
54	Request	-	-	-
55	Role	Y	Y	-
56	Scenario	Y	Y	-
57	Sequence Diagram	-	-	-
58	State	-	-	Y
59	Static	Y	-	-
60	Sterotype	-	Y	-
61	Structure	-	Y	-
62	Superstate	-	Y	-
63	Swimlanes	Y	Y	-
64	Tagged Values	Y	Y	-
65	Use Case	Y	Y	-
66	Use Case Diagram	Y	Y	-
67	XMI	Y	Y	-
68	xUML	Y	Y	-
69	Workflow	Y	Y	-
70	Visibility	Y	Y	-

Y-Yes.

TABLE. IV. CRITERIA FOR CONTROLLED AND UNCONTROLLED LANGUAGE IN PROBLEM AS WELL AS SOLUTION DOMAIN

Sr. No.	***Parameter in POS***	***Value per sentence***	***Controlled or Uncontrolled***
1	NN	> 10	Uncontrolled
2	VB	>5	Uncontrolled
3	VBD	>7	Uncontrolled
4	VBG	>5	Uncontrolled
5	VBN	>5	Uncontrolled
6	VBP	>5	Uncontrolled
7	VBZ	>5	Uncontrolled

REFERENCES

[1] Dr. Prasanth Yalla and Nakul Sharma, Combining Natural Language Processing and Software Engineering, In. Proc. International Conference in Recent Trends and Sciences (ICRTES), March 14-15, 2014, Pages 370-373, ISBN: 978-93-5107-223-2. (Conference Proceedings)

[2] Dr. Prasanth Yalla and Nakul Sharma, Parsing Natural Language Text for Use Case description, In. Proc. International Conference of Computer and Big Data, (CSIBIG 2014), March 7-8, 2014. Page: 210-212, ISBN-978-1-4799-3063-0 (Conference Proceedings).

[3] Nakul Sharma, Dr. Prasanth Yalla, "Issues in Developing UML Diagrams from Natural Language Text", In. Proc. Recent Advances In Telecommunications, Informatics And Educational Technologies, Pages 139-145, ISBN: 978-1-61804-262-0.

[4] Alister Cockburn, 2001, Use Case Template, Addison-Wesley, (Book).

[5] Walter F. Tichy, Mathias Landhabuer and Sven J. Korner, Universal Programmability- How AI Can Help?, In Proc. 2nd International Conference NFS sponsored workshop on Realizing Artificial Intelligence Synergies in Software Engineering, May 2013. (Conference Proceedings).

[6] Viliam Simko, Petr Kroha, Petr Hnetynka, "Implemented domain model generation", Technical Report, Department of Distributed and Dependable Systems, Report No. D3S-TR-2013-03.

[7] Bures T., Hnetynka P., Kroha P., Simko. V., "Requirement Specifications Using Natural Languages", Charles University, Faculty of Mathematics and Physics, Dept. of Distributed and Dependable Systems, Technical Report No-D3S-TR-2012-05, December 2012.

[8] F Meziane, N. Athanasakis, S. Ananiadou, "Generating Natural Lanuage Specifications from UML Class diagrams", Requirement Engineering Journal, 13(1):1-18, Springer-Verlag, London.

[9] Reynaldo Giganto, "Generating Class Models through Controlled Requirements", New Zealand Computer Science Research Conference (NZCSRSC) 2008, Apr 2008, Christchurch, New Zealand.

[10] Priyanka More and Rashmi Phalnikar, Generating UML Diagrams from Natural Language Specifications, International Journal of Applied Information Systems, Foundation of Computer Science, Vol-1-No-8, Apr-2012. (Journal)

[11] Imran Sarwar Bajwa and M. Abbas Choudhary, Natural Language Processing based auto-mated system for UML diagrams generation In. Proc. 18th National Computer Conference (NCC-2006), Page No-1-6. (Conference Proceedings)

[12] Imran S Bajwa, Marj. G. Lee, Behzad Bordbar, "SVBR Business Rules Generation from Natural Language Specification". In. Proc. Artificial Intelligence for Business Agility-Papers from AAAI Spring Symposium (SS-11-03, Pg. No. 2-8.

[13] Vidhu Bhala, "Conceptual Modeling of Natural Languag Functional Requirements, Journal of System Software , Sciencedirect, (2013), http://dx.doi.org/10.1016/j.jss.2013.08.036.

[14] Mosa Elbendak, Paul Vickers, Nick Rossiter, "Parsed use case descriptions as a basis for object-oriented class model generation", Journal of System and Software, 1209-1223.

[15] Grady Booch, James Rambaugh and Ivar Jacobson, The Unified Modeling Language User Guide, Addison Wesley Longman, Inc., Second Edition, ISBN 0-201-57168-4 (Book).

[16] Helmut Vieritz, Daniel Schilberg, Sabina Jeschke, "Access to UML Diagrams with the HUTN", In. Proc. ASSETS'12, ACM, October 22–24, 2012, Boulder, Colorado, USA,978-1-4503-1321-6/12/10.

Automatic Fuzzy-based Hybrid Approach for Segmentation and Centerline Extraction of Main Coronary Arteries

Khadega Khaled
Department of Information Technology
Cairo University
Giza, Egypt

Mohamed A. Wahby Shalaby
Department of Information Technology
Cairo University
Giza, Egypt

Khaled Mostafa El Sayed
Department of Information Technology
Cairo University
Giza, Egypt

***Abstract*—Coronary arteries segmentation and centerlines extraction is an important step in Coronary Artery Disease diagnosis. The main purpose of the fully automated presented approaches is helping the clinical non-invasive diagnosis process to be done in fast way with accurate result. In this paper, a hybrid scheme is proposed to segment the coronary arteries and to extract the centerlines from Computed Tomography Angiography volumes. The proposed automatic hybrid segmentation approach combines the Hough transform with a fuzzy-based region growing algorithm. First, a circular Hough transform is used to detect initially the aorta circle. Then, the well-known Fuzzy c-mean algorithm is employed to detect the seed points for the region growing algorithm resulting in 3D binary volume. Finally, the centerlines of the segmented arteries are extracted based on the segmented 3D binary volume using a skeletonization based method. Using a benchmark database provided by the Rotterdam Coronary Artery Algorithm Evaluation Framework, the proposed algorithm is tested and evaluated. A comparative study shows that the proposed hybrid scheme is able to achieve a higher accuracy, in comparison to the most related and recent published work, at reasonable computational cost.**

***Keywords*—Automatic segmentation; coronary arteries; computed tomography angiography; centerlines extraction**

I. INTRODUCTION

Over the past 15 years, it was reported that the ischemic heart disease and stroke are the leading causes for sudden death all over the world [1]. Coronary artery disease (CAD) is a problem of having narrow (stenosis) left and right arteries, commonly known as coronary atherosclerosis disease. These arteries are responsible for providing the cardiac muscle with oxygenated blood. Unfortunately, millions of healthy-looking human being may have CAD with no symptoms [1]. Therefore, there is a crucial need to have CAD diagnosis methodologies with a high degree of accuracy. In order to achieve this goal, a computed tomography angiography (CTA) scan is employed to capture very high quality images for the heart and its coronary arteries. CTA is a type of medical exam, in which a CTA scan is combined with an injection of a contrast media to produce pictures of blood vessels in a part of a human's body [2].

The key challenges of analysis process of coronary arteries are the narrow tubular structures and the large size of 3D captured cardiac volume [3]. The radiologist takes a large time in the diagnosis process due to these two problems. Hence, the development of an automated system for quantitative vascular shape analysis, based on coronary CTA images, is crucially needed to assist the radiologist in the diagnosis of coronary atherosclerosis. These automated coronary arteries shape analysis (ACASA) systems should be able to achieve high decision accuracy at short time for the sake of patients' life. This ACASA system has mainly two phases: 1) coronary arteries segmentation; and 2) centerline extraction phases [3].

Blood vessels segmentation from medical images is an essential phase in dealing with many medical applications, such as cardiac vessel diagnosis, i.e., stenosis of coronary arteries [4]. Automatic or semi-automatic image segmentation methods [3] are useful for the isolation and shape analysis of coronary arteries captured by CTA. Automatic segmentation is the process of extracting the object boundaries automatically by a computer. On the other hand, semi-automatic segmentation refers to the process whereby this automated segmentation phase is followed by user interaction for adjustment of the segmented object's boundaries. Despite of the increased data size of medical images, the automation of the diagnosis process is required. The latest advances in computer technology and reduced costs have made it possible to develop such systems [3]. Semi-automatic segmentation methods are extremely costly in time and effort. Automatic segmentation method, if sufficiently accurate, could give faster segmentation process.

As mentioned earlier, CTA [2] is a kind of medical CT scan injection of a contrast media to produce pictures of blood vessels. The contrast of CTA is injected through an intravenous (IV) line started in patient's arm. It is a type of X-ray that uses a computer to make cross-sectional images of body organ i.e. cardiac. However, input of CTA cardiac image can be a stack of 2D slices have only two dimensions (x and y) called 3D cardiac volume or be a 3D image of real cardiac object has third dimension, the depth (z) [4].This third dimension allows for rotation and visualization from multiple perspectives. It is found from the literature review that the previous proposed

schemes could be categorized based on two main factors: 1) dimensionality of the processed dataset; and 2) the level of automation of coronary arteries segmentation process. Table 1 shows the main categories of cardiac image segmentation methods. In addition, cardiac image segmentation methods could be categorized into six main methods: 1) histogram based methods; 2) statistical model based methods; 3) region based methods; 4) graph based methods; 5) deformable model based methods; and 6) atlas based methods [4]. Some of these methods are useful in coronary arteries segmentation. It is seen from the literature review that many techniques have been proposed using the 3D cardiac CTA volume dataset [5]-[10].

TABLE. I. CARDIAC IMAGE SEGMENTATION METHODS CATEGORIZATION

Dimensionality / **Automation levels**	**2D**	**3D**
Automatic	***2D-Automatic methods***	***3D-Automatic methods***
Semi-Automatic	***2D-Semi-Automatic methods***	***3D-Semi-Automatic methods***

In [5], a hybrid proposed approach for the automatic two-dimensional segmentation of coronary arteries from cardiac CTA volumes using Bayesian driven level set models and multi-scale vessel filtering. Using automation way, segmentation of the whole coronary tree from cardiac CTA volumes and the extraction process of the centerlines are describe in [6], the first steps of the segmentation algorithm consist of the detection of the aorta and the entire heart region then candidate coronary artery components are detected in the heart region after masking of the cardiac blood pools. Using the whole tree segmentation all the centerlines of the coronary arteries are extracted using a fast-marching level set algorithm. An automatic seeding method for coronary artery segmentation and skeletonization is proposed in [7], fuzzy connectedness theory is used to separate the coronary arteries from 3D CTA images based on the connectivity of the contrast agent in the vessel lumen and this step show the strength of fuzzy concept. In [8], an automatic method for extracting center axis representations centerlines of coronary arteries in contrast enhanced CTA volume scans using medialness-based vessel tree extraction algorithm which starts a tracking process from the ostia locations until all the branches are reached. Tracking method is proposed in [9] for tracking coronary arteries in CTA volume through 2D slices from ostium to the end, this method works based on the fact that each coronary artery has continuous pixels through slices from the start to the end point. In [10], volumetric region-growing algorithm used to segment the left coronary arteries tree, a sequential 3D thinning algorithm used as skeletonization method to extract arteries centerlines. Fig. 1 show the coronary ostium, the left main artery (LM), the left anterior descending (LAD) and the left circumflex (LCX) branches in anatomy representation (A) and in CT slice image (B).

In [5]-[10] most recent 2D automatic segmentation methods are presented. The main advantage of these methods is minimal user interaction so less time and less human effort, however, the accuracy needs to be better. Two-dimensionality segmentation methods offers short time to segment long vascular segment imaging such as the entire aorta or lower extremity arteries from the number of 2D slices. On the other hand, 3D segmentation methods better for smaller areas requiring higher spatial resolution such as carotid bifurcation from 3D image [11].

The semi-automatic approach combines the Hessian matrix based vesselness filter with two dimensional region growing algorithm for segmentation of the coronary arteries in CTA volume proposed in [12], centerlines of the segmented arteries are extracted using an in-house fast marching based method. In [13], a novel method presented for the automated extraction of coronary artery centerlines in 3D CTA image using a neural network (CNN) classifier for removing extraneous paths in the detected centerlines after using minimal path method to detect the optimal flow path of centerline. The main disadvantage of semi-automatic approaches whether 2D or 3D segmentation methods is computational cost and time for radiologist's diagnoses process and this can be effect the patient's health. Optimized particle filtering approach for the extraction of full coronary trees from 3D cardiac CTA image proposed in [14], this approach relies on a Bayesian model combining data likelihood with radius and direction priors along the coronary arteries following a centerline-based tracking design. In [15], a fully automatic coronary artery centerline tracking algorithm for 3D cardiac volume is proposed. In this algorithm, a complex continuous wavelet transform with the Gaussian kernels is used to reduce noise effect of CTA slices. Then, a multiple hypothesis tracking approach is applied to segment 3D vessel structures, and the tracking procedure is completed by applying a presented branch searching approach based on region growing algorithm and a mathematical morphology operation.

Finally, it could be seen from this literature that the 2D automatic methods for coronary arteries segmentation and centerlines extraction are preferable to be used in an environment that requires less time and reasonable accuracy.

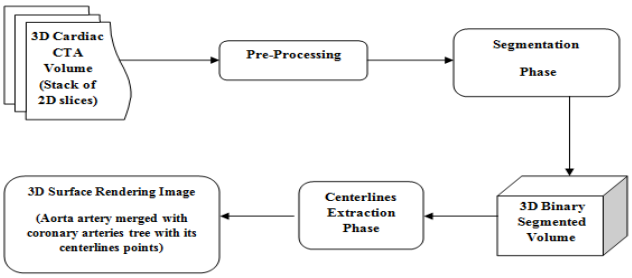

Fig. 1. Global view of hybrid proposed scheme.

It is well known that the Hough transform is an important technique used in image analysis and digital image processing as shape detection algorithm [16]. The classical Hough transform was involved for line detection in an image, but later the Hough transform has been extended to extract positions of special shapes, most ordinarily circles or ellipses. Hough transform as edge based segmentation method which can be used automatically to detect the aorta artery, that is, take a circle shape in CTA volume. The aorta is the main artery of the heart, which provides oxygenated blood to the heart and the rest of the body. Aorta artery is the root of two main coronary arteries from the original points known as "ostia points", the

main coronary arteries are Right Coronary Artery (RCA) and Left Main artery (LM), and those two coronary arteries provide oxygen rich blood to the cardiac muscle. LM artery divides on Left Anterior Descending (LAD) and the Left Circumflex Artery (LCX) as main arteries. The main goal of the segmentation process is to partition an image into regions. As mentioned earlier, region growing is one of region-based image segmentation methods and it is found to be effective approach in blood vessels segmentation process. The idea of region growing algorithm [17] is testing the neighboring pixels of initial seed points and determines whether the pixel neighbors in 2D or voxel neighbors in 3D should be added to the region in the iteration process. The aim of applying region growing in CTA volume is extracting the coronary arterial tree in each 2D slices have coronary arteries region. In this paper, a new approach is proposed for Automatic segmentation and centerline extraction for main coronary arteries from 3D cardiac volume. In this scheme, a new 2D based region growing algorithm is proposed to be able to achieve more accurate segmented arteries at a reasonable computational cost. Impressed by the ability of fuzzy C-means clustering (FCM) technique to meet different challenges in different research fields [18], our new 2D based region growing algorithm uses the FCM for determining the seed points. This new growing algorithm is used to produce a 3D volume binary data, which leads to faster extraction process of centerlines using skeletonization approach [19] .

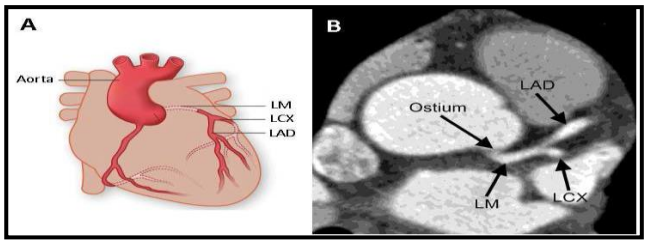

Fig. 2. (A) Aorta and LCA anatomy. (B) Example of a CT slice image showing the coronary ostium, the left main artery (LM), the left anterior descending (LAD) and the left circumflex (LCX) branches [10].

The rest of this paper is organized as: In Section 2, the overall proposed scheme is discussed. Segmentation phase is proposed in Section 3.Then centerline extraction phase is explained in Section 4. The comparisons and experimental results are presented in Section 5. Finally, conclusion and further work are in Section 6.

II. The Proposed Hybrid Scheme

The proposed scheme consists of two main phases, segmentation and centerlines extraction. Segmentation phase has been conducted by integrating the circular Hough transform approach with 3D volume region growing approach. In our region growing approach, the FCM algorithm has been utilized to detect the region growing seed points. This resulted in segmented arteries as a 3D binary volume. This binary 3D segmented volume simplifies the centerlines extraction phase. Therefore, in the second phase, a skeletonization method is utilized to extract the centerlines points of the 3D binary segmented volume. The main phases are depicted in Fig. 2.

The CTA scans are viewed as a series of consecutive two dimensional slices of the full 3D cardiac volume. Processing of such volumetric images on a slice by slice basis requires further processing to stack and interpolate results into 3D volume. CTA database is provided by the Rotterdam Coronary Artery Algorithm Evaluation Framework [20]. The CTA volume for each patient consist of a large number of 2D images larger than 200 slices for cardiac CTA are required to scan the complete coronary tree. In order to achieve a better computing time and memory management, first, all images are resized; the size of each axial image 512x512 is reduced to 256×256 pixels [21]. Second, pulmonary vessels are removed by a morphological erosion operator using spherical kernel with a radius of one voxel. The reason for using morphology operation is to enhance the contrast of medical images by removing noisy pixels/voxels which is essential in blood vessels segmentation to be accurate.

III. Segmentation Phase

Automatic image segmentation methods are helpful for the isolation and shape analysis of coronary arteries in CTA cardiac volume. Three main automatic steps in this phase: 1) aorta detection; 2) ostia detection; and 3) region growing segmentation.

A. Aorta Detection

The segmentation of coronary arteries is introduced by an automatic detection of ascending aorta artery, which is employed as an initial mask for ostia detection. An accurate segmentation of the ascending aorta is very important for more automatic seeding of heart coronaries segmentation. These ostia points reside at the lateral sides of the ascending aorta. The main features of the ascending aorta help in detecting and distinguishing it from the other similar structures found in a CTA image slice such as descending aorta. Two main features of the ascending aorta are shape and diameter size. The ascending aorta has a circular shape [22] that expands from the aortic arch down to the aortic root. The ascending aorta diameter in healthy patients is less than 2.1 cm/m2, while the diameter of the descending aorta is less than 1.6 cm/m2, so the ascending aorta diameter is bigger than the descending aorta diameter [23]. Depending on this features the proposed method segmenting the ascending aorta partially using circular Hough transform then full segmented with coronary arteries segmentation process using region growing. The partially segmented part of ascending aorta circle in the first several axial slices is used to detect the ostia points to segment the whole aorta with main arteries tree. Aorta detection is performed slice by slice to segment the ascending aorta from consecutive CTA image slices until the difference of the distance of the circle centers between two successive slices is equals to zero as stop condition, (1) :

$$d=\sqrt{(Cx(i)-Cx(i-1))^2+(Cy(i)-Cy(i-1))^2} \quad (1)$$

Where, Cx and Cy are vectors contain the x coordinates and y coordinates of centers of detected i circles, d is Euclidean distance. It is the distance measure between two aorta circles centers of two successive slices to select the detected aorta

circle in target slice. Target slice used to begin segment the coronary arteries. Fig. 3(b) shows example of the pre-processing result of one original slice Fig. 3(a) and 3(c) for aorta detection result.

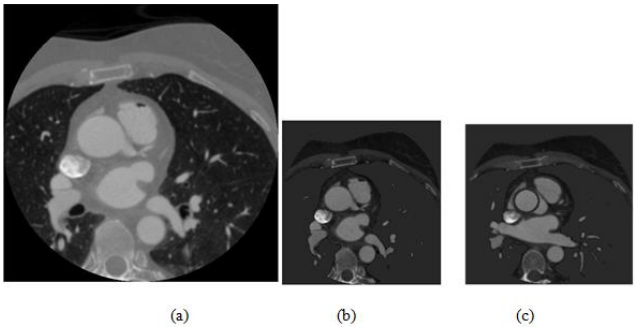

Fig. 3. (a) original slice, (b) preprocessed slice and (c) Aorta detected circle.

Once the circle of the aorta is determined, ostia points can be detected using FCM. The extracted aorta circle points from circular Hough transform help FCM technique to detect the accurate ostia points from all circle points as explained in the following.

B. Ostia Detection

After the circular region of the aorta is segmented, the ostia point of the left and right coronary trees can be detected. The segmentation of the coronary arteries is preceded by an automatic detection of the coronary ostia in which the origins of the coronary arteries is located. This method is initialized by automatically placing a single seed point in the ascending aorta on top of each coronary ostia. The main focus of this paper is that the coronary segmentation starts from the automatically detected ostia locations. More specifically, the extraction of coronary arteries centerlines relies on the vessel segmentation algorithm which starts from each ostia points and works only inside the heart mask. The ostia locations, opening points of left and right main coronary artery from the aorta are detected through an angle search regions. This regions defined in the polar coordinate system [21] is used to distinguish between the ostia of the left and right coronary trees. Based on the normal anatomy of the coronary arteries, the range of ΘL for the left Ostiaϵ [-90º, 45º] and for the right Ostia ϵ [45º, 135º]. FCM [18] used here to detect optimum left ostia point and right point in Θ range from -90º to 135º with two centers. It is based on minimization of the following objective function:

$$J_m = \sum_{i=1}^{N} \sum_{j=1}^{C} u_{ij}^{m} \left|\left|X_i - C_j\right|\right|^2 , 1 \leq m < \infty \qquad (2)$$

Where, m is any real number greater than 1, u_{ij} is the degree of membership of x_i in the cluster j, x_i is the ith of d-dimensional measured data, c_j is the d-dimension center of the cluster, and ||*|| is any norm expressing the similarity between any measured data and the center. Fuzzy partitioning is carried out through an iterative optimization of the (2) shown above, with the update of membership u_{ij} and the cluster centers c_j. FCM implemented on the measured data extracted from the aorta detection part, where x_i contains the x and y coordinates of points in Θ range of detected aorta circle.

C. Region Growing segmentation

Region growing method integrates only the neighboring voxels that satisfies a homogeneity criterion starting from an initial set of one or more seeds. Substantially, a region growing algorithm begins at the seed points and increases iteratively the size of the seeds check region. While the region grows, the algorithm has to decide which pixels/voxels are included into the segmented object and which are not. This decision depends on a similarity measure and the precise segmentation result is dependent on the choice of seed points. The centerline tree of the coronary arteries is computed through the region growing algorithm which has started a segmentation process from the coronary ostia locations detected using FCM as seed points until all the main vessels are extracted. Beginning from this seed points, axial aortic cross-sections are subsequently segmented by a 2D region growing technique. The coronary arteries are the only tubular structures that originate from the aorta. Segmentation of a thinner and a smaller object of the main coronary arteries is accomplished using a region-growing algorithm starting from the two seed points already detected using FCM on the aorta wall, a region growing is achieved for each segmented 2D cross section. The final output in such regions is this derived from the continuous vessel axis based on the cross sections. The result of region growing segmentation process consider as 3D binary volume of segmented 2D slices that contain the segment regions of main coronary arteries. Fig. 4 shows the 3D segmented binary volume that contains 2D slices of the main coronary arteries has all been successfully segmented: LM, LAD and LCX.

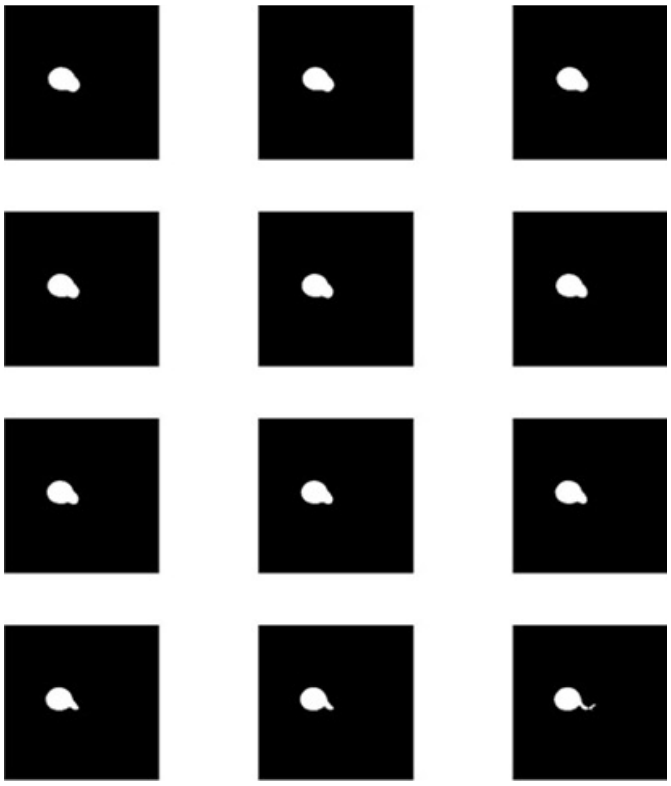

Fig. 4. 3D binary segmented volume.

IV. CENTERLINES EXTRACTION PHASE

There are a variety of methods proposed for image skeleton extraction. The suitable technique to extract the skeleton of segmented volumetric data especially for the binary segmented volume of 3D tubular object is iterative thinning because it is normally only applied to binary images, and produces another binary image as output. The 3D Thinning is an iterative layer by layer erosion technique for producing medial axis i.e. skeleton from 3D objects. A 3D binary volume is a mapping process that assigns the value of 0 or 1 to each point in the 3D space. The input of thinning operation is 3D binary volume representing a segmented voxel level tree object to extract its centerlines by iteratively deletes or removes some object points that changes some "1" points to zero until it produces only one voxel wide centerlines directly. The proposed algorithm by Lee, *et al.* [24] used to extract the centerline of the segmented coronary arteries in 3D binary volume using parallel thinning algorithm. With the 3D volumetric data at hand, it is certainly useful to create a 3D view of the coronary arteries. Once segmentation is achieved using region growing, coronaries can be visualized as 3D surfaces, and various measurements can be performed conveniently in a 3D sense. The final output of proposed scheme is 3D view of aorta artery merged with coronary arteries tree with its centerlines points. Fig. 5 shows the 3D segmented left coronary tree centerlines extracted and visualized with the aorta. Fig. 5(a) shows the left coronary tree, and 5(b) shows the left coronary tree and right coronary artery, respectively. Finally, Table 2 contains the Pseudo code of the proposed fuzzy-based hybrid scheme.

Fig. 5. (a) 3D surface rendering of LM, LAD and LCX with aorta. (b) 3D surface rendering of LM, LAD, LCX and RCA with aorta.

TABLE. II. PSEUDO CODE OF THE PROPOSED HYBRID MODEL

Begin

Preprocessing

For each slice:
extract the header information of dicom slice image. Output : info struct
extract the slice image pixels values.
resize the size of slice image from 512x512 pixels to 256×256 pixels
convert gray level unit of slice image to HU unit by :
HU_Image = (Resized_Image * info.RescaleSlope)+ info.RescaleIntercept
remove Pulmonary vessels by a morphological erosion operator
End_For

Aorta detection

Set X [x1,x2,x3 . . . x_i] = 0 where X is the vector contains the x_i coordinate of circle center in $slice_i$ if CHT success to detect circle in it.
Set Y [y1,y2,y3 . . . y_i] = 0 where Y is the vector contains the y coordinator of circle center in $slice_i$ if CHT success to detect circle in it.
For each slice:
Detection for the circles in the slice using CHT. Output : [r c rad] where r is vector of row coordinates of the circles, c is vector of column coordinates of the circles and rad is vector of radiuses of the circles.
Set X(i) = c(i)
Set Y(i) = r(i)
Check largest diameter to differ the ascending and descending aorta.
Output : aorta circle
Check the difference of the distance of the aorta circles centers between two successive slices is equal zero as stop condition Eq. (1). Output :Initial segmentation of aorta circle

Ostia Detection

Set the left Ostia ΘL ϵ [-90º, 45º] and the right Ostia ΘR ϵ [45º, 135º]
For each Θ = -90:1:135
Get All the x_i coordinate and the y_i coordinate in each Θ range by :
$x_i = X(i) + rad(i) * cosd(\Theta)$
$y_i = Y(i) + rad(i) * sind(\Theta)$
End_For

Set All_Points = [x_i, y_i]
Clustering for the All_Points data using FCM using Eq(2). Output : the left and right ostia points.
End_For

Region growing segmentation

Apply 2D region growing algorithm which has started a segmentation process from the coronary Ostia locations detected using FCM as seed points until all the main vessels are extracted. Output: 3D binary volume contains the segmented aorta with main coronary arteries.

Centerlines extraction

Apply Lee *et al.* algorithm [24] to extract the centerlines points of the segmented coronary arteries in 3D binary segmented volume using parallel thinning algorithm.
End

V. COMPARISONS AND RESULTS

The proposed scheme was implemented using MATLAB. The described methods were applied to segment the three main coronary arteries (LAD, LCX and RCA) and extract its centerlines. The 32 CTA datasets divided into training and testing datasets. The datasets were provided by [20] as mentioned before. Datasets acquired from two 64-slice scanners were randomly selected and included in this database, 20 cases from Sensation 64, and 12 cases from Somatom Definition (Siemens Medical Solutions, Forchheim, Germany). Image quality was scored as: 1) poor, which refers to presence of image-degrading artifacts and evaluation only possible with low confidence and they are 6 cases; 2) moderate, which refers to presence of artifacts but evaluation possible with moderate confidence are 11 cases; and 3) good, which refers to the absence of any image degrading artifacts related to motion and noise and they are 15 cases.

The evaluation focuses on two main categories: the overlap between the automatically created centerline and the reference centerline and the average distance between those two centerlines. The error measurements proposed in [20] are overlap (OV), overlap until first error (OF), overlap with the clinically relevant part of the vessel (OT), and average inside (AI). The proposed hybrid scheme is evaluated in a similar way as done in [25]. These measurements are based on point-to-point correspondence between the detected centerline and the ground truth. A centerline point is claimed to be detected correctly if its distance to the corresponding ground truth point is not more than a threshold which is set to the radius at that point [20]. Instead of annotating the radius at each centerline point, we set the threshold to 2.5 mm, which is approximately

the radius of the proximal segment of a coronary artery [25]. This threshold used to calculate OV and OF measurements. The overlap for the clinically relevant part (OT) calculated using the distal segment with a radius less than 0.75 mm and this threshold is excluded in [20].

TABLE. III. COMPARISON OF EVALUATION RESULTS OBTAINED BY THE PROPOSED METHOD WITH AND WITHOUT FCM ALGORITHM

Method	OV(%)	OF(%)	OT(%)	AI(mm)
Proposed scheme without FCM	85%	64%	88%	0.4mm
Proposed scheme with FCM	**91%**	**82%**	**94%**	**0.2mm**

In order to show the importance of using FCM in the proposed hybrid approach for ostia points' detection, the proposed scheme is implemented with and without the FCM technique. The 24 testing datasets have been used to calculate the above mentioned performance metrics. Table 3 contains the overall achieved values for the three arteries. It is clearly seen from Table 3 that the fuzzy-based hybrid proposed scheme is able to achieve results which are significantly much better than the proposed method without using FCM technique.

One of the advantages of the proposed approach is that the segmentation process is fully automated. Thus, the proposed hybrid method does not require any user interaction steps. The fuzzy-based segmentation process results in a 3D binary volume, which facilitate the extraction automatically of the centerlines points. This 3D binary output decreases the computational cost of the centerline extraction phase. The proposed hybrid segmentation method only depends on CHT algorithm and region growing approach after pre-processing steps which applies a morphological operation. In addition, the use of FCM technique made improvement in the segmentation phase and centerlines extraction phase. In segmentation, FCM detects the optimum seed points and that helped region growing algorithm to be accurate of segmented coronary arteries. The binary segmentation result of region growing has many advantages, fast to compute, easy to store and simple to process so it help the centerline extraction phase to be simple and fast. In centerlines extraction phase, FCM extracted the first centerline point as the accurate start point of centerline. It is known that the FCM gives best result for overlapped data set, unlike k-means where data point must exclusively belong to one cluster center, each data point is assigned with a membership to each cluster center. Main goal of centerline extraction step is tracking the center axis of the coronary arteries starting from the aorta surface to distal part of arteries. The centerlines points and radii of arteries considered important information to help radiologist to diagnose the place of stenosis. This shows the importance of being able to detect centerlines points more accurately.

Then to show the effectiveness of the fuzzy-based hybrid proposed scheme, a comprehensive comparative study have been conducted. In which, two comparisons are held between the fuzzy-based hybrid proposed scheme and most recent, as well as, related published work. First, in [25] a model-driven scheme was presented, in which the prior information embedded in a combined shape model with both heart chambers and coronary arteries are employed, and then the centerlines extracted using a machine learning based vesselness measurement. The results obtained for the 24 testing datasets are shown in Table 4. As it is seen from this table, the proposed fuzzy-based hybrid scheme achieves consistently higher accuracy than the model-driven method [25].

TABLE. IV. QUANTITATIVE COMPARISON OF THE PROPOSED METHOD AND MODEL-DRIVEN APPROACH

	Model-driven Method [25]				Proposed fuzzy-based hybrid Method			
LAD	**OV**	**OF**	**OT**	**AI**	**OV**	**OF**	**OT**	**AI**
LCX	87%	76%	92%	0.61mm	**88%**	**76%**	**92%**	**0.3mm**
RCA	71%	65%	89%	0.49mm	**94%**	**86%**	**94%**	**0.2mm**
Over ALL	82%	74%	94%	0.56mm	**92%**	**85%**	**96%**	**0.3mm**

Second, Table 5 contains the overall achieved performance metrics, using the training and testing datasets, of our fuzzy-based hybrid scheme and scheme presented in [15]. In addition, Table 5 contains also the needed processing times for both schemes. As mentioned in [15], the main disadvantage of centerlines tracking algorithm is having difficulties to detect the ostium points of the coronary arteries due to the anomalous origins of coronary trees of some datasets like dataset 17 and 26. Our proposed scheme is able to overcome this problem by using FCM technique, which has better ability to detect the accurate ostia points from segmented aorta for each dataset. Hence, the proposed hybrid scheme is able to detect the center lines with a higher accuracy at a lower computational cost.

TABLE. V. QUANTITATIVE COMPARISON OF THE PROPOSED METHOD AND CENTERLINES TRACKING APPROACH [15]

Method	OV(%)	OF(%)	OT(%)	Processing Time
Centerlines tracking method [15]	60.3%	81.6%	58.5%	8 min
Fuzzy-based hybrid scheme	**95%**	**89%**	**96%**	**30s**

It can be concluded from our comparative study that in quantitative experiments, the average extraction results of overlap measures and accuracy measure using our proposed scheme are better than results of model-driven approach [25] and centerlines tracking approach [15].In addition, the computational time is enhanced by using the 3D binary volume. The whole scheme takes about 30sincluding 20s for aorta detection, 1s for arteries segmentation and 9s for centerline extraction. For comparison, the proposed approach takes about 9s to extract the centerlines points from a 3D binary volume which is already the fastest among all automatic centerlines extraction algorithms that participated in the MICCAI challenge [20].

VI. Conclusion and Future Work

In this paper we proposed a fuzzy-based hybrid approach for automatic coronary arteries segmentation and centerlines extraction process in CTA cardiac volume. The main arteries have been segmented from detected aorta artery using circular Hough transform. FCM has been used to detect the seeds points for region growing algorithm. Using FCM helped to extract the accurate start point of centerline. Centerlines have been extracted from a 3D binary volume of segmented arteries using skeleton based method. The proposed approach has been evaluated using 32 CTA datasets provided by the Rotterdam Coronary Artery algorithm evaluation framework. A comprehensive comparative study has been conducted. From which, it is found first that the fuzzy-based hybrid proposed scheme is outperform a non-fuzzy technique. Then, quantitative evaluation results showed that the proposed approach is capable of achieving much higher accuracy, at reasonable computational cost, for coronary arteries centerlines extraction in CTA volume in comparison to the other recent schemes. The average OV, OF, and OT measures for centerlines extraction results of three main arteries are 95%,89% and 96%, respectively of 32 datasets, while the average AI distance measure is 0.2 mm by comparison with the ground truth. Future work involves searching the branches of main arteries and measuring the diameters and cross sectional areas of segmented vessels at different locations, so that a quantitative estimation of stenosis can be provided.

References

[1] "World Health Organization." [Online]. Available: http://www.who.int/mediacentre/factsheets/fs310/en/. [Accessed: 10-May-2017].

[2] R. Ambinder, D. Gladstone, R. Jones, Y. Kasamon, S. Shanbhag, and L. Swinnen, "John Hopkins Medicine," Sidney Kimmel Compr. cancer Cent.

[3] F. Kirbas, C. Quek, "A review of vessel extraction techniques and algorithms," Comput. Surv., vol. 36, no. 2, pp. 81–121, 2004.

[4] N. Shameena and R. Jabbar, "A Study of Preprocessing and Segmentation Techniques on Cardiac Medical Images," Int. J. Eng. Res. Technol., vol. 3, no. 4, pp. 336–341, 2014.

[5] Y. Yang, A. Tannenbaum, and D. Giddens, "Automatic segmentation of coronary arteries using Bayesian driven implicit surfaces," Proc. IEEE Int. Symp. Biomed. Imaging, pp. 189–192, 2007.

[6] P. Kitslaar, M. Frenay, E. Oost, J. Dijkstra, B. Stoel, and J. H. C. Reiber, "Connected Component and Morpholgy Based Extraction of Arterial Centerlines of the Heart (CocomoBeach)," Blood, pp. 1–8, 2008.

[7] C. Wang and O. Smedby, "An automatic seeding method for coronary artery segmentation and skeletonization in CTA," Insight J., 2008.

[8] H. Tek, M. a Gulsun, S. Laguitton, L. Grady, D. Lesage, and G. Funka-Lea, "Automatic Coronary Tree Modeling," Midas J. - Proc. MICCAI Work. - Gd. Chall. Coron. Artery Track., p. <http://hdl.handle.net/10380/1426>, 2008.

[9] V. Mohan, G. Sundaramoorthi, A. Stillman, A. Tannenbaum, and others, "Vessel segmentation with automatic centerline extraction using tubular tree segmentation," Proc. MICCAI Work. Cardiovasc. Interv. Imaging Biophys. Model., 2009.

[10] S. Salles, F. P. Salvucci, and D. Craiem, "A reconstruction platform for coronary arteries, finite element mesh generation and patient specific simulations," J. Phys. Conf. Ser., vol. 332, p. 12048, 2011.

[11] Bouraoui, Bessem, et al. "3D segmentation of coronary arteries based on advanced mathematical morphology techniques." Computerized medical imaging and graphics 34.5 (2010): 377-387.

[12] İ. Öksüz, D. Ünay, and K. Kadıpaşaoğlu, "A Hybrid Method for Coronary Artery Stenoses Detection and Quantification in CTA Images," 3D Cardiovasc. Imaging, 2012.

[13] Funka-Lea, P. Sharma, S. Rapaka, and Y. Zheng, "Coronary centerline extraction via optimal flow paths and CNN path pruning," Lect. Notes Comput. Sci. (including Subser. Lect. Notes Artif. Intell. Lect. Notes Bioinformatics), vol. 9902 LNCS, pp. 317–325, 2016.

[14] D. Lesage, E. D. Angelini, G. Funka-Lea, and I. Bloch, "Adaptive particle filtering for coronary artery segmentation from 3D CT angiograms," Comput. Vis. Image Underst., vol. 151, pp. 29–46, 2016.

[15] N. Salehi and A. R. Naghsh-nilchi, "Computer Methods in Biomechanics and Biomedical Engineering : Imaging & Visualization Automatic 3-D tubular centerline tracking of coronary arteries in coronary computed tomographic angiography," Comput. Methods Biomech. Biomed. Eng. Imaging Vis., vol. 1163, no. March 2017, pp. 1–12, 2016.

[16] B. M. Almezgagi, M. A. W. Shalaby, and H. N. Elmahd, "Improved Iris Verification System," vol. 14, no. 1, 2014.

[17] Fan, Jianping, et al. "Seeded region growing: an extensive and comparative study." Pattern recognition letters 26.8 (2005): 1139-1156.

[18] M. A. W. Shalaby . Thesis, "Fingerprint Recognition : a Histogram Analysis Based Fuzzy C-Means Multilevel," no. March, 2012.

[19] K. Palágyi and A. Kuba, "A Parallel 3D 12-Subiteration Thinning Algorithm," Graph. Model. Image Process., vol. 61, no. 4, pp. 199–221, 1999.

[20] M. Schaap et al., "Standardized evaluation methodology and reference database for evaluating coronary artery centerline extraction algorithms," Med. Image Anal., vol. 13, no. 5, pp. 701–714, 2009.

[21] G. Yang et al., "Automatic centerline extraction of coronary arteries in coronary computed tomographic angiography," Int. J. Cardiovasc. Imaging, vol. 28, no. 4, pp. 921–933, 2012.

[22] S. C. Saur, C. Kühhnel, T. Boskamp, G. Székely, and P. Cattin, "Automatic ascending aorta detection in CTA datasets," Bild. für die Medizin 2008, pp. 323–327, 2008.

[23] R. Erbel and H. Eggebrecht, "Aortic dimensions and the risk of dissection.," Heart (British Cardiac Society), vol. 92, no. 1. pp. 137–42, 2006.

[24] T. C. Lee, R. L. Kashyap, and C. N. Chu, "Building Skeleton Models via 3-D Medial Surface Axis Thinning Algorithms," CVGIP: Graphical Models and Image Processing, vol. 56, no. 6. pp. 462–478, 1994.

[25] Y. Zheng, J. Shen, H. Tek, and G. Funka-Lea, "Model-driven centerline extraction for severely occluded major coronary arteries," Lect. Notes Comput. Sci. (including Subser. Lect. Notes Artif. Intell. Lect. Notes Bioinformatics), vol. 7588 LNCS, no. Lcx, pp. 10–18, 2012.

An Improvement of Power Saving Class Type II Algorithm in WiMAX Sleep-mode

Mehrdad Davoudi
Dept. of Electrical Engineering
Islamic Azad University,
Science and Research Branch
Tehran,
Iran

Mohammad-Ali Pourmina
Dept. of Electrical Engineering
Islamic Azad University,
Science and Research Branch
Tehran,
Iran

Ahmad Salahi
Dept. of Telecommunication Engineering
Iran Telecommunication Research Center
Tehran, Iran

***Abstract*—Because of the fact that users can connect to a WiMAX (IEEE 802.16) network wirelessly with large-scale movement capability, it is inevitable that they cannot access electrical power sources at their desired time. As a result, a mechanism is needed to reduce power consumption; and therefore three power saving classes have been defined in WiMAX that each one is designed for a specific application. Although using a suitable power saving class (PSC) can reduce power consumption significantly, but lack of cross-layer coordination can reduce the efficiency of the power saving mechanism. Since real-time services which are related to power saving class type II (PSC II) have great importance and vast applications, an improved PSC II algorithm for WiMAX is proposed in this paper which not only guarantees WiMAX quality of service (QoS), but also makes the cross-layer coordination using a proactive buffer resulting in less power consumption. There is also a comparison made between the performance of the proposed algorithm and the predefined PSC II algorithm in WiMAX using computer simulations and it shows that using the proposed algorithm reduces power consumption by 60 percent, while WiMAX QoS is still guaranteed.**

Keywords*—WiMAX; IEEE 802.16; sleep mode; power saving class type II (PSC II); proactive buffer; quality of service (QoS)

I. Introduction

Considering the widespread usage of smartphones, tablets, laptops, etc. as devices to connect to internet and also vast coverage of wireless and cellular networks, nowadays mobile users tend to connect to the internet wirelessly. Wireless networks like cellular networks or WiMAX not only give users a large-scale movement capability, but also provide them with a high-speed and broadband internet connectivity. Despite these advantages, a fundamental challenge still remains; since users of these networks are mobile, probable unavailability of electrical power sources for them at their desired time is inevitable. As a result, designing a mechanism to reduce power consumption is vital, so that users can stay connected to the network, needless of recharging their devices.

In this article, the main goal is to propose an improved PSC II algorithm which saves more power than WiMAX predefined PSC II algorithm and yet guarantees WiMAX QoS. The approach to reach this goal is to design a proactive buffer to impose delay to delay-tolerable sporadic traffic generated by application layer such as keep-alive messages, so that the device stays more in sleep mode; and therefore more power is saved, without applying harsh changes to QoS parameters that result network instability and undesirable performance.

The reason to choose this subject is because PSC II aims to reduce power consumption in real-time services such as VoIP, IPTV, etc. and since these services are widely used, saving power in them gives users the ability to have a longer experience using these services, needless of recharging their devices.

In order to better understand the subject, there will be an insight about WiMAX power saving mechanisms in Section II and the literature review will be in Section III. In Section IV there will be an explanation about the proposed algorithm (methodology), Section V will be the results and comparison and there will be the conclusion and future works in Section VI.

II. Power Saving Mechanisms in WiMAX

A. Idle mode

Idle mode allows the Mobile Station (MS) to save power by restricting listening intervals (in which the MS is actively transmitting data) and completely turning off the air interface as well. This provides the network with a useful method called paging. The main role of paging is to create an alarm when there is downlink traffic [1]. When idle mode is activated, the air interface of Base Station (BS) and MS are powered off.

B. Sleep mode

In sleep mode, unavailability intervals are related to the BS, and the MS receives sleep mode parameters from BS. Unlike idle mode, in sleep mode the MS stays connected to the BS. This can help the device return to normal operation mode faster. There are two main states in sleep mode and the MS switches between them [2].

In the first state, the sleep window is activated. In fact, sleep window is a time span in which power is saved. In the second state, listening window is activated and the MS checks if any downlink traffic should be received from the BS or not.

Unlike idle mode which has only one operation mode, in sleep mode there are three different operation modes called “power saving class (PSC)”, each designed for a specific

application. They are named power saving class type one (PSC I), PSC II and PSC III.

PSC I is designed to save power in Best-Effort (BE) and Non-Real-Time Variable Rate (NRT-VR) services and consists of listening window and sleep window. The length of the listening window in this power saving class is fixed and a MS associated with PSC I checks if there are any buffered packets for it in the listening window. If there were buffered packets, the MS will return to normal operation mode to receive the packet. Otherwise, the sleep window will be activated, so that the device will save power. Then this procedure repeats and the length of sleep window is doubled until it reaches the maximum length defined in WiMAX standard [3].

PSC II is designed for unsolicited grant services and also Real-Time Variable Rate (RT-VR) services. Similar to PSC I, PSC II is also consisted of listening window and sleep window. Unlike PSC I, the length of listening and sleep windows are both fixed and the summation of them is called a sleep cycle. A MS associated with PSC II can still transmit data packets without returning to normal operation. As a result, the length of listening window should be long enough to receive all packets arrived during a single sleep cycle in PSC II [4].

As shown in Fig. 1, unlike PSC I and PSC II, PSC III consists only of a single sleep window and it is used for multicast services. By activating this PSC, a single sleep window with defined length in WiMAX standard starts and then the MS returns to normal operation mode [5].

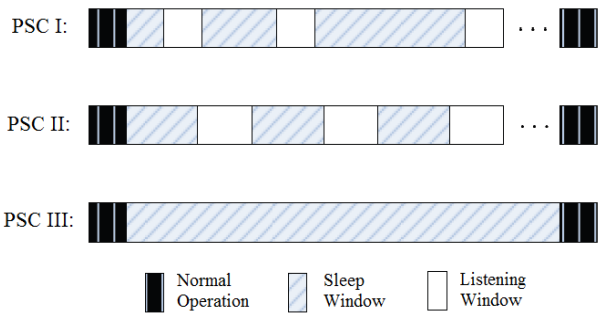

Fig. 1. WiMAX power saving classes.

III. Literature Review

Many researches have been done to reduce power consumption in WiMAX, each using a specific approach and we will point out some of the major ones. As in [6] a power saving mechanism for WiMAX was proposed to maximize energy efficiency. They have actually proposed a theoretic frame based on semi-Markov decision process along with a performance study on the power saving procedure. In [7] a power saving mechanism called Maximum Unavailability Interval (MUI) was proposed to increase energy efficiency in PSC II for WiMAX. They believe that their mechanism can calculate the maximum unavailability interval. They proposed a mathematical technique to reduce calculation complexity too. In [8] a research has been done to improve sleep mode's performance by applying a proactive algorithm to uplink traffic and also an efficient approach to numerically calculate power saving parameters has been proposed. In the end, they proved that a proper scheduling and a controllably delayed uplink traffic can have a huge positive impact on system performance and power saving procedure. In [9] a power saving mechanism has been proposed to guarantee delay parameter of QoS that synchronizes sleep cycles by imposing a slight delay. Based on WiMAX cross-layer design, a power saving strategy has been proposed in [10], in which they evaluated WiMAX power saving performance, as well as that of mobile stations in sleep mode by a Markov chain model. Then, they found the relationship between network load and power consumption and in the end they proposed a method to calculate power saving parameters. In [11] a power saving method for WiMAX was proposed to increase unavailability intervals in a MS which is using PSC II. This method configures sleep window's scheduling in a way that maximizes unavailability intervals. They also proved analytically that their method saves 20 percent more power in comparison with the predefined PSC II in WiMAX. [12] was a research aiming to design a scheduling algorithm for real-rime services in order to maximize unavailability intervals in PSC II. Using an Adaptive Bandwidth Reservation (ABR) algorithm, they reduced calculation complexity and proved that their proposed algorithm not only maximizes unavailability intervals, but also reduces power consumption significantly.

IV. Methodology

As explained in Section II, an MS associated with PSC II can transmit data packets without existing sleep mode. But some control packets (e.g. keep alive messages or time synchronization messages) that are sent to MAC layer of WiMAX (shown in Fig. 2) by application layer will terminate sleep mode. As a result, the MS will return to normal operation and this lack of cross-layer coordination will reduce the positive effect of sleep mode to save power.

In order to solve this problem we have made some changes in the predefined PSC II algorithm of WiMAX to make the cross-layer coordination between MAC and application layer. Therefore, we have implemented a proactive buffer between MAC and application layers to impose delay to control packets, so that the MS will longer stay in sleep mode and as a result, more power is saved.

WiMAX supports 2.5, 4, 5, 8, 10, 12.5 and 20 millisecond packet lengths [13]. Since the overhead of 5 millisecond packets cause PSC II operate optimally in saving power [14], [15], we have adjusted transmitted packet lengths to 5 milliseconds.

An assumption made in the simulations is to use UGS scheduling when sleep mode is activated. Since this transmission scheduling method is delay-sensitive, it can evaluate our proposed algorithm well; meaning if our proposed algorithm is proper, packets will be transmitted without problem. Otherwise, network delay will be increased and the network will be unstable. Moreover, the real-time traffic will no longer be real-time, resulting in network failure. One last assumption is that the MS moves in the BS's coverage area in random vector-like paths.

Major changes that we have made in the predefined PSC II of WiMAX are mostly related to sleep control (sleep-ctrl) and higher layer packets (hl-pk) states in WiMAX MAC layer.

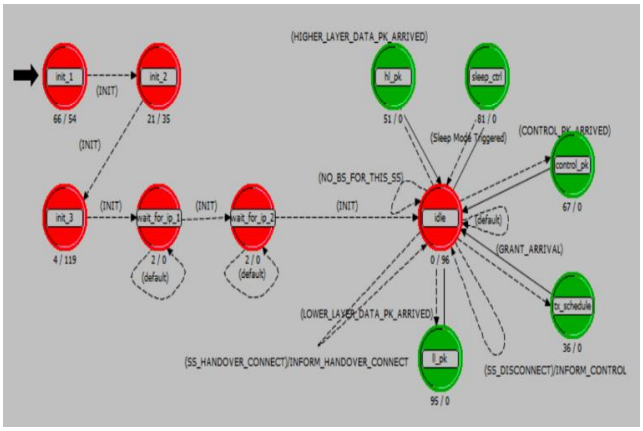

Fig. 2. WiMAX MAC layer.

A. Defining the buffer

Since the length of control packets from application layer to MAC layer is 4 milliseconds [16] and generally there are two types of control packets in WiMAX real-time services named time synchronization and keep alive messages [17] that are delay-tolerable [18], therefore we have set the buffer length to 100 milliseconds. As a result, there will be a queue of 25 control packets which will be delayed 100 milliseconds. This buffer length is neither too short to make a congestion inside the buffer, nor too long to exceed the packet delay bound of control packets and failing the network accordingly [19].

In order to optimally design the buffer, we should consider the fact that this buffer (like other common buffers) is actually a memory and it is only capable of recognizing the incoming packet sizes, not their types. So we have set a condition for the buffer to only let the 4 millisecond packets enter the queue; so that no extra delay would be applied to our 5 millisecond data packets by the buffer. (For a service like VoIP, even if we apply the 100 millisecond delay to data packets, if there were no more than 50 millisecond delay in other parts of the network, the service would still be real-time and functioning properly. [20])

Sleep window's duration in the predefined PSC II of WiMAX is 10 milliseconds [21]. According to our trial and error, if the buffer length and sleep cycle's duration are equal, the cross-layer coordination is best made; and therefore the sleep mode would function optimally. So the other change we have made in the predefined PSC II of WiMAX is to increase the sleep cycle's duration to 100 milliseconds; meaning that sleep window and listening window's duration should each be 50 milliseconds. Another obvious point to mention about the buffer is that it should be activated only when the sleep mode is triggered.

V. Results and Comparison

As mentioned before, in this section a comparison is made between the performance of the proposed PSC II algorithm and the predefined PSC II algorithm in WiMAX, when a real-time VoIP service with PCM quality speech is simulated in one hour duration in the network. This service is actually the service offered by most of social media applications (e.g., WhatsApp, telegram, etc.).

In this comparison, the first scenario (scenario 1) indicates the performance of the predefined PSC II algorithm in WiMAX and the second scenario (scenario 2) refers to the proposed algorithm (all simulations are run by OPNET simulator).

A. Power consumption

As shown in Fig. 3, power consumption for scenario 1 is 30 dBm, while for scenario 2 is 25.8 dBm; meaning that the power consumption for the proposed algorithm is 4.2 dBm less than that of the predefined PSC II of WiMAX.

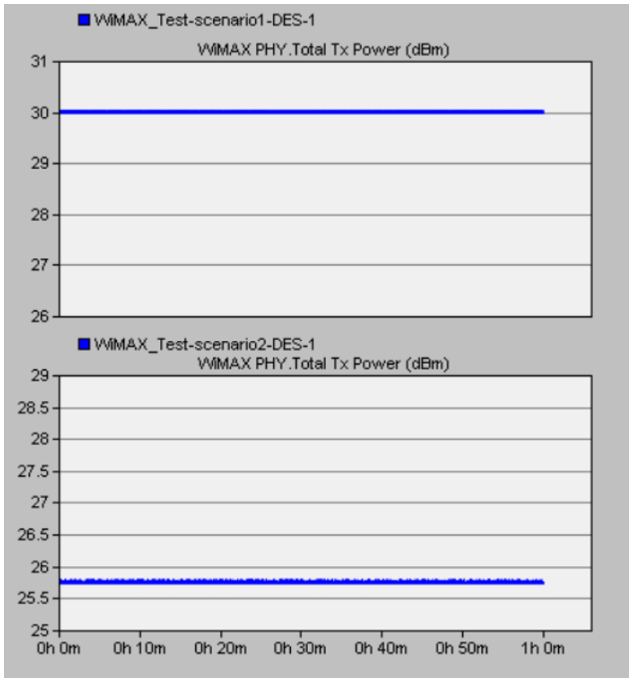

Fig. 3. Comparison of power consumption

In fact, power consumption for scenario 1 is 1 watt, while for scenario 2 is about 0.4 watts; meaning that the proposed algorithm saves about 60 percent more power.

B. Delay

Fig. 4 shows that both scenarios have 2.4 milliseconds (0.0024 seconds) delay. This means that the proposed algorithm has not imposed any extra delay to the network. QoS for WiMAX real-time services indicates that a delay less than 100 milliseconds is excellent and a delay less than 150 milliseconds is acceptable [22]. In fact, using UGS scheduling has not made any problems for the proposed algorithm and the delay in scenario 2 is far less than 100 milliseconds. As a result, the performance of the proposed algorithm is excellent in the field of delay.

C. Network load

As shown in Fig. 5, average network load for both scenarios is nearly the same and as expected, for both scenarios at their steady state stability, average network load is about 200,000 bits per second (25 kilobytes per second) which is actually the bit rate of a PCM quality speech VoIP service. Furthermore, since the network load has reached a steady state stability, we can conclude that no network failure has occurred.

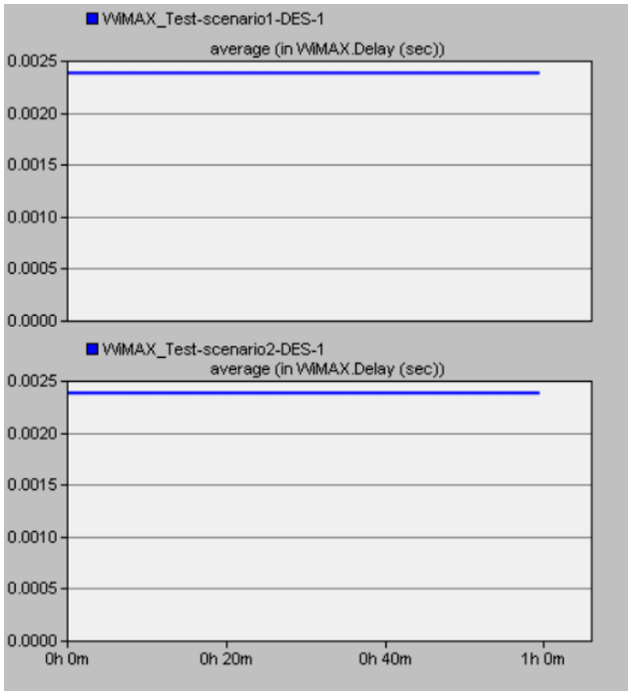

Fig. 4. Comparison of delay.

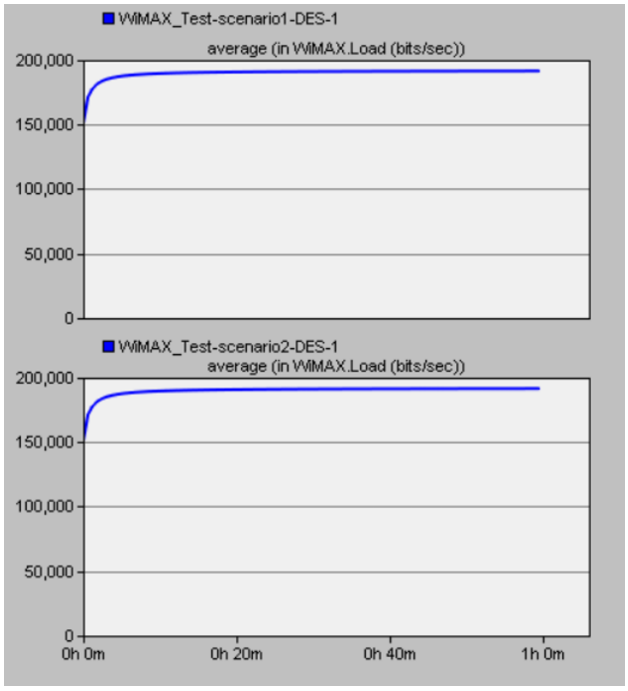

Fig. 5. Comparison of network load.

D. Dropped packets

From Fig. 6, it is clear that at the beginning of the simulation, dropped packets for both scenarios is 0.59 packets per second. But towards the end of simulation, average dropped packets is about 0.5 and 0.8 packets per second for scenario 1 and scenario 2, respectively. As a result, an average of 0.3 packets per second in the proposed algorithm is dropped more than that of the predefined PSC II algorithm of WiMAX. QoS for WiMAX real-time services indicates that at most 5 percent of packets can be dropped per second [22]. Since we chose that data packet lengths in the proposed algorithm to be 5 milliseconds and also 0.8 packets are dropped per second, one can conclude that 0.4 percent of packets are dropped in the proposed algorithm which is 4.6 percent less than the highest acceptable value in WiMAX QoS.

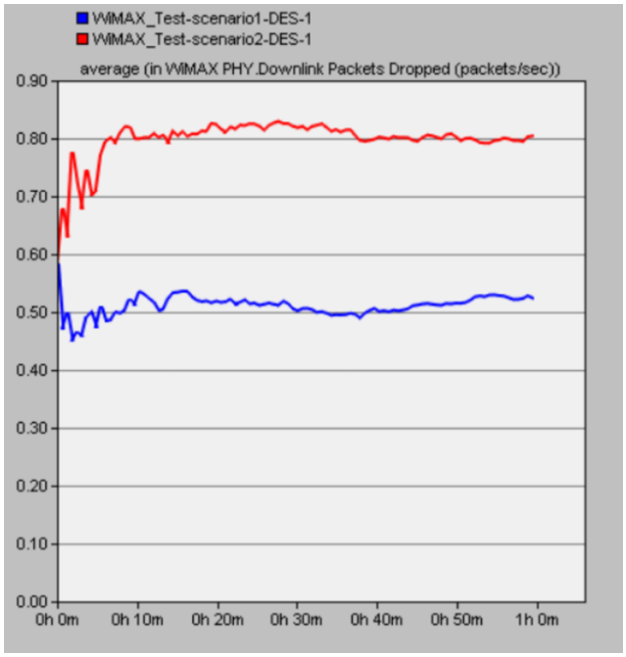

Fig. 6. Comparison of dropped packets.

E. Block error rate (BLER)

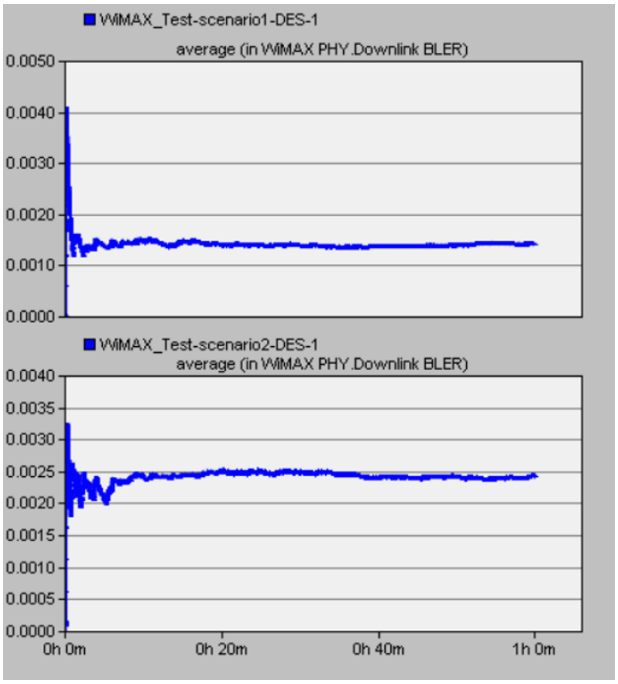

Fig. 7. Comparison of block error rate.

Fig. 7 shows that although the Block Error Rate (BLER) at the beginning of the simulation for scenario 2 is less than that of scenario 1, but towards the end of simulation, BLER is

about 0.0014 and 0.0024 for scenario 1 and scenario 2 respectively. This means that BLER for the proposed algorithm is about 0.001 more than that of the predefined PSC II of WiMAX, but the BLER for the proposed algorithm still guarantees the QoS of WiMAX real-time services [22].

F. Signal to noise ratio (SNR)

As shown in Fig. 8, average SNR for scenario 1 and scenario 2 is 4.2 and 3, respectively and as expected, the SNR for the proposed algorithms is less than that of the predefined PSC II of WiMAX.

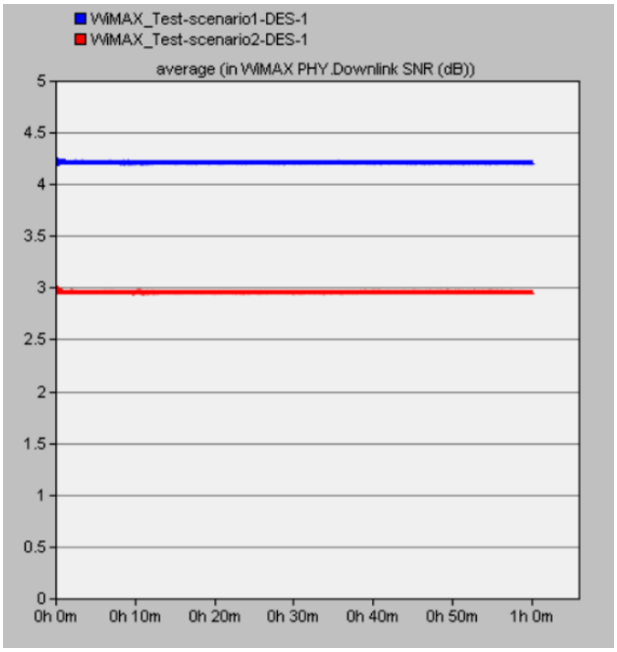

Fig. 8. Comparison of signal to noise ratio.

Since in this simulation the value of noise power is constant, it is the signal power that has made the difference. As expected, because cross-layer coordination has been made in the proposed algorithm (scenario 2), sleep mode has done a better job saving power; so it has used less signal power to transmit data packets accordingly. As a result, SNR has been decreased in the proposed PSC II algorithm. WiMAX QoS for real-time services indicates that this signal to noise ratio is quite enough for a WiMAX network to operate properly [22].

VI. Conclusion and Future Work

In this article a PSC II algorithm for WiMAX sleep mode is proposed to replace the predefined PSC II of WiMAX. Although PSC II can save power when using WiMAX, but lack of cross-layer coordination reduces the positive effect of WiMAX PSC II, thus we decided to make the cross-layer coordination by implementing a proactive buffer that delays delay-tolerable control messages like time synchronization and keep alive messages sent to MAC layer by application layer. In fact, we have made changes in the predefined PSC II algorithm of WiMAX (e.g., applying the buffer between MAC layer and application layer, alteration of sleep window and listening window length, etc.) to develop a new algorithm that makes the cross-layer coordination and saves more power accordingly.

We have also evaluated the performance of the predefined WiMAX PSC II algorithm and the proposed algorithm by comparing power consumption, delay, network load, dropped packets, block error rate (BLER) and signal to noise ratio (SNR) using OPNET simulator.

The comparison indicates that the proposed algorithm saves about 60 percent more power and no extra delay has been imposed to the network; moreover, network load has not been changed tangibly. The comparison also shows that 0.3 packets per second are dropped more in the proposed algorithm which is acceptable by WiMAX QoS. Also in the proposed algorithm, the block error rate is 0.001 more than that of the predefined WiMAX PSC II, but this is still acceptable by WiMAX QoS for real-time services. At last, the comparison of SNR shows that the proposed algorithm has less signal to noise ratio as expected; since less signal power has been used, regarding the constant noise power.

As a summarized conclusion one can say that the proposed algorithm saves 60 percent more power and it does not impose any extra delay to the network and it does not change the network load; but it increases the dropped packets and block error rate and also decreases the signal to noise ratio which are all acceptable by WiMAX QoS for real-time services.

A point that makes this research different from other related researches is the percentage of saved power which is 60 percent. Also the fact that no extra delay has been imposed to the network and no tangible alteration has been made in network load; meaning that the reason of less power consumption is cross-layer coordination; not imposing extra delay or reducing network load.

From the results and comparison, one can anticipate that since the proposed algorithm has done a good job saving power in a single connection between one mobile station and a base station, it can also perform well in a multiple connection where there are more than one mobile stations. This requires a research team to investigate the performance of the proposed algorithm when there are more than one mobile stations in a WiMAX network.

References

[1] S. Ahmadi, “An overview of next-generation mobile WiMAX technology,” IEEE Communications Magazine, vol. 47, no. 6, 2009.

[2] B. Kim, J. Park and Y.-H. Choi, “Power Saving Mechanisms of IEEE 802.16e: Sleep Mode vs. Idle Mode,” Springer, Frontiers of High Performance Computing and Networking, pp. 332-340.

[3] J. Jang, K. Han and S. Choi, “Adaptive Power Saving Strategies for IEEE 802.16e Mobile Broadband Wireless Access,” IEEE Communications, 2006. APCC '06. Asia-Pacific Conference, 2006.

[4] W.-H. Liao and W.-M. Yen, “Power-saving scheduling with a QoS guarantee in a mobile WiMAX system,” Journal of Network and Computer Applications, vol. 32, no. 6, p. 1144–1152, 2009.

[5] O. J. Vatsa, M. Raj and R. Kumar, “Adaptive Power Saving Algorithm for Mobile Subscriber Station in 802.16e,” IEEE, Communication Systems Software and Middleware, 2007. COMSWARE 2007. 2nd International Conference, 2007.

[6] L. Kong, G. K. Wong and D. H. Tsang, “Performance study and system optimization on sleep mode operation in IEEE 802.16e,” IEEE Transactions on Wireless Communications, vol. 8, no. 9, 2009.

[7] T.-C. Chen and J.-C. Chen, “Maximizing Unavailability Interval for Energy Saving in IEEE 802.16e Wireless MANs,” IEEE Transactions on Mobile Computing, vol. 8, no. 4, pp. 475 - 487, 2009.

[8] K. D. Turck, S. Andreev and S. D. Vuyst, "Performance of the IEEE 802.16e Sleep Mode Mechanism in the Presence of Bidirectional Traffic," Communications Workshops, 2009. ICC Workshops 2009. IEEE International Conference, 2009.

[9] Y. Wu, Y. Le and D. Zhang, "An Enhancement of Sleep Mode Operation in IEEE 802.16e Systems," Vehicular Technology Conference, 2009. VTC Spring 2009. IEEE 69th, pp. 1-6, 2009.

[10] J. Xue and Z. Yuan, "An Adaptive Power Saving Strategies based on Cross-layer Design in IEEE 802.16e," Journal of Networks, vol. 5, no. 3, pp. 359-366, 2010.

[11] S. Kwon and D. Cho, "Enhanced power saving through increasing unavailability interval in the IEEE 802.16e systems," IEEE Communications Letters, vol. 14, no. 1, 2010.

[12] C.-Y. Wu, H.-J. Ho and S.-L. Lee, "Minimizing energy consumption with QoS constraints over IEEE 802.16e networks," Computer Communications, Wireless Green Communications and Networking, vol. 35, no. 14, p. 1672–1683, 2012.

[13] M. Ergen, Mobile Broadband: Including WiMAX and LTE, Berkeley, CA, USA: Springer, 2009.

[14] A. Bestetti, G. Giambene and S. Hadzic, "MAC layer performance assessments," IEEE Wireless Pervasive Computing, 2008. ISWPC 2008. 3rd International Symposium, pp. 490-494, 2008.

[15] W. Hrudey, Steaming Video and Audio Content Over Mobile WiMAX Networks, British Columbia, Canada: School of Engineering Science Simon Fraser University, PhD Dissertation, 2009.

[16] J. Wang, M. Venkatachalam and Y. Fang, "System architecture and cross-layer optimization of video broadcast over WiMAX," IEEE Journal on Selected Areas in Communications, vol. 25, no. 4, 2007.

[17] M. Sukru Kuran, G. Gur and T. Tugcu, "Applications of the cross-layer paradigm for improving the performance of WiMax," IEEE Wireless Communications, vol. 17, no. 3, 2010.

[18] A. Alamdar Yazdi, S. Sorour and S. Valaee, "Optimum Network Coding for Delay Sensitive Applications in WiMAX Unicast," INFOCOM 2009, IEEE, pp. 2575-2580, 2009.

[19] B. Li and S.-k. Park, "Maximizing power saving with state transition overhead for multiple mobile subscriber stations in WiMAX," Frontiers of Information Technology & Electronic Engineering, vol. 17, no. 10, p. 1085–1094, 2016.

[20] S. Jadhav, H. Zhang and Z. Huang, "Performance Evaluation of Quality of VoIP in WiMAX and UMTS," IEEE, Parallel and Distributed Computing, Applications and Technologies (PDCAT), 12th International Conference, pp. 375-380, 2011.

[21] W. F. N. W. Group, WiMAX Forum Network Architecture—Stage 2: Architecture Tenets, Reference Model and Reference Points—Release 1, Version 1.2, New York, USA: WiMAX Forum, 2008.

[22] I. 8. W. Group, IEEE Standard for Local and Metropolitan Area Networks, Part 16: Air Interface for Fixed and Mobile Broadband Wireless Access Systems, Amendment 2: Physical and Medium Access Control Layers for Combined Fixed and Mobile Operation in Licensed Bands, New York, USA: IEEE Computer Society, 2006.

ASCII based Sequential Multiple Pattern Matching Algorithm for High Level Cloning

Manu Singh
School of ICT,
Gautam Buddha University
Greater Noida, Uttar Pradesh, India

Vidushi Sharma
School of ICT,
Gautam Buddha University
Greater Noida, Uttar Pradesh, India

***Abstract*—For high level of clones, the ongoing (present) research scenario for detecting clones is focusing on developing better algorithm. For this purpose, many algorithms have been proposed but still we require the methods that are more efficient and robust. Pattern matching is one of those favorable algorithms which is having that required potential in research of computer science. The structural clones of high level clones comprised lower level smaller clones with similar code fragments. In this repetitive occurrence of simple clones in a file may prompt higher file level clones. The proposed algorithm detects repetitive patterns in same file and clones at higher level of abstraction like file. In genetic area, there are a number of algorithms that are being used to identify DNA sequence. When compared with some of the existing algorithms the proposed algorithm for ASCII based sequential multiple pattern matching gives better performance. The present method increases overall performance and gradually decline the number of comparisons and character per comparison proportion by repudiating (avoid) unnecessary DNA comparisons.**

Keywords—Pattern matching; ASCII based; high level clone; file clone

I. INTRODUCTION

A software system is constantly changing, and consistent maintenance is required to help it adapt to the new changes. Designs, software upgrades, compilers, hardware upgrades and so forth all influence the working of software. Because of standard adjustments in code, redundancies happen in code and programming will be more mind boggling and troublesome in keeping up. Now and then this excess is known as cloning. Cloning may occur at various abstraction levels and have unusual source [1]. Literature study portrays half cloning in the source codes [2]. In literature, several techniques used to identify simple clone fragments [3] but detection clones at higher levels remains a promising area till now. One of the promising area in clone detection is pattern matching. pattern matching is the act of checking the occurrences of a particular pattern of characters in a large file.

This paper investigates the applicability of a new technique of pattern matching approach called ASCII based Pattern Matching algorithm, for detection of high level clone in source code. High Level Clones are classified [4] in structural clone, concept clone, behavioural clone [5] and domain model clone. This classification depicts that structural clones are formed by similar fragments of code at low level. This approach avoids lengthy comparisons in string sequence and reduces the effort for each character comparison at each attempt. The proposed algorithm gives better results as compared to other algorithms.

The rest of the paper is organized as: Related work is explained in Section II. Proposed algorithm is explained in Section III. Then simulation results are presented in Section IV. Experimental results of proposed algorithm are discussed in Section V. Section VI explain graphically the effect of increasing pattern size on performance indices. Section VII discusses comparative analysis of proposed algorithm with another algorithm. Section VIII analyse the impact of cumulative pattern size increment on no. of comparison. Then final performance analysis of proposed algorithm is given in Section IX. Concluding remarks are given in Section X.

II. RELATED WORK

There are various string matching techniques which mainly deal with problem of identifying occurrences of a substring in a given string or locate the occurrences of specific pattern in a sequence. In this section, we explore these different types of string matching techniques. Some techniques are based on algorithms of exact matching in string, such as Brute-force algorithm, Bayer-Moore algorithm, Knuth-Morris-Pratt algorithms [6], [7] and some are based on approximate string matching algorithms, dynamic programming is mostly used approach. In An indexed based K-Partition Multiple Pattern Matching Algorithm (IBKPMPM) [8] choose the value of k and divide both the string and pattern into number of substring of length k, each substring is called as a partition. We compare all the first characters of all the partitions, if all the characters are matching while we are searching then we go for the second character match and the process continues till the mismatch occurs or total pattern is matched with the sequence. In index based forward backward multiple pattern matching algorithm (IFBMPM) [9] patterns matching technique the characters in the given patterns are matched one by one in the forward and backward until a mismatch occurs or a whole pattern matches. In the Multiple Skip Multiple Pattern Matching Algorithm (MSMPMA) [10] technique the algorithm search the input text to find the all occurrences of the pattern based upon the skip technique. To get starting location of the matching Index is used; it compares the Text characters from the well-defined point with the pattern characters, and based on the match numbers decides the skip value (ranges 1 to m-1). In IBSPC [11] indexes have been used for the DNA sequence. Least occurring character index will be used to search for the pattern in the string. In Index Based Algorithm [12], on the basis of

frequently occur character index table is created and then align pattern with string and matched occurrence of patterns with multiple times one by one from left to right in the file.

This paper proposed the most efficient approach for finding similarity between multiple pattern, till date. To further increase the performance of pattern matching an ASCII based multiple pattern matching algorithm using ascii value comparison between pattern and substring is proposed. It is a simple approach for finding multiple occurrences of patterns from a given file. This algorithm gives better results when compare it with existing algorithms. This approach provides best results with the DNA sequence dataset. Proposed algorithm is implemented in VB.NET and results are compared with already existing algorithms. Experimental results of applying the technique to DNA sequences show the effectiveness of the proposed technique.

III. PROPOSED ALGORITHM

The proposed approach has been used ASCII value of characters for comparison. The algorithm considered a DNA sequence string S of 1024 characters as input. First of all, extract substring from string S equal to the pattern length m. Calculate the ASCII sum of all substrings. Suppose the given pattern is P. Compare the ASCII sum of both the pattern and substring, If ASCII sum of both the pattern and substring match so start comparing the pattern and substring character by character. If characters are not matched then skip the rest comparison of characters of substring and aligned the pattern with the next substring of the string. This process Continue till substring is less than the pattern length. By above example we can conclude that comparing ASCII values reduces the number of comparisons as when ASCII sum is not match then there is no need to compare substring and pattern character by character.

A. ASCII Based Multiple Pattern Matching Algorithm –

Input: String S of n characters and Length of pattern P of m characters.

Output: The number of occurrences of Pattern in String, its location and the number of characters compared.

```
Dim QueryASCIITable As String, patternASCIIValue As Int, _noOfComparison = 0
Step1: Dim count As Integer = 0, qStringarr As String (), patternarr As String (), tempstr As String
Dim queryIndex As Int32 = 0, blFound As Boolean = True
        If String.IsNullOrEmpty (String_S) Then
                qStringarr = String_SArray
'Array of substring
        If String.IsNullOrEmpty (Pattern_P) Then
                patternarr = m_Pattern_PArray
'Array of Pattern string
Step 2: ['Store the ASCII value of each size]
         For a As Integer = 0 To qStringarr.Length - 1
        If qStringarr.Length - a >= patternarr.Length Then
tempstr()=(ArraySelect(qStringarr,a,a+patternarr.Length)).ToArray()
QueryASCIITable.Add (a, GetASCIISum (tempstr), tempstr))
        End If
        Next
Step 3: [Store the ASCII value of pattern]
        patternASCIIValue = GetASCIISum(patternarr)
Step 4 : While (queryIndex < QueryASCIITable.Count - 1)
         If patternASCIIValue=QueryASCIITable(queryIndex).Key Then
 _noOfComparison += 1
 For patternIndex As Integer = 0 To patternarr.Length - 1
 _noOfComparison += 1
 If patternarr (patternIndex) = QueryASCIITable (queryIndex).Value (patternIndex) Then
 Continue For
 Else
 blFound = False
 Exit For
 End If
 Next
 If blFound Then
 indexarrfound.Add (queryIndex)
        End If
        End If
 queryIndex += 1
 End While
```

B. Performance Indices

Pattern matching algorithm efficiency can be judged by using certain performances indices. To make the comparisons we have used following performance indices:

1) No. of Occurrences: If we are given an array of text T (1……n) of length n and the pattern is an array P (1…m) of length m such that m<=n then the number of occurrences of pattern will be (n-m+1).

2) No. of Comparisons: Objective of pattern matching algorithm is to reduce the number of character comparison in worst and average case analysis.

3) Best Case: The best case of this algorithm will be, when the pattern matches in the first shift. Therefore, best case is, $T(n)=\Omega(m)$.

4) Worst Case: Let in worst case situation the pattern matches at every shift in the text then there will be 'm' comparisons in each shift, so the total number of comparisons will be 'm(n-m+1)'. So the worst time complexity of this algorithm will be , $T(n)=O(m(n-m+1))$.

5) Comparisons per Character (CPC): CPC is used as a measurement factor. Complexity is decreased when CPC decreased. CPC ratio can be calculated as CPC = (Number of comparisons/file size).

IV. SIMULATION RESULTS

The algorithm was implemented using VB.NET, and it was tested using different DNA sequence with different file sizes. However, the proposed algorithm is compared with other algorithms. They are MSMPMA, Brute-Force, Trie-matching and Index Based algorithm. These algorithms are selected due to common features with the proposed algorithm as follows:

1) Multiple string matching

2) No pre-processing operations: As the proposed algorithm compares the ASCII value of the character rather than the character itself. Thus it will not take any pre-processing time and hence no pre-processing operation is required before comparison due to which this algorithm will become more efficient as compared to other algorithms.

3) Maintaining different type of files: The implementation and comparison with other algorithms process is carried out When text file size = 1024 bytes, using different patterns and sizes in implementation process. The results are obtained and can be grouped in various sections.

V. Performance Analysis of ASCII based algorithm

The DNA Sequence data has been taken from the Multiple Skip Multiple Pattern Matching algorithm MSMPMA [9] for testing the proposed algorithm. After implementation of the proposed ASCII based multiple pattern matching algorithm for the 1024 character and finding the no of occurrences, no of comparisons and CPC ratio it has been concluded that the number of comparisons reduces as the pattern size of DNA increases and are shown below in Table 1.

TABLE I. Experimental Results of Proposed Algorithm

S. N	Pattern	No. of Character	No. of Occurrence	No. of Comparison	CPC Ratio
1	A	1	259	516	0.5
2	AG	2	53	278	0.27
3	CAT	3	11	131	0.128
4	GACA	4	6	127	0.124
5	AACGC	5	2	2	0.001

VI. Effect of Increasing Pattern Size on Different Performance Indices

After the implementation of the proposed algorithm, the following points could be concluded from the obtained results in table below.

The result indicates that to find pattern with one char length from 1024 DNA data sequence proposed algorithm required 516 no. of comparisons (almost half). It means proposed algorithm requires 0.50 comparisons/character to search one-character pattern.

Further table indicates that when pattern increased in size, the no. of comparisons to find the pattern is decreased. Therefore, it can be said that this is very beneficial for detection of high level clones because high level cloning is found at coarser level not at the fine level.

When the pattern length increased, Comparison per Character decreased, and it is a well-known fact that Complexity time is affected by Comparison per Character. It depicts that the complexity is also decreased when pattern size increased.

If we take in consideration the number of pattern occurrences, we can say that the complicity is less than O(n), since We need less number of comparisons for the second match and less for the third and so on.

The number of comparisons which affects the processing time rapidly decreased after the first match, and the total number of comparisons for all occurrences will be less than the text file size.

A. Analysis on the Basis of Occurrence

Fig. 1 depicts that number of occurrences decreased when pattern size increased. Generally when pattern size increase there is less probability to find pattern in file and at that time algorithm that can search large pattern in less number of comparisons is required.

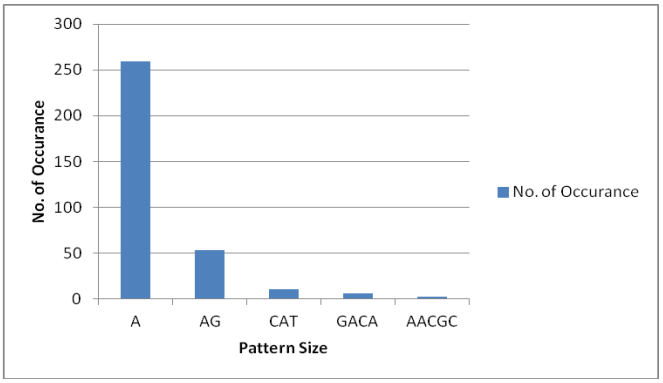

Fig. 1. Relation between pattern size and number of occurrences

B. Analysis on the Basis of Comparisons

The impact of increasing pattern size on number of comparisons have been displayed in Fig. 2. As the graph shows that when small pattern size is searched in file, number of comparisons is at its highest level but as the pattern size increased number comparisons decreased gradually.

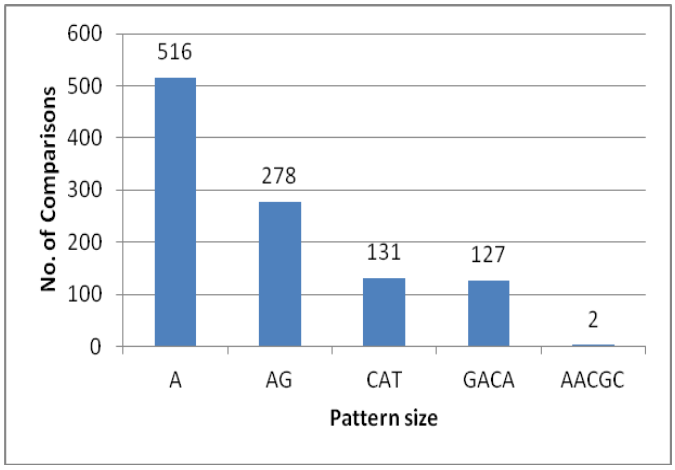

Fig. 2. Relation between pattern size and number of comparisons

C. Analysis on the Basis of Comparisons Per Character

The impact of increasing pattern size on comparison per character can be noticed in Fig. 3. When the pattern length increased, Comparison per Character decreased. Complexity time is affected by Comparison per Character. It depicts that the complexity is also decreased when pattern size increased.

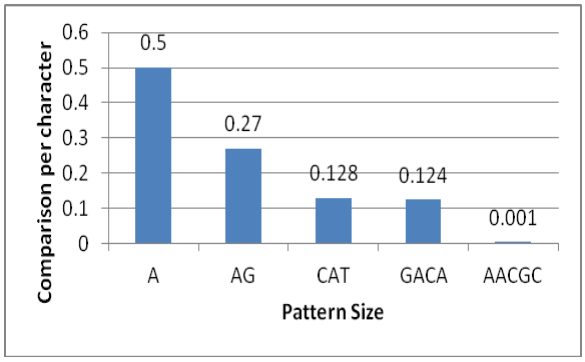

Fig. 3. Relation between pattern size and comparison Per character

VII. Comparative Analysis of ASCII based Algorithm with Other Existing Algorithms

As we have collected the data for various existing algorithm [10], [12] and drawn the comparative analysis in Tables 2.1, 2.2 and 2.3 with respect to the various existing algorithm.

TABLE II. (1) PATTERN=A (M=1)

Name of Algorithm	No. of Occurrences	No. of Comparisons	Comparisons per Character
MSMPMA	259	1024	1
Brute-Force	259	1024	1
Naïve String Search	259	1024	1
Trie-matching	259	1025	1.001
Index Based	259	774	0.75
ASCII Based	259	516	0.503

TABLE II. (2) PATTERN=AG (M=2)

Name of Algorithm	No. of Occurrences	No. of Comparisons	Comparisons per Character
MSMPMA	53	1230	1.201
Brute-Force	53	1282	1.252
Naïve String Search	53	1281	1.250
Trie-matching	53	1284	1.254
Index Based	53	414	0.404
ASCII Based	53	278	0.271

TABLE II. (3) PATTERN=CAT (M=3)

Name of Algorithm	No. of Occurrences	No. of Comparisons	Comparisons per Character
MSMPMA	11	1298	1.268
Brute-Force	11	1318	1.287
Naïve String Search	11	1321	1.290
Trie-matching	11	1310	1.279
Index Based	11	224	0.218
ASCII Based	11	131	0.128

Among them our algorithm which gives very good performance. It can be analysed that ASCII based algorithm gives improvements to other algorithms are following:

1) Decreases number of comparisons in average and best case analysis.
2) Appropriate for very large size input file.

VIII. Analysing the Impact of Cummulative Pattern Size Increment on Number of Comparison

Table 3 given below compare the total number of comparisons of different algorithms [13] with randomly selected different pattern sizes ranges from 1 to 8 in cumulative manner. As the size of pattern increasing in cumulative manner, the number of comparisons in proposed algorithm are lesser as compared to other pattern matching algorithms.

TABLE III. COMPARISON OF DIFFERENT ALGORITHMS USING DNA SEQUENCE FOR CUMULATIVE PATTERN [13]

	No. of Comparison							
Pattern	**Brute Force**	**MSM PMA**	**IFBM PM**	**IBMP M**	**Pair count**	**Boyer Moore**	**Index Based**	**ASCI I Base d**
A	**1024**	**1024**	**518**	**259**	**259**	**1024**	**774**	**516**
A+AG	**2308**	**2254**	**1142**	**777**	**506**	**1758**	**1188**	**794**
A+AG+CAT	**3626**	**3552**	**1709**	**1319**	**802**	**2365**	**1389**	**925**
A+AG+CAT+GACA	**5002**	**4911**	**2323**	**1933**	**1060**	**2869**	**1661**	**1052**
A+AG+CAT+GACA+AACGC	**6390**	**6286**	**2939**	**2540**	**1332**	**3235**	**1946**	**1054**
A+AG+CAT+GACA+AACGC+GACAAG	**7799**	**7680**	**3573**	**3163**	**1613**	**3611**	**2229**	**1058**
A+AG+CAT+GACA+AACGC+GACAAG+TCGGGTG	**9189**	**9070**	**4224**	**3797**	**1890**	**3811**	**2501**	**1060**
A+AG+CAT+GACA+AACGC+GACAAG+TCGGGTG+CCAAAAAA	**10538**	**10419**	**4822**	**4377**	**2163**	**4168**	**2759**	**1094**

The current technique gives good performance in reducing the number of character comparisons compared with other popular methods and existing algorithms. The results of proposed ASCII based multiple pattern matching algorithm and other existing algorithms for pattern size three also plotted in the graph as shown in Fig. 4.

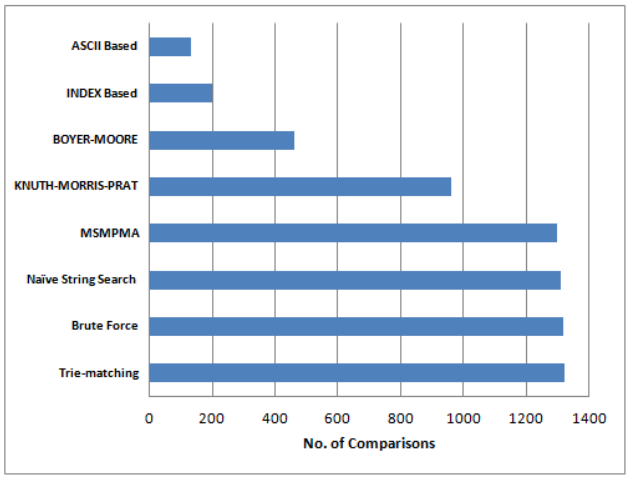

Fig. 4. Comparison of different algorithms for pattern [CAT]

This shows the reduction in number of comparison when pattern size is three-character long. Towards X-axis we have taken total number of comparisons whereas towards Y-axis it shows the names of all the algorithms.

IX. Performance Analysis of the Proposed Algorithm

Performance analysis of an algorithm is performed and explained by using the following measures.

1) Number of Occurrences: The number of occurrences of pattern will be (n-m+1).As the proposed algorithm is based on the ASCII values of the characters, it does not required any pre-processing time and consumes less space in memory as compared to Brute-Force Algorithm because Brute-Force algorithm requires extra CPU registers to hold the intermediate value, but the proposed algorithm do not require any extra register because it directly compares the ASCII value for any comparison thus we can say that it is more efficient as compared to Brute-Force and all the other algorithms.

2) Number of Comparisons: The number of character comparison in worst and best case analysis are shown in Table 4 and discusses as follows:

a) *Best Case*: The best case of this algorithm will be, when the pattern matches in the first shift. Therefore, best case is, T(n)=O(m).

b) *Average Case*: The average case of this algorithm will be, T (n) =Ω (m).

c) Worst Case: Let in worst case situation the pattern matches at every shift in the text then there will be 'm' comparisons in each shift, so the total number of comparisons will be 'm(n-m+1)'. So the worst time complexity of this algorithm will be, T(n)=O(m(n-m+1)).

TABLE IV. Comparison of Different Algorithms [14]

Algorithm	Pre-processing Time Required	Running Time	Best Case	Worst Case
Brute-Force Algorithm	NO	O(n-m+1) m	O(m)	O(n-m+1) m)
Knuth-Morris Prat	YES	O(n+m)	O(n)	Θ (n.m)
Boyer-Moore	YES	O (n\m)	O(m)	O(n-m+1) m+ Σ
ASCII Based	NO	O (n-m+1)	O(m)	O(m(n-m+1)

Degenerating property, i.e., of pattern is used by the proposed algorithm (in the same pattern sub-patterns appearing more than one time) and improves the worst-case complexity. The fundamental thought behind proposed algorithm is: at whatever point we identify a mismatch (after some matches), we definitely know a portion of the characters in the text of next window. We take advantage about this majority of the data to evade matching those characters that we know will in any case match.

X. Conclusion

We proposed a new algorithm which can be used for pattern matching in DNA sequences. This approach is suitable for unlimited size of input sequence. It reduces the total number of comparison as well as the CPC ratio when compared with other popular algorithms. The proposed algorithm gives very good performance with the other algorithms. Based on the experimental work our approach provides good performance related to DNA sequence dataset. Our proposed algorithm reduces the total number of comparison as well as the CPC ratio when compared with the some of the best known popular algorithm. In future, the proposed algorithm detects repetitive patterns at higher level of abstraction like file.

References

[1] H. A. Basit, S. Jarzabek, " A Case for Structural Clones ", International Workshop on Software Clones , 2009.

[2] B. S Baker, "On Finding Duplication and Near duplication in Large Software System ", Proceedings of 2nd IEEE Conference of Reverse Engineering , 1995.

[3] William S. Evans , Christopher W. Fraser and Fei Ma , " Clone Detection via Structural Abstraction ", Software quality journal Vol. 17, No. 4, 2009.

[4] M. Singh, V. Sharma, "High Level Clones Classification" International Journal of Engineering and Advanced Technology (IJEAT) ISSN : 2249 – 8958, Vol. 2, Issue - 6, August 2013.

[5] M. Singh, V. Sharma, "Detection of Behavioral Clone International Journal of Computer Applications (0975 – 8887) Vol. 102 – No.14 , 2014.

[6] Bayer R. S., J. S. Moore, "A Fast String Searching Algorithm " , Communications of the ACM , pp. 762-772 ,1977 7.

[7] Knuth D., Morris.J ,Pratt.V.R., "Fast Pattern Matching in Strings ", SIAM Journal on Computing Vol. 6 (1), 1977.

[8] Raju Bhukya, DVLN Somayajulu,"An Index Based KPartition Multiple Pattern Matching Algorithm", Proc. Of International Conference on Advances in Computer Science 2010 pp 83-87.

[9] Raju Bhukya, DVLN Somayajulu,"An Index Based Forward Backward Multiple Pattern Matching Algorithm", World Academy of Science and Technology. June 2010, pp347- 355

[10] Ziad A.A Alqadi, Musbah Aqel & Ibrahiem M.M.EI Emary, Multiple Skip Multiple Pattern Matching algorithms. IAENG

[11] Raju Bhukya, DVLN Somayajulu," Index Multiple Pattern Matching Algorithm using DNA Sequence and Pattern Count", International Journal of Information Technology and Knowledge Management July-December 2011, Volume 4, No. 2, pp. 431-441

[12] M. Singh, V. Sharma, "Index based detection of file level clone for high level cloning", International Journal of Computer Science Engineering and Information Technology Research (IJCSEITR) ISSN(P): 2249-6831; ISSN(E): 2249-7943 Vol. 5, Issue 4, Aug 2015, 63-70

[13] Raju Bhukya, DVLN Somayajulu, "Multiple Pattern Matching Algorithm using Pair-count", IJCSI International Journal of Computer Science Issues, July 2011, Vol. 8, Issue 4, No 2, pp. 453-465.

[14] Diwate. R.B., , Alaspurkar.S. J., " Study of Different Algorithms for Pattern Mining", International Journal of Advanced Research in Computer Science and Software Engineering 3(3), March - 2013, pp. 615-620

Mobile Malware Classification via System Calls and Permission for GPS Exploitation

Madihah Mohd Saudi
Faculty of Science and Technology (FST),
Universiti Sains Islam Malaysia (USIM),
Bandar Baru Nilai, 71800 Nilai,
Negeri Sembilan, Malaysia

Muhammad 'Afif b. Husainiamer
Faculty of Science and Technology (FST),
Universiti Sains Islam Malaysia (USIM),
Bandar Baru Nilai, 71800 Nilai,
Negeri Sembilan, Malaysia

***Abstract*—Now-a-days smartphones have been used worldwide for an effective communication which makes our life easier. Unfortunately, currently most of the cyber threats such as identity theft and mobile malwares are targeting smartphone users and based on profit gain. They spread faster among the users especially via the Android smartphones. They exploit the smartphones through many ways such as through Global Positioning System (GPS), SMS, call log, audio or image. Therefore to detect the mobile malwares, this paper presents 32 patterns of permissions and system calls for GPS exploitation by using covering algorithm. The experiment was conducted in a controlled lab environment, by using static and dynamic analyses, with 5560 of Drebin malware datasets were used as the training dataset and 500 mobile apps from Google Play Store for testing. As a result, 21 out of 500 matched with these 32 patterns. These new patterns can be used as guidance for all researchers in the same field in identifying mobile malwares and can be used as the input for a formation of a new mobile malware detection model.**

Keywords—Mobile malware; Global Positioning System (GPS) exploitation; system call; permission; covering algorithm; static and dynamic analyses

I. INTRODUCTION

Currently, Android smartphone is the most and widely used worldwide and many new mobile malwares are designed to attack it. Mobile malwares is defined as malicious software that is built to attack mobile phone or smartphone system without the owner consent. Examples of the mobile malwares are Slembunk and Santa Claus, where they are able to collect sensitive and confidential information and control smartphone with root exploitation. They tarnish the infected victim reputation and have caused loss of money, productivity and confidential information. Furthermore, McAffee has also reported that 37 million of malwares have been detected in apps stores in year 2016.[1] Apart from SMS, call log, audio and picture exploitation, Global Positioning System (GPS) has been used by many attackers to exploit smartphones. Through GPS, attackers know the victims' details such as satellite information and every movement can be monitored by them. In early year 2017, Google has released a patch (CVW-2016-8467) to overcome security vulnerabilities related with GPS exploitation in Nexus 6 and 6P phones.[2] Currently, not much work has been done to detect GPS exploitation in smartphone. Therefore, this paper objective is to detect mobile malware attacks for GPS exploitation based on system call and permission patterns. A covering algorithm is used as a basis for the proposed patterns. Then the proposed patterns are evaluated to prove its effectiveness.

This paper is organized as: Section 2 presents related work on mobile malware architecture, features and detection techniques. Section 3 describes the methodology used in this research. Section 4 presents the results of experiment carried out in this research. Section 5 includes the summary and potential future work of this paper.

II. RELATED WORK

There are many ways how mobile malwares can be categorized. Work done by Altaher classified android malware based on weighted bipartite graph [1]. He used API and permission for the classification but the dataset used for the experiment only limited to 500 dataset. A bigger and more recent dataset would be a good improvement for this work. As for Feizollah and colleagues, they used feature selection for mobile malwares features extraction [2]. These are based on four main features which are static, dynamic, hybrid and application metadata features. The paper provides a comprehensive review on feature selection for mobile malwares and it is used as guidance for our experiment in this paper. Hybrid feature which combines static and dynamic analyses has been applied due to its comprehensive and systematic feature. System call and permission that are related with GPS exploitation have been extracted and categorized in different patterns and details explained in Section 4 in this paper. Work by Manuel and colleagues also used hybrid feature in their experiment [3]. While works by [4]-[6] used static analysis only, which would give a better a performance if dynamic analysis is integrated in future (hybrid technique).

Apart from that, few research papers by [7]-[9], they discussed about Location Based Services (LBS) or GPS usage for Android smartphone. As for Singhal and Sungkla, they discussed about the implementation of LBS to give multiple

[1] B. Snell, "Mobile threat report what's on the horizon for 2016", 2016. [Online]. Available: https://www.mcafee.com/us/resources/reports/rp-mobile-threat-report-2016.pdf. [Accessed: 30- May- 2017]

[2] Tom Mendelsohn, "Google plugs severe android vulnerability that exposed devices to spying | Ars Technica," 2017. [Online]. Available: https://arstechnica.com/security/2017/01/google-plugs-severe-android-bootmode-vulnerability/. [Accessed: 30-May-2017].

services to the user based on their location through Google Web Services and Walk Score Transit APIs on Android. While Ma and colleagues, have developed a tool called as Brox to detect location information leakage in Android by integrating static analysis and Vanjire and colleagues have developed an Android application to locate nearest friends and family members location. There are also many works related to Android malwares analysis such as by [2], [6], [10]-[13]. However, none of the existing works discuss in detailed on how to detect and overcome GPS exploitation for smartphone. This is among the challenges for future work.

III. METHODOLOGY

The dynamic and static analyses and classification of GPS exploitation for system call and permission are summarized as in Fig. 1. The experiment was conducted in a controlled lab environment as illustrated in Fig. 2. No outgoing network connection is allowed to avoid any spread of the mobile malwares.

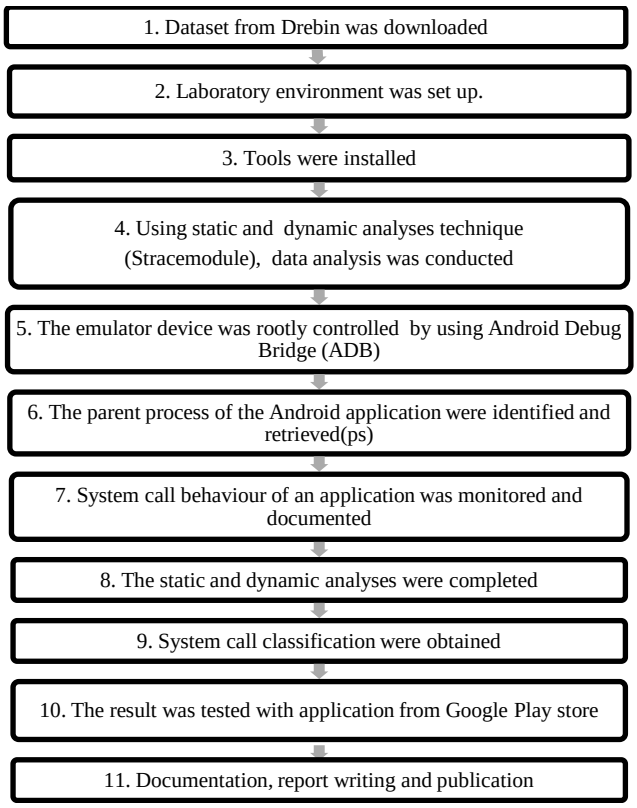

Fig. 1. Research processes.

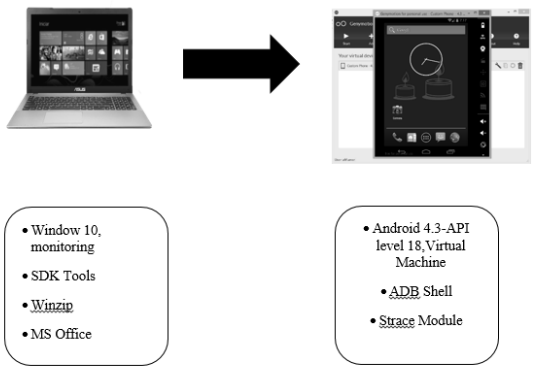

Fig. 2. Lab architecture.

TABLE. I. SOFTWARES USED

Software	Function
Genymotion	Android emulator
Microsoft Excel	Display log dataset in xlsx format Tabulate result recorded
WinZip	Unzip compressed file
ApkTool	Decompile apk resource file into a folder
Strace	Learn application behavior effectively through system calls
Android SDK	Conduct the dynamic analysis
Android Studio	Build application

Table 1 displays the softwares used for the experiment. For this research, the training dataset consists of 179 different types of mobile malwares from 5560 Drebin dataset [4]. While for the testing, 500 mobile applications (apps) have been randomly selected from Google Play Store. The Drebin dataset includes all dataset from the Android Malware Genome Project. It is among the largest malware dataset, free and widely used by many researchers such as by [2], [6], [10]-[13].

The dynamic analysis was used to capture the system call while static analysis was used to capture permission. Then all the extracted system calls and permissions were classified by using covering algorithm. For the dynamic analysis, the apk was installed in Genymotion and being controlled by Android Debug Bridge (ADB). Then the running processes and system calls of the apk were identified and extracted. Fig. 3 displays an example of a screen shot for the system calls captured and Fig. 4 displays an example of a screen shot for the permissions captured. As for the static analysis, the permissions were extracted in the Genymotion where Dexplorer being installed inside it.

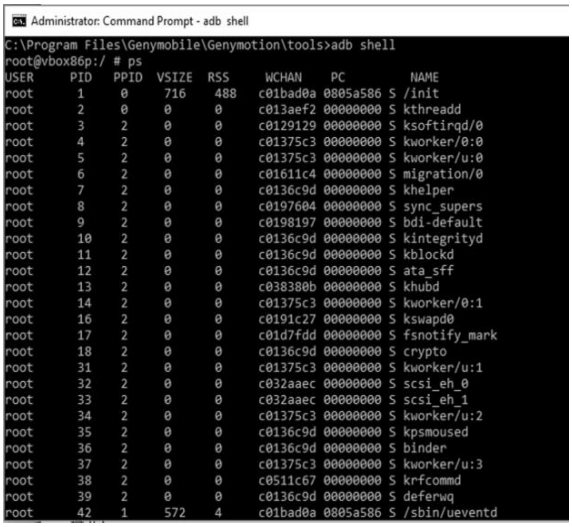

Fig. 3. Screenshot of system call captured.

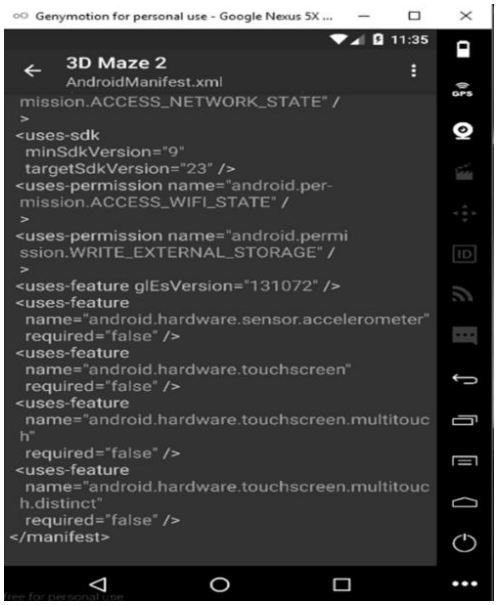

Fig. 4. Screenshot of permissions captured.

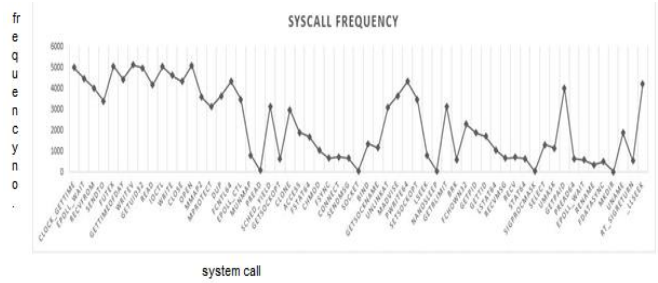

Fig. 5. System calls frequency.

Fig. 5 displays an example of the system calls frequency. Once all the permissions and system calls have been extracted, percentage of occurrence and covering algorithm were applied. These are crucial to verify the extracted dataset and to produce pattern. The percentage of occurrence is developed to compare the similarity between the extracted system calls and permissions. This is useful to avoid redundancy. Each of the system call occurrence is written as 1 to indicate the presence of the system call and 0 for vice versa. Then, the total of the presence and absence of the system calls and permissions were calculated and being compared with the existing dataset.

Once above steps are completed, the output became the input for the covering algorithm. The covering algorithm is used to generate system call and permission pattern for each apk. It identifies rules that have been set by the researchers. In this experiment, specific to general rule induction for covering algorithm has been applied as the following:

1) The extracted system calls and permissions are being picked up and generalized by repeatedly dropping condition.

2) If all the system calls and permissions covered by the set rule, then removed it and continue until all the system calls and permissions are covered.

3) When dropping the condition, make sure to choose the maximize rule coverage.

IV. FINDINGS

Thousands of system calls and permissions have been extracted, but the focus of this paper is on GPS exploitation. There are 58 system calls and 41 permissions out of 5560 samples that have been discovered that could be used together with genuine system calls for GPS exploitation. These system calls representation are shown in Table 2 and permissions representations are shown in Table 3.

TABLE. II. SYSTEM CALLS REPRESENTATION

Nominal Data	System call	Nominal Data	Systemcall
m1	clock_gettime()	m32	getsockname()
m2	epoll_wait()	m33	unlinkat()
m3	recvfrom()	m34	madvise()
m4	sendto()	m35	pwrite64()
m5	futex()	m36	setsockopt()
m6	gettimeofday()	m37	lseek()
m7	writev()	m38	nanosleep()
m8	getuid32()	m39	getrlimit()
m9	read()	m40	brk()
m10	ioctl()	m41	fchown32()
m11	write()	m42	getpid()
m12	close()	m43	gettid()
m13	open()	m44	lstat64()
m14	mmap2()	m45	recvmsg()
m15	mprotect()	m46	recv()
m16	dup()	m47	stat64()
m17	fcntl64()	m48	sigprocmask()
m18	epoll_ctl()	m49	select()

Nominal Data	System call	Nominal Data	Systemcall
m19	munmap()	m50	umask()
m20	pread()	m51	getpaid()
m21	sched_yield()	m52	pread64()
m22	getsockopt()	m53	rename()
m23	clone()	m54	fdatasync()
m24	access()	m55	mkdir()
m25	fstat64()	m56	uname()
m26	chmod()	m57	rt_sigreturn()
m27	fsync()	m58	_llseek()
m28	connect()		
m29	sendmsg()		
m30	socket()		
m31	bind()		

TABLE. III. FORTY-ONE PERMISSIONS

Nominal Data	Permission	Nominal Data	Permission
p1	access_course_location	p22	install_packages
p2	access_fine_location	p23	install_shortcut
p3	access_gps	p24	internet
p4	access_location_extra_commands	p25	kill_background_process
p5	access_network_state	p26	modify_audio_setting
p6	access_wifi_state	p27	read_calendar
p7	battery_stat	p28	read_call_log
p8	bluetooth	p29	read_contact
p9	bluetooth_admin	p30	read_external_storage
p10	call_phone	p31	read_logs
p11	camera	p32	read_phone_state
p12	change_network_state	p33	read_settings
p13	change_wifi_multicast_state	p34	read_sms
p14	change_wifi_state	p35	receive_boot_complete
p15	clear_app_cache	p36	receive_mms
p16	control_location_updates	p37	receive_sms
p17	delete_packages	p38	record_audio
p18	disable_keyguard	p39	restart_packages
p19	expand_status_bar	p40	write_external_storage
p20	get_accounts	p41	write_settings
p21	get_tasks		

TABLE. IV. SIX TOP PERMISSIONS USED TO EXPLOIT GPS

ACCESS_COURSE_LOCATION
ACCESS_FINE_LOCATION
GET_ACCOUNTS
READ_EXTERNAL_STORAGE
READ_PHONE STATE
WRITE_EXTERNAL_STORAGE

Table 4 shows permission classification that mostly used together with system call to exploit GPS that have been extracted from the Drebin dataset. Through dynamic analysis, numerous system calls per application have been encountered until the execution was stopped. Based on system calls presence during dynamic analysis, logs of dataset were recorded.

Table 5 shows the top 10 system calls classification that widely used with permission and system call to exploit GPS that have been extracted from Drebin dataset.

Table 6 shows list of patterns which have been produced based on mostly used for GPS exploitation.

TABLE. V. TOP TEN SYSTEM CALLS USED FOR GPS CONNECTION

chmod() epoll_wait() ioctl() read() access()	socket() bind() connect() recv() writev()

TABLE. VI. THIRTY-TWO PATTERNS FOR POSSIBLE GPS EXPLOITATION

Pattern Representation	Pattern
GPS1	p1+p2 +p20+p30+p32+p40+ m2+m9+m10+m24+m26
GPS2	p1+p2 +p20+p30+p32+p40+ m2+m9+m10+m24+m26+m7
GPS3	p1+p2 +p20+p30+p32+p40+ m2+m9+m10+m24+m26+m7+m28
GPS4	p1+p2 +p20+p30+p32+p40+ m2+m9+m10+m24+m26+m7+m28+m30
GPS5	p1+p2 +p20+p30+p32+p40+ m2+m9+m10+m24+m26+m7+m28+m30+m31
GPS6	p1+p2 +p20+p30+p32+p40+ m2+m9+m10+m24+m26+m7+m28+m30+m31+m46
GPS7	p1+p2 +p20+p30+p32+p40+ m2+m9+m10+m24+m26+m7+m28+m30+m46
GPS8	p1+p2 +p20+p30+p32+p40+ m2+m9+m10+m24+m26+m7+m28+m31
GPS9	p1+p2 +p20+p30+p32+p40+

	m2+m9+m10+m24+m26+m7+m28+m31+m46
GPS10	p1+p2 +p20+p30+p32+p40+ m2+m9+m10+m24+m26+m7+m28+m46
GPS11	p1+p2 +p20+p30+p32+p40+ m2+m9+m10+m24+m26+m7+m30
GPS12	p1+p2 +p20+p30+p32+p40+ m2+m9+m10+m24+m26+m7+m30+m31
GPS13	p1+p2 +p20+p30+p32+p40+ m2+m9+m10+m24+m26+m7+m30+m31+m46
GPS14	p1+p2 +p20+p30+p32+p40+ m2+m9+m10+m24+m26+m7+m30+m46
GPS15	p1+p2 +p20+p30+p32+p40+ m2+m9+m10+m24+m26+m7+m31
GPS16	p1+p2 +p20+p30+p32+p40+ m2+m9+m10+m24+m26+m7+m31+m46
GPS17	p1+p2 +p20+p30+p32+p40+ m2+m9+m10+m24+m26+m7+m46
GPS18	p1+p2 +p20+p30+p32+p40+ m2+m9+m10+m24+m26+m28
GPS19	p1+p2 +p20+p30+p32+p40+ m2+m9+m10+m24+m26+m28+m30
GPS20	p1+p2 +p20+p30+p32+p40+ m2+m9+m10+m24+m26+m28+m30+m31
GPS21	p1+p2 +p20+p30+p32+p40+ m2+m9+m10+m24+m26+m28+m30+m31+m46
GPS22	p1+p2 +p20+p30+p32+p40+ m2+m9+m10+m24+m26+m28+m30+m46
GPS23	p1+p2 +p20+p30+p32+p40+ m2+m9+m10+m24+m26+m28+m31
GPS24	p1+p2 +p20+p30+p32+p40+ m2+m9+m10+m24+m26+m28+m31+m46
GPS25	p1+p2 +p20+p30+p32+p40+ m2+m9+m10+m24+m26+m28+m46
GPS26	p1+p2 +p20+p30+p32+p40+ m2+m9+m10+m24+m26+m30
GPS27	p1+p2 +p20+p30+p32+p40+ m2+m9+m10+m24+m26+m30+m31
GPS28	p1+p2 +p20+p30+p32+p40+ m2+m9+m10+m24+m26+m30+m31+m46
GPS29	p1+p2 +p20+p30+p32+p40+ m2+m9+m10+m24+m26+m30+m46
GPS30	p1+p2 +p20+p30+p32+p40+ m2+m9+m10+m24+m26+m31
GPS31	p1+p2 +p20+p30+p32+p40+ m2+m9+m10+m24+m26+m31+m46
GPS32	p1+p2+p20+p30+p32+p40+ m2+m9+m10+m24+m26+m46

TABLE. VII. PERCENTAGE OF APPLICATIONS THAT MATCH WITH SYSTEM CALLS AND PERMISSION BASED ON GPS EXPLOITATION

Pattern	**Google play applications**	**Application name**	**Application types**	**Percentage**
GPS 1	21	A1	Game	4.2%
		A2	Downloader	
		A3	Game	
		A4	Game	
		A5	Entertainment	
		A6	Game	
		A7	Music	
		A8	Location	
		A9	Launcher	
		A10	Game	
		A11	Education	
		A12	Game	
		A13	Entertainment	
		A14	Communication	
		A16	Map	
		A17	Weather	
		A18	Travel	
		A19	Browser	
		A20	Map	
		A21	Map	
		A22	Comic	
GPS 2	21	A23	Game	4.2%
		A24	Downloader	
		A25	Game	
		A26	Game	
		A27	Entertainment	

		A28	Game	
		A29	Music	
		A30	Location	
		A31	Launcher	
		A32	Game	
		A33	Education	
		A34	Game	
		A35	Entertainment	
		A36	Communicatio n	
		A37	Map	
		A38	Weather	
		A39	Travel	
		A40	Browser	
		A41	Map	
		A42	Map	
		A43	Comic	
GPS 3	1	A45	Downloader	0.2%
GPS 4	1	A46	Downloader	0.2%
GPS 5	0	None	0	0%
GPS 6	0	None	0	0%
GPS 7	0	None	0	0%
GPS 8	0	None	0	0%
GPS 9	0	None	0	0%
GPS 10	0	None	0	0%
GPS 11	2	A47	Games	0.4%
		A48	Downloader	
GPS 12	0	None	0	0%
GPS 13	0	None	0	0%
GPS 14	0	None	0	0%
GPS 15	0	None	0	0%
GPS 16	0	None	0	0%
GPS 17	0	None	0	0%
GPS 18	1	A49	Downloader	0.2%
GPS 19	2	A50	Game	0.4%
		A51	Downloader	
GPS 20	0	None	0	0%
GPS 21	0	None	0	0%
GPS 22	0	None	0	0%
GPS 23	0	None	0	0%
GPS 24	0	None	0	0%
GPS 25	0	None	0	0%
GPS 26	2	A52	Game	0.4%
		A53	Downloader	
GPS 27	0	None	0	0%
GPS 28	0	None	0	0%
GPS 29	0	None	0	0%
GPS 30	0	None	0	0%
GPS 31	0	None	0	0%
GPS 32	0	None	0	0%

From 32 proposed patterns for potential GPS exploitation, only 21 of them which were downloaded from Google Play Store matched with our proposed patterns as summarized in Table 7.

Then from Table 7, the categories of these 21 apps are summarized in Table 8.

TABLE. VIII. CATEGORIES OF THE MATCHED MALICIOUS APPLICATIONS

No	Malicious Application	Type
1	Apps1	Game
2	Apps2	Downloader
3	Apps3	Games
4	Apps4	Game
5	Apps5	Entertainment
6	Apps6	Game
7	Apps7	Music
8	Apps8	Location
9	Apps9	Launcher
10	Apps10	Game
11	Apps11	Education
12	Apps12	Game
13	Apps13	Entertainment
14	Apps14	Communication
15	Apps15	Map
16	Apps16	Weather
17	Apps17	Travel
18	Apps18	Browser
19	Apps19	Map
20	Apps20	Map
21	Apps21	Comic

V. CONCLUSION

Based on the analysis results in this paper, it can be concluded that each of the executed mobile application has its own system call and permission. GPS has been identified as one of the features and has been used for different purposes. Thirty-two possible patterns for GPS exploitation of system calls and permissions combination are presented in this paper. Without users' consent, their confidential information especially that is related with their location or GPS can be easily exploited by the attackers. Thus based on 21 mobile apps that matched with our patterns, it is proven that GPS feature in the Android smartphone can be exploited by android mobile malware through permission and system call. For future work, this research can be used as guidance for other researchers to extend their work with the same interest and domain. These 32 patterns can be used as a database and input for the formation of a new model to detect mobile attacks exploitation via GPS. Furthermore, automatic for system call and permission extraction is another challenge to be tackled in future.

ACKNOWLEDGMENT

The authors would like to express their gratitude to Ministry of Higher Education (MOHE), Malaysia and Universiti Sains Islam Malaysia (USIM) for the support and facilities provided. This research paper is funded under grant: [FRGS/1/2014/ICT04/USIM/02/1].

REFERENCES

[1] A. Altaher, "Using Weighted Bipartite Graph for android malware classification", International Journal of Advanced Computer Science and Applications, vol. 8, no. 4, 2017.

[2] A. Feizollah, N. Anuar, R. Salleh and A. Wahab, "A review on feature selection in mobile malware detection", Digital Investigation, vol. 13, pp. 22-37, 2015.

[3] M. Egele, T. Scholte, E. Kirda and C. Kruegel, "A survey on automated dynamic malware-analysis techniques and tools", ACM Computing Surveys, vol. 44, no. 2, pp. 1-42, 2012.

[4] D. Arp, M. Spreitzenbarth, H. Malte, H. Gascon, and K. Rieck, "Drebin: effective and explainable detection of android malware in your pocket," Symp. Netw. Distrib. Syst. Secur., no. February, pp. 23–26, 2014. http://doi.org/10.14722/ndss.2014.23247.

[5] H. Kang, J. Jang, A. Mohaisen, and H. K. Kim, "Detecting and classifying android malware using static analysis along with creator information," Int. J. Distrib. Sens. Networks, vol. 11, no. 6, p. 479174, Jun. 2015. http://doi.org/10.1155/2015/479174.

[6] S. Wu, P. Wang, X. Li, and Y. Zhang, "Effective detection of android malware based on the usage of data flow APIs and machine learning," Inf. Softw. Technol., vol. 75, pp. 17–25, Jul. 2016. http://doi.org/10.1016/j.infsof.2016.03.004

[7] M. Singhal and A. Shukla, "Implementation of location based services in android using GPS and web services," Int. J. Comput. Sci. Issues, vol. 9, no. 1, pp. 237–242, 2012.

[8] Ma, S., Tang, Z., Xiao, Q., Liu, J., Duong, T. T., Lin, X., & Zhu, H. (2013). Detecting GPS information leakage in android applications. Global Communications Conference (GLOBECOM), 2013 IEEE, 826–831. http://doi.org/10.1109/GLOCOM.2013.6831175.

[9] S. Vanjire, U. Kanchan, G. Shitole, and P. Patil, "Location based services on smart phone through the android application," Int. J. Adv. Res. Comput. Commun. Eng., vol. 3, no. 1, 2014. Retrieved from http://www.ijarcce.com/upload/2014/january/IJARCCE3B__A_unmesh_Location.pdf.

[10] M. Lindorfer, M. Neugschwandtner, L. Weichselbaum, Y. Fratantonio, V. van der Veen, and C. Platzer, "ANDRUBIS -- 1,000,000 apps later: A view on current android malware behaviors," in 2014 Third International Workshop on Building Analysis Datasets and Gathering Experience Returns for Security (BADGERS), 2014, pp. 3–17. http://doi.org/10.1109/BADGERS.2014.7.

[11] Hashim, H. A.-B., M. Saudi, M., & Basir, N. (2015). A systematic review analysis of root exploitation for mobile botnet detection. Lecture Notes in Electrical Engineering, 315, 925–938. http://doi.org/10.1007/978-3-319-07674-4.

[12] A. Karim, R. Salleh, M. K. Khan, T. Schreck, J. Hoffmann, and I. Witten, "SMARTbot: A behavioral analysis framework augmented with machine learning to identify mobile botnet applications," PLoS One, vol. 11, no. 3, p. e0150077, Mar. 2016. http://doi.org/10.1371/journal.pone.0150077.

[13] Bhatt, M. S., Patel, H., & Kariya, S. (2015). A survey permission based mobile malware detection, 6(5), 852–856.

A Review and Proof of Concept for Phishing Scam Detection and Response using Apoptosis

A Yahaya Lawal Aliyu
Faculty of Science and Technology (FST),
Universiti Sains Islam Malaysia (USIM),
71800 Nilai, Negeri Sembilan, Malaysia.

Madihah Mohd Saudi
Faculty of Science and Technology (FST),
Universiti Sains Islam Malaysia (USIM),
71800 Nilai, Negeri Sembilan, Malaysia.

Ismail Abdullah
Faculty of Science and Technology (FST),
Universiti Sains Islam Malaysia (USIM),
71800 Nilai, Negeri Sembilan, Malaysia.

***Abstract*—Phishing scam is a well-known fraudulent activity in which victims are tricked to reveal their confidential information especially those related to financial information. There are various phishing schemes such as deceptive phishing, malware based phishing, DNS-based phishing and many more. Therefore in this paper, a systematic review analysis on existing works related with the phishing detection and response techniques together with apoptosis have been further investigated and evaluated. Furthermore, one case study to show the proof of concept how the phishing works is also discussed in this paper. This paper also discusses the challenges and the potential research for future work related with the integration of phishing detection model and response with apoptosis. This research paper also can be used as a reference and guidance for further study on phishing detection and response.**

Keywords*—Phishing; apoptosis; phishing detection; phishing response

I. Introduction

As online technology is growing at a faster level, so have other numerous online activities such as advertising, gaming, and e-commerce. As online financial activities are on the rise, so have online fraudulent activities in which phishing is playing a major role for illegally obtaining private individual details. Phishing activities against financial institutions have become a regular occurrence leading to a rising concern about how to increase security on these sectors which could relate to banks and online shopping such as Ebay and Amazon. Fraudulent schemes conducted via the Internet are generally difficult to trace and prosecute, and they cost individuals and businesses millions of dollars each year. From computer viruses to web site hacking and financial fraud, Internet crime became a larger concern than ever in the 1990s and early 2000s. In response to such issue, different anti phishing tools were developed in order to counter such illegal online activities [1].

As for the phishing activities, it has also been evolving on a rapid level in order to evade other anti-phishing tools that are been developed to counter the phishing tricks. Phishing emails are also known to contain links to the infected website. Phishing email directs the user to the infected website where they are asked to type in their personal information such as username and password of account details, so that the website will hack the information related to whatever the user enters. Phishing email is also sent to a large number of people and the phishers will also try to count the percentage of people who read that email and entered the information. It is very difficult to find that the individuals are actually visiting an actual site or malicious site. Phishing is also understood to be a sort of brand spoofing or carding. As a result researchers are attempting to reduce the risk and vulnerabilities of such fraudulent phishing activities [2]. Some researchers also define phishing as a new type of network attack. The attacker creates a replica of an existing Web page to fool users for example by using specially designed e-mails or instant messages into submitting personal, financial, or password data to what they think is their service provides' Website [3]. According to [4], phishing is a social engineering crime which is carried out by impersonating a trusted third party in order to attain access to private data or information. These are numerous definitions by different researchers depending on their point of view relating to their research. It could also depend on the trends the researchers are facing during their study due to the fact that the phishing techniques are always changing. It is important to understand why phishing has taken a lot of interest on targeting financial sectors. Numerous reports have shown that financial sectors are always under constant attacks through phishing techniques. According to Laidlaw and colleagues the share of phishing messages intended against the financial sector which consist of banks, payment systems and online stores have been rapidly on the rise for several quarters in a row [5]. In their porting period, it has raised to 50.96% of the total number of reported phishing attacks against various organizations, which is 4.73% higher than the value for the second quarter of 2016 as displayed in Fig. 1.

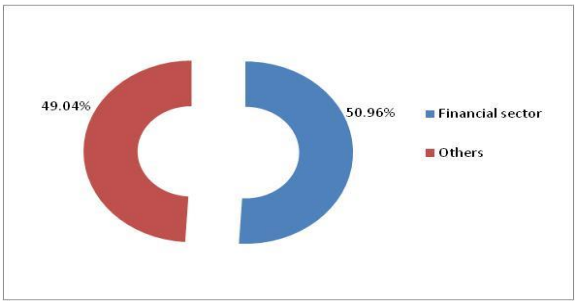

Fig. 1. Phishing target distribution of 3rd quarter (Q3) of 2016.

This research is funded by Ministry of Higher Education (MOHE), Malaysia and Universiti Sains Islam Malaysia (USIM).

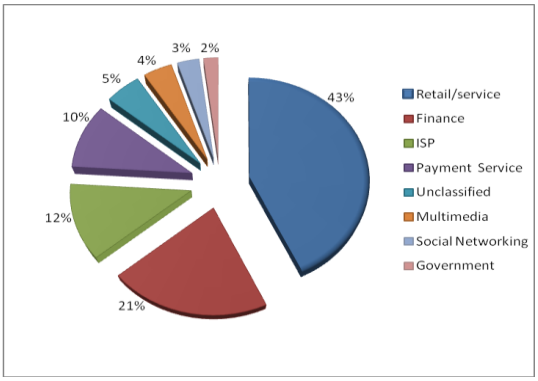

Fig. 2. Most recently targeted industries by phishing.

According to [6] there are many cyber-attacks targeted retail service sector, financial and payment service as displayed in Fig. 2. Financial gain is still known to be one of the major reasons behind most cybercriminal activities and there is no sign of this problem changing in the coming years or near future. Cybercriminals are continuously trying to make money. This is proved by the black market industry which has risen around different payments and card fraud. Cybercriminals have no problem coming up with different scams to make money [7].

Based on the phishing implication to financial sectors, therefore this paper aims to evaluate existing works related with the phishing detection and response techniques together with apoptosis. This paper also comes with a proof of concept (POC) on how the phishing attacks the victim. POC is important to help researcher to have a better understand on the phishing architecture. Hence the researcher will be able to grasp the idea how to detect and protect against phishing in future. This paper is organised as follows: Section 2 presents the related works with existing phishing detection methods and challenges. Section 3 explains the Apoptosis concept and benefits in applying it for protection against phishing. While Section 4 explains the POC of phishing attacks and Section 5 concludes and discusses future work for this paper.

II. Related Works

Different anti-phishing techniques have being on the rise in recent times due to the coming of advanced technological tools leading to an increase in phishing strategies invented by the perpetrators. Table 1 summarised the related works on anti-phishing tools.

In regards to the proposed research, despite the fact that there are existing works been implemented, applying the apoptosis concept against phishing activities will hopefully make improvements on the security aspect which will consist of not relying on black listing or white listing of website for threat identification. For the proposed research, implementing apoptosis should be able to identify any phishing threat through analysing of any slight change of message patterns within a network which could be either in the form of Domain Name Server (DNS) or a malware based phishing software from fraudsters. Another improvement to hoping to be made by using apoptosis concept is to improve protection against phishing by using its optimisation capability in which it will be able to measure its performance and policies to attempt to improve itself by reacting to any system changes by the user.

TABLE. I. Challenges Faced by Different Anti-Phishing Methods

Phishing Detection Tools	**Methods Used for detection**	**Challenges for improvement**
Proof Point [8]	• Offers a comprehensive solution for data protection and governance through an integrated, security-as-a-service platform.	Proofpoint solutions are complex and can include numerous modules that work together
CANTINA [9]	• Examine the content of a web page to find out whether it is legitimate or not. • Makes use of the well-known TF- IDF (term frequency/inverse document frequency) algorithm used in information retrieval.	Phishers are able to design their attacks to avoid CANTINA'S heuristic detection.
Auntie Tuna[10]	• It used with web browser plug-in that provides anti-phishing alerts whenever a user browses. • Indexes the target site's content and watches for this content to appear at incorrect sites which will identify a sign of active phishing.	Need to keep signature up to date against malware based phishing.
PhiGARO [11]	• It checks up on victims of phishing and prevents further harm related to the incident.	Depends on reports of phishing incidents from users.
Anomaly Based Phishing detection tool[12]	• Examine the anomalies in web pages, particularly, the difference between a web site's identity and its structural features and HTTP transactions.	False positives can become difficult using anomaly based setup.

Other limitations could be found in other phishing detection tools such as Anomaly based Phishing detection system which compares the fake website with the legitimate website by using Document Object Model (DOM) objects and Hyper Text Transfer Protocol (HTTP) transactions. The limitations noted are firstly, the network can be in an unprotected state as the system builds its profile, secondly if malicious activity looks like normal traffic to the system it will never send an alarm and false positives can become cumbersome with an anomaly based setup [12]. Although, some anti-phishing tools are useful, they also tend to have some limitations due to other circumstances. Also, as explained by [13], they described these flaws as follows:

- The attack could takes place at the necessary time for new (zero-day) phishing websites to be reported and hence added to the blacklist at that same time.
- The blacklist method may sometimes mislead to inform on a False Negative (FN) results showing that, the email or website is mistakenly identified as phishing.
- The white list method on the other hand is a collection of trustworthy URLs. This method however is a time consuming process. In addition, this method could cause an increased level of False Positive (FP) results, consequently letting phishing emails or websites to pass through; FP is meant to show that, the email or website is inaccurately identified as a legitimate.

Based on the limitations of all these anti-phishing tools that are mentioned, this research intends to come up with a new model on how to identify phishing activities based on using apoptosis algorithm which consist of a new phishing classification and also to optimise the accuracy of phishing detection rate by constructing new parameters. There are numerous phishing tools that are being developed due to the growing complication of phishing activities. One of these anti-phishing tool is the Logo Image Based Approach for Phishing Detection by [14]**.** This tool was built to capture screenshot and then commence with the approach in order to remove the logo. It focuses on to detect replaced images of the logo from downloaded image such as from image income of a query webpage by getting a screenshot to extract the logo. After capturing the screenshot, it will give the actual web content that is usually utilised for optimising the website loading speed.

Another phishing detection method is known as Feature Extraction or Feature Selection for Text Classification which is also a case study for phishing detection which was proposed by [15]. This tool deals with a lot of text classification which could be represented by thousands of token making the classification problem difficult. Therefore, dimensionality reduction is required to make the data representation much shorter and easier. This will make it possible to differentiate between emails. The techniques include feature extraction in which the original feature space is modified into a more compressed new space. Meanwhile, in feature selection technique, the original feature is chosen which will be used for the training and testing of the classifiers. The features that are discarded will not be used for the computations.

A research carried out on a phishing tool that was being performed by [16] is known as fMRI consisting of a study of Phishing and Malware Warning which measures the user's security performance together with the underlying neural activity with the task of distinguishing between a legitimate and phishing website. The phishing control experiment was built to take charge for stimuli offered for the phishing experiment whereby participants are instructed to observe the images shown on the screen without performing any active task. The neural activities were observed in which there were numerous indication of what was called top-down control and attention modulation system. The result of this phishing experiment showed significant activity in phishing activity during the study. It proved that such increased control might be critical for carrying out important judgment relating to the legitimacy of a website.

In regards to curbing out the problems of phishing, some authors are of the opinion that despite the benefits of online security tools, the people tend to be part of the problems which is also an issue to be solved in order to successfully reduce the online fraud effect. The researchers carried out a survey by using established questionnaires in order to evaluate information such as personality characteristics, impulsivity, web and computer based behaviour, previously experienced phishing consequences. In this survey, it was shown that people that are suspicious of others and also showing distrust on people have a low level of being affected by phishing attacks [17].

Dynamic analysis is to be utilised to carry out a test to observe how a phishing dataset will behave once sent by using email client server in the lab architecture. As for the proposed study, apoptosis method detection model aims to improve identification of any suspicious pattern related to phishing through the use of the dynamic analysis process in which any slight suspicious occurrence will be detected even if the fraudsters come up with new phishing procedure. The identity extractor will be further improved using the dynamic process. As for the page classifier, it may sometimes be bypassed due to being in an unprotected state while building its profile but improvement through implementing the apoptosis concept will be able to solve and rectify such limitation through its optimisation capability.

III. APOPTOSIS COMPUTING CONCEPT

For the apoptosis concept to be applied, it is important to note that it is divided into two parts. These parts are known as intrinsic and extrinsic apoptosis. Intrinsic apoptosis is known to be a reaction or response to damages that are internal such as damaged chromosomes or DNA. As for extrinsic apoptosis, it normally occurs as cellular immune response when invaded by external threat [18]. This research will use the extrinsic concept because that is the same process as being attacked by phishing from an external source.

As for the proposed research on phishing scam detection method using Apoptosis, it is meant to rectify these limitations by utilising its autonomous capability which consist of self-configuration, healing, optimisation and protection to provide full time protection against phishing related to financial frauds. Implementing the apoptosis concept is meant to overcome such weakness through its constant monitoring ability. The research proposes for a model is simplified. The process will consist of two phases. The PDA (Phishing Detection Apoptosis) consists of two phases. In regards to phase 1 in the PDA model, after the detection and Analysis, the PDA classification process will consist specifically of phishing site or email. After the analysis, the phishing mail or site will be classified followed by the data matching process which will perform the task of identifying and merging the records which corresponds with the same entities. The sample model can be seen in the Fig. 3.

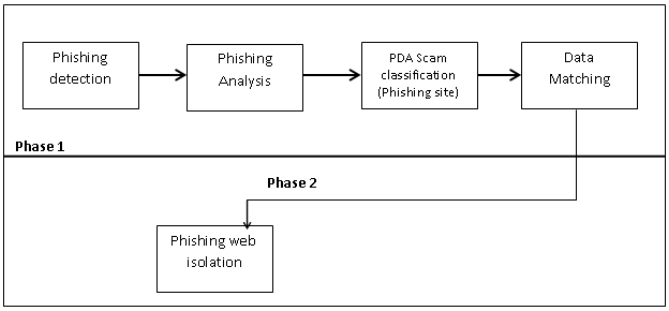

Fig. 3. Phishing Detection Apoptosis (PDA) Model.

Since multi-cellular computing is about virtual interaction rather than physical interaction, a computer only needs to be separated from communication and connection with any other computer. As a result, in computing issues, there should be more focus on quarantining an infected computer by cutting it off from the net. Rapid detection of infection is very important. Any infected computer, on average, could have the capability of infecting less than one other computer. Or else, the epidemic of infection may grow to other systems. Therefore the priority must be to detect infection quickly [19].

In describing Apoptosis implementation by [20], he explained it as a mechanism of a human immune system based on apoptosis that is adopted to build an Intrusion Detection System (IDS) to protect computer networks. Based on his work, features were selected from network traffic using Fisher Score. Also in relation to the selected features, the record/connection is classified as either an attack or normal traffic by the proposed methodology. Simulation results demonstrates that the proposed AIS based on apoptosis performs better than existing AIS for intrusion detection.

In issues that relate to the discipline of Natural Computing, the Apoptosis example can be observed within the context of Artificial Immune Systems [21]. Therefore the conception related to Apoptosis is utilised and embedded into computer system security in which a system is designed and developed from numerous types of small units and in this instance, if one becomes "damaged" through a computer malware, it will either initiate, or will be instructed to initiate Apoptosis concept without affecting other connected system components. This is similar to the analogy of being an animal cell that is invaded by a virus and the immune system knowing it is a foreign body and therefore will attack it. Inventing such type of artificial immune system for a self-managing autonomic computer system, such as a system with the ability to self-configuring, self-healing, self-optimising and self-protecting, is now been stated as a kind of a Holy Grail inspiring a different types of research papers. The autonomic computing paradigm is based on the biological metaphor of the Autonomic Nervous System in that it is self-managing without conscious input from the user, and is gaining ground as a way of designing and building systems capable of dealing with increasing cost and complexity [22].

The benefit of using this detection method is due to its interesting feature of being autonomic (acting involuntarily) without conscious control. It will be used on because Apoptosis detection tends to give full protection from any kind of threat.

The reason for such anticipated efficiency is also because it consists of self-managing cell which it uses for functional measurement with event correlation [23]. Some of its attributes are as follows:

- Self-configuration: The system must be able to readjust itself automatically, either to support a change in circumstances or to assist in meeting other system objectives.
- Self-healing: In reactive mode, the system must effectively recover when a fault occurs, identify the fault, and, when possible, repair it. In proactive mode, the system monitors. Vital signs to predict and avoid health problems, or to prevent their reaching undesirable levels.
- Self-optimization: The system can measure its current performance against the known optimum and has defined policies for attempting improvements. It can also react to the user's policy changes within the system.
- Self-protection: The system must defend itself from accidental or malicious external attacks, which requires an awareness of potential threats and the means to manage them.

Another interesting feature of Apoptosis as an autonomous system is the awareness of its components through its interconnectivity with other systems.

IV. FINDINGS

A case study using client server to perform a sample of phishing scam called phishing testis to shows the proof of concept (POC) on how the phishing works. Reverse engineering process and dynamic analysis were conducted to analyse the code using the architecture as illustrated in Fig. 4.

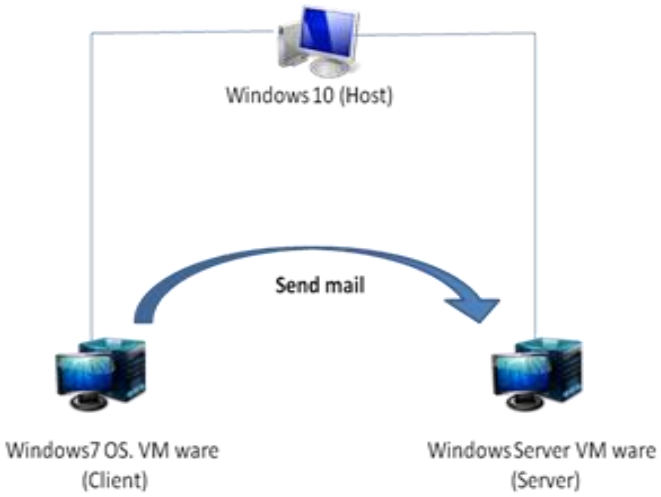

Fig. 4. Lab architecture.

TABLE. II. SOFTWARES FOR TESTING

Software	Function
MS Windows 10	To serve as a Host
MS Mail Server 2012	To receive the email
VM ware	To build virtual system in Host (Windows 10)
Windows 7	To function as Client
Process Monitor	To perform the analysis (Dynamic)
Process explorer	To perform the analysis (Dynamic)
Wireshark	To monitor the network traffic

The reverse engineering was performed in a controlled lab environment by using Windows 10 as the host for installing the testing tools. Windows 7 was used as the client and windows Server 2012 (Mail Server) was utilised as the server. Most of the software tools that were used for this experiment are freeware that can be downloaded freely from the internet. The tools are listed in Table II. The test was conducted within the virtual machine without the network connection. The phishing email dataset used was obtained from the malware traffic analyst website [24]. There are more than 2000 samples that can be freely downloaded for project uses. The dataset used for the test was a .pcap file.

After attaching the phishing mail sample to the virtual mail and sent to the server, numerous activities were observed using dynamic analysis tools. Both the client and server were used within a virtual network of the VM ware. For this experiment, outgoing network was not required. Further analysis showed that the phishing dataset attachment was able to successfully create a thread in which stolen information could be sent through. It also showed a buffer overflow in the result section which might cause loading of files to be slow with the following path at the registry.

HKCU\Software\Windows\CurrentVersion\Internet Settings\Connections\DefaultConnection.

For issue related to computer security, a buffer overflow is a strange activity where a program, during writing of data to a buffe's boiundry and overwrites adjacent memory locations.

Many fraudsters exploit buffer overfloe to gain access to a victims computer in order to gain access to information. The result is shown in Fig. 5. The file activity also made the outlook to do a "Thread Create" in the operation section which opens a registry key. This thread is known to be a holding place of information known to be related to single use program which may be handled by multiple users. Phishers may exploit this operation to retrieve information when using malware based phishing.

Based on the test conducted, it shows that phishing techniques can cause minimal distortions to make a system vulnerable to information theft. Therefore, implementing an efficient phishing detection model is to be performed in order to increase protection against phishing. As for future work, based on 4 concepts of the apoptosis, the concepts are listed and explained as follows:

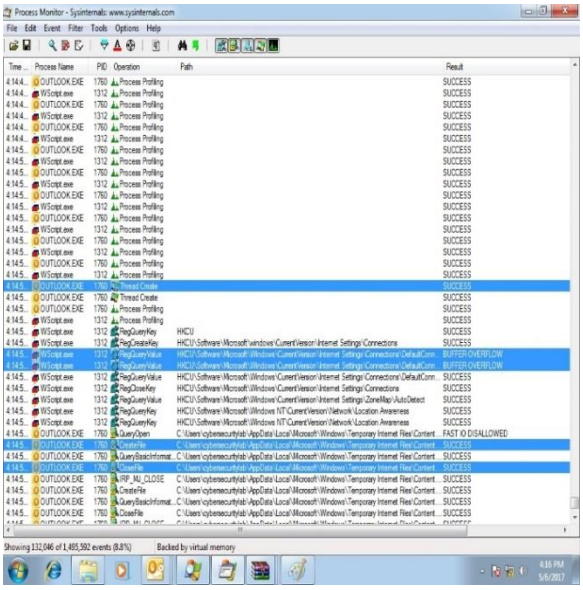

Fig. 5. Screen shot result after sending phishing email.

- Self- Protection: - In regards to this Apoptotic concept which is also known as Autonomic Defence System (ADS), it consist of very useful attributes comprising of protection of information system, actuators for implementing appropriate response, sensors for detecting attacks and lastly a controller for coordinating the sensors with the actuators.
- Self- Healing: - This concept enables the system to be able to automatically recover from any fault. Since fault detection is very important in order to develop an effective self- Healing system, the aim of this part of the system is to be able to do self-repair of components that might have failed without the need to bring down the whole system in order to ensure resource availability is maintained.
- Self- Configuration: - This concept enables the system to be able to adapt to any changes within its software environment or physical topology. This concept will also improve system reliability through rectification of human configuration errors which will in turn, reduce time wasting, therefore, making system resource available [25].
- Self- Optimisation: - For this concept, the system will be able to manage the systems complexity by responding to dynamic changes in order to improve the systems performance. The key aspects in optimisation are its resource utilisation and workload management. The main aims of these activities are to enable maximisation of system's operation.

These have been mapped to phishing detection and response technique as summarised in Table III.

TABLE. III. APOPTOSIS MAPPING TO PHISHING TECHNIQUE

Apoptosis Concept	Map to Phishing Detection and Response Technique
Self-protection	Defend against fake Domains sent by fraudsters
Self healing	Being able to recover from any malware based phishing file attack to the system
Self configuration	Automatically able to readjust itself to support the system (Improvement against any new phishing pattern)
Self-optimisation	Automatically adapt to any change, mostly against system complexities.

V. CONCLUSION

Phishing activities are evolving on a very fast level due to numerous innovations in online technology in recent times. Most malware programmers and online fraudsters are now inventing ways of bypassing many online security tools. For these reasons, it is highly required that online security is designed especially in the dynamic field sector. By utilising the use of Artificial Immune Systems such as Apoptotic computing, there is a high expectation of acquiring efficient result because of its method in detecting any malicious activity on a computer device or network. By thorough research, Apoptotic security concept will be implemented in order to hopefully increase the efficiency of protecting different fraudulent (Phishing) activities by identifying irregularities in both networks and system behavior within the online financial network.

This study will also aid other researchers to assist with coming up with new innovated ideas on how Artificial Immune Systems can be further developed in order to attain a more effective protection against online fraudulent activities. The model to be developed in this study will hopefully aid in coming up with the idea on reducing the effect of phishing on financial sectors. By utilising dynamic analysis for this study, a higher advantage will be attained against other anti-phishing tools especially the ones that rely on static analysis. Based on the findings on the proof of concept and other tests to be carried out for future analysis, the apoptosis model will be applied in order to observe the level of efficiency on how it will be able to detect any phishing pattern on a computer network with the aim of attaining a proper validation outcome.

ACKNOWLEDGEMENT

The authors would like to express their gratitude to Ministry of Higher Education (MOHE), Malaysia and Universiti Sains Islam Malaysia (USIM) for their support and facilities provided. This research paper is supported by grants: [USIM/FRGS/FST/32/50114] and [PPP/USG-0216/FST/30/16916].

REFERENCES

[1] Candid Wueest, "The state of financial Trojans 2014," Symantec Corporation, pp. 1-24, 2015.

[2] V. Suganya, "A Review on Phishing Attacks and Various Anti Phishing Techniques," Int. J. Comput. Appl., vol. 139, no. 1, pp. 975–8887, 2016.

[3] U.Naresh, "Intelligent Phishing Website Detection and Prevention System by Using Link Guard Algorithm," IOSR J. Comput. Eng., vol. 14, no. 3, pp. 28–36, 2013.

[4] Whittaker, C., Ryner, B., and Nazif, M. "Large-Scale Automatic Classification of Phishing Pages". In NDSS , Vol. 10, pp. 1, 2010.

[5] S .Laidlaw and M .Hillick, "Profiling cyber threats detected in a target environment and automatically generating one or more rule bases for an expert system usable to profile cyber threats detected in a target environment". U.S. Patent 9,503,472. Cyberlytic Limited, 2016.

[6] Anti-Phishing Working Group, "Phishing Activity Trends Report 1 Quarter," Most, no. March, pp. 1–12, 2010.

[7] R. Mohamad, A. Building, and N. A. Ismail, "Journal of Internet Banking and Commerce," J. Internet Bank. Commer., vol. 15, no. 1, pp. 1–11, 2010.

[8] H. Proofpoint, C. Help, and A. Proofpoint, "Why Today ' s Phishing Attacks are Harder to Detect and How Proofpoint Can Help Why Today ' s Phishing Attacks," no. 2, pp. 1–16.

[9] Y. Zhang, J. Hong, and L. Cranor, "Cantina: a content-based approach to detecting phishing web sites," Conf. World Wide Web, pp. 639–648, 2007.

[10] C. Ardi and J. Heidemann, "AuntieTuna : Personalized Content-based Phishing Detection," no. February, 2016.

[11] M. Husak and J. Cegan, "PhiGARo: Automatic phishing detection and incident response framework," Proc. - 9th Int. Conf. Availability, Reliab. Secur. ARES 2014, pp. 295–302, 2014.

[12] P. Ying and D. Xuhua, "Anomaly based web phishing page detection," Proc. - Annu. Comput. Secur. Appl. Conf. ACSAC, pp. 381–390, 2006.

[13] M. M. Al-daeef, N. Basir, and M. M. Saudi, "An anti-phishing tool to verify urls in email content," vol. 10, no. 3, pp. 1378–1382, 2015.

[14] H. Thakur and S. Kaur, "Logo Image Based Approach for Phishing Detection," vol. 6913, no. December 2016, pp. 129–139.

[15] M. Zareapoor and S. K. R, "Feature Extraction or Feature Selection for Text Classification: A Case Study on Phishing Email Detection," Int. J. Inf. Eng. Electron. Bus., vol. 7, no. 2, pp. 60–65, 2015.

[16] A. Neupane, N. Saxena, K. Kuruvilla, M. Georgescu, and R. Kana, "Neural Signatures of User-Centered Security: An fMRI Study of Phishing, and Malware Warnings," Proc. 2014 Netw. Distrib. Syst. Secur. Symp., no. February, pp. 1–16, 2014.

[17] M. Jakobsson, "The Human Factor in Phishing," Priv. Secur. Consum. Inf. 07, http//www.informatics.indiana.edu/markus/papers/aci.pdf, vol. 7, pp. 1–19, 2007.

[18] Z. Hongmei, "Extrinsic and Intrinsic Apoptosis Signal PathwayReview," Apoptosis Med., pp. 3–22, 2012.

[19] R. Sridevi and G. Jagajothi, "Apoptosis Inspired Intrusion Detection System," vol. 8, no. 10, pp. 1890–1896, 2014.

[20] D. Jones, "Implementing biologically-inspired Apoptotic behaviour in digital objects : An Aspect-Oriented Approach," no. March, 2010.

[21] M .Saudi, M.Woodward, J.Cullen and M .Noor, "An overview of apoptosis for computer security ". In Proc. International Symposium on Information Technology ITSim2008., 2008.

[22] R. Sterritt, "Apoptotic computing: Programmed death by default for computer-based systems," Computer (Long. Beach. Calif)., vol. 44, no. 1, pp. 59–65, 2011.

[23] T. Spotlight, C. Technologies, H. Education, S. Technologies, and S. Technologies, "Autonomic Computing When You Should Expect It," pp. 2001–2002, 2015.

[24] A source for Pcap abd Malware Samples. "Malware Traffic Analysis ". N.p., 2017. Web. 6 May 2017

[25] Dai. Y, Marshall. T & Guan. X, "Autonomic and Dependable Computing: Moving Towards a Model-Driven Approach," Journal of Computer Science., vol. 2, pp. 497-500, 2005.

Identifying Top-k Most Influential Nodes by using the Topological Diffusion Models in the Complex Networks

Maryam Paidar[1], Sarkhosh Seddighi Chaharborj[1, 2], Ali Harounabadi[3]
[1]Department of Computer Software, Islamic Azad University, Bushehr branch, Bushehr, Iran
[2]School of Mathematics and Statistics, Carleton University, Ottawa, Canada
[3]Department of Computer Software, Islamic Azad University Central Tehran Branch, Iran

***Abstract*—Social networks are sub-set of complex networks, where users are defined as nodes, and the connections between users are edges. One of the important issues concerning social network analysis is identifying influential and penetrable nodes. Centrality is an important method among many others practiced for identification of influential nodes. Centrality criteria include degree centrality, betweenness centrality, closeness centrality, and Eigenvector centrality; all of which are used in identifying those influential nodes in weighted and weightless networks. TOPSIS is another basic and multi-criteria method which employs four criteria of centrality simultaneously to identify influential nodes; a fact that makes it more accurate than the above criteria. Another method used for identifying influential or top-k influential nodes in complex social networks is Heat Diffusion Kernel: As one of the Topological Diffusion Models; this model identifies nodes based on heat diffusion. In the present paper, to use the topological diffusion model, the social network graph is drawn up by the interactive and non-interactive activities; then, based on the diffusion, the dynamic equations of the graph are modeled. This was followed by using improved heat diffusion kernels to improve the accuracy of influential nodes identification. After several re-administrations of the topological diffusion models, those users who diffused more heat were chosen as the most influential nodes in the concerned social network. Finally, to evaluate the model, the current method was compared with Technique for Order Preferences by Similarity to Ideal Solution (TOPSIS).**

Keywords*—Topological Diffusion; TOPSIS; Social Network; Complex Network; Interactive and Non-interactive Activities; Heat Diffusion Kernel

I. INTRODUCTION

Most networks existing around us are of complex type. These include neural networks, social networks, organizational networks, computer networks, etc. [1]. Today, social networks have drawn attention more than the others. Every social network is composed of two elements of users and relationships: Users are defined as any entity participating in a relationship and are called Nodes; relationships are the connections between entities and are called Edges. Different types of relationships (work, family, friends, etc.) can exist between nodes [2].

Development of social networks accelerates the spread of different types of information, including rumors, news, ideas, advertisements, etc. People's decisions to refuse or accept information depends on the diffusion or spread method of the information [3]. Therefore, choosing the individuals intended for spreading the information gains much importance. So far, several models have been proposed in social networks for identification of those individuals who have social influence among people. Many existing social influence models for the definition of influence diffusion are based solely on the topological relationship of social networks nodes. The ideas of topological diffusion models can be used in the process of diffusion and spread of influence, and it can be evaluated through topological relationships among nodes in a social network [4], [5].

In this paper, it is attempted to examine the social influence regarding the heat diffusion kernel phenomenon, i.e., the dynamical equations are modeled based on heat diffusion. In fact, the heat diffusion process finds the influential nodes in complex networks using heat transfer laws based on interactive and non-interactive activities. Therefore, users who receive heat more than others and have a greater increase in temperature curve are identified as the most influential nodes in a social network. Then, through defining the modified heat diffusion kernels, the accuracy of the identification of the influential nodes can be increased.

II. RELATED WORK

Doo & Liu in [3] proposed a model of social influence based on activities. Activity-based social influence is very effective in finding nodes in the social networks. In their paper, three types of topological diffusion, i.e., the Linear Threshold models (LT), Independent Cascade model (IC) and heat diffusion model have been fully expressed.

The authors in [6] carried out in 2015 for the first time the problem of influence maximization as a combination optimization problem. They considered two influences spread models, i.e. independent cascade and the linear threshold and evaluated these models extensively. But authors in [7] focused on the linear threshold model and presented a standard greedy algorithm in which the selection of a node with the maximum edge is increased repeatedly. The authors in [8] discussed mostly the time-critical influence maximization, where each node wants to reach maximize influence spread within a given deadline.

The authors in [9] presented three diffusion models together with three algorithms for selection of the best people. Their paper presented a new approach for analyzing social networks; subsequently, complexity analysis shows that the proposed model is also scalable to great social networks.

The authors in [10] designed a two-stage greedy algorithm (GAUP[1]) to find the most effective nodes in a network; GAUP initially computes the preferences of the user to a pattern that has latent feature model based on SVD[2] or a model based on vector space, then to find top-K nodes in the second stage, it utilizes a greedy algorithm.

A new technique [11] known as Technique for Order Preferences was presented by Similarity to Ideal Solution (TOPSIS weighted) to improve the ranking of node spread. With this method, the authors in [12] not only considered different centrality measures as the multi-attribute to the network but also proposed a new algorithm to calculate the weight of each attribute; and to evaluate its performance in four real networks they used the Susceptible– Infected–Recovered (SIR) model to do the simulation. Hu, *et al*.'s experiments on four real networks showed that the proposed method could rank the spreading ability of nodes more accurately than the original method.

III. METHOD

Social network models can be described by mathematical tools, such as graph and matrix. The most important property of graphs is their topological capability in which a vertex is created for each user, and if two users are friends with each other, the two vertices are connected. If a direction is attributed to each edge, the said network is called "directed", in which the order of vertices in an edge is important. Each row in the matrix corresponds to a vertex, and each column in the matrix also corresponds to a vertex. If there is a relationship/edge between two vertices of an edge, number 1 is used; otherwise, number 0 is inserted [13].

Users can send text, photo or video and like their friends, or write comments for them; hence, the users' activities can be divided into two categories: the interactive activities, i.e., those user activities that include nodes other than themself, and the non-interactive activities, which include only himself and not someone else. As an example, permission for commenting on the profile picture of another person is an interactive activity because it is implemented between two nodes and the picture in the profile page is a non-interactive activity because it includes only the node itself. If i is taken as a row and j as a column of a matrix, assume that IA_{ij} represents some interactive activities from node v_i to the neighboring node v_j and NIA_i are some non-interactive activities at node v_i. Upon combination of interactive and non-interactive activities, there are several methods for spreading heat diffusion kernel. Interactive and non-interactive activities are defined as $\left(IA_{ji} / \sum_{k:(v_j, v_k)\in E} IA_{jk} \right)$ and $\left(1-\left(NA_i / MAX\ (NA)\right)\right)$, respectively. The *MAX(NA)* is defined as the largest number of non-interactive activity in V [3]. Fig. 1 is an example of the topological structure of Twitter social network displaying top 10 users. The positive integer numbers on the edges represent the number of interactive activities, and positive integer numbers with underline at each node represent the number of non-interactive activities implemented by that node.

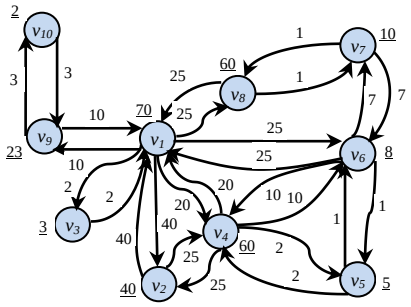

Fig. 1. A sample of social network (interactive and non-interactive activities).

Topological diffusion, as one of the processes of influence diffusion in social networks, exhibits the spread of influence through topological relationships between nodes. Heat diffusion model is one of such topological diffusion models. In this model, it is assumed that at the initial time t_0, in a social network of n nodes, all heat nodes except the node v_i has primary heat of zero. Node v_i which has some heat, is selected as a heat source and at time t_1, v_i diffuses the heat equally between all its neighbors. At time t_2, nodes with non-zero heat diffuser their heat to all their neighbors. With the repetition of this process for a period t for all n nodes, the influence of each node is found.

Suppose that $G = (V , E)$ represents a directional graph of social network, $V = \{v_1, v_2, ..., v_n\}$ is a set of vertices representing the number of users, and $E = \{(u,v)|u,v \in V\}$ is a set of edges representing the friendship relationship between users [14]. The heat at vertex v_i at time t is defined by the function $H_i(t)$; heat flows from a high-temperature node to a low-temperature node following the edges between vertices. In the directional graph, at time interval Δt, vertex v_i diffuses the heat to the amount of $DH_i(\Delta t)$ through output edges to next nodes. At the same time, the vertex v_j, receives the heat $RH_i(\Delta t)$ through input edges. Heat variations at vertex $V \in v_i$ between the time interval t and $t+\Delta t$ is defined with the sum of the differences between the heat that received, and the heat diffuses to, all its neighbors.

$$H_i(t+\Delta t) - H_i(t) = RH_i(\Delta t) - DH_i(\Delta t). \quad (1)$$

$DH_i(\Delta t)$ and $RH_i(\Delta t)$ are defined as (2) and (3):

$$RH_i(\Delta t) = \alpha \Delta t \sum_{j:(v_j, v_i)\in E} H_j(t) \left(\frac{IA_{ji}}{\sum_{k:(v_j, v_k)\in E} IA_{jk}} \right). \quad (2)$$

$$DH_i(\Delta t) = \alpha \Delta t\, H_i(t) \left(1 - \beta \frac{NA_i}{MAX\ (NA)} \right). \quad (3)$$

[1] Greedy Algorithm based on Users' Preferences (GAUP)

[2] Singular Value Decomposition (SVD)

Parameter α, called heat diffusion coefficient, controls the rate of heat transfer. Value of α is a real number between 0 and 1. If α tends to 0, heat transfer would be difficult, and the heat will not spread everywhere. If α tends to 1, without heat loss, all heat will be distributed among all neighbors, i.e., if α is big, the heat is diffused rapidly from one node to another. In this paper, the value of α is taken as 0.5, which means that the heat is transferred with a little loss between nodes. β in (3) is used as a weight for non-interacting activities and takes a real number between 0 and 1. If β is considered 0, it means that some of the non-interacting activities are ignored and have no effect on the heat diffusion process. But if β is set to 1, in heat diffusion process, node v_i loses its heat with a lower rate; in this paper, in all curves, the value of β is taken to be 0.5. Equation (2) and (3) can be combined with equation of heat variation (1) and obtain (4).

$$H_i(t+\Delta t)-H_i(t)=\alpha\Delta t\left(\sum_{j:(v_j,v_i)\in E}\begin{matrix}H_j(t)\left(\frac{IA_{ji}}{\sum_{k:(v_j,v_k)\in E}IA_{jk}}\right)-\\ H_i(t)\left(1-\beta\frac{NA_i}{MAX\ (NA)}\right)\end{matrix}\right). \quad (4)$$

In general, for n nodes, it can be written as (5):

$$H(t+\Delta t)-H(t)=\alpha\Delta t K H(t). \quad (5)$$

In (5), K is an $n\times n$ matrix representing the heat diffusion kernel from graph G, and $H(t)$ is a column vector representing heat distribution at time t in graph G, which is defined for primary heat source $H(0)$. Now the limit of (5) is taken on Δt when Δt approaches zero and gives (6).

$$\lim_{\Delta t\to 0}\frac{H(t+\Delta t)-H(t)}{\Delta t}=\lim_{\Delta t\to 0}\alpha K H(t),$$

$$\rightarrow \frac{dH(t)}{dt}=\alpha K H(t), \quad (6)$$

Then we take integral of both sides of (6):

$$\int\frac{dH(t)}{dt}=\int\alpha K dt. \quad (7)$$

Now if we take the *ln* of both sides of (7), the heat equation is defined as (8):

$$\rightarrow H(t)=e^{\alpha K t}H(0). \quad (8)$$

Then, using heat change equations *RH* and *DH*, two types of heat diffusion kernel are provided. Now, through MATLAB software, curves are drawn and with the help of curves, the most influential node can easily be found.

The first defined kernel is called heat diffusion kernel based on interactive and non-interactive activities. Matrix K is defined as:

$$K(i,j)=\begin{cases}IA_{ji}/\sum_{k:(v_j,v_k)\in E}IA_{jk} & ;\ (v_j,v_i)\in E\\ -\left(1-\beta\left(NA_i/MAX\ (NA)\right)\right) & ;\ i=j \text{ and } d_i>0\\ 0 & ;\ \text{otherwise.}\end{cases} \quad (9)$$

Fig. 2(a) illustrates the topological structure of heat diffusion based on interactive and non-interactive activities. This graph has been calculated and plotted using (9) and Fig. 1. As shown in the figure node v_1 neighbors six nodes v_2, v_3, v_4, v_6, v_8 and v_9. Two nodes v_4 and v_6 have four neighboring nodes; nodes v_1, v_2, v_5 and v_6 neighbor node v_4 and nodes v_1, v_4, v_5 and v_7 are four neighbors of node v_6. Each of nodes v_2, v_5, v_7, v_8 and v_9 is directly related to two nodes. Finally the nodes v_3 and v_{10} have one neighbor, it means that the node v_1 is the only neighbor of node v_3 and node v_9 is the only neighbor of node v_{10}.

Fig. 2(b) is the diagram of heat diffusion in which, as an example, node v_7 has been chosen as the heat source and is plotted by using (8) the diagram of heat diffusion. X-axis is the time line and Y-axis is the amount of heat at each node. The heat diffusion in this diagram is such that initially (at time zero), the heat source has a lot of heat and the rest of the nodes are without heat. At time 1, v_7 diffused heat to its neighbors (v_6 and v_8), and these two nodes gain heat. But node v_6 receives more heat and goes up. In this manner, the heat source reduces with time due to diffusion of heat to other nodes and the other nodes also receive heat from their neighbors and increase. Node v_1 receives more heat because it is directly linked with six nodes and increase more than all nodes; so it is obvious that it is ascending in the diagram. But nodes v_3 and v_{10} with just one neighbor will be the lowest limit of the diagram. A point worthy to note in this diagram is that in the time interval 10, two nodes v_2 and v_4 are higher than node v_6; the reason for that is that these two nodes receive more heat than node v_6; hence in the diagram, nodes v_2 and v_4 have higher increases.

The degree of each node is one of the influential factors for information diffusion. If d_j represents the degree of each node, the weight on the edges connected to node v_j is calculated as (10):

$$Weight\ v_j=\frac{1}{d_j}. \quad (10)$$

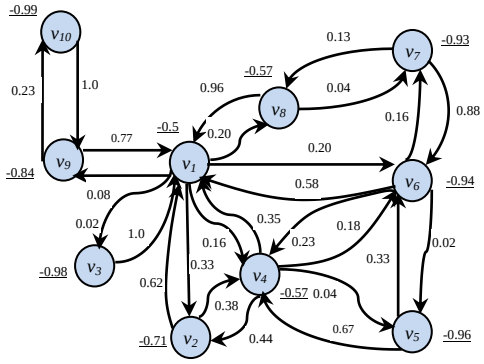

(a) Topological structure

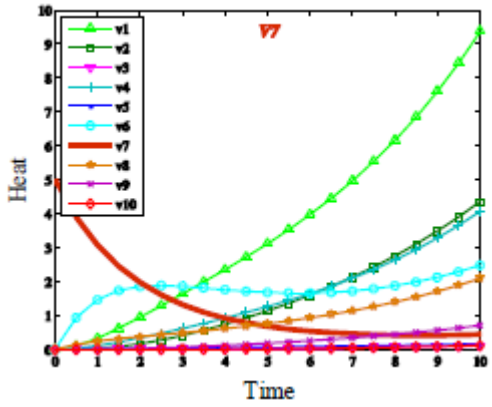

(b) Diagram of heat diffusion with heat source v_7

Fig. 2. Heat diffusion based on interactive and non-interactive activities.

Therefore, $RH_i(\Delta t)$ can be changed into (11):

$$RH_i(\Delta t) = \alpha \Delta t \sum_{j:(v_j, v_i) \in V} \frac{H_j(t)}{d_j}. \quad (11)$$

Now a new kernel called heat diffusion kernel can define through (11) and (3) based on the non-interactive activities.

$$RH_i(\Delta t) = \alpha \Delta t \sum_{j:(v_j, v_i) \in V} \frac{H_j(t)}{d_j}. \quad (11)$$

$$DH_i(\Delta t) = \alpha \Delta t H_i(t) \left(1 - \beta \frac{NA_i}{MAX\ (NA)}\right). \quad (3)$$

Matrix K changes as (12):

$$K(i,j) = \begin{cases} 1/d_j & ; \ (v_j, v_i) \in E \\ -\left(1 - \beta\left(NA_i / MAX\ (NA)\right)\right) & ; \ i = j \text{ and } d_i > 0 \\ 0 & ; \ \text{otherwise.} \end{cases} \quad (12)$$

Fig. 3(a) is drawn using (12) and Fig. 1. As it was mentioned above, d_j represents the degree of each node meaning that if the degree of each node is calculated based on (10), weight of the edge between nodes is obtained. As an example, vertices v_6 and v_8 are two neighbors of node v_7; therefore, the weight of 0.5 is assigned to $E(v_7, v_6)$ and $E(v_7, v_8)$, respectively, which means half of the heat of v_7 is transferred to v_6 and the other half to v_8. Node v_{10} has just one friend, which is vertex v_9. Thus, the weight of $E(v_{10}, v_9)$ is equal to 1. It means that the whole heat of v_{10} is diffused to v_9. Similarly, the edge weight between vertices is calculated.

For example, node v_7 is considered as a heat source and the heat diffusion diagram is plotted in Fig. 3(b) using (8). The heat diffusion process in this diagram is as follows: at time interval zero, the heat source has high heat, and the rest of the nodes are without heat.

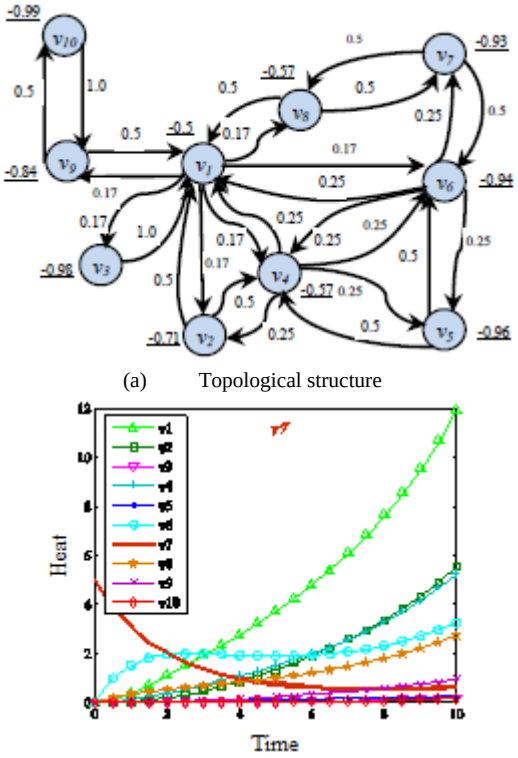

(a) Topological structure

(b) Diagram of heat diffusion with heat source v7

Fig. 3. Heat diffusion based on non-interactive activities.

With the passage of time, heat of the source reduces due to heat diffusion to other nodes; accordingly, heat increases in two nodes v_6 and v_8, which are directly related to heat source (v_7). But as shown, finally, it is node v_6, with more links to other nodes, which finally receives more heat and goes higher than node v_8. From time interval 4 onwards, node v_1 increases and surpasses all other nodes, even the heat source. Node v_1, with links to more nodes, receives higher heat. Therefore, expectedly, it follows an ascending trend.

A comparison of Fig. 2(b) and Fig. 3(b) diagrams indicates that in both diagrams, node v_1 is higher than all others; therefore, it is selected as the most influential node. But, as previously mentioned, the y-axis represents the receipt of the amount of heat; where each node receiving more heat goes higher.

Now, a comparison of node v_1 in both diagrams reveals that node v_1 in diagram Fig. 2(b) is higher than in diagram Fig. 3(b); therefore, it can be stated that diagram Fig. 2(b) has received more heat. It is thereupon implied that the heat diffusion kernel based on interactive and non-interactive activities (9) acts better than the heat diffusion kernel based on non-interactive activity (12); because the nodes in heat diffusion kernel based on interactive and non-interactive activity have received more heat. It is now attempted to obtain a modified kernel by combination of kernels in such a way that the most influential node receives more heat (i.e., it is higher in the y-axis). This core is expressed as (13):

$$K(i,j)=\begin{cases}\left(1+IA_{ji}\right)/\left(\sum_{k:(v_j,v_k)\in E} IA_{jk}+\dfrac{1}{d_j}\right); & (v_j,v_i)\in E\\ -\left(1-\beta\left(NA_i/MAX\ (NA)\right)\right) \quad ; \quad i=j \text{ and } d_i>0 & \\ 0 \quad ; \quad \text{otherwise.} & \end{cases} \tag{13}$$

Fig. 4(a), is the topological structure of the proposed kernel drawn using Fig. 1 and (13). As can be seen, the weight on the edges varies when (13) is applied. Heat diffusion diagram with heat source v_7 using (8) is indicated in Fig. 4(b). In this diagram also the heat source has a descending trend over time due to heat diffusion to other nodes; and still, node v_1 with more links has higher heat and increases more than other nodes. Accordingly, node v_1 is selected as the most influential node in the proposed kernel similar to the previously presented kernels.

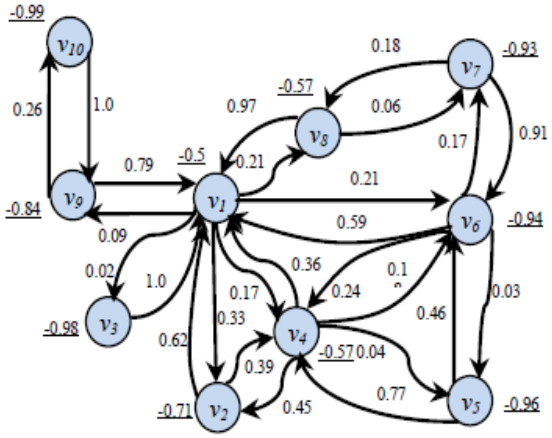

(a) The topological structure of proposed kernel

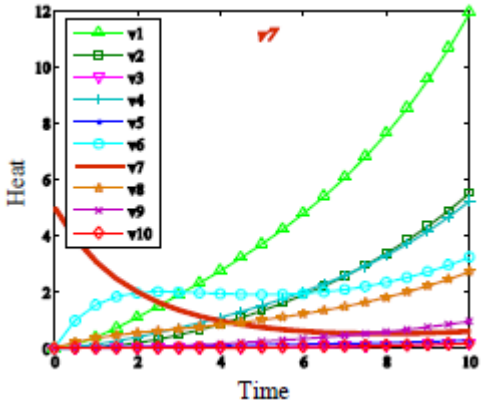

(b) Diagram of heat diffusion with heat source v7

Fig. 4. Heat diffusion of proposed kernel.

Heat diffusion kernel based on interactive and non-interactive activities is compared with the proposed kernel in two diagrams Fig. 2(b) and 4(b) in Fig. 5. In this diagram, too, node v_7 is selected as a heat source; continuous line represents the heat source of proposed method, and a dotted line represents the heat source of the method of interactive and non-interactive activities. Node v_1 (as the most influential node) for the proposed method is indicated as triangular and for the case of interactive and non-interactive method is shown as a circle. As seen in the diagram of Fig. 5, the triangular curve is higher than the circle curve, i.e. node v_1 in the proposed method receives more heat, and therefore triangular curve has higher increase. So the proposed kernel acts better than the heat diffusion kernel based on the interactive and non-interactive activities.

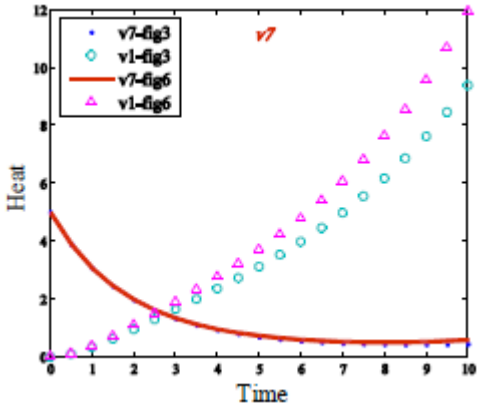

Fig. 5. Comparing best kernel with proposed kernel.

IV. Evaluation

In this section, two real data sets, Revije.paj and EIES.paj, are selected; then using Pajek software, the data is analyzed and implemented using MATLAB software. After that, TOPSIS method, which is a multiple criterion decision-making method, and is defined based on positive ideal solution and negative ideal solution, is used for evaluation. TOPSIS model evaluation and prioritization procedure will be as follows [4]:

The first step is development of a decision matrix; that is, using *m* criteria, *n* indexes will be evaluated.

The second step is normalization of the decision matrix. To that end, (14) is used, which is a vector method.

$$r_{ij}=\frac{x_{ij}}{\sqrt{\sum_{j=1}^{m} x_{ij}^{2}}} \quad ; \quad i=1,\ldots,m \quad ; \quad j=1,\ldots,n. \tag{14}$$

The third step is making weighted normalized decision matrix where the weight of criteria is calculated by (15).

$$v_{ij}=w_j\times r_{ij} \quad ; \quad i=1,\ldots,m \quad ; \quad j=1,\ldots,n. \tag{15}$$

In the fourth step, the positive and negative ideals are calculated. The highest performance of each index (positive ideal) and the lowest performance of each index (negative ideal) are represented by A^+ and A^-, respectively. These two indexes are calculated in (16) and (17).

$$A^{+}=\left\{\left(\max_i \ v_{ij} \mid j\in K_b\right)\left(\min_i \ v_{ij} \mid j\in K_c\right)\right\}. \tag{16}$$

$$A^{-}=\left\{\left(\min_i \ v_{ij} \mid j\in K_b\right)\left(\max_i \ v_{ij} \mid j\in K_c\right)\right\}. \tag{17}$$

In the fifth step, Euclidean distances of each criterion from the positive ideal and negative ideal are calculated by (18) and (19), respectively.

$$S_i^+ = \sqrt{\sum_{j=1}^{n}\left(v_j^+ - v_{ij}\right)^2} \quad ; \quad i = 1,\ldots,m \quad ; \quad j = 1,\ldots,n. \quad (18)$$

$$S_i^- = \sqrt{\sum_{j=1}^{n}\left(v_j^- - v_{ij}\right)^2} \quad ; \quad i = 1,\ldots,m \quad ; \quad j = 1,\ldots,n. \quad (19)$$

The sixth step is the calculation of ideal solution, i.e., the relative closeness of each criterion to the ideal solution, which is obtained by (20).

$$C_i = \frac{S_i^-}{S_i^- + S_i^+} \quad ; \quad i = 1,\ldots,m. \quad (20)$$

Prioritization is based on the value of C_i^+ where this value can be $0 \le C_i^+ \le 1$. When this value is closer to one, it indicates the highest rank, and when this value is close to zero it indicates the lowest rank.

A. Revije Data Set

Revije is a data set of Slovenian magazines and journals published in 1999 and 2000[3] [15]. 124 different magazines and journals were listed, and over 100,000 people were asked to read magazines and journals. A typical network is created from this data set in which the magazines are the vertices. In this network, edges are directed and weighted; the ring at vertices corresponds to the readers of the magazine. If a reader has read two or more magazines, then those magazines are linked together, and the weight on that indicates the number of readers of two magazines. The topological structure of this data set is shown in Fig. 6.

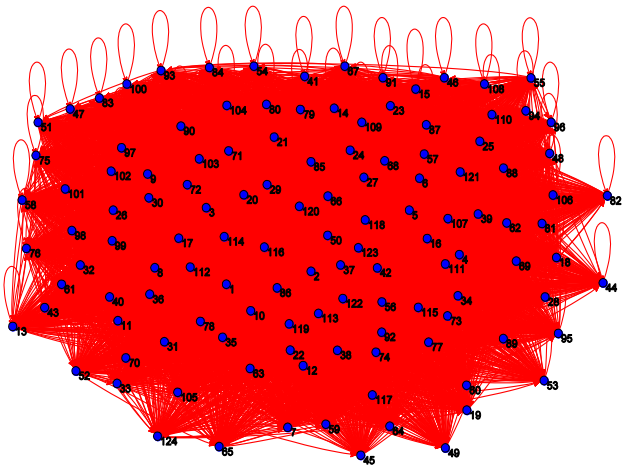

Fig. 6. The topological structure of Revije data set.

The data set of magazines and journals have interactive and non-interactive activities and include 124 vertices and 12068 edges. The highest degree of nodes is 123, which is related to nodes v_1, v_2, v_4, v_6, v_{27}, v_{42}, v_{113} and v_{119} and the lowest degree is 18, which belongs to node v_{50}. Ten highest nodes prioritized by TOPSIS model are shown in Table 1.

Node v_4 which has the highest priority in TOPSIS model is considered as the heat source. Top 10 nodes with the heat source v_4 for Revije data set are shown in Table 2, in the order of priority.

TABLE. I. THE ARRANGEMENT OF 10 SUPERIOR NODES BY THE TOPSIS MODEL FOR REVIJE DATA SET

Priority / Model	1	2	3	4	5	6	7	8	9	10
Model TOPSIS	v_4	v_1	v_{119}	v_{116}	v_3	v_{27}	v_{122}	v_2	v_{120}	v_{39}

TABLE. II. THE ARRANGEMENT OF 10 SUPERIOR NODES WITH THE HEAT SOURCE V_4 FOR REVIJE DATA SET

Priority / Method	1	2	3	4	5	6	7	8	9	10
Heat diffusion kernel based on interactive and non-interactive activity	v_4	v_{119}	v_1	v_{116}	v_{27}	v_{122}	v_{120}	v_{39}	v_2	v_3
Heat diffusion kernel based on the non-interactive activity	v_4	v_{119}	v_1	v_3	v_{116}	v_{39}	v_2	v_{120}	v_{27}	v_{122}
Proposed heat diffusion kernel	v_4	v_{119}	v_1	v_{116}	v_{27}	v_{122}	v_{120}	v_{39}	v_2	v_3

By comparing Tables 1 and 2, it can be seen that in all methods, node v_4 is the priority, but other priorities are different. For example, the second priority in TOPSIS method is node v_1 and in the heat diffusion method, node v_{119}. Hence, the heat diagrams of Revije dataset for two nodes v_1 and v_{119} are drawn in Fig. 7 and from that, the most influential node will be determined. For readability of the diagrams, the heat source (node v_4) is drawn only for the proposed heat diffusion kernel; heat diffusion kernel based on interactive and non-interactive activities are shown with φ_1, heat diffusion kernel based on non-interactive activity is shown by φ_2, and the proposed heat diffusion kernel is shown by φ_3.

As shown in Fig. 7, nodes v_1 and v_{119} are compared for the above-mentioned heat diffusion models, in both diagrams (a) and (b). Fig. 7(b) which is related to the node v_{119}, receives more heat compared with diagram Fig. 7(a) and thus has a higher ascending trend. So node v_{119} is more influential than node v_1 and has a higher priority. Hence, for advertisement and news diffusion, firstly node v_{119} and then node v_1 are selected.

[3] http://vlado.fmf.uni-lj.si/pub/networks/data.

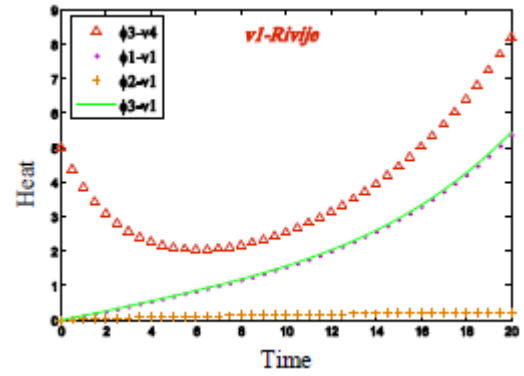

(a) Comparing node v_1 for all three diffusion models

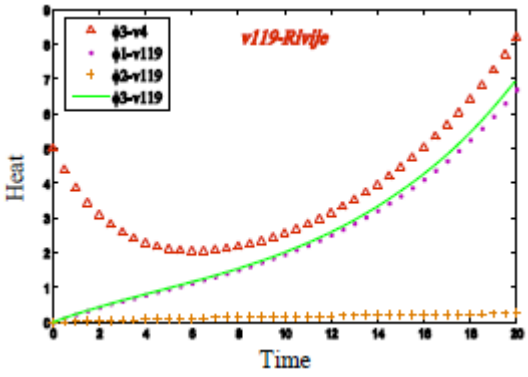

(b) Comparing node v_{119} for all three diffusion models

Fig. 7. Comparing the second priority for models presented in Revije.

B. EIES Data Set

EIES data set[4] [15] of Wasserman and Faust data collection is the second set of real data that has been considered in this paper. This data set also has interactive and non-interactive activities; its communication network is directional, weighted and has 32 nodes and 460 edges. Node v_1 with the degree 29 and node v_{25} with the degree 6 are highest and lowest degree in this data set, respectively. Fig.8 shows the topological structure of the data set.

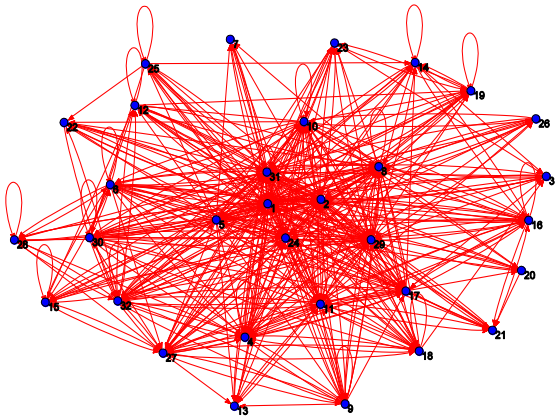

Fig. 8. The topological structure of EIES data set.

TABLE. III. THE ARRANGEMENT OF 10 SUPERIOR NODES BY THE TOPSIS MODEL FOR EIES DATA SET

Priority / Model	1	2	3	4	5	6	7	8	9	10
Model TOPSIS	v_1	v_{29}	v_8	v_2	v_{32}	v_{31}	v_{11}	v_{24}	v_{10}	v_4

TABLE. IV. THE ARRANGEMENT OF 10 SUPERIOR NODES WITH THE HEAT SOURCE V_4 FOR EIES DATA SET

Priority / Method	1	2	3	4	5	6	7	8	9	10
Heat diffusion kernel based on interactive and non-interactive activity	v_1	v_{32}	v_{29}	v_8	v_2	v_{31}	v_{11}	v_{24}	v_{27}	v_{10}
Heat diffusion kernel based on the non-interactive activity	v_1	v_{32}	v_{24}	v_{31}	v_2	v_{29}	v_5	v_8	v_{11}	v_{10}
Proposed heat diffusion kernel	v_1	v_{29}	v_{32}	v_8	v_2	v_{31}	v_{11}	v_{24}	v_{27}	v_{10}

In Table 3, the top 10 nodes based on the TOPSIS model are shown in the order of priority.

According to Table 3, node v1 in TOPSIS model has the highest priority; accordingly, in Table 4, the order of priorities of 10 superior nodes for data set EIES is indicated using v_1 as the heat source.

Comparing Tables 3 and 4, it can be seen that the priority in all methods belongs to node v_1, but other priorities vary. For example, the second priority in some methods is v_{29} while in some other ones, it is v_{32}. Thus, the diagram of heat diffusion of data set EIES for two nodes v_{29} and v_{32} is drawn in Fig. 9. Then, the most influential node is found from the diagrams. For readability of diagrams, the heat source (node v_1) is drawn just for the proposed heat diffusion kernel; heat diffusion kernel based on interactive and non-interactive activities are shown by φ_1, the heat diffusion kernel based on non-interactive activity is shown by φ_2 and proposed heat diffusion kernel is shown by φ_3.

By comparing the two diagrams (a) and (b) in Fig. 9, it is clear that the two diagrams have little difference. Now, if this is compared to diagram (c), which is related to node v_8 (third priority of TOPSIS model); for data set EIES, it can be stated that node v_8 has lower priority compared with node v_{32}. Therefore, nodes v_{29}, v_1 and v_{32} have the best condition for diffusion in social networks and they are more appropriate for spreading ideas and news or advertisements.

[4] http://vlado.fmf.uni-lj.si/pub/networks/data.

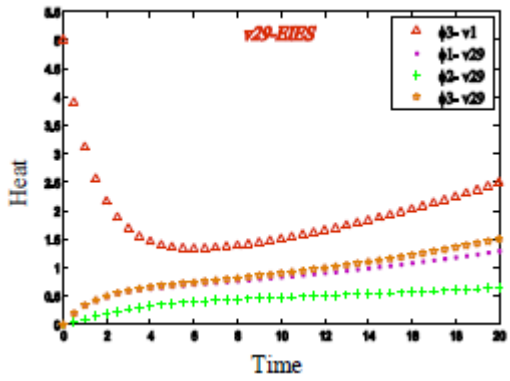

(a) Comparing node v_{29} for all three diffusion models

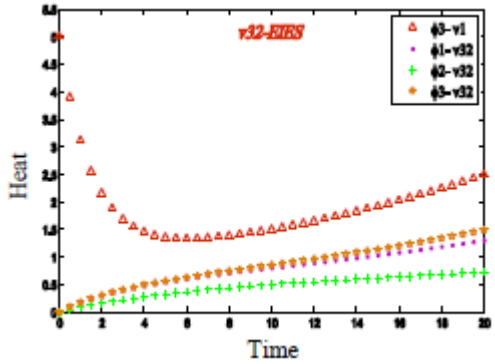

(b) Comparing node v_{32} for all three diffusion models

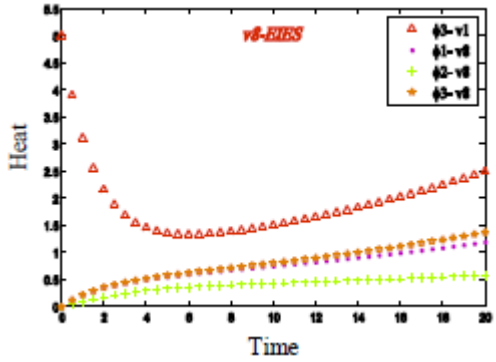

(c) Comparing node v_8 for all three diffusion models

Fig. 9. Comparing top nodes with heat source v_1 for models presented in EIES.

V. CONCLUSIONS

The most obvious problem in the field of social networks is finding *k* influential nodes in a network of individuals so as to benefit from the influence of these individuals in the entire network and diffuse the news in entire network to the most neighbors in the best and fastest possible way. Earlier, in the Methods section, three different heat diffusion kernels were defined: heat diffusion kernel based on interactive and non-interactive activities, heat diffusion kernel based on non-interacting activity and proposed heat diffusion kernel; this was followed in Experiments and Evaluation section by finding influential nodes for two data sets Revije and EIES (more specifically, node v_4 for Revije data set and node v_1 for EIES data set). Now in this section, the best heat diffusion kernel is depicted using Fig. 10. As stated previously, for readability of diagrams, the heat diffusion kernel based on interactive and non-interactive activities are shown by φ_1, the heat diffusion kernel based on non-interactive activity is shown by φ_2 and proposed heat diffusion kernel is shown by φ_3.

In Fig. 10(a), the diagram with the heat source for node v_4 in Revije data set is shown, where the diffusion kernel related to φ_3, which is the proposed diffusion kernel, is higher; in other words, since the proposed kernel has higher heat compared to the other two kernels, it has an ascending trend. In this diagram, heat diffusion kernel based on the non-interacting activity is lower than the other kernels.

In Fig. 10(b), the diagram with the heat source for node v_1 in data set EIES is drawn in which again the proposed diffusion kernel (φ_3) has increased more compared to the other two kernels, i.e., in EIES data set, the proposed kernel has higher heat. On the other hand, in this diagram also the heat diffusion kernel based on non-interactive activity is lower than the other kernels.

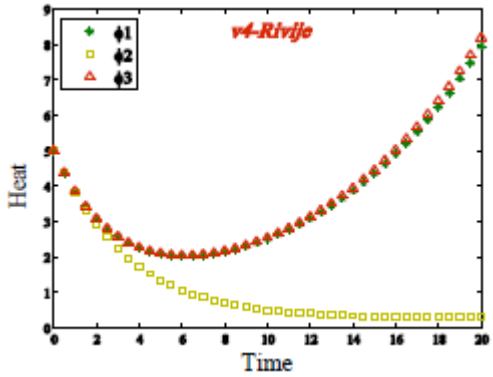

(a) The heat source of node v_4 for Revije data set

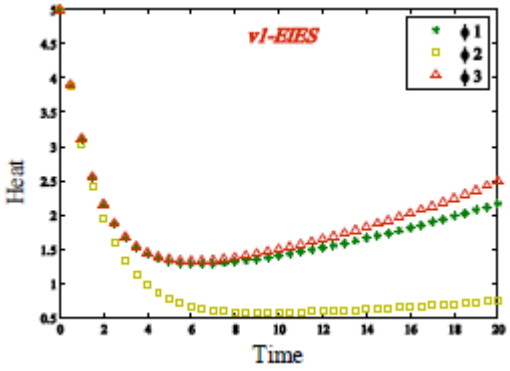

(b) The heat source of node v_1 for EIES data set

Fig. 10. Comparison of kernels to determine the highest priority of the kernel.

Therefore, proposed heat diffusion kernel in both data set Revije and EIES have higher increase and more heat. Thus, the order of kernels from the lowest to the highest priority can be concluded as the following:

1) Heat diffusion kernel based on the non-interactive activity.
2) Heat diffusion kernel based on interactive and non-interactive activity.
3) Proposed heat diffusion kernel.

REFERENCES

[1] S. Boccaletti, V. Latora, Y. Moreno, M. Chavez, and D. U. Hwang, "Complex networks: Structure and dynamics," *Physics Reports*, vol. 424, no. 4, pp. 175-308, Feb. 2006.

[2] M. E. Newman, "The structure and function of complex networks", SIAM review, vo1. 45, no. 2, pp. 167-256.و 2003.

[3] M. Doo, and L. Liu, "Extracting top-k most influential nodes by activity analysis," *In Information Reuse and Integration (IRI), 2014 IEEE 15th International Conference on*, 2014, pp. 227-236.

[4] R. M. Bond, C. J. Fariss, J. J. Jones, A. D. Kramer, C. Marlow, J. E. Settle, and J. H.Fowler, "A 61-million-person experiment in social influence and political mobilization", *Nature*, vol. 489, no. 7415, pp. 295-298, September 2012.

[5] I. Anger, and C. Kittl, "Measuring influence on Twitter", In Proceedings of the 11th International Conference on Knowledge Management and Knowledge Technologies, ACM, no. 31, September 2011.

[6] D. Kempe, J. Kleinberg, and É. Tardos, "Maximizing the spread of influence through a social network," *Theory of Computing*, vol. 11, no. 4, pp. 105-147, April 2015.

[7] Z. Lu, L. Fan, W. Wu, B. Thuraisingham, and K. Yang, "Efficient influence spread estimation for influence maximization under the linear threshold model," *Computational Social Networks*, vol. 1, no. 1, pp. 2, Dec 2014.

[8] W. Chen, W. Lu, and N. Zhang, "Time-critical influence maximization in social networks with time-delayed diffusion process," *In AAAI*, vol. 2012, pp. 1-5, July 2012.

[9] H. Ma, H. Yang, M. R. Lyu, and I. King, "Mining social networks using heat diffusion processes for marketing candidates selection," *In Proceedings of the 17th ACM conference on Information and knowledge management*, 2008, pp. 233-242.

[10] J. Zhou, Y. Zhang, and J. Cheng, "Preference-based mining of top-K influential nodes in social networks," *Future Generation Computer Systems*, vol. 31, pp. 40-47, Feb 2014.

[11] Y. Du, C. Gao, Y. Hu, S. Mahadevan, and Y. Deng,. "A new method of identifying influential nodes in complex networks based on TOPSIS", *Physica A: Statistical Mechanics and its Applications*, vol. 399, pp. 57-69, April 2014.

[12] J. Hu, Y. Du, H. Mo, D. Wei, and Y. Deng, "A modified weighted TOPSIS to identify influential nodes in complex networks," *Physica A: Statistical Mechanics and its Applications*, vol. 444, pp. 73-85, Feb 2016.

[13] J. Scott, "Social network analysis", *Sage*, 2012.

[14] P. Van Mieghem, "Graph spectra for complex networks", Cambridge University Press. 2010, pp. 13-17.

[15] V. Batagelj and A. Mrvar (2006). Pajek datasets.

Grid Connected PV Plant based on Smart Grid Control and Monitoring

Ibrahim Benabdallah
Faculty of Sciences of Tunis
Laboratory of Electric and Energetic Systems
El-Manar University, 10609
Tunis-Tunisia

Abeer Oun
Faculty of Sciences of Tunis
Laboratory of Electric and Energetic Systems
El-Manar University, 10609
Tunis-Tunisia

Adnène Cherif
Faculty of Sciences of Tunis
Laboratory of Electric and Energetic Systems
El-Manar University, 10609
Tunis-Tunisia

***Abstract*—Today, smart grid is considered as an attractive technology for monitoring and management of grid connected renewable energy plants due to its flexibility, network architecture and communication between providers and consumers. Smart grid has been deployed with renewable energy resources to be securely connected to the grid. Indeed, this technology aims to complement the demand for power generation and distributed storage. For this reason, a system powered by a photovoltaic (PV) has been chosen as an interesting solution due to its competitive cost and technical structure. To achieve this goal, a realistic smart grid configuration design is presented and evaluated using a radial infrastructure. Three-voltage models are used to demonstrate the grid design. Smart Meters are included via a SCADA to acquire and monitor the electrical signal characteristics during the day and to evaluate it through a statistical report. An operational data center (ODC) is used to collect the SMs statistical report and to review the demand-offer (DO) powers balance. The obtained results with Matlab/Simulink are validated by the famous ETAP software.**

Keywords*—*Distributed generation systems (DGS); smart grid (SG); smart meters (SM); photovoltaic systems (PVS)

I. Introduction

The integration of renewable energy sources, such as photovoltaic systems (PVS) into the electrical power grid (either low or medium voltage) throws up several technical troubles like instability, energy quality degradation, signal parameter fluctuation (current, voltage and frequency) and the renowned phenomenon of mismatch between load supply and demand. The economic problem of PV integration is the high installation cost due to lower PV penetration rate of these decentralized power stations. Indeed, electricity grids are stable systems contrarily to renewable energy plants (PV and Wind) which are decentralized, unpredictable and their connection to the grid could lead to instability while coupling them. These phenomena limit the integration of renewable energies into conventional grids and harm their sustainability [1]-[2].

This work aims to study these problems and propose some appropriate solutions to optimize production, control connection and stability via flexible smart grid architecture.

That is why it is indispensable to upgrade an ingenious power grid. There is twice, dealing ways to overpass this issue. The first way is the costly extension of transmission and distribution power systems to congregate overload demand shape. Or else, integrating decentralized renewable energy generators in co-generation seems to be the backing solution. Conversely, from the reviewed literature, earlier studies had proved that with the considerable integration, several drawbacks [3]-[7] concerning reliability of these systems appears to be real boundaries towards their integration.

With the considerable advancement reached in digital communication and IT technologies the concept of smart grid (SG) submerged. Its main concern is creating a communication between the power utility and the grid components throughout smart meters (SM). The main actors of the SG are SM, digital sensors, monitoring and control tools, automated actuators and bidirectional protection devices from production to plug or downstream path. Hence, the traditional grid is modernized into the bidirectional smart grid [8]-[10].

II. Related Works

Many simulations and modeling works have been conducted based on smart grid backbone structure over the last decade. In general, They discuss smart grid concept and applications, design, sizing and optimal placement of the energy mix, small scale test-bed implementations in order to choose the best strategy to its implementation, voltage stability, overall system integration rate, global losses and many other factors which help economical and technical decision-making [11].

One of the key features of the SG is the demand response dispatch. In this same context a smart grid is conceived by the authors in [12] by performing the smart demand-response dispatching. It implicitly promotes the reliability and sustainability of the power supply and lowering the peak demand. They presented a survey of potentials and benefits when enabling technologies such as energy controllers, smart meters and communication systems with reference to real industrial studies courses.

For example, authors of [13] conducted a systematic review of communication and networking technology architecture for a smart grid. Several technologies are used for the evaluation of the quality of service (QoS), control and management strategies.

In [14], a storage application based on renewable energies for green vehicle (P2V) and vehicle-to-grid (V2G) is developed. This study analyzed all service interactions between energy operators and other actors in smart grids such as consumers, distribution and transport.

Other study such as [15] is interested to present the solutions of the connection and the integration of renewable energy sources in the electric grid and their architectures.

In this context, we can note the work of [16] which used a Data Center Networks DCN as an efficient power management of SMART Grids modeled on OPNET 14.5 software. Besides, Data Center Networks (DCNs) cost-effectiveness and implementation challenges are discussed.

In [17] a new platform using SCADA software and XBEE wireless communication based on smart grid is presented. It combines software and hardware simulation. The implemented algorithm performs communication between buses and the ODC via Xbee.

III. METHODOLOGY

In this paper, we present two main novelties in comparison with last cited works. At first, we will present an improved electrical grid model dedicated to any smart grid based on power load profiles estimation which can be integrated with grid connected PV plants and conventional power generation stations. At a second plan, a realistic case study of a 500KW grid connected PV plant is developed. The PV chain is based on steady state modeling of the PVS connected to the MV level by means of the LV/MV transformer to the point of connection (POC).

The paper is divided as: Section VI presents an overview of the overall system design. Section V highlights interactions of the smart grid platform under variable daily climatic changes and sustainable load profiles. In Section IV, a validation using ETAP software is performed. Finally, in the last section conclusions are picked out from the presented work.

IV. GENERAL SYSTEM DESIDN

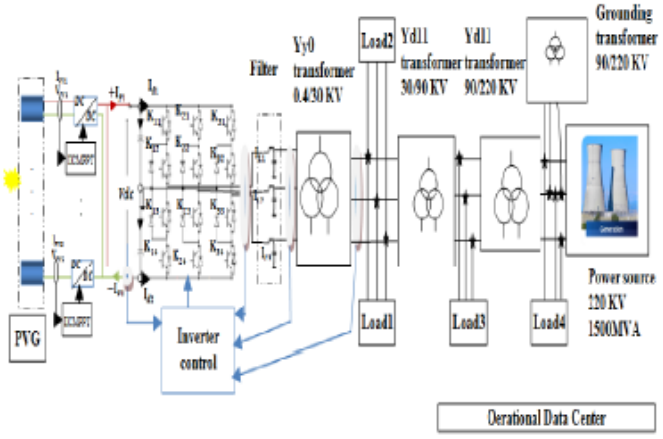

(a)

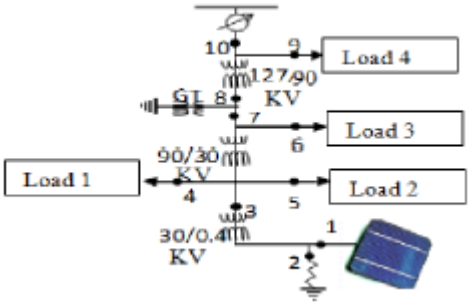

(b)

Fig. 1. (a) Overall System design (b) Equivalent one line diagram grid

The grid model described by Fig. 1(a) is composed of a conventional HTB power source delivering 220 KV per-phases and directly deserves "load 4". Then, the voltages are stepping down from 220 KV to 90 KV by transformer 3. The grounding transformer generates neutral wire. ''load 3" is the equivalent overall set of loads connected at 90 KV. Transformers 2 raised down the voltage from 90 KV to 30KV where "load1" and "load 2" are connected. The PVG is coupled to the POC throughout the first transformer. The observation and data operation center intercept wireless broadcast SMs information.

A. Traditional power source

A traditional power source produces typically from 35KW (micro turbine) to 400 MW (combined cycle gas) depending on load needs [18]. The power source is modeled as a set of ideal voltage source with internal inductance and resistance connected in (Yg) [19]. The short circuit level parameter leads us to indirectly compute the internal impedance:

$$L = \frac{V^2_{PS}}{P_{sc}} * \frac{1}{2\pi f} \quad (1)$$

$V_{PS} = 220KV, Psc = 1500MVA, \mathrm{f} = 50hz$

Once we evaluate L, R is then calculated from $\frac{X}{R}$.

B. Transformers

In every leg of the transformer we have an entrance winding and an output one. Thus, they are in number of 6 winding, two for every leg.

Consequently, we have six resistances modeling joule effect, and six self and mutual inductance modeling inter and intra magnetic effects.

The equation of the transformer model is given by [19], [20]:

$$\begin{bmatrix} V_1 \\ V_2 \\ V_3 \\ V_4 \\ V_5 \\ V_6 \end{bmatrix} = \begin{bmatrix} R_1 * I_1 \\ R_2 * I_2 \\ R_3 * I_3 \\ R_4 * I_4 \\ R_5 * I_5 \\ R_6 * I_6 \end{bmatrix} + \sum_{j=1}^{6} \begin{bmatrix} L_{1j} * \frac{dI_{1j}}{dt} \\ L_{2j} * \frac{dI_j}{dt} \\ L_{3j} * \frac{dI_{3j}}{dt} \\ L_{4j} * \frac{dI_{4j}}{dt} \\ L_{5j} * \frac{dI_{5j}}{dt} \\ L_{6j} * \frac{dI_{6j}}{dt} \end{bmatrix} \quad (2)$$

With:

R_i Windings' resistances, i=1..6.

L_{ii}, L_{ij} Are proper and mutual Windings' inductances?

i, j =1..6.

The parameters are calculated from the open and short-circuit tests applied to the transformer.

C. Equivalent Load profiles

Constant load profiles in every step voltage level correspond to four constant averaged and dispatchable loads that we have registered in MS-XL files. Their voltage and frequency are respected taking into account specificities in term of grid codes. Table1 shows their specified power values in kW and Kvar.

TABLE. I. LOAD PROFILES VALUES

Load n°	P_Kw	Q_Kvar
1	3000	350
2	1000	240
3	30000	1000
4	20000	1100

Loads are modeled using constant PQ loads.

D. Smart meters

The main role of Smart meters is to detect the electrical power characteristics and communicate them to the ODC. SM screens display broadcast waves:

$$\begin{cases} V_A = |V_A| \\ V_B = |V_B| e^{\frac{i2\pi}{3}} \\ V_C = |V_C| e^{\frac{i4\pi}{3}} \end{cases} \Rightarrow \begin{cases} V_{ASM} = \frac{|V_1|}{\sqrt{2}}\sqrt{3} \\ V_{BSM} = \frac{|V_2|}{\sqrt{2}}\sqrt{3} \\ V_{CSM} = \frac{|V_3|}{\sqrt{2}}\sqrt{3} \end{cases} \begin{cases} I_{ASM} = \frac{|I_1|}{\sqrt{2}} \\ I_{BSM} = \frac{|I_2|}{\sqrt{2}} \\ I_{CSM} = \frac{|I_3|}{\sqrt{2}} \end{cases} \quad (3)$$

$$\begin{cases} PQ_A = \frac{1}{2} V_A I_A^* \\ PQ_B = \frac{1}{2} V_B I_B^* \\ PQ_C = \frac{1}{2} V_C I_C^* \end{cases} \Rightarrow \begin{cases} P = PA + PB + PC \\ Q = QA + QB + QC \end{cases} \quad (4)$$

V_A, V_B, V_C are phase voltages.

V_{ASM} , V_{ASM} , V_{ASM} are smart meters broadcasted voltages.

I_{ASM} , I_{BSM} , I_{CSM} are smart meters broadcasted currents.

PQ_A , PQ_B , PQ_C are smart meters broadcasted branch powers.

PQ are smart meters broadcasted overall powers.

E. Line feeders

The transmission line is modeled as a balanced three-phase PI section in which the resistance, inductance, and capacitance are computed function of its length [19], [21]. The model is composed by a series resistance and inductance modeling cables length effects. Two parallel capacitance per-phase modeling interactions between the three wires. Finally, two capacities are modeling ground connections.

F. PV Generator model

The equivalent PVS model presents the average daily irradiance profile calculated from NASA surface meteorology and solar energy (34° 00'N and 9° 00'E), for a typical day, multiplied by the calculated total area landed by PV panels and taking into account GED system efficiency.

V. SIMULATION RESULTS

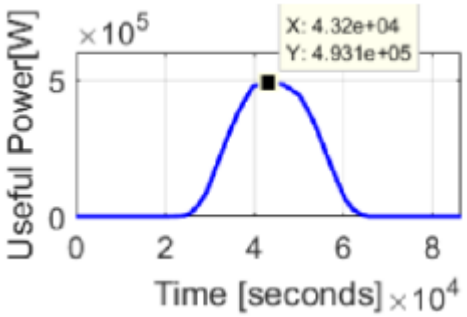

Fig. 2. Useful Power

Fig. 1(b) is the equivalent one line grid diagram in which the power source delivers 220 KV. The three transformer substations emulate the three voltage levels. The grounding transformer operates at 90KV voltage and generates the neutral wire. The uninterruptible equivalent loads are prescript in Table 1 expected to be fed from the generation power source and renewable PVG.

Fig. 2 presents the response of useful Power System after multiplying the irradiance by the area and the efficiency of the entire PV chain. At maximum power point the irradiance corresponds to 500W/m². The chain efficiency is about 15%. The output power is computed as the irradiance multiplied by the area and the efficiency.

Real power is equal to 6250*500* 15.8/100 = 493.75KW labeled in Fig. 2.

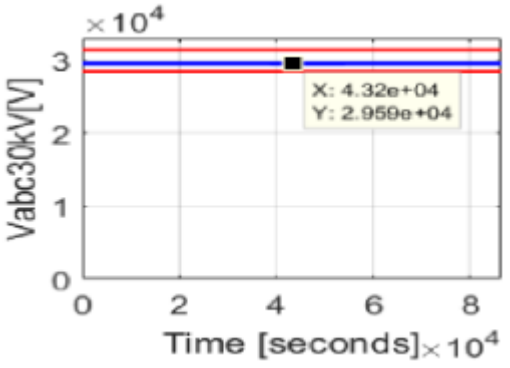

(a)

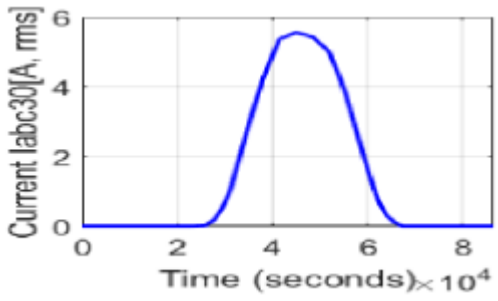

(b)

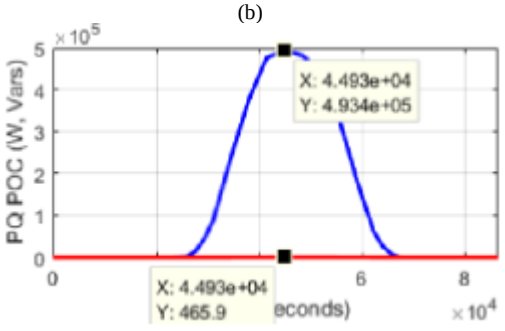

(c)

Fig. 3. (a) Bus 3 POC voltage (b) Bus 3 POC Current (c) Node3 received Power curve at POC

Fig. 3(a), 3(b), and 3(c) show the point of connection curves characteristics at Bus 3. Limits in red symbolize the boundaries of allowable variations in Fig. 3(a) and similarly for the voltage in all figures. The voltage signal remains quasi-invariable all through the day hours, even with irradiance changes. Active power is about 493 kW whereas reactive one is 466 Var.

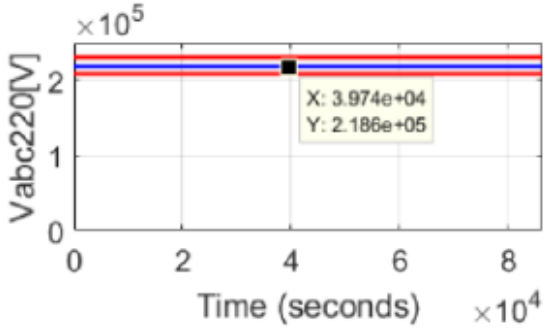

(a)

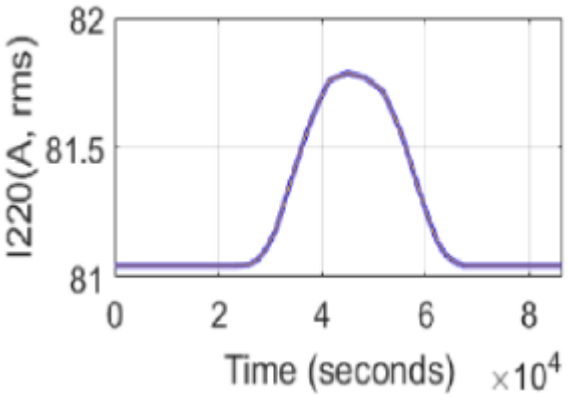

(b)

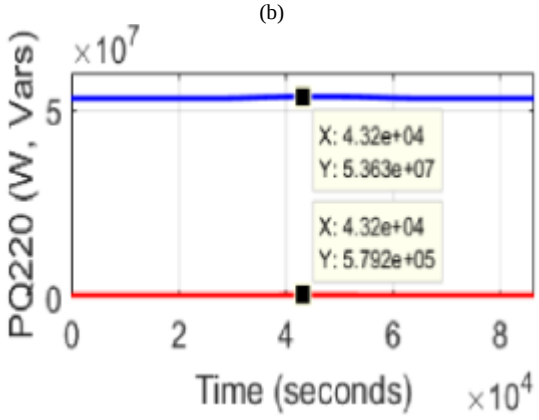

(c)

Fig. 4. (a) Bus 10 Generator voltage (b) Bus 10 Generator current (c) Bus 10 Generator Power

Fig. 4(a), 4(b), and 4(c) show 220 KV production level characteristics at Node10. The main generator produces about 53.63 MW active power and 579.2 Kvar reactive power already in 24 hours. The powers meet load demands either with existence of renewable power or not.

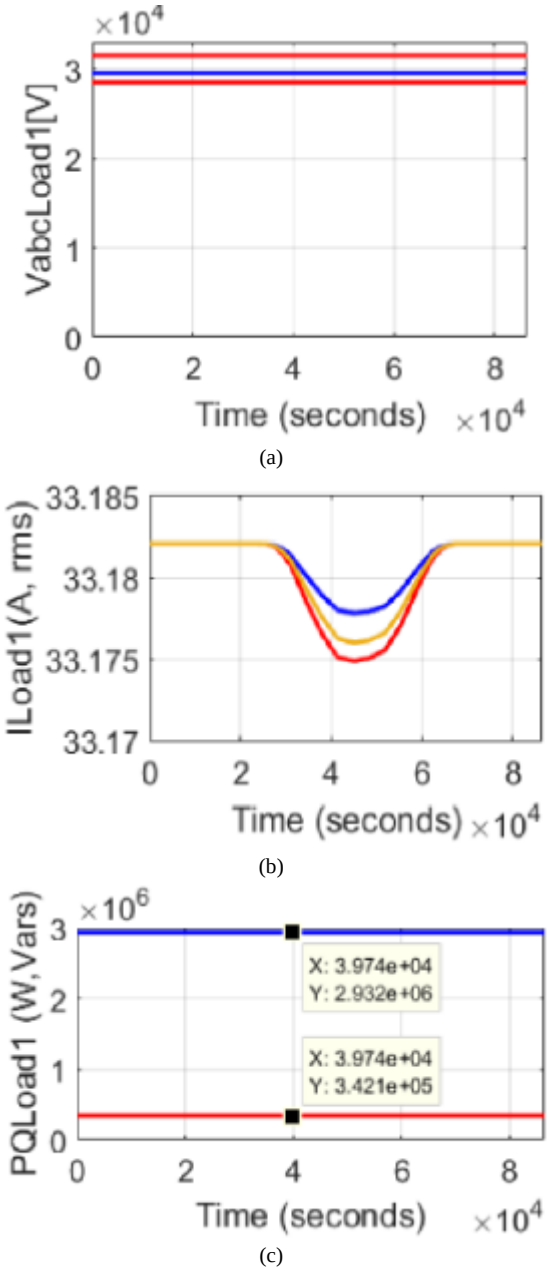

Fig. 5. (a) Bus 4 Voltage curve (b) Bus 4 Current curve (c) Bus4,"load1" power curve

Fig. 5(a), 5(b) and 5(c) show first load profile characteristics named "load1" at 30KV level, respectively, the voltage, current and received power at Node 4. Received real power to load1 is about 2.932MW and reactive power is 342.1 Kvar. The constant charge keeps Z unchangeable, even with current variation the voltage powers meet the requirements of Table 1.

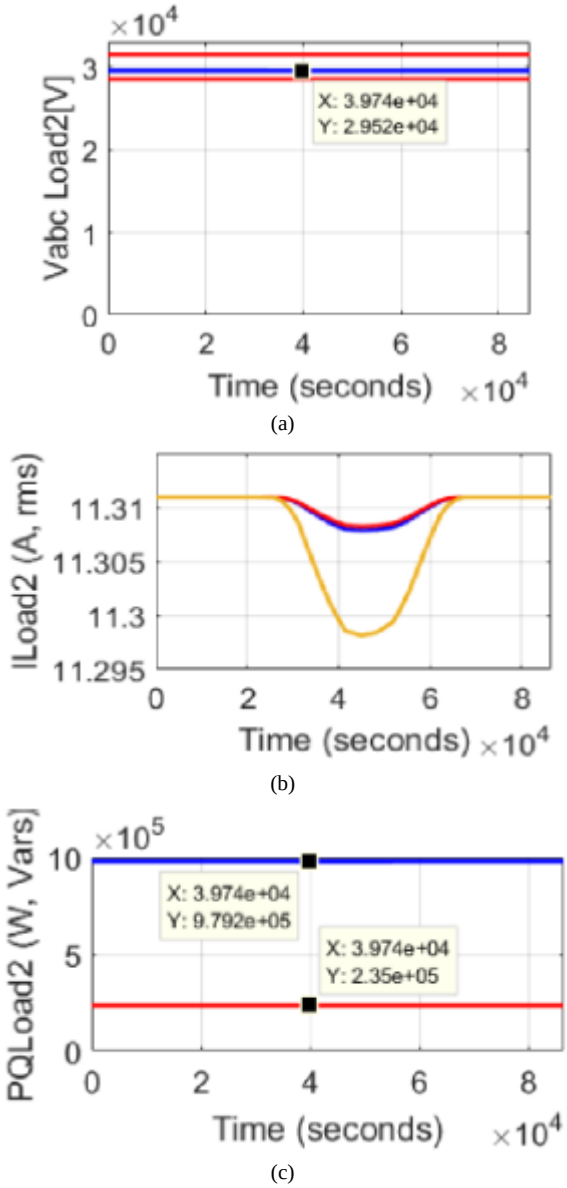

Fig. 6. (a) load2 voltage curve at Bus 6 (b) load2 current curve at Bus 6 (c) load2 power curve at Bus 6

Fig. 6(a), 6(b), and 6(c) present the second load profile characteristics named "load2" at 90KV level, respectively Bus 6 voltage, current and received power. Powers value is 979.2KW and 235 Kvar satisfy the load needs.

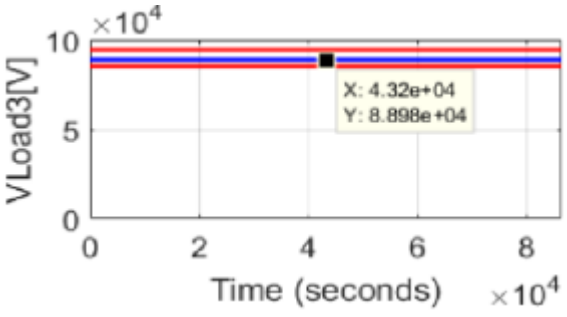

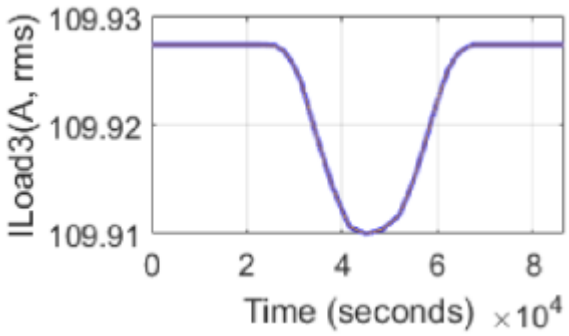

(b)

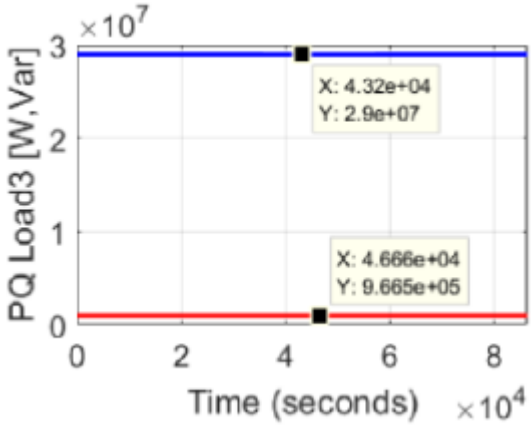

(c)

Fig. 7. (a) load3 power curve at Bus 9 (b) load3 current curve at Bus 9 (c) load3 power curve at Bus 9

Fig. 7(a), 7(b) and 7(c) are the third load profile named "load3" at 220 KV level, Bus9 characteristics. Same as load 2 the consumption demand is guaranteed; powers values 29 MW and 966.5 Kvar.

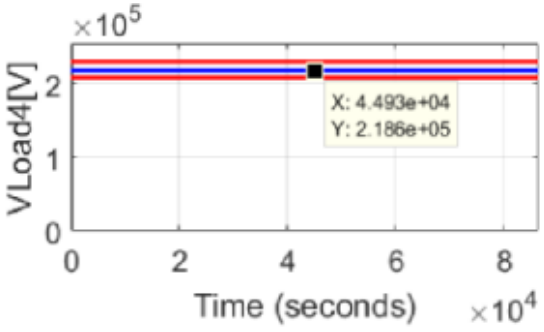

(a)

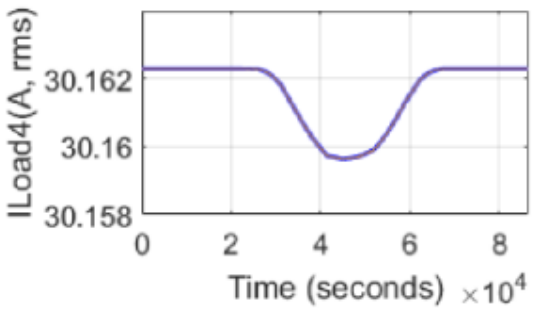

(b)

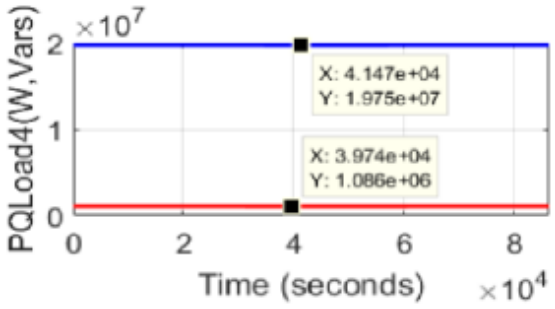

(c)

Fig. 8. (a) load4 voltage curve at Bus 5 (b) load4 current curve at Bus 5 (c) load4 power curve at Bus 5

Fig. 8(a), 8(b) and 8(c) introduce the fourth load profile characteristics named "load4" at 30KV level, respectively, the voltage, current and received power at Bus5. Received real power for load4 is about 19.75MW and reactive real power is 1.086 MVar. The constant charge keeps PQ unchangeable even with current variation. The voltage changes slightly and remains inside regulatory limits.

The power of the traditional generator and the PV system represents the total production from both sides. Thence coherence of power dispatching with the load needs is maintained and the sustainability of the grid even in high load demands is guaranteed with a minimum of losses.

We have to always find the power equation balance given by:

$$[P_{Bus10+Bus3}] = [P_{Bus4+Bus5+Bus6+Bus9}]$$
$$[Q_{Bus10+Bus3}] = [Q_{Bus4+Bus5+Bus6+Bus9}] \quad (5)$$

To depict the information, digital sensor agents are used. Each agent acts rapidly to send the required data from all smart agent groups. The received data were treated and monitored in the data center. To assess the extracted wave forms and power flows the intelligent actuators and wireless communications are included. These included component deals to detect abnormalities, helps decision-making and self-healing of smart grid.

VI. Results Validation on ETAP Software

Fig. 9 presents the identical grid architecture modeled in MATLAB software aiming to validate the obtained results by comparing the output results pertaining to power flows through the grid then prove the DO response equilibrium.

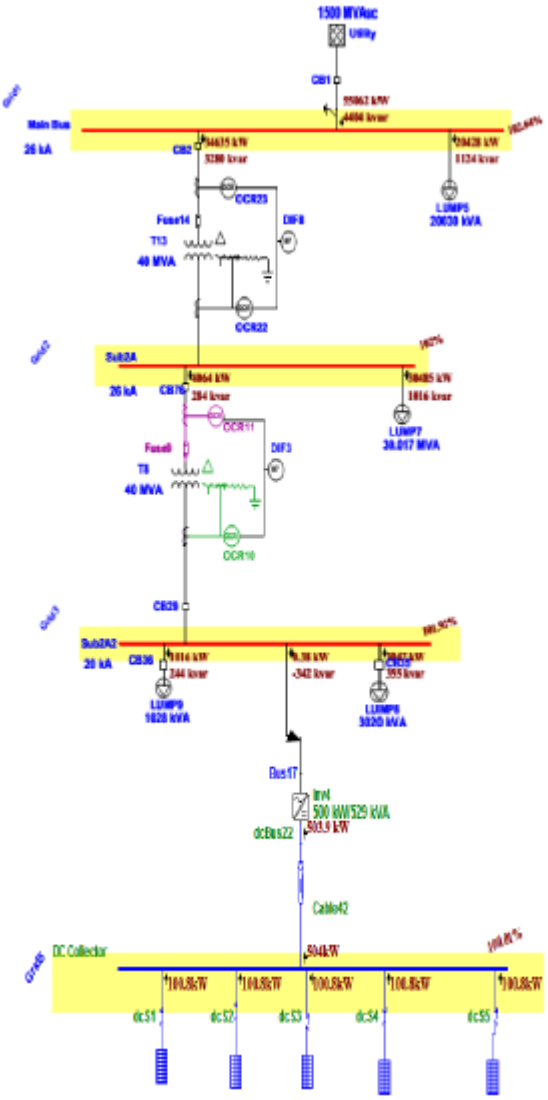

Fig. 9. One line diagram load flow analysis on ETAP

Fig. 9 presents the identical grid architecture modeled in MATLAB software aiming to validate the obtained results by comparing the output results pertaining to power flows through the grid then prove the DO response equilibrium

TABLE. II. COMPARISON OF RESULTS MATLAB VS ETAP

Bus	P_MAT. Kw	P_ET.Kw	Q_MAT.Kvar	Q_ET.Kvar
1	493	504	0.6931	0
3	493	503.9	0.466	0
4	2932	3047	342.1	355
5	979.2	1016	235	244
6	29000	30485	966.5	1016
9	19750	20428	1086	1124
10	53630	55062	579.2	4404

The similar outcome results of Table 2 are by a very small margin acquired excluding Bus 10 for the reactive produced powers (579.2-4404 Kvar), which correspond to the transformers and cable losses (of different models), are less in Matlab simulation case. DO equilibrium has been proved and results have been drawn in Fig. 10.

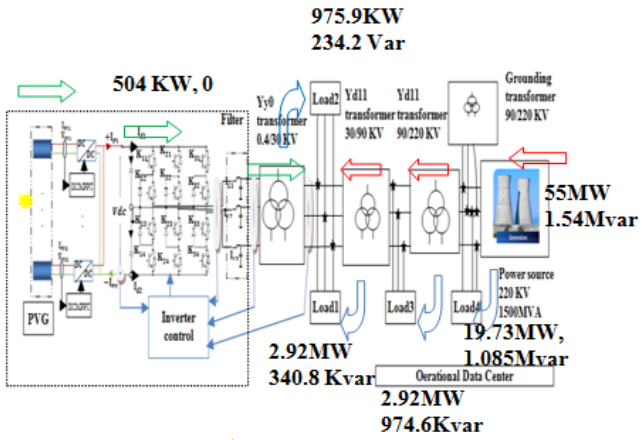

Fig. 10. DO equilibrium.

VII. CONCLUSIONS

In this paper, we have proposed an accurate distribution system based on smart grid technology. The presented system was treated and discussed in detail under various climatic conditions. Several assumptions were assessed and explained throughout the smart meter data.

To supervise and manage the required energy demand and the energy supply, an accurate platform was proposed. The proposed platform aimed to collect and treat the information according to smart meters.

Moreover, obtained results presented in the above section prove the reliability and sustainability of our proposed design.

The future works are aimed at implementing our accurate model in an embedded system using a Raspberry PI prototype.

REFERENCES

[1] Xi Fang, Satyajayant Misra, Guoliang Xue, Dejun Yang, "The New and Improved Power Grid: A Survey", IEEE Communications Surveys & Tutorials, Vol. 14, No. 4, pp. 944-980, 2012.

[2] Wided Medjroubia, Ulf Philipp Müllerb, Malte Scharfb, Carsten Matkea, David Kleinhansa, "Open Data in Power Grid Modelling: New Approaches Towards Transparent Grid Models", Elseiver Energy Reports, Vol.3, pp. 14-21, November 2017.

[3] Hany E. Farag ,E.F. El-Saadany,Ramadan El Shatshat,Aboelsood Zidan, "A generalized power flow analysis for distributed systems with high penetration of distributed generation", Elseiver, Electric Power Systems Research, Volume 81, Issue 7, pp.1499-1506, July 2011.

[4] Abbas Azarpour, Suardi Suhaimi, Gholamreza Zahed, Alireza Bahadori, "A Review on the Drawbacks of Renewable Energy as a Promising Energy Source of the Future", IEEE power & energy magazine, Vol. 38, Issue 2, pp 317–328, February 2013.

[5] Jan von Appen, Martin Braun, Thomas Stetz,Konrad Diwold and Dominik Geibel, "The Challenge of High PV Penetration in the German

Electric Grid", IEEE Power and Energy Magazine,Vol. 11 Issue: 2, pp. 55-64, 2013.

[6] Rakibuzzaman Shah, N. Mithulananthan, R.C. Bansal, V.K. Ramachandaramurthy, "A review of key power system stability challenges for large-scale PV integration", ELSEVIER, Renewable and Sustainable Energy Reviews, vol. 41, issue C, pp. 1423-1436, 2015.

[7] J. Arrinda, J. A. Barrena, M. A. Rodríguez, A. Guerrero, "Analysis of massive integration of renewable power plants under new regulatory frameworks", IEEE International Conference on Renewable Energy Research and Application (ICRERA), Octobre 2015.

[8] Steve G. Hauser, Kelly Crandall, "Chapter 1 – Smart Grid is a Lot More than Just "Technology", Sience Direct, Smart Grid, Integrating Renewable, Distributed & Efficient Energy, pp. 3–28, November 2012 .

[9] Jayavardhana Gubbi, Rajkumar Buyya, Slaven Marusic, Marimuthu Palaniswami, "Internet of Things (IoT): A vision, architectural elements, and future directions", Elseiver, Future Generation Computer Systems, Vol.29, Issue 7, pp. 1645-16602013, September 2013.

[10] Smita Mahindrakar, Ravi K. Biradar, "Internet of Things: Smart Home Automation System using Raspberry Pi", International Journal of Science and Research (IJSR), Vol. 6, Issue 1, pp. 901-905, January 2017.

[11] N. Phuangpornpitak, S. Tia, "Opportunities and Challenges of Integrating Renewable Energy in Smart Grid System", Elseiver Energy Procedia, Vol.34, pp. 282-290, 2013.

[12] Pierluigi Siano, "Demand response and smart grids—A survey", Elsevier, Renewable and Sustainable energy Reviews, Vol. 30, pp. 461-478, February 2014.

[13] Jingcheng Gaoa, Yang Xiao,Jing Liua,Wei Liangb,C.L. Philip Chenc, "A survey of communication/networking in Smart Grids", Elsevier, Future Generation Computer Systems, Vol.28, Issue 2, pp. 391-404, February 2012.

[14] Junjie Hu, Hugo Morais, Tiago Sousa,Morten Lind, "Electric vehicle fleet management in smart grids: A review of services, optimization and control aspects", Elsevier, Renewable and Sustainable Energy Reviews, Volume 56, pp. 1207-1226 , April 2016.

[15] Y. V. Pavan Kumara, Ravikumar Bhimasingua, "Key Aspects of Smart Grid Design for Distribution System Automation: Architecture and Responsibilities", Elsevier, SMART GRID Technologies, Vol. 21, pp. 352-3592015, 2015.

[16] Okafor Kennedy .C, Udeze Chidiebele. C, E. C. N. Okafor, C. C. Okezie, "Smart Grids: A New Framework for Efficient Power Management in Datacenter Networks", (IJACSA) International Journal of Advanced Computer Science and Applications, Vol. 3, No. 7, 2012.

[17] Aryuanto Soetedjo, Abraham Lomi, Yusuf Ismail Nakhoda, "Smart Grid Testbed using SCADA Software and Xbee Wireless Communication", (IJACSA) International Journal of Advanced Computer Science and Applications, Vol. 6, No. 8, 2015.

[18] Thomas Ackermann, Go¨ran Andersson, Lennart Soder, "Distributed Generation: a definition", Electric Power Systems Research, Vol. 57 pp. 195–204, 2001.

[19] Ben Abdallah, I., Jraidi, M., Hamrouni, N., Cherif A., "Modeling, Control and Simulation of a grid connected PV system", IEEE 2014 International Conference on Electrical Sciences and Technologies in Maghreb (CISTEM), April2015.

[20] Mamdouh Abdel-Akher, Karar Mahmoud, "Implementation of three-phase transformer model in radial load-flow analysis", Elseiver, Ain Shams Engineering Journal, Vol.4, Issue 1, pp. 65-73, March 2013.

[21] Semlyen, A and Deri, A, "Time domain modeling of frequency dependent three- phase transmission line impedance", IEEE Transactions on Power Apparatus and Systems,Vol. 104(6), pp.1549 – 1555, July 1985.

Modeling and FPGA Implementation of a Thermal Peak Detection Unit for Complex System Design

Aziz Oukaira*, Ouafaa Ettahri and Ahmed Lakhssassi
Université du Québec en Outaouais, Gatineau, (PQ), 18X 3X7, Canada.

***Abstract*—This paper, presents the modelization and the implementation of a thermal peak detection unit for complex system design. The modelization step starts with modeling the formula of the heat source using Simulink/Matlab tool, is the main objective of this work. Then the input temperature, the angles, the distance as well as certain frequencies, will be obtained from this formula using the GDS (gradient Direction Sensor) method based on RO (Ring Oscillator). Before the transition to the implementation in FPGA board, the use of VHDL code is necessary to describe the thermal peak detection unit, in order to verify and validate the whole module. This work offers a solution to thermally induced stress and local overheating of complex systems design which has been a major concern for the designers during the design of integrated circuit. In this paper a DE1 FPGA board cyclone V family 5CSEMA5F31C6 is used for the implementation.**

Keywords*—Thermal peak; complex system design; MATLAB; GDS; RO; FPGA; DE1

I. Introduction

Integrating complex systems on a single System on Chip (SoC) has become possible with the evolution of technology. The high integration in the SoC systems increase the power density of power consumed and dissipated, which increase the internal temperature of the chip. The more the chip shrinks, the more it is overheated. It is known that high temperatures as well as thermal variations reduce the life and reliability of semiconductor layers of complex systems. In theory current technologies limit the maximum temperature to 125 degrees Celsius, but practically checking this restriction is not an easy task. The designer must take into account many aspects such as maximum voltages, the effect of heat sinks and ventilators. There has been recently huge interest by several research studies on the detection and management of thermal peaks [1]-[5]. This research is similar in general purpose but differs greatly in the techniques used and the methodology applied, it all depends on the conditions considered in the study and the nature of the electronic system. A good study was done in [6] and a new technique was introduced. This paper models and implements in a FPGA board a thermal peak detection unit for circuits of high-complexity and high-density. On complex systems, the heat is accumulated from one cycle to another throughout their operation [7] which requires a deep study at the junction level. As a result the high temperatures as well as the variation of the thermal gradient reduce the lifetime and the reliability of semiconductor thin films. Regardless of the type of FPGA card used, the maximum temperature allowed by current technologies is 125°C like mentioned earlier [8]. In order to meet this requirement, the designer must deal with several aspects at the same time, such as total dissipated power, heat dissipation effect, cooling mode, PCB position, ambient temperature and the influence of the equipment used in proximity.

The GDS (gradient Direction Sensor) method [9]-[10] presents a good and easy solution to localize the thermal peak, in the simplest case it consists of three well positioned sensors that convert signals from electrical signal to frequencies in order to locate the thermal peak. Despite the use of the GDS method, the originality of this work rests on the modeling and implementation of a network of thermal sensors each one is actually a ring oscillator (RO) composed of six inverters to characterize the thermo mechanical stress of a complex system, Ring Oscillator (RO) and the GDS are explained in detail in [11] and [12]. Our methodology consists on the Development of a VHDL code to model the thermal peak localization equation under Matlab tool, using the GDS (gradient Direction Sensor) technique explained before, from each cell composed of three sensors we can obtain information on the temperature distribution and partly on the position of the heat source. This help to predict the thermal peak and to evaluate the thermo mechanical stress associated [13]. This means that, with the aid of a sensor network, it's easy to know the temperature values in some places in the structure, but this operation can only be possible after the conversion of the electrical signal to the frequency values, which is obtained after calculation, gives information on the thermal gradient direction. Based on this information the prediction of the temperature value associated with the heat source and the thermo mechanical stress distribution in the entire IC structure can be feasible. This approach is used as a methodology to model and implement the thermal peak detection equation to predict the temperature of a single heat source Ts on the surface of a given complex system. In Section 2, the development of the thermal peak localization model is discussed. Section 3 describes the implementation of VHDL code of the thermal peak detection unit on the FPGA board to verify and validate the results obtained.

II. The Modelization of the Thermal Peak Localization Unit

A. Description of the GDS method adopted

The GDS method is in general a technique for evaluating a single heat source on the chip surface. This method has been studied and analyzed for its applicability as inverse engineering problem which is capable of detecting the thermal peaks and associated thermo-mechanical stress on the critical surface areas of large VLSI devices. In order to obtain information

about heat source parameters, one only needs to know from where the phenomenon is distributed and sometimes how fast it is changing. The geometrical coordinates and an estimation of the investigated heat source can be obtained by applying the GDS method [1], [5]. In order to calculate the temperature of the heat source, the thermal peak detection module designed makes it possible to obtain this information by having at its input the angles, the distance h as well as certain frequencies. Although this module is optional, it is VHDL coded in order to have a thermal peak detection unit offering a plurality of services. The formula of the heat of this module is:

$$\frac{\frac{H}{a}(fc_1 - fa_1)(\sqrt{3} + \tan\alpha_2)(1 + \tan^2\alpha_1)}{\sqrt{3}(1 - \tan\alpha_1 \tan\alpha_2) - (\tan\alpha_1 + \tan\alpha_2)} + fa_1 \leftrightarrow Ts \quad (1)$$

Equation (1) of localization of the thermal peak, takes in consideration the angles α1 and α2, and the frequency fc1 and fa1 represents the description of a single heat source Ts with the GDS method. In order to obtain the temperature value of a single punctual heat source, the distance between the sensor and this source should be calculated. Two sensor cells are required for this purpose (Fig. 1). The cells are placed at a given distance H and each of them gives information about angle α1 and α2 in direction of the heat source. Under the consideration that "a" is relatively small, we can assume that the heat source and the center of the cells from a triangle in which the length of one side and values of the angles adjacent to this side are known, like illustrated in the following Fig. 1.

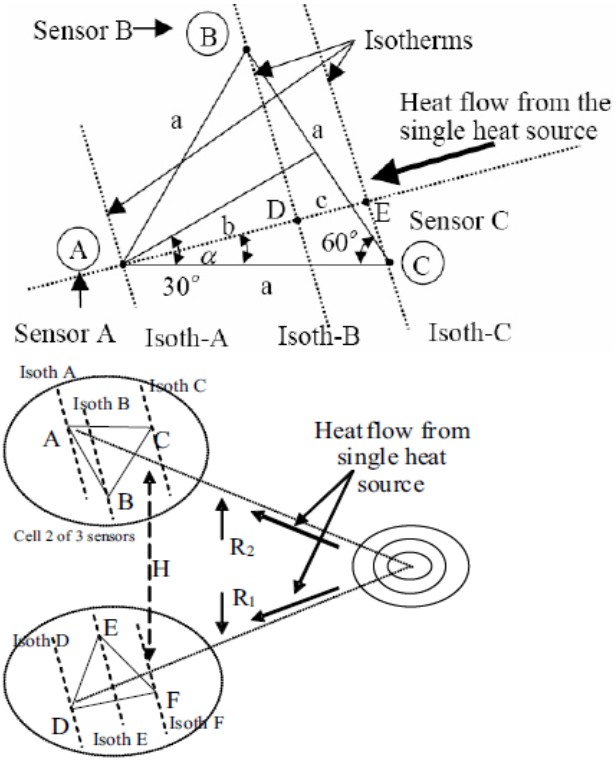

Fig. 1. The principle of detection by GDS of a source of heat based on three sensors RO.

This module based on the GDS method will be designed and tested afterwards using VHDL code.

B. *The modelization of the thermal peak localization unit using Simulink*

The following Fig. 2 to 7 shows the representation and modeling of (1) in order to detect and localize the thermal peak by Simulink ™ blocks.

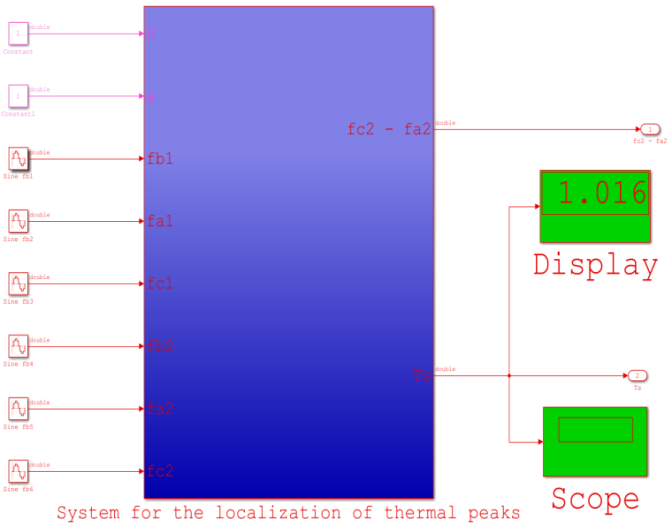

Fig. 2. Calculation system with Matlab/Simulink.

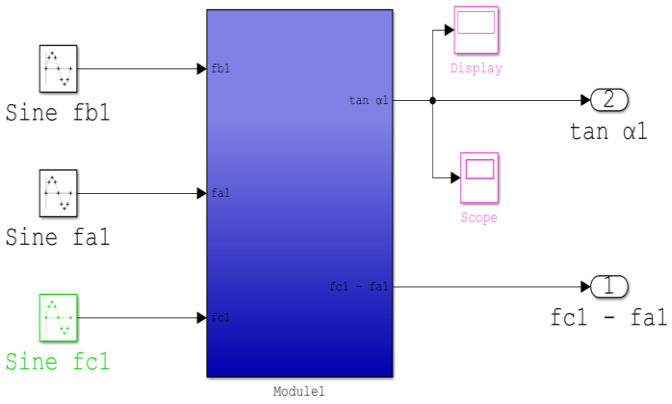

Fig. 3. The Simulink block subsystem of the first computing module.

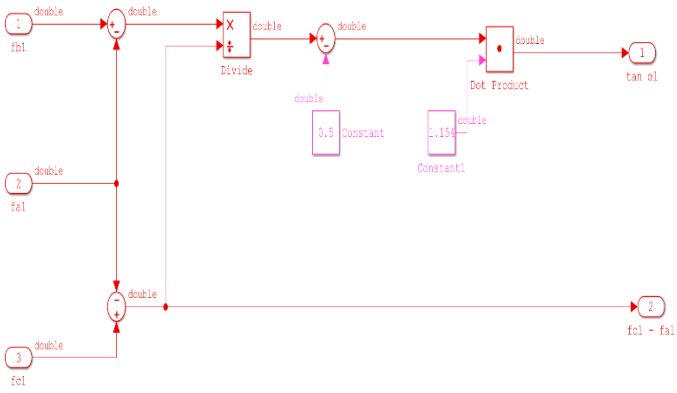

Fig. 4. The Simulink blocks of the first module.

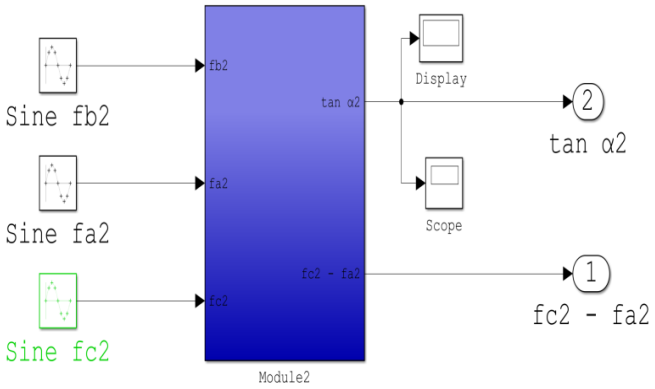

Fig. 5. The Simulink block subsystem of the second computing module.

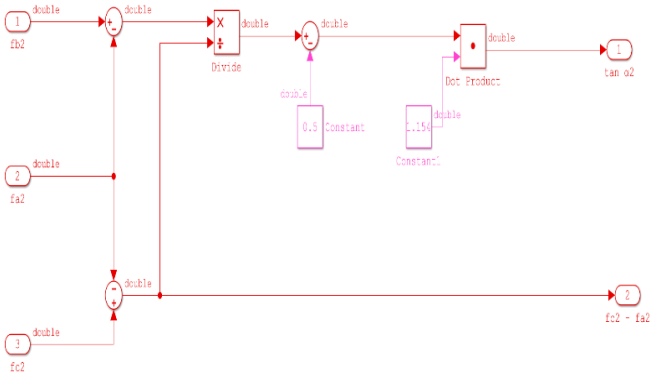

Fig. 6. The Simulink blocks of the second module.

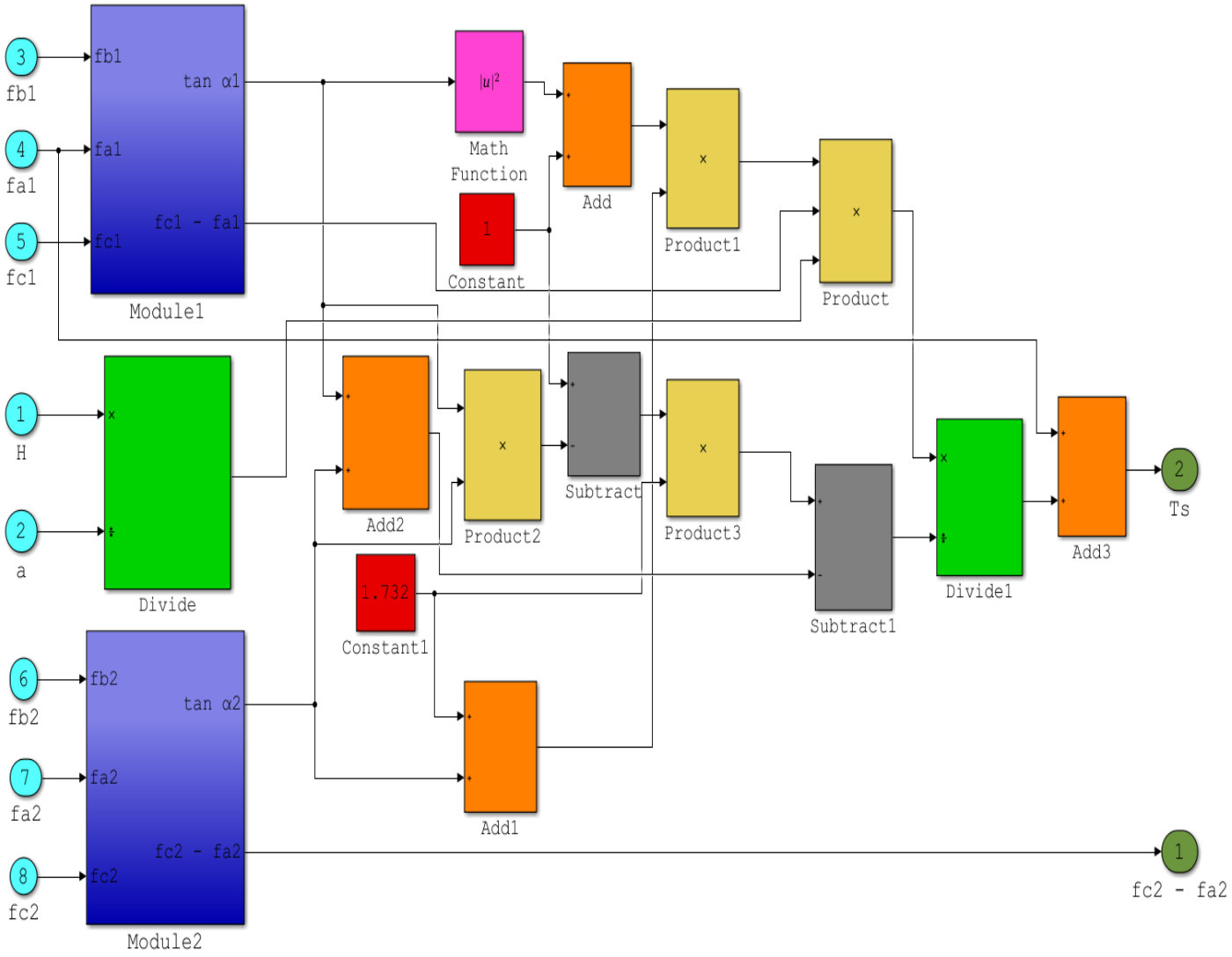

Fig. 7. Structure of the thermal peak detection module under Matlab / simulink

Fig. 7 shows the modeling of all the Matlab/Simulink blocks in which the estimation and localization of the temperature of the heat source Ts is calculated.

C. *Tests and results of the thermal peak module using the display option*

To test the realized thermal peak localization module under Matlab/Simulink of the heat source Ts introduced before in (1), the relation between the temperature and the frequency given

in Fig. 8 is used, this study is found in [12] for T=25 °C, f=1 MHz. As an example it can be assumed that $fa_1 = fc_1 = 1$ MHz this new values should be replaced with those in (1) with this new value we will get Ts=1°C at the end. To validate the module the same thing is done the frequencies fc_1 and fa_1 are replaced with the value 1 MHz and we get Ts=1.016 °C like shown in the display of Fig. 2. The answer corresponds to that obtained in (1). The flowing Table 1 explains this.

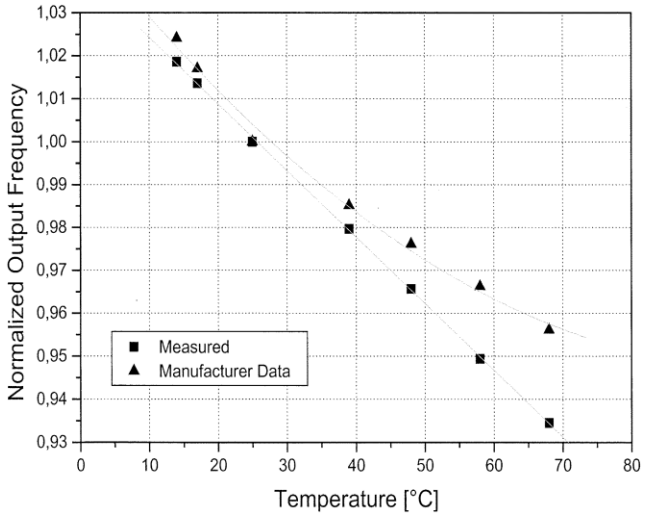

Fig. 8. Normalized ring-oscillator frequency response versus temperature.

The Fig. 8 shows the thermal evolution as a function of the frequency of the ring oscillator. For example, at 25 °C f=1 MHz, this information is used to test and validate our modelization in comparison with the heat equation as mentioned in the following table:

TABLE I. TEST TABLE OF OUR MODELIZATION IN COMPARISON WITH THE EQUATION OF A SINGLE HEAT SOURCE AT 25 °C

Test case	Ts (°C) from equation (1)	Ts (°C) from modelization
$fa_1 = fc_1 = 1$ MHz	1	1.016

According to this table practically the same value is shown in option display, see Fig. 2 theoretically found by the equation (1), this validates the thermal peak detection unit module in a complex system based on (1) using Simulink of Matlab.

D. Tests and results of the thermal peak module using the scope option

This section shows how much information can be found on the location of the thermal peak at the same frequency and the same temperature of the ring oscillators knowing that this type of sensor can only determine the necessary information if it receives sinusoidal signals, therefore a sinusoidal signal as an input of our module should be defined in this case, Fig. 9 shows the results found.

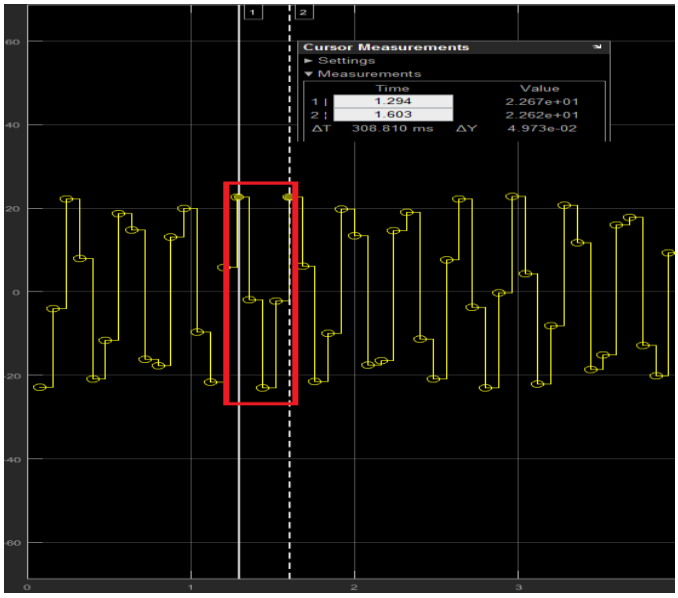

Fig. 9. Simulation of the thermal peak detection module shown by scope.

The simulation shown in Fig. 9 also confirms the correct functioning of the calculation module, as mentioned before in the results displayed by the scope option, within a timeframe of 308 ms, the module receives five information in order to characterize the thermal peak, this result validates the techniques and the methodology adopted to model (1). These found results will be used after in the implementation in the FPGA card to confirm and validate the good operation of the module.

III. EXPERIMENTAL IMPLEMENTATION AND RESULTS

The main purpose of this section is the implementation and validation of the modelization results and simulation by Matlab /Simulink. VHDL code is used to describe the module to facilitate the development of its architecture for its implementation in complex system design. This architecture is modeled in high-level language, and simulated to assess its performance and finally implemented on FPGA. The simulation results are validated by using the software Modelsim under Quartus Prime, which allows simulating the behavior of the system in time. Our design flow will be divided into three main parts: simulation, synthesis, and implementation of the VHDL code on FPGA. A description of each part will be presented in the next paragraphs.

A. Creation and simulation of the VHDL code

This part, presents the description of the thermal peak detection unit using a VHDL code editor. The code editor used is Modelsim. Fig. 10 shows the top-level module of our module.

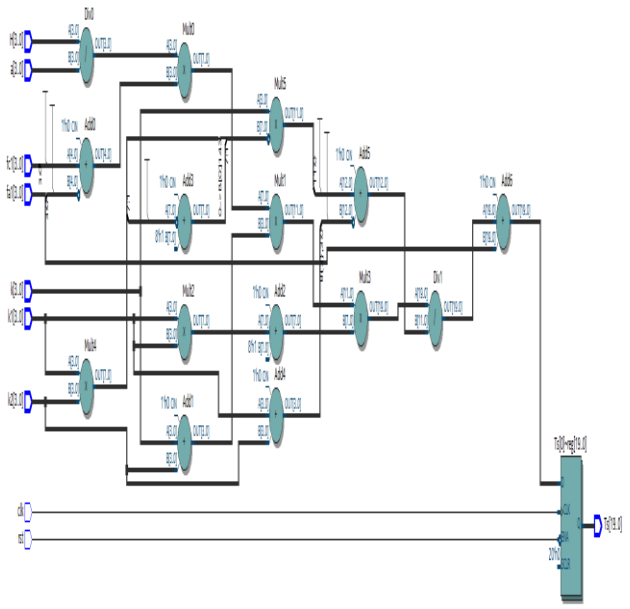

Fig. 10. Top level of the thermal peak detection module.

After generating the two .vhd files (the primary file system and the "Test Bench" file) with the "System Generator" the role of the Quartus Prime Navigator comes in order to synthesize the design and generate the RTL files as shown in Fig. 11.

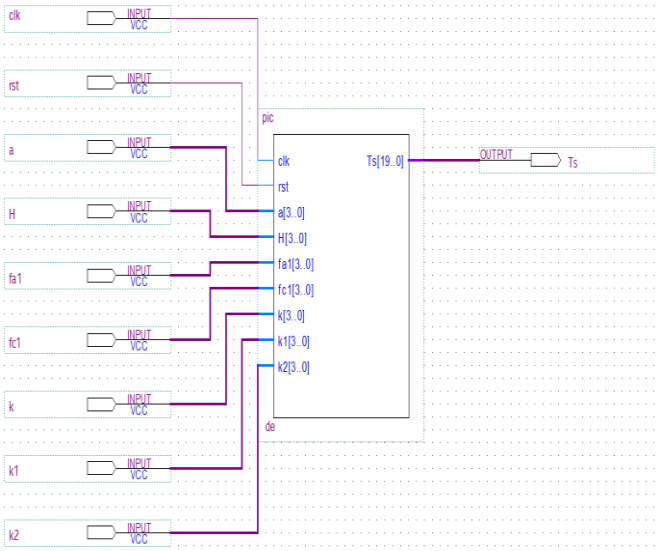

Fig. 11. Structure of the thermal peak detection module in Quartus Prime tool.

The structure of the thermal peak detection module after synthesis with Quartus Prime from Altera is shown in Fig. 11. The VHDL code implemented was validated based on the modelization designed before. In this part the simulation will be run with the same conditions used in Tab. I, to validate the experimental results. Fig. 12 shows the results found by the simulation using the Modelsim tool.

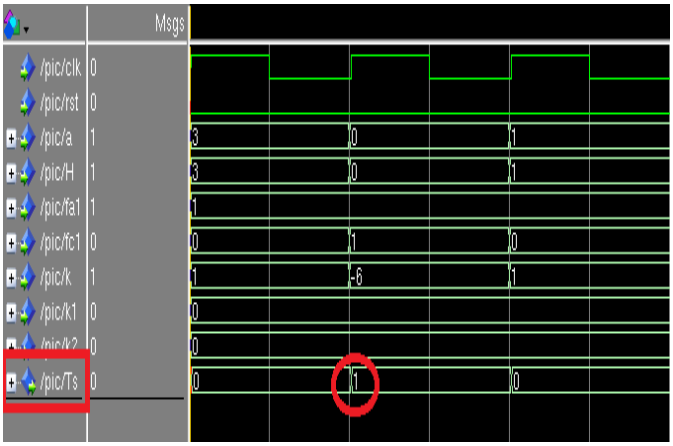

Fig. 12. Display results of simulation the VHDL code.

The value circled in red in Fig. 12, validates the VHDL code since it is the same value of Ts found before as shown in the comparison between our modelization and (1) shown in Fig. 2 and Table 1. This means that the VHDL code is correct and the modelization step is designed correctly. In this paper, an equation of single heat source based on GDS (gradient Direction Sensor) method for thermal peak detection is modeled, simulated and verified with a VHDL code and a 'test bench' at the laboratory LIMA the results found meet the initial specifications.

B. Implementation and downloading of the VHDL code on DE1

Once compiled after the assignment of the pins, the program is ready to be downloaded on the card DE1 cyclone V a family and 5CSEMA5F31C6 as a device. Fig. 13 shows that the VHDL code is downloaded successfully on the card.

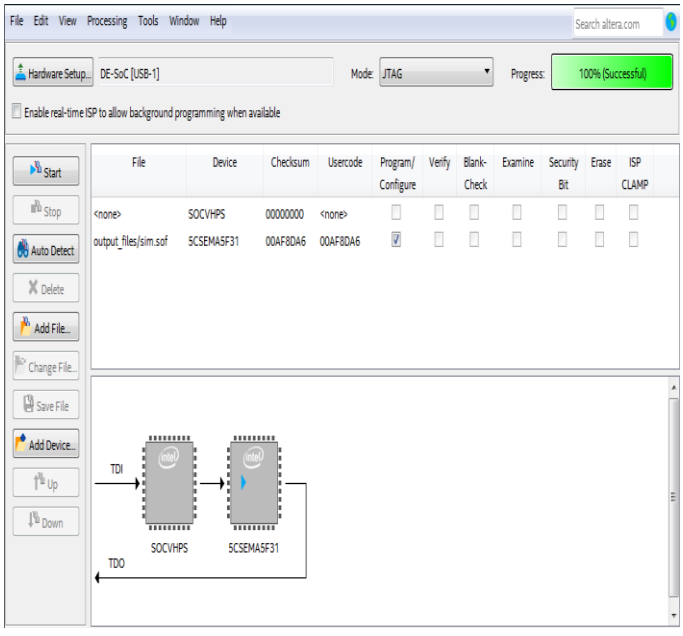

Fig. 13. Downloading the code of DE1 Altera cyclone V.

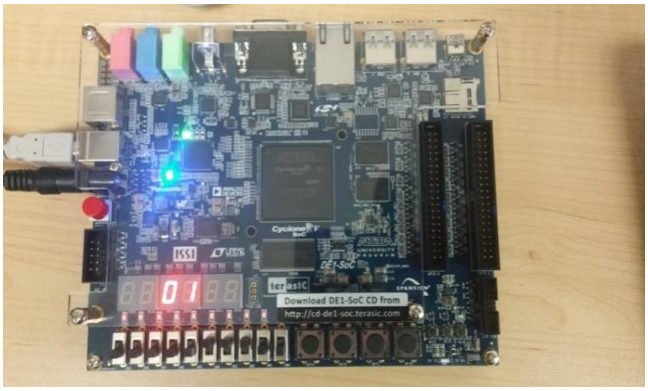

Fig. 14. The value shown on the LCD after the implementation of DE1 Altera cyclone V.

After the download, the program was running and then the outputs were shown. The clock is at 50 MHz, so the outputs should change with a frequency of 50 MHz and the following Fig. 14 shows the value (1°C) at 15 second after implementation on LCD reader without floating point.

Fig. 14 shows that the value displayed on the LCD matches the results found before. The simulation and implementation on DE1 FPGA board can be applied in any kind of environment to get improved performance with respect to the conventional schematic; it is also able to keep the temperature constant at the desired value regardless of changes in the load or environment. Thus, the overshooting problem can be solved up to great extent. One of the important issues in the field of electronics is overheating problems especially when it comes to integrated and complex systems and microsystems, but the mean question is how to perform thermal monitoring, to indicate overheating situations, without control. The traditional approach consists of many sensors all over the chip, and then their output can be shown simultaneously and be compared to the reference voltage recognized as the level of overheating. The idea of the proposed method is to predict the local temperature and gradient along the given distance in some places only on the monitored surface and evaluates obtained several real-time information in a short area in order to predict the temperature of the heat source. Therefore, in the case of a SoC device, there is no place on the layout for complicated unit to perform calculations such as described in paper [10], but there is also no need, because we only want to detect overheating situations. These peaks are essential when monitoring the thermal matrix to avoid a critical induced thermo-mechanical stress. In addition, in most cases, overheating occurs in only one location.

IV. Conclusion

In this paper, a new method to evaluate and predict thermal peak of complex system design, based on the GDS method. In this work a thermal peak detection unit was designed using the heat equation of a single heat source. The modelization of this unit was designed by simulink/Matlab, and was described with a VHDL coder, after the simulation, the unit was implemented on the DE1 FPGA board. Thus, the factors of the heat equation requiring special attention during the development of a thermal peak detection unit, we can mention the number of sensors, their proximity, their spatial distribution and their network interconnections. The application of this method will be the basis for future developments of the detection algorithm for several sources of heat. These architectures were modeled in high-level language, simulated to evaluate their performance and implemented on FPGA. The implementation of more complex design systems, the purpose of the applications that will be integrated using this work is to get more information in real-time, this will help the designers to react at the right time, also the proposed module, bringing other benefits such as support to characterize and locate each thermal peak. This will show other types of information, and communication methods on thermal peak in a reliable way and integrate them without any analog device.

References

[1] Bougataya, M, Lakhsasi, A, & Massicotte, D, “VLSI thermo-mechanical stress analysis by gradient direction sensor method”, In Electrical and Computer Engineering, IEEE Canadian Conference, pp. 710-713, (May. 2015).

[2] Janicki, M, Zubert, M, & Napieralski, A, “Application of inverse problem algorithms for integrated circuit temperature estimation”, Microelectronics journal, pp. 1099-1107, (1999).

[3] Lopez-Buedo, S, & Boemo, E, “Making visible the thermal behaviour of embedded microprocessors on FPGAs: a progress report”, In Proceedings of the ACM/SIGDA 12th international symposium on Field programmable gate arrays, pp. 79-86, (2005).

[4] Velusamy, S, Huang, W, Lach, J, Stan, M, & Skadron, K, “Monitoring temperature in FPGA based SoCs, In Computer Design: VLSI in Computers and Processors, Proceedings, IEEE International Conference, pp. 634-637, (Oct. 2005).

[5] Wójciak, W., & Napieralski, A, “Thermal monitoring of a single heat source in semiconductor devices the first approach”, Microelectronics journal, pp. 313-316, (1997).

[6] V. d'Alessandro, M. De Magistris, A. Magnani, N. Rinaldi, S. Grivet-Talocia, & S. Russo, “Time domain dynamic electrothermal macromodeling for thermally aware integrated system design”, In Signal and Power Integrity (SPI), 17th IEEE Workshop, pp. 1-4, (May. 2013).

[7] Jaeger, R. C, Suhling, J. C, Carey, M. T, & Johnson, R. W, “A piezoresistive sensor chip for measurement of stress in electronic packaging”, In Electronic Components and Technology Conference IEEE, Proceedings, pp. 686-692, (June. 1993).

[8] Oukaira, A, Lakhssassi, A, Fontaine, R, & Lecomte, R, “Thermal Model Development for LabPET II Scanner Adapter Board Detector Module”, Proceedings of the COMSOL Conference, pp. 1-5, (Oct. 2015).

[9] Sayde, M, Lakhssassi, A, Bougataya, M, Terkawi, O, & Blaquiere, Y, “SoC systems thermal monitoring using embedded sensor cells unit”, In Circuits and Systems (NWSCAS), 55th IEEE International Midwest Symposium, pp. 1052-1055, (Aug. 2012).

[10] Lakhssassi, A, Bougataya, M, Boustany, C, & Massicotte, D, “Thermal stress monitoring using gradient direction sensors”, In Circuits and Systems (NEWCAS-TAISA), 6th IEEE International Northeast Workshop, pp. 177-180, (June. 2008).

[11] Lakhssassi, A, M, Bougataya, “VLSI Thermal Analysis and Monitoring”, In-Tech, Kirchengasse, A-1070 Vienna, Austria, pp. 441-456, (2009).

[12] Lopez-Buedo, S, Garrido, J, & Boemo, E. I, “Dynamically inserting, operating, and eliminating thermal sensors of FPGA-based systems”, IEEE Transactions on components and packaging technologies, pp. 561-566, (2002).

[13] Bougataya, M, Lakhsasi, A, Savaria, Y & Massicotte, D, “Thermomechanical Stress Analysis of VLSI devices by partially coupled finite element methods”, IEEE Proceedings; ISBN, pp. 509-513, (May. 2004).

Quizrevision: A Mobile Application using the Google MIT App Inventor Language Compared with LMS

Mohamed A. Amasha
Department of Computer Teacher Preparation-Damietta, Egypt

Shaimaa Al-Omary
Department of Curricula and Teaching Methods (Arabic Language)
Cairo, Egypt

***Abstract*—At Qassim University, the Blackboard (https//:lms.qu.edu.sa) Learning Management System (LMS) is used. An exploratory study was conducted on 105 randomly selected students attending Qassim University. Of these, 91 students (87%) affirmed that they did not use the LMS as a study aide. This paper describes the means by which the MIT App Inventor language could be used to develop a mobile application (app) for the Android operating system. The app, Quizrevision, enables students to review course knowledge and concepts. An online survey was used to investigate students' perceptions and gather their feedback regarding the use of Quizrevision as a study aide, as compared to the LMS. An achievement test was used to examine the improvement of students' scores. Data was collected from 114 students taking the Phonetics course (Arab 342) in the Arabic Language Department (ALD) of Qassim University; 63 of them (55.27%) were male, and 51 (44.73%) were female. Descriptive statistics, *chi-square*, and *t-test* were used to analyze the data. The results indicated that the Quizrevision app supported the students' achievement. There was a positive attitude towards using the Quizrevision app, as well as higher engagement in using the app as compared with using the LMS. In addition, findings confirm that students prefer using m-learning apps rather than using LMSs for reviewing course concepts and knowledge. Furthermore, student scores improved after using the app.**

***Keywords*—Quizrevision; mobile application; LMS; e-learning; e-course; MIT APP Inventor; Android devices**

I. Introduction

Nowadays, the development and progress of information technology (IT) has resulted in many technological innovations that can be employed in the educational process [17]. Accordingly, many countries have already adapted their educational system to employ these technologies. Typically, universities, colleges and other educational institutions start presenting their training program via the internet, in a model known as e-learning. E-learning is a modern style of education that helps to simplify the educational process [12]. It enables both the teacher and the students to communicate within interactive educational environments. In this respect, e-learning is a significant aide in improving teaching and learning processes [11]. Boticki, Baska, Seow and Looi (2015) studied the design of a mobile learning platform called samEx as a virtual bages in elementary school. They discussed the design and analyzed the data regarding student use. Qun wu (2015) carried out a study to design a smartphone app to teach English Level 2 vocabulary, and investigated its effectiveness as a tool in helping college students classified as speaking English as a foreign language (EFL) to learn English vocabulary. Guerrero, Ochoa and Collazos (2010) conducted a study in improving grammar skills in elementary school students. They presented the design of a collaborative learning activity and designed a software application to support teaching grammar through mobile devices. Yang, Li and Lu (2015) investigated the interactions of internet and presentation mode on students' concentration and achievement in learning conceptual knowledge through mobile phones in the classroom setting. Previous studies in the same field did not address any application in the Arabic language or their influence on students of the Arabic Language Department. Furthermore, they did not address the advantages of designing mobile applications using the MIT App Inventor language. Finally, there is no research that compares the use of mobile applications and learning management systems, either in general or in the Arabic department specifically.

In this paper, we examined what motivated students in the Arabic Language Department (ALD) to interact using modern technology. In addition, we tried to leverage the widespread use of smart devices among students. Quizrevision was designed as a trial with a sample of ALD students (114) over a period of one academic year, to support and complement the learning process. We discuss the design of Quizrevision and analyze student feedback regarding use of the application. We hoped to see an improvement in students' scores after they used the app. We hope this study will pave the way for other researchers to use this technology to design other tools for reviewing Arabic language courses.

II. Theoretical Background

The development of e-learning is highly associated with the development of communication and information technology, which are becoming widely used in education [4]. This rapid development spurs educational researchers to search for new methods, which suit the characteristics of this development and help students to learn; e-learning cannot be overlooked, as it is the fastest-growing methodology [35]. Mobile learning, or m-learning, is considered a new phase in e-learning. Both the great development in communication and education technology, as well as the spread of e-knowledge among students at schools and universities has led to the emergence of new learning systems, such as m-learning. M-learning enables easy access to content, and it provides many opportunities for learning outside the classroom [4]. The widespread use of e-learning has led to the appearance of

learning management systems, which manage, monitor, and design learning. LMS systems also manage e-courses and follow up on student achievement [9]. Students are encouraged to use the LMS in studying the e-content [33]. In spite of the appearance of the social media and Web 2.0 tools (such as Facebook, Twitter, Linkdin, Wiki, and RSS) [18], [19] many universities prefer using LMS [27]. The many possibilities of the system as an integrated e-environment help to integrate social networks with it. As such, communication via both the system and the social network can be employed through m-learning, which is considered to be a model for m-learning [29].

A. App Inventor (AI)

App Inventor (AI) is an open-source, web-based system that enables developing a mobile application for Android operating system (OS) devices. It is an online development environment (ODE). Google Inc. and the Massachusetts Institute of Technology (MIT) developed AI in 2012. AI is a visual drag-and-drop programming tool [25]. Furthermore, it relies on a web-based graphical user interface (GUI) builder [7]. With this programming tool, programmers can produce and develop educational applications for mobile phones. AI is widely used because it utilizes an integrated programming editor that contains several tools to help programmers in producing and designing their apps [32]. It relies on a type of programming known as a blocks-based programming language [6]. AI helps both teacher and learner to create their apps on Android devices as fun, quick prototypes, with educational games and quizzes for classmates. AI can be used online through browsers like Chrome or Firefox.

B. Mobile learning (m-learning)

Nowadays, e-learning and m-learning have become key concepts in education as part of the technological revolution [8]. M-learning is considered the most well-known emerging technology, of those that support e-learning and online learning [13]. M-leaning enables learners to learn anywhere, at any time, through using cell phones, PDAs and smartphones to facilitate the exchange of information between teachers and students. The next-generation LMS should be mobile-friendly, personalized, customizable, adaptive, intuitive, integrated, and designed to enhance student learning. Furthermore, there are plenty of universities and institutions that use mobile phones in learning, since they allow students to surf the internet during lectures. Additionally, others use mobile phones to capture what is on the board [21].

C. Learning management systems (LMS)

Learning management systems (LMS) have become the most prevalent educational environment, since they organize and manage e-learning processes [34]. Recently, many universities have begun using an LMS in their educational systems. There are currently two brands of LMS. The first is open-source software, called Moodle. The second is commercial software, called Blackboard [15]. Blackboard includes several tools, such as learning and teaching activities, assignments, e-content, course organization, discussion board and virtual classroom [9] [26]. In addition, an LMS can be integrated with traditional educational methods to create blended learning. It can also support distance education [12]. It is generally agreed that an LMS helps to shift from traditional learning to e-learning by adopting content design standards such as IEEE, IMS, and SCORM. It requires an internet connection and can perform the following tasks: administration, publishing and writing reports. Moreover, an LMS consists of the following main parts: admission, e-course, synchronous learning, non-synchronous learning, e-test, discussion forums and electronic supervision. In fact, the first generation of e-learning is called “classic e-learning” and consists of adding a computer and the internet to the LMS. The second generation of e-learning is called “advanced e-learning”; it consists of mobile and wireless access in addition to VR/AR.

III. HYPOTHESES

This paper aims to use the MIT App Inventor language to develop a mobile app that enables students to review course knowledge and concepts, following participation in the course entitled the Phonetics course (Arab 342). The study aims to gather student feedback about using Quizrevision as a reviewing tool compared to an LMS. The study poses the following hypotheses:

H1: Students have positive attitudes towards using Quizrevision in reviewing the course entitled the Phonetics course (Arab 342).

H2: Students prefer using an m-learning app over an LMS for reviewing the course.

H3: There are statistically significant differences (at $p < 0.05$) between males and females regarding the use of m-learning as a reviewing tool for the course.

H4: The degree of students achievement have been improved and there is a statistically significant difference (at $p < 0.05$) between the mean scores of the pre- and post-tests following use of the Quizrevision app as a reviewing tool.

IV. METHODOLOGY

A. Instructional Material Design

The project was carried out using student in an ALD course, Phonetics course (Arab 342). We conducted interviews with a cohort of professors (15) from ALD at Qassim University. Thirteen (86.8%) agreed on the difficulty of this course and stressed the importance of a good review before the exam. Professors of ALD compiled the content of the course and then arranged it according to the relative importance of each part, based on the professors’ opinion. The content appeared as a booklet before its final form. It was divided into five parts: 1) important definitions; 2) phonetics; 3) the place of articulation; 4) illustrated explanation; and 5) test yourself. These sections would enable the students to fully review the content of the course. The app included a presentation of the behavioral goals for each part of the app and what the student should have learned by the end of the course. The app was designed to allow the students to navigate easily through links to access information. Furthermore, the app provided students with feedback through the Test Yourself icon. Before the programming process, the content was offered to a group of professors (the jury) in the Arabic

language, so they could express their opinions about its validity and how it was related to the preset targets. Hence, the validity of the content for the app was achieved.

B. Project Approach

The App Inventor language was selected as Quizrevision's design language. The following procedures were required: First, a Gmail account was created. Second, Java 1.6 was downloaded from http://www.java.com before starting. To design and develop the app, we used the block editor and inventory palette components (user interface, layout, media, and sensors). AI included the block editor, which was implemented as a Java Web application to start designing the application. It required installing Java on the desktop. AI exported a file package as an APK file, which could be published and distributed on Android devices. In addition, AI provided a QR code for the APK file.

To design the Quizrevision app and write the code that would help to solve the research problem, the problem inputs, mathematical and logical processes were identified and the problem outputs were specified. Hence, a flowchart was drawn to illustrate the steps required to implement the program. Fig. 1 shows the research algorithm. The flowchart was converted into a group of commands using MIT's App Inventor language.

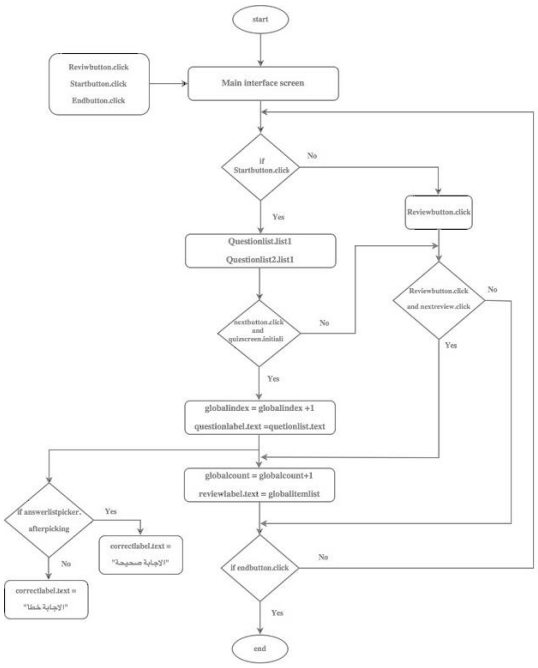

Fig. 1. The research flowchart

After the app was designed, it was published and run on the desktop, and then on the Android devices after launching the MIT AI2 Companion on the device and then scanning the barcode or typing in the code to connect for live testing of the app. The results of the app after publishing were compared with Fig. 2. In addition, Fig. 3 shows the MIT App Inventor block code.

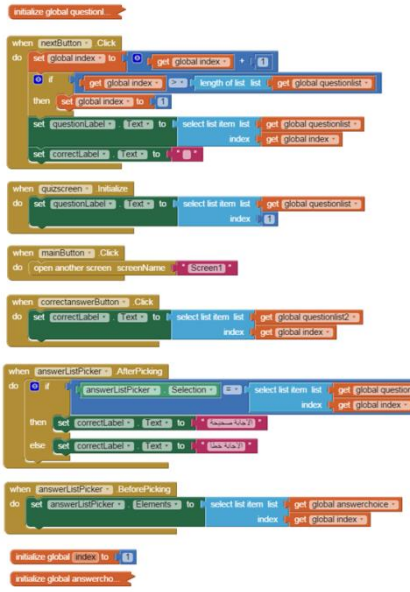

Fig. 2. MIT APP Inventor code

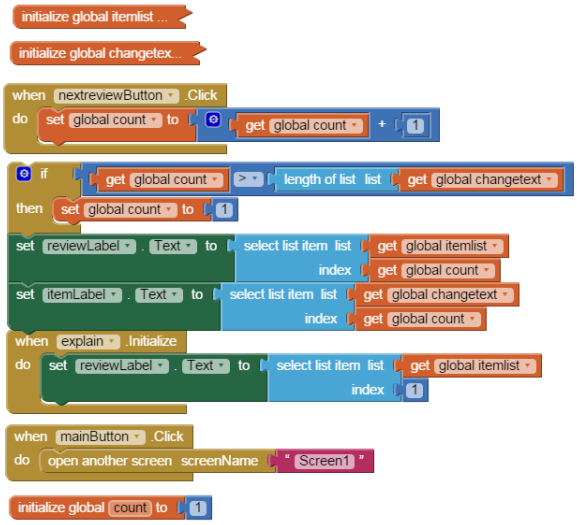

Fig. 3. MIT App Inventor code

As the code was written, the app was reviewed and prepared for publishing. Therefore, to publish the app, a Google Play developer account was created by the developer console. Then the APK file was uploaded to Google Play through "upload your first APK to production". The app properties were organized by store listing and were free. Accordingly, the app was published in Google Play under the name "quiz revision ARAB 342". The main interface menu and the app's icon in Google Play are shown in Fig. 4 and 5. After the course was completed in the 11th week, four weeks were devoted to reviewing the course. Two lectures per week were reviewed. The students were asked to bring their tablets and to download the application from Google Play. During the last week, they used the app to take a comprehensive test.

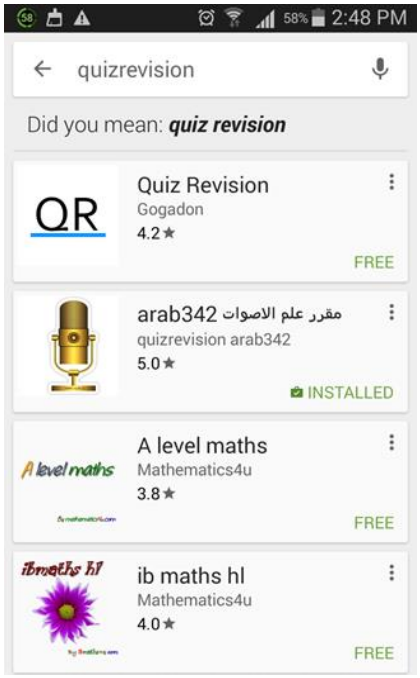

Fig. 4. App icon in Google Play

Fig. 5. Main menu in the user interface

C. Participants

Data was collected from 114 students at Qassim University; they contributed to the survey voluntarily. They comprised 114 college students, as shown in Fig. 6. Of these, 63 (55.27%) were male and 51 (44.73%) were female. All participants took the phonetics (Arab 342) course, at ALD at Qassim University. After they completed the course, Quizrevision was presented to them to review the course concepts and information. A link to the online questionnaire (http://goo.gl/forms/gKOQQ9Pe6y) was sent to them through e-mail and they were asked to complete the questionnaire.

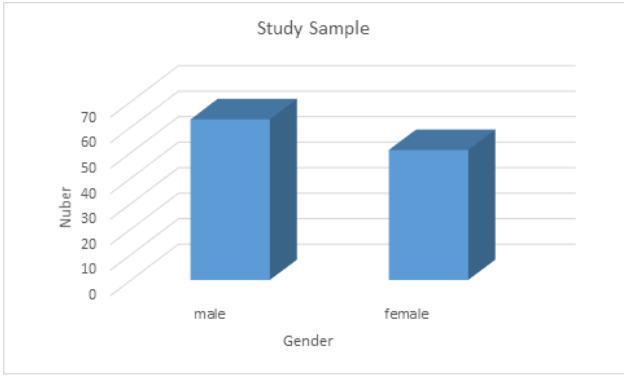

Fig. 6. Study participants

D. Measurement Instrument

A questionnaire was designed for the purposes of this study and distributed to some selected professors to express their opinions about the questionnaire and to edit its contents. The questionnaire consisted of 23 items with six constructs as follows:

1) *Usage and accessibility (UA),*
2) *Clarity of content (CC),*
3) *Effectiveness of learning (EL),*
4) *Compared with LMS (CL),*
5) *Attitude toward using the app (AU), and*
6) *Impression of app (IP).*

The measurement items were based on a five-point type Likert scale, ranging from strongly disagree (1) to strongly agree (5). The internal consistency reliability was 0.87 and Cranach's α (≥ 0.98), which was used to evaluate the reliability of the instrument. Therefore, the questionnaire had acceptable reliability for the application.

V. Results

A. Analysis of Measurement

Both discrimination and internal consistency validity were collected for measurement after Cranach's α (≥ 0.98) was computed. Discrimination validity ranged from 0.735 to 0.935. Discrimination was confirmed by examining the correlation coefficient among constructs of the measurement to exclude any weak or negative items; no item was excluded. The correlation matrix between constructs is shown in Table 1.

TABLE I. Correlation Matrix between Constructs

Constructs	UA	CC	EL	CL	AU	IP
UA	-					
CC	.876**	-				
EL	.804**	.862**	-			
CL	.780**	.796**	.914**	-		
AU	.735**	.768**	.869**	.868**	-	
IP	.801**	.829**	.881**	.916**	.882**	1.00

2-tailed p values; * $p < 0.05$, ** $p < 0.01$.

Usage and accessibility (UA), Clarity of content (CC), Effectiveness of learning (EL), Compared with LMS (CL), Attitude toward using the app (AU), Impression of app (IP)

The internal consistency validity was collected to ensure there were associations between constructs and the questions of the instrument as a whole. As shown in Table 2, the value of the internal consistency validity ranged from 0.843 to 0.935. The value refers to an acceptable value of internal consistency validity which is statistically significant (at $p < 0.05$) in general. Acceptable value reliability is 0.70. Therefore, the measurement items had both validity and reliability and there was a strong correlation between the correlation coefficient and items of each construct.

TABLE II. DISCRIMINATION VALIDITY OF CONSTRUCTS

Constructs	AV	Cronbach's Alpha
UA	15.78	.843**
CC	11.30	.883**
EL	18.92	.935**
CL	14.71	.922**
AU	14.79	.883**
IP	11.29	.929**

2-tailed p values; *p < 0.05, **p < 0.01.

B. Hypothesis Testing

In order to examine the research hypotheses, the constructs of the instrument were analyzed and descriptive statistics and chi-square(x^2) were collected, as shown in Table 3. Test results showed that the mean (SD) value ranged from 3.60 (1.544) to 4.16 (1.229), the x^2 value ranged from 26.70 to 122.35, and all the values were statistically significant (at $p < 0.05$). Regarding the first hypothesis of the research, students had a positive attitude toward using Quizrevision in reviewing the Phonetics course (Arab 342) course. The researchers used the constructs *Attitude toward using the app* (AU) and *Impression of app* (IP) to test the first hypothesis. As shown in Table 3, all items of AU and IP were significant, as follows: AU→x^2 (b1=34.86, b2=36.26, b3=26.70, b4=32.14, $p < .05$). The results indicate that students used the app while reviewing the course material; this gave them self-confidence, thus they had a positive attitude toward using the app IP→x^2 (b1= 51.61, b2=43.45, b3=32.57, $p < .05$). According to the results shown in Table 3, the students indicated they had a positive impression of the app. For the second research hypothesis, students preferred using the m-learning app rather than the LMS to review the course. We used the constructs *Effectiveness of learning (EL) compared with LMS (CL)* to examine the second hypothesis. The results, displayed in Table 3, show that all items the constructs EL and CL were significant, as follows: (EL)→x^2 (b1=61.11, b2=44.86, b3=61.08, b4=72.88, b5=64.38, $p < .05$). The students ensured that using the app as a reviewing tool provided them with quick feedback to support their knowledge and grasp of course concepts. According to the results in Table 3, (CL)→x^2 (b1=51.96, b2=97.84, b3=50.56, b4=56.96, $p < .05$). The students reported that they preferred using the app over the LMS, since it is more interesting and attractive.

TABLE III. MEANS, STANDARD DEVIATIONS (SD), CHI-SQUARE AND RELIABILITY FOR CONSTRUCTS OF THE INSTRUMENT

Constructs	Measurement instrument	Mean (SD)	Construct reliability	Chi Squared[a]
Usage and accessibility	I can easily use the Quizrevision app and navigate inside it.	3.88 (1.489)	.843	90.85
	I can get information easily using the app.	4.16 (1.229)		122.35
	I can easily download the app from Google Play.	3.89 (1.352)		77.75
Clarity of content	It helps me to learn and review, any place, anytime.	3.99 (1.346)	.883	93.32
	The content of the app is clear and orderly.	3.88 (1.252)		60.93
	Fonts, shapes, and graphics are clear.	3.79 (1.421)		53.55
	The app instructions are clear and understandable.	3.79 (1.417)		58.81
Effectiveness of learning	It motivates me to learn the content and to review it.	3.86 (1.327)	.935	61.11
	It helps me to fulfill my educational goals.	3.82 (1.294)		44.86
	The app facilitates performing the course activities.	3.74 (1.517)		61.08
	I can recognize differences between sounds and their pronunciation.	3.84 (1.461)		72.88
	It provides quick feedback to support my knowledge.	3.84 (1.430)		64.38
Compared with LMS	It is easier than LMS.	3.66 (1.539)	.922	51.96
	It is more interesting and attractive than LMS.	3.82 (1.549)		97.84
	Unlike LMS, I can use it anywhere without an internet connection.	3.60 (1.544)		50.56
	Unlike LMS, it helps me to memorize the content even	3.64 (1.529)		56.96

Constructs	Measurement instrument	Mean (SD)	Construct reliability	Chi Squared[a]
	after finishing my course.			
Attitude toward using the App	I believe that using the app while reviewing gives me self-confidence.	3.73 (1.285)	.883	34.86
	It develops my ability to recover course information and concepts.	3.69 (1.358)		36.26
	It improves my skills in understanding the course content.	3.66 (1.296)		26.70
The impression of the App	I have a positive attitude toward using the app.	3.71 (1.288)		32.14
	It is easy to use the app through my mobile device.	3.75 (1.436)	.929	51.61
	It is easy to test myself through the app.	3.80 (1.311)		43.45
	I have a positive impression of the app.	3.74 (1.262)		32.57

[a] chi-squared used to test time trends; *df* = 4

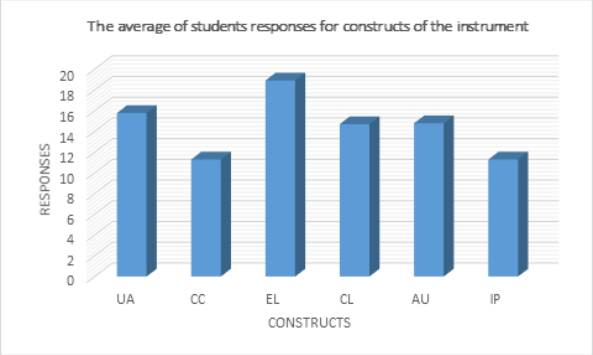

Fig. 7. Student responses for constructs of the instrument

TABLE IV. INDEPENDENT SAMPLES TEST

Constructs	Gender	Mean (SD)	MD	*t-value*	df	Sig.(2-tailed)
(UA)	Male	16.22 (4.77)	0.98	1.041	112	0.300*
	Female	15.24 (5.34)				
(CC)	Male	11.54 (3.87)	0.54	0.717	112	0.475*
	Female	11.00 (4.14)				
(EL)	Male	19.10 (6.52)	0.39	0.321	112	0.749*
	Female	18.71 (6.37)				
(CL)	Male	14.98 (5.67)	0.61	0.571	112	0.569*
	Female	14.37 (5.72)				
(AU)	Male	14.98 (5.67)	0.61	0.571	112	0.569*
	Female	14.37 (5.72)				
(IP)	Male	11.38 (3.88)	0.2	0.281	112	0.779*
	Female	11.18 (3.83)				

2-tailed p values; *p < 0.05, **p < 0.01.

In order to examine the third hypothesis of the research, the t-test value was calculated, which shows the difference between the participants (at p < 0.05) in the groups (male, female) regarding constructs of the instrument. Table 4 shows that participants in the groups have a score of: male (16.22), female (15.24); the mean difference (MD) is 0.98 while sig. = 0.300 > 0.05, t-value is 1.041, and *p*=0.01. Therefore, there is no statistical significance (at p < 0.05) between the test groups' opinions of the construct of UA. This result means that students have a positive impression of the construct of *Usage and accessibility* (UA), and the opinions of the two groups are the same. (Note: mean difference =MD, standard deviation=SD, freedom of degree=DF). As shown in Table 4, there is no statistical significance (at p < 0.05) between the test groups' opinions of the construct of CC, while sig. =.475 > 0.05 and *t*-value is .717, *p*=0.01; accordingly, the students agree on the construct of *Clarify the content* (CC). The students agree on the construct EL, as shown through the t-value of .321, *p*= .749. We can ensure that there is no statistical significance (at p < 0.05) between the test groups' opinions about the construct of EL. Table 4 shows that the students preferred the Quizrevision app to the LMS, with a t-value of 0.571, *p*=0.01. Therefore, there is no statistical significance (at p < 0.05) between the groups' opinions about the construct of CL. The participants in the test groups have the same opinion of using the app. The results in Table 4 illustrate that the *t-value* is 0.571, *p*=0.01. They agree on using Quizrevision as a reviewing tool because it enables them to develop their skills in recognizing course information and concepts. They also agree on the ease of learning the course through the app. There is no statistical significance (at p < 0.05) between the groups' opinions about the construct of IP, where t-value is .281, *p*=0.001. The Student responses for constructs of the instrument are shown in Fig. 7.

TABLE V. T-TEST AND DESCRIPTIVE RESULTS

Gender	Pre-group Mean (SD)	Post-group Mean (SD)	t-value	df	Sig.(2-tailed)
Male	24.22 (7.56)	44.62 (3.56)	18.63	61	0.000*
Female	31.71 (5.93)	47.25 (1.89)	16.55	49	0.000*

*P <.05. **p<.01.

To examine the fourth hypothesis of the research, which provides for "The degree of students achievement have been improved and there is a statistically significant difference (at p < 0.05) between the mean scores of the pre- and post-tests after using the Quizrevision app as a reviewing tool." The t-test value was used to validate the hypothesis; results are shown in Table 5. There is a statistically significant difference between the mean scores of the study group score after using Quizrevision in reviewing the course. This indicates that the

fourth hypothesis of the study is confirmed, in terms of the effectiveness of the proposed program in knowledge acquisition of the proposed unit for the students. This result is due to the degree to which the students improved after using the app as a reviewing tool.

VI. CONCLUSIONS

The purpose of this study was to provide students of the Phonetics course (Arab 342) with an alternative tool for reviewing that would enable them to review course knowledge and concepts. We were interested in motivating students to interact using modern technology. Moreover, the scores of students were improved after using the app. We used MIT's App Inventor language to design the application. The app, Quizrevision, was designed to provide students in the Phonetics course (Arab 342), with quick feedback to support their knowledge and to be used as a reviewing tool. Moreover, the app enables students to recognize differences between sounds and their pronunciation. Consequently, our findings confirm that students prefer using m-learning apps rather than LMS for revision.

VII. FUTURE WORK

The application will be a base for series of other researches in Arabic courses and it will be a support for using e-learning at universities**.**

REFERENCES

[1] A. Rabiee, Nazarian Z., & Gharibshaeyan , R., "An Explanation for Internet Use Obstacles Concerning E-Learning in Iran". *International Review of Research in Open and Distance Learning, 14*(3), p361-376, 2013.

[2] C.Chang, Shen H.-Y., & Liu , E. Z.-F. "University Faculty's Perspectives on the Roles of E-Instructors and Their Online Instruction Practice". *International Review of Research in Open and Distance Learning, 15*(3), p72-92, 2014.

[3] C.Gautreau, "Motivational Factors Affecting the Integration of a Learning Management System by Faculty. *Journal of Educators Online, 8*(1), p1-25, Jan, 2011.

[4] C.Keller & Cernerud , L.,"Students' Perceptions of E-learning in University Education". *Journal of Educational Media, 27*(1/2), p55-67, 2002.

[5] D.Coşkunçay & özkan, s., "A model for instructors' adoption of learning management systems: empirical validation in higher education context" . *Turkish Online Journal of Educational Technology, 12*(2), p13-25, 2013.

[6] D.Meehan & Sabin , M., "QuizPower: a mobile app with app inventor and XAMPP service integration". *SIGITE '13 Proceedings of the 14th annual ACM SIGITE conference on Information technology education* (New York: ACM. pp. 103-108). 2013,doi:10.1145/2512276.2512300

[7] D.Wolber, Abelson, H., Spertus, E., & Looney, L. "*App Inventor 2", 2nd Edition.* O'Reilly Media, October 2014.

[8] H.J. Jung, "Fostering an English Teaching Environment: Factors Influencing English as a Foreign Language Teachers' Adoption of Mobile Learning". *Informatics in Education, 14*(2), p219-241, 2015.

[9] H.Twakyondo & Munaku, M., "Blackboard (Web resource); Moodle (Computer software); Chuo Kikuu cha Dar es Salaam; Learning Management System (Computer software); Courseware; Open source software. *International Journal of Computing & ICT Research, 6*(2), p33-45, Dec,2012.

[10] I. Boticki, Baksa, J., peter seow, & chee-kit looi, "Usage of a mobile social learning platform with virtual badges in a primary school". *Computers & Education, 86*, p120–136, August, 2015.

[11] J.Sae-Khow, "Developing of Indicators of an E-Learning Benchmarking Model for Higher Education Institutions". *Turkish Online Journal of Educational Technology - TOJET, 13*(2),p35-43, 2014.

[12] K. Al-Busaidi A., "An empirical investigation linking learners' adoption of blended learning to their intention of full e-learning". *Behaviour & Information Technology, 32*(11), p1168-1176, 2013. doi:10.1080/0144929X.2013.774047.

[13] K. F. Hashim, Tan, F. B., & Rashid, A.,"Adult learners' intention to adopt mobile learning: A motivational perspective". *British Journal of Educational Technology, 46*(2), p381-390, 2015.

[14] K. M. titi & Muhammad A., "Improvement Quality of LMS Through Application of Social Networking Sites". *International Journal of Emerging Technologies in Learning, 8* (3), p48-51, 2013.

[15] K.Georgouli, Skalkidis, I., & Guerreiro, P. A "Framework for Adopting LMS to Introduce e-Learning in a Traditional Course. *Educational". Technology & Society, 11*(2), p227-240, . 2008.

[16] L.A. Guerrero, Ochoa, S., & Collazos, C., "A mobile learning tool for improving grammar skills". *Procedia - Social and Behavioral Sciences, 2*(2), p1735-1739, 2010.

[17] L.Carter , Salyers , V., Carter , A., Myers , S., & Barrett , P. The Search for Meaningful E-Learning at Canadian Universities: A Multi-Institutional Research Study. *International Review of Research in Open and Distance Learning, 15*(6), p313-347, 2014.

[18] M. A. Amasha; Salem Alkhalaf ,."Using RSS 2.00 as a Model for u-Learning to Develop e-Training in Saudi Arabia, International journal of information and communication technology education: an official publication of the Information Resources Management Association 6(7):6 · July 2016.

[19] M.A.Amasha, Salem Alkhalaf. "A Model of an E-Learning Web Site for Teaching and Evaluating Online", International Journal of Advanced Computer Science and Applications (IJACSA), 4(12), 2013. arXiv preprint arXiv:1501.05578

[20] M.Demirbilek, Investigating Attitudes of Adult Educators towards Educational Mobile Media and Games in Eight European Countries. . *Journal of Information Technology Education, 9*, p235-247, 2010.

[21] M.Sarrab, AL-Shihi, H., & AL-Manthari, B., "System Quality Characteristics For Selecting Mobile Learning Applications". *Turkish Online Journal of Distance Education (TOJDE). , 16* (4), p18-27, Oct, 2015.

[22] P.Ling & Ze, Z., "Developing Digital Learning Resources for the College Market in China". *Publishing Research Quarterly, 4*, p354-363, 2011.

[23] Q.Wu, "Designing a smartphone app to teach English (L2) vocabulary". *Computers & Education, 85*, p170–179, July 2015.

[24] S. B. Asselin, "Learning and assistive technologies for college transition". *Journal of Vocational Rehabilitation, 40*(3), p 223-230, 2014.

[25] S. Papadakis, Kalogiannakis, M., Orfanakis, V., & Zaranis, N., "Novice Programming Environments". Scratch & App Inventor: a first comparison. *IDEE '14 Proceedings of the 2014 Workshop on Interaction Design in Educational Environments* (p. 1). New York ,NY, USA: ACM. doi: 10.1145/2643604.2643613

[26] S.Alkhalaf, Mohammed A. Amasha, Amal Al-Jarallah. "Using M-learning as an Effective Device in Teaching and Learning in Higher Education in Saudi Arabia". International Journal of Information and Education Technology, 7(6). Jun,2017.

[27] S.D. "Using disruptive technologies to make digital connections: stories of media use and digital literacy in secondary classrooms". *Educational Media International, 51*(2), p109-123, 2014.

[28] S.Gabarre, C., Din, R., Shah, P. M., & Karim, A. A. "Using Mobile Facebook As An LMS: Exploring Impeding Factors". *GEMA Online Journal of Language Studies, 13*(3), 99-115. 2013.

[29] S.Wichadee, "Factors Related to Faculty Members' Attitude and Adoption of a Learning Management System". *Turkish Online Journal of Educational Technology, 14*(4), p53-61,2015.

[30] S.Williams van Rooij, .Open-source learning management systems: a predictive model for higher education. *Journal of Computer Assisted Learning, 28*(2), p114-125, Apr 2012.

[31] X.Yang, Li, X., & Lu, T. "Using mobile phones in college classroom settings: Effects of presentation mode and interest on concentration and achievement". *Computers & Education, 88*, p292–302, October 2015.

[32] Y.C. Hsu & Ching, Y.-H. "Mobile App Design for Teaching and Learning: Educators' Experiences in an Online Graduate Course". *International Review of Research in Open and Distance Learning, 14*(4), p117-139, 2013 .

[33] Y.Lin, Chung , P., Yeh , R., & Chen , Y., "An Empirical Study of College Students' Learning Satisfaction and Continuance Intention to Stick with a Blended e-Learning Environment" *International Journal of Emerging Technologies in Learning, 11*(2), p63-66, 2016.

[34] Z.Bogdanovic, Barac, D., Jovanic, B., Popovic, S., & Radenkovic, B. "Evaluation of mobile assessment in a learning management system". *British Journal of Educational Technology, 45*(2), 231–244, 2013. doi:10.1111/bjet.12015

[35] Z.Wan, Compeau, D., & Haggerty, N. "The Effects of Self-Regulated Learning Processes on E-Learning Outcomes in Organizational Settings". *Journal of Management Information Systems, 29* (1), p307-340, 2012.

A Systematic Literature Review to Determine the Web Accessibility Issues in Saudi Arabian University and Government Websites for Disable People

Muhammad Akram
College of Graduate Studies
Universiti Tenaga Nasional
Jalan IKRAM-UNITEN, 43000 Kajang, Selangor,
Malaysia

Rosnafisah Bt Sulaiman
College of Information Technology
Universiti Tenaga Nasional
Jalan IKRAM-UNITEN, 43000 Kajang, Selangor,
Malaysia

***Abstract*—Kingdom of Saudi Arabia has shown great commitment and support in past 10 years towards the higher education and transformation of manual governmental services to online through web. As a result number of university and e-government websites increased but without following the proper accessibility guidelines. Due to this many disable peoples may not be fully benefited the contents available on university and government websites. According to the World Health Organization (WHO) report, there are more than one billion people all over the world facing different kind of disabilities. Almost 720,000 Saudi nationals are disable which is about 4% of total Saudi population. The objective of this study is to review the existing literature to identify the web accessibility issues in Saudi Arabian university and government websites through a systematic literature review. Several scholarly databases were searched for the research studies published on web accessibility evaluation globally and in Saudi Arabia from 2009 to 2017. Only 15 (6 based on Saudi Arabia and 9 global) research articles out of 123 articles fulfilled the selection criteria. Literature review reveals that web accessibility is a global issue and many countries around the world including Saudi Arabia are facing web accessibility challenges. Moreover web accessibility guidelines WCAG 1.0 and WCAG 2.0 are not addressing many problems which are faced by user and some guidelines were not effective to avoid the user problems. However, findings in this study open a new dimension in web accessibility to do extensive research to determine the web accessibility criterions/standards in context of Saudi Arabia.**

Keywords*—Web accessibility; disability; e-government; web contents accessibility guidelines; WCAG 1.0; WCAG 2.0; accessibility evaluation

I. INTRODUCTION

Websites play a vital role to get the information in different fields of life such as, education, employment, government, commerce, health care etc. These websites should be accessible for all users including disable people so that they can utilize all provided services. According to the report published on disability by the WHO, there are more than one billion people worldwide live with different kinds of disabilities [1]. These disable persons are considered as people who have long term or permanent physical, cognitive, mental, intellectual, psychological or sensory impairments which constitute a barrier or obstacle for them to fully, equally, and effectively participate in all society activities as other people [2]. Like other countries, Saudi Arabia also have reasonable number of disable person. According to the news published on Saudi national newspaper, there are almost 720,000 Saudi nationals are disable. It is around 4% of total Saudi population [3].

In 2006 [2], UN assembly passed a treaty for disable people's rights which aims to promote and protect their rights. It covers a number of key areas such as employment, education, health and accessibility. The elementary issue of article 9 of the convention entails countries to determine and eradicate obstacles and barriers that hinder disabled people from accessing their environment, transportation, public facilities, services and information technologies (ICT). The United Nations have recently extended these efforts to include web accessibility in Article 9, Section-2, paragraph-h. According to United Nation treaty collection [4], about 187 countries already signed the treaty and Saudi Arabia signed this treaty in June 2008 and makes the legislation which addresses the disability issues. This law was mainly addressing the employment and skills development which did not clearly contain the rules for web accessibility.

Study which was conducted by the UK office for disability studies noted that the main reason of using Internet by disable people was to use the services provided by the government web sites [5].

It is very important to design and implement governmental and university websites by following the web accessibility guidelines. It will ensure that disable people can also benefit from services provided by governmental website. Therefore, in this paper we have reviewed the existing research studies conducted in Saudi Arabia and globally to identify the web accessibility issues in both university and governmental websites. Accessibility issues are highlighted and proposed the further need of in-depth research to design the web accessibility guide lines in context of Saudi Arabia. The rest of research paper is organized into seven sections: Section 2 briefly explains the web accessibility and principles of web content accessibility guidelines 2.0. Section 3 describes about the legislation on web accessibility. Section 4 discuss about the e-services provided by the Saudi government and universities. Section 5 discuss about existing research studies conducted on web accessibility. Section 6 talk about the research

methodology which is adopted to complete this study. Section 7 presents the discussion and recommendation. Section 8 gives the conclusion and future work.

II. Web Accessiblity and Principles of Web Content Accessibility Guideline 2.0 (WCAG 2.0)

According to the Information Resources Management Association (IRMA) web accessibility is *"making web content available to all individuals, regardless of any disabilities or environmental constraints they experience"* [6].

World Wide Web Consortium establishes the Web Accessibility Initiative (WAI) in 1997 to design web accessibility guidelines. In 1999, they finalized and recommended to use Web Content Accessibility Guidelines (WCAG 1.0) to design websites [7]. At the end of 2008, WCAG-2.0 was published that applies broadly to more advance technologies [8]. WCAG 2.0 contains 12 guide lines which are based on four main principles; 1) perceivable 2) operable 3) understandable and 4) robust. These guidelines are shown in Table 1 below:

TABLE. I. PRINCIPLES OF WEB CONTENT ACCESSIBILITY GUIDELINE 2.0

Principles	Guidelines
Principle 1: Perceivable	• Website should provide the alternative text for all non-text contents. • If there is any multimedia file in web site then web designer must include the caption for those files. • Website contents should be presented in such a way that if someone use assistive technology then meaning of contents not loose. • All the information which is available on website should be very easy to read and hear.
Principle 2: Operable	• It should be possible that user can perform all available operations in website using keyboard. • Website did not have any data or contents which can be the reason of seizures. • Help should be available for users to search different contents in website and to navigate different available pages in website.
Principle 3: Understandable	• All available contents in website must be readable and easily understandable for all different type of users. • All website contents should appear and operate in predictable way. • Support should be available for users to avoid making mistakes and if mistakes are done from user than there should be mechanism to correct them.
Principle 4: Robust	• All designed website should have compatibility to run on different type of browsers and also different assistive tools can be used.

The goal of these guidelines is to promote and achieve web accessibility for people suffering with different kind of disabilities.

WCAG 2.0 encompasses a series of checkpoints under 12 guidelines. W3C working group assigned priority levels to each checkpoint on bases of its impact on accessibility. Total three priority level was defined and for each there are numbers of checkpoints those need to be satisfied to achieve corresponding conformance level [8] which are listed in the following Table 2:

TABLE. II. CONFORMANCE LEVEL AND CHECKPOINTS

Conformance level	Total number of checkpoints
"Single-A": Satisfied all checkpoints of Priority1.	25
"Double-A": Satisfied all checkpoints of Priority 1 and 2.	25 + 13 = 38
"Triple-A": Satisfied all checkpoints of Priority 1, 2, and 3.	38 + 24 = 62

III. Legislation on Web Accessibility

Strong legislation can surely produce the better web accessibility results and countries those have strict laws or policies on web accessibility with actual execution of law provides the more protection to disable people [5]. Many countries worldwide are continuously working to set up the legislation that all governmental websites should be accessible for all citizens including the people with disability. According to W3C [9], 19 countries already have done their national legislation on web accessibility, Table 3 shows the web accessibility legislation for some of them.

TABLE. III. LEGISLATION ON DISABILITY

County	Legislation
United Kingdom	• The disability discrimination act 1995 • Special educational needs and disability act 2001
United States of America	• Americans with disabilities act (ADA)
Australia	• Disability discrimination act 1992
Canada	• Canadian human rights act of 1977
Germany	• Act on Equal Opportunities for Disabled Persons of 27 April 2002
Ireland	• The Disability Act, 2005
Israel	• The Equal Rights for People with Disabilities Law 5758-1998
Italy	• Provisions to support the access to information technologies for the disabled
New Zealand	• Human Rights Amendment Act 2001
Portugal	• Resolution of the Council of Ministers Concerning the Accessibility of Public Administration Web Sites for Citizens with Special Needs

Source: W3C, Policies Relating to Web Accessibility

However, Thailand has updated the Web Content Accessibility Guidelines 2.0 (WCAG 2.0) according to their own country requirements and named it: Thailand Web Content Accessibility Guidelines (Th-WCAG) [10], [11]. Now these guidelines gives the roadmap for web developers to

design websites focusing the accessibility issues and also decision makers take help to form any policy related to web accessibility. The countries those are struggling to establish their own web accessibility guidelines can modify the web content accessibility guidelines designed by W3C according to their local context as Thailand has done.

IV. Background on E-Service Provided by Saudi Government and Saudi Universitiess.

A. Internet Users:

Internet facility becomes available in KSA since 1997 [10] and its users are gradually increasing due the increase in Saudi population, improvement in infrastructure, reduction in Internet usage cost and continues improvement in quality of service. According to the internet live stats, total numbers of internet users in Saudi Arabia was about 4.7 million in year 2000 (2.2% of total Saudi population) and increased to about 20.8 million in year 2016 (64.7% of total Saudi population) [12]. These users are mainly divided into following four main categories 1) users using e-government services 2) user using university websites 3) user doing online shopping 4) user using social websites.

B. E-Services:

E-services or e-government is a process of shifting the manual government services to online by using information and communication technology. This transformation from manual to online is important because it provides easy access for all stakeholders to government e-services, reduce the personal cost, save time, increase service and increase the efficiency [6], [13].

The Kingdom of Saudi Arabia has shown great interest and commitment towards the transformation of manual governmental services to online. A Royal Decree [6] was issued to the Ministry of Communication and Information Technology (MCIT) in 2003 to make plans to provide all government services online through internet to all its stakeholders. In response to the Royal Decree, MCIT, Ministry of Finance (MOF) and Communication and Information Technology Commission (CITC) worked together and prepare a plan for e-government and named it Yesser. Moreover many other e-government projects have been started and implemented e.g. national smart identity card, e-payment through "Sadad", social insurance, portal for e-government, public key infrastructure, e-participation, e-procurement etc. By 2016, [14] around 2974 service are provided by all Saudi government agencies, whereas 2668 services are electronic based and only 306 services are traditional services. Saudi government divided its services in different categories for its beneficiaries; Table 4 shows the total number of services provided by government according to its category until May 2017.

According to the UN e-government survey 2016 [15], KSA belongs to the countries which have high e-government development index (EGDI). Table 5 shows the EGDI ranking of Saudi Arabia and its components: Online Service Index (OSI), Telecommunication Infrastructure Index (TII) and Human Capital Index (HCI).

TABLE. IV. Number of E-services provided by Saudi government and its beneficiaries

E-Service Category	**Beneficiaries**			
	Individual	***Business***	***Public entities***	***Visitors***
Information and Communication Technology	16	12	16	0
Economy and business	172	288	149	2
Training, education, and culture	412	54	52	2
Travel and Tourism	31	11	6	11
Islamic affairs	57	38	32	5
Labor	42	42	18	0
Insurance and pension	45	47	12	0
Social life	110	6	13	2
Housing and municipality	183	127	54	1
Health and environment	99	61	31	2
Utilities	39	33	13	0
Transportation	40	85	16	0
Traffic and safety	36	23	18	0
Personal documentations	123	34	42	1

TABLE. V. E-government development index (EGDI) of Saudi Arabia

EGDI World Ranking 2016	**Asian Ranking**	**EGDI Level**	**EGDI Value**	**OSI**	**HCI**	**TII**
44	9	High	0.6822	0.6739	0.5733	0.6822
TII and its components per 100 inhabitants						
Fixed-telephone subscriptions	Mobile-cellular telephone subscriptions	Mobile-cellular telephone subscriptions	Fixed (wired)-broadband subscriptions	Wireless broadband subscriptions		
63.70	13.36	179.56	10.36	70.60		

Source: UN E-Government Survey 2016

C. Saudi Universities:

Saudi Arabian government has shown great commitment and support towards the higher education in past 10 years and continuation in coming years. Moreover most of these institutions have adopted the e-learning and online centric programs.

Saudi Arabia has total 73 colleges and universities, among them about 26 are public sector universities which are fully funded by government [16]. King Saud University is first university which was established in 1957 and University of Jeddah is the newest university established in 2014.

Student's enrolment in both public sector and private sector universities is gradually increasing due to the continues increase in universities during past 10 years. In 2001, total numbers of students in higher education programs were 432,000 and become 1.5 million in 2014. Moreover it is estimated that students' number will reach 2.537 million in 2022 [17].

All colleges and universities have their own website and most of the website are bilingual (English and Arabic). These websites are not only used by current students, it can be accessed by prospective students, alumni students, program advisory committee, student's family members, international user etc. So it is very important that users with disability can also access the website same as the normal user can access because most of the universities are providing the online services to students such as online library, online course registration, current student's surveys and alumni surveys. E-learning was started in 2002 in Saudi Arabia [18] and since it is gradually shifting their traditional teaching system to web based learning in higher education programs. Now most of the universities in kingdom have adopted BlackBoard as Learning Management System (LMS) and smart classroom automation techniques [19]. Both faculty members and students are required to use LMS during their regular class activities e.g. organizing virtual classes, online attendance, uploading assignments, student grades etc. This transformation from traditional teaching style to e-learning demands to improve the web accessiblity of university and college websites. However exiting research studies shows that university website have many web accessibility issues which need to be handle properly.

V. Existing Research Studies on Web Accessibility

Literature review reveals that many research studies have been conducted in past two decades on web accessibility around the world and few are done in Saudi Arabia as well. Following five research studies fulfilled the selection criteria which are completed since 2010 to explore the web accessibility issue for disable people in Saudi Arabia.

In 2010, Mukhtar M. Rana, et al., [20] used automatic web accessibility analysis tools JAWS and Supernova to evaluate the web accessibility of home page of 25 Saudi university websites against the web accessibility guidelines provided by World Wide Web consortium. Functional accessibility analysis on university websites shows that, navigation and orientation, text equivalent and styling are partially implemented and average errors are 24.30%, 28.15% and 38.02% respectively. Moreover scripting and HTML standards are completely implemented with average errors 0% in scripting and 8.53% HTML standards. Study concluded that 80% university websites in Saudi Arabia are not following the web accessibility guidelines also web developers are not fully aware of the web accessibility guidelines. Another study [21] was conducted to identify the challenges which affect the web accessibility of Saudi Arabian university websites by doing interviews from 15 experts in 9 Saudi universities. Study identified the eight main challenges which need to address to improve the web accessibility. However one of the core challenges was the negative attitude toward addressing the disability issues. Web accessibility in Saudi Arabian university is continues challenge which need to address properly by doing further research to explore the problems faced by disable user and consider user's problem during designing the university websites

Hend S. Al-Khalifa [10] evaluated the accessibility of Arabic version of 36 Saudi government websites to check the conformance level with WCAG 2.0. Each homepage was inspected manually with the help of evaluation tool WAVE toolbar and web developer toolbar. It is noted that each governmental website has violated the web accessibility guidelines and no website is following minimum guidelines of WCAG 2.0. According to the Saudi national portal; currently 2974 services provided by all Saudi government agencies, whereas 2668 services out of 2974 are electronic based which clearly give the indication of importance for improvement of web accessibility in governmental websites.

Addin Osman [22] performed a systematic literature review to evaluate the available automatic web accessibility tools and the web accessibility of website globally and in Saudi Arabia based on the web content accessibility guidelines. Study reveals that it is required to improve the accessibility of websites globally and in Saudi Arabia and web accessibility awareness among web masters and decision makers in Saudi Arabia. Knowledge about web accessibility for decision makers and web developer is also an important factor which can affect the improvement of web accessibility.

Majed Alshamari [23] examined the homepage of three popular online shopping websites in Saudi Arabia using accessibility evaluation tools: AChecker, TAW, MAUVE, EvalAcess and Functional Assessment Evaluation 2.0. Study concluded that selected websites have navigation errors, readability errors, HTML errors, and input assistance and timing errors. Moreover they suggested some recommendation and point out that involvement of web accessibly experts in evaluation can give better results.

Table 6 below present the summary of all reviewed article on web accessibility conducted globally and in Saudi Arabia. Web accessibility is a global issue and especially in developing countries web accessibility situation is not very good as compared to developed countries.

Developing countries including Saudi Arabia needs to put web accessibility as a high priority issue to solve because disable user are not fully get benefited from the eservice provided by government and universities due to poor web accessibility.

TABLE. VI. SUMARY OF EXISTING RESEARCH STUDIES ON WEB ACCESSIBILITY

Author, Year	Objective/Purpose of Study	Research Methodology	Results/Output
Addin Osman (2017) [22] Saudi Arabia	To evaluate the web accessibility of website globally and in Saudi Arabia based on the web content accessibility guidelines.	Systematic Literature Review	Researcher concluded that it is required to improve the accessibility of websites globally and in Saudi Arabia specifically. It is required to check the web accessibility of website in Saudi Arabia.
Majed Alshamari (2016) [23] Saudi Arabia	To evaluate the supporting tools used by disable people to access the websites and accessibility analysis of three popular e-commerce website using automatic tools.	Five automatic accessibility evaluation tools AChecker, TAW, Eval Access, MAUVE and FAE was used to test the accessibility of selected e-commerce websites.	Result shows that selected websites have navigation errors, readability errors, HTML errors, and input assistance and timing errors. Moreover involvement of web accessibly experts in evaluation can give better results.
Asmaa Alayed et. al. (2016) [21]. Saudi Arabia	To identify the challenges which affect the web accessibility of Saudi Arabian university websites.	Interviews were conducted from 15 experts in 9 Saudi universities.	Identified the eight main challenges which need to address to improve the web accessibility.
Hend S. Al-Khalifa (2012) [10] Saudi Arabia	To evaluate the Saudi Arabian government websites on the bases of the guidelines provided by the W3C.	Comprehensive literature review and assess the home page of Saudi government websites	Found many accessibility errors and no governmental website is following minimum guidelines of WCAG 2.0
Mukhtar M. Rana et al. (2011) [20] Saudi Arabia	To evaluate the accessibility of 21 Saudi university websites using assistive technologies such as JAWS and Supernova.	Qualitative approach Screen readers JAWS and Supernova were used.	The research revealed that 80% of universities have low accessibility standards and could not achieve minimum 'A' conformance
Mohd Hanapi et al. (2010) [24] Malaysia	To evaluate the accessibility of nine Malaysian e-government website on the bases of guidelines provided by the World Wide Web Consortium (W3C) and also to identify that webmasters have knowledge of W3C guidelines.	• Nine Malaysian government websites was chosen to evaluate the web accessibility. • Automatic tool Bobby was used to evaluate the websites. • Only the main page of these websites was tested. • Interviews conducted with webmasters and website developers.	No single government website is following W3C proposed guidelines. Also most of the webmasters did not have clear idea of W3C proposed guidelines.
Yakup Akgul et al. (2016) [25] Turkey	Homepage of twenty five Turkish government websites was evaluated to check the web accessibility for disable people	• TML and CSS validity was checked by automatic evaluation tools, Markup Validation Service and CSS validator service. • Web accessibility was checked by AChecker, eXaminator, TAW, Total Validator, WAVE, Web Accessibility Assessment Tool, Eval Access, Cynthia Says, MAGENTA, HERA, Amp and Sort Site	Mostly websites did not meet minimum level of web accessibility requirements. Moreover only four web sites (about 16%) are using proper HTML5 DOCTYPE and only five websites (about 20%) have some use of ARIA.
Solomon Adelowo Adepoju et al. (2016) [26] Nigeria	To evaluate the accessibility and performance of Nigerian e-Government websites.	Automatic tools: TAW and site analyzer was used to measure the conformance level of e-government with WCAG.	None of the Nigerian government websites are fully following the accessibility guidelines.
Basel Al Mourad et al. (2013) [27][28]. Dubai	To evaluate the accessibility of 21 Dubai e-Government websites for conformance level with WCAG 1.0 by using automatic tools.	Main page of the 21 e-Government website was evaluated by using accessibility evaluation tool: TAW (Test de Accesibilidad Web)	Result shows that many e-Government websites in Dubai did not meet the minimum accessibly conformance level. Main issues are text equivalents are not provided for non-text elements and no static equivalent for dynamic elements.
Muhammad Bakhsh et al. (2012) [29] Pakistan	To evaluate the web accessibility of home page of 45 central government web portals in Pakistan on the bases of W3C guidelines.	Automatic web accessibly checking tools: Functional accessibility evaluator (FAE) and total validator were used to measure the conformance level with WCAG 2.0.	Researcher s found that W3C guidelines are not fully followed for the development of central government web portals. Navigation is one of an importance factor to fully explore the contents of any website for its users including disable people but result shows that only 2.63% websites are fully and 97.37% are partially implemented.

Aidi Ahmi et al. (2016) [30] Malaysia	To evaluate the main page of 25 Malaysian governmental websites for the WCAG 2.0 and Section 508 guidelines	• Twenty five Malaysian government websites was chosen to evaluate the web accessibility. • Automatic tool WAVE and AChecker was used to evaluate the websites. • Only the main page of these websites was tested. .	Study reported three different types of problems 1) known problems 2) likely problems 3) potential problems Also Most of the ministry websites are not designed by following the WCAG 2.0 and Section 508
Humaira Nazar et al. (2017) [31] Pakistan	To evaluate the accessibility of main page of 15 banking websites in Pakistan for compliance with WCAG 1.0 and WCAG 2.0 using automatic accessibility tools.	• Fifteen Pakistan banking websites was chosen to test the web accessibility. • Automatic tools: Markup validation service, ACheker, Valet and Eval was used • Only homepage was analyzed.	Four parameters was test during evaluating the websites and it is found the no web site is following WCAG 1.0 and WCAG 2.0 properly.
Joanne et al. (2009) [5] EU, Africa and Asia	To evaluate the accessibility of governmental website located in Europe, Asia and Africa.	Automatic web accessibility tool TAW was used to evaluate the websites of six federal governmental agencies in 12 countries for compliance with WCAG 1.0	Results shows that web accessibility is a global issue but countries those have strong accessibility law have better web accessibility situation.
Abdulmohsen et al. [32]	To evaluate the e-Government websites of Saudi Arabia and Oman for conformance level with Web Content Accessibility Guidelines.	13 Saudi e-Government websites and 14 Omani e-Government websites was evaluated by tools: Multiweb, LYNX and W3C validator service.	It is concluded that less importance to provide the services for people with special need is key factor and GCC countries need to review policies make their e-Government websites more accessible.

Fig. 1 shows that 87% of reviewed articles are using automatic web accessibility evaluation tools to evaluate the homepage of websites, 7% have used the literature review technique and only 6% completed their studies on the bases of interviews. Fig. 2 shows that 14 automatic web accessibility evaluation tools were used in reviewed articles and TAW is the mostly used tool followed by AChecker and EvalAccess.

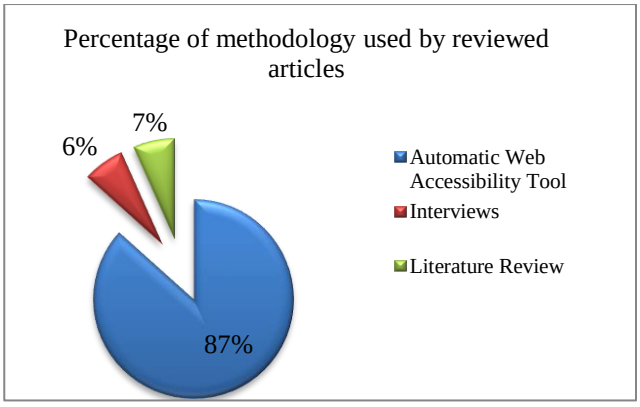

Fig. 1. Percentage of methodology used by authors.

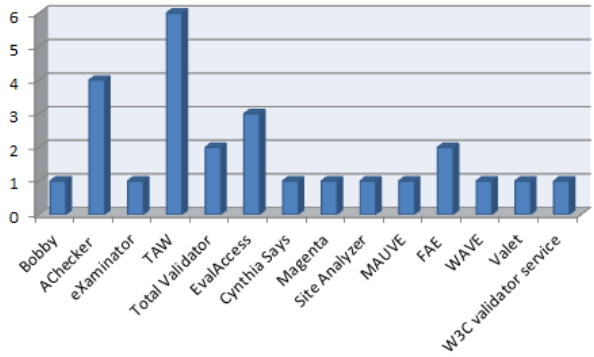

Fig. 2. Usage of automatic web accessibility tools.

VI. Research Methodology

In this paper systematic literature review (SLR) methodology is used for the identification and critically evaluation of exiting literature in the scope of web accessibility.

A. Formation of Research question

First step in SLR is to form the research questions which need to be address. Three research questions have been defined to determine the web accessibility issue in Saudi Arabia and other countries.

Research question 1: What are the main principles of Web Content Accessibility Guideline 2.0 (WCAG-2.0) proposed by the World Wide Web Consortium (W3C) to improve the web accessibility?

Research question 2: What is the compliance level of university and government websites against WCAG-2.0 globally?

Research question 3: What is the compliance level of Saudi Arabian university and government websites compare to WCAG-2.0?

B. Identification of relevant publications/articles

Second step in SLR is to identify the relevant studies in the area of web accessibility. So we have following search strategy for the identification of studies.

1) Selection Period: Articles was selected from 2009 to 2017.

2) Keywords used to search the relevant articles: Web accessibility, disability, e-government, web contents accessibility guidelines, WCAG 1.0, WCAG 2.0, accessibility evaluation.

3) Scholarly databases searched: Google scholar, Google search engine, EBSCO host, IEEE Explorer, Science Direct, The Elsevier, Springer Link, ACM digital Library, Wiley and Emerald.

4) Study Population: Saudi Arabia, UAE, Malaysia, Turkey, Pakistan, Nigeria, UK, France, Germany, Switzerland, China, India, Cambodia, Philpines, South Africa.

5) Outcome: 25 research studies were selected for review.

Identification of relevant research studies in the area of web accessibility is achieved in three layers. Table 7 show the layer model which is divided into basic layer, intermediate layer and advanced layer.

VII. Discussion and Recomendation

Analysis of 15 reviewed articles discloses that web accessibility is a global issue and mostly countries including Saudi Arabia is not properly following the guidelines provided by the World Wide Web consortium.

Disable people around the world are not able to fully benefit from services provided by government and universities due to low web accessibility. Web accessibility need to be a key priority for Saudi government because eelectronic service share in Saudi e-government is 89.7% and mostly Saudi universities have adopted BlackBoard as learning management system (LMS) and smart classroom techniques. Following are the factors which affects the web accessibility of websites:

Literature review explore that many web accessibility issues needs to handle properly in Saudi Arabia and around the world e.g. Navigation errors, orientation issue, timing errors, text equivalent to graphics, content and scripting, validity of HTML and CSS, use of HTML5, interface design, content and scripting.

A. *Effect of web accessibility legislation and proper law execution*

Web accessibility legislation is an important factor which needs to address by most of the countries including Saudi Arabia. In [5], reported that countries those have strict web accessibility legislation with proper implementation have improved web accessibility situation for disable peoples. Saudi Arabia [10] signed UN treaty for disable people's rights in June 2008 and makes the legislation by focusing the disability issues but without clearly defined the rules for web accessibility.

B. *Lack of web accessibility knowledge*

Web developers and policy makers' awareness of WCAG 1.0 and WCAG 2.0 are very important to improve web accessibility but [21], [24] reported that many web developers are unaware of web accessibility guidelines.

TABLE. VII. Layered Model for Identification of Relevant Research Studies

Layers	Description	Output
Basic Layer	Research studies identification Criteria: • Study population: International • Search Area: Web Accessibility • Publication Year: Not restricted • Databases: EBSCO host, IEEE Explorer, Science Direct, The Elsevier, Springer Link, ACM digital Library, Wiley and Emerald.	Total Article searched: 123 • International: 88 • Based on Saudi Arabia: 35
Intermediate Layer	Initial screening Criteria: • Publication Title • Publication Year • Scope • Keyword Articles Excluded 67	• International: 39 on Saudi : 17
Advance Layer	High level screening Criteria: • Publication Title • Publication Year • Specific Keywords Articles Excluded 52	• International: 9 on Saudi : 6

Moreover, André Pimenta [33] made comparisons of problems faced by users with web accessibility guidelines and proved that web accessibility guidelines are not addressing many problems which are faced by user. However disability types vary from country to country, few countries (e.g. UK, Australia, US, Canada) already developed their own accessibility guidelines based on their country's context. Recently, Ontario, one of the provinces of Canada, adapted its own accessibility guidelines based on provincial context to improve the web accessibility for disable peoples [34].

Saudi Arabia also needs to review their policies related to web accessibility and to develop their own web accessibility guidelines according the country context, culture and disability types. This can be achieved by doing in-depth research with following objectives: 1) Evaluate national portals those provide e-governance services and university websites for web accessibility 2) Accumulation of barriers faced by different types of disable people 3) Categorizations of barriers into discrete problems 4) Mapping the discrete problems with WCAG 2.0 guidelines.

VIII. Conclusion and Future Work

Web accessibility is one of the main factor to access the quality of any website and if accessibility guidelines are not properly followed then many disable users will not be able to use the services provided by the website. According to the UN e-government survey 2016, Saudi Arabia belongs to the countries those have high level of e-government development index (EGDI). However web accessibility needs to be a top priority issue for Saudi Arabia to address properly so that its 4% disable citizen can get full benefit from the e-services provided by government.

In this study, a systematic literature review is conducted on selected research studies performed in Saudi Arabia and outside of Saudi Arabia to explore the web accessibility issue in the governmental and university websites. It is found that no website is following the World Wide Web consortium's web accessibility guidelines. Legislation in this regard can play a vital role to improve the web accessibility. It is also noted that some countries have legislation but still facing web accessibility issue due to not proper implementation of web accessibility law.

This paper provides a strong foundation for future work to evaluate the national Saudi portals those provide e-governance services and university websites for web accessibility issues by involving the disable users, web developer, web designer and policy makers. To accumulate the barriers faced by different types of disable people. Then categorize the barriers into discrete problems and to map the discrete problems with WCAG 2.0 guidelines to explore which problem are covered by WCAG 2.0 and which user problems are missing. To address the missing problems will be helpful to do the legislation for web accessibility and to improve the existing web accessibility guidelines according to the local Saudi context.

References

[1] World Health Organization and World Bank, "World Report on Disability", 2011, available at, www.who.int disabilities world report 2011 report.pdf .

[2] United Nations Development Group, Inter-Agency Support Group for the CRPD Task Team, "Including the rights of persons with disabilities in United Nations programming at country level", July 2010, available at, www.undg.org/docs/11534/Disability---G - Annexes.pdf .

[3] KSA has 720,000 disabled, Published by ArabNews, December 2012, available online at http://www.arabnews.com/ksa-has-720000-disabled.

[4] United Nations Treaty Collection, available at.

[5] https://treaties.un.org/Pages/ViewDetails.aspx?src=TREATY&mtdsg_no=IV-15&chapter=4&clang=_en

[6] Kuzma, Joanne and Yen, Dorothy and Oestreicher, Klaus (2009) Global e-government Web Accessibility: An Empirical Examination of EU, Asian and African Sites. In: Second International Conference on Information and Communication Technologies and Accessibility, 7th to 9th May 2009, Hammamet, Tunisia.

[7] R. Kurdi, E. Nyakwende and D. Al-Jumeily, "E-Government Implementation and Readiness: A Comparative Study between Saudi Arabia and Republic of Korea," 2015 International Conference on Developments of E-Systems Engineering (DeSE), Duai, 2015, pp. 279-284. doi: 10.1109/DeSE.2015.30.

[8] Web Accessibility Initiative (WAI), available at, http://www.w3.org/wai .

[9] http://www.w3.org/WAI/WCAG20/ .

[10] Policies Relating to Web Accessibility, available at

[11] https://www.w3.org/WAI/Policy/ [Accessed April 22, 2017].

[12] Al-Khalifa, H.S. (2012) The Accessibility of Saudi Arabia Government Web Sites: An Exploratory Study. Universal Access in the Information Society, 11, 201-210. http://dx.doi.org/10.1007/s10209-010-0215-7.

[13] Mitsamarn, Namnueng, Waragorn Gestubtim, and Sirilak Junnatas. "Web accessibility: a government's effort to promote e-accessibility in Thailand." Proceedings of the 1st international convention on Rehabilitation engineering & assistive technology: in conjunction with 1st Tan Tock Seng Hospital Neurorehabilitation Meeting. ACM, 2007.

[14] Saudi Arabia Internet Users, Internet Live Stats, http://www.internetlivestats.com/internet-users/saudi-arabia/ [Accessed March 13, 2017].

[15] Alshehri M. & Drew S. "Challenges of e-Government Services Adoption in Saudi Arabia from an e-Ready Citizen Perspective", World Academy of Science, Engineering and Technology, 2010, 66: 1053-1059].

[16] Government Service, avialable at, https://www.saudi.gov.sa/wps/portal/ [Accessed May 12, 2017].

[17] UN E-Government Survey 2016, available at, http://workspace.unpan.org/sites/Internet/Documents/UNPAN96407.pdf [Accessed April 20, 2017].

[18] List of Universities and colleges in Saudi Arabia, https://en.wikipedia.org/wiki/List_of_universities_and_colleges_in_Saudi_Arabia .

[19] Nader Habibi, Is Saudi Arabia training too many graduates, University World News: The global window on higher education, Issue No: 376. July 17, 2015. http://www.universityworldnews.com/article.php?story=20150714013422488 [Accessed: April 04, 2017].

[20] Al-Asmari AM, Rabb Khan MS. E-learning in Saudi Arabia: Past, present and future, Near and Middle Eastern Journal of Research in Education 2014:2 http://dx.doi.org/10.5339/nmejre.2014.2

[21] Afifa Jabeen Quaraishi, More Saudi universities boarding e-learning bandwagon, arab news. News published May 10, 2012. http://www.arabnews.com/more-saudi-universities-boarding-e-learning-bandwagon.

[22] Masood Rana, Mukhtar; Fakrudeen, Mohammed; Rana, Uzma; "Evaluating Web Accessibility of University Web Sites in the Kingdom of Saudi Arabia." International Journal of Technology, Knowledge & Society. 2011, Vol. 7 Issue 3, p1-15. 15p.

[23] Asmaa Alayed, Mike Wald and Ea Draffan, Challenges to Enhancing Web Accessibility in Saudi University Websites: An exploratory Study, WEB 2016, The Fourth International Conference on Building and Exploring Web Based Environments, June 2016, Lisbon, Portugal, pages 6-9.

[24] Addin Osman, Web-Accessibility Automatic Checking Tools and Evaluation in Saudi Arabia: A Systematic Literatrue Review, International Journal of Engineering Science and Innovative Technology (IJESIT), Volume 6, Issue 1, January 2017, pp 14 – 17.

[25] Alshamari, M. (2016) Accessibility Evaluation of Arabic E-Commerce Web Sites Using Automated Tools. Journal of Software Engineering and Applications , 9, 439-451. http://dx.doi.org/10.4236/jsea.2016.99029

[26] Mohd Hanapi Abdul Latif and Mohamad Noorman Masrek, Accessibility Evaluation on Malaysian E-Government Websites, Journal of e-Government Studies and Best Practices, Vol. 2010 (2010).

[27] Yakup AKGÜL and Kemal VATANSEVER, "Web Accessibility Evaluation of Government Websites for People with Disabilities in Turkey," Journal of Advanced Management Science, Vol. 4, No. 3, pp. 201-210, May 2016. doi: 10.12720/joams.4.3.201-210.

[28] Solomon Adelowo Adepoju, Ibrahim Shehi Shehu, and Peter Bake, "Accessibility Evaluation and Performance Analysis of e-Government Websites in Nigeria," Vol. 7, No. 1, pp. 49-53, February, 2016. doi: 10.12720/jait.7.1.49-53

[29] Basel Al Mourad and Faouzi Kamoun (2013), " Accessibility Evaluation of Dubai e-Government Websites: Findings and Implications" Journal of E-Government Studies and Best Practices, Vol. 2013 (2013), Article ID 978647, DOI: 10.5171/2013. 978647,

[30] http://creativecommons.org/licenses/by/3.0/.

[31] Faouzi Kamoun, Mohamed Basel Almourad, (2014) "Accessibility as an integral factor in e-government web site evaluation: The case of Dubai e-government", Information Technology & People, Vol. 27 Issue: 2, pp.208-228, doi: 10.1108/ITP-07-2013-0130.

[32] M. Bakhsh and A. Mehmood, "Web Accessibility for Disabled: A Case Study of Government Websites in Pakistan," *2012 10th International Conference on Frontiers of Information Technology*, Islamabad, 2012, pp. 342-347. doi: 10.1109/FIT.2012.68

[33] Aidi Ahmi and Rosli Mohamad, Evaluating Accessibility of Malaysian Ministries Websites using WCAG 2.0 and Section 508 Guidelines, Journal of Telecommunication electronic and computer engineering, Volume 8, No. 8, pp 177-183, 2016.

[34] Humaira Nazar, M. Shahzad Sarfraz and Umar Shoaib, Web Accessibility Evaluation of Banking Website in Pakistan, International Journal of Computer Science and Information Security (IJCSIS), Volume 15, No. 1, pp 642-650, January 2017.

[35] Abanumy A, Al-Badi A, and Mayhew P "e-Government Website Accessibility: InDepth Evaluation of Saudi Arabia and Oman" The Electronic Journal of e-Government Volume 3 Issue 3 pp 99-106.

[36] André Pimenta Freire, "Disabled people and the Web: User-based measurement of accessibility", PhD thesis, University of York, September 2012.

[37] Accessibility laws, Ontario Canada, December 2015, available at https://www.ontario.ca/page/accessibility-laws

Secure Encryption for Wireless Multimedia Sensors Network

Amina Msolli
Laboratory of Micro-Optoelectronics and Nanostructures (LMON),
Faculty of Sciences,
Monastir University,
Tunisia

Abdelhamid Helali
Laboratory of Micro-Optoelectronics and Nanostructures (LMON),
Faculty of Sciences,
Monastir University,
Tunisia

Haythem Ameur
Laboratory of Micro-Optoelectronics and Nanostructures (LMON),
Faculty of Sciences,
Monastir University,
Tunisia

Hassen Maaref
Laboratory of Micro-Optoelectronics and Nanostructures (LMON),
Faculty of Sciences,
Monastir University,
Tunisia

***Abstract*—The security in wireless multimedia sensor network is a crucial challenge engendered by environmental, material constraint requirements and the energy consumption. Standard encryption algorithms do not agree with the real-time applications on this network. One of the solutions to the challenges mentioned above is to maintain the safety and reduce the energy consumption. In this article, a new approach with a high-energy efficiency, a high level of security and a big robustness against the statistics and differential attacks is presented in this paper. The new approach called Shift-AES admits simple operations such as the substitution, the transposition by or-exclusive and shift. It keeps the principle of Shannon for the diffusion and the confusion. Some criteria to measure the performances of the approach such as the visual inspection, histogram analysis, entropy images, the correlation of two adjacent pixels, the analysis against differential attacks, and the analysis of performance at the level run-time and throughput are successfully realized. The experimental evaluation of the proposed algorithm Shift-AES proves that the algorithm is ideal for wireless multimedia sensor network. With a satisfactory level of security, best term timeliness and throughput of transmission, compared with the AES standard encryption algorithm, this approach allows us to increase the lifetime of the network.**

Keywords*—Wireless Multimedia Sensor Network (WMSN); image encryption; Shift-AES; security

I. INTRODUCTION

The wireless sensor network (WSN) has evolved very quickly in the scientific research field during the last years. This type of network is the result of a fusion of two poles of the modern computing: the embarked systems and the wireless communications. A wireless sensor network is established by a set of sensor nodes. These sensor nodes are deployed in a geographical zone in a random way. The environmental data is obtained, harvested and transmitted with nodes towards the sink in an autonomous way. The communication between the user and the network takes place through a satellite and the internet.

A node sensor is specified by a sensor unit, a processing unit, and a wireless transmission unit. All these units are fed by a battery. Therefore, in a wireless sensor network, every node captures the physical quantities (such as temperature, humidity, heat, power ...), transforms them into a digital greatness to attribute all data processing and storage and then transmitted.

The field of sensor network applications is more and more widened due to the technical developments facing the domains of electronics and telecommunications. These developments include the reduction in the size and cost of the sensors, as well as the expansion of the ranges of available sensors (movement, temperature ...) and the evolution of the wireless communication mediums, besides civil applications (environment, buildings, industries, transport, medical, commercial, etc.). Indeed, the sensor network applications can be military (intrusion detection, localization fighters, enemy position, weapons, etc. on a battlefield, underwater ...) or the development of other low-cost devices such as micro-cameras expanded areas of wireless sensor network application.

Thus a new generation of the network named Wireless Multimedia Sensor Network has appeared (WMSN) [1]-[3]. In this type of network, nodes are equipped with multimedia devices such as cameras, wireless microphones: often deployed in harsh environments and the energy limitation are factors which make the wireless sensor networks very vulnerable again and subject to several types of attacks, hence the safety in the WSN being of crucial importance. Consequently, the symmetric key encryption algorithm with weak power consumption is necessary for this type of network. Contrary to the public key, encryption algorithm is a fundamental technology and is used widely in the world. But it has its material limits such as the memory and the battery power, cannot therefore be applied to sensor networks [4].

One of the solutions to the challenges mentioned above to preserve the safety and reduce energy consumption presented in this paper. Is presented in this paper: a new approach with high-energy efficiency, a high level of security and a big robustness against the statistics and differential attacks. The new approach called Shift-AES admits simple operations as the substitution, the transposition by or-exclusive and shift. It maintains the principle of Shannon for the diffusion and the confusion. Certain criteria to measure the performances of the approach such as the visual inspection, histogram analysis, entropy images, the correlation of two adjacent pixels, the analysis against differential attacks, and the analysis of performance at the level run-time and throughput are successfully carried out. The experimental evaluation of the proposed algorithm Shift-AES proves that the algorithm is ideal for wireless multimedia sensor network. Because it has a satisfactory level of safety, better term in speed of execution and throughput of transmission, compared with the AES standard encryption algorithm. Hence this approach allows us to increase the lifetime of the network.

The rest of the paper is planned in five parts. First, a bibliographical study on related work for cryptographic algorithms is presented. Afterwards a brief description of the symmetric key cryptographic algorithm AES in Section III. Then, the proposed approach (Shift-AES) is described in Section IV. Section V discusses the results of experimental performances and security analysis, and finally the paper is concluded.

II. Related Works

Cryptography is a very vast domain allowing information data protection to ensure the confidentiality, the integrity and the authenticity. This protection is made by means of a secret or a key. Depending on keys, there are two encryption techniques the public key encryption, and the secret key encryption. The public key encryption, called also the asymmetric cryptography, consists of two keys, the public key is of use to the encryption and the private key ensures the decryption. The use of the asymmetric cryptography allows the abolition of the problem of secure transmission of key. But it remains less successful compared with symmetric cryptography because it consumes more processing times and a large key size for the same level of security.

The private key encryption, also called symmetric cryptography, uses a single key for the encryption and the decryption of the data. It admits less mathematical problems. This encryption mode is established of two main types: by stream and by block.

Cryptography by stream: The encryption of the data is made character-by-character or bit by bit. This type has for advantages the insensitivity in the phenomenon of the propagation of the errors, because as if one erroneous bit there is only. But it puts a secure channel for key distribution, a large size of keys similar to the size of data.

Cryptography by block: The data divide into blocks according to the size of the key. As well as the encryption of the data bases itself on a model of repeated conscript round, where from the result of a block depends on the previous result.

This paper is focused on the symmetric cryptography by block because it is more adapted to the wireless sensor network. The most popular algorithms of this approach are DES, the Triple DES, the AES and the Blowfish.

A. Data Encryption Standard (DES)

DES (Data Encryption Standard) [5] is an American national standard data encryption adapted from the American National Standards Institute (ANSI) in the 1977.

The operation principle of DES is based on 16 rounds. The encryption algorithm operates on blocks of 64 bits, an initial key size of 64 bits contains only 56 bits effective [6] and other 8-bits of parity allow errors to be detected and do not enter the encryption process. First step, the input undergoes a permutation then a fraction in two blocks of 32 bits. The encryption undergoes in the round process. At each round, both halves of 32-bit input and a sub-key undergo several transformations of permutation, substitution and or-exclusive. There are six various permutation operations used in the key extension and the encryption process. Furthermore, the decryption process is similar to the encryption, except that the inverse order of round sub-key is taken.

Nowadays numerous registered attacks show the weaknesses of DES and its insecurity [7], [8].

B. Triple DES (3-DES)

During the development of key safeties, the triple-DES algorithm replaces the DES to correct their weaknesses. It was standardized for the norm EFT of the ANSI X9.17 [5], ISO 8732 and PEM for the key management. The Triple DES algorithm is equivalent to DES when admitting three equal keys ($k_1 = k_2 = k_3$). The length of the key is 168 bits or each key with a length of 56 bits. The principle of the triple DES algorithm is based on the encryption and the decoding by every key according to the following Equation (1):

$$\text{Ciphertext} = DES_{k_3}\{DES_{k_2}^{-1}\{DES_{k_1}(Plaintext)\}\} \quad (1)$$

where DES_{k_i} is the DES encryption with (a) key k_i with i = 1 and 3, and $DES_{k_2}^{-1}$ is the decryption by using the key k_2.

C. Advanced Encryption Standard (AES)

The AES (Advanced Encryption Standard) [9], [10], is a new standard of symmetric encryption by block developed to replace the former Data Encryption Standard (DES) which was published by the National Institute of Standards and Technology (NIST) of the United States as Federal Information Processing Standard Pub 197 (FIPS 197) on 26 November 2001. After a standardization process of five years, the NIST adopted the Rijndael algorithm as AES. The AES algorithm is composed of three main parts: encryption, decryption and key extension. Extension Key generates a schedule Key derived from the secret key which is used in the encryption and decryption procedures.

The AES algorithm is used to realize four different simple transformations applied in succession to the bits of data blocks,

in a number of iterations, called rounds. These transformations are: SubBytes, ShiftRows, MixColumns and AddRoundKey represented more exactly in the following section. The AES algorithm is capable of using cryptographic keys of 128, 192 and 256 bits to encrypt and decrypt data in blocks operating on 128 bits. The number of rounds depends on the corresponding cryptographic keys 10, 12 and 14.

D. Blowfish

The Blowfish encryption algorithm [11] was proposed by Bruce Schneier in the 1993. The Blowfish algorithm uses a key of variable length (32 bits - 448 bits) with a 64-bit block size.

The Blowfish algorithm is constituted by logical or-exclusive operation between halves of the inverted blocks of input, the sub-keys and a function. This function consists of four S-box connected between them by operations of or-exclusive and two modulo 2^{32} additions. This process is repeated 16 times, except in the last round, replaced by a simple reversal block and XOR.

In the same direction of the symmetric cryptography by block, there may be mentioned other algorithms such as: IDEA [12], RC 6 [13], TEA [14], SEA [15], etc.

III. Advanced Encryption Standard (AES)

The AES is an encryption algorithm used to protect electronic data. AES in special peculiarities adapted for WSN applications [16]-[19]. Consequently, the secure AES implementation can greatly influence the nodes of networks resources extremely limited.

AES is based on a matrix N_b x N_k of bytes referred to as ("state"). The number of lines N_b is equal to the size of the data block / 32, which equals 4. Similarly for the key, the number of columns is N_k = key length / 32. The algorithm undergoes various transformations. These transformations (sub Bytes, Shift Rows, Mix Columns and add Round Key) run in a number of iterations proportional to the size of the key.

1) *SubByte:* SubByte is a non-linear substitution function of byte in GF (2^8). Every byte of the State is replaced by another one by means of a substitution table (S-box). S-box which is derived from the multiplicative inverse of a finite field.

2) *ShiftRows:* ShiftRows is a permutation function. Each line of the State is moving towards the left by an offset equal to the line number.

3) *MixColumns*: MixColumns is a mixing function. This processing operates in the State column by column. The four bytes in each column of the State are combined by using an invertible linear transformation. This processing returns the column as a polynomial of four words over GF (2^8). The MixColumns transformation in charge of multiplying a constant matrix with the State as shown in the following equation (2), which is equivalent to GF (2^8) to multiply the fixed polynomials with the polynomial of the column modulo $x^4 + 1$.

$$\begin{pmatrix} b_{0,x} \\ b_{1,x} \\ b_{2,x} \\ b_{3,x} \end{pmatrix} = \begin{pmatrix} 02 & 03 & 01 & 01 \\ 01 & 02 & 03 & 01 \\ 01 & 01 & 02 & 03 \\ 03 & 01 & 01 & 02 \end{pmatrix} \begin{pmatrix} a_{0,x} \\ a_{1,x} \\ a_{2,x} \\ a_{3,x} \end{pmatrix} \quad (2)$$

4) *AddRoundKey:* AddRoundKey is an XOR function. For each round, a sub-key is diverted from the main key in the help Rijndael key schedule, XORed with the State matrix.

During the decryption, the AES algorithm reverses the encryption by performing the inverse transformation by taking the block of 128 bits of encrypted image and to convert it to an image light by the application of the four opposite operations. AddRoundKey is the same for the encryption and the decryption. However, the other three functions are reversed in the decryption process: inverse SubBytes (InvSubBytes), inverse ShiftRows (InvShiftRows), and inverse MixColumns (InvMixColumns).

IV. Proposed Approach (Shift-AES)

Wireless multimedia sensor network allows defining several constraints. The constraints of the multimedia are the real-time execution, the quantity of enormous information, etc. One of the constraint of the network is the physical constraint of the sensor node or a supply of battery and a small memory size. The proposed approach reconciles between the various constraints.

After the exhaustive research on the AES, it is noted that the MixColumns processing consumes more processing time because it counts on the operations of addition and multiplication. This transformation indicates a weakness in the wireless multimedia sensors network. The aim of the intervention is to minimize as much as possible the run time, whereby decreasing the arithmetic operations.

The idea of the approach is based on the AES algorithm with shifts instead of the arithmetic operations named the Shift-AES. In this approach, the MixColumns process of the AES algorithm is replaced by another shift transformation of columns. The principle of shift makes an order of shift

- α: shift for the first column
- η: shift for the second
- β: shift for the third
- ɣ: shift for the fourth column,

To determine the security in the cryptography, it is necessary to keep the capacities of confusion and diffusion by the best choice of the shift parameters (α, η, β, ɣ). The experimental study below allows us to select the exact parameter values, as shown in Fig. 1. Therefore, this approach maintains the principle of Shannon for the diffusion and better reduces the execution time.

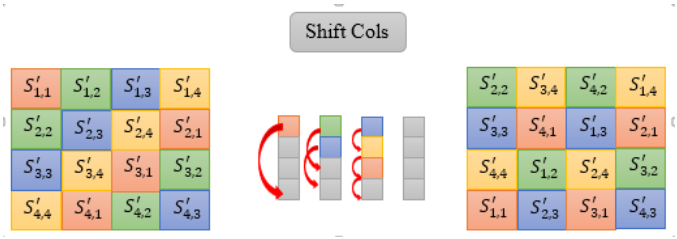

Fig. 1. The Transformation Shift-Cols after the whole processing SubByte and ShiftRows of AES.

After the application of Shift-AES, a better earning in run time is achieved. To improve the entropy of the approach, a modification of the general structure of Shift-AES is realized. ShiftCols transformation enhances the various transformations in the process of iterations of encryption. Tables 1 and 2 represent the algorithm of the general structure of the Shift-AES approach and Shift-Cols.

TABLE. I. STRUCTURE OF THE PROPOSÉD CIPHER ALGORITHM SHIFT-AES

Algorithm 1 : Pseudo code cipher Shift-AES

Input : Clair image, key
Output : cipher image
Procedure :
S_Box ⟵ Initialize Shift-AES
Expansion key ⟵ Initialize Shift-AES
image ⟵ Initialize Shift-AES
l ⟵ Number of image blocks initialize Shift-AES
k ⟵ image size initialize par Shift-AES
For l = 1 **to** k **do**
State ⟵ image(l)
State ⟵ AddRoundKey(State, key)
For r=1 **to** (Nr-1) **do**
State ⟵ ShiftCols(State)
State ⟵ SubBytes(State, S_Box)
State ⟵ ShiftRows(State)
State ⟵ AddRoundKey(State, key)
End for
State ⟵ SubBytes(State, S_Box)
State ⟵ ShiftRows(State)
State ⟵ AddRoundKey(State, key)
C ⟵ State(l)
End for
Cipher_Image =C

TABLE. II. STRUCTURE OF SHIFT-COLS ALGORITHM

Algorithm 2 : Process ShiftCols (state)

Input : state, offset_Shift
Output : state
Procedure :
 	
Nb=4
Offset_Shift=1
For col = 0 **to** 3 **do**
Offset_Shift (col) ⟵ Offset-Shift + col
State(row, col) ⟵ State(((row + offset_Shift(col)) mod Nb), row)
End for

V. EXPERIMENTAL PERFORMANCE RESULTS AND ANALYSIS OF SAFETY

In this section, a study of experimental performance is defined to verify the results stemming from the statistical analysis of the security and to prove the efficiency of the proposed approach. The experimental result involves the collection of all the test standard images required for the simulation trial. Then, the new Shit-AES approach is feigned and tested on the standard images to estimate their performances. The evaluation parameters [20] are made by the histogram, entropy image, the correlation, its resistance against the differential attack and the run time. These quantitative parameters are the most suitable and the most used for the analysis.

A. Experimental results

The simulation of several test standard images of different size and dimension allows us to observe a total invisibility in the coded image, with the parameters $\alpha = 3$, $\eta = 2$, $\beta = 1$, $\gamma = 0$ shifts below (choice of parameters is below). The simulation results of the Shift-AES approach are very satisfactory. The visual inspection of the images in Fig. 2 allows to count the proposed Shift-AES approach, because it is effective in hiding the information contained in them.

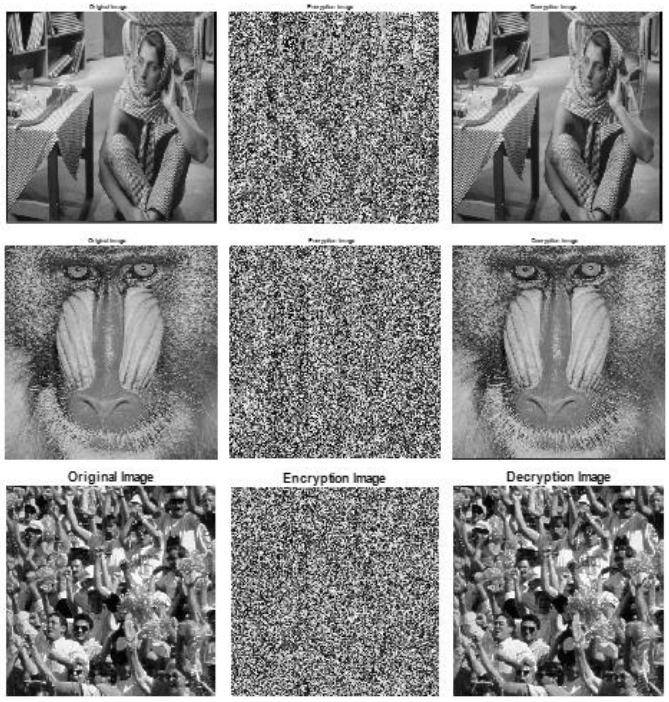

Fig. 2. Encryption and decryption of the standard images (Woman, Mandrill, and Crowd respectively) with the proposed Shift-AES approach.

B. Statistical analysis of the security

The statistical analysis of the security provided the analysis of the histogram, the entropy and the correlation of the original and encrypted images to have the efficiency of the proposed approach. So, it analyzes the robustness of approach against any statistical and differential attack by the parameters NPCR (Number of Pixels Exchange Rate) and UACI (Unified Average Changing Intensity).

1) Histogram of the image: The histogram of the image is the most recently used way to prove the effect of the proposed encryption algorithm. If the histogram of encrypted image does not contain a statistical similarity to the original image, then, it avoids the data leakage to the opponent. The histogram illustrates the random distribution of pixels in a digital image by the number of pixels at each level of gray intensity.

The simulation of the selected standard images Woman, Mandrill, and Crowd respectively, of various dimensions 256x256 and 512x512 by Shit-AES algorithm allows to calculate the histograms of the original images and encrypted, as shown in Fig. 3. The comparison of analysis histogram shows a total difference in the content of pixels intensity between the original image as well as the encrypted images. The histograms of the coded images are almost uniform and appreciably different compared with the histograms of the original images. These rather adequate results hide the information during transmission and defend against the statistical attacks.

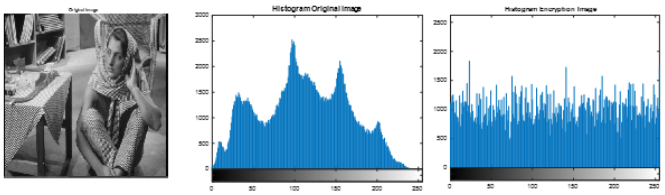

a) Original image of Woman, histogram of original image and histogram of encrypted Woman image, respectively.

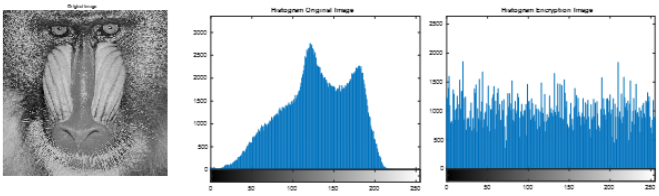

b) Original image of Mandrill, histogram of original image and histogram of encrypted Mandrill image, respectively.

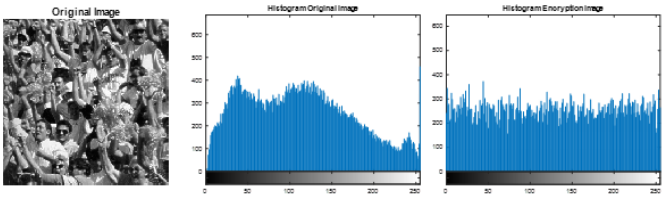

c) Original image of Crowd, histogram of original image and histogram of encrypted Crowd image respectively

Fig. 3. Histogram of the standard images (Woman, Mandrill, and Crowd respectively) of original and encrypted with the proposed AES-Shift approach.

2) Image entropy: The digital images are a combination of discrete values of the pixels, organized together to form a visual perception of the image. The entropy allows to analyze the information contained in random data. The entropy of an image calculated by the Equation (3):

$$E = -\sum_{i=1}^{N} X_i\,(log2(X_i)) \quad (3)$$

Where E is the entropy of the image expressed in bits, X is the probability of the level of intensity in the image and N is the total number of intensity levels.

The ideal value of the entropy of a random source of 2^8 intensity levels is eight according to (3). In fact, the entropy of the encrypted images has to be approximately eight. The measures of entropy are presented in Table 1. The result proves that the entropy of the encrypted images is around eight.

Table 3 indicates the percentage of entropy between the entropy of encrypted image and the original one. The average value of entropy is 12.13% for standard images with different extensions and dimensions.

TABLE. III. IMAGE ENTROPY

Images	**Dimensions**	**Entropy of the images**		
		original	***encrypted***	***%***
lena.jpg	256x256	7.5691	7.9247	4.6980
cameraman.tif	256x256	7.0097	7.7758	10.9291
peppers.png	512x384	6.9917	7.8668	12.5162
football.jpg	320x256	6.7134	7.8466	16.8796
pout.tif	240x291	5.7599	7.6106	32.1307
rice.png	256x256	7.0115	7.9402	13.2453
woman.jpg	512x512	7.6631	7.9638	3.9239
mandrill.png	512x512	7.3579	7.9550	8.1150
The average value of the entropy		7.0095	7.8604	12.1392

3) Correlation of adjacent pixels: Another parameter analyzes the safety and studies the performance of the new approach, it is the correlation of adjacent pixels in vertical and horizontal direction.

Equations (4) and (5) allows to calculate the coefficients of vertical and horizontal correlations of the original image and the encrypted image.

$$cov(x,y) = E\big(x - E(x)\big)\big(y - E(y)\big) \quad (4)$$

$$r_{xy} = \frac{cov(x,y)}{\sqrt{D(x)}\sqrt{D(y)}} \quad (5)$$

Where x and y are the gray level values of two adjacent pixels in the image. The results are mentioned in Table 4. The correlation values show a difference between the original and encrypted image. For example, in vertical direction, the original image admitted a correlation coefficient of about 0.9894 while in the coded image the value is equal to 0.0577.

TABLE. IV. COMPARISON CORRELATION COEFFICIENT VERTICAL AND HORIZONTAL

Direction	**original Image**	**encrypted Image**
Vertical	0.9894	0.0577
Horizontal	0.9995	0.5740

There is another procedure to calculate the correlation of two adjacent pixels. This method selects 1024 pairs of two adjacent pixels in vertical direction of a standard image Lena 256x256 size. The numerical calculation is made by the discrete Equations (6), (7) and (8);

$$E(x) = \frac{1}{N}\sum_{i=1}^{N} x_i \quad (6)$$

$$D(x) = \frac{1}{N}\sum_{i=1}^{N}(x_i - E(x))^2 \quad (7)$$

$$cov(x,y) = \frac{1}{N}\sum_{i=1}^{N}(x_i - E(x))\,(y_i - E(y)) \quad (8)$$

Fig. 4 illustrates a distribution of the correlation coefficient of two adjacent pixels in the original and encrypted image. The simulation results show that the coefficients are strongly correlated with the original image, while in the encrypted image the coefficients are scattered, that is to say, a negligible correlation in the encrypted image.

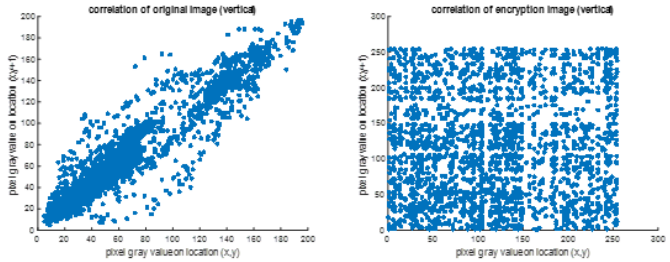

Fig. 4. Correlation coefficient of two adjacent pixels to the original and encrypted image respectively.

4) Differential attack: Among the principle of security in the wireless communication is the confidentiality of the information during transmission against attacks.

To guarantee the safety in the proposed Shift-AES approach, it is necessary to verify the resistance against differential attacks through the common parameters: NPCR and UACI [21]. These parameters test the influence of the change of a single pixel in the original image on the encrypted image.

NPCR (Number of Pixels Exchange Rate) and UACI (Unified Average Changing Intensity) are defined as follows by (9) and (10):

$$NPCR = \frac{\sum_{i,j} D(i,j)}{W \times H} \times 100\% \quad (9)$$

$$UACI = \frac{1}{W \times H}\left[\sum_{i,j} \frac{C_1(i,j) - C_2(i,j)}{225}\right] \times 100\% \quad (10)$$

Where W and H are the C_1 and C_2 dimensions. C_1 and C_2 are two corresponding encrypted images to the original image and that modified by a single pixel. Thus, D is a bipolar matrix determined from C_1 and C_2.

In the simulation, the Lena original image on a dimension 256x256 is used as an image test to estimate the proposed Shift-AES algorithm according to the influence of change of a pixel to 256 gray levels. The obtained quantitative results are NPCR = 99.63% and UACI=30.71%. These quantitative and qualitative results imply that a small change in the original image will be translated by a significant modification in the encrypted image, whereby the effectiveness of Shift-AES has the resistance against differential attacks.

a) Choice of shift parameters

The choice of the offsets is realized to obtain the good performance. A study on the shift is summarized in Table 5. The study is done on a cameraman image of 256x256 size. The six combinations of the shift values represent all the existing possibilities.

The evaluation of the proposed AES-Shift algorithm is successfully realized by some statistical criteria well known as the statistical analysis and differential attack parameters. Shift-AES is designated as an ideal and robust algorithm in the wireless multimedia sensor network. Because it demonstrates a robust against the statistical, differential attack and an efficiency in the histogram, entropy and the correlation of adjacent pixel analysis.

5) Performance of approach Shift-AES:

Execution time: The search for security in the wireless multimedia sensor network imposes crucial another issue as the energy consumption which must be considered during the multimedia real-time application and under the constraints of hardware sensor node. In this sense it is necessary to try always to decrease the run time most rather possible.

In this section, the evaluation of the Shift-AES algorithm is performed by comparing the execution time of the standard AES algorithm with the proposed Shift-AES algorithm, through several image tests of different sizes on disk and by comparing the encryption time in relation to different key sizes.

Fig. 5 shows that the execution time of the Shift-AES approach is more successful and shorter compared with the time of the AES algorithm, in the different sizes of images. This result supports the efficiency of Shift-AES in the wireless multimedia sensor network.

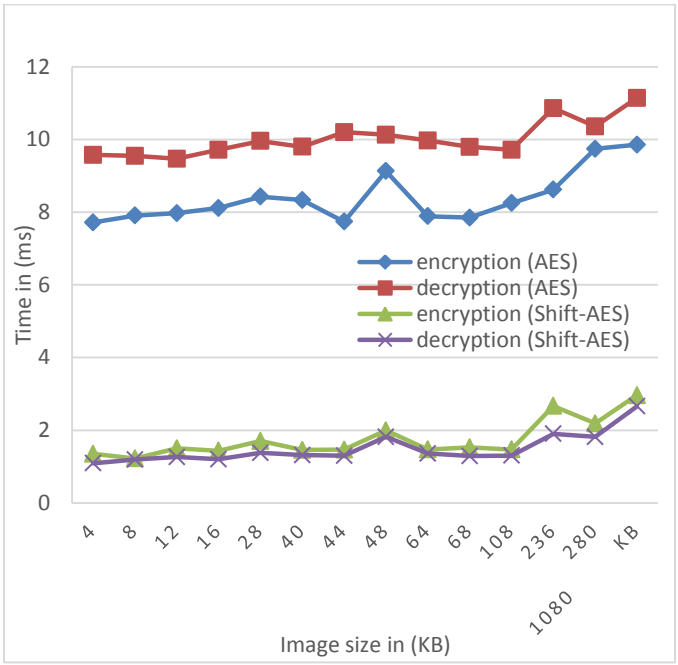

Fig. 5. Comparison of execution time in ms between AES and Shift-AES for different image sizes on disk.

Furthermore, to evaluate the performance of the similarity between the energy consumption and the safety. Simulations

are made between the different key sizes of security and the execution time for a standard image Lena of size 256x256. The simulation (Fig. 6) gives an execution time at the Lena image encryption of approximately 7 ms, 8 ms and 10 ms for key size 128 bits, 192 bits and 256 bits respectively, for the AES algorithm while in the Shift-AES approach the run time is approximately 1.3 ms, 1.4 ms and 1.5 ms. Fig. 7 specifies that the proposed approach called Shift-AES consumes less energy than that AES. Hence this approach increases the lifetime of the wireless multimedia sensor network.

TABLE. V. CHOICE OF SHIFT PARAMETERS FOR COLUMNS

	α=0, η=1,(low) β=2, γ=3	**α=1, η=3,(low) β=1, γ=3**	**α=1,(low) η=2,(up) β=3,(low) γ=1(up)**	**α=3, η=2,(low) β=1, γ=0**	**α=0, η=2,(low) β=0, γ=2**	**α=1,(up) η=2,(up) β=2,(low) γ=1(low)**
Entropy (cipher image)	7.7758	7.7572	7.7490	**7.7829**	7.7671	7.7566
NPCR (%)	99.55	99.48	99.53	**99.79**	99.72	99.68
UACI (%)	**29.88**	30.84	31.15	31.51	30.70	32
horizontal Correlation (cipher image)	0.6116	**0.1870**	0.3854	0.3034	0.4641	0.4219

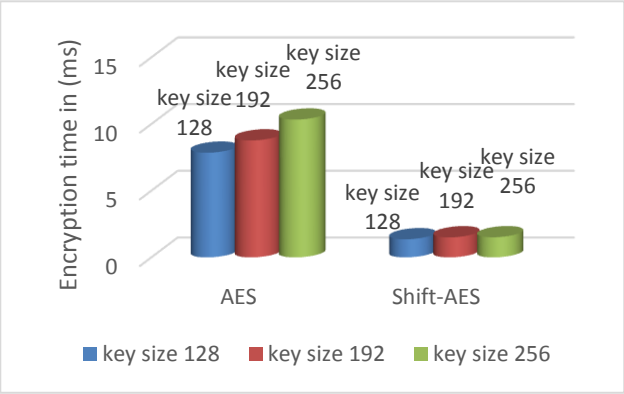

Fig. 6. Comparison encryption time between AES and AES-Shift for the different key sizes.

Throughput: The throughput is another parameter that can examine the performance of the approach. The throughput is similar at the speed of encryption and decryption. The throughput is the division between the global data size to be encrypted and the time total execution of encryption so of deciphering, it is expressed in megabytes per second.

Fig. 7 explains the evolution of throughput according to the size of images. Shift-AES appeared better to favor that the AES algorithm especially for the large data size, because if the throughput increases then the energy consumption reduces.

VI. CONCLUSION

This paper proposes a new approach named Shift-AES with simple operations for the real-time applications in wireless multimedia sensor network. An experimental performance is defined to verify the results of the analysis and prove the effectiveness of the proposed Shift-AES approach. The simulation of several standard image tests of different size and dimension allows us to observe:

5) A total invisibility in the encrypted image.

6) A difference in the content of pixel intensity between the original image and encrypted, in the histogram.

7) A percentage average value of the entropy of the images is about 12.13%, expresses the resistance against the attacks statistics.

8) A random distribution of correlation coefficients of two adjacent pixels in the encrypted image.

9) The robustness against the differential attacks appeared to the NPCR = 99.63% and UACI=30.71% .

10) A rapidity of execution equal to 1.3 ms instead of 7 ms compared with the standard algorithm.

11) And an increase of throughput and speed of transmission.

This rapidity and increase of throughput allow to decrease the energy consumption. Consequently, increase the lifetime of the network. More energy high efficiency, a high level of security and robustness against statistics and differential attacks.

These results are quite adequate to conclude that Shift-AES is a very satisfying and ideal algorithm for the wireless multimedia sensor network.

Future works focus to apply this new approach in various modes of encryption known to have the safest mode and implement the proposed approach on sensors nodes to estimate the energy consumption.

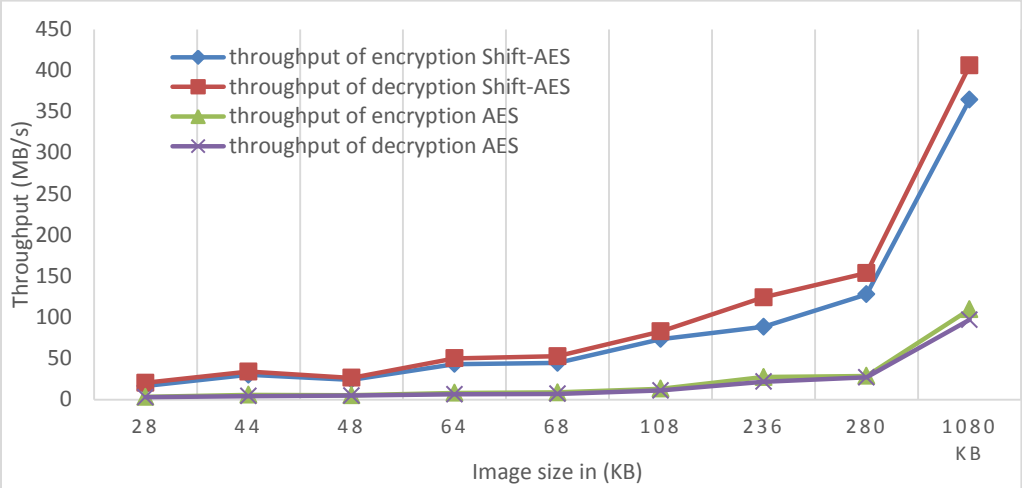

Fig. 7. Comparison of throughput between AES and Shift-AES.

REFERENCES

[1] Ian F. Akyildiz, Tommaso Melodia, Kaushik R. Chowdhury, "A Survey On Wireless Multimedia Sensor Networks", Computer Networks (ELSEVIER), Vol 51, Pages 921-960, 2007.

[2] K.Kalaivani, B.R. Sivakumar, "Surey On Multimedia Data Security", International Jounal Of Modeling and Optimization, Vol 2, February 2012.

[3] Viral Patel, Krunal Panchal, "Survey on Security in Multimedia Traffic in Wireless Sensor Network", International Journal of Engineering Development and Research (IJEDR), vol. 2, pp. 3906-3910, Dec 2014.

[4] Yun Zhou, Yuguang Fang, Yanchao Zhang , "Securing wireless sensor network s: a survey," IEEE Communications Surveys and Tutorials, vol. 10, No.3, 3rd Quarter, 2008.

[5] Standard, Data Encryption. "Data encryption standard." Federal Information Processing Standards Publication, 1999.

[6] DataEncryptionStandard(DES).Available:http://csrc.nist.gov/publications/fips/fips46-3/fips46-3.pdf.

[7] W.Stallings, "Cryptography and Network Security 4th Ed," Prentice Hall, PP. 58-309, 2005

[8] Coppersmith, D. "The Data Encryption Standard (DES) and Its Strength against Attacks."I BM Journal of Research and Development, pp. 243 -250 May 1994

[9] FIP 197: Announ cing the Advanced Encryption Standard , Nov . 26,. 200 I. http://csrc.nist.gov/publications/fips/fipsI97/fips-197.pdf

[10] J. Daemen and V. Rijmen , "AES Proposal : Rijndael, AES Algorithm", Submission, September 3, 1999.

[11] Schneier, B., "Description of a New Variable-Length Key, 64-Bit Block Cipher (Blowfish)", Fast Software Encryption, Cambridge Security Workshop Proceedings (Dec. 1993), Lecture Notes in Computer Science (LNCS), Springer-Verlag, Vol. 809, pp. 191-204, 1993, ISBN 3-540-58108-1.

[12] X. Lai and J. Massey, "A proposal for a new block encryption standard", In Proceedings of the EUROCRYPT 90 Conference, pp. 3 89-404, 1990.

[13] R.L. pavan, M.J.B. Robshaw, R.Sidney, and Y.L. Yin. "The RC6 Block Cipher". Ver 1.1, August 1998.

[14] Wheeler, D.J., & Needham, R.J, "TEA, a tiny encryption algorithm", In Fast Software Encryption – Proceedings of the 2nd International Workshop,1008, (1994)

[15] Abdelfatah A. Yahya and Ayman M. Abdalla, "A Shuffle Image-Encryption Algorithm", Journal of Computer Science, Vol 4, p. 999-1002, 2008

[16] Ankit Srivastava, Dr. N. Revathi Venkataraman, "AES-128 Performance in Tinyos with CBC Algorithm (WSN) ," International Journal of Engineering Research and Development, vol. 7, pp. 40-49, June 2013.

[17] Ortega Otero, Tse.J, Manohar.R. , "AES Hardware-Software Co-design in WSN," Asynchronous Circuits and Systems (ASYNC), 2015 21st IEEE International Symposium on, pp. 85 – 92, May 2015.

[18] P.D. Khambre,S.S.Sambhare, P.S. Chavan, "Secure Data in Wireless Sensor Network via AES (Advanced Encryption Standard)", International Journal of Computer Science and Information Technologies, vol. 3, 2012.

[19] Hyeopgeon Lee, Kyounghwa Lee, Yongtae Shin, "Implementation and Performance Analysis of AES-128 CBC algorithm in WSNs", Advanced Communication Technology (ICACT), 2010 The 12th International Conference on (Volume:1), pp. 243 – 248, Feb 2010.

[20] Abdulkarim Amer Shtewi, Bahaa Eldin M. Hasan, Abd El Fatah .A. Hegazy," An Efficient Modified Advanced Encryption Standard (MAES) Adapted for Image Cryptosystems", International Journal of Computer Science and Network Security, Vol 10(2), Pages 226-232, February 2010.

[21] Yue Wu, Joseph P. Noonan, , and Sos Agaian, "NPCR and UACI Randomness Tests for Image Encryption", Journal of Selected Areas in Telecommunications (JSAT),pp.31-38, April 2011.

Towards Efficient Graph Traversal using a Multi-GPU Cluster

Hina Hameed
Systems Research Lab, Department of Computer Science,
FAST National University of Computer and Emerging Sciences
Karachi, Pakistan

Sehrish Hina
Systems Research Lab, Department of Computer Science,
FAST National University of Computer and Emerging Sciences
Karachi, Pakistan

Nouman M Durrani
Systems Research Lab, Department of Computer Science,
FAST National University of Computer and Emerging Sciences
Karachi, Pakistan

Jawwad A. Shamsi
Systems Research Lab, Department of Computer Science,
FAST National University of Computer and Emerging Sciences
Karachi, Pakistan

***Abstract*—Graph processing has always been a challenge, as there are inherent complexities in it. These include scalability to larger data sets and clusters, dependencies between vertices in the graph, irregular memory accesses during processing and traversals, minimal locality of reference, etc. In literature, there are several implementations for parallel graph processing on single GPU systems but only few for single and multi-node multi-GPU systems. In this paper, the prospects of improvement in large graph traversals by utilizing multi-GPU cluster for Breadth First Search algorithm has been studied. In this regard, a DiGPU, a CUDA-based implementation for graph traversal in shared memory multi-GPU and distributed memory multi-GPU systems has been proposed. In this work, an open source software module has also been developed and verified through set of experiments. Further, evaluations have been demonstrated on local cluster as well as on CDER cluster. Finally, experimental analysis has been performed on several graph data sets using different system configurations to study the impact of load distribution with respect to GPU specification on performance of our implementation.**

***Keywords*—Graph processing; GPU cluster; distributed graph traversal API; CUDA; BFS; MPI**

I. INTRODUCTION

Data processing accompanied with GPGPU techniques is being employed to process large amount of data with limited resources in several application domains throughout the globe. However, there are several challenges when it comes to graph processing. These include dependencies between vertices in the graph, irregular memory accesses during graph processing, and scalability to larger data sets.

As graph problems grow larger in scale and more ambitious in their complexity, they easily outgrow the computation and memory capacities of single processors [1]. Given the success of parallel computing in many areas of scientific computing, parallel processing appears to be necessary to overcome the resource limitations of single processors in graph computations.

Utilization of parallel architectures became a viable mean in order to improve graph processing performance. However, besides the inherent complexities in graph traversal, parallelism is challenging in several aspects such as: finding the correct step to introduce parallelism in the algorithm, expensive memory accesses, communication overheads, poor locality of reference, and complex load balancing, etc.

Utilization of the distributed GPU clusters will make mining of large graphs faster and cheaper. Many Big Data applications such as Social networks analysis, traffic management, and disaster management systems that rely on graph traversals might be able to perform better, faster, and cheaper. In this context, Breadth First Search (BFS) and Single Source Shortest Path (SSSP) algorithms are important graph traversal algorithms which find their applications in several application domains such as the all pairs' shortest path algorithm, s-t shortest path algorithm, etc.

Since, motivated from the usability of BFS and potential of distributed graph processing, in this paper, a DiGPU - an API providing efficient implementations of these algorithms on distributed GPU clusters has been proposed.

DiGPU is a flexible user friendly CUDA-based implementation of BFS, which can be executed both on single node as well as multi-node systems. DiGPU can also be run on single node multi-GPU systems. For this purpose, it incorporates Unified Virtual Access (UVA) between host and device and Peer-to-Peer direct access between devices. In this work, the BFS algorithm has been implemented on single-node single GPU system as well as on single node multi-GPU systems. Further, the multi-node implementation of DiGPU has also planned that will help in efficient computation of large graphs.

This research has been supported by NVIDIA Teaching and Research Center Awards.

In this regard, the initial implementation has been tested on two types of experimental setups. The traditional hardware cluster comprises of combinations of NVIDIA Tesla K40 and NVIDIA GTX-780 GPUs. A test system on the GPU nodes of Georgia State University cluster has also been setup for further testing.

In summary, following are the main contributions of this paper:

1) The design and development of DiGPU has been proposed. It is an open source software module for distributed graph computations on a heterogeneous GPUs cluster.

2) The functions provided by DiGPU would become building blocks for many applications performing intensive graph computations or analysis. Availability of these building blocks will facilitate a user with the ease of designing graph applications.

3) A hybrid model has been developed. The model utilizes UVA and Peer-to-Peer access between GPUs on same node and CUDA-aware-MPI on different nodes of cluster.

4) Different experiments have been performed to study the impact of load-distribution according to specifications of GPUs on the cluster.

DiGPU will be beneficial for the community in computing large graphs over a series of GPU clusters. Our initial results are encouraging. In this work, it has been aimed to provide an open source version of DiGPU, to perform graph analysis which would make our work a true example of reusable graph building blocks for graph research community. The performance has been evaluated through an extensive evaluation over a large dataset and involving varying GPUs with heterogeneous computational power.

The rest of the paper is organized as: Section II covers the background and related work in this area; Section III illuminates our methodology and approach toward the research problem; Section IV contains details about our initial experimental setup; Section V lists down the results of our preliminary experiments and Section VI concludes this paper.

II. BACKGROUND AND RELATED WORK

This section extensively covers the related work that has previously been done regarding GPU implementations of SSSP and BFS algorithms.

A. Breadth First Search

The classic queue-based parallel BFS initiates the computation with a root node, putting that node in an empty queue. During each iteration, the head of queue is pulled out and all of the connected nodes are visited. Neighbor nodes visited for the first time are placed at the end of the queue. The output of the algorithm is an array storing the distance from the source or predecessor, for each vertex. The best time complexity reported for sequential algorithm is O(V+E).

The queue is a current level set of vertices. For each vertex in the current level, all its neighbors must be visited. The set of all neighbors composes the Next Level Frontier Set (NLFS). From the NLFS only new vertices are selected to build the queue for the next level. The BFS visit is divided into levels with a distance from the root that increases at each subsequent level [2].

Vibhav, *et al*. [2] performed BFS implementation for vertex compaction process. At particular time, small number of vertices may be active. They used prefix sum for assigning threads to active vertices only. They carried out experiments on various types of graphs and compared the results with the best sequential implementation of BFS and experiment shows lower performance on low degree graphs.

P. Harish, *et al*. [3] proposed accelerated large graph algorithm using CUDA. The proposed algorithms is capable of handling large graphs. In their implementation, one thread is assigned to every vertex. They have used frontier array, visited array and cost array which stores the minimum count of edges of every vertex from the source vertex S. During each iteration, every vertex checks frontier array index for itself and in case of positive values updates the cost of itself and its neighbors. But this algorithm's performance slacks due to large degree at few vertices. Also, since it loops the kernel which causes the more lookups to device memory, hence slowing down the kernel execution time.

Lijuan, Luo [4] proposed effective GPU implementation of BFS for designing an efficient queue structure. A hierarchical kernel arrangement is used in order to reduce synchronization overhead. Their experimentation results present similar computational complexity as the fastest CPU version with a potential speedup of up to and they claim to 10 times.

S. Hong, *et al*. implemented a novel warp-centric [5] method for reducing the inefficiency. Many graph algorithms suffer severe performance degradation in case of highly irregular graphs, i.e. when the distribution of degrees (number of edges per node) is highly skewed. Instead of assigning a different task to each thread, their approach allocates a chunk of tasks to each warp and executes distinct tasks in serial. They have utilized multiple threads in a warp for explicit SIMD operations only, thereby preventing branch-divergence altogether.

A. Grimshaw, *et al*. report [6] deals with parallel BFS on GPU clusters. Their work resorts to a duplicate removal procedure by using a heuristic that removes a high percentage of duplicates at the CTA level. In contrast, our algorithm also eliminates every duplicate in the Next Level Frontier Set (at a global level). They have used four GPUs that have a unified memory address space with a reduced latency, compared with a standard network interconnection.

Level Synchronous BFS [7] ensures the correctness of the computation by synchronization at the end of each level in a parallel implementation, . The number of levels is of the same order of the diameter of the graph, in real-world graphs, the computation is dominated by only two or three levels, for which the next level set of vertices is very large.

D. Merril, *et al*. [8] suggested that work-efficient parallel BFS algorithm should perform O(n+m) work. In order to achieve O(n+m) complexity, each iteration should examine only the edges and vertices in that iteration's logical edge and vertex-frontiers, respectively. For each iteration, tasks are

mapped to unexplored vertices in the input vertex-frontier queue. Their neighbors are inspected and the unvisited ones are placed into the output vertex-frontier queue for the next iteration. The typical approach for improving utilization is to reduce the task granularity to a homogenous size and then evenly distribute these smaller tasks among threads, by expanding and inspecting neighbors in parallel.

Leiserson and Schardl [2] designed an implementation for multi-socket systems that incorporates a novel multi-set data structure for tracking the vertex-frontier. In other implementations, hardware's full-empty bits are used for efficient queuing into an out-of core vertex frontier. Both approaches perform parallel adjacency list expansion, relying on runtimes to throttle edge-processing tasks in-core. Luo, *et al*. [4] present an implementation for GPUs that relies upon a hierarchical scheme for producing an out-of-core vertex frontier.

Talking about frameworks and APIs multi-GPU CUDA implementations of BFS have been provided in Medusa [9] and GunRock [10]. Both are graph processing frameworks capable of performing on multiple-GPUS on a single node. Medusa uses two schemes for multi-GPU execution: Replication – division of the graph into equal-sized partitions and store each partition on one GPU and maintain replicas of the head vertices of all cross-partition edges in the partitions where the tail vertices reside. Each cross partition edge is replicated in its tail partition, so messages are emitted directly from the replicas and every edge can access its head and tail vertices directly. The execution of is performed on each partition independently and the replicas are updated on each graph partition after execution. The update requires costly PCIe data transfer, which becomes a bottleneck. Multi-hop replication, on the other hand, alleviates the overhead of inter-GPU communication by reducing the number of times of replica update, as multi-hop replicas aren't updated after every iteration.

In Gunrock's BFS implementation; Merrill, *et al*.'s expand method [11] has been used. During the advance stage, this implementation sets a label value for each vertex to show the distance from the source, and/or sets a predecessor value for each vertex that shows the predecessor vertex's ID. The base implementation uses atomics during advance to prevent concurrent vertex discovery. When a vertex is uniquely discovered, its label (depth) and/or predecessor ID is set. Gunrock's fastest BFS uses the idempotent advance operator, thus avoiding the cost of atomics and uses heuristics within its filter that reduce the concurrent discovery of child nodes.

B. Distributed Breadth First Search

In graph algorithms, the CPU execution time is only a small fraction of the overall execution time due to low arithmetic intensity. While dealing with a distributed environment, data might reside in a remote memory location, spending a large proportion of time in sending and receiving data. Furthermore, graph algorithms do not have a regular communication pattern; messages' size and the number of sending and receiving parties vary throughout their execution. It can be rightly stated that the bottleneck of a distributed BFS is the communication. The optimization of the communication among tasks is crucial for an efficient BFS algorithm on a distributed architecture [2].

In a distributed cluster of GPUs, it is not possible to use an algorithm based on the static mapping of vertices on arrays (adjacency lists). The current and the next level frontier must be an array of exactly |V| elements. Then, a trivial static mapping makes use of a thread for each vertex in the graph. But for large graphs, the number of vertices |V| might be too high to store a global array of size |V| in the memory of a single node. In distributed environments, vertices are scattered among multiple nodes and each node only holds a subset of the whole graph. The number of edges assigned to tasks need be balanced.

P. Harish [12] and S. Hong [5] use the aforementioned static mapping. The authors in [4] use a global bitmask array to mark visited vertices which reduces the size of the global masking array to great extent but this solution is not much scalable. The maximum size of the graph that could be processed will be limited by the maximum size of the array that fits the memory of GPU.

All the shared memory optimizations speed up the visit of local vertices. In the distributed problem, however, the time spent to execute this operation is only a small fraction of the total running time which is dominated by the part of the algorithm that copes with non-local vertices [2].

The multi-node multi-GPU implementations of BFS have been presented by E Mastrostefano, *et al*. [2] and SYSTAP's Blazegraph, both of which are not open source. Therefore, a DiGPU implementation has been proposed to perform distributed graph traversal using BFS. The next section describes the design and implementation of the proposed graph traversal algorithm.

III. METHODOLOGY AND IMPLEMENTATION

The purpose of this section is to elaborate the design and implementation of DiGPU. DiGPU is a flexible user friendly CUDA-based implementation of BFS, which can be executed both on a single node and a multi-node system. For this purpose, it incorporates Unified Virtual Access (UVA) between host and device, and Peer-to-Peer direct access between devices. The BFS algorithm has been implemented on single-node single GPU system as well as on single node multi-GPU systems.

A. Module Overview

DiGPU provides following features to the user shown in Fig. 1:

1) *_SetDataFilePath*, to take the complete path of the location of graph data set.

2) *_CreateGraph*, to read and parse graph dataset and create adjacency list from it.

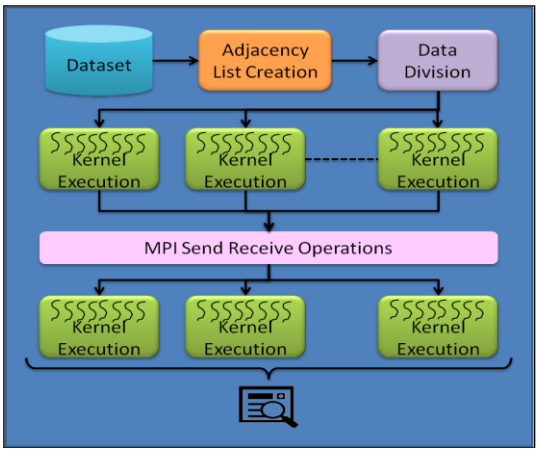

Fig. 1. Generic flow of processing in the DiGPU API

3) _ClustScan, *to examine the cluster and propose the suitable launching configurations.*

4) *_SetConfigs*, to set system information, how many nodes have been connected and how many devices every node has.

5) *_BFS*, to perform breadth first search on the created graph, with randomly selected node as root node.

_BFS utilize the following functions to perform intended operations:

a) Queue operations maintaining consistency through atomic operations, *_enqueue*, *_dequeue*, *_copyQueue*, and *_mergeQueue.*

b) *mapThreads* maps created threads to the nodes in next level frontier set. This also handles the load distribution part.

c) *CUDA Kernels*.

d) *_send* & *_receive* are the functions for data exchange among nodes using MPI.

Fig. 2 illuminates the generic flow of the API core functions. Dataset is read and parsed and then converted into an offset array and adjacency list shown in Fig. 3. The offset array and adjacency list are divided among available devices and kernels (repeatedly). The results are then combined and presented. The flow of distributed BFS in DiGPU presented in Fig. 2 also explains the order of execution of functions to accomplish BFS traversal of a graph.

B. Data Structure and Graph Representation

The adjacency list representation of graph has been used in our implementation, as there is a constraint of limited memory while working with GPUs, adjacency list is the better option than adjacency graph as it consumes lesser space.

For a graph G = (V, E), an array 'Va' of size 2|V| is used to store vertices of the graph, whereas, another array 'Ea' of |E| elements is used to hold the edges. Provided i = 0 …. |V|-1, 2Va[i] represents the offset of neighbors of node i in the Ea array and 2Va[i]+1 represents the number of neighbors of node i. Where, node b is the neighbor of node 'a' if there is a directed edge from 'a' to 'b'.

Fig. 3 represents the graph structure used in our proposed system. The offset array holds the nodes of graph in form of pairs, one index represents the index where the first neighbor of a node is located in the adjacency list and the second one is the count of neighbors of that node. For instance, in Fig. 3, node 1 has its first neighbor at 2nd index, and the 3 following it shows that it has a total of three neighbor nodes.

C. Parallel Breadth First Search – Single Node

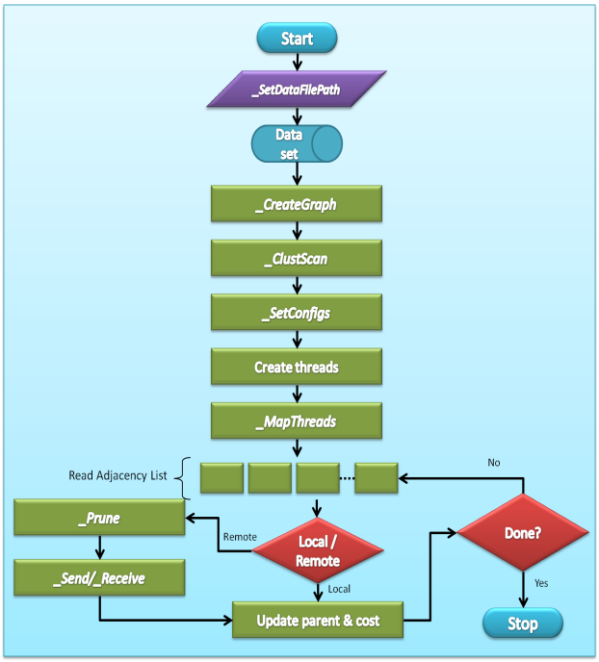

Fig. 2. Flow Diagram of Distributed BFS in DiGPU

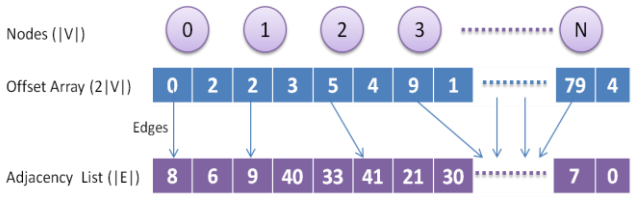

Fig. 3. Adjacency list representation of graph data

TABLE I. P2P ACCESS STATUS OF GPU DEVICES IN CDER CLUSTER

From	To	Access Allowed
GPU0	GPU1	Yes
GPU1	GPU0	Yes
GPU2	GPU3	Yes
GPU3	GPU2	Yes

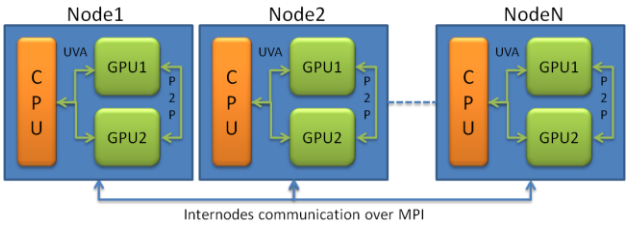

Fig. 4. Representation of Distributed Multi-GPU Cluster

The algorithm proposed in [12] has been extended for multiple GPUs on a single node. The algorithm requires one thread to be created in order to process one vertex. Two arrays namely, frontier Fa and visited Xa each of size |V| are used to store the BFS frontier and the nodes that have been visited vertices. An array to stores the minimal number of edges of each vertex from the source vertex S, the cost array Ca is also used. In every iteration, each vertex checks its entry in the frontier array Fa. If it is positive, it fetches its cost from the cost array Ca and updates all the costs of its neighbors if more than its own cost plus one using the edge list Ea. The vertex removes its own entry from the frontier array Fa and adds to the visited array Xa. It also adds its neighbors to the frontier array if the neighbor is not already visited. This process is repeated until the frontier is empty. The algorithm terminates when all the levels of the graph are traversed and frontier array is empty.

This implementation has also been extended for shared-memory multi-GPUs, utilizing the CUDA Peer-to-Peer (P2P) Direct Access (Table 1). The offset array was divided equally amongst the GPU devices on the node (which enable P2P access with other devices). The adjacency list is then divided such that each device gets the complete set of those nodes which are adjacent to the nodes assigned to it.

Host keeps track of the allocations and utilizing the Unified Virtual Addressing facilitated by CUDA the devices could know which device has their desired node if they are missing any, and then using P2P access that device gets a copy of it.

D. Distributed Multi-GPU Approach

The distributed graph traversal has been implemented on multi-GPU cluster, following and eventually extending the work presented by Mastrostefano, *et al*. [10] towards a hybrid model. The cluster setup represented in Fig. 4 shows that it has multiple nodes, each node having more than one GPU devices. The system perform as a shared memory implementation within a node, using Peer-to-Peer direct access when devices are communicating with each other and Unified Virtual Addressing while host and device are communicating. The system follow distributed approach across the nodes, i.e., communication using *_send* and *_receive* functions.

IV. Experimental Setup

The experimental setups have been used to perform the experimentation of the proposed DiGPU system. Details of these setups have been explained as follows:

A. Cluster Setups

Fours clusters have been used to perform our experiments for DiGPU. The details of hardware specifications of utilized clusters are enlisted below:

1) NVIDIA Research Center (SysLab) Cluster – FAST NUCES

This cluster consisting of following devices have been set up specifically for our experimentation purpose shown in Table 2:

- Standalone PCs with:
  - NVIDIA Tesla K40 and GTX-780
  - NVIDIA GTX-780 and GTX-780
  - NVIDIA Tesla K40 and NVIDIA Tesla
- Multi-node cluster with the nodes listed above.

2) DER Cluster – Georgia State University

This cluster has 19 nodes out of which three nodes have CUDA supported GPU cards:

- GPU07 – 1 GeForce GTX TITAN Black
- GPU11 – 4 GeForce GTX 770
- GPU10 – 4 Tesla K20c.

Above nodes have:

- Processors Dual Intel Xeon E5-2650 with 64 GB memory
- Operating system CentOS 6.7.
- CUDA 7.5

TABLE II. Configurations of Clusters Involved in Experiments

Configuration	Nodes	GPUs/node	GPU Specifications	P2P Access Status
A	1	4	4 GeForce GTX 770	Refer Table 1
B	1	4	4 Tesla K20	Refer Table 1
C	2	2	1 Tesla K40c 1 GeForce GTX 780	Enabled between devices of 1 node
D	1	2	1 Tesla Kxxx 1 GeForce GTX 7xx	Enabled

TABLE III. BREADTH FIRST SEARCH EXECUTION TIMES

Experimental Setup	Vertices	Edges	Processing Time (sec)
Single Node – Single GPU	2394385	5021410	1635.9
Single Node – 2 GPUs	2394385	5021410	1089.3

TABLE IV. DISTRIBUTED BFS USING HYBRID MODEL EXECUTION TIMES

Experimental Setup	Dataset	Processing Time (sec)
CDER cluster – Configuration A	WikiTalk ~ $2.3x10^6$ vertices	349.325377
	Synthetic Graph – $10x10^6$ vertices	772.945530
CDER cluster – Configuration B	WikiTalk ~ $2.3x10^6$ vertices	363.795705
	Synthetic Graph – $10x10^6$ vertices	607.428377
SysLab cluster – Configuration C	WikiTalk ~ $2.3x10^6$ vertices	849.862036
	Synthetic Graph – $10x10^6$ vertices	1809.419021
CDER cluster – Configuration D	WikiTalk ~ $2.3x10^6$ vertices	1003.844756
	Synthetic Graph – $10x10^6$ vertices	4346.329110

3) Cloud Intances

For our preliminary results, two categories of Amazon Web Services EC2 GPU instances have been used with following specifications:

- High Frequency Intel Xeon E5-2670 (Sandy Bridge) Processor
- NVIDIA Grid GPUs, each with 1,536 CUDA cores and 4GB of video memory
- Ubuntu LTS 14.04
- CUDA 7.0

B. Datasets

Both synthetic datasets and real-world graph have been used to experiment in this research. PaRMAT [13] is used to generate synthetic graphs of various sizes to perform impact analysis of load distribution based on GPU specifications. Experiments have been performed on graphs as large as 10M vertices.

WikiTalk dataset from SNAP [14] has been used as a real-world graph to test the implementation. Each registered user of Wikipedia has a talk page, which could be edited by either them or other users to communicate and discuss updates to various articles on Wikipedia. In this SNAP WikiTalk dataset, there is information extracted from all user talk page changes and converted in the form of a network.

The network contains all the users and discussion from the inception of Wikipedia till January 2008. Nodes in the network represent Wikipedia users and a directed edge from node i to node j represents that user i at least once edited a talk page of user j. The dataset represents a directed graph, with 2,394,385 nodes and 5,021,410 edges [14].

V. RESULTS

This section explains the outcomes of the testing of proposed Hybrid Model for DiGPU and also presents the implications of proposed load-balancing based of specifications of GPUs.

A. Preliminary Results – PRAM Algorithm Implementation

The results in Table 3 are preliminary results which had been obtained using a primitive single node PRAM implementation of BFS using Harish's algorithm [12]. The results had been computed using Amazon AWS instances on the WikiTalk graph dataset.

B. Distributed BFS – Hybrid Model Implementation

Hybrid model has been tested on several datasets for all four experimentation setups, the major and important results are those which have been obtained from the 10M vertices synthetic graph and WikiTalk dataset. These results have been summarized in Table 4.

Traversed Edges per Second (TEPS) is a metric well known to measure performance related to graph operations. The results of execution of DiGPU hybrid model on local SysLab cluster (Configuration C) have been represented in the form of TEPS in Table 5. The TEPS for each graph traversal instance in Table 4 show improvement with increase in number of vertices in the graph. This depicts that even though there is network latency issue DIGPU's is scalable for large graphs and the given set of results show improvement in performance with increase in graph size.

Fig. 5 is the visual representation of the comparison amongst the four experimentation benches, in terms of Thousand TEPS. Setup A, B, C all three have four GPU devices but Fig. 5 clearly indicates that Setup C lags behind both Setup A and B. The reason is network latency introduced by the switch used to connect nodes at SysLab. An improvement might be observed if there would have been an Infiniband switch. Also, on test bed Setup C, only one node offers P2P access between the two GPUs in it.

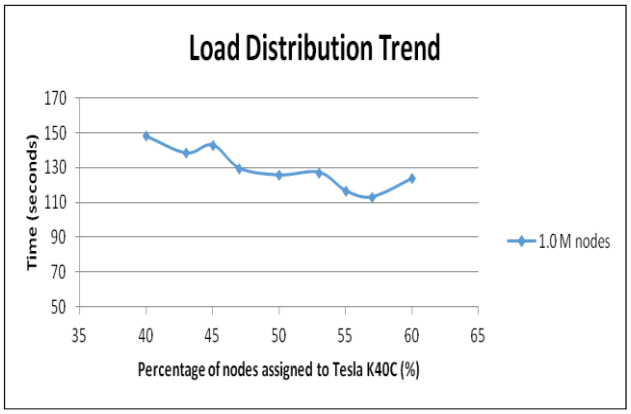

Fig. 5. . Load Distribution Trend Synthetic Graph of 1 million nodes

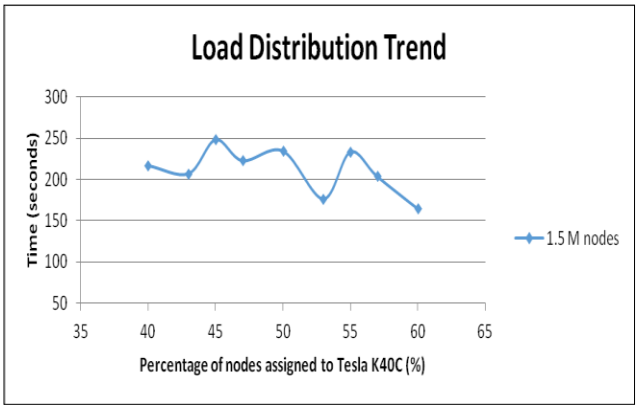

Fig. 6. Load Distribution Trend Synthetic Graph of 1.5 million nodes

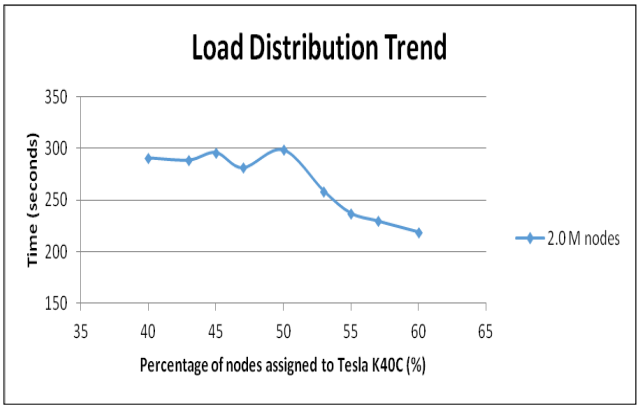

Fig. 7. Load Distribution Trend Synthetic Graph of 2 million nodes

TABLE V. PERFORMANCE OF HYBRID MODEL ON LOCAL CLUSTER WITH VARYING DATA SIZES

Dataset	Processing Time (sec)	Traversed Edges Per Second
Synthetic Graph – $1.0x10^6$ nodes	206.004216	4854.269584
Synthetic Graph – $1.5x10^6$ nodes	274.754027	5459.428625
Synthetic Graph – $2.0x10^6$ nodes	413.738531	4833.970853
Synthetic Graph – $2.5x10^6$ nodes	533.307219	4687.729531
Synthetic Graph – $3.0x10^6$ nodes	595.089924	5041.254907
Synthetic Graph – $10x10^6$ nodes	1809.419021	5526.635833

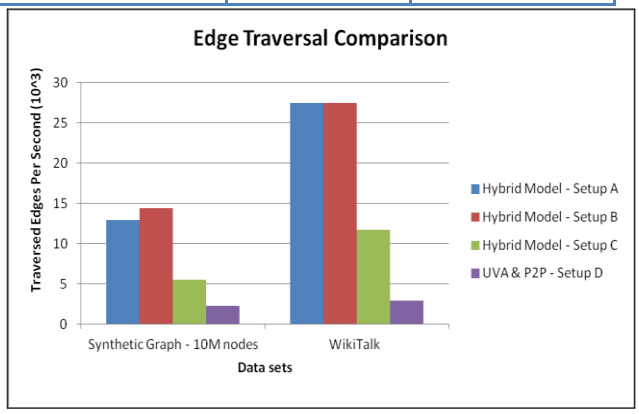

Fig. 8. TEPS Comparison of Experimental Setups

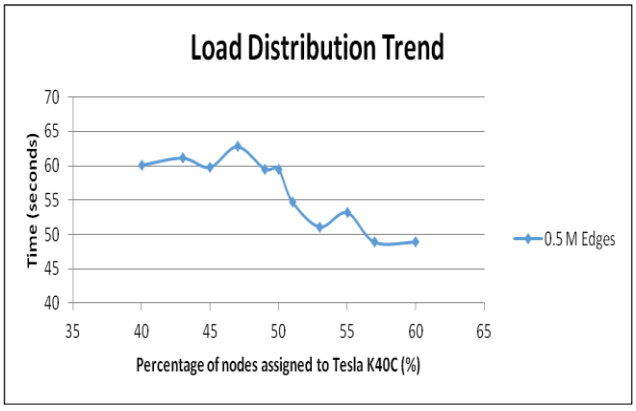

Fig. 9. Load Distribution Trend Synthetic Graph of 0.5M nodes

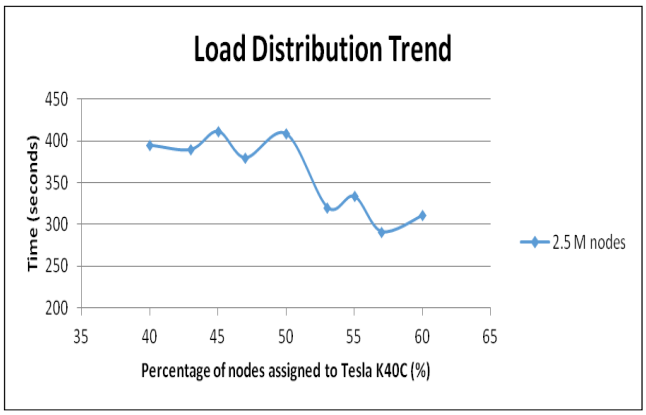

Fig. 10. Load Distribution Trend Synthetic Graph of 2.5 million nodes

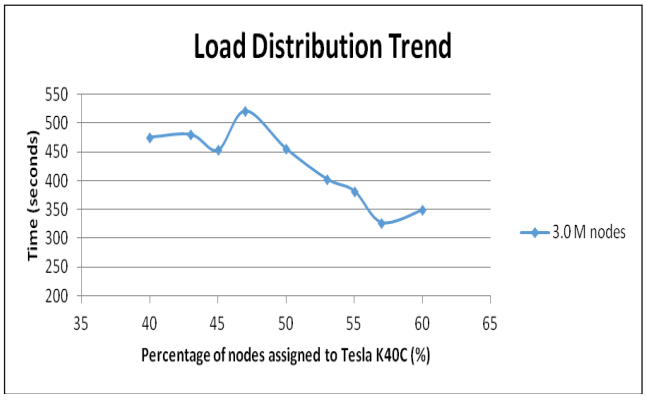

Fig. 11. Load Distribution Trend Synthetic Graph of 3 million nodes

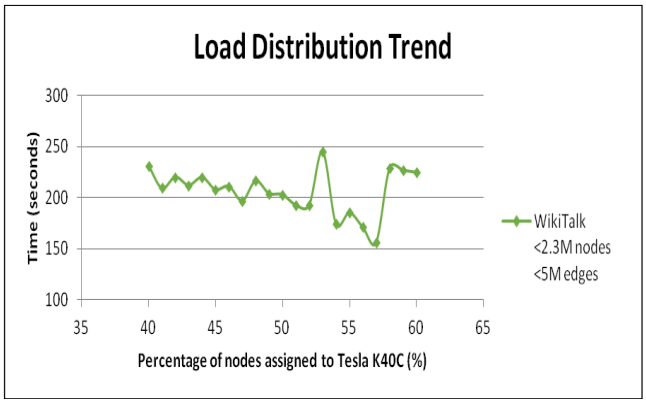

Fig. 12. Load Distribution Trend of Real World graph of WikiTalk

C. Load Distribution

Load distribution experiments have been performed on six synthetic graphs of varying sizes on SysLab systems having Tesla K40c and GeForce GTX 780 GPUs.

Graphs in Fig. 6 to 12 show that execution time improved when the distribution of load was in favor of Tesla device. This is due to the fact that Tesla is better device with more computation power, better memory bandwidth, more CUDA cores and larger memory when compared to GeForce GTX 780 device.

Load distribution using GPU specification represents improvement in execution time of graph traversal. Performance of Hybrid model is better on CDER cluster than SysLab setups which is obviously due to network latencies [15].

VI. Conclusion and Future Work

DiGPU is a software module for multi-node, distributed cluster graph traversal in form of Breadth First Search on GPUs. Results show that our proposed Hybrid Model for graph traversal in multi-GPU clusters performs better than its PRAM and single node UVA-P2P counterpart. Though UVA-P2P on a single node is the base case of the hybrid model its performance is greatly affected by infrastructure, for instance the bandwidth of interconnects between the GPUs and also the processor in the node. The bottleneck in performance is network latency which is inherent in a distributed cluster. But for a cluster with a better interconnect between its nodes or when there are multiple GPUs on a node amongst which not all are paired with each other, our Hybrid Model implementation works better, and our results from experiments performed on CDER cluster clearly support that.

Our motivation behind this research was to explore aspects of improvement in graph analysis, the experiments performed to study the impact of GPU specifications also show a trend in favour of the better GPU device when more nodes are allocated to it, and after a certain increment in load distribution ratio the results begin to deteriorate which is explainable as there would definitely be more communication due to large imbalance in communication.

Acknowledgment

This research has been supported by NVIDIA Teaching and Research Center awards. The authors also acknowledge the Georgia State University, for providing us the testing environment. The authors would like to thank Mr. Muhammad Rafi, and Mr. Ali Ahmed for their valuable input.

References

[1] Lumsdaine, Andrew, et al. "Challenges in parallel graph processing." Parallel Processing Letters 17.01 (2007): 5-20.

[2] Vibhav Vineet and P. J. Narayanan,“Large graph algorithms for massively multithreaded architecture” in Proc. HiPC, 2009.

[3] S. Kumar, A. Misra, R. S. Tomar,“A Modified Parallel Approach to Single Source Shortest Path Problem for Massively Dense Graphs Using CUDA”, Int. Conf. on Computer & Comm. Tech. (ICCCT), IEEE, 2011.

[4] L. Luo, M. Wong, and W.-M. Hwu, An Effective GPU Implementation of Breadth-First Search, in Proc. DAC, 2010, pp. 52-55.

[5] S. Hong, S.K. Kim, T. Oguntebi, and K. Olukotun, “Accelerating CUDA Graph Algorithms at Maximum Warp,” in Proc. PPoPP, 2011, pp. 267-276

[6] Hong, Sungpack, Tayo Oguntebi, and Kunle Olukotun. "Efficient parallel graph exploration on multi-core CPU and GPU." Parallel Architectures and Compilation Techniques (PACT), 2011 International Conference on. IEEE, 2011.

[7] Merrill, Duane, Michael Garland, and Andrew Grimshaw. "Scalable GPU graph traversal." ACM SIGPLAN Notices. Vol. 47. No. 8. ACM, 2012.

[8] A. Grimshaw, D. Merrill, M. Garland, “High Performance and Scalable GPU Graph Traversal”, Technical Report, Nvidia, 2011.

[9] Wang, Yangzihao, et al. "Gunrock: A high-performance graph processing library on the GPU." Proceedings of the 20th ACM SIGPLAN Symposium on Principles and Practice of Parallel Programming. ACM, 2015.

[10] Mastrostefano, Enrico, and Massimo Bernaschi. "Efficient breadth first search on multi-GPU systems." Journal of Parallel and Distributed Computing 73.9 (2013): 1292-1305.

[11] Leskovec, Jure, and Andrej Krevl. "{SNAP Datasets}:{Stanford} Large Network Dataset Collection." (2014).

[12] P. Harish and P. J. Narayanan, “Accelerating large graph algorithms on the GPU using CUDA”, High Performance Computing – HiPC 2007, S. Aluru, M. Parashar et al. (Eds.), Springer Berlin Heidelberg 2007, pp. 197-208.

[13] Khorasani, Farzad and Vora, Keval and Gupta, Rajiv, " PaRMAT: A Parallel Generator for Large R-MAT Graphs", Proceedings of the 24th International Conference on Parallel Architectures and Compilation Techniques, 2015.

[14] Bernaschi, Massimo, et al. "Enhanced GPU-based distributed breadth first search." Proceedings of the 12th ACM International Conference on Computing Frontiers. ACM, 2015.

[15] Durrani, Muhammad Nouman, and Jawwad A. Shamsi. "Volunteer computing: requirements, challenges, and solutions." Journal of Network and Computer Applications 39 (2014): 369-380.

A Japanese Tourism Recommender System with Automatic Generation of Seasonal Feature Vectors

Guan-Shen Fang
Department of Information Engineering
Hiroshima University
Hiroshima, Japan

Sayaka Kamei
Department of Information Engineering
Hiroshima University
Hiroshima, Japan

Satoshi Fujita
Department of Information Engineering
Hiroshima University
Hiroshima, Japan

***Abstract*—Tourism recommender systems have been widely used in our daily life to recommend tourist spots to users meeting their preference. In this paper, we propose a content-based tourism recommender system considering travel season of users. In order to characterize seasonal variable features of spots, the proposed system generates seasonal feature vectors in three steps: 1) to identify the vocabulary concerned through Wikipedia; 2) to identify the trend over all spots through Twitter for each season; and 3) to highlight the weight of words contained in each identified trend. In the decision of recommendation, it does not only match the user profile with features of spots but also takes user's travel season into account. The effectiveness of the proposed system is evaluated by a series of experiments, *i.e.* computer simulation and questionnaire evaluation. The result indicates that: 1) those vectors certainly reflect the similarity of spots for designated time period, and 2) with using such vectors of spots, the system successfully realized a tourism seasonal recommendation.**

***Keywords*—Tourism recommender system; seasonal feature vector; Wikipedia; Twitter**

I. Introduction

In recent years, tourism recommender system is widely used to support users' choices of tourist spots. Unlike commodity such as books or movies, many of the features of Japanese spots change following season. A typical example is the famous tourist spot Niseko in Hokkaido, Japan, whose red leaves attract visitors in autumn. In winter, the snow makes its scene totally different so that visitors may enjoy skiing. Therefore, the decision of spots made for the user must not only fit his interest, but also realize the seasonal fashion.

In this paper, we focus on content-based seasonal recommendation. Although content-based recommendation has been applied successfully in the tourism domain [2], [3], [4], [5], they seldom produce recommendation considering season.

We propose a content-based seasonal tourism recommender system which fits the designated season of travel. For example, for a user who likes Matsushima island because of cherry-blossom viewing and wishes to travel in spring, the system can recommend other spots with the attraction of cherry-blossom viewing. However, such spots may not be the recommendations of another user who wishes to travel in autumn even if is fond of Matsushima's sea and coast. In order to characterize the dynamically changed seasonal features, the proposed system generates seasonal feature vector for each spot for a given season. Its generation consists three steps. Firstly, it identifies the vocabulary concerned through Wikipedia[1] document about the spot. The reason for using Wikipedia is that each tourist spot has its unique document which introduces its detail features (see Fig. 1 which shows the description about the spot "Ritsurin Garden" in Kagawa prefecture including seasonal features for each season). Secondly, it identifies the trend (*i.e.*, seasonal variance of features for a designated period) over all spots in Japan through Twitter[2]. Finally, for the words (*i.e.*, the features) in the vocabulary, it highlights the ones contained in the identified trend which corresponds to the given season. With these vectors of spots, the proposed system match them with user's profile which presents his/her preference to decide the recommendations for the travel period of user.

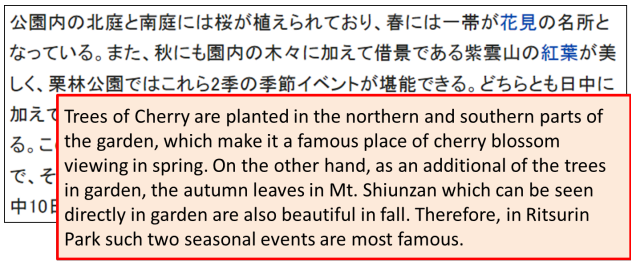
公園内の北庭と南庭には桜が植えられており、春には一帯が花見の名所となっている。また、秋にも園内の木々に加えて借景である紫雲山の紅葉が美しく、栗林公園ではこれら2季の季節イベントが堪能できる。どちらとも日中に
加えて
る。こ
で、そ
中10
Trees of Cherry are planted in the northern and southern parts of the garden, which make it a famous place of cherry blossom viewing in spring. On the other hand, as an additional of the trees in garden, the autumn leaves in Mt. Shiunzan which can be seen directly in garden are also beautiful in fall. Therefore, in Ritsurin Park such two seasonal events are most famous.

Fig. 1. A part of the Wikipedia article about Ritsurin Park. A detailed description of the main features is included.

As the implementation, the proposed system gathered 6,057 Wikipedia documents to cover almost all sightseeing spots in Japan. On the other hand, it also collected more than 500 thousands tweets that are published during 7 months. In the experiments we conducted a series of experiments including both a computer simulation and a questionnaire evaluation.

The contribution of current paper is as follows:

- For a designated season, it provides a method to generate seasonal feature vector for sightseeing spot as the characterization of its features. The experimental results demonstrate that the property of those vectors certainly reflect the similarity of spots.
- The proposed recommender system provides the user a

[0] A preliminary extended abstract [1] of this paper appears in the proceedings of the 4th International Symposium on Computing and Networking (CANDAR).

[1] http://ja.wikipedia.org
[2] https://www.twitter.com

recommendation of spots with awareness of the travel season. The experiment of questionnaire shows that the seasonal recommendations have higher precision of user's actual choices than the one without applying seasonal feature vectors.

The remainder of this paper is organized as: Section II overviews related works. Section III describes the detail of the proposed system including the generation of seasonal feature vectors and recommendation process as well. Section IV represents the implementation of the prototype system. Section V represents the method of evaluation and shows its results. Finally, a conclusion is given and future works are discussed in Section VI.

II. Related Work

A. Content-based Tourism Recommendation

Content-based tourism recommendation systems try to recommend spots similar to those users have liked in the past (*i.e.*, history) [6]. From the history, user's profile is built to represent his preference. On the other hand, the features of spots are characterized in order to match with user's profile to decide the recommendation. Some of existing researches aim to provide the user an appropriate tour plan to meet his/her constraints, such as time or cost [7], [8], [3]. The features of spots are given from experts of tourism, which simply includes available time, normal visiting time and geographical information, etc.. Therefore, the recommendation of the tour plan turns to an integer programming problem or traveling salesman problem to approximate a combination of spots with minimization of the travel path or time wasted in movement. Győrödi *et al.* [9] proposes a spot recommendation with a mobile application. In order to determine user's interest and features of spot, they use tags such as food, music etc., which can be established by users and assigned to a specific spot. The recommendation is produced by matching such tags of the given user and spots.

In existing content-based researches much efforts are made to provide tourist spots or plan to meet user's needs. However, the travel season which is an essential factor in decision of spots is seldom taken into account.

By utilizing the proposed method not only in content-based recommendations but also in some hybrid approaches [10], [11], [12], a seasonal recommendation can be easily realized.

B. Tourism Recommendation using Wikipedia

In many recent researches of tourism recommendation, Wikipedia is integrated as an external source in identification of spots. It is effective at reducing the cost of manually construction or maintenance of spots' information. A common idea is to take advantage of geographic information included in Wikipedia documents about spots to filter users' geo-tagged photos (e.g., photos in Flickr) and extract their visiting trajectories of spots [13], [14], [15]. Techniques such as T-pattern tree [16] are exploited to mine the traveling patterns potentially contained in extracted trajectories. Additionally, in Wikipedia since categories are assigned to each tourist spot, some of researches further transform user's trajectories into sequences of categories to represent user's preference [14], [15].

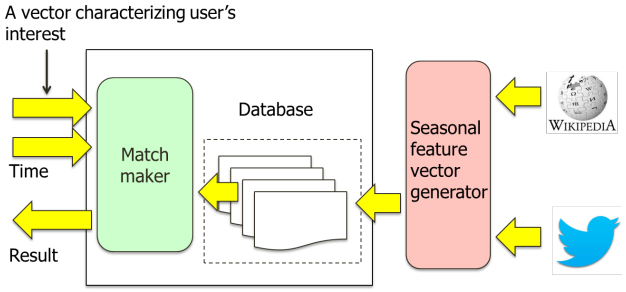

Fig. 2. Components in proposed tourism recommender system.

Although in many existed researches Wikipedia is used to combine with SNS to improve the performance of recommendations, few researches take advantage of the content of textual article in Wikipedia, even the detailed description of both permanent and seasonal features is contained.

C. Identification and Analysis of Tweets for Tourism

Recently, Twitter has been paid much attention as a source of data mining and characterization of spots for tourism informatics. In order to detect tourism related tweets which are posted at specific spots, Shimada *et al.* [17] applies a Support Vector Machine(SVM) to their gathered tweets. Their idea is that the target tweets are similar on their textual content. With the aid of geo-tag, Oku *et al.* [18] proposes another SVM-based method of detection of tweets relevant to tourism, and extract temporal features of spots from them. They regard tweets issued within a week as a single document and obtain a temporal feature vector for each week by calculating the TF-IDF weight of keywords contained in such documents. However, it does not generate vectors to cover a sufficient number of spots because it is solely based on tweets. Similarly, Menchavez *et al.* [19] focus on the identification of tourism related tweets and a Naive Bayes based sentiment analysis to mine the opinions when tourists visit spots in Philippines. Furthermore, such mined opinions are classified into positive and negative polarity and presented at the geographical map as references for tourists. Similar study is done by Claster *et al.* [20] for Thailand, in which the sentiment analysis of tweets is applied in time-series. Although the problem definitions of previously mentioned researches are different with the current paper, the objectives are similar which aim to discover useful information of tourism via Twitter.

In such researches, many efforts have made to reduce the noise in tweets. However, due to the irregularity of tweets, many meaningless words like punctuation or prefix are always extracted and significantly influence the accuracy of the analysis. In addition, those techniques based on machine learning are sometimes difficult to conduct for minor spots having few related tweets. Since in this paper the proposed system uses Wikipedia as the corpus combined with Twitter, it is free of the influence from such noise. Furthermore, for the minor spots which are seldom tweeted Wikipedia can cover their features and avoid the failure of their recommendation.

III. Seasonal Recommendation of Tourist Spot

In this section, we represent the proposed recommendation system in detail. Fig. 2 shows the architecture, which consists of two processes: 1) to generate seasonal feature vectors for each spot; 2) to identify user's preference as profile, and match it with such vectors of spots to produce recommendation. Following subsections detail each part.

A. Generation of Seasonal Feature Vectors

Firstly, the time axis is assumed to be separated into several ranges so that the features of spots are regarded to be invariant, as in the year end season, the season of cherry-blossom viewing or the bathing season. Each range is called a **season**. The proposed system generates one seasonal feature vector (SFV, for short) of each spot for each season. SFV is calculated by extending the basic feature vector (BFV, for short), in such a way that it reflects the trend of words in each season. More concretely, BFV is a vector of TF-IDF weights (defined bellow) and SFV is its extension.

Let O be the set of spots and d_i be the Wikipedia document about spot $o_i \in O$. Generally d_i is a summarization of the entire information of o_i. Therefore, the reader should note that d_i is the union of statements on spot o_i relevant to various seasons. In other words, in order to generate SFV for each season, the system needs to distinguish word sets relevant to each season in document d_i. Let W_i be the set of words included in document d_i and $W = \bigcup_i W_i$ (*i.e.*, W is the set of words included in Wikipedia documents about O). Then, the term frequency (TF, for short) weight of word w_j in document d_i is defined as

$$TF_{i,w_j} = \frac{n_{i,w_j}}{\sum_{w \in W} n_{i,w}}$$

and the inverse document frequency (IDF, for short) weight of word w_j over $|O|$ documents is defined as

$$IDF_{w_j} = \log\left(\frac{|O|}{m_j}\right)$$

Where, n_{i,w_j} is the number of occurrences of w_j in d_i and $m_j (\leq |O|)$ is the number of documents containing w_j. With these notions, the BFV $\vec{v}_i^b$ of spot o_i is defined as:

$$\vec{v}_i^b = \{(w_j, TF_{i,w_j} \times IDF_{w_j}) \mid w_j \in W_i\}. \quad (1)$$

The words which are frequently mentioned in d_i and seldom contained in other documents would have high weights in BFV.

For a given season, the key idea is to extend the definition of the TF weight in (1) by considering the trend of words. Let t_k be a collection of tweets issued in season s_k. By considering t_k as a single document, the TF weight of word w_j in season s_k is defined as follows:

$$TF'_{k,w_j} = \frac{n'_{k,w_j}}{\sum_{w \in W} n'_{k,w}} \quad (2)$$

Where, n'_{k,w_j} is the number of occurrences of word w_j in t_k. Because W is the set of words contained in Wikipedia documents about O, *the proposed system omits words in tweets which do not appear in any Wikipedia document*. With the above notions, SFV $\vec{v}^s_{i,k}$ of spot o_i for season s_k is defined as

$$\vec{v}^s_{i,k} = \{(w_j, ((1-\alpha)TF_{i,w_j} + \alpha TF'_{k,w_j}) \times IDF_{w_j}) \mid w_j \in W_i\} \quad (3)$$

Where, $0 \leq \alpha \leq 1$ is an appropriate parameter. Note that for o_i, only for the word $w_j \in W_i$ it has TF_{i,w_j} to be non-zero. If word $w_j \in W_i$ has not tweeted in specific season s_k, $TF'_{k,w_j} = 0$; otherwise $TF'_{k,w_j} > 0$, then we say that w_j is highlighted in s_k.

B. Identification of User's Preference and Recommendation Process

Although an analysis of user's history of tweets would help us to extract his/her preference on the features of sightseeing spots, it may fail for the users who even do not have Twitter accounts or seldom tweet about travel. In order to fit such users, the proposed system extracts user's preference in an explicit way that it directly asks the user for a history of travel. In other words, the user answers two easy questions when he/she begins to use the system: 1) the season that he/she wishes to travel; 2) the most favorite spot that he/she has visited during assigned season until now. Assume that user u chooses tourist spot $o_{i'}$ and the period of season $s_{k'}$. His/her profile which presents preference is defined by the SFV $\vec{v}^s_{i',k'}$ as $\vec{U_{k'}}$. Although the user profiling is simple, it effectively characterizes user's seasonal preference and is with various benefits: first, it does not suffer the cold start problem; second, such questions are easy to answer and time-saving.

With the constructed user profile, the proposed system matches it with SFVs of spots to decide recommendations for season $s_{k'}$. To quantify the correspondence of $o_{i'}$ and a given spot $o_l (o_l \neq o_{i'})$ in $s_{k'}$, the system calculates their cosine similarity as follows:

$$Sim_{i',l} = \frac{\vec{U_{k'}} \cdot \vec{v}^s_{l,k'}}{|\vec{U_{k'}}||\vec{v}^s_{l,k'}|}, \quad for\ each\ o_l \neq o_{i'}, o_l \in O.$$

The spots with Top-t similarities are the recommendations to user u in $s_{k'}$ as a ranking. Note that the recommendations vary for different seasons designated.

IV. Implementation of a Prototype System

A. Datasets Description

Since the objective of recommendation is entire tourist spots in Japan, for this prototype system, we focus on 6,057 spots given in the category of "tourist spots in Japan" in Wikipedia, and download the Japanese document for each of them from the Wikipedia server. The prototype system uses only nouns as words in each document d_i. The set of words W_i in d_i is obtained by conducting the morphological analysis using MeCab [3] with the default IPA dictionary. From all collected Wikipedia documents, 608,390 words are extracted overall, in average 100.5 words for a document. The relationship of the count of spots and the size of words which are extracted from

[3] http://mecab.sourceforge.net/

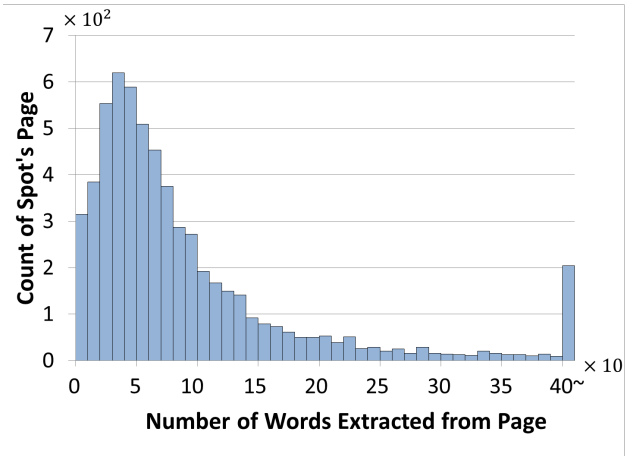

Fig. 3. The counts of spots with various sizes of words extracted from their documents.

TABLE I. THE NUMBER OF MINOR SFVS FOR EACH s_k WHEN $\ell = 3$.

$\alpha < 1.0$	$\alpha = 1.0$						
	Sep.	Oct.	Nov.	Dec.	Jan.	Feb.	Mar.
61	220	199	205	175	274	601	191

their documents is shown in Fig. 3. It represents that most spots are introduced in detail in their Wikipedia documents.

A set of tweets relevant to tourism is gained from Twitter using Twitter Streaming API. More concretely, 50 million Japanese tweets issued from September 2013 to March 2014 are acquired. For each of the tweet, its textual content is matched with the names of collected spots. As a result, about 500 thousands tweets containing at least one name of 6,057 spots are regarded as tweets relevant to the tourism and extracted as a part of dataset. Although it may contain tweets which are not relevant to tourism and may miss tweets relevant to the tourism, we didn't evaluate the precision of such a naive extraction since it is the out of scope of this paper. Let T be the resulting set of tweets.

B. Parameter Assignments

Considering seasons always last more than one month with different periods of time, assume that one year is divided into 12 disjoint seasons of (almost) equal length in the way that the first season is from January 1st to January 31st, the second season is from February 1st to February 28th (or 29th), and so on. More precisely, seven documents, which represent the trend of each season, is derived from T because collected tweets are for seven months. For a given season and its corresponding document in T, the prototype system generates one SFV for each spot. As a result, in all spots' SFVs 170,978 words are highlighted by Tweets, 28.3 words for one spot's SFVs in average.

Finally, another task is to identify appropriate value for α in (3). The value α is assumed more than 0 without loss of generality. Recall that W_i is the word set contained in the Wikipedia document about spot o_i. Relatively, let W'_k be the word set contained in tweets in season s_k. When $\alpha < 1$, the L^0-norm of SFV $\vec{v}^s_{i,k}$ coincides with $|W_i|$ which is independent

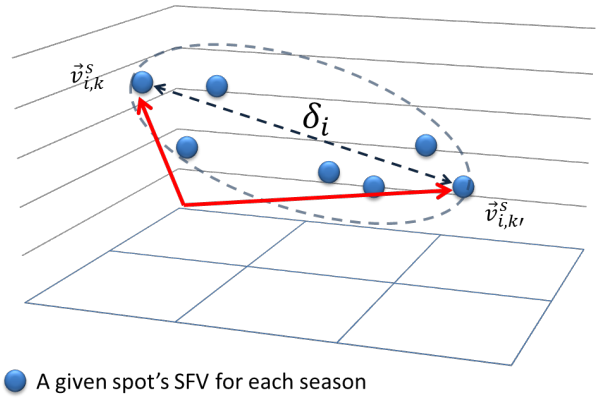

Fig. 4. Diameter of spot in the vector space.

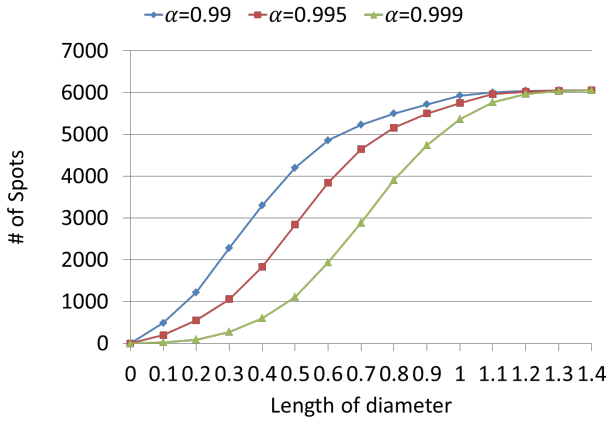

Fig. 5. Distributions of the diameters of spots with $\alpha = 0.99$, 0.995 and 0.999.

of α and k, but when $\alpha = 1$, it coincides with $|W_i \cap W'_k|$ which varies depending on k. It may cause failure of recommendation for some spots which are lack of vocabulary in their Wikipedia documents and have been seldom tweeted. Such spots are defined as **minor** if the L^0-norm of its SFV is smaller than or equal to ℓ. Table I shows the number of minor spots for given α and k. Although the number of minor ones is 61 when $\alpha < 1$, it exceeds 170 by increasing α to 1. Thus, in the following, the prototype system will restrict our attention to the case of $\alpha < 1$.

Next, consider the variance of SFVs in various α to decide its assignment. Let Ω be the vector space spanned by all SFVs (of all spots). In the following, each vector is normalized by the length in the L^2-norm to have an unit length in Ω. Therefore, each spot o_i is mapped to a point by SFV $\vec{v}^s_{i,k}$ in Ω for each season s_k. This implies that the "intensity" of the variance of SFVs is characterized by

$$\delta_i = \max_{k \neq k'} \{ |\vec{v}^s_{i,k} - \vec{v}^s_{i,k'}| \} \quad (4)$$

Where, $|\cdot|$ denotes the L^2-norm. See Fig. 4 for the illustration. δ_i is affected by α and called the **diameter** of o_i hereafter.

Fig. 5 illustrates the cumulative distributions of δ for $\alpha = 0.99$, 0.995 and 0.999, where the horizontal axis is the length of the diameter and the vertical axis is the accumulative size of the spots having diameter less or equal to a specific value. It indicates that the diameter follow Gaussian distribution and its mean and variance of diameter certainly increase as α increases. In general, a large δ implies that for corresponding spot its seasonal features are well highlighted in SFVs.

Additionally, for each of the word sets $W_i \setminus W'_k$ and $W_i \cap W'_k$, we observe its average weight of words in SFVs. When $\alpha = 0.995$, a comparison is made that the two averages are both at range of 2.3×10^{-4}. As α increased to 0.999 the words in $W_i \setminus W'_k$ are weighted as one-fifth as the ones in $W_i \cap W'_k$ overall. It implies that although in the latter case the seasonal features are well highlighted, static features which do not relate with the seasons are weakened significantly and with failures of characterization. On the other hand, it is observed that the average distance of a spot's BFV to its nearest neighbor is almost 1.2, which is nearly twice of the average of all spots' δ in the case of $\alpha = 0.995$(almost 0.55). Therefore, α is fixed to 0.995.

V. Evaluation

In this section, the effectiveness of the proposed system is evaluated with respect to the following two aspects: 1) whether the proposed SFV certainly extracts and characterizes seasonal features from Wikipedia and Twitter; and 2) whether the proposed system effectively provides seasonal tourist spot's recommendation.

A. Variance of SFVs

1) Evaluation Methodology: In this section, rather than a direct observation of the difference of SFVs for a given spot, the evaluation of time transition of the similarity of spots is conducted. They are obtained by applying the K-means method [21] to SFVs of all spots. More concretely, if the spots contained in a cluster in season s_k are separated into several clusters in other seasons, those spots are given similar SFVs for s_k and the set of words characterizing the cluster should represent the feature of those spots for s_k. Considering the size of spots is over 6,000, the value of K is setted to 70 in the process of clustering. This evaluation examines the mean of each resulting clusters and focus on several typical ones for the convenience of presentation.

2) Result: From the resulting clusters, four typical clusters, say C_r, C_i, C_s and C_c, are identified. Their details are summarized in Table II. Note that each of these four clusters is defined only for a specific season. Since *red leaves* and *cherry-blossom* have higher popularities than *illumination* and *snow* in Japan, the corresponding ones also have larger sizes than the others.

Results on the time transition of the similarity of spots are summarized in Fig. 6. The left-most figure of the first line in Fig. 6 shows the result of cluster C_r and the other three figures concern with clusters C_i, C_s and C_c, respectively. In November, all spots in C_r form a distinct cluster, but in other seasons, they separate into different ones. It indicates that the common features of those spots are *highlighted* in November, although they have various features in other seasons. Similar phenomenon can also be found in other clusters. On the other hand, several spots in C_c are also confirmed to remain in the same cluster through all seasons. It indicates that SFVs of those spots are close with each other in vector space Ω regardless of the transition of seasons.

TABLE II. Details of Four Typical Clusters

	relevant features	season	# of spots
C_r	`red leaves, waterfall`	November	109
C_i	`illumination,cafe`	January	36
C_s	`snow,event`	January	35
C_c	`cherry-blossom,park`	March	61

TABLE III. The value of $\xi(30, k)$ with $k \in$ { Sep, Oct, Nov, Dec, Jan, Feb, Mar }.

	Sep.	Oct.	Nov.	Dec.	Jan.	Feb.	Mar.
C_r	5	5	**5**	5	5	4	4
C_i	−8	4	4	4	**4**	4	4
C_s	6	4	4	5	**8**	3	3
C_c	11	10	11	11	12	13	**13**

B. Impact on Recommendation

1) Evaluation Methodology: In this subsection, the performance of the proposed seasonal tourism recommender system is evaluated with simulated users. Although a questionnaire evaluation is also conducted in the next subsection, here we aim to compare and observe the difference between recommendations which are generated with considering season (*i.e.*, SFV) and without season (*i.e.*, BFV) in detail. The evaluation focuses on the aforementioned clusters C_r, C_i, C_s and C_c, and regards the mean of SFVs contained in each cluster as the preference of users[4]. In other words, there are four users who are fond of *red leaves*, *illumination*, *snow* and *cherry-blossom*, with the spots in clusters C_r, C_i, C_s and C_c as the answers respectively. The performance as the proposed system is evaluated by analyzing the Top-t spots' recommendation to the designated points for each season k. Such a subset of spots is denoted as Q_t^k hereafter. As comparison, according to the cosine similarity of the corresponding BFVs to the designated points, the Top-t spots (denoted as P_t) are also calculated.

For the mean of a given cluster C, the goodness of a subset X concerned is measured by $|C \cap X|$. Thus, the advantage of using SFV instead of ordinary BFV can be measured by calculating

$$\xi(t, k) \stackrel{\text{def}}{=} |Q_t^k \cap C| - |P_t \cap C|, \tag{5}$$

which depends on the value of parameter t and the selection of season k.

2) Result: Table III summarizes the results for $t = 30$, where the emphasized numbers designate the seasons in which the corresponding clusters are defined (e.g., cluster C_r is defined for November). The result implies that by using SFVs, the proposed system can recommend more spots to fit simulated users' preferences and the effect is maximized when the designated season coincides with the one defining the cluster.

[4]A typical scenario assumed in this paper is that the user designates an interested spot as the preference with a hoped travel season and the system returns a set of spots as recommendation.

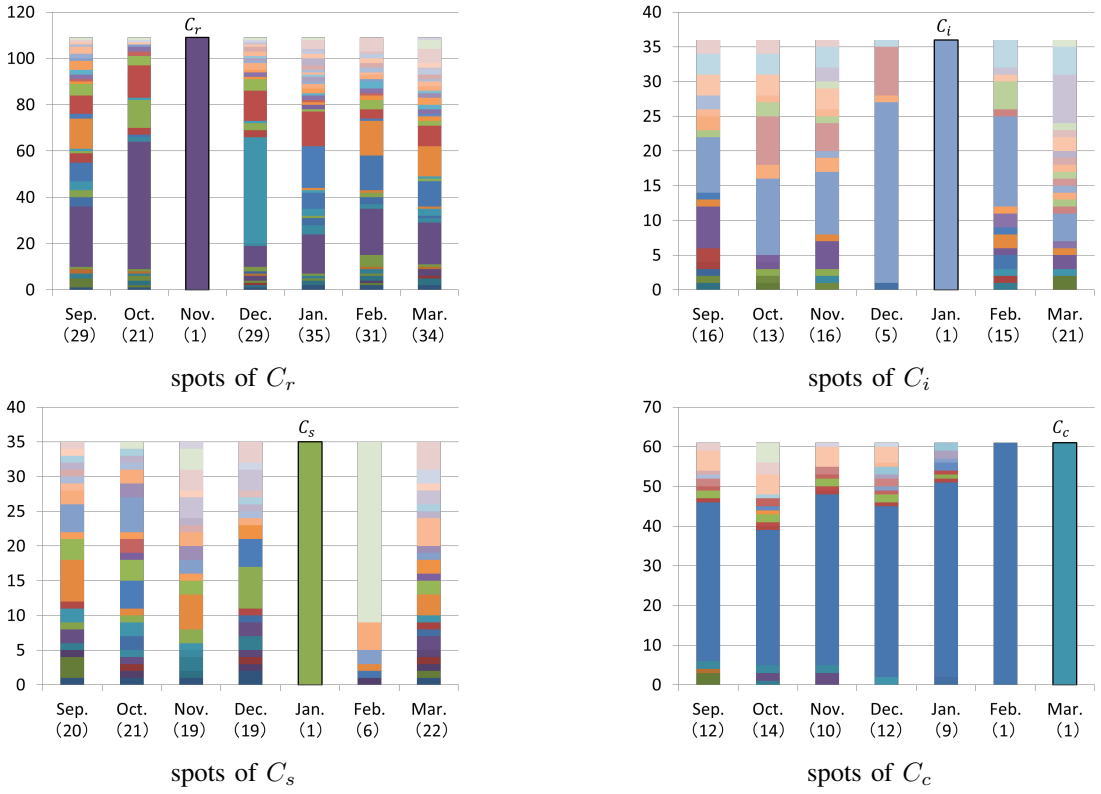

Fig. 6. The distributions of clusters for the spots that are included in C_r, C_i, C_s and C_c. The bars with various colors represent different clusters and their lengths depend on the sizes of focused spots. For a given cluster and a season, the number of clusters that focused spots separate into is also given in parentheses at the bottom.

TABLE IV. THE VALUE OF $\xi(t,k)$, WHERE THE VALUE OF t IS FIXED TO BE EQUAL TO THE CORRESPONDING CLUSTER SIZE

	Sep.	Oct.	Nov.	Dec.	Jan.	Feb.	Mar.
C_r	6	8	**7**	8	9	-4	2
C_i	-15	-5	0	0	**0**	-3	0
C_s	7	6	4	5	**9**	4	4
C_c	8	8	11	10	8	17	**17**

Recall that the value of $\xi(t,k)$ depends on parameter t. Table IV summarizes the results for each cluster, where the value of t is fixed to be equal to the cluster's size, e.g., let $t = 109$ for cluster C_r. Comparing with Table III, in each row a larger gap of $\xi(t,k)$ is observed for each season. It indicated that there are various $Q^k_{|C|}$ for given cluster C. In other words, if the designated season is not relevant with given C, fewer spots that contained in C will be recommended.

C. Questionnaire Evaluation

1) Evaluation Methodology: Finally, a two-steps' seasonal tourism questionnaire is conducted to evaluate whether the proposed system can provide a seasonal recommendation of spots in an actual case. Recall that the proposed system extracts user's preference from his visited favorite tourist spot in Section III-B. Therefore, as the first step of the questionnaire, participant selects the spot and the season (*i.e.* month) $s_{k'}$ that he/she wishes to travel. According to his/her selections, system generates a list of recommendations for $s_{k'}$ denoted as $Q'^{k'}_t$. For comparison, another recommendation list P'_t using BFVs instead of SFVs of spots are generated. Here t denotes the number of spots that are included in the recommendations, *i.e.* the lengths of $Q'^{k'}_t$ and P'_t. $Q'^{k'}_t$ and P'_t are randomly combined into one list of recommendations, as $Q'^{k'}_t \cup P'_t$. In the second step, from $Q'^{k'}_t \cup P'_t$ the participant chooses at most 5 spots that he/she wishes to visit in $s_{k'}$. Since in following we focus on entire participants and their experimental results, the superscript k' in $Q'^{k'}_t$ is omitted for convenience.

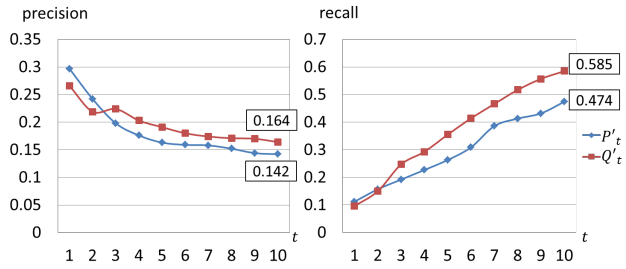

Fig. 7. Precision and recall of Q'_t and P'_t following t.

As quantification, this evaluation calculates average precision and recall of all participants' choices in Q'_t and P'_t as follows:

$$precision = E(\frac{h_t}{t})$$

$$recall = E(\frac{h_t}{H})$$

TABLE V. THE NUMBERS OF TRIALS WITH EACH $s_{k'}$ HAVING BEEN CHOSEN. FOR EXAMPLE, 10 QUESTIONNAIRES ARE SUBMITTED WITH $s_{k'} = Dec.$.

month	Jan.	Feb.	Mar.	Sep.	Oct.	Nov.	Dec.
# of trials	6	6	12	11	14	5	10

TABLE VI. THE SIZES OF SPOTS CHOSEN FROM P'_t AND Q'_t BY ALL PARTICIPANTS

	P'_t	Q'_t	$Q'_t \cup P'_t$	$Q'_t \cap P'_t$
$t = 5$	52	61	107	6
$t = 10$	91	105	185	11

Where, h_t is the size of spots having been chosen from $Q'_t \cup P'_t$ by a participant, and H is such size of spots with $t = 10$.

In this evaluation, 55 participants' cooperation is received, including 17 college students major in information engineering and 38 second-year high school students, and 64 spots are chosen as their favorite spots overall, *i.e.* 64 trials by 55 participants. Table V summarizes the favorite spots having been chosen by the participants with various $s_{k'}$.

2) Result: Table VI shows the detail of participants' choices from recommendations $Q'_t \cup P'_t$. In either case of t, the size of spots having been chosen in Q'_t is higher than P'_t. It represents that participants prefer the recommended spots in Q'_t than P'_t. Also note that from $Q'_t \cup P'_t$, 107 and 185 spots are chosen when $t = 5$ and $t = 10$ respectively, which contain duplicated spots in Q'_t and P'_t. More concretely, in all trials 6 spots are chosen from $Q'_t \cap P'_t$ when $t = 5$ by participants, and 11 spots with $t = 10$ respectively. In average, almost 2.89 spots are chosen from $Q'_t \cup P'_t$ in one trial.

The results of precision and recall are given in Fig. 7. It represents that when $t \leq 2$, although the precision of Q'_t is worse than P'_t, the recall of Q'_t and P'_t are almost at the same level. This phenomenon represents that the users who wish to visit the spots in the top of Q'_t are with little interest to the spots having been included in P'_t. Furthermore, such users tend to choose fewer spots overall than the ones who have not chosen the spots in the top of Q'_t. On the other hand, in the case of $t > 2$, proposed seasonal recommendation outperforms the ordinary recommendation only utilizing BFV. Also considering the fact that in most of the recommender systems the list of recommendations often includes more than 3 spots, the spots recommendations provided by the proposed system more fit user's demand than ordinary ones without considering travel season.

VI. CONCLUDING REMARKS

This paper proposes a seasonal tourism recommender system using Wikipedia and Twitter to provide a list of tourist spots as seasonal recommendation. The effectiveness of the proposed system is experimentally evaluated by detailed observation of seasonal feature vector of spot and questionnaires of users' actual choices of spots. The results of evaluations indicate that SFVs certainly characterize the variable seasonal features of the spots. More concretely, the variance of SFVs follows Gaussian distribution and the similarity of SFVs reflects the similarity of the features of the corresponding spots in a designated season. Further more, the result of questionnaire verifies that in most of the case the proposed system successfully provides seasonal spots recommendations to fit user's demand in tourism.

A future work is to extend the proposed recommender system to extract and characterize *spatial-temporal* features of the spot. Another issue is to integrate user modeling techniques into proposed recommender system, in order to improve the accuracy of recommendations. On the other hand, we also consider that in some hybrid recommender systems like [11], [22], our proposed method can be used as a component to improve them to achieve a seasonal recommendations. In future, we wish to combine the proposed method with such approaches and evaluate the performance of recommendations.

REFERENCES

[1] G.-S. Fang, S. Kamei, and S. Fujita., "Automatic generation of temporal feature vectors with application to tourism recommender systems," in *Proceedings of the 4th International Symposium on Computing and Networking*, 2016.

[2] G. Büyüközkan and B. Ergün, "Intelligent system applications in electronic tourism," *Expert systems with applications*, vol. 38, no. 6, pp. 6586–6598, 2011.

[3] Y. Kurata, Y. Shinagawa, and T. Hara, "Ct-planner5: a computer-aided tour planning service which profits both tourists and destinations," in *Workshop on Tourism Recommender Systems, RecSys*, vol. 15. ACM, 2015, pp. 35–42.

[4] Ángel García-Crespo, J. L. López-Cuadrado, R. Colomo-Palacios, I. González-Carrasco, and B. Ruiz-Mezcua, "Sem-fit: A semantic based expert system to provide recommendations in the tourism domain," *Expert Systems with Applications: An International Journal*, vol. 38, no. 10, pp. 13 310–13 319, September 2011.

[5] M. Zanker, M. Jessenitschnig, and W. Schmid, "Preference reasoning with soft constraints in constraint-based recommender systems," *Constraints*, vol. 15, no. 4, pp. 574–595, 2010.

[6] P. Lops, M. De Gemmis, and G. Semeraro, "Content-based recommender systems: State of the art and trends," in *Recommender systems handbook*. Springer, 2011, pp. 73–105.

[7] D. Herzog and W. Wörndl, "A travel recommender system for combining multiple travel regions to a composite trip," in *Workshop on New Trends in Content-Based Recommender Systems*. Citeseer, 2014, pp. 42–48.

[8] R. A. Abbaspour and F. Samadzadegan, "Time-dependent personal tour planning and scheduling in metropolises," *Expert Systems with Applications*, vol. 38, no. 10, pp. 12 439–12 452, 2011.

[9] R. Győrödi, C. Győrödi, and M. Deridan, "An extended recommendation system using data mining implemented for smart phones," *International Journal of Computers and Technology*, vol. 11, no. 3, pp. 2360–2372, 2013.

[10] A. Garca-Crespo, J. Chamizo, I. Rivera, M. Mencke, R. Colomo-Palacios, and J. M. Gmez-Berbs, "Speta: Social pervasive e-tourism advisor," *Telematics and Informatics*, vol. 26, no. 3, pp. 306 – 315, 2009.

[11] G. Fenza, E. Fischetti, D. Furno, and V. Loia, "A hybrid context aware system for tourist guidance based on collaborative filtering," in *Fuzzy Systems (FUZZ), 2011 IEEE International Conference on*. IEEE, 2011, pp. 131–138.

[12] J. M. Noguera, M. J. Barranco, R. J. Segura, and L. MartíNez, "A mobile 3d-gis hybrid recommender system for tourism," *Information Sciences: an International Journal*, vol. 215, pp. 37–52, December 2012.

[13] R. Baraglia, C. Frattari, C. I. Muntean, F. M. Nardini, and F. Silvestri, "A trajectory-based recommender system for tourism," in *International Conference on Active Media Technology*. Springer, 2012, pp. 196–205.

[14] C. Lucchese, R. Perego, F. Silvestri, H. Vahabi, and R. Venturini, "How random walks can help tourism," in *European Conference on Information Retrieval*. Springer, 2012, pp. 195–206.

[15] K. H. Lim, "Recommending tours and places-of-interest based on user interests from geo-tagged photos," in *Proceedings of the 2015 ACM SIGMOD on PhD Symposium*. ACM, 2015, pp. 33–38.

[16] F. Giannotti, M. Nanni, F. Pinelli, and D. Pedreschi, "Trajectory pattern mining," in *Proceedings of the 13th ACM SIGKDD international conference on Knowledge discovery and data mining*. ACM, 2007, pp. 330–339.

[17] K. Shimada, S. Inoue, and T. Endo, "On-site likelihood identification of tweets for tourism information analysis," in *Proceedings of the IIAI International Conference on Advanced Applied Informatics*, 2012, pp. 117–122.

[18] K. Oku, K. Ueno, and F. Hattori, "Mapping geotagged tweets to tourist spots for recommender systems," in *Proceedings of the IIAI 3rd International Conference on Advanced Applied Informatics*, 2014, pp. 789 – 794.

[19] J. C. L. Menchavez and K. J. P. Espinosa, "Fun in the philippines: Automatic identification and sentiment analysis of tourism-related tweets," in *2015 IEEE International Conference on Data Mining Workshop (ICDMW)*, Nov 2015, pp. 660–667.

[20] W. B. Claster, M. Cooper, and P. Sallis, "Thailand–tourism and conflict: Modeling sentiment from twitter tweets using naïve bayes and unsupervised artificial neural nets," in *2010 Second International Conference on Computational Intelligence, Modelling and Simulation*, 2010, pp. 89–94.

[21] C. Elkan, "Using the triangle inequality to accelerate k-means." in *ICML*, T. Fawcett and N. Mishra, Eds. AAAI Press, 2003, pp. 147–153.

[22] C. Tan, Q. Liu, E. Chen, H. Xiong, and X. Wu, "Object-oriented travel package recommendation," *ACM Trans. Intell. Syst. Technol.*, vol. 5, no. 3, pp. 43:1–43:26, Sept. 2014.

A Survey of Big Data Analytics in Healthcare

Muhammad Umer Sarwar*, Muhammad Kashif Hanif†, Ramzan Talib‡, Awais Mobeen§, and Muhammad Aslam¶
Department of Computer Science,
Government College University, Faisalabad, Pakistan

***Abstract*—Debate on big data analytics has earned a remarkable interest in industry as well as academia due to knowledge, information and wisdom extraction from big data. Big data and cloud computing are two most important trends that are defining the new emerging analytical tools. Big data has various applications in different fields like traffic control, weather forecasting, fraud detection, security, education enhancement and health care. Extraction of knowledge from large amount of data has become a challenging task. Similarly, big data analysis can be used for effective decision making in healthcare by some modification in existing machine learning algorithms. In this paper, drawbacks of existing machine learning algorithms are summarized for big data analysis in healthcare.**

Keywords*—Big data; Analytics; Healtcare; Analytical tools; Machine learning

I. Introduction

According to Sutherland and Shan, big data is based on three main properties, i.e., volume, velocity, and variety [1]. A large volume of data is being produced by various sources like astronomy, environmental data, transportation data, stock market transactions, census, airline traffic, internet images etc. The rate at which data is being generated from different resources is referred to velocity. Variety is different types of data including text, audio, images, video etc. In statistical perspective, big data is not big just in volume only but it is also big in terms of dimensions. Dimensions are also termed as features. Existing traditional methods of data mining can hardly give useful information. There is need for modification in existing machine learning methods for better data extraction and decision making [2].

Recently, the trend in healthcare is now diverting from cure to prevention due to rapid increase in data. Scientist have focused to make improvement in reliability and efficiency of healthcare systems to minimize the curing cost in healthcare and also to deliver better medication to patients. Hospitals and healthcare system are good warehouse of big data like patient history, test reports, medical image [3]. It is challenging task to cope with large amount of unstructured data and missing values. Improvements in existing data mining and machine learning approaches can help to develop personalized medicines which can cure and prevent diseases [4]. Existing traditional machine learning algorithms works on centralized databases which requires a lot of time to train and analyze large amount of data. Similarly, it is not feasible to store and process big data on single machine. Therefore, there is need to parallelize existing approaches and modify these approaches with hybrid approaches that have enough capabilities to overcome the challenge of storing and processing large data set in distributed environment [1].

A lots of research has been carried out in healthcare domain to train the system and predict the expected result for the patient. Microarray data has become a major interest area in healthcare domain in recent few years. There are thousands of dimensions in microarrays data that require huge amount of processing in terms of cost and time [5]. Dimension reduction techniques are applied to extract relevant information from large dimensions.

II. Big Data

Data is considered as much important as oil. However, oil in unprocessed form is hardly of use. Similarly, data in unprocessed form in not useful. Important information can be extracted from data by using different analytical methods. According to Hermon [3], big data analytics can bring the revolution in healthcare industry. This data in healthcare provide opportunity to perform predictive analysis. Big data analytics has a great potential to process large amount of data in parallel and solution of hidden problems can also be find. This analytical approach can be implemented to minimize cost of processing time on large amount of data. For example, any disease that has occurred earlier in any parts of the world, prediction of that disease can be done efficiently. Although, clinics and hospitals can reprocess the data to analyze and calculate the patient preferences. In predictive analysis, we implement different statistical methods, data mining, and machine learning approaches to analyze, process, and predict the conclusion for undiscovered data. Healthcare domain has a lot of possibilities to provide better cure for disease using different analytical tools.

Processing of big data can be organized into four layers (Fig. 1). To process large amount of data collected from different sources which can be in different formats is a challenging task. Due to unstructured data, traditional database management system cannot be use for knowledge extraction form data. Big data may include structured, semi-structured, and unstructured data [6]. First, we collect data that is generated from different origins and then collect and store it into one common platform. Most commonly, we use Apache Hadoop that is open source framework to provide Hadoop Distributed File System (HDFS) for distributed storage and fault tolerance [7]. MapReduce is the programming model of Hadoop which can be used to process huge amount of data as quick as possible [8]. The dataset is partitioned into training and testing subsets [9]. Machine learning algorithm can be implemented to perform intelligent analysis on input data and produce information that can be used to produce reports in processing layer.

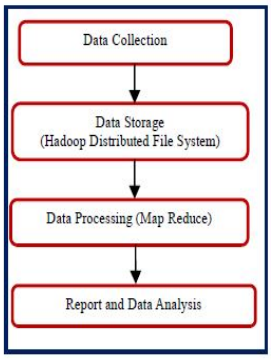

Fig. 1. Big data processing

III. Analysis and Prediction using Machine Learning Approaches

In industry, how the market is growing can be predicted using data analysis. Prediction is done using machine learning algorithms. Different factors are investigated in making prediction. There should be a prior knowledge about the class about which the prediction model is going to work. Two types of learning approaches used in healthcare are supervised and unsupervised learning. To deal with large amount of features, we apply dimensionality reduction approaches to obtain relevant features. Dimensionality reduction eliminates the unnecessary features to speed up computation and prediction for accurate decision [1]. In the following section of paper, different data mining approaches are summarized.

A. Feature Selection and Evaluation

Initially, data pre-processing is performed to reduce the noise and redundant data to speedup computation. As the dataset is divided into training and testing subsets, the training subset is used for the feature extraction and selection.In this manner, subset from given features are selected.These features are derived from pixel intensity,colors and geometric features such as contours, edges and shapes [9]. These features are further used for elimination of redundant and noisy features. This step will help for model interpretation. Different approaches can be used to obtain optimal feature subset.

- **Complete search**
  This search guarantees the best solution. It can be applied for finding optimal solution of big data problems. Heuristic approaches like branch and bound helps to minimize the searching whole feature space.

- **Sequential search**
  In this type of search, heuristic approach is applied [10]. This approach search either from whole feature set or null feature subset to obtain optimal solution by adding or removing features, respectively. Added features cannot be removed and removed features cannot be added. This approach does not guarantee for optimal solution. However, solution of this approach become acceptable due to less processing time.

- **Random Search**
  Random features are selected to start this search. Local optimal solution can be achieved using randomness. Performance of random search can be increased by integrating with sequential search for generation of random subset like simulated annealing and random start hill climbing algorithm.

Feature evaluation step involves values that are assigned to feature subset depending on specific criteria. Similarity is determined using class labels for classification. Finding irrelevant features is a challenging task in clustering. The concept behind feature evaluation claims: “Good features subsets contains features highly correlated with class, yet uncorrelated with each other” [11]. Commonly used for feature evaluation are wrapper, filter, and hybrid appraoches.

Wrapper approach has ability to provide optimal solution which can be tuned for classifier learning. Algorithm performs searching to select particular feature subset based on criterion function (Fig. 2) [12]. Computational cost increases since algorithm is run at each iteration. This technique involves high computational cost and not suitable for solving big data problems.

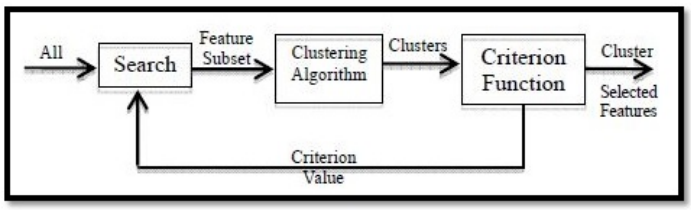

Fig. 2. Wrapper approach

Filter approach can be used to determine relevance between selected features (Fig. 3). Subset production is not used for classifier learning. Therefore, generic result is produced instead of specific algorithm tuning [12]. Its suitability becomes high for solving big data problems. This approach performs batter than other approaches like Relief attributes estimator [13].

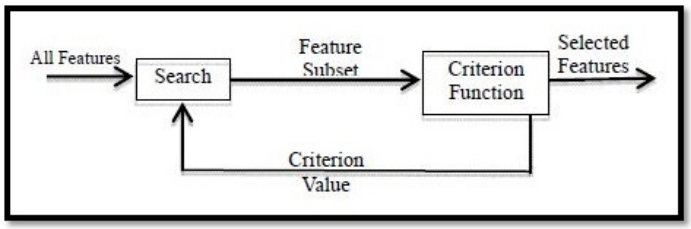

Fig. 3. Filter approach

Hybrid approach performs evaluation on features and make a feature subset by choosing the best among them in further iterations. Comparison between different types of features subsets is performed for optimal learning of algorithm [14]. Hybrid approaches have gain more importance as compared with other approaches. It involves trade-off between time and efficiency. From healthcare aspect, it is more suitable approach than other approaches. There is scope of sub-optimal solution [15].

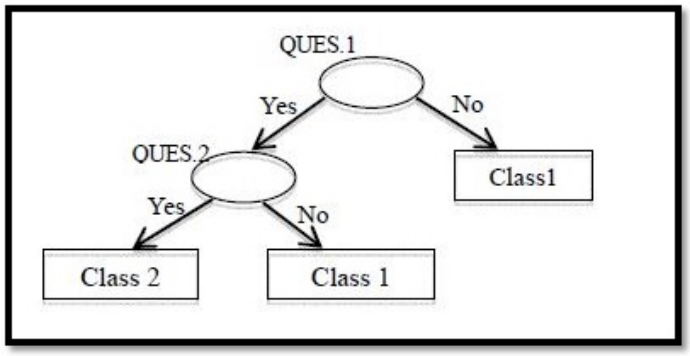

Fig. 4. Classification by decision tree

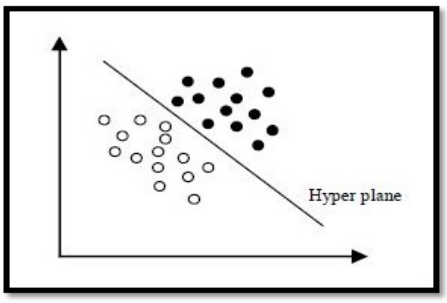

Fig. 5. Classification by support vector machine

B. Classification

Classification model classifies input data and target class is used by classifier for training and testing purpose [16]. Input is given to machine learning algorithm; target class data is also given for performing correct decision by classifier that involve features of input data based on classifier model for target class. After training of classifier, next phase is testing in which input data is given to perform prediction about target class. Due to increase in volume of big data, existing classification approaches have some limitations and involve high processing cost [1]. Commonly used classification techniques in healthcare domain are decision tree, support vector machine, neural network, k-nearest neighbour, and Bayesian approach [17].

A decision tree is a tree like structure used for classification [18]. Decision tree is applied for gaining accurate and fast results due to its simple structure. It difficult to construct decision tree with huge amount of data because a lot of time is required to construct it. Decision tree is most commonly classification approach in healthcare domain for problem solving by assigning class label to patient. Fig. 4 represents a sample decision tree.

Support Vector Machine (SVM) is a statistical model used for classification. SVM is capable for making decisions on large data set.SVM is very beneficial specially multidomain applications in big data environment. SVM is mathematically complex and computational expensive [19]. Multi-level or binomial classification can be performed using SVM [20]. SVM is most popular approach among existing machine learning techniques. The performance of SVM degrades on larger data set that consist of noisier data. This method performs prediction very fast after training [21]. Prediction is done based on hyper plane and support vector that performs separation in higher dimensional space. To overcome problem of noisy data, SVM is combined with other machine learning techniques for obtaining better results [22]. Fig. 5 shows SVM classification is represented by hyper plane for decision making.

In traditional machine learning techniques, Neural Network (NN) depicted lot of variation. In NN, weights of connecting links are adjusted between neurons until reaching optimal value. NN is most commonly used for problem solving is Multilayer Perceptron (MLP) [23]. It works similar to human brain. First, NN is trained to perform classification. After completion of training, testing is performed on input data. Major drawback of using NN is computation time for large data set. Memory requirement also increases as size of data set increases. NN is suitable for gaining optimal results but it requires more time for larger data set. There is need to adopt hybrid approach to minimize computational time by combining NN with other approaches to overcome issue of computational time for larger data set [24].

Convolutional Neural Network (CNN) is the advance form of NN. CNN is a multilayer neural network that takes input in vector form. However in case of medical images pixels or voxels are information source.In standard multi-layer neural network, Convolutional layers interlard with sub-sampling layer followed by fully connected layer is designed to batter use of spatial information by taking 2D or 3D images as input [25].

K-Nearest Neighbour (KNN) is a simple classification model that works according to nearest neighbor of existing class label [26]. In KNN, value of k is computed to find nearest neighbor where k represents number of nearest neighbours. To obtain accurate results, optimization algorithms are applied to minimize computational cost. KNN provides better results when compared with Bayesian method in various applications [26].

Bayesian method works according to Bayes theorem.Bayes theorem provide mathematically grounded tools to find out the uncertainty of a model [27]. For larger data set, Bayesian classifier can perform better in classification [28]. Naive Bayesian model provide high accuracy only when attributes values are independent [17]. It is a statistical model and provides high accuracy. This appraoch assumes all attributes are independent according to each other. This classifier can perform well in healthcare either by pre-processing or without pre-processing.

C. Clustering

Clustering groups similar data together to make clusters. Target class label is not provided initially in clustering. There exists higher similarity within same cluster. Different clusters have lower similarity between data points. Traditional approaches that are being used for similarity measures are Jaccard measure, Pearson correlation, euclidean distance and Cosine [15], [29]. There is no need for previous information about data is required to work upon clustering. It is suitable for applying on microarray data in which very little information is required about genes. Tapia et al. implemented genetic algorithm on expression data to analyze it [30]. It has capability to

represent information in compact form without losing much information by producing optimal clusters with reference to big data [31]. There exists different clustering algorithms.

Partitioned clustering involves predefined number of clusters. In this technique, data set is classified into predefined number of partitions. There is none of empty partition and data belongs to exactly one cluster. This approach can be further classified based on cluster centroid and similarity measures, i.e., K-Medoids and K-Means. In K-Medoids, medoids are used instead of centroid. Center point of a cluster is medoid that exist in data set. Belciug et al. applied clustering for detection of breast cancer to obtain better accuracy [32].

In hierarchical clustering, it is not necessary to pre-define number of clusters [31]. There are two main categories of hierarchical clustering with respect of working. Agglomerative technique is a bottom up technique in which every data point is assumed as cluster while two different clusters are merged on the basis of few similarity measures [33]. Desired cluster can be obtained after some iterations. Major drawback of this appraoch is integration cannot be rollback. Divisive technique is top-down technique in which all data points are treated as a cluster. After some iterations, cluster is further classified into two classes based on some measures [33]. Required number of clusters can be achieved by repeatedly running this algorithm. This approach also has major drawback that once cluster is divide into sub-clusters, these cannot be grouped together to make original cluster. In hierarchical clustering algorithms, iterations can be stop by gaining desired number of clusters.

IV. Fusion of Different Classifier

All existing traditional data mining techniques have not capability to perform better classification for big data in healthcare domain. Therefore, there is need to merge the distinct techniques together to perform better classification [34]. One popular approach for requiring relationship between data is Association. It is necessary to obtain relationship between diseases for finding similar treatment. Apriori algorithm is applied in association to find relationship between items and also to perform separation between similar as well as different items. PSO optimization approach is mostly combined with SVM to perform optimization first on feature set and then classifier is applied to separate data [33]. KNN is fused with fuzzy logic to decrease computation time [35]. It is better to combine different techniques in healthcare domain for obtaining better classification.

V. Related Work

Different researchers are investigating to improve performance of existing approaches by combining with other techniques. From few recent years, modification in traditional machine learning approaches has earned remarkable interest in healthcare domain. To increase classifier accuracy, different fusion techniques have been proposed. Few traditional machine learning related works in healthcare domain is discussed. Chest disease is classified using artificial neural network [36]. Chronic illness classification has been carried out [34]. For targeting high-dimensional data, conventional method of filter has been modified [37]. Distributed K-Nearest Neighbour has been applied for learning [38]. For detection of Parkinsons disease, fuzzy approaches have been fused with K-Nearest Neighbour to better classification [35]. To find irregular relationship in health data set, Association has been implemented [39]. Different big data processing platforms have been applied for classification. To reduce drawbacks of traditional approach, Map Reduce application of decision tree method has been proposed [40].

VI. Conclusion

Due to rapid enhancement in big data prediction and analysis, healthcare domain has got a valuable attention from recent few years. Existing traditional machine learning approaches take much time in computation when data set volume increase. Similarly, in healt care domain huge data is collected from different sources and researchers always try to make problem simpler to patient. In big data, we can find remarkable and hidden information that can help in understanding the nature of problem more deeply.

References

[1] S. Suthaharan, "Big data classification: Problems and challenges in network intrusion prediction with machine learning," *SIGMETRICS Perform. Eval. Rev.*, vol. 41, no. 4, pp. 70–73, 2014.

[2] B. P. RAO, "of the notes: Brief notes on big data: A cursory look," 2015.

[3] R. Hermon and P. A. Williams, "Big data in healthcare: What is it used for?" 2014.

[4] W. Raghupathi and V. Raghupathi, "Big data analytics in healthcare: promise and potential," *Health Information Science and Systems*, vol. 2, no. 1, p. 1, 2014.

[5] O. H. Fang, N. Mustapha, and M. N. Sulaiman, "Integrating biological information for feature selection in microarray data classification," in *Second International Conference on Computer Engineering and Applications (ICCEA)*, vol. 2. IEEE, 2010, pp. 330–334.

[6] P. Groves, B. Kayyali, D. Knott, and S. Van Kuiken, "The big data revolution in healthcare," *McKinsey Quarterly*, vol. 2, 2013.

[7] S. Chandra and D. Motwani, "An approach to enhance the performance of hadoop mapreduce framework for big data," in *Micro-Electronics and Telecommunication Engineering (ICMETE), 2016 International Conference on*. IEEE, 2016, pp. 178–182.

[8] K. R. Satish and N. Kavya, "Big data processing with harnessing hadoop-mapreduce for optimizing analytical workloads," in *International Conference on Contemporary Computing and Informatics (IC3I)*. IEEE, 2014, pp. 49–54.

[9] A. S. Panayides, C. S. Pattichis, and M. S. Pattichis, "The promise of big data technologies and challenges for image and video analytics in healthcare," in *Signals, Systems and Computers, 2016 50th Asilomar Conference on*. IEEE, 2016, pp. 1278–1282.

[10] M. A. Hall, "Correlation-based feature selection for machine learning," Ph.D. dissertation, The University of Waikato, 1999.

[11] H. Liu and H. Motoda, *Computational methods of feature selection*. CRC Press, 2007.

[12] Y. Saeys, I. Inza, and P. Larrañaga, "A review of feature selection techniques in bioinformatics," *bioinformatics*, vol. 23, no. 19, pp. 2507–2517, 2007.

[13] M. A. Hall, "Correlation-based feature selection of discrete and numeric class machine learning," 2000.

[14] H. Liu and L. Yu, "Toward integrating feature selection algorithms for classification and clustering," *IEEE Transactions on knowledge and data engineering*, vol. 17, no. 4, pp. 491–502, 2005.

[15] R. Dharavath and A. K. Singh, "Entity resolution-based jaccard similarity coefficient for heterogeneous distributed databases," in *Proceedings of the Second International Conference on Computer and Communication Technologies*. Springer, 2016, pp. 497–507.

[16] G. Kesavaraj and S. Sukumaran, "A study on classification techniques in data mining," in *Fourth International Conference on Computing, Communications and Networking Technologies (ICCCNT)*. IEEE, 2013, pp. 1–7.

[17] D. Tomar and S. Agarwal, "A survey on data mining approaches for healthcare," *International Journal of Bio-Science and Bio-Technology*, vol. 5, no. 5, pp. 241–266, 2013.

[18] D. Wang, X. Liu, and M. Wang, "A dt-svm strategy for stock futures prediction with big data," in *IEEE 16th International Conference on Computational Science and Engineering (CSE)*. IEEE, 2013, pp. 1005–1012.

[19] S. Suthaharan, "Support vector machine," in *Machine Learning Models and Algorithms for Big Data Classification*. Springer, 2016, pp. 207–235.

[20] B. Schölkopf, A. J. Smola, R. C. Williamson, and P. L. Bartlett, "New support vector algorithms," *Neural computation*, vol. 12, no. 5, pp. 1207–1245, 2000.

[21] G. Cavallaro, M. Riedel, M. Richerzhagen, J. A. Benediktsson, and A. Plaza, "On understanding big data impacts in remotely sensed image classification using support vector machine methods," *IEEE journal of selected topics in applied earth observations and remote sensing*, vol. 8, no. 10, pp. 4634–4646, 2015.

[22] Y. Tang and J. Zhou, "The performance of pso-svm in inflation forecasting," in *2015 12th International Conference on Service Systems and Service Management (ICSSSM)*. IEEE, 2015, pp. 1–4.

[23] B. Chandra and R. K. Sharma, "Fast learning for big data applications using parameterized multilayer perceptron," in *IEEE International Conference on Big Data*. IEEE, 2014, pp. 17–22.

[24] V. Bijalwan, V. Kumar, P. Kumari, and J. Pascual, "Knn based machine learning approach for text and document mining," *International Journal of Database Theory and Application*, vol. 7, no. 1, pp. 61–70, 2014.

[25] D. S. S. Kevin Zhou, Hayit Greenspan, *Deep Learning for Medical Image Analysis*, 1st ed. joe Hayton, 1 2017.

[26] A. Gelman, J. B. Carlin, H. S. Stern, and D. B. Rubin, *Bayesian data analysis*. Chapman & Hall/CRC Boca Raton, FL, USA, 2014, vol. 2.

[27] Y. Gal and Z. Ghahramani, "Dropout as a bayesian approximation: Representing model uncertainty in deep learning," in *international conference on machine learning*, 2016, pp. 1050–1059.

[28] G. J. Torres, R. B. Basnet, A. H. Sung, S. Mukkamala, and B. M. Ribeiro, "A similarity measure for clustering and its applications," *Int. J. Electr. Comput. Syst. Eng.*, vol. 3, no. 3, pp. 164–170, 2009.

[29] J. J. Tapia, E. Morett, and E. E. Vallejo, "A clustering genetic algorithm for genomic data mining," in *Foundations of Computational Intelligence Volume 4*. Springer, 2009, pp. 249–275.

[30] A. Fahad, N. Alshatri, Z. Tari, A. Alamri, I. Khalil, A. Y. Zomaya, S. Foufou, and A. Bouras, "A survey of clustering algorithms for big data: Taxonomy and empirical analysis," *IEEE transactions on emerging topics in computing*, vol. 2, no. 3, pp. 267–279, 2014.

[31] J. Han, J. Pei, and M. Kamber, *Data mining: concepts and techniques*. Elsevier, 2011.

[32] K. Sasirekha and P. Baby, "Agglomerative hierarchical clustering algorithm–a review," *International Journal of Scientific and Research Publications*, vol. 3, no. 3, p. 1, 2013.

[33] C. Xiang, Y. Xiao, P. Qu, and X. Qu, "Network intrusion detection based on pso-svm," *Indonesian Journal of Electrical Engineering and Computer Science*, vol. 12, no. 2, pp. 1502–1508, 2014.

[34] C.-H. Jen, C.-C. Wang, B. C. Jiang, Y.-H. Chu, and M.-S. Chen, "Application of classification techniques on development an early-warning system for chronic illnesses," *Expert Systems with Applications*, vol. 39, no. 10, pp. 8852–8858, 2012.

[35] W.-L. Zuo, Z.-Y. Wang, T. Liu, and H.-L. Chen, "Effective detection of parkinson's disease using an adaptive fuzzy k-nearest neighbor approach," *Biomedical Signal Processing and Control*, vol. 8, no. 4, pp. 364–373, 2013.

[36] O. Er, N. Yumusak, and F. Temurtas, "Chest diseases diagnosis using artificial neural networks," *Expert Systems with Applications*, vol. 37, no. 12, pp. 7648–7655, 2010.

[37] L. Yu and H. Liu, "Feature selection for high-dimensional data: A fast correlation-based filter solution," in *ICML*, vol. 3, 2003, pp. 856–863.

[38] R. Mall, V. Jumutc, R. Langone, and J. A. Suykens, "Representative subsets for big data learning using k-nn graphs," in *IEEE International Conference on Big Data*. IEEE, 2014, pp. 37–42.

[39] Y. Ji, H. Ying, J. Tran, P. Dews, A. Mansour, and R. M. Massanari, "Mining infrequent causal associations in electronic health databases," in *IEEE 11th International Conference on Data Mining Workshops*. IEEE, 2011, pp. 421–428.

[40] W. Dai and W. Ji, "A mapreduce implementation of c4. 5 decision tree algorithm," *International Journal of Database Theory and Application*, vol. 7, no. 1, pp. 49–60, 2014.

An Image Encryption Technique based on Chaotic S-Box and Arnold Transform

Shabieh Farwa*, Tariq Shah†, Nazeer Muhammad*, Nargis Bibi‡, Adnan Jahangir*, and Sidra Arshad†
*Department of Mathematics, COMSATS Institute of Information Technology, 47040, Wah Cantt, Pakistan
†Department of Mathematics,Quaid-i-Azam University, Islamabad, Pakistan
‡Department of Computer Science, Fatima Jinnah Women University, Rawalpindi, Pakistan

***Abstract*—In recent years, chaos has been extensively used in cryptographic systems. In this regard, one dimensional chaotic maps gained increased attention because of their intrinsic simplicity and ease in application. Many image encryption algorithms that are based on chaotic substitution boxes (S-boxes) have been studied in the last few years but some of them appear to be vulnerable to robustness. We, in this paper, propose an efficient scheme for image encryption that utilizes a composition of chaotic substitution based on tent map with the scrambling effect of the Arnold transform. The proposed construction algorithm for substitution box is, on one hand, straightforward and saves computational labour, while on the other, it provides highly efficient performance outcomes. The understudy scheme uses an S-box, that is based on 1-D chaotic tent map. We partially encrypt the image using this S-box and then apply certain number of iterations of the Arnold transform to attain the fully encrypted image. For decryption we apply the reverse process. The strength of the proposed method is determined through the most significant techniques used for the statistical analysis and it is proved that the anticipated algorithm shows coherent results.**

***Keywords*—Chaos; image encryption; tent map; S-box; Arnold transform; statistical analyses**

I. Introduction

Transmitting large amount of confidential information over the communication media has raised the security challenges. The growing demand for comparatively safer and more reliable crypto-systems has created new research problems in the field of cryptography and has engaged scientists from relevant backgrounds to design improved encryption algorithms. In recent years, it has been developed that the chaotic systems exhibit the most legitimate features to fit for cryptographic applications therefore chaos based algorithms have been widely used in digital multimedia applications including image ciphering, data hiding, watermarking and steganography [1]-[12].

Edward Lorenz in 1960's introduced the study of chaotic dynamics [13], [14]. The development of chaotic theory proved that the chaos based systems have capability to produce high level of confusion and diffusion in substitution-permutation networks. The basic characteristics of the chaotic maps such as ergodicity, broadband spectrum and high sensitivity to the initial conditions attracted the attention of researchers to incorporate them in high-security encryption algorithms used in modern communication. In the last few years many chaotic-encryption algorithms have been studied [15]-[18].

Substitution box, the most indispensable component in block ciphers, is widely used in image encryption applications [19]-[24]. However, many recent researchers ignore the encryption option in communication process of image and signal processing [25]-[31]. Recently Zhang, *et al*. [32] studied an S-box-only image cipher based on chaotic map and proposed that the S-box-only image encryption algorithms are vulnerable against cryptographic robustness. Keeping this in view, we in this paper, propose an image encryption scheme that is not just based on the chaotic S-box but further utilizes a composition of the chaotic substitution with the Arnold transform's scrambling effect. The scheme is as follows, we apply the chaotic tent map to synthesize an S-box. Firstly the plain image is encrypted using the chaotic S-box, then the Arnold transform is applied on this encrypted image in order to attain high level of perplexity and randomness. For decryption purposes we first apply the inverse Arnold transform and then the inverse S-box. The proposed method is tested and we prove that it can be used to produce required security level in the internet applications for safe handling of the confidential information.

The material presented in this paper is organized as: In Section 2 we explain in detail the major properties of the tent map and its use in the construction of a substitution box. In Section 3 the concepts regarding the Arnold transform are presented. Section 4 presents the detailed algorithm used for the image encryption. In Section 5 we test the strength of the proposed scheme using statistical analyses and lastly Section 6 presents the conclusion.

II. Chaos-based S-Box

The intent of this section is to present the main algorithm used to design the chaotic S-box. We use the tent map to construct the substitution box. In the following subsections we discuss in detail, the properties of the underlying map and the detailed algorithm used to form the chaotic S-box.

A. Chaotic tent map

Tent map is a 1-D chaotic map $\phi : [0,1] \to [0,1]$ defined by:

$$\phi(x_n) : \begin{cases} \mu x_{n-1} & ; \ 0 \leq x < \frac{1}{2} \\ \mu(1 - x_{n-1}) & ; \ \frac{1}{2} \leq x \leq 1, \end{cases}$$

Where, $\mu \in \mathbb{R}^+$ and ϕ has chaotic behaviour when $\mu = 2$. For the desired purpose regarding construction of S-box, we assume $\mu = 2$. One can observe through Fig. 1 that the graph of the bifurcation diagram of tent map is in tent shape, representing chaotic behaviour.

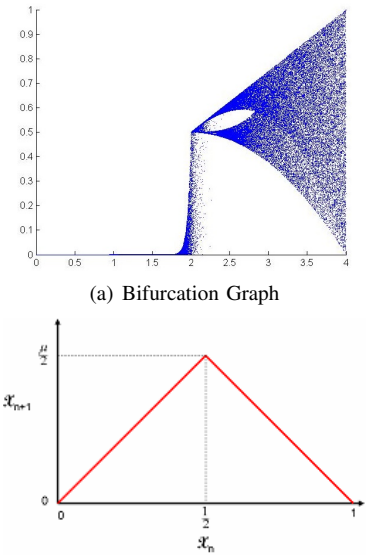

(a) Bifurcation Graph

(b) Tent-shape Diagram

Fig. 1. Bifurcation graph of Tent map.

B. Algorithm for S-box

The formation of the S-box is then subsequent to the following steps:

- Partition the output interval $I = [0, 1]$ into 256 subintervals $I_m = [m\Delta, (m + 1)\Delta)$; $0 \leq m \leq 255$, where $\Delta = \frac{1-0}{256}$.
- Set the initial condition. Her we choose $x_0 = 1$.
- Apply ϕ for 256 times and assign the output interval number by using ψ, i.e. if $\phi(x_n) \in I_m$ then $\psi(n) = m$.
- If a region is repeated then definitely some region is missed also. Remove this error by assigning the leftover regions (in ascending order) to keep $\psi : GF(2^n) \rightarrow GF(2^n)$ bijective.
- The images of ψ produce the required S-box (see Table I).
  The performance parameters of the newly developed S-box are shown in the Table II, which clearly show that our proposed S-box exhibits extra-ordinary properties. It is worth-mentioning at this stage, that if we compare our algorithm with some of well-prevailing chaotic S-boxes as presented in [33]-[35], it is crystal clear that the performance indices such as nonlinearity, strict avalanche, bit independence, linear and differential approximation probabailities of our S-box are much better than the models discussed in [33]-[35]. However our scheme is very simple and direct as compared to the aforementioned methods.

III. Arnold Transform

Arnold transform is used for encryption of digital images to increase the spread of pixel intensities [36]. For any square image of size $M \times M$, encryption of the Arnold transform can be given as:

$$\begin{bmatrix} \acute{a} \\ \acute{b} \end{bmatrix} = \begin{bmatrix} \vartheta & \vartheta \\ \vartheta & \tau \end{bmatrix} \begin{bmatrix} a \\ b \end{bmatrix} (mod\, M), \tag{1}$$

Where, (a, b) and $(\acute{a}, \acute{b})$ represent the pixel coordinates of the input image and encrypted data respectively, such that $(\vartheta, \tau) = (1, 2)$. Fig. 2 shows the effect of 10 iterations of the Arnold Transform's application on the test image "House".

The Arnold transform encryption is worked on periodic boundary treatment. The image encryption using k number of iterations of Arnold transform may be written as:

$$I(\acute{a}, \acute{b})^k = I\Lambda(a, b)^{k-1} (mod\, M), \tag{2}$$

Where, Λ is the Arnold transform matrix given in (1) and I is an $M \times M$ encrypted image data for k number of iterations: $k = 1, 2, ..., n$, such that $I(\acute{a}, \acute{b})^0 = I(a, b)$. Periodicity of encryption is dependent on the size of a given image. The encrypted image data can be reversed on application of the inverse Arnold transform to I with same number of iterations k as follows:

$$I(a, b)^k = I\Lambda^{-1}(\acute{a}, \acute{b})^{k-1} (mod\, M). \tag{3}$$

IV. Image Encryption Scheme

In this section we present the scheme used for the image encryption. It comprises of the following two steps:

- Use chaotic substitution box to partially encrypt the plain image.
- Apply 10 iterations of the Arnold transform on this partially encrypted image to obtain the fully encrypted image.

We selected three benchmark images, house (256×256), cameraman (256×256) and Lena (512×512). By following the above stated scheme the images are encrypted. We obtain the decrypted images by applying the inverse Arnold transform and inverse S-box, respectively. Fig. 3 to 5 show the results obtained from encryption and decryption of images.

V. Statistical Analysis of the Proposed Method

In this section we evaluate the forte of our method by some useful analysis such as contrast Table III, correlation Table IV, homogeneity Table V, number of pixels change rate (NPCR) and unified average change intensity (UACI) Table VI. We discuss these security parameters one by one and present the numerical results also.

A. Contrast

Contrast is a measure used to identify objects in an image. A strong encryption technique produces high level of contrast. Table III shows that our encryption scheme is quite efficient to attain acceptably high level of contrast.

TABLE I. CHAOTIC S-BOX

79	159	193	124	249	12	24	49	99	199	112	224	62	125	251	9
18	36	72	144	222	67	134	243	25	51	103	206	98	196	119	238
34	68	136	239	32	65	130	248	8	16	33	89	137	242	26	52
104	209	93	187	148	230	50	66	132	247	22	60	95	150	236	19
38	77	155	100	200	55	110	221	69	138	235	40	80	160	191	128
255	1	2	5	11	23	46	115	197	152	223	39	78	157	203	139
232	54	90	135	241	27	56	113	226	58	117	234	42	84	169	172
166	179	153	205	101	202	107	214	82	165	180	151	212	92	185	141
229	75	105	211	88	176	181	192	127	250	0	3	10	4	17	29
57	91	145	240	31	63	126	252	6	13	45	53	121	216	83	167
190	158	195	120	233	30	61	122	244	44	47	94	189	133	245	20
41	111	164	182	147	217	76	178	210	116	207	123	218	97	177	220
71	109	161	188	146	237	28	86	131	219	59	118	227	70	108	156
204	129	225	87	142	246	43	73	81	163	194	140	231	48	96	201
143	253	254	7	14	15	21	35	37	74	149	213	85	170	184	186
171	168	174	162	198	173	228	64	102	154	208	106	215	114	183	175

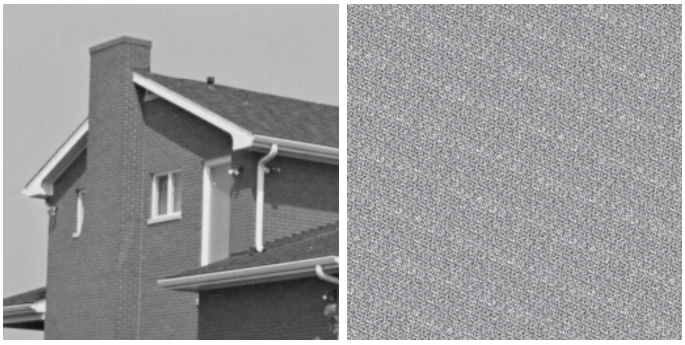

(a) Plain image (b) Encrypted image

Fig. 2. 10 iterations of Arnold transform's application on the test image (House)

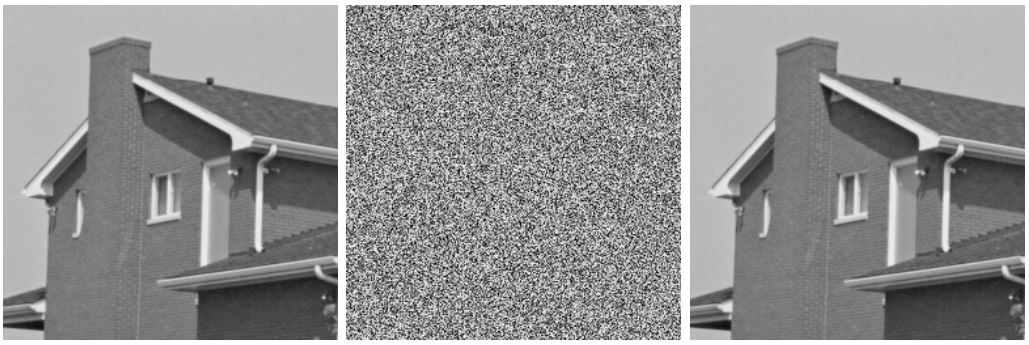

(a) Plain image (b) Encrypted (c) Decrypted

Fig. 3. House: Plain, encrypted and decrypted images

TABLE II. PERFORMANCE INDICES FOR S-BOX

Analysis	**Max**.	**Min**.	**Average**	**Square deviation**		
Nonlinearity	106	102	**104.5**			
SAC	0.609375	0.421875	**0.514648**	0.0191304		
LP	162					**0.132813**
DP					**0.046875**	
BIC		94	**103.214**	3.17757		

TABLE III. CONTRAST ANALYSIS

	Contrast	
Test images	Plain	Encrypted
House (256 × 256)	0.1826	8.0021
Cameraman (256 × 256)	0.5871	11.2393
Lena (512 × 512)	0.2287	10.8693

B. Correaltion

In order to examine the encryption effect of the proposed method we perform correlation analysis on both the plain and the encrypted images. It is quite clear that for an efficient encryption, the correlation of the encrypted image should be reduced as compared to the plain image. The correlation coefficient is given by,

$$r_{xy} = \frac{E((x-\mu_x)(y-\mu_y))}{\sqrt{\delta_x \delta_y}},$$

Where, μ and δ represent the expected value and variance. The value of correlation coefficient close to zero guarantees better

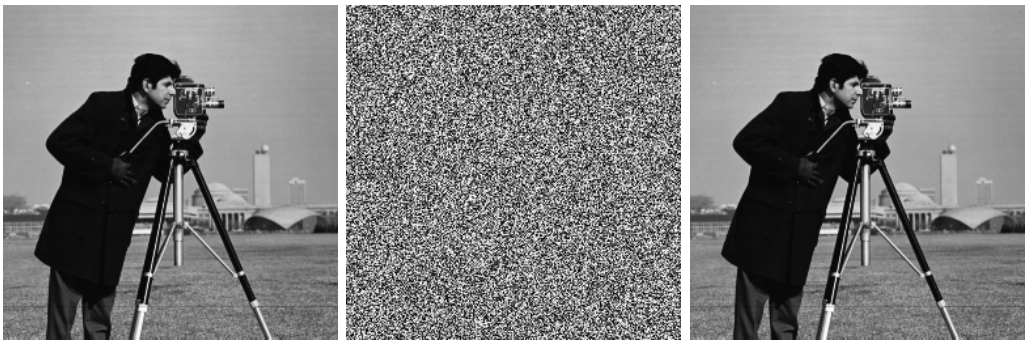

(a) Plain image (b) Encrypted (c) Decrypted

Fig. 4. Cameraman: Plain, encrypted and decrypted images

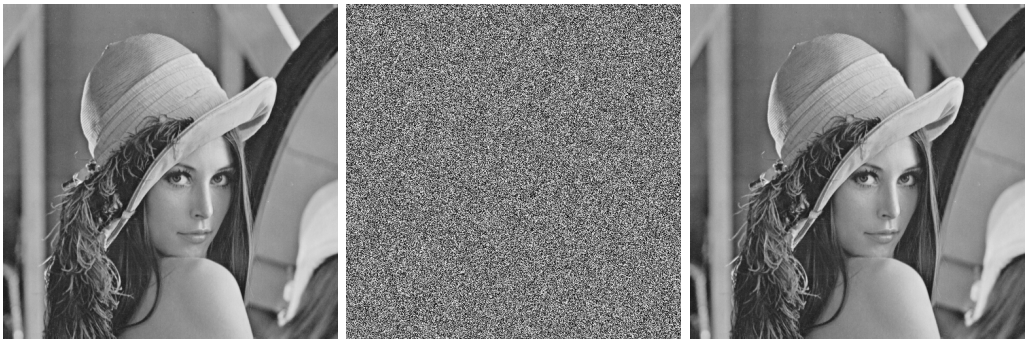

(a) Plain image (b) Encrypted (c) Decrypted

Fig. 5. Lena: Plain, encrypted and decrypted images

encryption quality. The analysis is performed on three images, house (256×256), cameraman (256×256) and Lena (512×512). Results arranged in Table IV witness the effectiveness of the proposed method.

TABLE IV. CORRELATION ANALYSIS

	Correlation Coefficient	
Test images	Plain	Encrypted
House (256×256)	0.9497	-0.0166
Cameraman (256×256)	0.9227	0.0034
Lena (512×512)	0.9505	-0.0033

C. Homogeneity

Gray level co-occurrence matrix (GLCM) depicts the ability of combinations of pixel brightness results in tabular form. The closeness of the distribution in the (GLCM) to its diagonal is measured through the homogeneity analysis. The smaller is the homogeneity measure, the better is encryption. The numerical results shown in the following table witness the effectiveness of the proposed method.

TABLE V. HOMOGENEITY ANALYSIS

	Homogeneity	
Test images	Plain	Encrypted
House (256×256)	0.9250	0.4210
Cameraman (256×256)	0.8952	0.3849
Lena (512×512)	0.9050	0.3876

D. Differential analysis

A desirable feature of a cryptosystem is to show high sensitivity to single-bit change in the plain image. For this purpose two measures, NPCR and UACI, are commonly used. NPCR stands for the number of pixels change rate of encrypted image as a result of one pixel change in the plain image. NPCR can be defined as the variance rate of pixels in the encrypted image that occurs through the change of a single pixel in original image. However UACI means unified average intensity of differences between the plain and encrypted images. The percentage values for both these measures are given by the following formulae.

$$NPCR = \frac{\sum_{i,j} D_{ij}}{W \times H} \times 100, \tag{4}$$

$$UACI = \frac{1}{W \times H}\left[\frac{\sum_{i,j} C_{ij} - \acute{C}_{ij}}{255}\right] \times 100. \tag{5}$$

In above C and $\acute{C}$ represent the encrypted images obtained as a result of single bit change in the original image. In (4) and (5), W and H represent the width and the height of the images C and $\acute{C}$.

An efficient encryption scheme is one that produces higher values of both NPCR and UACI. The results obtained in our case are shown in Table VI.

TABLE VI. DIFFERENTIAL ANALYSIS

Test images	NPCR%	UACI%
House (256 × 256)	0.9958	0.3347
Cameraman (256 × 256)	0.9960	0.3346
Lena (512 × 512)	0.9959	0.3345

VI. CONCLUSION

In this work, an image encryption scheme is proposed that is extremely simple and highly effective. It has been established in some recent research work that the S-box only encryption techniques are not secured enough to resist cryptographic robustness therefore we introduced the combination of the chaotic S-box with certain iterations of the Arnold transform. The strength of the proposed method is then analyzed through several techniques that proves high effectiveness of our scheme as shown in listed tables.

REFERENCES

[1] Ghebleh, M., Kanso, A.: A robust chaotic algorithm for digital image steganography. Commun. Nonlinear Sci. Numer. Simul. 19(6), 1898-1907 (2014)

[2] Zhou, Y., Bao, L., Chen, C.L.P.: A new $1-D$ chaotic system for image encryption. Signal Processing 97, 172-184 (2014)

[3] Aziz, M., Tayarani-N, M.H., Afsar, M.: A cycling chaos-based cryptic-free algorithm for image steganography. Nonlinear Dyn. 80(3), 1271-1290 (2015)

[4] Cavusoglu, U., Kacar, S., Pehlivan, I., Zengin, A.: Secure image encryption algorithm using a novel chaos based S-box, Chaos, Solitions and Fractals, 95, 92-101 (2017)

[5] Muhammad, N., Bibi, N., Qasim, I., Jahangir, A., Mahmood, Z. Digital watermarking using Hall property image decomposition method. Pattern Analysis and Applications, 1–16, (2017)

[6] Muhammad, N., Bibi, N., Zahid M, Dai-Gyoung K. Blind data hiding technique using the Fresnelet transform. SpringerPlus, 4(1), 1–15, (2015)

[7] Muhammad, N., Bibi, N., Digital image watermarking using partial pivoting lower and upper triangular decomposition into the wavelet domain. IET Image Processing, 9(9), 795–803, (2015)

[8] Muhammad, N., and D. G. Kim, A novel Fresnlet based robust data hiding algorithm for medical images, 2012 IEEE International Conference on Imaging Systems and Techniques Proceedings, Manchester, 213-216, (2012)

[9] Muhammad, N., and Dai-Gyoung Kim. An Efficient Data Hiding Technique in Frequency domain by using Fresnelet Basis. Proceedings of the World Congress on Engineering. Imperial College London, UK.Vol. 2. (2012)

[10] Muhammad, N., Bibi, N., Zahid, M., Tallha, A., Syed, R-N., Reversible Integer Wavelet Transform for Blind Image Hiding Method 10.1371/journal.pone.0176979, (2017)

[11] Muhammad, N., Bibi, N., Zahid, M., Tallha, A., Syed, R-N.: Reversible Integer Wavelet Transform for Blind Image Hiding Method, PLOS ONE, (2017)

[12] Jamal, S.S., Shah, T., Hussain, I.: An efficient scheme for digital watermarking using chaotic map, Nonlinear Dyn. 73(3), 14691474 (2013)

[13] Edward, N. L. Deterministic Nonperiodic Flow, Journal of the Atmospheric Sciences, 20(2), 130141, (1963)

[14] Edward, N. L. Atmospheric predictability as revealed by naturally occurring analogues, Journal of the Atmospheric Sciences, 26(4), 636646, (1969)

[15] Zhu, Z., Leung, H. Optimal synchronization of chaotic systems in noise, IEEE Trans. Circ. Syst.-I: Fund. Th. Appl. 46, 1320-1329

[16] Chen, G. R., Mao, Y. B., Chui, C.K. A symmetric image encryption scheme based on 3D chaotic cat maps, Chaos Solitons Fract. 21(3), 749761, (2004)

[17] Wong, K.W., Kwok, B., Law, W. A fast image encryption scheme based on chaotic standard map, Phys. Lett. A 372(15), 26452652, (2008)

[18] Khan, M., Shah, T. An efficient chaotic image encryption scheme, Neural Computing and applications, 26(5), 1137-1148, (2015)

[19] Wang, D., Zhang, Y. B. Image encryption algorithm based on S-boxes substitution and chaos random sequence, International Conference on Computer Modeling and Simulation, Guangzhou, China 110113, (2009)

[20] Venkatachalam, S. P., Vignesh, R., Sathishkumar, G. A. An improved S-box based algorithm for efficient image encryption, International Conference on Electronics and Information Engineering, India 1, 428431, (2010)

[21] Xu, Z. H., Shen, G., Lin, S. Image encryption algorithm based on chaos and S-boxes scrambling, Adv. Mater. Res. 171172, 299304, (2011)

[22] Wang, Y., Lie, P., Wong, K. W. A Method for Constructing Bijective S-Box with High Nonlinearity Based on Chaos and Optimization, Int J. Bifurcation Chaos 25, 1550127, (2015)

[23] Xiao, D., Fu, Q., Xiang, T., Zhang, Y. Chaotic Image Encryption of Regions of Interest, Int J. Bifurcation Chaos 26, 11, (2016)

[24] Farwa, S., Shah, T., Idrees. L. A highly nonlinear S-box based on a fractional linear transformation, SpringerPlus. 5: 1658, (2016)

[25] Muhammad N, Bibi N, Jahangir A, Mahmood Z. Image denoising with norm weighted fusion estimators. Pattern Analysis and Applications. 2017:1-10.

[26] Mahmood Z, Muhammad N, Bibi N, Ali T. A Review on state-of-the-art Face Recognition Approaches. Fractals. 2017;25(02):1750025.

[27] Bushra M, Muhammad N, Muhammad S, Tanzila S, Amjad R. Extraction of breast border and removal of pectoral muscle in wavelet domain. Biomedical Research-ind 2017;28(10): 1-3.

[28] N. Muhammad, et al. Image de-noising with subband replacement and fusion process using bayes estimators, Computers and Electrical Engineering, 2017, http://dx.doi.org/10.1016/j.compeleceng.2017.05.023.

[29] Mughal, B., Sharif, M., Muhammad, N,. Bi-model processing for early detection of breast tumor in CAD system, The European Physical Journal Plus, 6(132), (2017), 10.1140/epjp/i2017-11523-8.

[30] Nargis, B., Nazeer M., Kleerekoper. A, and Cheetham, B. Equation Method for correcting clipping errors in OFDM signal, SpringerPlus, splus-016-0294. ,

[31] Nargis, B., Nazeer M., Kleerekoper. A, and Cheetham, B. Inverted Wrap-Around Limiting with Bussgang Noise Cancellation Receiver for OFDM Signals, Circuits, Systems, and Signal Processing, (2017), 10.1007/s00034-017-0585-7.

[32] Zhang, Y., Xiao, D. Cryptanalysis of S-box-only chaotic image ciphers against chosen plaintext attack, Nonlinear Dyn. 72(4): 751-756, (2013)

[33] zkayanak, F., zer, A. B.: A method for designin g stron S-boxes based on chaotic Lorenz system. Phys. Letters A, 374(36), 3733-3738 (2010)

[34] Khan, M., Shah, T., Mahmood, h., Gondal, M. A.: An efficient method for the construction of block cipher with multi-chaotic systems. Nonline ar Dynamics, 71(3), 489-492 (2013)

[35] Gondal, M. A., Raheem, A., Hussain, I.: A scheme for obtaining secure S-boxes based on chaotic Bakers map. 3D Res., 5-17 (2014).

[36] Muhammad, N., Bibi, N. Kim, D. G.: A Fresnelet-Based Encryption of Medical Images using Arnold Transform, International Journal of Advanced Computer Science and Applications. A 1(1), 131140, (2013)

Fault-Tolerant Model Predictive Control for a $Z(T_N)$-Observable Linear Switching Systems

Abir SMATI, Wassila CHAGRA and Moufida KSSOURI
University of Tunis El-Manar, Science Faculty of Tunis
Laboratory of Analysis and Control Systems, 1060 Tunis, Tunisia

***Abstract*—This work considers the control and the state observation of a linear switched systems with actuators faults. A particular problem is studied: the occurrence of non-observable subsystem in the switching sequence. Hence, the accuracy of the state estimations will decrease affecting the observer-based fault detection algorithms. In this paper, we propose a solution based on a constrained switching control in a predictive scheme. An extension to fault-tolerant control is derived, using several hybrid observers for estimation and fault detection and a reconfigurable finite control set model-predictive controller. The paper includes experimental results applied to a multicellular converter to demonstrate the efficiency of the method.**

Keywords*—Switching systems; $Z(T_N)$-Observability; finite control set predictive control; fault tolerant control; multicellular converter

I. Introduction

Hybrid dynamic systems (HDS) represent a particular type of supersystems that contain both continuous and discrete subsystems. A linear switching system (LSS) is a class of HDS in which the interaction between its linear subsystems follows a discrete switching law [1]. The first proposed classical approaches are based on pulse width modulation (PWM) as an open loop control. Its drawback is the presence of several oscillations around the set points. Others approaches can be found in the litterature with additional purposes like in [2], the author proposes a binary Lyapunov-based control with a commutation limiting constraint to extend switching components durability. Also, finite control set predictive control (FCS-PC) are presented in [3].

Continuous and descrete state estimation need the LSS observability, which led the researchers to find solutions to different problems caused by its switching behavior. Some of those problems suppose that the continuous and discrete states are unknoun and were treated using a sliding mode observer [4]. The other problems consider only the estimation of discrete states where some of the proposed solutions use either a sliding mode input reconstruction [5] or Petri networks [6]. These approaches use output measurements and the estimated continuous state to determine the operating discrete state of the LSS. In a different context, Luenberger-based observer structures for HDS are researched in [7]. All these works assume that all LSS subsystems are observable. In the general case, this is not always true. Some LSS contain unobservable subsystems. Consequently, an extension of the observability property for HDS called $Z(T_N)$-observability is investigated in [8] to allow observer design with partial observability of the targeted LSS.

A particular domain of interest in the HDS control research topic is the fault tolerant control (FTC). Faults are symptoms of noncritical abnormal behaviors of the system. However, if a fault persists it may lead to a failure (critical anomaly) that may destroy the system. The dynamic of HDS may involve high commutation frequencies, reducing switching component lifespan and causing occasional malfunctions. The switch is stuck open or stuck closed, reducing the ability to control the HDS. Solutions are needed to minimize faults impact, to prevent failures and to ensure acceptable performance level of the faulty HDS.

Two major approaches investigate FTC for HDS, passive and active. Passive schemes are based on robust control schemes with limited need to observers, but active schemes involve some kind of fault detection isolation and estimation (FDIE) algorithm to ensure appropriate fault compensation by the FTC module. The isolation and estimation parts require the observability of the HDS. Partial observability or unobservability of some HDS subsystem will hinder the ability of FTC design using classical controller design approaches. In some cases, only fault detection (FD) or fault isolation (FDI) are possible. $Z(T_N)$-observability comes handy in this case, allowing performant active FTC designs if favourable control sequences are ensured.

Getting back to the FDIE step, a popular solution is to design a bank of residual generators. Residual generators are particular observers designed to react only to a specified subset of faults and ignoring the remaining ones. Fault detection is ensured if the residual signals react and converge to a pattern called fault signature, and fault isolation is possible if multiple distinct patterns exist, with a one-to-one ratio with the faults to detect. Fault estimation is achieved if some laws exist linking residual amplitudes with fault severity. Observer based FDIE are model-based, requiring knowledge of the targeted system. One should note that some authors address the FDIE problem in a more general fault detection and diagnosis (FDD) context. Rigorously speaking, diagnosis is performed after system failures and involve artificial intelligence approaches to reconstruct failure causes, while FDIE and FTC are running in real-time and should (hopefully) avoid failures with appropriate actions.

The HDS FTC is complex, since different model types are involved. HDS FTC designs are usually hybrid also. In [9], an observation technique with a higher order sliding mode is used to estimate the residual vector. Additionally, the system is modeled as a discrete automaton and a diagnoser (event-based fault reconstructor [10]) is designed to detect continuous faults.

It can be said, considering the previous works on the

topic that an observability ensuring constraint of the switching sequence can lead to a guaranteed performance of the FTC for HDS. Finite control set predictive control (FCS-PC) is a suitable framework to deal with multiple constraints on the control and will be the basis of the proposed contribution.

In this paper, a predictive active FTC scheme for LSS is used to limit the impact of faults and to maintain an acceptable accuracy of the supporting FDI module. Several predictive control algorithms associated with each expected fault are designed. The suitable controller is selected upon the evaluation of the residual vector obtained from the residual generators bank designed according to [11]. The strategy adopted in this article is multilayered and covers several areas: FDI, observation and control of LSS. The main motivation is to propose an FTC solution for partially observable LSS. In the predictive scheme, a constraint is maintained in the algorithm to ensure $Z(T_N)$-observability and to increase the FDIE convergence rate.

The rest of the paper is organized as: Section 2 presents the proposed FTC strategy. Section 3 presents the Finite control set predictive control algorithm. Section 4 discusses the observability aspect and contains a background for $Z(T_N)$-observability. Section 5 presents FDI procedure. Section 6 includes the experimental results and validates the proposed strategy. Finally, conclusions are given in Section 7.

II. Fault Tolerant Control Scheme

Consider a linear continuous switched system described by:

$$\begin{cases} \dot{x}(t) = A(u(t))x(t) + B(u(t)) \\ y(t) = Cx(t) \end{cases} \quad (1)$$

Where, $x(t) = [x_1(t), x_2(t), ..., x_n(t)]$ the state vector, $y(t) \in \mathbf{R}^l$ is the measured output vector, $u(t) = [u_1(t), u_2(t), ..., u_m(t)]$ with $u_i = \{0, 1\}$ is a discrete input. C is 1 $\times$ n matrix and $A(u), B(u)$ are respectively n$\times$ n, n$\times$ 1 matrices that change for every new set of the vector $u(t)$.

From (1) and (2) it is possible to deduce another state representation of the switched system described by the following subsystem:

$$\begin{cases} \dot{x}(t) = A_s x(t) + B_s \\ y(t) = Cx(t) \end{cases} \quad (2)$$

Where, $s = \{0, 1, ..., N-1 = 2^m - 1\}$ is a discrete state or a configuration mode corresponding to a set of $u(t)$ and A_s, B_s are respectively n$\times$ n, n$\times$ 1 constant matrices.

In general, the failures that may happen when dealing with the switched systems are of two types. Failures with effects on the continuous states of the system and failures that affect the hybrid behavior or the discrete states which are treated in this work.

When a fault occurs on a discrete input, a change may appear in the transition to a configuration mode that should not be used by the system under normal circumstances. Also, some of the subsystems may be unobservable and the fault may alter the switching sequences that make the continuous states observable and consequently, the state estimation becomes inaccurate.

In this paper, we focus on failures affecting the discrete states of a switching system. The procedure followed here is to detect the failure in a first step, then to use an input sequence enabling its isolation in a second step and finally to reconfigure the controller to take into account the changes in the system behavior. The isolation sequence is needed because the failure may affect the controller that may choose some sequences making the system non observable. Therefore, after fault detection, a different control sequence must be used to satisfy the $Z(T_N)$-observability until the fault is isolated.

The fault tolerant control strategy adopted here is based on two major blocs as presented in Fig. 1 the controller bloc and the fault detection bloc.

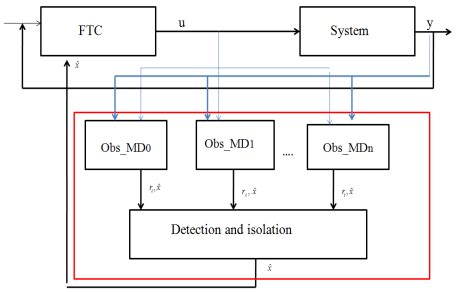

Fig. 1. Fault tolerant control scheme.

The controller bloc is based on several predictive algorithms where each one is related to a predetermined fault model of the process. Whereas, the fault detection bloc is constituted of several hybrid observers Obs_MD_i where $i = 0, 1, ..., m$ is the i^{th} actuator fault, with a detection and isolation bloc. Each observer is associated with a faulty model of the process (Obs_MD_0 is associated to the healthy system), and generates two outputs: the estimated state vector $\hat{x}$ and a residual estimate r_i. The fault detection and isolation procedure is used to detect and identify the fault based on the estimated residual given by all the observers and delivers to the controller bloc the estimated states and the fault if any. The latter reconfigures the control algorithm after receiving the information about the nature of the fault, otherwise the bloc uses the healthy system control algorithm. In order to obtain good results with the proposed FTC scheme, the process must present some redundancies that enable the controller to find solutions to compensate the fault. Further informations about each bloc of the FTC strategy are given in the following sections.

III. Finite Control Set Predictive Control for Switched Systems

Generally, the predictive control algorithm is based on a discrete model. In the case of hybrid systems it is possible to use several discrete models where each one corresponds to a different configuration mode of the system. Suppose that the system states are accessible, the discrete sub-models can be obtained from the next approximation for one step horizon:

$$\dot{x}(t) \simeq \frac{\hat{X}(k+1, s^{k+1}) - X(k)}{T_e} \quad (3)$$

Where, $\hat{X}(k+1, s^{k+1})$ denotes the predicted state over an horizon $H_p = 1$ for a future active mode s^{k+1} and T_e is the sampling time.

After replacing the subsystem (2) into (3) and having $x(t) = X(k)$ when $t = kT_e$, one can obtain the following approximated discrete subsystems:

$$\hat{X}(k+1, s^{k+1}) \simeq (I + T_e A_{s^{k+1}})X(k) + T_e B_{s^{k+1}} \quad (4)$$

Where, $I \in \mathbb{R}^{n \times n}$ is the identity matrix. Note that for N subsystems, one has N future possibilities. When $H_p = 2$, there will be others N future possibilities for every mode in the previous horizon ($H_p = 1$). So, in total there will be N^2 future possibilities to be selected by the controller leading to N^2 discrete models to be computed. If one expand even more the prediction horizon, it will lead to N^{H_p} discrete models to be computed. That will increase the complexity of the algorithm without having a major improvement [3]. In the following, H_p will be equal to 1 to avoid complexity in the control algorithm.

If the LSS system is controllable, then a cost function for every subsystem is needed to ensure a minimal difference between the outputs and its references. Its expression has the following form:

$$F_{s^{k+1}} = (\hat{X}(k+1, s^{k+1}) - X_{ref})\, Q\, (\hat{X}(k+1, s^{k+1}) - X_{ref})^T \quad (5)$$

Where, X_{ref} is a vector containing the reference output and $Q \in \mathbb{R}^{n \times n}$ is a weighting matrix. The results are N cost functions for every future mode $s = 0, 1, ..., N-1$. The configuration associated to the minimal cost function will be selected by the controller and will be applied on the process each sample time following the next steps:

- Get $X(k)$
- Compute $F_{s^{k+1}}$ for all $s = 0 \dots N$
- Apply $s_{opt} = argmin[F_{s^{k+1}} : s = 0 \dots N]$ to the process.

Stability analysis and proof can be found in [12] and experimental control results with measured continuous state are presented in [13] to attest the efficacy of the predictive algorithm. As reported previously, this paper considers the case where the continuous states are estimated and the LSS is subject to actuator fault. Therefore, feedback control with measured states is not the objective here.

IV. Observer Design for Hybrid Systems

Matrices $A(u)$ and $B(u)$ in (1) can be expressed as follows:

$$A = \overline{A}_0 + \overline{A}_1 u_1 + \ldots + \overline{A}_j u_j \quad (6)$$

$$B = \overline{B}_1 u_1 + \ldots + \overline{B}_j u_j \quad (7)$$

Where, $\overline{A}_{j=1,\ldots,m}$ are n$\times$ n constant matrices and $\overline{B}_{j=1,\ldots,m}$ are n$\times$ 1 constant matrices.

Then, the switched system (1) can be rewritten as follows [14]:

$$\dot{x}(t) = \overline{A}_0 x(t) + \sum_{j=1}^{m} u_j(t)(\overline{A}_j x(t) + \overline{B}_j) \quad (8)$$

Let consider that for some values of the vector $u(t)$, the state vector is not fully observable, meaning that some of its elements are not observable. Moreover, some elements are observable for another combination of $u(t)$.

The system is then said to be $Z(T_N)$-observable, and verifies the following conditions [15]:

(1) Each element of the state vector is observable within at least one time interval.

(2) The components of the state vector that are not observable in a time interval where another one is observable must remain constant during that time.

(3) A time trajectory T_N including time intervals verifying conditions **1** and **2** is used in a way that all the components of the state vector are observable within it.

Remark 4.1: In the case of system (8) the first condition is met if each element of the vector state $x(t)$ is observable for at least one value of $u(t)$. Then the second condition is verified if for the same input $u(t)$ the elements that are unobservable are constant. Finally, the third condition is verified if the sequence of inputs used to control the system contains all the combinations that meet the two previous conditions for all the elements of $x(t)$. The system (8) is said to be Z(T_N) observable.

The observers used in our predictive strategy are based on a hybrid observer proposed in [16]:

$$\dot{\hat{x}}(t) = \overline{A}_0 \hat{x}(t) + \sum_{j=1}^{m} (u_j(t)(\overline{A}_j \hat{x}(t) + \overline{B}_j + K_j(y - \hat{y})) \quad (9)$$

Where, K_j are the correction matrix gains.

From the above equations the dynamics of the error $e = x(t) - \hat{x}(t)$ are:

$$\dot{e}(t) = \tilde{A}_0 e + \sum_{j=1} u_i \tilde{A}_j e \quad (10)$$

With $\tilde{A}_j = \overline{A}_j - K_j C$ for all $j = 0, 1 \ldots m$.

The Lyapunov function is given by: $V(x(t)) = e(t)^T H e(t)$ where H is a positive-definite matrix i.e ($H > 0, H^T = H$).

The dynamic of the Lyapunov function is given by:

$$\dot{V} = e^T((\tilde{A_0}^T H + H\tilde{A_0}) + \sum_{i=1}^{m} u_i(\tilde{A_i}^T H + H\tilde{A_i}))e \quad (11)$$

It can be seen from equation (11), that if we manage to find H and K_j that verifies $\dot{V} < 0$, we can achieve error convergence of the observer.

Remark 4.2: It can be noted that the decreasing rate of the estimation error depends not only on the parameter of the observer but also on the chosen configuration sequences, because of the $Z(T_N)$-observability of the system. Indeed, the difference $x_j - \hat{x}_j$ decreases rapidly if the combinations of $u(t)$ for which x_j is observable are used more often. Otherwise, the difference decreases more slowly. When using estimated values as feedback in a closed loop predictive control strategy,

if the $Z(T_N)$-observability is not taken into account through a convenient sequence of control, then estimation and control results will be affected negatively. A modification to the control algorithm is needed to use adequate control sequence in order to improve the state estimation.

V. Fault Detection and Isolation

The fault detection and isolation procedure is based on the following equation:

$$R_i(k+1) = |r_i(k+1) + \lambda R_i(k)|; 0 < \lambda < 1;\ i = 1, ..., m \tag{12}$$

With $R_i(0) = r_i(0)$, λ a forgetting factor, $r_i = y - \hat{y}_i$ is the residual given by the observer associated to the i^{th} fault and $\hat{y}_i$ is the estimated measured output given by the same observer ($i = 0$ corresponds to a no fault status).

Remark 5.1:

• When a fault i occurs, it sets the value of u_i of the switched system to a permanent value.

• An observer associated to a fault i is based on equation (9) with its input u_i equal to the value set by the fault.

Remark 5.2 : The observer associated to the healthy system is not affected by the fault occurrence, its input u_i remains connected to the controller.

Assumption 5.1:

• The discrete fault i is detectable, meaning that its occurrence causes a change in the dynamic behavior of the system.

• The occurrence of the discrete fault i improves the estimated states given by the observer related to the fault i.

Theorem 5.1: Assuming that each observer is well defined, if there is not a fault occurrence then there is a real positive value ε_0 such that:

$$lim_{k\to+\infty} R_0 \leq \varepsilon_0 \tag{13}$$

Given **assumption 5.1**, the occurrence of a fault i leads to:

$$lim_{k\to+\infty} R_i \leq \varepsilon_i \tag{14}$$
$$lim_{k\to+\infty} R_0 \geq \varepsilon_0 \tag{15}$$
$$lim_{k\to+\infty} R_{j\neq i} \geq \varepsilon_{j\neq i} : j = 1, ..., m \tag{16}$$

Proof: In the case of a healthy system when the fault $i = 0$, then **remark 4.2** is verified leading to:

$$|r_0(+\infty)| < ... < |r_0(k)| < |r_0(k-1)| < ... < |r_0(0)| \tag{17}$$

So, there exists a real value r_{max} such that:

$$lim_{k\to+\infty} |r_0(k)| \leq r_{0_{max}} \tag{18}$$

Also, (**??**) can be expanded to become:

$$R_i(k+1) = |r_i(k+1) + \lambda r_i(k) + \lambda^2 r_i(k-1) + \lambda^3 r_i(k-1) + ... + \lambda^{k+1} r_i(0)|; 0 < \lambda < 1;$$

Since $0 < \lambda < 1$, so $lim_{k\to+\infty}\lambda^k = 0$, then:

$$lim_{k\to+\infty} R_0(k+1) \leq |r_{0_{max}} + R_{0_{max}}| \tag{19}$$

Where, $R_{0_{max}}$ is a maximum real value containing the weighted sum of the r_0 new values (the residual values that are close to the instant $(k+1)$ which proves (**??**).

Following **remark** 5.1, in the case of a fault occurrence, the same reasoning can be followed to prove (**??**) because the input u_i of the faulty system and that of the observer associated to the fault i are equal, which leads to:

$$lim_{k\to+\infty} R_i(k+1) \leq |r_{i_{max}} + R_{i_{max}}| \tag{20}$$

Where, $r_{i_{max}}$ and $R_{i_{max}}$ are real values.

Also, following **Remark 5.2**, for every control input u_i different from the value set by the fault the observer related to the healthy system does not take it into account leading to:

$$lim_{k\to+\infty} R_0(k+1) \geq |r_{0_{max}} + R_{0_{max}}| \tag{21}$$

Which proves (**??**) That also can be said about the other observers that have an input $u_{j\neq i}$ set permanently to a fixed value, see **Remark 5.1**, but their other inputs are connected to the controller. So, for every control input value u_j different from the value of u_j of the j^{th} observer, the latter does not take it into account leading to:

$$lim_{k\to+\infty} R_j(k+1) \geq |r_{j_{max}} + R_{j_{max}}| \tag{22}$$

Where, $r_{j_{max}}$ and $R_{j_{max}}$ are real values, which prove equation (16).

From **Theorem 5.1**, let consider $\tilde{R}_i$ as a threshold value of R_i used to generate a localization signature of the i^{th} fault as follows:

$$sg_i = \begin{cases} 0\ if R_i > \tilde{R}_i \\ 1\ if R_i < \tilde{R}_i \end{cases} \tag{23}$$

Where, $sg_i = 1$ corresponds to the appearance of the i^{th} fault and $sg_i = 0$ means that the corresponding fault did not occur.

The choice of λ in (12) affects the sensibility of the detection. Indeed, a small value attenuates the contribution of the residual's old values and increases the variation speed of R_i, which let appear several peaks that can alter the detection of the fault. In the contrary, a bigger value attenuates the peaks and slow down the variation speed of R_i. Thus, the time taken in the procedure of detection and isolation of the fault is slower but the accuracy is better.

VI. Application to a Three Cellular Converter

The FTC developed above is applied on a real three cellular converter located in LAMIH (Laboratory of Industrial and Human Automation Control, Mechanical Engineering and Computer Science), Valenciennes, France. Multicellular converters are typical examples of hybrid systems, constituted of the association of several cells separated by capacitors. Each cell is formed by two complementary switches where each one has a binary value (0 if open and 1 if closed), which results in a hybrid behavior of the process. Its main objective is to decrease the power supply to a sustainable level for the load when the power source is so elevated. The converter distributes the elevated power between several cells

which limits the constraint voltages on the semiconductor components. Moreover, it is possible to control the output current if the semiconductors are manipulated using a suitable control technique. A three cell converter, Fig. 2, has two capacitors, eight operating modes for every combination value of its switches, see Table I, and four output voltage levels.

TABLE I. MODE CONFIGURATION OF A THREE CELLS CONVERTER

	u_3	u_2	u_1	V_s
Mode 0	0	0	0	0
Mode 1	0	0	1	V_{c1}
Mode 2	0	1	0	V_{c1}
Mode 3	0	1	1	V_{c2}
Mode 4	1	0	0	V_{c1}
Mode 5	1	0	1	V_{c2}
Mode 6	1	1	0	V_{c2}
Mode 7	1	1	1	E

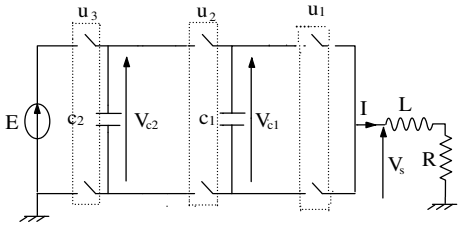

Fig. 2. Structure of a three cell converter with RL load.

The process is described by the following equation:

$$\begin{pmatrix} \frac{dV_{c_1}}{dt} \\ \frac{dV_{c_2}}{dt} \\ \frac{dI}{dt} \end{pmatrix} = \begin{pmatrix} 0 & 0 & \frac{u_2-u_1}{C_1} \\ 0 & 0 & \frac{u_3-u_2}{C_2} \\ \frac{u_1-u_2}{L} & \frac{u_2-u_3}{L} & -\frac{R}{L} \end{pmatrix} \begin{pmatrix} V_{c_1} \\ V_{c_2} \\ I \end{pmatrix} + \begin{pmatrix} 0 \\ 0 \\ \frac{E}{L}u_3 \end{pmatrix} \tag{24}$$

Where, $u_i \in \{0,1\}$ with i = 1, 2, 3 are binary input variables, $X = [V_{c1}\ V_{c2}\ I]^T$ is the state vector containing the capacity voltages and the output current, E is the the supply voltage, C_1, C_2 are the capacity values and $R-L$ represents the load.

In general, industrials use an open loop control when dealing with the multicellular converters to reduce the cost of the capacitor voltage sensors. The drawback is the appearance of several oscillations in the output responses with a slow dynamic before attaining the output references. Therefore, an alternative solution would be using closed loop controller with state observers to estimate the capacitor voltages. But, it can be deduced from (**??**) that the system is not observable for any combination input, as the rank of the observability matrix is inferior to 3. Fortunately, the three cell converter presents several transition modes that meet $Z(T_N)$-observability [17]. That will be exploited by the FCS-PC algorithm in order to achieve a proper estimation and acceptable reference tracking. As discussed in **Remark 5.2**, as long as the sequences insure the $Z(T_N)$- observability of the process, the estimation error decreases resulting in an improvement of the real output responses. But, in our case the predictive controller may choose some input combinations that will slow down the convergence rate like mode 0 and mode 7, because they do not satisfy the first condition of $Z(T_N)$ observability mentioned in Section 4. Also, the transitions between mode 1 and mode 6 and between mode 3 and mode 4 do not satisfy the third condition of the Z(T_N) observability. Because in the first transition, both mode 1 and mode 6 have $\dot{V}_{c_2} = 0$, and in the second transition, mode 3 and mode 4 have both $\dot{V}_{c_1} = 0$ as can be seen in (**??**). Moreover, the convergence is greatly affected by the switches commutation frequencies. Indeed, for a high frequency the observer cannot lose its minimum dwell time in the estimation. Two step are needed to overcome this problem: the first one is to remove mode 0 and mode 7 from the control algorithm. The controller will rely on the input redundancy of the converter to find alternative solutions to attain its objective. The second one is to use a restriction in the same algorithm to prevent transition between the modes having the commutation of two or three switches simultaneously which will decreases the commutation frequency and in the same time will prohibit the transitions not satisfying the $Z(T_N)$-observability. The resulting switching sequences that will be used by the controller is given in Fig. 3. One can find in [3], the modifications in the control algorithm that can be made to allow or to prohibit transitions between operating modes.

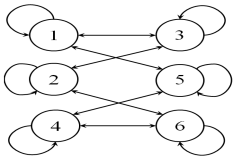

Fig. 3. Transitions allowed to use from a current mode to a future mode.

A. Materials and methods

The process used to validate the presented FTC approach is constituted of three legs connected to a R-L load ($R = 200\Omega, L = 1H$). We used a three-cell converter, located in the first leg, see Fig. 4. The value of the capacitors between

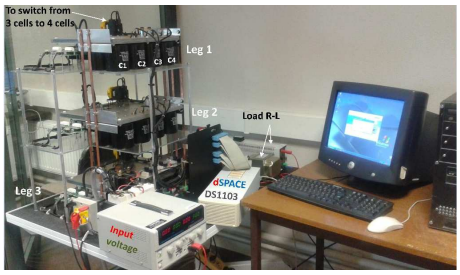

Fig. 4. Photography of the experimental setup.

the cells are $C_1 = C_2 = 720\mu F$. The switches are bipolar transistors (IGBTs) model SKM100GB12V. The current and the voltage measurements are obtained from voltage sensors and current transduction. The source voltage of the converter is $E = 30V$ supplied by a rectifier.

A Matlab program file containing the FTC algorithm was compiled and run by a DSPACE card DS1103. The latter will be used to control the switch gates via its binary outputs after receiving the measurements of the current.

B. Experimental results

1) Predictive control for three-cell converter: Hereafter, the experimental results obtained after using control sequences that meet the conditions of the converter $Z(T_N)$-observability, see Fig. 5 that shows a zoomed view of the inputs switching. Fig. 6 shows, respectively, the capacity voltages V_{c_1}, V_{c_2} and the current load I where the output references are $V_{c_{1ref}} = 10\,V$, $V_{c_{2ref}} = 20\,V, I_{ref} = 0.08\,A$. The sampling period used is $T_e = 7\ 10^{-4} s$.

The parameters of the observer (9) are obtained by pole placement [16] as follows:

$$K_0 = 10^2 \begin{pmatrix} 0 \\ 0 \\ 8.55 \end{pmatrix}, K_1 = 10^4 \begin{pmatrix} 13.4625 \\ -6.75 \\ 0 \end{pmatrix},$$

$$K_2 = 10^4 \begin{pmatrix} -6.7125 \\ 6.7125 \\ 0 \end{pmatrix}, K_3 = 10^4 \begin{pmatrix} -6.75 \\ -13.4625 \\ 0 \end{pmatrix}$$

The matrices $\overline{A}_0, \overline{A}_1, \overline{A}_2, \overline{A}_3, \overline{B}_1, \overline{B}_2$ and $\overline{B}_3$ for three cell converter can be found in [16]. The error estimation of V_{c_1} and

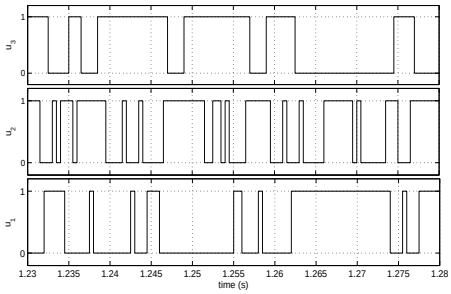

Fig. 5. Control inputs with transitions satisfying the Z(T_N) observability.

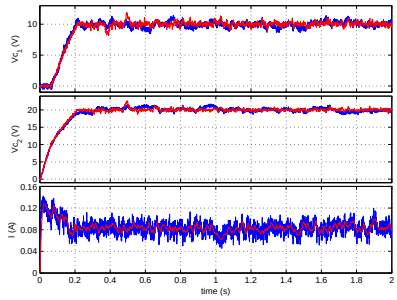

Fig. 6. Experimental results of the capacitor voltages and the output current; (blue line) measured values and (red line) estimated values.

V_{c_2} displayed in Fig. 7 are acceptable and in the same time, the real outputs values in Fig. 5 follow closely enough their references. However, the imposed restrictions on the control algorithm do not come without drawbacks, as it can be seen in the current I response where the fluctuation rate around its reference is significant but remains acceptable.

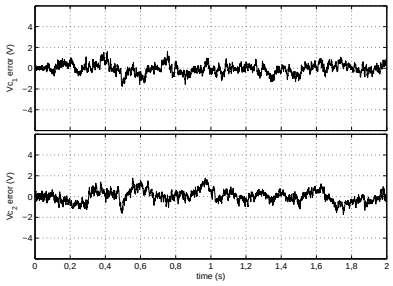

Fig. 7. V_{c_2} and V_{c_1} estimation error.

2) Fault tolerant predictive control: Hereafter, the results of the proposed fault tolerant control strategy are shown. As discussed previously, the study focuses on the discrete failure that may happen to the multicellular converter when one or several switches fail to open or to close when needed.

In the literature, very few works cover the problem. In fact, some studies are only restricted to the fault identification without considering the control of the system. One of the reasons can be related to how we can use the remaining operating modes after the appearance of the fault. That issue was solved here using several predictive control algorithms, hence the contribution made in this paper.

The application is restricted to the case where one cell is stuck closed (stuck open, respectively) with a different cell each time to cover all the potential cases. To that end, 7 observers were used, where three are affected respectively to the failure stuck closed of u_1, u_2 and u_3, three to the failure stuck open and the last one affected to the non faulty converter. All the observers are based on (**??**), where the faulty input $u_{i=\{1,2,3\}}$ of every observer is equal to 1 if stuck closed or 0 if stuck open and the non faulty inputs are driven by the controller.

TABLE II. CAPACITY VOLTAGES RESPONSES AFTER THE APPEARANCE OF A FAILURE

	$u_3u_2u_1$	modes	$\dot{V}_{c_2}$	$\dot{V}_{c_1}$
u_3 stuck close	1 0 0	4	I/c	0
	1 1 0	6	0	I/c
	1 0 1	5	I/c	$-I/c$
u_2 stuck close	0 1 0	2	$-I/c$	I/c
	0 1 1	3	$-I/c$	0
	1 1 0	6	0	I/c
u_1 stuck close	0 0 1	1	0	$-I/c$
	0 1 1	3	$-I/c$	0
	1 0 1	5	I/c	$-I/c$
u_3 stuck open	0 1 1	3	$-I/c$	0
	0 0 1	1	0	$-I/c$
	0 1 0	2	$-I/c$	I/c
u_2 stuck open	0 0 1	1	0	$-I/c$
	1 0 1	5	I/c	$-I/c$
	1 0 0	4	I/c	0
u_1 stuck open	0 1 0	2	$-I/c$	I/c
	1 0 0	4	I/c	0
	1 1 0	6	0	I/c

All the potential failures and their consequences on the system states are described by Table II. Note that the current I always flows in one direction because of the load. Considering that, one can see that in some cases it is possible to control at least two states of the system. For example, when u_3 is

stuck close, V_{c_2} can increase or remain invariable but cannot decrease. However, V_{c_1} is not affected by the failure of u_3, as can be seen from equation (24), so it is controllable and the same can be said for the current since it depends on V_{c_1}. Also, when u_1 is stuck close, V_{c_1} cannot increase and V_{c_2} is not affected by the failure, so it is controllable along with the output current.

There are other cases where it is not possible to control any of the outputs of the converter. For example, when u_2 is stuck closed (respectively stuck open), we can see that V_{c_1} cannot decrease and V_{c_2} cannot increase (respectively V_{c_1} cannot increase and V_{c_2} cannot decrease) and consequently the current I is not controllable.

When u_3 is stuck open, the current source is disconnected and the current I provided by the capacities will obviously decrease until disappearing. When u_1 is stuck open, V_{c2} is not affected, so we can suppose that it is controllable unlike V_{c1}. But, in reality that is not true because the path enabling the discharge of the capacities are cut off, so V_{c_2} cannot decrease. Further explanation on that case will be given after displaying the states responses of the converter.

The detection and isolation of the fault in this experimentation is based on Table III where $\tilde{R}_0$ and sg_0 are associated to the healthy mode, $\tilde{R}_1$, $\tilde{R}_2$, $\tilde{R}_3$ and sg_1, sg_2, sg_3 are respectively associated to u_1, u_2, u_3 stuck closed and $\tilde{R}_4$, $\tilde{R}_5$, $\tilde{R}_6$ and sg_4, sg_5, sg_6 are respectively associated to u_1, u_2, u_3 stuck open. Following **Theorem 5.1**, it is save to

TABLE III. FAULT DETECTION AND LOCALIZATION

$\tilde{R}_0 = 1.2$	sg_0	1	0	0	0	0	0	0
$\tilde{R}_1 = 1.3$	sg_1	x	1	0	0	0	0	0
$\tilde{R}_2 = 1.3$	sg_2	x	0	1	0	0	0	0
$\tilde{R}_3 = 1.3$	sg_3	x	0	0	1	0	0	0
$\tilde{R}_4 = 1.3$	sg_4	x	0	0	0	1	0	0
$\tilde{R}_5 = 1.3$	sg_5	x	0	0	0	0	1	0
$\tilde{R}_6 = 1.3$	sg_6	x	0	0	0	0	0	1
current fault	f	0	1	2	3	4	5	6

prioritize the signature of the healthy system over the others signatures. So, when $sg_0 = 1$ all the other signatures are ignored and the current fault f is 0 meaning that the converter operates properly. When sg_0 pass from 1 to 0 that means the appearance of a fault. In that case, sg_0 will hold to its value and an isolation input sequence will replace the control sequence for a time delay corresponding to the minimum dwell time for the stabilization of R_i related to all the observer. After that, the faulty cell and its type is identified (stuck close if $1 \leq f \leq 3$ or stuck open if $4 \leq f \leq 6$).

The application will proceed as follows: initially, the three cell converter will operate without fault. After 4 seconds $u_{i=\{1,2,3\}}$ is stuck close (open respectively). When the signature sg_0 pass from 1 to 0, a PWM (pulse wave modulation) input sequence is triggered to isolate the faulty cell, and when that happens the controller will be reconfigured to an appropriate control algorithm. The PWM signal was chosen with a duty cycle qual to 0.5 because the input sequence in that case does not use mode 0 or mode 7 [17]. That choice will improve the estimation since it will reduce the use of sequence unfavourable to $Z(T_N)$-observability. Also, a switching frequency $fs = 5hz$ of the PWM sequence was chosen to offer the time needed for the convergence of the observer associated to the failure and the divergence of the others.

The detection and localization results of some fault cases are displayed in Fig. 8, 9 and 10 when u_1 is stuck closed and in Fig. 11, 12 and 13 when u_3 is stuck closed.

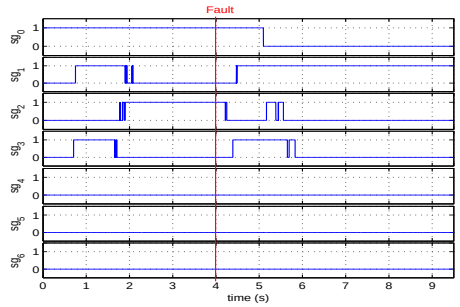

Fig. 8. Signature evolutions when u_1 is stuck closed.

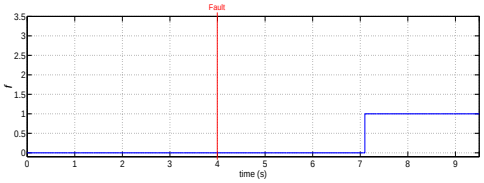

Fig. 9. Fault localization when u_1 is stuck closed.

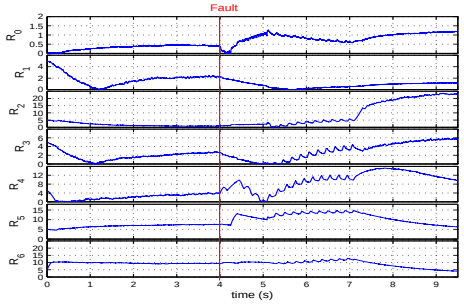

Fig. 10. R_i evolution when u_1 is stuck closed.

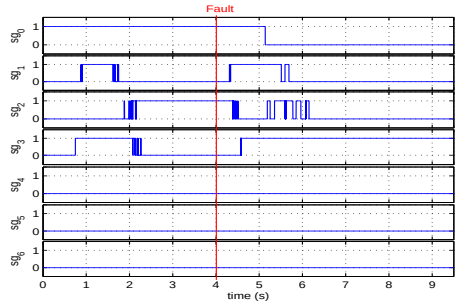

Fig. 11. Signature evolutions when u_3 is stuck closed.

We can see that some signatures commute to 1 even when there is no fault or there is a different fault. For example, Fig. 11 where we have sg_2 equal to 1 when the converter operates

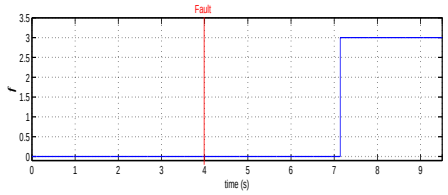

Fig. 12. Fault localization when u_3 is stuck closed.

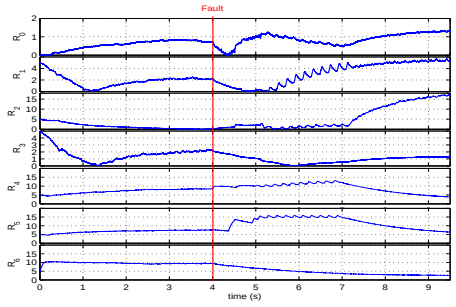

Fig. 13. R_i evolution when u_3 is stuck closed.

correctly. That is because R_2 increases until reaching its threshold value, see Fig. 13, which is caused by the controller setting u_2 to 1. In that case the observer of the converter and the one related to the fault are similar since they use the same (**??**) with the same input $u_2 = 1$. When the controller set u_2 to 0, R_2 will increase because its corresponding observer has u_2 equal to 1, sg_2 changes to 0 when the controller maintains $u_2 = 0$ for enough time until R_2 increases over its threshold.

The fault localization was set to 3.1 seconds after the fault detection (i.e., when $sg_0 = 0$) to identify accurately the fault. The reason is related to the slow variation of $R_{i=0,\dots,6}$ because the value of λ in equation (12) was taken big enough to filtrate the measurement noises that can tamper the results. However, some faults can be isolated after only 2.1 seconds, like when u_1 or u_3 are stuck closed. Indeed, each fault changes the input sequences favourable to $Z(T_N)$-observability, so the isolation time is not the same for each different fault.

When a fault occurs, some transitions will be discarded which compels the system to use a very reduced number of configuration modes. Table II includes the remaining configuration modes to use for each fault case.

When the failure is identified, the control algorithm will consider only those modes and removes the others when computing the minimal value of the cost function. That will prevent the use of wrong sequences that target a healthy process and use only the sequences that aim to control the corresponding faulty process. Also, in order to improve the control results, the one commutation restriction on the switches used when the converter operates correctly was removed from the algorithm.

The input control and the outputs of the converter are shown in Fig. 15 to 24. It can be seen the change in the shape of the switching commutation after the appearance of the fault, then the PWM sequence is used, and finally the switching sequence to control the faulty system.

The output results when u_1 is stuck closed are presented in

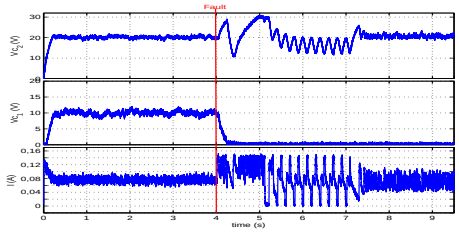

Fig. 14. Experimental results using the proposed FTC when u_1 is stuck closed.

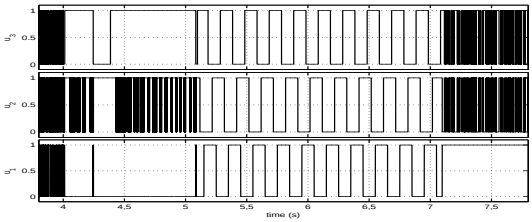

Fig. 15. Experimental results for inputs control applied to the converter when u_1 is stuck closed.

Fig. 14 where it can be seen after the appearance of the fault that the responses move away from their references for 3.1 seconds where only R_1 is under its threshold value, in that instant the information is given to the controller to modify its algorithm taking into account the fault as can be seen in Fig. 15. The FTC is able then to return V_{c_2} and I to their reference values but was not able to do the same to V_{c_1}. The latter cannot increase because it is connected permanently to the load so when $u_2 = 0$ the capacity C_1 discharges and when $u_2 = 1$ it will not charge because the current heads to the load without passing through C_1.

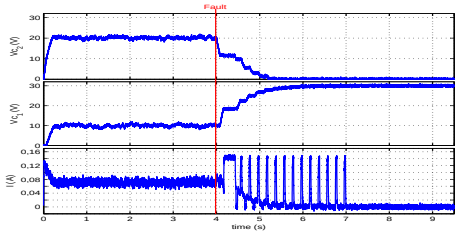

Fig. 16. Experimental results using the proposed FTC when u_2 is stuck closed.

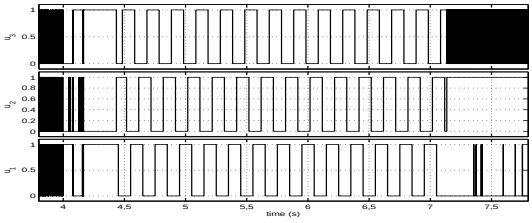

Fig. 17. Inputs control applied to the converter when u_2 is stuck closed.

Fig. 16 describes the evolution of the system states when u_2 is stuck closed. It can be seen in Fig. 17 that there is not a single input combination able to control V_{c_1} and V_{c_2} as explained previously in Table II, but we can also see that there is one combination for which the current increases very

fast, that is when all the superiors switches are closed. So, the voltage output commutes between $0Volt$ and E and so I commute between 0 A and E/R.

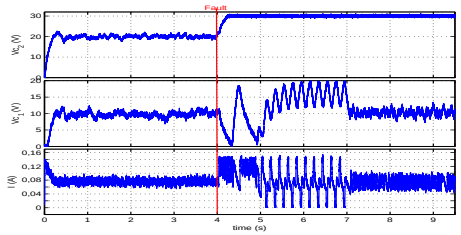

Fig. 18. Experimental results using the proposed FTC when u_3 is stuck closed.

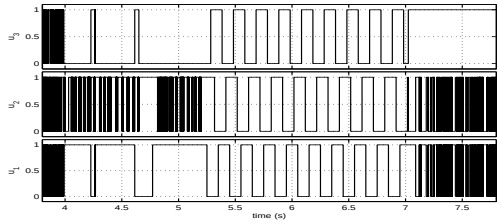

Fig. 19. Inputs control applied to the converter when u_3 is stuck closed.

The output results when u_3 is stuck closed are presented by Fig. 18. It can be seen after the appearance of the failure that the responses lose their tracks and remain that way until R_3 pass under its threshold value and the others are above their threshold values. At that time, the information is given to the controller to modify its algorithm taking into account the fault as can be seen in Fig. 19. The FTC is able then to return V_{c_1} and I to their reference values but was not able to do the same to V_{c_2} because the latter cannot decrease. That makes sense since the capacity C_2 is connected permanently to the source E because of the failure.

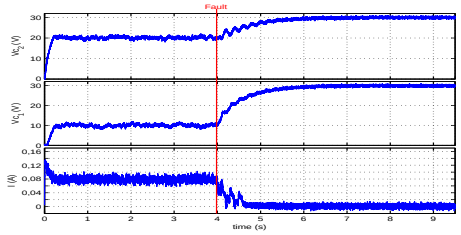

Fig. 20. Experimental results using the proposed FTC when u_1 is stuck open.

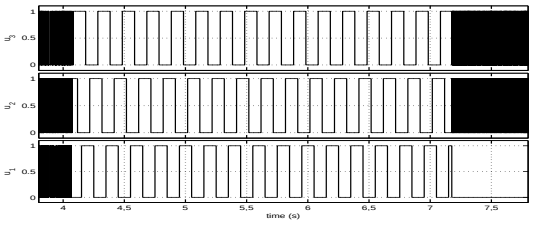

Fig. 21. Inputs control applied to the converter when u_1 is stuck open.

Fig. 20 shows the evolution of the system states without a possibility to be controlled after the appearance of the fault as can be seen in Fig. 21. Indeed, even if V_{c_2} can increase or decrease (see Table II) which is not the case with V_{c_1} since it can only increase leading at some point to $V_{c_1} \geq V_{c_2}$. At that instant, the current I stops flowing from C_2 to C_1 so it becomes equal to zero and V_{c_2} becomes invariable.

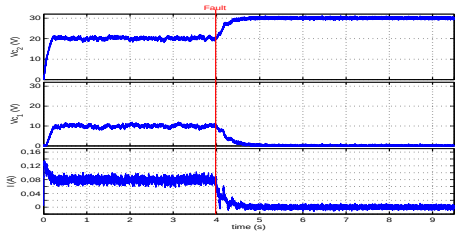

Fig. 22. Experimental results using the proposed FTC when u_2 is stuck open.

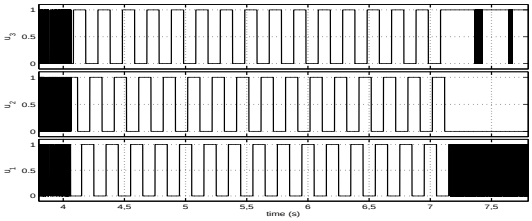

Fig. 23. Inputs control applied to the converter when u_2 is stuck open.

The analysis in the case of u_2 is stuck open in Fig. 22 and 23 is analog to that when u_2 is stuck closed the two capacity voltages are not be controllable C_1 and C_2. The first cannot decrease and the second cannot increase. Thus, the current can not controllable.

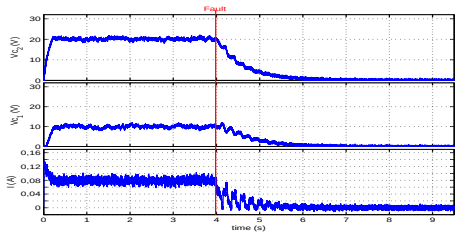

Fig. 24. Experimental results using the proposed FTC when u_3 is stuck open.

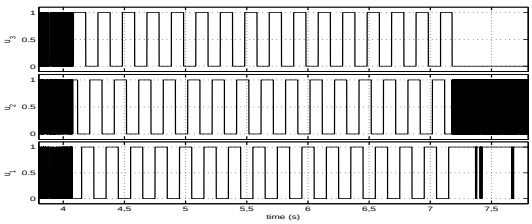

Fig. 25. Inputs control applied to the converter when u_3 is stuck open.

In the case where u_3 is stuck open, see Fig. 24 and 25, the source power is disconnected so V_{c_2} decreases and the current that remains in the capacities will gradually decrease until reaching zero.

As can be seen, after the appearance of the fault, the proposed FTC strategy is able to control some of the system's

states when they are controllable. But in the other cases, the system states are not controllable, either because of the disconnection of the power source, or because of the path allowing the discharge of the capacities are cut off. A solution can be found with a modification in the structure of the converter similar to the solution suggested in [18]. For example it is possible to incorporate alternative switchers for used when u_1 is stuck open to allow the discharge of the capacities and another one is used when u_3 is stuck open to prevent the disconnection of the power source. In that case, the converter will operate with two cells leading to another new configuration that did not exist before the fault.

Nevertheless, the results in the controllable fault cases are acceptable, the load current along with the remaining controllable capacitor voltage is well maintained around their references.

VII. Conclusion

The presented work covers multiple areas: control, observation, fault detection and isolation of hybrid systems. The main objective is to build an FTC strategy based on a predictive controller having a finite control set to apply on a linear switching system.

This paper focuses on a certain class having non-observable subsystems, hence the contribution made in this work. A solution can be found when using the $Z(T_N)$-observability approach in order to identify the fault. However, controlling the system after that is another difficult problem. In fact, the fault compel the controller to use a very reduced number of operating modes. Consequently, the objective was partially reached because of the non controllability of the system's states in some fault cases. A part from that, the proposed method is able to control the hybrid system despite its $Z(T_N)$-observability nature before and after the appearance of a failure as shown by the experimental results. Future works can focus on reducing the detection and isolation time and search a FTC strategy based on a different control technique than the predictive algorithm.

References

[1] D. Liberzon and A.S. Morse, *Basic problems in stability and design of switched systems*, IEEE Control Systems, Vol.19, No.5, pp.59–70, 1999.

[2] J.V Gorp, M. Defoort and M. Djemai, *Binary signals design to control a power converter*, 50th IEEE Conference on Decision and Control and European Control Conference (CDC-ECC), pp.6794–6799, 2011.

[3] A. Smati, D. Berdjag, W. Chagra, M. Defoort and M. Ksouri, *Predictive control for multicell converter*, 2nd International Conference on Automation,Control, Engineering and Computer Science Proceedings of Engineering and Technology (PET), 2015.

[4] J.V. Gorp, M. Defoort, K. Veluvolu and M. Djemai, *Hybrid sliding mode observer for switched linear systems with unknown inputs*, Journal of the Franklin Institute, vol.351,(7), pp.3987–4008, 2014.

[5] N. Orani, A. Pisano, M. Franceschelli, A. Giua and E. Usai, *Robust reconstruction of the discrete state for a class of nonlinear uncertain switched systems*, Nonlinear Analysis : Hybrid Systems, vol.5,(2), pp.220–232, 2011.

[6] F. Arichi, M. Djemai and B. Cherki, *Active mode detection for a class of hybrid dynamic systems*, International Conference on Systems, Signal Processing and Electronics Engineering (ICSSEE'2012), pp.210–215, 2012.

[7] A. Alessendri and P. Coletta, *Design of Luenberger observers for a class of hybrid linear systems*, IHybrid systems: computation and control. Lecture notes in computer science, pp.7–18, 2001.

[8] A. Balluchi, L. Benvenuti, M. D. Di Benedetto, A. L. Sangiovanni-Vincentelli, *Design of observers for hybrid systems*, Hybrid Systems: Computation and Control, pp.76–89, 2002.

[9] J.V. Gorp, M. Defoort, M. Djemai and N. Manamanni, *Hybrid Observer for the Multicellular Converter*, 4th IFAC Conference on Analysis and Design of Hybrid Systems, pp.259–264, 2012.

[10] M. Sampath, R. Sengupta, S. Lafortune, K. Sinnamohideen and D. Teneketzis, *Failure diagnosis using discrete event models*, Decision and Control, Proceedings of the 33rd IEEE Conference on, vol.3,(2), pp.3110–3116, 1994.

[11] A. Takrouni, N. Zanzouri, V. Cocquempot and M. Ksouri, *Robust Diagnosis for Hybrid Dynamical Systems*, International Journal of Engineering and Innovative Technology, Vol. 3, (9), pp. 312–318, 2014.

[12] M. S. Branicky , *Multiple Lyapunov functions and other analysis tools for switched and hybrid systems*, IEEE Transactions on Automatic Control, vol.43, pp.475–482, 1998.

[13] P. Lezana, R. Aguilera and D. E. Quevedo , *Model Predictive Control of an Asymmetric Flying Capacitor Converter*, IEEE Transactions on Automatic Control, Vol.56, No.6 pp.1839 –1846, 2009.

[14] L. Hetel, M. Defoort and M. Djema, *Binary Control Design for a Class of Bilinear Systems: Application to a Multilevel Power Converter*, IEEE Transaction on control systems technology, Vol. 24, pp. 719 – 726, 2015.

[15] J. Lygeros, K. Johansson, S. Simic, J. Zhang and S. Sastry, *Dynamical Properties of Hybrid Automata*, IEEE Transactions on Automatic Control, Vol.48, pp.2–17, 2003.

[16] P. Riedinger, M. Sigalotti, J. Daafouz, K. Johansson, S. Simic, J. Zhang and S. Sastry, *On the algebraic characterization of invariant sets of switched linear systems*, Automatica, Vol.46, No.6, pp.1047–1052, 2010.

[17] J.V. Gorp, M. Defoort, M. Djemai and N. Manamanni, *Hybrid Observer for the Multicellular Converter*, 4th IFAC Conference on Analysis and Design of Hybrid Systems, pp.259–264, 2012.

[18] S. Meradi, K. Benmansour, M. Djemai, M. Tadjine and M.S. Boucherit, *Fault Detection and sliding mode reconfiguration for the Multi-cellular Converter three cells*, 4th International conference on electrical engeneering, pp. 615–620, 2012.

Impact of Distributed Generation on the Reliability of Local Distribution System

Sanaullah Ahmad
Electrical Engineering Department
IQRA National University (INU)
Peshawar,Pakistan

Azzam Ul Asar
Electrical Engineering Department
CECOS University
Peshawar,Pakistan

Sana Sardar
Electrical Engineering Department
IQRA National University (INU)
Peshawar,Pakistan

Babar Noor
Electrical Engineering Department
IQRA National University (INU)
Peshawar,Pakistan

***Abstract*—With the growth of distributed generation (DG) and renewable energy resources the power sector is becoming more sophisticated, distributed generation technologies with its diverse impacts on power system is becoming attractive area for researchers. Reliability is one of the vital area in electric power system which defines continuous supply of power and customer satisfaction. Around the world many power generation and distribution companies conduct reliability tests to ensure continues supply of power to its customers. Uttermost reliability problems in power system are due to distribution network. In this research reliability analysis of distribution system is done. The interruption frequency and interruption duration increases as the distance of load points increase from feeder. Injection of single DG unit into distribution system increase reliability of distribution system, injecting multiple DG at different locations and near to load points in distribution network further increases reliability of distribution system, while introducing multiple DG at single location improves reliability of distribution system. The reliability of distribution system remains unchanged while varying the size of DG unit. Different reliability tests were done to find the optimum location to plant DG in distribution system. For these analyses distribution feeder bus 2 of RBTS is selected as case study. The distribution feeder is modeled in ETAP, ETAP is software tool used for electrical power system modeling, analysis, design, optimization, operation, control, and automation. These results can be helpful for power utilities and power producer companies to conduct reliability tests and to properly utilize the distributed generation sources for future expansion of power systems.**

***Keywords*—Electric power system reliability; distributed generation; reliability assessment**

I. Introduction

The electricity demand is usually fulfilled by the power generated in electrical power plants. Fig. 1 shows a traditional power plant with the transmission and distribution section. The output power capacities depend upon size and type of generation. These capacities typically range from hundreds of MW to few GW [1] . Such large scale generating plants are located at a distance from load centers. Transmission lines and distribution feeders are used to transmit power from the point of generation to the load points [2], [3]. The fundamental characteristic of power system is to provide economical and reliable electricity to its customers. Presently, the operation of power system is considerably influenced by energy obtained from renewable resources such as photovoltaic and wind energy system. The major challenges that electrical utilities are going through is to provide power to the customers with lower rates and by increasing the market value of services they provide with right amount of reliability and lowering the maintenance cost, operational and constructional cost [4]. Reliability is divided into system adequacy and security [5]. The adequacy is associated to meet the customer demand in the presence of sufficient electric power generation. The term security is associated to the capability of power system for its response to instability and transients that occurs in the system.

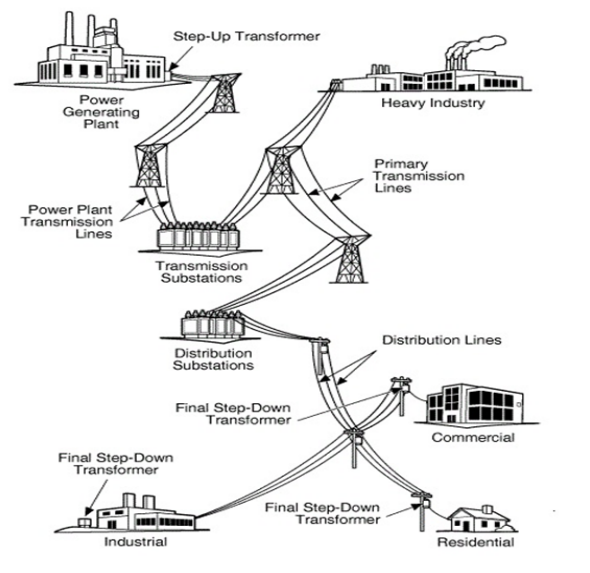

Fig. 1. Traditional Power System.

Distributed Generation is a new technique based on renewable energy resources which will possibly participate as a vital entity of electric Power System. Distributed Generation can also be considered as power generation unit injected to distribution network by neglecting the transmission lines, hence

decreasing the technical losses [6], [7]. The power generated from these DGs is not connected to the national grids as they range from few kilowatts (KW) to several megawatts (MW) [8], [9]. Radial distribution systems are much modest but are more exposed to outages instead of interconnected system. During normal operating conditions the loads accomplish its required power demand, but if any fault occurs, the circuit trips causing failure to power flow. Despite the fact that distribution systems have localized effects, statistics shows that distribution system failure affects the system as much as 85 to 90 percent towards the unavailability of supply to load as compared with failure of other parts of electric power system [10]. Amalgamation of DG in the distribution system will provide an extra power for operation of loads even under faulty conditions. The placement of DG and protection devices will affect the reliability of system with respect to DG penetration [11].

Researchers are eager to develop such systems which are feasible, economical and time saving to cope with the increasing power demand and improve power system reliability. In this regard, distributed generation is considered to be the power paradigm for the new millennium. Distributed generation has a vital impact on power system, for this purpose, distributed generation source is connected to distribution system causing variation in power flow and reliability factors. This depends on the optimal location, size and number of distributed generation. Power generation and utility companies are looking for techniques to reduce costs and still provide the acceptable level of reliability necessary for the customers satisfaction. One solution is to add distributed generation with right configurations into distribution system. In this research the impact of distributed generation on the reliability of distribution system will be analyzed.

II. Distributed Generation Technologies

Energy resources are categorized as non-renewable (conventional) and renewable (non conventional) energy resources. Technologies based on renewable energy include PV modules, geo-thermal system and wind turbines. Where as co-generation plants, fuel cells and heat engines are the technologies based on non-conventional resources [12]. Fig. 2 shows different conventional and non-conventional energy resources are integrated with distribution system. In [13] a new plan is presented to solve the network re-configuration problem in the existence of distributed generation (DG) with an aim of minimizing losses in real power and voltage profile improvement in distribution system. In the existing power system the generated power is transmitted to load centers through long transmission lines, causing technical losses. These losses can be minimized by injecting the distributed generation near to load centers, eliminating transmission losses and hence improving the voltage profile. Many benefits have been derived from integration of DG units into the distribution networks by power system planners and policy makers [14]. These benefits depend upon the characteristics of DG units such as photovoltaic (PV), wind generating system and reciprocating engines, type of loads, local renewable sources and network pattern. This study comprehensively reviews various research works on the technical, environmental and economic benefits of renewable DG integration such as reduction in line-loss, reliability enhancement, economic benefits and optimizing environmental pollution. In [15], [16] the authors have discussed

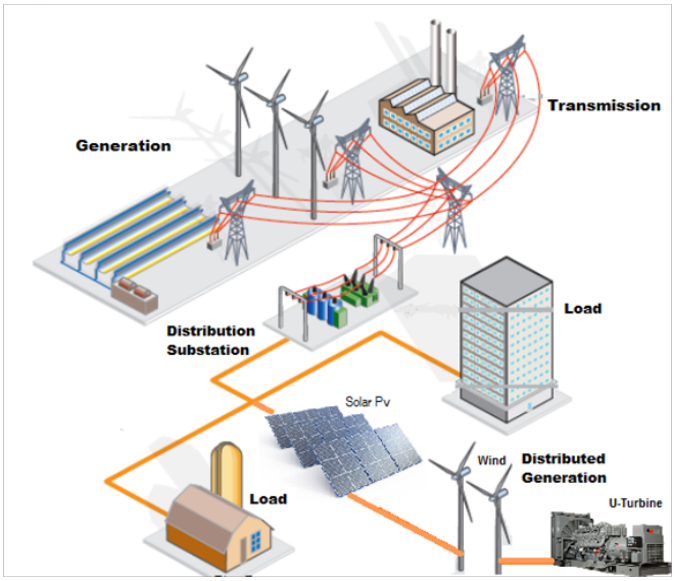

Fig. 2. Distribution System with Distributed Generation.

that maximum reliability improvement is obtained when the placement of Distributed generation is close to the customer premises, making available maximum access in provisions of customer numbers. The authors in [17] have shown that if the customer interruptions due to any fault in the system are followed by some planned techniques, likely by injecting DG units to the distribution system will improve the reliability of the system. The results reveal that the reliability of the distribution network does improve by injecting DG to the system.

III. Reliability of Electric Power system

The reliability of power has a great importance for its customers. The power quality issue can be defined by customer perspective as any state of supplied electricity that causes a fault in equipment or a device. Power reliability can be considered as a voltage quality. The utility can perform its duty utmost by providing a sufficient voltage to the customers. Utilities generally have no concern with the current obtained by the users at the end. For the perfect power quality it is necessary to have an ideal sinusoid with unvarying frequency and amplitude. When the source voltage is disturbed due to the transient character, its amplitude and frequency will be distorted. Due to this change low power quality will be obtained [18].

Generation stations comprises of different generating units which convert the mechanical energy to electrical energy by driving the turbine coupled with a generator. Steam is used to drive prime mover; this steam is formed inside boiler excited via natural gas, nuclear fuel, oil and coal. The capability of electricity generating plants is to supply continuous electricity that the customers require is submitted to as adequacy of system. System adequacy has the following basic conditions which if met, guarantee the system adequacy. In first condition

the generating capacity of a plant should always be greater than system losses in addition to demand of the load.

Generation capacity >Demanded load+System losses

For second condition the system should be able for the transportation of demand of the load to the consumer end without interrupting or overloading the equipments.

Demanded load → Consumer end

The third condition is to serve the consumer within a specific voltage range.

Acceptable voltage range → Consumers served

Distribution system falls just after the transmission system. Here, high voltages of the transmitted power are then stepped down to distribution level voltages, from where loads are served. Reliability has always been a secondary concern. However capacity planning is of main concern. A distribution system which is planned solely for capacity and least amount of protection standard, costs approximately 40 percent -50 percent of a usual overhead design. such system has no protection, absence of switching sections, tie switches are not present, no fuses and lack of lightning protection. Any capital spent ahead of such a minimal capacity design is spent for reliability improvement. Analyzing the viewpoint, approximately 50 percent of distribution systems expenditure is for capacity and 50 percent is for reliability. For residential consumers with 90 minutes of interrupted power/year, about 70 to 80 minutes will be attributable by distribution network [19].

Since past decades, less consideration to distribution network is established towards the reliability modeling and assessment of the electric power generating system. For measuring system performance, various measures of reliability have been defined by IEEE, these measures are actually done with reliability indices which includes frequency of outages, system availability, outage duration and response time. Some of these reliability indices are defined in [20].

IV. Mathematical modeling and Evaluation of Power System Reliability.

The techniques required for analyzing a distribution system is dependent upon type of system considered. The main concern of this chapter is to evaluate the basic techniques. These basic techniques are agreeable for analyzing radial distribution systems. However, some complex techniques are required for ring or meshed systems. Reliability studies are usually carried out assuming the generation and transmission system points, having infinite capacity and are 100 of reliable [21]. While discussing distribution systems, they may likely be radial networks or to some extent meshed networks [19]. In radial distribution system, components including over head lines, underground cables, bus bars and isolators are connected in series. In such system costumers could be connected to load point and need all the components to be operated.

A. Components Modeling

The indices in [20] are generally used to evaluate the distribution system's reliability indices illustrated below:

Expected Failure Rate **(λ):**

(λ) is load interruption frequency. Expected failure rate is the sum of rate of

active failures (λ_a) and passive failure (λ_b). Equation is given below:

$$\lambda = \lambda_a + \lambda_b$$

In active failure rate the protective devices operates around the failed components i.e a short-circuit fault or the failure of component which restores after repair and replacement. While on the other hand, the protective device does not operate around a failed components in passive failure rate i.e an open circuit fault.

Mean Time to Repair (MTTR):

(r), is the time in hours, needed to restore a component outage to its normal operating condition is termed as Mean time to repair.

$$\text{MTTR} = \text{r}$$

Expected Repair Rate (μ):

Expected repair rate is the frequency of repair and is denoted by (μ) (occurrence per year).

$$\mu = 8760 / \text{MTTR}$$

Mean Time to Failure (MTTF):

Mean time to failure is probable time (in years) the component will remain in failed condition.

$$\text{MTTR} = \text{m}$$

$$\text{MTTF} = 1 / \lambda$$

Mean Time Between Failures (MTBF):

Mean time between failures is the expected time in years a component fails. Fig. 3 shows the difference between MTTR, MTTF and MTBF.

$$\text{MTBF} = \text{MTTF} + \text{MTTR} / 8760$$

B. Network Modeling:

Physical networks are translated to reliability networks through network modeling, based on parallel and series configurations. Network modeling is not a state based technique but is a component base method. The two primary component configurations in network modeling are:

1) Series configuration.
2) Parallel configurations.

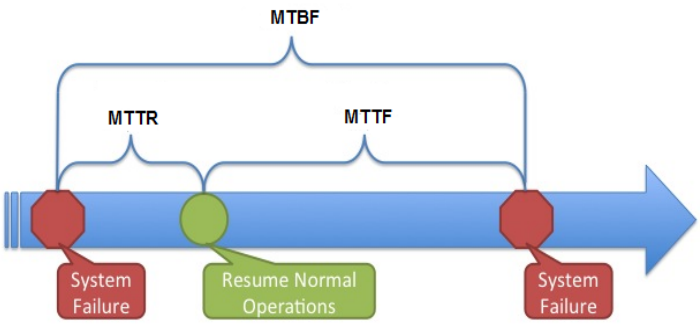

Fig. 3. MTTR, MTTF and MTBF.

1) Series Configuration: The series connection is shown below in Fig. 4 and 5:

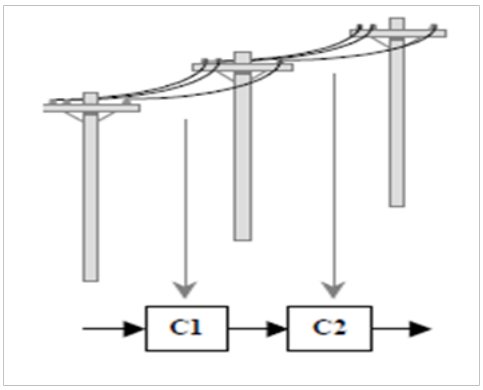

Fig. 4. Series Configuration of Network Modeling.

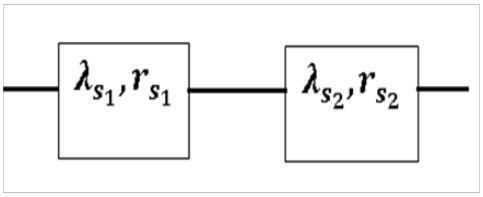

Fig. 5. Block diagram of Series Components.

$$\lambda_{sysytem}=\lambda_{s1}+\lambda_{s2} \quad (1)$$

$$\gamma_{system}=\frac{\lambda_{s1}*\gamma_{s1}+\lambda_{s2}*\lambda_{s2}+(\lambda_{s1}*\gamma_{s1})(\lambda_{s2}*\gamma_{s2})}{\lambda_{system}} \quad (2)$$

2) Parallel Configuration: The parallel connection is shown in Fig. 6 and 7:

Fig. 8 shows how series and parallel components in a network are reduced.

$$\lambda_{system} = \frac{\lambda_{s1}*\lambda_{s2}(\gamma_{s1}+\gamma_{s2})}{(1+\lambda_{s1}*\gamma_{s1}+\lambda_{s2}*\gamma_{s2})} \quad (3)$$

$$\gamma_{system} = \frac{\gamma_{s1}*\gamma_{s2}}{\gamma_{s1}+\gamma_{s2}} \quad (4)$$

λ_{s1} : failure rate of first series component.
λ_{s2} : failure rate of second series component.
λ_{system} : failure rate of system.

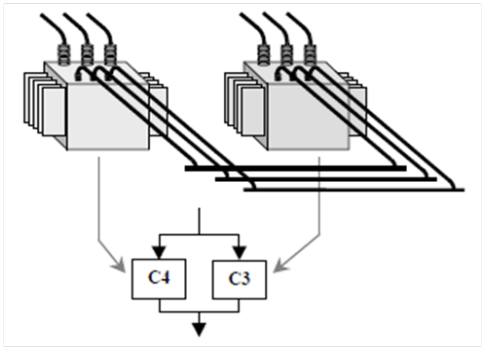

Fig. 6. Parallel Configuration of Network Modeling.

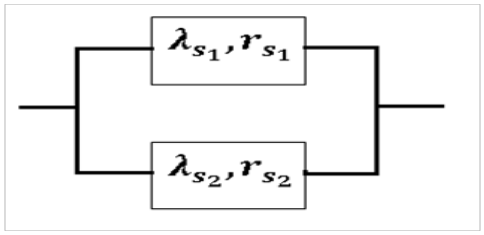

Fig. 7. Block diagram of Parallel Components.

γ_{s1} :outage duration of first series component.
γ_{s1} :outage duration of second series component.
γ_{system} :outage duration of system.

Equation 01, 02, 03 and 04 are generally approximations and are applicable for component failure in transmission and distribution networks. These equations are universally used in reliability evaluation of distribution system [22].

In series network configuration, the probability of availability of path is equivalent to the multiplication of availabilities of individual component. In parallel networks, the probability of an unavailable pathway is equivalent to the multiplication of unavailability of the individual component.

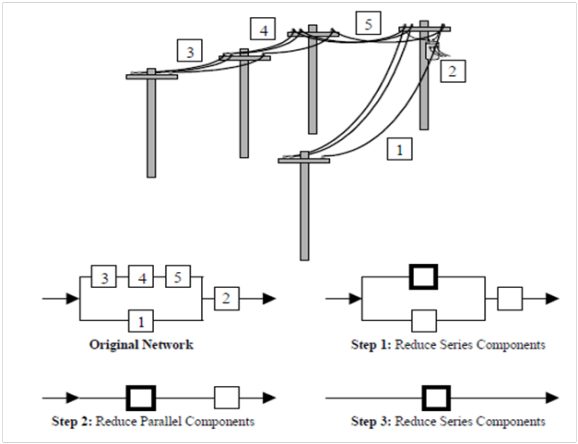

Fig. 8. Reduction of a Series and Parallel Component into Equivalent Network.

C. System Modeling

This research focuses on reliability model of radial distribution network, in which WTG, a DG source, is modeled as

negative load for different reliability tests. However, several DG technologies either renewable or non-renewable energy resources can be modeled as voltage source and uninterrupted power source.

1) Modeling of DG Unit: Modeling DG as a negative load adding reactive power and real power into the network as shown in Fig. 9, whatever the system voltage is, this load will transport power to the system. Provided that DG is connected to a source, it will transfer power to the system in either peak hours or net metering mode. From viewpoint of utility, DG can be modeled as a negative load. While utilities will possibly need DG units for disconnecting it from the system when no utility source is connected, for ensuring safety, permitting faults to clear and avoiding the problems related with islanded operation.

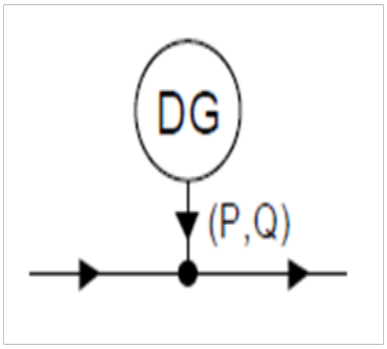

Fig. 9. DG as a Negative Load.

V. Evaluation of Electric Power System Reliability

The Institute of Electrical and Electronic Engineers (IEEE) defines the generally accepted reliability indices in its standard number P1366, Guide for Electric Distribution Reliability Indices. IEEE-P1366 lists several important definitions for reliability including what are momentary interruption events, momentary interruptions and sustained interruptions[20]. These indices are classified as:
1) Load based (point) reliability indices.
2) System based reliability indices.

A. Load Point Reliability Indices

1) Average Failure Rate at Load Point i,λ_i (failure per year)::

$$\lambda_i = \sum_{j \in N_e} \lambda_{e,j}$$

λ_i =Average failure rate at point i.
$\sum$ =Summation function.
N_e=Total number of elements whose fault will interrupt load point i.
$\lambda_{e,j}$ =Average failure rate.

2) Annual Outage Duration at Load Point i,U_i (hour per year):

$$U_i = \sum_{j \in N_e} \lambda_{e,j} . \gamma_{i,j}$$

U_i=Annual outage duration at load point i.
$\sum$ =summation.
$\lambda_{e,j}$ =Average failure rate.
N_e =Total number of elements whose fault will interrupt load point i.
$\gamma_{i,j}$ =Failure duration at load point i due to a failed element j.

3) Average Outage Duration at Load Point i,r_i (hours):

$$\text{Average outage duration at load point } i, \quad \gamma_i = \frac{\text{Annual outage duration at load point } i, U_i}{\text{Average failure rate at load point } i, \lambda_i}$$

B. System based Indices

1) System Average Interruption Frequency Index (SAIFI):

$$SAIFI = \frac{\sum (N_i)}{N_T}$$

$\sum$ =Function used for summation.
N_i=Total number of interrupted customers.
N_T= Total number of customers served.

SAIFI can also be written as:

$$SAIFI = \frac{SAIDI}{CAIDI}$$

2) System Average Interruption Duration Index (SAIDI):

$$SAIDI = \frac{\sum (\gamma_i * N_i)}{N_T}$$

$SAIDI$ = System average interruption duration index.
$\sum$ =Function of summation.
N_i =Total number of customers interrupted.
N_T =Total number of customers served.
γ_i =Restoration time in minutes.

3) Customer Average Interruption Duration Index (CAIDI):

$$CAIDI = \frac{\sum (\gamma_i * N_i)}{N_i}$$

$CAIDI$ = Customer average interruption duration index.
$\sum$ =Function of summation.
N_i =Total number of customers interrupted.
γ_i =Restoration time in minutes.

4) Average Service Availability Index (ASAI):

$$ASAI = \frac{(customer\ hours\ of\ availble\ service)}{Customer\ hours\ demanded}$$

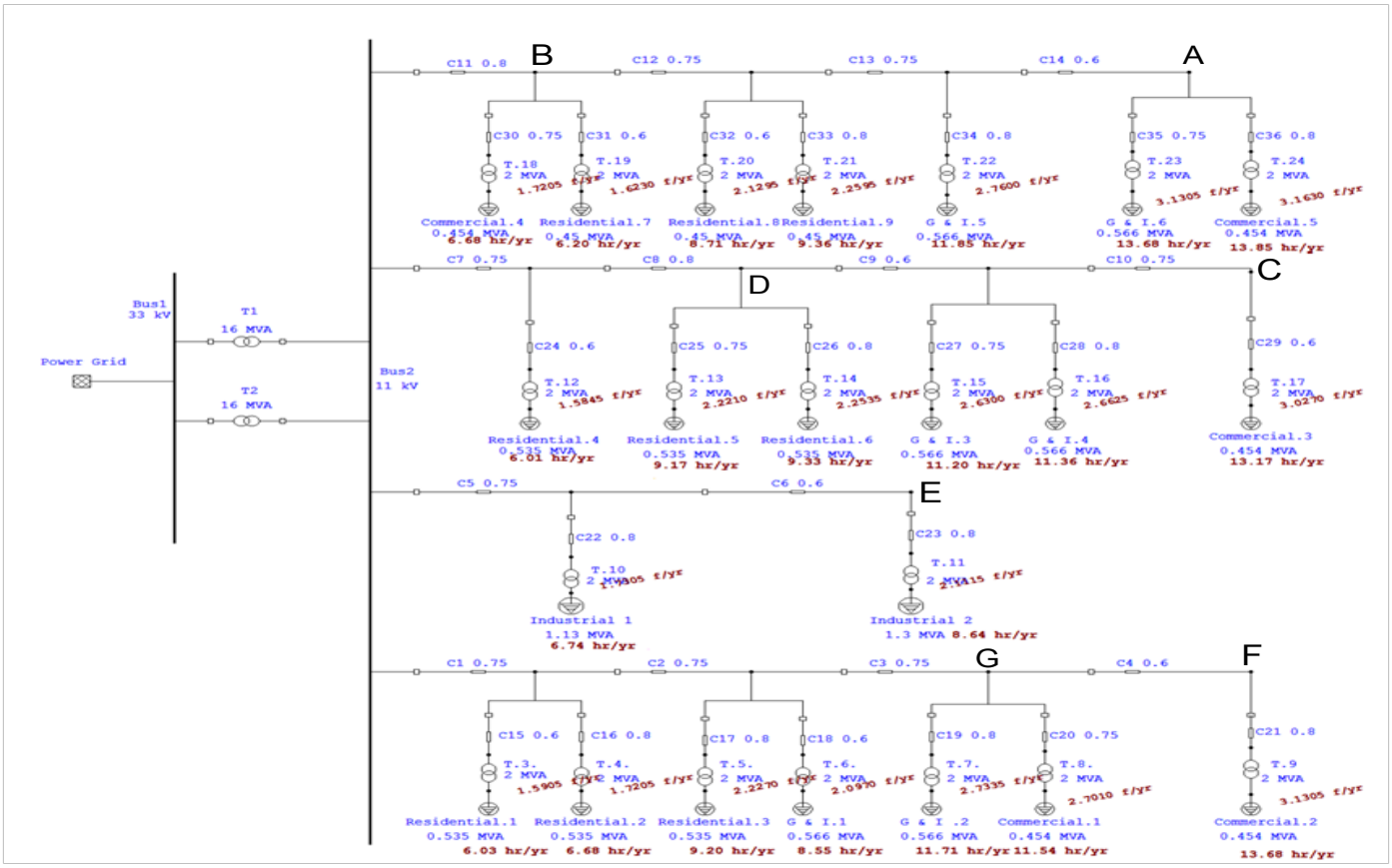

Fig. 10. RBTS bus 2 Modeled in ETAP.

5) Average service unavailability index (ASUI):

$$ASUI = 1 - ASAI$$

VI. Research Methodology

The reliability evaluation of an electric power system is quite a tough job. For the ease of students to make hand calculations and to fully understand the reliability of power system including all the basic components, a test system by Roy Billinton was introduced for educational intention [23]. The distribution system developed by Roy Billinton Test System (RBTS) is used in this research. The RBTS is a six bus distribution test system, consists of two generator buses, five load buses, nine transmission lines, circuit breakers, connecting feeders/conductors, and eleven generation units.This work focuses on DG as a source rather than technology and is assumed that DG is used with its full capacity. Wind turbine generator of 1 MW and 5 MW are considered as DG source, Moreover DG is connected to distribution system with a circuit breaker in order to isolate DG in fault conditions. Reliability data of Wind turbine is based on operational observations.

A. Modeling in ETAP

ETAP software was selected for reliability analysis. Electric Transient Analysis Program (ETAP) is an electrical power system tool which has complete integration of AC and DC systems [24]. The reliability analysis by means of ETAP helps to evaluate distribution system reliability with extremely efficient analytical algorithms, for this purpose RBTS bus 2 as shown in Fig. 10 was modeled and analyzed in ETAP. Fig. 11 shows the flow chart that how results were calculated.

VII. Results and Discussion

Under different scenarios six cases were analyzed which shows diverse impacts of DG on reliability, varying number, size and location of the DG unit(s) and its affect on the reliability of the traditional distribution system were analyzed.

1) Case 01: Reliability Analysis without DG: The data showed in Table 1 is the distance of different load points from feeder, annual outage rate, average outage duration and annual duration. The load near to the feeder experience lesser number of outage durations, on other hand, as the distance of load points increases from feeder the value of outage durations are also increased. This makes the system vulnerable to outages. Table 2 illustrates different system indices of the whole distribution system.

2) Case 02: Reliability Analysis with One DG: After injection of DG in distribution network at point A . The System Reliability indices shows improvement, as the interruption frequency and interruption duration is decreased as presented in Table 3.

3) Case 03: Impact of DG Size on Reliability: Varying the size of DG has no effect on system reliability indices as shown

TABLE I. LOAD POINT INDICIES WITHOUT DG

S.no	Type of customer	Distance from feeder. (km)	Average outage rate. (f/ yr)	Average outage duration. (hr)	Annual outage duration.(hr/ yr)
Residential					
1	Residential 1	1.35	1.5905	3.79	6.0335
2	Residential 2	2.35	2.2535	4.14	9.3335
Commercial					
1	Commercial 2	3.65	3.1305	4.37	13.6825
2	Commercial 4	1.55	1.7205	3.88	6.6835
3	Commercial 5	3.7	3.1630	4.38	13.8450
Industrial					
1	Industrial 2	2.15	2.1115	4.09	8.6355

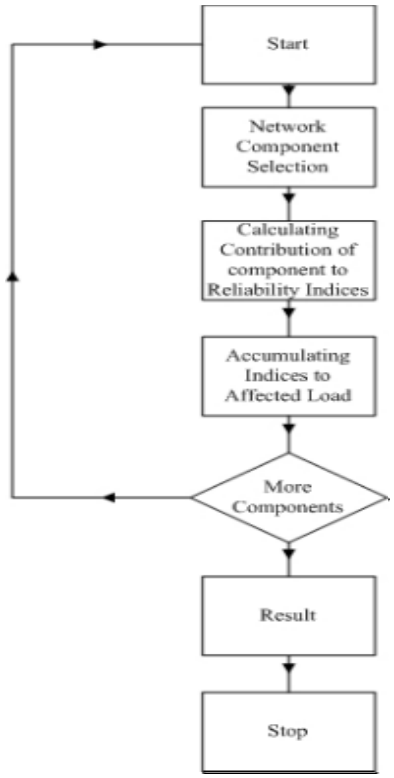

Fig. 11. Flow chart.

TABLE II. SYSTEM INDICIES WITHOUT DG

S no.	System indices	Results
01	SAIFI (f/ Customer. Yr)	1.9772
02	SAIDI (hr/ Customer. Yr)	7.9568
03	CAIDI (hr/ Customer interruption)	4.0240
04	ASAI (pu)	0.9991
05	ASUI (pu)	0.00091

TABLE III. SYSTEM INDICES WITH ONE DG

	At point 'A'	
S no.	System indices	Results
01	SAIFI (f/ Customer. Yr)	1.1979
02	SAIDI (hr/ Customer. Yr)	6.0093
03	CAIDI (hr/ Customer interruption)	5.016
04	ASAI (pu)	0.9993
05	ASUI (pu)	0.00069

TABLE IV. SYSTEM INDICES VARYING SIZE OF DG

	At point 'A'		
S no.	System indices	1MW	5MW
01	SAIFI (f/ Customer. Yr)	1.1979	1.1979
02	SAIDI (hr/ Customer. Yr)	6.0093	6.0093
03	CAIDI (hr/ Customer interruption)	5.016	5.016
04	ASAI (pu)	0.9993	0.9993
05	ASUI (pu)	0.00069	0.00069

TABLE V. SYSTEM INDICES AFTER INJECTING DG AT DIFFERENT LOCATION

	SAIFI	SAIDI	CAIDI	ASAI (pu)	ASUI (pu)
Without DG	1.9772	7.9568	4.024	0.9991	0.00091
At point A	1.1979	6.0093	5.016	0.9993	0.00069
At point B	1.3236	6.6311	5.010	0.9992	0.00076
At point C	1.2041	6.0391	5.015	0.9993	0.00069
At point D	1.2110	6.0721	5.014	0.9993	0.00069
At point E	1.3290	6.6514	5.005	0.9992	0.00076
At point F	1.2537	6.2863	5.014	0.9993	0.00072
At point G	1.2564	6.2997	5.014	0.9993	0.00072

in Table 4 the interruption frequency and interruption duration remains same while changing the capacity of DG unit.

4) Case 04: Injection at Different Locations (Optimum Location): DG has been injected at several different locations and system reliability indices have been recorded individually, Injecting DG at seven different locations in distributed network the indices showed that best or optimum location for injecting DG was Point A. The recorded indices are shown in Table 5.

5) Case 05: Multiple DG Injection at Same Location: Injecting multiple DGs at the same point (i.e point A). Not much variation in system reliability indices were observed comparing them with injection of single DG at same point. Table 6 illustrate this saying.

6) Case 06: Multiple DG injection at Different Locations: Multiple DG were injected at different locations and system reliability indices were recorded. The indices showed that system reliability indices were improved when the DG units were injected at two different point i.e point A and point F. Table 7 depicts the recorded indices. —

TABLE VI. SYSTEM INDICES FOR MULTIPLE DG INJECTION AT SAME LOCATION

	At point 'A'		
S no.	System indices	Single DG	Multiple DG
01	SAIFI (f/ Customer. Yr)	1.1979	1.1980
02	SAIDI (hr/ Customer. Yr)	6.0093	6.0095
03	CAIDI (hr/ Customer interruption)	5.016	5.016
04	ASAI (pu)	0.9993	0.9993
05	ASUI (pu)	0.00069	0.00069

TABLE VII. SYSTEM INDICES FOR MULTIPLE DG INJECTION AT DIFFERENT LOCATIONS

S no.	System indices	Multiple DG at Point A	DG at Point A & F
01	SAIFI	1.1980	1.1224
02	SAIDI	6.0095	5.6428
03	CAIDI	5.016	5.027
04	ASAI (pu)	0.9993	0.9994
05	ASUI (pu)	0.00069	0.00064

VIII. CONCLUSION

Reliability assessment is the most vital element in planning and designing of distribution systems that must function in an economic way with minimum interruption of customer loads. With increase in distributed generation and renewable energy technologies researchers are more interested to analyze its effect on power systems.

In this research work the reliability analysis of radial distribution system with and without distributed generation has been done. The reliability indices depict that interruption frequency and interruption duration of load points were high as the distance of load point increases from feeder. A wind turbine generator as a distributed generation sources was injected in distributed system and different reliability tests were performed. The injection of one distributed generation unit near to load center has showed positive impacts on reliability, while injecting multiple distributed generations at different locations in distribution system has further increased the reliability of distribution system. Results showed that increasing the size of distributed generation Unit from 1 MW to 5 MW does not affect or change the reliability of distribution system. After caring out different reliability tests the optimum location was selected for DG unit to be planted.

From the results it can be concluded that proper injection of distributed generation into distribution system at a proper location increase the reliability of distribution system. Distribution system reliability can further be enhanced by injecting multiple distributed generations at different locations and near to load center s in distribution system.

A. Future Work

In future several DG technologies either renewable or non-renewable energy sources can be modeled as voltage sources and uninterrupted power sources. This research work can also help distribution companies to evaluate the reliability of a real distribution network and also helps the DISCOs to inject distributed generation with most appropriate type, size and in proper location to enhance reliability of distribution system.

REFERENCES

[1] H. Iyer, S. Ray, and R. Ramakumar, "Assessment of distributed generation based on voltage profile improvement and line loss reduction," in *2005/2006 IEEE/PES Transmission and Distribution Conference and Exhibition*. IEEE, 2006, pp. 1171–1176.

[2] P. Chiradeja and R. Ramakumar, "An approach to quantify the technical benefits of distributed generation," *IEEE Transactions on energy conversion*, vol. 19, no. 4, pp. 764–773, 2004.

[3] H. B. Puttgen, P. R. Macgregor, and F. C. Lambert, "Distributed generation: Semantic hype or the dawn of a new era?" *IEEE power and energy magazine*, vol. 1, no. 1, pp. 22–29, 2003.

[4] M. Čepin, *Assessment of power system reliability: methods and applications*. Springer Science & Business Media, 2011.

[5] B. Roy, A. Ronald, and R. Norman, "Reliability evaluation of power systems," 1996.

[6] G. Pepermans, J. Driesen, D. Haeseldonckx, R. Belmans, and W. Dhaeseleer, "Distributed generation: definition, benefits and issues," *Energy policy*, vol. 33, no. 6, pp. 787–798, 2005.

[7] V. M. Quezada, J. R. Abbad, and T. G. S. Roman, "Assessment of energy distribution losses for increasing penetration of distributed generation," *IEEE TRANSACTIONS ON POWER SYSTEMS PWRS*, vol. 21, no. 2, p. 533, 2006.

[8] T. Q. D. Khoa, P. tt Binh *et al.*, "Optimizing location and sizing of distributed generation in distribution systems," in *2006 IEEE PES Power Systems Conference and Exposition*. IEEE, 2006, pp. 725–732.

[9] P. Dondi, D. Bayoumi, C. Haederli, D. Julian, and M. Suter, "Network integration of distributed power generation," *Journal of power sources*, vol. 106, no. 1, pp. 1–9, 2002.

[10] T. Dorji, "Reliability assessment of distribution systems," *Master of Science in Electric Power Engineering, Norwegian University of Science and Technology*, 2009.

[11] M. Al-Muhaini and G. T. Heydt, "Evaluating future power distribution system reliability including distributed generation," *IEEE Transactions on Power Delivery*, vol. 28, no. 4, pp. 2264–2272, 2013.

[12] A. A. Sahito, M. Uqaili, A. Larik, and M. A. Mahar, "Nonlinear controller design for buck converter to minimize transient disturbances," *Science International*, vol. 26, no. 3, pp. 1033–1037, 2014.

[13] A. Apparao and K. Bhashna, "Optimal allocation of dg considering loss minimization and voltage profile using pso."

[14] J. P. Lopes, N. Hatziargyriou, J. Mutale, P. Djapic, and N. Jenkins, "Integrating distributed generation into electric power systems: A review of drivers, challenges and opportunities," *Electric power systems research*, vol. 77, no. 9, pp. 1189–1203, 2007.

[15] B. Das, B. C. Deka, and C. Bimal, "Impact of distributed generation on reliability of distribution system," *IOSR Journal Electrical and Electronics Engineering*, vol. 8, no. 1, pp. 42–50, 2013.

[16] S. Ahmad, S. Sardar, B. Noor, and A. ul Asar, "Analyzing distributed generation impact on the reliability of electric distribution network," *International Journal of Advanced Computer Science & Applications*, vol. 1, no. 7, pp. 217–221, 2016.

[17] P. Mazidi and G. Sreenivas, "Reliability assessment of a distributed generation connected distribution system," *International Journal of Power System Operation and Energy Management (IJPSOEM), Nov*, 2011.

[18] R. E. Brown, *Electric power distribution reliability*. CRC press, 2008.

[19] R. Billinton and S. Jonnavithula, "A test system for teaching overall power system reliability assessment," *IEEE Transactions on Power Systems*, vol. 11, no. 4, pp. 1670–1676, 1996.

[20] Transmission, D. Committee *et al.*, "Ieee guide for electric power distribution reliability indices," *IEEE Std 1366-2003*, 2003.

[21] A. M. L. da Silva, A. M. Cassula, R. Billinton, and L. A. F. Manso, "Integrated reliability evaluation of generation, transmission and distribution systems," *IEE Proceedings - Generation, Transmission and Distribution*, vol. 149, no. 1, pp. 1–6, Jan 2002.

[22] R. Allan *et al.*, *Reliability evaluation of power systems*. Springer Science & Business Media, 2013.

[23] R. Billinton, S. Kumar, N. Chowdhury, K. Chu, K. Debnath, L. Goel, E. Khan, P. Kos, G. Nourbakhsh, and J. Oteng-Adjei, "A reliability test system for educational purposes-basic data," *IEEE Transactions on Power Systems*, vol. 4, no. 3, pp. 1238–1244, 1989.

[24] "Etap," http://www.etap.com/, accessed: 2017-03-15.

Security Issues in the Internet of Things (IoT): A Comprehensive Study

Mirza Abdur Razzaq
Department of Computer Science
Shah Abdul Latif University
Khairpur, Pakistan

Muhammad Ali Qureshi
Department of Telecommunication Engineering
University College of Engineering and Technology
The Islamia University of Bahawalpur, Pakistan

Sajid Habib Gill
Department of Computer Science
NCBA & E Rahim Yar Khan Campus
Rahim Yar Khan, Pakistan

Saleem Ullah
Department of Computer Science & IT
Khwaja Fareed University of Engineering and IT
Rahim Yar Khan, Pakistan

***Abstract*—Wireless communication networks are highly prone to security threats. The major applications of wireless communication networks are in military, business, healthcare, retail, and transportations. These systems use wired, cellular, or adhoc networks. Wireless sensor networks, actuator networks, and vehicular networks have received a great attention in society and industry. In recent years, the Internet of Things (IoT) has received considerable research attention. The IoT is considered as future of the internet. In future, IoT will play a vital role and will change our living styles, standards, as well as business models. The usage of IoT in different applications is expected to rise rapidly in the coming years. The IoT allows billions of devices, peoples, and services to connect with others and exchange information. Due to the increased usage of IoT devices, the IoT networks are prone to various security attacks. The deployment of efficient security and privacy protocols in IoT networks is extremely needed to ensure confidentiality, authentication, access control, and integrity, among others. In this paper, an extensive comprehensive study on security and privacy issues in IoT networks is provided.**

***Keywords*—Internet of Things (IoT); security issues in IoT; security; privacy**

I. Introduction

Internet of Things (IoT) has attracted considerable attention during the past few years. The concept of IoT was firstly proposed by Kevin Ashton in 1999. Due to rapid advancements in mobile communication, Wireless Sensor Networks (WSN), Radio Frequency IDentification (RFID), and cloud computing, communications among IoT devices has become more convenient than it was before. IoT devices are capable of co-operating with one another. The World of IoT includes a huge variety of devices that include smart phones, personal computers, PDAs, laptops, tablets, and other hand-held embedded devices. The IoT devices are based on cost-effective sensors and wireless communication systems to communicate with each other and transfer meaningful information to the centralized system. The information from IoT devices is further processed in the centralized system and delivered to the intended destinations. With the rapid growth of communication and internet technology, our daily routines are more concentrated on a fictional space of virtual world [1]. People can work, shop, chat (keep pets and plants in the virtual world provided by the network), whereas humans live in the real world. Therefore, it is very difficult to replace all the human activities with the fully automated living. There is a bounding limit of fictional space that restricts the future development of internet for better services. The IoT has successfully integrated the fictional space and the real world on the same platform. The major targets of IoT are the configuration of a smart environment and self-conscious independent devices such as smart living, smart items, smart health, and smart cities among others [2]. Nowadays the adoption rate of the IoT devices is very high, more and more devices are connected via the internet. According to appraisal [3], there are 30 billion connected things with approximate 200 billion connections that will generate revenue of approximately 700 billion euros by the year 2020. Now in China, there are nine billion devices that are expected to reach 24 billion by the year 2020. In future, the IoT will completely change our living styles and business models. It will permit people and devices to communicate anytime, anyplace, with any device under ideal conditions using any network and any service [4]. The main goal of IoT is to create Superior world for human beings in future. Fig. 1 shows the concept of IoT with their capabilities.

Unfortunately, the majority of these devices and applications are not designed to handle the security and privacy attacks and it increases a lot of security and privacy issues in the IoT networks such as confidentiality, authentication, data integrity, access control, secrecy, etc. [5]. On every day, the IoT devices are targeted by attackers and intruders. An appraisal discloses that 70% of the IoT devices are very easy to attack. Therefore, an efficient mechanism is extremely needed to secure the devices connected to the internet against hackers and intruders.

The rest of the paper is organized as: Section II discusses IoT applications while Section III provides a brief overview of security requirements followed by security threats in IoT are discussed in Section IV. Section V provides analysis of different attacks and their possible solutions and finally the paper is concluded in Section VI.

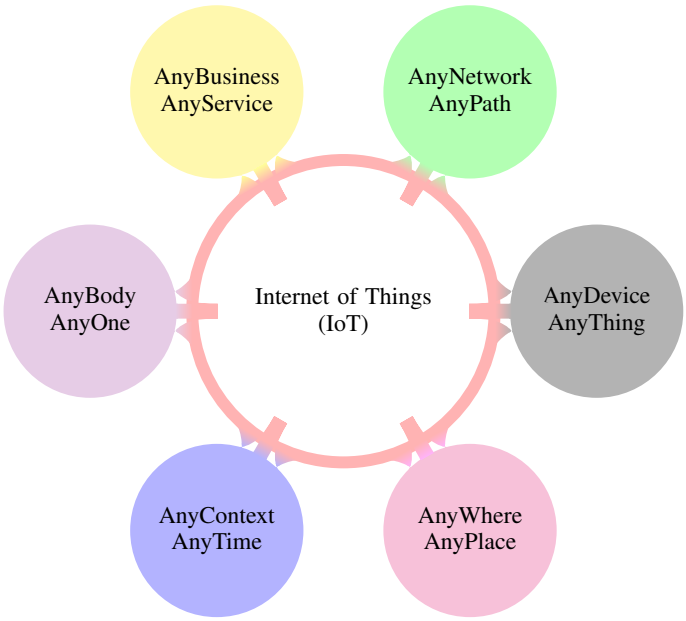

Fig. 1. Definition of IoT.

II. IoT Applications

The main objectives of IoT are the configuration of a smart environment and self-conscious independent devices such as smart living, smart items, smart health, and smart cities among others [2]. The applications of IoT in industries, medical field, and in home automation are discussed in the following section.

A. IoT in Industries

The IoT has provided a fair opportunity to build significant industrial systems and applications [6], in an intelligent IoT transportation system, the authorized person can monitor the existing location and movement of a vehicle. The authorized person can also predict its future location and road traffic. In earlier stage, the term IoT was used to identify unique objects with RFID. Latterly, the researchers relate the term IoT with sensors, Global Positioning System (GPS) devices, mobile devices, and actuators. The acceptance and services of new IoT technologies mainly depend upon the privacy of data and security of information. The IoT permits many things to be connected, tracked and monitored so meaningful information and private data collected automatically. In IoT environment, the privacy protection is a more critical issue as compared to traditional networks because numbers of attacks on IoT are very high.

B. IoT in Personal Medical Devices

The IoT devices are also widely used in healthcare systems for monitoring and assessment of patients [7]. To monitor the medical condition of a patient, Personal Medical Devices (PMDs) are either planted in patients body or it may attach to patients body externally. PMDs are small electronic devices that are becoming very common and popular. The market value of these devices is projected to be around 17 billion dollars by 2019 [8]. These devices use a wireless interface to perform communication with a base station that is further used to read status of the device, medical reports, and change parameters of the device, or update status on the device. Wireless interface causes a lot of security and privacy threats for the patient. The wireless interface of such devices is very easy to cyber-attacks that may jeopardize the patients security, privacy, and safety. In the case of health care, the primary goal is to ensure the security of network in order to prevent the privacy of patient from malicious attacks. When attackers attack mobile devices, they have their predefined goals. Usually, their aim is to steal the information, attack on devices to utilize their resources, or may shut down some applications that are monitoring patients condition.

There are many types of attacks on medical devices that include eavesdropping in which privacy of the patient is leaked, integrity error in which the message is being altered, and availability issues which include battery draining attacks. Some cyber security threats related to security, privacy, and safety of medical data of patient are discussed as follows:

1) PMDs are critical to any task that uses battery power. Hence these devices must support a limited encryption. If the device is a part of different networks then confidentiality, availability, privacy, and integrity will be at high risk.
2) As PMDs have no authentication mechanism for wireless communication. So the information stored in the device may be easily accessed by unauthorized persons.
3) Absence of secure authentication also uncovers the devices to many other security threats that may leads to malicious attacks. A hostile may launch Denial of Service (DoS) attacks.
4) The data of patient is sent over transmission medium which may be altered by unauthorized parties, as a result privacy of a patient may loss.

C. IoT in Smart Home

The IoT smart home services are increasing day by day [9], digital devices can effectively communicate with each other using Internet Protocol (IP) addresses. All smart home devices are connected to the internet in a smart home environment. As the number of devices increases in the smart home environment, the chances of malicious attacks also increase. If smart home devices are operated independently the chances of malicious attacks also decreases. Presently smart home devices can be accessed through the internet everywhere at any time. So, it increases the chances of malicious attacks on these devices.

A smart home consists of four parts: service platform, smart devices, home gateway, and home network as shown in Fig. 2. In the smart home, many devices are connected and smartly shares information using a home network. Consequently, there exists a home gateway that controls the flow of information among smart devices connected to the external network. Service platform uses the services of service provider that deliver different services to the home network.

III. Security Requirements

In IoT, all the devices and people are connected with each other to provide services at any time and at any place. Most

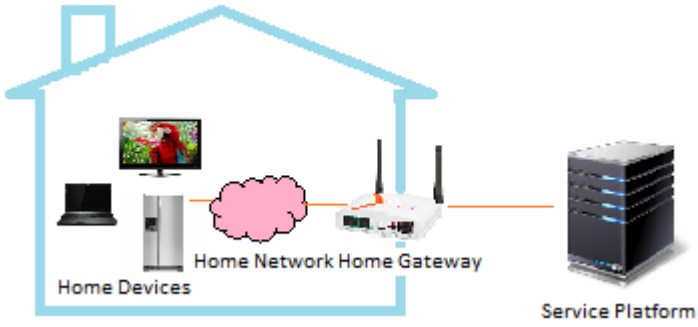

Fig. 2. Elements of a smart home in IoTs.

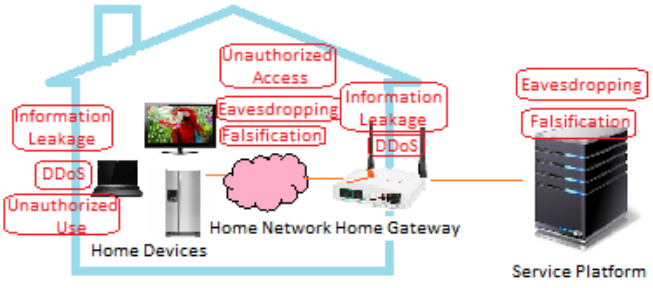

Fig. 3. Threats in smart home in IoTs.

of the devices connected to the internet are not equipped with efficient security mechanisms and are vulnerable to various privacy and security issues e.g., confidentiality, integrity, and authenticity, etc. For the IoT, some security requirements must be fulfilled to prevent the network from malicious attacks [7], [10], [11]. Here, some of the most required capabilities of a secure network are briefly discussed.

- **Resilience to attacks:** The system should be capable enough to recover itself in case if it crashes during data transmission. For an example, a server working in a multiuser environment, it must be intelligent and strong enough to protect itself from intruders or an eavesdropper. In the case, if it is down it would recover itself without intimation the users of its down status.
- **Data Authentication:** The data and the associated information must be authenticated. An authentication mechanism is used to allow data transmission from only authentic devices.
- **Access control:** Only authorized persons are provided access control. The system administrator must control access to the users by managing their usernames and passwords and by defining their access rights so that different users can access only relevant portion of the database or programs.
- **Client privacy:** The data and information should be in safe hands. Personal data should only be accessed by authorized person to maintain the client privacy. It means that no irrelevant authenticated user from the system or any other type of client cannot have access to the private information of the client.

IV. IoT Security, Privacy, Threats and Challenges

The era of IoT has changed our living styles [12]. Although the IoT provides huge benefits, it is prone to various security threats in our daily life. The majority of the security threats are related to leakage of information and loss of services. In IoT, the security threats straightforwardly are affecting the physical security risk. The IoT consists of different devices and platform with different credentials, where every system needs the security requirement depending upon its characteristics. The privacy of a user is also most important part because a lot of personal information is being shared among various types of devices [13], [14]. Hence a secure mechanism is needed to protect the personal information.

Moreover, for IoT services, there are multiple types of devices that perform communication using different networks. It means there are a lot of security issues on user privacy and network layer. User privacy can also be uncovered from different routes. Some security threats in the IoT are as follows:

1) **E2E Data life cycle protection:** To ensure the security of data in IoT environment, end-to-end data protection is provided in a complete network. Data is collected from different devices connected to each other and instantly shared with other devices. Thus, it requires a framework to protect the data, confidentiality of data and to manage information privacy in full data life cycle.
2) **Secure thing planning:** The interconnection and communication among the devices in the IoT vary according to the situation. Therefore, the devices must be capable of maintaining security level. For example, when local devices and sensors used in the home-based network to communicate with each other safely, their communication with external devices should also work on same security policy.
3) **Visible/usable security and privacy:** Most of the security and privacy concerns are invoke by misconfiguration of users. It is very difficult and unrealistic for users to execute such privacy policies and complex security mechanism. It is needed to select security and privacy policies that may apply automatically.

A. Security Threats in Smart Home

Smart home services can be exposed to cyber-attacks because majority of the service provider do not consider security parameters at early stages. The possible security threats in a smart home are eavesdropping, Distributed Denial of Service (DDoS) attacks and leakage of information, etc. Smart home networks are threatened by unauthorized access. The possible security threats to smart home are discussed as follows (see Fig. 3).

1) Trespass: If the smart door lock is effected by malicious codes or it is accessed by an unauthorized party, the attacker can trespass on smart home without smashing the doorway as shown in Fig. 4. The result of this effect could be in the form of loss of life or property. To get rid of such attacks, passwords should be changed frequently that must contain at

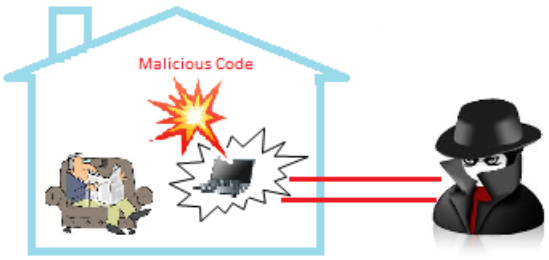

Fig. 4. An example of Trespass attack, hacking a door lock.

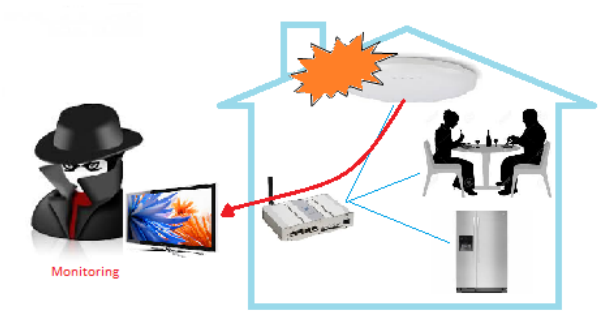

Fig. 5. An example of monitoring personal information.

least ten characters because it is very difficult for attackers to break the long password. Similarly, authentication mechanism and access control may also be applied.

2) Monitoring and personal information leakage: Safety is one of the important purposes of a smart home. Hence there are a lot of sensors that are used for fire monitoring, baby monitoring, and housebreaking, etc. If these sensors are hacked by an intruder then he can monitor the home and access personal information as shown in Fig. 5. To avoid from this attack, data encryption must be applied between gateway and sensors or user authentication for the detection of unauthorized parties may be applied.

3) DoS/DDoS: Attackers may access the smart home network and send bulk messages to smart devices such as Clear To Send (CTS) / Request To Send (RTS). They can also attack targeted device by using malicious codes in order to perform DoS attacks on other devices that are connected in a smart home as shown in Fig. 6. As a result, smart devices are unable to perform proper functionalities because of draining resources due to such attacks. For avoidance from this attack, it is very important to apply authentication to block and detect unauthorized access.

4) Falsification: When the devices in smart home perform communication with the application server, the attacker may collect the packets by changing routing table in the gateway as shown in Fig. 7. Although the SSL (secure socket layer) technique is applied, an attacker can bypass the forged certificate. In this way, the attacker can misinterpret the contents of data or may leak the confidentiality of data. To secure the smart home network from this attack, SSL technique with proper authentication mechanism should be applied. It is also important to block unauthorized devices that may try to access smart home network.

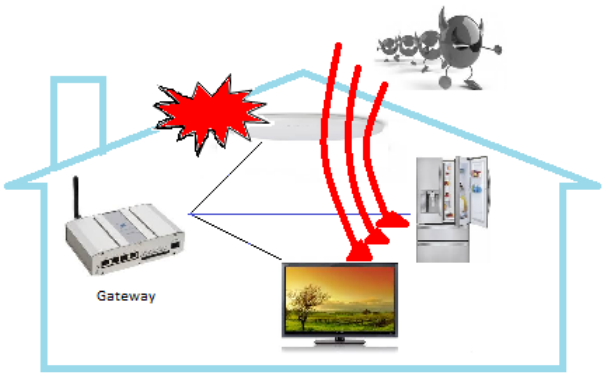

Fig. 6. An example of DDoS attack.

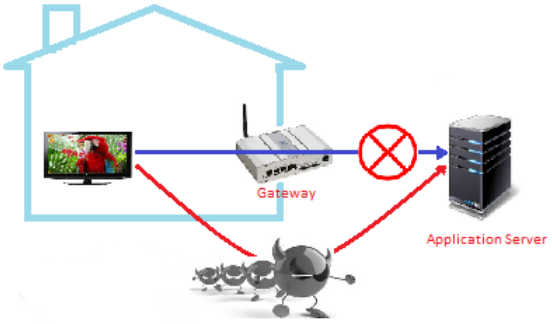

Fig. 7. An example of falsification.

The IoT is a concept that depicts future where the physical objects connected to internet communicate with each other and identify themselves for other devices [15]. The IoT system consists of smart objects, smartphones, tablets and intelligent devices etc. as shown in Fig. 8. Such systems use RFID, Quick Response (QR) codes or wireless technology to perform communication between different devices.

The IoT helped to build connections from human to human, human to physical objects, and physical object to other physical objects. As per appraisal from IDC, there will be 30 billion internet connected devices by 2020. This rapid growth of internet data needs more valuable and secure network.

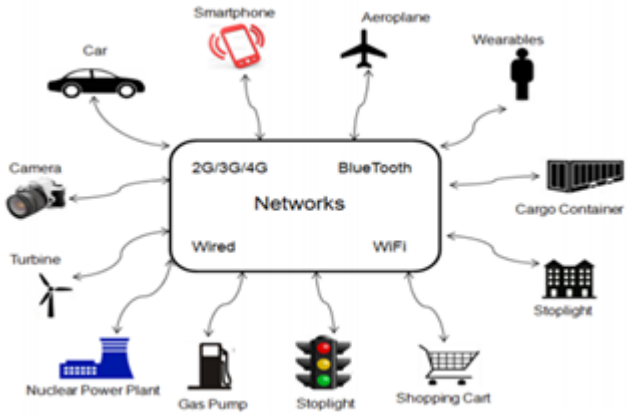

Fig. 8. Example of IoT system [16].

B. IoT Challenges

The security concern is the biggest challenge in IoT. The application data of IoT could be industrial, enterprise, consumer or personal. This application data should be secured and must remain confidential against theft and tampering. For example, the IoT applications may store the results of a patients health or shopping store. The IoT improve the communication between devices but still, there are issues related to the scalability, availability and response time. Security is a concern where the data is securely transmitted over the internet. While transporting the data across international border, safety measure act may be applied by government regulation such as Health Insurance Portability and Accountability (HIPA) act. Among different security challenges, the most important challenges relevant to IoT are discussed.

1) ***Data Privacy****:* Some manufacturers of smart TVs collect data about their customers to analyze their viewing habits so the data collected by the smart TVs may have a challenge for data privacy during transmission.

2) ***Data Security****:* Data security is also a great challenge. While transmitting data seamlessly, it is important to hide from observing devices on the internet.

3) ***Insurance Concerns****:* The insurance companies installing IoT devices on vehicles collect data about health and driving status in order to take decisions about insurance.

4) ***Lack of Common Standard****:* Since there are many standards for IoT devices and IoT manufacturing industries. Therefore, it is a big challenge to distinguish between permitted and non-permitted devices connected to the internet.

5) ***Technical Concerns****:* Due to the increased usage of IoT devices, the traffic generated by these devices is also increasing. Hence there is a need to increase network capacity, therefore, it is also a challenge to store the huge amount of data for analysis and further final storage.

6) ***Security Attacks and System Vulnerabilities****:* There has been a lot of work done in the scenario of IoT security up till now. The related work can be divided into system security, application security, and network security [17].

a) System Security: System security mainly focuses on overall IoT system to identify different security challenges, to design different security frameworks and to provide proper security guidelines in order to maintain the security of a network.

b) Application security: Application Security works for IoT application to handle security issues according to scenario requirements.

c) Network security: Network security deals with securing the IoT communication network for communication of different IoT devices.

In the next section, the security concerns regarding IoT are discussed. The security attacks are categorized into four broad classes.

V. Analysis of Different Types of Attacks and Possible Solutions

The IoT is facing various types of attacks including active attacks and passive attacks that may easily disturb the functionality and abolish the benefits of its services. In a passive attack, an intruder just senses the node or may steal the information but it never attacks physically. However, the active attacks disturb the performance physically. These active attacks are classified into two further categories that are internal attacks and external attacks. Such vulnerable attacks can prevent the devices to communicate smartly. Hence the security constraints must be applied to prevent devices from malicious attacks. Different types of attack, nature/behavior of attack and threat level of attacks are discussed in this section. Different levels of attacks are categorized into four types according to their behavior and propose possible solutions to threats/attacks.

1) **Low-level attack:** If an attacker tries to attack a network and his attack is not successful.
2) **Medium-level attack:** If an attacker/intruder or an eavesdropper is just listening to the medium but dont alter the integrity of data.
3) **High-level attack:** If an attack is carried on a network and it alters the integrity of data or modifies the data.
4) **Extremely High-level attack:** If an intruder/attacker attacks on a network by gaining unauthorized access and performing an illegal operation, making the network unavailable, sending bulk messages, or jamming network.

The Table I presents different types of attacks, their threat levels, their nature/behavior, and possible solution to handle these attacks.

VI. Conclusion

The main emphasis of this paper was to highlight major security issues of IoT particularly, focusing the security attacks and their countermeasures. Due to lack of security mechanism in IoT devices, many IoT devices become soft targets and even this is not in the victim's knowledge of being infected. In this paper, the security requirements are discussed such as confidentiality, integrity, and authentication, etc. In this survey, twelve different types of attacks are categorized as low-level attacks, medium-level attacks, high-level attacks, and extremely high-level attacks along with their nature/behavior as well as suggested solutions to encounter these attacks are discussed.

Considering the importance of security in IoT applications, it is really important to install security mechanism in IoT devices and communication networks. Moreover, to protect from any intruders or security threat, it is also recommended not to use default passwords for the devices and read the security requirements for the devices before using it for the first time. Disabling the features that are not used may decrease the chances of security attacks. Moreover, it is important to study different security protocols used in IoT devices and networks.

TABLE I. A SUMMARY OF DIFFERENT TYPES OF ATTACKS AND THEIR THREAT LEVELS, THEIR NATURE AND SUGGESTED SOLUTIONS

Type	Threat level	Behavior	Suggested Solution
Passive	Low	Usually breach data confidentiality. Examples are passive eavesdropping and traffic analysis. Hostile silently listen the communication for his own benefits without altering the data.	Ensure confidentiality of data and do not allow an attacker to fetch information using symmetric encryption techniques.
Man in the Middle	Low to Medium	Alteration and eavesdropping are the examples of this attack. An eavesdropper can silently sense the transmission medium and can modify the data if encryption is not applied and steal the information that is being transmitted. Hostile may also manipulate the data.	Apply data confidentiality and proper integration on data to ensure integrity. Encryption can be also applied so that no one can steal the information or modify the information or encode the information before transmission.
Eavesdropping	Low to Medium	The information content may be lost by an eavesdropper that silently senses the medium. For example in medical environment, privacy of a patient may be leaked.	Apply encryption on all the devices that perform communication.
Gathering	Medium to High	Occurs when data is gathered from different wireless or wired medium. Examples are skimming, tampering and eavesdropping. Data is being collected to detect messages. Messages may also be altered.	Encryption can be applied to prevent this kind of attack. Identity based method and message authentication code can also be applied in order to prevent the network from such malicious attacks.
Active	High	Effects confidentiality and integrity of data. Hostile can alter the integrity of messages, block messages, or may re-route the messages. It could be an internal attacker.	Ensure both confidentiality and integrity of data. To maintain data confidentiality, symmetric encryption can be applied. An authentication mechanism may be applied to allow data access to only authorized person.
Imitation	High	It impersonate for an unauthorized access. Spoofing and cloning are the examples of this attack. In spoofing attack a malicious node impersonate any other device and launch attacks to steal data or to spread malware. Cloning can re-write or duplicate data.	To avoid from spoofing and cloning attacks, apply identity based authentication protocols. Physically unclonable function is a countermeasure for cloning attack.
Privacy	High	Sensitive information of an individual or group may be disclosed. Such attacks may be correlated to gathering attack or may cause an imitation attack that can further lead to exposure of privacy.	Apply anonymous data transmission. Transmit sample data instead of actual data. Can also apply techniques like ring signature and blind signature.
Interruption	High	Affects availability of data. This makes the network unavailable.	Applying authorization, only authorized users are allowed to access specific information to perform certain operation.
Routing diversion	High	Only the route is diverted showing the huge traffic and the response time increased.	Ensure connectivity based approach so no route will be diverted.
Blocking	Extremely High	It is type of DoS, jamming, or malware attacks. It sends huge streams of data which may leads to jamming of network, similarly different types of viruses like Trojan horses, worms, and other programs can disturb the network.	Turn on the firewall, apply packet filtering, anti-jamming, active jamming, and updated antivirus programs in order to protect the network from such attacks.
Fabrication	Extremely High	Affects the authenticity of information. Hostile can inject false data and can destroy the authenticity of information.	Data authenticity can be applied to ensure that no information is changed during the transmission of data.
DoS	Extremely High	Malicious user may modify the packets or resend a packet again and again on network. User can also send bulk messages to devices in order to disturb the normal functionalities of devices.	Apply cryptographic techniques to ensure security of network. Apply authenticity to detect the malicious user and block them permanently. In this way, the network is prevented from damage.

REFERENCES

[1] J. S. Kumar and D. R. Patel, "A survey on internet of things: Security and privacy issues," *International Journal of Computer Applications*, vol. 90, no. 11, 2014.

[2] M. Abomhara and G. M. Køien, "Security and privacy in the internet of things: Current status and open issues," in *Privacy and Security in Mobile Systems (PRISMS), International Conference on*. IEEE, 2014, pp. 1–8.

[3] S. Chen, H. Xu, D. Liu, B. Hu, and H. Wang, "A vision of iot: Applications, challenges, and opportunities with china perspective," *IEEE Internet of Things journal*, vol. 1, no. 4, pp. 349–359, 2014.

[4] L. Atzori, A. Iera, and G. Morabito, "The internet of things: A survey," *Comput. Netw.*, vol. 54, no. 15, pp. 2787–2805, Oct 2010.

[5] M. M. Hossain, M. Fotouhi, and R. Hasan, "Towards an analysis of security issues, challenges, and open problems in the internet of things," in *Services (SERVICES), 2015 IEEE World Congress on*. IEEE, 2015, pp. 21–28.

[6] L. Da Xu, W. He, and S. Li, "Internet of things in industries: A survey," *IEEE Transactions on industrial informatics*, vol. 10, no. 4, pp. 2233–2243, 2014.

[7] L. M. R. Tarouco, L. M. Bertholdo, L. Z. Granville, L. M. R. Arbiza, F. Carbone, M. Marotta, and J. J. C. de Santanna, "Internet of things in healthcare: Interoperatibility and security issues," in *Communications (ICC), IEEE International Conference on*. IEEE, 2012, pp. 6121–6125.

[8] A. Mohan, "Cyber security for personal medical devices internet of things," in *Distributed Computing in Sensor Systems (DCOSS), 2014 IEEE International Conference on*. IEEE, 2014, pp. 372–374.

[9] S. Yoon, H. Park, and H. S. Yoo, "Security issues on smarthome in iot environment," in *Computer Science and its Applications*. Springer, 2015, pp. 691–696.

[10] R. H. Weber, "Internet of things–new security and privacy challenges," *Computer law & security review*, vol. 26, no. 1, pp. 23–30, 2010.

[11] S. Babar, P. Mahalle, A. Stango, N. Prasad, and R. Prasad, "Proposed security model and threat taxonomy for the internet of things (iot)," in *International Conference on Network Security and Applications*. Springer, 2010, pp. 420–429.

[12] Y. H. Hwang, "Iot security & privacy: threats and challenges," in *Proceedings of the 1st ACM Workshop on IoT Privacy, Trust, and Security*. ACM, 2015, pp. 1–1.

[13] M. A. Qureshi, A. Aziz, B. Ahmed, A. Khalid, and H. Munir, "Comparative analysis and implementation of efficientdigital image watermarking schemes," *International Journal of Computer and Electrical Engineering*, vol. 4, no. 4, p. 558, 2012.

[14] M. Abdur Razzaq, R. A. Sheikh, A. Baig, and A. Ahmad, "Digital image security: Fusion of encryption, steganography and watermarking," *International Journal of Advanced Computer Science and Applications (IJACSA)*, vol. 8, no. 5, 2017.

[15] S. Singh and N. Singh, "Internet of things (iot): Security challenges, business opportunities & reference architecture for e-commerce," in *Green Computing and Internet of Things (ICGCIoT), 2015 International Conference on*. IEEE, 2015, pp. 1577–1581.

[16] K. Rose, S. Eldridge, and L. Chapin, "The internet of things: An overview," *The Internet Society (ISOC)*, pp. 1–50, 2015.

[17] H. Ning, H. Liu, and L. T. Yang, "Cyberentity security in the internet of things," *Computer*, vol. 46, no. 4, pp. 46–53, 2013.

A Two-Stage Classifier Approach using RepTree Algorithm for Network Intrusion Detection

Mustapha Belouch
Laboratory of Applied Mathematics and Informatics, FSTG, Cadi Ayyad University, Marrakesh, Morocco

Salah El Hadaj
National School of Trade and Management Cadi Ayyad University, Marrakesh, Morocco

Mohamed Idhammad
LabSIV, Department of Computer Science, FSA, Ibn Zohr University Agadir, Morocco

***Abstract*—In this paper, we present a two-stage classifier based on RepTree algorithm and protocols subset for network intrusion detection system. To evaluate the performance of our approach, we used the UNSW-NB15 data set and the NSL-KDD data set. In first phase our approach divides the incoming network traffics into three type of protocols TCP, UDP or Other, then classifies into normal or anomaly. In second stage a multiclass algorithm classify the anomaly detected in the first phase to identify the attacks class in order to choose the appropriate intervention. The number of features is reduced from over 40 to less than 20 features, according to the protocol, using feature selection techniques. The detection accuracy of 88,95% and 89,85% was achieved on the complete UNSW-NB15 and NSL-KDD data set, respectively using individual classifier, results are better as compared to the recent work on these data sets.**

***Keywords*—Intrusion detection; REPTree; UNSW-NB15; NSL-KDD**

I. Introduction

The emerging Internet of Things together with the rapid growth of computer networks, connected devices, web applications and cloud computing, highlight now, more than ever, the need for accurate and efficient network security. With the aim to protect confidentiality, integrity and availability against the numerous threats and cyber-attacks, firewalls, authentication methods, intrusion detection and prevention systems have been developed over the years.

An Intrusion Detection System (IDS) is used to identify an unauthorized or malicious action which can compromise the confidentiality, integrity or availability of an information resource [1]. In case of such a detection, the IDS requires the network administrator to intervene. An IDS can be classified based on the type of intrusions that detects with the two primary ones being a misuse intrusion and an anomaly based one. A misuse detection algorithm can only detect known attacks based on the stored intrusion database signature. In an anomaly based detection system, a trained algorithm creates a model of normal activities and activities that deviate from these models are classified as an anomaly [2]. While a misuse or signature based detection is preferred for commercial products due to its high predictability and accuracy, an anomaly detection system is considered as a more effective way to address novel attacks [3].

Unfortunately, modern attacks are continuously changing and enable diverse intrusion mechanisms. The attacks are becoming more intelligent and self-adaptable, able to deal with the current securities of conventional network administrations. This sophistication in threats is very dynamic, which in turn makes it critical for newer security measure adoptions.

An efficient, accurate and real-time IDS is required to present low false positive ratio, high true positive ratio and at the same time entail low detection and response time and maintain a high detection attack rate. Detection response time and overhead are two of the most challenging issues of a modern IDS since computer networks and data information are continuously changing and increasing, making a real-time intrusion detection is a critical feature of a modern IDS [4].

For evaluating the efficiency of an IDS, a modern comprehensive data set that contains contemporary normal and attack activities is required [5]. By analysing an IDSs response to various important outbound and inbound traffic, critical information can be extracted and efficient training of an IDS can be achieved. The NSL-KDD dataset which is an improved version of the original KDDCUP'99 dataset [3], and the UNSW-NB15 is a modern datasets with realistic attacking and normal activities [6].

The proposed anomaly based IDS uses machine learning algorithms for intrusion detection and prediction. Binary and multi-class classification is performed for both normal/attack activities and attack possible states. A true negative state (TN) is considered when the IDS identifies an activity as a normal one with the actual activity being normal. A false positive (FP) case is considered when the IDS identifies an activity as an attack but the actual activity is a normal one. A false positive (FP) is a false alarm, and in a false negative (FN) situation, which is the most critical one, the IDS fails to identify an actual attack.

The remainder of this paper is structured as: Section 2 presents related works currently used in the domain. Section 3 describes the proposed method and the techniques and algorithms used for our approach. Experimental and comparison results are provided in Section 4. Finally, Section 5 provides the final conclusions.

II. Related Work

Since Denning firstly proposed an intrusion detection model [7], many research efforts have been focused on how to effectively and accurately develop most advanced and modern

detection models. Artificial intelligence and machine learning techniques were exploited to identify the underlying patterns and models utilizing training datasets. The most commonly used methods are focused on rule based induction, classification and data clustering.

Based on a previous study [8], many detection algorithms reported high detection rates with relative low false positives. By examining specific datasets such as the KDDCUP'99 one [3], two critical issues can be identified. Firstly, the KDD dataset includes a huge number of redundant records, which causes a significant bias in the learned algorithms towards the most frequent records. Secondly, the difficulty level of the records is quite questionable since about 98% of the records in the train set and 86% of the records in the test set are correctly classified within all the 21 learners.

The new version of KDD dataset, the NSL-KDD, is publicly available and although this dataset still suffers in some of the issues discussed by McHugh [9] it can be considered as an adequate benchmark for evaluating intrusion detection methods. A standard KDDTrain+ and KDDTest+ is presented in [3], in order to train and test algorithms in such a way that researchers can easily compare their results. In this work, we compare our proposed method with other two state-of-the-art methods using the same and complete dataset.

In [6], a recent dataset, the UNSW-NB15, includes real-world normal and abnormal network traffic in a synthetic environment. This dataset was utilized in [5] for statistical and evaluation purposes by comparing five different algorithms DT, LR, NB, ANN, and EM clustering, for measuring their performance in terms of accuracy and False Alarm Rate (FAR) against the KDD99 dataset. The evaluation results showed that the DT technique achieved the best efficiency. Furthermore, the results of the two datasets were also compared showing that the efficiency techniques using the KDD99 data set were better than when using the UNSW-NB15 dataset. As a consequence, the UNSW-NB15 dataset can be considered more complex and a better representative of the modern attack and normal network traffic, making it more appropriate for the evaluation of existing and the proposed NIDS methods.

Many researchers have chosen the NSL-KDD dataset since it is publicly available. A binary classifier is used in [4], [10]–[14] to identify the incoming network traffic as normal or attack. On the other side, some works propose a multi-class classifier for classifying the incoming network traffic into five categories; normal, DoS, U2R, R2L or Probe [15]–[24]. In [12], [17], [20], [23], [25], researchers used a random portion of the NSL-KDD for the training and testing dataset but without clearly denoting which subpart of the NSL-KDD was used (KDDTrain+ or KDDTest+). As a result, the comparison of these methods is inefficient because of the different used datasets for both the training and testing. Other works report the use of the same datasets for training and testing allowing a high accuracy results from 94,7% to 99,7% [12], [26].

The work in [10] utilizes a fuzzy classification over the NSL-KDD using the KDDTrain+ and KDDTest+ for training and testing, respectively, without discrimination of the attack types, with an overall achieved accuracy of 82,74%. In [27], three types of detection agents were generated according to TCP, UDP and ICMP protocols with a reported accuracy rate at 91.21% on the KDDCUP'99 dataset. After preprocessing, 32 attributes for the TCP detection agent were selected, 21 attributes for the UDP detection agent and 18 attributes for the ICMP detection agent were chosen. The training time of the proposed method was 194 seconds. In [13], the NSL-KDD was divided to TCP, UDP and ICMP and feature selection was applied, with a reported low accuracy only in the UDP subset.

A number of researchers have employed different feature selection techniques to reduce the number of features and to eliminate irrelevant features from the NSL-KDD data set. The work in [13] combines information gain and a genetic algorithm for selecting 17, 10 and 5 features for the TCP, UDP and ICMP, respectively. A deep belief network, a gain ration and a chi-square were used to select only 13 features based on the proposed work in [15]. Principal component analysis was also used in [19] to reduce the selected features to 23. The authors in [24] apply a combining classifier with NBTree and RandomTree algorithm in the NSL-KDD dataset for detecting the normal and attack traffic with an achieved accuracy of 89,24% along 41 attributes. In [5], a different multiclass classifier is applied to identify normal traffic or nine attack types: Fuzzers, Analysis, Backdoor, DoS, Exploit, Generic, Reconnaissance, Shellcode and Worm. The highest result of 85,56% was achieved using a Decision Tree algorithm with all the attributes.

III. Proposed Research Method

The proposed method introduces a novel approach of model creation for better results in terms of accuracy and training time using individual classifiers instead of combining multiple algorithms. The system architecture is explained throughout this Section along with a the data preprocessing techniques and the classification algorithm. A detailed analysis of the NSL-KDD and UNSW-NB15 datasets that were exploited in the training and testing of the proposed model are presented in the experimental section.

A. Proposed Architecture

The architecture of the proposed approach is shown in Fig. 1 where the intrusion detection model is based on two main stages and on a Reduced Error Pruning Tree (REPTree) algorithm for classification and identification of the incoming network traffic.

In the first stage, the incoming traffic flow is firstly classified upon its protocol as TCP, UDP and other. The reason for such protocol classification lays on the different protocol formats which subsequently defines the different needed features for each one. Data pre-processing is applied to each of the three subsets to eliminate any unrelated features and noisy outliers. The network traffic is defined as normal or attack in this stage, in order to speed up the control of the network.

In the second stage, a pre-trained multiclass classifier is launched whenever an attack was identified by the first classifier for identifying the attack type and providing the appropriate response.

In a network traffic dataset the distribution of connections of various protocols is not even. Since connections in some protocols are more frequent against others, this protocol imbalance affects the pre-processing. The proposed TCP, UDP and

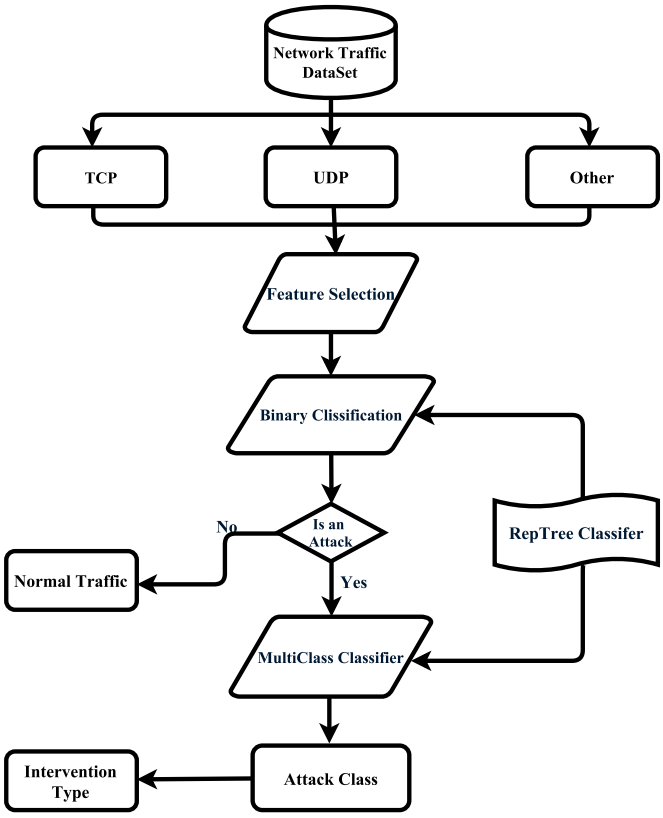

Fig. 1. Proposed architecture.

Other protocol discrimination reduces this effect of protocol imbalance in the dataset.

Feature selection is used also to reduce the size of the analyzed dataset through deleting the unrelated, redundant or irrelevant features. The combination of information gain and consistency through an evolutionary search method was used for the proposed feature selection. Since attributes are filtered by measuring the information gain with respect to the class, the required resources for dataset tuple classification are minimized. The information required conveyed by a tuple of a probability distribution D is given by:

$$Info(D) = -\sum_{i=1}^{\infty} p_i log(p_i) \quad (1)$$

Where, P_i is the probability that an arbitrary tuple D belongs to a class C_i and Info (D) is the entropy of the tuple in D. If we partition a set of samples T on the basis of a non-categorical attribute X into sets $T_1, T_2, \ldots T_m$, then the information needed to identify the class of an element of T is given by:

$$Info(X,T) = \sum_{i=1}^{m} \frac{|T_i|}{|T|} \times Info(T_i) \quad (2)$$

The information gain, $Gain(X,T)$, is then defined as:

$$Gain(X,T) = Info(T) - Info(X,T) \quad (3)$$

TABLE II. DISTRIBUTION OF ATTACKS IN EACH PROTOCOL ON DATASETS

Data set		CLASS	TCP	UDP	Other	Total
NSL-KDD	Training	DoS	42,188	892	2,847	58,630
		Probe	5,857	1,664	4,135	
		U2R	49	3	0	
		R2L	995	0	0	
	Testing	Dos	6,739	14	706	12,832
		Probe	1,864	317	240	
		U2L	67	0	0	
		L2R	2,367	514	4	
UNSW-NB15	Training	Backdoor	272	28	1,446	83,341
		Analysis	564	0	1,436	
		Fuzzers	11,761	4,945	1,478	
		Shellcode	557	576	0	
		Reconnaissance	5,100	3,586	1,805	
		Exploits	19,689	624	13,080	
		DoS	2,281	358	9,625	
		Worms	115	15	0	
		Generic	486	39,229	285	
	Testing	Backdoor	51	6	526	45,332
		Analysis	58	0	619	
		Fuzzers	3,713	1,098	1251	
		Shellcode	193	185	0	
		Reconnaissance	1,865	1,304	327	
		Exploits	7,754	250	3,128	
		DoS	1,055	169	2,865	
		Worms	38	6	0	
		Generic	520	18,303	48	

A ranker algorithm ranks the features in the data set based on their redundancy and relevancy and allowed us to select the appropriate number of features based on our requirements.

To evaluate the performance we used the 10-fold cross validation technique. After randomly dividing the training dataset into 10 distinct parts, the model is trained with 9 parts and one part is selected for testing in each iteration. The value of 10 was chosen empirically due to its adequate performance in estimation error, low bias, low overfitting and low variance.

B. Reduced Error Pruning Tree

Decision tree classifiers like ID3, C4.5, CART, build a decision tree model based on instances of the training dataset. The root and the internal nodes in a decision tree represent the attributes and the leaf nodes represent the classes. However, a decision tree classifier can generate large decision trees that are overfitted to the training set. This effect limits the performance of the classifier and requires more resources in terms of memory allocation. This issue was solved by optimizing the size of the decision tree after applying pruning. The pruning, known also as reduced error pruning, was achieved by the method proposed by Quinlan [28]. While traversing the internal nodes from downwards to upwards, a procedure that checks and replaces each internal node with the most frequent class is initiated, without affecting the trees accuracy. The procedure continues pruning the nodes until any further pruning would decrease the accuracy.

REPTree is considered a fast decision tree learner which builds a decision/regression tree using information gain as the splitting criterion, and prunes it using the reduced error pruning method. Reduced Error Pruning results in a more accurate and simple classification tree, even in cases with large amount of training and testing data.

IV. EXPERIMENTS AND RESULTS

To evaluate the performance of our proposed two stage classifier, a series of experiments on the NSL-KDD and the

TABLE I. NORMAL / ATTACK NSL-KDD AND UNSW-NB15

Data Set		TCP		UDP		Other		Total
		Normal	Attack	Normal	Attack	Normal	Attack	
NSL-KDD	Training	53,600	49,089	12,434	2,559	1,309	6,982	125,973
	Testing	7,842	11,038	1,776	845	93	950	22,544
UNSW-NB15	Training	39,121	40,825	13,922	49,361	2,957	29,155	175,341
	Testing	27,848	15,247	8,097	21,321	1,055	8,764	82,332

TABLE III. THE SELECTED FEATURES FOR EACH PROTOCOL

Data set	Protocol	Selected Features	No. of selected features
NSL-KDD	TCP	2,4,5,32,33,34,36,37,39	9
	UDP	2,4,5,7,22,28,29,32,33,34,35,39	12
	Other	2,34,5,28,32	6
UNSW-NB15	TCP	1,3,5,7,8,12,16,19,21,22,24,26,27, 28,30,31,34,35,36,40	20
	UDP	6,7,8,9,10,11,12,13,17,27,32,35	12
	Other	6,7,8,9,10,11,12,13,17,27,32,35	12

TABLE VIII. PERFORMANCE COMPARISON ON NSL-KDD

Classifier	Accuracy	Train (s)	Test (s)
NBTree+RandomTree [24]	89.24	50.29	0.93
REPTree	**89.85**	**1.17**	**0.24**

TABLE IX. PERFORMANCE COMPARISON ON UNSW-NB15

Classifier	Accuracy	Train (s)	Test (s)
Decision Tree [5]	85.56	7.66	0.84
REPTree	**88.95**	**2.69**	**0.37**

UNSW-NB15 dataset were performed. In these experiments, we implemented and evaluated the proposed methods in the Weka data mining software on a 2.5 GHz Intel Core i5 CPU with 4 GB RAM.

The NSL-KDD dataset includes 41 features with normal classes and 4 types of attacks: Probe, R2L, U2R and Denial of Service Attack (DoS) [3]. The generated datasets, KDDTrain+ and KDDTest+ include 125,973 and 22,544 instances, respectively. During the performance evaluation of the first classifier we used binary class labels (normal or attack) as shown in Table I, where for the second classifier we selected only attack-type labeled classes, as shown in Table II.

The UNSW-NB 15 dataset involves nine attack categories and 49 features [6]. This dataset was divided into 175,341 and 82,332 records for training and testing, as shown in Tables I and II, respectively.

Both used datasets NSL-KDD and UNSW-NB 15 are publicly available, the volume and distribution of the training and testing dataset are presented in Table I for the binary classification and in Table II for the multi-class classification for each protocol.

For the comparison results, we employed also four different learning algorithms for the training and testing dataset in order to compare them against the REPTree classifier. We used all 40 features of the NSL-KDD dataset and 42 features of the UNSW-NB15, where the overall accuracy and the performance of the classification is expressed in terms of precision and training time, respectively. The selected features are given in Table III for each protocol.

An assessment was also performed utilizing a reduced dataset (KDDTrain+ and KDDTest+ datasets from the NSL-KDD and UNSW-NB15) since computational speed is essential for IDS systems running on routers and network appliances. The training and testing was conducted using the reduced feature set shown in Table III for each dataset and for each protocol. The features were selected based on the information gain feature ranking and consistency through an evolutionary search method. The results are presented in Tables IV to VII where the classification accuracy for the selected features is proved to be better when compared with the all features approach.

Furthermore, we performed four experimental series over the two datasets based on the selected features of Table III. We also compared the results with decision tree, neural network, nave Bayes and random tree approaches. The average values of the results are shown in Tables IV to VII and the respective comparison in terms of accuracy, train and test time are shown in Tables VIII and IX.

In the case of binary classification, using the UNSW-NB15 dataset of Table IV, the REPTree algorithm performed the best with the nave Bayes presenting the worst performance. The highest detection accuracy was achieved on the Other protocols and low accuracy achieved on TCP protocol. Similar results are obtained with the NSL-KDD dataset in Table V with the high detection rate evident on the Other protocols and the lowest on UDP protocol.

For the multi-class classification results on the UNSW-NB15 dataset, Table VI shows a better accuracy with decision for REPTree and lower accuracy when using nave Bayes or neural networks and prediction was very difficult on other protocols. The efficiency of detection is quite high in UDP and substantially lower on TCP protocol. Table VII shows results on the NSL-KDD dataset, REPTree algorithm achieved the best accuracy detection and prediction was difficult on UDP protocol.

Table VIII shows the comparison results of the proposed model against the combined method of Random Tree and NBTree classifiers [24]. The results show a quite same accuracy performance but with the advantage of better training and testing time performance. Table IX shows the comparison of results for the UNSW-NB15 dataset with the best accuracy obtained in [5]. Our model presents the best performance in terms of accuracy and training and testing time.

V. CONCLUSION

In this paper, we proposed a two stage classification network intrusion detection system based on the REPTree algorithm. The NSL-KDD dataset and UNSW-NB15 dataset were used to evaluate the performance of our novel detection algorithm. Network traffic if firstly divided into different classes according to the different network protocol. In the first stage we classify the incoming network traffic into normal or attack classes. In case of attack traffic, the second classifier identifies the type of the attack for providing the best necessary

TABLE IV. BINARY CLASSIFICATION ON UNSW-NB15

UNSW-NB15	All Features				Feature selection			
N/A	TCP	UDP	Other	Accuracy	TCP	UDP	Others	Accuracy
DT	81.13	89.30	98.58	86.13	82.01	92.17	99.69	87.74
ANN	84.13	85.06	99.66	86.31	71.96	90.03	99.30	81.67
NB	70.64	87.34	99.50	80.04	71.90	87.82	99.69	80.90
RandomTree	81.35	90.25	98.64	86.59	81.17	91.77	99.42	87.13
RepTree	83.48	90.12	99.85	87.80	**84.48**	**91.88**	**99.85**	**88.95**

TABLE V. BINARY CLASSIFICATION ON NSL-KDD

NSL-KDD	All Features				Feature Selection			
N/A	TCP	UDP	Other	Accuracy	TCP	UDP	Others	Accuracy
DT	85.47	84.5	94.82	85.78	78.67	84.50	94.82	80.09
ANN	82.59	52.68	94.82	79.67	75.28	55.32	93.95	73.82
NB	78.51	72.22	95.11	78.54	72.43	73.29	95.11	73.57
RandomTree	78.41	84.50	95.68	79.91	83.25	73.52	96.26	82.72
RepTree	87.07	85.73	95.20	87.29	**90.02**	**85.76**	**97.12**	**89.85**

TABLE VI. MULTI-CLASS CLASSIFICATION ON UNSW-NB15

UNSW-NB15	All Features				Feature Selection			
Attacks	TCP	UDP	Other	Accuracy	TCP	UDP	Other	Accuracy
DT	81.03	98.27	27.21	78.73	85.13	98.13	35.69	81.68
ANN	77.24	96.30	35.54	78.14	70.74	95.52	35.32	75.54
NB	83.60	93.68	8.70	73.86	76.00	97.13	32.56	77.53
RandomTree	83.76	93.40	21.30	76.21	79.11	98.04	31.16	78.74
RepTree	81.39	97.97	29.74	79.20	**84.46**	**98.11**	**34.81**	**81.28**

TABLE VII. MULTI-CLASS CLASSIFICATION ON NSL-KDD

NSL-KDD	All Feature				Feature Selection			
Attacks	TCP	UDP	Other	Accuracy	TCP	UDP	Other	Accuracy
DT	79.77	38.93	99.57	78.54	74.09	38.93	99.57	73.66
ANN	73.32	38.93	99.57	72.99	79.44	38.93	99.57	78.26
NB	71.95	38.69	99.05	71.76	77.48	38.69	99.05	76.52
RandomTree	69.39	38.46	98.63	69.51	77.68	38.46	99.57	76.71
RepTree	71.43	38.93	99.57	71.37	**85.64**	**38.93**	**99.57**	**83.59**

response. Extensive evaluation and comparison results showed that the proposed two stage classifier model yields better results in terms of speed of detection and prediction accuracy rate.

Attacks classification experiments on both NSL-KDD and UNSW-NB15 are still not perfect especially for UDP and Other protocols. In future work, we will improve the detection accuracy in these protocols.

REFERENCES

[1] P. Dokas, L. Ertoz, V. Kumar, A. Lazarevic, J. Sri- vastava, P.-N. Tan, *Data mining for network intrusion detection*, in: Proc. NSF Workshop on Next Generation Data Mining, 2002, pp. 21-30.

[2] A. K. Ghosh, J. Wanken, F. Charron, *Detecting anomalous and unknown intrusions against programs*. in: Proc. Computer Security Applications Conference, 1998, pp. 259-267.

[3] M.Tavallaee,E.Bagheri,W.Lu,A.-A.Ghorbani, *A detailed analysis of the KDD CUP 99 data set.* In : Computational Intelligence for Security and Defense Applications, 2009. CISDA 2009. IEEE Symposium on. IEEE, 2009. p. 1-6.

[4] H. M. Harb, A. S. Desuky, *Adaboost ensemble with genetic algorithm post optimization for intrusion detection*. Update 2 (2011) 1.

[5] N. Moustafa, J. Slay, *The evaluation of network anomaly detection systems: Statistical analysis of the UNSW-NB15 data set and the comparison with the KDD99 data set.* Information Security Journal: A Global Perspective (2016).

[6] N. Moustafa, J. Slay, *Unsw-nb15: a comprehensive data set for network intrusion detection systems (UNSW- NB15 network data set)*. in: Military Communications and Information Systems Conference, 2015, pp. 1-6.

[7] D. E. Denning, *An intrusion detection model*, IEEE Transactions on software engineering (2) (1987) 222-232.

[8] S.X.Wu,W.Banzhaf, *The use of computational intelligence in intrusion detection systems: A review*.Applied Soft Computing 10 (1) (2010) 1-35.

[9] J. McHugh, *Testing intrusion detection systems: a critique of the 1998 and 1999 darpa intrusion detection system evaluations as performed by lincoln laboratory*. ACM Transactions on Information and System Security 3 (4) (2000) 262-294.

[10] P. Krömer, J. Platoš, V. Snáš, A. Abraham, *Fuzzy classification by evolutionary algorithms*. in: IEEE International Conference on Systems, Man, and Cybernetics, 2011, pp. 313-318.

[11] M. Panda, A. Abraham, M. R. Patra, *Discriminative multinomial naive bayes for network intrusion detection*. in: International Conference on Information Assurance and Security, 2010, pp. 5-10.

[12] M. Panda, A. Abraham, M. R. Patra, *A hybrid intelligent approach for network intrusion detection*. Procedia Engineering 30 (2012) 1-9.

[13] S. Sethuramalingam, E. Naganathan, *Hybrid feature selection for network intrusion*. International Journal on Computer Science and Engineering 3 (5) (2011) 1773-1780.

[14] J. Koshal, M. Bag, *Cascading of C4.5 decision tree and support vector machine for rule based intrusion detection system*. International Journal of Computer Network and Information Security 4 (8) (2012) 8.

[15] M. A. Salama, H. F. Eid, R. A. Ramadan, A. Darwish, A. E. Hassanien, *Hybrid intelligent intrusion detection scheme*. in: Soft computing in industrial applications, 2011, pp. 293-303.

[16] P. Natesan, P. Rajesh, *Cascaded classifier approach based on adaboost to increase detection rate of rare network attack categories*. in: International Conference on Recent Trends In Information Technology, 2012, pp. 417-422.

[17] R. S. Naoum, N. A. Abid, Z. N. Al-Sultani, *An enhanced resilient back-propagation artificial neural network for intrusion detection system*. International Journal of Computer Science and Network Security 12 (3) (2012) 11.

[18] R. S. Naoum, Z. N. Al-Sultani, *Learning vector quantization (LVQ) and k-nearest neighbor for intrusion classification*. World of Computer Science and Information Technology Journal 2 (3) (2012) 105-109.

[19] F. E. Heba, A. Darwish, A. E. Hassanien, A. Abraham, *Principle components analysis and support vector machine based intrusion detection system*. in: International Conference on Intelligent Systems Design and Applications, 2010, pp. 363-367.

[20] Y. Zhang, L. Wang, W. Sun, R. C. Green II, M. Alam, *Distributed intrusion detection system in a multi-layer network architecture of smart grids*. IEEE Transactions on Smart Grid 2 (4) (2011) 796-808.

[21] S.Joseph,etal., *Feature reduction using principal component analysis for effective anomaly-based intrusion detection on nsl-kdd*. International Journal of Engineer- ing Science and Technology 1 (2) 1790-1799.

[22] S. Mukherjee, N. Sharma, *Intrusion detection using naive bayes classifier with feature reduction*. Procedia Technology 4 (2012) 119-128.

[23] S. Kumar, S. Nandi, S. Biswas, *Research and application of one class small hypersphere support vector machine for network anomaly detection*. in: International Conference on Communication Systems and Networks, 2011, pp. 1-4.

[24] J. Kevric, S. Jukic, A. Subasi, *An effective combining classifier approach using tree algorithms for network intrusion detection*. Neural Computing and Applications (2016) 1-8.

[25] C.R.Pereira,R.Y.Nakamura,K.A.Costa,J.P.Papa, *An optimum-path forest framework for intrusion detection in computer networks*. Engineering Applications of Artificial Intelligence 25 (6) (2012) 1226-1234.

[26] G. MeeraGandhi, K. Appavoo, S. Srivasta, *Effective network intrusion detection using classifiers decision trees and decision rules*. International Journal of Advanced Network and Application 2.

[27] S. Teng, H. Du, N. Wu, W. Zhang, J. Su, *A cooperative network intrusion detection based on fuzzy SVMs*. Journal of Networks 5 (4) (2010) 475.

[28] J. R. Quinlan, *Simplifying decision trees*. International journal of man-machine studies 27 (3) (1987) 221-234.

[29] H. Kopka and P. W. Daly, *A Guide to LaTeX*, 3rd ed. Harlow, England: Addison-Wesley, 1999.

Comprehensive Understanding of Intelligent User Interfaces

Sarang Shaikh
and M. Ajmal Sawand
Sukkur Institute of Business Administration,
Sukkur, Sindh, Pakistan

Najeed Ahmed Khan
NED University of Engineering and Technology,
Karachi, Pakistan

Farhan Badar Solangi
Federal Board of Revenue,
Islamabad, Pakistan

***Abstract*—This paper represents basic discussion for one of the latest advances in the technology, known as *Intelligent User Interface (IIUI)* which is a combination of two major fields of computer science, namely, HCI & Artificial Intelligence. The paper first discusses basic definitions, motivation to this research and UIMS *(User Interface Management System)* along with example of user interface models to understand user interfaces in detail. The four major classes *(with their examples)* of these interfaces have been taken as a method for this study. The overall discussion summarizes some basic principles used to create these interfaces, components that are important in the generation of IUIs and decision making process in IUI for the reader to understand working of IIUIs.**

***Keywords*—Intelligent user interfaces; HCI; artificial intelligence; IIUI**

I. Introduction

Intelligent User Interfaces refers to the study and use of the two major fields of the Computer Science that are *Human Computer Interaction (HCI)* and *Artificial Intelligence (AI)*. HCI provides efficient user interfaces designing techniques and AI is used to automate or to build intelligence in those interfaces. Basically the term *IIUIs* suggests that an interface or interface like system, which is interacting with the user, must generate some output that the user considers it an intelligence, e.g., if the user dont know how to copy files in the windows operating system then in the windows help there must be assistance available for this when user searches for this, if user clicks the wrong button then an automatic message must be appeared for the help of the user, if the user has previously selected some options on the interface based on those options the system must understand the interests of the user and generates output according to it.

Moreover, the intelligent systems with interfaces cannot be called as IIUIs because they are intelligent in machine point of view but not in users point of view. IIUIs directly deals with users goals, requirements, efficiency, effectiveness, etc. these type of interfaces are quite frequent now a days due to advancement in the technology. These are basically dynamically generated, run time decision makers for the users according to users input, etc. Below in the paper, different information for these type of interfaces in provided, that might be helpful in understanding this new technology. Now the road map for rest of the paper. Section II will explain state of the art, Section III will discuss section II in more detailed way, Section IV will explain decision making process in IIUIs, Section V will conclude the whole study and Section VI will suggest some future work for this study.

II. State of the Art

Since inception of the computers, these machines were only used for business and mathematical calculations. These were performing efficiently for such selected functions because the inputs were limited and constrained based. As computer is information processing tool so it is important to make computer efficient and effective in processing information and interpreting user inputs correctly. For this, the need of the user interface had been possibly a main issue in the computers because computer machines only understand binary (machine) code but that code cannot be interpreted by humans easily. If human tries to input that code, it is time consuming task. High level languages solved this problem to some extent for humans but human still need an interface to communicate (to provide) correct input for the correct functions in the computers.

Basically user interfaces is a complete study in the field of *Human Computer Interaction*. The very first type of interaction was input through punch cards and output was printed on some paper or anything else, after that keyboards were used for input and monitors were used for output. At that time the first interface was created known as *Command Line Interface (CLI)*. That was a command based interface in which user inputs the command in textual format and machine understands it by converting it into machine code. That interface worked quite best at that time for simple processing or calculations because the inputs were limited and interaction was simple. As time passes, the computer became more general and application programs like word processors and spread sheets were developed. It is a clear matter of understanding that for such type of programs interaction through CLI is quite difficult so a new and advance way of interaction was developed known as *Graphical User Interface (GUI)*. In which mouse and icons were used to interact.

Today, the technology is being so advanced that task like image processing, face detection, emotion and speech recognition, body behavior detection, automation of machines, etc is demanding for a new type of interactive user interfaces that can provide facility to the human and the machines to interact in these technologies. No doubt, GUIs are the most effective way of interaction but they are static and fixed interfaces. Advance technologies are dynamic, they are working in real time scenarios so they also require real time and dynamic interfaces to interact. So with the help of Artificial Intelligence

and Human Computer Interaction such type of interfaces are being created known as *IIUIs*. These interfaces change their behavior according the real time scenario on which it is implemented. In [1], authors have discussed the historical background and presented introduction of IIUIs, moreover they have tried their level best to make these interfaces understand.

A. Understanding User Interfaces

First of all, we need to understand what is an interface? *An interface provides a means of communication between two or more objects* i.e., in computer systems the command line or graphical user interfaces helps the human to communicate with machine by giving the inputs, at the same time it helps the machine to give output to the human using some hardware. Similarly, we need to cope up what is intelligence means in this context? In the perspective of interfaces, *the intelligence might be in predicting what the user wants to do, and presenting information with this prediction in mind*. It means to use information in a proper and intelligent way.

Since, the intelligence in the interfaces varies from user to user because for every user there are different requirements and understanding levels. Intelligence is just like a future step which is one step forward from us, when we reach to it intelligence finishes. Point here is, what components of the interface should be intelligent. The main points are discussed below:

1) **System Functionality:** The interface must have the information about the user tasks and how to interact with the system. With this information, the interface can be intelligent.
2) **Intelligent about the user:** The interface must be intelligent about the user by using user models. This is done when system uses different modes for input and output to the human like voice, visual, etc.
3) **Interface must be sensitive about needs of user:** By using different user models, the system must understand on run time that what is the need of the user? One specific case can be system detects that user wants help while attempting some particular task. For e.g. if the user is continuously pressing the wrong button then system must generates some hints about the correct button or highlight the correct button which should be pressed or generates some messages [2].

B. User Interface Management Systems (UIMS)

Every user interface management system uses some user interface models because these models create notations for UIMS which describes the user interfaces and their implementations. There are various types of techniques are being developed for explanation of user interfaces, these techniques are divided into two major parts. One is about the design of the interface and another one is about the implementation of the interface. Design techniques are not of such importance because they just show the thoughts of a designer but implementation techniques are most important because they produce the executables for the interfaces. The techniques used in UIMS represent the no. of interfaces that can be created by UIMS, for creating general UIMS it is required that the design techniques must support max no. of user interfaces. Basically the term UIMS represents also an user interface.

The selection of the user model for UIMS is very important because user model decides what service or features should be provided in the user interfaces. For example, if the user model is divided into different components then UIMS should have to apply design and implementation tools for each component. This defines that before designing the UIMS for user interface, the user model should be designed first. The best user model ever known is **Seeheim Model**. The best thing about this model is that it is a generalized model; it can be integrated with any UIMS without having any issues of design or implementation for that model. This is helpful in studying just the model not different UIMSs [3].

This model divides the design and implementation of user interfaces into three components:

1) **Presentation Component:** Deals with the physical view of the user interfaces, including input and output devices, interaction and display techniques, screen arrangement. It deals directly with the hardware devices and it serves as a lexical part of the interfaces.
2) **Dialogue Control Component:** Deals with the communication between user and the computer system. This component is responsible for structure of the inputs, commands, dialogues provided by the user. This is known as syntactic level of the user interfaces.
3) **Application Interface Model Component:** This is a logical part of the user interfaces, in which the interaction between the user and all remaining application procedures is handled. The information processed by the user is understandable to the machine in this component and according to it the computer works and generates the output. Fig. 1 explains working of above mentioned basic components of UIMS.

All of these components communicate with each other by passing tokens same as in compilers [4]. The token contains the name and values; the name of the token defines the type of the token. The token going from user to the application program is called an input token whereas the token going back from application program to the user is called an output token. For e.g. while interaction performed in the interface like text box, drop down menu or button, the token names can be text box, drop down and button. The values can be those values which are entered by the user as an input into the interface.

C. Principles for creating IIUIs

When combining automation, i.e., artificial intelligence with user interfaces generates some key problems. E.g. poor assumptions for users goals and requirements, insufficient consideration for automated tasks, poor timing for tasks and wrong analysis of the automated decisions and actions. For this some principles have been defined which helps in understanding user requirements and creating effective interfaces.

1) **Developing significant value added automation:** To provide intelligent interfaces, which provide original value over solutions achievable with direct manipulation.

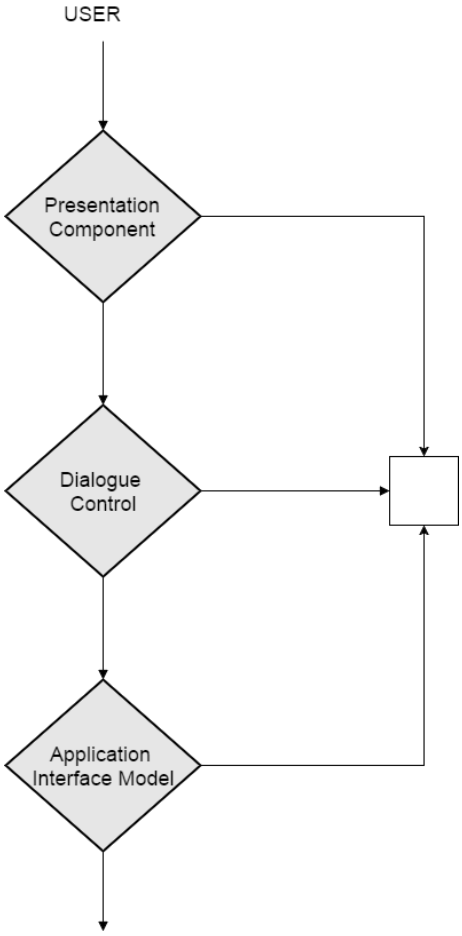

Fig. 1. User interface model [1].

2) **Considering uncertainty about users goals:** Computers are often uncertain about the goals of the users. So different ways for inferring the intentions of the users can employed by the system.
3) **Considering the status of users attention in the timing of services:** The timing of the automated actions can be major factor as cost for the actions. Agents should apply users attention models to check for timing costs and benefits.
4) **Inferring ideal actions in lights of costs, benefits and uncertainty:** Automated actions taken against users goals are directly related with costs and benefits. The cost for those actions can be controlled by considering some expected values / assumptions for the costs.
5) **Employing dialogues to resolve key uncertainties:** If a system hasnt any knowledge about users intentions tasks, it should be able to involve user in a detail dialogue to understand users actions while keeping costs minimum.
6) **Allowing efficient direct invocation and termination:** In some cases of uncertainties, system can take poor decisions about an intelligent interface. There should be several ways to provide options to the user during communication to start or terminate or control that automated service.
7) **Minimizing the costs of poor guesses about actions and timings:** The design and implementation of intelligent interfaces must be in a way such that there must be minimum costs for poor decisions taking by the system.
8) **Continuing to learn by observing:** Intelligent interfaces must be designed to work with users needs and they have ability to adopt new users goals during interaction.

D. Components of Intelligent Interfaces

Below are the components defined for intelligent interfaces, which helps in constructing efficient interfaces and also to understand above described principles [5].

1) The User Model:

Definition: This is an important part of the intelligent interfaces which creates the bases for the design and implementation of the interface. Without this component the system would not have any information regarding what the user will do? It also describes how to present the information, how and what type of help interface has to give and how the user will interact with the interface?

Characteristics:

- The system tries to adjust its behavior according to the users.
- The system takes responsibility to confirm the user-system communication.
- System ensures that various users with various requirements can use the interface.

Importance of the User Models: It helps the interface to decide what to ask, how to ask from the user, how to interpret the responses generated by the user and how to resolve ambiguity created by users actions. It helps the interface to provide help and advice to the user, to evaluate relevance of the tasks performed by the user, to recognize and correct misconceptions in the users mind. It helps the interface to understand users information seeking style by recognizing users goals and plans. It helps the interface to provide output to the user, deciding what to present and how to present.

2) The Multimodal Communication:

Definition: The use of different ways of communication in the interfaces is known as multimodal communication. These ways can be mouse, natural language entered by typing or voice, gesture, point on screen using pen, etc. This component always requires help of user model because depending on input and output of the user the way of communication is selected whether it should be textual, visual or vocal.

Characteristics:

- It enables the users to access the system naturally by using advance interaction ways like gestures or voice input.
- It gives the user more freedom such that the user is not restricted to sit in front of the system.

Importance of the Multimodal Communication: It is most important that the situations like when user is not able or user

don't want to use all of his senses for interaction. For example: If user has to closely look to the system for long duration, so the visual output would be not a good idea. Instead of this the voice or sound output would be better so that user can pay attention for long time.

3) Plan Recognition:
Definition: Plan recognition is used in intelligent interfaces to decide what user plans to do. It uses the system information, the user model and actions of the user to recognize plans of the user. For example: If there is a taxi automation system, the user wants to select the vehicle for 04 peoples and send it. When user will select no. of passengers, the interface will automatically suggest that which vehicle will be suitable? Or it will notify the user that you will send car for 04 peoples. So you want to send this time or not?
Characteristics:

- To recognize plans of the users before the user enters any goal or intention.
- To predict the user actions and provide guidance along the way.

Importance of the Plan Recognition: To automate user actions so that user doesnt want to select each and every option every time. To use past history of users actions so that it can inform the user for taking correct and efficient decisions.

4) Dynamic Presentation:
Definition: This component helps to display data for different users in different ways in which they want. The display of the data should be in an understandable way. Display depends upon the user model of the user such that what is requirement of the user. Different users have different requirements.

Characteristics:

- This component allows the display of the data either not to be in detail or not to be so short. But it must be in an effective style according to the user demands.
- This helps for display of different types of data in different formats.

Importance of the Dynamic Presentation: This helps in displaying data in an intelligent manner. For users who want to see just one table, this will show it. Instead, if user want to see 10 tables then that will also be displayed dynamically on run time.

5) Natural Language:
Definition: This is one of the best techniques to create effective and automated interfaces. The user selects the options or enters the inputs in simple natural language that he/she knows, instead of remembering commands for each task and input. The user enters the task what he wants to happen.
Characteristics:

- It will completely remove the GUI based style because there will be no more menus or lists for selecting different actions or performing tasks.
- There will be no list of commands for the system.

Importance of the Natural Language: It will help the users to communicate directly in their own language. Users dont need to memorize commands or huge menus creation will be removed. Communication will be simple and effective.

6) Intelligent Help:
Definition: Intelligent help presents the users helps which they want at the particular time or situation. This component is very useful in complex systems where asking for help returns in more information than necessary or information that is not according to the users needs.
Characteristics:

- Some plan recognition techniques can be used in intelligent help to acquire about users tasks and then to provide specific help according to the query.
- This feature requires the knowledge for application functionality.

Importance of the Intelligent Help: It is important feature for intelligent interfaces because it will help the users in an efficient manner by providing automatic help during any communication problem. It will generate error messages or help messages or hints to reduce the extra time taken by users [6], [7], [8].

III. Discussion

This section involves the discussion about some IIUIs studied and evaluated as an example from various sources. Basically there are four type of general interfaces or classes defined as an example below:

1) Direct Manipulation Interface Adaptation: In these type of interfaces, the user models are used to predict the goals or tasks of the user or to identify the patterns of the users inputs. Due to these type of predictions the intelligence can be easily adapted in four ways defined below: [3]

- **Speculative Execution:** The predicted users actions are already started to be carried out such that when user inputs a command or action the earlier phases for completing that command is already done or on the way towards completion, due to this phase.
- **Pattern Completion:** If the several input behavioral patterns are clear and same then different commands can be combined to create a big or general command.
- **Rapid Issue:** The commands that are used to execute several predicted actions or action that are performed by the user can be allowed to be accessed by the user in a rapid manner.
- **Assistance:** The system can offer help by using the knowledge it have about users goals or tasks.

Below is the practical example of these type of interfaces created and implemented by Microsoft and the UNIX systems. The very first example is *Davison and Harisch* system for predicting UNIX commands [9]. This system is based on Probabilistic User Model, which contains likeliness for the commands which are previously issued commands. This system outputs the top five predictions according to the user input for commands. This system proved to be efficient 75 percent. The second one example is MS Windows 95 and MS Office 97. In MS Windows 95, there were separate user accounts

facility, in which according to the input account of the user whether guest or any other account, the privileges of providing menus, permissions, etc was controlled. This was a type of personalized adaption. The recent files or human input history was easily and rapid accessible by the user. The menus were designed for the ease of the user with each option and rapid access. The help was available for each task related to the users input.

2) Informative Interfaces: Now a days, the use of data or information is increasing day by day, this is possible because of www or the internet. This type of interfaces deals with intelligence with the data. Intelligence of the data basically defines filtering in the data that which data should be display by the interface to the user according to its query [10], [11]. There are basic two main methods for filtering information:

- **Content Based Filtering:** This type of filtering uses objects descriptor relationship over the information, such as documents words relationship. It observes that which type of information is demanded by the user and after providing that information, it again observes that which type of data user is selecting from that provided information. An example for this type of interface is *SySkill and Webert*, this system recommends the web pages on a given topic provided by the user according to its likeness.
- **Collaborative Filtering:** This type of information filtering is used when objects are available but the descriptors are not or it can be clearly defined that when the interests of the user are not clearly defined. Firstly this filtering analysis the interests of the user, then it analysis the interests of other user profiles also. Finally, based on both of these analysis it suggests the information or data on that given topic asked by the user. This basically works on current user as well as other profiles interests. This type of filtering is quite helpful in film or music or art data filtering. An example of this type of interface is *FilmFinder*, that provides users the films that they might like.

There is a common informative interface based system known as *Langs News Weeder*. This system provides information about stories and web pages. Content based filtering is used to predict the interests of the current user accessing that system and collaborative filtering is used to provide general information on that topic from others profiles also of the same interests.

3) Generative Interfaces: This type of interface is used to generate new data according to previously recorded data values. The main purpose of this system is to improve the quality of the data by reducing data entry time for a human; this will surely help the beginners doing any task in case of performance. An example is provided to understand further this interface, the system is known as *Clavier* [12]. This system basically works on arrangement of air craft parts. When it is provided with lists of parts, from the past successive arrangements it lists out the most efficient arrangement which was perfect and containing all parts. Another example of this is *Hermens and Schlimmers Generative Interfaces*. This system is used to fill out repetitive forms. Each time the user fills a form the new form is generated on the basis of previous forms data with default values from previous data. Previous data is just like a training for generative interfaces [13].

4) Programming By Demonstration (PBD) Interfaces: This type of interface is used to communicate simple repetitive programs or tasks generated by user without implementing that programs. The user just has to tell the tasks to the system and all the work is done by the system. The basic example for this type of interfaces or systems is a simple *Macro Reader*, when user clicks the play button; it continuously records until the user clicks the stop button. To create PBD systems, there are few things that must be understood well [14].

- **Representation of User Tasks:** This is concerned with the input data by the user to the PBD system. The data should be accurate to be processed such that system can create meaningful information from that input. For example: by clicking a mouse or menu item must also send some textual information to process to the system, rather than just to send co-ordinates of the clicks.
- **Representation of Predictions:** This is important in how to represent the predictions done by the system to the user. The best way to solve this is to provide information to the user which is easily under stable by the user. For example: when user is going to click a button, the message is generated by the system prediction that you are going to click Button ID 01 to process. This is quite awkward in case of user, instead of this the button must be highlighted or some graphical change when user is going to click that button. This is more supportable by the user.
- **The Domain Knowledge:** The knowledge of the user tasks that which type of actions users can take. For example: in case of macro recorder, the user can start recording, stop recording, play recording, re-recording, save the recording, etc.
- **Termination Conditions:** This is about performance or efficiency of the PBD system, that how much it can support user interaction / usage in case of providing information. For example: on each click to provide the user each and every message, is not right. The user will be get irritated on seeing message on each iteration. For example: while recording a voice, if user speaks a letter, then system will generates message that you spoke a letter, proceed to further. This is not an efficient way.

IV. Decision Making in Intelligent Interface Systems

The IIUIs have to make several decisions during communication, the level up to that interface is considered to be intelligent depends upon its decision making during run time communication with the user, the tasks performed, nature of the application, etc. All of these factors are combined together and called adaptive of the IIUIs. The more intelligent interface is the more adaptive [15]. The adaptation strategy can also be called as decision making process. There are some attribute about the decision making process which can be helpful for a intelligent interface system [16], [17], [18]. Fig. 2 elaborates

process of decision making in IIUIs. Furthermore, this process includes some of basic decision making factors discussed below:

1) **What to Adapt:** This refers to the adaption or acceptance of the content of the information, sequences of the interaction, objects and techniques of the interactions. That is why it is called user computer interaction or known as *Adaptation Constituents*.
2) **When to Adapt:** During the run time adaptation in user computer interaction, it is important to analyze or monitor the time because the adaptation decisions are based on time. These are known as *Adaptation Determinants* i.e., requirements of the tasks, users sensory load, etc.
3) **Why to Adapt:** This depends upon the goals of the user; designer has to adapt such interfaces for communication according to requirements of the user. This is commonly known as *Adaption Goals*.
4) **How to Adapt:** Adaptation is done by some proper way known as *Adaptation Rules*. These rules combine the adaptation constituents, determinants & goals to create interfaces according to it.

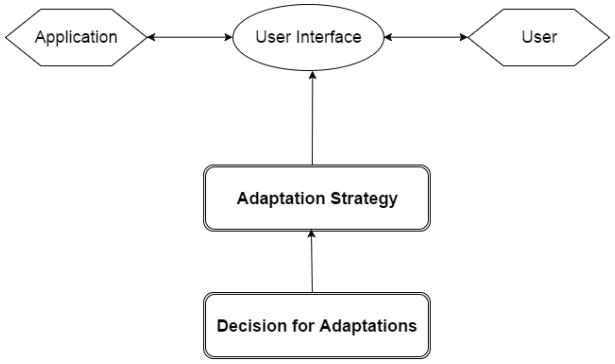

Fig. 2. Adaption at the highest level [2].

Although these attributes are quite important in decision making process, but not efficient in this way. Because these attributes are just used to create adaptation rules nothing else. In the case of existing systems, this approach fails because the adaptation rules become hard coded due to these attributes. They cant be used for multiple interfaces at a time. We have to change complete rules for another interface to be created. This will surely make the decision making process very inefficient [19].

The adaptation determinants that are used in decision making usually involves characteristics of user and information and task that is being to be performed. Different models like task user model, dialogue model and application model are used to manage these characteristics. Also based on the requirements of the application different determinants can be effectiveness, efficiency, graphic designs, etc. [20], [21], [22]. This is not fix that I any one set determinants for a application then that cant be changed. For every researcher or developer there are different determinants and their characteristics for a same application. User models are being used to represent determinants and their characteristics.

The adaptation rules are used to operate a system, these are basically hard coded and cant be changed dynamically. So it is quite a big issue that rules cant be modified, until and unless they are not to be re created again. These rules guide a system at different levels of human computer interaction. For example: If the task / sub goal requires spatial information, then it is better to use visual media resources, If the thing that has to be displayed is a analysis of complex structure of the system, then use network charts [23], If the number of secondary values of a object is 8 then interaction object selected must be a list box [24].

The above discussion suggests that adaptation rules are being generated on the basis of fixed determinants, constituents & goals. This makes it specific for a system, there rules are not flexible to be applied on any system. If any one of them needs modification then all of the four things will be modified. Because they all are inter linked with each other. As explained diagramatically in Fig. 3.

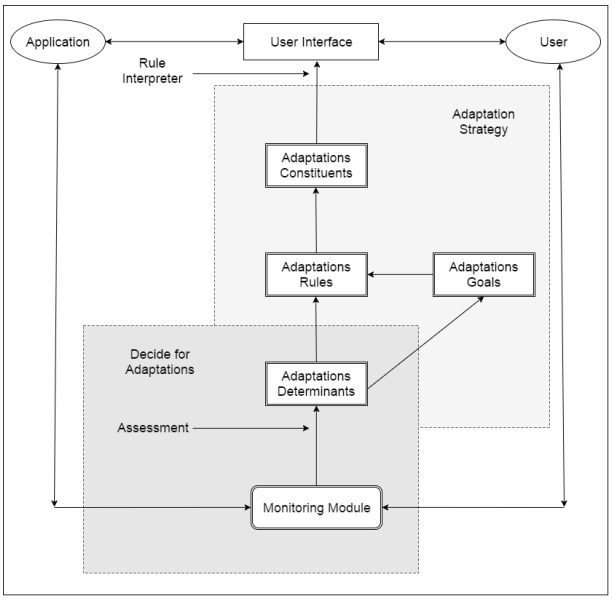

Fig. 3. Decision making in IIUIs [2].

V. Conclusion

Today in the era of technology there is a need for such type of interfaces because today computers are not limited just to the office or scientific computing or calculation, but it has become an important part of our lives. We, humans, are entirely dependent on each task on this machine whether it is to type a document, to drive the car, to study something, to calculate something, to make presentations, the internet; a huge invention of computers, online shopping, online music, etc. Also in the field of medical sciences, surgery, analysis of the internal body, to cure serious diseases, etc. In every field of human life, this machine is involved. If up to such level, this machine is involved then the interaction must be as efficient as possible. CLI or GUIs are also very good interaction styles, but they are static and limited. They cant perform multi-tasking like IIUIs or systems. When the user has to work with speech recognition, face detection, analysis of information, intelligent searching like Google, natural language processing like Google translator. When the user doesn't want to repeat

the same options every time when the user trying to see it's previous tasks & many tasks like these. So, nowadays there is a huge need for different intelligent interfaces that can meet user criteria because the expectation of the user towards the technology is increasing day by day. Finally, concluded that the need of intelligence in machines is increasing day by day so advances in the Artificial Intelligence & Human Computer Interaction is quite needed.

VI. Future Work

As this paper is a comprehensive and introductory survey of IIUIs, so one of the major future work is to make this paper as a base and find a research problem. The research problem can be either related to applications of these interfaces or further enhancement of these interfaces in terms of studies. Furthermore, this paper will create basis for other researchers of same domain for work in coming future.

References

[1] Ross, E., *Intelligent user interfaces: Survey and research directions*, University of Bristol, Bristol, UK, 2000.

[2] Horvitz, E., *Principles of mixed-initiative user interfaces*, Proceedings of the SIGCHI conference on Human Factors in Computing Systems. 1999. ACM.

[3] Sullivan, J., J.W. Sullivan, and S.W. Tyler, *Synergistic Use of Direct Manipulation and Natural Language*, IIUIs. 1994.

[4] Green, M. (1986), *A survey of three dialogue models.*, ACM Transactions on Graphics (TOG), 5(3), 244-275.

[5] Keolle, D., *IIUIs. 2000 [cited 2017-05-05];*, Available from: http://web.cs.wpi.edu/Research/airg/IntInt/intint-paper-intro.html.

[6] Tyler, S.W., et al., *An intelligent interface architecture for adaptive interaction*, Readings in IIUIs. 1991. ACM

[7] Chin, D.N., *Intelligent interfaces as agents*, Readings in IIUIs, 1998: p. 358.

[8] Kass, R. and T. Finin., *General user modeling: A facility to support intelligent interaction*, Readings in IIUIs. 1991. ACM

[9] Davison, B.D. and H. Hirsh., *Predicting sequences of user actions*, Notes of the AAAI/ICML 1998 Workshop on Predicting the Future: AI Approaches to Time-Series Analysis. 1998.

[10] Langley, P., *Machine learning for adaptive user interfaces*, KI-97: Advances in artificial intelligence. 1997. Springer.

[11] Langley, P., *User modeling in adaptive interface*, UM99 User Modeling (pp. 357-370). Springer Vienna.

[12] Hinkle, D., & Toomey, C., *Clavier: Applying Case-Based Reasoning to Composite Part Fabrication*, IAAI.

[13] Hermens, L.A. and J.C. Schlimmer., *A machine-learning apprentice for the completion of repetitive forms*, Artificial Intelligence for Applications, 1993. Proceedings., Ninth Conference on. 1993. IEEE.

[14] Cypher, A., & Halbert, D. C., *Watch what I do: programming by demonstration*, MIT press.

[15] Szekely, P. (1989), *Structuring programs to support intelligent interfaces*, (No. ISI/RS-89-231). UNIVERSITY OF SOUTHERN CALIFORNIA MARINA DEL REY INFORMATION SCIENCES INST.

[16] Zhuang, S., *Adaptive User Interfaces [cited 2017-05-10];*, Available from: https://susiezhuang.wordpress.com/2012/06/08/adaptive-user-interfaces/.

[17] Dieterich, H., et al., *State of the art in adaptive user interfaces*, Human factors in information technology, 1993. 10: p. 13-13.

[18] Stephanidis, C., C. Karagiannidis, and A. Koumpis, *Decision making in IIUIs*, Proceedings of the 2nd international conference on IIUIs. 1997. ACM.

[19] Arens, Y., Hovy, E. H., & Vossers, M. (1992), *On the knowledge underlying multimedia presentations*, (No. ISI/RR-93-370). UNIVERSITY OF SOUTHERN CALIFORNIA MARINA DEL REY INFORMATION SCIENCES INST.

[20] Sutcliffe, A. and P. Faraday, *Designing presentation in multimedia interfaces*, Proceedings of the SIGCHI Conference on Human factors in computing systems. 1994. ACM.

[21] Mackinlay, J. (1988), *Search architectures for the automatic design of graphical presentations*, ACM SIGCHI Bulletin, 20(1), 76.

[22] Chappel, H. and M. Wilson, *Knowledge-based design of graphical responses*, Proceedings of the 1st international conference on IIUIs. 1993. ACM.

[23] Bernsen, N. O. (1992), *Matching information and interface modalities: An example study*, Working Papers in Cognitive Science.

[24] Bodart, F., & Vanderdonckt, J. (1994, August), *On the problem of selecting interaction objects*, BCS HCI (pp. 163-178).

A Review of Bluetooth based Scatternet for Mobile Ad hoc Networks

Khizra Asaf*, Muhammad Umer Sarwar†, Muhammad Kashif Hanif‡, Ramzan Talib§, and Irfan Khan¶
Department of Computer Science,
Government College University, Faisalabad, Pakistan

***Abstract*—Bluetooth based networking is an emerging and promising technology that takes small area networking to an enhanced and better level of communication. Bluetooth specification supports piconet formation. However, scatternet formation remains open. The primary challenge faced for scatternet formation is the interconnection of piconets. This paper presents a review of the proposed approaches and the problems confronted for establishing scatternet for ad hoc networks specifically MANET. In this work, a comparison of the Blue layer algorithm with MMPI interface based algorithm on Bluetooth scatternet formation. The enhancement in the developed MMPI framework makes it a good option for scatternet applications.**

***Keywords*—Bluetooth; ad hoc network; piconet; scatternet; MANET**

I. Introduction

Bluetooth is a basis for transformative wireless ad hoc connectivity. It is among the technologies that can serve as a communication tool even when cellular network is not working or destroyed. Bluetooth permits the devices to make a short range network called *piconet*. Piconet has the capability to support up to eight bluetooth devices. One device takes the master device role and the other devices become the slave. The network topology resulted by the interconnection of piconets is known as *scatternet*. Bluetooth standard permits multiple tasks for the same node. It can act both as a master in one piconet and slave in even more than one piconet at the same time.

In last decade, traditional cell phones are upgraded to smart phones at a remarkable rate. This noticeable up-gradation is due to the substantial increase in functionality of the smart phones. Mobile applications are playing a vital role for the betterment of the world in almost every field of life. The applications are designed and developed with the deliberation for the need and demand of time. Today, everyone is familiar with the natural incidents as well as with the planned attacks. Thus, it emerges to focus on more efficient ways for personal safety and assistance. In this regard, communication technologies and mobile applications have played a vital role.

Mobile wireless technology is flagging the way for mobile ad hoc networks and bluetooth is supposed to be a reasonable option. It empowers and supports multi-hop communication. Scatternets are the best way to achieve high data transfer capacity by forming as many piconets as conceivable in a scatternet. Indeed, scatternets are considered as a preferential and recommended topology for establishing a point to the multi point piconet.

Different applications can be hosted and presented for one hop communication using bluetooth technology. However, scatternet formation is a problem that has still not been dealt yet. Bluetooth based scatternet formation faces some technical difficulties such as routing, interlinking piconets, and scheduling. Routing is suggested as one of the procedural issues in scatternet formation. Nodes can connect and disconnect with the network at random times. This feature of node mobility can create problems in network enactment. Moreover, bluetooth specification does not provide any particular protocol for establishing scatternet. The problem of scatternet formation turns to be significantly difficult if the starting nodes have no acquaintance with their ambiances [1]. The process of encountering network is a frequency hopping structure; nodes in immediacy must coordinate among frequency hopping configurations and timing before being available for the communication mode.

Mainly two processes are defined for building a scatternet: 1) piconets should be interlinked to form a network; and 2) the bridge nodes must maintain connectivity between piconets. The remaining paper is organized as: Background information on Bluetooth based mobile ad hoc networks is presented in Section II. Related work is described in Section III. Section IV compares compares Bluelayer algorithm and MMPI interface algorithm. Finally, the paper concludes the outcomes in Section V.

II. Background

A. Mobile ad-hoc network (MANET)

Ad-hoc networks have been a fascinating and worth considering research zone for almost two decades. A Mobile Ad-hoc network commonly known as MANET is a developing wireless network. Mobile nodes associate on the ex-temporal basis and are considered as self-forming as well as self-healing network. This feature enables peer-level dynamic infrastructure between mobile nodes. Fig. 1 shows an ad-hoc network formed by the interconnection of piconets.

In ad hoc network, each node uses the same station to execute multi-hop progressing. Each node plays the role of a host and a router to path the packets to and from nodes beyond the communication range [3]. The unusual aspects of MANET empower it to provide major assistance's in an environment of vibrant structure formation.

B. Piconet

Bluetooth devices connect in an ad hoc manner and form a network called piconet. A piconet may consist of minimum two devices. This number can be extend up to a maximum of eight

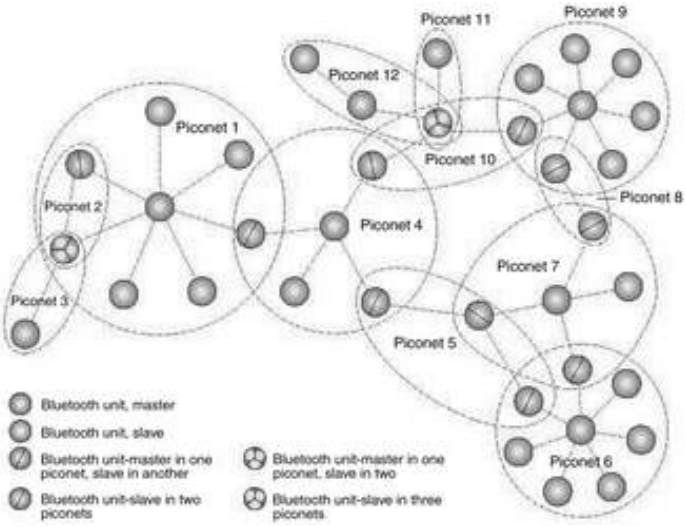

Fig. 1. Mobile ad hoc network [2].

devices. Fig. 2 shows a piconet formed by the combination of a single master and its slaves. In a piconet, one member will act as a master while the other members act as slave in the network. Every piconet has a single master and hops individualistically. The unit establishing piconet is a master and the devices discovered are the slaves. The hopping classification is decided by the master of the particular piconet. In point of fact, the limit of slaves connected to a master is applicable for active devices not for connected devices. Only seven slaves can be active at the same time. The remaining connected devices have to be in a state called parked state. Piconet can be single slave and multi-slave. Single slave piconet has only one slave while multi-slave piconet has many slaves but not more than seven.

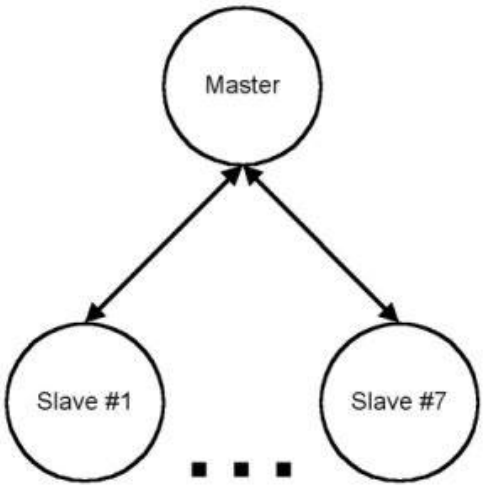

Fig. 2. Piconet with a master and seven slaves [4].

C. Scatternet

Scatternet is a network of interconnected piconets. This type of interlinked network can increase networking tractability and expedite new applications. Fig. 3 depicts a scatternet formed by interconnection of the two piconets. A peer to peer connection is created in scatternet. It is formed when a member of one piconet behaves as a slave in another piconet. A single device is permissible to act as a bridge for numerous piconets [5]. The participating member can either be a master or a slave. A device can perform as a slave device in more than one piconet. However, it can act as a master device only in one piconet. The device existing in two piconets works as transmit device. This intermediate device forwards data packets among the piconets using the concept of time division multiplexing (TDM) or time sharing. Point to multi-point competency is required for the device to be a part of scatternet communication. Scatternet permits communication among more than eight devices thus increasing the number of devices in a network. It makes intelligent use of bandwidth.

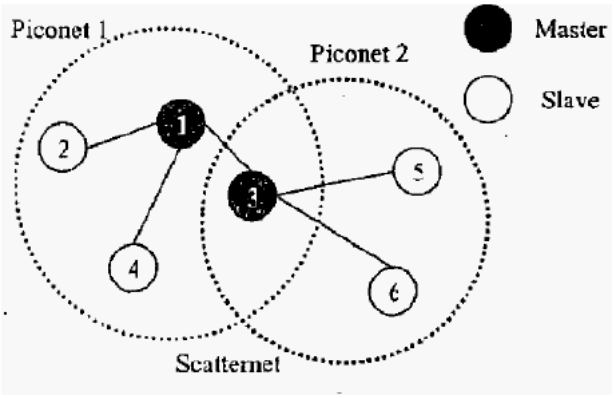

Fig. 3. Scatternet formed by overlapping of piconets [6].

III. Related Work

Different researchers have proposed various algorithms for scatternet formation. The way piconets are interlinked and the method for formation of a scatternet significantly affect performance. Numerous topology establishment algorithms are suggested for creating multiple ad hoc networks. Scatternet models have classified as tree-based or mesh topology. Tree structure allows a single route for each node pair whereas mesh topology allows multiple paths between the nodes. The algorithms are classified into two categories [7]. One deals with the restriction of all the nodes in the radio range and other deals with both types of nodes; within and outside the radio range.

A. Tree Topology

Different approaches exists for tree building algorithms. Tree scatternet formation (TSF), SHAPER, and SFX are mostly used. Multi-hop scatternets form a tree-like structure. The term tree compromises the master-slave linkage. TSF is a simple algorithm for building a tree-shaped structure. The root of the tree becomes the master. In TSF, all the nodes of the network lies within the communication range and can communicate with each other. TSF targets at dynamic situations. The connectivity, communication efficiency and healing power enrich the working of TSF algorithm [8].

Considering the SHAPER algorithm for scatternet formation is a more genuine and convincing approach. It is a

distributed self-healing algorithm which offers QoS support. SHAPER is the first flexible algorithm among scatternet formation algorithms. It can adapt and adjust the topology in a multi-hop state according to the mobility and disasters of nodes [9]. SHAPER works for the nodes even when they are not in the bluetooth radio range. This algorithm provides the network with self-healing capability in case of any trouble.

SFX was built using SHAPER algorithm by extending the realistic conditions to a coherent and corroborated explanation. SFX was proposed with the aim to develop and uphold a bluetooth node tree with an appropriate organization of piconets. The merging technique in SFX is exceedingly asymmetrical and is a significant peculiarity to SHAPER algorithm [10]. SFX builds a parallel structure and permits any number of trees to merge with the same tree at the same time. The principal idea of SHAPER was implemented for SFX. However, some of its features were ignored to avoid the unnecessary complexity. In SHAPER, four distinct merge processes were involved. However, SFX consists of only a single procedure to be handled making it much easier to implement.

B. Mesh topology

Mesh topology is based on tree shaped structure. The tree shaped structure is generated initially which is converted to mesh shaped topology. The mesh topology was proposed to decrease the route lengths of a standard tree to a sufficient extent [7]. The backward connection mechanism is used in this topology to create multiple paths among the nodes of the network. Master/Slave Web (MSW) and Slave/Slave Web (SSW) coordinate to generate a mesh scatternet.

MTSF is a mesh topology scatternet formation algorithm presented for the establishment of a scatternet. MTSF was capable of managing addition and deletion of nodes in a network [11]. It removes the restriction of bluetooth radio range. Thus, building a larger scatternet. MTSF has three phases. In the initial phase, nodes get to know their neighbors. This period is called the discovery phase and is common in almost all the algorithms. Clusters of piconets are formed in second phase. The piconets are interlinked in the third stage.

BlueMesh is a protocol for scatternet establishment. It forms a mesh of devices having diverse paths between nodes. BlueMesh does not restrict the bluetooth devices to be available in the broadcast range for scatternet formation. It is found to be operational and quick regarding scatternet generation. Furthermore, it provides the benefit of comparing the shortest route among multiple paths between any two member nodes. BlueMesh consists of two phases. The first phase is device discovery phase and the second phase is responsible for forming piconets and interconnecting the piconets to form a scatternet [12].

IV. Comparison

This section presents the comparison of BlueLayer and Mobile Message Passing Interface algorithms.

A. BlueLayer

BlueLayer diminishes complications of topology establishment outlays. This algorithm was designed in a way to take benefits of tree shaped and mesh shaped topologies [13]. In BlueLayer, a web-shaped topology is formed. It can identify new roots during the phase of scatternet formation. Every new source creates and possesses a confined web shaped sub-net by coordinating with other roots. Three pre configured network factors are assumed to generate separate web shaped sub-nets.

(a)Scatternet Formation Procedure;
Initialization:the first root sets k1=k*v,connects up-to 7 slaves and generates new masters;
if *a downstream master is connected,* **then**
  $k_1 = k_1 - 1$, each new master propagates (k_1, k, v) in its downstream direction ;
  if $k_1 = 0$, *the* k_1^{th} *master becomes a new root* **then**
    $v = v + 1$ and $k_1 = k * v$, the new root propagates (k_1, k, v) in its downstream direction and executes a return connection procedure for the first root;
    if *a leaf node is connected* **then**
      the leaf node starts the return connection procedure for its upstream roots to build their own sub-nets;
      else
        each node continuously propagates (k_1, k, v) in its downstream direction
      end
    end
  end
end
(b)Return Connection Procedure;
Initialization: The leaf master node propagates an initial return variable $r = 1$ in its upstream direction;
if *the upstream master is reached* **then**
  $r = r + 1$ until the immediate upstream root is reached;
  if $r > k_1/2$ *at its upstream root node* **then**
    the root retains its role as a root and gather nodes information of its downstream master until all its downstream masters notifications as well as the algorithm stops;
    else
      the root switches its role to a master and deliver its affiliated information to its upstream root
    end
  end
end

Algorithm 1: The Pseudo code of Bluelayer scatternet formation

Scatternet shape significantly influences routing protocol strategy. Therefore, the tier-ring addressing scheme has been presented to attain self-routing protocol. This protocol comprises of two phases; address query phase and a forwarder decision phase. First phase trace and pinpoint a destination and the second phase decide the ideal master as a forwarder.

B. Mobile Message Passing Interface

Mobile Message Passing Interface (MMPI) is a library presented for implementing the functionality of MPI on bluetooth empowered mobile devices. It offers point to point and global communication. The library was designed mainly for

```
Routing algorithm();
Initialization:Node S sends packets to destination D
  with the tier ring address;
if the master node M of S node has routing information
  to node D then
    node M sends packets to node D directly;
    else
      node M calculates the distance of all its one-hop
        masters to node D by equation(1) and decides
        the optimal forwarder with the minimum
        distance to node D;
      if more than two neighboring masters have
        equal distance then
        node M randomly selects a master as the
          optimal forwarder;
      end
    end
end
```

Algorithm 2: The Pseudo code for Forwarder decision

piconets. A solution was presented that provided the same functionality as offered by MMPI library and was implemented over a Scatternet [14]. For scatternet formation, a significant advancement of the MMPI library is required to organize the network setup as well as to permit intercommunication of the devices. The enhancement made in the library encompasses some distinctive modules while holding all of its unique functionality. MMPI node and CommsCenter are among the significant parts of the enhanced MMPI library. The CommsCenter class is considered as the heart of the library as it takes raw information and interprets it into MPPI messages. The MMPI node level delivers the interface between the MMPI class and the CommsCenter. This class is also responsible for device discovery process at the initial level. With this, the interface to the library is the MMPI class. Data is provided through a defined order that is started at the CommsCenter and lasting up to MMPI class.

```
Data: list of all MMPI capable devices
Initialize list of devices to send to bridge node;
foreach deviceinthelist do
    create master connection;
    add bridge node to routing table;
    else if add node to routing table then
        create slave connection;
        add slave node to routing table;
        send slave message;
        else if after bridge node then
            add device to list of devices to send to
              bridge node;
            add node to routing table;
        end
    end
end
add number of devices to bridge message;
add list of devices to bridge message;
```

Algorithm 3: Establishing initial connections at the root node

Scatternet formation is initiated at the root node. First, an inquiry is performed for the devices offering MMPI provision. Then, the root node selects the number of piconets vital to support the scanned MMPI nodes. A bridge node is selected among the network and a list of the addresses of the nodes are sent to bridge node by the root node. The bridge node then selects the master of the second piconet and send it the list of the other devices. The master of the second piconet then establish connections with each device of the list to form a scatternet. Message routing system broadcasts a validation message. A message routing table is used to send a message through the network. Every node has a table of all other nodes and the nodes are routed using the provided index.

```
Data: list of devices sent by root node
Initialize list of devices to send to additional master;;
foreach deviceinthelist do
    if second master then
        create master connection ;
        add second master to routing table;
    end
    else
        add node to routing table;
    end
end
add number of devices to Master message;
add list of devices to the Master message;
send Master message;
```

Algorithm 4: Establishing connections at the bridge node

The idea of the scatternet is an integral as well as a required part of Bluetooth aspect. It is suggested as the best approach to get high data broadcast capability. Scatternet is indeed a preferred way for point to multipoint communication and fulfills the requirement of MANET in an accepted way. Keeping in view the components required for scatternet formation, Bluelayer algorithm is a good approach as it exhibits good network scalability and routing competence for scatternet. On the other side, MMPI library is capable of supporting ad hoc networks of more than eight devices using the scatternet framework.

V. Conclusion

Bluetooth specification facilitates piconet formation. Conversely, it does not provide any answer for scatternet development. Blue layer proposes an approach to alleviate the communication as well as computation disbursements for forming a scatternet. It capably creates various sizes of topology formations thus achieving scalable network along with good routing adeptness. On the other side, enhancement in the MMPI library makes it adept and proficient for parallel computing on ad hoc networks. The improvement in the developed framework alleviates the limitation of node thus making it available for scatternet applications.

References

[1] T. Salonidis, P. Bhagwat, L. Tassiulas, and R. LaMaire, "Distributed topology construction of bluetooth wireless personal area networks," *IEEE Journal on Selected Areas in Communications*, vol. 23, no. 3, pp. 633–643, 2005.

[2] "wirelessadhocnetwork," [Online; accessed May 27, 2017]. [Online]. Available: http://www.technologymedia.co.th

[3] A. K. Sanghi, D. Singh, and H. Rathore, "A study of wireless environment by means of multiple wireless nodes," *International Journal of Computer Applications on Wireless Communication and Mobile Networks*, no. 7, pp. 31–35, 2012.

[4] "Piconet," [Online; accessed May 27, 2017]. [Online]. Available: http://www.edgefxkits.com

[5] M. Medidi and A. Daptardar, "A distributed algorithm for mesh scatternet formation in bluetooth networks." in *International Conference on Wireless Networks*. Citeseer, 2004, pp. 295–301.

[6] "Bluetooth devices forming a scatternet out of two piconets." [Online; accessed May 27, 2017]. [Online]. Available: www.researchgate.net

[7] C.-M. Yu, S.-K. Hung, and Y.-C. Chen, "Forming mesh topology for bluetooth ad hoc networks," in *Consumer Electronics (ISCE), 2013 IEEE 17th International Symposium on*. IEEE, 2013, pp. 123–124.

[8] A. OLUWARANTI, "Evaluation of tree scatternet formation algorithm for enhanced bluetooth scatternet," *Journal of Sustainable Technology*, vol. 2, no. 2, pp. 28–36, 2015.

[9] F. Cuomo, T. Melodia, and I. F. Akyildiz, "Distributed self-healing and variable topology optimization algorithms for qos provisioning in scatternets," *IEEE Journal on Selected Areas in Communications*, vol. 22, no. 7, pp. 1220–1236, 2004.

[10] M. Methfessel, S. Peter, and S. Lange, "Bluetooth scatternet tree formation for wireless sensor networks," in *Mobile adhoc and sensor systems (MASS), 2011 IEEE 8th international conference on*. IEEE, 2011, pp. 789–794.

[11] S. Sunkavai and B. Rarnalmurthy, "Mtsf: a fast mesh scatternet formation algorithm for bluetooth networks," in *Global Telecommunications Conference, 2004. GLOBECOM'04. IEEE*, vol. 6. IEEE, 2004, pp. 3594–3598.

[12] C. Petrioli, S. Basagni, and I. Chlamtac, "Bluemesh: degree-constrained multi-hop scatternet formation for bluetooth networks," *mobile Networks and Applications*, vol. 9, no. 1, pp. 33–47, 2004.

[13] C.-M. Yu and Y.-B. Yu, "Joint layer-based formation and self-routing algorithm for bluetooth multihop networks," *IEEE Systems Journal*, 2016.

[14] B. J. Donegan, D. C. Doolan, and S. Tabirca, "Mobile message passing using a scatternet framework," *International Journal of Computers Communications Control*, vol. 3, no. 1, pp. 51–59, 2008.

Data Provenance for Cloud Computing using Watermark

Muhammad Umer Sarwar*, Muhammad Kashif Hanif†, Ramzan Talib‡ Bilal Sarwar§, and Waqar Hussain¶
Department of Computer Science,
Government College University, Faisalabad, Pakistan

***Abstract*—The term data is new oil which has become a proverb due to large amount of data generation from various sources. Processing and storing such tremendous amount of data is beyond the capabilities of traditional computing system. Cloud computing preferably considered next-generation architecture due to dynamic resource pools, low cost, reliability, virtualization, and high availability. In cloud computing, one important issue is to track and record the origin of data objects which is known as data provenance. Major challenges to provenance management in distributed environment are privacy and security. This paper presents data provenance management for cloud computing using watermarking technique. The experiment is performed by using both visible and hidden watermarks on shared data objects stored in cloud computing environment. The experimental results demonstrate the efficiency and reliability of proposed technique.**

***Keywords*—Cloud computing; data provenance; watermark; security; visible watermark; invisible watermark**

I. Introduction

During the last 20 years, continuous development in web technology has produced a huge collection of data. Before 2020, people and linked data objects will approximately generate the billions gigabytes of data that will have an influence on daily life [1]. It would be difficult to manage such a huge volume of data with traditional processors. Organizations have started to manage such large amount of data by shifting their services over the cloud. According to *Gartner's 2011 CIO Agenda Survey*, most of organizations will depend on the cloud computing more than half of their IT Services before 2020. This prototype shifting reduced the costs to manage the software and hardware resources.

Cloud computing provide accessibility of data, files, programs, and services from web browser over internet. Cloud computing stores the software, programs, and other computing applications to a central location. The management of resources on cloud have security challenges. One of the important issue is to ensure data integrity. It is dangerous to guarantee data integrity in cloud computing for results assembling process [2]. One possible solution to ensure data security is *Data Provenance*. In cloud computing, the term data provenance is defined as the original source of shared data objects.

In this paper, a watermarking technique is used to store provenance information of shared data objects in cloud computing. This technique will help to find the original source of data objects in cloud computing. The experiment is performed by implementing the presented watermarking technique in an open source platform known as *ownCloud* [3]. This approach is used to answer the following questions related to data security in cloud computing: What is the original source of data object? Who is the owner of data object? How much reliable is the original source? Who modified the data object? Finally, the efficiency and reliability of proposed technique is measured.

The rest of the paper is structured in different sections. Section II presents related work. Section III describes cloud computing along with its architecture and security challenges. In Section IV, data provenance and techniques for maintaining provenance are presented. Proposed methodology is presented in Section V. Section VI discusses the results. Finally, we conclude the work with outcomes in Section VII.

II. Related Work

The rapid and large increase in data poses the problems of data security in cloud computing. Numerous watermarking techniques have been proposed by the researchers for ensuring the security of shared data. These techniques are categorized on the basis of types of watermark like digital watermark, visible watermark, invisible watermark, and cover type [4]. These techniques can also be characterized by data provenance, data lineage, usability, and robustness [4].

A few watermarking techniques have been used in order to ensure the data security and integrity [5], [6]. Some researchers have used watermarking techniques for data provenance that includes fragile [7] and novel [8] watermarking. In these techniques, some important issues like data security, usability, robustness, distortion, and capacity are taken under consideration. However, these techniques lacks to solve the data provenance problem to optimum level. Sarwar et al. presented a package watermarking technique to ensure data provenance in database systems [9].

Tiwari and Sharma studied various semi fragile watermarking algorithms by using different methods like image quality matrices, insertion and verification methods [10]. Zhang et al. proposed a gray scale watermark pre-processing technique. Their work provides robustness of video watermarking for copyright protection. This approach almost maintains the same bit rate and also provides good visual quality [11]. Some researchers have worked on the problem of data provenance [12], [13]. However, their work only emphasis on the semantic analysis of data provenance information.

III. Cloud Computing

Cloud computing is relatively a new computing model which provides high performance computational services at a minimal cost. Some famous organizations in the field of

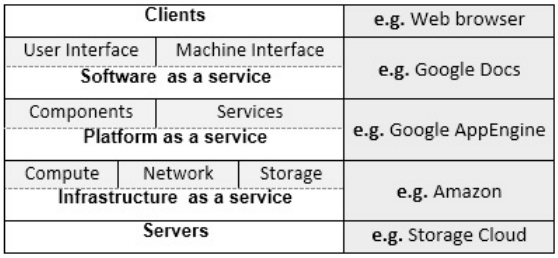

Fig. 1. Cloud computing architecture.

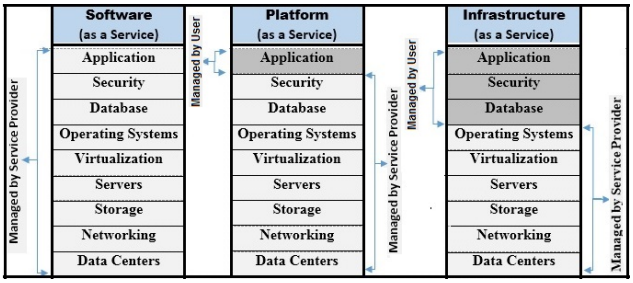

Fig. 2. Cloud computing services (CIO Research Center, 2010) [19].

IT such as Google, Microsoft, and Amazon have shifted their cloud services over the Internet [14]. Cloud computing is called the fifth utility in the line of electricity, water, telephone and gas [15]. It provides the facility of storing and accessing files from any where in the world based on access permissions. Main advantage of cloud computing is to allow the users to carry out their every day computing operations using cloud computing [16]. The term cloud computing is defined by the researchers in various ways. Buyya, et al. [17] defined cloud computing is distributed computer system consisting of the collection of interconnected and virtualized computers that are supplied with strength and can be obtained as one or more conventional Service Level Agreements (SLA) based processing resources through negotiation between service providers and consumers. According to Vaquero, et al. [18], clouds are a large amount of virtualized resources (such as hardware, development platforms, and services) that can be accessed in a functional and accessible manner. These resources can be dynamically reconfigured to fit an adjustable load scale enabling an optimum consumption of resource. This resource pool is abused by a pre-use payment model where the warranty is offered by the infrastructure provider through custom service level agreements.

Cloud computing can be classified into three well-known and frequently used service models. These models are known as Software as a Service (SaaS), Platform as Service (PaaS), and Infrastructure as Service (IaaS). Fig. 1 shows hierarchy of these services with examples. These service model provides specific features and functionalities. The major difference between these service models is depicted in Fig. 2. SaaS is famous and well-known type of cloud service for common users. SaaS applications are hosted on remote server and are managed by the service provider. These applications are accessible to users through a web browser on Internet. Some well known SaaS applications are Google Apps and DropBox. PaaS is similar to SaaS in many ways. Instead of delivering the applications over the web, PaaS provides an environment for users to create their own applications. However, rest of the computing elements except applications are managed by the PaaS service provider as shown in Fig. 2. Example of PaaS application is Google App Engine. IaaS is the most flexible cloud computing model and allow users to run any applications. These applications can be run on the hardware of IaaS service provider. IaaS offers web-based access to computing power and storage. In this service model, the user does not need to control PaaS infrastructure or SaaS services. Famous applications of IaaS includes Google Engine, Amazon Web Services, and Microsoft Azure.

The cloud computing is categorized in public, private, and hybrid clouds. Private clouds are organized within premises and accessible only to a single organization. Public clouds are deployed off premises and accessible by any user within or outside the organization. Hybrid cloud may be either internal or external. Hybrid cloud contains the characteristics of both private and public clouds [14]. Fig. 3 Illustrates these cloud deployment types [20].

Fig. 3. Cloud deployment models [20].

Although cloud computing is emerging rapidly but at the same time there are severe security challenges. Some security issues have reduced the adoption of cloud computing among its users. One important problem in cloud computing is to ensure the trustworthiness of data object. Thus, increase in demand of cloud computing has raised a few security problems for both of its users and service providers. How the users can ensure the unique ownership of their uploaded data object in the cloud? Every user wishes to know about the availability of their data objects in the cloud [21].

IV. Data Provenance

With the huge growth of data, finding origin and transformation of data becoming an important and challenging task. In many applications like cloud computing, database, and social media network, it is a challenging task to find out the origin of data object. The original source of shared data object in cloud computing is very important in order to take any decision. The term "data provenance" means a procedure to trace and record the origin of data products. The importance of the data source is increasingly recognized by both users and publishers of that data product for a long time. The original source of shared data objects in cloud can be used by scientists or scholars to determine the real ownership who is working on these data products. Likewise, medical research requires severe product quality data checks because errors can harm people's health.

The term data provenance is defined as history of ownership of a shared data object. Provenance can also help to find out the authenticity of a shared data object in cloud computing. In other words, provenance is a term used in

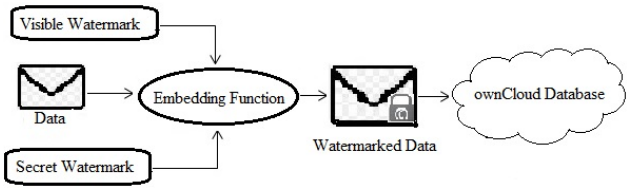

Fig. 4. Watermark embedding process.

diverse areas which describes the history of an object since its creation. In cloud computing, data is shared widely and anonymously. Therefore, the source of data object is required to verify the authenticity of that data product. Cloud users face severe security challenges from both inside and outside the cloud. In fact they have to face some threats from cloud service providers. If the source is provided in cloud computing, users can gain more control over their data. Additionally, cloud users can detect what went wrong with respect to data under its control. In particular, cloud users may be able to verify that nothing has gone wrong with its data products.

Currently, there is no way to trust on the data provenance information in the cloud computing. However, numerous novel techniques are designed and implemented in cloud computing. Some issues of data security and governance in cloud computing are discussed in [22]. A data security framework for cloud computing networks is proposed [23]. Younis and Kifayat provides a survey on secure cloud computing for critical infrastructure [24]. Chen and Zhao [25] analyzed privacy and data security issues in the cloud computing by focusing on privacy protection, data separation, and cloud security. According to a survey [12], characteristics of nine different data provenance techniques are summarized in [12].

V. Methodology

Data security is one of the biggest concerns about cloud computing. Numerous different techniques are introduced by the computing researchers for data protection as already discussed in Section IV. However, there are still some gaps in those techniques which require enhancement. In this section, the main focus is to explain how watermarking technique can be used to maintain original ownership about data in cloud computing. The proposed watermarking technique for data provenance is practically examined using a free and open-source cloud software known as ownCloud. ownCloud is a file sharing server that permits its users to store data objects in a centralized location, much like Dropbox [26]. These data objects can be any type of images or text documents.

In this paper, two important watermarking techniques are used to secure the shared data objects in cloud computing. First technique is to embed the visible watermark which can be seen by everybody who is seeing the data object. This type of watermark ensures trustworthiness of data packets in the cloud. Second technique is to insert the hidden watermark which provides backup facility in case when visible watermark fails to prove trustworthiness of data. Both visible and hidden watermarks are embedded in the data objects when these data packets are created or added for the first time in the cloud. The process of embedding both visible and hidden watermarks in the host data object consists of two steps as shown in Fig. 4. In first step, both types of watermarks are embedded in the data object. Then, in second phase, watermarked data objects are stored in the database of relevant cloud like ownCloud. The experiment is performed with six different images using an open source free cloud known as ownCloud. These images are taken randomly and then both visible and invisible watermarks are embedded in them according to proposed formula which is described in next paragraphs.

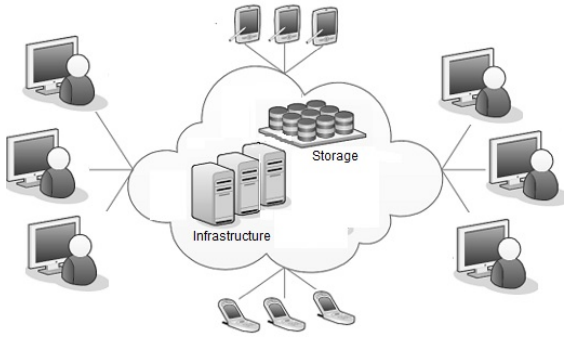

Fig. 5. Cloud computing network.

ownCloud inherits the characteristics of IaaS, a well-known service model of cloud computing as already discussed in Section III. Fig. 5 represents a network diagram between ownCloud and its users. Actually ownCloud infrastructure is installed at a centralized server computer and configured with a static IP address. Then, different kinds of nodes or clients like desktop computers, mobile phones, and laptops are deployed in a network. These clients can access the ownCloud interface through an IP address. All clients can upload and access their data to ownCloud through a web enabled-interface.

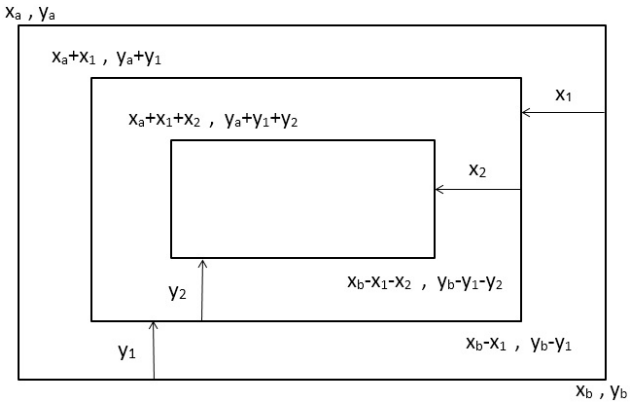

Fig. 6. Watermark placement in images.

Fig. 6 shows the strategy that is adopted to embed both visible and hidden watermarks on the uploaded data object like images. In order to perform the experiment, the whole image is divided into three rectangles. The hidden watermark in inserted into the innermost rectangle while visible watermark is placed into the outer rectangle adjacent to the outermost boundary of the image.

$$x_i = (x_{i-1})/(i \times 10) \quad (1)$$

$$y_i = (y_{i-1})/(i \times 10) \tag{2}$$

Where, $i \geq 1$, x_0, and y_0 is width and height of original image, respectively.

$$\sum_{i=1}^{l} x_i, \sum_{i=1}^{l} y_i \tag{3}$$

$$x_b - \sum_{i=1}^{l} x_i, y_b - \sum_{i=1}^{l} y_i \tag{4}$$

Where, $l \geq 1$

In (1) and (2), the gap between these rectangles in an image is calculated which separates the inner rectangle from outer one. Equation (1) calculates the width of inner rectangle which is reduced by ten percent w.r.t the width of outer rectangle, whereas (2) calculates height of inner rectangle. After calculating the gap from outer most layers, coordinates of first and last point of inner rectangle are calculated in (3) and (4). In this way, the whole area of the image is partitioned into three rectangles and both visible and invisible watermarks are embedded in outer and inner rectangle, respectively.

TABLE I. IMAGE UPLOADING TIME IN CLOUD (SEC)

Sr. No	without watermark	with watermark
1	0	0.27
2	0	0.31
3	0	0.33
4	0	3.57
5	0	5.98
6	0	7.65

VI. RESULT AND DISCUSSION

In this paper, the adopted methodology exposes an interesting open research question on data provenance in cloud computing. Data is increasing in huge amount, it is essential for provenance information to be shared along with the data object. In this work, a watermarking technique is used to store the provenance information about shared data objects in cloud computing. Data objects which are created by the cloud users are stored in the database of ownCloud in two steps. In first step, data is embedded with both visible and hidden watermark and in second step, watermarked data finally stores in ownCloud database.

In this section, a criteria is introduced to evaluate the efficiency and reliability of the adopted methodology. This criteria takes decision upon the results that are generated from the proposed watermarking technique. The efficiency of the proposed watermarking technique is measured in terms of time required to upload a data object from client's local machine to cloud database. For one data object, it's time to watermark the input data object and then to store that watermarked object in ownCloud database. In Table I, it can be seen that for all six different images, time required to upload the watermarked image is greater than that of without watermark image. Another aspect is the size of the uploaded image which is increased when both visible and invisible watermarks are embedded in it.

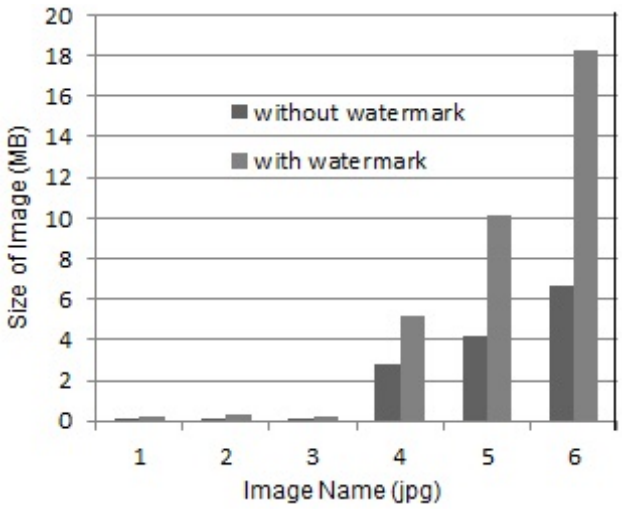

Fig. 7. Size of original and watermarked images.

Size difference of all six images with and without watermarks is depicted graphically in Fig. 7. On the other hand, reliability depends on the nature of watermarks that are embedded on the shared data object in cloud computing. In this scenario, two dissimilar watermarks are used i.e. visible watermark is different from hidden watermark in every aspect. This feature enhances security of data objects in cloud computing.

VII. CONCLUSION

The main focus throughout this paper is on the problem of determining the trustworthiness of data in cloud computing. In order to trust on the cloud data, there is a need to track the origin of data object. To address this problem, a watermarking technique is proposed which stores the information about the origin of data product. This technique uses two important types of watermarks that are visible watermark and hidden watermark. By adopting this methodology, shared data object in the cloud can be safe from the malicious attack that may change or lose the real ownership of that data object. Finally, the efficiency and reliability of this adopted approach is evaluated by calculating the time required to embed both visible and hidden watermarks on data objects. In this paper, the problem of data provenance is focused within a same cloud computing environment. In the near future, some other techniques are expected to ensure the trustworthiness of shared data objects among different cloud computing environments simultaneously.

REFERENCES

[1] S. Sakr, A. Liu, D. M. Batista, and M. Alomari, "A survey of large scale data management approaches in cloud environments," *IEEE Communications Surveys & Tutorials*, vol. 13, no. 3, pp. 311–336, 2011.

[2] C. Dai, D. Lin, E. Bertino, and M. Kantarcioglu, "An approach to evaluate data trustworthiness based on data provenance," in *Workshop on Secure Data Management*. Springer, 2008, pp. 82–98.

[3] A. Patawari, *Getting started with ownCloud*. Packt Publishing Ltd, 2013.

[4] R. Halder, S. Pal, and A. Cortesi, "Watermarking techniques for relational databases: Survey, classification and comparison." *J. UCS*, vol. 16, no. 21, pp. 3164–3190, 2010.

[5] K. Ramya, R. C. Devi, M. Revathi, and P. Annapandi, "Sensor data hiding based on image watermarking using interpolation technique over inter-packet delays." *Applied Mechanics & Materials*, no. 573, 2014.

[6] M. D. Swanson, M. Kobayashi, and A. H. Tewfik, "Multimedia data-embedding and watermarking technologies," *Proceedings of the IEEE*, vol. 86, no. 6, pp. 1064–1087, 1998.

[7] M. Schäler, S. Schulze, R. Merkel, G. Saake, and J. Dittmann, "Reliable provenance information for multimedia data using invertible fragile watermarks," in *British National Conference on Databases*. Springer, 2011, pp. 3–17.

[8] L. Zhang, Y. Zhu, and L.-M. Po, "A novel watermarking scheme with compensation in bit-stream domain for h. 264/avc," in *IEEE International Conference on Acoustics Speech and Signal Processing (ICASSP)*. IEEE, 2010, pp. 1758–1761.

[9] M. U. Sarwar, M. K. Hanif, R. Talib, and M. A. Abbas, "Ensuring data provenance with package watermarking," *International Journal of Advanced Computer Science and Applications*, vol. 8, no. 5, pp. 498–501, 2017.

[10] A. Tiwari and M. Sharma, "Semifragile watermarking schemes for image authentication-a survey," *International Journal of Computer Network and Information Security*, vol. 4, no. 2, pp. 43–49, 2012.

[11] J. Zhang, A. T. Ho, G. Qiu, and P. Marziliano, "Robust video watermarking of h. 264/avc," *IEEE Transactions on Circuits and Systems II: Express Briefs*, vol. 54, no. 2, pp. 205–209, 2007.

[12] Y. L. Simmhan, B. Plale, and D. Gannon, "A survey of data provenance techniques," *Computer Science Department, Indiana University, Bloomington IN*, vol. 47405, 2005.

[13] M. Greenwood, C. Goble, R. D. Stevens, J. Zhao, M. Addis, D. Marvin, L. Moreau, and T. Oinn, "Provenance of e-science experiments-experience from bioinformatics," in *Proceedings of UK e-Science All Hands Meeting 2003*, 2003, pp. 223–226.

[14] Y. Sun, J. Zhang, Y. Xiong, and G. Zhu, "Data security and privacy in cloud computing," *International Journal of Distributed Sensor Networks*, vol. 2014, 2014.

[15] R. Buyya, C. S. Yeo, S. Venugopal, J. Broberg, and I. Brandic, "Cloud computing and emerging it platforms: Vision, hype, and reality for delivering computing as the 5th utility," *Future Generation computer systems*, vol. 25, no. 6, pp. 599–616, 2009.

[16] W. Voorsluys, J. Broberg, and R. Buyya, "Introduction to cloud computing," *Cloud computing: Principles and paradigms*, pp. 1–44, 2011.

[17] B. Rajkumar, C. Yeo, S. Venugopal, J. Broberg, and I. Brandic, "Cloud computing and emerging it platforms," *Future Generation Computer Systems. Elsevier Press, Inc*, 2009.

[18] L. M. Vaquero, L. Rodero-Merino, J. Caceres, and M. Lindner, "A break in the clouds: towards a cloud definition," *ACM SIGCOMM Computer Communication Review*, vol. 39, no. 1, pp. 50–55, 2008.

[19] R. K. Perrons, "How the energy sector could get it wrong with cloud computing," *Energy Exploration & Exploitation*, vol. 33, no. 2, pp. 217–226, 2015.

[20] V. Zapolskas, "Securing cloud storage service," 2012.

[21] F. B. Shaikh and S. Haider, "Security threats in cloud computing," pp. 214–219, 2011.

[22] Z. Mahmood, "Data location and security issues in cloud computing," in *International Conference on Emerging Intelligent Data and Web Technologies (EIDWT)*. IEEE, 2011, pp. 49–54.

[23] A. Pandey, R. Tugnayat, and A. Tiwari, "Data security framework for cloud computing networks," *International Journal of Computer Engineering & Technology*, vol. 4, no. 1, pp. 178–181, 2013.

[24] M. Younis and K. Kifayat, "Secure cloud computing for critical infrastructure: A survey," *Liverpool John Moores University, United Kingdom, Tech. Rep*, 2013.

[25] D. Chen and H. Zhao, "Data security and privacy protection issues in cloud computing," in *Computer Science and Electronics Engineering (ICCSEE), 2012 International Conference on*, vol. 1. IEEE, 2012, pp. 647–651.

[26] B. Martini and K.-K. R. Choo, "Cloud storage forensics: owncloud as a case study," *Digital Investigation*, vol. 10, no. 4, pp. 287–299, 2013.

On FPGA Implementation of a Continuous-Discrete Time Observer for Sensorless Induction Machine using Simulink HDL Coder

Moez Besbes
Department of Electrical Engineering
ENIM, Road Ibn Eljazzar
5019 Monastir, Tunisia

Faouzi M'Sahli
Department of Electrical Engineering
ENIM, Road Ibn Eljazzar
5019 Monastir, Tunisia

Salim Hadj Sad
Department of Electrical Engineering
ENIM, Road Ibn Eljazzar
5019 Monastir, Tunisia

Monther Farza
Caen University
6 Bd Marechal Juin, 14050 Caen, France

***Abstract*—This paper deals with the design of a continuous-discrete time high gain observer (CDHGO) for sensorless control of an induction machine (IM). Only two weakly sampled stator current measurements are used to achieve a real-time estimation of the rotor flux, the mechanical speed and the load torque. The feasibility of implementing our algorithm on the FPGA target is discussed in term of the best word format choice for internal variables and in term of making up for problems attached with complex bloc diagram VHDL conversion. Before an eventual implementation on the Virtex FPGA board, a validation of the proposed observer is performed through the ModelSim software where we show that the waveforms of estimates bring closer the true ones.**

***Keywords*—Hig gain observer; FPGA; HDL coder**

I. Introduction

Due to their reliability, their low cost and their simple maintenance, induction motors (IM) remain the most used electric actuators in many industrial application (Hoisting cranes, roller conveyors, elevators, pumping...). In high performance IM drive systems, resolvers or encoders are usually required to determine the rotor position. Nonetheless, these sensors present several hindrances such as signal conditioning requirement, presence of noise measurement, increase of the installation cost and reduction of the total system robustness. To cope with such problem, many research efforts have been made in the last two decades to substitute the speed sensors by computational solutions. Therefore, the so called "speed sensorless control" is becoming standard solution in the area of induction machine drives despite of the persistent problems associated with it [1].

From only stator voltage and current measurements, different theoretical approaches of the nonlinear observers are exploited and experimentally carried out for providing an estimation of the mechanical speed, the rotor flux and the load torque. The extended Kalman filter (EKF) is one of the most famous algorithms used in speed sensorless IM drives and the lack of its theoretical justification is recently resolved under some assumptions in [2]. After providing a convergence analysis in the mean square sense, the authors have validated experimentally the implementation of the EKF algorithm in the stochastic environment. The technique of sliding mode observer (SMO) is used in [3] for jointly recovering the rotor flux, the mechanical speed and the load torque. It is shown that the flux and speed estimations are sensible to the stator resistance. The model reference adaptive system (MRAS) scheme based sensorless indirect stator flux oriented controlled IM drive is more recently proposed in [4]. The experimental results confirm that the estimated rotor speed converges to the real value despite of the large variations of the inertia moment. In [5], an adaptive backstepping observer (BO) for speed and rotor flux Backstepping control of IM drives is experimentally tested using the DSpace DS1104 board. The adaptation mechanism designed has contributed to reduce the sensitivity of the system performances against the abrupt change of the rotor constant time. The interconnected high gain observer (HGO) characterised by its simple implementation and its few number of design parameters have been applied in sensorless control IM in [6]. The applicability of the designed observer has been showed through the experimental robustness tests w.r.t the parameters variations.

In the majority cases, the implementation of the previous nonlinear observer algorithms has been eventually achieved through two digital supports: The software solution (DSP and microcontrollers) and the hardware solutions (FPGA). If the use of the DSP (software digital controllers) present the feature of design flexibility, attractive cost and ability to implement complex tasks, such selection remains limited in some industrial drive applications because of their fixed internal architecture which leads to fully serialize the treatment. On the other hand, field programmable gate arrays (FPGAs) are showed by several recent research studies as good candidates to achieve high control performances in industrial control applications [7], [8], [9]. Not only because that their specific architecture offers a significant integration density but also, due to the possibility to exploit the inherent algorithm parallelism. Such the feature can considerably reduce the execution time

of the algorithm computing.

Among the solutions for fast prototyping high performance control algorithms, Simulink HDL (Hardware Description Language) Coder is a suitable software to generate HDL codes (VHDL or Verilog) from fixed point Simulink models [10]. By exploiting its model blocks, users have to build the Simulink model with provided library to generate HDL codes which facilitate the implementation of complex control systems that require dedicated multipliers and computing units.

It is well-known that the digital implementation of nonlinear observers when using continuous-time measurements requires a fast sampling processes and large memory which may increase the cost and reduce the reliability.

In the contrast, using a relatively slow sampling process involves a degradation in the stability and the convergence properties of the state estimation error. By considering the availability of the output measurements only at the sampling instants, there have been several theoretical continuous-discrete nonlinear observer (CDNO) design approaches investigated in the last couple decades [11], [12], [13]. However, there are almost no work for the hardware implementation of the CDNO and a correspondent detail.

This paper deals with the feasibility study of a continuous-discrete time observer implementation on the FPGA board. The objective is to provide an estimation of the induction machine states through only two sampled currents measurement. We attempt to alleviate the necessary computational time by increasing the sample time and after that cancelling the request of a very fast $A\backslash D$ converter and a high computation hardware. The remainder of the paper is organised as follows. In the next section, we specify the class of nonlinear systems that correspond to the CDHGO design. In the third section, we detailed the induction machine model and the appropriate change of coordinates which allows reconstruct the IM state variables. We highlight in the fourth section our methodology and the steps to implement the underlying observer. Finally, the last section is devoted to illustrate some results obtained through ModelSim software.

II. Continuous-Discrete Time Observer Design

We consider the nonlinear systems which are diffeomorphic to the following bloc triangular form [14].

$$\begin{cases} \dot{z}(t) & = Az(t) + \varphi(u(t), z(t)) + B\epsilon(t) \\ y(t_k) & = Cz(t_k) = z^1(t_k) \end{cases} \quad (1)$$

with[1]:

$$z = \begin{pmatrix} z^1 \\ \vdots \\ z^{q-1} \\ z^q \end{pmatrix}; \varphi(u,z) = \begin{pmatrix} \varphi^1(u, z^1) \\ \varphi^2(u, z^1, z^2) \\ \vdots \\ \varphi^{q-1}(u, z^1, \cdots, z^{q-1}) \\ \varphi^q(u, z) \end{pmatrix}$$

$$A = \begin{pmatrix} 0_p & I_p & & 0_p \\ \vdots & \ddots & \ddots & \\ \vdots & & \ddots & I_p \\ 0_p & 0_p & \cdots & 0_p \end{pmatrix}, B = \begin{pmatrix} 0_p \\ \vdots \\ 0_p \\ I_p \end{pmatrix}$$

$$C = \begin{pmatrix} I_p & 0_p & 0_p \end{pmatrix}$$

Where, $z \in \mathcal{R}^n$ is the whole state vector and $z^i \in \mathcal{R}^p$ for $i \in [1, q]$. $u(t) \in U$ a compact subset of $\mathcal{R}^m$ and $y \in \mathcal{R}^p$ denote respectively the input and output of the system. Output measurements are supposed available only at the sampling time with respect the following condition:

$0 \leq t_0 < \cdots < t_k < t_{k+1} < \cdots$, for time-varying intervals $\tau_k = t_{k+1} - t_k$ and $\lim_{k\to\infty} t_k = +\infty$.

The function $\varphi(.)$ have a triangular structure and each $\varphi^i(.)$ for $i \in [1, q]$ is globally Lipschitz with respect to z uniformly in u. The $\epsilon(t)$ signal is considered as an unknown function denoting the system uncertainties.

Before giving the equations of the continuous-discrete time HGO, we need to satisfy the following assumptions :

A1. The state $z(t)$ is bounded, i.e. there exists a compact set $\Omega \in \mathcal{R}^n$ such that ? $\forall t \geq 0$, $z(t) \in \Omega$.

A2. The functions $\varphi^i(.)$ for $i = 1, \cdots, q$ are Lipschitz with respect to z uniformly in u, i.e. $\forall \rho > 0; ?\exists L > 0; ?\forall u$ such that $\|u\| \leq ?\rho$. $\forall (z, ?\bar{z}) \in ?\Omega \times \Omega : \|\varphi^i(u, z) - \varphi^i(u, \bar{z})\| \leq ?\|z - \bar{z}\|$.

A3. The unknown function $\varepsilon(t)$ is essentially bounded, i.e. $\|\varepsilon(t)\| \leq ?\delta$. The continuous-discrete observer that only uses the sampled time measurements is given by:

$$\dot{\hat{z}}(t) = A\hat{z}(t) + \varphi(u(t), \hat{z}(t)) + T_c(t) \quad (2)$$

with:

$T_c(t) = -\theta\Delta_\theta^{-1} e^{-\theta K^1 (t-t_k)} S^{-1} C^T (C\hat{z}(t_k) - y(t_k))$
$\Delta_\theta = diag(I_p, \frac{1}{\theta} I_p, ..., \frac{1}{\theta^{q-1}} I_p)$ θ is the sole synthesis parameter of the proposed observer. S is the explicit matrix solution of the algebraic Lyapunov equation: $S + A^T S + SA + C^T C = 0$. K^1 is the first element of the matrix K, where $K \in \mathcal{R}^{pqxp}$ is the rectangular matrix gain which is chosen such that $A - KC$ is Hurwitz. $K = \left[K^{1^T}, \cdots, K^{q^T}\right]^T = S^{-1}C^T = \left[\mathcal{C}_1^q I_{n_1} \ \cdots \ \mathcal{C}_q^q I_{n_q}\right]^T$, $K^i = k_i.I_p$ for $i = 1, ..., q$ and $\mathcal{C}_j^i = \frac{j!}{i!(j-i)!}$ for $1 \leq i, j \leq q$.

Theorem [14], [15] Consider the system (1) subject to assumptions A1, A2 and A3. Then, for every $u \in U$, for every $\theta > \theta_0$, there exists $\chi_\theta > 0$, $N_\theta(\tau_m, \tau_M) > 0$ such that if the

[1] in order to alleviate the written we omitted, at the next, the variable t

upper bound of the sampling partition diameter τ_M is chosen with $\tau_M < \chi_\theta$, then for every $\hat{x}(0) \in \mathcal{R}^n$, we have:

$$\| e(t) \| \leq \lambda \theta^{q-1} e^{\eta_\theta t} \| e(0) \| + N_\theta(\tau_m, \tau_M)\delta$$

with $0 < \tau_m < \tau_k = t_{k+1} - t_k < \tau_M$ and $e(t) = \hat{z} - z$. More detailed proof for estimation error convergence is illustrated in [14].

III. Observer Synthesis of the IM Model

The induction machine model can be represented in the fixed reference frame attached to the stator by the following expression:

$$\begin{cases} \dot{I} = KF(\omega)\Psi - \gamma I + \frac{1}{\sigma L_s} u \\ \dot{\Psi} = -F(\omega)\Psi + \frac{M}{T_r} I \\ \dot{\omega} = \frac{pM}{JL_r} I^T J_2 \Psi - \frac{1}{J} T_L \\ \dot{T}_L = \varepsilon_{T_L} \\ y(t_k) = I(t_k) \end{cases} \tag{3}$$

with

$T_r = \frac{R_r}{L_r}$, $\sigma = 1 - \frac{M^2}{L_r L_s}$, $K = \frac{M}{\sigma L_r L_s}$, and $\gamma = \frac{R_s}{\sigma L_s} + \frac{R_r M^2}{\sigma L_s L_r^2}$.
$F(\omega) = \frac{1}{T_r} I_2 - p\omega J_2$, with I_2 is the 2-dimensional identity matrix and $J_2 = \begin{pmatrix} 0 & -1 \\ 1 & 0 \end{pmatrix}$ $u = [u_{\alpha_s}, u_{\beta_s}]^T$, $I = [I_{\alpha_s}, I_{\beta_s}]^T$, $\Psi = [\Psi_{\alpha_r}, \Psi_{\beta_r}]^T$

where

- u_{α_s}, u_{β_s}, I_{α_s}, I_{β_s}, Ψ_{α_r} and Ψ_{β_r} are respectively, the stator voltages, the stator currents and the rotor fluxes,
- R_s, R_r are stator (resp. rotor) per-phase resistances,
- L_s, L_r are stator (resp. rotor) per-phase inductances and M is the mutual inductance,
- ω, T_L, J and p denote respectively the mechanical speed, the load torque, the motor moment of inertia and the number of pairs of poles,
- ε_{T_L} is an unknown real value.

The main goal consists in achieving the estimation of the state variables of the IM such as angular speed, rotor flux and the load torque. Only both sampled stator currents and the voltage supplies are used in the continuous-discrete HGO for reconstructing the state of the system. In such design, we assume that the stage operation of the IM is so far to unobservability neighbourhood (for more detail see observability analysis in [17]). We introduce the following notations: $x = \begin{pmatrix} x^1 \\ x^2 \\ x^3 \end{pmatrix}$ with $x^1 = \begin{pmatrix} x_1^1 \\ x_2^1 \end{pmatrix}$, $x^2 = \begin{pmatrix} x_1^2 \\ x_2^2 \end{pmatrix}$, $x^3 = \begin{pmatrix} x_1^3 \\ x_2^3 \end{pmatrix}$,

where:

$x_1^1 = I_{\alpha_s}$, $x_2^1 = I_{\beta_s}$, $x_1^2 = \Psi_{\alpha_r}$, $x_2^2 = \Psi_{\beta_r}$, $x_1^3 = \omega$ and $x_2^3 = T_L$.

So, the IM model can be written under the following standart form:

$$\begin{cases} \dot{x}(t) = f(x(t), u(t)) + B_1 \bar{\epsilon}(t) \\ y(t_k) = Cx(t_k) = x^1(t_k) \end{cases} \tag{4}$$

with $f(.)$ can be easily deduced from (3), $B_1^T = [0_{1\times 5} \ \ 1]$ and $\bar{\epsilon}(t) = \epsilon_{T_L}$.

Now, in order to transform system (3) into the considered class (1), we propose the following Lipschitzian diffeomorphism:

$$\Phi : \mathcal{R}^6 \to \mathcal{R}^6, x \mapsto z = \begin{pmatrix} z^1 \\ z^2 \\ z^3 \end{pmatrix} = \Phi(x) = \begin{pmatrix} \Phi^1(x) \\ \Phi^2(x) \\ \Phi^3(x) \end{pmatrix} \tag{5}$$

where Φ^k for $k = 1, 2, 3$ are defined as follows:

$$\begin{cases} z^1 = \Phi^1(x) = I \\ z^2 = \Phi^2(x) = KF(w)\psi \\ \qquad\quad = K\left(\frac{1}{T_r} I_2 - pwJ_2\right)\psi \\ z^3 = \Phi^3(x) = -pKJ_2\left(\dot{w}\psi + w\dot{\psi}\right) \end{cases} \tag{6}$$

The time derivative of the above states allows us to have :

$$\begin{cases} \dot{z}^1 = z^2 + \varphi^1(u, z^1) \\ \dot{z}^2 = z^3 + \varphi^2(z^1, z^2) \\ \dot{z}^3 = \varphi^3(z) + b(z)\epsilon(t) \\ y(t_k) = Cz(t_k) = z^1(t_k) \end{cases} \tag{7}$$

with $z = \begin{pmatrix} z^1 \\ z^2 \\ z^3 \end{pmatrix}$; $z^k = \begin{pmatrix} z_1^k \\ z_2^k \end{pmatrix}$

for $k = 1, .., 3$;

The nonlinear functions $b(.)$ and $\varphi^k(.) \in \mathcal{R}^2$, $k = 1, 2, 3$ are defined as follows:

$$\begin{cases} \varphi^1(u, z^1) = -\gamma z^1 + \frac{1}{\sigma L_s} u \\ \varphi^2(z^1, z^2) = \frac{1}{T_r}\left(-z^2 + \frac{MN}{T_r} z^1\right) \\ \varphi^3(z) \triangleq \frac{\partial \Phi^3}{\partial x^1}(.)\dot{x}^1 + \frac{\partial \Phi^3}{\partial x^2}(.)\dot{x}^2 + \frac{\partial \Phi^3}{\partial x_1^3}(.)\dot{x}_1^3 \\ b(z) \triangleq \frac{\partial \Phi^3}{\partial x_2^3}(.) \end{cases}$$

Thereafter, the IM model (3) can be written in the form (1) as follows:

$$\dot{z} = \begin{pmatrix} 0 & I_2 & 0 \\ 0 & 0 & I_2 \\ 0 & 0 & 0 \end{pmatrix} z + \begin{pmatrix} \varphi^1(.) \\ \varphi^2(.) \\ \varphi^3(.) \end{pmatrix} + \begin{pmatrix} 0 \\ 0 \\ b(z) \end{pmatrix} \epsilon \tag{8}$$

So, we can adapt a continuous-discrete observer in the z-coordinate as given in (2). When, using the inverse transformation $x = \phi^{-1}(z)$ and considering the new variable r such

as $r = F(\omega)\Psi$, the observer can be re-written in the original coordinates as the following form:

$$\begin{cases} \dot{\hat{I}} = K\hat{r} - \gamma\hat{I} + \frac{1}{\sigma L_s}u - 3\theta_1 e^{-3\theta_1(t-t_k)}(\hat{I}_k - I_k) \\ \dot{\hat{r}} = -pJ_2(\frac{M}{T_r}\hat{I} - \hat{r})\hat{\omega} + \frac{1}{T_r}(\frac{M}{T_r}\hat{I} - \hat{r}) \\ \qquad\qquad -3\frac{\theta_1^2}{K}e^{-3\theta_1(t-t_k)}(\hat{I}_k - I_k) \\ \dot{\hat{\omega}} = -\frac{1}{J}\hat{T}_L - \frac{pM}{JL_r}\hat{I}^T J_2(\frac{1}{T_r}I_2 - pJ_2\hat{\omega})^{-1}\hat{r} \\ \qquad\qquad -\frac{\theta_1^3}{pK}\left(F(\omega)\right)^{+} e^{-3\theta_1(t-t_k)}(\hat{I}_k - I_k) \end{cases} \tag{9}$$

The flux estimate can be easily reconstructed from the expression of $\hat{r}$ i.e. $\hat{\Psi} = \frac{1}{K}F(\omega)^{-1}\hat{r}$.

Now, the load torque estimation and its derivative is obtained by another HGO which is designed and placed in cascade according to (9):

$$\begin{cases} \dot{\hat{\hat{\omega}}} = -\frac{1}{J}\hat{T}_L - \frac{pM}{JL_r}\hat{I}^T J_2\Psi - \frac{1}{J}\hat{\tau_L} - 3\theta_2(\hat{\hat{\omega}} - \hat{\omega}) \\ \dot{\hat{\tau}}_L = \tau_{L_p} + 3J\theta_2^2(\hat{\hat{\omega}} - \hat{\omega}) \\ \dot{\hat{\tau}}_{L_p} = J\theta_2^3(\hat{\hat{\omega}} - \hat{\omega}) \end{cases} \tag{10}$$

IV. Simulation Results

To highlight the performance of the CDHGO w.r.t to the CHGO, we compared the estimates of both algorithm with a weak sample time choice ($T_e = 5.10^{-3}s$). The estimation results of the mechanical speed and load torque are illustrated in Fig. 1 whereas reconstruction of the stator currents and the rotor flux is given in Fig. 2.

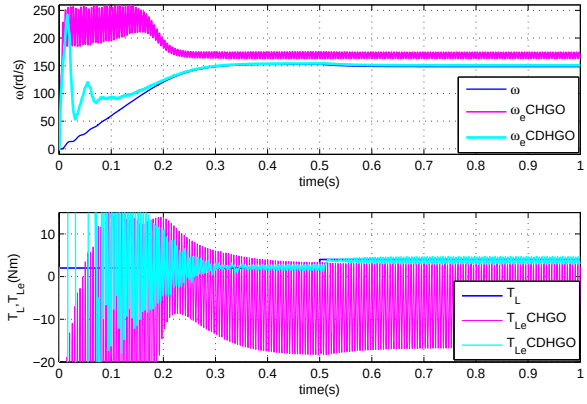

Fig. 1. The mechanical speed and the load torque estimation ($T_e = 5.10^{-3}s$).

Note that the first curve of all figure legends represents the state variables of IM given by the underlying model. The second signals refers to continuous HGO (CHGO) algorithm where the third one results from the CDHGO routine. We recall that the sole measurements signals used in both observer algorithms (i.e. the stator currents) are only available at the sample instant. We can show that the CDHGO performs well the reconstruction of the output signal (Fig. 2 graph a and b) whereas the current estimate waveforms is not perfectly sinusoidal in the case of CHGO. Such observation is also visible for the rotor flux estimation. In Fig. 1, whether for mechanical speed or load torque, we can remark that the CHGO presents many oscillations even in the steady state

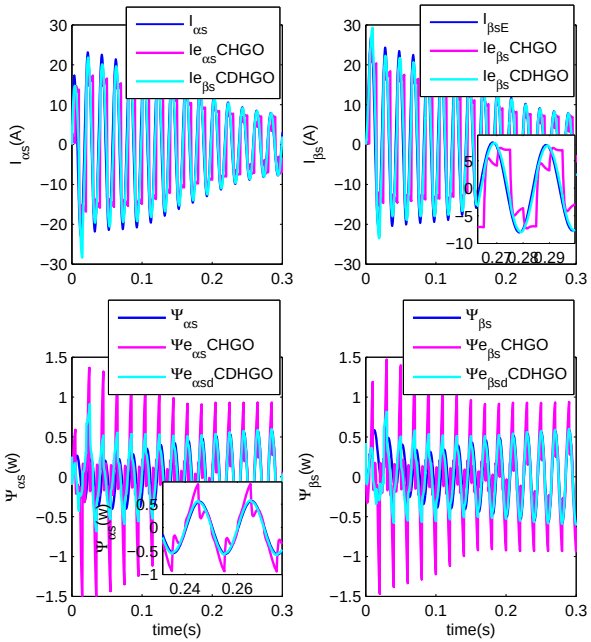

Fig. 2. The stator currents and the rotor flux estimation ($T_e = 5.10^{-3}s$).

regime. In contrary, in spite of some overshoots showed at the transient, the application of CDHGO achieves a quite estimation of these inaccessible states.

V. Implementation Methodology and Validation

The evaluation of the proposed observer in such AC drive application is achieved using an experimental setup shown in Fig. 3. It consists of an induction machine supplied by a voltage source inverter (VSI) and it is associated with a load and an incremental encoder. The system works without a speed sensor, while only the inverter input voltage and output currents are measured. The VHDL code is generated with HDL coder from Matlab-Simulink. The specification of the word format for the observer design is directly tuning with the fixed point toolbox. It is worth noticing that some inversion module of the observer algorithm are replaced by lookup table method which can alleviate the computational time [16]. The switching signals of the inverter are provided by the FPGA Virtex board. These PWM (pulse width modulation) control signals are generated by the triangular waveform modulator. Note that the frequency of triangular signal is constrained by the switching time of power switches accommodated in the three phases inverter. In our case, we have specified the PWM frequency at 2Khz.

The two sampled stator current measurements are provided by the ADC (analogue digital converter) with 12-bit resolution. In order to perform experimentally the underlying continuous-time high gain observer, the implementation has required the development of several tasks. In the first step, we used the solver with the variable-step (ode45). In this case, all blocs such as the adder, the gain, the multiplier and so on are configured in the default way. It means that we adopted the double precision format to obtain acceptable results with low

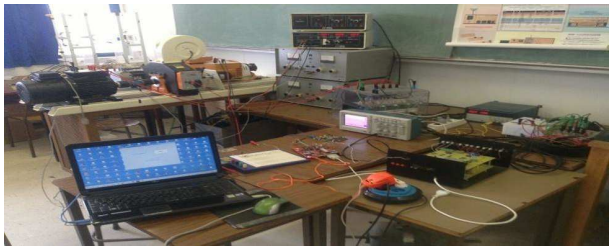

Fig. 3. Induction machine test bench.

ripple and best accuracy. In the second step, we switched to the discrete solver. So, a particular attention has been taking in the choice of each couple (W, F)[2] for all internal variables. Then, a VHDL file is generated using the HDL Coder Toolbox. Finally, in order to validate our observer design we have exploited the ModelSim software. At this stage, we have taking int account the size of the allowed resources that is indicated by the ISE software and this though and optimisation of the couple (W, F).

The characteristics of the involved IM are given as follows: $P = 1.5kw$, $p = 2$, $L_s = .13H$, $M = .083H$, $L_r = .069H$, $R_s = 3.9\Omega$, $R_r = 3.9\Omega$, $J = 0.22kgm^2$.

After several simulation, we have choose the both HGO design parameters as follows: $\theta_1 = 800$ and $\theta_2 = 200$.

The sample time T_e is specified as $5\ 10^{-3}s$. To illustrate the performance of the designed observer, a step load torque is applied at $0.25s$ with the value $T_L = 10Nm$. Both CDHGO algorithm and IM discrete model (by using Euler approximation of (3)) are implemented in Virtex FPGA board and the comparison is carried out between the estimated states and the true ones. The curves obtained by ModelSim software for each estimated state are illustrated in Fig. 4. The graphs (a) (b) (c) and (d) correspond respectively to α component of the rotor flux, β component of the rotor flux, mechanical speed and the load torque. In all graphs, the first curve represent the true state, where the second refers to CDHGO estimates. We can show that despite some overshoots at the transient, each component of the estimated flux track well the true one. Moreover, a good agreement can be recorded from the mechanical speed and the load torque in one side and these estimates in the other side.

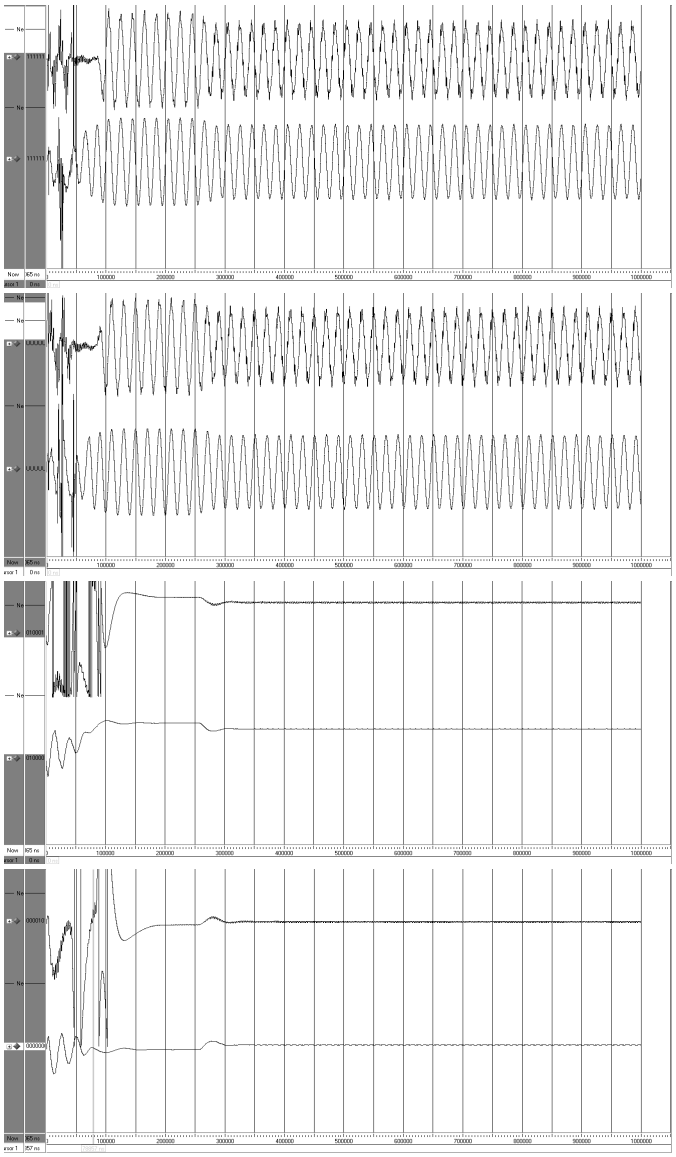

Fig. 4. Estimation results provided by Modelsim for rotor flux (ϕ_α, ϕ_β), mechanical speed ω and the load torque T_L.

VI. Conclusion

The FPGA implementation of a CDHGO with less knowledge as possible of output measurements is studied in this paper. Precisely, for an induction motor application, we have focus at the estimation of the rotor flux, the mechanical speed and the load torque by using only the two weakly sampled stator currents. After a comparison with the continuous version of the HGO algorithm when the sample frequency is imperfect, the sampled output observer design shows the best reconstruction of the original output signal as well as more realistic estimation of the missing states. Driving profit from the advanced Matlab Simulink tools such as HDL Coder and Fixed point toolbox, the implementation of the nonlinear observer is achieved and validation results are obtained through ModelSim soft-ware. Now, with the success of the CDHGO implementation, it is possible to use a lower cost digital hardware that can works with a relatively low sample frequency.

[2]W:Word length, F: Fractional part

References

[1] J. Holtz, Sensorless control of induction machines-With or without signal injection" IEEE Trans. Ind. Electron., 53(1):7-30, 2006.

[2] F. Alonge, T. Cangemi, F. D'Ippolito, A. Fagiolini, and A. Sferlazza, Convergence Analysis of Extended Kalman Filter for Sensorless Control of Induction Motor, IEEE Trans. Ind. Electron., 62(4):2341-2352, 2015

[3] Malek Ghanes and Gang Zheng, On Sensorless Induction Motor Drives: Sliding-Mode Observer and Output Feedback Controller, injection" IEEE Trans. Ind. Electron., 56(9):3404-3412, 2009.

[4] Youssef Agrebi Zorgani, Yassine Koubaa, Mohamed Boussak, MRAS state estimator for speed sensorless ISFOC induction motor drives with Luenberger load torque estimation, ISA Transactions,61:308-317, 2009.

[5] Trabelsi, R., A. Kheder, M. Faouzi Mimouni and F. M'sahli, An Adaptive Backstepping Observer for on-line rotor resistance adaptation. Int. J. Sciences and Techniques IJ-STA 4(1): 1246-1267, 2010.

[6] M. Ghanes, J. De Leon, A. Glumineau, Observability study and observer-based interconnected form for sensorless induction motor Proc. 45th IEEE Conf. Decision and Control, 1240-1245.

[7] E. Monmasson, L. Idkhajine, M. N. Cirstea, I. Bahri, A. Tisan, and M. W. Naouar, FPGAs in industrial control applications, IEEE Trans. Ind. Inf., 7(2): 224243, 2011.

[8] L. Idkhajine, E. Monmasson, and A.Maalouf, Fully FPGA-based sensorless control for synchronous AC drive using an extended Kalman filter, IEEE Trans. Ind. Electron., 59(10):3908-3918, 2012.

[9] J. Guzinski and H. Abu-Rub, Speed Sensorless Induction Motor Drive With Predictive Current Controller, IEEE Trans. Ind. Electron., 60(2):699-675, 2013.

[10] Z. Ma, J. Gao, and R. Kennel, FPGA Implementation of a Hybrid Sensorless Control of SMPMSM in the Whole Speed Range, IEEE Trans. Ind. Electron., 9(3):1253-1261, 2013.

[11] M. Nadri, H. Hammouri, and R. Grajales, Observer design for uniformly observable systems with sampled measurements, IEEE Trans.Auto. Contr. 58: 757762, 2013.

[12] T. Ahmed-Ali, V. V. Assche, J.-F. Massieu, and P. Dorleans, Continuous-discrete observer for state affine systems with sampled and delayed measurements, IEEE Tran. Auto. Cont. 58:10851091, 2013.

[13] M. Farza, M. M'Saad, M. L. Fall, E. Pigeon, O. Gehan, and K. Busawon, Continuous-Discrete Time Observers for a Class of MIMO Nonlinear Systems IEEE Trans Auto. Contr., 59(4), 2014.

[14] M. Farza, I. Bouraoui, T. Menard, R. Ben Abdennour, M. M'Saad, Sampled output observer design for a class of nonlinear systems, Proc. of Eur. Cont. Conf. (ECC), Strasbourg, France, June 24-27, 2014.

[15] I. Bouraoui, M. Farza, T. Menard, R. Ben Abdennour, M. M'Saad, H. Mosrati, Observer design for a class of uncertain nonlinear systems with sampled outputsApplication to the estimation of kinetic rates in bioreactors, Automatica, 55:7887, 2015.

[16] Y.P.Siwakoti, G.E.Town, Desing of FPGA-controlled Power Electronics and Drives Using MATLAB Simulink, Proc.of IEEE ECCE-Asia, 571-577, 2013.

[17] A. Dib, M. Farza, M. M'Saad, Ph. Dorlans, J.F. Massieu, High gain observer for sensorless induction motor, IFAC Proc. 44(1):674-679, January 2011.

[18] M. Farza, M'Saad, M. Triki, and T. Maatoug. High gain observer for a class of non-triangular systems. Systems & Control Letter, 60(1):27-35, 2011.

[19] G. Beasanon and H.Hammouri, On uniform observation of non uniformly observable systems, Systems Control Lett.29:9-19, 1996.

[20] M. Besbes, S.H. Sad, F M'sahli, FPGA implementation of high gain observer for induction machine using Simulink HDL coder, Proc. IEEE CEIT, 2015.

A Feature Selection Algorithm based on Mutual Information using Local Non-uniformity Correction Estimator

Ahmed I. Sharaf
Dept. of Computer Science
Computers & Informations Faculty
El-Mansoura University, Egypt

Mohamed Abu El-Soud
Dept. of Computer Science
Computers & Informations Faculty
El-Mansoura University, Egypt

Ibrahim El-Henawy
Dept. of Computer Science
Computers & Informations Faculty
Zagazig University, Egypt

***Abstract*—Feature subset selection is an effective approach used to select a compact subset of features from the original set. This approach is used to remove irrelevant and redundant features from datasets. In this paper, a novel algorithm is proposed to select the best subset of features based on mutual information and local non-uniformity correction estimator. The proposed algorithm consists of three phases: in the first phase, a ranking function is used to measure the dependency and relevance among features. In the second phase, candidates with higher dependency and minimum redundancy are selected to participate in the optimal subset. In the last phase, the produced subset is refined using forward and backward wrapper filter to ensure its effectiveness. A UCI machine repository datasets are used for validation and testing. The performance of the proposed algorithm has been found very significant in terms of classification accuracy and time complexity.**

Keywords*—Feature subset selection; irrelevant features; mutual information; local non-uniformity correction

I. Introduction

In many applications of machine learning, the number of samples and dimensions of most datasets have grown rapidly [1]. Since the computational power, processing time and classification accuracy depend on the size of data therefore, reducing the dataset represents a challenge for researches. The primary motivation of reducing dimensions of data and minimizing the set of features is to decrease the training time and to enhance the classification accuracy of the algorithms [2], [3], [4]. Feature subset selection provides an approach for dimensions reduction and data minimization by replacing the original set of features with a compact subset that acts similar to the original one. This approach has been used in several applications in engineering, economy and medical sciences [5], [6], [7], [8].

Feature subset selection is categorized into two main approaches in terms of evaluation strategy [1]: First, the wrapper approach which depends on searching the whole search space to find the optimal subset [9]. This approach finds every combination of subsets to determine the accuracy by the classifier predication function. Thus, the quality of this subset is calculated without any modification of the learning algorithm. Since the produced subset is optimized for a particular classification algorithm therefore, the main advantage of the wrapper approach is the high accuracy. On the other hand, searching every combination consumes the computational power. The wrapper approach may also suffer from over-fitting to the learning algorithm. This drawback may also occur, when any parameter changes in the learning model [10].

Second, the filter approach depends on ranking each feature according to a specific evaluation function using distance, information and statistical measures. Many techniques have been proposed to calculate the feature relevance including: Fishers Discriminate Ratio [11], the Single Variable Classifier [12], Mutual Information [13], the Relief Algorithm [14], Rough Set Theory [15] and Data Envelopment Analysis [16]. The main advantage of the filter approaches is the computational efficiency and scalability in terms of the data dimensionality. Even though the filter approach is faster than the wrapper it suffers from lack of information between the features and the classifier. This approach may also select irrelevant or redundant features because of the limitation of the evaluation function [17].

Information theory [18] has been applied in many filter approaches to determine the relevance and redundancy of features. In feature subset selection process, mutual information is used to measure relevance and redundancy of features effectively. It has been applied by many researchers to characterize the information content of features [13], [19], [20]. The primary contribution of this research is to generate a compact feature subset with high accuracy and to keep the time complexity as minimum as possible. This paper is organized as: Section II introduces the related work and the limitations of the previous work. In Section III, the preliminaries and essential knowledge of information system, mutual information, conditional entropy and feature significance are discussed. In Section IV, the proposed algorithm is illustrated in detail. In Section V, the experiment and final results are presented. Finally, the paper is concluded in Section VI.

II. Related Work

Authors proposed many approaches for the enhancement of feature subset selection using several methods. Mutual information was first proposed by Battiti, et al. [13] to improve the selection process by providing a novel algorithm called Mutual Information Feature Selection (MIFS). The MIFS used mutual information among features and between each feature and the

decision class to determine the best k features from the original set. The MIFS used the traditional greedy algorithm to select the optimal candidate set. The MIFS introduced the concept of relevance and redundancy using mutual information. Battiti proved that mutual information could be very useful for feature selection problems, and illustrated that his proposed MIFS is suitable for any classification issues. However, this method is not suitable for non-linear ones. Kwak and Choi [21] analyzed the work presented by Battiti and proposed an enhancement of the MIFS method. Kwak and Choi introduced MIFS-U that enhanced the estimation of information between input features and decision classes obtained from the MIFS. However, they neglected the behavior of the selected features together and focused on individual features.

Peng and Long [19] proposed a different method for solving feature selection problem based on min-redundancy and max-relevance mRMR. This method consists of two steps: in the first step, the best candidate elements are selected using the mRMR first order incremental criteria. In the second one, the wrapper filter is applied to search the obtained candidate set using backward and forward selections algorithms. However, this method searches the complete search space to find the compact subset of features which is a high computational cost. Therefore, it is necessary to reduce the search space with any reduction method or refine the candidate feature set.

The presented methods are all incremental methods that search for one feature at a time according to specific criteria. This strategy neglects the relationship among feature groups and could select one element to represent the group if it is better than the other candidates.

III. Preliminaries

In this section, a brief introduction to information theory, basic principles and concepts are presented. An Information System IS is defined as quadruple such that $IS = (U, A, V, f)$ where U denotes a non-empty set contains the whole set of objects, A denotes the finite non-empty set of features, V represents the combination of all feature domains $V = \bigcup_{a \in A} V_a$ and V_a is the domain of a specific feature $a \in A$, and f represents the mapping function $f : U \times A \to V$ that produces a unique values of each feature with each object belongs to the universe. Let there is subset called P such that $P \subseteq A$, then for each P there is an associated indiscernible relation defined as $IND(P) = \{(u, v) \in U \times U \mid \forall a \in P, f(u, a) = f(v, a)\}$, it is clear that $IND(P)$ is an equivalence relation on the universe U for $P \subseteq A$. The universe is divided into a various number of classes (granules) by this relations such that $U/IND(P) = \{[u]_p \mid u \in U\}$ where $[u]_p$ is the equivalence class calculated by u with respect to subset P. For any given $P \subseteq A$, there is a binary relation called $SIM(P)$ that defined as follows $SIM(P) = \{(u, v) \in U \times U \mid \forall a \in P, f(u, a) = f(a, v)\}$. Let $S_p(u)$ is the maximal set of instances that possibly indistinguishable the universe U by the set P such that $S_p(u) = \{v \in U \mid (u, v) \in SIM(P)\}$. A member $S_p(u)$ from $U/SIM(P)$ is called an information granule. [22].

The information entropy among random variables is defined as the required amount of information to describe this variable x [18], [23]. The entropy of a discrete random variable $X = (x_1, x_2, , x_n)$ is denoted as $H(X)$ and defined as follows:

$$H(X) = -\sum_{i=1}^{n} P(x_i) lg(P(x_i)) \tag{1}$$

Where x_i represents the possible values of x and $P(x_i)$ states for the probability of x_i. In the case of discrete random variable then:

$$P(x_i) = \frac{Number\_of\_instances(x_i)}{total\_number\_of\_instances} \tag{2}$$

The base of the used logarithm is two because the unit of measuring entropy are bits. For any two discrete random variables called X and Y with corresponding probability distribution $P(x; y)$. The conditional entropy is defined as:

$$H(X|Y) = -\sum_{x_i \in X}^{X_m} \sum_{y_i \in Y}^{Y_n} P(x, y) lg(P(x, y)) \tag{3}$$

The mutual information is defined as the amount of information that variable X contains about variable Y and is represented as follows:

$$I(X; Y) = \sum_{X_i \in X}^{X_m} \sum_{y_j \in Y}^{Y_n} P(x, y) lg \frac{P(x, y)}{P(x).P(y)} \tag{4}$$

The mutual information indicates the level of shared information between two random variables. Mutual information could be used to decrease computation by representing a relation between the entropy and the conditional entropy as follows:$I(X; Y) = H(X) - H(XY) = H(Y) - H(YX) = H(X) + H(Y) - H(X, Y)$. The high value of mutual information means that the two random variables are closely related to each other. Otherwise, if the mutual information value equals to zero, then the two variables are very independent of each other. Replacing Y with F_n and D defines both the feature to class and the feature to features terms respectively. Although the mutual information is a stable measure of obtaining the uncertainty, it is not a monotonic function. Therefore, Dai, et. al [24] presented a monotonic mutual information measure for incomplete decision tables as follows:

$$H(D|B) = -\sum_{i=1}^{|U|} \sum_{j=1}^{m} \frac{|T_B(u_i)| \cap |Y_j|}{|U|} log \frac{|T_B(u_i) \cap |Y_j|}{|T_B \cap (u_i)|} \tag{5}$$

Dai, et. al proved that this new formulation is a monotonic function that could be used for measuring uncertainty effectively. Mutual information is also used to determine the significance of a specific feature $b_i \in B$ such that $B \subseteq C$ with respect to D as follows:

$$sig(b_i, B, D) = I(D; B) - I(D; B - \{b_i\}) \tag{6}$$

The value of $sig(b_i, B, D)$ represents the change of mutual information if the feature b_i is removed from the subset B. The higher value of the mutual information is, the more significant

the feature is. If $sig(b_i, B, D) = 0$ then the feature b_i is dispensable.

IV. A Mutual Information based Uncertainty Measure

In this section, the ranking function is introduced to obtain the uncertainty of knowledge. The main properties and features are presented to illustrate the validity of the ranking function. In order to obtain the uncertainty for a target decision, measuring the feature dependency and the redundancy among features. Let $IS = (U, C \cup D)$ is a given information system, the uncertainty of knowledge is formulated as follows:

$$h(c) = \frac{\sum_{i=0}^{m} I(C, D_i)}{\sum_{i=0}^{m} I(C, D_i) + \sum_{j=0}^{n} I(C, C_j)} \tag{7}$$

Where, $I(C, D_i)$ and $I(C, C_j)$ represents the mutual information between the decision and a specific feature and the mutual information between a certain feature and the other features respectively.The proposed function $h(C)$ represents a relation between feature redundancy and decision dependency

Property 1. *Let $IS = (U, F \cup D)$ is an information system such that U represents the all space of objects, F is condition classes (features) set and D is the decision set. For $\forall A, B \subseteq C$, if $A \subseteq B$ then $h(A) \leq (B)$.*

Proof: Assume the universe of objects $U = \{x_1, x_2, ..., x_n\}$, the classification of U induced by subset A is $U/T_A(X) = \{T_A(X_1), T_A(X_2), ..., T_A(X_n)\}$, the classification induced by the set B is $U/T_B(X) = \{T_B(X_1), T_B(X_2), ..., T_B(X_n)\}$ and the classification produced by the decision D is $U/IND(D) = \{D_1, D_2, ..., D_m\}$. Since $A \subseteq B$ then the classification produced by the subset B is better than the classification produced by the subset A or simply $T_B(X) \subseteq T_A(X) i.e : |T_B(X)| \leq |T_A(X)|$. This equation is reformulated as follows: $T_A(X) = (T_A(X) \cap D_j) \cup (T_A(X) \cap (U - D_j))$ and similarly with subset $T_B(X) = (T_B(X) \cap D_j) \cup (T_B(X) \cap (U - D_j))$. From the inequality, we have $(T_B(X) \cap D_j) \leq (T_A(X) \cap D_j)$ and $(T_B(X) \cap (U - D_j)) \leq (T_A(X) \cap (U - D_j))$ respectively. Consequently from the monotonicity of $f(x, y) = -xlog\frac{x}{x+y}$ [24], we obtain that $-\frac{|T_B(X) \cap D_i|}{|U|} log\frac{|T_B(X) \cap D_i|}{|T_B(X)|} \leq -\frac{|T_A(X) \cap D_i|}{|U|} log\frac{|T_A(X) \cap D_i|}{|T_A(X)|}$. Hence, $H(D|B) \leq H(D|A)$ according to definition (x). Substituting with equation(x) then $h(A) \leq h(B)$. ■

Property 2 (Maximum Value)**.** *Let $IS = (U, C \cup D)$ is a given information system, the maximum value of $h(f)$ is one and occurs when $P(f, f_i) = P(f)P(f_i), \forall 0 < i < n - 1$ where n is the number of features.*

Property 3 (Minimum Value)**.** *Let $IS = (U, C \cup D)$ is a given information system, the minimum value of $h(f)$ is zero and occurs when $P(f, D_i) = P(f)P(D_i), \forall 0 < i < m - 1$ where m is the number of decision classes.*

A. Feature selection algorithm

In feature selection process based on mutual information, the tolerance classes must be computed for the complete decision system. This process is an exponentially time consuming that affects the total time performance. In order to design an effective feature selection algorithm based on mutual information for a decision system, a fast algorithm for assembling granules from a given decision system is introduced initially. This algorithm is mainly based on decomposition and mutual information estimation. Computing the mutual information is a very complex task especially for large dimensions or samples. Determining mutual information using the traditional method is a time-consuming task with an exponentially time complexity $O(n^2)$. Therefore, a non-parametric mutual information estimator based on Local Non-uniformity Correction (LNC) is used [25]. The main idea of LNC based algorithm is to calculate an average correction term $\overline{LNC}$ for all each point $x_i \in X$. The correction term $\overline{LNC}$ is used to adapt the value of Kraskov estimated mutual information [26]. The correction term is computed based the volume of max-norm rectangle $V(i)$ produced by the PCA analysis of the k_{th} nearest neighbors of each point x_i.

Algorithm 1 Mutual Information Estimation using LNC

1: **Input:** $X = \{x^1, x^2, ...x^m\}$ where X is the sample of point, d is the dimension size, k is the k-nearest neighbor and α is a threshold.
2: **Output:** $\hat{I}_{LNC}(X)$
3: Calculate $\hat{I}_{KSG}(X)$ using KSG estimator with k nearest neighbors.
4: **for all** $x_i \in X$ **do**
5: Find the k_{th} nearest neighbors of x^i as $\{knn_1{}^i, knn_2{}^i, ..., knn_k{}^i\}$
6: Apply PCA on the k_{th} nearest neighbors
7: Calculate the volume corrected rectangle $V(i)$, and volume of max-norm rectangle $\overline{V(i)}$
8: **if** $\overline{V(i)}/V(i) \leq \alpha$ **then**
9: $LNC_i = log(\overline{V(i)}/V(i))$
10: **else**
11: $LNC_i = 0$
12: **end if**
13: **end for**
14: Calculate $\overline{LNC} = \sum_{i=1}^{m} LNC_i/m$
15: $\hat{I}_{LNC}(X) = \hat{I}_{KSG}(X) - \overline{LNC}$
16: **return** $\hat{I}_{LNC}(X)$

The LNC estimator works typically for any dimensions d, for example to compute the mutual information $I(X; Y)$ using the LNC algorithm. Let the dimension parameter $d = 2$, the input array equals to $X = [[x_1, x_2, \ldots], [y_1, y_2, \ldots]]$, the K_{th} nearest neighbors $k = 3$ and threshold $\alpha = 0.25$. The time complexity of Algorithm 1 is determined as follows: for step(3) it is $O(Nk + d)$ which can be approximated to $O(N)$ since both k and d are relatively less than N. For step (5) it is $O(k)$, for step (6) it is $O(k^3)$, and the complexity of steps (7-12) are $O(1)$. Then the overall complexity becomes $O(N).(O(k) + O(k^3) + O(1))$ that yields to $O(Nk) \approx O(N)$.

B. Proposed Method

In this section, the feature subset selection is proposed in detail.

The proposed algorithm consists of three main blocks. In the first block from step(1) to step(12), the proposed measure

Algorithm 2 A Hybrid Mutual Information based Feature Selection Algorithm

Input: $IS = (U, C \cup D)$.
Output: Red The reduced subset.

1: Calculate $h(c_i), \forall c_i \in C$ using Algorithm 1.
2: Sort the features in descending order using radix sorting and then denote the result by $S = \{a_1, a_2, ...a_n\}$
3: Calculate $U/SIM(C)$.
4: **for all** $a_i \in S$ **do**
5: Calculate $U/SIM(C - \{a_i\})$.
6: Calculate $sig(a_i, C, D)$
7: **if** $(sig(b_i, C, D) == 0)$ **then**
8: $\bar{R} = \bar{R} \cup \{a_i\}$
9: **else**
10: $R = R \cup \{a_i\}$
11: **end if**
12: **end for**
13: Let $R' = R$
14: Calculate $U/SIM(R')$.
15: Construct an input sequence subset $P = \{a_1, a_2, ...a_k\}$ such that $k = |R'|$ and $k \leq n$.
16: **for all** $a_i \in P$ **do**
17: Calculate $U/SIM(R \cup \{a_i\})$.
18: Calculate $sig(a_i, R, D)$
19: **if** $(sig(a_i, R, D) \neq 0)$ **then**
20: $R' = R' \cup \{a_i\}$
21: **end if**
22: **end for**
23: Let $Red = R'$
24: Construct an input sequence subset $Q = \{a_1, a_2, ...a_l\}$ such that $l = |R'|$ and $l \leq n$.
25: **for all** $a_i \in R'$ **do**
26: Calculate $U/SIM(R' - \{a_i\})$.
27: Calculate $sig(a_i, R', D)$
28: **if** $(sig(a_i, R', D) \neq 0)$ **then**
29: $Red = Red - \{a_i\}$
30: **end if**
31: **end for**
32: **return** Red

is computed for each feature according to Eq.(7). Since the computation of mutual information is a time expensive process, an effective estimator is used to calculate this formula based on Local Non-uniformity Correction (LNC) and KSG estimator. Afterwards, radix sort is used to sort the features according to the value of $h(c_i)$ in a descending order. The radix sort is used to minimize the total computational cost as it is a linear time sorting. Then, the granules of information are obtained using Pawlak definitions with respect to the complete set of features [27]. Then, the significant of each feature is computed to construct an initial subset of features. If the significance of a feature equals to zero then its considered to be an irrelevant feature. Otherwise, the relevant feature is added to the optimal subset of features called R. In the second block from step(13) to step(22), the obtained subset R is refined using forward wrapper filter. The granule of information is calculated to determine the significance of the non-participated features. Each feature is joined to the generated subset R to study it's significant. Once the feature is considered a significant one with respect to R, then it should be merged to R. The last block from step(23) to step(32) is a backward wrapper, which makes it similar to the second block but with reverse effect.

The complexity analysis of the proposed algorithm is determined as follow: the time complexity of step(1) is $O(n|U|)$. For step(2), the radix sort is applied with a complexity of $O(n)$. For step(3), the time complexity is $O(n|U|)$. From step(4) to step(12) the complexity is $O(n) \times (O(|U|) + O(1))$ which is approximated to $O(n|U|)$. From step(13) to step(22), a forward wrapper filter is applied to determine the effect of any irrelevant feature to granules obtained by the classification of subset R. The complexity of the forward wrapper is $O(k|U|)$ where $k \leq n$. Then, a backward wrapper is used to refine the generated subset with a complexity of $O(l|U|)$ where $l \leq n$. Hence, to total complexity of proposed algorithm is $O(n|U|) + O(n) + O(n|U|) + O(k|U|) + O(l|U|)$ which approximately equals to $O(n|U|)$.

V. Experimental Results and Discussion

In this section, datasets description, numeric results and comparative studies are presented.

A. Dataset Description

Five datasets are used to benchmark and evaluate the proposed approach. These public datasets are used for benchmarking and validation of selection algorithms. A brief discussion of the used datasets is listed in Table I.

TABLE I. Description of Benchmarking Dataset

Dataset Name	Features Count	Instances Count
Breast Cancer Wisconsin	9	699
Glass	9	214
Ionosphere	34	351
Iris	4	150
Liver Disorder	6	345

The iris dataset is a very popular benchmarking dataset that contains information about iris plant. The Iris dataset contains three classes of 50 instances per class represents an iris category (Setosa, Versicolour, and Virginica). Also, the feature set includes a sepal length, sepal width, petal length, and petal width. The second dataset contains experimental information about breast cancer. Dr. William H. Wolberg collected this dataset from the University of Wisconsin Hospitals, Madison. There are nine features in this dataset out of ten features excluding the sample identifier. Each instance could be classified in the binary decision (benign or malignant). The missing values are replaced with the average value of the corresponding feature in order to prevent exceptions. The Liver Disorder dataset that contains blood measures tests. This dataset contains six features and 345 instances. Each instance could be classified into the binary decision. Finally, the Glass dataset that includes nine features and 214 instances with seven decision classes per instance. The numeric experiment is implemented using Python Scikit-learn [28] package. All comparative studies with the other methodologies are implemented on WEKA [29] software. The experiment is executed on an Intel(R) Core (TM) i7-2400 CPU 3.10GHz platform and MS Windows 10 installed.

B. Numeric Results And Comparative Studies

In this section, the numeric results of the experiment are presented. The proposed method is implemented on five datasets as described in Table I and achieved a high accuracy over the other methods. The Naive Bayes classifier is used to determine the accuracy of the proposed algorithm. The comparison is based on some standard methods such as Information Gain, Gain Ratio, Chi-Square, Best First Approach and Symmetrical Uncertainty. Also, the mRMR, MIFS, MIFS-ND and MIFS-U are also used for the ionosphere dataset. For the breast cancer dataset, the proposed method achieved the highest accuracy among the other methods as shown in Fig. 1. The minimum accuracy achieved by symmetric uncertainty method, then the best first method. All of the chi-squares, gain ratio and information achieved the same accuracy. The minimum scored accuracy is 91.04% and the maximum accuracy is 92.09%.

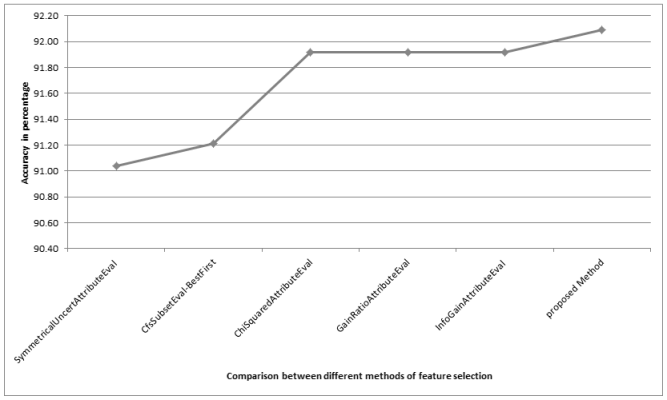

Fig. 1. A comparison between different methods of feature selection for breast cancer dataset.

For the glass dataset, the proposed method archived the highest accuracy as shown in Fig. 2. The minimum accuracy achieved by chi-square, gain ratio, information gain and symmetric uncertainty. The best first feature selection scored 49.53% accuracy and the proposed method scored 54.67%.

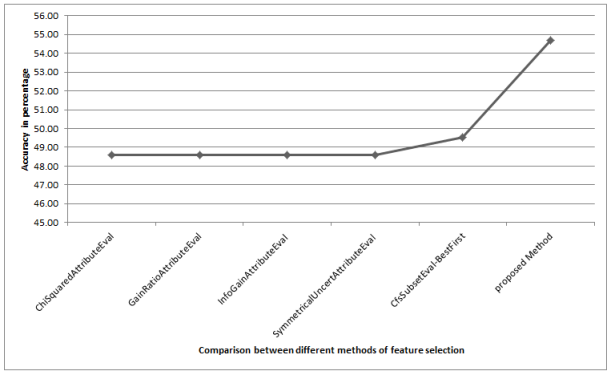

Fig. 2. A comparison between different methods of feature selection for the glass dataset.

For the ionosphere dataset, the proposed method achieved the best accuracy over the other methods as shown in Fig. 3. The MIFS-U achieved the best accuracy for only three features. The MIFS-ND scored the best accuracy over the all other methods. The proposed method scored the best accuracy from the other methods for the both the ten and fifteen features. The minim accuracy achieved for 15 features is 92% by MIFS, and the maximum accuracy is 94.3% by the proposed method.

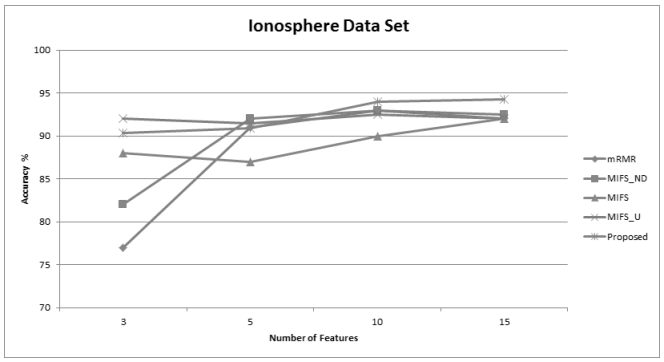

Fig. 3. A comparison between different methods of feature selection for the ionosphere dataset.

For the liver disorder dataset, the proposed method scored the best accuracy as shown in Fig. 4. The minimum accuracy achieved by most of the selections methods (chi-square, gain ratio, info gain and symmetric uncertainty). Then the best first scored accuracy of 58.55%. The best scored accuracy 58.84% achieved by the proposed method.

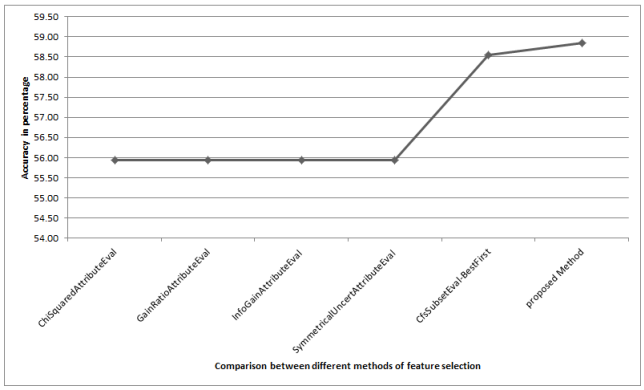

Fig. 4. A comparison between different methods of feature selection for the liver disorder dataset.

VI. Conclusion

In this paper, a feature subset selection algorithm is proposed based on mutual information and LNC estimator. Although information theory has used before for solving feature selection. The proposed method ranks the features according to $h(c)$ that represents the relation between features redundancy and decision dependency. A Mutual information estimator based on LNC is used to reduce the overall time complexity. Five dataset from the UCI machine repository are used for testing and validating the proposed algorithm. Naive Bayes classifier is used to compare the obtained feature subsets. Final results are compared to Information Gain, Chi-square, Best first methods. The results of Ionosphere datasets are compared to mRMR, MIFS, MIFS-ND and MIFS-U. The

obtained results from the comparative study illustrate the efficiency and accuracy of the proposed method. Reducing total time complexity of mutual information algorithms is also achieved.

REFERENCES

[1] G. Chandrashekar and F. Sahin, "A survey on feature selection methods," *Computers & Electrical Engineering*, vol. 40, no. 1, pp. 16 – 28, 2014.

[2] Y. Zhang, C. Yang, A. Yang, C. Xiong, X. Zhou, and Z. Zhang, "Feature selection for classification with class-separability strategy and data envelopment analysis," *Neurocomputing*, vol. 166, pp. 172–184, 2015. [Online]. Available: http://www.sciencedirect.com/science/article/pii/S0925231215004609

[3] L. Yu and H. Liu, "Feature selection for high-dimensional data: A fast correlation-based filter solution," in *ICML*, vol. 3, Conference Proceedings, pp. 856–863.

[4] A. Arauzo-Azofra, J. L. Aznarte, and J. M. Bentez, "Empirical study of feature selection methods based on individual feature evaluation for classification problems," *Expert Systems with Applications*, vol. 38, no. 7, pp. 8170–8177, 2011. [Online]. Available: http://www.sciencedirect.com/science/article/pii/S095741741001523X

[5] G. M. U. Din and A. K. Marnerides, "Short term power load forecasting using deep neural networks," in *Computing, Networking and Communications (ICNC), 2017 International Conference on*. IEEE, 2017, pp. 594–598.

[6] Y. Zhang, D.-w. Gong, and J. Cheng, "Multi-objective particle swarm optimization approach for cost-based feature selection in classification," *IEEE/ACM transactions on computational biology and bioinformatics*, vol. 14, no. 1, pp. 64–75, 2017.

[7] J. Yu, J. Yu, A. A. Almal, S. M. Dhanasekaran, D. Ghosh, W. P. Worzel, and A. M. Chinnaiyan, "Feature selection and molecular classification of cancer using genetic programming," *Neoplasia*, vol. 9, no. 4, pp. 292–IN3, 2007. [Online]. Available: http://www.sciencedirect.com/science/article/pii/S1476558607800996

[8] S. Sasikala, S. A. a. Balamurugan, and S. Geetha, "A novel feature selection technique for improved survivability diagnosis of breast cancer," *Procedia Computer Science*, vol. 50, pp. 16–23, 2015. [Online]. Available: http://www.sciencedirect.com/science/article/pii/S1877050915005062

[9] I. Guyon, S. Gunn, M. Nikravesh, and L. A. Zadeh, *Feature extraction: foundations and applications*. Springer, 2008, vol. 207.

[10] G. Brown, A. Pocock, M.-J. Zhao, and M. Luján, "Conditional likelihood maximisation: a unifying framework for information theoretic feature selection," *Journal of Machine Learning Research*, vol. 13, no. Jan, pp. 27–66, 2012.

[11] S. Wang, D. Li, X. Song, Y. Wei, and H. Li, "A feature selection method based on improved fishers discriminant ratio for text sentiment classification," *Expert Systems with Applications*, vol. 38, no. 7, pp. 8696–8702, 2011.

[12] I. Guyon and A. Elisseeff, "An introduction to variable and feature selection," *Journal of machine learning research*, vol. 3, no. Mar, pp. 1157–1182, 2003.

[13] R. Battiti, "Using mutual information for selecting features in supervised neural net learning," *Neural Networks, IEEE Transactions on*, vol. 5, no. 4, pp. 537–550, 1994.

[14] H. Zheng and Y. Zhang, "Feature selection for high-dimensional data in astronomy," *Advances in Space Research*, vol. 41, no. 12, pp. 1960–1964, 2008.

[15] J. Liang, F. Wang, C. Dang, and Y. Qian, "A group incremental approach to feature selection applying rough set technique," *IEEE Transactions on Knowledge and Data Engineering*, vol. 26, no. 2, pp. 294–308, 2014.

[16] Y. Zhang, A. Yang, C. Xiong, T. Wang, and Z. Zhang, "Feature selection using data envelopment analysis," *Knowledge-Based Systems*, vol. 64, pp. 70–80, 2014.

[17] Y. Saeys, I. Inza, and P. Larrañaga, "A review of feature selection techniques in bioinformatics," *bioinformatics*, vol. 23, no. 19, pp. 2507–2517, 2007.

[18] T. M. Cover and J. A. Thomas, *Elements of information theory*. John Wiley & Sons, 2012.

[19] H. Peng, L. Fulmi, and C. Ding, "Feature selection based on mutual information criteria of max-dependency, max-relevance, and min-redundancy," *Pattern Analysis and Machine Intelligence, IEEE Transactions on*, vol. 27, no. 8, pp. 1226–1238, 2005.

[20] P. A. Estevez, M. Tesmer, C. A. Perez, and J. M. Zurada, "Normalized mutual information feature selection," *IEEE Transactions on Neural Networks*, vol. 20, no. 2, pp. 189–201, 2009.

[21] N. Kwak and C. Chong-Ho, "Input feature selection for classification problems," *IEEE Transactions on Neural Networks*, vol. 13, no. 1, pp. 143–159, 2002.

[22] Q. Zhang, Q. Xie, and G. Wang, "A survey on rough set theory and its applications," *CAAI Transactions on Intelligence Technology*, vol. 1, no. 4, pp. 323–333, 2016. [Online]. Available: http://www.sciencedirect.com/science/article/pii/S2468232216300786

[23] R. Togneri and J. Christopher, *Fundamentals of information theory and coding design*. CRC Press, 2003.

[24] J. Dai, W. Wang, Q. Xu, and H. Tian, "Uncertainty measurement for interval-valued decision systems based on extended conditional entropy," *Knowledge-Based Systems*, vol. 27, pp. 443–450, 2012. [Online]. Available: http://www.sciencedirect.com/science/article/pii/S0950705111002334

[25] S. Gao, G. Ver Steeg, and A. Galstyan, "Efficient estimation of mutual information for strongly dependent variables." in *AISTATS*, 2015.

[26] A. Kraskov, H. Stögbauer, and P. Grassberger, "Estimating mutual information," *Phys. Rev. E*, vol. 69, p. 066138, Jun 2004. [Online]. Available: http://link.aps.org/doi/10.1103/PhysRevE.69.066138

[27] Z. Pawlak, "Rough sets," *International Journal of Computer & Information Sciences*, vol. 11, no. 5, pp. 341–356, 1982. [Online]. Available: http://dx.doi.org/10.1007/BF01001956

[28] F. Pedregosa, G. Varoquaux, A. Gramfort, V. Michel, B. Thirion, O. Grisel, M. Blondel, P. Prettenhofer, R. Weiss, V. Dubourg *et al.*, "Scikit-learn: Machine learning in python," *Journal of Machine Learning Research*, vol. 12, no. Oct, pp. 2825–2830, 2011.

[29] M. Hall, E. Frank, G. Holmes, B. Pfahringer, P. Reutemann, and I. H. Witten, "The weka data mining software: An update," *SIGKDD Explor. Newsl.*, vol. 11, no. 1, pp. 10–18, Nov. 2009. [Online]. Available: http://doi.acm.org/10.1145/1656274.1656278

Sentiment Analysis Using Deep Learning Techniques: A Review

Qurat Tul Ain*, Mubashir Ali*, Amna Riaz†, Amna Noureen‡, Muhammad Kamran‡, Babar Hayat* and A. Rehman*
*Department of Computer Science and Information Technology,
The University of Lahore, Gujrat, Pakistan
†Department of Information and Technology,
University of Gujrat, Gujrat, Pakistan
‡Department of Computer Engineering,
EME, NUST, Islamabad, Pakistan

***Abstract*—The World Wide Web such as social networks, forums, review sites and blogs generate enormous heaps of data in the form of users views, emotions, opinions and arguments about different social events, products, brands, and politics. Sentiments of users that are expressed on the web has great influence on the readers, product vendors and politicians. The unstructured form of data from the social media is needed to be analyzed and well-structured and for this purpose, sentiment analysis has recognized significant attention. Sentiment analysis is referred as text organization that is used to classify the expressed mind-set or feelings in different manners such as negative, positive, favorable, unfavorable, thumbs up, thumbs down, etc. The challenge for sentiment analysis is lack of sufficient labeled data in the field of Natural Language Processing (NLP). And to solve this issue, the sentiment analysis and deep learning techniques have been merged because deep learning models are effective due to their automatic learning capability. This Review Paper highlights latest studies regarding the implementation of deep learning models such as deep neural networks, convolutional neural networks and many more for solving different problems of sentiment analysis such as sentiment classification, cross lingual problems, textual and visual analysis and product review analysis, etc.**

***Keywords*—Sentiment analysis; recurrent neural network; deep neural network; convolutional neural network; recursive neural network; deep belief network**

I. Introduction

A. Sentiment Analysis

Sentiment analysis refers to the management of sentiments, opinions, and subjective text [1]. Sentiment analysis provide the comprehension information related to public views, as it analyze different tweets and reviews. It is a verified tool for the prediction of many significant events such as box office performance of movies and general elections [2]. Public reviews are used to evaluate a certain entity, i.e., person, product or location and might be found on different websites like Amazon and Yelp. The opinions can be categorized into negative, positive or neutral. The purpose of sentiment analysis is to automatically determine the expressive direction of user reviews [3]. The demand of sentiment analysis is raised due to increase requirement of analyzing and structuring hidden information which comes from the social media in the form of unstructured data [4].

1) Features of Sentiment Analysis: Sentiments contains a variety of featured values like tri-grams and bi-grams by means of polarities and combinations. So sentiments are being assessed both as negative and positive aspects through the numerous support vector machines, by using training algorithms. The neural networks are implemented in sentiment analysis to compute belongingness of labels. To help out data extraction at context level the conditional dependencies among several edges and nodes of acyclic graph operated by Bayesian networks are used. By optimizing words and sentences, learning and data accuracy can be attained on social media platform. At word root level, data tokenization is used to produce negative and positive aspects of data. Techniques are being used to decrease the errors in sentiment analysis to attain higher level of precision in data for social media. [5]

2) Sentiment Analysis as multidisciplinary Field: The sentiment analysis is multidisciplinary field, because it includes numerous fields such as computational linguistics, information retrieval, semantics, natural language processing, artificial intelligence and machine learning [6]. The classification for the approaches of sentiment analysis can be done in three extraction levels a) feature or aspect level; b) document level; and c) sentence level [5].

3) Techniques for Sentiment Analysis: Sentiment analysis relies on two types of techniques, i.e., lexicon based and machine learning based techniques [5].

a) Machine learning based techniques: This type of techniques are implemented by extracting the sentences and aspect levels. The features consist of Parts of Speech (POS) tags, n-grams, bi-grams, uni-grams and bag-of-words. Machine learning contains three flavors at sentence and aspect, i.e., Nave Bayes, Support Vector Machine (SVM) and Maximum Entropy.

b) Lexicon based or corpus based techniques: These techniques are based on decision trees such as k-Nearest Neighbors (k-NN), Conditional Random Field (CRF), Hidden Markov Model (HMM), Single Dimensional Classification (SDC) and Sequential Minimal Optimization (SMO), related to methodologies of sentiment classification.

Machine learning approach has three categories: i) supervised; ii) semi supervised; and iii) unsupervised. This approach

is capable of automation and can handle huge amount of data therefore these are very suitable for sentiment analysis.[6].

B. Deep learning

Deep Learning was firstly proposed by G.E. Hinton in 2006 and is the part of machine learning process which refers to Deep Neural Network [7]. Neural network is influenced by human brain and it contains several neurons that make an impressive network. Deep learning networks are capable for providing training to both supervised and unsupervised categories [8].

Deep learning includes many networks such as CNN (Convolutional Neural Networks), RNN (Recurrent Neural Networks), Recursive Neural Networks, DBN (Deep Belief Networks) and many more. Neural networks are very beneficial in text generation, vector representation, word representation estimation, sentence classification, sentence modeling and feature presentation. [9].

1) Applications of Deep Learning: Deep architecture consists of numerous levels of non-linear operations. The capability of modeling the tasks of hard artificial intelligence makes the expectations that deep architecture will be act good in semi supervised learning such as Deep belief network (DBN) and will attain prominent success in Natural language processing community[10]. The Deep Learning consists of improved software engineering, enhanced learning procedures and accessibility of computing power and training data [11]. It is inspired by neuro science and has splendid impact on a range of applications like speech recognition, NLP (Natural Language Processing) and computer vision. One of the basic challenge of deep learning research is the way of learning the structure of model and the quantity of layers and quantity of hidden variables for each layer [12].

While dealing with varying functions, the architecture of deep learning shows full potential and requires labeled samples in high amount for data capturing by deep architecture. Deep learning networks and techniques have been implemented widely in various fields such as in visual classification, pedestrian detection, off-road robot navigation, object categories, acoustic signals and Time series predictions tasks [13]. A very motivating approach in natural language processing has explored that complex multi-tasking such as semantic labeling can be highly performed by using deep architectures[13].

In terms of data, deep learning efforts to learn high level abstractions by exploiting the hierarchical architectures. It is a promising approach and has been extensively applied in artificial intelligence field, like computer vision, transfer learning, semantic parsing, natural language processing and many more. Now a days, deep learning is prosperous because of three main and important reasons, i.e., improved abilities of chip processing (GPU units), extensively lower expenditure of hardware and significant enhancements in machine learning algorithms [14].

C. Combining Sentiment Analysis and Deep Learning

Deep learning is very influential in both unsupervised and supervised learning, many researchers are handling sentiment analysis by using deep learning. It consists of numerous effective and popular models and these models are used to solve the variety of problems effectively [15]. The most famous example Socher has used is the Recursive Neural Network (RNN) for the representation of movies reviews from the website rottentomatoes.com [16].

By following the effort of [17], many researchers has performed sentiment classification by using neural networks. For example, Kalchbrenner [18] anticipated a DyCNN (Dynamic Convolutional Neural Network) which use a pooling operation, i.e, dynamic k-max pooling on linear sequences. Kim [19] use CNN to learn sentiment-bearing sentence vectors.

Furthermore, Paragraph vector is proposed by Mikolov, *et al*. [20] which performs better sentiment analysis than bag-of-words model and ConvNets for learning the SSWE (sentiment specific word embedding). Recently [21] has applied ConvNets on characters rather than directly applying on word embeddings. Another composition model for the classification of sentiments is LSTM which can simply take flow on one input direction [22].

In this paper, Section II covers the detailed literature review and Section III presents the conclusion whereas, Section IV shows the analysis phase been analyzed in literature review.

In the Literature Review section, various studies of sentiment analysis using Deep Learning techniques are discussed. This review is conducted on the basis of numerous latest studies in the field of sentiment analysis.

II. Literature Review

For the accurate classification of sentiments, many researchers have made efforts to combine deep learning and machine learning concepts in the recent years. This section briefly describes the numerous studies, related to sentiment analysis of web contents about users opinions, emotions, reviews toward different matters and products using deep learning techniques.

Sentiment analysis tasks can be performed efficiently by implementing different models such as deep learning models, which have been extended recently. These models include CNN (convolutional neural networks), RNN (recursive neural network), DNN (deep neural networks), RNN (recurrent neural networks) and DBN (deep belief networks). This section describes the efforts of different researchers toward implementing deep learning models for performing the sentiment analysis [23]. Several researchers have used more than one model in their study, and these are mentioned under the hybrid neural network section.

A. Convolutional Neural Networks (CNN)

The CNN (convolutional neural network) [24] includes pooling layers and sophistication as it gives a standard architecture to map the sentences of variable length into sentences of fixed size scattered vectors.

This study [25] has proposed a novel convolutional neural network (CNN) framework for visual sentiment analysis to predict sentiments of visual content. CNN has been implemented using Caffe and Python on a Linux machine. Transfer learning approach and hyper-parameter has been used in biases and weights are utilized from pre-trained GoogLeNet. As CNN

enhance its performance by increasing its size and depth, so a very deep CNN model, inspired by GoogLeNet is proposed with 22 layers for sentiment analysis. It is optimized by using SGD (Stochastic gradient descent) algorithm. The strategy with 60 epochs has been performed for training the network as GoogLeNet has performed 250 epochs. For experimental work, a dataset of twitter containing 1269 images is selected and back propagation is applied. Amazon Mechanical Turk (MTurk) and popular crowd intelligence is used to label the images. Five workers were involved to generate sentiment label in favor of every image. The proposed model was evaluated on this dataset and acquired better performance than existing systems. Results shows that proposed system achieve high performance without fine-tuning on Flickr dataset. However AlexNet was used in previous works and GoogleNet provided almost 9% performance progress than AlexNet. By converting GoogLeNet in to visual sentiment analysis framework, the better feature extraction was achieved. Stable and reliable state were achieved by using hyper parameters.

The authors [26] have proposed the system of deep learning for sentiment analysis of twitter. The main focus of this work was to initialize the weight of parameters of convolutional neural network and it is critical to train the model accurately while avoiding the requirement of adding new feature. A neural language is used to initialize the word embedding and is trained by big unsupervised group of tweets. For further refining the embedding on bulky supervised corpus, a conventional neural network is used. To initialize the network, previously embedded words and parameters were used, having same architecture and training on supervised corpus as of Semeval-2015. The components used in proposed work are activations, sentence matrix pooling, softmax and convolutional layers. To train the network, stochastic gradient descent (SGD) and non-convex function optimization algorithms were used and to calculate the gradients back propagation algorithm was used. Dropout technique were used to enhance the neural networks regularization. The deep learning model is applied on two tasks: message level task and phrase level task from Semeval-2015 to predict polarity and achieve high outcomes. By applying six test-set, the proposed model lies at first rank in terms of accuracy.

A detailed research by [27] has presented an overview of sentiment analysis related to Micro-blog. The purpose of this effort was to get the opinions and attitudes of users about hot events by using Convolutional Neural Network (CNN). The use of CNN overcomes the problem of explicit feature extraction and learns implicitly through training data. To collect the data from target, the input URL and focused crawler have been used, 1000 micro-blog comments were collected as a corpus and divided into three labels, i.e., 274 neutral emotions, 300 negative emotions and 426 positive emotions. The proposed model has been compared with the previous studies as those had studies used CRF, SVM and additional traditional algorithms to perform sentiment analysis with a high price. However, the performance proves that the proposed model is reasonable and sufficient to enhance the accuracy in terms of emotion analysis.

Research by [28] was motivated through the need of controlling of comprehensive social multimedia content and employ both textual and visual SA techniques for combined textual-visual sentiment analysis. A convolutional neural network (CNN) and a paragraph vector model were used for both the image and textual SA accordingly. The proposed model was termed as rule based sentiment classifier VADER. After conducting the wide range of experiments on manually labeled and weakly labeled visual tweets, it was concluded that mutual textual-visual features outperformed the sentiment analysis algorithms which were only depend on Visual contents. It was demonstrated that how models of one domain to a different domain can be transmitted easily. Getty Images had been selected to crawl data and Caffe was used to tune the CNN model. Tweets were gathered through Twitter API. To make sentiment labels for chosen visual tweets, the Mechanical Turk (AMT) and crowd intelligence had been employed. The results recommend that the joint textual-visual model has performed better than the both single visual and textual sentiment analysis models.

In study by [15], the researcher has represented a seven-layer framework to analyze the sentiments of sentences. This frame work depends on CNN (Convolutional neural network) and Word2vec for SA and to calculate vector representation, respectively. Word2vec have been proposed by Google. The Dropout technology, Normalization and Parametric Rectified Linear Unit (PReLU), have been used to progress the correctness and generalizability of proposed model. The framework was verified on the data set from rottentomatoes.com which contains movie review excerpts' corpus, the dataset consists of five labels positive, somewhat positive, neural, negative and somewhat negative. By comparing the proposed model with previous models such as Matrix-Vector recursive neural network (MV-RNN) and recursive neural network (RNN), the proposed model outperformed the previous models with the 45.5 % accuracy. In Table I, we have presented the analysis of best studies following the convolutional neural network.

B. Recursive Neural Network (RNN)

The recursive neural network (RNN) [24] lies in supervised learning. It contains a tree structure which is settled before training and the nodes can have different matrices. There is no need of reconstruction of input in RNN.

The proposed work [29] builds a Treebank for chines sentiments of social data to overcome the deficiency of labeled and large corpus in existing models. To predict the labels at sentence level i.e positive or negative, the Recursive Neural Deep Model (RNDM) was proposed and achieved high performance than SVM, Nave Bayes and Maximum Entropy. 2270 movie reviews were collected from the website and Chinese word segmentation tool ICTCLAS was used to segment these reviews. Five classes were settled for each sentence and standford parser applied for sentence parsing. The proposed model improved the prediction of sentiment labels of sentences by concluding 13550 chines sentences and 14964 words. ME and NB performs higher with contrastive conjunction structure than baselines with great margin.

In this study [30], a model comprising RNTN (Recursive Neural Tensor Network) and Sentiment Treebank has been proposed to correctly clarify the compositional effects at different levels of phrases, i.e., positive and negative phrases.The proposed model was compared with all the existing models.

TABLE I. ANALYSIS OF CONVOLUTIONAL NEURAL NETWORKS

Researcher Name and Year	Model Used	Purpose	Data Set	Results
J.Islam and Y. Zhang 2016 [25]	Convolutional Neural Networks (CNN)	Visual SA	1269 images from twitter	GoogleNet gave almost 9 % performance progress than AlexNet.
A. Severyn and A. Moschitti, 2015 [26]	Convolutional Neural Networks (CNN)	Phrase level and message level task SA	Semeval-2015	Compared with official system ranked 1st in terms of pharse level subtask and ranked 2nd in terms of message level.
L. Yanmei and C. Yuda, 2015 [27]	Convolutional Neural Networks (CNN)	Micro-Blog SA	1000 micro-blog comments (HuaQiangu)	Proposed model can effectively improve the accuracy of emotional orientation, validation.
Q. You, J. Luo, H. Jin, and J. Yang, 2015 [28]	Convolutional Neural Networks (CNN)	Textual-visual SA	Getty Images, 101 keywords	Joint visual and textual model outperforms the early single fusions.
X. Ouyang, P. Zhou, C. H. Li, and L. Liu, 2015 [15]	Convolutional Neural Networks (CNN)	Sentiments of sentences	rottentomatoes.com (contains movie review excerpts)	The proposed model outperformed the previous models with the 45.5% accuracy.

TABLE II. ANALYSIS OF RECURSIVE NEURAL NETWORKS

Researcher Name and Year	Model Used	Purpose	Data Set	Results
C. Li, B. Xu, G. Wu, S. He, G. Tian, and H. Hao, 2014 [29]	Recursive Neural Deep Model (RNDM)	Chines sentiments analysis of social data	2270 movie reviews from websites	Performs higher (90.8%) than baselines with a great margin.
R. Socher, A. Perelygin, and J. Wu, 2013 [30]	RNTN (Recursive Neural Tensor Network)	Semantic Compositionality	11,855 single sentences from moview review (Pang and Lee 2005)	The RNTN achieved 80.7% accuracy in sentiment prediction , an improvement of 9.7 % over baselines (bag of features).
W. Li and H. Chen, 2014 [31]	Recursive Neural Network (RNN)	Identifying Top Sellers In Underground Economy	Russian carding Forum)	Results have been indicated that Deep learning techniques accomplish superior outcomes than shallow classifiers. Carding sellers have fewer ratings than malware sellers.

In existing models, the meaning of long phrases cannot be expressed effectively by semantic word spaces, so for sentiment detection, more rich and supervised evaluation and training resources are needed as it requires more influential composition models. The RNTN achieved 80.7% accuracy in sentiment prediction by performing fine-grained labeling over all the phrases and outperformed previous models.

This study [31] has contributed a generalized and scaled framework to recognize top carding/malware sellers. The model is based on deep learning for sentiment analysis and used in thread classification and snowball sampling to assess the quality of sellers service/product by analyzing the customer feedback. The evaluation of proposed model has been conducted on Russian carding forum and a web crawler was used to gather the conversation stuff from the forum. A sentiment tree bank has been used and it was trained by using recursive neural tensor network on online review corpus. For evaluating the validity and effectiveness, two experiments were conducted in which proposed model was compared with Nave Bayes, KNN and SVM based models. This study has searched out the sellers who are highly rated for malicious services/products and the effectiveness of deep learning for recognizing these sellers. Results have been indicated that Deep learning techniques accomplish superior outcomes than the shallow classifiers and it was established that the carding sellers have fewer ratings than malware sellers. Table II, presenting the analysis of best approaches based on recursive neural network.

C. Deep Neural Networks (DNN)

In this study [32], author has proposed a model for sentiment analysis considering both visual and textual contents of social networks. This new scheme used deep neural network model such as Denoising auto encoders and skip gram. The base of the scheme was CBOW (Continuous Bag-Of-Words) model. The proposed model consisted of two parts CBOW-LR (logistic regression) for textual contents and was expanded as the CBOW-DA-LR. The classification was done according to the polarity of visual and textual information. Four datasets were evaluated, i.e., Sanders Corpus, Sentiment140, SemEval-2013 and SentiBank Twitter dataset. The proposed model outperformed the CBOWS+SVM and FSLM (fully supervised probabilistic language model). Perhaps the ESLAM (extended fully supervised probabilistic language model) in term of small training data had outperformed the current model. The feature learning and skip grams both required large datasets for best performance.

In this study [33], deep neural network architecture has been proposed to evaluate the similarity of documents. The architecture was trained by using several market news to

TABLE III. ANALYSIS OF DEEP NEURAL NETWORKS

Researcher Name and Year	Model Used	Purpose	Data Set	Results
C. Baecchi, T. Uricchio, M. Bertini, and A. Del Bimbo, 2016 [32]	deep neural networks (CBOW-DA-LR)	Visual and Textual SA	4 datasets: Sanders Corpus, Sentiment140, SemEval-2013 and SentiBank Twitter Dataset	CBOW-DA-LR model obtained superior classification accuracy than previous models.
H. Yanagimoto, M. Shimada, and A. Yoshimura, 2013 [33]	Deep Neural Network (DNN)	Document Similarity Estimation	T&C News	The proposed method accomplished superior performance in terms of similarity estimation of articles according to polarity.

produce vectors foe articles. The T&C news have been used as dataset. The cosine similarity was calculated among labeled articles and the polarity of documents was considered but contents were not considered. The proposed method accomplished superior performance in terms of similarity estimation of articles according to polarity. In Table III, we have presented the summarized analysis of two approaches using the deep neural network.

D. Recurrent Neural Networks (Recurrent NN)

The Recurrent neural network (RNN) [24] is an influential model in language modeling because it doesnt represent the context of fixed-length that contaminate all history words .

In this study [34], the HBRNN (hierarchical bidirectional recurrent neural network) has been developed to extract the reviews of customers about different hotels in a complete and concise manner. To model the sequential long term information, HBRNN has used the terminology of RNN and the prediction process was done at review level by HBRNN. The experimental data was taken from DBS text mining Challenge 2015. HBRNN performance was improved through networks parameters along with the fine tuning and the model was compared with LSTM (long shot term memory) and BLSTM (Bidirectional LSTM). After performing the experiments, the evaluation recall, F1 scores and precision was made on highly biased data. The development, test set and train splits were used for comparing outcomes with benchmark systems, tenfold cross validation used to present the performance of HBRNN. The main challenges that was resolved is lack of online reviews with high quality and lack of high skewness in the reviewed data. Experimental Results on the dataset proved that HBRNN performed better than other methods. This model can be applied to other opinion mining activities which consists of huge data volume. This contribution [35] has been done to overcome the issue of dataset of Bangla as it is standard and large for SA (Sentiment Analysis) tasks. The issue has been resolved by providing a significant dataset for sentiment analysis of 10,000 BRBT (Bangla and Romanized Bangla Text). The Deep Recurrent model especially LSTM (Long Short Term Memory) was used to test the dataset by using two loss functions, i.e., binary and categorical cross-entropy. Data were gathered from different sites like YouTube, Face book, Twitter and others. The experiments were conducted to prepare dataset of one mark for another (and the other way around) to investigate the fact whether it contributes towards the better outcomes.

This author [36] proposed a sequence model to focus on the embedding of reviews having temporal nature toward products as these reviews had less focus in existing studies. The combination of gated recurrent units with recurrent neural network is used to learn dispersed representations of products and users. For sentiment classification these representations fed into machine learning classifier. The approach was evaluated on three datasets collected from Yelp and IMDB. Each review labeled according to rating score. To train the network the back-propagation algorithm with Adam stochastic optimization method has been used. Results show sequence modeling of dispersed product and user representation learning improves the performance sentiment classification of document-level and the proposed approach achieves high-tech results on the benchmark datasets. The result of proposed model compared with many baselines including recursive neural networks, user product neural network, word2vec, paragraph vector and algorithm JMARS. We have also made an analysis of some approaches based on Recurrent Neural Network and this analysis is presented in tabular form in Table IV.

E. Deep Belief Networks (DBN)

Deep belief networks (DBNs) [37] includes several hidden layers, composed by RBM (restricted Boltzmann machines). DBN has been proved efficient for feature representation. It utilizes the unlabeled data and fulfills the deficiencies of labeled analysis issues.

In this paper [38], a new deep neural network structure has been presented termed as WSDNNs (Weakly Shared Deep Neural Networks). The purpose of WSDNNs is to facilitate two languages to share sentiment labels. The features of language specific and inter language have been presented through building multiple weakly shared layers of features. The datasets from Prettenhofer and Stein have been used containing four languages French, German, English and Japanese. In comparison with existing studies the proposed work address the challenge of shortening overlap among feature spaces of both source and target language data through cross lingual information transfer process using backpropogation. DNNs used for transformation of information from source to target language. The experiments have been conducted for sentiment classification tasks of cross multilingual product reviews of Amazon. results concluded that the proposed approach is more effective and powerful in terms of cross lingual sentiment classification than the previous studies.

TABLE IV. ANALYSIS OF RECURRENT NEURAL NETWORKS

Researcher Name and Year	Model Used	Purpose	Data Set	Results
R. Silhavy, R. Senkerik, Z. K. Oplatkova, P. Silhavy, and Z. Prokopova, 2016 [34]	HBRNN (hierarchical bidirectional Recurrent Neural Network)	Sentiment Analysis of Customer Reviews	150,175 labelled reviews from 1500 hotels (DBS text mining Challenge 2015)	The experimental results explored that that HBRNN outperformed all other methods.
A. Hassan, M. R. Amin, A. Kalam, A. Azad, and N. Mohammed, [35]	Deep Recurrent model especially LSTM (Long Short Term Memory)	Sentiment Analysis on Bangla and Romanized Bangla Text (BRBT)	9337 post Samples from different social sources	Ambiguous Removed with 78% accuracy. Ambiguous converted to 2 scored highest with 55% accuracy.
T. Chen, R. Xu, Y. He, Y. Xia, and X. Wang , 2016 [36]	Recurrent Neural Network (RNN-GRU)	Learning User and Product Distributed Representations	Three datasets collected from Yelp and IMDB.	Results have been indicated that proposed model outperformed many baselines including recursive neural networks, user product neural network , word2vec, paragraph vector and algorithm JMARS

Another study by [17] has used deep belief network with word vector for the political detection in Korean articles. The proposed model has used SVM for bias calculation, five stage pipeline for detection of political bias, python web crawler to gather news articles, KKMA for morpheme analysis, word2Vec and scikit-learn package. The dataset contained 50,000 political articles from 01 Jan, 2014 to 28 Feb, 2015. Results showed 81.8% accuracy by correctly predicting labels and the results contained mean square error of 0.120.

This research [37] has proposed a deep belief network with feature selection (DBNFS) to overcome the vocabulary problems, the network has used input corpus along with numerous hidden layers. Chi-Squared technique of feature selection was used to improve the Deep Belief Network (DBN) for the purpose of decreasing complexity of vocabulary input and for eliminating irrelevant features. By applying Chi-Squared technique, the learning phase of DBN was enhanced to DBNFS. In this work, two new tasks features, selection and reduction were used along with many other tasks of existing classification approaches, such as data portioning, feature extraction, model training and model testing. Performance of DBNFS was demonstrated and training time and accuracy of proposed DBNFS was also compared with other algorithms. Five Dataset of sentiment classification were used for estimation, datasets are books (BOO), electronics (ELE), DVDs (DVD), kitchen appliances (KIT) and movies reviews (MOV). For fair comparison, the parameters of learning were same as of existing works. Accuracy was evaluated by comparing the amount of features before and after the feature selection and reduction. The accuracy results were compared with the previous works and were proved better DBNFS than DBN. The training time was also lower in DBNFS than DBN. Training time was improved due to simple deep structure and proposed feature selection method. The only drawback of DBN was that it is costly plus time consuming. Summarized analysis of existing approaches for sentiment analysis by using DBN is presented in Table V.

F. Hybrid Neural Networks

This study [8] has proposed two deep learning techniques for the sentiment classification of Thai Twitter data, i.e., Convolutional Neural Network (DCNN) and Short Term Memory (LSTM). Data processing was conducted properly. Data was collected from the users and their followers of Thai Twitter. After filtering the data, only the users with Thai tweets and tweets with Thai characters were selected. Five experiments were conducted to achieve finest parameters for deep learning, to compare the deep learning with classical techniques and to achieve the words sequence importance. Three-fold cross validation was used to verify the process. The results concluded that the accuracy is high in DNN than LSTM and both techniques of deep learning are higher in accuracy than SVM and Nave Bayes but lesser than Maximum Entropy. Higher accuracies were found in original sentences than shuffled sentences so the words sequence is important.

In this research study [39] a hybrid model has proposed which consists of Probabilistic Neural Network (PNN) and a two layered Restricted Boltzmann (RBM). The purpose of proposing this hybrid deep learning model is to attain better accuracy of sentiment classification. The polarity, i.e., negative and positive reviews vary according to different context in order to solve this type of problem this model performs well, neutral reviews are not considered. Experiments have done with datasets of Pang and Lee and Blitzer, *et al*., binary classification implemented on every dataset. The accuracy has been enhanced for five datasets by comparing with the existing state-of-the-art Dang, *et al*. [13]. There are no outer resources in proposed approach such as POS tagger and sentiment dictionary etc therefore it is faster too than competitor. To attain a reduced number of features the dimensionality reduction has been implemented as previous study used a complex strategy for feature selection. Approaches based on hybrid neural networks are presented in summarized form in Table VI.

TABLE V. ANALYSIS OF DEEP BELIEF NETWORKS

Researcher Name and Year	Model Used	Purpose	Data Set	Results
G. Zhou, Z. Zeng, J. X. Huang, and T. He, 2016 [38]	WSDNNs (Weakly Shared Deep Neural Networks)	Cross-Lingual Sentiment Classification	Four languages reviews from amazon, each language consists of 1000 negative and 1000 positive reviews	Proposed approach is more effective and powerful than the previous studies by applying experiments on 18 tasks of cross lingual sentiment classification.
T. Mikolov, K. Chen, G. Corrado, and J. Dean, 2013 [17]	Deep Belief Networks Along with word vector	Political Detection in Korean articles	50,000 political articles	Results showed 81.8% accuracy by correctly predicting labels.
P. Ruangkanokmas, T. Achalakul, and K. Akkarajitsakul, 2016 [37]	Deep Belief Network with Feature Selection (DBNFS)	Feature Selection	Five sentiment classification datasets (1 is movie reviews and other four are multi-domain). Total 2,000 labeled reviews (1,000 negatives and 1,000 positives).	The accuracy results are compared with previous works and proved better DBNFS than DBN.

G. Other Neural Networks

In this study [40] to overcome the complexity in word-level models the character-level model have been proposed. The motivation of proposed model CDBLSTM is an existing model that is DBLSTM neural networks [41]. The focus of this work is only on textual content and on the polarity analysis of tweets in which a tweet is classified into two classes, i.e., positive and negative. There can be more options than positive and negative such as natural and finer but here the model is restricted only to positive and negative classes to compare with existing published results. The tweets are encoded from character level and trained by the use of CCE (categorical cross-entropy). Experiments were conducted on two datasets, first one is latest benchmark dataset for SemEval 2016 and the second one is provided by GO dataset. Adam algorithm was implemented to train all the models and the learning rate settled to 0.1. Final predictions were obtained by the model of logistic regression. Results demonstrate that proposed approach is competent for the polarity problems. By applying different experiments results shows that CDBLSTM performs better than DBLSTM and by comparing the results with Deep Convolutional Neural Network (DCNN) [42] which performs well on twitter SPC (sentiment polarity classification). The 85.86% accuracy was achieved on STS (Stanford Twitter Sentiment) corpus and 84.82% on SemEval-2016. In this study [41], author has proposed TF-IDF, GR, and RBFNN for sentiment classification on Hinglish text. Many studies have worked on sentiment analysis of various languages such as English, Turkish, Flemmish, Spanish, Arabic and Chinese but no work has been done on Indic language. To fill this gap, the sentiments were classified in Hinglish language as it contains Hindi words along with the English. Dataset has creep from Facebook comments and viz. news, five methods of feature selection information gain, chi-square, t-statistics, association and gain ratio have been implemented on DTM (Document-Term Matrix) and TF-IDF (Term Frequency-Inverse Document Frequency). Many classifiers have used such as SVMs (Support Vector Machine), RBFNet (Random Forest, Radial Basis Function Neural Network), Naive Bayes, J48 (Decision Tree), CART, JRip, Logistic Regression (LR) and Multi-layer Perception (MLP) methods for the classification of data. Total 840 experiments were performed on datasets and best results were achieved. The proposed triumvirate approach was proved efficient for sentiment classification of Hinglish text.

This contribution [42] overcomes the problem that occurs in effectively analyzing the emotions of customers toward companies in blog sphere. A neural network (NN) based technique is proposed which subordinate the advantages of Semantic orientation index and machine learning methods for the classification of sentiments effectively and quickly. The input of neural network is semantic orientation indexes. While considering the fault tolerance ability the BPN (back-propagation neural network) is selected as basic learner of proposed method. Data was collected from the blogs of real world such as from “LiveJournal” and “Review Center”. Segmentation of words, SO indexes calculations, neural network trainings and performance evaluations have been conducted. Training and test sets were settled of datasets. The overall accuracy (OA), performance evaluation matrices and F1 were used. Results concluded that proposed method has enhanced the performance of classification and saved training time as compared to traditional ML and IR.

This contribution [43] proposed a data driven supervised approach for the purpose of feature reduction and development of lexicon specific to twitter sentiment analysis about brand. Statistical analysis and n-gram were used for twitter specific

TABLE VI. ANALYSIS OF HYBRID AND SOME OTHER NEURAL NETWORKS

Researcher Name and Year	Model Used	Purpose	Data Set	Results
P. Vateekul and T. Koomsubha , 2016 [8]	Convolutional Neural Network (DCNN) and Short Term Memory (LSTM).	Sentiment Analysis on Thai Twitter Data	3,813,173 tweets (33,349 negative tweets and 140,414 positive tweets)	Higher in accuracy than SVM and Nave Bayes lesser than Maximum Entropy Higher accuracies in original sentences than shuffled sentences
R. Ghosh, K. Ravi, and V. Ravi, 2016 [39]	Probabilistic Neural Network (PNN) and a two layered Restricted Boltzmann (RBM)	Better accuracy of sentiment classification	Pang and Lee and Blitzer, *et al*. (1000 negative and 1000 positive reviews on each of DVDs, Books (BOO), Kitchen appliances (KIT) and Electronics (ELE).	The proposed model attains accuracies in following manner: MOV = 93.3%, BOO = 92.7%, DVD = 93.1%, ELE = 93.2%, KIT = 94.9%
R. Goebel and W. Wahlster, 2011 [40]	Deep Bi-directional Long Short-Term Memory Neural Networks (DBLSTM)	Sentiment Analysis of Social Data	SemEval 2016 and the second one is provided by Go dataset (1.6 million tweets)	85.86% accuracy was achieved on STS (Stanford Twitter Sentiment) corpus 84.82% on SemEval-2016.
K. Ravi and V. Ravi, 2016 [41]	Radial Basis Function Neural Network (RBFNN)	Sentiment classification on Hinglish text	300 news articles from viz. news and facebook.	The proposed approach performed better sensitivity than specificity in terms of news dataset. The proposed approach performed better specificity than sensitivity in terms of fb dataset.
L.-S. Chen, C.-H. Liu, and H.-J. Chiu, 2011 [42]	Back Propagation Neural Network (BPN)	Sentiment classification in the blogosphere	LiveJournal and Review Center have been used to collect reviews	Results concluded that proposed method enhance performance of classification and save training time as compared to traditional ML and IR.
M. Ghiassi, J. Skinner, and D. Zimbra, 2013 [43]	Dynamic Artificial Neural Network (DANN)	Twitter brand sentiment analysis (for justinbieber brand)	Total 10,345,184 tweets related to justinbieber brand	Results concluded that: More than 80% tweets dont have sentiment. Reduced feature set with characterize 97.3% of all messages in the 10,345,184 Justin Bieber Twitter corpus. Only six expressions were found related to Justin Bieber brand out of 181 and other were found twitter specific. Facilitates the Justin Bieber brand to identify the issues and views about the brand.

lexicon and feature reduction accordingly. The existing models SVM and nave Bayes were used for twitter specific lexicon to compete with the existing studies. The classification was done in proposed model by using artificial neural networks for twitter specific lexicon and this difference outperformed the existing models. The input matrix was parse matrix. Datasets were divided into training and test datasets to achieve better accuracy. The feature engineering phase was done through preprocessing activities for transforming the documents in simple form and to produce the vector presentation. The data was collected from Twitter API v1.0. The proposed model was applied on Justin Bieber Twitter corpus and it was established that the emotions contain high explanatory power as compared to existing studies. The proposed model has reduced the features of Justin Bieber corpus and enhanced the classification accuracy and high amount of coverage. Only six expressions were found related to Justin Bieber brand out of 181 and others were found twitter-specific. The proposed model has facilitated the Justin Bieber brand to identify the issues and views about the brand.

III. CONCLUSION

Sentiment analysis refers to the management of sentiments, opinions, and subjective text. The demand of sentiment analysis is raised due to the requirement of analyzing and structuring hidden information, extracted from social media in form of unstructured data. The sentiment analysis is being implementing through deep learning techniques. Deep learning consists of numerous effective and popular models, these models are used to solve the variety of problems effectively. Different studies have been discussed in this review to provide a deep knowledge of the successful growing of deep learning applications in the field of sentiment analysis. Numerous problems have been resolved by having high accuracy of both fields of sentiment analysis and deep learning.

TABLE VII. ANALYSIS OF ALL THE BEST STUDIES DISCUSSED IN THIS REVIEW

Researcher Name and Year	Model Used	Purpose	Data Set	Results
J.Islam and Y. Zhang 2016 [25]	Convolutional Neural Networks (CNN)	Visual SA	1269 images from twitter	GoogleNet gave almost 9% performance progress than AlexNet.
R. Silhavy, R. Senkerik, Z. K. Oplatkova, P. Silhavy, and Z. Prokopova, 2016 [34]	HBRNN (hierarchical bidirectional Recurrent Neural Network)	Sentiment Analysis of Customer Reviews	150,175 labelled reviews from 1500 hotels (DBS text mining Challenge 2015)	The experimental results explored that that HBRNN outperformed all other methods.
G. Zhou, Z. Zeng, J. X. Huang, and T. He, 2016 [38]	WSDNNs (Weakly Shared Deep Neural Networks)	Cross-Lingual Sentiment Classification	4 languages reviews from Amazon, each language consists of 1000 negative and 1000 positive reviews	Proposed approach is more effective and powerful than the previous studies by applying experiments on 18 tasks of cross lingual sentiment classification
P. Vateekul and T. Koomsubha , 2016 [8]	Convolutional Neural Network (DCNN) and Short Term Memory (LSTM)	Sentiment Analysis on Thai Twitter Data	3,813,173 tweets (33,349 negative tweets and 140,414 positive tweets)	Higher in accuracy than SVM and Nave Bayes lesser than Maximum Entropy Higher accuracies in original sentences than shuffled sentences
R. Ghosh, K. Ravi, and V. Ravi, 2016 [39]	Probabilistic Neural Network (PNN) and a two layered Restricted Boltzmann (RBM)	Better accuracy of sentiment classification	Pang and Lee and Blitzeret al (1000 negative and 1000 positive reviews)	The proposed model attains accuracies in following manner: MOV = 93.3%, BOO = 92.7%, DVD = 93.1%, ELE = 93.2%, KIT = 94.9%
Q. You, J. Luo, H. Jin, and J. Yang, 2015 [28]	Convolutional Neural Networks (CNN)	Textual-visual SA	Getty Images, 101	keywords Joint visual and textual model outperforms the early single fusions
W. Li and H. Chen, 2014 [31]	Recursive Neural Network (RNN)	Identifying Top Sellers In Underground Economy	Russian carding Forum	Deep learning techniques accomplish superior outcomes than shallow classifiers carding sellers have fewer ratings than malware sellers.
H. Yanagimoto, M. Shimada, and A. Yoshimura, 2013 [33]	Deep Neural Network (DNN)	Document Similarity Estimation	T& C News	The proposed method accomplished superior performance in terms of similarity estimation of articles according to polarity.
T. Mikolov, K. Chen, G. Corrado, and J. Dean, 2013 [17]	Deep Belief Networks Along with word vector	Political Detection in Korean articles	50,000 political articles	Results showed 81.8% accuracy by correctly predicting labels

IV. ANALYSIS

This review has described ample of studies related to sentiment analysis by using deep learning models as summarized in Table VII. After analyzing all these studies, it is established that by using deep learning methods, sentiment analysis can be accomplished in more efficient and accurate way. As the sentiment analysis is used to predict the views of users and deep learning models are all about the prediction or mimic of human mind, so the deep learning models provide more accuracy than shallow models. Deep learning networks are better than SVMs and normal neural networks because they have more hidden layers as compared to normal neural networks that have one or two hidden layers. Deep learning networks are capable to provide training in both supervised/unsupervised ways. Deep-learning networks carry out automatic feature extraction and doesnt involve human intervention therefore it can save time because feature engineering is not needed. Sentiment Analysis comprises different kinds of problem statements. The capability of settling in the task variations by having little alterations in system itself includes a feather in strength of Deep Learning standard. This method also has some limitations as well, as compared to previous models such as SVM. It requires large data sets and is tremendously costly to train. These complex models can obtain weeks to train by using machines equipped with expensive GPUs.

REFERENCES

[1] A. V. Yeole, P. V. Chavan, and M. C. Nikose, Opinion mining for emotions determination, ICIIECS 2015 - 2015 IEEE Int. Conf. Innov. Information, Embed. Commun. Syst., 2015.

[2] B. Heredia, T. M. Khoshgoftaar, J. Prusa, and M. Crawford, Cross-Domain Sentiment Analysis: An Empirical Investigation, 2016 IEEE 17th Int. Conf. Inf. Reuse Integr., pp. 160165, 2016.

[3] F. Luo, C. Li, and Z. Cao, Affective-feature-based sentiment analysis using SVM classifier, 2016 IEEE 20th Int. Conf. Comput. Support. Coop. Work Des., pp. 276281, 2016.

[4] M. Haenlein and A. M. Kaplan, An empirical analysis of attitudinal and behavioral reactions toward the abandonment of unprofitable customer relationships, J. Relatsh. Mark., vol. 9, no. 4, pp. 200228, 2010.

[5] J. Singh, G. Singh, and R. Singh, A review of sentiment analysis techniques for opinionated web text, CSI Trans. ICT, 2016.

[6] E. Aydogan and M. A. Akcayol, A comprehensive survey for sentiment analysis tasks using machine learning techniques, 2016 Int. Symp. Innov. Intell. Syst. Appl., pp. 17, 2016.

[7] M. Day and C. Lee, Deep Learning for Financial Sentiment Analysis on Finance News Providers, no. 1, pp. 11271134, 2016.

[8] P. Vateekul and T. Koomsubha, A Study of Sentiment Analysis Using Deep Learning Techniques on Thai Twitter Data, 2016.

[9] Y. Zhang, M. J. Er, N. Wang, M. Pratama, and R. Venkatesan, Sentiment Classification Using Comprehensive Attention Recurrent Models, pp. 15621569, 2016.

[10] S. Zhou, Q. Chen, and X. Wang, Active deep learning method for semi-supervised sentiment classification, Neurocomputing, vol. 120, pp. 536546, 2013.

[11] L. Deng, G. Hinton, and B. Kingsbury, New types of deep neural network learning for speech recognition and related applications: an overview, 2013 IEEE Int. Conf. Acoust. Speech Signal Process., pp. 85998603, 2013.

[12] S. Bengio, L. Deng, H. Larochelle, H. Lee, and R. Salakhutdinov, Guest Editors Introduction: Special Section on Learning Deep Architectures, IEEE Trans. Pattern Anal. Mach. Intell., vol. 35, no. 8, pp. 17951797, 2013.

[13] L. Arnold, S. Rebecchi, S. Chevallier, and H. Paugam-Moisy, An Introduction to Deep Learning, Esann, no. April, p. 12, 2011.

[14] Y. Guo, Y. Liu, A. Oerlemans, S. Lao, S. Wu, and M. S. Lew, Deep learning for visual understanding: A review, Neurocomputing, vol. 187, pp. 2748, 2016.

[15] X. Ouyang, P. Zhou, C. H. Li, and L. Liu, Sentiment Analysis Using Convolutional Neural Network, Comput. Inf. Technol. Ubiquitous Comput. Commun. Dependable, Auton. Secur. Comput. Pervasive Intell. Comput. (CIT/IUCC/DASC/PICOM), 2015 IEEE Int. Conf., pp. 23592364, 2015.

[16] R. Socher and C. Lin, Parsing natural scenes and natural language with recursive neural networks, Proc. , pp. 129136, 2011.

[17] T. Mikolov, K. Chen, G. Corrado, and J. Dean, Efficient Estimation of Word Representations in Vector Space, Arxiv, no. 9, pp. 112, 2013.

[18] N. Kalchbrenner, E. Grefenstette, and P. Blunsom, A Convolutional Neural Network for Modelling Sentences, Acl, pp. 655665, 2014.

[19] Y. Kim, Convolutional Neural Networks for Sentence Classification, Proc. 2014 Conf. Empir. Methods Nat. Lang. Process. (EMNLP 2014), pp. 17461751, 2014.

[20] T. Mikolov, K. Chen, G. Corrado, and J. Dean, Distributed Representations of Words and Phrases and their Compositionality, Nips, pp. 19, 2013.

[21] Z. Wu, T. Virtanen, T. Kinnunen, E. S. Chng, and H. Li, Exemplar-based unit selection for voice conversion utilizing temporal Information, Proc. Annu. Conf. Int. Speech Commun. Assoc. INTERSPEECH, pp. 30573061, 2013.

[22] K. S. Tai, R. Socher, and C. D. Manning, Improved semantic representations from tree-structured long short-term memory networks, Proc. ACL, pp. 15561566, 2015.

[23] A. A. Al Sallab, R. Baly, and H. Hajj, Deep Learning Models for Sentiment Analysis in Arabic, no. November. 2015.

[24] C. Z. Jiajun Zhang, Neural Networks in Machine Translation: An Overview, IEEE Intell. Syst., pp. 17241734, 2015.

[25] J. Islam and Y. Zhang, Visual Sentiment Analysis for Social Images Using Transfer Learning Approach, 2016 IEEE Int. Conf. Big Data Cloud Comput. (BDCloud), Soc. Comput. Netw. (SocialCom), Sustain. Comput. Commun., pp. 124130, 2016.

[26] A. Severyn and A. Moschitti, Twitter Sentiment Analysis with Deep Convolutional Neural Networks, Proc. 38th Int. ACM SIGIR Conf. Res. Dev. Inf. Retr. - SIGIR 15, pp. 959962, 2015.

[27] L. Yanmei and C. Yuda, Research on Chinese Micro-Blog Sentiment Analysis Based on Deep Learning, 2015 8th Int. Symp. Comput. Intell. Des., pp. 358361, 2015.

[28] Q. You, J. Luo, H. Jin, and J. Yang, Joint Visual-Textual Sentiment Analysis with Deep Neural Networks, Acm Mm, pp. 10711074, 2015.

[29] C. Li, B. Xu, G. Wu, S. He, G. Tian, and H. Hao, Recursive deep learning for sentiment analysis over social data, Proc. - 2014 IEEE/WIC/ACM Int. Jt. Conf. Web Intell. Intell. Agent Technol. - Work. WI IAT 2014, vol. 2, pp. 13881429, 2014.

[30] R. Socher, A. Perelygin, and J. Wu, Recursive deep models for semantic compositionality over a sentiment treebank, Proc. , pp. 16311642, 2013.

[31] W. Li and H. Chen, Identifying top sellers in underground economy using deep learning-based sentiment analysis, Proc. - 2014 IEEE Jt. Intell. Secur. Informatics Conf. JISIC 2014, pp. 6467, 2014.

[32] C. Baecchi, T. Uricchio, M. Bertini, and A. Del Bimbo, A multimodal feature learning approach for sentiment analysis of social network multimedia, Multimed. Tools Appl., vol. 75, no. 5, pp. 25072525, 2016.

[33] H. Yanagimoto, M. Shimada, and A. Yoshimura, Document similarity estimation for sentiment analysis using neural network, 2013 IEEE/ACIS 12th Int. Conf. Comput. Inf. Sci., pp. 105110, 2013.

[34] R. Silhavy, R. Senkerik, Z. K. Oplatkova, P. Silhavy, and Z. Prokopova, Artificial intelligence perspectives in intelligent systems: Proceedings of the 5th computer science on-line conference 2016 (CSOC2016), vol 1, Adv. Intell. Syst. Comput., vol. 464, pp. 249261, 2016.

[35] A. Hassan, M. R. Amin, A. Kalam, A. Azad, and N. Mohammed, Bangla Text (BRBT) using Deep Recurrent models.

[36] T. Chen, R. Xu, Y. He, Y. Xia, and X. Wang, Using a Sequence Model for Sentiment Analysis, no. August, pp. 3444, 2016.

[37] P. Ruangkanokmas, T. Achalakul, and K. Akkarajitsakul, Deep Belief Networks with Feature Selection for Sentiment Classification, Uksim.Info, pp. 16, 2016.

[38] G. Zhou, Z. Zeng, J. X. Huang, and T. He, Transfer Learning for Cross-Lingual Sentiment Classification with Weakly Shared Deep Neural Networks, Proc. 39th Int. ACM SIGIR Conf. Res. Dev. Inf. Retr. - SIGIR 16, pp. 245254, 2016.

[39] R. Ghosh, K. Ravi, and V. Ravi, A novel deep learning architecture for sentiment classification, 3rd IEEE Int. Conf. Recent Adv. Inf. Technol., pp. 511516, 2016.

[40] R. Goebel and W. Wahlster, Integrated Uncertainty in Knowledge Modelling and Decision Making, Proc. Int. Symp. Integr. Uncertain. Knowl. Model. Decis. Mak. (IUKM 2011), vol. 1, pp. 362373, 2011.

[41] A. Graves, N. Jaitly, and A. R. Mohamed, Hybrid speech recognition with Deep Bidirectional LSTM, 2013 IEEE Work. Autom. Speech Recognit. Understanding, ASRU 2013 - Proc., pp. 273278, 2013.

[42] C. N. dos Santos and M. Gatti, Deep Convolutional Neural Networks for Sentiment Analysis of Short Texts, Coling-2014, pp. 6978, 2014.

[43] K. Ravi and V. Ravi, Sentiment classification of Hinglish text, 2016 3rd Int. Conf. Recent Adv. Inf. Technol. RAIT 2016, pp. 641645, 2016.

Cloud Computing: Pricing Model

Aferdita Ibrahimi, Ph.D. Student,
Faculty of Contemporary Sciences and Technologies
South East European University
Tetovo, Macedonia

***Abstract*—Cloud computing is the elemental aspect for online security of computing resources. It helps on-demand dividing of resources and cost between a major number of end users. It provides end users to process, manage, and store data so fast with reasonable prices. This is significant to know the causes of embarrassment between clients in relation to cloud computing services, particularly when it comes to a new price method. The price presents an important element, an indicator that often shows the quality of services, but on the other hand, the salesman with its offer on services has an impact directly on clients' decisions to use them. For both providers and users of cloud services, identifying the common factors in cloud services pricing is critical. In this paper will be shown various pricing model for cloud computing, and how they affect in different resources, their comparison, also the pricing model for two platforms: 1) Google Cloud Computing; and 2) Amazon Web Services.**

***Keywords*—Component; Cloud Computing pricing model; comparison of pricing model; Google Cloud platform and Amazon Web Service pricing model**

I. Introduction

This paper shows the importance of various prices models that the Cloud technology use, and it's use in many situations. Nowadays, Cloud Computing has become an essential part of the digital world. A Cloud is a sample of similar and distributed system that has an accumulation of inter-connected and virtually computers, which presents as one or more unified computing resources based on a convention between the service provider and consumers [1].

The use of Cloud Computing and the services offered by many company is increasing a lot every day. Today, we might see that needs and demands are increasing for these kinds of things, that allow us to have our space without having the need to secure hardware for storage or for various services, which will give a cost of thousands to have under our proprietary. However, a massive use of these services and multiple offers showed from different cloud platforms, provides various services as for compute, storage, big data, analytics, database, etc. often create confusion for the prices to the consumers. How many affects have prices in the use of these services? What are the kinds of pricing model that Amazon Web Services and Google Cloud Platform have?

Computing is a sample consisting of services that are similar to traditional benefits such as water, power, etc. In this model, users access services without having a need to connect with the main services. So, the principal part of it is Cloud computing [2].

Cloud computing is suitable for business owners because it gives the users to plan for their provision and allows enterprises to raise their resources only when there is an expansion in service demand [3]. The main part of it is that users don't have to know all the things about it or to have great ability to use them [2].

We can say that cloud providers form an oligopoly, with their equilibrium prices is like a Cournot equilibrium, which gives prices above the competitive price (is the time when prices equal production costs), but when it comes to decreasing resource costs, it changes a lot [4]. Even though Cloud service plays a key role in the success of cloud computing, exciting pricing models cannot respond quickly to market changes [5].

Pricing model in Cloud Computing is inclinable than other models, having its pricing scheme. Cloud Computing focuses to accomplish and to assure the quality of service (QoS) for clients [6].

The rest of the paper is organized as: Section 2 presents Overview of Cloud Computing. Section 3 describes Cloud Computing Pricing model. Section 4 shows Comparison of the Cloud Computing Pricing model and pricing model for cloud platforms: Amazon Web Service and Google Cloud. Section 5 has the Conclusion and the last section presents References used in the paper.

II. Overview of Cloud Computing

Cloud computing is a significant model for computing recourses, for instance, networks, storage, application, and services. As a service, it provides some facilities, like a cheap cost of services, high performances, scalability [7].

For many years cloud computing has become a lower cost for corporate computing market, as software, hardware, processing power, and storage capacity become more commoditized [8].

Using it gives a way to share computing resources that include applications, computing, storage, networking, development and deployment platforms which users can use it at any time [9].

Paradigms of Cloud Computing are being discussed based on the technical, business, and human factors, analyzing how business and technology strategy is being influenced by the following aspects of cloud computing: Architecture, Security, Costs, Hardware/software trends, Organizational/Human Factors [10].

Essential characteristics of cloud computing platforms are [11]:

1) The provider will take care of fluctuation demand (Dynamism).

2) Everything (OS, the plug-ins, web security or the software platform) should be in place without any worry of end-user (Abstraction).

3) A company dealing with Payroll Management may require more resources at the end or beginning of the month (Resource Sharing).

4) Pay-as-you-go ensures users that will never pay anything extra. Users will have the possibility to save money.

There were a lot of websites that started with cloud computing, for instance, the first one was in 1999 called Salesforce.com, which provided an application for delivering enterprise using the website. On the other hand, the second one who introduced Amazon Web Service in 2002 was the Amazon, after that Google Docs in 2006 was another factor to take the attention of public for cloud computing. In 2006, Amazon's Elastic Compute Cloud (EC2) gave the opportunity to companies and individuals to rent computers on which they could run their computer applications. Eucalyptus in 2008 with the source called AWS API created private clouds, followed by Open Nebula which was the first open source software for distributing private and hybrid clouds. In November 2009, Windows Azure from Microsoft entered with cloud computing. Today, you may see a major number of sources who use cloud computing [12], [13].

Using cloud computing helps to raise their profits with minimal output, and this is not just a distribution among different businesses; it is also the one that offers the best service to its clients [14].

Cloud Services provides many platform; in this case, would be taken to compare prices models for:

1) Google Cloud Platform: This platform provides to the people their chance to build, test, and deploy an application using reliable infrastructure. This platform can take from computing, storage, and application services for the web, mobile and backend solutions [15]. Google Cloud Platform provides services for Compute, Storage & Database, Networking, Big Data, Internet of Thing, Machine Learning, Identity & Security, Management Tools, and Development Tools [16].

2) Amazon Web services: Amazon Web Services (AWS) is a secure cloud services platform, offering computing power, database storage, content delivery and other functionality to help businesses scale and grow [17]. AWS has been operating since 2006, and from that time it had spent millions of dollars building and managing the large-scale, reliable, and efficient IT infrastructure that powered one of the world's largest online retail platforms. Nowadays the Amazon serves hundreds of thousands of customers worldwide, can say that it had arrived at its goal [18]. Amazon provides services for Compute, Storage, Database, Networking & Content Delivery, Developer Tools, Management Tools, Analytics, Security, Identity & Compliance, Mobile Services, Application Services, Messaging, Business Productivity, Desktop & App Streaming, Software, Migration, Artificial Intelligence, Contact Center, Game Development, and Internet of Things [19].

The principal part of Cloud Computing is Cloud Platform, in that part developers write applications that run in the cloud or they just can use services offered by the cloud, or both of them [20]. Amazon and Google are the first that offer cloud computing platforms. They have invested a lot for delivering scalable compute, storage and database services. Both provide web services accessed through simple API endpoints that can take infrastructure, store data, or create a network [21].

The aim of this paper is to offer descriptions and information about prices models for cloud computing and to show few differences between them, to help potential customers to know more about it.

III. CLOUD COMPUTING PRICING MODEL

The price presents an essential element, an indicator that often shows the quality of services, but on other side also setting prices from the salesman has an impact directly on clients' decisions to use them. For both providers and users of cloud services, identifying the common factors in cloud services pricing is critical.

We all know that in the market, customers should have the ability to compare their options and choose the best, while providers will have to show their pricing models to standard their schemes, in order to raise their quality of services [22].

A cloud computing provider's typical goal is to maximize its revenues with its employed pricing scheme, while for customers is to obtain the highest level of quality of service (QoS) feasible for a reasonable price. Therefore, satisfying both parties requires an optimal pricing methodology [23].

Anyway, the pricing model is a relationship between providers and customers, for which they should agree with it. Providers have their accounting system to calculate the price for the cloud services. All of them try to make benefit from it, while customers try to have the maximum service for lower prices. So, the price is an important element for the company, because this has an effect directly to the consumer and organization profit [6]. We could say that pricing is the key of what a service provider will accept from an end user instead of their services [23].

Fig. 1 presents a model for cloud computing cost accounting which addresses cost accounting issues in the production of cloud services. Services provider has infrastructure cloud, which allows them building platforms and services on top of it [24].

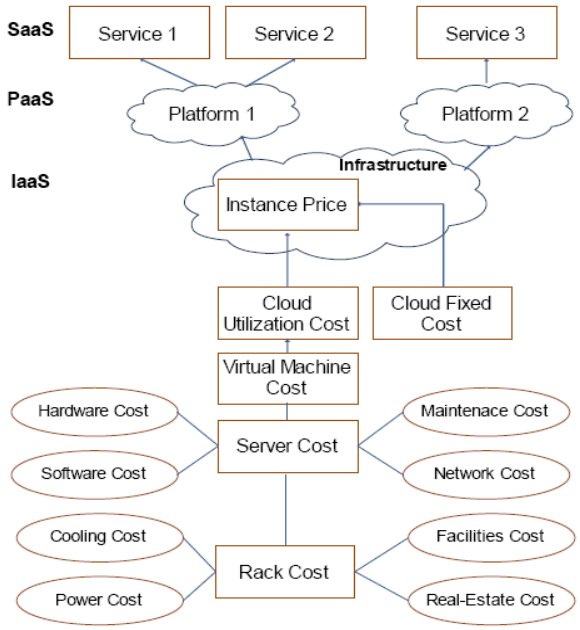

Fig. 1. Cloud computing cost accounting model.

Pricing in Cloud Computing has two impact aspects. First, pricing has its root in system design and optimization, resource-consumption based pricing is particularly sensitive to how a system is designed, configured, optimized, monitored, and measured. Second, pricing also has its root in economics, where key concepts such as fairness and competitive pricing in a multi-provider marketplace affect the actual pricing [25].

Cloud computing is a substantial practice for the online provisioning of computing resources as services. This technology allows sharing of resources and costs among a large number of end users. It provides end users to process, manage, and store data efficiently at very high speeds. Clients don't have to install any software and can access their data from any computer till the internet connection is available [23]. The interaction between systems and economy on price model has an important implication on cloud computing that should be explored by researchers [25].

The definitions and a short description of pricing schemes which varies depending on the services are shown below [6]:

1) Time-based: Pricing based on how long a service is being used.

2) Volume based: Pricing based on the capacity of a metric.

3) Flat rate: A fixed tariff for a specified amount of time.

4) Priority pricing: Services are labeled and priced according to their priority.

5) Edge pricing: A calculation is done based on the distance between the service and the user.

6) Responsive pricing: Charging is activated only on service congestion.

7) Session-oriented: Based on the use given to the session.

8) Usage-based: Based on the general use of the service for a period, e.g. a month.

9) Content-based: Based on the accessed content.

10) Location-based: Based on the access point of the user.

11) Service type: Based on the usage of the service.

12) Free of charge: No charge for the services.

13) Periodical fees: Payment of time to time quantities for the use of a service.

14) Pre-paid: The payment for the service will be in advance.

15) Post-paid: The payment for the service will be after it's use.

16) Online: The accounting performed while the user makes use of a service.

17) Offline: After the use of the service, the accounting process should proceed.

Price also is considered a key element in economic term with many factors which affect it [25]. The influencing factors for pricing in cloud computing [6], [23]:

1) Initial costs: This is the amount of money that the service provider spends annually to buy resources.

2) Lease period/contract time: This is the period in which the customer will lease resources from the service provider. Service providers usually offer lower unit prices for longer subscription periods.

3) QoS: This is the set of technologies and techniques provided by the service provider to enhance the user experience in the cloud, such as data privacy and resource availability. The better QoS offered, the higher the price will be.

4) Age of resources: This is the age employed by the service provider. The fee will be lower if the recourse is older than the others and this is because it can maintain their consumption which facilitates their financial value.

5) The cost of maintenance: This is the amount of money that the service provider spends on maintaining and securing the cloud annually.

6) The rate of depreciation: This is the rate at which the hardware of service provider is expected to lose its financial value.

Consumers have to be sure that the service they are paying for has to be delivered to them unbreakable. They can use SLAs (Service Level Agreements) between the consumers and providers to do it. An efficient economic model is being a challenge for enterprise working in the field of cloud computing [26].

Two pricing schemes for cloud are [27]:

1) Static pricing (fixed): This repair all prices for the whole time horizon. The cloud computing services are highly time dependent, so the time interval of offered service is predetermined.

2) Dynamic pricing.

These are two important criteria to decide the cost of query: availability when a user demands something from the cloud, a query is fired to the cloud and time horizon, i.e., when request a query.

The difference between fixed and dynamic is that in fixed pricing, each resource type has a predefined price, set by the

seller, while using dynamic pricing, computes each request according to the pricing mechanism used [28].

Fixed pricing mechanisms sets prices that do not differentiate in function of customer characteristics are not volume dependent and are not based on real-time market conditions. The mechanisms used are pay-per-use, subscription and menu pricing. In pay-per-use, the customer pays in function of the time or quantity he consumes for a product or service. For example, if they listen an online music he could be charged, or online newspaper may charge him for every article read. When he uses a subscription, the customer pays a flat fee for using a product or to profit from a service [29].

Fixed prices were easier to understand and more straightforward for users. Anyway, they could not be fair to all users [23]. Also, supports assurances for consumers, lets consumers know how much they will pay, is more consistent, reduces risks, makes profit estimation easy. However, disadvantages of fixed pricing model is that sometimes it is unfair for consumer because if the user doesn't consume the resource extensively, he/she may pay more than his/her real utilization. Moreover, it doesn't allow provider to change price for any account, unfair for them, it could happen that consumer may pay less than his/her real utilization [30]. Consumers also might be charged for resources they have not consumed. Their usage stops if they reach the maximal limit [22].

Dynamic price is based on pricing mechanism whenever there is a request. Sometimes the price of the resources is determined according to demand and supply [6]. Using dynamic pricing a firm delays its pricing decisions until after discoveres the market condition, so that it can fit prices accordingly, when demand is ample, set a high price, and when demand is weak, set a low price. But, many firms do not adjust prices to respond to market conditions [31]. Dynamic pricing is the monopolist that sells a single product and have perfect information about the demand distribution [22].

This model supports sellers to maximize profits with each consumer, fair for a consumer as it allows him to pay according to the offered QoS, and they could set the price according to a current state of the market. However, this model has also disadvantages such as consumers are not interested in this model, the one that pays more feel inequality, creating him negative opinions for dynamic pricing [30].

We have many business models based on different service models that define the price of services in the cloud [6].

A. Pricing model

Pricing is the process of determining what a service provider will receive from an end user in exchange for their services [23]. The service gives a price for resources that go to the costumer, reducing customer base and decreasing in revenue and profits [6].

Prices that are being used increasingly are pay-per-use and subscription [23], [32].

If customer use pay-per-use then he/she will pay only for what he/she is using, for a period of a particular service, it helps them to do business and consume the resource [6]. In pay-per-use model, the customers pay for the amount they consume of a product or the amount of time they use for a certain service [23]. It is the most used model, in which the consumer is charged a fee for a used unit for a specified duration. The unit used may be a certain computing unit of hardware, software or application, for example, GB or CPU [33]. Pay-per-use is called a piece of cloud concept heart [34].

Fixed-price model, sometimes called subscription, charges the user for using a service unit for a fixed price, usually in period of month or year [33]. Subscription is used from user paying just for accessing the software as an online service [6]. It is one of the pricing models, and customer subscribes it with a particular service provider for a fixed price [23]. The consumer has to sign a contract with all the criteria for using the service unit [35].

When we consider these two techniques: subscription and pay-per-use, we would say that subscription is more likely to be used in a time when customers don't like the time to complete the service, giving the firm a lot of costs. So, they should invest or cover that large capacity cost only when they get enough revenue from customers. However, pay-per-use generates higher revenue if revenue is reasonably low, while subscription pricing is considerable [36].

IV. COMPARISON OF CLOUD COMPUTING PRICING MODEL

Based on data obtained from the various publication of prices scheme (static or fixed and dynamic) in Cloud Computing shown in Section 3, will be presented with differences, and advantages and disadvantages of them.

The following table presents the differences between fixed and dynamic pricing:

TABLE. I. DIFFERENCES BETWEEN FIXED AND DYNAMIC PRICING

	Differences between Fixed and Dynamic Pricing
Fixed pricing	• The resource has a predetermined price, set by provider • Could not be fair to all consumer
Dynamic pricing	• The resource will be count for each request based on pricing mechanism used. • Fair for consumer

In Table 1, the main difference between this two pricing scheme has been presented, which shows the way how they make prices for a resource or a particular service differs from other. In fixed pricing, the resource has a predetermined price, given by provider, while dynamic, calculate pricing for each request based on the mechanism used. Using static pricing, the customer cannot change the price after its determination, while in dynamic pricing, the price will change depending on their demand. Then, another difference between them is the way how they treat their customer, fixed pricing could not be fair, while in dynamic pricing, it is.

The following table presents the advantages of fixed and dynamic pricing:

TABLE. II. ADVANTAGES OF FIXED AND DYNAMIC PRICING

	Fixed pricing	**Dynamic pricing**
Advantages	Better to enforce on consumers rationing risk	Firm delays its pricing decisions until after market recealed its conditions
	Easier to understand and more forthright for users	Fair for consumers
	Supports securities, more stable, reduce risks	Supports provider to maximize profits with each consumer
	Makes profit estimation easy	Setting price based on the current state of the market.

Both, fixed and dynamic pricing have their advantages that characterize them in their use. For instance, while fixed price is more forthright for the user, dynamic pricing is fair for it; while static pricing supports securities, dynamic pricing supports provider to maximize profits with each consumer.

The following table shows the disadvantages of fixed and dynamic pricing:

TABLE. III. DISADVANTAGES OF PRICING SCHEME

	Fixed pricing	**Dynamic pricing**
Disadvantages	Produce prices that do not vary in function of customer	Enforces a price risk on consumers
	Are not based on real-time market conditions	Consumer might pay higher price than can pay
	Could not be fair to all users	Many firms don't suit prices to respond to market conditions
	Doesn't allow provider to change price for any reason	Many users are not interested in this model
	Unfair for provider (consumer may pay less than his/her real utilization)	Consumer who pay more feel inequality
	Consumers might be charged for resources they have not consumed	
	Could be stopped if consumers reach the maximal limit	

Besides the advantages shown in Table 2, fixed and dynamic pricing also have their disadvantages. Table 3 shows some of the disadvantages of these pricing schemes. For example, one for fixed pricing is that it charges it's consumer for resources they have not consumed, while in dynamic pricing they might pay more than they can pay.

The table below, shows the comparison of some pricing model. All pricing models presented belongs to the pricing scheme: static and dynamic.

Table 4 presents some pricing model for cloud computing, for which the description is for each of them, the way how they treat customers, advantages and disadvantages and their implementation. From the model shown in the table, many of them are as the theoretical study with simulation.

B. Google Cloud Platform vs. Amazon Web Services: Pricing Model

Amazon Cloud Platform and Google platform offer a lot of cloud services, and both of them have their way how the users have to pay services that they offer: "Pay-as-you-go" for Amazon and "pay only for what you use" for Google [37], [38].

The challenge for service providers is to provide better services for a reasonable price to users. The pricing should be on customer's perceived value instead of production costs of services [6].

Amazon Web Services (AWS) provides a pay-as-you-go approach paying it only for a particular service you need, without having any problem with contracts or complex licensing. It is the same how people use water or electricity, paying just for the period that you use it and has not an additional cost or termination fees [37].

Below you may find the way how two platforms offer their product and how they set the price. While both of them have services for a virtual machine, they indeed have differences between each other.

For Google Compute Engine product, Google platform offers two categories of machine types: predefined machine types, which have preset virtualized hardware properties and a set price; and custom machine types where they take the price according to the number of vCPUs and memory that the virtual machine instance uses.

Below are presented billing model which applies to all types, predefined or custom [43]:

1) Charging all types for a minimum of **10 minutes**. For example, if you run your virtual machine for 2 minutes, you will be billed for 10 minutes of usage.

2) After 10 minutes, instances are charged in **1-minute increments, rounded up to the nearest minute.** An instance that lives for 11.25 minutes charges for 12 minutes of usage.

Amazon EC2 (Amazon Elastic Compute Cloud) provides to the consumers a model pay only for you, where they calculate pricing per instance-hour consumed, so each partial instance-hour consumed will be billed as a full hour. This service offers instance in four ways of paying [44]:

1) On-demand instance.
2) Reserved instance.
3) Spot instance.
4) Dedicated hosts.

TABLE. IV. COMPARISON OF PRICING MODEL

Pricing model	Operation (description)	Features and Fairness	Advantages (A) Disadvantages (D)	Implementation
Pay-as-you-go [6]	Price is set by a service provider and remains constant. This model is static	Unfair to the client. He might pay more than necessary	(A) - Resources/Services are available during reservation period, and the price is known (D) – Over-provisioning and Under-provisioning' problems may occur. The price is unchangeable [29]	Implemented [37]
Subscription [30]	Price is based on the period of subscription	Sometimes consumer might pay more for a resource	(A) - It is good for consumer When utilize extensively Resources/Services (D) - Consumer may pay more than the real utilization cost when he/she does not use Resources/Services properly	Implemented [38]
Dynamic resource pricing [28]	It is a dynamic pricing model used for federated cloud and facilitates sellers to provide multiple resource types.	Resource payments are assigned based on demand and supply.	(A) - It can balance the number of successful requests and the number of allocated resources depending on the market condition [28]. (D) - Less scalability of high demand in the market than fixed pricing	Theoretical study With simulation
Pay-for-recourses	It is a static model which will set by cloud provider	Fair for both customers and the service provider	(A)- Offers maximum utilization of the service provider's resources (D)	Implemented [38]
Hybrid pricing [23]	Price changed according to the job queue wait times (static/dynamic)	Fair to customers because of the price authority entity, which dynamically adjusts prices within static limits	(A) - Simple and has lower computational overhead (D) - Must reach an agreement on common base price and variation limits	Implemented
Dynamic auction [35]	This mechanism used the approach of pricing, truthfulness and dynamic adjustment mechanisms	Dynamic adjustments tolerate fluctuation of users' distributions.	(A) - Dynamic adjustments tolerate fluctuation of users' distributions.	Theoretical study with simulation
A novel financial, economic model [39]	This model is dynamic, usage-based.	It is fair for service provider and consumer.	(A) –It provides a high level of Quality of Service for clients. (D) – Does not consider maintenance costs and assumes the price charged for assets for customers	Theoretical study with simulation
Pricing algorithm for cloud computing [23]	It is a real time pricing This model is dynamic	Fair for provider because it reduces costs and maximizes revenues	(A) - Reduces the costs of the providers; maximizes revenues (D) - Model is almost fixed and cannot adapt to rapid changes in supply and demand in the market	Theoretical study with simulation
Costumer-based pricing [6, 40]	In this dynamic price is set according to consumer requirements and needs	This model is fair for clients if it is taken into account	(A) – Considerate Cloud Computing (D) - vendors try to charge prices lower than their competitors.	Implemented
Cost-based pricing [6, 41]	In this model, the priority is to increase the profit.	This model is not fair to consumer	(A) Easy to calculate the price (D) – Determining the price by the provider without the customer's influence.	Implemented
Double sided combinational auction to resource allocation [11, 42]	This model is for service allocation that enables users and providers to deal through double-sided combinational auction.	Users and service providers should be satisfied by the resource allocation mechanism	(A) - suitable for cases requiring various services and where many participants exist (D) - doesn't make optimization of energy consumption	Theoretical study with simulation
Value-based pricing [30]	This model is dynamic. Service prices are defined depending on the customer's point of view	It is fair to consumer	(A) – Increases revenues (D) – Hard to implement	Implemented

Genetic model for pricing in cloud computing markets [23]	It is real-time based pricing. This model is dynamic	Biased toward the service provider; the algorithm considers increasing revenues	(A) - Achieves very high revenues, Stable against noises, Flexible, Easy to implement (D) - Assumes that the market behaves rationally, which might cause the model to underperform in very high and very low demand conditions	Theoretical study with simulation
Competition-based pricing [28, 40]	In this model price assigned according to competitors' prices. This model is dynamic.	A fair model because the price assigned according to competitors' prices.	(A) – Easy to implement (D) – Ignores the cloud customers	Implemented
Datacenter net profit optimization with individual job deadlines [23]	This is a job scheduling based model. This model is dynamic.	Biased toward the service provider; it mainly reduces costs and increases	(A) - Maximizes revenues for the service provider and minimizes electricity (D) - Considers only static job arrivals and departures and assumes	Theoretical study with simulation

V. CONCLUSION

This paper presents Cloud Computing and its pricing model. Firstly, describes two main schemes for pricing: fixed and dynamica, then in Section 4 a comparison between how they set the price and their advantages and disadvantages. Then, in Section 3, two pricing models: pay-per-use and subscription are presented which are the most used models.

Aside from in Section 4, you might find the comparison of some of the pricing models and their characteristics, where you can find their description, fairness, advantages and disadvantages, and their implementation.

In the end, shows two platforms: Amazon and Google cloud, where there is also presented the main pricing model with an example of how their platform set the price for a particular product.

REFERENCES

[1] Buyya, Rajkumar, et al. "Cloud computing and emerging IT platforms: Vision, hype, and reality for delivering computing as the 5th utility." *Future Generation Computer systems* 25.6 (2009): 599-616.

[2] IEEE UCC,"*The 5th IEEE/ACM International Conference on Utility and Cloud Computing"* IEEE UCC 2012, Chicago, Illinois, US, available at http://cloudcomputing.ieee.org/conferences/calendar/view/144/23.%202012

[3] Zhang, Qi, Lu Cheng, and Raouf Boutaba. "Cloud computing: state-of-the-art and research challenges." *Journal of Internet services and applications* 1.1 (2010): 7-18.

[4] Kash, Ian A., and Peter B. Key. "Pricing the Cloud." *IEEE Internet Computing* 20.1 (2016): 36-43.

[5] Wang, Wei, Ben Liang, and Baochun Li. "Revenue maximization with dynamic auctions in IaaS cloud markets." *The quality of Service (IWQoS), 2013 IEEE/ACM 21st International Symposium on*. IEEE, 2013.

[6] Mazrekaj, Artan, Isak Shabani, and Besmir Sejdiu. "Pricing Schemes in Cloud Computing: An Overview." *INTERNATIONAL JOURNAL OF ADVANCED COMPUTER SCIENCE AND APPLICATIONS* 7.2 (2016): 80-86.

[7] Mell, Peter, and Tim Grance. "The NIST definition of cloud computing." (2011)..

[8] Wyld, David C. "The utility of cloud computing as a new pricing-and consumption-model for information technology." *International Journal of Database Management Systems* 1.1 (2009): 1-20.

[9] Judith Hurwitz, Marcia Kaufman, Fern Halper: Cloud Services for Dummies –IBM Limited Edition, John Wiley & Sons, Inc, New Jersey, 2012

[10] Gorelik, Eugene. *Cloud computing models*. Diss. Massachusetts Institute of Technology, 2013.

[11] Basant Narayan, Cloud Computing for Beginners, Techno-Pulse, 2010

[12] Dikaiakos, Marios D., et al. "Cloud computing: Distributed Internet computing for IT and scientific research." *IEEE Internet Computing* 13.5 (2009): 10-13.

[13] Ivan Zapevalov, *"The Basics of Cloud Computing"* Conseil Européen pour la Recherche Nucléaire, pp. 7, Geneva, Switzerland, available at http://ais-grid-2013.jinr.ru/docs/24/1-CloudComputing_IZ.pdf. 2013

[14] Aljabre, Abdulaziz. "Cloud computing for increased business value."*International Journal of Business and Social Science* 3.1 (2012).

[15] Google Cloud Platform, *"Why Google,"* https://cloud.google.com/why-google/

[16] Google Cloud Platform, *"Products,"* available at https://cloud.google.com/products/

[17] Amazon Web Services, available at http://aws.amazon.com/what-is-aws/

[18] Mathew, Sajee. "Overview of Amazon Web Services." *Amazon Whitepapers*(2014).

[19] Cloud products & services – Amazon Web Service available at https://aws.amazon.com/products/

[20] Chappell, David. "A short introduction to cloud platforms." *David Chappell & Associates* (2008).

[21] Google cloud vs. Amazon, https://cloud.google.com/docs/compare/aws/, last accessed 18.08.2016

[22] Bitran, Gabriel, and René Caldentey. "An overview of pricing models for revenue management." *Manufacturing & Service Operations Management*5.3 (2003): 203-229.

[23] Al-Roomi, May, et al. "Cloud computing pricing models: a survey."*International Journal of Grid & Distributed Computing* 6.5 (2013): 93-106.

[24] Jäätmaa, Jaakko. "Financial aspects of cloud computing business models." (2010).

[25] Wang, Hongyi, et al. "Distributed Systems Meet Economics: Pricing in the Cloud." *HotCloud* 10 (2010): 1-6.

[26] Chawla, Chetan, and Inderveer Chana. "Day-ahead Pricing Model for Smart Cloud using Time-Dependent Pricing." *International Journal of Computer Network and Information Security* 7.11 (2015): 9.

[27] Kamra, Varun, Kapil Sonawane, and Pankaja Alappanavar. "Cloud computing and its pricing schemes." International Journal of Computer Science and Engineering 4.4 (2012): 577.

[28] Mihailescu, Marian, and Yong Meng Teo. "Dynamic resource pricing on federated clouds." In *Proceedings of the 2010 10th IEEE/ACM International Conference on Cluster, Cloud and Grid Computing*. IEEE Computer Society, 2010.

[29] Osterwalder, Alexander. "The business model ontology: A proposition in a design science approach." (2004).

[30] Ali, Taj-Eldin Suliman M., and Hany H. Ammar. "Pricing Models for Cloud Computing Services, a Survey."

[31] Cachon, Gérard P., and Pnina Feldman. "Dynamic versus static pricing in the presence of strategic consumers." *Retrieved April* 15 (2010): 2011.

[32] Weinhardt, Christof, et al. "Cloud computing–a classification, business models, and research directions." *Business & Information Systems Engineering* 1.5 (2009): 391-399.

[33] Weintraub, Eli, and Yuval Cohen. "Cost Optimization of Cloud Computing Services in a Networked Environment." *International Journal of Advanced Computer Science and Applications* 6.4 (2015): 148-157.

[34] Weinman, Joe. "The Economics of Networking and the Cloud." *IEEE Cloud Computing* 3.3 (2016): 12-15.

[35] Samimi, Parnia, and Ahmed Patel. "Review of pricing models for grid & cloud computing." *Computers & Informatics (ISCI), 2011 IEEE Symposium on*. IEEE, 2011.

[36] Cachon, Gérard P., and Pnina Feldman. "Pricing services subject to congestion: Charge per-use fees or sell subscriptions?." *Manufacturing & Service Operations Management* 13.2 (2011): 244-260.

[37] AWS Pricing, https://aws.amazon.com/pricing/, last accessed 19.08.2016

[38] Pricing, Cloud Pub/Sub Documentation, Google Cloud Platform, https://cloud.google.com/pubsub/pricing, last accessed 20.08.2016

[39] Sharma, Bhanu, et al. "Pricing cloud compute commodities: a novel financial economic model." *Proceedings of the 2012 12th IEEE/ACM international symposium on cluster, cloud and grid computing (CCGrid 2012)*. IEEE Computer Society, 2012.

[40] Rohitratana, Juthasit, and Jörn Altmann. "Agent-based simulations of the software market under different pricing schemes for software-as-a-service and perpetual software." *International Workshop on Grid Economics and Business Models*. Springer Berlin Heidelberg, 2010.

[41] Lehmann, Dipl-Wirtsch-Ing Sonja, and Peter Buxmann. "Pricing strategies of software vendors." *Business & Information Systems Engineering* 1.6 (2009): 452-462.

[42] Fujiwara, Ikki, Kento Aida, and Isao Ono. "Applying double-sided combinational auctions to resource allocation in cloud computing."*Applications and the Internet (SAINT), 2010 10th IEEE/IPSJ International Symposium on*. IEEE, 2010.

[43] Google compute engine, https://cloud.google.com/compute/pricing, last accessed 25.05.2017

[44] Amazon EC2 Pricing, https://aws.amazon.com/ec2/pricing/, last accessed 25.05.2017

Cryptography: A Comparative Analysis for Modern Techniques

Faiqa Maqsood[1]
Dept. Computer Science & Information Technology
Superior University
Lahore, Pakistan

Muhammad Mumtaz Ali[3]
Dept. Computer Science & Information Technology
Superior University
Lahore, Pakistan

Muhammad Ahmed [2]
Dept. Computer Science & Information Technology
Superior University
Lahore, Pakistan

Munam Ali Shah[4]
Dept. Computer Science
COMSATS Institute of Information Technology
Islamabad, Pakistan

***Abstract*—Cryptography plays a vital role for ensuring secure communication between multiple entities. In many contemporary studies, researchers contributed towards identifying best cryptography mechanisms in terms of their performance results. Selection of cryptographic technique according to a particular context is a big question; to answer this question, many existing studies have claimed that technique selection is purely dependent on desired quality attributes such as efficiency and security. It has been identified that existing reviews are either focused only towards symmetric or asymmetric encryption types. Another limitation is found that a criterion for performance comparisons only covers common parameters. In this paper, we have evaluated the performance of different symmetric and asymmetric algorithms by covering multiple parameters such as encryption/decryption time, key generation time and file size. For evaluation purpose, we have performed simulations in a sample context in which multiple cryptography algorithms have been compared. Simulation results are visualized in a way that clearly depicts which algorithm is most suitable while achieving a particular quality attribute.**

***Keywords*—Cryptography; symmetric; asymmetric; encryption; decryption**

I. Introduction

Cryptography is the art of secret writing which is used since Roman times to hide information secret or keeping message secure. To keep information secret, a widely-used method is an encryption/decryption. Basically, encryption/decryption are the fundamental functions of cryptography. In encryption, a simple message (plain text) is converted into unreadable form called ciphertext. While in decryption, a ciphertext is converted into the original text (plaintext). Both of these functions are used to secure message against who is not authorized to view the message contents [1]-[3]. The simple working of encryption and decryption functions is shown in Fig. 1.

Symmetric and asymmetric are widely accepted types of cryptography [4] in which symmetric (also called symmetric key cryptography) is focused towards ensuring secure communication between sender and receiver by using same secret key, whereas asymmetric cryptography (also called public key cryptography) secures communication by using public and private keys [5], [6]. Private key is hold individually in communication while public key is known to everyone due to public nature. Fig. 2 and 3 shows the symmetric and asymmetric cryptography, respectively.

To secure the communication, key size is the most important parameter in symmetric and symmetric cryptography. The key size of symmetric cryptography is less than the asymmetric cryptography which make symmetric cryptography less secure for more sensitive data [7], [8].

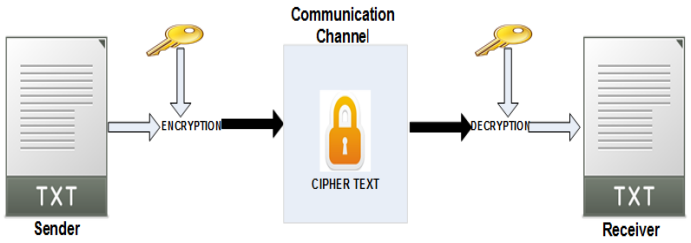

Fig. 1. Working of encryption and decryption.

The computational time of asymmetric cryptography is greater than the symmetric cryptography which makes encryption/decryption more complex for a large amount of data [9], [10]. Due to larger key size and greater computational time of asymmetric cryptography, public key cryptography is used once for key exchange only and further encryption/ decryption is done by symmetric key cryptography [11], [12].

The computational time of cryptography techniques is further classified as encryption/decryption time, key generation, and key exchange time. Encryption/decryption time is calculated by converting a plaintext (message) into ciphertext and vice versa [13], [14]. Key generation time is depending on the size of key length which is different for symmetric and asymmetric cryptography. Key exchange time is depending on the communication channel between sender and receiver [15], [16].

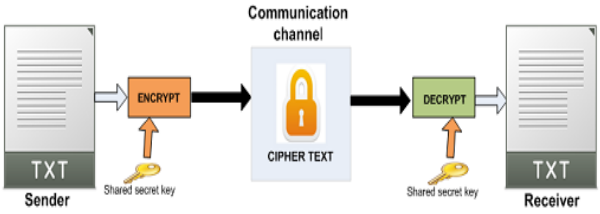

Fig. 2. Symmetric Cryptography

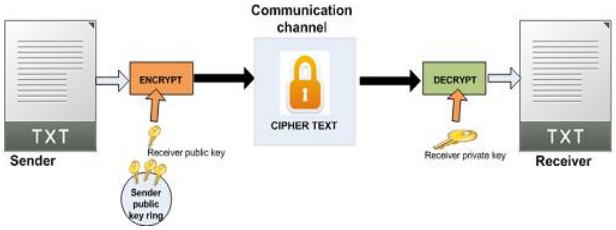

Fig. 3. Asymmetric cryptography.

There are designed many cryptographic algorithms used for encryption and decryption [17], [18]. As we already described, the cryptography schemes are classified as symmetric and asymmetric algorithms. In our paper, symmetric algorithms include but not limited; DES (Data Encryption Standard), 3DES (Triple Data Encryption Standard), AES (Advanced Encryption Standard). Asymmetric algorithms include RSA (Rivest, Shamir and Adleman), Elgamal, and ECC (Elliptic Curve Cryptography) [19]. Fig. 4 describes the taxonomy of cryptography techniques.

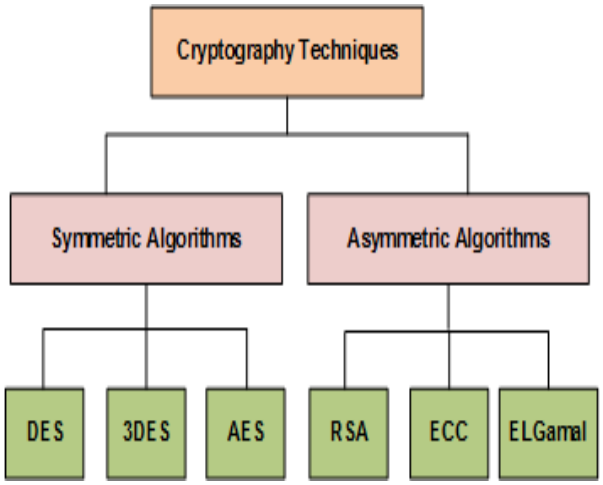

Fig. 4. Taxonomy of cryptography techniques.

In this paper, we describe the literature review of the cryptographic schemes including symmetric and asymmetric. We also evaluate the performance of described cryptographic systems on different file sizes. Performance analysis shows that the asymmetric algorithms take much time for encryption and decryption as compare to symmetric algorithms.

The main objective of this paper is to provide the performance evaluation of cryptographic schemes including symmetric and asymmetric algorithms. We use different evaluation parameters such as encryption/decryption time, and key generation time.

The rest of the paper is organized as: Section II discussed existing state of the art cryptographic schemes. Performance evaluation and results discussion of cryptographic schemes is presented in Section III. Section IV concludes the paper and future work.

II. Literature Review

There are many cryptography algorithms used to secure information such as DES, 3DES, Blowfish, AES, RSA, ElGamal and Paillier [2]. All of these algorithms are unique on it's way. However, the problem is that how to find the best security algorithm which provides the high security and also take less time for a key generation, encryption, and decryption of information. Security algorithms will depend on pros and cons of each algorithm, requirement and suitable for different application [25], [32], [33].

In paper [7], it has been evaluated that performance of two algorithms DES and Blowfish on basis of certain parameters such as encryption speed, power consumption, and security analysis. Experiment result showed that performance of Blowfish is fastest than DES and AES algorithm [34]. However, in [35] results showed that AES performance is good than Blowfish.

In [18] some of the cryptography algorithms details are given such as AES, DES, 3DES, RC6, Blowfish and RC2. Furthermore, the performance of these security algorithms is also evaluated and experiment is performed on text file and image. The result is showed that all algorithms slow in performance as compare to Blowfish as increased the packet size. However, selecting the image as the type of data instead of text file then Blowfish, RC6, and RC2 the algorithm has consumed more time than AES, DES and 3DES algorithms. The result showed that DES is still faster in performance than 3DES [18].

In this paper, [36] take the different size of a file for performance evaluation of cryptography algorithm. The experiment is performed on single processor and cloud computing. The result is proved that cryptography algorithm works faster in cloud computing than a single processor computer. AES with small input file has highest Speed up ratio, MD5 the least while RSA is the most time-consuming [36]. In author [37] evaluated the performance of different cryptography algorithms such as DES, AES, and 3DES to find the encryption and decryption time and throughput for different hardware. These algorithms are used to calculate the time of encryption. Encryption time is increasing as when the size of data increases. Therefore, the speed of encryption increase depends on file (in bytes) not on the data type of a file [38]. The throughput of 3DES has less as compare to AES, text files and images used for performance evaluation [39]. Dot net frame used for implementation of DES 3DES that take more processing time as compare to AES algorithm [37]. Only a single parameter is used to measure the encryption time. For future work of this paper is measure the encryption time by using the different parameter.

DES performance is not faster for software use. However, the performance of DES is faster on hardware [40] [12]. The performance of AES, DES, and Blowfish has been evaluated by using different size of text file in term of encryption and decryption speed. Future work of this paper shows better result by using the better simulator for implementation [41]. In this paper [42], RSA, DES and AES are discussed. Analyses are performed on the basis of some parameter such as usage of memory, computation time and output byte. Text file used for evaluation and implementation of result which showed that DES and AES are the minor difference for file encryption time while encryption time of RSA is longest and also consumed the high memory.

Mobile client and server used for evaluating the performance of RSA and ECC cryptography algorithm [43]. WTLS (Wireless Transport Layer Security) security protocol is used for performance evaluation. In experiment, the result showed that RSA is faster for client side but performance is slow at the server side as compare to ECC (Elliptic Curve Cryptosystem) performance. RSA, ElGamal and Paillier have been used for performance evaluation based on a parameter such as the encrypted file size, decrypted file size, encryption time, decryption time and throughput. Experimental result showed that encryption time of RSA is better than ElGamal but decryption time of ElGamal is better as compared to RSA. Result also showed that throughput of RSA encryption process is better and throughput in the decryption process of ElGamal performance is better than RSA. Overall performance according to the chosen parameter RSA is better than all other two algorithms paillier and ElGamal [29].

In [44] paper analysis is performed and RSA with different key size and word length variable in term of encryption and decryption process require memory size and execution time. Experiment result showed that RSA execution time is slow and need more memory requirement as compare to ECC. Key agreement and key distribution is the main problem in DES algorithm but in RSA encryption and decryption, both operations consume more time. The result showed in a simulation that RSA is slower in performance than DES and evaluated that RSA algorithm throughput of is not better than DES algorithm. In this paper, simulation result showed that power consumption and throughput of DES algorithm is much better than another algorithm [45].

III. State of the Art of Cryptography Schemes

A. Symmetric Cryptography

Symmetric cryptography is placed in the category of cryptography schemes in which a shared key is used to convert a plaintext into cipher text. A same secret key is shared by both sender and receiver. Followings are the symmetric cryptography schemes.

- DES (Data Encryption Standard): DES stands for Data Encryption Standard. DES introduced in early 1970 at IBM. The early design of DES is based on Horst Feistel. DES is a symmetric cryptographic algorithm used for encryption and decryption of message [20]. In DES, only one secret key is used for both encryption and decryption. The key size of DES is 56-bit. To perform encryption/decryption, the sender and receiver must have the same key. The DES performs encryption on a block of 64-bit [13]. The DES algorithm is most widely used in many applications [21] and some popular use in military, commercial, and security of communication system [7], same as DES but key size is different from DES. The key size of 3DES is 168 bit. The 3DES algorithm performs operation three times on each block of data. It is slower than DES [22].
- AES (Advanced Encryption Standard): AES stands for Advanced Encryption Standard which is the advancement of 3DES algorithm [23]. It was introduced in 1997 by the NIST (National Institute of Standards and Technology). Basically, AES is based on the Rijndael cipher developed by two cryptographers, Joan Daemen and Vincent Rijmen. AES is different from DES and 3DES due to variables key sizes such as 128, 192, and 256 bits [21]. Same like DES and 3DES, AES also performs encryption on blocks which are 128-bit [13]. AES algorithm use in small devices for encrypting a message to send over a network. Some other applications are monetary transaction [24] and security applications [15] [25].

B. Asymmetric Cryptography

Asymmetric cryptography is also in the category of cryptography schemes. Unlike symmetric cryptography, two keys are used: one is public and second is private. The public key is shared by anyone in the cryptographic system while the private key is kept secret by authenticated user. Followings are the asymmetric cryptography algorithms.

- RSA (Rivest, Shamir and Adleman): RSA stands for Rivest, Shamir and Adleman who introduced the RSA algorithm in 1977 [26]. RSA is an asymmetric cryptographic algorithm [2] which is also used for encryption and decryption of the message. RSA is widely used in transferring of keys over an insecure channel. Due to asymmetric nature, there are two keys used in the algorithm. One is public key and second is a private key. The public key is openly accessible to everyone in the cryptosystem and the private key is kept secret by authorized person. RSA provides confidentiality, integrity, authenticity, and non-repudiation of data [27] [23]. RSA is more commonly used in electronic industry for online money transfer [19]. In future, RSA can be used in Java cards [28].
- ElGamal: ElGamal algorithm was introduced in 1985 by Taher ElGamal [29]. ElGamal is an asymmetric key encryption algorithm that is based on the Diffie-Helman key exchange as an alternative to RSA for public key encryption. ElGamal is also used in digital signature generation algorithm called ElGamal signature scheme [20][30][31]. A homomorphic algorithm named paillier used for its semantic security [6].
- ECC (Elliptic Curve Cryptography): ECC stands for Elliptic Curve Cryptography. ECC introduced in 1985 by Neal Koblitz and Victor S. Miller. ECC lies in the category of the asymmetric scheme that is based on

elliptic curves. The applications of ECC are encryption, digital signatures and pseudo-random generators [32].

IV. Performance Evaluation

In this section, we present experimental setup and experimental results of symmetric and asymmetric algorithms.

A. Experimental Setup

The algorithms are implemented using the Java (Eclipse Platform Version: 3.3.1.1) Experiments are performed on Intel Pentium processor with a 2.34 GHz and 1 GB of memory. We used different size of text files in our experiments such as 32 KB, 126 KB, 200 KB, 246 KB and 280 KB.

B. Experimental Result

We evaluate the performance of symmetric and asymmetric algorithms by using parameters such as encryption time, decryption time and key generation time. Symmetric algorithms include DES and AES while asymmetric algorithms include RSA and ElGamal.

Encryption time is the time required by any encryption function to convert plaintext into ciphertext [44]. Decryption time is the time required to convert again cipher text into plain text. Similarly, key generation time is the time taken by key generation function to generate keys. All these functions generate different times according to the size of text files and key length in any algorithm. Table 1 shows the generation time of symmetric and asymmetric keys.

TABLE. I. Key Sizes with their Generation Time

Cryptography Algorithms		***Key Size (bits)***	***Generation Time (milliseconds)***
Symmetric	DES	56	29 ms
	AES	128	75 ms
Asymmetric	RSA	1024	287 ms
	ElGamal	160	86 ms

C. Symmetric Cryptography

In this section, we analyzed the encryption and decryption time of symmetric algorithms. Fig. 5 shows the encryption time of DES and AES algorithms performed on different file sizes. It is obvious from the Fig.5 that the encryption time of AES algorithm is lower than comparing to DES algorithm.

In Fig. 6, the performance results show that the decryption time of AES is also lower than the decryption time of DES. To conclude, the performance of AES algorithm in the context of encryption/decryption time is much better than the DES algorithm.

Table 2 shows the encryption and decryption time of symmetric and asymmetric algorithms with their different file sizes. Performance results show that when we increase the size of text files, the encryption and decryption time is also increased.

TABLE. II. File Size with their Encryption and Decryption Times

Cryptography Algorithms	***File size (kilo bytes)***	***Encryption Time (in Seconds)***	***Decryption Time (in Seconds)***
DES	32	0.27	0.44
	126	0.83	0.65
	200	1.19	0.85
	246	1.44	1.23
	280	1.67	1.45
AES	32	0.15	0.15
	126	0.46	0.44
	200	0.72	0.63
	246	0.95	0.83
	280	1.12	1.10
RSA	32	0.13	0.15
	126	0.52	0.43
	200	0.74	0.66
	246	1.11	0.93
	280	1.39	1.23
ElGamal	32	0.45	0.43
	126	1.03	0.85
	200	1.41	1.13
	246	1.75	1.30
	280	1.83	1.64

D. Asymmetric Algorithms

In this section, we analyzed the performance of asymmetric algorithms in term of encryption and decryption time. Fig. 7 shows the encryption time of RSA and ElGamal algorithms performed on different file sizes. It is obvious from the Fig. 7 that the encryption time of RSA algorithm is lower than comparing to ElGamal algorithm.

In Fig. 8, the performance results show that the decryption time of RSA is also lower than the decryption time of ElGamal. To conclude, the performance of RSA algorithm in the context of encryption/decryption time is much better than the ElGamal algorithm.

E. Symmetric and Asymmetric Algorithms

In this section, we analyzed the performance of symmetric and asymmetric cryptographic algorithms in term of encryption/decryption time and key generation time.

- *Encryption Time:* Fig. 9 shows the encryption time of DES, AES, RSA, ElGamal on different file sizes. It is clear from the figure that encryption time of DES algorithm is more than all other schemes such as AES, RSA, and ElGamal. The RSA encryption time is less than all other schemes. To conclude that, the encryption time of asymmetric algorithms is less than the symmetric algorithms.

- *Decryption Time:* Fig. 10 shows the decryption time of DES, AES, RSA, ElGamal on different file sizes. The decryption time of RSA algorithm is much than all other schemes such as DES, AES, and ElGamal.
- *Key Generation Time*: Fig. 11 shows the key generation time of symmetric and asymmetric algorithms. Key generation time is depending on the bit length of a key. The more in length, the increase in time. The RSA algorithm takes more time to generate the key because of key length 1024 bits while DES algorithm takes less time because of key length 56 bits.

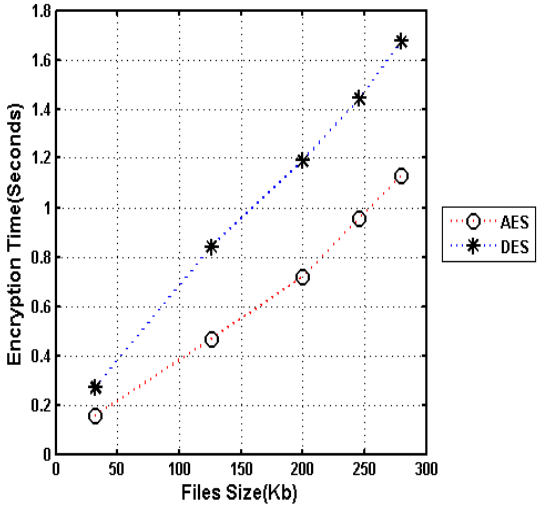

Fig. 5. Encryption Time (AES and DES).

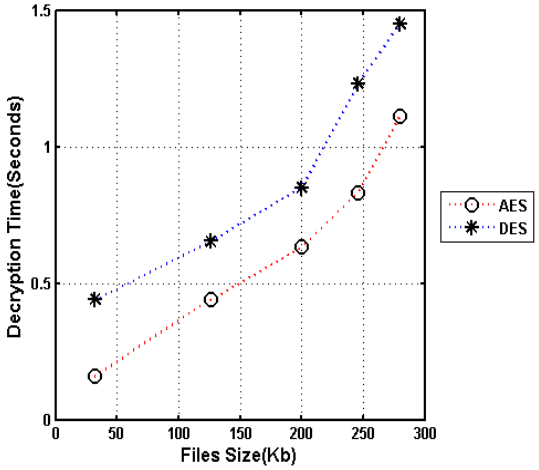

Fig. 6. Decryption Time (AES and DES).

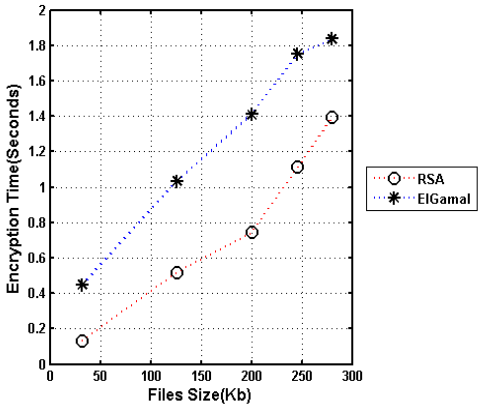

Fig. 7. Encryption Time (RSA and ElGmal).

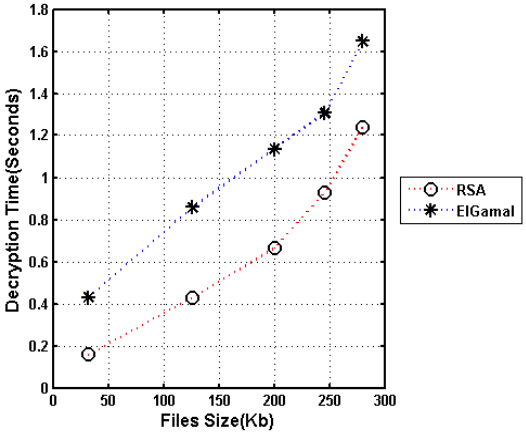

Fig. 8. Decryption Time (RSA and ElGmal).

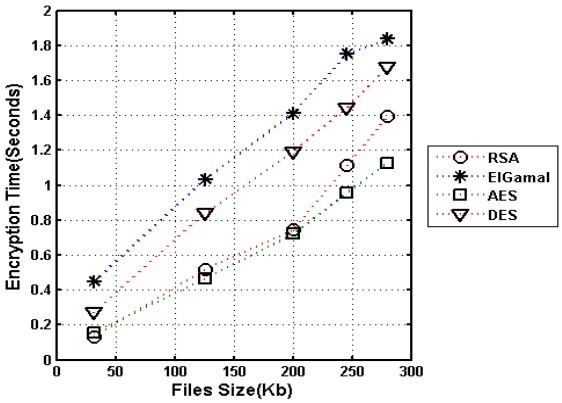

Fig. 9. Encryption Time (DES, AES, ElGmal and RSA).

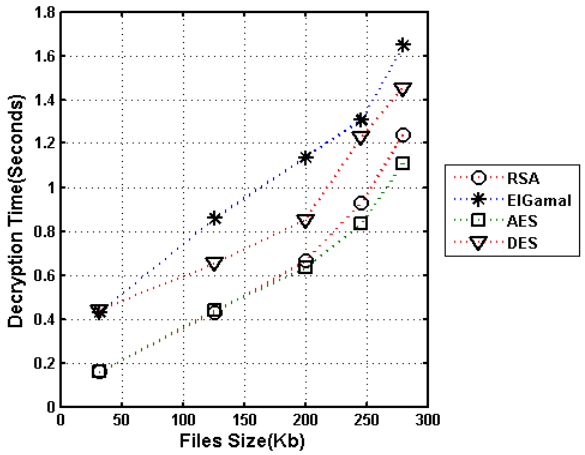

Fig. 10. Decryption Time (DES, AES, ElGmal and RSA).

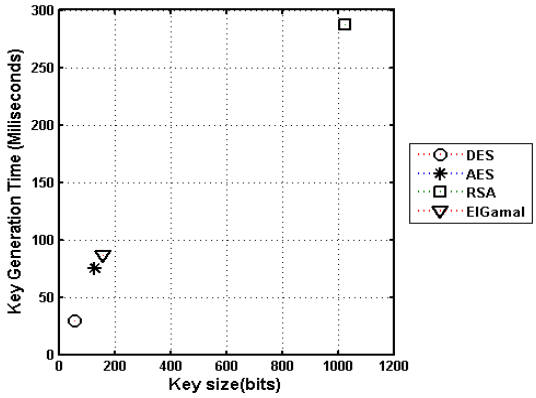

Fig. 11. Key Generation Key (DES, AES, ElGmal and RSA).

V. CONCLUSION

In this work, we analyzed the performance of symmetric and asymmetric cryptography schemes. We used encryption time, decryption time and key generation time to evaluate the cryptographic schemes. The performance results show that the symmetric schemes are computationally inexpensive when compared with asymmetric schemes. The key generation time is depending on the key length of bits. In future, we plan to elaborate more symmetric and asymmetric schemes and extend our performance analysis results.

REFERENCES

[1] Jitendra Singh Chauhan and S. K. Sharma, "A Comparative Study of Cryptographic Algorithms," Int. J. Innov. Res., pp. 24–28, 2015.

[2] A. Al Hasib and A. A. M. M. Haque, "A comparative study of the performance and security issues of AES and RSA cryptography," Proc. - 3rd Int. Conf. Converg. Hybrid Inf. Technol. ICCIT 2008, vol. 2, no. November 2001, pp. 505–510, 2008.

[3] C. Narasimham and J. Pradhan, "Evaluation of Performance Characteristics of Cryptosystem Using Text Files.," J. Theor. Appl. Inf. Technol., vol. 4, no. 1, 2008.

[4] M. Mikhail, Y. Abouelseoud, and G. Elkobrosy, "Extension and Application of El-Gamal Encryption Scheme," 2014.

[5] A. Naureen, A. Akram, T. Maqsood, R. Riaz, K. H. Kim, and H. F. Ahmed, "Performance and security assessment of a PKC based key management scheme for hierarchical sensor networks," IEEE Veh. Technol. Conf., pp. 163–167, 2008.

[6] S. Farah, M. Y. Javed, A. Shamim, and T. Nawaz, "An experimental study on Performance Evaluation of Asymmetric Encryption Algorithms," Recent advaces Inf. Sci., vol. 8, pp. 121–124, 2012.

[7] R. Tripathi and S. Agrawal, "Comparative Study of Symmetric and Asymmetric Cryptography Techniques," Int. J. Adv. Found. Res. Comput., vol. 1, no. 6, pp. 68–76, 2014.

[8] B. Padmavathi and S. R. Kumari, "A Survey on Performance Analysis of DES , AES and RSA Algorithm along with LSB Substitution Technique," Int. J. Sci. Res., vol. 2, no. 4, pp. 170–174, 2013.

[9] G. Singh, "A Study of Encryption Algorithms (RSA, DES, 3DES and AES) for Information Security," *Int. J. Comput. Appl.*, vol. 67, no. 19, pp. 975–8887, 2013.

[10] A. Patil and R. Goudar, "A Comparative Survey Of Symmetric Encryption Techniques For Wireless Devices," *Int. J. Sci. Technol. Res.*, vol. 2, no. 8, pp. 61–65, 2013.

[11] C. Science and M. Studies, "An Efficient Password Security Mechanism Using Two Server Authentication and Key Exchange," pp. 50–53, 2015.

[12] A. Levi and E. Savas, "Performance evaluation of public-key cryptosystem operations in WTLS protocol," *Proc. - IEEE Symp. Comput. Commun.*, pp. 1245–1250, 2003.

[13] S. S. and K. Annapoorna Shetty, "A Review on Asymmetric Cryptography – RSA and ElGamal Algorithm," *Int. J. Innov. Res. Comput. Commun. Eng.*, vol. 2, no. Special issue 5, p. 98, 2014.

[14] T. Nie, C. Song, and X. Zhi, "Performance evaluation of DES and Blowfish algorithms," *2010 Int. Conf. Biomed. Eng. Comput. Sci. ICBECS 2010*, 2010.

[15] D. Elminaam, "Performance evaluation of symmetric encryption algorithms," *Int. J. Comput. Networks*, vol. 8, no. 12, pp. 280–286, 2008.

[16] A. S. Wander, N. Gura, H. Eberle, V. Gupta, and S. C. Shantz, "Energy Analysis of Public-Key Cryptography on Small Wireless Devices," *Third IEEE Int. Conf. Pervasive Comput. Commun.*, p. 3, 2005.

[17] S. Singh and R. Maini, "Comparison of data encryption algorithms," *Int. J. Comput. Sci. …*, vol. 2, no. 1, pp. 125–127, 2011.

[18] D. Li, Y. Wang, and H. Chen, "The research on key generation in RSA public-key cryptosystem," *Proc. - 4th Int. Conf. Comput. Inf. Sci. ICCIS 2012*, pp. 578–580, 2012.

[19] H. Mathur and P. Z. Alam, "Cryptology Algorithm," *Int. J. Elmerging Trends Technol. Comput. Sci.*, vol. 4, no. 1, pp. 4–6, 2015.

[20] D. Sukhija, "Performance Evaluation of Cryptographic Algorithms : AES and DES," vol. 3, no. 9, pp. 582–585, 2014.

[21] M. Panda, "Performance Analysis of Encryption Algorithms for Security," pp. 840–844, 2016.

[22] E. Barker, A. Roginsky, G. Locke, and P. Gallagher, "Transitions: Recommendation for Transitioning the Use of Cryptographic Algorithms and Key Lengths," *NIST Spec. Publ.*, no. January, pp. 800–131, 2011.

[23] H. O. Alanazi, B. B. Zaidan, a. a. Zaidan, H. a. Jalab, M. Shabbir, and Y. Al-Nabhani, "New Comparative Study Between DES, 3DES and AES within Nine Factors," *J. Comput.*, vol. 2, no. 3, pp. 2151–9617, 2010.

[24] A. K. Mandal and C. Parakash, "Performance Evaluation of Cryptographic Algorithms : DES and AES," 2012.

[25] A. Sterbenz and P. Lipp, "Performance of the {AES} Candidate Algorithms in {Java}," *Third {Advanced Encryption Stand. Candidate Conf. April 13--14, 2000, New York, NY, USA*, pp. 161–168, 2000.

[26] R. L. Rivest, A. Shamir, and L. Adleman "A Method for Obtaining Digital Signatures and Public- Key Cryptosystems." Communications of the ACM, vol. 26, no. 1, pp. 96–99, 1983.

[27] M. E. Student, "Algorithms for Secure Cloud," vol. 3, no. 6, pp. 1–9, 2014.

[28] G. Bernabé and N. Clarke "Study of RSA Performance in Java Cards," 2013 .

[29] P. Nalwaya, V. P. Saxena, and P. Nalwaya, "A cryptographic approach based on integrating running key in feedback mode of elgamal system," *Proc. - 2014 6th Int. Conf. Comput. Intell. Commun. Networks, CICN 2014*, pp. 719–724, 2014.

[30] X. Li, X. Shen, and H. Chen, "ElGamal digital signature algorithm of adding a random number," *J. Networks*, vol. 6, no. 5, pp. 774–782, 2011.

[31] H. Chen and J. Lin, "Digital Signature Scheme," 2009.

[32] M. S. Anoop, "Elliptic Curve Cryptography," *Infosecwriters*, pp. 1–11, 2015.

[33] R. H. Rathod and C. Dhote, "Comparison of symmetric key encryption algorithms," International Journal of Research in Information Technology (IJRIT), 2014.

[34] O. Verma, R. Agarwal, D. Dafouti, and S. Tyagi, "Peformance analysis of data encryption algorithms," in Electronics Computer Technology (ICECT), 2011 3rd International Conference on, vol. 5. IEEE, 2011, pp. 399–403.

[35] A. Jeeva, D. V. Palanisamy, and K. Kanagaram, "Comparative analysis of performance efficiency and security measures of some encryptionalgorithms," International Journal of Engineering Research and Applications (IJERA) ISSN, pp. 2248–9622, 2012.

[36] P. Arora, A. Singh, and H. Tyagi, "Evaluation and comparison of security issues on cloud computing environment," World of Computer Science and Information Technology Journal (WCSIT), vol. 2, no. 5, pp. 179–183, 2012.

[37] M. Mittal, "Performance evaluation of cryptographic algorithms," International Journal of Computer Applications, vol. 41, no. 7, pp. 1–6, 2012.

[38] R. Masram, V. Shahare, J. Abraham, and R. Moona, "Analysis and comparison of symmetric key cryptographic algorithms based on various file features," International Journal of Network Security & Its Applications, vol. 6, no. 4, 2014.

[39] S. Kansal and M. Mittal, "Performance evaluation of various symmetric encryption algorithms," in Parallel, Distributed and Grid Computing (PDGC), 2014 International Conference on. IEEE, 2014, pp. 105–109.

[40] S. Soni, H. Agrawal, and M. Sharma, "Analysis and comparison between aes and des cryptographic algorithm," International Journal of Engineering and Innovative Technology, vol. 2, no. 6, pp. 362–365, 2012.

[41] J Thakur and N. Kumar, "Des, aes and blowfish: Symmetric key cryptography algorithms simulation based performance analysis," International journal of emerging technology and advanced engineering, vol. 1, no. 2, pp. 6–12, 2011.

[42] S. M. Seth and R. Mishra, "Comparative analysis of encryption algorithms for data communication 1," IJCST, vol. 2, 2011.

[43] A. Levi and E. Savas, "Performance evaluation of public-key cryptosystem operations in wtls protocol," in Computers and Communication, 2003.(ISCC 2003). Proceedings. Eighth IEEE International Symposium on. IEEE, 2003, pp. 1245–1250.

[44] K. B. R. P.R.Vijayalakshmi, "Performance analysis of rsa and ecc in identity-based authenticated new multiparty key agreement protocol," International Conference on Computing, Communication and Applications (ICCCA), 2012.

[45] A. Aman, J. Attri, A. Devi, and P. Sharma, "Comparative analysis between des and rsa algorithms," International Journal of Advanced Research in Computer Science and Software Engineering, 2012.

Facial Expression Recognition using Hybrid Texture Features based Ensemble Classifier

M. Arfan Jaffar
College of Computer and Information Sciences,
Al Imam Mohammad Ibn Saud Islamic University (IMSIU),
Riyadh, Saudi Arabia

***Abstract*—Communication is fundamental to humans. In the literature, it has been shown through many scientific research studies that human communication ranges from 54 to 94 percent is non-verbal. Facial expressions are the most of the important part of the non-verbal communication and it is the most promising way for people to communicate their feelings and emotions to represent their intentions. Pervasive computing and ambient intelligence is required to develop human-centered systems that actively react to complex human communication happening naturally. Therefore, Facial Expression Recognition (FER) system is required that can be used for such type of problem. In this paper, FER system has been proposed by using hybrid texture features to predict the expressions of human. Existing FER system has a problem that these systems show discrepancies in different cultures and ethnicities. Proposed systems also solve this type of problem by using hybrid texture features which are invariant to scale as well as rotate. For texture features, Gabor LBP (GLBP) features have been used to classify expressions by using Random Forest Classifier. Experimentation has been performed on different facial databases that demonstrate promising results.**

Keywords*—Expression classification; ensemble; adaboost; facial; features

I. INTRODUCTION

Communication is fundamental to humans. Many scientific research studies have shown that most of the human communication (55% to 93%) is non-verbal [1], [2]. Along with the movement of the head, facial expressions are the main part of the non-verbal communication [3]. Facial expressions are one of the most compelling, of course, excellent means for people to communicate their feelings and emotions to clarify and to strain their understanding, disagreements, and intentions. The next generation computing, such as, pervasive computing and ambient intelligence, needs to develop human-centered systems that enthusiastically respond to complex human communication happening naturally [4]. Traditional HCI ignore bulk of information communicated through non-verbal ways and just caters for user's intentional input. FER plays a key role in the development of interfaces that can understand the emotional expressions and emotional responses of the user [5], [6]. The effective application areas of FER are: affective computing (autism syndrome diagnosis, analysis of depression, pain detection, stress recognition, drowsiness detection, etc.), smart media (smart home, smart meeting), video conferencing and visual surveillance, lie detection, psychiatry, emotion and paralinguistic communication, robotics, computer games (e.g. Microsoft Kinect), medicine, expression driven facial animation (e.g. facial movements in the film Avatar, Cartoons for children), security, HCI, facial image fusion for gender conversion and different age groups' fusion [7]-[9], etc. Thus, there is a strong interest for both academia and industry, and it makes the researchers to pursue for the goal to develop robust and efficient FER systems.

To develop a reliable and robust system for the FER is still a difficult and challenging problem [10], [11]. The FER is innately data driven. The challenge of generalization and robustness for various ethnicities and cultural variations can only be reasonably addressed if a representative database of such variations is available. But, there is no database constructed yet by keeping this problem in view. A good number of traditional expression recognition systems, trained over a benchmark data set and tested over the corresponding one, can offer an optimal performance. It is observed that while being in physical/practical environment such systems reflect a substantial decline in their performance due to in-appropriation or insufficiency of training datasets for facial expression patterns which could be expected in feature [12]. An expression can be demonstrated by so many combinations of facial expression patterns. Each of the images in facial expression datasets represents a single common expression i.e. disgust, but a variety of facial expression patterns easily observable. So, it is too difficult to engender such all possible patterns and to use these as training data even when the construction of an expression recognition system is based on a large number of facial images. This is nearly impossible to consider all possible future variations in facial expression patterns ahead-in-time. Thus, based on existing datasets, the highest recognition performance is never expected in practical environments. Although, some efforts have been made to construct naturalistic databases but they still have many limitations along with publically accessibility issues [13]. However, researchers in the FER community are agreed that spontaneous data gathering with real-life environments is very monotonous task. Consequently, the process for data base construction requires new methods those could expedite its creation process and represent the actual real conditions. Furthermore, the construction of robust algorithms with reliability is also required. Under such sort of situation when these databases are not available in absolution, an incremental learning along with dynamically weighted majority voting based solution is proposed. Head movements, pose variations and illumination variations are frequently encountered while dealing with spontaneous expressions. This problem is

addressed by using a feature set that is robust against in-plane image rotations and illumination variations.

II. PROPOSED METHOD

Proposed method has been divided into three different phases. First phase is to extract region of interest (ROI) and in this case is to extract the face portion only that is used for facial expression recognition. Hairs, or head or neck and other parts of bodies has no involvement in facial expression recognition therefore, face extraction is the most important step. In the second phase, the most suitable features that represent the facial expression are important. So in this phase texture and geometrical features has been extracted for the decision of expression. In the third phase, intelligent classifier has been used to decide the expression type by using the features extracted in second phase. Fig. 1 shows proposed method.

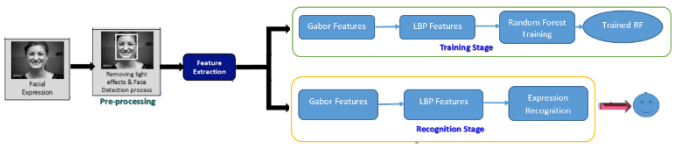

Fig. 1. Proposed method.

A. Preprocessing to extract Face part

First step in proposed method is to extract face from whole image. Most of the time during photography or image acquisition, it is not common to take only face image. Always whole body image or some time head with neck is also taken in the images. Facial expressions are only available on the faces. Therefore, it is important to extract the face part from the images. Proposed method used one of the standard method available in the literature to extract face part by using voila and Jones method. Proposed system did not require any other step as preprocessing except this face part extraction. Result of voila jones method has been shown in Fig. 2 that has been taken from MUG database.

Fig. 2. Face extraction using Viola and Jones method.

B. Feature Extraction

Feature represents the characteristics of an object to distinguish from other objects. Facial image also contains some characteristics, six based upon it can be distinguished and can be identified the expression as well. So some impressive types of features are required that can be used for all type of images as well as for all ethnicities and cultural people so there should be no discrepancies in different cultures and ethnicities. Most of the times, frontal faces are not available, some posed either left or right faces available. Similarly, it is not necessary to take picture from same distance from camera. Sometimes, it has been taken from long distances and some time from very short distances so scaling is also a factor to consider during features extraction. So such type of features is required that are rotation invariant as well as scale in variant. Texture features is special type of features extraction that can be used to handle such type of variations. So hybrid texture features have been used by extracting Gabor based features and local binary patterns (LBP) features.

C. LBP Features using Gabor Filter

Gabor filter can be used to extract texture information. Texture shows a specific pattern and facial images have some specific pattern that represents a specific expression. Like laughing has specific pattern that always remain same for all faces similarly most the time sad also has some specific pattern, smile also has a specific pattern. Therefore, texture is the most suitable for features extraction in the case of facial expression. So the characteristics of texture can be represented by a spatial frequencies and it can also be represented by their orientations. There are different types of Gabor filter that can be applied on images to extract texture features [14]-[18]. But in facial expression 2-D Gabor filter is most suitable due to nature of images that are in 2-D form. Gabor filter is a Gaussian kernel function and that can be modulated by a sinusoidal wave of precise frequencies and orientation [19]-[21]. To represent the 2-D Gabor filter, following equations can be used:

$$g(x,y) = \frac{1}{2\pi\sigma_x\sigma_y} e\left[-\frac{1}{2}\left(\frac{\bar{x}^2}{\sigma_x^2}+\frac{\bar{y}^2}{\sigma_y^2}\right)\right] e(2\pi jW\bar{x})$$

$$\bar{x} = x.\cos\theta + y.\sin\theta and \bar{y} = x.\sin\theta + y.\cos\theta$$

Where, variables x, and y are the spatial variables, σ_x and σ_y represents are the scaling parameters of the filter, and W is the central frequency of the complex wave. Gabor filter bank is a combination of different Gabor filters applied at different scales, frequencies and orientation. It is possible to generate different filter banks with different orientation and scales. In this paper, Gabor filter bank has been created by applying two frequencies, two scales, and two orientations. For this purpose, following values has been used for generation of filter bank. After calculating these filters, convolution is required to apply on the original images. So these eight filters are convolved with the original images so it returns eight new convolved images. After applying Gabor filter bank, there are magnitude values of the Gabor transform. These magnitudes represent changes very slowly with displacement. Thus there is required a process to encode these magnitude values. LBP can be used to encode these magnitude values. Basic advantage of LBP encoding over magnitude images is to improve and enhance the information in the Gabor filtered images. Applying local binary pattern on Gabor is actually a representation approach based on multi-resolution spatial histogram combining local intensity distribution with the spatial information, therefore, it is robust

to noise and local image transformations. Additionally, instead of directly using the intensity to compute the spatial histogram, multi-scale and multi-orientation Gabor filters are used for the decomposition of an image, followed by the local binary patterns (LBP) operator. LBP operator on each pixel of the image to get LBP coded image and then represented as a histogram of that code. The Gabor and LBP combination further improves the representational power of the spatial histogram greatly (Fig. 3).

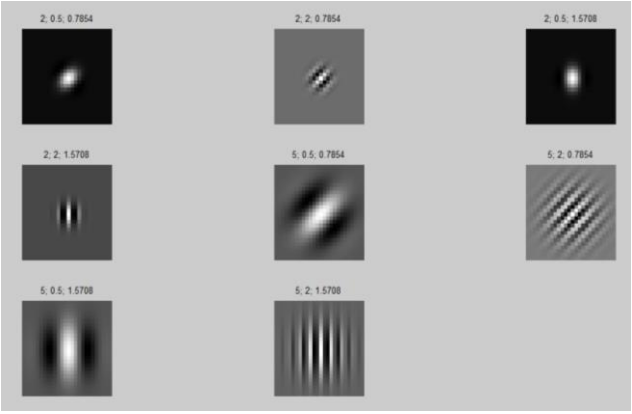

(a) Gabor Filters with 2 orientations and 4 scales

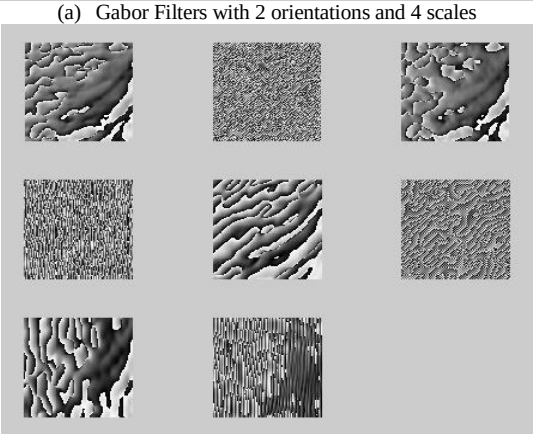

(b) Implementation of LBP on Gabor filter

Fig. 3. Gabor Filters and Implementation on LBP.

III. Classification using Adaboost

Classification is the process to differentiate into classes by using some characteristics. In the literature, many different classifiers are available that can be classified individually. Ensemble classification used different weak classifiers and combine intelligently to combine those classifiers to improve the performance of classification. One of the most important ensemble classifier is AdaBoost that is also known as adaptive boosting. This AdaBoost was proposed by [14] and it improves the simple classifier by using the iterative procedure. In this iterative procedure, during each iteration, there is a process to improve the misclassified samples. This procedure increased weights of misclassified patterns and decrease the weights of correctly classified samples during each iteration. In this way, weak classifiers given more preferences and these weak classifiers are forced to learn more by using difficult samples [14]. In this way, classification performance improves during this iterative weight adjustment procedures [27]. These adaptive weights can be used for the classification of new samples. In this way, algorithm supposed that the training set contains m samples and these samples are labelled as -1 and +1. In this way, classification of the new sample can be find out by using voting for all classifiers Mt with weights αt. Mathematically, it can be written as:

$$H(x) = sign(\sum_{t=1}^{T} \alpha_t . M_t(x))$$

Pseudocode of the AdaBoost is given in Fig. 4.

Require: I (a weak inducer), T (the number of iterations), S (training set)
Ensure: $M_t, \alpha_t; t = 1, \ldots, T$
1: $t \leftarrow 1$
2: $D_1(i) \leftarrow 1/m; i = 1, \ldots, m$
3: **repeat**
4: Build Classifier M_t using I and distribution D_t
5: $\varepsilon_t \leftarrow \sum_{i:M_t(x_i) \neq y_i} D_t(i)$
6: **if** $\varepsilon_t > 0.5$ **then**
7: $T \leftarrow t - 1$
8: exit Loop.
9: **end if**
10: $\alpha_t \leftarrow \frac{1}{2} \ln(\frac{1-\varepsilon_t}{\varepsilon_t})$
11: $D_{t+1}(i) = D_t(i) \cdot e^{-\alpha_t y_t M_t(x_i)}$
12: Normalize D_{t+1} to be a proper distribution.
13: $t++$
14: **until** $t > T$

Fig. 4. Pseudo code of Adaboost Classifier.

IV. Results and Discussion

For performance evaluation two different datasets has been used to evaluate proposed method. To validate results accuracy has been used as quantitative measure and results has been presented in the form of confusion matrix. After face detection each face image was resized to [150 x 150] before the extraction of feature vector. These datasets contain different types of expressions like some are spontaneous and some are posed so it is a mixture of different expressions. Some sample images have been shown in Fig. 5. JAFFE database which consists of 213 facial expression images of Japanese females and MUG database which consists of both posed and induced expressions are used in the experimentation. The MUG database consists of 86 subject's image sequences. Out of which 51 subjects are males and 35 subjects are females.

Results has been shown in the form confusion matrix where ANG, DIS, FEA, HAP, SAD, SUR and NEU represents the anger, disgust, fear, happy, sad, surprise and neutral expressions, respectively. In this paper, hybrid texture features have been extracted by using Gabor and LBP. Random Forest classifier has been used for prediction of expressions.

For experimentation, three different types of experiments have been conducted by using different ratios of training and testing data like 60-40 ratio mean 60 percent for training and 40 percent for testing similarly 50-50 and 40-60 percent so that there should no biasness in the results. These tests have been conducted 10 times and then results have been shown by taking average of all these differently 10 times. Results have been shown in Table 1 on JAFFE database and Table 2 shows results on MUG database.

Fig. 5. Sample Images from datasets.

TABLE. I. CONFUSION MATRIX ON JAFFE DATASET

	ANG	DIS	FEA	HAP	SAD	SUR	NEU
ANG	**96.0%**	1.0%	0.0%	0.0%	1.0%	1.0%	0.0%
DIS	5.89%	**87.66%**	2.25%	1.20%	2.0%	1.0%	0.0%
FEA	2.12%	0.0%	**91.63%**	1.0%	1.0%	4.24%	0.0%
HAP	0.0%	1.0%	0.0%	**95.38%**	1.50%	0.0%	2.22%
SAD	3.22%	0.0%	0.66%	3.22.0%	**91.0%**	2.0%	0.0%
SUR	0.0%	0.0%	0.0%	2.0%	1.33%	**91.0%**	5.67%
NEU	0.0%	1.0%	0.67%	1.0%	3.33%	0.0%	**94.0%**
						Average	**92.38%**

Table 1 shows results of proposed method on JAFFE dataset. It shows that approximately it achieves good results for all expression. As table shows that on anger accuracy is 96%, disgust 87.66%, fear 91.63%, happy 95.38%, sad 91%, surprise 91% and neutral 94%. Average results of all these has been shown that 92.38% that is good for this problem. These results has been shown on three experiments and then taken average results of all those three experiments. This shows that proposed method works well specially by extracting features of hybrid Gabor LBP features. These GLBP features plays important role in good accuracy and recognition rate.

TABLE. II. CONFUSION MATRIX ON MUG DATASET

	ANG	DIS	FEA	HAP	SAD	SUR	NEU
ANG	**95.15%**	0.64%	0.0%	0.0%	1.91%	2.30%	0.0%
DIS	2.55%	**91.08%**	0.0%	3.18%	1.0%	0.91%	1.27%
FEA	0.0%	0.0%	**92.07%**	1.0%	1.0%	2.75%	3.18%
HAP	2.4%	1.27%	0.0%	**96.09%**	0.0%	0.0%	0.60%
SAD	3.18%	0.0%	1.47%	1.91%	**92.14%**	0.0%	0.0%
SUR	0.0%	1.64%	3.46%	3.18%	1.0%	**90.72%**	0.0%
NEU	2.18%	1.0%	0.0%	1.0%	2.83%	1.99%	**91.0%**
						Average	**92.60%**

Table 2 shows results of proposed method on MUG dataset. It shows that approximately it achieves good results for all expression. As table shows that on anger accuracy is 95.15%, disgust 91.08%, fear 92.07%, happy 96.09%, sad 92.14%, surprise 90.72% and neutral 91%. Average results of all these has been shown that 92.60% that is good for this problem. These results have been shown on three experiments and then taken average results of all those three experiments. This shows that proposed method works well specially by extracting features of hybrid Gabor LBP features. These GLBP features plays an important role in good accuracy and recognition rate.

Table 3 shows comparison of different methods on both JAFFE and MUG datasets. It has been compare with existing methods like F. Wallhoff used DCT features with SVM and hidden Markova model (HMM) and it achieved 61.7% on JAFFE and 63.5 on MUG datasets. Similar other results have been shown in this table. Proposed method also shows 92.38% on JAFFE and 92.60 on MUG datasets that is the highest from all other existing methods.

TABLE. III. COMPARISON WITH EXISTING METHODS

Methodology	Recognition (%) JAFFE dataset	Recognition (%) MUG dataset
Wallhoff, F [21] (DCT+SVM-SFFS+HMM)(5-fold)	61.7	63.5
Xiao, R [22] (Multiple Manifold)	78.5	79.2
Samad, R [23] (Gabor+PCA+SVM)	81.7	82.4
Samad, R [24] (Edge-Gabor+PCA+SVM)	91.7	92.2
Zhang, L [25] (SIFT_FAP+AdaBoost)	63.6	65.4
Khan, R.A [26] (LBP-Pyramid+SVM)(10-fold)	91.36	92.13
Khan, R.A [26] (LBP-Pyramid+2NN)(10-fold)	91.28	92.20
(Proposed System) (GaborLBP) (10-fold)	**92.38**	**92.60**

V. CONCLUSION

Facial expressions are the most of the important part of the non-verbal communication and it is the most promising way for people to communicate their feelings and emotions to represent their intentions. Pervasive computing and ambient intelligence required to develop human-centered systems that actively react to complex human communication happening naturally. Therefore, Facial Expression Recognition (FER) system is required that can be used for such type of problem. In this paper, FER system has been proposed by using hybrid texture features to predict the expressions of human. Existing FER systems has a problem that these systems show discrepancies in different cultures and ethnicities. Proposed system also solves this type of problem by using hybrid texture features which are invariant to scale as well as rotation. For texture features, Gabor LBP (GLBP) features have been used to classify expressions by using AdaBoost Classifier. Experimentation has been performed on different facial

databases that demonstrate promising results. In the future, deep learning will be explored in this domain.

REFERENCES

[1] Lapakko, D., Three cheers for language: A closer examination of a widely cited study of nonverbal communication. Communication Education, 1997. 46(1): p. 63-67.

[2] Mehrabian, A., Nonverbal communication. 1977: Transaction Publishers.

[3] Bull, P., Nonverbal communication. The Psychologist, 2001. 14: p. 644-647.

[4] Jaimes, A., N. Sebe, and D. Gatica-Perez. Human-centered computing: a multimedia perspective. in Proceedings of the 14th annual ACM international conference on Multimedia. 2006. ACM.

[5] Zeng, Z., et al., A survey of affect recognition methods: Audio, visual, and spontaneous expressions. Pattern Analysis and Machine Intelligence, IEEE Transactions on, 2009. 31(1): p. 39-58.

[6] Scherer, K.R., T. Bänziger, and E. Roesch, A Blueprint for Affective Computing: A sourcebook and manual. 2010: Oxford University Press.

[7] Bettadapura, V., Face expression recognition and analysis: the state of the art. arXiv preprint arXiv:1203.6722, 2012.

[8] Ekman, P., Telling Lies: Clues to Deceit in the Marketplace, Politics, and Marriage (Revised Edition). 2009: WW Norton & Company.

[9] Poria, S., A. Mondal, and P. Mukhopadhyay, Evaluation of the Intricacies of Emotional Facial Expression of Psychiatric Patients Using Computational Models, in Understanding Facial Expressions in Communication. 2015, Springer. p. 199-226.

[10] Valstar, M.F., et al. The first facial expression recognition and analysis challenge. in Automatic Face & Gesture Recognition and Workshops (FG 2011), 2011 IEEE International Conference on. 2011.

[11] Valstar, M., et al., Fera 2015-second facial expression recognition and analysis challenge. Proc. IEEE ICFG, 2015.

[12] Chin, S. and C.-Y. Lee, Exaggeration of facial expressions from facial motion capture data. Chinese Optics Letters, 2010. 8(1): p. 29-32.

[13] Zhang, L., Towards spontaneous facial expression recognition in real-world video. 2012.

[14] Gangardiwala, A. and R. Polikar. Dynamically weighted majority voting for incremental learning and comparison of three boosting based approaches. in Neural Networks, 2005. IJCNN'05. Proceedings. 2005 IEEE International Joint Conference on. 2005.

[15] Muhlbaier, M.D., A. Topalis, and R. Polikar, Learn. NC: Combining Ensemble of Classifiers With Dynamically Weighted Consult-and-Vote for Efficient Incremental Learning of New Classes. Neural Networks, IEEE Transactions on, 2009. 20(1): p. 152-168.

[16] Kotsia, I. and I. Pitas, Facial expression recognition in image sequences using geometric deformation features and support vector machines. Image Processing, IEEE Transactions on, 2007. 16(1): p. 172-187.

[17] Pantic, M. and L.J. Rothkrantz, Expert system for automatic analysis of facial expressions. Image and Vision Computing, 2000. 18(11): p. 881-905.

[18] Braathen, B., et al. An approach to automatic recognition of spontaneous facial actions. in Automatic Face and Gesture Recognition, 2002. Proceedings. Fifth IEEE International Conference on. 2002.

[19] Berretti, S., et al., 3D facial expression recognition using SIFT descriptors of automatically detected keypoints. The Visual Computer, 2011. 27(11): p. 1021-1036.

[20] Fang, T., et al., 3D/4D facial expression analysis: an advanced annotated face model approach. Image and Vision Computing, 2012. 30(10): p. 738-749.

[21] Wallhoff, F., et al. Efficient recognition of authentic dynamic facial expressions on the feedtum database. in Multimedia and Expo, 2006 IEEE International Conference on. 2006. IEEE.

[22] Xiao, R., et al., Facial expression recognition on multiple manifolds. Pattern Recognition, 2011. 44(1): p. 107-116.

[23] Samad, R. and H. Sawada, Extraction of the minimum number of Gabor wavelet parameters for the recognition of natural facial expressions. Artificial Life and Robotics, 2011. 16(1): p. 21-31.

[24] Samad, R. and H. Sawada. Edge-based Facial Feature Extraction Using Gabor Wavelet and Convolution Filters. in MVA. 2011.

[25] Zhang, L., D. Tjondronegoro, and V. Chandran. Discovering the best feature extraction and selection algorithms for spontaneous facial expression recognition. in Multimedia and Expo (ICME), 2012 IEEE International Conference on. 2012

[26] Khan, R.A., et al., Framework for reliable, real-time facial expression recognition for low resolution images. Pattern Recognition Letters, 2013. 34(10): p. 1159-1168.

[27] K.J. Archer and R.V. Kimes. Empirical characterization of random forest variable importance measures. Computational Statistics & Data Analysis, 52(4):2249–2260, 2008.

Web Service for Incremental and Automatic Data Warehouses Fragmentation

Ettaoufik Abdelaziz
RITM Lab., ESTC, CED Engineering Sciences
ENSEM, Hassan II University
Casablanca, Morocco

Mohammed Ouzzif
RITM Lab., ESTC
Hassan II University
Casablanca, Morocco

***Abstract*—The data warehouses (DW) are proposed to collect and store heterogeneous and bulky data. They represent a collection of thematic, integrated, non-volatile and histories data. They are fed from different data sources through transactional queries and offer analytical data through decisional queries. Generally, the decisional queries execution cost on large tables is very high. Reducing this cost becomes essential to enable decision-makers to interact in a reasonable time. In this context, DW administrators use different optimization techniques such as fragmentation, indexing, materialized views, and parallelism. On the other hand, the volume of data residing in the DW is constantly evolving. This can increase the complexity of frequent queries, which can degrade the performance of DW. The administrator always has to manually design a new fragmentation scheme from the new load of frequent queries. Having an automatic fragmentation tool of DW becomes important. The approach proposed in this paper aims at an incremental horizontal fragmentation technique of the DW through a web service. This technique is based on the updating of the queries load by adding the new frequent queries and eliminating the queries which do not remain frequent. The goal is to automate the implementation of the incremental fragmentation in order to optimize the new queries load. An experimental study on a real DW is carried out and comparative tests show the satisfaction of our approach.**

***Keywords*—Data warehouse; horizontal fragmentation; incremental fragmentation; frequent queries; web service**

I. INTRODUCTION

Business intelligence is a sector in full development. It is a management term that refers to the means, tools and methods that support the process of collecting, consolidating, modeling, analyzing and restoring information [1]. To store heterogeneous and voluminous data, data warehouse (DW) has been proposed [2]-[4]. It is very promising technology and is being accepted rapidly across all domains of the industries [1]-[5]. DW is an essential component of almost every modern enterprise information system [6]. It provides a new and wide idea of the company and gives better performance of database [7]. It can be defined as a model of a concrete business system representing a set of all of the states of that system during a given interval of time [8]. It is represented by multidimensional cubes supporting a large volume of data that can reach several thousand gigabytes (terabyte). Each dimension of the cube represents an axis of analysis and each element of the cube represents the fact analyzed. The DW is modeled according to one of the three models, star schema, snowflake schema and constellation schema. In the star modeling case, the measurements are represented by a fact table and each measurement dimension represented by a dimension table [9]. The fact table contains attributes representing quantitative data named measurements and foreign keys referencing the dimension tables, whereas the dimension table contains attributes representing qualitative data that can be used as the analysis axis.

The DW are often questioned by complex decisional queries. These queries invoke a very large fact table and include joins between the fact table and several dimension tables. In order to reduce the cost of this queries kind, the DW Administrator uses different optimization techniques. Horizontal fragmentation (HF) is one of the most used techniques; it consists of partitioning a dataset of DW to several disjoint partitions. This partitioning is madding from an attributes list and selection predicates extracted from the query load noting that the number of fragmentation sub-schemes of fact table can be very large. It is given by $N=\prod_{i=1}^{g} mi$ where, mi represents the number of fragments of dimension table and g represents the number of dimension tables participating in fragmentation process [10]. To avoid the explosion of this number, the problem of HF schema selection is handled under the maximum number of fragments constraint required by the administrator. The selection of a DW HF schema has been proven to be NP-complete problem [11]-[15]; there is not an exact solution to this kind of problem. For this purpose, several works have treated the HF schema selection problem using different algorithms and different methods in order to select a schema close to the most optimal schema. Gacem, *et al*. in [14] grouped these works into four categories: 1) predicate-guided works; 2) affinity-guided works; 3) cost-guided works; and 4) classification-guided works.

During the analysis of different works, we found that several works propose the HF schema selection approaches based on a static selection carried out manually by the DW's administrator. Few studies propose a static selection using the DW's administration tools [10]-[16]. In [17] the authors propose an approach for selecting an incremental HF scheme. This approach is based on the manual adaptation of the current HF schema to the new frequent queries. But it does not take into account the queries participating in the selection process of the current schema and which do not remain frequent. In this paper, we propose an approach for selecting an automatic and incremental HF schema using a web service. It is based on

the adaptation of the current HF schema to changes appeared in the frequent queries load.

In Section 2 we give a brief overview of related work on the static selection problem of a HF schema and on the interaction between DW and web service. Then we present our approach of automatic and incremental selection of a HF schema in Section 3. Section 4 presents our experimental study on a physical DW. And we will conclude with a conclusion and perspectives.

II. Selection of Optimization Techniques

We want to offer a lightweight but powerful and online data warehouse performance optimization tool. The DW performance is considered the main concern for designers [9]. This performance is based on optimization of the queries execution time. The fragmentation, indexing and materialized views are a set of techniques used to improve the queries execution cost. The fragmentation is used in case of very huge fact and dimension tables, both of these tables can be physically partitioned. Whereas materialized views store aggregated data to yield faster access of data and reduced query response time [4]. It is a redundant structure that duplicates data in DW and occupies a supplement memory space. The space constraint forces to select an optimal subset of materialized views to attain the balance between query cost and space limits [4]. The indexing belongs also to the redundant structure; it represents data structures allowing direct and rapid access to the tuples of a voluminous relation. It optimizes queries by minimizing the amount of data to be used in calculations. Optimizing queries execution time consists in selecting and implementing one or several optimization techniques. This selection can be isolated, sequential or combined. The first case consists in implementing one optimization technique at a time. Whereas the second case consists of implementing two or more techniques sequentially and third case joint selection of two or more optimization techniques by exploiting the dependencies between them.

A. Selection of a HF schema

The selection of an HF schema consists in partitioning the DW schema into several disjoint sub-schemas in order to optimize the queries load executed on DW. The combination of these sub-schemas produces the full source data without loss or addition of information. There are three types of fragmentation [11]:

1) Horizontal fragmentation (HF) consists of partitioning a table following a selection predicate.

2) Vertical fragmentation (VH) allows partitioning a table according to a projection query.

3) Mixed fragmentation (MF) allows partitioning a table by combining HF and VF.

In data warehouses field, we talk about the primary horizontal fragmentation (PHF) and derived horizontal fragmentation (DHF). The PHF consists on partitioning the dimension tables whereas the DHF consists on partitioning the fact table according to the fragmentation schema of dimension tables.

Typically, DW's administrators use different optimization algorithms to select an optimal schema. Thus, the administrator always has to determine the frequent queries load. The selection of an optimal schema of HF can be static or incremental.

1) Static selection

The process of static selection has following parameters in entrance:

- A data warehouse schema
- A set of frequent queries
- A constraint W describes the maximum number of fragments.

The static selection of HF schema consists of selecting a set of tables to fragment and determinate the sub-partitions for each table selected in order to minimize the total queries execution cost under the maximum number of fragments. The static selection of HF schema remains less efficient since it does not adapt to the queries load evolution. In this case, the process of static selection mast be triggered and a new HF schema should be generated.

Several research studies deal with the queries optimization problem [2]-[6], [12]-[15], [18]-[22]. We will introduce below some works dealing with static selection of fragmentation schema and will also present some algorithms used in this context. We will focus on the HF of DW.

In [15], the authors treat the HF of DW using a method based on the algorithm of ant colonies. They proposed a cost based approach. This approach differs from existing approaches since it does not start with the direct application of an HF schema selecting algorithm, but it adds a new brick to map the HF selection problem. Then they solve the mapped problem by exploiting all the research conducted to solve this problem kind. On the other hand, the authors propose in [18] an XML data warehouses performance optimization technique by fragmentation and distribution on a grid. To do this, they used a method to adapt the most widely used fragmentation techniques in the relational domain to XML DW. The final fragmentation schema is generated by an original fragmentation method based on the k-means classification technique to control the number of fragments. Finally, they proposed a distribution approach of a XML data warehouse on a grid whereas in [14], the authors propose a scalable approach based on classification and election for a fragmentation supporting bulky loads. To this effect, they proposed a method for reducing the input queries load in order to minimize the selection problem complexity and the queries execution time. The proposed approach is based on two principles steps: 1) the queries classification to reduce the load size; and 2) the election to produce a new load that substitutes the initial load. This new load will be used as a main load to split the DW. From their part, the authors in [12] are interested to implementing a DW horizontal fragmentation approach. This approach represents the following characteristics: 1) cost model based approach; 2) it allows control of the generated number of fragments; and 3) DW fragmentation is performed from a maximum number of fragments set by the

administrator according to the following scenario: PHF of the dimension tables according to which the DHF from the fact table is performed. The authors have demonstrated that this scenario is most appropriate for data warehouses, as it improves selections operations on dimension tables and the joint operations between facts and dimensions whereas in [19], the authors propose a method based on a classification algorithm to reduce the number of predicates in the data warehouses before fragmentation. The proposed method encompasses four phases: 1) a preliminary phase for determinate the set of predicates selection; 2) a coding phase for coding the predicates as binary matrices; 3) a classification phase of these predicates using the k-means algorithm; and a final phase 4) to reduce the number of predicates. All works that we have cited in this section are based on static selection of HF schema. They do not evolve as the query load changes.

2) Incremental selection

The works deal with the selection of HF schema which is based on static selection. This selected schema does not remain validate when a new frequent costly query coming integrated the frequent queries load. The incremental selection of an HF schema represents a solution of static selection limits. The process of incremental selection has following parameters in entrance:

- The current HF schema.
- A set of frequent queries.
- A set of new frequent queries.
- A set of queries that does not remain frequent.
- A constraint W describes the maximum number of fragments.

The incremental selection of HF schema consists on adapting the current HF schema to new frequent queries load. This adaptation is realized by execution of splitting operation when new frequent query coming integrates the frequent queries load, or by merging when an old frequent query does not remain frequent.

Very little works have dialed with dynamic and an incremental optimization of DW performance [17]-[23]. In [17], the authors have opted for the incremental selection of a fragmentation schema. They have presented an incremental HF approach. This approach is based on splitting of partitions in order to adapt the current fragmentation schema with the newly queries load. The authors have proved that this approach is very important than the selection of new fragmentation schema because this last requires the merging of all fragments followed by several splitting operations.

B. Methods of implementation

After selection of one or several optimization techniques, an implementation of the generated schema represents the next step. This implementation can be carried out manually by DW's administrators or automatically by DW administration tools and tuning tools.

1) Manual Implementation

In order to implement the selected DW fragmentation the administrator must seizes the necessary scripts then execute them in DW. These scripts are represented by scripts of fragmentation and scripts for rewriting queries. This task is difficult and requires an expertise of the administrator and an additional time.

In the most works that we have quoted, the administrators implement manually the selected schemas. This implementation is realized in the following steps:

- Generating HF schema by using one or several optimization algorithms or using other method.
- Seizing the scripts of fragmentation.
- Seizing the scripts of rewriting queries.
- Executing the some scripts in DW.

2) Automatic implementation

The automatic implementation of selected HF schema represents an approach to reducing the manual efforts and to minimizing the implementation time.

Very little works propose an automatic fragmentation approach. In [24], the authors propose a method based on exploitation of recent statistical data access for dynamic fragmentation in DW. This fragmentation is represented by the automatic selection and automatic implementation of selected schema whereas in [17], the authors propose the ParAdmin tool of administration and tuning of DW. Among other things, this tool assists the administrator in HF task and indexing task. To do this, it implements various algorithms for selecting an HF schema and different algorithms for selecting a binary join index (BJI) configuration. Similarly, the proposed tool supports isolated selection of HF technique, and multiple selections of HF and BJI. On their part, in [16] the authors present a tool named AdminFIC. This tool allows a combined selection of a fragmentation schema and BJI based on selection attributes classification. The selection of each technique is carried out by the genetic algorithm guided by a cost model.

The two proposed tools allow implementing a new HF schema. Even if this implementation will improve the DW performance, it is very expensive from the implementation view point on an already fragmented DW. The fragmentation of this latter requires several mergers of old partitions followed by several partitioning operations.

C. Data warehouses and web services

A web service can be represented by set of features exposed on internet or on intranet, either by applications or for applications in real time and without human intervention. Previous works have treated the combine between DW and web services. In [25], the authors presented a new distribution of DW called data web house (DWH). This pattern of DW distribution is based on Web service. For their part, the authors in [26] proposed an architecture of DW oriented web service. This architecture is based on construction of mini-cubic SOLAP for mobile customer whereas in [27], the authors has presented a prototype named Data warehouse fed with Web Services (DaWeS), and they have explored how ETL using the mediation approach benefits this trade-off for enterprises with

complex data warehousing requirements. The pricipal gol of this approach is to reduce the manual effort. For their part the authors in [28], discussed the combinaison between web service and DW. This discution is based on opportunities for using DW at real-time through a web service in terms of data modeling, acquisition and analysis, analyses and designs the real-time data warehouse architecture.

In our approach, we use a web service for monitoring and improving automatically the DW performance and reduce both the manual efforts and the implementation cost.

III. PROPOSED APPROACH

In order to control and improve DW performance we present a new approach based on automatic and incremental fragmentation using a web service. However, the web service selects and implements an HF schema, and then it monitors the DW performance to avoid any degradation kind. This approach offers a remote administration and an automatic implementation of an HF schema. The web service allows the administrator to:

- View the DW state.
- View the frequent queries load.
- Be aware of new queries that integrate the load of frequent queries and queries that remain more frequent.
- Set the used optimization algorithm (the genetic algorithm in our case).
- Set the value of maximum number of fragments (W).
- Set the value of storage space reserved for redundant structures (indexes and materialized views).

We define our approach of automatic and incremental HF by taking inspiration from the works of Bouchakri, *et al*. [10] who presented a manual incremental HF approach and did not deal with the case of queries that are no longer frequents.

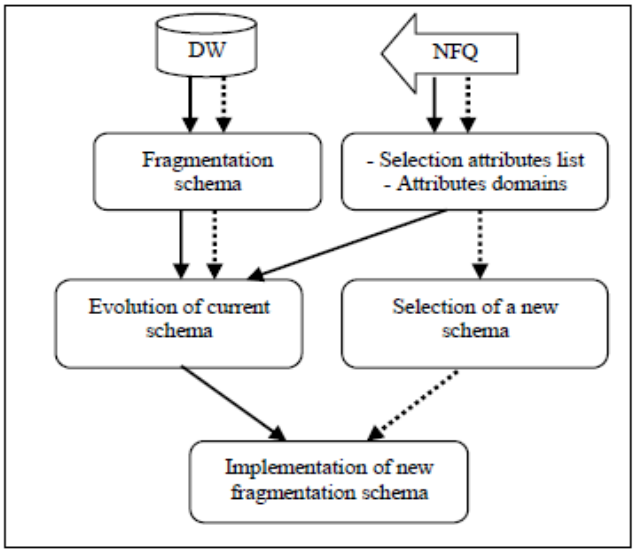

Fig. 1. General description of proposed approach.

Our approach follows the process of Fig. 1: First, the set of new queries are detected then the new frequent queries (NFQ) are determined. The NFQ determines a new fragmentation attributes or adds new domain extensions to the old attributes.

A. Queries treatment

The web service uses a module for queries management. This module is responsible for processing all requests querying the DW. This treatment takes place in the following steps:

- Establish the frequent queries list.
- Compare the new list with the frequent queries list saved.
- Determine the list of NFQ.
- Determine the queries list that is no longer frequents.
- For each NFQ, determine the fragmentation attributes list and the selection predicates list.

1) Establish the frequent queries list: In order to retrieve the queries list that is querying it, Oracle stores all queries information in a view named: V$SQLAREA. The execution of a projection on this view makes it possible to construct a most frequent queries list that interrogates the DW. Fig. 2 presents an example of projection result on the V$SQLAREA view:

SELECT sql_text, sql_id, executions, first_load_time
FROM V$SQLAREA
ORDER BY executions DESC;

The execution of this query returns the result illustrated in Fig. 2.

	SQL_TEXT	SQL_ID	EXECUTIONS	FIRST_LOAD_TIM
1	select Product_level,count(*) from ACTVA...	8abzzt38ucz0v	14	2017-01-06/12:19:12
2	select Customer_level,Avg(Unitssold) from ...	5bcd1r3tg41wr	5	2017-01-06/12:17:07
3	select Product_level,Sum(Dollarcost) from ...	g131jvzakhdjn	4	2017-01-06/12:19:01
4	select Product_level,Sum(Dollarcost) from ...	2hzx8q6uqb0r7	4	2017-01-06/12:24:38
5	select Time_level,count(*) from ACTVARS ...	1kndd08f9x5vv	4	2017-01-06/12:14:24
6	select Channel_level,count(*) from ACTVA...	4md677zxrztnj	3	2017-01-06/12:22:21

Fig. 2. Example of most frequent queries list.

The "SQL_TEXT" field represents the query body, the "SQL_ID" field represents the query identifier, the "EXECUTIONS" field represents the executions count of query, and the "FIRST_LOAD_TIME" field represents the hour of query first execution. This last allow us to build the frequent queries list from a given date.

2) Compare the new list with the frequent queries list saved: The web service uses a table dedicated to saving the information of the frequent queries load. This information will be used later to update the queries load by comparing this queries list to the current list of frequent queries. In our approach, two queries are considered identical if they use the same selection attributes with the same predicates.

Consider the following three queries Q1, Q2 and Q3:

Request Q1

```
SELECT MAX(Prix)
FROM Product P, Purchase A, Suppliers S
WHERE P.IdP = A.IdP  AND P.IdF = S.IdF
      AND P.NomProduct ='P5'
      AND  F.Ville  = 'Casablanca';
```

Request Q2

```
SELECT MAX(Prix)
FROM Product P, Purchase A, Suppliers S
WHERE P.IdP = A.IdP  AND P.IdF = S.IdF
      AND P.NomProduit ='P4'
      AND  F.Ville  = 'Rabat';
```

Request Q3

```
SELECT AVG(Prix)
FROM Product P, Purchase A, Suppliers S
WHERE P.IdP = A.IdP  AND P.IdF = S.IdF
      AND P.NomProduit='P5'
      AND  F.Ville  = 'Casablanca';
```

The two queries Q1 and Q3 use the same selection attributes with the same predicates. They are considered identical even if the two queries use two different aggregation functions. On the other hand, the query Q2 uses other selection predicates; it is different from the two queries Q1 and Q3. The Table 1 shows an example of saving data for the three queries Q1, Q2, and Q3.

TABLE. I. QUERIES DATA SAVING TABLE

Request	ibute	predicate
Q1	NomProduit	P5
Q1	Ville	Casablanca
Q2	NomProduit	P4
Q2	Ville	Rabat
Q3	NomProduit	P5
Q3	Ville	Casablanca
Q3	Ville	Casablanca

From Table 1 data, the web service generates the domain of each selection attribute. AN example of attributes domains presentation is illustrated in Table 2.

TABLE. II. ATTRIBUTES DOMAINS

Ville	NomProduit
Casablanca	P4
Rabat	P5

When the web service detects a NFQ, it updates the queries information table. This update allows adding a new selection attributes or define a new extension of the old attributes in order to trigger the optimization task.

3) Determine the list of NFQ: An NFQ is a detected request and does not belong to the current list of frequent queries. An NFQ determines either new selection attributes or domain extensions of the old attributes.

4) Determine the queries list that are no longer frequents: A query that does not remain frequent is a query belonging to the old load of frequent queries. For this purpose, this query must be present in the query table filled in by the web service since it participated in the selection process of the fragmentation current schema. On the other hand, this query will not be selected from the frequent queries determined from the V$SQLAREA view.

5) For each NFR, determine the fragmentation attributes list and the selection predicates list: Each query is processed as a character string. Any selection attribute "AtS" of any NFQ must be presented in one of the following forms: "WHERE AtS", "HAVING AtS", "AND AtS", and "OR AtS". The selection attributes and the join attributes are distinguished by the fact that the join attributes are compared to other join attributes, while the selection attributes are compared by values. These values represent the selection predicates. The selection criterion is written as follows: "AtS opr PrS", where AtS represents a selection attribute, "PrS" represents a selection predicate and "opr" designates one of the following comparison operators {=, <,>, <>, ≤, ≥,IN, NOT IN}.

Consider the following query Q4:

Request Q4

```
SELECT AVG(Prix)
FROM Product P, Purchase A, Fournisseurs F
WHERE P.IdP = A.IdP  AND P.IdF = A.IdF
      AND P.NomProduit ='P5'
      AND  (F.Ville  = 'Casablanca' OR F.Ville='Rabat');
```

From the query Q4, the module extracts the attributes list {NomProduit, Ville} and the selection predicates list {P5, Casablanca, Rabat}.

In order to consider the NFQ in the DW optimization process, two optimization methods can be defined: 1) implementation of a new fragmentation schema; and 2) the fragmentation current schema adaptation.

B. Implementation of a new fragmentation scheme (INFS)

Several research works treat the implementation of a new HF schema through the use of different optimization algorithms. The major problem encountered is that the INFS does not take into account the fragmentation previous scheme.

The INFS improves the DW performance, but it is very expensive from the implementation view point on an already fragmented DW. It requires several merge operations of the old partitions for reconstruct the no fragmented DW. Then use several partitioning operations for implement the new fragmentation schema.

C. Adaptation of current schema of fragmentation

In order to take into account the execution of a NFQ, an adaptation of the fragmentation current schema must be performed. This adaptation can be achieved by bursting of the DW fragments in the appearance case of the new attributes or the new selection predicates, and by fusions in the disappearance case of the former attributes or the fragmentation predicates. Under Oracle, is used the SPLIT PARTITION function to split a fragment into two, and the MERGE PARTITION function to combine two fragments.

The SPLIT function increases the number of fragments, whereas the MERGE function decreases the number of fragments.

The adaptation of the fragmentation schema can be implemented in four different ways:

1) Splitting fragments

Consider a DW containing a facts table named Purchase and a dimension table named Product. The Product table data before and after fragmentation is shown in Fig. 3. The Products table is partitioned according to the model shown in Fig. 4.

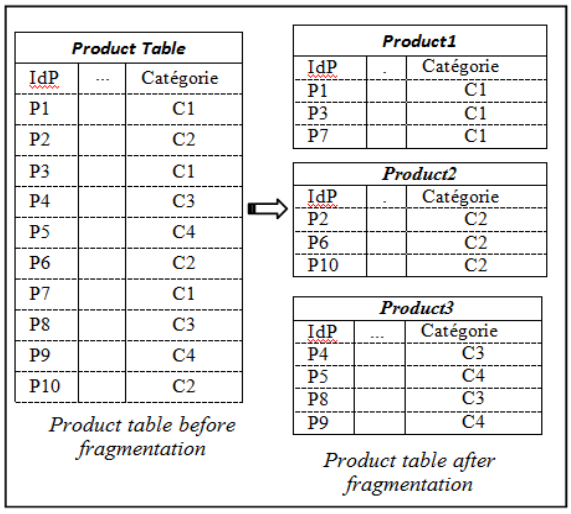

Fig. 3. Product table before and after fragmentation.

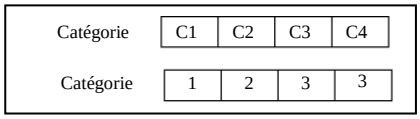

Fig. 4. Fragmentation schema of Product table.

Consider the following query Q5:

Request Q5

```
SELECT AVG(Prix)
FROM Purchase A, Product P
WHERE A.Idp = P.IdP
   AND P.Categorie = 'C3'
```

The query Q1 is an NFQ, the response time optimization of this query leads to the application of the fragmentation schema illustrated in Fig. 5. The adaptation of the current fragmentation scheme must be carried out by the application of the function SPLIT on the third fragment of the Product table (Product3) and will produce a new fragment. The result of this adaptation is presented in Fig. 6.

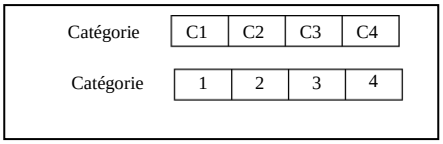

Fig. 5. New fragmentation schema.

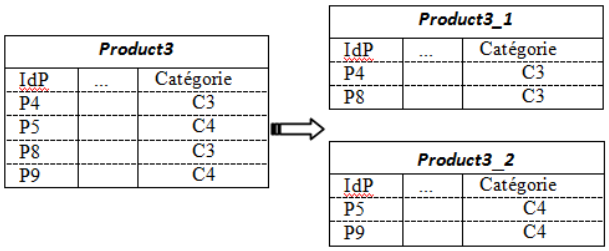

Fig. 6. Products table fragmented according to the new fragmentation scheme after application of the SPLIT function.

2) Splitting followed by fusion

If the number of fragments generated exceeds the maximum number of fragments (W), and if the web service does not detect other requests that do not remain frequent, it proceeds to classify the selection attributes according to their use frequencies by the queries. Then, it merges the sub-domains the months used until obtaining an HF schema that respects the W constraint. The following code represents the algorithm used to adapt the HF schema to the new frequent queries load.

Algorithm1: Splitting followed by fusion algorithm

```
input :
   Q : NFQ (New Frequent Query)
   FQL : Frequent Queries Load
   A: Set of fragmentation attributes
   P : Set of fragmentation predicates
   W : maximum number of fragments
output :
   Adapted fragmentation scheme
Begin
   Extract = { Predicates_Extract(Q)}
   For each predicate Pi in Extract Do
      Split = {add new fragments}
   End For
   FQL =  FQL + Q // updating the queries load
Calculate(FN) // Fragments number
   If FN>W Then
      Sort = {Scheduling of sub-domains}
      Do
         Merge = { Grouping of fragments }
      Until FN<=W
   End If
End
```

3) Merging fragments

Consider the DW shown in Fig. 3 which is fragmented according to the fragmentation schema shown in Fig. 4. Assume that the Q6 query that participated in the fragmentation process, no longer frequent, and also the other frequent queries using the same selection predicates do not exist.

Request Q6

```
SELECT AVG(Prix)
FROM Purchase A, Product P
WHERE A.Idp = P.IdP
   AND P.Categorie = 'C2'
```

The fragment dedicated to the selection predicate "C2" is no longer useful and can deteriorate the response time of other requests. The grouping of this fragment with other fragments reduces the number of fragments loaded when executing the most frequent queries, which reduces the joins number to be performed for respond to queries. For example, if a request queries the DW with the clause "WHERE P.Categorie<> 'C1' ". The response to this query requires access to two fragments (Product2 and Product3) instead of a single fragment, which consumes extra time.

The response time optimization of other requests leads to the implementation of the HF schema illustrated in Fig. 7. The adaptation of the fragmentation current schema must be carried out by applying the MERGE function to group the two fragments (Product2 and Product3). The result of this adaptation is presented in Fig. 8.

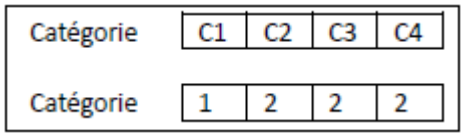

Fig. 7. New fragmentation schema for merging.

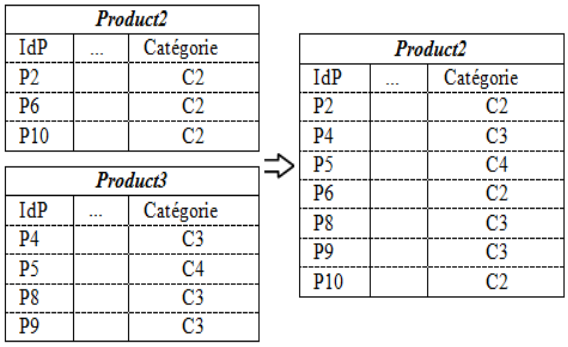

Fig. 8. Product table fragmented according the new fragmentation schema after application of MERGE function.

4) Fusion followed by splitting

Executing the fragment merging operation reduces the number of fragments. In this case, the web service triggers the optimization process of the other frequent queries. This process begins with the scheduling of the sub-domains which are constituted by several selection predicates. This classification is carried out following the use of frequency of the sub-domains by the queries. Then, it proceeds to the bursting the most used sub-domains until obtaining a new fragmentation schema. This new schema increases the number of fragments that does not exceed the W value.

The following code illustrates the algorithm used to adapt the HF schema to the new load of frequent queries:

Algorithm 2 : Fusion followed by splitting algorithm

```
Input :
   NFQ :  Non Frequent Query
   FQL : Frequent Queries Load
   A:  Set of fragmentation attributes
   P : Set of fragmentation predicates
W : maximum number of fragments
Output :
   Adapted fragmentation scheme
Begin
   Q = FQL – NFQ
Extract = { Predicates_ Extract(NFQ)}
   For  each predicate Pi in Extract  DO
      For each  Qi in Q DO
         If Qi does not use Pi Then
          Merge = { Grouping fragments of predicate Pi}
         End If
      End For
   End For
   FQL =  Q  // updating the frequent queries load
Calculate (FN) //fragments number
   If FN<W Then
  Sort = { Scheduling of sub-domains}
      DO
         Split = {add new fragments}
      Until  FN=W
   End If
End
```

IV. TESTS AND RESULTS

We performed tests on APB1 benchmark generated under Oracle 11g. We use an already fragmented DW (static fragmentation) according to an HF schema generated from load of ten queries presented in Table 3.

In first step, we fixed the maximum number of fragments (W) to 10 then we started by executing new queries set illustrated in Table 4. First, we executed query Q11 several times. The web service detects the presence of an NFQ and triggers the selecting process of optimization. We have successively executed the new queries set presented in Table 4. Then we retrieved the execution cost of each request in different cases: static fragmentation, implementation of a new HF schema and adaptation of the current schema. In second step we varied the maximum number of fragments (W) and we executed simultaneously a set of new queries illustrate in Table 4 then we retrieved the execution cost in the three cases.

To calculate the queries execution cost, we used the method EXPLAIN PLAN offered by the Oracle optimizer.

TABLE. III. FREQUENT QUERIES LOAD LIST

Request	Attribute
Q1	class_level
Q2	family_level
Q3	line_level 3
Q4	division_level
Q5	year_LEVEL
Q6	class_LEVEL, retailer_level
Q7	year_LEVEL, class_level
Q8	month_level, retailer_level
Q9	year_level, retailer_level, line_level
Q10	month_level, division_level, all_level

TABLE. IV. NEW FREQUENT QUERIES LIST

Request	Attribute
Q11	group_level
Q12	year_level, month_level, class_level, group_level
Q13	month_level, group_level, retailer_level, all_level
Q14	month_level, division_level
Q15	customer_level

A. Queries execution cost

1) Variation of Query

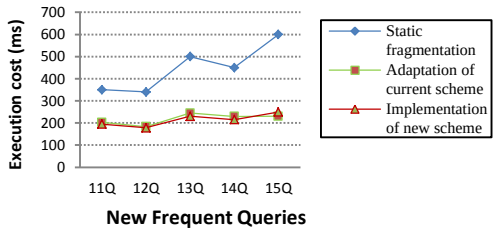

Fig. 9. Execution cost of new queries.

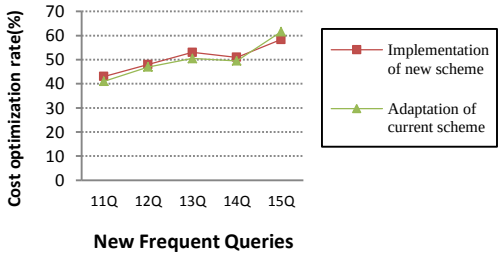

Fig. 10. Reduction rate of new queries execution cost.

Fig. 9 shows the execution time of new frequent queries in three cases: 1) static fragmentation; 2) implementation of new fragmentation schema; and 3) adaptation of the current fragmentation schema whereas Fig. 10 shows the reduction rate of the execution cost of new frequent queries.

We notice that the adaptation of the current schema and the INFS have the best cost compared to the static fragmentation. This is caused by the fact that the INFS generates a new optimal schema optimizing the total execution cost of the queries load. Thus the adaptation of the current schema generates, generally, a fragment for each frequent request. This results show the incremental fragmentation impact on DW performance.

2) Variation of W

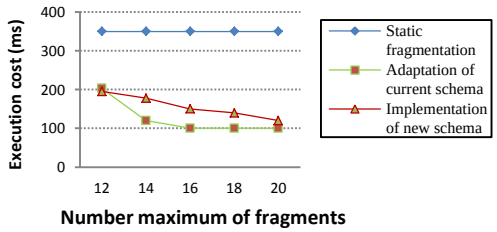

Fig. 11. Execution cost by varying W.

In order to see the influence of the W constraint on the optimization in the incremental fragmentation case, we have varied it and for each value we have executed both the list of new frequent queries illustrated in Table 4. We have noted the execution cost. The results illustrated in Fig. 11 show that the best cost is obtained by the approach of adapting the current fragmentation scheme. This is demonstrated by the fact that when executing a list of new frequent queries, the INFS approach generates a fragmentation scheme optimizing the cost of the whole load of frequent queries whereas the approach of current schema adaptation optimizes the total cost of the list of frequent new queries by generating new fragments under the maximum number of fragments constraint.

B. Incremental fragmentation implementation time

In second test, we recovered the incremental fragmentation implementation time through the web service. We compared the implementation time of a new HF scheme with the adaptation time of the current schema. For this purpose we have executed the new queries successively several times. In the other hand, we recovered the incremental fragmentation implementation time through the web service for different values of W. We compared the implementation time of a new HF schema with the adaptation time of the current schema. For this purpose we have executed the simultaneously a set of new frequent queries several times for each value of W.

The results obtained are summarized in the following illustrations:

1) Variation of Query

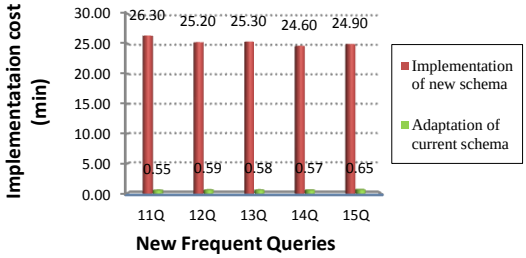

Fig. 12. Implementation cost of an incremental HF schema in the case of new frequent queries.

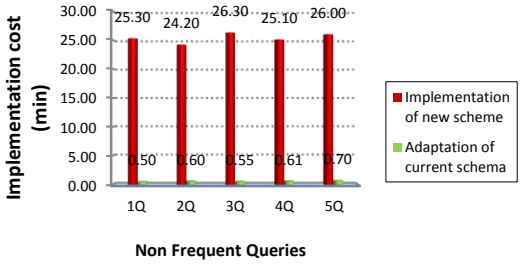

Fig. 13. Implementation cost of incremental HF schema in the case of queries that are no longer frequent.

Fig. 12 shows the implementation cost of incremental HF schema for different new queries detected by the web service. Whereas Fig. 13 illustrates the implementation time of the HF schema in the case of queries which participated in the first fragmentation process and which do not remain frequent. The two figures illustrate the implementation time of a new

schema and the adaptation time of the current schema. The results obtained show that the implementation total cost of a new incremental HF schema is very expensive compared to the adaptation total cost of the current HF schema. This is proved by the fact that the INFS requires several merge operations of the old partitions for reconstruct the no fragmented DW. Then trigger an optimization algorithm or other method for generating a new optimal schema. And finally, execute several partitioning operations for implementing the new fragmentation schema in DW. The INFS cannot benefit from the old fragmentation schema. But, the adaptation of the current schema requires just the execution of some operations of partitioning, fusion or both. These operations are not very expensive.

2) Variation of W

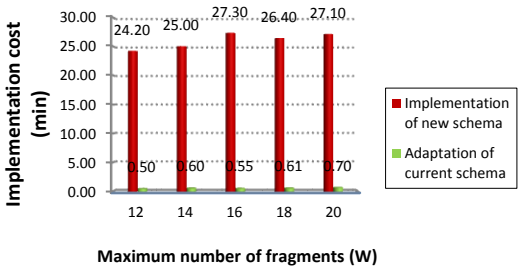

Fig. 14. Implementation cost of incremental HF schema for different values of W.

3) Variation of Number of New Frequent Queries

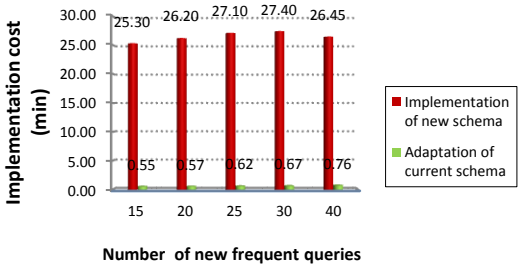

Fig. 15. Implementation cost of incremental HF schema for different number of new frequent queries.

Fig. 14 shows the implementation cost of incremental HF schema by the web service for different values of W, and Fig. 15 shows the implementation cost of incremental HF schema by the web service for different number of new frequent queries.

It is noted that the implementation cost of adaptation of the current schema does not vary much when we change the maximum number of fragments or the number of new frequent queries executed simultaneously. But the cost of implementing a new schema is very high compared to the cost of adapting the current schema. The cost of implementing a new schema can be written as follows: $CT_{imp} = C_{sel} + C_{imp}$.

4) C_{sel} : Represents the cost of selecting the new schema, it depends on the optimization algorithm and/or any other method used to select a schema close to the optimal schema. This selection generally requires a high cost compared to the implementation cost.

5) C_{imp}: Represents the implementation cost of the selected schema, it is the time needed to run the partitioning and/or merge scripts in the adaptation of the current schema case, and the time needed to execute the partitioning script in the INFS case.

In the adaptation approach, the C_{sel} is null because in this case the current schema is always validate. Thus, the web service product other fragments optimizing the new frequents queries. But in the INFS approach, the web service does not takes in the account the current schema, it proceeds by merging all fragments then splitting them until generating the schema already selected.

V. CONCLUSION

The goal of this work is to improve the DW performance. However, the proposed approach is based on incremental selection and automatic implementation of HF schema using a web service. Two incremental selection scenarios were proposed: 1) selection of a new HF schema; and 2) adaptation of the current schema to evolution of the frequent queries load. Both scenarios optimize queries execution cost. The implementation of the selected schema is completed automatically by the web service. The implementation cost of the selected schema according to second scenario is very low, which favors this scenario. Our approach differs from existing approaches since it makes it possible to monitor and improve automatically the DW performance. In the other works, the DW's administrators, generally, have to implement fragmentation manually, which requires a lot of time and an expertise. Very few works offer locally installed administration tools. On the other hand, although our approach allows improving the DW performance in reasonable time, it increases the availability of the latter since it will be manageable through the web.

We plan to study the possibility to automate the optimization of a varied queries load by combining fragmentation with other optimization techniques.

REFERENCES

[1] P. Muley, Exploring the Scope of Data Warehouse and Business Intelligence Applications in Indian Higher Education Sector, IOSR Journal of Business and Management (IOSR-JBM) e-ISSN: 2278-487X, p-ISSN: 2319-7668. Volume 18, Issue 7 .Ver. I, PP 59-63, July 2016.

[2] M. K. Sohrabi*, V. Ghods, *Materialized View Selection for a Data Warehouse Using Frequent Itemset Mining*, Journal of Computers, Volume 11, Number 2, pp 140-148, March 2016.

[3] R. Nath, K. Hose, T. Pedersen, O Romero, A Programmable Semantic Extract-Transform-Load Framework for Semantic Data Warehouses, Journal of Information Systems March 3, 2017

[4] A Gosaina, Heena, *Materialized Cube Selection using Particle Swarm Optimization algorithm*, 7th International Conference on Communication, Computing and Virtualization 2016. s. Published by Elsevier.

[5] M. Shahid, U. Sheikh, B. Raza, M. Shah, A. Kamran, A. Anjum, Q. Javaid, *Application of Data Warehouse in Real Life: State-ofthe-art Survey from User Preferences' Perspective*, (IJACSA) International Journal of Advanced Computer Science and Applications, Vol. 7, No. 4, pp. 415-426, 2016

[6] BiriArun, T.V. V. Kumar, Materialized View Selection using Artificial Bee Colony Optimization, International Journal of Intelligent Information Technologies (IJIIT), vol. 13, issue 1, pp. 26-49, 2017

[7] A. Mateen, L. Chaudhary, *Reduce The Wastage of Data During Movement in Data Warehouse*, International Journal of Computer Applications (0975 – 8887) Volume 152 – No.8, pp. 20-24, October 2016

[8] I. Bojicic, Z. Marjanovic, *Domain/Mapping Model: A Novel Data Warehouse Data Model*, International Journal of Computers, Communications & Control (IJCCC) ·pp. 166-182, February 2017

[9] E. Sidi, M. El Merouani, E. A. Abdelouarit, *Star Schema Advantages on Data Warehouse: Using Bitmap Index and Partitioned Fact Tables*, International Journal of Computer Applications (0975 – 8887), Volume 134 – No.13, January 2016

[10] K. BOUKHALFA, L. BELLATRECHE, P. RICHARD, *Fragmentation Primaire et Dérivée: Étude de Complexité, Algorithmes de Sélection et Validation sous ORACLE10g*, LISI(Rapport de Recherche, N° 01 - 2008), Mars, 2008.

[11] L. BELLATRECHE, Techniques d'optimisation des requêtes dans les data warehouses, *Sixth International Symposium on Programming and Systems* (PS 2003), 2003, pp. 81-98.

[12] K. BOUKHALFA, L. BELLATRECHE, S. CAFFIAU, De l'optimisation de requêtes aux outils d'administration des entrepôts de données, RSTI - ISI (Ingénierie des Systèmes d'Information) (ISI 2009), vol. 13, n. 6/2008 , 2009.

[13] P. Kling, M. T.Ozsu, and D K. audjee, (2010). Distributed xml query processing: Fragmentation, localization and pruning. Technical report, University of Waterloo.

[14] A. Gacem, K. Boukhalfa, Nouvelle Approche Scalable Dédiée au Charges Volumineuses pour la fragmentation des Entrepôts de Données, *Proceedings of Maghreb Conference on Advances in Decision-making Systems* (ASD2013, pp. 61-73, 2013)

[15] M. BARR, L. BELLATRECHE, Approche dirigée par les fourmis pour la fragmentation horizontale dans les entrepôts de données relationnels, Revue : Nature & Technologie . n° 06, pp. 16- 24, Janvier 2012.

[16] R. BOUCHAKRI, *Une approche dirigée par la classification des attributs pour fragmenter et indexer des entrepôts de données*, Ph.D. Thesis, Ecole nationale Supérieure d'Informatique (ESI), Oued Semar, Alger, 2009.

[17] R. BOUCHAKRI, L. BELLATRECHE, Z. FAGET, Algebra-Based Approach for Incremental Data Warehouse Partitioning, *Proceedings of the 25th International Conference on Database and Expert Systems Applications* (DEXA 2014, pp. 441-448, 2014).

[18] Mahboubi H., *Optimisation de la performance des entrepôts de données XML par fragmentation et répartition*, Ph.D. Thesis, EDIIS, Universite Lumière Lyon 2, 2009.

[19] M. GHORBEL, K. TEKAYA, A. ABDELLATIF, Reducing the number of predicates for approaches to distribution of data warehouses, Revue des sciences et technologies de l'information, Volume 21 n°1 - pp.81-102, 2016

[20] S. Aissi, M. Gouider, T. Sboui, L. Ben Said, Enhancing spatial data arehouse exploitation: A SOLAP recommendation approach, *Proceeding of 17th IEEE/ACIS International Conference on Software Engineering, Artificial Intelligence, Networking and Parallel/Distributed Computing (SNPD)*, 30 May-1 June 2016, Shanghai, China

[21] S. Gawali1, M. Vaidya, Selection and Maintenance of Materialized View Using Genetic Algorithm, International Journal Of Engineering And Computer Science ISSN:2319-7242 Volume 5 Issue 8 pp. 17715-17717, 2016

[22] V. Bhatnagar, N. Dahiya, M. Singh, Efficient Materialized View Selection for Multi-Dimensional Data Cube Models, International Journal of Information Retrieval Research, Volume 6 Issue 3, pp.52-74 July 2016

[23] M. Hamad, Y. Turky, *A Dynamic Warehouse Design Based on Simulated Annealing Algorithm*, Journal of Advanced Computer Science and Technology Research, Vol.6 No.1, pp1-8, March 2016

[24] H. Derrar, M. Ahmed-Nacer, O. Boussaid, *Exploiting data access for dynamic fragmentation in data warehouse*, International Journal of Intelligent Information and Database Systems 7(1):34 - 52, January 2013

[25] Z. Luo, Z. Kai-song, J Qiong, X. Hong-xia 1,Z. Kai-peng, Application of the Web Service Technology on the Data Warehouse System, Journal of Wuhan University of Technology, 2004

[26] E. Dubé, T. Badard, Y. Bédard, *A web service oriented architecture for the delivery of SOLAP mini-cubes to mobile clients*, International Journal of Geomatics and Spatial Analysis, Volume 19/2, pp.211-230, 2009

[27] J. Samuel, Towards a Data Warehouse fed with Web Services, Proceeding of *European Semantic Web Conference ESWC: The Semantic Web*: *Trends and Challenges* pp 874-884, 2014

[28] L. Jun, H. ChaoJu, Y. HeJin, Application of Web services on the real-time data warehouse technology, *Proceeding of International Conference on Advances in Energy Engineering* (ICAEE), 19-20 June 2010.

Cost Optimization of Replicas in Tree Network of Data Grid with QoS and Bandwidth Constraints

Alireza Chamkoori
Department of Computer Engineering
Khormoj Branch
Islamic Azad University, Iran

Farnoosh Heidari
Department of Electrical Engineering
Bushehr Branch
Islamic Azad University, Bushehr, Iran

Naser Parhizgar
Department of Electrical Engineering
Shiraz Branch
Islamic Azad University, Shiraz, Iran

***Abstract*—Data Grid provides resources for data-intensive scientific applications that need to access a huge amount of data around the world. Since data grid is built on a wide-area network, its latency prohibits efficient access to data. This latency can be decreased by data replication in the vicinity of users who request data. Data replication can also improve data availability and decreases network bandwidth usage. It can be influenced by two imperative constraints: Quality of Service (QoS) that is locally owned by a user and bandwidth constraint that globally affects on link that might be shared by multiple users. Guaranteeing both constraints and also minimizing replication cost consisting communication and storage costs is a challenging task. To address this problem, the authors propose to use a dynamic algorithm called Optimal Placement of Replicas to minimize replication cost and coupled with meeting both mentioned constraints. It is also designed as heuristic algorithms that are competitive with optimal algorithm in performance metrics such as replication cost, network bandwidth usage and data availability. Extensive simulations show that the Optimal algorithm saves 10% cost compared to heuristic algorithms and provides local responsiveness for half of the user requests.**

Keywords*—Hierarchical data grid; replication cost; replica optimal placement; communication cost; storage cost; cost minimization; QoS and bandwidth constraints

I. Introduction

Data-intensive scientific applications are increasingly growing because of recent development in distributed systems (such as peer to peer systems, grid, cloud computing, etc.). These applications need extreme-scale repositories and computing resources. For example, astronomy projects-Virtual Observations[1] and protein simulation-Bio-Grid[2] require analysing a huge amount of data. The data generated from such an experiment, with a network of sensors or an instrument is stored at a master storage site and is moved to other sites all over the world. *Data grid* is a suitable distributed system to provide computational facilities and repositories in large scale for users. It offers a scalable infrastructure for management of massive storage resources and data that are distributed across network.

Each data grid has its own model that is the manner of resource organization such as data resources which can be either single or distributed, data size, and sharing model of data. Data grids usually follow four common models: *monadic*, *hierarchical*, *federation*, and *hybrid* [1]. In this paper, it has been focused on hierarchical model that consists of several levels (tiers). In the first level, data is generated and stored. Then, the data is distributed to other levels if it is requested. This model is usually found in current data grids [1]. One example for this model is LCG (Large Hadron Collidor Grid) project in which scientists likely need to access a huge amount of raw data that can reach several petabytes. Also, most of these data are read only; because they are the input data to the application for analysis, classification, and other purposes.

Data grid, building on wide-area network and resulting in high latency as its consequence, utilizes efficient techniques to deliver data to users with guaranteed QoS that has either local or global influence on user satisfaction. The local influence is due to QoS that is requested by user and the global influence is because of constraint on the link bandwidth may be shared by multiple users. One of the technique to guarantee QoS is data replication in multiple locations which allows user to access data from a server in her vicinity.

Clearly, in one hand, data replication not only reduces data access cost and provides the guaranteed QoS, but also promotes data availability in many applications. On the other hand, replication cost borne by user can increase if a suitable replication strategy is not taken. Thus, replication cost and access cost are two potentially conflicting objectives that should be addressed whilst the constraints in the system are satisfied.

This paper discusses the aim of addressing the above problem called *Replica Placement Optimization* with QoS and bandwidth constraints. Here some assumptions in this problem, which are compatible with the characteristics of real data grid are also discussed. It is assumed that all objects are initially stored in the root of tree and access to the objects is based on the *Closest* policy in which the user requests are served only by the closest replica in the path from request node up to the root [2]. The objective of this problem is to minimize communication and storage costs whilst QoS constraint (number of hops) and link bandwidth limitation are respected.

Several works investigate replica placement on parallel and distributed systems with regular structures such as tree, hyper cube, ring, etc. [3]. But, neither this deals with QoS guarantee nor with bandwidth constraints. Moreover, the objective function of these work is not similar to that of us. Cidon et al. [4] studied an optimal placement of replicas and minimized communication and storage costs without any constraints.

[1] www.birncommunity.org
[2] www.biogrid.jp

Karlsson et al. [5] have taken into account bandwidth limitations and proposed several heuristic algorithms to tackle NP-complete problem. But, they do not consider QoS constraint. Wu et al. [6] investigated a problem in which the objective function is to minimize the number of replicas with QoS in terms of a range limit (i.e., hops number). Rehn-Sonigo [7] proposed a major extension [6], with the same objective function but with an additional constraint, i.e., link bandwidth. Our work is different with both of these previous works in terms of the objective function.

The main objective of our algorithms is to minimize replication cost, which includes communication and storage costs whilst the desired QoS of user in terms of distance between the client (i.e., user) and server is guaranteed. It is also considered bandwidth constraint as a global QoS that belongs to the network and can influence on all clients in the data grid system. Further, proposed several heuristic algorithms and compared with the optimal one in three aspects that are important in data grid: *replication cost*, *network bandwidth usage*, and *data availability*.

The rest of the paper organized as: Section II presents related work in replica placement in data grid environments. The basic preliminaries are provided and also formulated replica placement optimization problem in Section III. Section IV dedicated to proposed algorithms. The experimental results are given in Section V. Finally, Section VI concludes the paper.

II. Related Work

Replica placement problem has been well investigated in literature. This problem can be categorized based on network structure: *general graph* and *tree*. The problem in former category is known to be a NP-hard K-center problem and has been dealt in two steps discussed as: In first step, with considering the desired objective function, a spanning tree is extracted. In the second step, the replicas are placed in the extracted tree to optimize the objective function. In this regard, many works considered QoS as a constraint whilst considering replication cost as an objective function [8], [9]. Our work does not fall into this line of research.

In the latter structure, this problem either can be reduced to NP-problem or can be optimally solved, which depends on the defined objective function and constraints in these problems. Researchers have exhaustively studied this problem mainly for two categories as follows:

Replica Placement without Constraint: Early work on this category has done by Wolfson and Milo [10], where the multicast write policy is employed to optimally allocate k replicas in different topology. We also propsed algorithm to place k replicas in data grid tree network [11], [12]. Kalpakis et al. [13] discussed the replica placement problem when a general objective function takes into account read, write, and storage costs and uses a minimum spanning tree to propagate updates among the replicas. Cidon et al. [4] studied an instance of the problem with the objective function aimed at finding the optimal number of replicas, where the communication and storage costs are considered. Also a similar instance was studied of the problem and an algorithm with the lower time complexity in the context of data grid systems [14].

Replica Placement with Constraints: The constraints in replica placement can be on server capacity, link bandwidth, and QoS [2]. Tang et al. [15] have been the first author to consider actual QoS constraint in replica placement problem. They studied this problem in graph and tree networks. Several works considered this constraint in data grid tree network where the objective function is either replication cost minimization or load balance on servers [6], [16]. Also, Shorfuzzaman et al. [17] investigated the placement of k replicas with QoS constraint in data grid tree network such that the replication cost, which is a summation of write, read, and storage costs is minimized. Rehn-Sonigo [7] proposed a theoretical algorithm to balance load on servers such that QoS and link bandwidth constraints are satisfied.

Most work listed above do not provide both QoS and bandwidth constraints simultaneously. A dynamic algorithm is proposed to optimize replication cost including communication and storage costs such that QoS and bandwidth constraints are guaranteed. Although [7] and our work are similar in constraints (QoS and link bandwidth), our objective function is to minimize communication and storage costs whilst the objective function of [7] is aimed at balancing load on servers. Moreover, three heuristic algorithms is proposed to replicate data based on either read cost or storage cost.

III. Premilinaries and Problem Formulation

The system model is represented as a rooted undirected tree $T_r = (V, E)$, where $V(|V| = n)$ is the set of nodes. A node is a server if it has a replica of the object else it is a client. E is the set of edges, which represents links in tree. r is the root of tree and all objects i $m(1 \leq i \leq m)$ are initially stored in it. The size of each object i is denoted by O_i. Let $r_i(v)$ and $S(v)$ be two functions representing the number of read requests issued by node v for object i and storage cost of placing a replica of object at node v, respectively. Also, let $d(u, v)$ be a non-negative cost between nodes u and v and assigned to link $(u, v) \in E$. It can be interpreted as delay, link cost or number of hops. Also each link $(u, v) \in E$ owns a bandwidth limit $bw(u, v)$ that cannot be exceeded. Let $t(v)$ the sub-tree rooted by node v, and $t'(v) = t(v) - v$, i.e. the forest of trees rooted at v's children.

It is defined in two constraints: QoS and link bandwidth. The required QoS is termed by $q(v)$ that should be guaranteed. With no less of generality, it can be considered the distance (i.e., the number of communication hops) between a client and server as QoS. Thus,

$$\forall c \in clients, \forall v \in servers, d(c, v) \leq q(c) \qquad (1)$$

where distance $d(c, v)$ is the number of hops between client c and server v. According to (1) if object i is retrieved by client c from server v within distance $d(c, v) \leq q(c)$, then QoS requirement is met; otherwise it is violated.

Other constraint in our system model is bandwidth limitation and it is defined as follows. Assume that the node v_l in distance of l links is an ancestor of node c and also $S_r(t(c), v_l)$ denotes the total requests issued from $t(c)$ to node v_l for the desired object. Based on this constraint, $S_r(t(c), v_l)$ should not

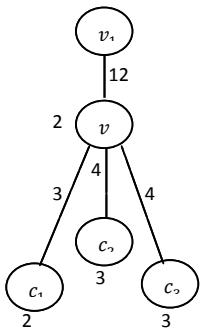

Fig. 1. An example of bandwidth constraint.

exceed the bandwidth of all links between node c and v_l. This translates into:

$$\forall c \in clients, \forall v \in servers, S_r(t(c), v_l) \leq bw(c, v_l) \quad (2)$$

where $l \in path[c, v_l]$.

An example of bandwidth constraint is illustrated in Fig. 1. Consider tree $t(v_1)$ that holds the desired object in its root (i.e, v_1). The number attached to node represents the requests per time unit of that node for the desired object. For example, node c_1 owns 2 requests for object in node v_1. Label on the link shows its bandwidth. For example, link bandwidth between v and v_1 is 12. Suppose sub-tree rooted in v making 10 (2+3+3+2) requests must be passed through the link between v and v_1 to reach object at v_1. In this case, there is not bandwidth restriction because $S_r(t(v), v_1) = 10 \leq bw(v, v_1) = 12$. Another example: Let us increase the requests of node v from 2 to 6. In this case, since $S_r(t(v), v_1)$ exceed from 10 to 14, the link bandwidth constraint is violated because $S_r(t(v), v_1) = 14 > bw(v, v_1) = 12$. A simple solution to remove this limitation is to retrieve a replica of object from v_1 and store it in node v.

In the following, is calculated the total cost and defined the replica placement optimization problem. Consider a resident set RP_i hosting replicas of object i for tree T_r. To minimize the total cost of this set, $Cost(RP_i, T)$, includes two types of costs: *communication* and *storage* cost.

A read cost of RP_i is the cost of serving all read requests issued from $v \in V$ and defined as

$$\sum_{v \in V} r_i(v) \times O_i \times d(v, v_l) \quad (3)$$

where $v_l \in RP_i$ is the closest ancestor of node v that contains object i and $d(v, v_l)$ equals the hops number on l links.

The storage cost of RP_i is the cost of hosting object i at all nodes in RP_i and formalized as

$$\sum_{v \in RP_i} O_i \times S(v) \quad (4)$$

Thus, the total cost for the set RP_i for tree T is

$$Cost(RP_i, T) = \sum_{v \in V} r_i(v) \times O_i \times d(v, v_l) + \sum_{v \in RP_i} O_i \times S(v) \quad (5)$$

Replica Placement Optimization Problem: Given a tree network $T_r(V, E)$, with m objects, find a subset $RP_i \subseteq V$ for all objects i ($1 \leq i \leq m$) such that the total cost $Cost(RP_i, T)$ given in (5) is minimized and constraints in (1) and (2) are satisfied.

IV. Proposed Algorithms

In this section, an algorithm called Replica Placement Optimization is suggested that works in two phases in order to solve the optimization problem described in the previous section. In the first phase, the cost parameter is computed for each node and then determined whether it is potential to host a replica in itself or not. The computed cost parameter will serve phase 2 to determine the optimal placement of replicas. In the following, two phases are presented in details.

A. Phase 1: Bottom-Up Cost calculation

Let $C^i_{min}(t(v), v_l)$ denote the minimum cost (calculated based on (5)) of the sub-tree $t(v)$ with the assumption that the issued requests from $t(v)$ are processed by node v_l that is the lowest ancestor of node v. Also assume that the *candidate nodes set* associated to $C^i_{min}(t(v), v_l)$ is termed by $C^i_{set}(t(v), v_l)$. This set contains potential nodes that can host a replica of object i. By traversing the tree T_r in breadth first order from bottom to top, $C^i_{min}(.)$ and $C^i_{set}(.)$ for two distinguished cases are calculated as follows:

Case (a): As shown in Fig. 2, assume that node v is a leaf. It has two ways to access object i in v_l, which is its lowest ancestor. 1) It reads object i for one time and locally stores it. Thus, node v incurs the read cost from v_l through link (v, v_l) for one time in addition to the storage cost of object i. This cost is called *storing cost* and is computed as $C^i_{sl}(v, v_l) = O_i \times d(v, v_l) + O_i \times S(v)$ and node v is added to $C^i_{set}(v, v_l)$. Since a request from v to v_l is passed through links $l \in path[v, v_l]$ to read the desired object for one time, the value $S_r(v, v_l)$ is increased by one. This modification helps us to control link bandwidth constraint. 2) It reads the object whenever it needs, and incurs read cost for $r_{v,i}$ times. This cost is called *reading cost* and is computed as $C^i_{rl} = r_{v,i} \times O_i \times d(v, v_l)$. So, node v is not added to $C^i_{set}(v, v_l)$ and $S_r(v, v_l)$ is increased by $r_{v,i}$ because all requests $r_{v,i}$ passed through links $l \in path[v, v_l]$. By considering the defined QoS for each node and the link bandwidth, $C^i_{min}(.)$ for each leaf is calculated as follows.

If the distance between v and its ancestor v_l is more than $q(v)$ (i.e., $d(v, v_l) > q(v)$) or the issued requests $r_{v,i}$ exceeds than bandwidth of any links $l \in path[v, v_l]$, then the object i is retrieved from node v_l and replicated at node v (in fact, node v has only one way to access object in v_l). Thus, $C^i_{min}(v, v_l) = C^i_{sl}(v, v_l)$ and the remaining parameters, $C^i_{set}(v, v_l)$ and $S_r(v, v_l)$, corresponds to the parameters that are defined in the *storing cost*. Otherwise, *reading cost* and *storing cost* are calculated for node v and then the minimum cost is considered. In fact, in this case, node v has two ways to access its desired object. Thus, $C^i_{min}(v, v_l) = min(C^i_{sl}(v, v_l), C^i_{rl}(v, v_l))$, and based on the minimum cost, other parameters, $C^i_{set}(v, v_l)$ and $S_r(v, v_l)$, are calculated, respectively.

Case(b): As illustrated in Fig. 3, node v is a non-leaf. Similar to leaf v, it is with two alternatives to access object i in

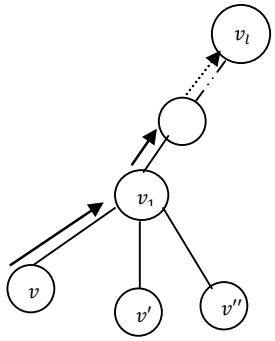

Fig. 2. The rational of dynamic algorithm for leaf nodes of tree.

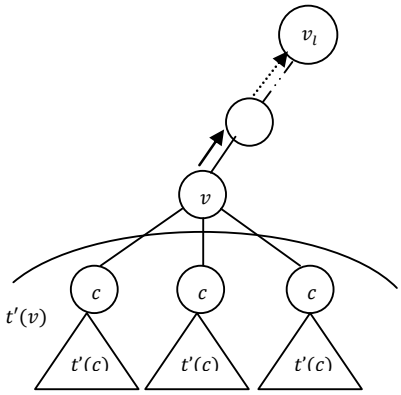

Fig. 3. The rational of dynamic algorithm for non-leaf nodes of tree.

node v_l. 1) Node v reads object i from v_l and stores in itself. Thus, *storing cost* is calculated as described for leaves. In contrast to leaf, we have $t'(v) \neq \emptyset$ and replication cost of $t'(v)$ is the minimum replication cost for children $c \in t'(v)$ with this assumption that node v contains replica of object i. Therefore, *storing cost* for non-leaf is calculated as $C^i_s(v, v_l) = O_i \times (d(v, v_l)+S(v))+\sum_{c\in t'(v)}(C^i_{min}(c, v))$. Similar to the *storing cost* incurred for leaf, $C^i_{set}(v, v_l)$ contains node v and $S_r(v, v_l)$ is increased by one. Thus: $C^i_{set}(v, v_l) = \cup_{c\in t'(v)} C^i_{set}(c, v) \cup v$ and $S_r(v, v_l) = S_r(v, v_l) + 1$, where $\cup_{c\in t'(v)} C^i_{set}(c, v)$ indicates the optimal candidate nodes set of $t'(v)$ if v contains replica of object i. 2) Node v reads object from v_l instead of storing in itself and its cost equals to *reading cost* described for a leaf. Since, in this case, node v does not contain replica of object i, the replication cost of $t'(v)$ is the minimum replication cost of children $c \in t'(v)$ with the assumption that v_l has a replica. Therefore, reading cost for non-leaf is $C^i_r(v, v_l) = r_{v,i} \times O_i \times d(v, v_l) + \sum_{c\in t'(v)}(C^i_{min}(c, v_l))$, and its corresponding parameters $C^i_{set}(v, v_l)$ and $S_r(v, v_l)$ are given by $C^i_{set}(v, v_l) = \cup_{c\in t'(v)} C^i_{set}(c, v_l)$ and $S_r(v, v_l) = S_r(v, v_l) + r_{v,i}$ (see how these parameters are calculated for a leaf that incurs *reading cost*).

Thus, based on the defined constraints for nodes and links, $C_{min}(v, v_l)$ for non-leaf nodes is calculated as follows. If one of constraints is violated ($q_v < d(v, v_l)$ or $bw(v, v_l) < r_{v,i}$), then v has to read object and replicate in itself, and $C_{min}(v, v_l) = C_s(v, v_l)$. If $d(v, v_l) \leq q(v)$, $C_{min}(v, v_l)$ is the minimum of *storing* and *reading* costs. If ($C_{min}(v, v_l) = C_s(v, v_l)$), it is not required to investigate the link constraint because in storing cost case, only one request goes up through links $l \in path(v, v_l)$ that can process at least one request. Otherwise, if ($C_{min}(v, v_l) = C_r(v, v_l)$), it is possible the link constraint violation happens. To handle this violation, in the following subsection, an algorithm called Bandwidth Constraint Handling with Minimal Cost (BCHMC) and also three heuristic algorithms are suggested. Based on the above discussions, Algorithm 1 details Phase 1.

Algorithm 1: Cost Calculation: Phase 1

Input : T_r
Output: $C_{min}(v, v_l)$, $C_{set}(v, v_l), S_r(v, v_l)$

forall $v \in T_r$ *traversed in breadth first order* **do**
  if v *is a leaf* **then**
    if $q_v < d(v, v_l)$ *or* $bw(v, v_l) < r_{v,i}$ **then**
      $S_r(v, v_l) + +$, $C_{min}(v, v_l) \leftarrow C_{sl}(v, v_l)$
      $C_{set}(v, v_l) \leftarrow v$
    else
      Calculate $C_{min} \leftarrow min(C_{sl}(.), C_{rl}(.))$
      if $C_{min}(.) = C_{sl}(.)$ **then**
        $S_r(v, v_l) + +$, $C_{set}(v, v_l) \leftarrow v$
      else
        $S_r(v, v_l) = S_r(v, v_l) + r_{v,i}$
      end
    end
  else
    if $q(v) \leq d(v, v_l)$ *or* $bw(v, v_l) < r_{v,i}$ **then**
      $S_r(v, v_l) + +$, $C_{min}(v, v_l) \leftarrow C_s(v, v_l)$
      $C_{set}(v, v_l) \leftarrow \cup_{c\in child(v)}(c, v) \cup v$
    end
    if $(d(v, v_l) \leq q(v))$ **then**
      Calculate $C_{min} \leftarrow min(C_s(.), C_r(.))$
      if $C_{min}(.) = C_s(.)$ **then**
        $S_r(v, v_l) + +$,
        $C_{set}(v, v_l) \leftarrow \cup_{c\in child(v)}(c, v) \cup v$
      else
        $S_r(v, v_l) = \sum_{c\in child(v)} S_r(c, v_l) + r_{v,i}$
        if $bw(v, v_l) < S_r(v, v_l)$ **then**
          call Bandwidth Constraint Handling Algorithm
        else
          $C_{set}(v, v_l) \leftarrow \cup_{c\in child(v)}(c, v)$
        end
      end
    end
  end
end
Return $C_{min}(v, v_l)$, $C_{set}(v, v_l), S_r(v, v_l)$

B. Bandwidth Constraint Handling

In this section, at first introduced new terminologies and then propose an algorithm to solve bandwidth constraint violation for a non-leaf node v. For clarity in notations, node v is termed by v_f. As discussed above, bandwidth constraint happens when node v_f reads object from v_l and and its requests $S_r(v_f, v_l) = r_{v_f,i}+\sum_{c\in child(v_f)}(r_{c,i})$ increases more than the bandwidth of at least one of the links $l \in path[v_f, v_l]$.

Algorithm 2: Bandwidth Constraint Handling with Minimal Cost (BCHMC)

Input : T_r, $S_r(v, v_l)$
Output: $S_r(v, v_l), C_{min}(v, v_l)$, $C_{set}(v, v_l)$

1 **forall** $v \in R$ **do**
2 | $C_{over}(v) = C_s(v, v_l) - C_r(v, v_l)$
3 **end**
4 $R_{sort} \leftarrow$ sort node $v \in R$ based on $C_{over}(v)$
5 **while** $S_r(v_f, v_l) \leq bw(v_f, v_l)$ **do**
6 | select $v \in R_{sort}$
7 | **if** $(v = v_f)$ **then**
8 | | $S_r(v_f, v_l) = 1$
9 | | $C_{min}(v_f, v_l) = C_s(v_f, v_l)$
10 | | $C_{set}(v_f, v_l) = \cup_{c \in child(v)} C^i_{set}(c, v_f) \cup v_f$
11 | **else**
12 | | $S_r(v_f, v_l) = S_r(v_f, v_l) - (r_{v,i} - 1)$
13 | | $C_{min}(v, v_l) = C_s(v, v_l)$
14 | | $C_{set}(v, v_l) = \cup_{c \in child(v)} C^i_{set}(c, v) \cup v$
15 | **end**
16 **end**
17 Return $C_{min}(v, v_l)$, $C_{set}(v, v_l)$

Algorithm 3: Replica placement: Phase 2

Input : $C_{min}(.), C_{set}(.)$
Output: RP

1 RP$\leftarrow \emptyset$, $lev \leftarrow 1$, $v_{inv} \leftarrow c \in child(r)$
2 Procedure Replica Placement (v_{inv}, lev)
3 **forall** $v \in T_r$ *traversed in level order* **do**
4 | **if** $v_{inv} = Null$ **then**
5 | | Return;
6 | **else**
7 | | **if** $v_{inv} \in C_{set}(v_{inv}, v_{lev})$ *or* $C_{min}(v_{inv}, v_{lev}) = C_s(v_{inv}, v_{lev})$ *or* $C_{min}(v_{inv}, v_{lev}) = C_{sl}(v_{inv}, v_{lev})$ **then**
8 | | | RP$\leftarrow$RP$\cup v$
9 | | | Replica Placement($c \in child(v_{inv})$,1)
10 | | **end**
11 | | **if** $C_{min}(v_{inv}, v_{lev}) = C_r(v_{inv}, v_{lev})$ *or* $C_{min}(v_{inv}, v_{lev}) = C_{rl}(v_{inv}, v_{lev})$ **then**
12 | | | Replica Placement(RP)
13 | | **end**
14 | **end**
15 **end**
16 Return $S_r(v, v_l), C_{min}(v, v_l)$, $C_{set}(v, v_l)$

Note $S_r(v_f, v_l)$ is the summation of requests of node v_f (i.e. $r_{v_f,i}$) and requests of its children that do not contain the replica of object (i.e. $\sum_{c \in child(v_f)}(r_{c,i})$). Let R be a set that includes these nodes and defined as $R = v_f \cup c \in childe(v_f) \wedge c \notin C_{set}(v_f, v_l)$. Also, let $C_{ove}(v)$ be the *overhead cost* of replication for node $v \in R$, which is the difference between *storing cost* ($C_s(v, v_l)$) and *reading cost* ($C_r(v, v_l)$) of node v (i.e., $C_{ove}(v) = C_s(v, v_l) - C_r(v, v_l)$). To eliminate link bandwidth constraint, the BCHMC algorithm is proposed to select nodes from R to host a replica of object i. The rationale behind this algorithm is to select nodes $v \in R$ such that the summation of the overhead cost (i.e., $\sum_{v \in R}(C_{over}(v))$) is minimized and the constraint $S_r(v, v_l) \leq bw(v, v_l), l \in path[v, v_l]$ is satisfied.

To do so, as illustrated in Algorithm 2, overhead cost for all nodes $v \in R$ is first calculated and then these nodes are sorted based on $C_{over}(v)$ on ascending order and denoted by R_{sort}(Lines 1-4). To remove bandwidth constraint, nodes $v \in R_{sort}$ are selected until the condition $S_r(v_f, v_l) \leq bw(v_f, v_l)$ is satisfied for all links $l \in path[v_f, v_l]$. Clearly, if $v = v_f (v \in R)$, then a replica placed at v_f and the already selected nodes (i.e., $v \in R_{sor} \wedge v \neq v_f$) are not considered because by creating a replica in v_f, all requests made by v_f and its children $c \in child(v_f) \wedge c \notin C^i_{set}(v_f, v_l)$ are satisfied with this replica. Thus: $S_r(v_f, v_l) = 1$, $C_{min}(v_f, v_l) = C_s(v_f, v_l)$ and $C_{set}(v_f, v_l) = \cup_{c \in child(v_f)} C^i_{set}(c, v_f) \cup v_f$, where $c \in child(v_f) \wedge c \notin C^i_{set}(v_f, v_l)$ (Lines 5-10). Otherwise, if $v \neq v_f$[3], then a replica should be placed at v. As a result, $S_r(v_f, v_l) = S_r(v_f, v_l) - (r_{v,i} - 1)$ because at least one request from the selected node v goes up through links $l \in path(v, v_l)$, $C_{min}(v, v_l) = C_s(v, v_l)$ and $C_{set}(v, v_l) = \cup_{c \in child(v)} C^i_{set}(c, v) \cup v$ (Lines 11-14).

[3]Note in this condition, node v is a child of v_f that does not contain the replica of object i

C. Phase 2: Top-Down Replica Placement

Phase 2: as illustrated in Algorithm 3, it is a recursive approach that is fed by $C_{min}(.)$ and $C_{set}(.)$ computed in Phase 1. In this phase, an algorithm called *Replica Placement* is suggested to determine which node $v \in T_r$ contains a replica of the object. This algorithm begins at the root of tree and ends at leaves. In the proposed algorithm, assumed that lev is the distance between node v and node v_{inv}. Here, node v has a replica of the object and node v_{inv} is the node that should be investigated whether to host a replica or not, such that (5) is minimized and constraints are satisfied. Sine *Replica Placement* Algorithm starts from root r, we set $lev = 1$, $v = r$ and $v_{inv} = c \in child(r)$.

By starting from the right most child of r, if node $v_{inv} \in C_{set}(v_{inv}, v_{lev})$, then a replica is placed at v_{inv} and it is added to RP, i.e., the set of optimal placement of replicas. Also *Replica Placement* Algorithm is called with $lev = 1$, and $v_{inv} = c \in child(v_{inv})$. That is, Replica Placement ($child(v_{inv}), 1$) (lines 7-10). Otherwise, if $v_{inv} \notin C_{set}(v_{inv}, v_{lev})$, algorithm investigates the value of $C_{min}(v_{inv}, v_{lev})$ and based on this value two cases are considered: 1) If ($C_{min}(v_{inv}, v_{lev}) = C_r(v_{inv}, v_{lev})$), then node v_{inv} does not host a replica and the *Replica Placement Algorithm* is called with $lev = lev + 1$ and $v_{inv} = c \in child(v_{inv})$(lines 11-13). 2) Otherwise, if ($C_{min}(v_{inv}, v_{lev}) = C_s(v_{inv}, v_{lev})$), Replica Placement Algorithm works similar to the case as discussed above where $v_{inv} \in C_{set}(v_{inv}, v_{lev})$.

The time complexity of the algorithm to find an optimal placement of replicas is as follows. The algorithm works in two phases. In Phase 1, for each node $v \in T_r$, the values of $C_{min}(.)$ and $C_{set}(.)$ are calculated. So, the computation requires $O(n)$ if bandwidth constraint is not violated. If this

constraint happens (Lines 27-28), then Algorithm 2 is called and takes time complexity of $O(n)$. Thus, in worst case, the time complexity of Phase 1 is $O(n^2)$. In regard to Phase 2, for all nodes, the computed parameters in Phase 1 are compared and optimal placement of replicas is determined. Thus, this phase takes $O(n)$, and the total computation complexity of proposed algorithm is $O(n^2 + n) = O(n^2)$.

D. Heuristic Algorithms for handling Bandwidth Constraint

In this section, the authors propose three algorithms to address bandwidth constraint and then compare with Algorithm 2 in performance parameters in the next section. These algorithms are as follows:

Bandwidth Constraint Handling Based On Nodes Requests (**BCHNR**): Whenever link bandwidth constraint occurs for node v_f, it is handled as follows: First, all children of v_f not containing replica of object (i.e., $c \in childe(v_f) \wedge c \notin C_{set}(v_f, v_l)$) and node v_f are sorted based on their requests in descending order. Second, the first node in the sorted nodes list is selected and a replica of object is placed at this node. The node selection process is repeated until the bandwidth constraint is removed (i.e., $S_r(v_f, v_l) \geq bw(v_f, v_l)$).

Bandwidth Constraint Handling Based on Nodes Storage Cost (**BCHNSC**): When link bandwidth constraint happens for node v_f, this algorithm works as follows. First the storage cost of replication in all children of node v_f is calculated and then the children of v_f are sorted in ascending order of storage cost. Second, the nodes corresponding to these sorted values are chosen to host replica of the object. The node selection (to host replica) continues until the constraint $S_r(v_f, v_l) \geq bw(v_f, v_l)$ is removed.

Bandwidth Constraint Handling Based on Node Random Selection (**BCHNRS**): Similar to the above discussed heuristic algorithms, whenever the link bandwidth constraint is violated for node v_f, the children of v_f not containing replica are randomly selected to host object replica until the violation is omitted.

Bandwidth Constraint Handling Based on Node v_f (**BCHNV**): In this simple algorithm, if link bandwidth constraint happens for node v_f, then the desired object is replicated in node v_f; as a result the constraint is discarded.

V. Performance Evaluation

Extensive experiments have been done to evaluate optimal placement of replica Algorithm with QoS and bandwidth constraints, using different proposed algorithms that handle bandwidth constraint, with several criterion such as replication cost, network bandwidth usage and local availability of objects.

A. Simulation Setup

In this simulation, the tree is randomly generated and controlled by two parameters: number of nodes and the children of each node that effects the proposed algorithms that handle the bandwidth constraint. The number of nodes n ranges from 100 to 5000 and the number children of each node follows a uniform distribution in (1-5) for $n \leq 1000$ and [1-10] for $n > 1000$. It is set q with a fraction of the tree height h. That is, $q = 1/4h$, $q = 1/2h$, $q = 3/4h$ and $q = h + 1$. The last value of q implies the absence of QoS. The link bandwidth constraint is assigned as follows. Tree links in level 0 connecting a leaf to its father is assigned with a uniform distribution in the range (1, 10), and the link bandwidth of an immediate higher level of that leaf ($level1$) is set to (10, 30) for $n \leq 1000$ and (30-70) for $n > 1000$. Each higher levels links ($level \geq 2$) is assigned between 2 and 4 times the immediate corresponding lower level links. The value of other parameters following a uniform distribution is according to Table I.

TABLE I. Default System Parameter Settings

Parameter	Setting	Parameter	Setting
n	1-5000	$r_{i,v}$	1-10
m	100	$S(v)$	1-20
O_i	1MB-100MB	$d(u, v)$	1-5

B. Results

1) Normalized Replication Cost: It indicates the ratio of replication cost of the proposed algorithms to the **BCHNV** Algorithm as a benchmark. If this ratio is lower, the algorithm works better in finding a placement for the replicas in the tree network. From Fig. 4, observed that the BCHMC Algorithm has minimal normalized replication cost for all q and n values compared with other algorithms. Three observations we can make are as follows: 1) As n increases the normalized replication cost of the BCHMC algorithm decreases. The reason is that when tree size (i.e., n) increases, QoS and link bandwidth constraint violations happen more and the proposed optimal algorithm works better than other algorithms. As an example, for $q = 1/2$, the normalized cost replication decreases from 95% to below 90% when n increases from 100 to 5000. 2) As the requested QoS of nodes is tight (that is q is low), the normalized cost of replication in all proposed algorithms is small in comparison with the case in which QoS tend to be relaxed. This is because, in former case the QoS violation occurs more than the latter case. 3) As expected, the hierarchy between other proposed algorithms in normalized replication cost is respected, i.e., BCHNSC is better than BCHNR which in turn is better than BCHNRS especially n increases. The reason is that the BCHNSC algorithm works based on the storage cost whilst the other two algorithms act based on requests number.

2) Effective Network Usage: It is the ratio of the total data transferred through links to the total requested data for serving user requests. As this parameter decreases, the algorithm performs better in placing replicas in the tree. As shown in Fig. 5, data transferred below 50% through the links in the BCHMC algorithm for all n and q whilst this value for other heuristic algorithms is between 55% and 78%. BCHNR comes after BCHMC such that less than 60% of data is remotely read. In fact, it performs better than other heuristic algorithms. The reason is that the priority of this algorithm is to store replicas in nodes that have more requests. As results show, in regards to remaining heuristic algorithms therefore BCHNSC works better than BCHNRS, which is in turn better than BCHNV. Also, from Fig. 5 It is found that as q decreases, the network usage percentage improves because of more QoS violations, that results in more replicas being placed in the tree.

3) Local Access Percentage of Objects: It exhibits the percentages of user requests in the tree that are locally satisfied. As shown in Table II, by using BCHMC algorithm, more than

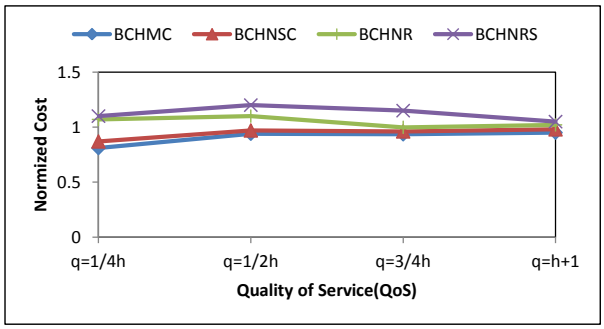

(a)

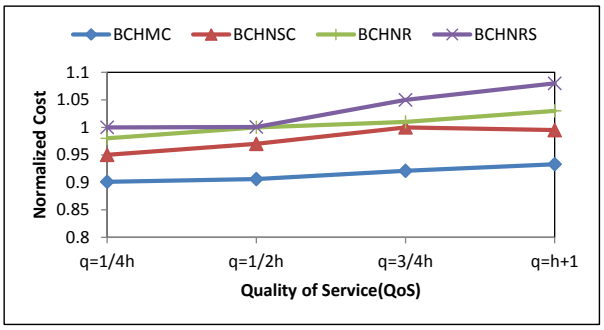

(b)

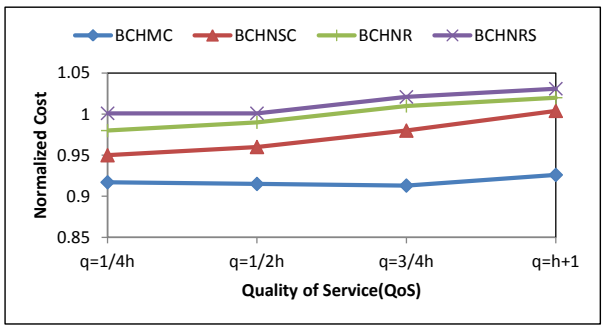

(c)

Fig. 4. Normalized Cost vs. Quality of service(QoS). (a) nodes number=100. (b) nodes number=1000. (c) nodes number=5000.

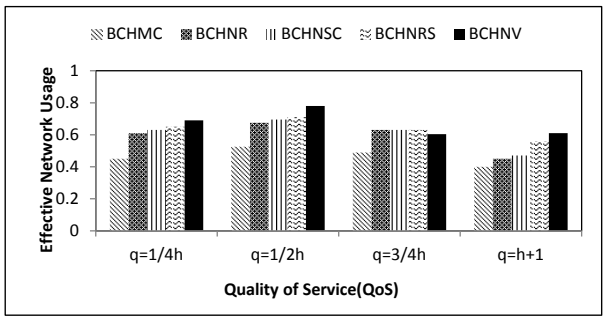

(a)

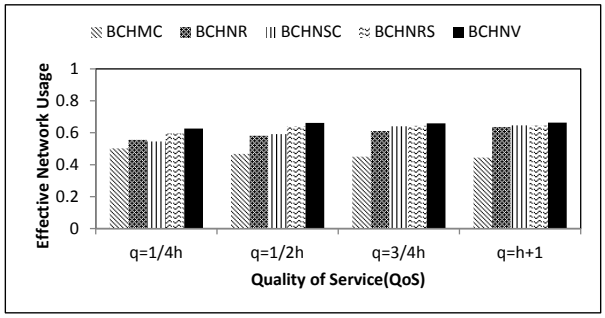

(b)

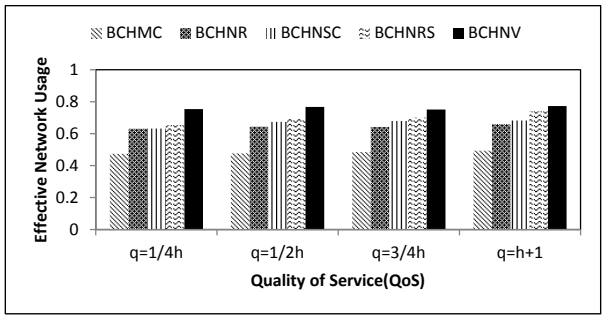

(c)

Fig. 5. Network Usage vs. Quality of service(QoS).(a) nodes number=100. (b) nodes number=1000. (c) nodes number=5000.

50% of requests are locally served and it always outperforms other proposed algorithms for all n and q. But the BCHNV algorithm has the worst performance because in this algorithm the link bandwidth constraint is removed by replication of data in the node v_f instead of its children. As a result, more than 70% of requests remotely access objects. It is also observed the BCHNR algorithm comes after BCHMC with regards to local responsiveness, where BCHNR services 35%-40% of requests locally. The reason is that, to remove bandwidth constraint, BCHNR selects nodes based on their read rate to replicates objects in those nodes. The other algorithms, BCHNSC and BCHNRS, rank next in this metric, respectively.

VI. Conclusions and Future Works

This paper studied a new replica placement algorithm in hierarchical data grid, that amid at replication cost optimization whilst QoS and bandwidth constraints take into consideration. This algorithm has low time complexity which makes it well-suited for data grid environment. The simulation showed that this algorithm compared with heuristic algorithms has suitable performance in terms of access cost, network bandwidth usage and data availability. The BCHMC algorithm replicates data in nodes with guaranteed constraints such that it saves cost by at least 10% compared to other heuristic algorithms. It also locally serve 50% of requests whereas at most only 40% of requests could be locally satisfied in other algorithms. As a future work, we plan to consider updating cost in the proposed algorithms and evaluate the effects of this cost on the performance criterion that are important in data grid environment.

Acknowledgment

The authors would like to thank Deepak C Poola for his helpful suggestions to improve our paper. This work has been done when the second author was with Islamic Azad University. Now, he is a PhD student at Melbourne University in CLOUDS laboratory.

TABLE II. LOCAL ACCESS PERCENTAGE OF OBJECTS

Algorithm	q=1/4h	q=1/2h	q=3/4h	q=h+1
BCHCMC	54.5%	87.4%	50.3%	50%
BCHNR	42.8%	41.4%	35.6%	38.4%
BCHNSC	31.8%	40%	31.8%	40.4%
BCHNRS	30.8%	39.4%	30%	33.7%
BCHNV	30%	31.4%	29%	30.4%

(a) Number of Nodes, n=100

Algorithm	q=1/4h	q=1/2h	q=3/4h	q=h+1
BCHCMC	52%	53.1%	50.8%	50%
BCHNR	38.4%	40.1%	36.6%	36.1%
BCHNSC	34.4%	35.7%	33%	31.2%
BCHNRS	32.4%	33.9%	31.6%	30.4%
BCHNV	30.4%	31.7%	28.9%	29.9%

(b) Number of Nodes, n=1000

Algorithm	q=1/4h	q=1/2h	q=3/4h	q=h+1
BCHCMC	56.7%	58.3%	52.4%	53.4%
BCHNR	40.1%	42.5%	37.7%	38.9%
BCHNSC	39.7%	41.7%	36.6%	35.6%
BCHNRS	38%	41%	30%	34.3%
BCHNV	30.1%	35.6%	34%	34.2%

(c) Number of Nodes, n=5000

REFERENCES

[1] S. Venugopal, R. Buyya, and K. Ramamohanarao, "A taxonomy of data grids for distributed data sharing, management, and processing," *ACM Comput. Surv.*, vol. 38, no. 1, Jun. 2006.

[2] A. Benoit, V. Rehn-Sonigo, and Y. Robert, "Replica placement and access policies in tree networks," *Parallel and Distributed Systems, IEEE Transactions on*, vol. 19, no. 12, pp. 1614–1627, 2008.

[3] O.Kariv and S. Hakimi, "An algorithmic approach to location problems. ii: The p-medians," *SIAM J.Applied Math*, vol. 37, no. 2, pp. 539–560, 1979.

[4] I. Cidon, S. Kutten, and R. Soffer, "Optimal allocation of electronic content," in *INFOCOM 2001. Twentieth Annual Joint Conference of the IEEE Computer and Communications Societies. Proceedings. IEEE*, vol. 3, 2001, pp. 1773–1780 vol.3.

[5] M. Karlsson and C. Karamanolis, "Choosing replica placement heuristics for wide-area systems," in *Proceedings of the 24th International Conference on Distributed Computing Systems (ICDCS'04)*, ser. ICDCS '04. Washington, DC, USA: IEEE Computer Society, 2004, pp. 350–359.

[6] J.-J. Wu, Y.-F. Lin, and P. Liu, "Optimal replica placement in hierarchical data grids with locality assurance," *Journal of Parallel and Distributed Computing*, vol. 68, no. 12, pp. 1517 – 1538, 2008.

[7] V. Rehn-Sonigo, "Optimal replica placement in tree networks with qos and bandwidth constraints and the closest allocation policy," Tech. Rep.

[8] J.-J. Wu, S.-F. Shih, H. Wang, P. Liu, and C.-M. Wang, "Qos-aware replica placement for grid computing," *Concurr. Comput. : Pract. Exper.*, vol. 24, no. 3, pp. 193–213, Mar. 2011.

[9] Z. Du, J. Hu, Y. Chen, Z. Cheng, and X. Wang, "Optimized qos-aware replica placement heuristics and applications in astronomy data grid," *Journal of Systems and Software*, vol. 84, no. 7, pp. 1224 – 1232, 2011.

[10] O. Wolfson and A. Milo, "The multicast policy and its relationship to replicated data placement," *ACM Trans. Database Syst.*, vol. 16, no. 1, pp. 181–205, Mar. 1991.

[11] M. Garmehi and Y. Mansouri, "Optimal placement replication on data grid environments," in *Information Technology, (ICIT 2007). 10th International Conference on*, Dec 2007, pp. 190–195.

[12] Y. Mansouri, S. T. Azad, and A. Chamkori, "Minimizing cost of k-replica in hierarchical data grid environment," in *Advanced Information Networking and Applications (AINA), 2014 IEEE 28th International Conference on*, May 2014, pp. 1073–1080.

[13] K. Kalpakis, K. Dasgupta, and O. Wolfson, "Steiner-optimal data replication in tree networks with storage costs," in *Database Engineering and Applications, 2001 International Symposium on.*, 2001, pp. 285–293.

[14] Y. Mansouri, M. Garmehi, M. Sargolzaei, and M. Shadi, "Optimal number of replicas in data grid environment," in *Distributed Framework and Applications, 2008. DFmA 2008. First International Conference on*, Oct 2008, pp. 96–101.

[15] X. Tang and J. Xu, "Qos-aware replica placement for content distribution," *Parallel and Distributed Systems, IEEE Transactions on*, vol. 16, no. 10, pp. 921–932, 2005.

[16] Y. Mansouri and R. Monsefi, "Optimal number of replicas with qos assurance in data grid environment," in *Asia International Conference on Modelling and Simulation*, 2008, pp. 168–173.

[17] M. Shorfuzzaman, P. Graham, and R. Eskicioglu, "Qos-aware distributed replica placement in hierarchical data grids," in *Advanced Information Networking and Applications (AINA), 2011 IEEE International Conference on*, 2011, pp. 291–299.